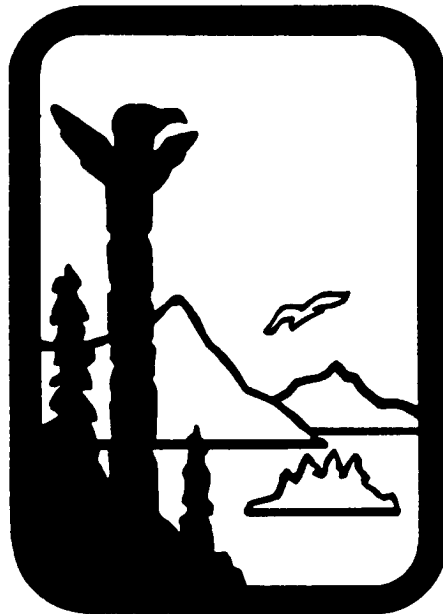


Alaska Department of Environmental Conservation



Amendments to: State Air Quality Control Plan

Vol. III: Appendix III.D.5.08

**{Appendix to Volume II. Analysis of Problems, Control Actions;
Section III. Area-wide Pollutant Control Program; D. Particulate
Matter; 5. Fairbanks North Star Borough PM2.5 Control Plan}**

Public Review Draft

November 14, 2014

**Sean Parnell
Governor**

**Larry Hartig
Commissioner**

(This page serves as a placeholder for two-sided copying)

Appendix III.D.5.08

Modeling Appendix

Speciated Modeled Attainment Test (SMAT).

Aerosol Chemistry in Fairbanks: A summary of prevailing conditions, May 27, 2011, by Richard E. Peltier (MPH, PhD), Dirigo Consulting LLC, Amherst, MA.

Using the CALPUFF dispersion model to characterize the Fairbanks Power Plant Plumes.

Fairbanks PM_{2.5} Non-Attainment Area WRF-ARW, Final Report, Reporting Period March 8, 2011- January 31, 2012, by Dr. Brian J. Gaudet, PI and Dr. David R. Stauffer, co-PI, Department of Meteorology, The Pennsylvania State University, University Park, PA.

Fairbanks Alaska PM_{2.5} Organic Composition and Source Apportionment Research Study, Final Report August 10, 2012, by Dr. Christopher P. Palmer (PhD), Department of Chemistry and Biochemistry, University of Montana, Missoula, MT.

Exploratory Research of Wintertime Aerosol Chemical Composition at a Ground Location in Fairbanks, Alaska, February 10, 2012, by Dr. Richard E. Peltier (PhD), University of Massachusetts.

Final Report to the U.S. Environmental Protection Agency, Stable Boundary Layers Representation in Meteorological Models in Extremely Cold Wintertime Conditions, Reporting Period September 1, 2008- January 31, 2010, by Dr. Brian J. Gaudet, PI and Dr. David R. Stauffer, co-PI, Department of Meteorology, The Pennsylvania State University, University Park, PA.

CMAQ Final Report- Phase I: "Fairbanks PM_{2.5} Non-Attainment Area CMAQ Modeling", December 1, 2011, reporting period March 1, 2011- October 31, 2011, by Dr. Nicole Molders (PhD) and Ketsiri Leelasakultum, Department of Atmospheric Sciences, College of Natural Science and Mathematics, Geophysical Institute, University of Alaska at Fairbanks.

Investigation of means for PM_{2.5} mitigation through atmospheric modeling, April 2011 Final Report Phase I, reporting period December 1, 2008-December 31, 2010, prepared by Dr. Nicole Molders (PhD), Huy N.Q. Tran and Ketsiri Leelasakultum, Department of Atmospheric Sciences, College of Natural Science and Mathematics, Geophysical Institute, University of Alaska at Fairbanks.

CMAQ Final Report- Phase II: "Fairbanks PM_{2.5} Non-Attainment Area CMAQ Modeling", reporting period January 1, 2012- December 31, 2012, by Dr. Nicole Molders (PhD) and Ketsiri Leelasakultum, Department of Atmospheric Sciences, College of Natural Science and Mathematics, Geophysical Institute, University of Alaska at Fairbanks.

Fairbanks PM_{2.5} Source Apportion Estimates, Winter 2008-2009.

Reconciling Trends in Carbon Measurements for Fairbanks, 2006-2010.

CMAQ First Quarterly Report- Phase II: "Fairbanks PM2.5 Non-Attainment Area CMAQ Modeling", reporting period January 1, 2012- April 30, 2012, by Dr. Nicole Molders (PhD) and Ketsiri Leelasakultum, Department of Atmospheric Sciences, College of Natural Science and Mathematics, Geophysical Institute, University of Alaska at Fairbanks.

The Fairbanks, Alaska PM2.5 Source Apportionment Research Study Winters 2005/2006-2012/2013 and Summer 2012, Final Report, Amendments 6 &7, December 23, 2013, by Tony J. Ward, PhD., Center for Environmental Health Sciences, University of Montana, Missoula, MT.

Characterization of PM2.5 from Fairbanks, AK: Organics Analysis for Residential Oil Burner Emissions, Interim Report June 2011, by Dr. Christopher P. Palmer (PhD), Department of Chemistry and Biochemistry, University of Montana, Missoula, MT.

(This page serves as a placeholder for two-sided copying)

5.8. Modeling Appendix

Introduction

This appendix provides the supplemental details of the photochemical transport modeling required as part of the Species Modeled Attainment Test (SMAT). Modeling efforts using PMF and CMB describe the early efforts to quantify the contributions to particulate matter concentrations in Fairbanks. Dispersion modeling results are presented to quantify the potential influence of point sources. Scientific analysis of sulfur formation and organic components of ambient aerosols provide further understanding related to contributing activities and atmospheric processes to PM_{2.5} formation. The photochemical transport modeling sections provide the methodology for converting meteorological model outputs and emission inventories to model-ready inputs. Photochemical model outputs are then presented in the form of episode averaged concentrations of PM_{2.5} components and gaseous SO₂. The resulting future design value concentrations are then calculated for the attainment tests.

Emissions Processing

Emission inventories were processed through the Sparse Matrix Operator Kernel Emissions (SMOKE) model version 2.7.5. The emissions sources were grouped into 8 different source sectors: point, home heating, onroad rate per vehicle (starting exhaust), onroad rate per distance (running exhaust, tire, and brake), onroad rate per profile (evaporative), nonroad including railroad, airport, and other area. All source sectors with the exception of the onroad mobile sources were processed through the following SMOKE program workflow: SMKINVEN, GRDMAT, SPCMAT, TEMPORAL, and SMKMERGE. An additional layer step is needed for point, home heating and airport sources with vertical distributions above the ground level.

Before the emissions processing can be initiated the meteorological data from the WRF model and the emissions inventory are converted to inputs for both the SMOKE and CMAQ models. The meteorological outputs from WRF are used to define the modeling grid (GRIDDESC) for both SMOKE and CMAQ. The Meteorology-Chemistry Interface Processor (MCIP) program version 3.6 was used to prepare the WRF outputs for use with SMOKE and CMAQ. The SMOKE model as configured in 5.8.4 was used to process episodic inventories for the 2008 baseline, 2015 projected baseline, 2015 control scenario, 2019 projected baseline, and 2019 control scenario.

SMOKE Processing Outline

- Meteorological input processing
- Point
 - Actuals
 - PTE
 - Vertical Layering
- Home Heating

- Processing as Point Sources
 - Spatial Allocations
 - Temporal Allocations
 - Speciation Changes
 - AP42
 - Omni
 - Vertical Layering
- Nonroad
 - Spatial Allocations
 - Temporal Allocations
- Other Area
 - Spatial Allocations
 - Temporal Allocations
- Airport
 - Spatial Allocations
 - Temporal Allocations
 - Vertical Layering
- Rate-Per-Vehicle
 - MOVES Lookup Tables
 - Activity Inputs
 - Spatial Allocations
 - Plugins Adjustments
- Rate-Per-Distance
 - MOVES Lookup Tables
 - Activity Inputs
 - Spatial Allocations
- Rate-Per-Profile
 - MOVES Lookup Tables
 - Activity Inputs
 - Spatial Allocations
 - Maintained year to year

SMOKE Emissions Processing Modifications for Fairbanks, AK PM_{2.5} SIP

In support of PM_{2.5} SIP modeling efforts in Fairbanks, Alaska, Sierra Research has created a modified version of the SMOKE-model. Model modifications were made in order to generate highly resolved home heating emissions and address bugs in the processing of onroad mobile source emissions from the MOVES model. The baseline source codes used in these projects were SMOKE version 2.7.5, MOVES 2010a, and SMOKE-MOVES 0.20 and 0.31. Processed emissions were evaluated using Verdi 1.31, custom NCL scripts, custom BASH and CSH SHELL scripts, and NCO programs on a custom-built computer (Intel i7 950 4 core/8 thread, 8 GB system memory, 1 TB hard disk drive) running Ubuntu 10.04 OS.

The modeling episodes span January 23 through February 11 and November 7 through November 22. The modeling domain covers 199x199 grid cells of 1.33x1.33km size comprising the bulk of the Fairbanks North Star Borough and 38 vertical layers up to 20km.

Area Source Modifications

Home heating emissions inputs to the SMOKE model were generated using a Fairbanks-specific heating demand model developed by Sierra Research. The home heating model is informed by multiyear phone surveys, in-home instrumentation data, device measurement studies, local land parcel data, census records and local day-specific meteorology. The home heating model can produce highly spatially resolved, hourly emissions for the 199x199 gridded model domain. To best preserve the temporal and spatial resolution of this inventory, an alternative approach to the standard SMOKE area source processing via spatial and temporal surrogates schemes was developed. The most efficient approach was to treat the home heating source input file as a large point source emissions inventory with hourly specified emissions.

Both an inventory input and hourly emissions input file were created to meet SMOKE's point source processing requirements: PTINV¹ and PTHOUR. The PTINV input was formatted per the ORL formatting guidelines². Descriptive, dummy text was applied to the facility information fields with the exception of the FIPS, SCC codes, pollutant CAS number, X location and Y location. In this instance, the PTINV file ultimately serves as a spatial allocation file. The PLANTID field is given a name specific to the grid cell where the home heating activity is located and which corresponds to the latitude and longitude specified by the X and Y location fields. Since hourly emissions data are imported with PTHOUR, the emission levels in the PTINV file are set to dummy values and not ultimately used. PTHOUR follows the EMS95 Wide format per the SMOKE guidelines.³

Changes to the SMOKE code were made to allow for the home heating sources to be processed using the PTINV and PTHOUR inputs while preserving the sector's identity as an area source. Code sections that received changes are noted below and comments were added within the source code. The initial code changes were made to the inventory importing routines within the smkinven⁴ program. Lines of code were added to read the HOUR_SPECIFIC_YN environment variable on lines 201 to 205 within the area source subsection of smkinven.f. Modifications were subsequently required on lines 249, 256, 273, 275, 401, and 424 related to the source category variable CATEGORY. For simplicity when the hour-specific emissions variable was set to true, the source category was changed from AREA to POINT before calling certain subroutines. The old category was stored in a separate variable and then recalled after these subroutines were completed. This category swapping was preferable to rewriting each of the subroutines to allow both POINT and AREA categories to use the PTHOUR emissions and PTINV inventory files. Subroutines impacted by this category swapping were the following:

¹ Variables, subroutines, and inputs are presented in all capitalized form for clarity.

² SMOKE v2.7 User's Manual: section 8.2.8.3 pages 408-412

³ SMOKE v2.7 User's Manual: section 8.2.7.2 pages 300-401

⁴ Executable programs and their source code files are presented in lowercase to distinguish them from variables, subroutines, and inputs.

RDINVSRCs, PROCINVSRCs, PROCINVEN, OPENINVOUT, WRINVCHR, SRCMEM, and WRINVE MIS.

Several other subroutines were impacted by the point as area and hourly emissions changes. The INITFINFO subroutine in file initinfo.f was modified on lines 61, 67 and 76 to read the hourly emissions flag. Conditional statements were placed or modified to correctly initialize variables associated with processing the hourly area source emissions and inventory data as for the treatment of the hourly area source emissions on lines 77, 112, 120, 166, 176, 187, 201, 203, 219, and 237.

The OPENINVIN subroutine was altered on line 121 to allow for hourly specified emissions outside of POINT sources. Conditional statements were added on lines 340 and 347 to avoid opening certain point source related files that were not required for the area source category. RDINVDATA was updated to add logic around the instances where hourly specific emissions were to be used and area source category inventories were being read. Line 225 was modified to determine whether the hourly specific emissions flag was set. Lines 362, 669, 691, 795, 855, 1171, 1188, 1389, 1393, 1458, 1460, 1479, and 1495 received modifications to their conditional statement logic to have the hourly specific area source files process more like point source files when the hourly specific emissions flag was set.

Due to the 8-character, SCC length limitations of the EMS95 Wide Format, the RDEMSPD subroutine in rdemspd.f had to be altered to extend the SCC size from 8 to 10 characters for EMS95 Wide emission files. Extending the SCC field width requires shifting all of the proceeding fields by the number of characters added to the SCC field. Changes occurred on lines 273 and 274 where the position of the field following the SCC code is defined: DATNAM. Both the start and end positions of the DATNAM field were increased by two, 381 to 383 and 396 to 398. There are no other fields that follow these in the EMS95 Wide format. Lines 680 and 721 are responsible for reading the SCC code from each line in the PTHOUR file. The values indicating the ending position of the SCC code were increased by two digits from 380 to 382.

Additional precision was also sought in the reading of the latitude and longitude entries, XLOC and YLOC, of the PTINV file. The RDINVDATA subroutine was modified to accept two additional digits of precision when reading latitude and longitude, line 214 in the file rdinvdata.f. Lines 1502 and 1503 were revised to preserve the desired precision of the XLOC and YLOC by using a formatted read statement instead of the existing code's usage of the function STR2REAL. Subroutine RDDATAORLPT in file rddatantipt.f was modified on lines 75 and 76 to extend the LAT and LON dimensions from 9 to 11.

A section of the subroutine WRPDEMIS that checks for missing emissions data and fills in those data with values based on annual emissions data was modified since the area emissions are now using hourly data only. An error would result due to the inability of the code to differentiate between missing emissions data and a zero emissions value. Line 319 was modified to set null emissions to zero.

Following changes to the smkinven source code, the smkinven program was compiled and tested with PTINV and PTHOUR area source inputs. Debug statements, log files for the smkinven program, and intermediate data files were inspected as part of the QA process to address any coding errors and resolve any bugs. The resulting intermediate files from the imported inventory and emission files were then passed to the grdmat, spcmat, and temporal programs.

The gridding program, grdmat, was updated to use the latitude and longitude information from the imported inventory file to grid the emissions. Sections of code were added on lines 172 and 199 to read the hourly-specific emissions flag and conditionally branch into point source spatial allocation subroutines even when the area category was being processed. Conditional statements were modified on lines 254, 299, 303, 641, 706, 726, and 756 to allocate sufficient memory for the number of sources and to call subroutines to convert the latitude and longitude to gridded outputs. Source code in.opengmat.f was modified on lines 87, 110 and 120 to setup the correct headers for the area source as points gridding matrix. Grdmat was then compiled and tested similarly to the smkinven program.

The speciation program, spcmat, received updates to correct for problems with processing the hourly area sources. Changes occurred on lines 152 and 166 to add reading of the hourly specified flag and a temporary variable for storing the source category. A line of code was added on line 186 to read the hourly emissions environment flag. Source code was added on line 271 to artificially switch the source code to POINTS before running the RDINVCHR subroutine that reads inventory characteristics. This is a more efficient solution than modifying the RDINVCHR code. A conditional statement in file asgntag.f line 179 was changed to allow both hourly point and area sources to use a set of SCC storage arrays required for the number of sources being processed. The profile assignment subroutine in asgnsprow.f was modified on lines 129, 190, 224, 234, 242, 314 and 361 to accommodate the changes to the rest of the spcmat program. Spcmat was compiled and tested using the existing intermediate files from smkinven.

No modifications were required to the temporal allocation program within SMOKE. Temporal was tested as is with some additional debug statements to ensure clean processing of the hourly area sources. Intermediate files and log files were also checked to determine the successful operation of the program.

With the completion of the smkinven, grdmat, spcmat, and temporal programs some minor changes to the smkmerge program was made to merge together the spatial, temporal, and speciated intermediate data files. Code was written on lines 206 and 219 to determine if hourly specific data were being merged. Next conditional statements on lines 393, 401, 404, 419, 429, 433, 452, 561, 565, 625, 657, 661, 666, 719, 720, 761, 766, 795, 924, 925, 939, and 951 were written to correctly call point source or area source subroutines depending on the state of the hourly specific data variable. The resulting code was compiled and extensively bug tested using intermediates generated from the previously mentioned intermediate programs. The outputs from smkmerge were plotted using the Verdi program and exported to both Excel and ArcGIS compatible file formats for spatial and temporal assessments. NCO software, ncl scripts, and BASH scripts were utilized in creating data summaries of the inventories generated from this process.

SMOKE-MOVES code changes, bug fixes, daily meteorology

The MOVES 2010a model was used to create onroad emissions inventory lookup tables for the Fairbanks PM_{2.5} nonattainment area. Local data was used for the configuration of the MOVES model for the two separate modeling episodes. Details on the operation of MOVES and post processing are described in the Emission Inventory Data CMAQ/SMOKE 2008 sections. The meteorological processing routines in the MET4MOVES code was changed to allow for daily processing of meteorology for use in the MOVES model and the MOVESMRG program. Lines 293 and 312 of met4moves.f were modified to indicate daily averaging methods were being used. Lines 163, 262, 266, and 269 of rdmetmoves.f were modified to allow for day specific averaging and storing of minimum and maximum while reading the MCIP processed meteorology fields.

Revisions to the SMOKE source code were made for the processing of the MOVES mobile source emissions inventory. These changes were necessary due to bugs from the preliminary nature of the releases of the software available at the time: SMOKE 2.7.5b and the SMOKE-MOVES processing tools version 0.20 – 0.31.

The MOVESMRG source code was modified to correct for errors that occurred during the reading and processing of the mobile source emissions inventory. These errors included the exceeding of arrays. The BLDSRCCELL subroutine in file bldsrcell.f allocates the source fractions to each grid cell. Conditional statements were added on line 82 and 87 to ensure the SRC variable falls between 1 and NSRC (the maximum number of sources) to prevent the NSRCCELLS array from exceeding its bounds.

For the core MOVESMRG source code a bug was addressed with the discrepancy between county codes used in movesmrg.f and in other subroutines resulting in an error in the arrays AVGMIN and AVGMAX. Parameter CNTYCOD was added on line 78 and used on line 546 to correctly address the county number for determining MINVAL and MAXVAL. Additional debug statements and warning messages were added to movesmrg.f on lines 546, 717 and 720.

Photochemical Modeling

Model outputs were extracted for the State Office Building grid cell in the modeling domain for all episode days. The episode averages and multi-episode averages are shown in tables below for the 2008 baseline, 2015 projected baselines, 2015 control scenarios. The 2015 year emissions are presented both with actual point source emissions (Actuals) and PTE-level point source emissions (PTE). Outputs are shown as for PM_{2.5} total, OC (organic carbon), EC (elemental carbon), SO₄ (sulfate), NO₃ (nitrate), NH₄ (ammonium), OTH (other), SOA (secondary organic aerosol), and SO₂ (gaseous sulfur dioxide).

Table 5.8-1. 2015 PM Species Concentrations Episode Averages and Multi-Episode Averages

Scenario	Averaging Period	PM _{2.5} (µg/m ³)	OC (µg/m ³)	EC (µg/m ³)	SO ₄ (µg/m ³)	NO ₃ (µg/m ³)	NH ₄ (µg/m ³)	OTH (µg/m ³)	SOA (µg/m ³)	SO ₂ (ppm)
2008 Baseline	Ep1 & Ep2	35.72	24.47	4.34	2.13	1.30	1.17	2.31	0.01	0.02
	Ep1	42.01	29.24	5.13	2.40	1.25	1.25	2.73	0.01	0.02
	Ep2	28.53	19.01	3.44	1.83	1.35	1.07	1.83	0.01	0.01
2015 Baseline Actuals	Ep1 & Ep2	33.91	23.36	3.82	2.20	1.23	1.17	2.13	0.01	0.02
	Ep1	39.59	27.66	4.52	2.48	1.20	1.27	2.47	0.01	0.02
	Ep2	27.42	18.44	3.01	1.88	1.27	1.07	1.73	0.00	0.01
2015 Baseline PTE	Ep1 & Ep2	36.90	23.48	3.91	2.72	1.26	1.35	4.18	0.01	0.02
	Ep1	42.82	27.81	4.65	3.02	1.21	1.44	4.69	0.01	0.02
	Ep2	30.12	18.53	3.07	2.37	1.32	1.25	3.59	0.01	0.02
2015 Controls Actuals	Ep1 & Ep2	30.80	20.70	3.46	2.18	1.18	1.15	2.13	0.01	0.02
	Ep1	36.04	24.61	4.11	2.46	1.15	1.24	2.47	0.01	0.02
	Ep2	24.82	16.23	2.72	1.86	1.22	1.05	1.73	0.00	0.01
2015 Controls PTE	Ep1 & Ep2	33.77	20.82	3.56	2.70	1.20	1.32	4.18	0.01	0.02
	Ep1	39.24	24.76	4.25	2.99	1.14	1.40	4.69	0.01	0.02
	Ep2	27.51	16.32	2.78	2.36	1.26	1.22	3.58	0.01	0.02

Relative response factors for each of the components of PM_{2.5}, gaseous SO₂, and SO₄* are calculated for 2015. SO₄* RRF represents the combined impacts of primary and secondary sulfate on PM_{2.5} using both modeled and measured estimates of sulfur. The method for calculating SO₄* is explained below. PM_{2.5} and SO₂ RRFs are calculated by dividing the modeled concentrations in the 2015 multi-episode 24-hour averaged concentration of a species by the 2008 multi-episode 24-hour averaged concentration:

$$RRF_i = \frac{[i_{2015}]}{[i_{2008}]}$$

where RRF is the relative response factor of species i and $[i]$ is the concentration of i for 24-hours averaged over all episode days in 2008 and 2015.

The SO_4^* RRF is calculated as the weighted average of the SO_4 and SO_2 RRFs. A process analysis study of the CMAQ-model for both the modeling episodes by Leelasakultum and Mölders found that nearly all of the sulfate is derived from primary emissions.⁵ Any RRF derived from the modeled SO_4 concentrations would overestimate the impacts of changes to primary SO_4 while ignoring the impacts of changes to gaseous SO_2 . In order to estimate the likely impacts of changes to SO_2 emissions on $PM_{2.5}$ a method was developed to account for the secondary formation of sulfate:

$$RRF_{SO_4^*} = \frac{([SO_{4(FRM)}] - [SO_{4(CMAQ)}]) \times RRF_{SO_2}}{[SO_{4(FRM)}]} + \frac{[SO_{4(CMAQ)}] \times RRF_{SO_4}}{[SO_{4(FRM)}]}$$

Where the variables are defined as follows:

- $RRF_{SO_4^*}$ is the relative response factor for both primary and secondary sulfate
- $[SO_{4(FRM)}]$ is the measured concentration of SO_4 averaged over FRM days for both episodes in $\mu g/m^3$
- $[SO_{4(CMAQ)}]$ is the modeled concentration of SO_4 averaged over FRM days for both episodes in $\mu g/m^3$
- RRF_{SO_2} is the relative response factor of gaseous SO_2
- RRF_{SO_4} is the relative response factor of primary SO_4 .

This method assumes that the sulfate concentrations calculated by CMAQ are due only to primary emissions and transport of sulfate. This assumption seems reasonable given the results of the process analysis study by Leelasakultum and Mölders.⁶

Table 5.8-2. 2015 PM and SO_2 Relative Response Factors - Episode Averages and Multi-Episode Averages

Scenario	Averaging Period	OC	EC	SO_4	NO_3	NH_4	OTH	SO_2	SO_4^*
2008 Baseline	Ep1 & Ep2	1.00	1.00	1.00	1.00	1.00	1.00	1.00	1.00
	Ep1	1.00	1.00	1.00	1.00	1.00	1.00	1.00	1.00
	Ep2	1.00	1.00	1.00	1.00	1.00	1.00	1.00	1.00
	Ep1 & Ep2	0.95	0.88	1.03	0.95	1.00	0.92	1.06	1.05

⁵ Fairbanks North Star Borough PM 2.5 Non-Attainment Area CMAQ Modeling Final Report Phase II DEC 2012 By Prof. Nicole Mölders (PhD, PhD) and Ketsiri Leelasakultum (MS) University of Alaska Fairbanks, Geophysical Institute, College of Natural Science and Mathematics, Department of Atmospheric Sciences

⁶ IBID

2015 Baseline Actuals	Ep1	0.95	0.88	1.03	0.96	1.01	0.90	1.06	1.05
	Ep2	0.97	0.88	1.03	0.94	1.00	0.95	1.06	1.04
2015 Baseline PTE	Ep1 & Ep2	0.96	0.90	1.27	0.97	1.15	1.80	1.29	1.28
	Ep1	0.95	0.91	1.26	0.97	1.15	1.72	1.26	1.26
	Ep2	0.97	0.89	1.30	0.97	1.16	1.96	1.33	1.32
2015 Controls Actuals	Ep1 & Ep2	0.85	0.80	1.02	0.91	0.98	0.92	1.05	1.04
	Ep1	0.84	0.80	1.02	0.92	0.99	0.90	1.05	1.04
	Ep2	0.85	0.79	1.02	0.90	0.98	0.95	1.05	1.04
2015 Controls PTE	Ep1 & Ep2	0.85	0.82	1.26	0.92	1.13	1.80	1.28	1.27
	Ep1	0.85	0.83	1.25	0.92	1.12	1.72	1.26	1.25
	Ep2	0.86	0.81	1.29	0.93	1.13	1.96	1.33	1.31

Ammonium and particle bound water RRFs are calculated based on the changes to sulfate and nitrate RRFs. Calculated future ammonium concentrations are fixed at $0.29 \times [\text{NO}_3] + 0.37 \times [\text{SO}_4]$. The ratios of 0.29 for $\text{NH}_4:\text{NO}_3$ and 0.37 for $\text{NH}_4:\text{SO}_4$ are fixed based on the 2006 – 2010 winter average (quarters 1 and 4) values used for SANDWICH. Particle bound water RRFs are calculated by attributing 1/3rd of the PBW to ammonium nitrate and 2/3rd of the PBW to ammonium sulfate as discussed in the precursors document in Appendix III.D.5.7. The equation to calculate the PBW RRF is shown below:

$$RRF_{PBW} = \frac{2}{3} \times RRF_{SO_4} + \frac{1}{3} \times RRF_{NO_3}$$

Where RRF_{PBW} , RRF_{SO_4} , and RRF_{NO_3} are the relative response factors for PBW, SO_4 and NO_3 respectively. The RRFs from model outputs averaged over both episodes are used to calculate the future design values for 2015 emissions scenarios.

Future design values calculated from the RRFs above with a $0.5 \mu\text{g}/\text{m}^3$ credit for voluntary measures are presented in table 5.8-3. Scenarios for the baseline projections and controls were simulated with actual point source emissions (Actual) and potential to emit levels (PTE). Three sets of design values are shown for each scenario depending on the treatment of sulfate: FDV, FDV SO_4 , and FDV SO_4^* . The FDV column calculates the design value based on RRFs for OC, EC, NO_3 and OTH with PBW and NH_4 RRFs derived as stated above. Per discussions with EPA regarding the model performance of SO_4 the sulfate RRF is held to 1.0. FDV SO_4 and FDV SO_4^* present scenarios where the sulfate RRF is used in the design value calculations. FDV SO_4 uses the RRF calculated from the model outputs for $[\text{SO}_4]$ with no modifications. Based on the model performance and process analysis assessment this approach likely does not account for secondary sulfate. FDV SO_4^* uses the RRF for SO_4^* in the design value calculation. This treatment of the design value should more accurately capture the influence of both secondary and primary sulfate on $\text{PM}_{2.5}$ concentrations.

Voluntary measure benefits are calculated as the weighted average of a 3% credit in onroad mobile source contributions and a 6% reduction in the remaining sources. The total needed

reductions based on the baseline design value of $44.7 \mu\text{g}/\text{m}^3$ and 24-hour $\text{PM}_{2.5}$ NAAQS of $35 \mu\text{g}/\text{m}^3$ would be calculated as $44.7 - 35 = 9.7 \mu\text{g}/\text{m}^3$. Using the inventory for the 2008 baseline onroad mobile sources contribute 13.7% of the direct $\text{PM}_{2.5}$ in the nonattainment area with all other sources contributing 86.7%. A 3% voluntary measure credit from mobile source would yield a reduction of $3\% * 13.7\% * 9.7 \mu\text{g}/\text{m}^3 = 0.04 \mu\text{g}/\text{m}^3$. A 6% voluntary measure benefit from all other sources would yield a reduction of $6\% * 86.7\% * 9.7 \mu\text{g}/\text{m}^3 = 0.5 \mu\text{g}/\text{m}^3$. A total voluntary credit of $0.5 \mu\text{g}/\text{m}^3$ is taken when rounding to the first decimal.

Table 5.8-3. Future Design Values for 2015 baselines (Actual and PTE) and Control Scenarios (Actual and PTE)

Scenario	FDV ($\mu\text{g}/\text{m}^3$)	FDV SO_4 ($\mu\text{g}/\text{m}^3$)	FDV SO_4^* ($\mu\text{g}/\text{m}^3$)
2015 Baseline Actual	42.4	42.8	43.0
2015 Baseline PTE	43.2	46.6	46.8
2015 Control Scenario Actual	39.6	39.8	40.1
2015 Control Scenario PTE	40.1	43.4	43.5

The treatment of Actual and PTE point sources along with the influence of sulfate can produce a range of results for the control run between $39.6 \mu\text{g}/\text{m}^3$ and $43.5 \mu\text{g}/\text{m}^3$. The PTE bias alone can cause the results to shift by $0.5 \mu\text{g}/\text{m}^3$ to $3.6 \mu\text{g}/\text{m}^3$ depending on the treatment of sulfate. This range of bias is caused by the significant contributions of sulfate and sulfur dioxide from point sources. The most realistic approximation of the FDV in 2015 would be $40.1 \mu\text{g}/\text{m}^3$ from the 2015 Control Scenario Actual with SO_4^* .

CMAQ-modeled outputs for 2019 baseline and control scenarios are shown in tables 5.8-4. Similar to 2015 the outputs are shown as averaged over both episodes and for individual episodes across $\text{PM}_{2.5}$ total, OC, EC, SO_4 , NO_3 , NH_4 , OTH, SOA, and SO_2 . Simulations for 2019 are presented only for the case where point sources are held to PTE levels. A 2019 baseline and control scenario are shown along with the 2008 baseline for comparison. The control scenario package contains the ARA OHH, WSCO, State standards, natural gas expansion, dry wood, and natural turnover. Credit for voluntary measures is taken following the RRF calculations below.

Table 5.8-4. 2019 PM Species Concentrations Episode Averages and Multi-Episode Averages

Scenario	Averaging Period	PM _{2.5} (µg/m ³)	OC (µg/m ³)	EC (µg/m ³)	SO ₄ (µg/m ³)	NO ₃ (µg/m ³)	NH ₄ (µg/m ³)	OTH (µg/m ³)	SOA (µg/m ³)	SO ₂ (ppm)
2008 Baseline	Ep1 & Ep2	35.72	24.47	4.34	2.13	1.30	1.17	2.31	0.01	0.02
	Ep1	42.01	29.24	5.13	2.40	1.25	1.25	2.73	0.01	0.02
	Ep2	28.53	19.01	3.44	1.83	1.35	1.07	1.83	0.01	0.01
2019 Baseline PTE	Ep1 & Ep2	37.16	23.84	3.79	2.76	1.26	1.36	4.15	0.02	0.01
	Ep1	43.02	28.14	4.49	3.07	1.21	1.46	4.64	0.02	0.01
	Ep2	30.47	18.91	2.99	2.41	1.31	1.26	3.59	0.02	0.00
2019 Controls PTE	Ep1 & Ep2	26.87	14.70	2.57	2.78	1.29	1.39	4.13	0.02	0.00
	Ep1	31.29	17.80	3.12	3.08	1.19	1.47	4.62	0.03	0.00
	Ep2	21.81	11.16	1.95	2.43	1.40	1.30	3.57	0.02	0.00

Relative response factors for 2019 are calculated in the same manner as for 2015 using 2008 as the base year with 2019 as the future year. Again no Actual level point source outputs are presented here.

Table 5.8-5. 2019 PM and SO₂ Relative Response Factors - Episode Averages and Multi-Episode Averages

Scenario	Averaging Period	OC	EC	SO ₄	NO ₃	NH ₄	OTH	SO ₂	SO ₄ *
2008 Baseline	Ep1 & Ep2	1.00	1.00	1.00	1.00	1.00	1.00	1.00	1.00
	Ep1	1.00	1.00	1.00	1.00	1.00	1.00	1.00	1.00
	Ep2	1.00	1.00	1.00	1.00	1.00	1.00	1.00	1.00
2019 Baseline PTE	Ep1 & Ep2	0.97	0.87	1.29	0.97	1.17	1.79	1.32	1.31
	Ep1	0.96	0.88	1.28	0.97	1.17	1.70	1.30	1.29
	Ep2	1.00	0.87	1.32	0.97	1.17	1.96	1.37	1.35
2019 Controls PTE	Ep1 & Ep2	0.60	0.59	1.30	0.99	1.19	1.79	1.43	1.38
	Ep1	0.61	0.61	1.28	0.95	1.17	1.69	1.39	1.35
	Ep2	0.59	0.57	1.33	1.03	1.21	1.95	1.50	1.43

Design values for 2019 are derived from the above RRFs with the same considerations for sulfate presented for each scenario in Table 5.8-6: FDV, FDV SO₄, and FDV SO₄*. The bias from PTE emissions is not calculated in the 2019 scenarios, but the influence is again expected to range from 0.5 µg/m³ to 3.6 µg/m³ depending on the sulfate RRF calculations. The previously calculated voluntary measure credit of 0.5 µg/m³ is also applied to the FDV values for 2019 in the table below.

Table 5.8-6. Future Design Values for 2019 baseline (PTE) and Control Scenarios (PTE)

Scenario	FDV ($\mu\text{g}/\text{m}^3$)	FDV SO ₄ ($\mu\text{g}/\text{m}^3$)	FDV SO ₄ * ($\mu\text{g}/\text{m}^3$)
2019 (PTE)	43.4	47.1	47.4
2019 Control Scenario (PTE)	33.5	37.3	38.3

Unmonitored Area Analysis

Areas in the nonattainment region away from the monitor sites require additional analysis to show attainment under a control scenario. These unmonitored areas are reviewed using a technique described as unmonitored area analysis (UMAA). The UMAA methodology blends photochemical model predicted concentrations of PM_{2.5} with interpolated ambient monitor data to produce a map of future concentrations throughout the nonattainment area. This approach takes advantage of modeled PM_{2.5} gradients between grid cells while making use of the existing monitor network's spatial fields. Three steps are recommended for UMAA; 1) interpolate ambient data, 2) adjust ambient spatial fields with modeled outputs, 3) adjust model-modified spatial fields with modeled cell-by-cell RRFs.⁷

1) Interpolation of Measured Ambient Concentrations

The interpolation of ambient monitored PM_{2.5} concentrations relies on data from monitor sites over the design period of 2006 – 2010 to produce a five year weighted average design value as described in the SMAT section of the SIP (Chapter 5.8.9.2). The only available monitor with FRM-derived speciated concentrations covering all winters for 2006 through 2010 was the State Office Building monitor. Several other temporary monitor sites were operated during that period. The measurements from these sites were compared against the total PM_{2.5} at the State Office Building monitor site during severe winter episodes to establish a ratio. These sites were then used in lieu of more permanent monitors to spatially interpolate PM_{2.5} concentrations. Since the data from these sites were not all speciated the total PM_{2.5} was used to establish the ratios between the State Office Building and the rest of the sites in the nonattainment area.

2) Adjusting Ambient Spatial Fields with Modeled Outputs

The spatial information from the monitors is adjusted with modeled outputs using the Voronoi Neighbor Averaging (VNA) technique. The VNA technique was applied in Excel as described in the BenMAP: Environmental Benefits Mapping and Analysis Program User's Manual.⁸

⁷ Guidance on the Use of Models and Other Analyses for Demonstrating Attainment of Air Quality Goals for Ozone, PM_{2.5}, and Regional Haze U.S. Environmental Protection Agency Office of Air Quality Planning and Standards Air Quality Analysis Division Air Quality Modeling Group Research Triangle Park, North Carolina - EPA -454/B-07-002 April 2007

⁸ BenMAP: Environmental Benefits Mapping and Analysis Program User's Manual, September 2008, Prepared for Office of Air Quality Planning and Standards, U.S. Environmental Protection Agency by Abt Associates Inc.

BenMAP software was not used due to the limited monitor availability during the modeling episodes. VNA operates as an inverse-distance weighted average of monitor values. The VNA method was coded to match the default options in BenMAP with no distance cutoff or maximum number of monitors. The $PM_{2.5}$ weighted average is calculated in a given grid cell as follows,

$$PM_{2.5i} = \frac{\frac{1}{d_1} * \frac{[obs_1]}{[model_1]} + \frac{1}{d_2} * \frac{[obs_2]}{[model_2]} + \dots + \frac{1}{d_n} * \frac{[obs_n]}{[model_n]}}{\frac{1}{d_1} + \frac{1}{d_2} + \dots + \frac{1}{d_n}} * [model_i]$$

Where $PM_{2.5i}$ is the adjusted $PM_{2.5}$ concentration in a grid cell i ; d_1 , d_2 , and d_n are the distances between the grid cell i and 1st, 2nd, and n^{th} monitors; obs_1 , obs_2 , and obs_n are the observed $PM_{2.5}$ concentrations at the 1st, 2nd, and n^{th} monitors; $model_1$, $model_2$, and $model_n$ are the modeled concentrations at the 1st, 2nd, and n^{th} monitor grid cells; $model_i$ is the modeled concentration in the grid cell i . The adjusted grid cells are calculated over the nonattainment area grid cells using the 2008 baseline model outputs.

3) Relative Response Factor Adjustments of Spatial Fields

Cell by cell RRFs were calculated for total $PM_{2.5}$ in the modeling domain for the 2015 and 2019 control scenarios. The total $PM_{2.5}$ RRF was used instead of the individual components due to the lack of speciated measurements away from the State Office Building monitor site. To be consistent with the methodology used in the FDV calculations the total $PM_{2.5}$ RRF in each grid cell was calculated as follows:

$$RRF_{PM} = \frac{OC_{future} + EC_{future} + NO3_{future} + NH4_{future} + OTH_{future} + SO4_{baseline}}{OC_{baseline} + EC_{baseline} + NO3_{baseline} + NH4_{baseline} + OTH_{baseline} + SO4_{baseline}}$$

Where the RRF_{PM} is the relative response factor for $PM_{2.5}$ for a future year control scenario in a grid cell; OC, EC, NO₃, NH₄, OTH, and SO₄ are concentrations of individual $PM_{2.5}$ species for either the future year or the baseline year. Note the SO₄ contribution to the RRF is held constant to match the RRF_{SO_4} calculation used in the attainment demonstration.

SMAT (Speciated Modeled Attainment Test)

EPA model guidance, “Guidance on the Use of Models and Other Analyses for Demonstrating Attainment of Air Quality Goals for Ozone, PM_{2.5}, and Regional Haze” (USEPA, 2007), recommends the Species Modeled Attainment Test (SMAT) to estimate future concentrations of daily PM_{2.5} concentration. The method combines monitoring data with outputs from simulation models to estimate future PM_{2.5} concentrations. It can be used to determine whether emission reductions will bring ambient concentrations to or below the National Ambient Air Quality Standard (NAAQS) ($\leq 35 \mu\text{g}/\text{m}^3$ for 24-hr PM_{2.5}). The SMAT is combined with other modeling techniques and relevant supplemental evidence to develop a technically-sound, weight-of-evidence recommendation on whether the proposed control strategies will meet the goal of pollution levels below the NAAQS.

SMAT recommends a nine-step process to take historically-measured PM_{2.5} concentrations, apply factors to represent changes from the historical period to a future year, and estimate the future PM_{2.5} design value (DV). The historically-measured PM_{2.5} concentrations are sampled from the top 25% of polluted wintertime days within a five-year period. For each major chemical component of PM_{2.5} (sulfates, nitrates, ammonium, organic carbon, elemental carbon; particle bound water, other primary particulate matter (Figure 1)), an air pollution model projects the change in concentration from the historical period to the future year. For instance, if the organic carbon concentration is projected to be in 2014 half of what it was in 2008, then the organic carbon concentration from the polluted days in the historical period is divided by two. The process is done for each chemical species and then summed across species to get the projected future PM_{2.5} after implementation of control strategies.

One important aspect of SMAT is how speciated PM_{2.5} measurements from the Speciated Trends Network (STN) monitor are melded with the standard federal reference method (FRM) measurement of total PM_{2.5} concentration. Care must be taken in this step because the STN monitor and FRM monitor use different measurement techniques. As the NAAQS are based on FRM monitored values, the speciated data from the STN monitor must be transformed into the values that would have been recorded by the FRM monitor. EPA modeling guidance in Section 5.1.4 describes this transformation technique, called Sulfate, Adjusted Nitrate, Derived Water, Inferred Carbonaceous material balance approach (SANDWICH), which follows the peer-reviewed, scientific methodology of Frank (2006) and references therein.

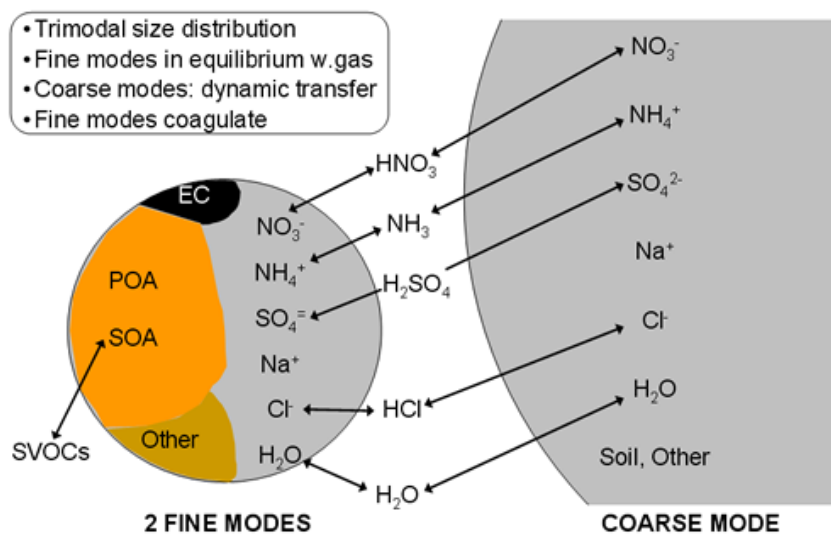


Figure 1: Major Components of PM_{2.5}

<http://www.epa.gov/AMD/ModelDevelopment/aerosolModule.html>

STEP 1:

The first step in the SMAT analysis is to identify the high observed PM_{2.5} days at each monitoring site for each year used for the baseline design value (DV). The baseline design value represents the pollution levels at the time the area violated the NAAQS and was designated nonattainment. In Fairbanks, the State Office Building is the only monitoring station that was used to determine a non-attainment area (NAA). Following the EPA emission inventory guidance (USEPA, 2005), 2008 was chosen as the base year, and following Section 3.1 of the EPA modeling guidance the baseline design value was calculated as an average of the 2006-2008, 2007-2009, and 2008-2010 three-year design values. The three-year design value is the same one as in the calculation of compliance with the PM_{2.5} NAAQS: an average of three consecutive years' worth of 98th percentiles. The baseline design value for the Fairbanks non-attainment area the design value is 44.7 μg/m³ (Table 1).

The baseline design value is not directly used in the calculation of the future year design value. Rather, the species-specific changes from the base (historical) year to the future year are applied to all the individual 24-hour averages in the 2006-2010 period and then the same procedure as used to calculate the baseline design value (98th percentiles for each year, three year design values, average of three year design values) is used to calculate the future design value (USEPA Update to the 24 hour PM_{2.5} NAAQS model attainment test, 2011). The baseline design value is not useless, however. The difference between the baseline design value and the NAAQS determines the overall reductions needed to reach attainment. After the amount of pollution reduction needed to reach attainment (9.2 μg/m³) is divided by the number of years between designation of nonattainment and the Moderate Area attainment date (5), we arrive at the one year's worth of progress value relevant for Reasonable Further Progress and Contingency Measures (1.84 μg/m³).

Table 1: The 98%-tile PM_{2.5} (μg/m³) concentration days and resulting 5-year rolling average DV for Fairbanks, excluding Exceptional Events¹.

Year	High Concentrations	98th Percentile	3- year design value
2006	51.9	42.2	
	42.2		
2007	51.6	33.1	
	34.1		
2008	114.5	46.7	40.7
	50.7		
2009	59.0	51.0	43.6
	52.7		
2010	83.2	51.8	49.8
	57.1		
5-yr Baseline Design Value			44.70

¹Exceptional Events for the 2009 data have been flagged by DEC and concurred by EPA. 2010 Exceptional Events have been flagged by DEC and are in the EPA concurrence process. If the 2010 data is not concurred on by EPA, the baseline design value will be 51.8 $\mu\text{g}/\text{m}^3$. These Exceptional Events become official when EPA acts on them in the Federal Register, which will come when the EPA acts upon this SIP revision.

STEP 2:

The intent of Step 2 is to develop the average $\text{PM}_{2.5}$ chemical speciation for representative polluted days. For Fairbanks we designated the top 25% of winter days during Quarter 1 and 4 of 2006-2010—as indicated by the $\text{PM}_{2.5}$ concentration from the FRM filter -- for this task as a balance of choosing the relevant polluted days and having a statistically strong dataset to use (Table 2). We develop a post-SANDWICH average speciation for Quarter 1 (January, February, and March) and Quarter 4 (October, November, and December) separately, according to EPA modeling guidance. We then use the average of the Quarter 1 and Quarter 4 speciated concentration because Fairbanks experiences polluted days across all winter months.

We developed the species concentration fractions from the STN monitor located at the same State Office Building location as the violating FRM monitor. As mentioned previously, the speciated concentration from the STN measurement cannot be directly used as the speciated concentration from the FRM. The speciated concentration must be converted into the concentration that would have been measured by the FRM monitor after accounting for the differences between the instruments. For example, the FRM measurements do not capture all ambient particles, loss of ammonium nitrate, and addition of particle bound water (PBW) from the STN speciation measurement. The SANDWICH method (Frank, 2006) carries out this conversion process and is described briefly below. We followed the SANDWICH method described from Frank and by EPA modeling guidance exactly in most cases, but made a couple changes specific to woodsmoke-dominated areas in consultation with the EPA Regional Office and in collaboration with other states with woodsmoke issues.

Table 2: The top 25% of high PM_{2.5} (µg/m³) days at the State Office Monitor for the years 2006-2010 for Quarter 4 (Q4) and Quarter 1 (Q1).

Q4 Date	Q4 FRM Concentration (µg/m ³)	Q1 Date	Q1 FRM Concentration (µg/m ³)
20081229	114.5	20100126	83.2
20071220	51.6	20090107	59
20091209	51	20090110	52.7
20081114	50.7	20060117	51.9
20081202	46.7	20100102	51.8
20091230	43.1	20100105	51.8
20091221	41.5	20100108	44.4
20101201	41.2	20060111	42.2
20091212	40.8	20080209	40.4
20081214	38.3	20090104	39
20081108	37	20100120	38.1
20101207	36.9	20060105	38
20091124	35.3	20100111	36.9
20081217	34	20070205	34.1
20071223	33	20070223	33.1
20061219	32.1	20060129	32.7
20061125	31.1	20100204	31.5
20071129	29.6	20100213	30.9
20081223	29.1	20070220	29.7
20081111	27.4	20070127	29.6
20081205	27.1	20090113	29.1
20071217	26.7	20100201	28.8
20091121	26.2	20100123	28.5
20081220	25.7	20070301	28.2
20091227	25.2	20090215	28
20101210	25.2	20090101	27.7
20091206	25.1	20060123	27.6
20061119	23.7	20100129	27.4
20081123	23.6	20070112	26.7
20061207	22.8	20090125	26.2
20071111	22.7	20100216	26

SANDWICH addresses the 7 major measured components of PM_{2.5}:

- Measured sulfate [SO_{4STN}]
- Adjusted nitrate [NO_{3FRM}] (retained on the FRM filter)
- Adjusted ammonium [NH_{4FRM}] (retained on the FRM filter)
- Measured elemental carbon [EC_{STN}] (corrected IMPROVE to NIOSH analysis)
- Organic carbonaceous mass estimated from a mass balance [OCMmb]
- Estimated particle bound water [PBW]
- Estimated other primary PM_{2.5} components [OPP]

Measured sulfate

There are no major differences in how the STN and FRM instruments measure sulfate. It is assumed that the sulfate measured by the STN is equal to what was captured by the FRM.

Retained Nitrate Mass

Nitrate volatilizes from the FRM filter but not the STN measurement. SANDWICH calculates the amount that would have volatilized if the amount of nitrate measured by STN had been deposited on the FRM filter. The volatilized nitrate mass concentration, ΔNO_3 , in units of $\mu g/m^3$ is

$$\Delta NO_3 = \frac{745.7}{T_R(K)} \times \frac{1}{24} \sum_{i=1}^{24} K_i^{1/2} \quad \text{Eq. 5.2 (USEPA, 2007) ; (Eq. 5, (Frank, 2006)).}$$

The dissociation constant for ammonium nitrate (K_i) is evaluated for every hour of every day of nitrate measurements we are using for the analysis. The hourly temperature and relative humidity data used for the associated equations (Frank, 2006) in determining K_i are from the Fairbanks Airport (PAFA). The reference temperature T_R in Eq. 5.2 is the daily average ambient temperature and then ΔNO_3 averaged to 24-hour. The retained nitrate [NO_{3FRM}] is estimated by

$$NO_{3FRM} = NO_{3STN} - \Delta NO_3.$$

A limit was applied to NO_{3FRM} as follows,

If $NO_{3FRM} < 0$, then $NO_{3FRM} = 0$.

The potential nitrate loss using local Fairbanks meteorology is shown in Figure 2. The graph is labeled as potential nitrate loss, because the loss of nitrate is bound by the nitrate on the filter (NO_{3FRM}). The amount of nitrate volatilization during the winter in Fairbanks is low. The maximum nitrate loss of all the days analyzed from 2006-2010 was $1.2 \mu g/m^3$ and was during the summer on exceptional event day.

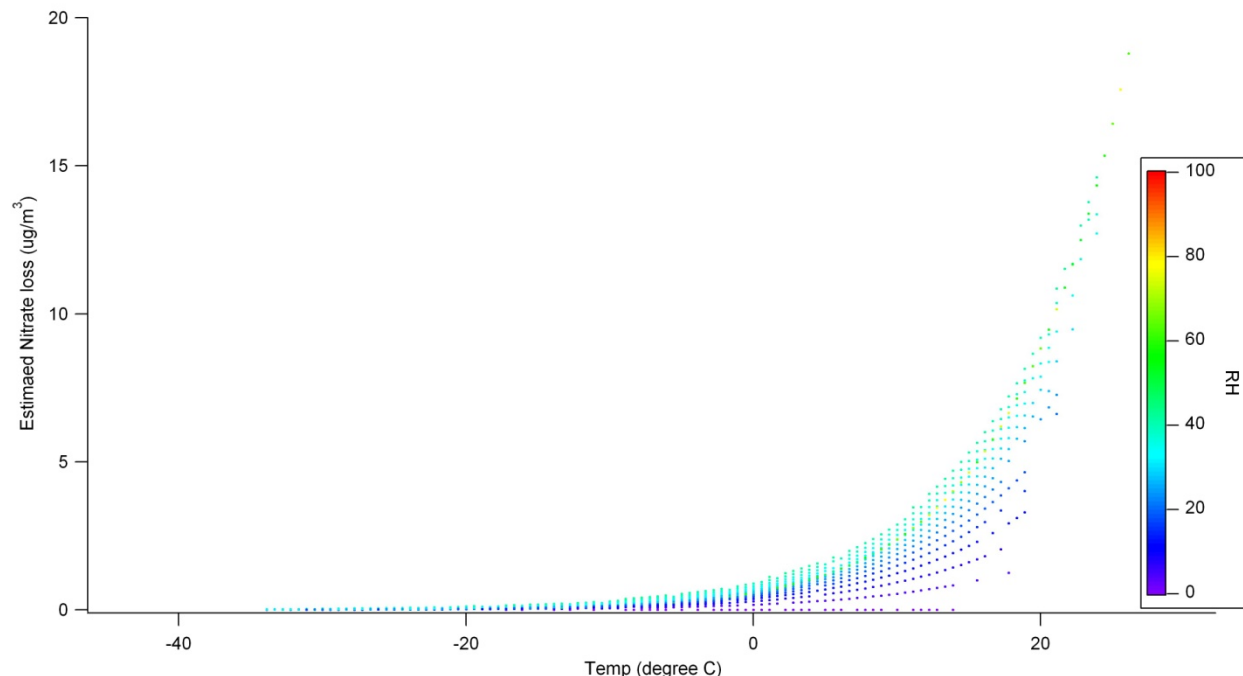


Figure 2: Fairbanks Potential 1-hr NO₃ loss as a function of temperature and relative humidity.

Adjusted Ammonium Mass

EPA modeling guidance recommends using the measured STN ammonia (NH₄) as the measured FRM ammonia. Many of the questions raised in the guidance about the validity of such a recommendation are not problems in Fairbanks because Fairbanks winters are very cold and the amount of ammonium nitrate volatilization is very small. Thus,

$$[\text{NH}_{4\text{FRM}}] \cong [\text{NH}_{4\text{STN}}].$$

In cases where the ammonia concentration exceeds the amount necessary to neutralize the FRM sulfate and nitrate, the ammonia concentration was adjusted to ensure charge balance. This is a deviation from the USEPA recommended adjustment, but has been noted in other adjusted ammonium concentration calculations (Turner, 2010). The adjustment used was:

$$\text{NH}_{4\text{FRM}} = 2 \times \text{SO}_4^{2-} + \text{NO}_{3\text{FRM}} - \text{H}^+ \text{ when } \text{H}^+ > 0 \text{ or else } \text{H}^+ = 0$$

The hydrogen ion concentration results from the calculation of particle bound water, as described below.

Elemental Carbon Mass

Elemental carbon (EC) concentrations as measured by the STN instrument are used directly as the concentrations for the FRM measurement. In October 2009, the STN instrument at the Fairbanks State Office Building changed its technique for measuring elemental and organic carbon; the MetOne SASS using the NIOSH analysis method was replaced with the URG 3000N using the IMPROVE analysis method. Since most of the measurements were made on the SASS sampler and NIOSH method and evidence of high wood smoke PM_{2.5} areas are more accurately measured by the NIOSH method, the EC

measurements from October 2009 on were corrected to reflect the NIOSH method (Hixson, 2011). Traditionally in the Lower 48 the NIOSH data is corrected to reflect the IMPROVE method, but the opposite makes sense for the particular case of a wood smoke dominated area with primarily NIOSH data in the 2006-2010 analysis timeframe.

$$\begin{aligned} EC_{FRM} &= EC_{SASS/NIOSH} && \text{(Before October 2009)} \\ EC_{FRM} &= (EC_{URG/IMPROVE} * 0.5722) + 0.2509 && \text{(After October 2009)} \end{aligned}$$

Other primary PM_{2.5} components

We calculate the other primary PM_{2.5} (OPP) directly as recommended by EPA modeling guidance:

$$OPP = 3.73 \times [Si] + 1.63 \times [Ca] + 2.42 [Fe] + 1.94 \times [Ti].$$

Particle Bound Water Mass

Because the STN speciation does not measure the particle bound water (PBW) that would be present in the PM_{2.5} if it were being measured by a FRM monitor, we calculate the PBW with the Aerosol Inorganic Model II (<http://www.aim.env.uea.ac.uk/aim/model2/model2a.php>). Inputs to the model are using the ammonia, nitrate, and sulfate concentrations as calculated above. As suggested by Frank (2006), the model is evaluated at 295K and 35% RH because these are the equilibrium atmospheric conditions under which the FRM filter is weighed in the laboratory. In the model we assume there is no ammoniated compound solid formation and use the following ion mass balance equation:

$$H^+ = [2 \times SO_4^{2-}] + NO_3^- - NH_4^+.$$

The measured sulfate, retained nitrate mass and adjusted ammonium mass allowed an estimated hydronium ion proton molar concentration and a PBW water mass was directly calculated from the AIM model.

Organic Carbonaceous Mass

SANDWICH estimates organic carbonaceous mass, [OCMmb], as the amount that is not explained by other chemical species:

$$OCMmb = [PM2.5_{FRM}] - \{[SO_{4STN}] + [NO_{3FRM}] + [NH_{4FRM}] + [EC_{FRM}] + [OPP] + [PBW] + 0.5\}$$

The STN instrument measures organic carbon directly, but the techniques to quantify the organic mass have considerable uncertainties. The mass balance technique is reasonable since all other species can be well-quantified and it is likely the remaining mass is organic carbon. As a benefit mass closure is assured. To guard against spurious results, the organic carbon mass is bound on the lower end by 70% of the measured organic carbon and on the upper end by 80% of the total mass. As with the elemental carbon concentration, organic carbon concentrations obtained with the URG/IMPROVE method were converted using the correlation in Hixson (2011) to the SASS/NIOSH method. When a bound is applied, the speciated concentration no longer adds up to the total concentration. When this happens all species are adjusted proportionally such that they add up to the total measured concentration by the FRM instrument. The upper bound was never invoked by the Fairbanks data set, while the lower bound was used on three

occasions (5% of the total dataset). The concentration closure adjustment in these three cases modified the sum of the species' concentration by less than 10%.

Quarterly average FRM-derived species concentration fractions

The SANDWICH process is done separately for every 24-hour measurement in the dataset. The top 25% polluted days in 2006-2010 for Quarter 1 and Quarter 4 represent 31 and 27 samples, respectively. The average speciation for Quarter 1 and Quarter 4 is presented in Table 3 and Figures 4-5. These values represent the chemical composition of PM_{2.5} on polluted wintertime days in Fairbanks for the baseline 2006-2010 period.

Table 3: Quarterly average percentage of SANDWICH'ed PM_{2.5}, calculated from the top 25% of PM_{2.5} days for years 2006-2010

	SO _{4STN}	NO _{3FRM}	NH _{4FRM}	PBW	EC _{URG/IM>SASS/NI}	OPP	OCMmb _{URG/IM>SASS/NI}
Q4	17.40%	3.64%	7.57%	5.82%	6.89%	1.25%	57.43%
Q1	19.15%	5.0%	8.54%	6.27%	6.19%	1.01%	53.82%

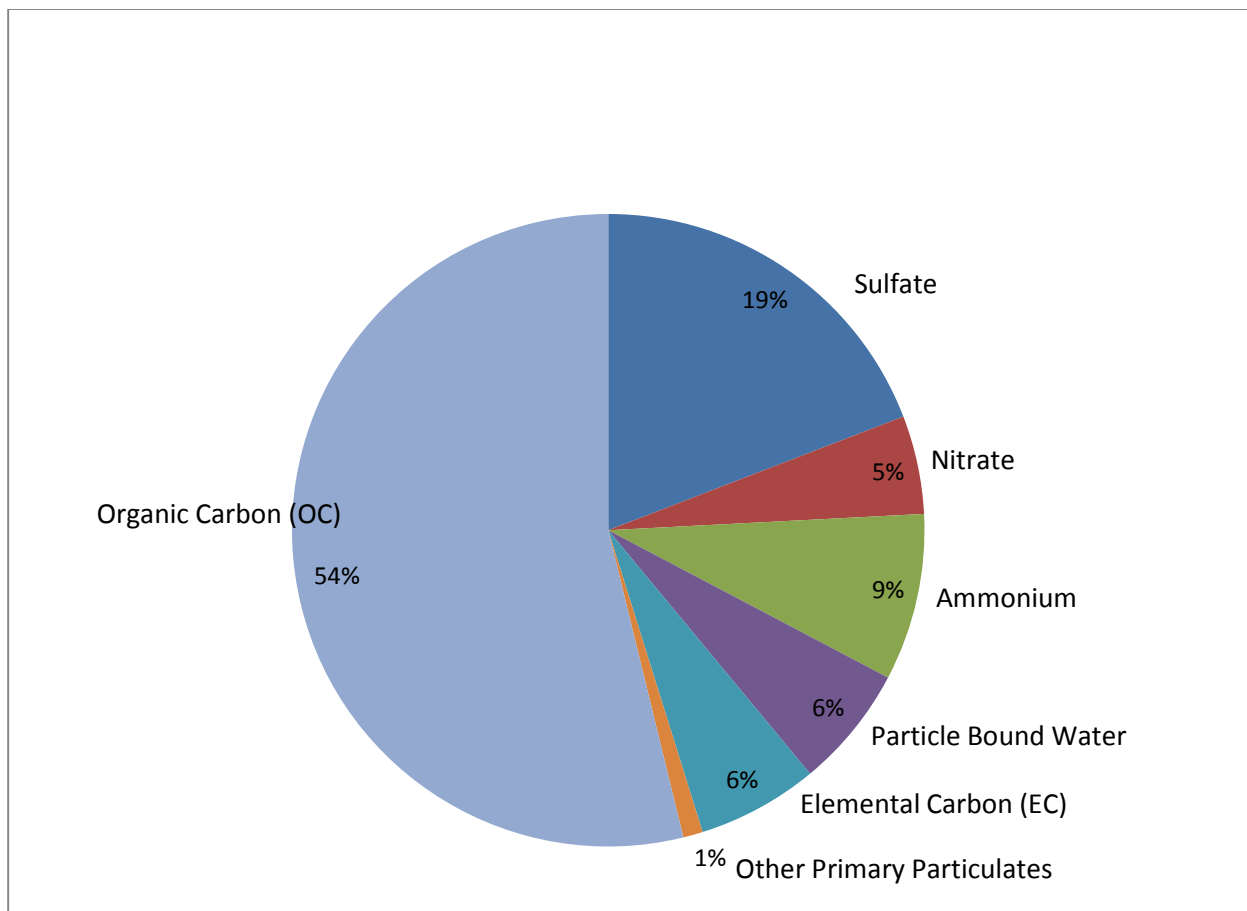


Figure 4: Quarter 1, FRM-derived species percentage of high 24-hr average PM_{2.5} days from the Fairbanks State Office Building for years 2006-2010.

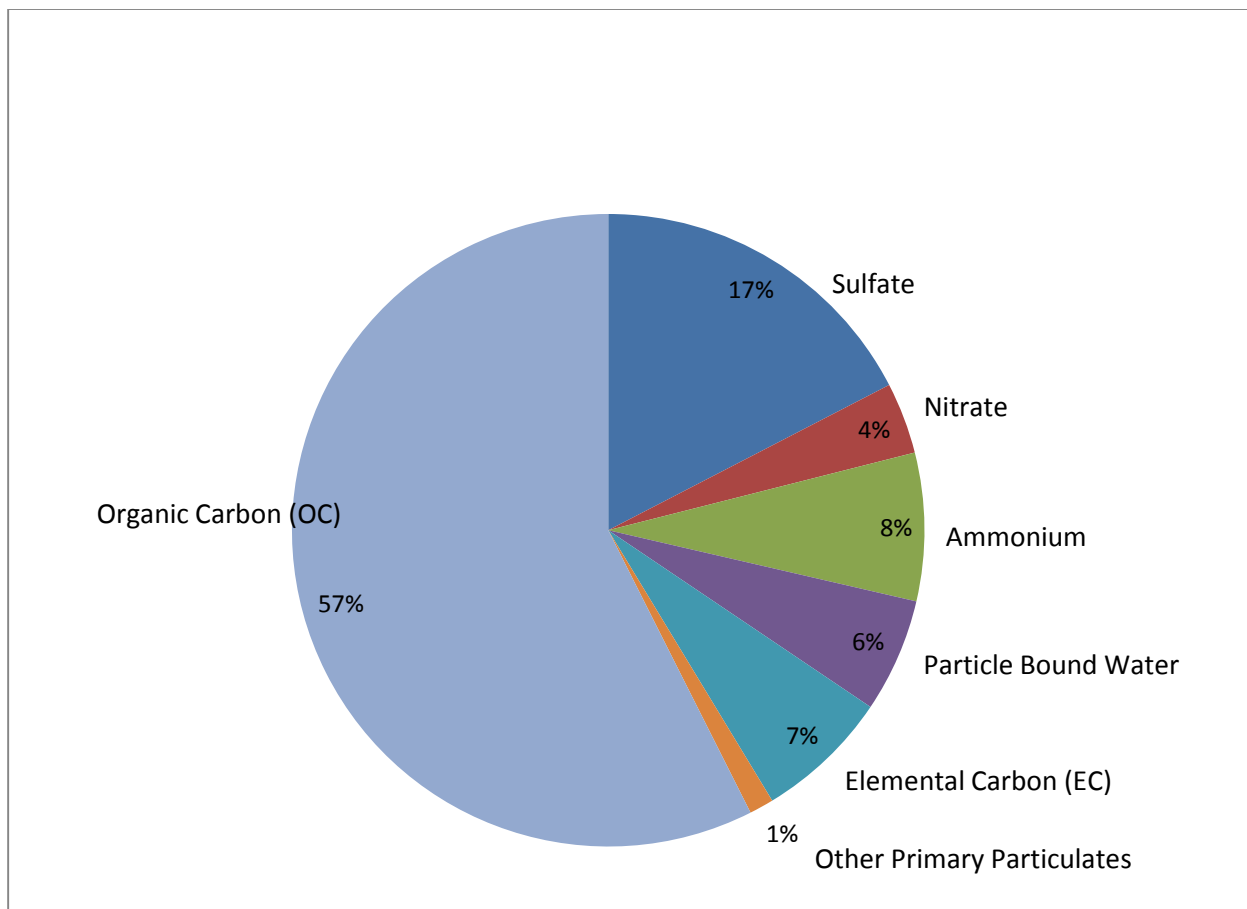


Figure 5: Quarter 4, FRM-derived species percentage of high 24-hr average PM_{2.5} days from the Fairbanks State Office Building for years 2006-2010.

After SANDWICH was complete and the Q1 and Q4 average species concentrations and percentages were calculated (Table 4), the average species percentage was multiplied by the baseline design value of 44.7 µg/m³ from Step 1. While not necessary for the model attainment test, this information has been helpful in guiding other parts of the attainment plan.

Table 4: Averaged Quarter 1 and 4, FRM-derived species percentage of high PM_{2.5} days and average concentration based on the baseline design value (DV) of 44.7µg/m³.

Species	Sulfate	Nitrate	Ammonium	Water	elemental carbon	OPP	Organic carbon
Q4 %	17.40	3.64	7.57	5.82	6.89	1.25	57.43
Q1 %	19.15	5.03	8.54	6.27	6.19	1.01	53.82
Average of Q1 and Q4 %	18.28	4.34	8.05	6.05	6.54	1.13	55.62
Average DV(µg/m ³)	8.17	1.94	3.60	2.70	2.92	0.50	24.86

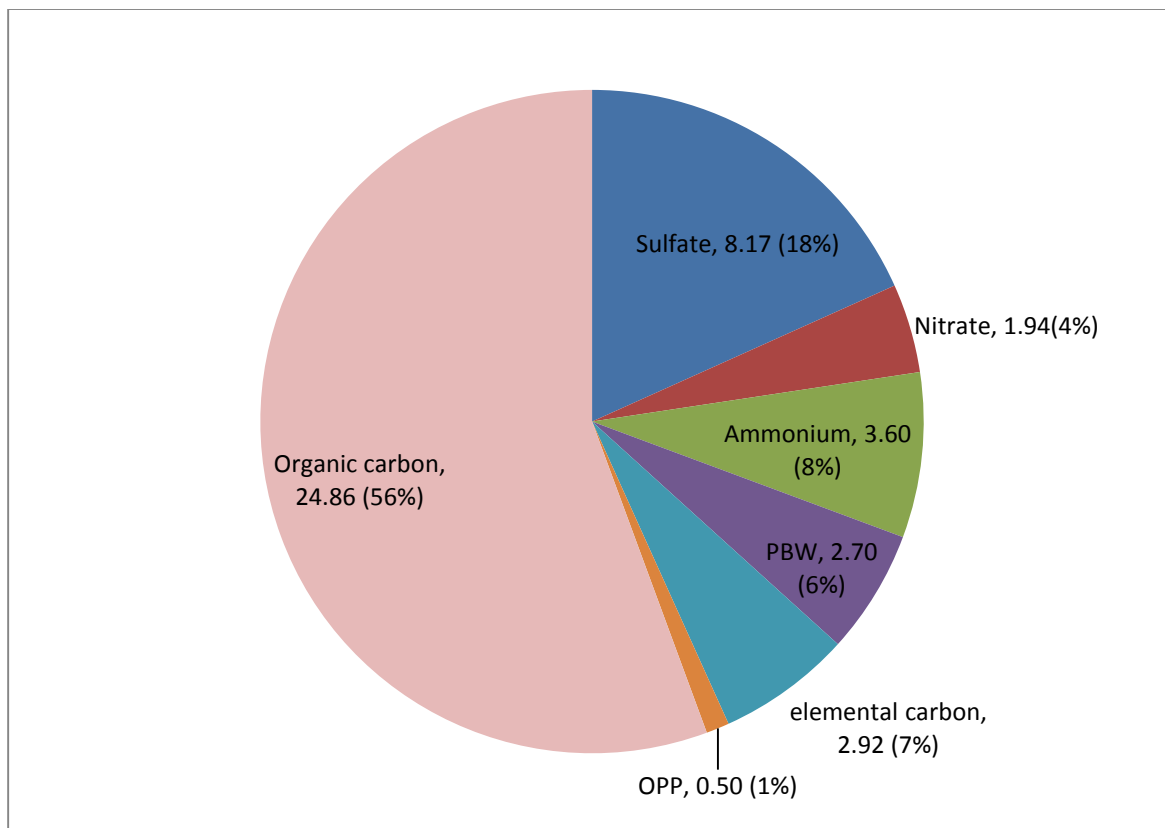


Figure 6: Averaged Quarter 1 and 4, FRM-derived species percentage of high PM2.5 days from years 2006-2010 and average concentration based on the baseline design value (DV) of 44.7 µg/m³.

Step 3: Calculate species concentration for each of the high ambient days

Step 3 calculates the concentration of chemical species on each of the high ambient days in 2006-2010. For example, the highest PM_{2.5} from 2006 was 51.9 µg/m³ on January 17th (see Table 1,STEP1), Using the Quarter 1 average speciation percentages (Table 4), we calculate the species concentrations in µg/m³ on that day at the Fairbanks State Office Building in Table 5:

Example for sulfate:

$$51.9 \mu\text{g}/\text{m}^3 - 0.5 \mu\text{g}/\text{m}^3 \text{ (blank filter)} = 51.4 \mu\text{g}/\text{m}^3 \times 0.1915 \text{ (SO}_4\text{, Q1 \% from Table 3)} = 9.84 \mu\text{g}/\text{m}^3$$

Table 5: PM_{2.5} Species concentrations in µg/m³ for the highest day in the year 2006

Date	FRM PM2.5	Blank	Non blank FRM	Sulfate	Nitrate	Ammonium	Water	Elemental Carbon	OPP	Organic Carbon
1/17/06	51.9	0.50	51.40	9.84	2.58	4.39	3.22	3.18	0.52	27.66

The same process is done for the top 25% of high days during the winter (Quarter 1 and 4) and all of these high days are listed in Table 2, STEP 2.

STEP 4: Calculate the component specific RRFs (Relative Response Factor)

The relative response factor is a ratio between the modeled projected concentrations divided by the present baseline modeled concentration for each species. Two episodes from 2008 are modeled using emissions from 2008 (present baseline) and then using emissions from 2015 (future baseline) plus emission reductions from emission reduction strategies (future control). The modeled concentrations from the 2015 future control case are divided by the modeled concentrations from the 2008 present baseline. This is done for each chemical species and for every grid cell of the modeling domain. The result is a table of RRFs similar to Table 5, which is just an illustration for explanatory purposes. The RRFs for the emission reductions proposed in this attainment plan are presented in Chapter 5.9. Concentrations in the both the present and future model runs are calculated as 24-hour average values for each component of PM for the baseline and each component of the future. Then the future components were divided by the baseline for the episode-long 24-hour PM species averages for all episode days except for the two model spin up days at the start of each episode. The resulting RRFs for the modeled State Office Building grid cell are in Table 6. Table 7 shows an example of data from the high days of 2008 with the species-specific RRFs applied in order to calculate the concentration of each PM_{2.5} chemical species in 2015 given a scenario of emission controls.

Example calculation:

Sulfate RRF = 2015 future modeled concentration / 2008 baseline modeled concentration = 0.89 RRF

Sulfate RRF = 8.78/9.82 = 0.89 RRF

Table 6: Relative Response Factor (RRF) example averaged over days in episode 1 and 2 derived from a present baseline 2008 simulation and future year control strategies.

Species	Sulfate	Nitrate	Ammonium	Water	Element Carbon	OPP	Organic Carbon
RRF	0.89	0.95	0.94	1.00	0.88	0.99	0.77

There are no RRFs for particle bound water or the blank, they do not change as control strategies changes. For example, in Table 6, the OCMmb (organic carbon mass balance) RRF is 0.77 and a large decrease in OC is observed from controls that largely only affect organic carbon.

STEP 5-6: Apply the component specific RRFs to the observed air quality by quarter

Step 5-7 are represented as an example in Table 7 for the year 2008, high PM_{2.5} days and the species are added together to calculate the future year PM_{2.5} species (step6). The left side of the Table 7 follows the exact same method as shown in Table 5 for January 17th, 2006. The FRM derived species concentrations based on the Sandwich method on the left and the right side is the future species concentrations based on the example RRFs in Table 6.

Example calculation for future sulfate:

Future Sulfate = 2008 FRM-derived species concentration x 2015 sulfate RRF = 17.66 µg/m³

Future Sulfate = 19.84 x 0.89 = 17.66 µg/m³

Table 7: Example RRF future year concentrations based on the RRFs in Table 5 and the top high days in year 2008.

Observed FRM PM 2.5	Blank	Non blk FRM	Observed Sulfate	Observed Nitrate	Observed Ammonium	Water	Observed Elemental Carbon	OPP	Observed Organic Carbon		Future Sulfate	Future Nitrate	Future Ammonium	Water	Future Elemental Carbon	Future OPP	Future Organic Carbon	Blank	Future FRM
114.5	0.50	114.00	19.84	4.16	8.62	6.64	7.85	1.42	65.47		17.66	3.95	8.11	6.64	6.91	1.41	50.41	0.50	95.58
50.7	0.50	50.20	8.74	1.83	3.80	2.92	3.46	0.63	28.83		7.78	1.74	3.57	2.92	3.04	0.62	22.20	0.50	42.37
46.7	0.50	46.20	8.04	1.68	3.50	2.69	3.18	0.58	26.53		7.16	1.60	3.29	2.69	2.80	0.57	20.43	0.50	39.03
40.4	0.50	39.90	7.64	2.01	3.41	2.50	2.47	0.40	21.47		6.80	1.91	3.20	2.50	2.17	0.40	16.54	0.50	34.02
40.4	0.50	39.90	6.94	1.45	3.02	2.32	2.75	0.50	22.91		6.18	1.38	2.84	2.32	2.42	0.49	17.64	0.50	33.78
38.3	0.50	37.80	6.58	1.38	2.86	2.20	2.60	0.47	21.71		5.86	1.31	2.69	2.20	2.29	0.47	16.72	0.50	32.03
37	0.50	36.50	6.35	1.33	2.76	2.13	2.51	0.46	20.96		5.65	1.26	2.60	2.13	2.21	0.45	16.14	0.50	30.94
34	0.50	33.50	5.83	1.22	2.53	1.95	2.31	0.42	19.24		5.19	1.16	2.38	1.95	2.03	0.41	14.81	0.50	28.44
32.6	0.50	32.10	5.59	1.17	2.43	1.87	2.21	0.40	18.43		4.97	1.11	2.28	1.87	1.95	0.40	14.19	0.50	27.27
25.9	0.50	25.40	4.86	1.28	2.17	1.59	1.57	0.26	13.67		4.33	1.21	2.04	1.59	1.38	0.25	10.53	0.50	21.84
23.7	0.50	23.20	4.44	1.17	1.98	1.45	1.44	0.23	12.49		3.95	1.11	1.86	1.45	1.26	0.23	9.61	0.50	19.99
23.5	0.50	23.00	4.40	1.16	1.96	1.44	1.42	0.23	12.38		3.92	1.10	1.85	1.44	1.25	0.23	9.53	0.50	19.82
23.4	0.50	22.90	4.39	1.15	1.96	1.44	1.42	0.23	12.32		3.90	1.09	1.84	1.44	1.25	0.23	9.49	0.50	19.74
21.5	0.50	21.00	4.02	1.06	1.79	1.32	1.30	0.21	11.30		3.58	1.00	1.69	1.32	1.14	0.21	8.70	0.50	18.14
19.8	0.50	19.30	3.70	0.97	1.65	1.21	1.19	0.19	10.39		3.29	0.92	1.55	1.21	1.05	0.19	8.00	0.50	16.71
19.5	0.50	19.00	3.64	0.96	1.62	1.19	1.18	0.19	10.23		3.24	0.91	1.53	1.19	1.03	0.19	7.87	0.50	16.46
14.4	0.50	13.90	2.22	0.00	0.80	0.77	0.76	2.07	7.28		2.22	0.00	0.80	0.77	0.76	2.07	7.28	0.50	14.40

Step 7: Sum the species components to get total PM_{2.5} concentrations for each day

The species concentrations from the future year are added together to arrive at the modeled projected concentrations given changes in emissions between 2015 and 2008 plus changes from emission controls. Table 7 is the result of this process for when or example RRFs (from Step5) are applied to our high ambient days (from Step1). It is an estimate of the PM_{2.5} concentration that would have been observed in 2006-2010 if the area had the pollutant emissions from 2015 and from the proposed emission control strategy. The result of this process for the emission controls proposed in this attainment plan is in Section Chapter 5.6 and Appendix 5.6.

Step 8: Determine future year 98th percentile concentrations for each site year.

The 98th percentile concentration is usually the 3rd highest concentration from a year for the sampling schedule followed in 2006-2010 but it depends on how many valid samples were obtained from the year [Appendix N reference]. For the 2006 PM_{2.5} data, the 2nd highest concentration is the 98th percentile and is the 3rd highest for 2007 through 2010. Table 8 identifies the 98th percentile for the future year control case.

Step 9: Calculate future 5 year 24-hr DV.

The future year control design value is calculated as an average of the 3-year design values from 2006-2008, 2007-2009, and 2008-2010. For our example case:

Table 8: Baseline and Future 5-year Design Values based example RRFs (Table 5)

Year	98%-tile	98%-tile
2006	42.2	36.6
2007	33.1	28.7
2008	46.7	39.0
2009	51.0	45.6
2010	51.8	44.9
Design Values	44.70	38.6

References

Frank, N.H. (2006): Retained Nitrate, Hydrated Sulfates, and Carbonaceous Mass in Federal Reference Method Fine Particulate Matter for Six Eastern U.S. Cities.

Hixson, M. (2011): Reconciling Trends in Carbon Measurements for Fairbanks 2006-2010.

Turner, J. (2010): PM_{2.5} Species Mass Fractions for the Species Modeled Attainment Test.

USEPA (2007): Guidance on the Use of Models and Other Analyses for Demonstrating Attainment of Air Quality Goals for Ozone, PM_{2.5}, and Regional Haze, EPA-454/B-07-002, United States Environmental Protection Agency, Office of Air Quality Planning and Standards, April 2007.

USEPA (2011): Attachment A and B. http://www.epa.gov/ttn/scram/guidance/guide/Update_to_the_24-hour_PM25_Modeled_Attainment_Test.pdf

USEPA(1993): Appendix N.

Aerosol Chemistry in Fairbanks: A Summary of Prevailing Conditions

May 27, 2011

Dirigo Consulting, LLC

Amherst, MA 01002

Principle: Richard E Peltier, MPH, PhD

1. Introduction

Atmospheric particulate matter (PM) is comprised of a variety of chemicals across a range of sizes and is nearly ubiquitous in the environment. It is also a dynamic component of the atmosphere that can undergo rapid chemical or physical transformation from a variety of stimuli. This leads to highly complex aerosol climatology that is dependent on a variety of contextual variables and therefore must be characterized with high precision and specificity.

The Fairbanks region in Alaska is a region of specific concern because of the relatively high concentrations of PM, especially in the winter. In recent years, the Fairbanks community has experienced a number of exceedances in which PM concentrations were above the federally-mandated standard. This paper will describe the current state of understanding of the conditions observed in the Fairbanks region. A specific focus of this document entails a detailed discussion of a specific component of PM – sulfur-containing aerosol – that is found in significant quantities of aerosol measured in this community.

2. General Overview on Particulate Matter

Ambient PM is ubiquitous in the lower troposphere and results from a variety of physical and chemical transformations. It can be formed as a primary pollutant from combustion and biogenic sources, as well

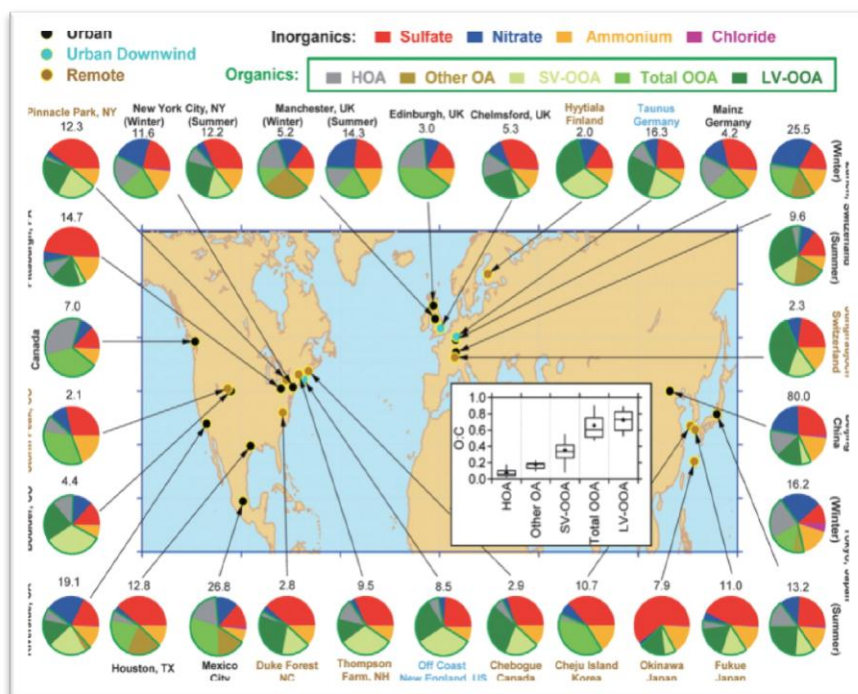


Figure 1: Measured worldwide distribution of aerosol composition, including differences in inorganic and organic components. Figure adapted from Jimenez, et al [1]

quite complex, and thus, our understanding of aerosol formation is also incomplete. PM is chemically complex in different regions of the world. Figure 1, adapted from Jimenez et al [1] confirms significant spatial variability of aerosol chemical components at the global and continental scale. In general, ammonium, sulfate, and secondary fractions of organic carbon comprise the majority of observed PM_{2.5} mass near the East coast of North America. In contrast, aerosol on the West Coast is more chemically variable, but is driven by nitrate, ammonium, and more volatile fractions of organics. Thus on continental scales,

as by resuspension of dust from crustal surfaces [2-4].

Secondary aerosol sources, i.e. those formed by precursor gases and/or particles, are substantially more complex, however. PM has also been shown to form as a secondary product from a variety of chemical reactions in the atmosphere [3, 5], with the most important reactions involving the secondary formation from petroleum combustion exhaust, biomass burning, and coal fired emissions. The diversity of possible atmospheric reactions makes unequivocal identification of aerosol sources

quite complex, and thus, our understanding of aerosol formation is also incomplete. PM is chemically complex in

significant spatial variability is observed in aerosol chemical composition. This implies that when assessing aerosol chemical exposure in different regions of North America, a $PM_{2.5}$ measure of exposure in one region is chemically different from a $PM_{2.5}$ measure of exposure in another region.

In general, particulate matter in Fairbanks is comprised of a mixture of ions, crustal material, and carbonaceous components, with relative levels of each component dependent, in part, on prevalent local sources and sinks, long-range transport of chemicals, and chemical processing. However, because of its geography and prevailing meteorology, we currently lack a full understanding of the chemical processing that typically occurs, especially during the winter months when there is a high demand for residential heating, strong inversions, and extremely cold temperatures. This white paper attempts to provide a summary of the current state of knowledge, provides an initial analysis of some of the existing data, and proposes some mechanisms for future study. A specific focus of this paper expands the understanding of sulfur chemistry, which drives a significant fraction of the aerosol composition in Fairbanks.

2 Sources of Aerosol Sulfur in Fairbanks

2.1 Sulfur Precursors

Sulfur is emitted into the atmosphere typically as gas-phase constituents from both biogenic and anthropogenic sources. Biogenic sources of sulfur include hydrogen sulfide (H_2S), carbonyl sulfide, dimethyl sulfide and a variety of mercaptans, all of which contain sulfur in the lowest oxidation state (-2). Anthropogenic sources of sulfur are extensive, though the largest source (by mass) is the release of sulfur dioxide stemming from the combustion of petro-fuels such as heating oil, diesel, and coal.

Observed particulate sulfur in Fairbanks comprises a significant fraction of total PM, though our understanding of sulfur sources remains incomplete. Sulfur can be present in three broad forms: as part of an organosulfur compound, as a sulfate salt, or other sulfur-metal or sulfur-metalloid complexes. The latter complexes are atypical and usually only found as a result of specific industrial sources and are often only of limited consequence for an urban community.

Atmospheric processing of these sulfur sources is equally diverse and includes a number of relevant pathways that lead to sulfur-containing particulate matter. There are a number of primary emission sources, such as the release of sea spray laden with sulfate, that do contribute to primary sources of sulfur to the atmosphere, though these are likely to have an insignificant impact on the Fairbanks regions since few sources are located nearby. This leaves secondary formation mechanisms that lead to the bulk of observed sulfur in particulate matter.

Specific sources of sulfur in Fairbanks are thought to include emissions from the three coal-fired power generation facilities (Atkinson Power Plant at UAF, the Chena Power Plant, and the Fort Wainwright Power Plant – a fourth plant in Eielson AFB also exists), on-road diesel fuel, and home heating oil. Long-range transport is not thought to contribute significantly to sulfur loading in Fairbanks because there are very few upwind regional sources of sulfur. Wood-burning does contribute to the overall loading of particulate matter, but it is not likely to directly contribute to the sulfate burden typically observed in Fairbanks. Thus, the available sulfur sources in Fairbanks are probably limited to these three main categories, though recent regulations have sharply reduced the quantity of sulfur in on-road diesel; the mechanisms of formation are also not yet fully understood, and thus a discussion of these mechanisms follows.

2.2 Secondary Sources of Sulfur: Homogeneous nucleation

Gas-to-particle conversion of precursor sulfur-containing gases can be a significant source of particulate laden with sulfate. Briefly, this process is initiated when a gas, such as SO_2 , is present in supersaturated conditions and spontaneously forms agglomerates (e.g. molecular clusters). These agglomerations, which are inherently unstable and continuously disintegrate, can interact with one another if an adequate number of agglomerates are formed. In a process similar to coagulation, these agglomerates can form larger particles that exceed (albeit briefly) a critical diameter that allows for vapor equilibrium between the newly-formed particle and the surrounding vapor. In this case, condensation is encouraged and allows for rapid growth of the particle governed by Kelvin theory, a complex ratio of saturation vapor pressure over a flat plane compared to that over a spherical particle.

Homogeneous nucleation typically depends on point sources of sulfur (usually SO_2) that are emitted in high concentrations in order for optimal conditions to be present for gas-to-particle formation to occur. Such sources might include coal- or residual oil-fired power generation facilities, high sulfur fuel use (mainly for heating purposes) or fugitive sulfur emissions from refining activities. This is relevant for Fairbanks because all of these sources are thought to have an impact on local aerosol climatology, though these processes are not yet fully understood. Even less empirical data are available on nucleation in extremely cold environments such as what Fairbanks experiences each winter, though nucleation events at cold temperatures would require higher vapor pressures than an equivalent event at warmer temperatures; essentially, this makes this process less likely a player in aerosol formation in Fairbanks. However, an open mind would be prudent in future assessment of homogeneous nucleation in this community because of the unusual and unique environmental conditions (rapid cooling, ice fog formation, rapid sublimation) that these gases meet soon after emission.

2.3: Heterogeneous nucleation

Heterogeneous nucleation, that is, the formation of sulfur-containing particles that involves precursor gases and other reactants, is a far more complex formation mechanism and likely to be a significant source of particulate-bound sulfur. Heterogeneous reactions are usually mediated by compounds that can either directly oxidize sulfur, or participate as catalysts in oxidation processing. Though gas-phase heterogeneous chemistry involving common oxidants (e.g. hydroxyl radical, ozone, organic peroxides, etc.) is typically quite slow, aqueous phase reactions are greatly accelerated and contribute to the bulk of the observed heterogeneous chemistry. Thus, the importance of available water is crucial for facilitating the formation of particle-bound sulfur compounds.

Heterogeneous formation of sulfur-containing particles likely plays at least some role in the climatology of aerosol chemistry in Fairbanks, however, this formation mechanism is poorly, if not at all, understood. Under more typical conditions, water droplets, or seed particles coated with liquid water (from vapor condensation, deliquescence, etc) serve as the reactor vessels that lead to sulfate aerosol formation. Sulfur dioxide, a common emission source of sulfur, is dissolved in these droplets and allows for much more rapid rates of conversion compared to typical gas-phase reactions. Oxidants, either formed in-situ or directly released, play an important role in mediating this oxidation, and they include ozone, peroxyradicals, hydroxyl groups, formaldehyde, oxides of nitrogen, and some metals and are summarized in Table 1.

Table 1: Possible oxidant reactions that may play a role in sulfur chemistry in Fairbanks

Oxidant component	Likely Local Source of oxidant in Fairbanks	Estimated relative reaction efficiency in Fairbanks in winter	Consideration of future measurement to better understand sulfur conversion?
Ozone	Photochemical production of ozone	low	Perhaps. Easy to do with instrumentation already in place.
Hydrogen peroxide	Mainly found dissolved in clouds/fog resulting from photochemistry	Unknown, likely moderate	yes
Organic Peroxides	VOC oxidation due to NO ₃ radical chemistry	low	Yes, surveys of representative organic peroxides might yield important information on sulfur conversion pathway.
Dissolved Oxygen	Naturally-occurring	Probably trivial	No, yield not likely to be significant and O ₂ concentration already known.
Metal catalysis (Fe ³⁺ , Cu ²⁺ , and Mn ²⁺)	Direct emission of metals	Unknown, possible synergy in presence of both metals.	Yes, but these metals already measured in speciation network; consider additional study of metal oxidation states.
Hydroxyl radical	Photochemical production from water vapor/droplets/crystals	Probably low	No, technically challenging to directly measure OH
Oxides of nitrogen	Direct emission	Low	Yes, despite low theoretical yield, research infrastructure already in place by investigators at UAF. Also, many local sources, especially in winter.
Formaldehyde (and other aldehydes)	Direct emission and secondary formation from VOC oxidation	unknown	Yes

Of these typical oxidant pathways, most are pH dependent, with lower sulfur conversion yields at higher pH [6]. They also vary depending on the precursor chemical concentrations present in the ambient environment. An exception to this is the pathway involving hydrogen peroxide which is relatively insensitive to changes in acidity, and maintains a high sulfur conversion yield independent of pH (assuming typical urban concentrations of constituent gases).

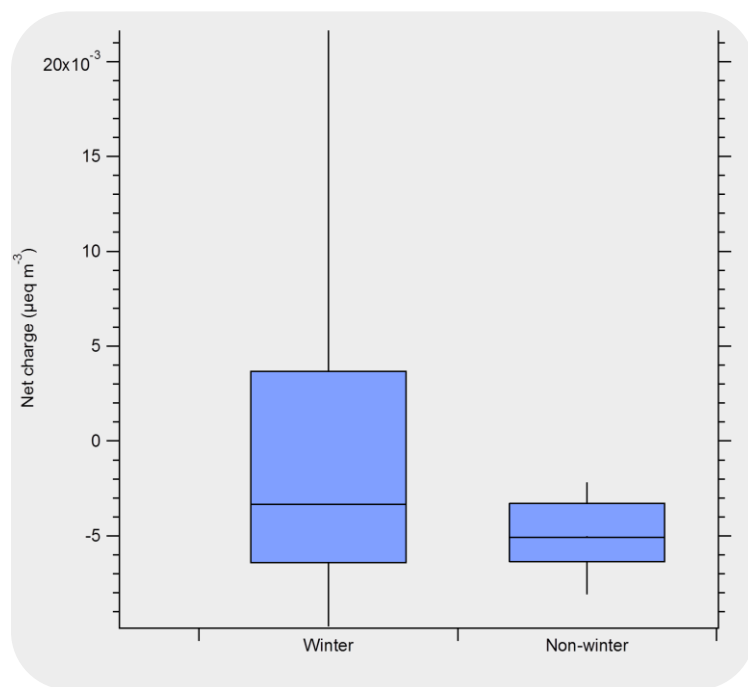


Figure 2: Net charge on aerosol resulting from sulfate (-2), nitrate (-1), and ammonium (+1) by season. Winter is defined as November- March; non-winter is all other months. Measurements less than zero suggest an apparently acidic aerosol.

Using data of fine sulfate, ammonium, and nitrate collected by FNSB from 2007-2010, we observe a somewhat different apparent aerosol acidity profile in the winter compared to the non-winter periods (Figure 2). While this approach only includes a fraction of the components that comprise a molar balance of aerosol (e.g. other aerosol species may change this balance), it appears that aerosol is generally acidic in both the winter periods (defined as November – March) and the non-winter periods (April – October). There is no significant difference between the two seasons, though there is a skewing of data during the winter towards more alkaline conditions that is not observed in the summer. This indicates an apparent excess of positively-charged components (e.g. ammonium ion) during the winter. In the case of positively charged aerosol, previous work [7, 8] has shown this to likely be

a result of biomass burning influence and suggests the presence of unmeasured organic acids as the anionic pair.

The majority of the scientific understanding on sulfur chemistry has been studied under acidic conditions. Only limited information on heterogeneous chemistry is available and seems to suggest that typical sulfur conversion reactions are not highly favored. Nonetheless, sulfur (mainly as sulfate) is most certainly observed in significant quantities in Fairbanks. Most research has investigated alkaline sulfate formation of sea salt in the presence of ozone, though this process is not expected to play any significant role in Fairbanks. Thus at present, the mechanism of heterogeneous sulfate formation in the winter in Fairbanks is not understood.

Of the mechanisms described in Table 1, the most likely candidates to play a significant role in sulfur conversion in Fairbanks appears to be that induced by hydrogen peroxide, organic peroxides, metal catalysis, oxides of nitrogen, and formaldehyde. This does not exclude the other sources of sulfur conversion chemistry, but they are not likely to play a large role in contributing to the observed sulfur in the region. While there are plausible primary sources of these components, there may also be unusual secondary chemistry at play that forms these reagents in-situ. A number of arctic studies [9-11] (and references therein) have suggested that halide chemistry, specifically interactions with chlorine and bromine species, play an important role in catalyzing oxidant formation, specifically in the presence of snowpack. Most existing studies, again, have taken place in remote areas (e.g. Barrow, AK, northern Finland, Greenland, etc), and have centered on investigating the fundamental mechanistic chemistry principles under pristine conditions and may not be fully transferable to a more complex urban

environment characterized by multiple sources of aerosol. However, this pathway may still be an important determinant in the formation of atmospheric constituents that can lead to sulfur conversion.

A unique possibility for further study of sulfur chemistry in the Fairbanks area relates to the widespread presence of ice fog in the vicinity of the Chena River during the winter. With low winter temperatures, most water bodies in the region freeze to solid ice (surfaces at least). The Chena River, which winds through the central downtown region, is injected by waste heat produced by the Chena Power Plant, a 29MW coal-fired facility. Coupled with winter dew points well below zero and low ambient temperatures, artificially warm river water rapidly evaporates, condenses, and freezes each day. This represents a significant mass transfer of water and dissolved components into the air, and may suggest a possible source for direct formation of aerosol from this process [12-14]. It also likely provides a large number of small particles, which in total, create a large surface area suitable for reactive chemistry. This is particularly important because it occurs in the immediate vicinity of the power plant; in the presence of a looping or fumigating plume, there is the potential for significant sulfur chemistry.

2.4 Sulfur losses

Particulate sulfur is lost through one of two ways: via transport out of the measurement domain (e.g. long-range meteorological transport), or loss to the surface by deposition (through direct contact with surfaces or induced by precipitation). Because it is very stable, sulfur bound as sulfate aerosol generally does not undergo further chemical processing that reduces concentration. Other sulfur species (e.g. organosulfur components) may be subjected to further chemical processing though this mechanism is not understood and depends on the initial chemical conditions, aerosol sources, and available atmospheric reactants. Because the region has relatively low annual precipitation, it is likely that sulfur losses in Fairbanks are most likely a result of long range transport out of the region.

3. Current Investigations and Open Questions

The Fairbanks region is characterized by almost entirely locally-generated particulate matter, with relatively low concentrations in summer and much higher concentrations in winter. For much of the United States, this seasonal pattern is reversed (with highest PM concentrations observed in the summer) and reflects the importance of photochemistry in the formation of PM. Fairbanks, however, lacks significant photochemistry in the winter suggesting that unique, alternative formation mechanisms drive the chemistry. While a number of studies have looked at atmospheric chemistry in arctic regions, to our knowledge, no studies have examined in detail the processing of urban pollutants in arctic regions. This is, in part, because there are relatively few cities located in arctic regions and there are comparatively few opportunities to conduct such investigations.

The Division of Air Quality of Fairbanks North Star Borough, has had a presence monitoring ambient particulate matter since 1999. It currently operates 4 monitoring stations, and includes measurements of PM₁₀ and PM_{2.5}, as well as measurements of carbon monoxide, SO₂, and chemical speciation. Recent efforts have begun the attempt to characterize the chemistry conditions prevalent in the Fairbanks region beyond the scope and capacity of the FNSB borough, and these are now summarized. As of the date of this document, many of the results summarized below are in progress and final data and analyses are not yet completed.

3.1 Measurements by FNSB

Measurements of elemental sulfur and particulate sulfate have been collected in Fairbanks since 2003. Figure 3 shows a simple time series of sulfate concentration. Of note, significant wintertime spikes in sulfate are apparent, with summer minima more typical. Also plotted on this figure is the ratio of directly measured elemental sulfur that is predicted stoichiometrically by sulfate (e.g. removal of four moles of oxygen per mole of sulfate), including a box-plot smoothed line to more clearly identify any patterning in the data. Despite the seasonal spikes in sulfate concentration, no

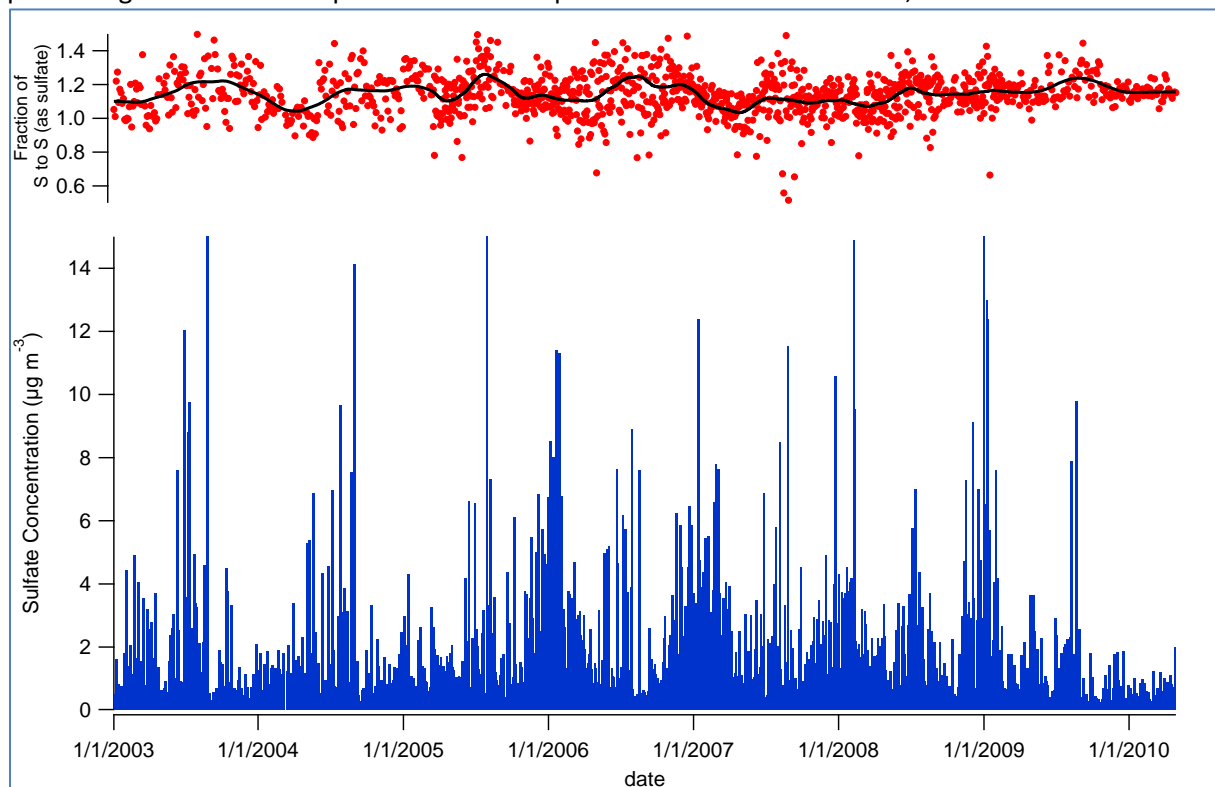


Figure 3: Time series of sulfate concentration (lower frame) and sulfur-to-sulfur ratio (upper frame, including box-smoothed line for visual aid) from Jan 2003-Jan 2010, as collected by FNSB.

pattern in this ratio is apparent, although it appears there is an unmeasured source of sulfur in Fairbanks that is not measured as sulfate. On the whole, the sulfur-to-sulfur (as sulfate) ratio is 1.15 and suggests an addition $\sim 15\%$ of sulfur cannot be attributed to sulfate. The ratio and sulfate concentration measurements are not correlated, suggesting that an independent factor is associated with this additional sulfur. Possible sources for this include organosulfur compounds or sulfur gases preferentially-adsorbed and reacted onto elemental filters. Additional work is continuing to understand this process.

3.2 Modelling approaches

Investigators from the University of Montana, Center for Environmental Health have recently concluded an intensive effort to characterize aerosol chemistry from 2008-2009 using modeling approaches. This study, which employs a Chemical Mass Balance model to identify relative sources of aerosol, utilized existing data provided by FNSB from five monitoring locations in the region. A secondary approach used archived filters for a chemical analysis of isotopes of carbon as well as levoglucosan, a marker for

biomass burning. Their results were recently summarized in a final report by Dr. Tony Ward (Ward, 2010).

Their CMB analysis identified 5 prevailing source profiles of aerosol representative of the Fairbanks region. While there was some site-to-site variability, winter time aerosol loading was most significantly impacted by woodsmoke (range: 62.7%-79.8%, depending on location). Sulfate aerosol was the second most prevalent component of PM (range: 9.8%-20.0%). Their findings also suggest that ammonium nitrate was also substantial (range: 5.1%-10.5%), with lesser contributions from automobile exhaust (range: not detected to 6.8%), diesel exhaust (range: not detected to 7.3%), and Unexplained (range: 0.5%-1.2%). While CMB modeling does not provide insight into specific chemistry, it does provide information towards the more important chemical processes that might be at play in the Fairbanks region.

This study also provided an analysis of ^{14}C carbon isotope ratio analysis that provides information on the sources of the observed carbon. ^{14}C analyses are particularly powerful because they can identify, at the atomic level, the likely age of the carbon elements. In this case, Ward's investigation provides confirmatory evidence that woodsmoke, or 'modern carbon' is a significant contributor to the aerosol loading in the Fairbanks region. This project investigated an additional dataset of levoglucosan, a sugar associated with woodsmoke. Their results were, again, consistent with the notion that woodsmoke contributes significantly to the aerosol mass loading for the Fairbanks airshed.

3.3 Denuder studies

Work at the Washington University in St Louis has begun to investigate the nature of denuder function in cold-weather environments. This study explores three main objectives: whether extreme cold temperate allows for SO_2 penetration through a denuder, whether water vapor interferes with denuder functionality, and whether long-term denuder loading plays a deleterious role in denuder efficiency. This work is still under development and not yet completed, but early results suggest that there is no significant effect on denuder function based on cold-temperate operating conditions, and that water vapor does, in fact, inhibit the denuder from efficient functioning.

3.4 Winter intensive characterization

In February and March of 2011, investigators from the University of Massachusetts established an intensive field monitoring site to provide a broad spectrum of chemical characterization measurements at a fast time resolution. This was an effort to establish more advanced chemical measurements throughout typical wintertime conditions in Fairbanks, and to capture both typical and atypical PM climatology in the region. The study collected hourly aqueous samples of dissolved $\text{PM}_{2.5}$ (including all typical ions), daily high-volume filter samples (for trace metal analysis), and hourly measurements of organic carbon and elemental carbon.

Preliminary data, which has not yet been validated, shows a time series of organic and elemental carbon during the study period (Figure 4). The data are characterized by highly distinct spikes of both organic and elemental carbon, with a good correlation between the two measurements ($r^2 = 0.53$). This suggests that a periodic event that leads to this chemistry consistently occurs and lowers the likelihood of industrial sources of OC or EC (such as power plant emissions or refinery effluent, which normally do not have a significant diurnal emissions profile). Ion measurements and trace metal results are still

pending.

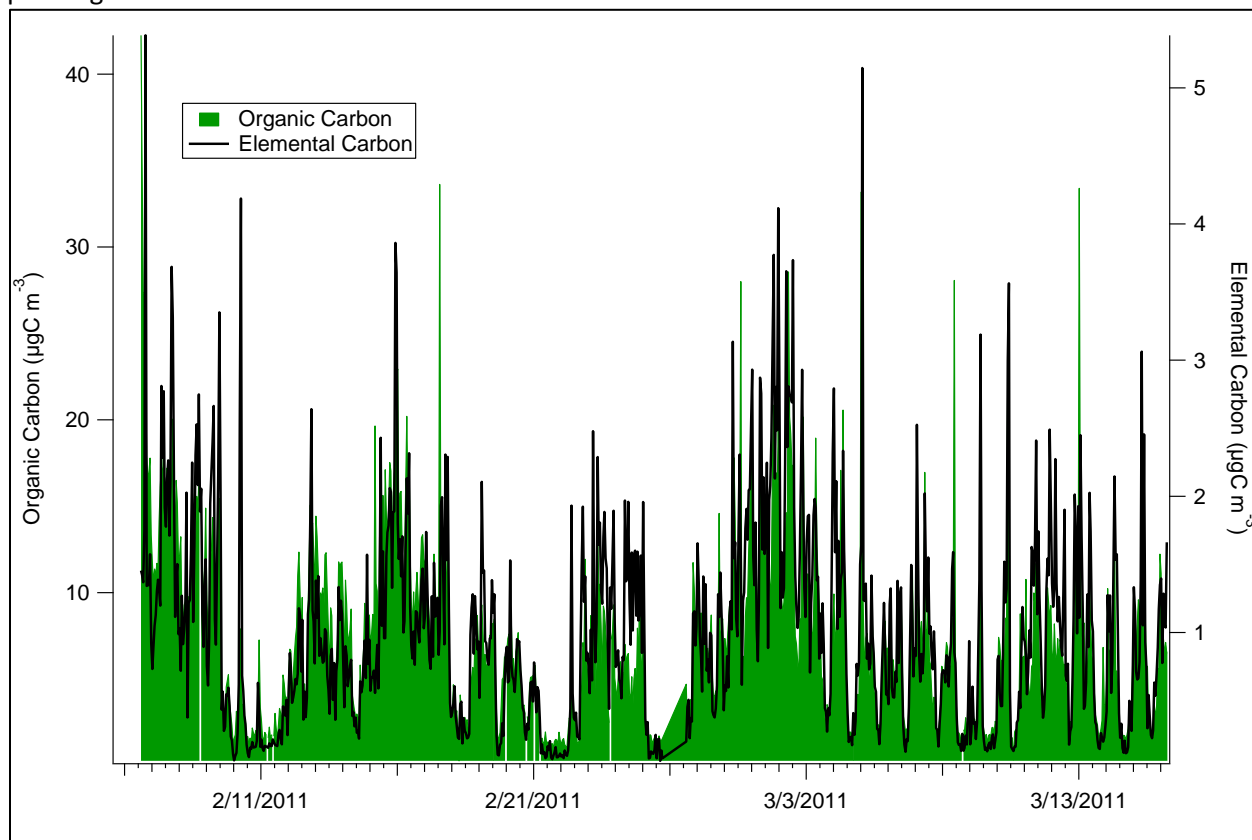


Figure 4: Time series of organic carbon and elemental carbon measured during this study in Feb-Mar 2011 in Fairbanks.

There appears to be a wintertime pattern of highly enhanced EC and OC, as well as a precipitous drop in the same concentration. Figure 5 presents the same data in an alternative approach, with all of the OC and EC data presented as box plots across each hour of the day. Both EC and OC exhibit a clear bimodal distribution, with apparent spikes in the late morning and the hours before midnight during the study period. There are several possible explanations for this finding, though the most probable one involves a link to residential heating using wood and/or oil. The latter possibility is important in the context of sulfur chemistry, since wood burning does not normally emit significant quantities of sulfur, and these data may be useful for further study of home heating oil use in that this emits both sulfate precursor as well as organic and elemental carbon, and thus their variability is likely to have a high degree of association.

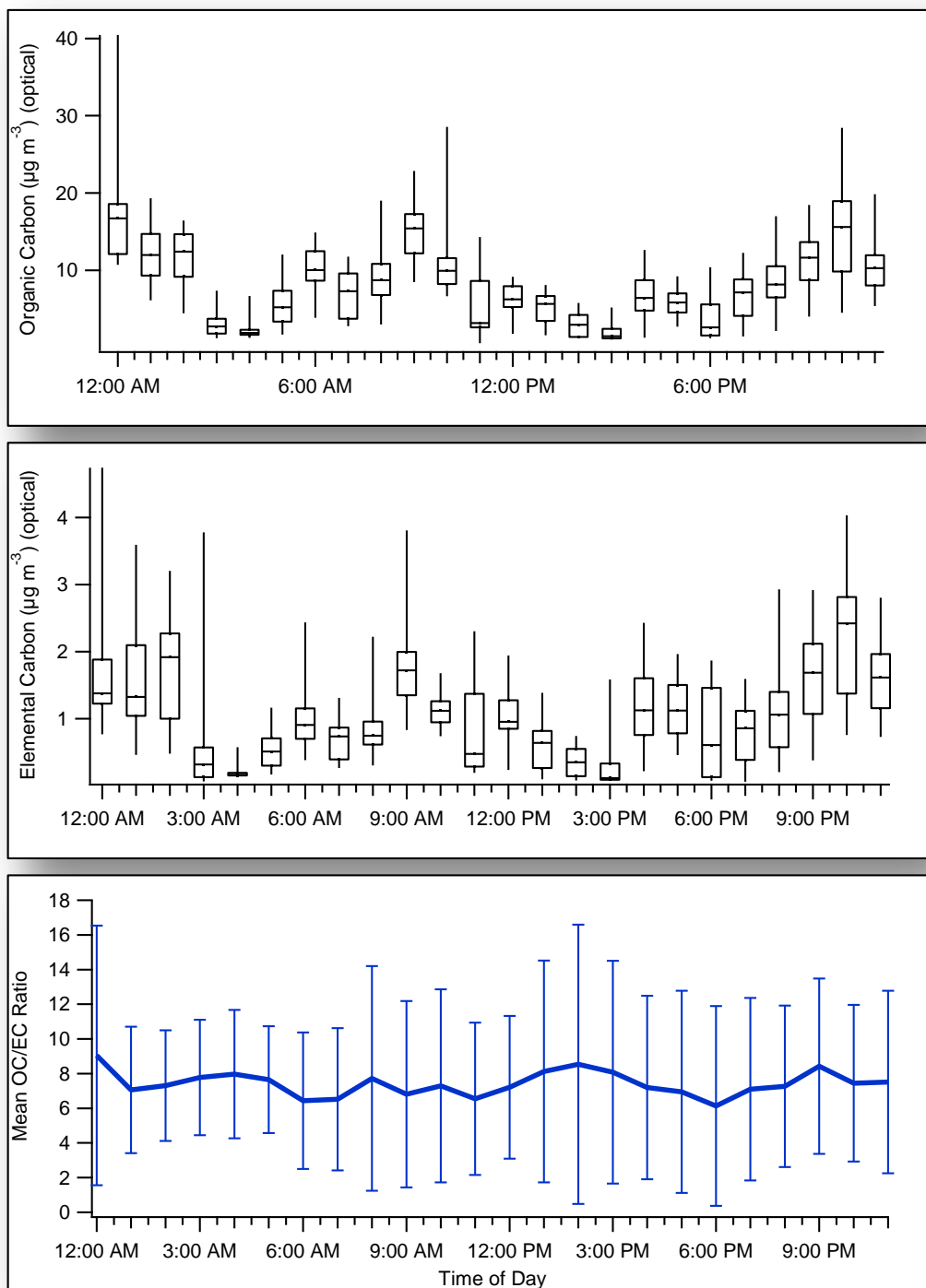


Figure 5: Hourly measurements of organic carbon (top), elemental carbon (middle), and mean OC/EC ratio (bottom). Box plots consist of median and 25th and 75th percentile; whiskers denote 10th and 90th percentiles. Data was collected over approximately 40 days in Feb-Mar 2011 in Fairbanks.

The data also include the mean OC-to-EC ratio for each hour. Overall, these ratios are quite large, with mean ratios approaching 8. The included error bars denote that there is no significant patterning in the data across the diurnal profile, which is inconsistent with the concentration plots of OC and EC. The EC

tracer method of estimating secondary organic aerosol [15, 16], which is an admittedly imperfect analytical approach, would suggest that the majority of the observed OC in the atmosphere is primarily emitted since the ratios are much higher than typical environments with active secondary organic aerosol formation mechanisms. It should be noted that the primary emissions profile of wood and oil burning, on-road diesel combustion, and other local sources of particulates in Fairbanks is not yet known. Additional work (described below) will inform whether the empirically measured ratio is entirely consistent with primary emissions, or if, in fact, secondary formation processes have an important role.

3.5 Fuel feedstock characterization studies

FNSB has recently contracted with Omni Environmental (Portland, OR) to chemically characterize a variety of local fuel feedstocks, including firewood, local on-road and heating oil fuel, and coal. By doing so, it is hoped that a chemical signature profile can be developed for each source indigenous to Fairbanks which, in turn, can be used to study and better understand the observed ambient conditions. As of the date of this paper, no results are yet available.

3.6 Open Questions

Several specific open questions remain that have not yet been addressed by the current efforts. It would be worthwhile to investigate the approaches to answering these questions, and to determine whether these efforts would inform FNSB in the best approach to establishing attainment status. These questions include:

- 1) To what degree does wintertime ice fog play a role in secondary aerosol chemistry?
- 2) Can the current emissions inventory of sulfur account for the observed sulfur (as sulfate or non-sulfate sulfur-containing components?)
- 3) Can PM be better apportioned to on-road diesel, home heating fuel oil, home heating biomass, and coal-fired power plant emissions, which likely comprise the bulk of PM emissions in Fairbanks?
- 4) How does extreme cold temperatures influence gas-to-particle conversion in the context of stack emissions (e.g. how does a rapidly cooling wet emissions stack perform)?
- 5) Can existing (or new) air quality models be better calibrated to on-the-ground observations? Are these model assumptions valid?

4.0 Future Plans on Attainment in Fairbanks

Currently, Sierra Research is working with FNSB staff to develop a comprehensive Implementation Plan to ensure compliance with federal air quality standards. Data from these, and future, investigations will provide significant guidance in the best approaches to developing efficient, and effecting plans to reduce the burden of particulate matter.

There are two complimentary approaches to a better understanding of air quality issues in the Fairbanks region, and both are equally important. The first approach includes better empirical understanding of local aerosol conditions through additional field characterization studies. This approach will result in a direct understanding of the critical mechanisms at play in this unique environment, and will do so with the least amount of scientific uncertainty. However, over the long term, additional field studies are probably unsustainable in that they are technically challenging, often limited to answering only a few, specific questions, and can be cost-prohibitive. Thus, computational chemistry modeling is an outstanding extension to field studies. They are cost-effective, highly repeatable, and can be adapted to changing conditions. By themselves however, models – especially those developed to operate in an

atypical aerosol milieu such as that of Fairbanks – need to be compared with on-the-ground measurements to provide operational efficacy and validation to ensure high confidence in their results. A number of these possible future studies are listed in Appendix A, though not all are specific to improving model guidance.

5.0 Summary and Conclusions

This paper has summarized the current state of the science associated with aerosol chemistry during the winter in Fairbanks, Alaska. It has also provided a brief summary of the studies to-date, and these results appear to be consistent with significant issues related to sulfur chemistry, as well as chemistry related to carbon (organic and elemental). Further, it identified likely and unlikely oxidation mechanisms for secondary formation (mainly in the context of sulfur conversion, though this process is not necessarily limited to this element).

Attainment of the National Ambient Air Quality Standards in Fairbanks will only be achieved with a better understanding of aerosol formation chemistry specific to the winter in Fairbanks. Without this understanding, most attempts to reduce emissions – e.g. through regulatory action – may be misguided and not achieve the intended targets. At this point, the understanding of chemical conditions in Fairbanks, specifically related to sulfur chemistry, is quite poor and needs significant improvement.

Cited References

1. Jimenez, J.L., et al., *Evolution of Organic Aerosols in the Atmosphere*. Science, 2009. **326**(5959): p. 1525-1529.
2. Kanakidou, M., et al., *Organic aerosol and global climate modelling: a review*. Atmospheric Chemistry and Physics, 2005. **5**: p. 1053-1123.
3. Seinfeld, J.H. and J.F. Pankow, *Organic atmospheric particulate material*, in *Annual review of physical chemistry, Volume 54, 2003*. 2003, Annual Review. p. 121-40.
4. USEPA. *Review of the national ambient air quality standards for particulate matter policy Assessment of scientific and technical information*. 2005; 514 p.]. Available from: Available online, Government web site, 2005: <http://purl.access.gpo.gov/GPO/LPS62787>
5. Jacobson, M.C., et al., *Organic atmospheric aerosols: review and state of the science*. Reviews of Geophysics, 2000. **38**(2): p. 267-94.
6. Seinfeld, J.H. and S.N. Pandis, *Atmospheric chemistry and physics : from air pollution to climate change*. 1998, New York: Wiley. xxvii, 1326 p.
7. Sullivan, A.P., et al., *Airborne measurements of carbonaceous aerosol soluble in water over northeastern United States: Method development and an investigation into water-soluble organic carbon sources*. Journal of Geophysical Research, 2006. **111**(D23): p. 1-14.
8. Peltier, R.E., et al., *Fine aerosol bulk composition measured on WP-3D research aircraft in vicinity of the Northeastern United States – results from NEAQS*. Atmospheric Chemistry and Physics, 2007. **7**(12): p. 3231–3247.
9. Huff, A.K. and J.P.D. Abbatt, *Gas-phase Br-2 production in heterogeneous reactions of Cl-2, HOCl, and BrCl with halide-ice surfaces*. Journal of Physical Chemistry A, 2000. **104**(31): p. 7284-7293.
10. Huff, A.K. and J.P.D. Abbatt, *Kinetics and product yields in the heterogeneous reactions of HOBr with ice surfaces containing NaBr and NaCl*. Journal of Physical Chemistry A, 2002. **106**(21): p. 5279-5287.
11. Simpson, W.R., et al., *Halogens and their role in polar boundary-layer ozone depletion*. Atmospheric Chemistry and Physics, 2007. **7**: p. 4375-4418.
12. Donaldson, D.J. and K.T. Valsaraj, *Adsorption and Reaction of Trace Gas-Phase Organic Compounds on Atmospheric Water Film Surfaces: A Critical Review*. Environmental Science & Technology, 2010. **44**(3): p. 865-873.
13. Fuzzi, S., P. Mandrioli, and A. Peretto, *Fog droplets - An atmospheric source of secondary biological aerosol particles*. Atmospheric Environment, 1997. **31**(2): p. 287-290.
14. Nilsson, E.D. and C. Leck, *A pseudo-Lagrangian study of the sulfur budget in the remote Arctic marine boundary layer*. Tellus Series B-Chemical and Physical Meteorology, 2002. **54**(3): p. 213-230.
15. Chu, S.H., *Stable estimate of primary OC/EC ratios in the EC tracer method*. Atmospheric Environment, 2005. **39**(8): p. 1383-1392.
16. Schauer, J.J., *Evaluation of elemental carbon as a marker for diesel particulate matter*. Journal of Exposure Analysis and Environmental Epidemiology, 2003. **13**(6): p. 443-453.

Appendix A

Future Research Initiatives: Fairbanks North Star Borough Region

Ice Fog Sample Collection

Method Summary: Develop highly mobile, high volume TSP samplers suitable for quick deployment to collect and characterize ice fog samples for a chemical analysis of potential aerosol formation processes. Samples could be collected and compared across periods of local wood- and fuel-burning influence, when gas-phase power plant emissions have a stronger downwelling impact, or when relatively clean air advects through the region. Samples would be taken in the immediate vicinity of the fog formation near the Chena River, as well as downwind of this fog after the crystals have phase sublimation.

Rationale: Because the chemical processing and formation mechanisms are, at this point, not fully understood, it has been hypothesized that ice fog crystals provide suitable reactive surface area for heterogeneous nucleation in the absence of known oxidant components. Collecting in-situ measurements with newly-formed fog crystals (and pre-existing particles and gases near the river), we can provide baseline concentration measurements of sulfur-containing fine particles. Additional measurements may provide insight into sulfur oxidation processes by assessing differential sulfur-containing particle concentrations downwind of the aerosol/fog mixture.

Spatial profiling of aerosol composition: Stationary Approaches

Method Summary: Develop and simultaneously deploy a set of 15-20 (or more) autonomous filter samplers capable of unattended, low-flow PM_{2.5} aerosol collection on Teflon filter media. Typical deployment schemes include weekly (or bi-weekly) filter changes with a ½ hour on, ½ hour off cycle that collects samples at low flow (4 lpm) throughout the week. Alternative approaches include more frequent filter changes (e.g. every 48 hours) with a continuous sample collected during each time period. Spatially distributed measurements can be scaled against 2-3 reference site measurements for components thought to have limited local variation (TBD) in order to account for instrument variability, instrument precision, or local emission effects. Study length will be 6-8 weeks during the winter, and can be coupled with 6-8 weeks during the summer for comparative purposes. Filter analysis by gravimetry and high resolution XRF for ~35 metals.

Rationale: The ability to discern spatial and temporal characteristics of particle composition, coupled with meteorological data, may provide important insight into the specific sources of aerosols in the region. Further, it will provide a dense dataset which may inform spatial models currently under production and use in the region with improved chemistry profiles and temporal variations.

Model Validation Studies

Method Summary: Chemical speciation measurements guided by the chemical modeling currently used by FNSB to identify predicted PM concentrations and future attainment. Speciation measurements depend on elements identified by the model as predictive of model efficacy and uncertainty and would be measured in different locations and across different times (e.g. different seasons, diurnal variations). Measurements could include chemical elements such as those measured by XRF, PM_{2.5} mass, or gas-

phase tracers. Both high spatial resolution models (e.g. smallest grid cells) and low spatial resolution models can be validated.

Rationale: Because of increased reliance on models to efficiently provide estimates or predictions of current and future aerosol climatology, it is essential to characterize the performance of these models in terms of precision and uncertainty through robust field measurements. This approach will provide either a) a mechanism to assess and possibly improve model performance for local conditions; b) provide evidence to invalidate model results based on field testing; or c) provide insight into reasons and locations where model predictions and field measurements are de-coupled.

Spatial profiling of aerosol composition: Mobile Approaches

Method Summary: Expand and enhance the analytical capabilities of the FNSB “Sniffer” vehicle with a wider range of chemical and physical characterization capacity (either permanently or for a specific study period). Relevant instruments for such an application might include high time resolution measurements of carbon monoxide, sulfur dioxide, particle size distribution (by SMPS and/or aerosol laser spectrometer), and short time integrated, high volume filter samplers.

Rationale: Expansion of analytical capacity provides FNSB staff with the capacity to better investigate aerosol chemical characteristics across a wide range of conditions, often in response to short-term prevailing environmental conditions (e.g. presence of strong or weak inversion, periodically located downwind of specific sources of interest, etc). The current Sniffer vehicle has yielded important findings, but is currently limited by analytical capacity and specificity.

Characterizing Organic Carbon (and tracers of combustion) in Fairbanks

Method Summary: Simultaneously characterize carbonaceous aerosol at three or more locations to provide chemical evidence describing multiple facets of carbon. A set of instrumentation will be established at each site, and will include aethelometers, Sunset Labs EC/OC (field instruments), and a custom-built filter sampler capable of multiple sample collections on quartz filters through either denuded or undenuded sample lines. The latter would be collected and analyzed (after extraction) by suitable speciation methods (e.g. GC/MS) for organic speciation, ¹⁴C isotopic dating, and levoglucosan analysis. Measurements to be conducted in the winter and summer.

Rationale: Organic carbon accounts for a large fraction of PM_{2.5} (and is even larger when converted to organic matter) and thus represents an important subject of study in order to move FNSB towards attainment. By undertaking more comprehensive chemical analyses with a specific focus on carbon-containing aerosol, FNSB is likely to better understand source contributions to this complex component, whether from fuel oil combustion, on-road diesel/gasoline, or wood-burning.

Using the CALPUFF Dispersion Model to Characterize the Fairbanks Power Plant Plumes.

Fairbanks has a significant PM_{2.5} nonattainment problem with design values increasing, in excess of 50 µg/m³ in recent years. Chemical speciation shows organic carbon (OC) levels amount to approximately 60% and sulfate levels of about 20% of the mass of PM_{2.5}. The dominant source of CO is thought to be from the wood burning and sources of sulfur from space heating oil, power plant fuel oil and coal. Upon analysis of the monitoring site filters, it is not clear whether the SO₂ and sulfate emissions are from fuel oil or from the coal because of the presence of winter time inversion layers.

The air quality model CMAQ, configured with the Penn State developed meteorological model WRF runs showed approximately 20% of the particulate matter composed of sulfate. It was not known whether the sulfur contribution to the PM_{2.5} was from fuel oil or from the coal. EPA region 10 suggested running a dispersion model to assess the plumes from the point sources located at the adjacent areas. ADEC and EPA agreed that CALPUFF would be an appropriate model to run to characterize the plumes from the power plants located within the vicinity of the nonattainment area.

CALPUFF is a non-steady-state meteorological and air quality modeling system used by the EPA for studies that include long range transport of pollutants. The model was configured with WRF inputs using mesoscale model interface program (MMIF) and was modified to handle 38 vertical layers representing Fairbanks with the lowest layer being 4 meters above ground level on a 1.33 x 1.33 km grid cell. Six point sources that are in the Fairbanks PM_{2.5} nonattainment area were modeled for the design episode January 23- February 10, 2008. These six point sources were:

- 1- Fort Wainwright (Facility ID 1121) – Coal is the fuel source, hourly emissions provided.
- 2- University of Alaska Fairbanks (Facility ID 315) Coal is the base fuel and distillate fuel oil is the secondary fuel used to satisfy increased loads, hourly emissions were provided.
- 3- GVEA is the electric utility and has two facilities Zehnder (Facility ID 109). Zehnder peaking facility north of downtown which burns high sulfur distillate fuel oil on an intermittent basis.
- 4- North Pole (Facility ID 110). North Pole is a larger facility and burns a mixture of high sulfur distillate fuel oil and naphtha (very low sulfur), hourly emissions provided for both.
- 5- Aurora Energy (Facility ID 315) is a power plant owned by the coal company, located in downtown Fairbanks, which burns a mixture of coal and distillate fuel oil. They sell the power to GVEA and they sell hot water and steam to office buildings and a limited number of homes in the downtown area. Only constant yearly emissions were provided.
- 6- Flint Hills Refinery (Facility ID 71) – is located in North Pole. It is a distillation refinery, no cracking; all heavy ends go back into the pipeline. Hourly emissions were provided.

Figure XX represents the modeling domain 201 x 201 in the X and Y direction with a grid cell size of 1.33 x 1.33 km. In addition to the gridded receptors, the model used discretely placed receptors at specific locations with vertical resolution of the WRF data's first 12 layers to obtain the average surface concentration of the entire domain. Summary of the six major point sources average surface concentration of PM_{2.5} and SO₂ is tabulated below.

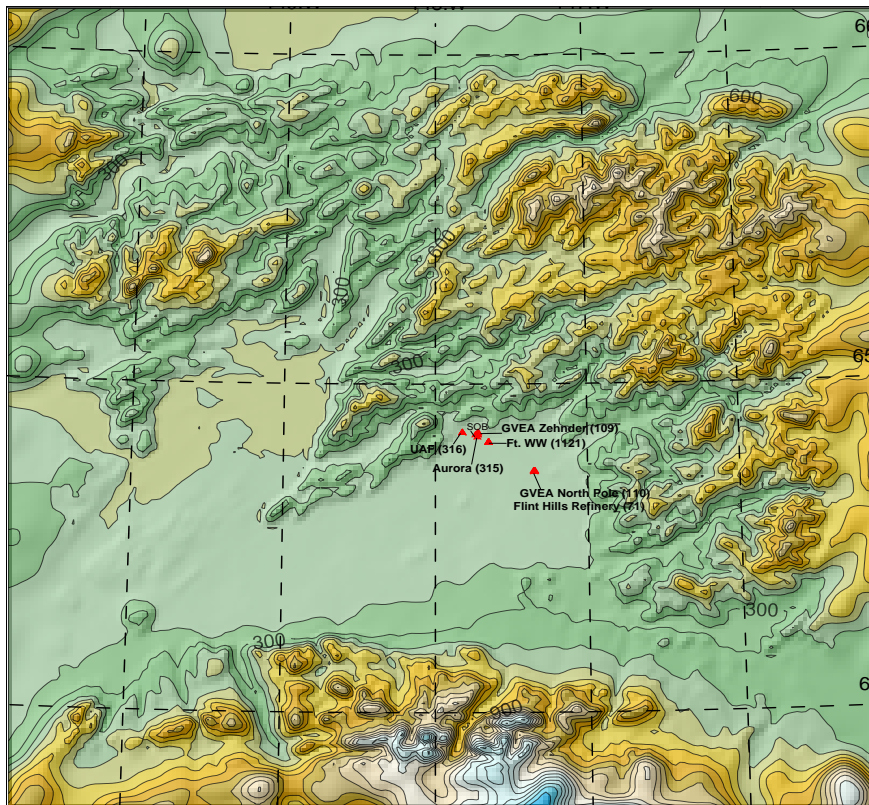


Figure XX: Fairbanks point source locations are represented by red triangles and are labeled by facility ID number and abbreviated name. The SOB (state office building) that houses the FRM (Federal Reference Method) monitor is labeled with a red triangle. The domain represented is 201 x 201, 1.33 km grid cells.

Table 1. Summary of six major Fairbanks point source plumes from CALPUFF for the episode (Jan. 23rd to Feb. 9th, 2008) average surface concentrations of PM_{2.5} and SO₂ in µg/m³.

Power Plant	Episode average SO ₂ (µg/m ³)	Episode average PM _{2.5} (µg/m ³)
UAF- 316	2.75	0.16
Aurora- 315	0.75	0.02
Zehnder-109	0.48	0.19
Flint Hills-071	0.016	0.38
GVEA NP-110	3.8	1.45
Ft. WW- 1121	14	1.6
Total surface concentration	21.8	3.8

CALPUFF modeling showed two largest sources that influence PM_{2.5} concentration at the downtown state office building site were, the GVEA North Pole and Ft. Wainwright power plants. Monitoring data from the state office building was selected for comparison because it was the only location for which January 2008 episode data was available. Average SO₂ concentration from all sites for the entire episode was 4.4 µg/m³ and the highest were from the two sources aforementioned. The cumulative effect of all six plants according to model output is estimated to be less than 10% of the PM_{2.5} surface concentration. In overall, whether use of vertical profiles, episode surface concentration averages for all power plants, or SOB specific concentrations, there was not more than 10% influence on the surface concentrations from the six power plants.

Final Report

To

Alaska Department of Environmental Conservation (ADEC)

Grant Number 127617

Reporting Period: 8 March 2011 – 31 January 2012

‘Fairbanks, North Star Borough AK PM2.5 Non-Attainment Area WRF-ARW’

Dr. Brian J. Gaudet, PI

Dr. David R. Stauffer, co-PI

The Pennsylvania State University

Dept. of Meteorology

University Park, PA 16802

bjg20@met.psu.edu

2 Apr 2012

EXECUTIVE SUMMARY

This final report describes work performed by the Department of Meteorology at the Pennsylvania State University under Grant Number 127617, 'Fairbanks North Star Borough PM2.5 Non-Attainment Area WRF-ARW Modeling', supported by the Alaska Department of Environmental Conservation (ADEC) and the Fairbanks / North Star Borough. The purpose of this project was to perform meteorological modeling of the region around Fairbanks and North Pole, AK, as part of the State Implementation Plan for fine particulate matter (PM2.5) analysis of the region. The Fairbanks / North Star region was designated a non-attainment area for the daily National Ambient Air Quality Standard (NAAQS) for PM2.5 by the Environmental Protection Agency (EPA); high PM2.5 concentrations for the area predominantly occur within stable boundary layers during periods of extreme cold and weak winds during the winter season. The air quality modeling component of the SIP utilizes atmospheric analyses generated by a meteorological model; therefore it is important to select a meteorological model configuration that can properly represent the structure and evolution of the local stable boundary layer in these conditions.

The simulations were to be performed with the Weather Research and Forecasting (WRF), Advanced Research WRF (WRF-ARW) model, a globally used and freely-available meteorological model. Initial WRF-ARW simulations for a period in Jan. – Feb. 2008 were performed by Penn State under the Regional Applied Research Effort (RARE) project funded by the EPA. During the RARE project an optimal set of physics options, grid configuration, and data assimilation strategy was developed and tested. For physics sensitivity tests data assimilation was only performed on the coarser two domains (12-km and 4-km horizontal grid spacing), while the finest domain (1-km horizontal grid spacing) was used for assessing sensitivity. It was concluded, however, that a final meteorological analysis to be provided to EPA should also have data assimilation on the finest domain, to provide a better fit to the observations.

For the current contract, the model setup from the RARE project was to be applied to the production of a new meteorological analysis covering the period 2-17 Nov. 2008. As in the final meteorological analysis of the RARE project, data assimilation for the current project uses data assimilation on all three domains. However, a few modifications to the data assimilation procedure were implemented to take advantage of data and source code not used in the RARE project: 1) the effective vertical resolution of the observations as seen by the data assimilation modules was increased; 2) a more vertically-consistent objective analysis procedure was used; 3) additional surface observations from non-standard sources (i.e., stations not present in the standard METAR-format database typically used for hourly meteorological reporting) were used

both for verification and in the data assimilation, in order to supplement the METAR observations in this relatively data-sparse region.

A test period (5 – 9 Nov 2008) was used to perform some initial evaluations of possible modified procedures. In particular, during the RARE project the data assimilation on Grid 3 for the final meteorological analysis only used the temperatures from the METAR surface stations, and not the winds. For the RARE project it was thought that, since the surface winds during the coldest episode would be expected to be weak and poorly sampled, and since the surface winds in these conditions might be expected to be thermally-driven, the best chance of accurately reproducing existing flows would be to only use the temperature (and moisture) fields from surface observations in data assimilation, while relying on the model itself to generate the proper wind fields. This led to realistic low-level flow patterns and generally satisfactory wind error statistics at non-calm locations. There did tend to be a positive near-surface temperature bias during periods of extreme cold and weak winds, which could have been a result of overestimated vertical mixing due to the model's positive near-surface wind speed bias. The extended surface dataset used in the current study provided an opportunity to determine if improved statistics could result if 1-km grid data assimilation of near-surface winds was included. This was one of the initial sensitivity tests performed for the test period.

The major findings of the current project are as follows:

- The use of near-surface winds in data assimilation during the test period, when compared to a control simulation, led to about a 20 degree improvement in the mean absolute error (MAE) of wind direction. Temperature and wind speed statistics were also improved, but the improvements were modest. The modest size of these improvements was hypothesized to be due to either insufficient horizontal resolution of the model topography, or too large of a region of influence of particular observations in the data assimilation procedure.
- A new simulation was performed in which the radius of influence of observations on the 1-km grid was reduced from 75 km to 30 km, and the strength of the relaxation coefficient was doubled. These experiments produced slightly better temperature statistics on average, but slightly worse wind speed statistics. Wind direction errors, however, were further reduced by the new simulation procedure by a substantial amount (about 19 degrees in MAE). It was decided to make this model configuration (experiment TWIND2X30) the basis of a simulation of the entire 2-17 Nov. 2008 episode.
- Previous experiments did not make use of calm wind observations in the data assimilation procedure; the possible presence of missing data or high instrument response thresholds imply that it might be preferable to retain model-generated flows in weak-

wind conditions rather than relax the flows towards a zero-magnitude wind vector by data assimilation. However, because it was desired to further reduce the model positive wind speed bias, an additional set of simulations over the 2-17 Nov. 2008 episode was performed, for which data assimilation did make use of calm wind reports (henceforth experiment TWIND2X30CALM). While the use of calm wind reports did reduce the positive near-surface wind bias of the model, the improvement was only on the order of 0.1 m s^{-1} . Meanwhile, TWIND2X30CALM had wind direction MAE scores that were about 14 degrees worse. Since wind direction by necessity can only be verified with non-calm wind observations, the implication was that the use of near-surface calm wind observations in data assimilation was degrading wind direction statistics at other observation locations without making a substantial improvement in wind speed statistics. Therefore, it was decided to deliver the results of TWIND2X30, rather than TWIND2X30CALM, to ADEC for use in subsequent air quality modeling.

- The Jan-Feb 2008 episode simulated during the RARE study was re-simulated using the TWIND2X30 procedure, and compared with corresponding statistics using the RARE configuration. Little statistical difference was found between the RARE and TWIND2X30 for variables other than wind direction, for which the TWIND2X30 configuration was about 12 degrees better in terms of MAE.
- Qualitatively, it was found that the meteorological analysis produced realistic topographical flows, and was capable of reproducing observed surface temperatures below $-40 \text{ }^{\circ}\text{C}$ in locations such as Woodsmoke. However, the model did tend to have a positive near-surface temperature bias during the coldest episodes at valley locations that could not be well-resolved by the model (e.g., Goldstream Creek). This was counteracted by periods when the model had a negative temperature bias, such as during the initial precipitation event of the 2-17 Nov. 2008 episode, such that the overall model temperature bias was quite small (less than a degree Celsius) for both simulated episodes.

1. INTRODUCTION

The region around Fairbanks and North Pole, AK, was designated by the Environmental Protection Agency (EPA) as a non-attainment area for fine particulate matter (PM_{2.5}, referring to particles with aerodynamic diameters equal to or less than 2.5 microns). This designation required that a State Implementation Plan (SIP) be developed. The violations occur predominantly during the cold season, when the meteorological conditions frequently become ideal for achieving high concentrations of any tracer released into the atmosphere. These ideal conditions, often present in combination, include the presence of extremely strong inversions capping a shallow layer of extremely cold air, light and variable winds, and very weak, intermittent turbulence (e.g., Benson 1970; Serreze et al. 1992; Mölders and Kramm 2010). These conditions, which frequently occur in the winter over inland Alaska, can be exacerbated in the region around Fairbanks, where a rough semicircle of ridges tends to isolate the airflow around Fairbanks from its surroundings, restricting the dispersal of pollutants.

2. EPA RARE STUDY BACKGROUND

The Regional Applied Research Effort (RARE) study was sponsored by the EPA to help the Fairbanks North Star Borough and the Alaska Department of Environmental Conservation (ADEC) develop a State Implementation Plan for the Fairbanks / North Pole PM_{2.5} non-attainment area. This project included meteorological modeling, meteorological observational, and trace gas and aerosol analysis modeling components. Penn State conducted the meteorological modeling component of this study from 1 Sep 2008 – 31 Jan 2010, with the specific focus being the extremely cold stable boundary layers in winter in the Fairbanks region. The meteorological portion of the project consisted of selecting and performing two twenty-day simulations down to 1-km horizontal grid spacing for two episodes from the 2007-2008 winter season characterized by high PM_{2.5} exceedance events in the Fairbanks region. One episode was to be characterized by near total darkness, while the second was to contain partial sunlight.

There were two components of the atmospheric modeling portion of the study. One was to produce the best possible analysis of the atmosphere (at approximately 1-km grid spacing) that could be used in conjunction with the parallel chemical and emissions modeling efforts to better understand the nature of the PM_{2.5} exceedance events of the Fairbanks / North Star Borough area. The other was to perform physics sensitivity studies on turbulence and land surface model parameterizations to determine the best-performing modeling configuration and physics suite for representing the stable atmospheric boundary layers in these conditions.

The tool used for the meteorological modeling component of the RARE project was the Weather Research and Forecasting (WRF) model (Skamarock et al. 2008), more specifically, the Advanced Research WRF dynamic core (WRF-ARW, henceforth simply called WRF). WRF contains separate modules to compute different physical processes such as surface energy budgets and soil interactions, turbulence, cloud microphysics, and atmospheric radiation. Since turbulent eddies in the SBL are typically much smaller than mesoscale model horizontal grid spacing (e.g., ten meters vs. a thousand or more meters), they cannot be modeled directly (e.g., Wyngaard 2004), but typically their effect is parameterized by a planetary boundary layer (PBL) scheme that predicts turbulent kinetic energy (TKE). Within WRF the user has many options for selecting the different schemes for each type of physical process. There is also a WRF Preprocessing System (WPS) that generates the initial and boundary conditions used by WRF, based on topographic datasets, land use information, and larger-scale atmospheric and oceanic models.

The RARE simulations used three one-way nested horizontal grids with horizontal grid spacing of 12 km, 4 km and 1.3 km, respectively. Grid 1 covers the entirety of Alaska and extends from Siberia to the northwestern continental United States (Figure 1). Grid 2 closely coincides with the extent of the Alaskan landmass south of the Brooks range; it includes the Anchorage region and the Gulf of Alaska in the south (Figure 2). Grid 3, centered around Fairbanks and extending south to the Alaska Range and north past the White Mountains and other uplands just north of Fairbanks, includes all of the non-attainment area within the Fairbanks North Star Borough (Figure 3 - Figure 4).

Many of the WRF namelist parameters used in the RARE study were taken directly from modeling studies performed by Penn State for studying the nocturnal stable boundary layers of central Pennsylvania (Stauffer et al. 2009; Seaman et al. 2012) using version 3.1 of WRF-ARW. Many of the grid-independent parameters are listed in Table 1. In particular, the extremely fine vertical grid spacing of the model levels near the surface is in order to adequately resolve the depth of stable boundary layers that may be only tens of meters deep, and within which the scale of the turbulent eddies may be even less. However, the near-surface vertical grid spacing in the RARE study was coarsened slightly from that of the central Pennsylvania studies both in order to prevent numerical instabilities from occurring over the extremely steep elevation gradients on the north edge of the Alaska Range, and to alleviate concerns about the model atmospheric grid spacing being on the order of the vegetation canopy height. The final near-surface vertical grid spacing was 4 m, increasing gradually with height above the surface (refer to Gaudet and Stauffer 2010).

Grid-dependent namelist parameters and WRF Preprocessing System (WPS) namelist parameters are listed in Table 2 and Table 3, respectively.

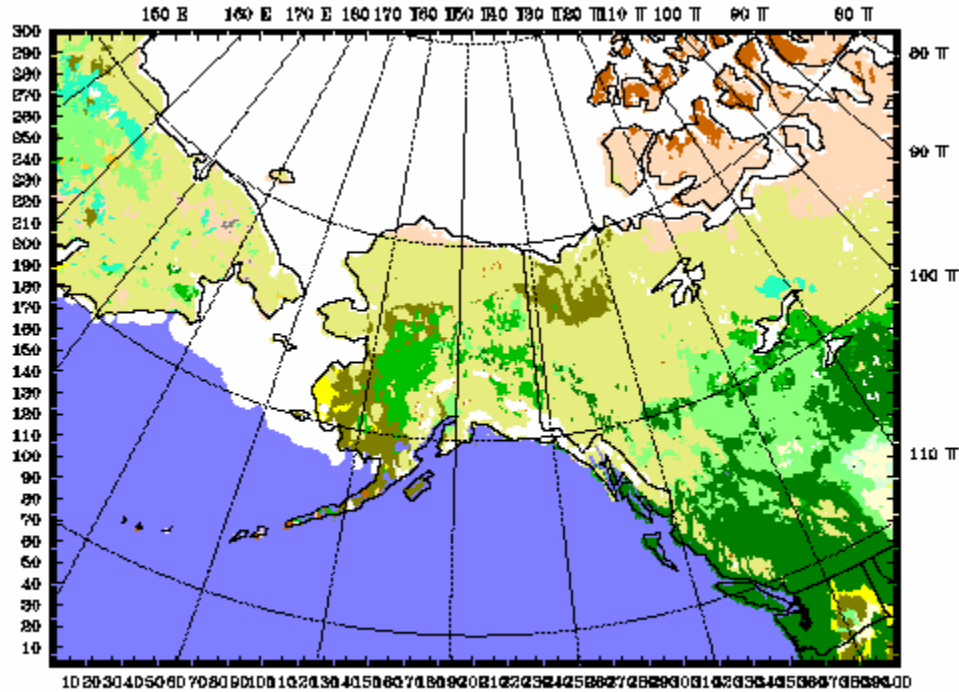


Figure 1: Grid 1 domain, showing land use variation. Colors indicate: light green – cropland/woodland mosaic; yellow – grassland; dark yellow – shrubland; mustard – mixed shrubland/grassland; leaf green – deciduous broadleaf forest; dark green – deciduous or evergreen needleleaf forest; forest green – mixed forest; light blue – water body; brown – herbaceous wetland; surf green – wooded wetland; tan – barren or sparsely vegetated; light gray – herbaceous tundra; avocado – wooded tundra; peach – mixed tundra; medium gray – bare ground tundra; white – snow or ice.

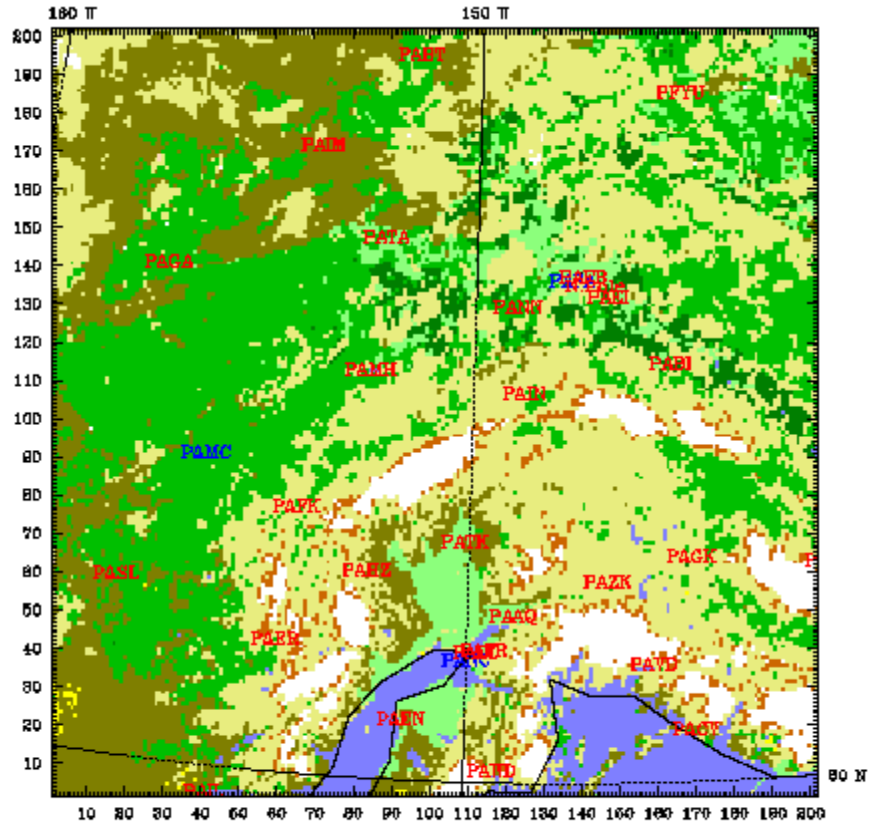


Figure 2: Grid 2 domain, showing land use variation. Color scale same as in Figure 1.

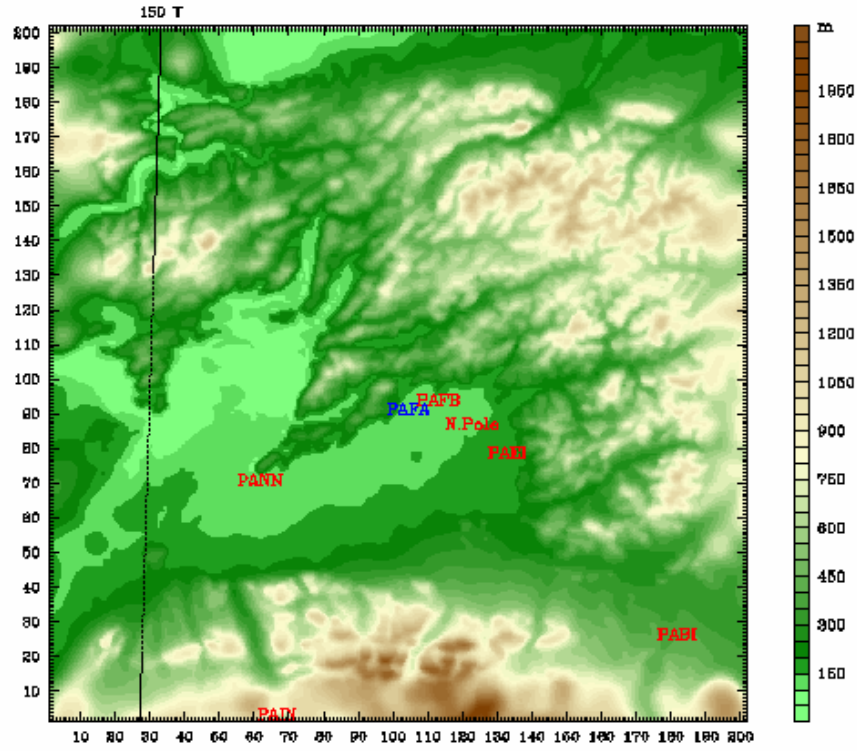


Figure 3: Grid 3 domain, showing topographic relief. METAR stations are shown in red; rawinsonde stations are shown in blue. Eielson AFB is denoted by PAEI; Fort Wainwright is denoted by PAFB. Location of community of North Pole is also indicated.

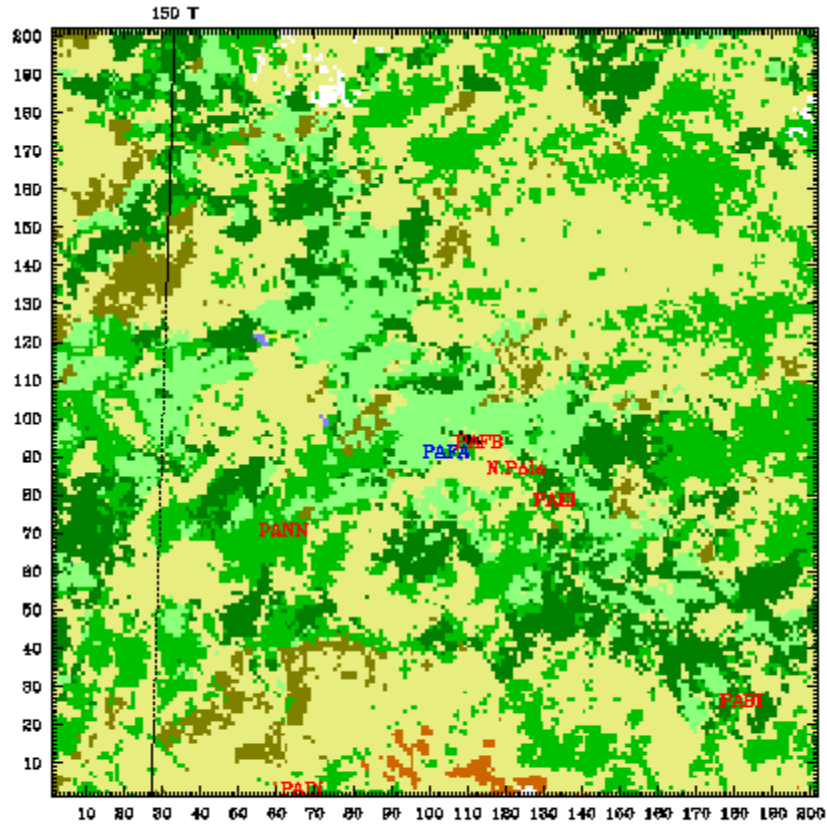


Figure 4: Grid 3 domain, showing land use variation. Color scale same as in Figure 1.

Table 1: Grid-independent features of WRF simulations.

nesting procedure	one-way concurrent
model top (hPa)	50
number of vertical layers	39
eta value of full levels	1.0, 0.9995, 0.999, 0.9984, 0.99705, 0.99415, 0.99155, 0.986, 0.78, 0.966, 0.95, 0.034, 0.918, 0.902, 0.886, 0.866, 0.842, 0.814, 0.78, 0.74, 0.694, 0.648, 0.602, 0.556, 0.51, 0.464, 0.418, 0.372, 0.326, 0.282, 0.24, 0.2, 0.163, 0.128, 0.096, 0.066, 0.04, 0.018, 0
approximate height above ground level of half levels (m)	2.0, 6.0, 10.5, 18.4, 35.5, 57.8, 90.9, 146.2, 228.3, 344.5, 478.7, 614.8, 752.7, 892.5, 1052.3, 1251.1, 1491.2, 1785.4, 2148.4, 2587.7, 3079.8, 3598.2, 4146.0, 4727.3, 5346.7, 6010.4, 6725.8, 7502.6, 8333.4, 9208.6, 10135.5, 11190.6, 12139.8, 13234.2, 14408.4, 15652.1, 16921.7, 18193.7
exclude nudging from the boundary layer	no
G for analysis nudging, when used (s^{-1})	0.0003
G for obs nudging, when used (s^{-1})	0.0004
obs nudging half-time window (hr)	2
specified, relaxed zone width	1, 9

Table 2: Grid-Dependent features of baseline model configuration

	Grid 1	Grid 2	Grid 3
horizontal extent	401 x 301	202 x 202	202 x 202
horizontal Δx (km)	12	4	1.33
i parent start	-	156	103
j parent start	-	106	106
time step (s)	24	8	4
sound step ratio	8	8	4
dampcoef	0.0	0.0	0.0
analysis nudging	yes	no	no
obs nudging	yes	yes	yes
surface obs nudging xy radius (km)	100	100	75
topographic dataset	USGS 10 m	USGS 2 m	USGS 30 s

Table 3: Grid-independent WRF Preprocessor System (WPS) features

projection	Lambert conformal
reference latitude, longitude	64.8, -148.0
true latitudes	50.0, 70.0
standard longitude	-148.0
initial conditions	0.5 degree GFS analyses
analysis interval (hr)	6

Two twenty-day episodes from the 2007-2008 winter season were selected in the RARE study. One episode was from 14 Dec 2007 to 03 Jan 2008, a time of year when there is little solar radiation in the Fairbanks area (approximately three hours of daylight per day near the solstice). During this episode the temperature rapidly decreased to near -40°C by 21 Dec, accompanied by rapid increases in PM_{2.5} concentrations, and then temperatures generally increased and PM_{2.5} decreased for the remainder of the episode. The second episode was from 23 Jan 2008 to 12 Feb 2008, when solar insolation was more significant (between five and eight hours of sunlight per day), and provides an example of ‘partial sunlight’ conditions. During this episode temperatures were initially relatively warm (near 0°C), decreased briefly to near -35°C by 27 Jan, rebounded slightly, and then decreased during the most extensive period of sub -35°C weather of the season. Consistent with the prolonged period of cold temperatures were recurring violations of the PM_{2.5} standard in the Fairbanks area.

In the initial period of a regional model simulation there is generally a period of several hours when the atmospheric state, whose initial conditions are usually provided by a global or coarser regional model, is still dynamically adjusting to the finer scale resolution and topography of the regional model. Therefore the model output from this initial ‘spin-up’ period is not completely reliable as an indicator of the true atmospheric state. However, if a regional model simulation is allowed to progress for too long without re-initialization (normally several days), it tends to drift away from the actual observed atmospheric state. Therefore, our method of obtaining realistic regional atmospheric analyses over an entire twenty-day episode was to divide each episode into four overlapping simulation segments. Each segment was around five days long with a twelve-hour overlap between each segment to avoid spin-up effects. (Specifically, the near total darkness episode was divided into successive segments of 6 days, 5.5 days, 5.5 days, and 4.5 days; the partial sunlight episode was divided into successive segments of 5 days, 5.5 days, 5.5 days, and 5.5 days). Initial conditions and most of the Grid 1 lateral boundary conditions were obtained from the half-degree Global Forecast System (GFS) zero-hour analyses (except for a few particular times during the near total darkness episode when the half-degree GFS product was unavailable, when one-degree GFS analysis was used).

Even with the overlapping simulation segment strategy, it is difficult to ensure that the interior of a regional model simulation remains close to observations for simulations of more than a day or so. Therefore, dynamic analyses of historical cases are often performed, in which a Four-Dimensional Data Assimilation (FDDA) strategy is applied throughout the model integration. Relaxation terms based on the differences between actual observations and the corresponding model fields at the observation sites (also known as the ‘innovations’) are added to the model’s predictive equations. In this way the model error is constrained based on available observations while the model still provides dynamic consistency and finer mesoscale structure not present in the observations. The version of FDDA used in these simulations is the multiscale, multigrid

nudging FDDA strategy developed by Stauffer and Seaman (1994) for the MM5 mesoscale model, and implemented in WRF as described in Deng et al. (2009). Nudging is also known as Newtonian relaxation, where the nudging relaxation terms are proportional to the innovation divided by a characteristic e-folding time inversely proportional to a nudging coefficient G . Nudging does not perform a direct insertion of observational information at a single point in space and time, but rather it applies the correction or innovation gradually in time and space based on the model terrain influences and prescribed / assumed weighting functions. For example, when a well-mixed PBL is present, one would generally want the influence of surface observations to be extended throughout the PBL, because in these conditions there is high correlation between errors in atmospheric fields at the surface and those anywhere within the PBL.

The multiscale multigrid FDDA method uses a combination of two forms of nudging: analysis nudging and observation ('obs') nudging. Analysis nudging is performed in model grid space where an objective analysis of observations (e.g., a modified Cressman scheme, Benjamin and Seaman 1985) is performed using the interpolated global analyses (e.g., from the GFS) as a background field. The resultant 'enhanced analysis' can then be used as the basis for analysis nudging. Analysis nudging is generally applied on coarser model domains where synoptic data can be used to produce a reasonable gridded analysis. Obs nudging is more attractive for finer-scale domains and asynoptic data. It is particularly effective where observational data density is sparse and corrections are applied only in the neighborhood of the observations, allowing the model to still add value in regions without any data by advecting observation information into the data-sparse regions and creating mesoscale structure not in the observations. In this case the nudging is performed in observation space, and the model field is interpolated to the observation site to compute the innovation that is then analyzed back to the model grid over some three-dimensional neighborhood in space, and over some time window. Quality control (QC) of observations is critically important for the success of both analysis nudging and observation nudging.

In the multiscale multigrid FDDA method applied in the RARE study, 3D-analysis nudging, as well as surface analysis nudging using higher temporal frequency surface data within the PBL (e.g., Stauffer et al. 1991), were performed on the outermost 12-km domain. Obs nudging is applied on at least the 12-km and 4-km domains. (Obs nudging is not applied on the finest 1.33-km model nest for the physics sensitivity studies described further below.) The finer domains thus have the benefit of improved lateral boundary conditions from the coarsest 12-km domain using both types of nudging, as well as the obs nudging performed directly on the 4-km nested domain. This project was one of the first applications of the multiscale FDDA strategy of Stauffer and Seaman (1994) in WRF. The newly developed OBSGRID module was used to produce gridded objective analyses similar to those produced by Rawins / Little_r in the MM5 system. The output files of OBSGRID can be used for 3D and surface analysis nudging and obs

nudging within WRF. OBSGRID takes as input raw WMO observations (both surface and upper air) and the output from WPS, which consists of large-scale gridded data (e.g., GFS output) horizontally interpolated to the model grid to be used in WRF. The outputs of OBSGRID relevant to this study include 1) pressure-level and surface objective analyses of the WMO observations (passing internal QC checks) using the GFS output interpolated to the model grid as background fields; the resultant analyses are then vertically interpolated to the WRF terrain-following “sigma” layers to be used for 3D analysis nudging; 2) surface analysis nudging files that can be directly used by WRF; 3) observation nudging files usable by WRF, and 4) files of the WMO observations including those passing the QC tests for use in the statistical verification software.

As mentioned above, for the physics sensitivity portion of the RARE study, 3D analysis nudging, surface analysis nudging, and obs nudging were performed on the 12-km domain (Grid 1); obs nudging was performed on the 4-km domain (Grid 2); and no nudging was performed on the 1.33- km domain (Grid 3). Thus Grid 3 has no direct FDDA tendencies and could be used to determine physics sensitivities, while still benefiting from improved lateral boundary conditions derived from the coarser grids that did have FDDA.

The following modifications were made to the WRF FDDA schemes for use in the baseline Alaska simulations. 1) The verification software was rewritten so that surface wind observations are verified against the third model half-layer from the ground (level closest to the 10-m observation level), while surface moisture and temperature observations are verified against the lowest model half-layer (level closest to the 2-m observation level). 2) A portion of the verification software that uses an assumed lapse rate to adjust model temperatures based on the difference between modeled and actual elevation was disabled, because this can lead to large errors in very stable conditions. 3) The surface analysis nudging and obs nudging codes were modified so that surface innovations for wind are computed and applied directly at the third model level. 4) Because surface wind observations directly relate to the third model layer and surface temperature and moisture observations directly relate to the lowest model layer, the similarity-based adjustments normally performed on model output for surface innovation computation was also disabled. 5) Hardwired vertical weighting functions for surface innovations were implemented into the surface analysis nudging and obs nudging codes, replacing the default functions that extend surface corrections to the model-predicted PBL height. The new functions had a vertical extent hardwired at about 150 m, which is a reasonable order of magnitude estimate for the maximum depth of nocturnal radiatively-driven stable boundary layers (SBL).

As a result of the physics sensitivity studies, the selected physics parameterizations included the Morrison cloud microphysics scheme (specifically designed for high-latitude simulations; Morrison et al. 2005), the RRTMG longwave / shortwave radiation package (Mlawer et al. 1997; Chen and Dudhia 2001), the Mellor-Yamada-Janjic PBL turbulence parameterization

(Janjic 2002) (as modified to be appropriate for the weak-turbulence conditions of very stable boundary layers), and the Rapid Update Cycle (RUC) land surface model (Smirnova et al. 2000). In particular, this physics suite seemed to have the best (least positive) temperature bias and best statistics during the periods when the surface temperatures were coldest and PM_{2.5} concentrations were the greatest. However, even with this physics configuration, the model's positive temperature bias could not be completely removed; furthermore, during other periods (such as the falling temperature periods in advance of a number of extremely cold episodes) the selected model physics suite seemed to have a negative temperature bias. It was thus strongly suggested that the actual meteorological analysis provided to the EPA be obtained from a final dynamic analysis simulation in which FDDA was also used to constrain the 1.33-km Grid 3 to the observations. However, there was concern that data assimilation of wind fields on Grid 3 would produce spurious low-level circulations in the model; furthermore, it was expected that the low-level circulations in both the actual atmosphere and the model would be driven by the low-level temperature fields. Thus, it was decided that in the delivered final dynamic analysis, that FDDA on Grid 3 would be done within all layers for temperature and moisture fields, but only within layers more than 150 m above the surface for wind fields. Also, the radius of influence for obs nudging on Grid 3 was reduced from the 100 km used on Grids 1 and 2 to 75 km. This value was obtained by computing the characteristic Grid 3 surface temperature innovation length scale through a correlation procedure that will be described in more detail in the next section.

3. WORK PLAN FOR NOV 2008 EPISODE

The current study covers the period 2-17 Nov 2008. Temperatures were relatively mild during the initial portion of this period (Figure 5), but then decreased to -17 °F (-27.2 °C) by the 7th, as recorded by a portable Beta Attenuation Mass (BAM) monitoring unit in the Fairbanks / North Star Borough region. Temperatures then rebounded for about 5 days before the next cold outbreak which bottomed out again at (-11 °F) (-24 °C) by the 14th. The low temperature periods corresponded to high PM_{2.5} concentrations as expected, especially towards the end of the study episode. However, the extremely cold temperatures, below (-22 °F) -30 °C, recorded during the Jan-Feb 2008 RARE episode did not occur during the Nov 2008 episode, and so the extreme effect of ice fog was not a factor. The final simulation of the episode was divided into four overlapping segments (12 UTC 01 Nov – 00 UTC 05 Nov; 12 UTC 04 Nov – 12 UTC 09 Nov; 00 UTC 09 Nov – 00 UTC 14 Nov; 12 UTC 13 Nov – 12 UTC 18 Nov). In order to facilitate the performance of initial sensitivity studies, an initial test period of 00 UTC 05 Nov – 12 UTC 09 Nov, encompassing one of the colder times during the Nov 2008 episode, was chosen.

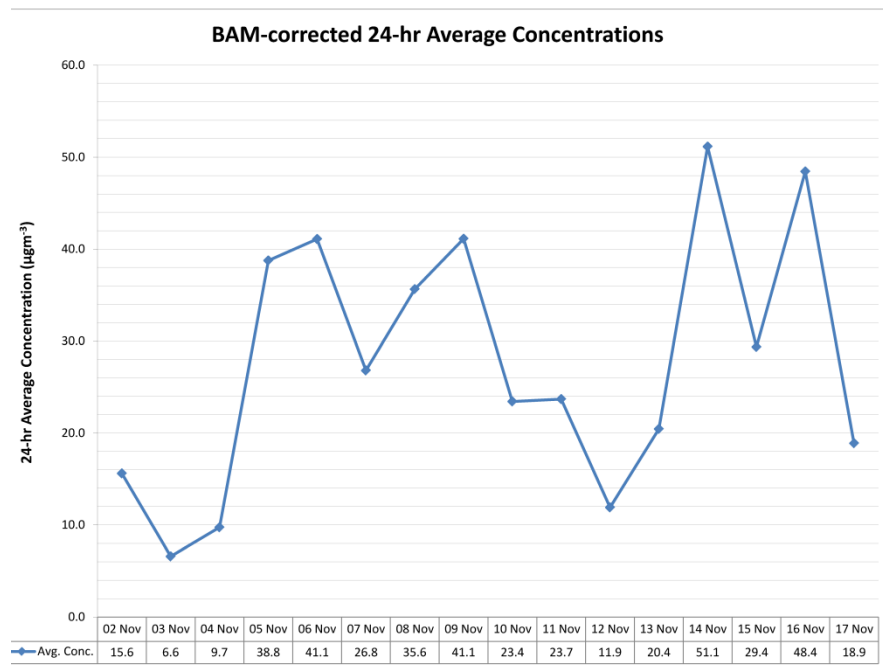
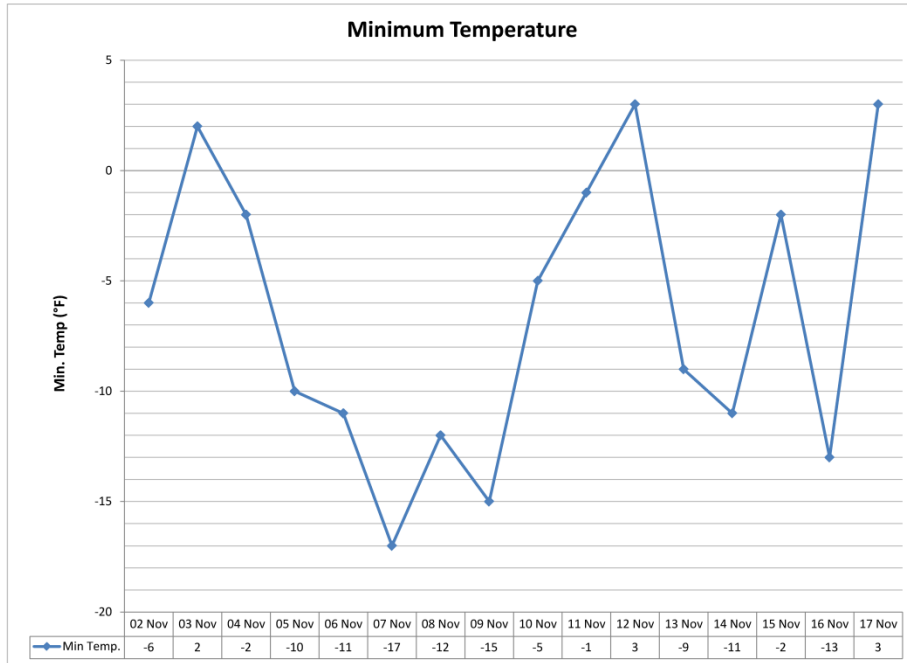


Figure 5 – Plot showing the daily minimum temperatures for the November episode in the Fairbanks region in Fahrenheit (top) and the BAM-corrected 24-hr average concentration of PM2.5 (bottom). Courtesy Bob Dulla, Sierra Research.

The grid configuration was taken directly from the EPA RARE study, although there are a few modifications relating to the use of observations for the November case as compared to the RARE study. The first involves the effective vertical resolution of the quality control procedure performed on the observations. The OBSGRID pre-processing software package compares point observations of a field such as temperature (either at a single level such as the surface or at multiple levels such as in a sounding) to the background analysis values of that field. For surface observations a direct comparison is performed between observed values of temperature and the background surface values. For sounding observations, if a vertical pressure level of the background analysis does not correspond to one of the pressure levels of that sounding, the observed sounding is interpolated in pressure space to the background pressure levels prior to the objective analysis and the values at the original observed sounding pressure levels are not retained. The result of this procedure is that the effective vertical resolution of sounding observations in the verification dataset and as used in the model is limited by the vertical resolution of the background analysis. In the GFS background fields the pressure levels are spaced 25 hPa apart near the surface, which corresponds to a distance in physical space of approximately 250 m. To alleviate this issue for the current study, a modified version of the GFS decoder, obtained from NCAR, permitted the generation of a background analysis with enhanced vertical resolution, with pressure levels spaced 5 hPa (~50 m) apart near the surface. It was hoped that the increased vertical resolution would improve the representation of the extremely shallow stable boundary layers characteristic of the winter season.

Another modification dealt with the specific objective analysis procedure used by OBSGRID. During the RARE project OBSGRID used either a Cressman scan procedure or a multiquadric analysis (Nuss and Titley 1994) depending on the number of observations at each vertical level. Since the RARE project, NCAR modified the OBSGRID code to provide the user with more flexibility in the objective analysis procedure. It was decided to use the Cressman method at each vertical level in order to produce more vertical consistency in the analysis; furthermore, each successive scan radius was set using the same method present in the Mesoscale Model version 5 (MM5) developed by the co-PI and others at Penn State.

Finally, a decision was made to make use of observations beyond those from the standard METAR observational dataset, in order to enhance the sparse local observational dataset. The total number of surface METAR stations within the Grid 3 domain is eight: Fairbanks (code PAFA), Eielson Air Force Base (PAEI), Ft. Wainwright (PAFB), Nenana (PANN), Delta Junction / Ft. Greely (PABI), McKinley Park (PAIN), Healy (PAHV), and Manley Hot Springs (PAML). Of these, only three could be said to lie in the focus region of the non-attainment area (Fairbanks, Eielson AFB, Ft. Wainwright). However, data from non-METAR surface stations for the period of Nov 2008 were located in the focus region during this project. The data quality from these stations is sometimes uncertain, and often standard METAR meteorological fields

(such as dewpoint) may be absent, but some of the data may be quite valuable, and many of them are used in the Meteorological Assimilation Data Ingest System (MADIS) that is run operationally by the National Weather Service. Stations from the non-METAR database are shown in Table 4.

Table 4: Non-METAR stations used for data assimilation and verification in current study. APRSWXNET – Automatic Position Reporting System as a WX NETWORK; RAWS – Remote Automated Weather Station; AKDOT – AK Department of Transportation; MADIS – Meteorological Assimilation Data Ingest System

Station	Database	Latitude	Longitude	Elevation (m)
Woodsmoke	Other MADIS	64.781	-147.284	145
Goodpasture	RAWS	64.238	-145.267	463
Healy (near Otto Lake Rd.)	APRSWXNET	63.839	-149.068	594
Two Rivers	APRSWXNET	64.873	-147.174	229
Fairbanks, near Farmer's Loop Rd. & Ballaine Rd.	APRSWXNET	64.879	-147.824	152
Goldstream Creek	APRSWXNET	64.894	-147.876	176
Livengood	RAWS	65.424	-148.722	137
Ester Dome	APRSWXNET	64.879	-148.055	708
Parks Hwy at Antler Creek	AKDOT	63.810	-148.965	462

A qualitative examination of the data from the non-METAR stations suggested that the temperature data are quite reasonable, although data gaps are more common than for most of the METAR stations. Most of these stations also provide wind data; while the actual values often seem quite plausible, the non-METAR stations overwhelmingly report zero wind speeds during the time period of this study. This is probably due to the relatively high start-up measurement threshold of the instruments used, making them inadequate to measure the very weak winds in the stable meteorological conditions. The one exception to this is Ester Dome, located 710 m above sea level on a ridge to the west of Fairbanks, which normally records a stronger flow. Many of the non-METAR stations also report pressure, but it was discovered that in some cases the pressure seemed to be reduced to the 1000-hPa level, whereas in other cases actual pressure was used. The value of pressure has some significance in that WRF uses potential temperature

as an internal variable, which is the temperature that would result if an air parcel is adiabatically compressed or expanded from its current pressure to the standard sea level pressure. An incorrect or misinterpreted pressure would lead to an erroneous potential temperature and thus an erroneous sense of the ‘warmth’ of a station. Thus, a decision was made to disregard any reported pressures from the non-METAR surface stations, and effectively use the model-predicted surface pressures to generate a self-consistent potential temperature field from the surface observations.

4. NEAR-SURFACE WIND ASSIMILATION

In the original RARE project a decision was made not to assimilate low-level wind data from surface stations on the 1.33-km (Grid 3). The reasoning was that the near-surface flow in these conditions was weak and predominantly thermally-forced (i.e., much of the existing wind circulation likely consists of topographically-forced drainage flows induced by air masses of varying temperatures). Thus, a numerical model may actually do a better job at capturing these flows than an observational network, especially a sparse observational network, and any data assimilation of observed near-surface winds within the model may erroneously override the development of these flows. The use of this data assimilation strategy in the RARE project did lead to realistic low-level flow patterns and produced generally satisfactory wind error statistics. However, the reported wind speed and wind directions statistics excluded cases where the observation wind report was calm. Including calm wind reports in the wind speed verification, by necessity, makes the wind speed bias more positive, because the model generated wind is never exactly zero. On the one hand, calm or near-calm conditions are common in extremely cold stable boundary layers, so representing them properly is of importance to this study. On the other hand, it is not clear how much of the positive model wind speed bias during calm wind reports is an artifact of insufficient instrument sensitivity. (More discussion on this issue will appear in the next section.) The reported surface temperature biases in the RARE project were also reasonable, but did tend to be positive during the periods of the weakest winds, which could be a direct consequence of positive model wind speed biases leading to too much turbulent mixing in the model. Because the extended dataset to be used in Nov 2008 case provided the potential for more surface data coverage over the Fairbanks region than that used in the Jan-Feb 2008, the possible use of near-surface wind data assimilation was revisited.

A comparison for the 5-9 Nov test period was performed between a simulation that used the RARE FDDA strategy on Grid 3, only nudging temperature and moisture near the surface (henceforth experiment T), and a simulation where additionally nudging of winds near the surface was performed (henceforth experiment TWIND). Statistics for the three local METAR stations are shown in Table 5. The wind speed statistics here include calm wind observations, but the wind direction statistics still do not, because wind direction cannot be defined in calm conditions. It can be seen that in experiment TWIND the wind speed RMSE statistics for all stations are reduced in comparison with experiment T; the reduction is modest but is about 10%

for Ft. Wainwright. The positive wind speed biases are also reduced, though their reduction is even more modest (no more than 0.02 m s^{-1}). Temperature statistics show a small sensitivity, although again Ft. Wainwright shows the greatest improvement in RMSE score. The biggest statistical difference between experiments T and TWIND resides in the wind direction RMSE scores, for which there is a 20 degree improvement for TWIND relative to T when the statistics for all stations are combined.

Table 5: Surface METAR statistics for experiments T and TWIND

Temperature (°C)	T RMSE (MAE for wind direction)	TWIND RMSE (MAE for wind direction)	T Bias	TWIND Bias
Fairbanks	1.71	1.72	-0.07	-0.15
Eielson AFB	1.83	1.80	1.20	1.18
Ft. Wainwright	1.36	1.32	0.05	-0.05
Three Stations	1.70	1.68	0.42	0.36
Relative Humidity (%)				
Fairbanks	4.21	4.31	-0.54	-0.59
Eielson AFB	7.39	7.50	3.59	3.70
Ft. Wainwright	17.55	17.89	-16.59	-16.96
Three Stations	9.31	9.49	-2.06	-2.11
Wind Speed (m s^{-1})				
Fairbanks	0.98	0.95	0.54	0.16
Eielson AFB	1.20	1.16	0.71	0.70
Ft. Wainwright	0.82	0.75	0.18	0.53
Three Stations	1.05	1.01	0.54	0.53
Wind Direction (degrees)				
Fairbanks	49.1	32.6	26.2	22.4
Eielson AFB	66.2	37.6	42.0	16.7
Ft. Wainwright	93.1	74.2	35.8	36.2
Three Stations	73.1	53.8	33.2	28.4

This statistical improvement in wind direction statistics suggested that using near-surface wind FDDA on the 1.33-km Grid 3 should be recommended, once a subjective analysis of the wind field in simulation TWIND revealed no irregularities.

Though the wind direction improvement in experiment TWIND was encouraging, the relatively small improvement in surface wind speed statistics, and the lack of substantial improvement in surface temperature statistics, was puzzling. An examination of the time series of the statistics during the test period (Figure 6 - Figure 13) suggests that while at Eielson AFB positive temperature biases are the norm during the early morning hours, this is not true at Fairbanks on 06 Nov, within one of a couple of prolonged periods of negative surface temperature biases at Fairbanks. (The time axes on the plots are in Coordinated Universal Time (UTC), so 00 UTC is 1500 Alaska Standard Time while 12 UTC is 0300 Alaska Standard Time, which correspond closely to the typical times of daily maximum and minimum temperatures, respectively.) Note that the location of the Fairbanks METAR is at the airport near the west end of the semi-circular topographical bowl in the region, while Eielson AFB is at the east end of this bowl and somewhat more distant from the neighboring ridges (Figure 3). If the time series of actual observed and modeled surface temperatures at the METARs are examined (Figure 14), it can be seen that for Eielson AFB and apparently for Ft. Wainwright the model is significantly too warm during the night (approximately -22°C versus the observed -25°C), consistent with the findings from the RARE study. (The gap during the night in the Ft. Wainwright observations is due to the fact that observations from that location are not typically reported during the night or on weekends.) However, on 06 Nov the Fairbanks observation reports a much warmer temperature (near -18°C) than the other stations, and it shows significant oscillations but no trend of decreasing temperatures during the night. The modeled temperature time series in Figure 14 shows much less variability among the three stations; however, there is a warm spike in the modeled temperature at Fairbanks near 12 UTC 06 Nov that is reflective of the observations.

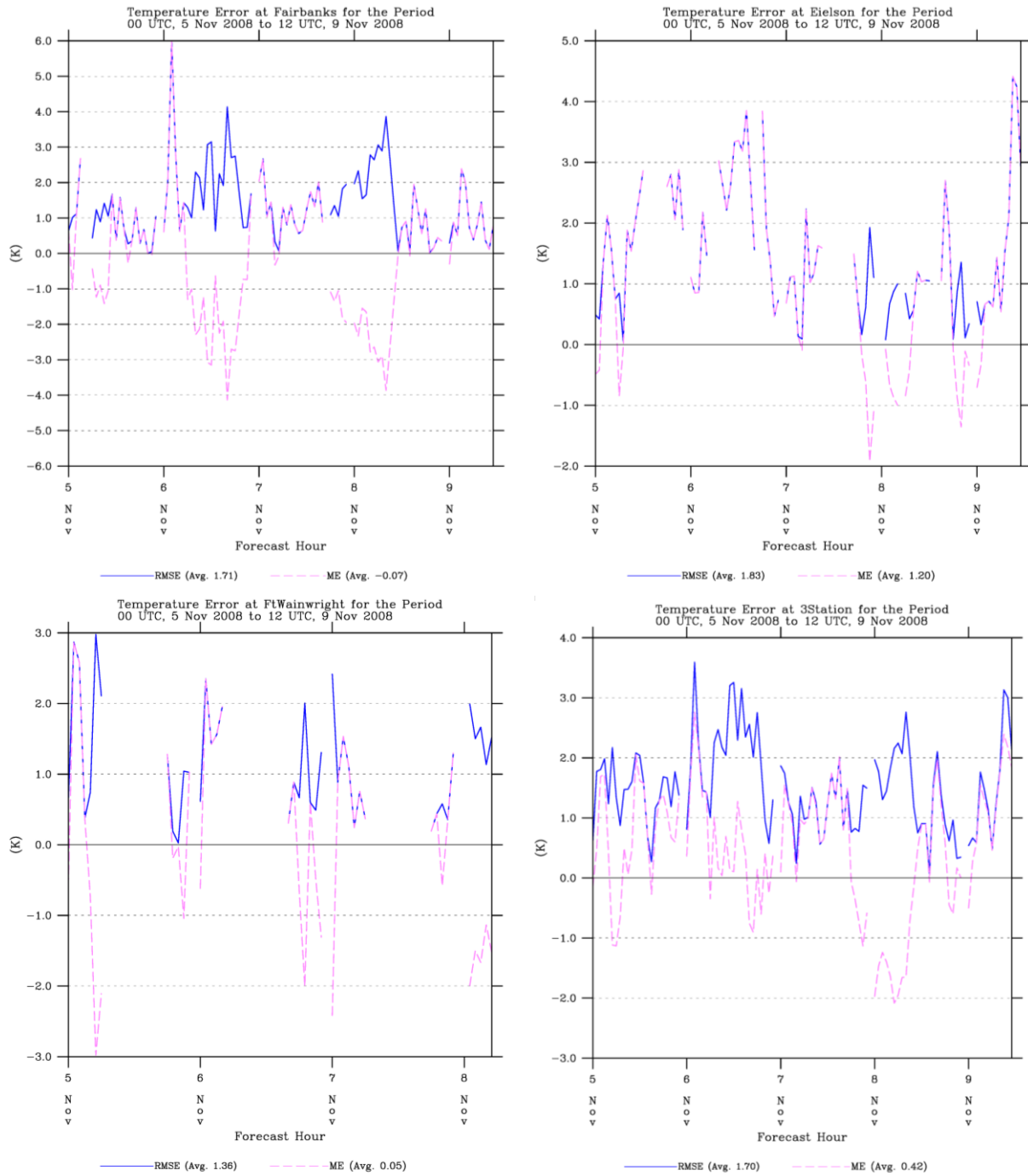


Figure 6: Temperature root mean square error (RMSE) and bias or mean error (ME) statistics for experiment T during the 00 UTC 5 Nov 2008 – 12 UTC 9 Nov 2008 test period at the local METAR surface stations. Statistics are for Fairbanks (top left), Eielson AFB (top right), Ft. Wainwright (bottom left) and all three stations combined (bottom right).

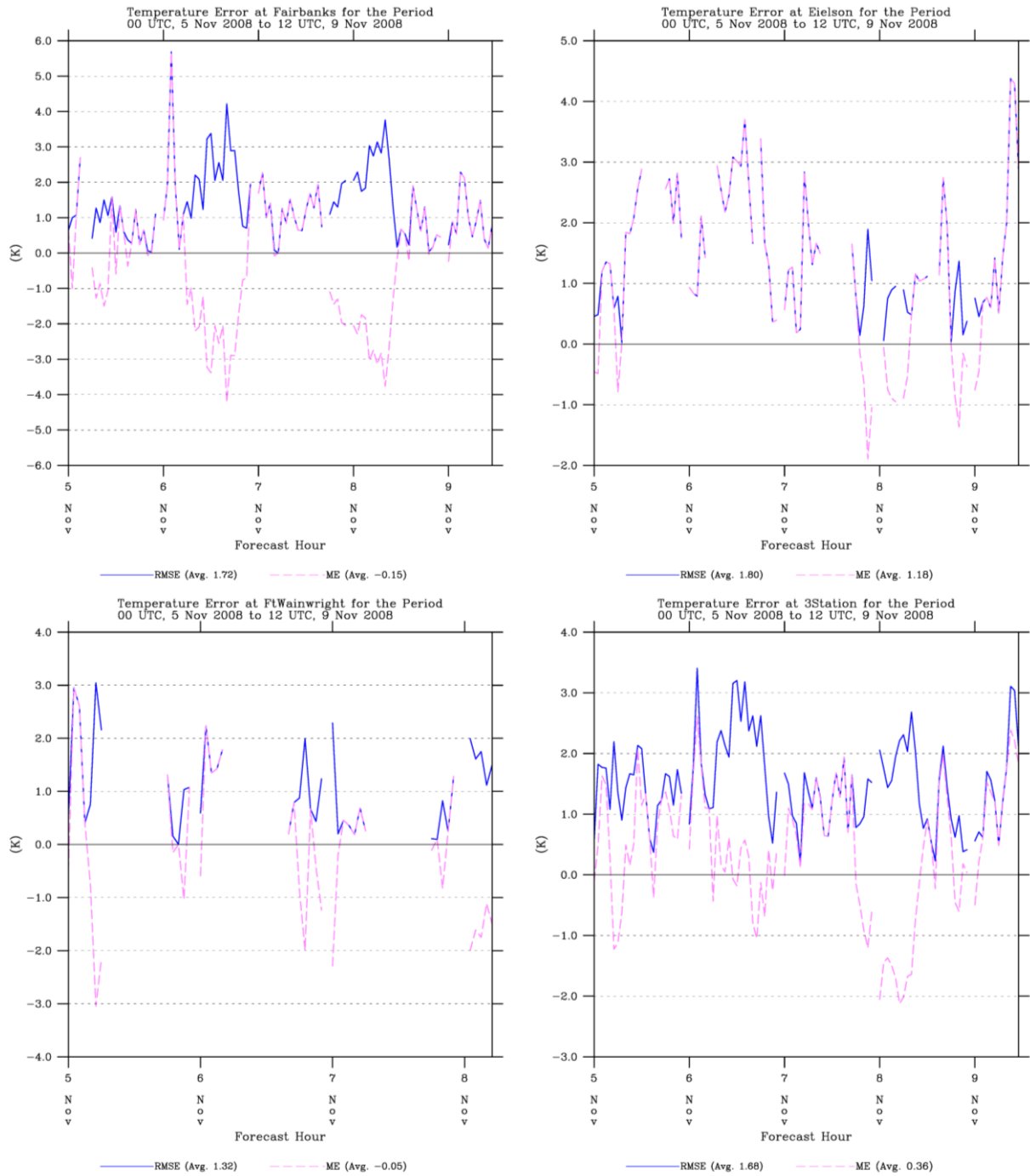


Figure 7: Same as Figure 6, but for experiment TWIND.

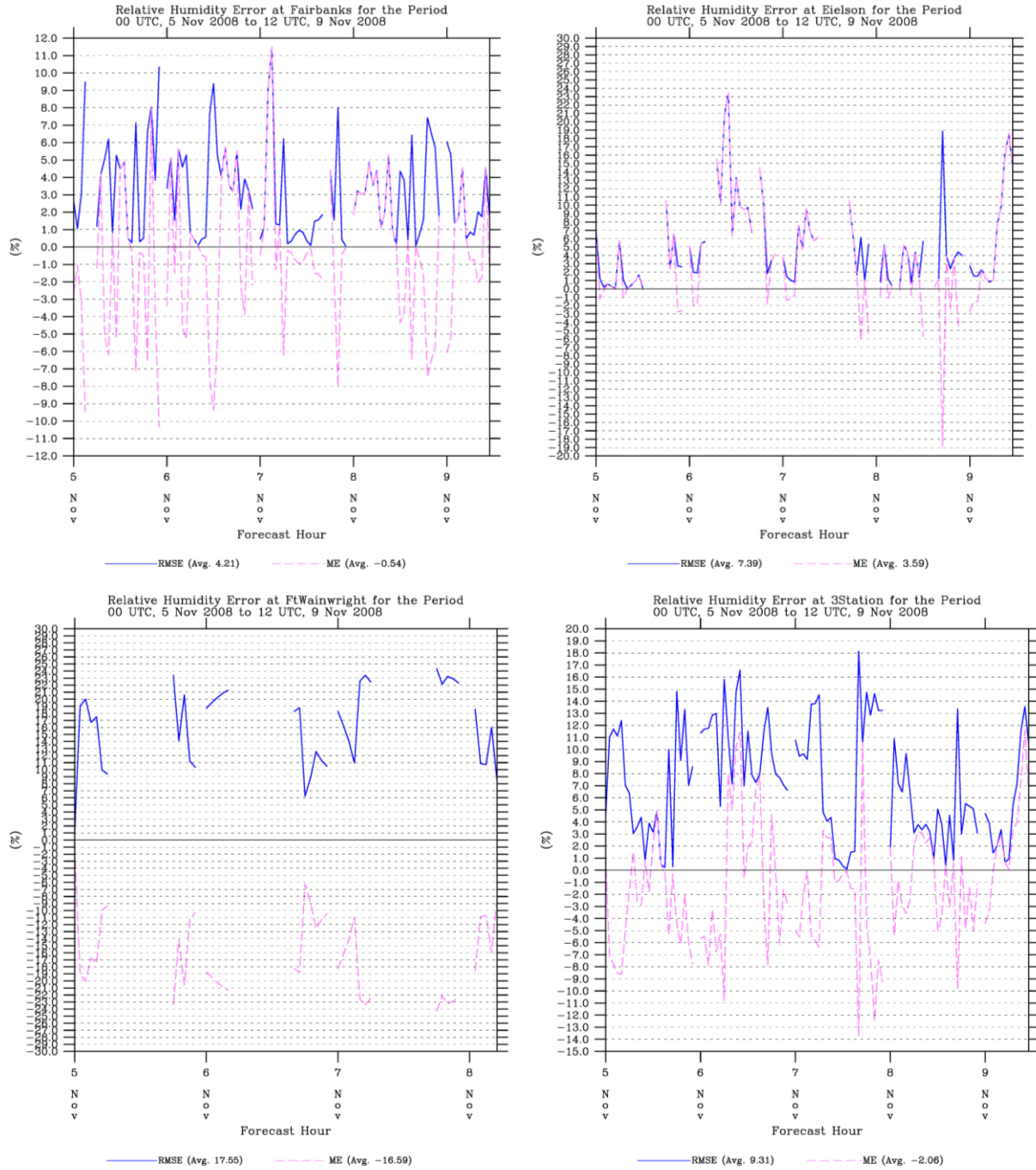


Figure 8: Relative humidity root mean square error (RMSE) and bias or mean error (ME) statistics for experiment T during the 00 UTC 5 Nov 2008 – 12 UTC 9 Nov 2008 test period at the local METAR surface stations. Statistics are for Fairbanks (top left), Eielson AFB (top right), Ft. Wainwright (bottom left) and all three stations combined (bottom right).

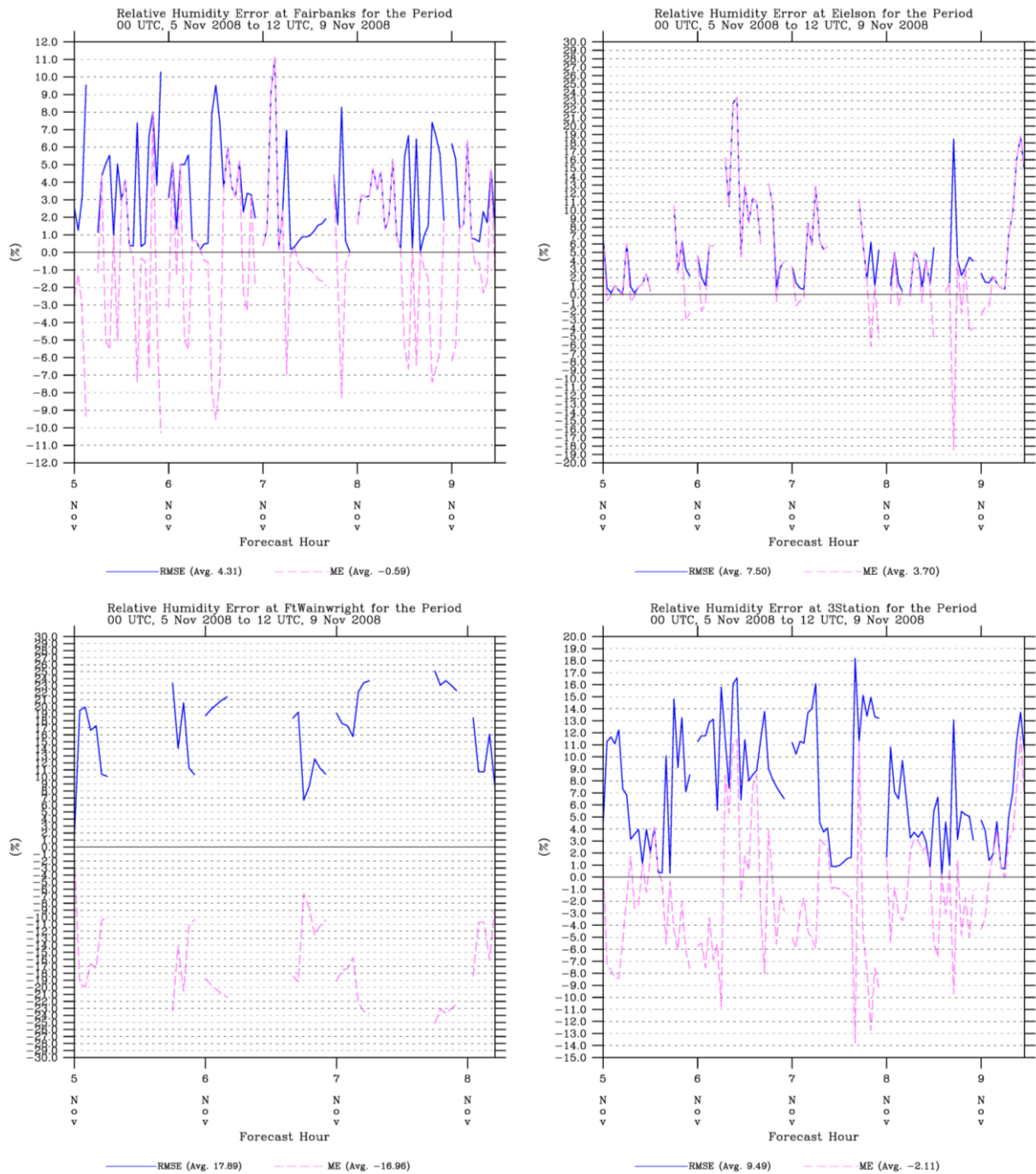


Figure 9: Same as Figure 8, but for experiment TWIND.

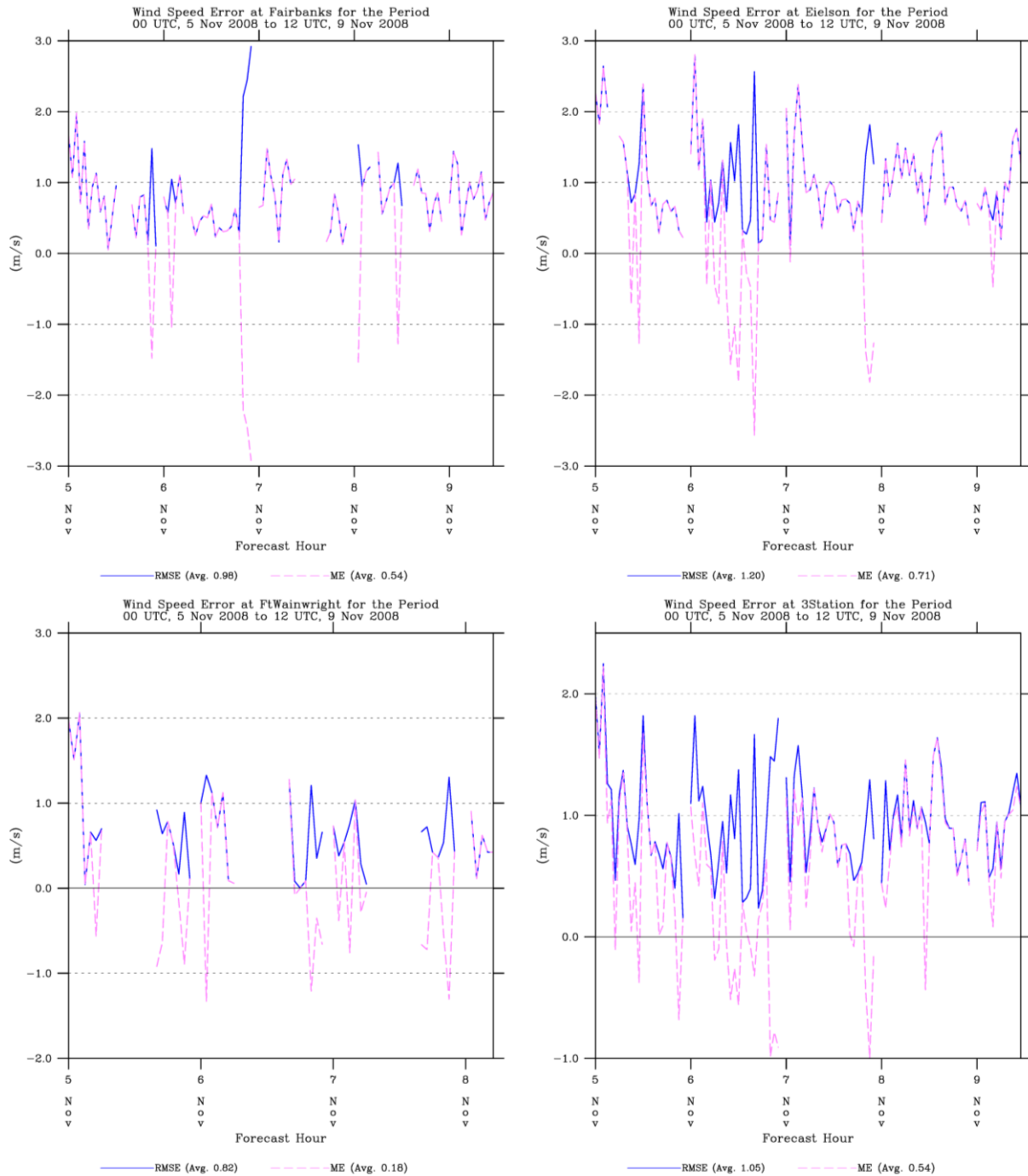


Figure 10: Wind speed root mean square error (RMSE) and bias or mean error (ME) statistics for experiment T during the 00 UTC 5 Nov 2008 – 12 UTC 9 Nov 2008 test period at the local METAR surface stations. Statistics are for Fairbanks (top left), Eielson AFB (top right), Ft. Wainwright (bottom left) and all three stations combined (bottom right).

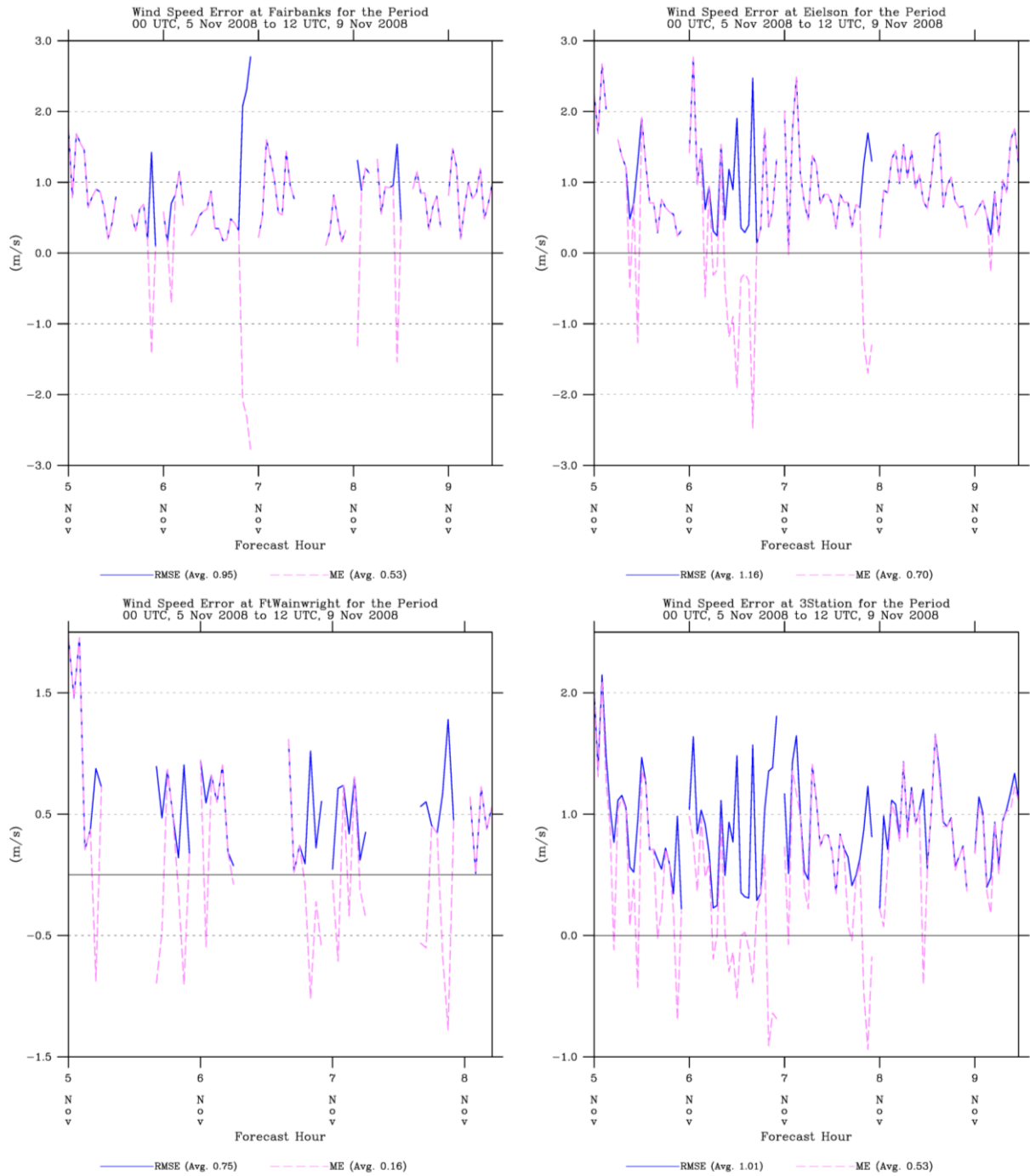


Figure 11: Same as Figure 10, but for experiment TWIND.

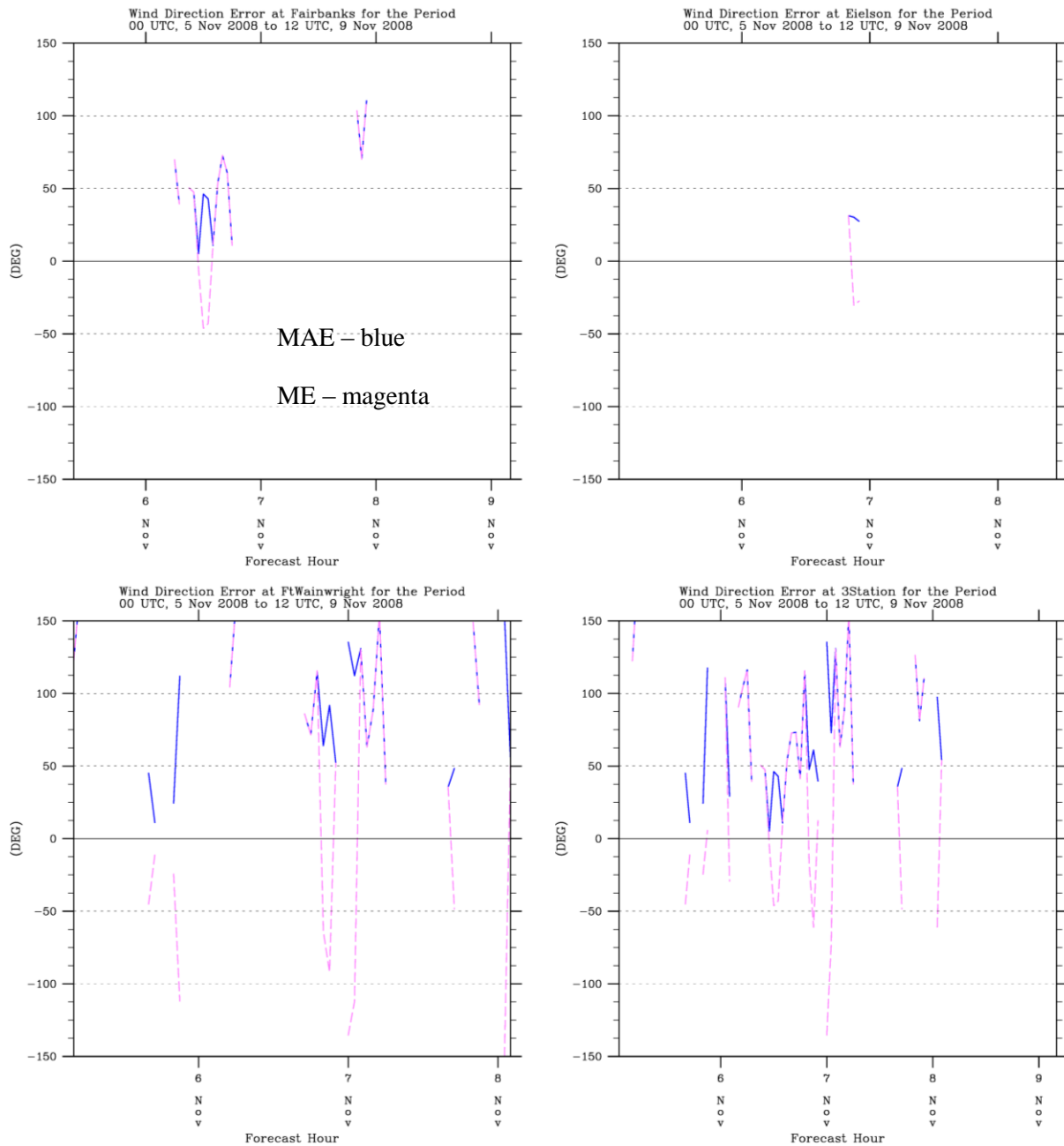


Figure 12: Wind direction mean absolute error (MAE) and bias or mean error (ME) statistics for experiment T during the 00 UTC 5 Nov 2008 – 12 UTC 9 Nov 2008 test period at the local METAR surface stations. Statistics are for Fairbanks (top left), Eielson AFB (top right), Ft. Wainwright (bottom left) and all three stations combined (bottom right).

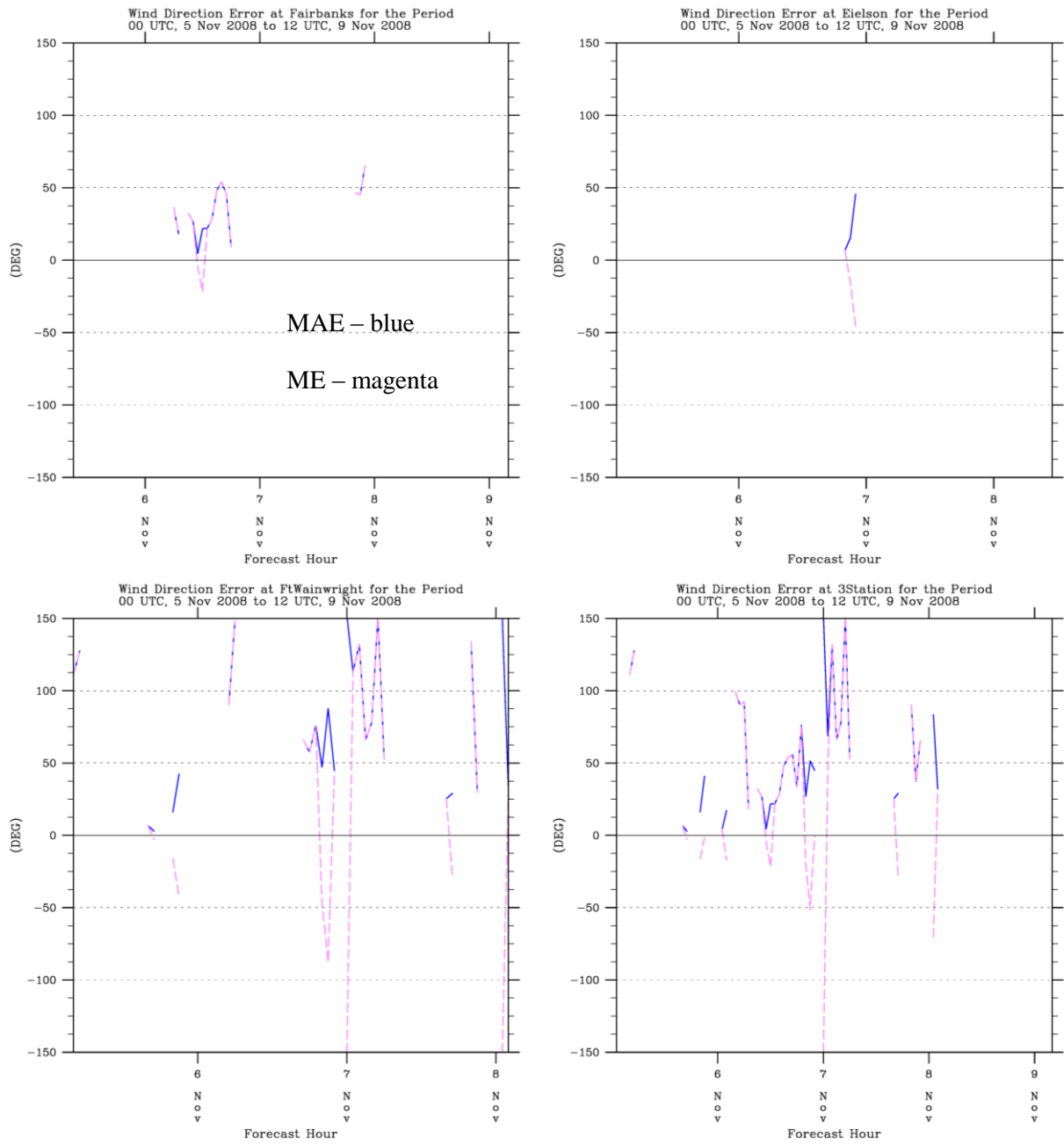


Figure 13: Same as Figure 12, but for experiment TWIND.

The corresponding time series of observed and modeled wind speeds (Figure 15) reveal that 06 Nov exhibits fairly strong wind speeds at Fairbanks (to about 4 m s^{-1} or about 8 knots), especially compared to the other stations, which is probably due to the fact that the Fairbanks station is

closest to the perimeter of the stagnant air within the topographic semicircle. The model successfully reproduces some of the increased wind speed at Fairbanks at this time ($2.2 - 2.8 \text{ m s}^{-1}$), but the maximum wind speed of 4.0 m s^{-1} is underestimated. It is plausible that the anomalously warm temperatures at Fairbanks for this case are a direct consequence of increased wind speeds at this location, which lead to increased turbulent mixing and prevent the occurrence of the cold surface temperatures shown at the more stagnant locations at Ft. Wainwright and Eielson AFB. A plausible explanation of the errors in the model predictions is that the model is insufficiently resolving the differences in topography and location among the three stations, and effectively blending the effects of the observations of all three stations. The conclusion, then, is that surface wind data assimilation on Grid 3 seems to be beneficial, especially for wind direction, but that the radius of influence of wind observations should probably be reduced.

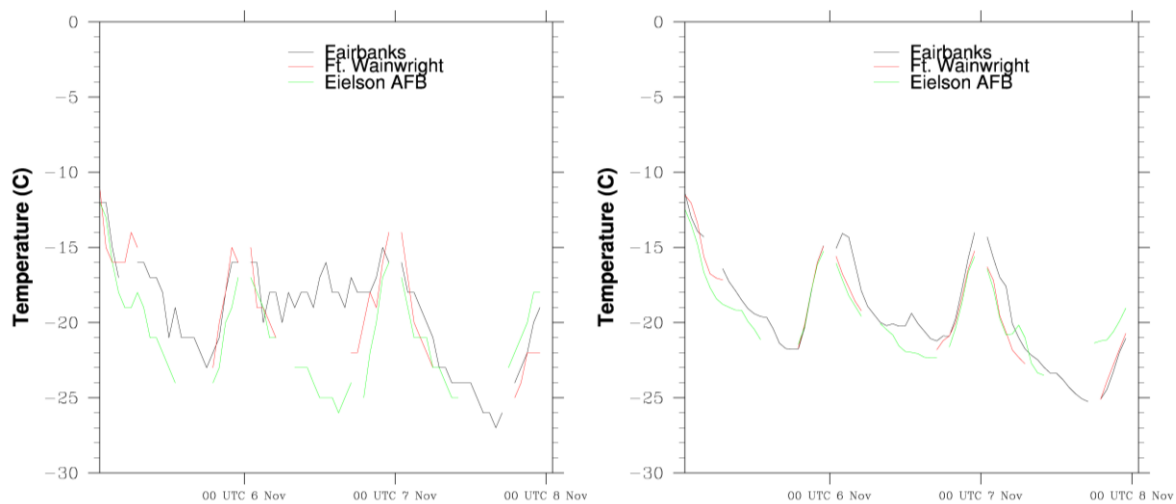


Figure 14: Time series of temperature for Fairbanks, Ft. Wainwright, and Eielson AFB from observations (left) and experiment TWIND (right)

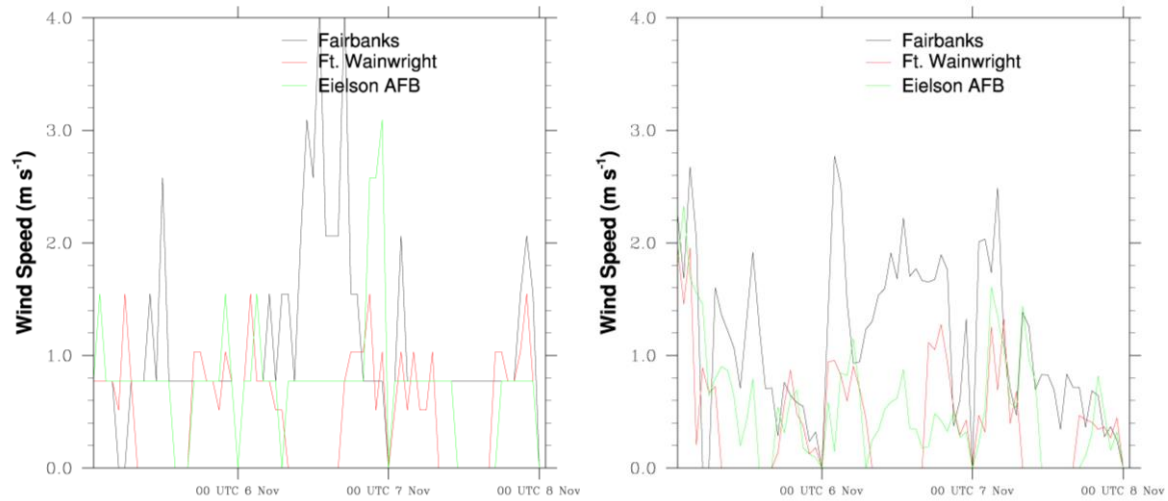


Figure 15: Same as Figure 14, but for wind speed

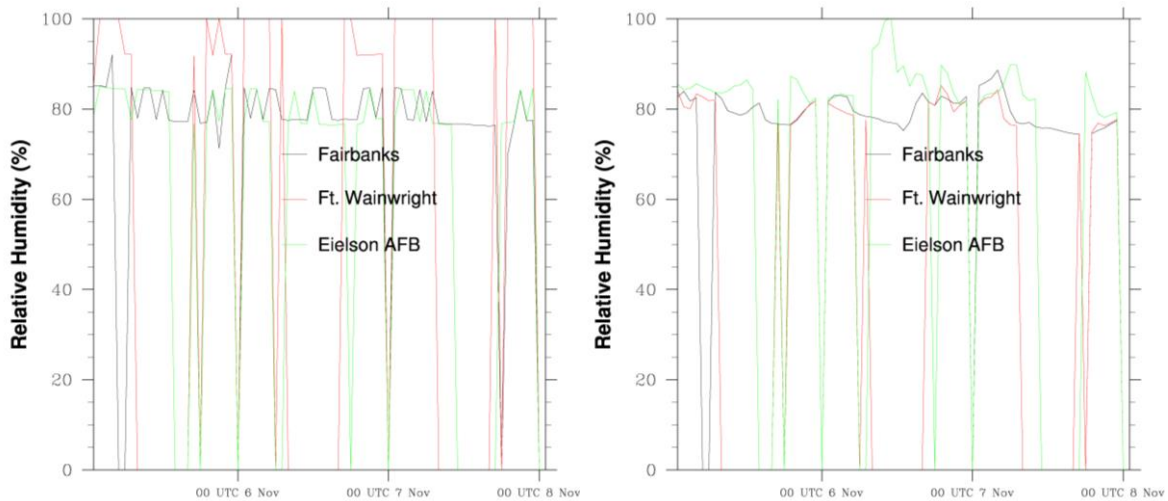


Figure 16: Same as Figure 14, but for relative humidity

Some insight into the characteristics of the relative humidity statistics can be found in Figure 16. The observations for stations other than Ft. Wainwright indicate relative humidity values are consistently near 80%. This is consistent with conditions near saturation with respect to ice but with relative humidity reported with respect to water saturation, when temperatures are on the order of -20 °C. However, Ft. Wainwright always reports relative humidity near 100% in these conditions. The model output at the Ft. Wainwright location tends to be closer to 80%, leading to the large positive relative humidity bias found in the Ft. Wainwright relative humidity

statistics. This could reflect the fact that Ft. Wainwright is erroneously reporting 100% relative humidity, based on the occurrence of ice crystals and other water condensate in the atmosphere, when in reality the atmosphere is ice saturated. However, it is interesting that the model does in fact produce conditions closer to water saturation near Eielson AFB during the day of 07 Nov, though the observations do not reflect this. Water saturation at temperatures as cold as -20°C is difficult to maintain because of the large numbers of ice nuclei at these temperatures; after nucleation, ice crystals tend to deplete all water vapor above the ice saturation value and deplete all remaining liquid water via the Bergeron-Findeisen process. However, it is possible to maintain water saturation at these temperatures if the air is pristine. So a full explanation of these differences is not known at present.

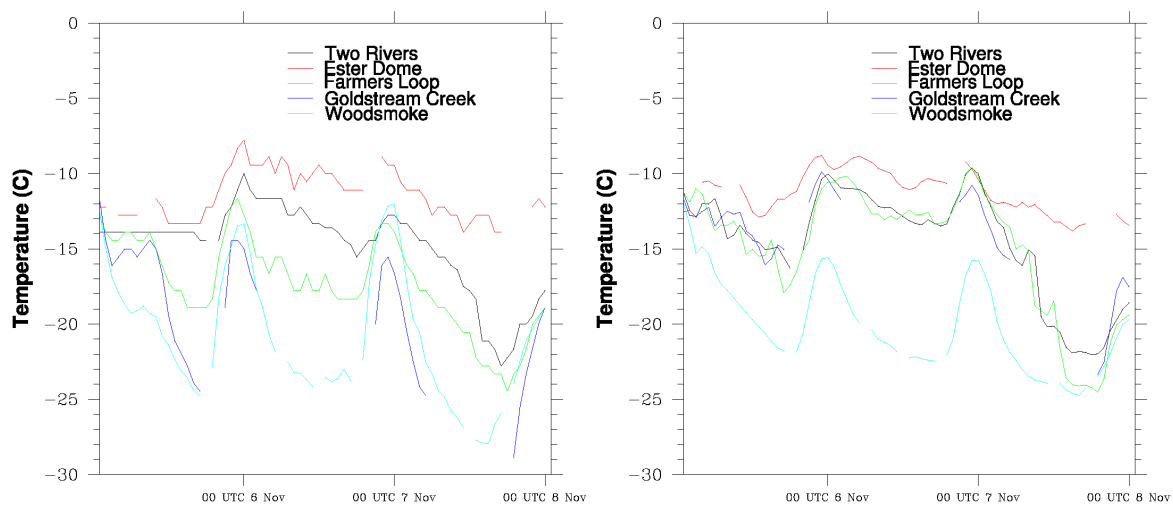


Figure 17: Time series of temperature for the local non-METAR surface stations from observations (left) and experiment TWIND (right).

Figure 17 shows the time series of observed and TWIND temperature at five non-METAR surface stations in the immediate Fairbanks region. The observed temperatures show that Woodsmoke and presumably Goldstream Creek behave like Eielson AFB and Ft. Wainwright, approaching -25°C at night. The location near Farmer's Loop Rd. behaves somewhat like the Fairbanks METAR station in that it has temperatures decreasing to only about -18°C at night. Two Rivers has even less of a nocturnal decrease of temperature, while Ester Dome remains near -10°C for most of the period. This seems to confirm that the warmest temperatures during these episodes occur on the ridges while the coldest temperatures occur within the low spots of local valleys. Of these stations, Ester Dome is predicted very well by the model, helping corroborate the model skill for the atmosphere above the near-surface stable boundary layer. Two Rivers and Woodsmoke are also fairly well predicted by the model; the latter performance is notable because it confirms that the model configuration is capable of reproducing observed surface

temperatures at least as low as about $-23\text{ }^{\circ}\text{C}$. These two stations also happen to be located at the east end of the Fairbanks / North Star Borough valley, near Eielson AFB. The model predicts approximately the same temperatures at Goldstream Creek and Farmer's Loop Rd. as at Two Rivers, but for Farmer's Loop Rd. and Goldstream Creek the resultant temperature is much too warm. It should be pointed out that these two stations are only about 2 km apart in physical distance, so it cannot be expected that a numerical model with 1.33-km horizontal grid spacing would be able to differentiate the temperature behavior between the two. All of the results considered together suggest that the model is able to predict the temperature evolution well in places both along the ridges and in the valley, but in other places the model is insufficiently resolving the actual difference in meteorological conditions between stations, whether the insufficient resolution is in the model terrain or in the way the model is treating observations in the data assimilation.

Statistics for wind speed are shown in Figure 18 for the non-METAR stations. This is an example of the fact that, other than Ester Dome, the wind instrumentation at these stations is generally not capable of recording what little wind is present. For Ester Dome itself, however, the magnitude of the wind speed peaks are well represented at the beginning of the test period. It can be seen that at the Woodsmoke station, the appropriately low model temperatures are accompanied by model wind speeds generally about 1 m s^{-1} or less, while the other stations have model wind speeds that are usually above 1 m s^{-1} .

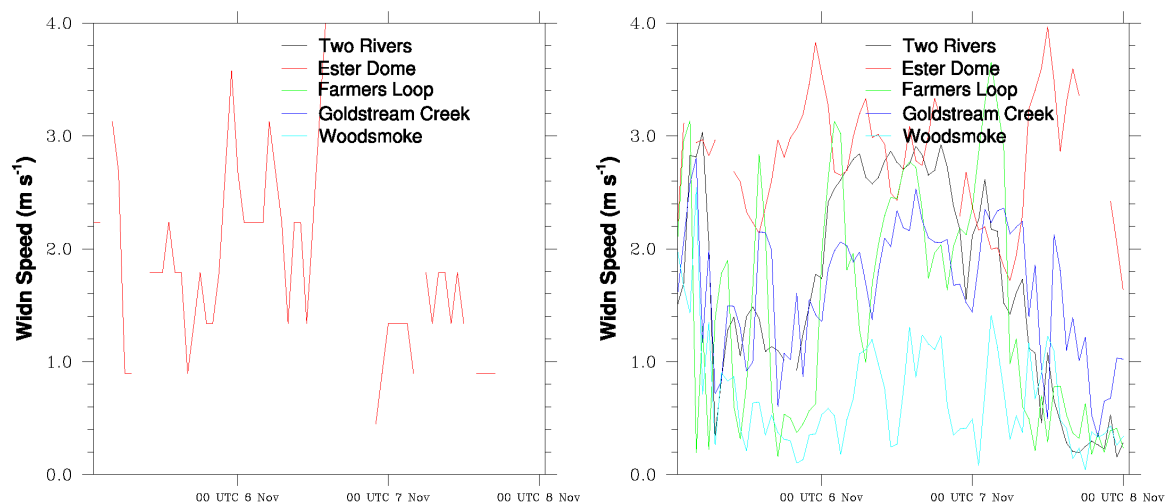


Figure 18: Same as Figure 17, but for wind speed.

Based on these results, it was decided to re-apply a procedure performed during the RARE study to derive an observation nudging correlation length scale based on the near-surface temperature field, and to use that radius of influence in subsequent model simulations. The procedure

consists of repeating the simulation with the same configuration, but with no FDDA of any sort performed on Grid 3. For each station on Grid 3, the temperature innovation (value of the observation minus the value of the model at that location) is computed at one hour increments. The correlation coefficient was then calculated between pairs of stations separated by known horizontal distances. Since the innovation for a variable is proportional to the nudging tendency for that variable, the typical distance over which innovations are correlated gives an indication of what the radius of influence should be. When this analysis was performed for the November case, it was discovered that the typical correlation distance was on the order of 30 km, substantially smaller than the 75 km value derived in the RARE project. (The ability to calculate a smaller radius of influence for the current study was aided by the presence of a denser surface observational network after the inclusion of the non-METAR stations.) It was thus decided to try a combination of a reduced radius of influence from 75 km to 30 km on Grid 3, along with a doubled value of the wind nudging strength on Grid 3 (from $4 \times 10^{-4} \text{ s}^{-1}$ to $8 \times 10^{-4} \text{ s}^{-1}$). The temperature nudging strength was left unaltered, because the extreme horizontal variability in the temperature field and its strong dependence on the local topography argue for a more conservative approach.

When the new experiment (henceforth TWIND2X30) was run on the test period, the results (Table 6 and Figure 19 - Figure 22) showed even more improvement in surface wind direction errors for the three local METAR stations, with an average decrease in MAE of 19 degrees. Temperature RMSE scores were slightly better for Fairbanks, somewhat worse for Ft. Wainwright, but substantially better for Eielson AFB. Since Eielson AFB is relatively distant from most of the other stations, this is an indication that the reduced radius of influence was in fact an improvement. Relative humidity errors are also generally improved. On the other hand, wind speed RMSE scores were made slightly worse, by up to 0.16 m s^{-1} for Ft. Wainwright.

Though there was no completely unambiguous choice, based on the test period results, for the optimal model configuration to produce the dynamic analysis for the entire 2-17 Nov 2008 episode, it was decided that, since the degradation in wind speed errors was slight while the improvement in wind direction errors was substantial, we would select the TWIND2X30 setup as the basis for further simulations.

Table 6: Surface METAR statistics for experiments TWIND and TWIND2X30

Temperature (°C)	TWIND RMSE (MAE for wind direction)	TWIND2X30 RMSE (MAE for wind direction)	TWIND Bias	TWIND2X30 Bias
Fairbanks	1.72	1.68	-0.15	0.33
Eielson AFB	1.80	1.45	1.18	0.95
Ft. Wainwright	1.32	1.43	-0.05	0.63
Three Stations	1.68	1.55	0.36	0.62
Relative Humidity (%)				
Fairbanks	4.31	4.46	-0.59	-0.61
Eielson AFB	7.50	5.43	3.70	2.49
Ft. Wainwright	17.89	16.22	-16.96	-15.33
Three Stations	9.49	8.36	-2.11	-2.26
Wind Speed (m s ⁻¹)				
Fairbanks	0.95	1.01	0.16	0.60
Eielson AFB	1.16	1.24	0.70	0.82
Ft. Wainwright	0.75	0.91	0.53	0.27
Three Stations	1.01	1.10	0.53	0.63
Wind Direction (degrees)				
Fairbanks	32.6	21.0	22.4	9.5
Eielson AFB	37.6	19.3	16.7	3.1
Ft. Wainwright	74.2	48.9	36.2	10.7
Three Stations	53.8	34.5	28.4	9.2

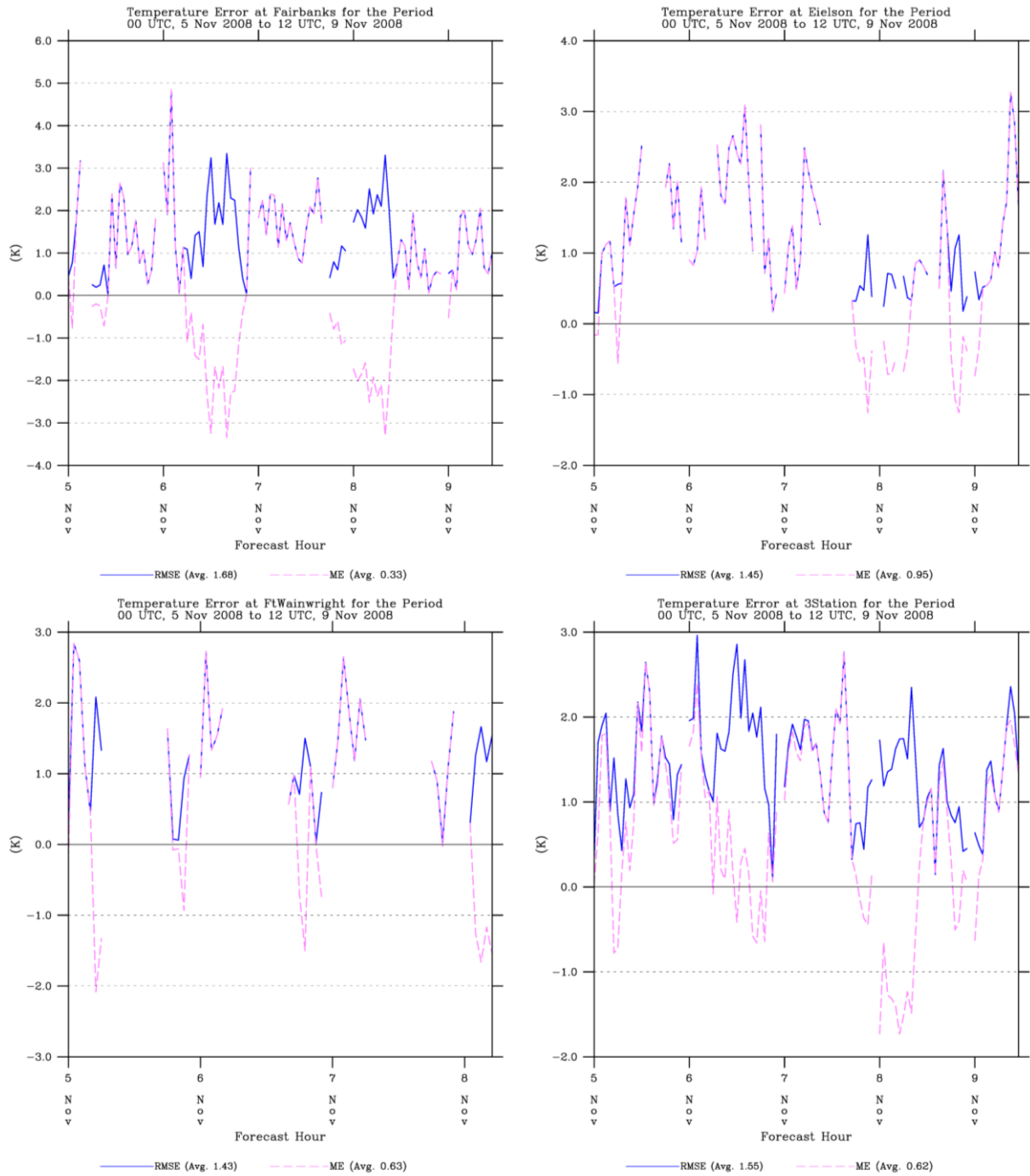


Figure 19: Same as Figure 6, but showing temperature statistics for experiment TWIND2X30.

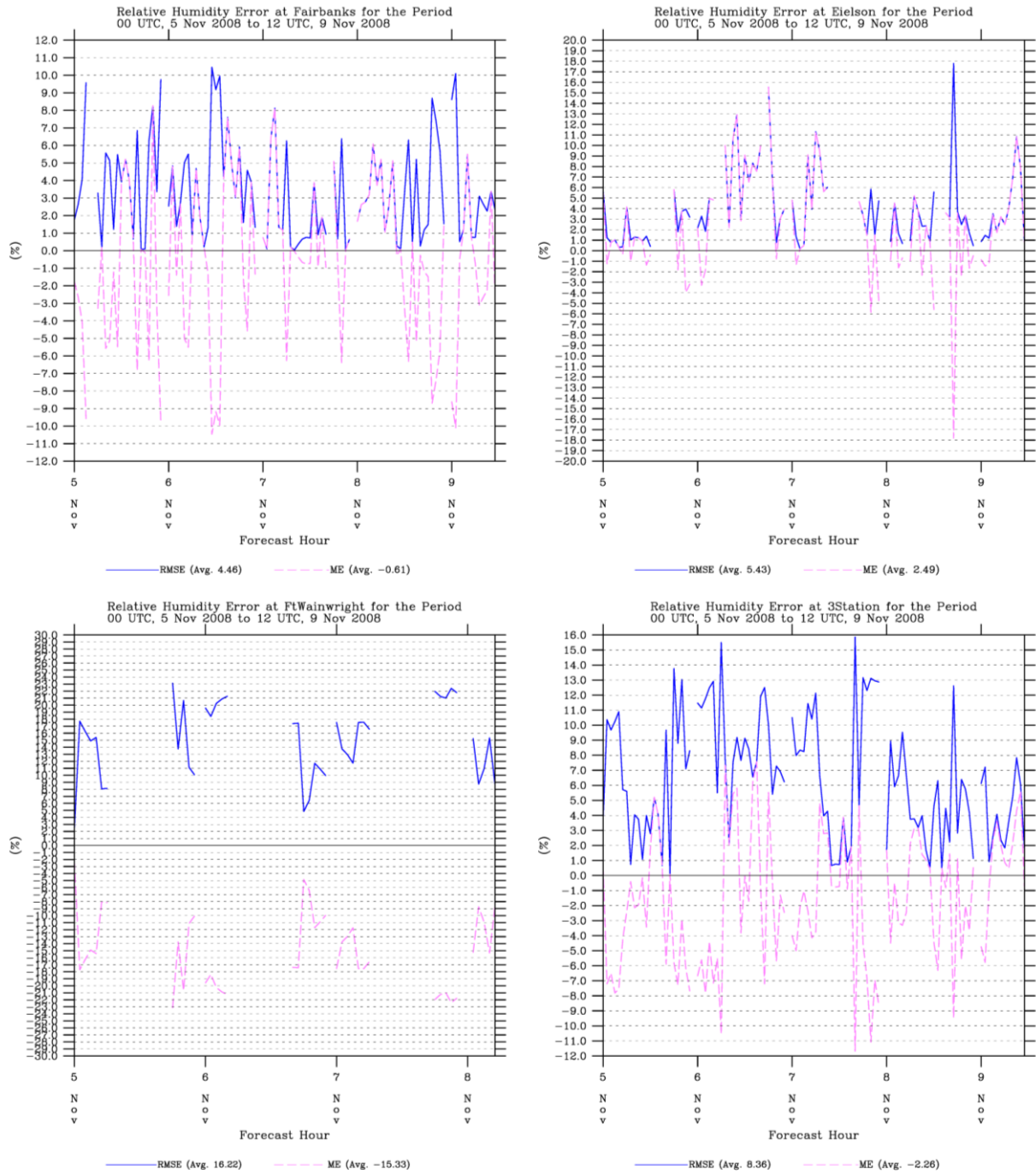


Figure 20: Same as Figure 8, but showing relative humidity statistics for experiment TWIND2X30.

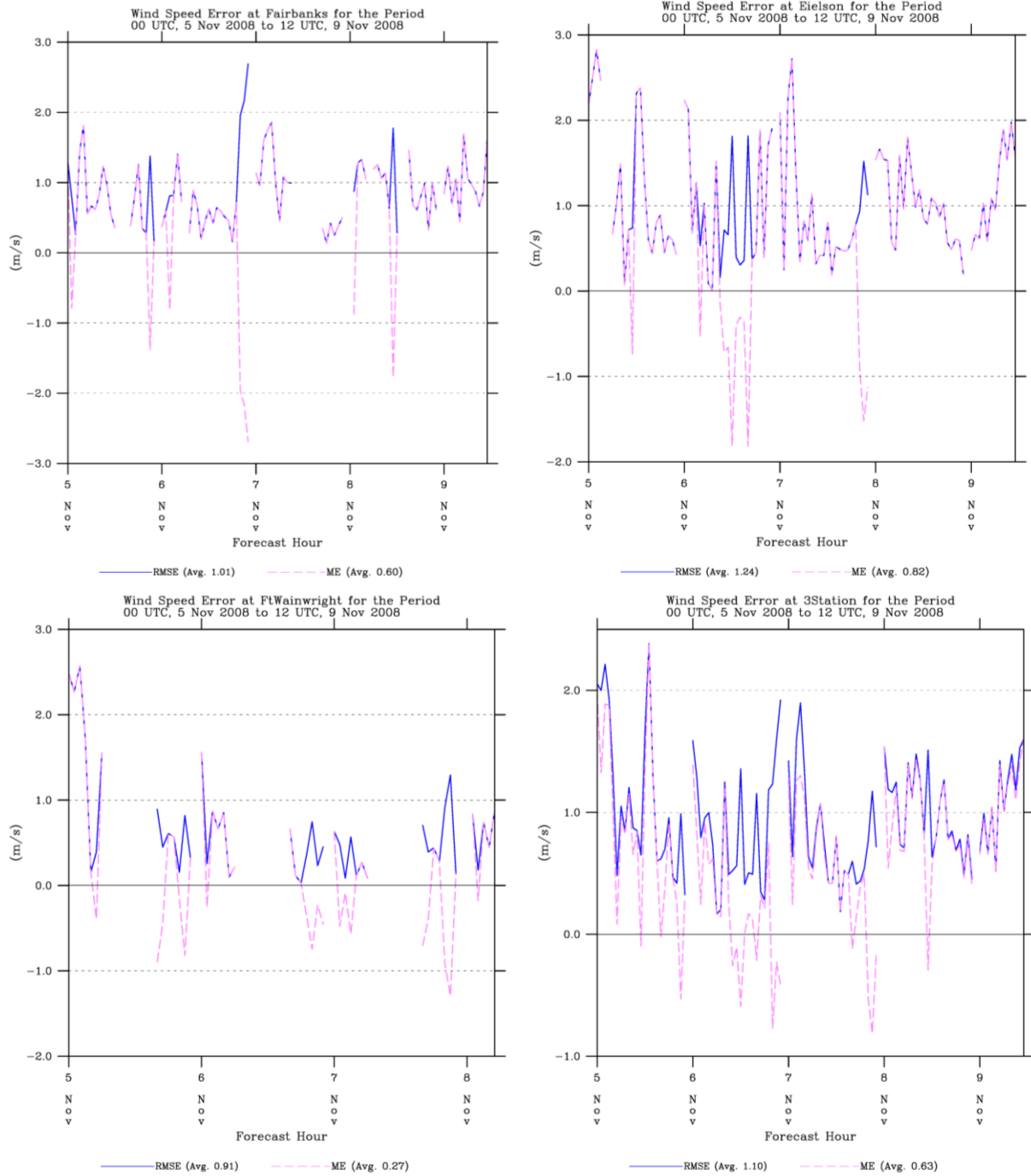


Figure 21: Same as Figure 10, but showing wind speed statistics for experiment TWIND2X30.

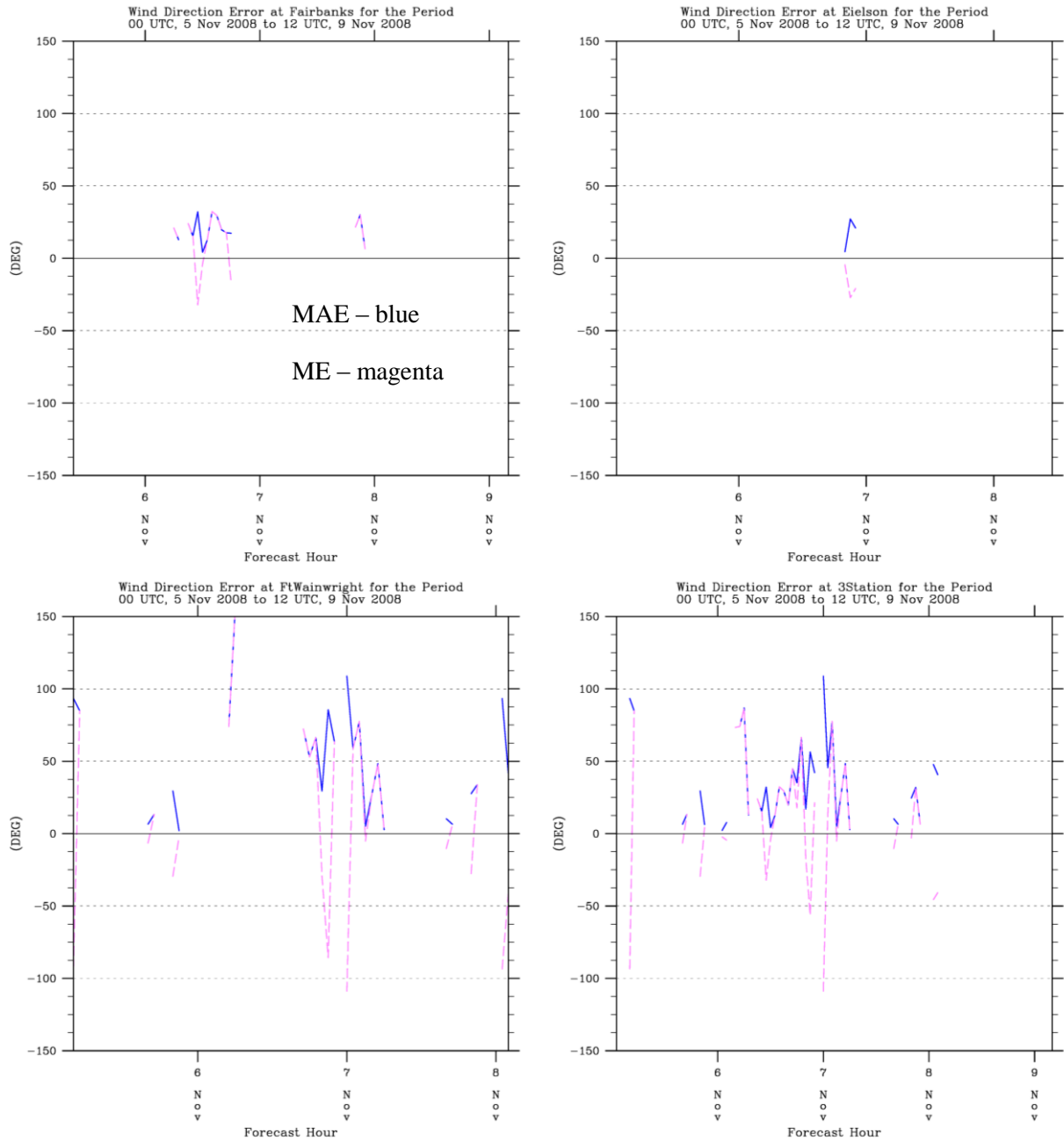


Figure 22: Same as Figure 12, but showing wind direction MAE and ME statistics for experiment TWIND2X30.

5. USE OF CALM WIND OBSERVATIONS

One issue of particular importance lies in the treatment of observations that report zero wind speed. It is often not clear, especially for non-METAR data, whether a report of zero wind speed indicates calm conditions, or indicates missing or faulty data. Furthermore, even if it is accepted that the data correctly represents calm conditions, in practice a report of calm generally indicates an actual wind speed that could have any value up to some minimum detection threshold. For automated METAR surface stations such as Fairbanks this threshold is 3 knots ($=1.543 \text{ m s}^{-1}$). This is on the order of the model positive wind speed biases, which suggests that a (not-well-known) component of the model positive wind speed bias may be due to the model capturing actual atmospheric flows that are below the observational threshold. Furthermore, observations of calm winds do not provide usable guidance on the direction of the flow that does exist, which is of great importance for dispersion applications, and for which the model may be the only reliable source of information.

Because of these considerations, the default obs nudging data assimilation strategy is not to use calm wind reports. For the typical case of dense surface observing networks and non-stagnant meteorological conditions, this is entirely satisfactory. However, in the particular application of near-surface transport under very stable conditions, when only a few meters per second of flow can have a great effect on the transport of pollutants, and where the presence of non-calm surface wind observations are infrequent, the assimilation of near-surface calm winds should be considered.

As noted above, the great majority of the surface wind observations for these stable episodes are calm reports. Since the model appears to have a positive wind speed bias in these conditions, nudging towards a zero velocity wind vector near the surface may have a beneficial effect on reducing a positive wind speed bias. On the other hand, also as noted above, an unknown portion of the positive wind speed bias in near-calm conditions is an artifact of the model always having a wind speed above zero while observations indicate a wind speed of exactly zero when the wind speed is below the instrument threshold. Furthermore, since a calm wind observation does not provide guidance as to the wind direction, within the radius of influence of a calm surface observation there is the potential to degrade model predictions of wind direction at locations where the wind speed is not actually calm.

Table 7: Surface METAR statistics for experiments TWIND2X30CALM and TWIND2X30 for the November test period.

Temperature (°C)	TWIND2X30CALM RMSE (MAE for wind direction)	TWIND2X30 RMSE (MAE for wind direction)	TWIND2X30CALM Bias	TWIND2X30 Bias
Fairbanks	1.51	1.68	0.22	0.33
Eielson AFB	1.43	1.45	0.93	0.95
Ft. Wainwright	1.50	1.43	0.70	0.63
Three Stations	1.48	1.55	0.57	0.62
Relative Humidity (%)				
Fairbanks	4.55	4.46	-0.87	-0.61
Eielson AFB	5.44	5.43	2.46	2.49
Ft. Wainwright	16.21	16.22	-15.30	-15.33
Three Stations	8.37	8.36	-2.38	-2.26
Wind Speed (m s ⁻¹)				
Fairbanks	0.97	1.01	0.54	0.60
Eielson AFB	1.18	1.24	0.72	0.82
Ft. Wainwright	0.96	0.91	0.29	0.27
Three Stations	1.07	1.10	0.57	0.63
Wind Direction (degrees)				
Fairbanks	31.4	21.0	20.9	9.5
Eielson AFB	31.0	19.3	4.97	3.1
Ft. Wainwright	83.7	48.9	5.9	10.7
Three Stations	57.1	34.5	11.3	9.2

A final sensitivity test to the effect of including calm wind reports in the data assimilation procedure of experiment TWIND2X30, henceforth experiment TWIND2X30CALM, was performed. Statistics for the two experiments performed over the test period are shown in Table 7. The assessment of the comparison is mixed. Overall temperature biases and wind speed biases are improved by about 10% in experiment TWIND2X30CALM (note however that a 10% improvement of wind speed bias in this case amounts to less than 0.1 m s^{-1} which is certainly less than the instrumentation precision), and temperature RMSE scores are improved by about 5%. However, both statistics are actually degraded for the Ft. Wainwright station. Furthermore, overall wind direction MAE statistics are over 20 degrees worse in experiment TWIND2X30CALM than in experiment TWIND2X30. Recall that in wind direction statistics calm wind observations are excluded from the verification dataset; therefore, a degradation of wind direction statistics in experiment TWIND2X30CALM means that the inclusion of calm wind reports in the data assimilation is having an adverse affect on the model-generated winds at other locations that are not reporting calm winds.

The decision between using simulation TWIND2X30CALM and TWIND2X30 was even more challenging than the decision between simulation TWIND and TWIND2X30. However, despite the beneficial reduction in the positive wind speed bias in TWIND2X30CALM, because of the importance of wind direction prediction to dispersion calculations in these conditions, and because wind direction was the variable that showed the most statistical variability between different experiments, a final decision was made to simulate the whole 2-17 Nov 2008 episode using the TWIND2X30 setup (although a parallel simulation of the entire episode using TWIND2X30CALM was also performed). The time series of the entire episode are presented in Figure 23 - Figure 26. It appears that the statistics for the whole 2-17 Nov 2008 episode are somewhat worse than the statistics for just the test period, particularly for the temperature statistics during 2-5 Nov, 13-14 Nov, and 17-18 Nov. These three periods of greater-than-typical temperature RMSE scores are actually characterized by negative temperature biases, and meteorologically are characterized by extensive cloudiness and frequent reports of snow. Failure of the model to properly represent these events and the cloudiness in particular could explain the negative temperature biases. The periods of coldest temperatures adjacent to these events have positive temperature biases at these stations, but these are generally of the order of $2 \text{ }^{\circ}\text{C}$ or less. The overall three-station temperature bias for the whole episode is negative ($-0.9 \text{ }^{\circ}\text{C}$), and the overall temperature RMSE of $2.4 \text{ }^{\circ}\text{C}$ is comparable to what was obtained in the RARE project. The overall wind speed bias for the whole Nov 2008 episode for the three METAR stations is almost exactly the same as it is for just the test period ($+1.0 \text{ m s}^{-1}$). The overall wind direction MAE of 41 degrees for these stations is slightly better than what we have observed in SBLs over central Pennsylvania using unfiltered wind data. These results give us confidence that our general model configuration is performing as intended, though possibilities for improvement still exist.

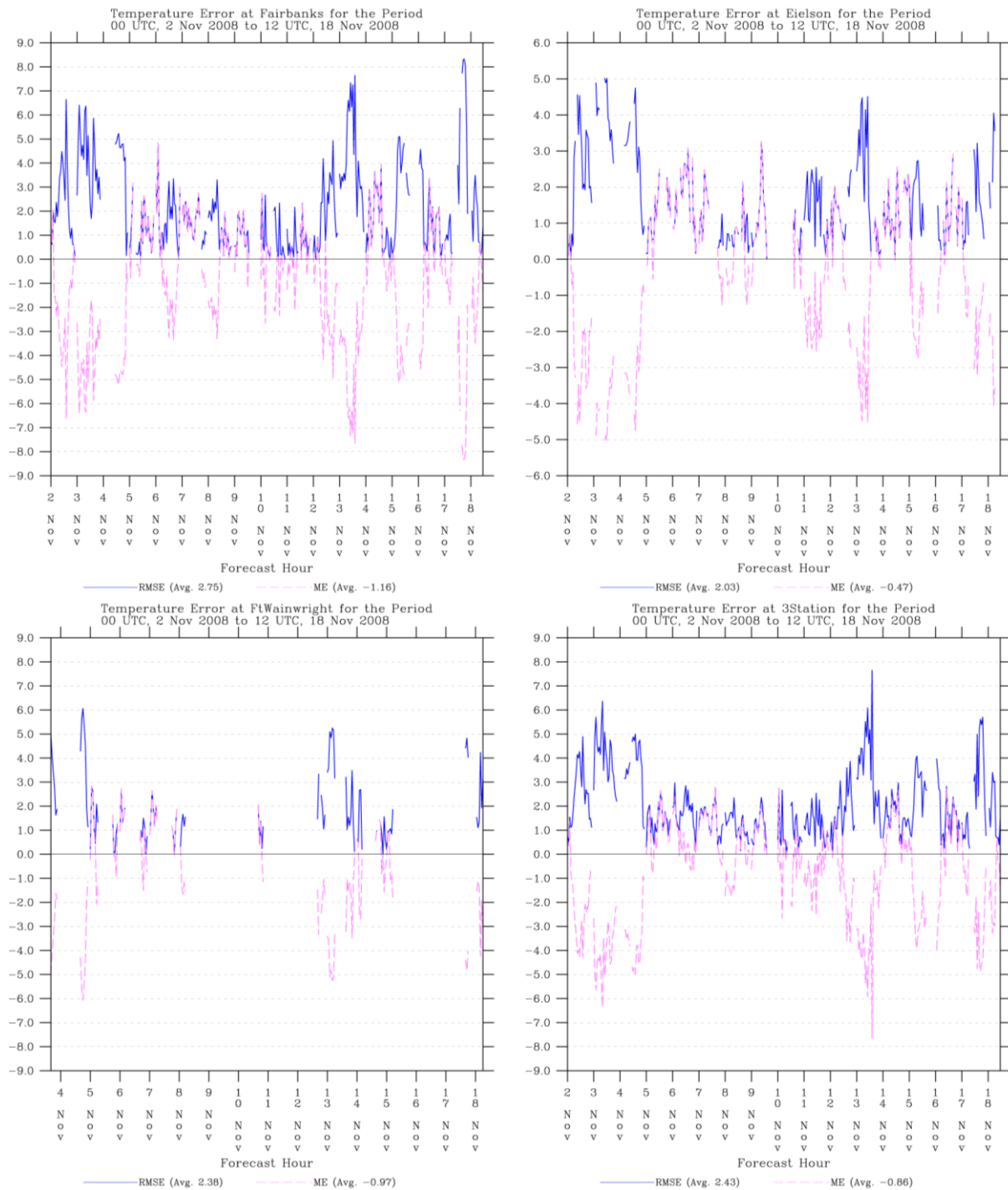


Figure 23: Temperature statistics for experiment TWIND2X30 over the entire 00 UTC 2 Nov 2008 – 12 UTC 18 Nov 2008 test episode at the local METAR surface stations.

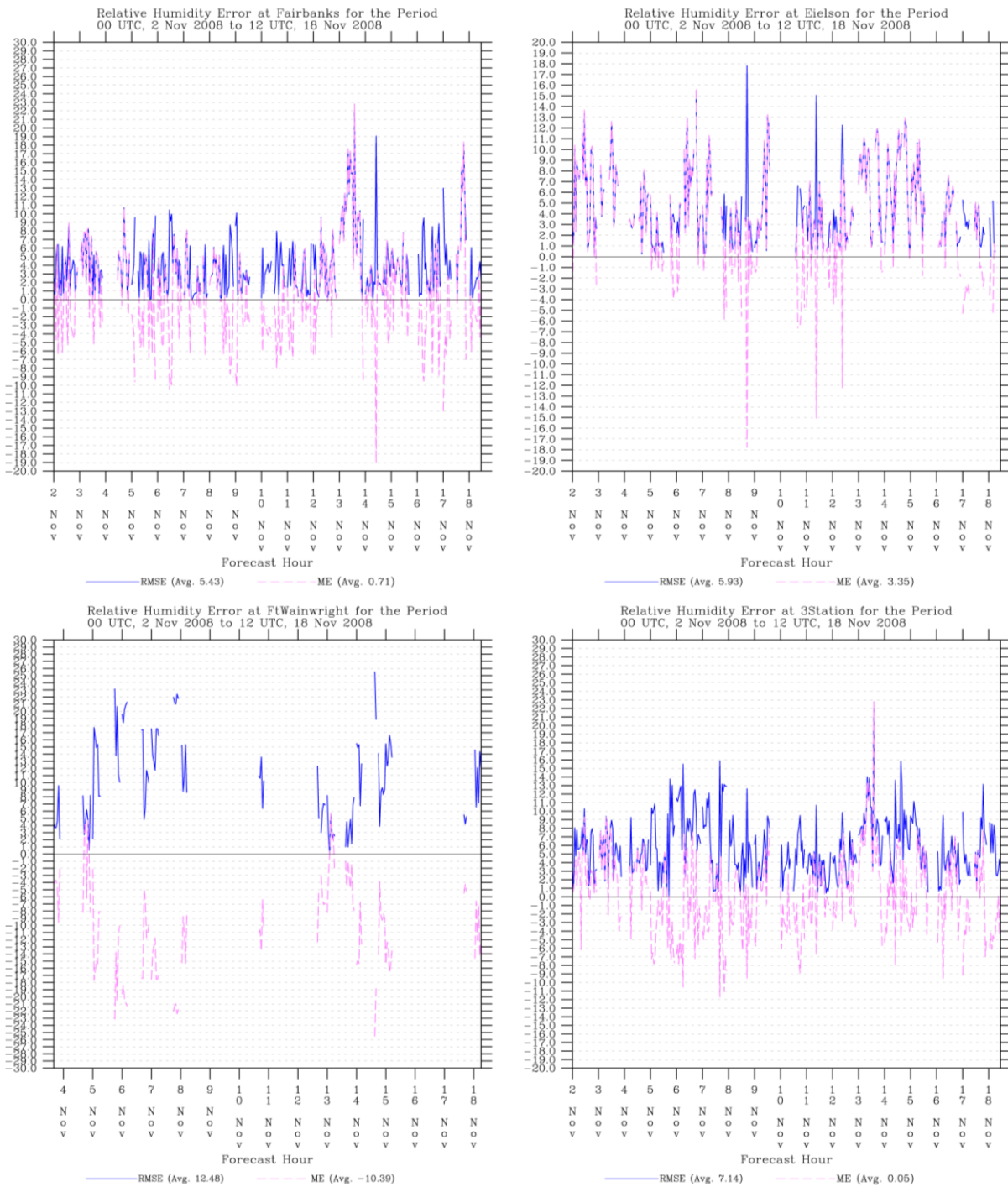


Figure 24: Same as Figure 23, but showing relative humidity statistics.

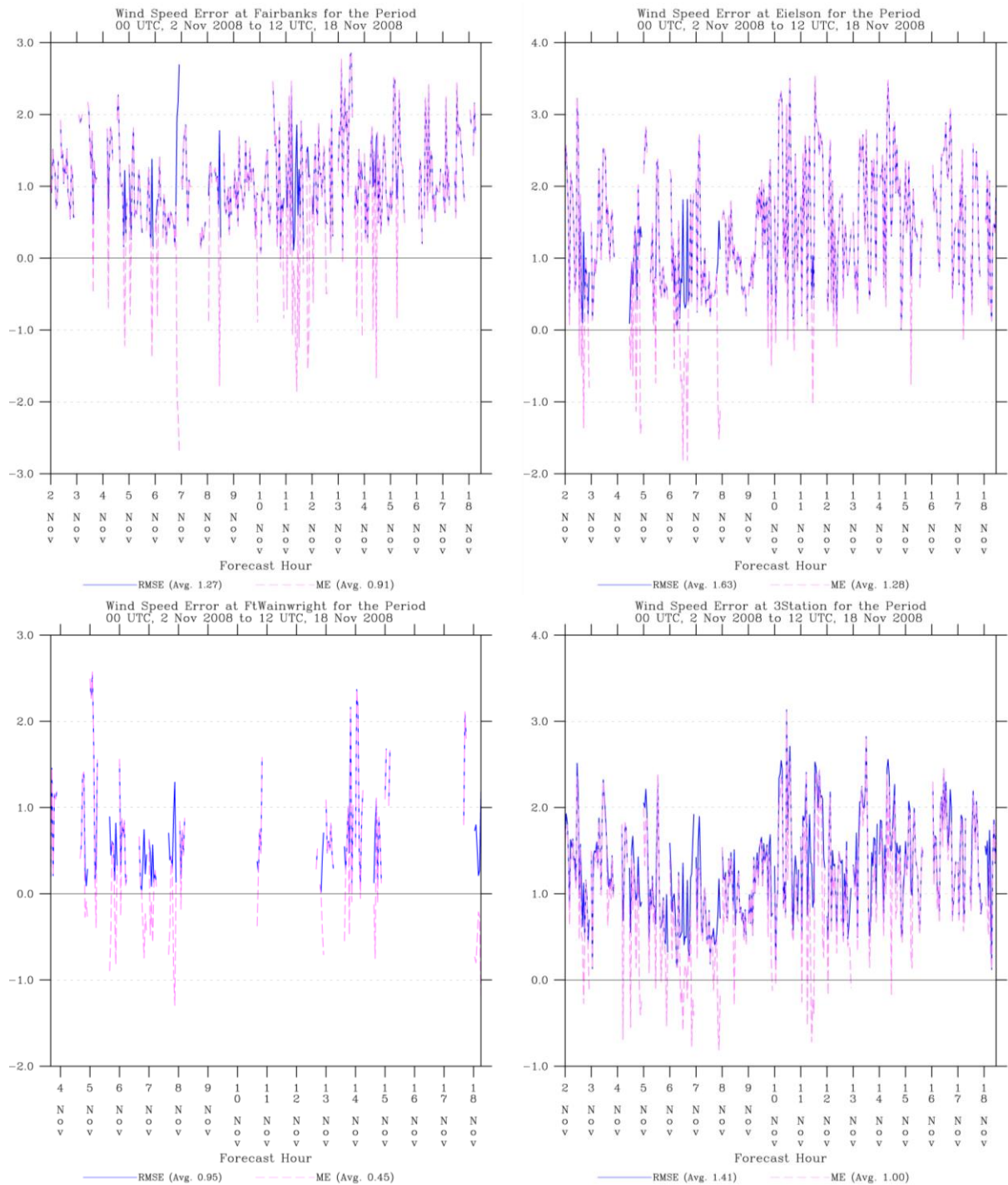


Figure 25: Same as Figure 23, but showing wind speed statistics.

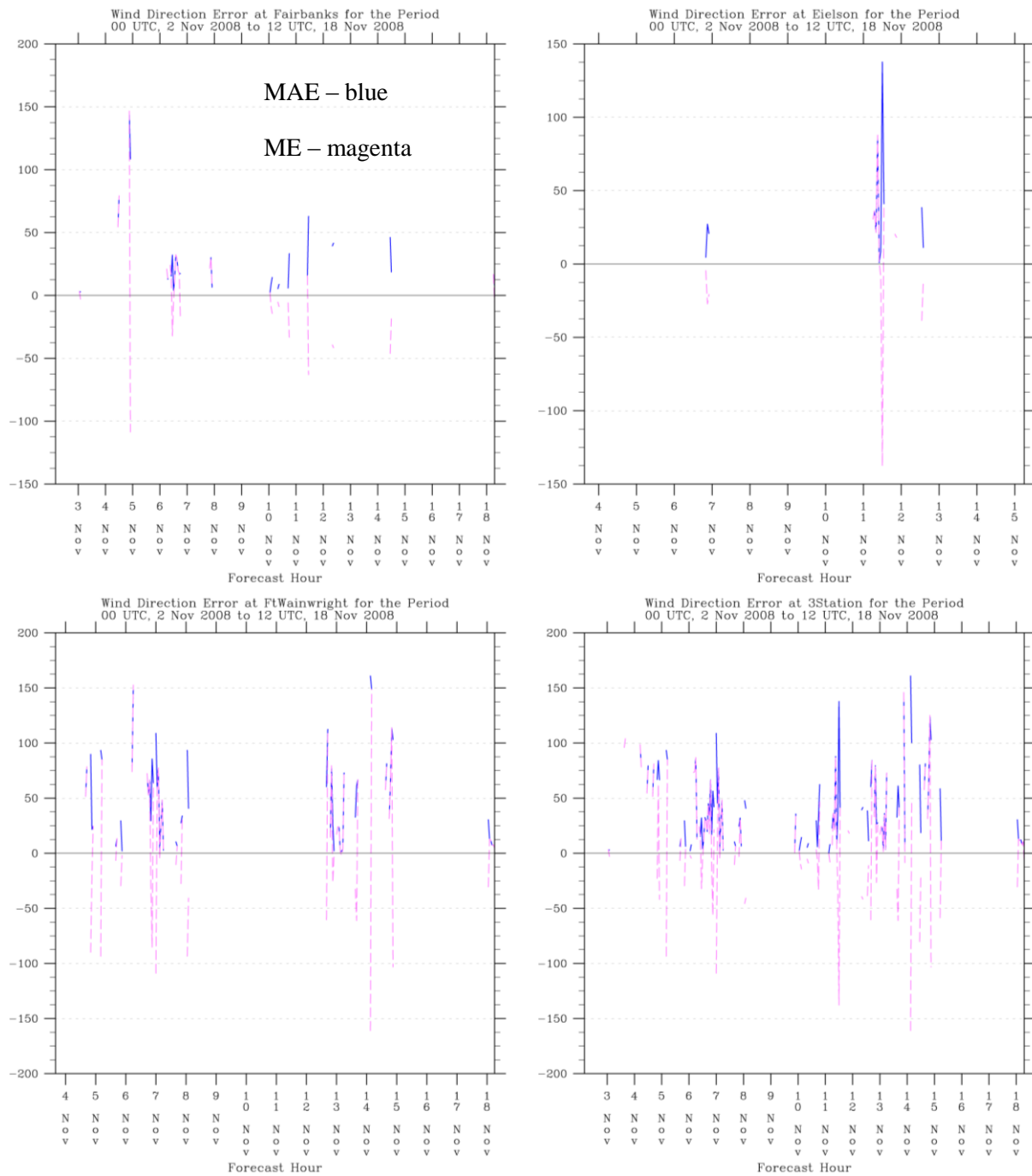


Figure 26: Same as Figure 23, but showing wind direction statistics.

For reference, a comparison between the statistics for the TWIND2X30CALM and TWIND2X30 model configurations for the entire November episode are presented in Table 8. Essentially, the same tendencies found for the November test period apply to the entire November episode as a whole. The superior configuration for temperature depends on statistic and station, and in all cases the sensitivity to calm wind inclusion is never more than about 0.15 °C. Positive wind speed biases are reduced by the inclusion of calms by on the order of 0.1 m s⁻¹ for Fairbanks and Eielson, but are actually increased at Ft. Wainwright. Again, the one substantial sensitivity is in wind direction error, for which TWIND2X30 has the better performance.

Finally, detailed time series of the statistics and modeled and observed values of surface meteorological variables, for both METAR and non-METAR stations, are presented in Appendix A for the TWIND2X30 simulation of the November episode that was provided to ADEC.

Table 8: Same as Table 7, but over entire November episode.

Temperature (°C)	TWIND2X30CALM RMSE (MAE for wind direction)	TWIND2X30 RMSE (MAE for wind direction)	TWIND2X30CALM Bias	TWIND2X30 Bias
Fairbanks	2.64	2.75	-1.30	-1.16
Eielson AFB	2.03	2.03	-0.46	-0.47
Ft. Wainwright	2.44	2.38	-0.94	-0.97
Three Stations	2.38	2.43	-0.92	-0.86
Relative Humidity (%)				
Fairbanks	5.49	5.43	0.75	0.71
Eielson AFB	6.01	5.93	3.42	3.35
Ft. Wainwright	12.39	12.48	-10.40	-10.39
Three Stations	7.17	7.14	0.10	0.05
Wind Speed (m s ⁻¹)				
Fairbanks	1.22	1.27	0.84	0.91
Eielson AFB	1.51	1.63	1.16	1.28
Ft. Wainwright	1.00	0.95	0.49	0.45
Three Stations	1.33	1.41	0.93	1.00
Wind Direction (degrees)				
Fairbanks	46.6	32.8	6.5	6.1
Eielson AFB	45.7	38.6	22.0	18.2
Ft. Wainwright	69.7	50.8	17.1	17.9
Three Stations	55.7	41.3	14.2	13.6

6. JAN-FEB 2008 EPISODE

The episode from 23 Jan – 12 Feb 2008 was re-simulated using the final model setup used for the 2-17 Nov 2008 episode (i.e., model configuration TWIND2X30, using the supplemental surface stations and enhanced vertical resolution in data assimilation). As mentioned previously, the Jan-Feb 2008 episode was considerably colder than the Nov 2008 case, with an extended period of temperatures reaching -35°C (see Figure 27). A comparison between the METAR station statistics for the TWIND2X30 re-simulation with the statistics from the original RARE project simulation is shown in Table 9. Generally the difference between the re-simulated and original statistics were slight for temperature, wind speed, and relative humidity (although at Ft. Wainwright the temperature RMSE increased by 0.5°C in the re-simulated case). Wind direction errors were substantially reduced in the re-simulated Jan – Feb 2008 episode, though, because in the original RARE configuration there was no assimilation of any surface wind observations on the finest domain. It appears that either model configuration has little, if any, overall temperature bias for the Jan-Feb episode. However, this reflects a cancellation between periods of positive temperature bias (generally the coldest temperature episodes) and periods of negative temperature bias (generally before the coldest episodes, often when precipitation is occurring).

A comparison of the METAR statistics between the TWIND2X30 versions of the Nov 2008 and Jan-Feb 2008 episodes (Table 10) shows that the TWIND2X30 version of the Jan-Feb 2008 episode arguably has better statistics than the Nov 2008 episode, despite the more extreme cold present in the former. However, the more negative temperature bias in the Nov 2008 versus the Jan-Feb 2008 episode is consistent with the relative absence of extreme cold periods in Nov 2008 and the configurations general tendency to have a negative temperature bias in milder winter conditions for the Fairbanks region. While the model tends to be too warm during the periods of the coldest temperatures, the coldest temperature periods also tend to be of short duration.

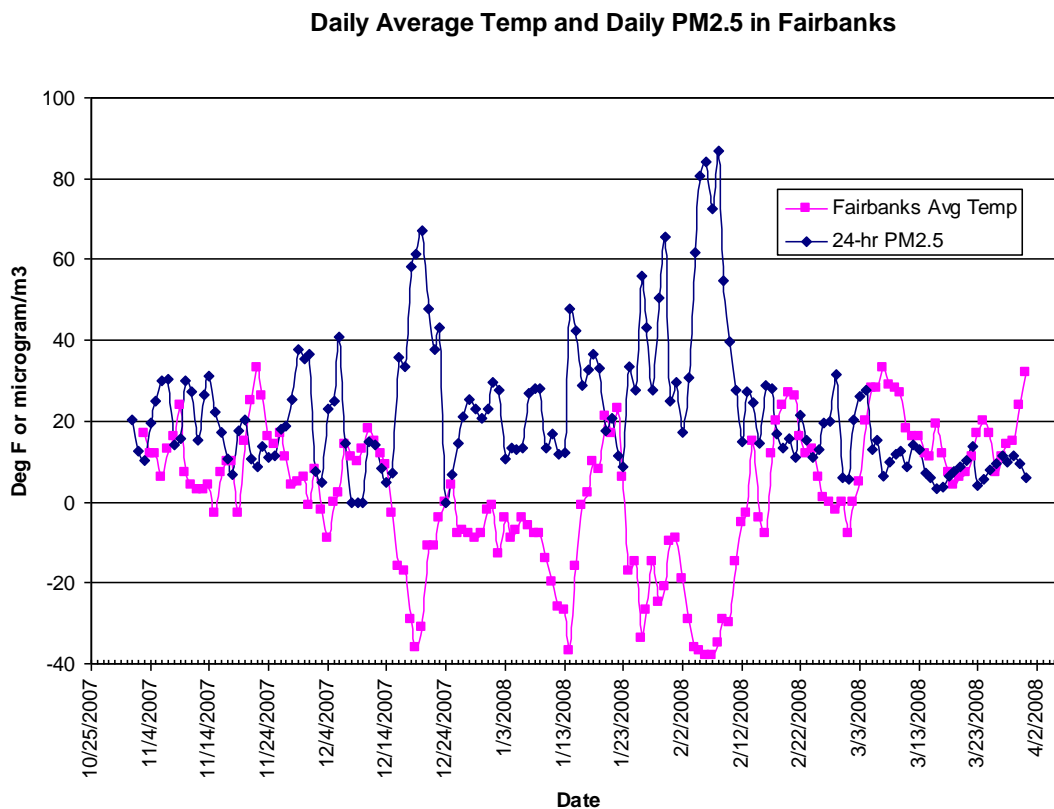


Figure 27: Measured daily average temperature (Fahrenheit) and 24-hr PM_{2.5} concentration in Fairbanks region during 2007-2008 winter season. Courtesy Robert Dulla, Sierra Research.

Temperatures for some of the local non-METAR stations are shown in Figure 28. Although the data record is a bit erratic, it is apparent that for the coldest period between 00 UTC on the 4th and 00 UTC on the 9th, the temperatures in Woodsmoke can be 10 °C or more colder than those in Two Rivers, which in turn can be 10 °C colder than those on Ester Dome. While the model surface temperature forecasts are not perfect (daytime temperatures at Two Rivers in particular seem to be too warm) the model configuration is certainly capturing a large part of the temperature variability and magnitude across these stations

Time series of statistics for the METAR stations for the rerun of the Jan – Feb 2008 case are shown in Figure 29 – Figure 32. While there are significant gaps in the data, it seems clear that the period from about 28 January through 31 January, as well as from about 4 – 11 February, exhibit positive temperature bias, corresponding to periods of low actual temperatures, while other periods tend to have a negative temperature bias (Figure 29). The largest temperature RMSE values for the positive and negative temperature bias periods are roughly comparable (exceeding 4 °C at times, but usually less than 3 °C). Wind speed biases tend to be positive

(Figure 31), but wind speed RMSE values seem to vary little on average between the warm and cold periods. These results are broadly consistent with those from the RARE project.

Appendix B contains more detailed time series of the statistics and modeled and observed surface field values for the Jan-Feb 2008 episode.

Table 9: Comparison of statistics for Jan-Feb 2008 between RARE configuration and TWIND2X30 configuration.

Temperature (°C)	Jan-Feb RARE RMSE (MAE for wind direction)	Jan-Feb RARE Bias	Jan-Feb TWIND2X30 RMSE (MAE for wind direction)	Jan-Feb TWIND2X30 Bias
Fairbanks	2.20	-0.03	2.22	-0.12
Eielson AFB	1.81	-0.07	2.05	-0.23
Ft. Wainwright	1.33	0.23	1.83	0.51
Three Stations	1.87	0.02	2.07	0.00
Relative Humidity (%)				
Fairbanks	8.07	2.74	8.15	2.55
Eielson AFB	11.45	-1.38	12.45	-2.49
Ft. Wainwright	16.85	-13.87	17.09	-13.67
Three Stations	11.98	-2.89	12.44	-3.32
Wind Speed (m s ⁻¹)				
Fairbanks	1.58	0.87	1.51	0.86
Eielson AFB	1.17	0.69	1.18	0.69
Ft. Wainwright	1.31	0.32	1.21	0.25
Three Stations	1.38	0.69	1.34	0.68
Wind Direction (degrees)				
Fairbanks	43.6	0.3	21.6	-5.6
Eielson AFB	55.7	-19.4	26.0	-10.3
Ft. Wainwright	66.4	18.9	40.3	3.4
Three Stations	54.6	1.9	29.2	-3.6

Table 10: Comparison of statistics for Nov 2008 and Jan-Feb 2008 episodes for TWIND2X30 model configuration.

Temperature (°C)	Nov 2008 RMSE (MAE for wind direction)	Nov 2008 Bias	Jan-Feb 2008 RMSE (MAE for wind direction)	Jan-Feb 2008 Bias
Fairbanks	2.75	-1.16	2.22	-0.12
Eielson AFB	2.03	-0.47	2.05	-0.23
Ft. Wainwright	2.38	-0.97	1.83	0.51
Three Stations	2.43	-0.86	2.07	0.00
Relative Humidity (%)				
Fairbanks	5.43	0.71	8.15	2.55
Eielson AFB	5.93	3.35	12.45	-2.49
Ft. Wainwright	12.48	-10.39	17.09	-13.67
Three Stations	7.14	0.05	12.44	-3.32
Wind Speed (m s ⁻¹)				
Fairbanks	1.27	0.91	1.51	0.86
Eielson AFB	1.63	1.28	1.18	0.69
Ft. Wainwright	0.95	0.45	1.21	0.25
Three Stations	1.41	1.00	1.34	0.68
Wind Direction (degrees)				
Fairbanks	32.8	6.1	21.6	-5.6
Eielson AFB	38.6	18.2	26.0	-10.3
Ft. Wainwright	50.8	17.9	40.3	3.4
Three Stations	41.3	13.6	29.2	-3.6

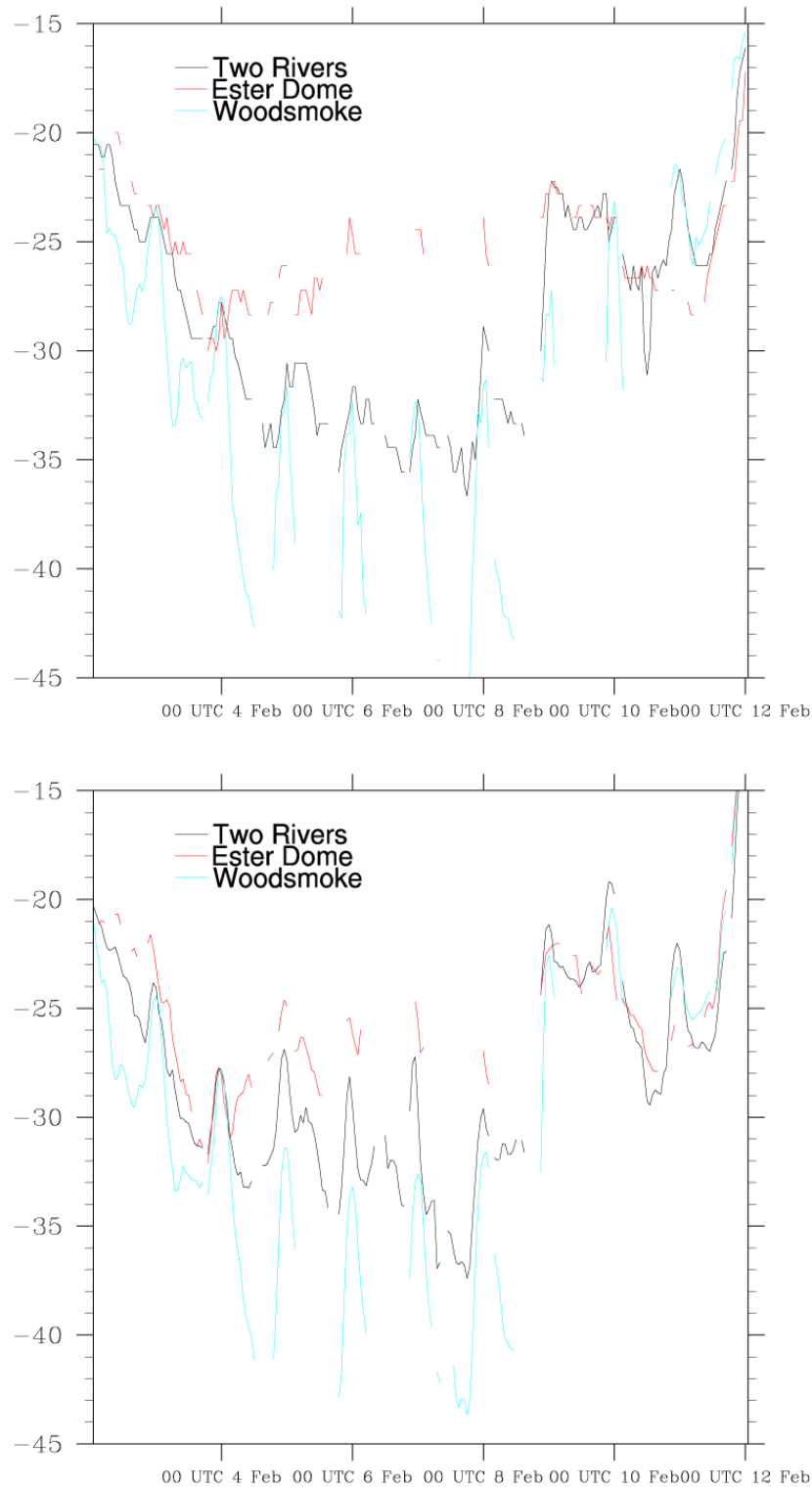


Figure 28: Observed (top) and model (bottom) surface temperatures (degrees Celsius) at non-METAR stations for 00 UTC 3 Feb -- 00 UTC 12 Feb

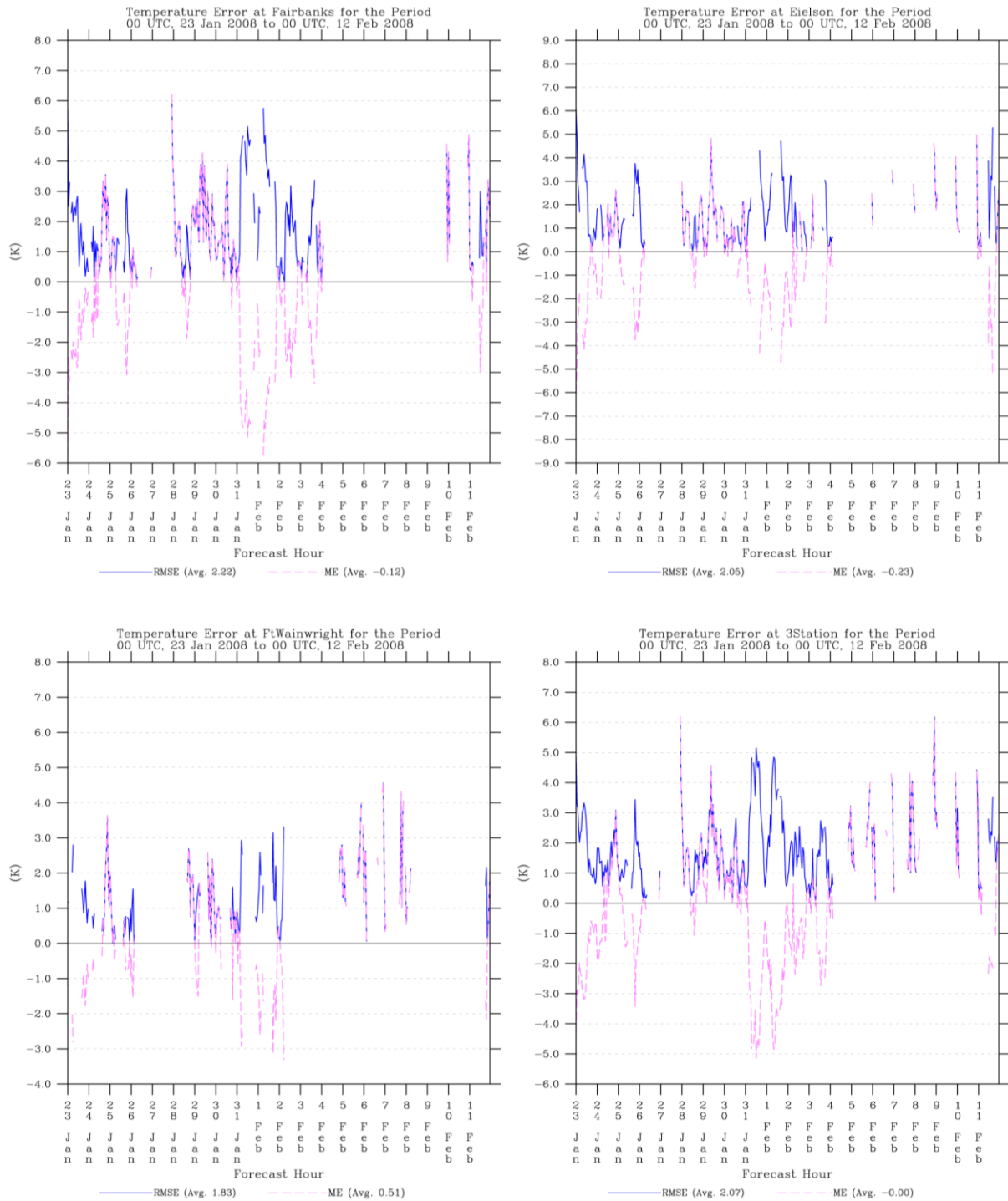


Figure 29: Temperature RMSE and Bias statistics for Jan-Feb 2008 episode at the local METAR surface stations using TWIND2X30 configuration.

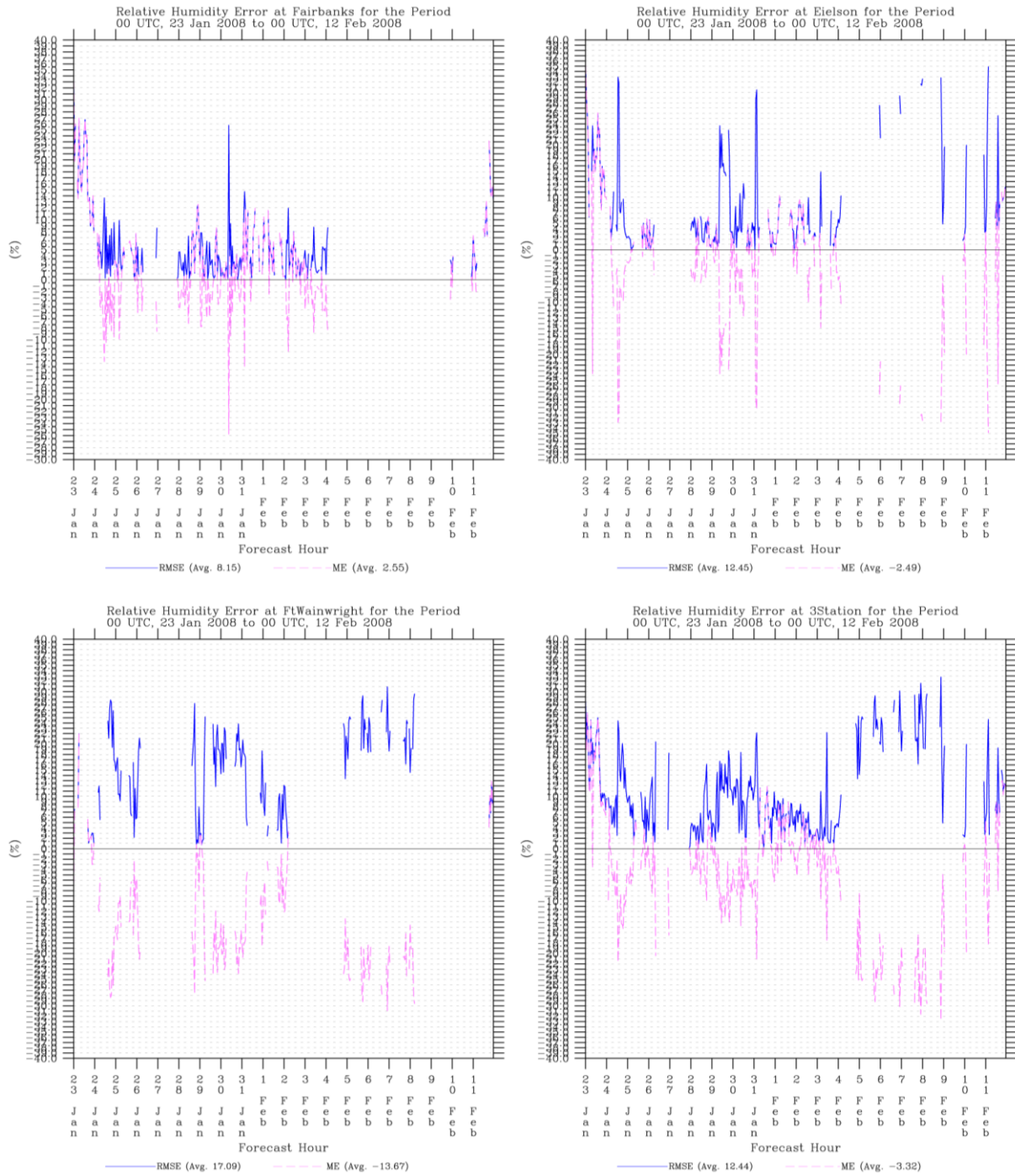


Figure 30: Same as Figure 29, but for relative humidity.

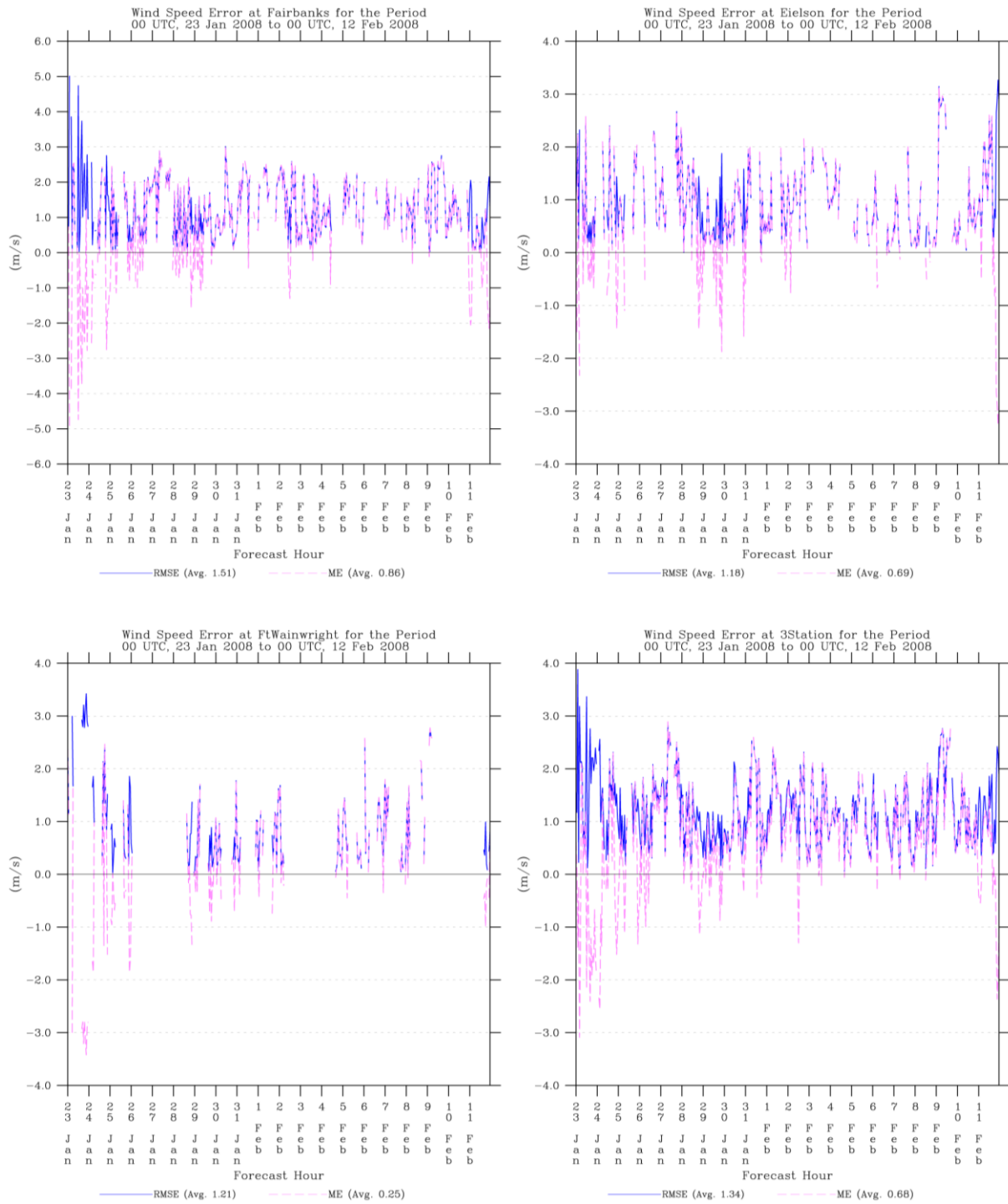


Figure 31: Same as Figure 29, but for wind speed.

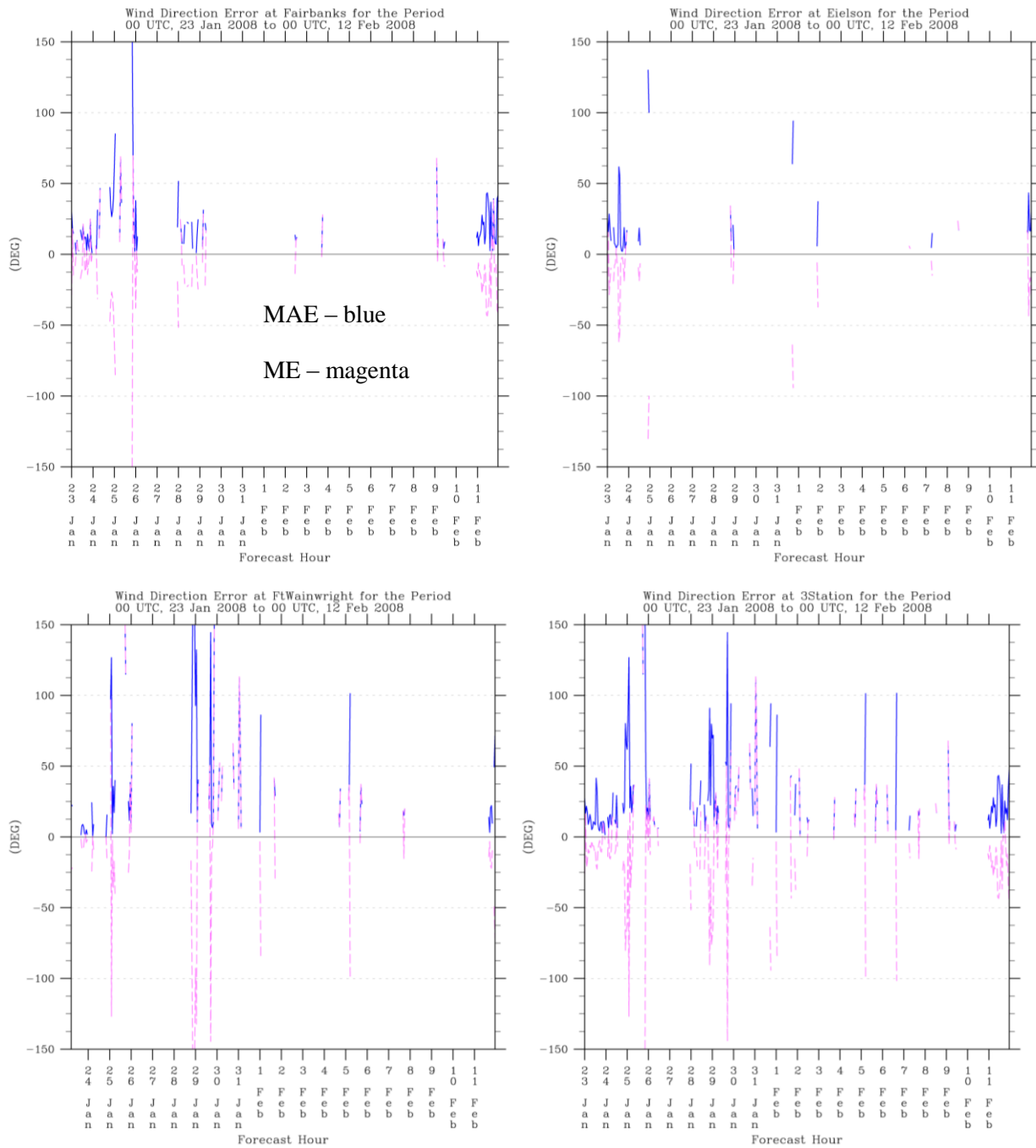


Figure 32: Same as Figure 29, but for wind direction MAE and ME statistics.

7. CONCLUSIONS

An episode extending from 2-17 November 2008 was simulated as part of the State Implementation Plan for the Fairbanks / North Star non-attainment region. The simulations were performed using the WRF-ARW model with essentially the same configuration as that used in the preliminary RARE study. However, initial decisions were made to increase the effective vertical resolution of the data assimilation near the surface, to use observation nudging towards surface wind observations even on the 1.33-km finest grid, and to make use of both standard METAR and non-METAR surface observations that were available for the period. These alterations to the procedure of the RARE study were made because, even though the statistics from that study were reasonably good, the model displayed a warm bias during the coldest, most stagnant conditions from that study, and concurrently the model wind speed bias was consistently positive. It was felt that these modifications would lead to the creation of a dynamic analysis that would be a closer fit to the actual state of the atmosphere.

The November episode was divided into four overlapping simulation segments using the discussed model configuration. A test period from 5-9 November was chosen for model sensitivity tests, including a comparison between the RARE study methodology and the proposed method of enhancing the data assimilation capabilities. Statistics indicated the benefits of the new data assimilation configuration, especially for wind direction. This configuration was then used for all subsequent simulations. However, the statistics also suggested that the model data assimilation was effectively blending the influence of neighboring observations in the Fairbanks region, leading to model simulations that did not possess all of the horizontal variability of the observations. A procedure taken from the RARE study was performed to determine an effective correlation length scale for surface temperature observation innovations; this led to new simulations in which the radius of influence was reduced from 75 km to 30 km, while the strength of the nudging coefficients was doubled. The new configuration (indicated by the label TWIND2X30) was then used to simulate the entire November episode, and generated the atmospheric analysis delivered to ADEC.

A positive wind speed model bias remained during stagnant, cold temperature conditions, though a portion of that bias is an artifact of the threshold of instrument detection, causing observations to frequently report dead calm conditions while model simulations produce non-zero wind speeds near the surface. While one procedure to reduce the positive wind speed bias would be to explicitly nudge towards the calm wind observations, it was found that this led to only minimal reductions in the wind speed bias, and using these reports in nudging had the undesirable effect of creating large increases in wind direction error at nearby stations not reporting dead calm conditions. Therefore, the decision was made to use the default procedure of not making explicit use of calm surface wind observations in the data assimilation procedure.

The Jan-Feb 2008 episode was then re-simulated using the TWIND2X30 configuration. Wind direction statistics for the METAR stations were improved with respect to the original simulations from the RARE project. Other fields did not show much change statistically. While model output at the location of the non-METAR station at Woodsmoke confirmed that the model could produce temperatures (nearly) as cold as observed temperatures around $-45\text{ }^{\circ}\text{C}$, at other locations the model had difficulty producing sufficient cooling, especially if the horizontal resolution was insufficient (e.g., Goldstream Creek).

At the METAR stations, overall temperature bias for both episodes was quite low (less than a degree Celsius), while the temperature RMSE was on average $2 - 2.5\text{ }^{\circ}\text{C}$, which seemed reasonable given the occasionally extreme meteorological conditions. Wind speed RMSE values seemed to be fairly consistent at $1.3 - 1.4\text{ m s}^{-1}$, while wind direction MAE values were on the order of $30 - 40$ degrees with the TWIND2X30 configuration.

**APPENDIX A – Detailed Time-Series Figures of 2-17 November 2008 Episode, for
TWIND2X30 Configuration**

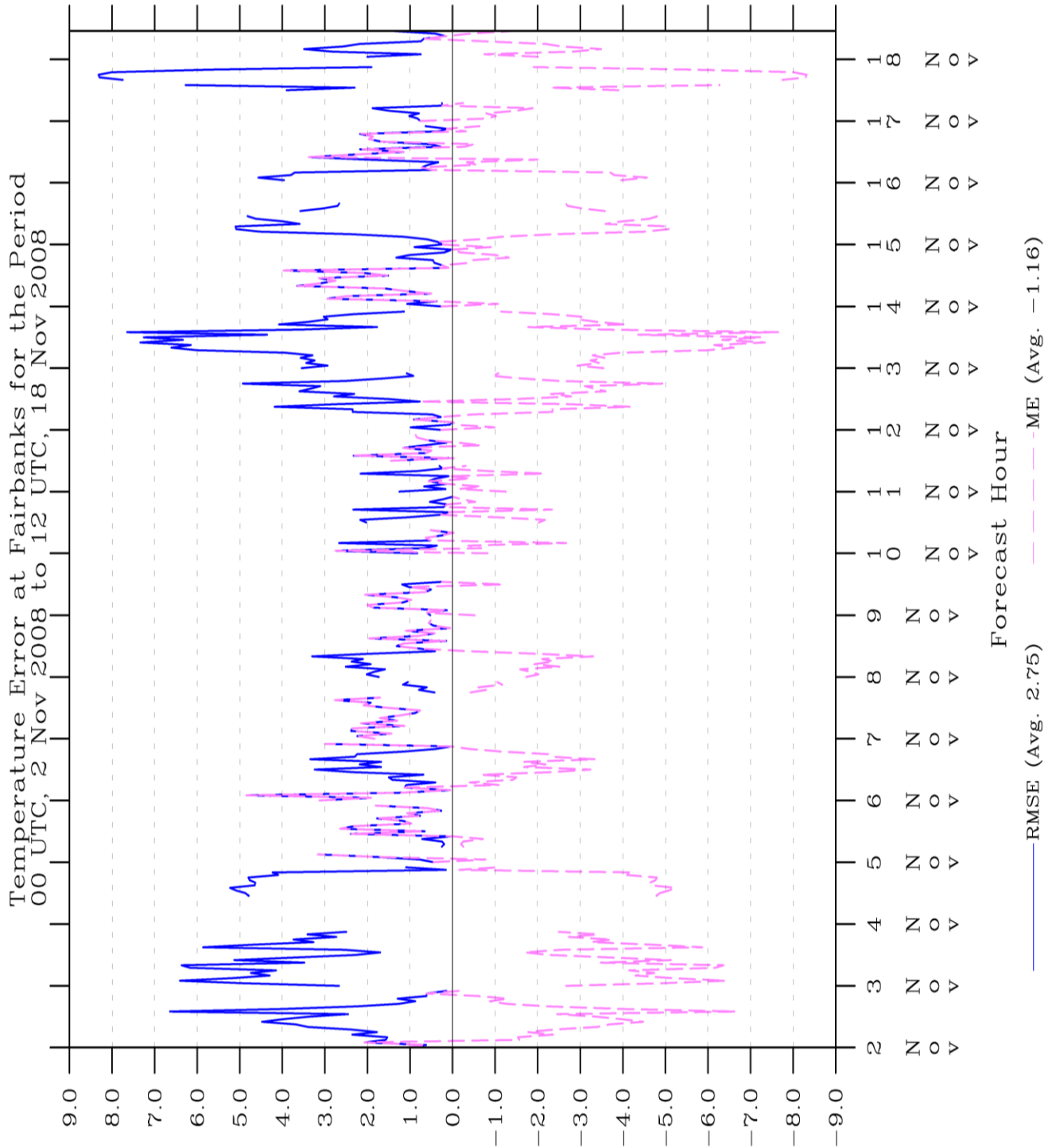


Figure 33: Time series of temperature statistics for Fairbanks in TWIND2X30.

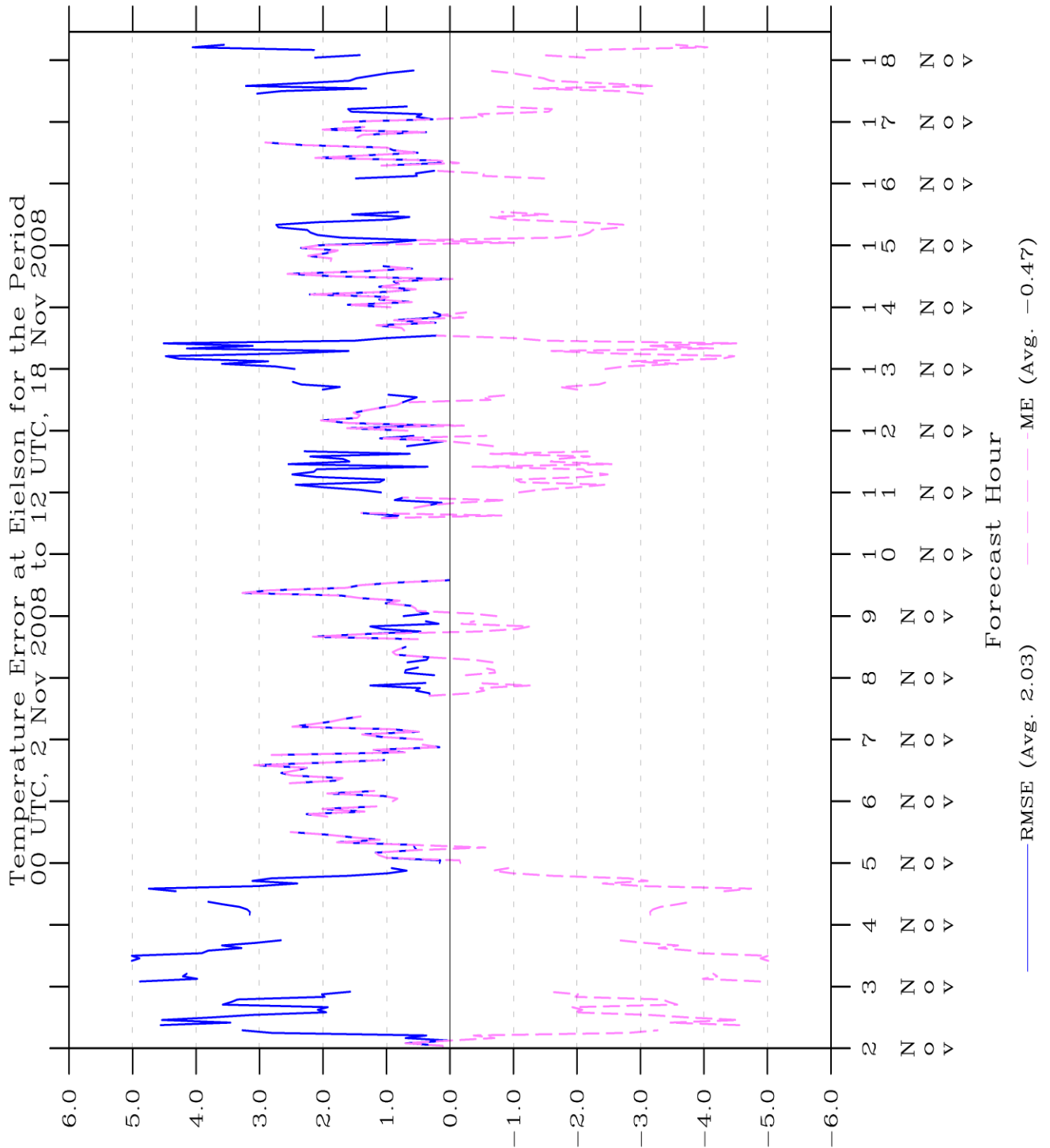


Figure 34: Time series of temperature statistics for Eielson in TWIND2X30.

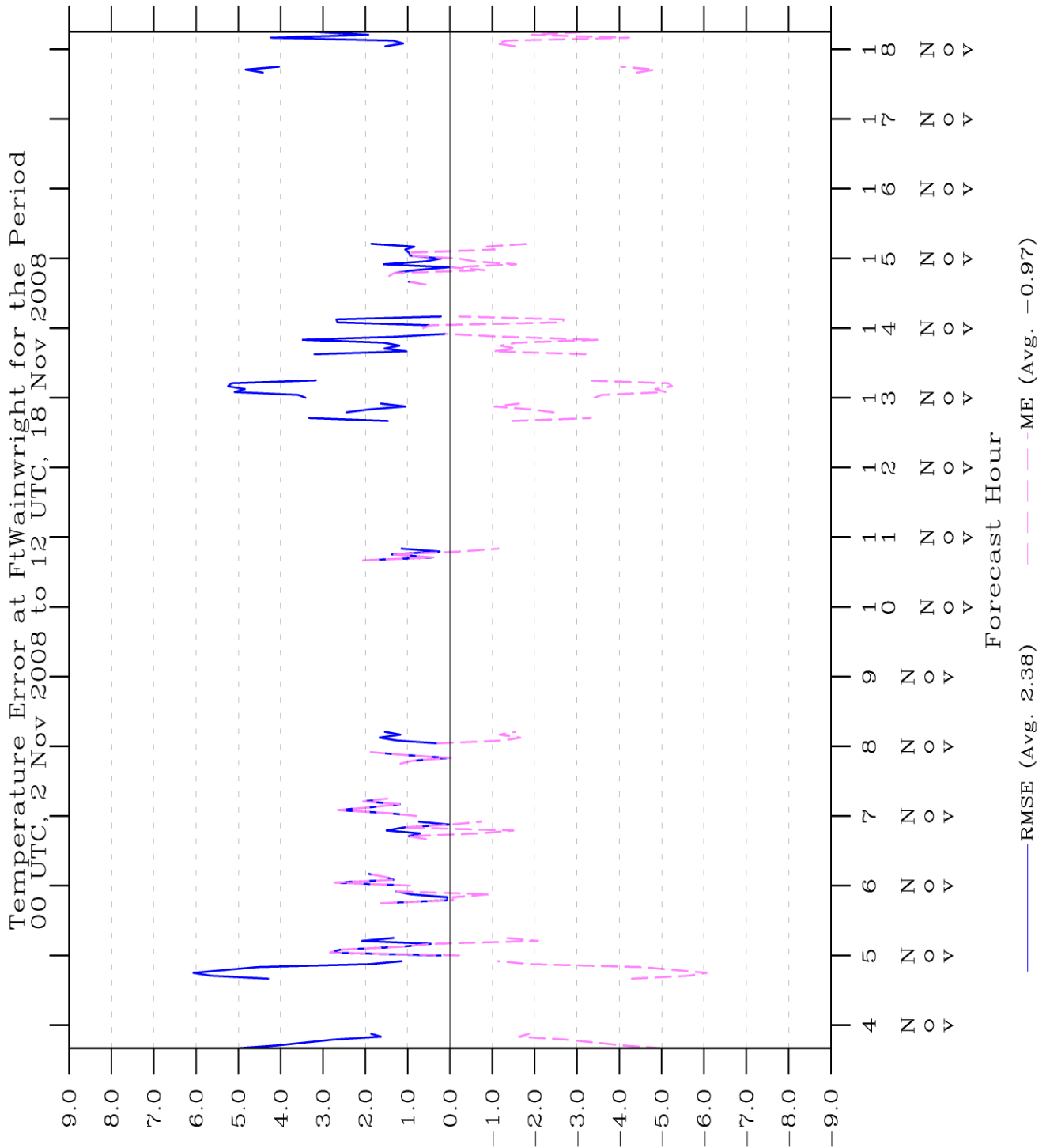


Figure 35: Time series of temperature statistics for Ft. Wainwright in TWIND2X30.

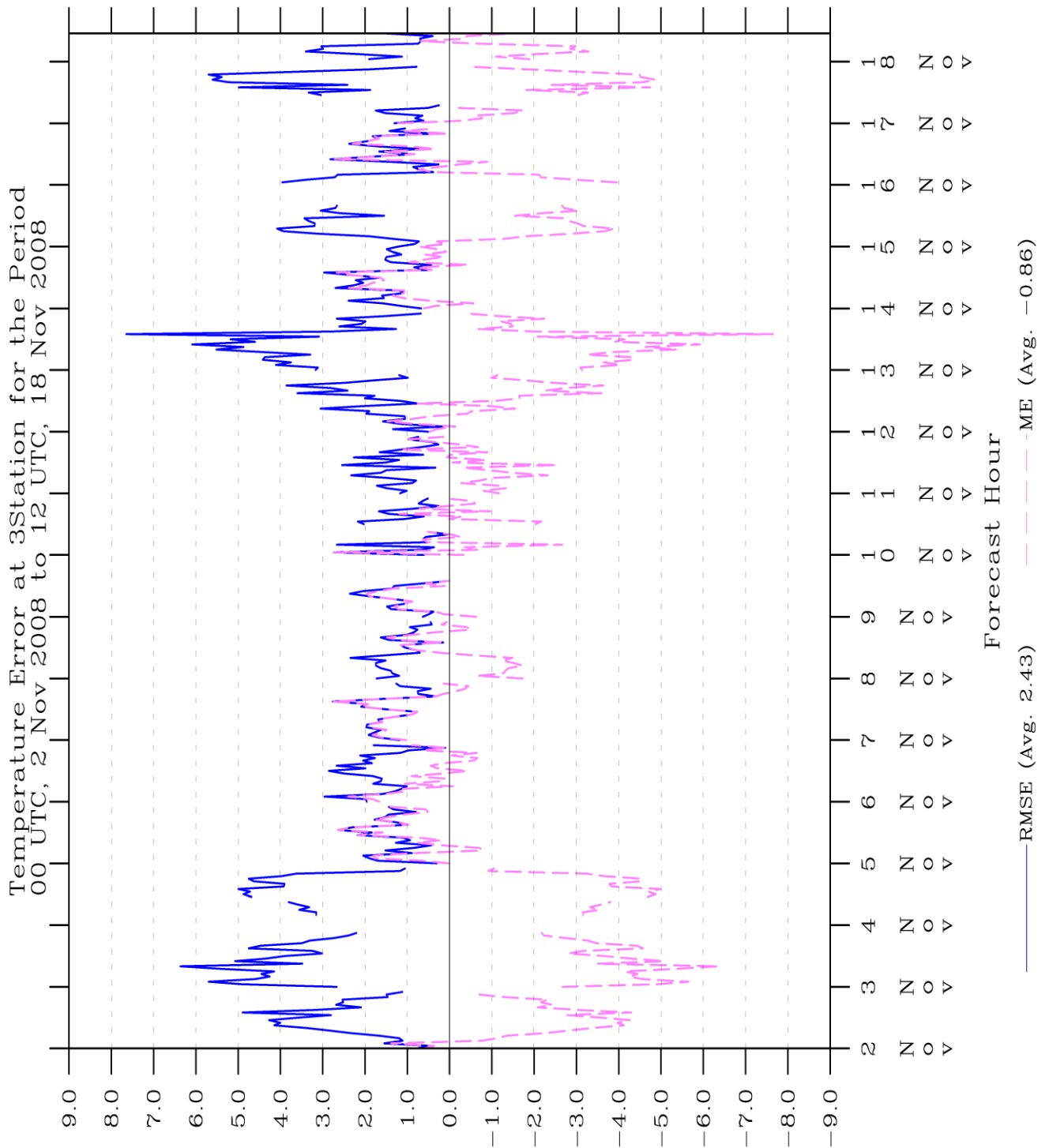


Figure 36: Time series of temperature statistics for all three stations in TWIND2X30.

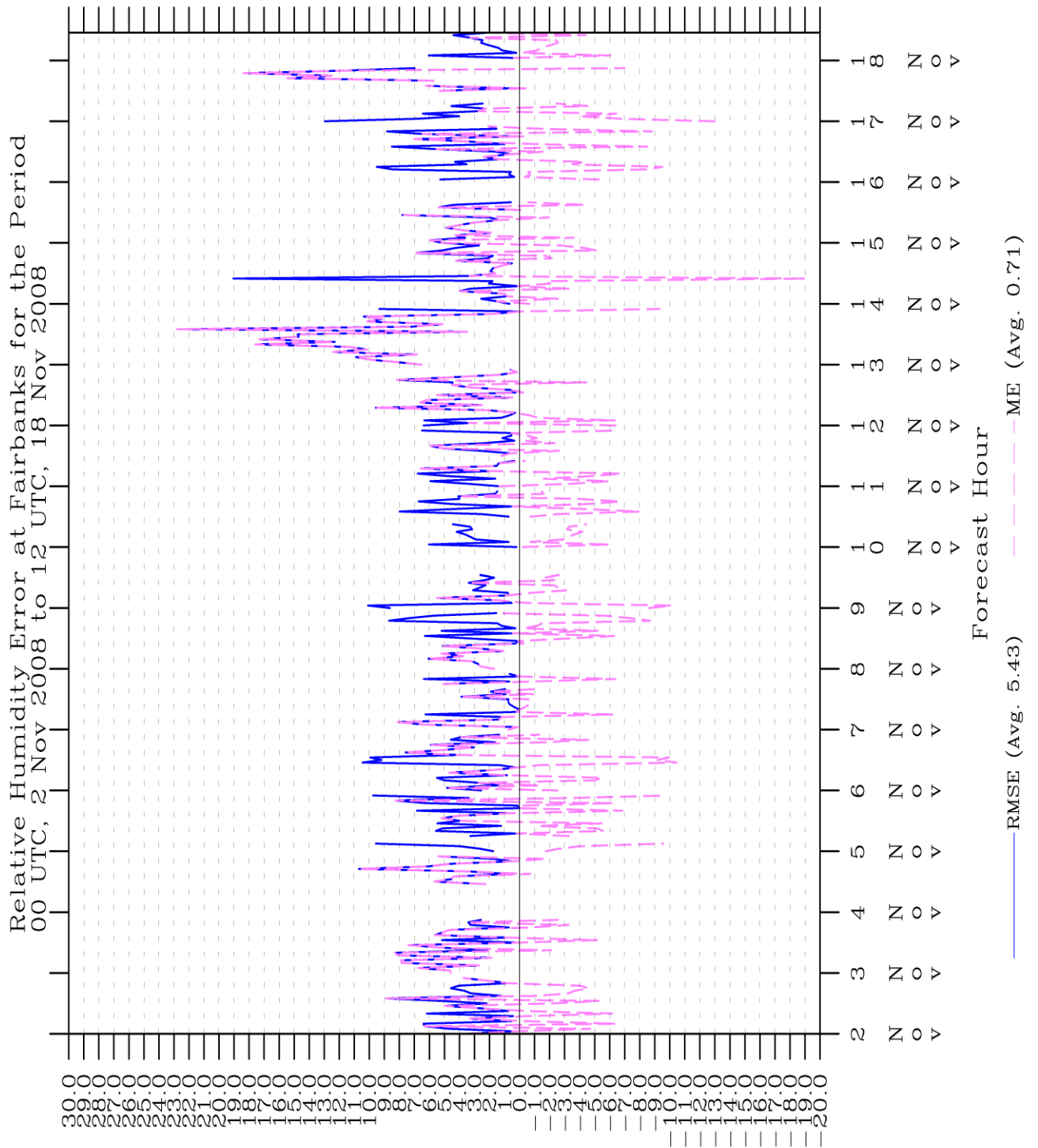


Figure 37: Time series of relative humidity statistics for Fairbanks in TWIND2X30.

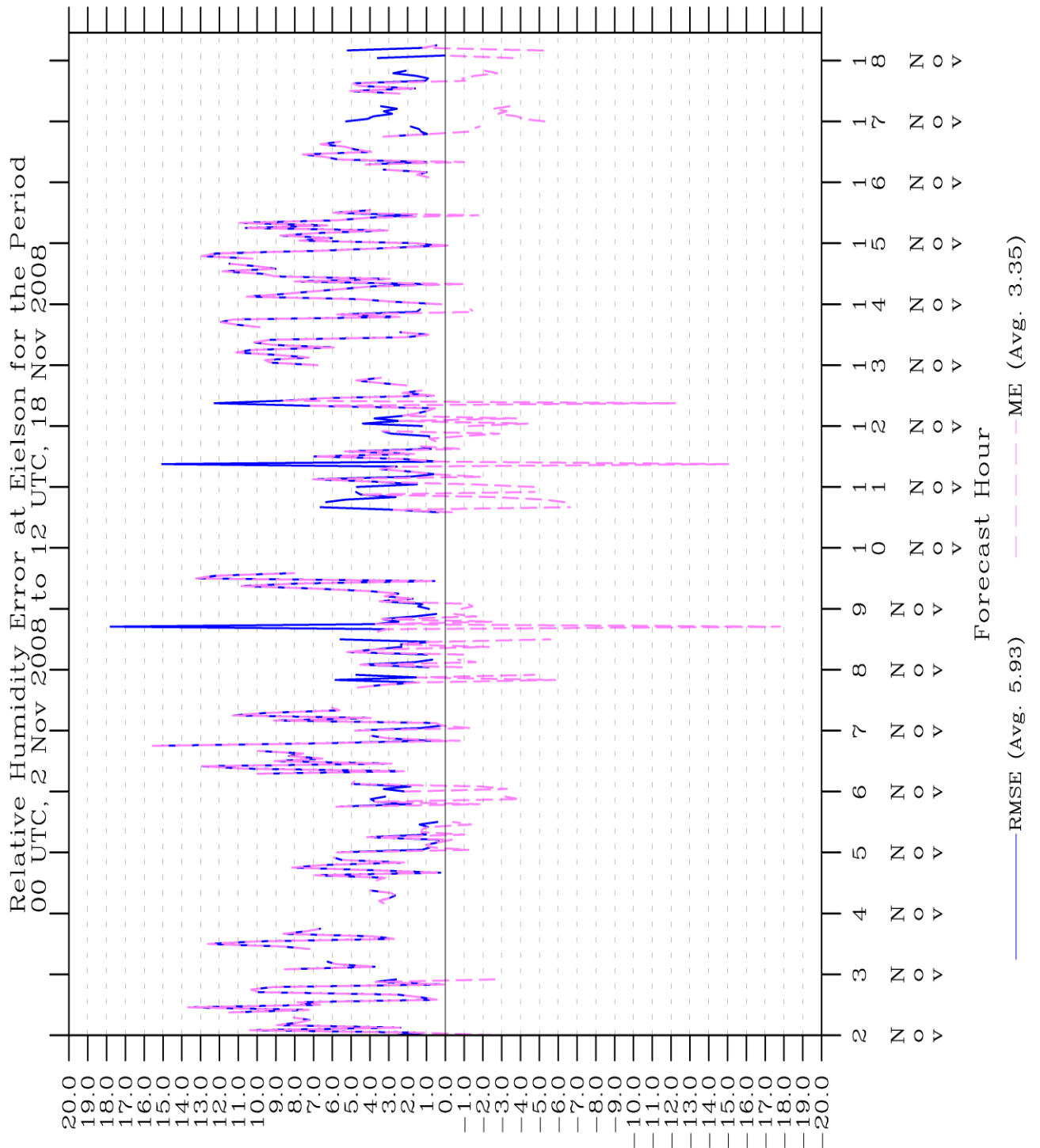


Figure 38: Time series of relative humidity statistics for Eielson in TWIND2X30.

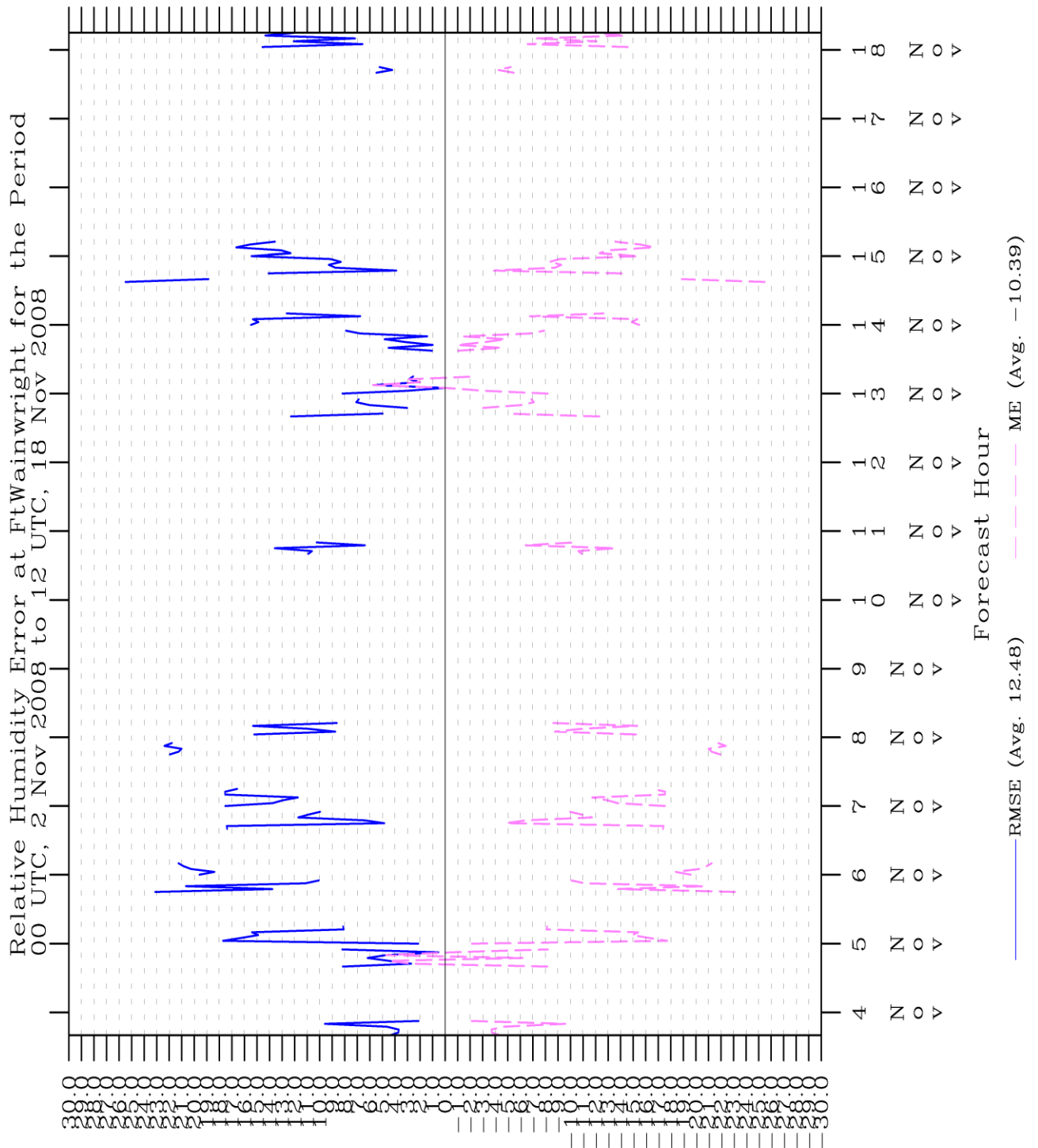


Figure 39: Time series of relative humidity statistics for Ft. Wainwright in TWIND2X30.

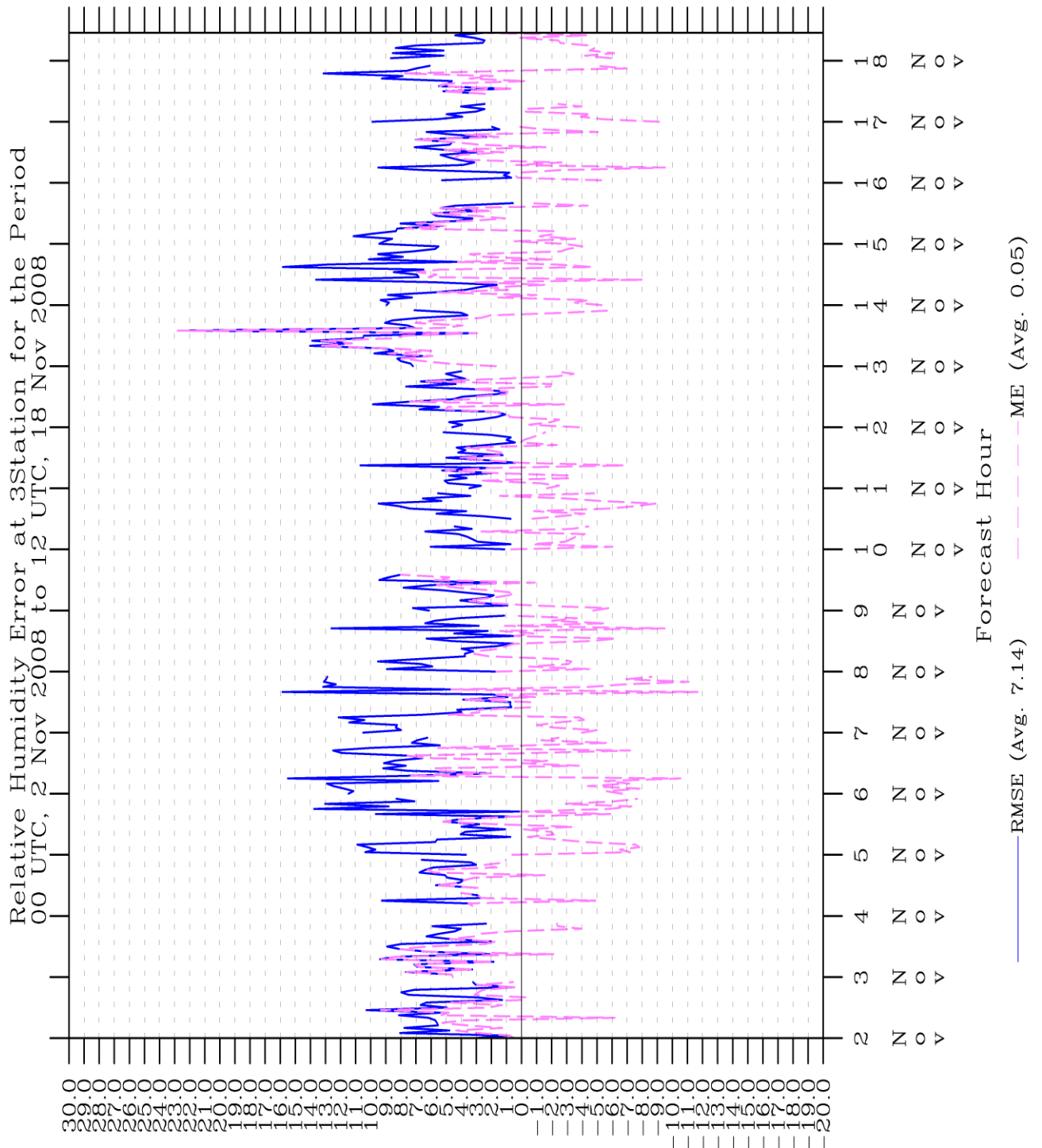


Figure 40: Time series of relative humidity statistics for all three stations in TWIND2X30.

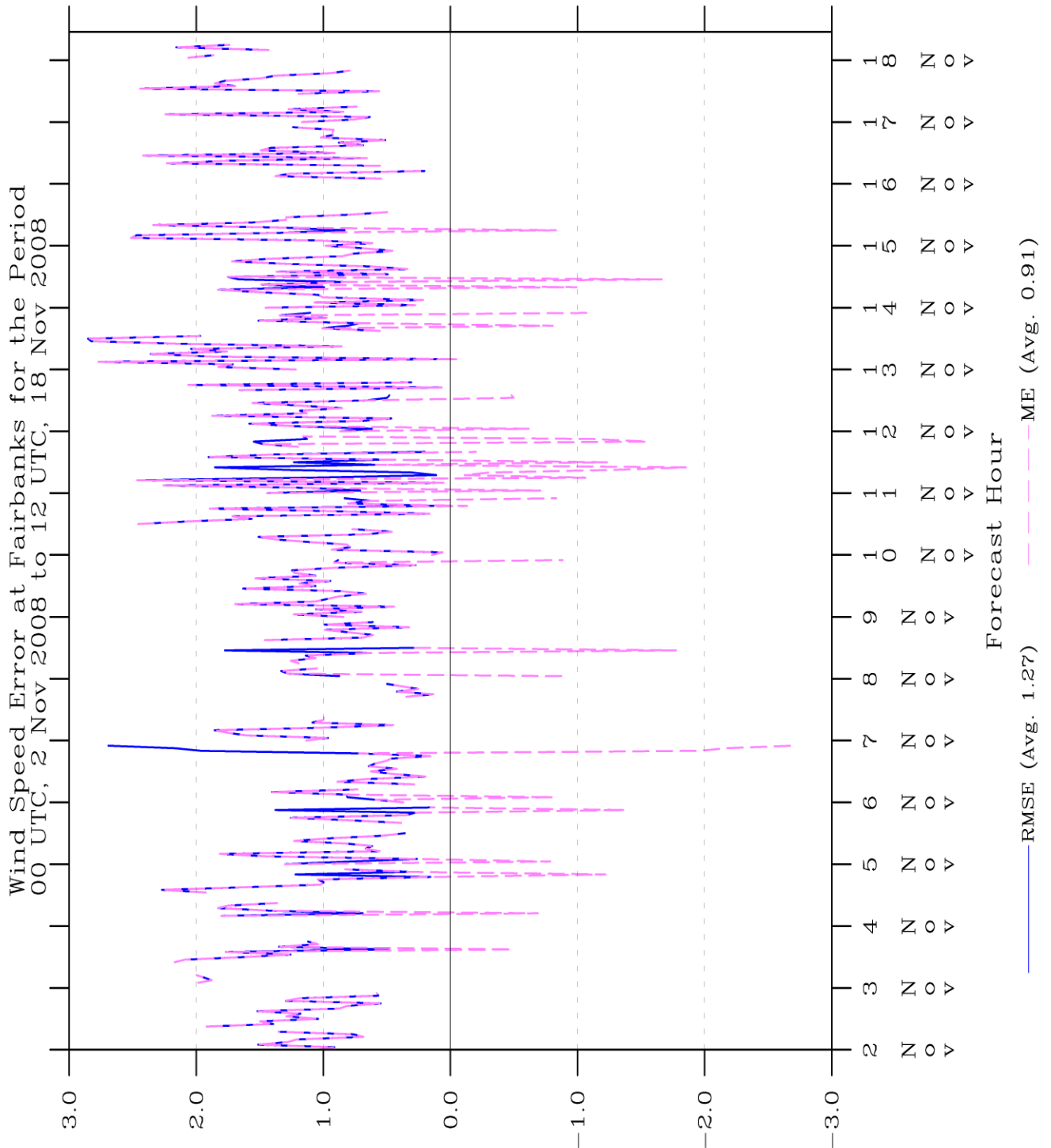


Figure 41: Time series of wind speed statistics for Fairbanks in TWIND2X30.

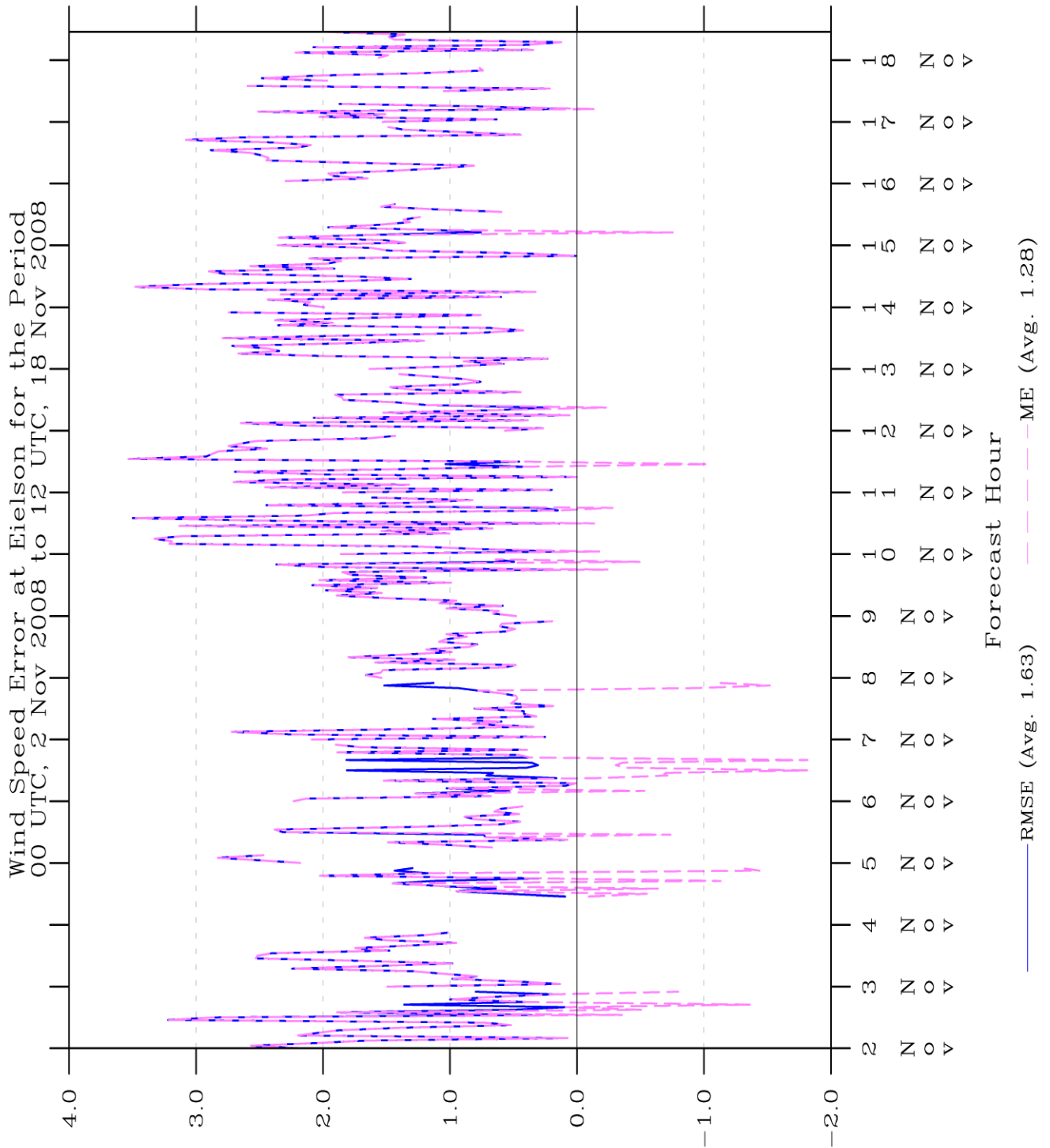


Figure 42: Time series of wind speed statistics for Eielson in TWIND2X30.

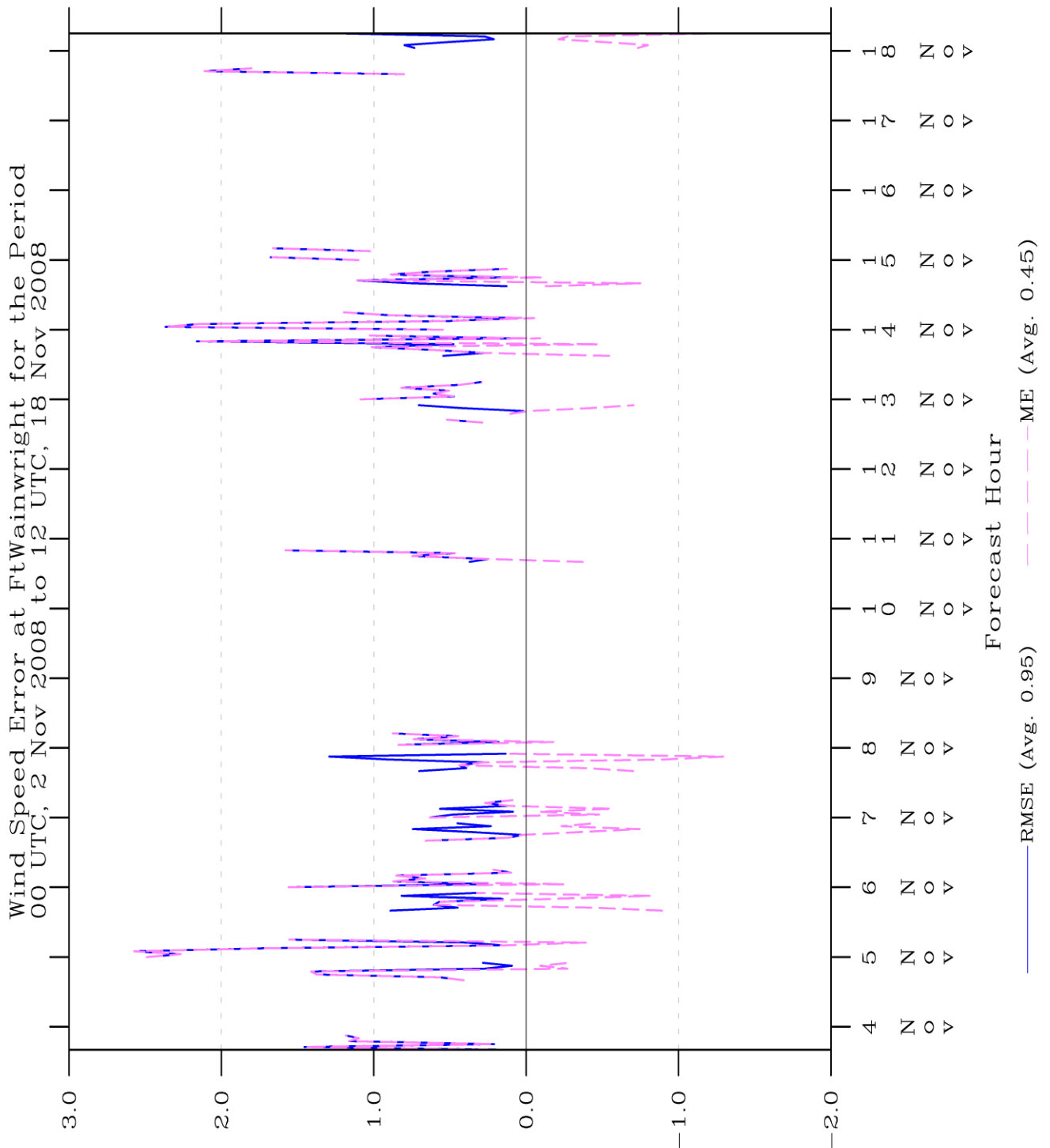


Figure 43: Time series of wind speed statistics for Ft. Wainwright in TWIND2X30.

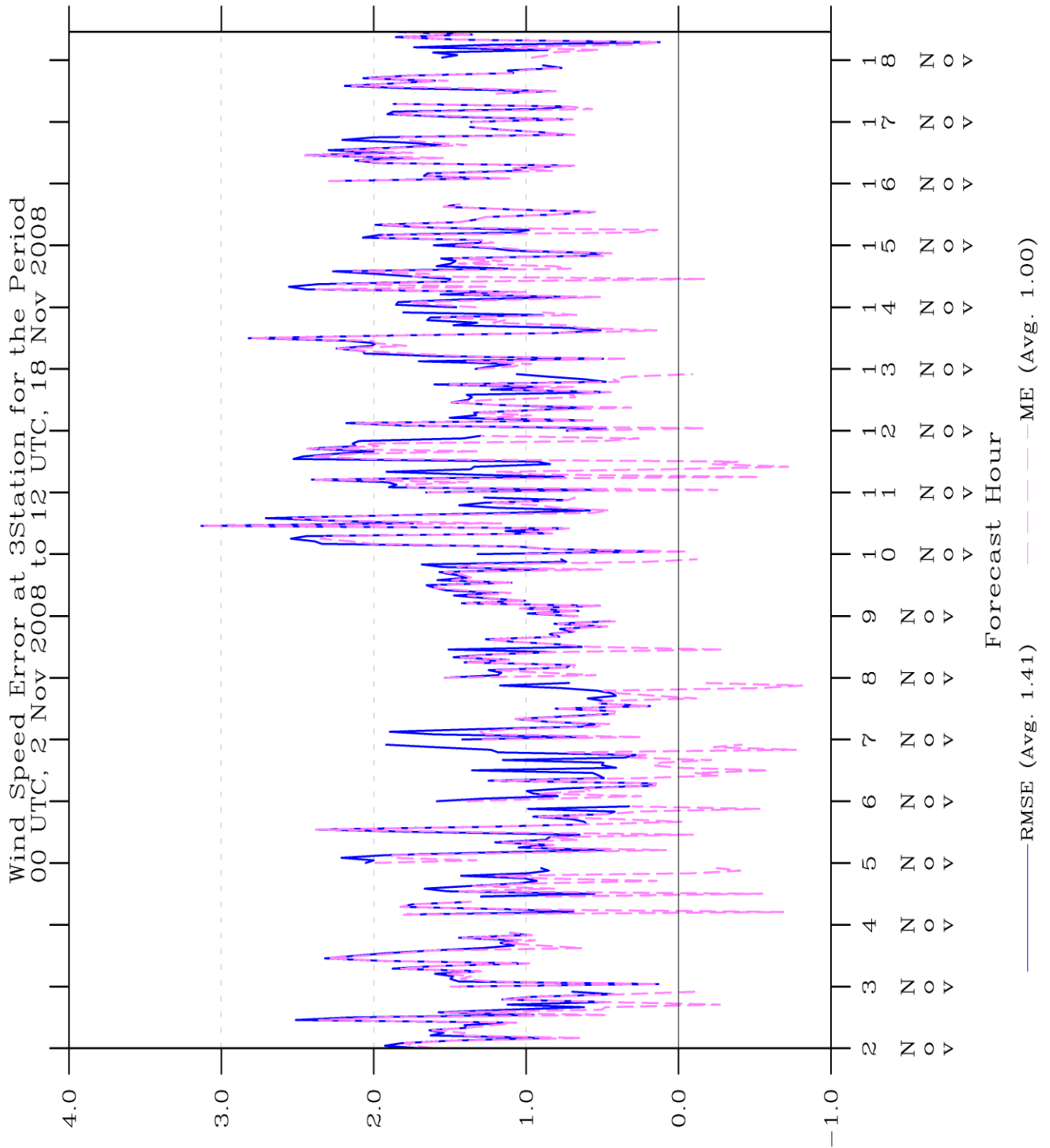


Figure 44: Time series of wind speed statistics for all three stations in TWIND2X30.

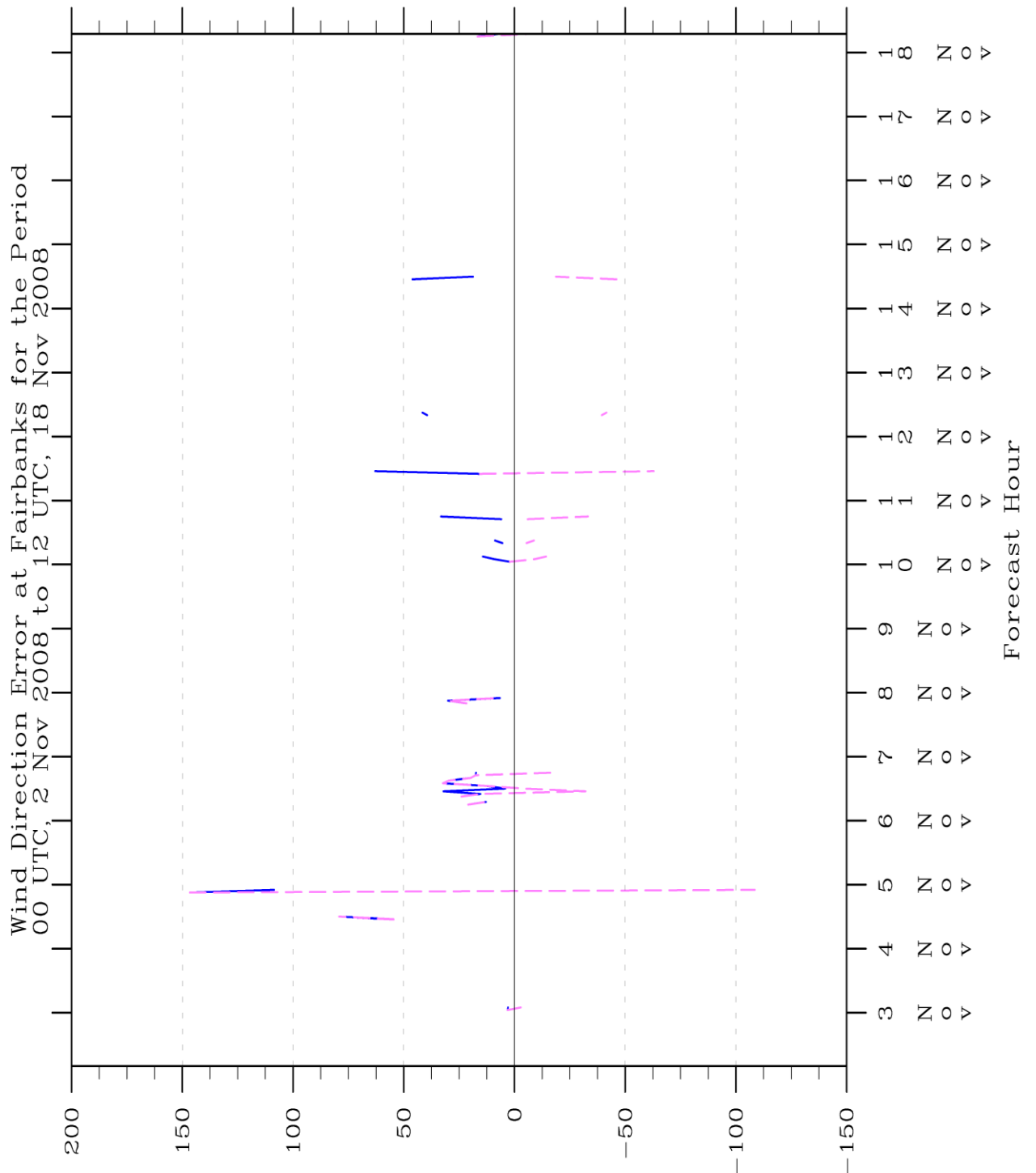


Figure 45: Time series of wind direction mean absolute error (blue) and mean error (magenta) statistics for Fairbanks in TWIND2X30.

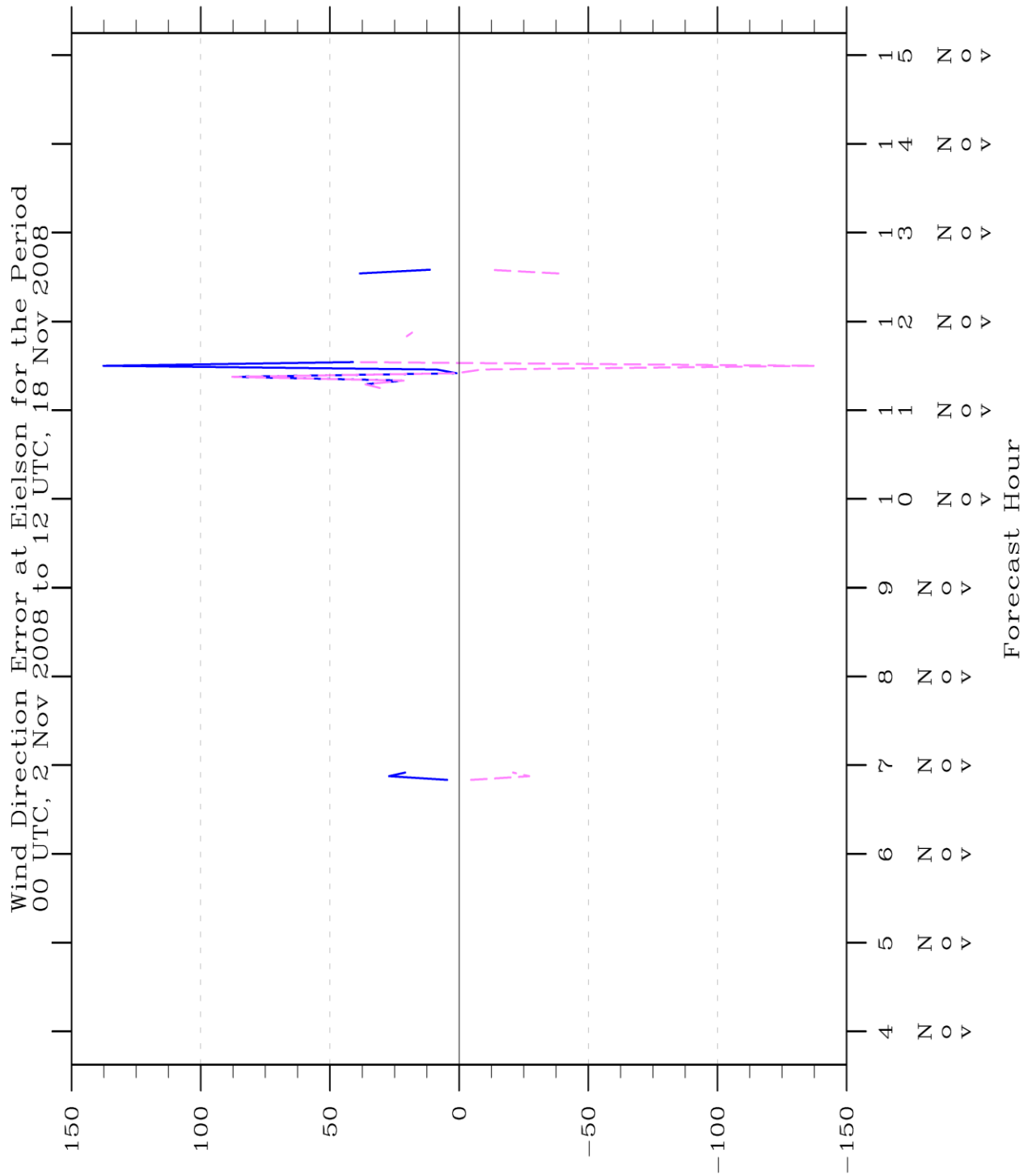


Figure 46: Time series of wind direction mean absolute error (blue) and mean error (magenta) statistics for Eielson in TWIND2X30.

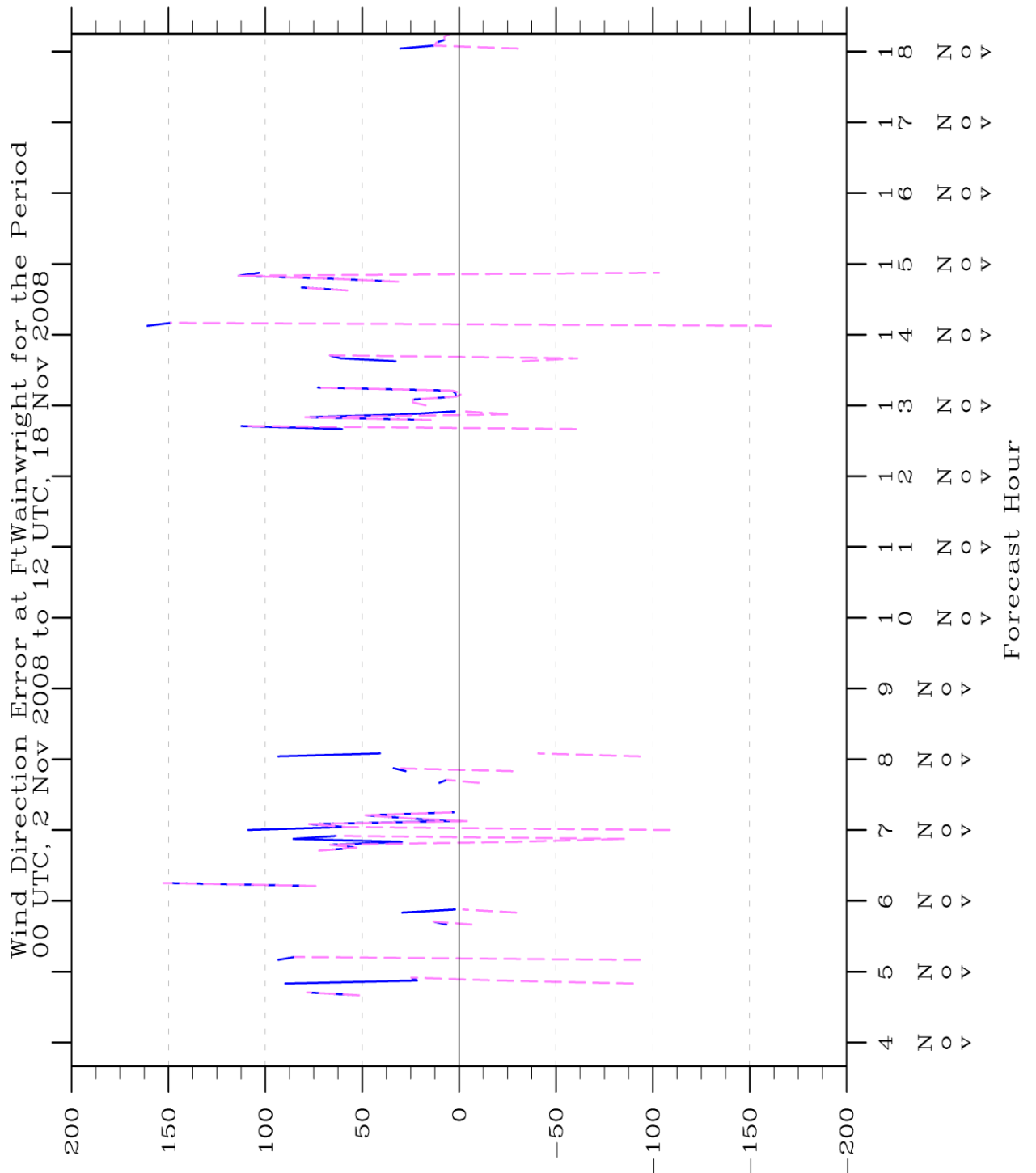


Figure 47: Time series of wind direction mean absolute error (blue) and mean error (magenta) statistics for Ft. Wainwright in TWIND2X30.

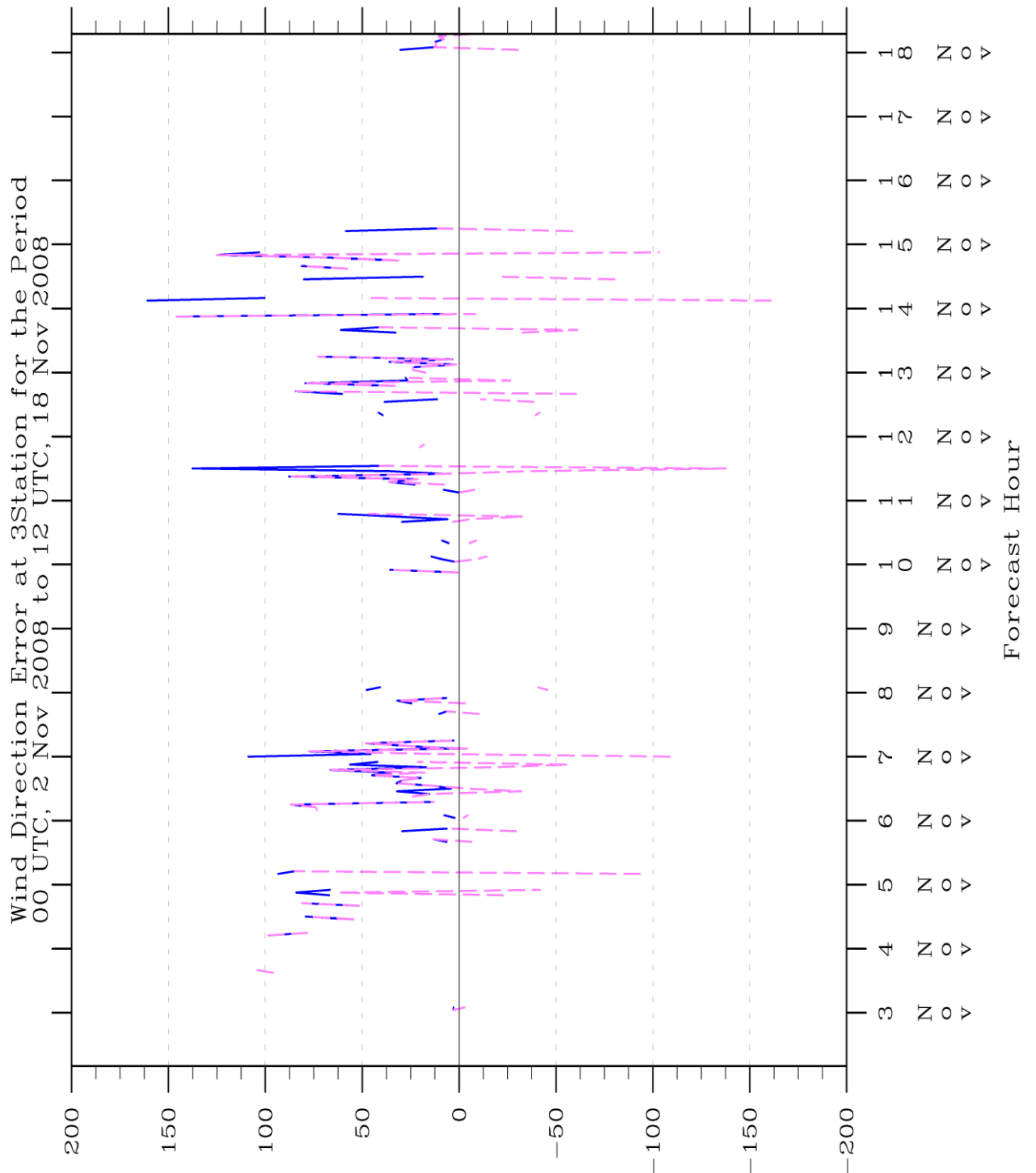


Figure 48: Time series of wind direction mean absolute error (blue) and mean error (magenta) statistics for all three stations in TWIND2X30.

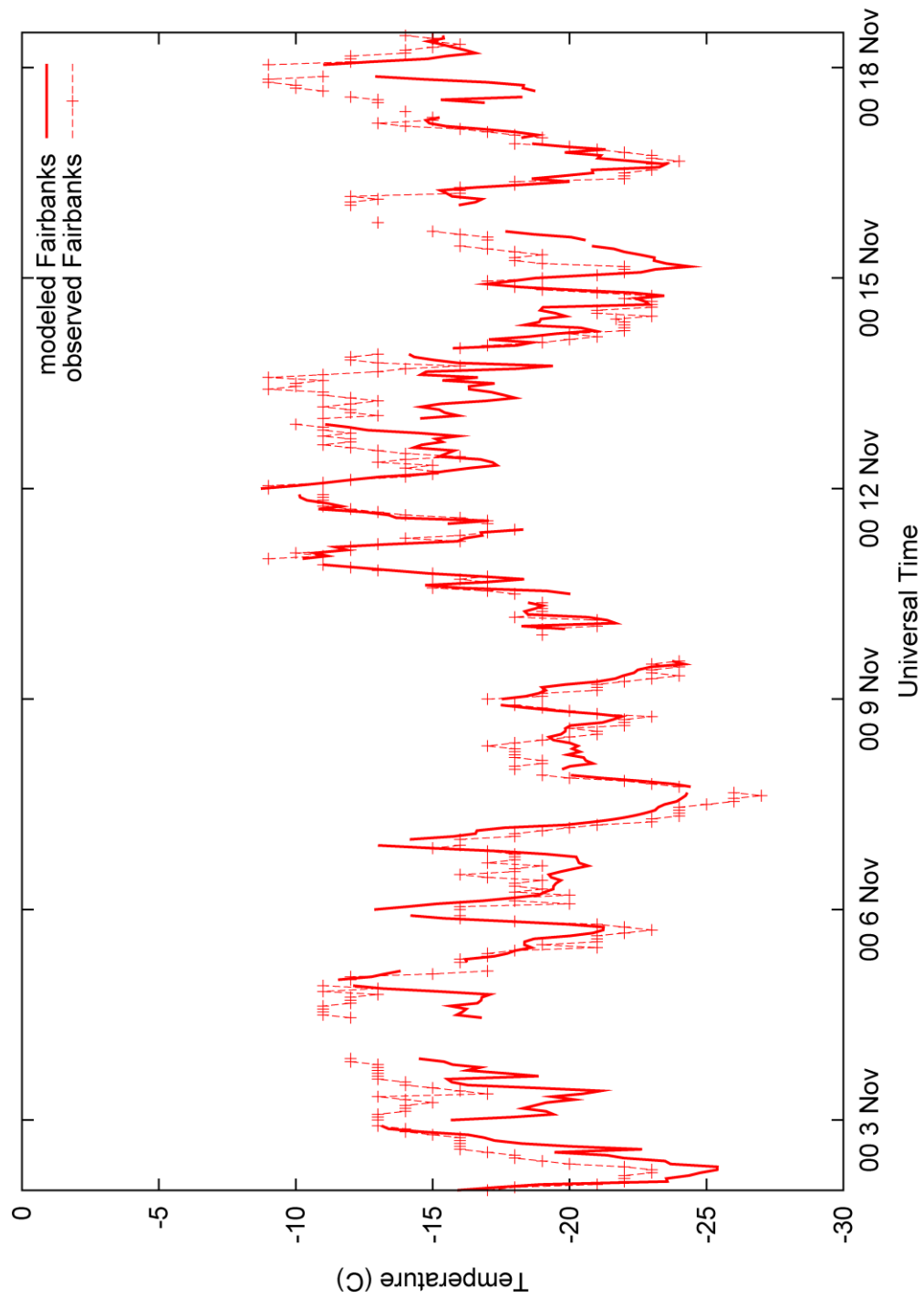


Figure 49: Time series of modeled and observed temperature for Fairbanks in TWIND2X30.

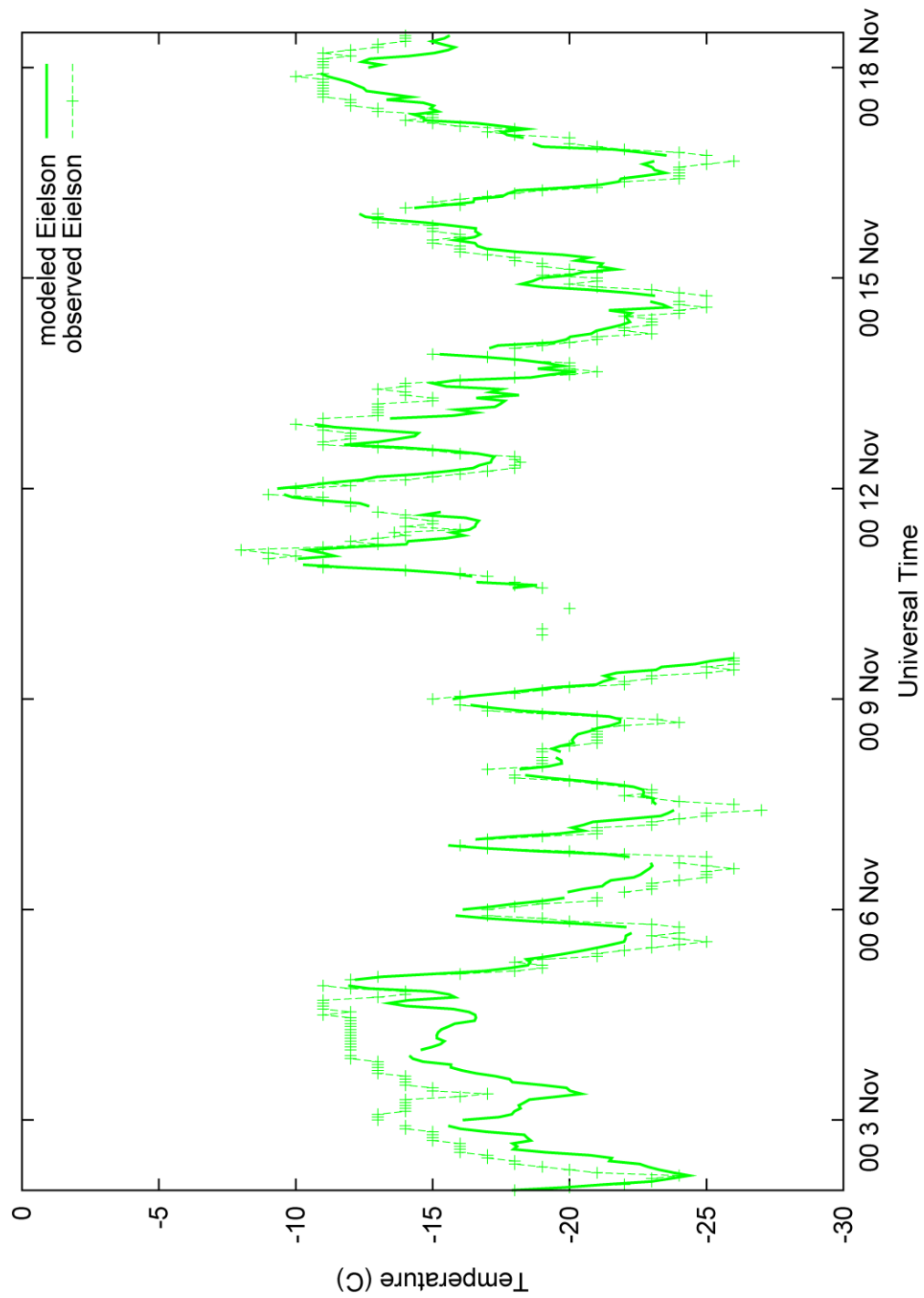


Figure 50: Time series of modeled and observed temperature for Eielson in TWIND2X30.

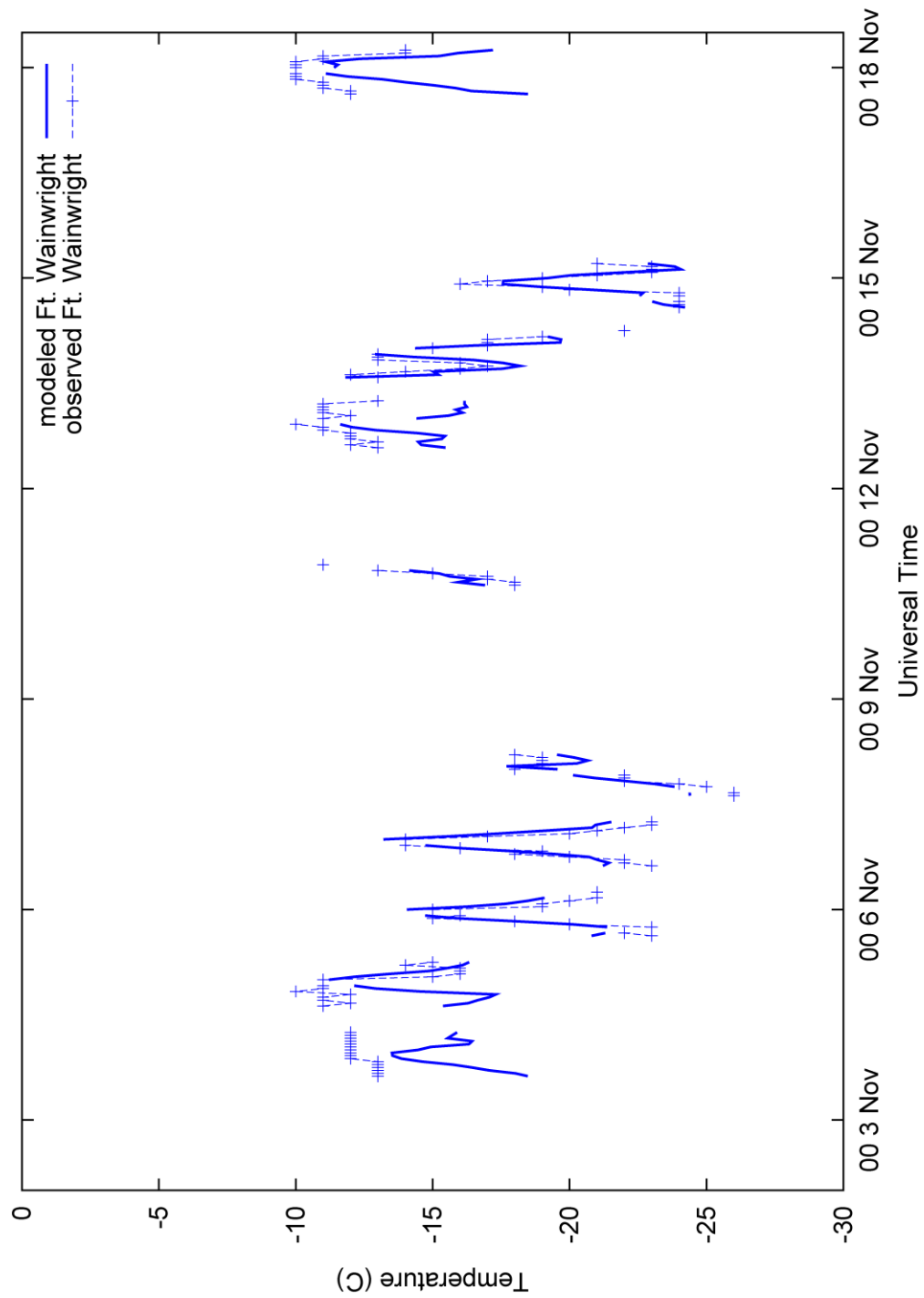


Figure 51: Time series of modeled and observed temperature for Ft. Wainwright in TWIND2X30.

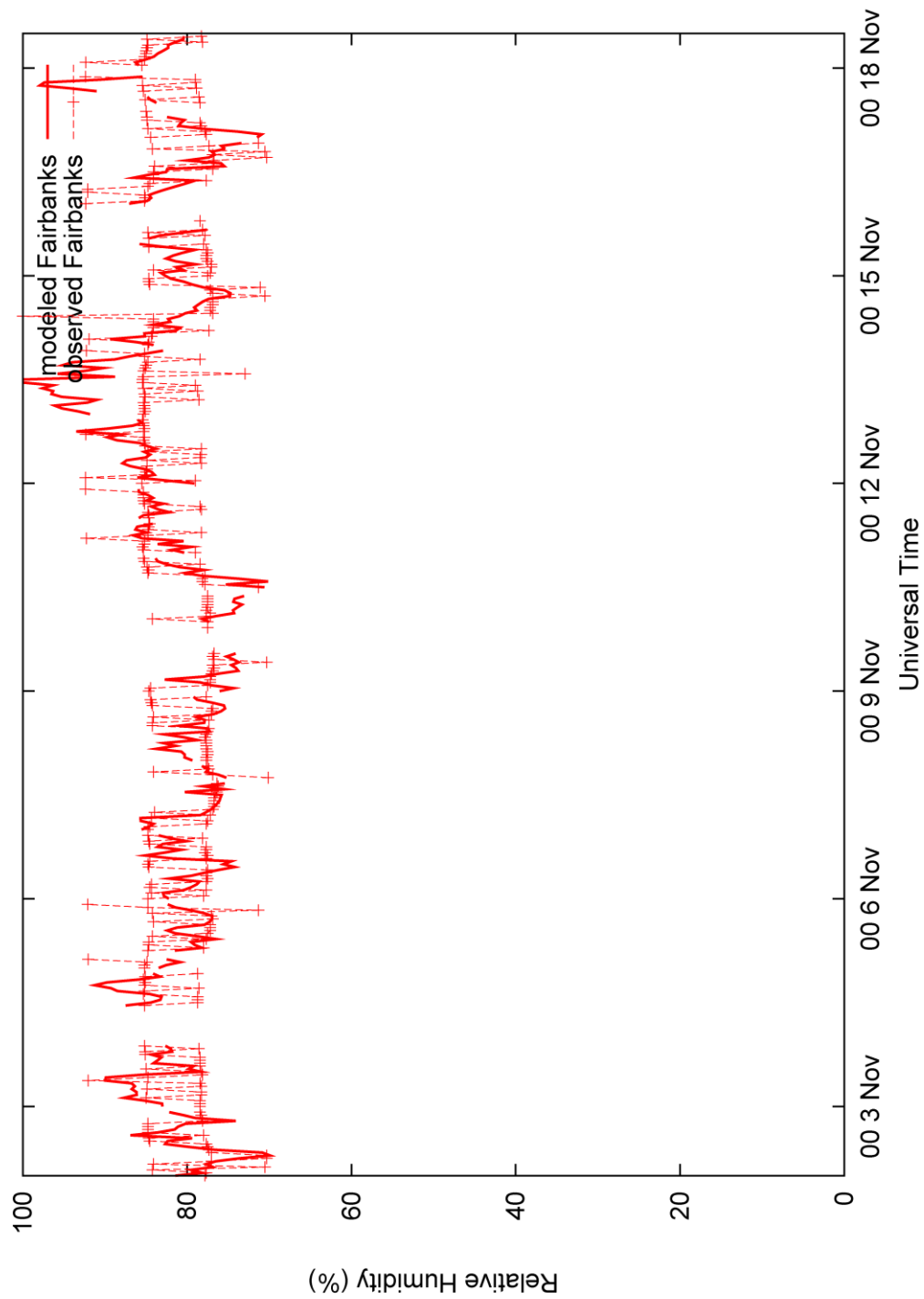


Figure 52: Time series of modeled and observed relative humidity for Fairbanks in TWIND2X30.

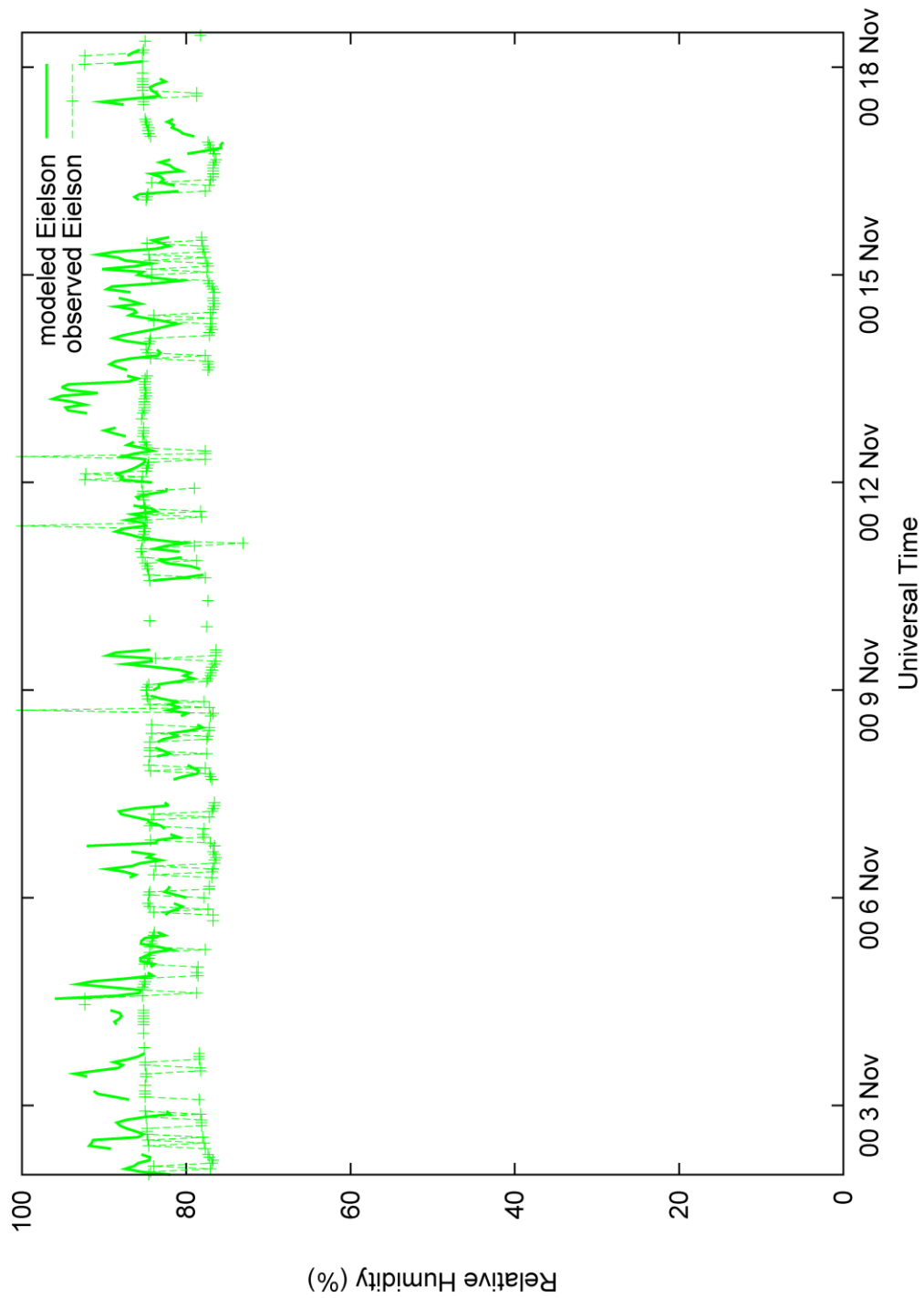


Figure 53: Time series of modeled and observed relative humidity for Eielson in TWIND2X30.

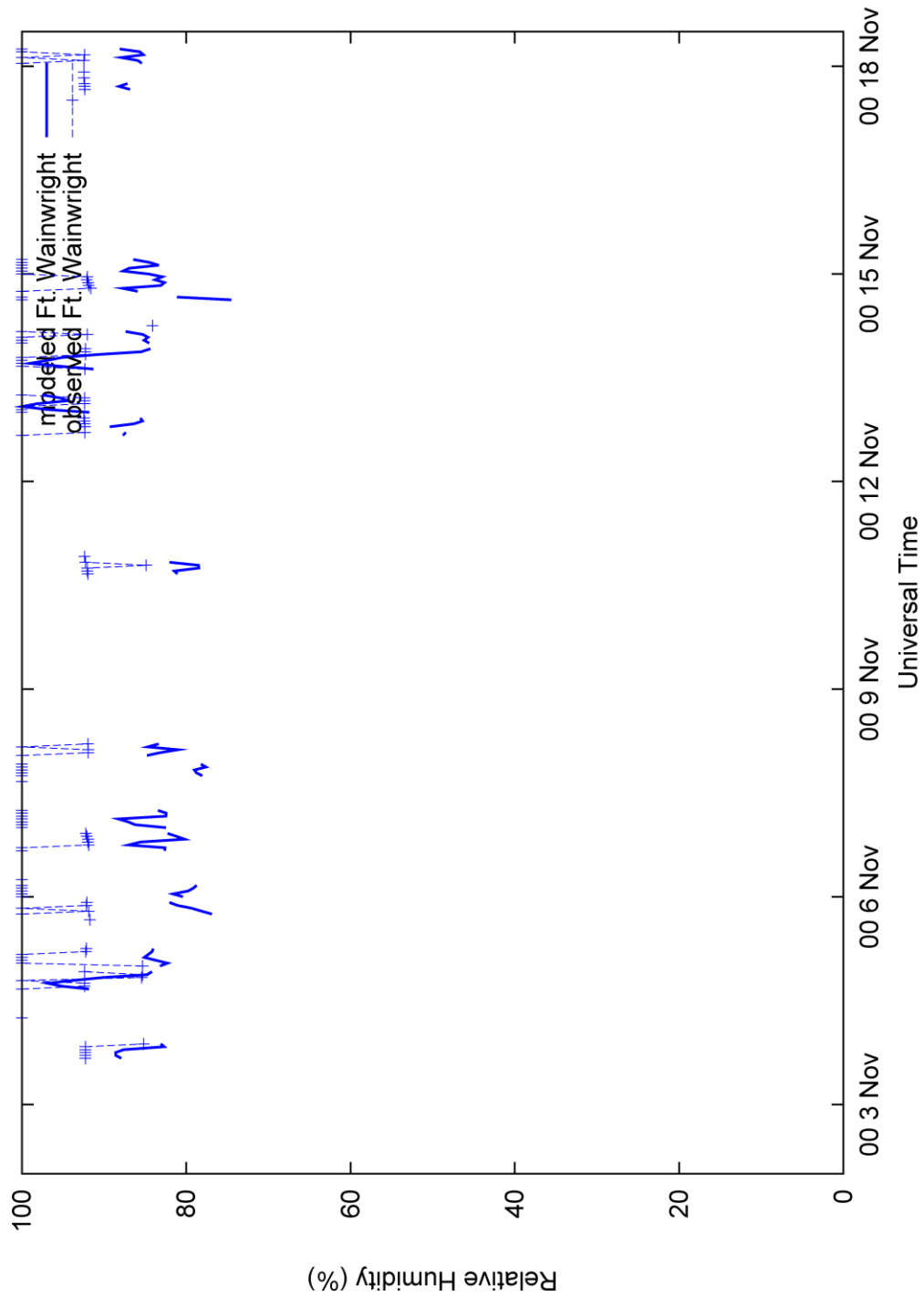


Figure 54: Time series of modeled and observed relative humidity for Ft. Wainwright in TWIND2X30.

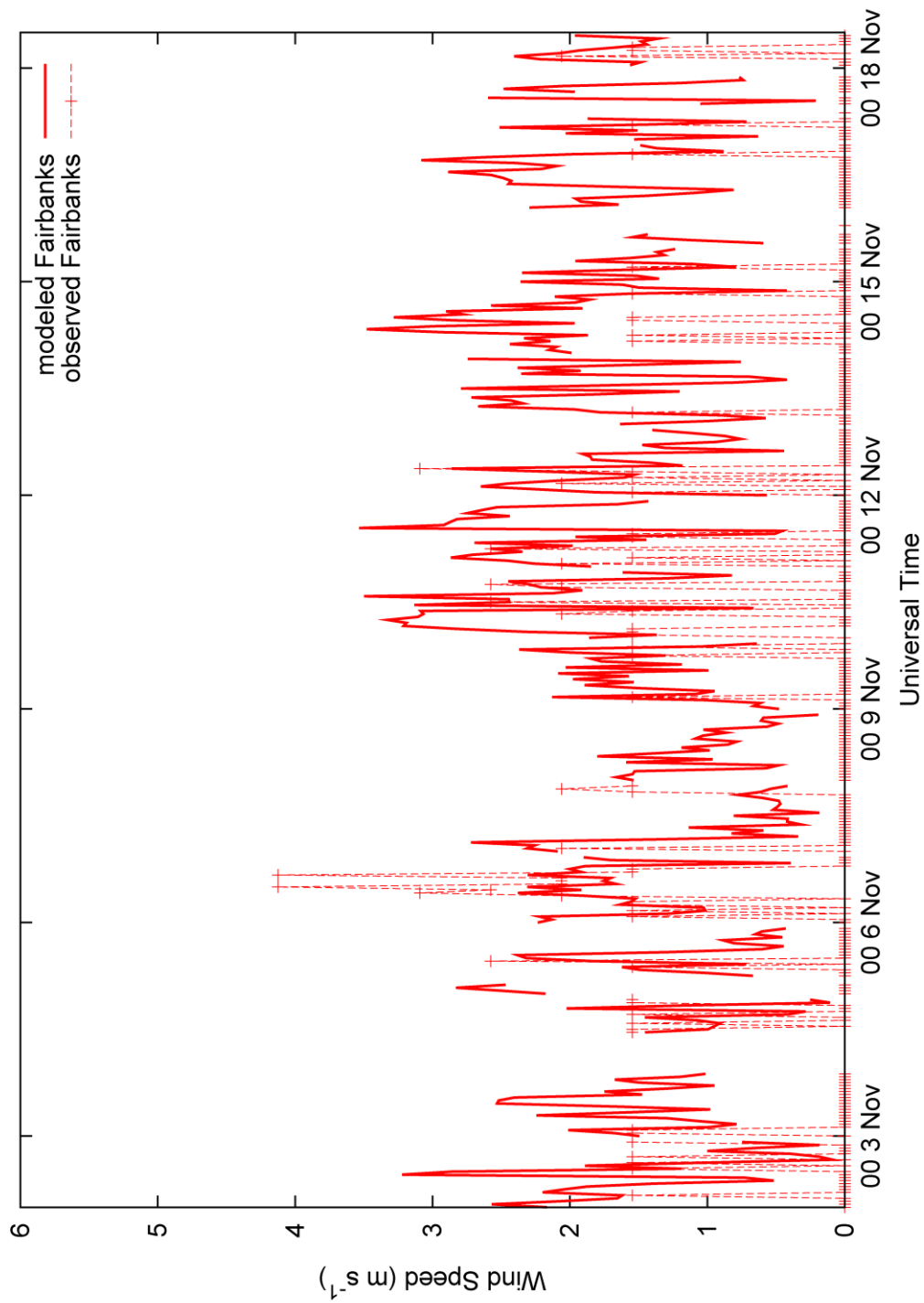


Figure 55: Time series of modeled and observed wind speed for Fairbanks in TWIND2X30.

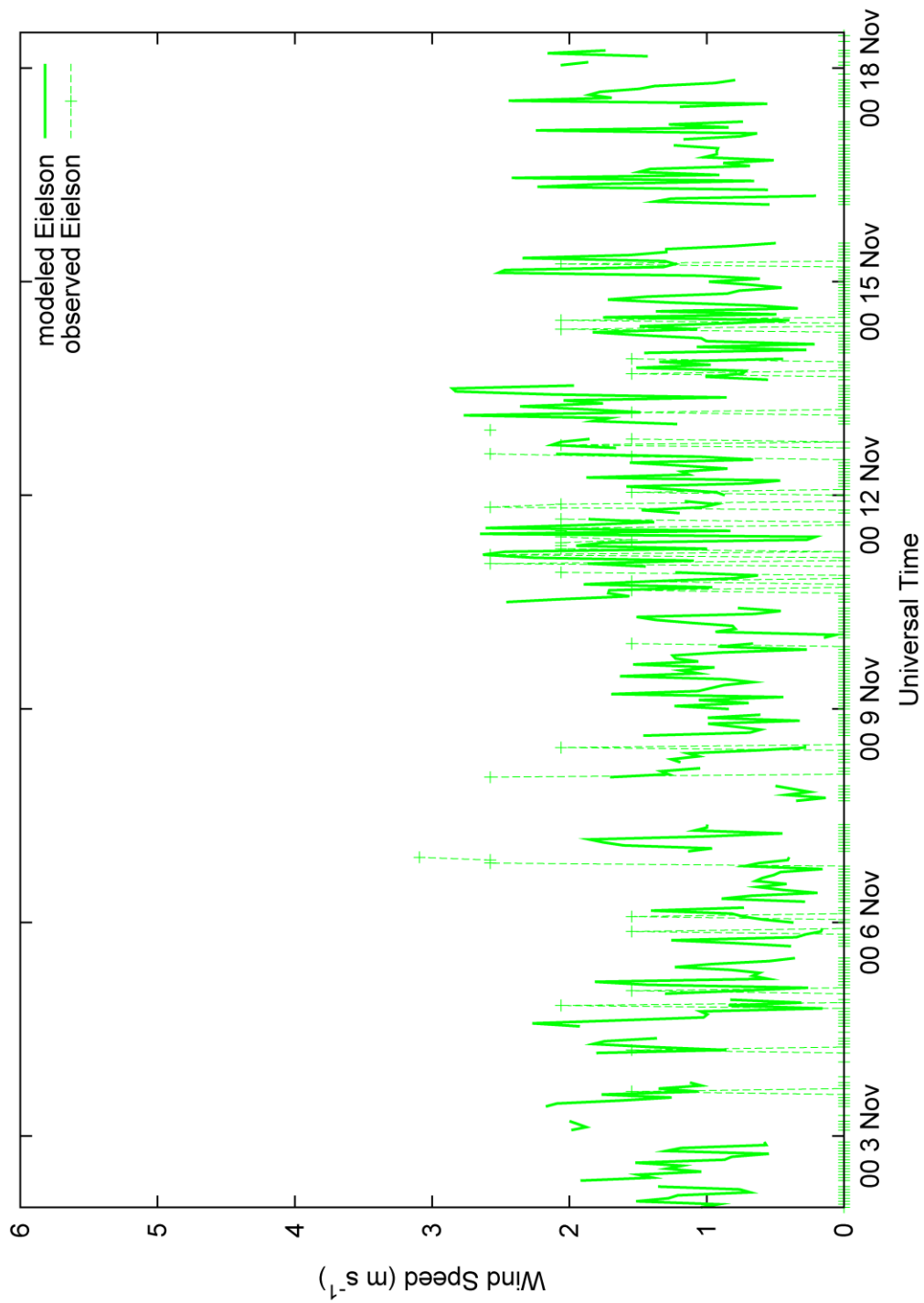


Figure 56: Time series of modeled and observed wind speed for Eielson in TWIND2X30.

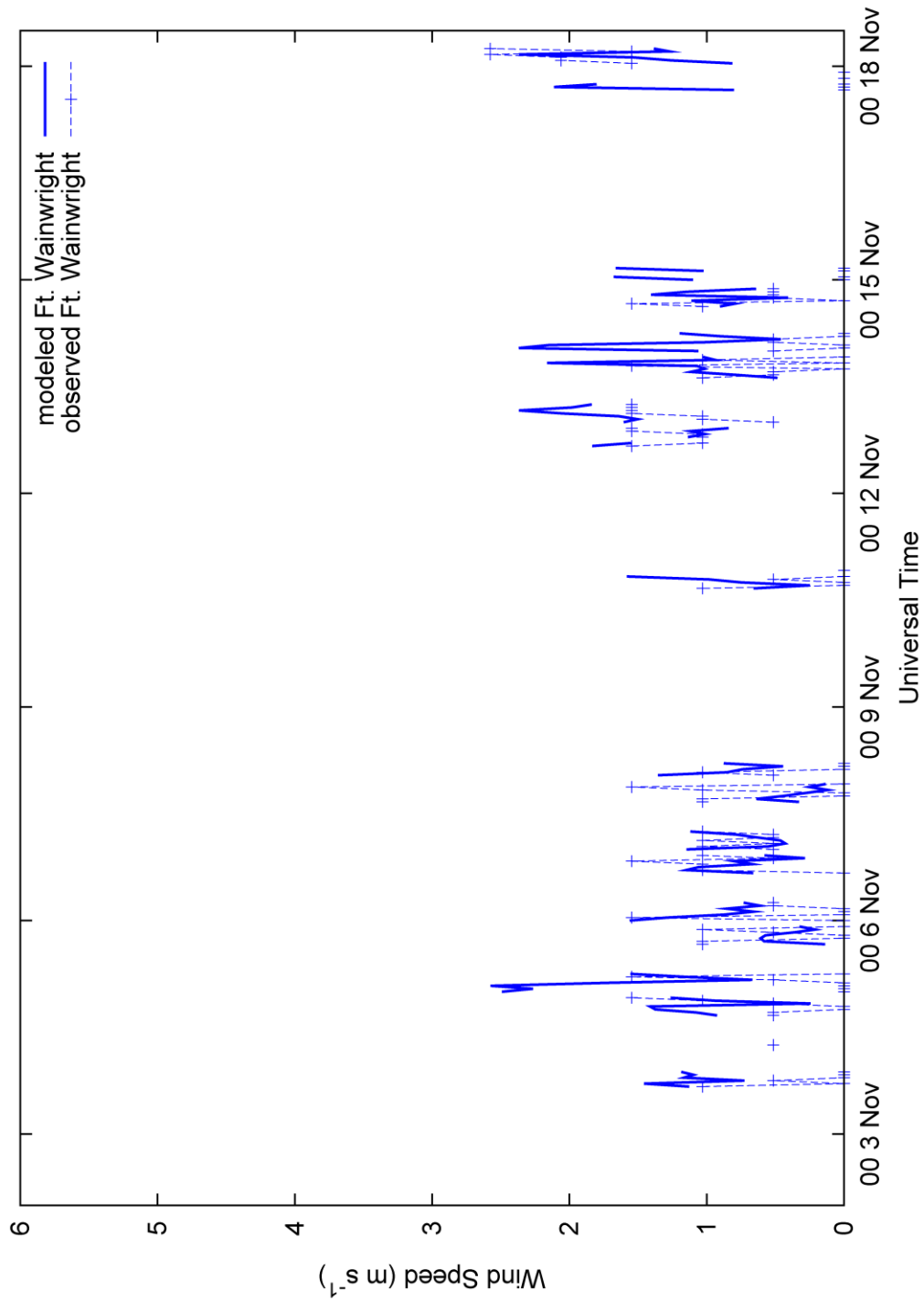


Figure 57: Time series of modeled and observed wind speed for Ft. Wainwright in TWIND2X30.

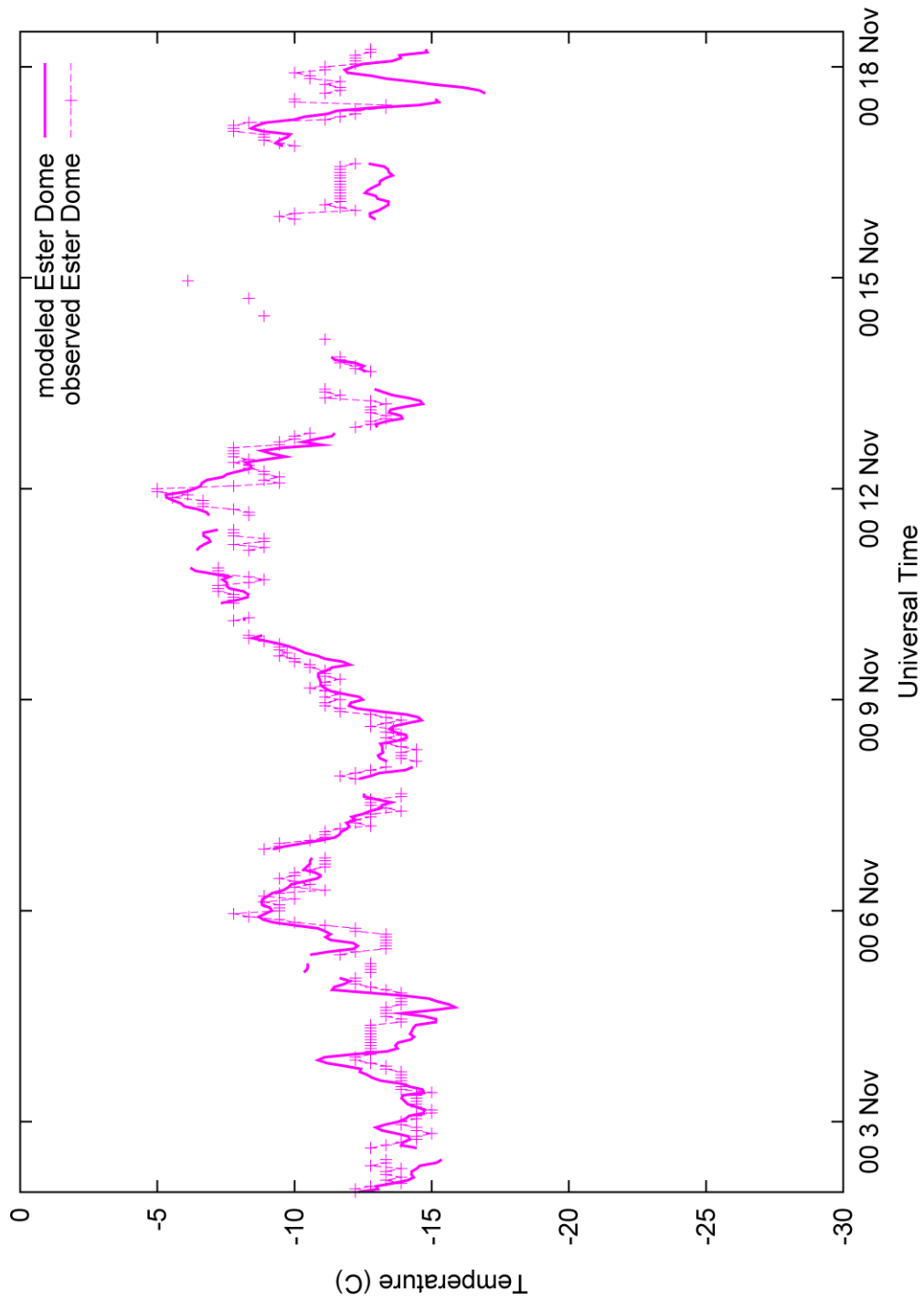


Figure 58: Time series of modeled and observed temperature for Ester Dome in TWIND2X30.

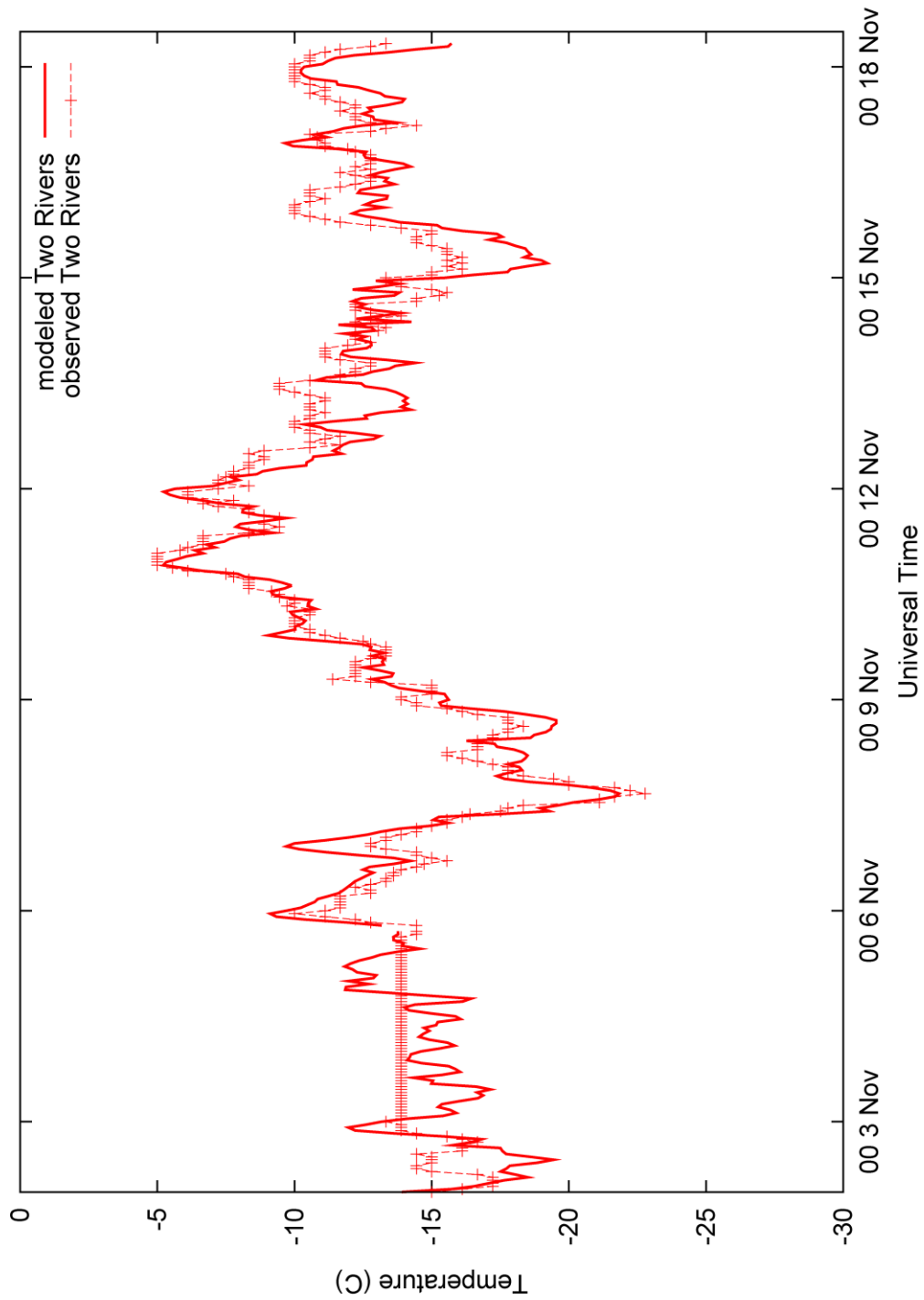


Figure 59: Time series of modeled and observed temperature at Two Rivers in TWIND2X30.

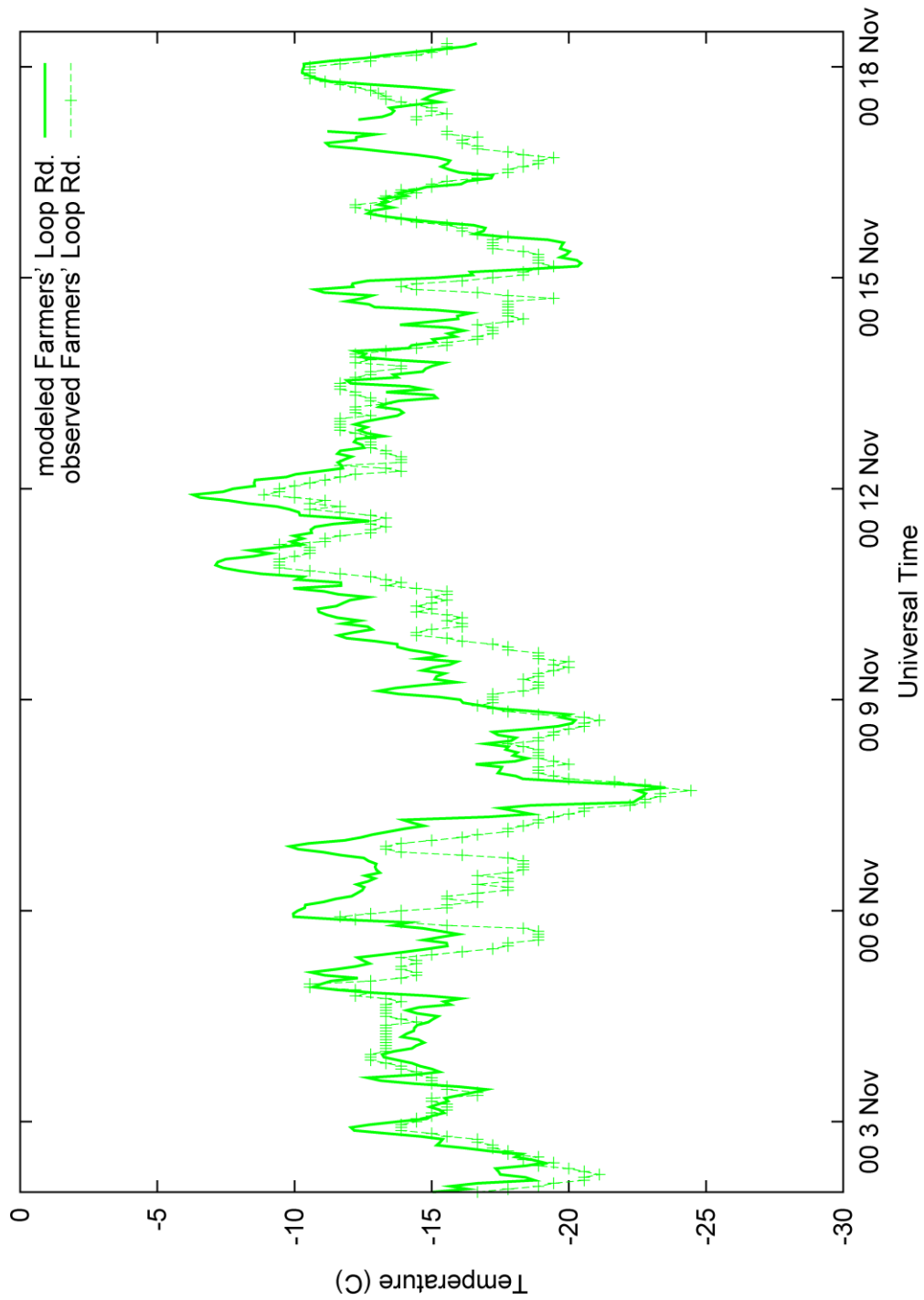


Figure 60: Modeled and observed time series of temperature for Farmers' Loop Rd. in TWIND2X30.

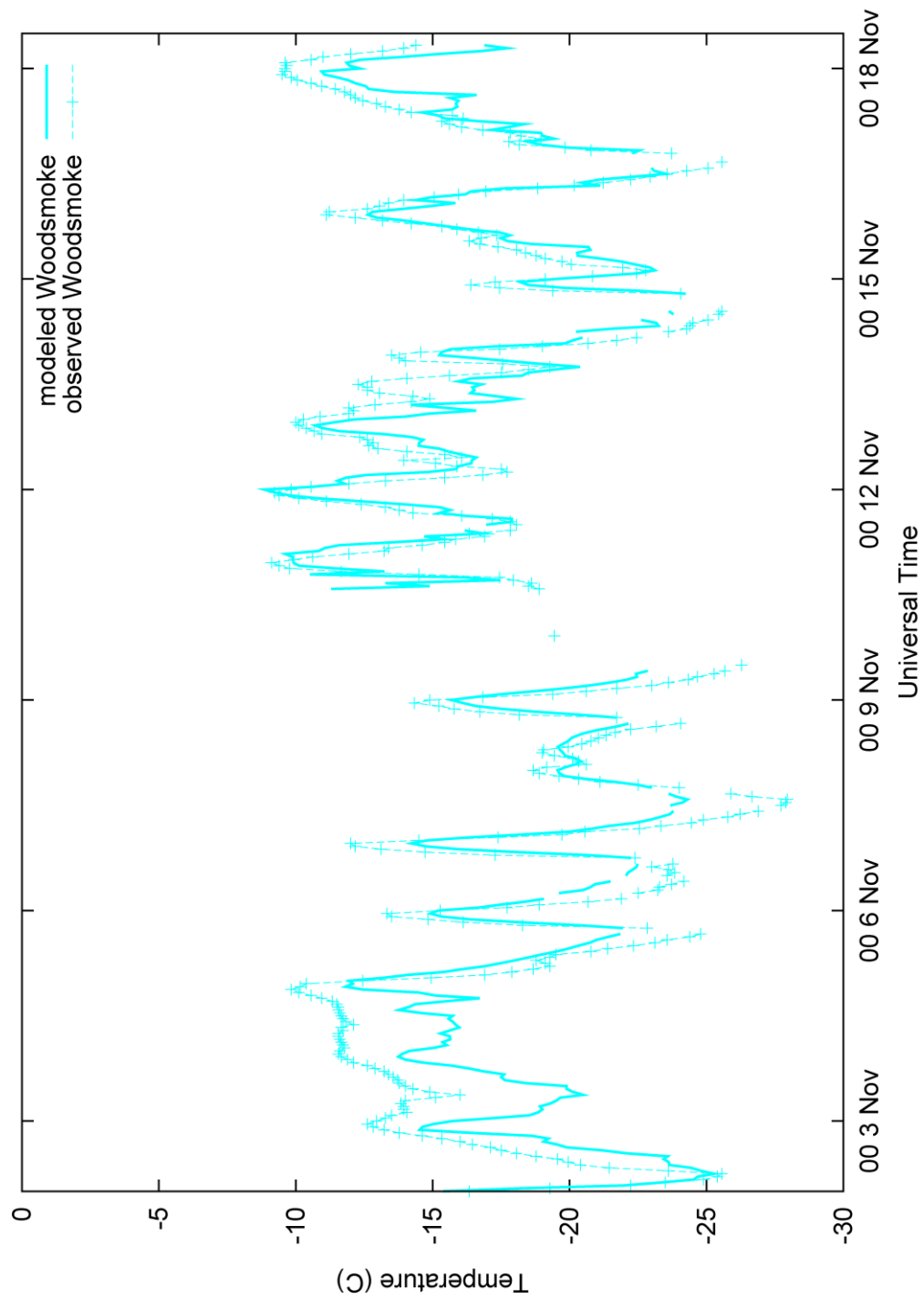


Figure 61: Time series of modeled and observed temperature for Woodsmoke in TWIND2X30.

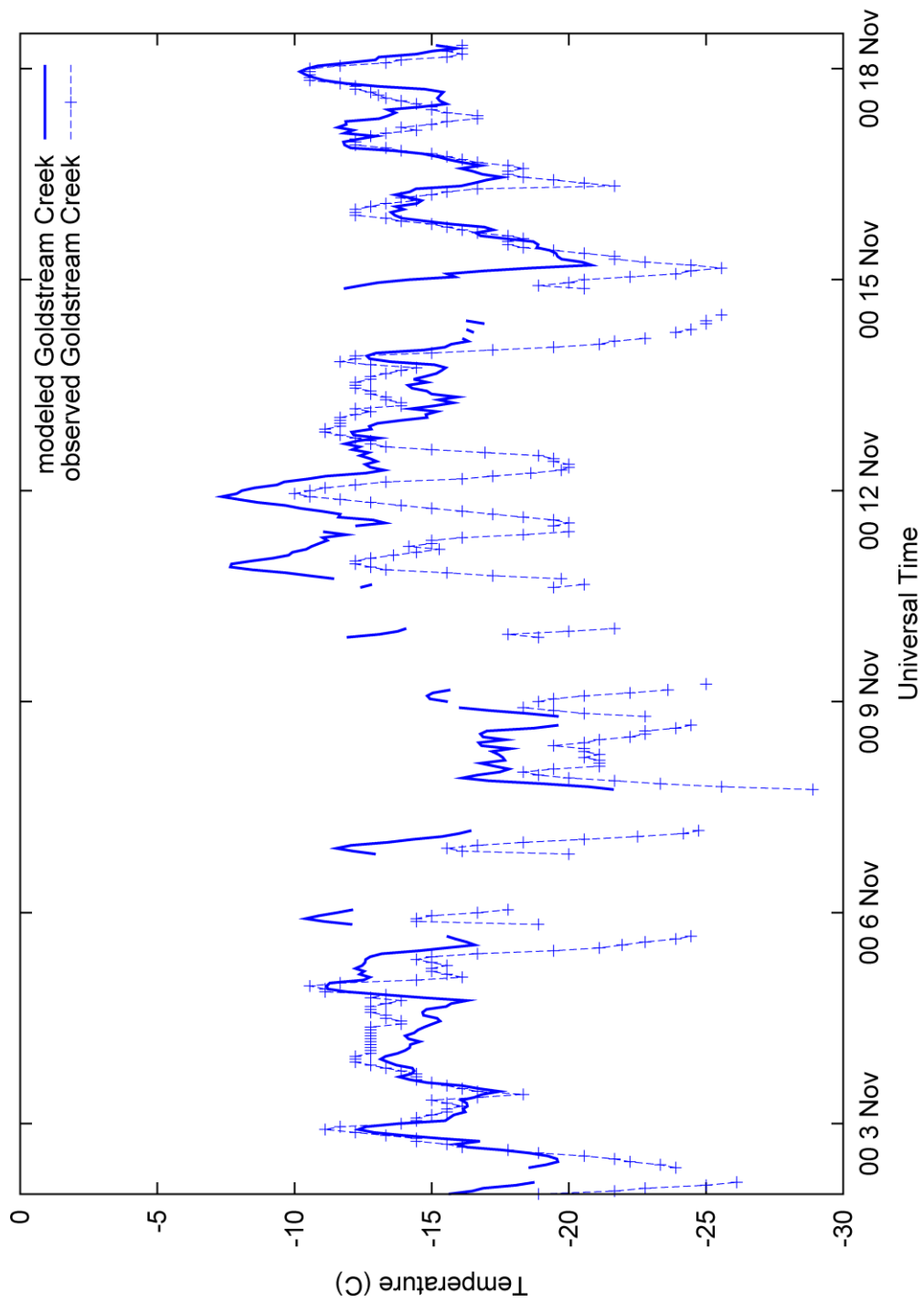


Figure 62: Time series of modeled and observed temperature for Goldstream Creek in TWIND2X30.

**APPENDIX B – Detailed Time-Series Figures of 23 Jan – 12 Feb 2008 Episode, for
TWIND2X30 Configuration**

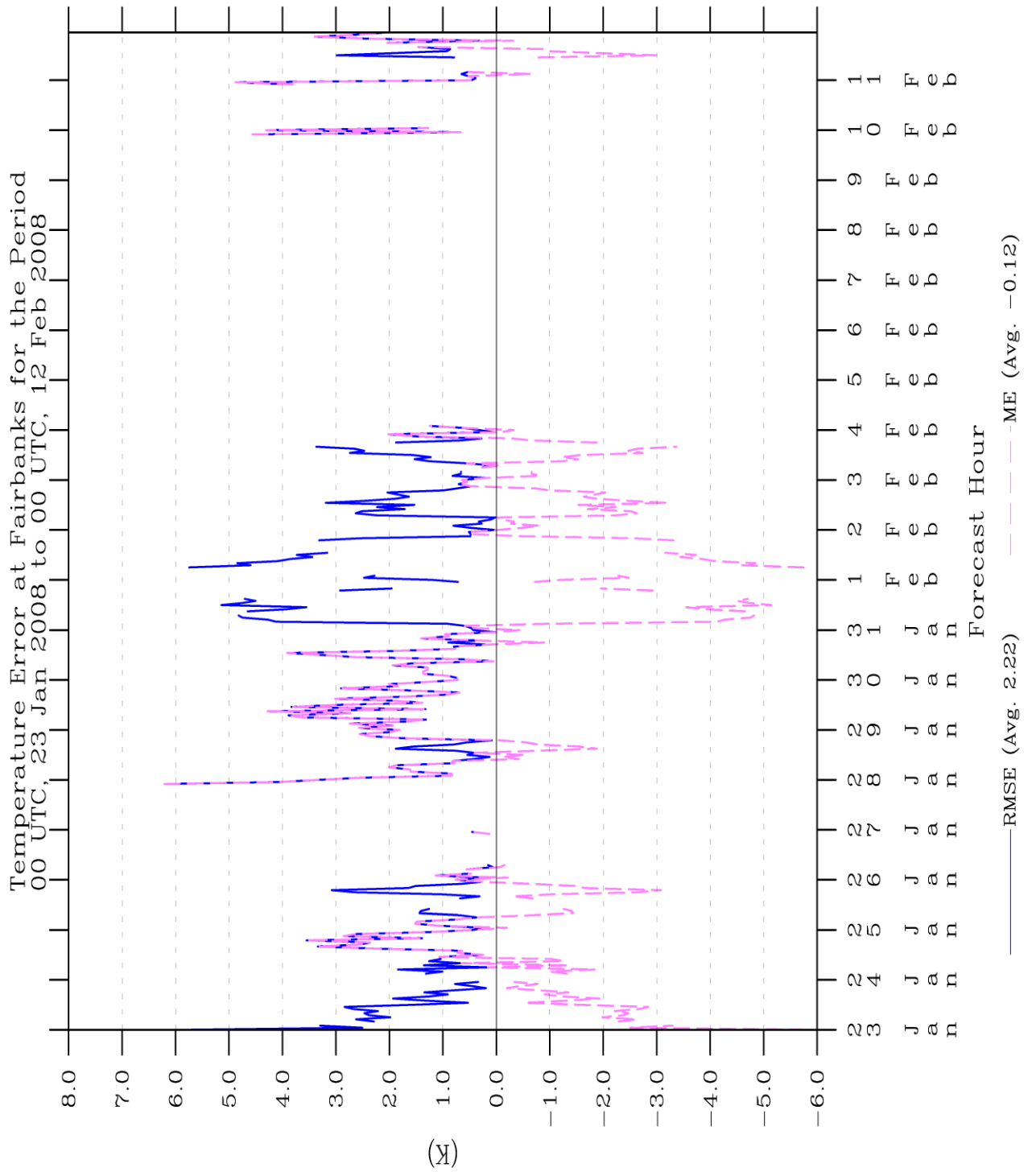


Figure 63: Time series of temperature statistics for Fairbanks in TWIND2X30

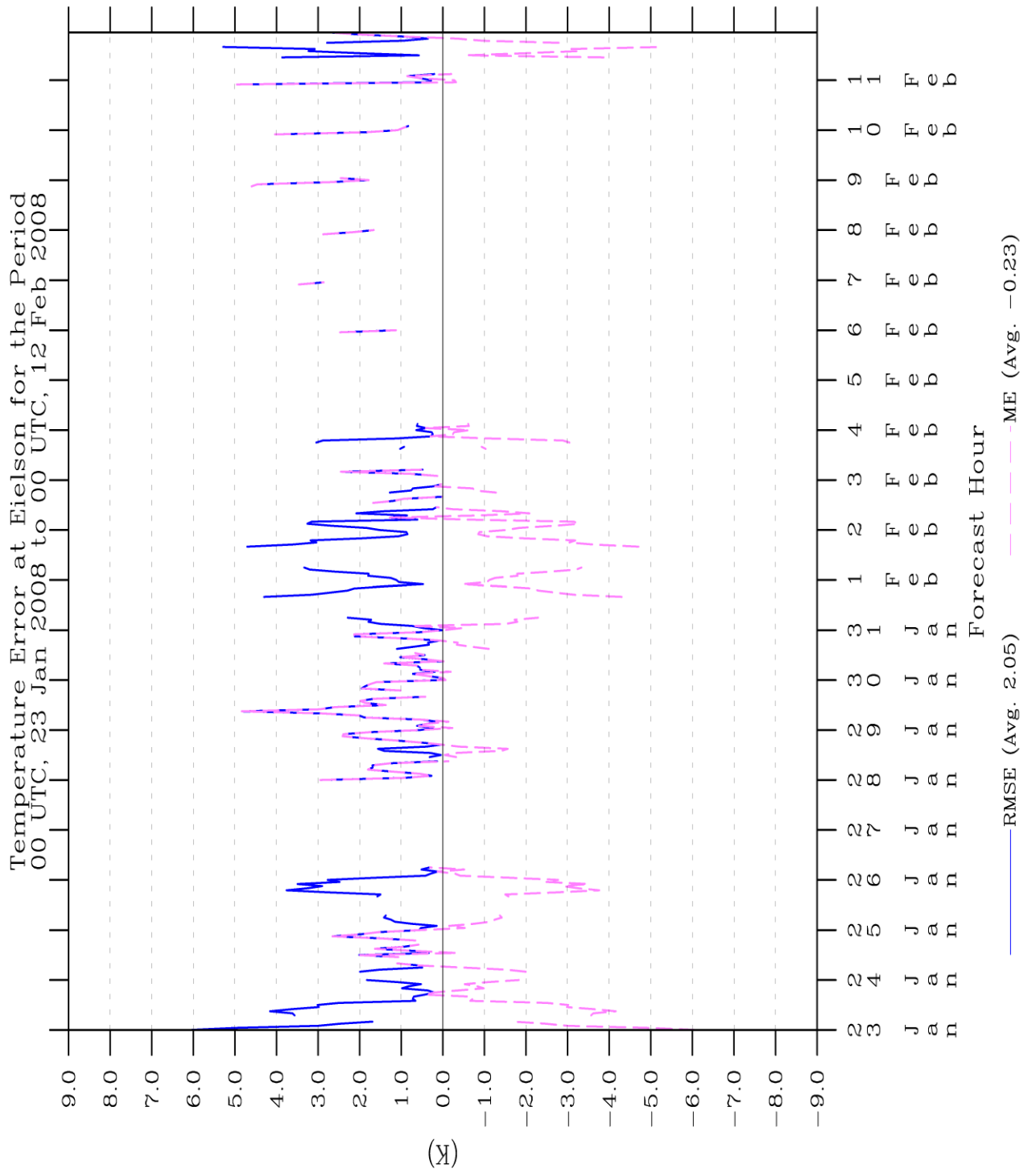


Figure 64: Time series of temperature statistics for Eielson in TWIND2X30.

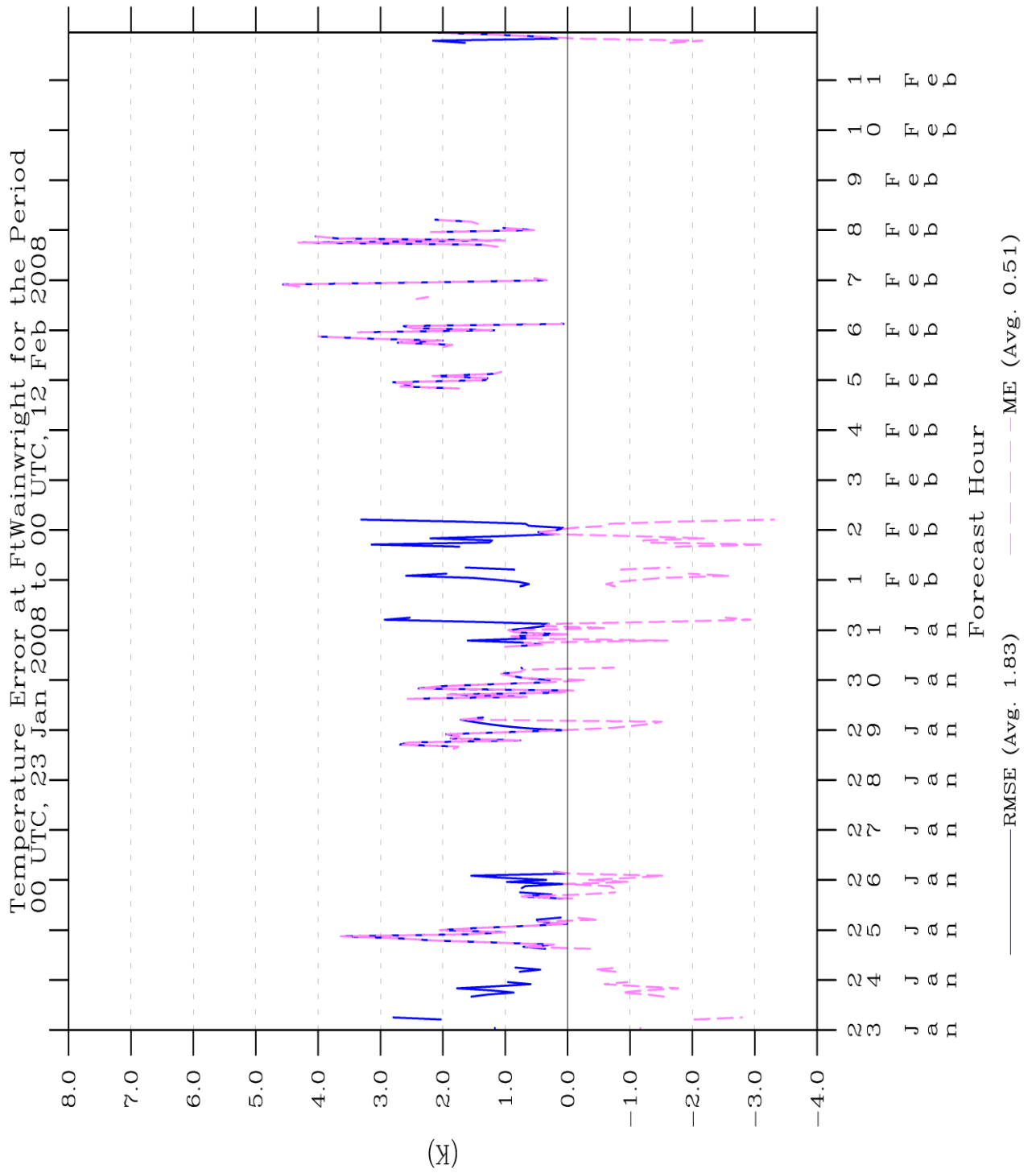


Figure 65: Time series of temperature statistics for Ft. Wainwright in TWIND2X30.

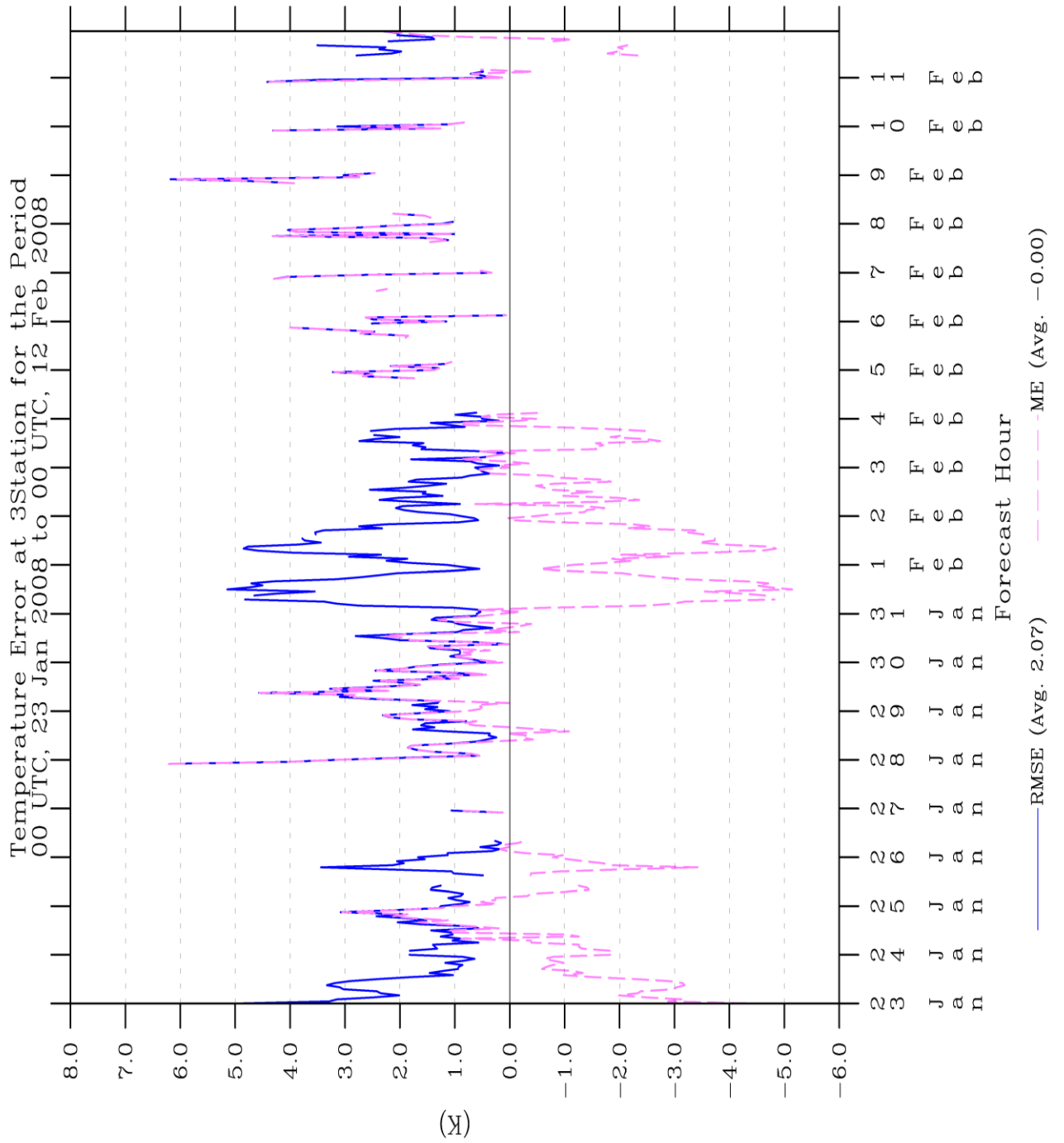


Figure 66: Time series of temperature statistics for all three stations in TWIND2X30.

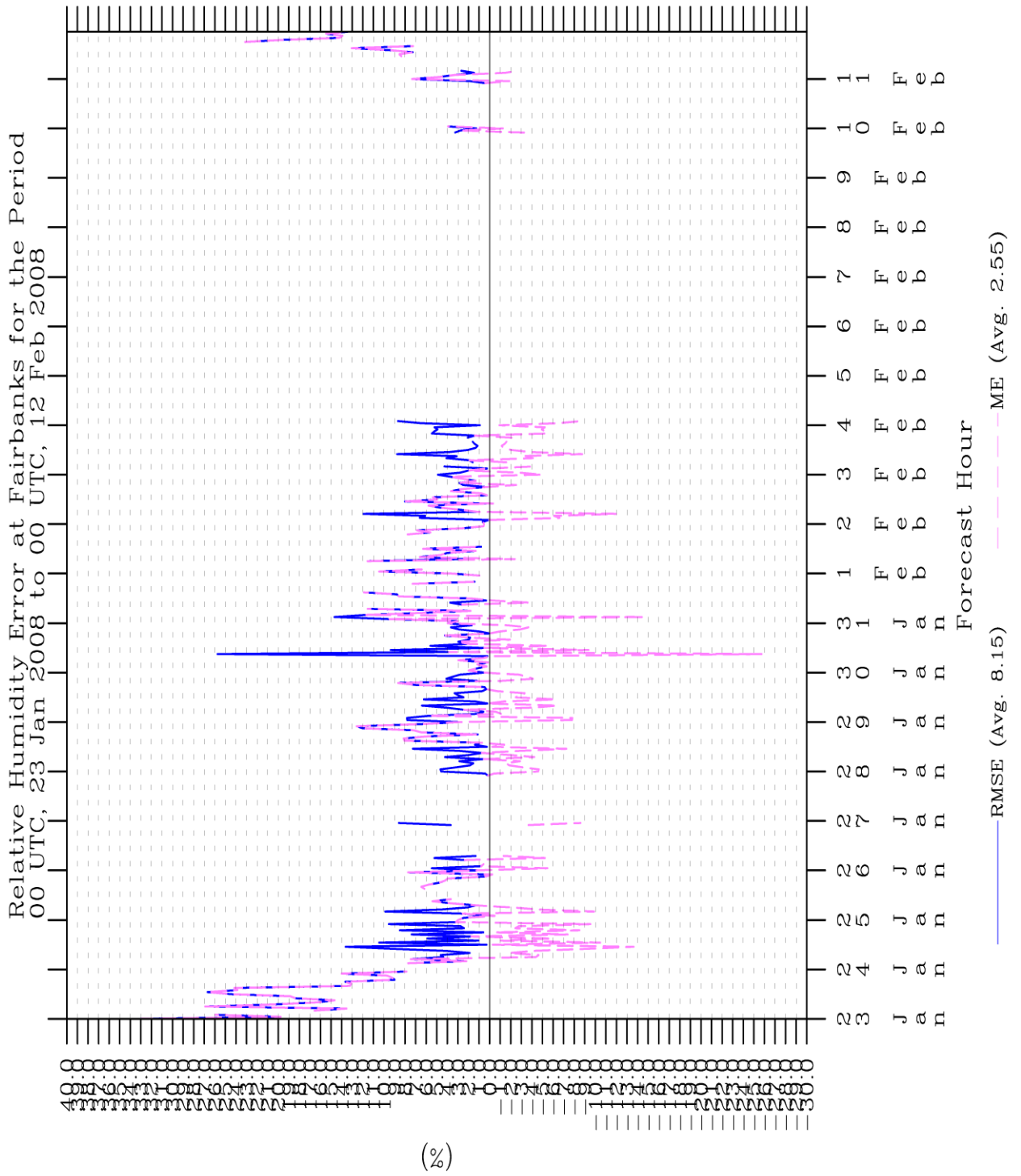


Figure 67: Time series of relative humidity statistics for Fairbanks in TWIND2X30.

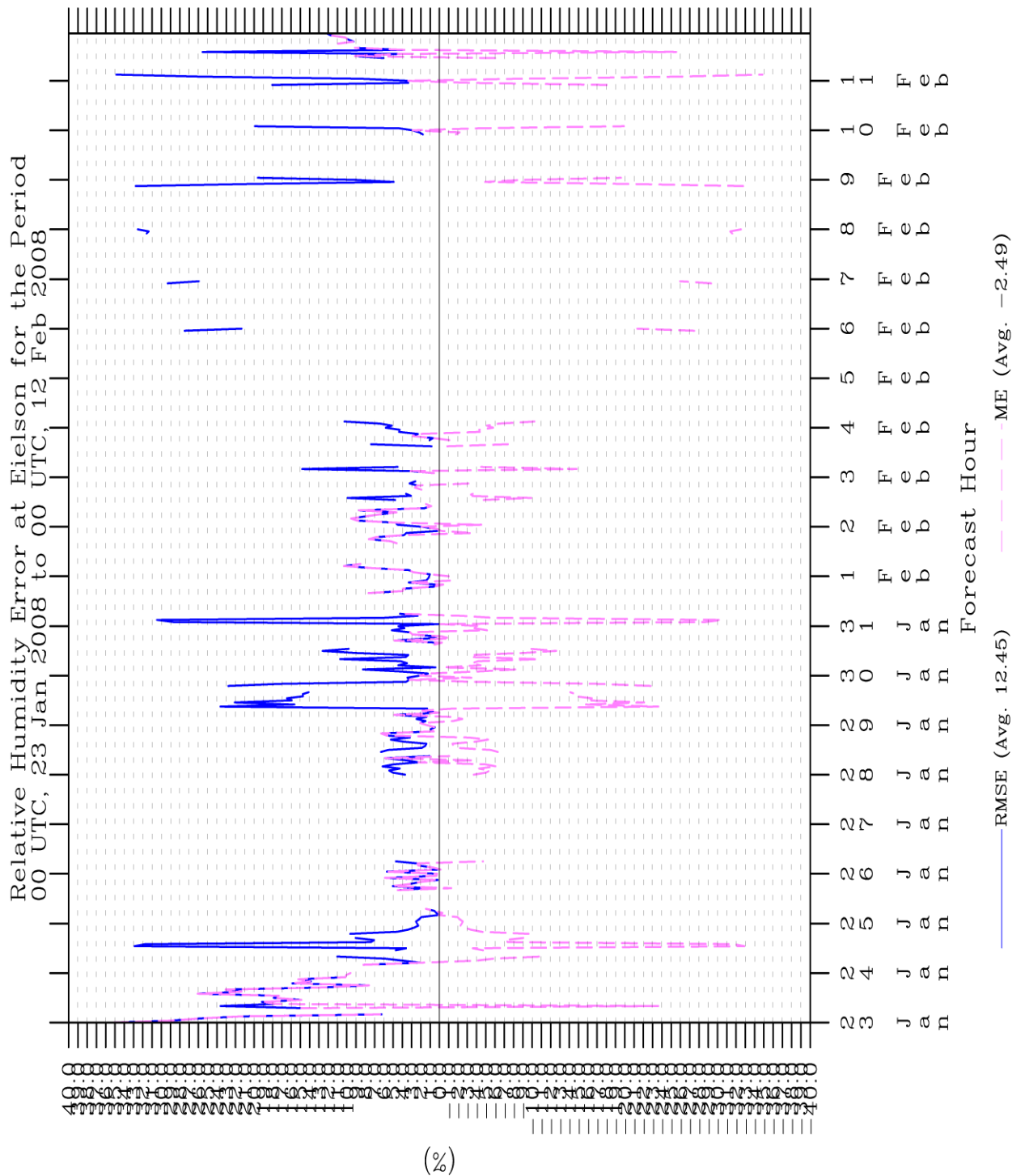


Figure 68: Time series of relative humidity statistics for Eielson in TWIND2X30.

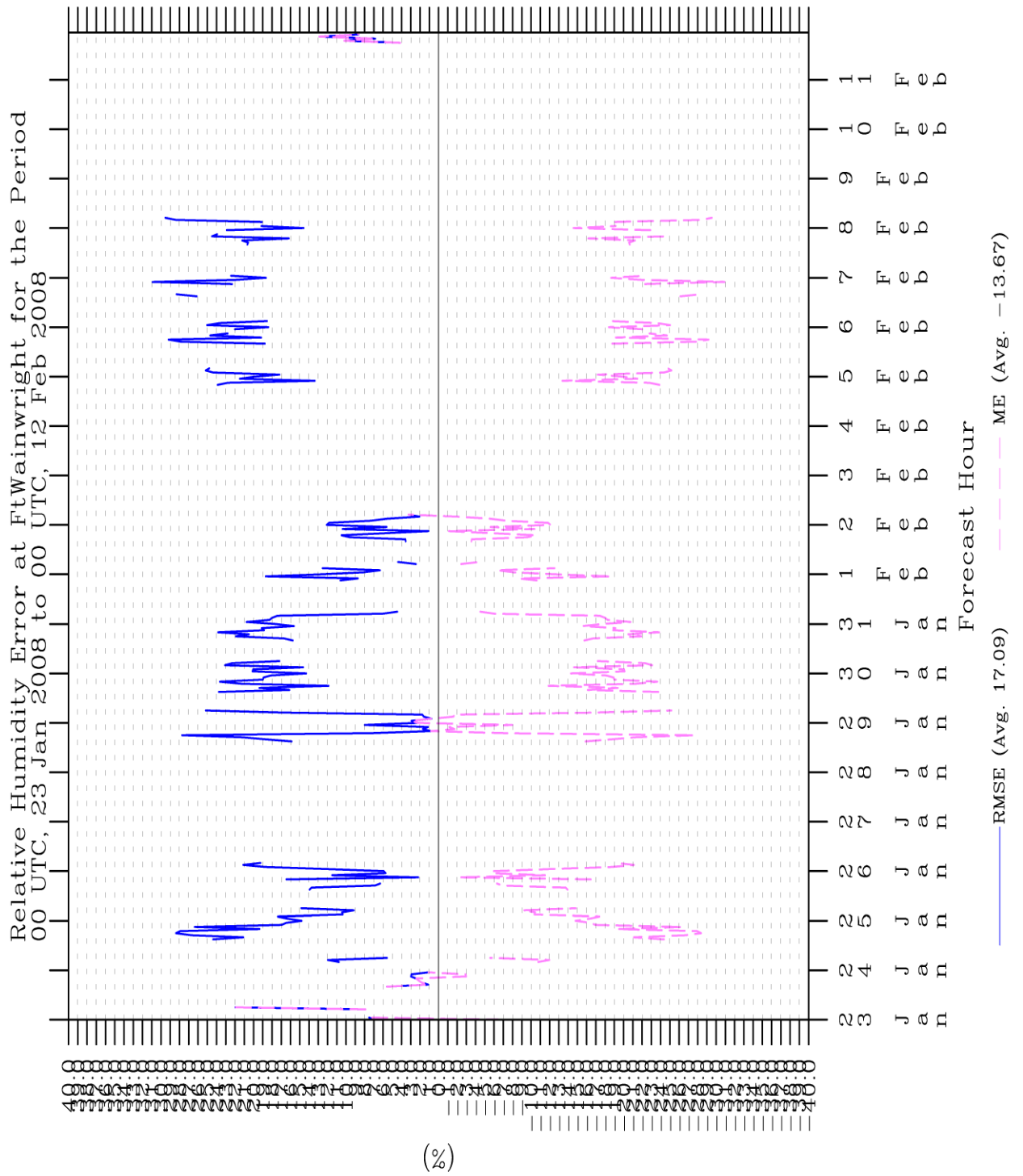


Figure 69: Time series of relative humidity statistics for Ft. Wainwright in TWIND2X30.

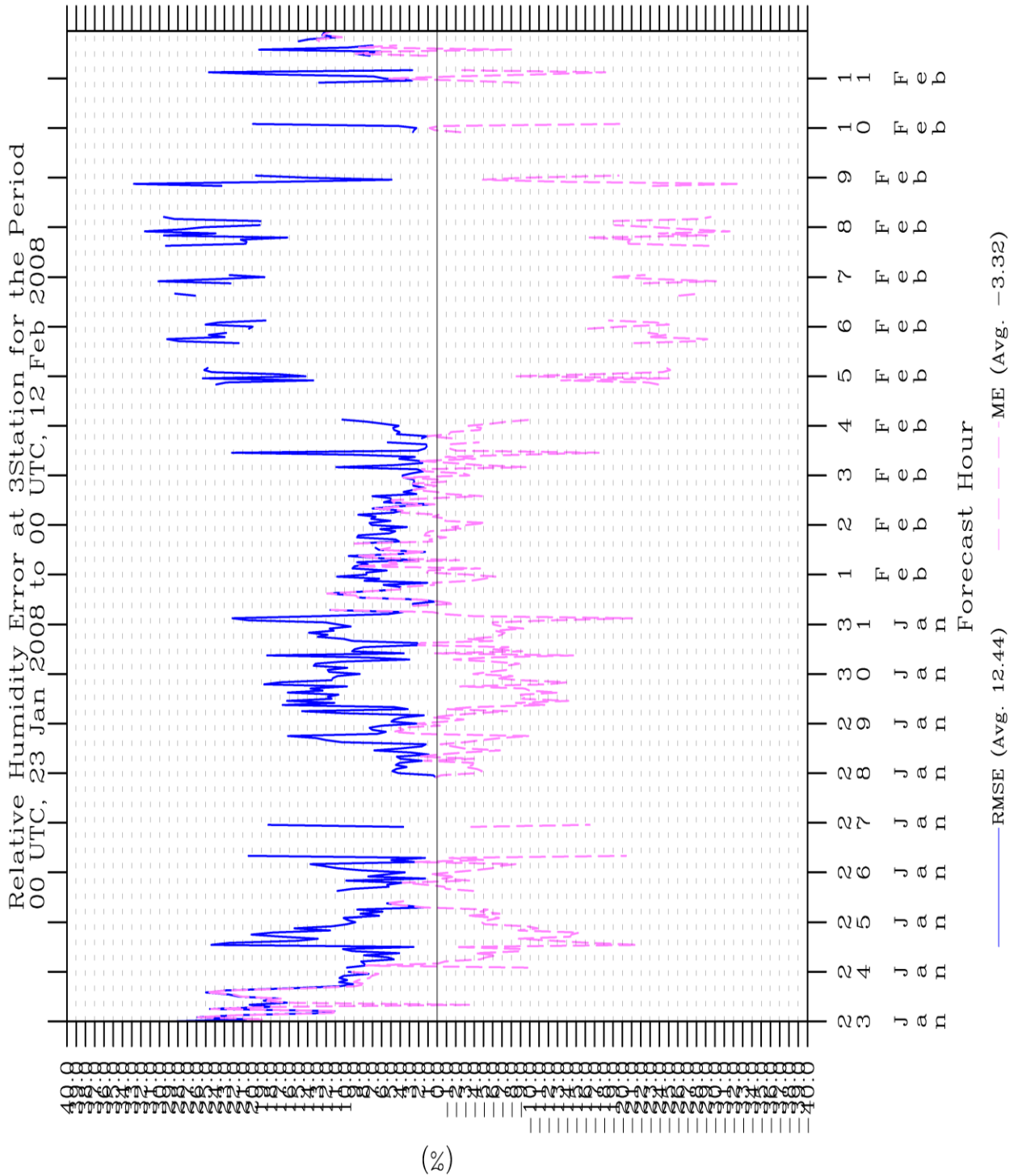


Figure 70: Time series of relative humidity statistics for all three stations in TWIND2X30.

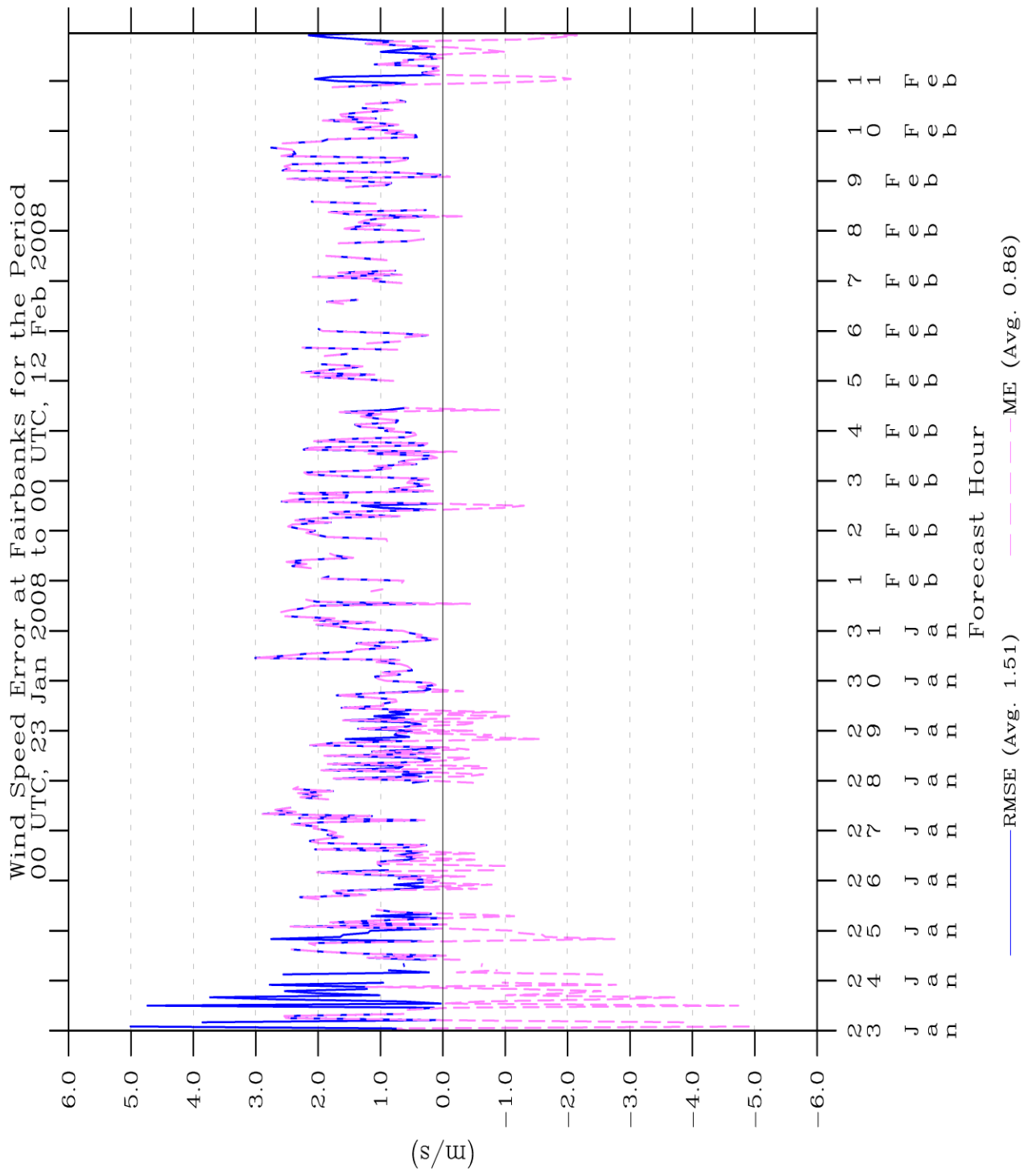


Figure 71: Time series of wind speed statistics for Fairbanks in TWIND2X30.

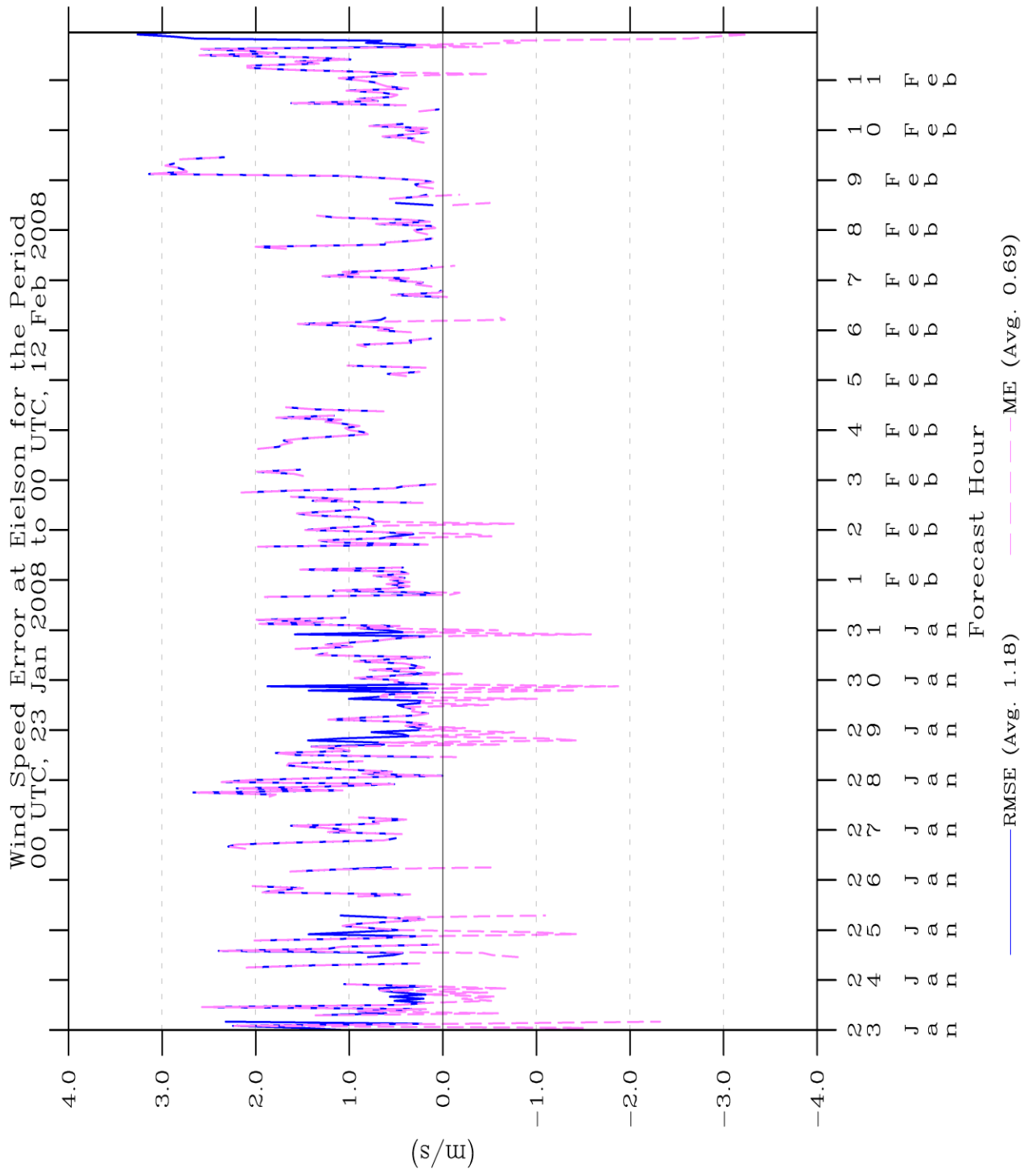


Figure 72: Time series of wind speed statistics for Eielson in TWIND2X30.

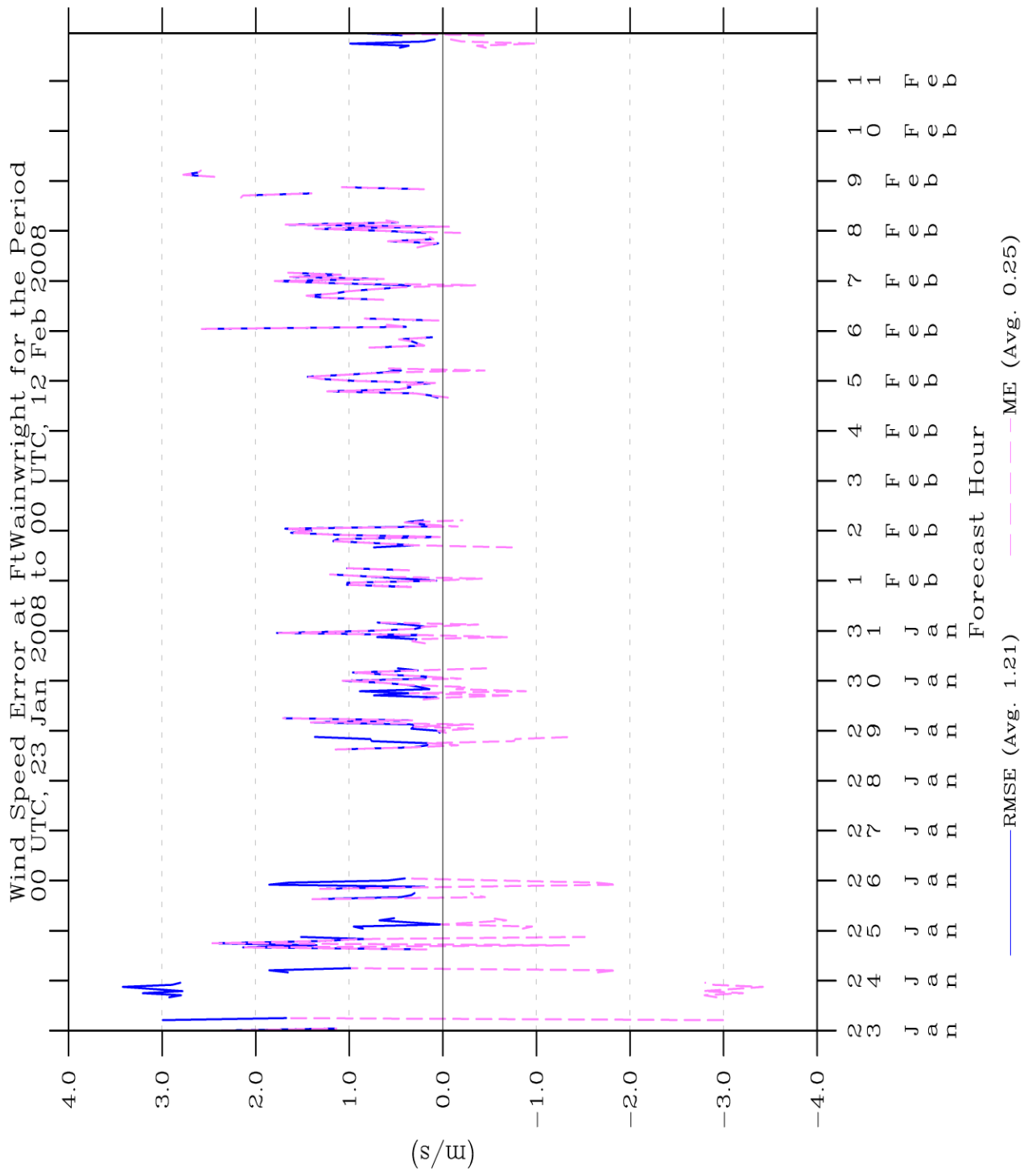


Figure 73: Time series of wind speed statistics for Ft. Wainwright in TWIND2X30.

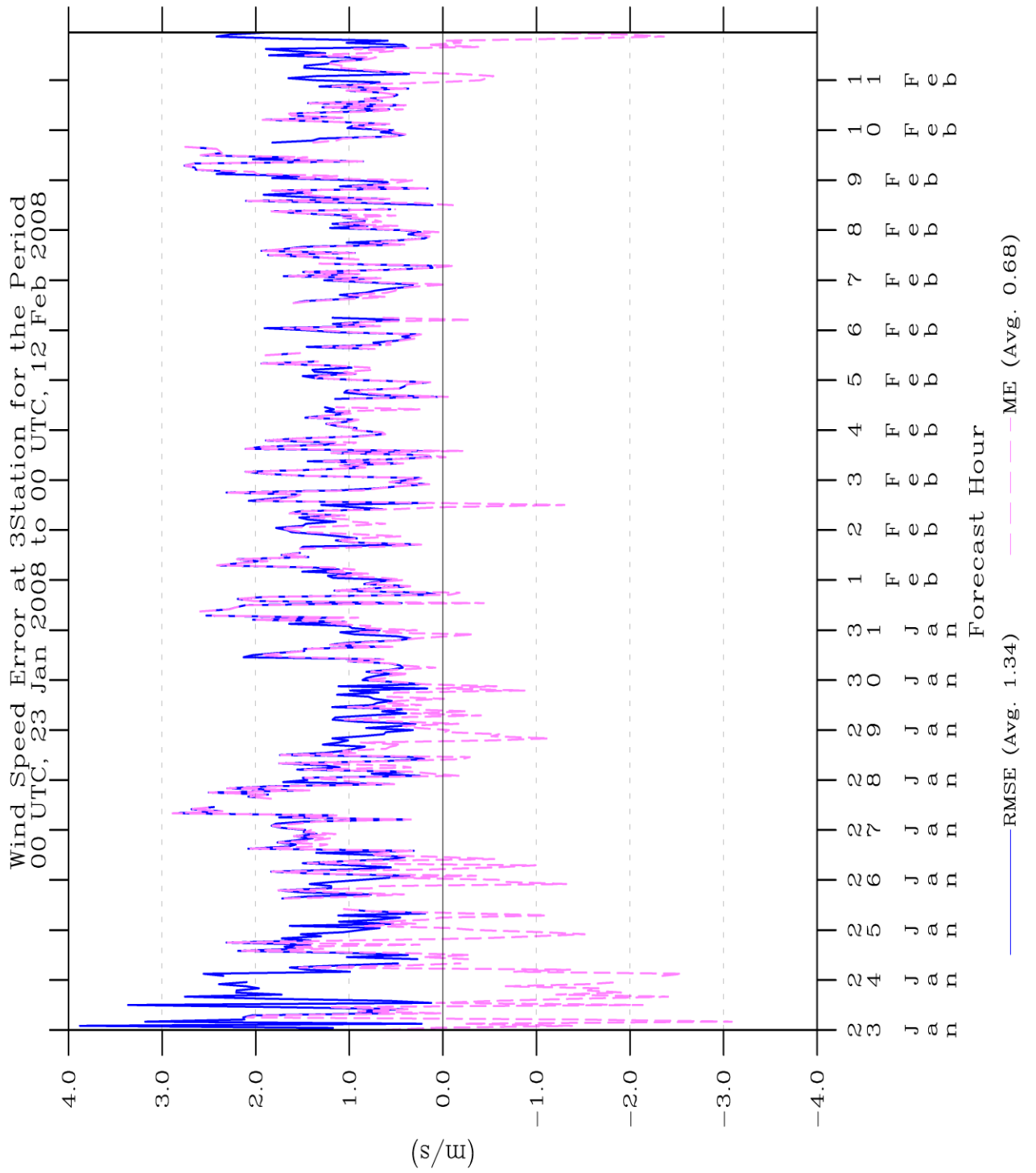


Figure 74: Time series of wind speed statistics for all three stations in TWIND2X30.

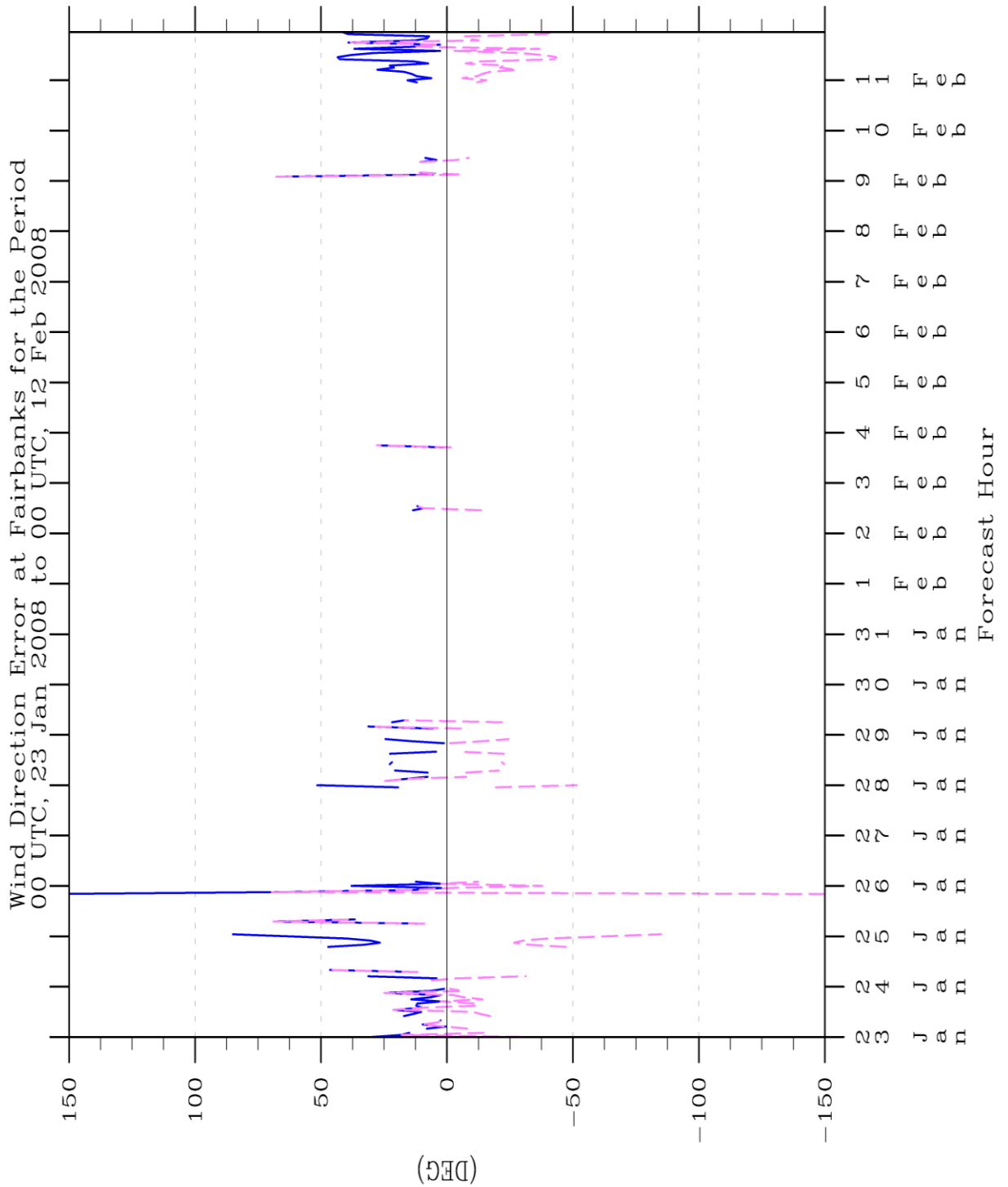


Figure 75: Time series of wind direction mean absolute error (blue) and mean error (magenta) statistics for Fairbanks in TWIND2X30.

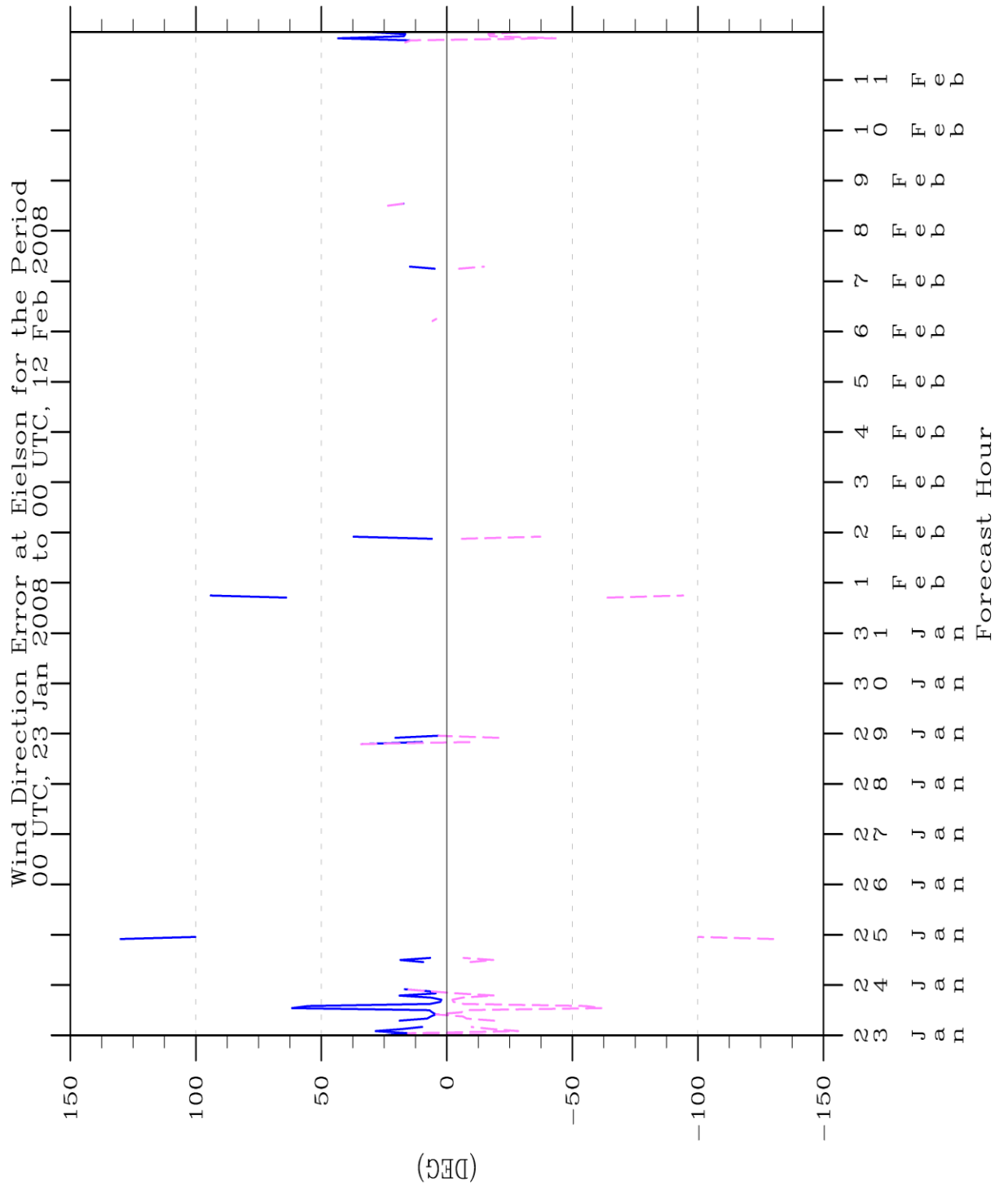


Figure 76: Time series of wind direction mean absolute error (blue) and mean error (magenta) statistics for Eielson in TWIND2X30.

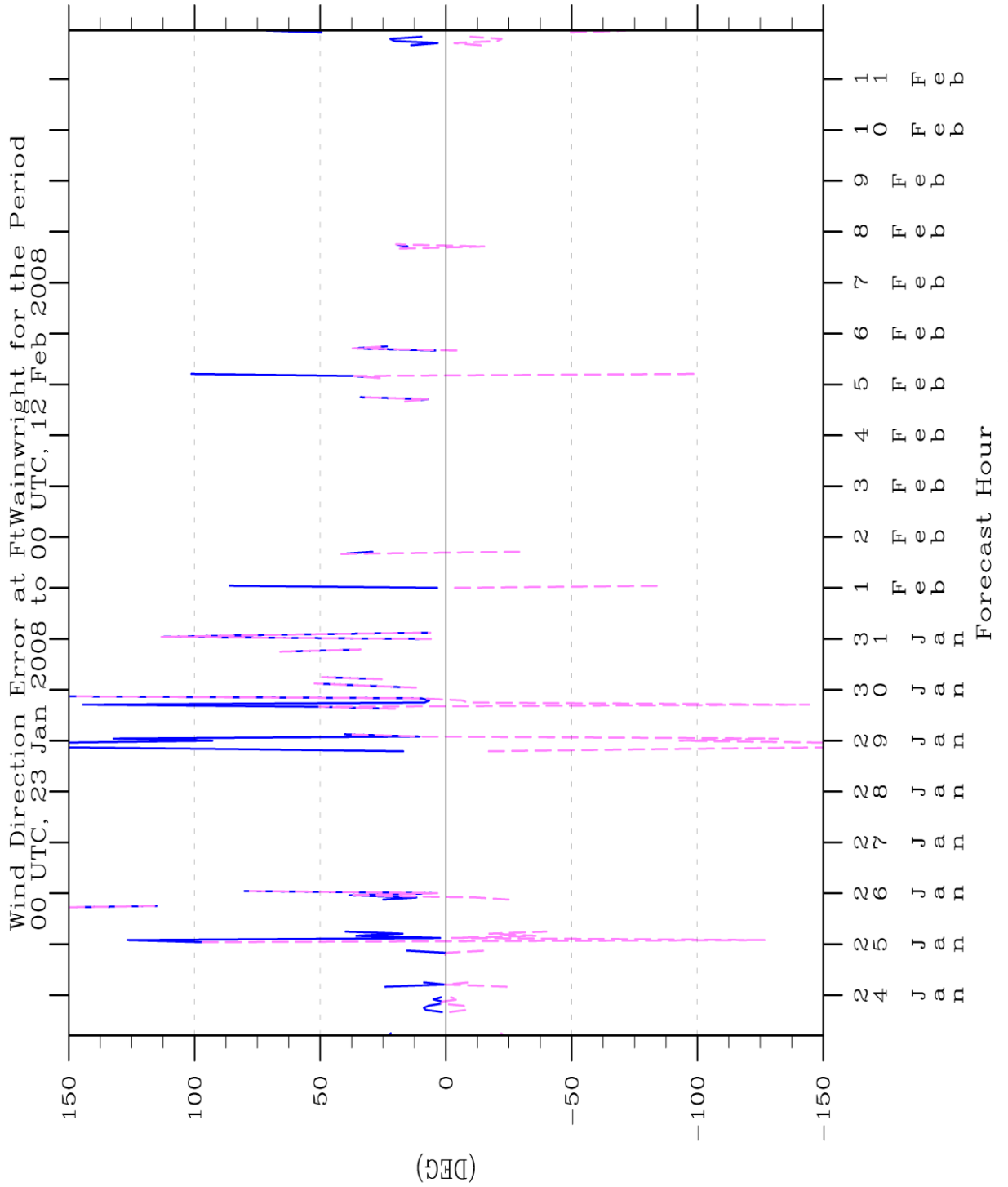


Figure 77: Time series of wind direction mean absolute error (blue) and mean error (magenta) statistics for Ft. Wainwright in TWIND2X30.

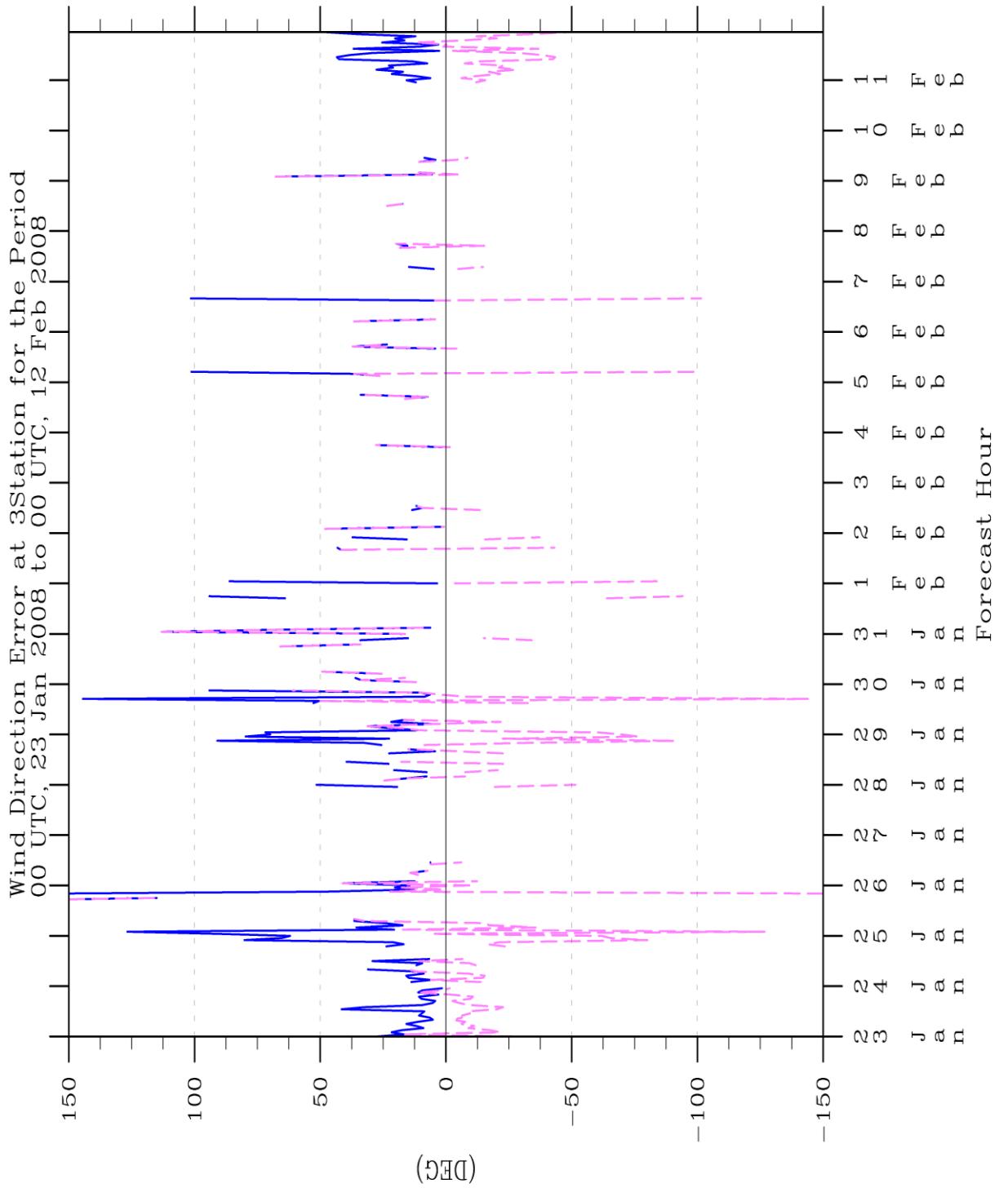


Figure 78: Time series of wind direction mean absolute error (blue) and mean error (magenta) statistics for all three stations in TWIND2X30.

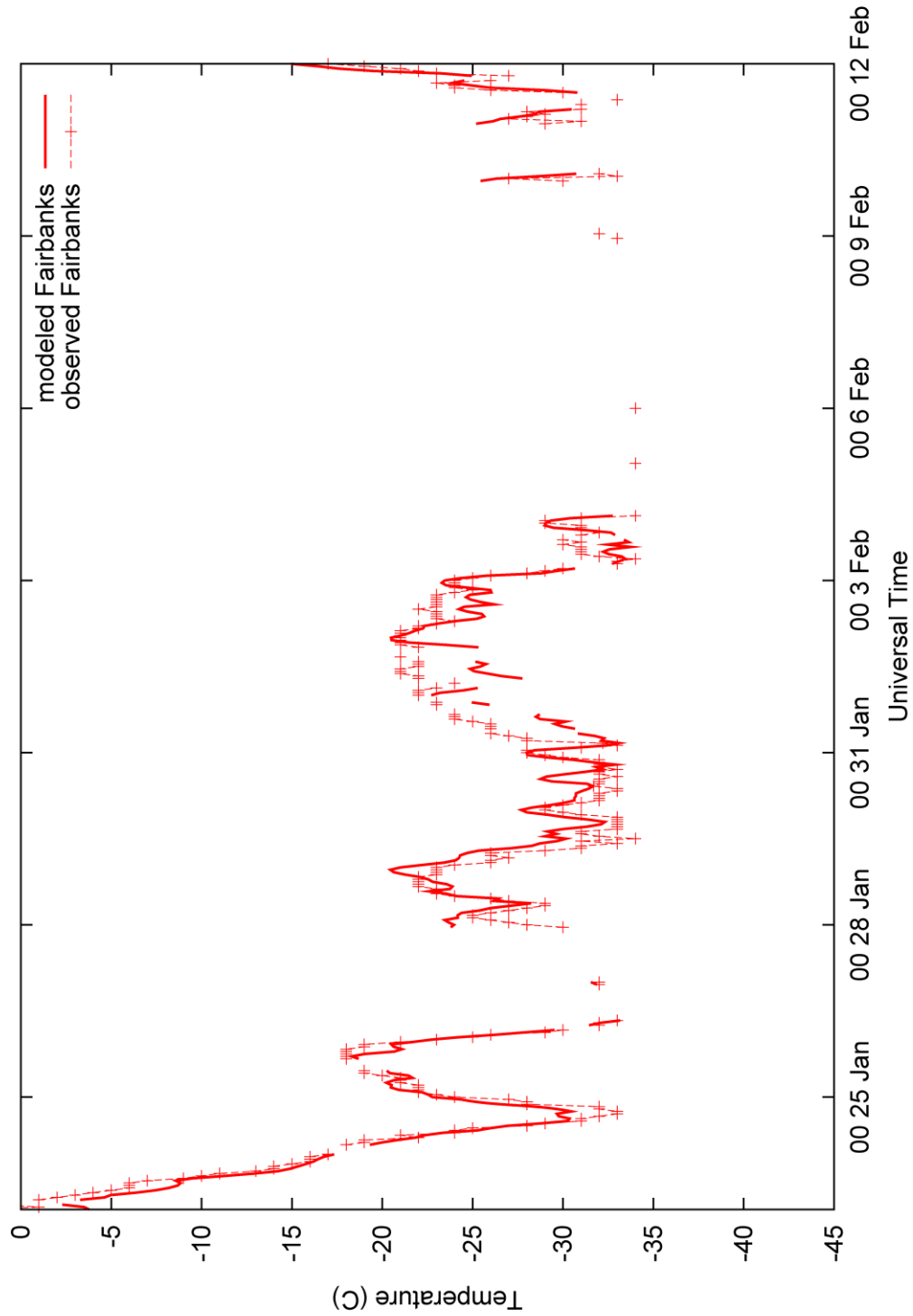


Figure 79: Time series of modeled and observed temperature for Fairbanks in TWIND2X30.

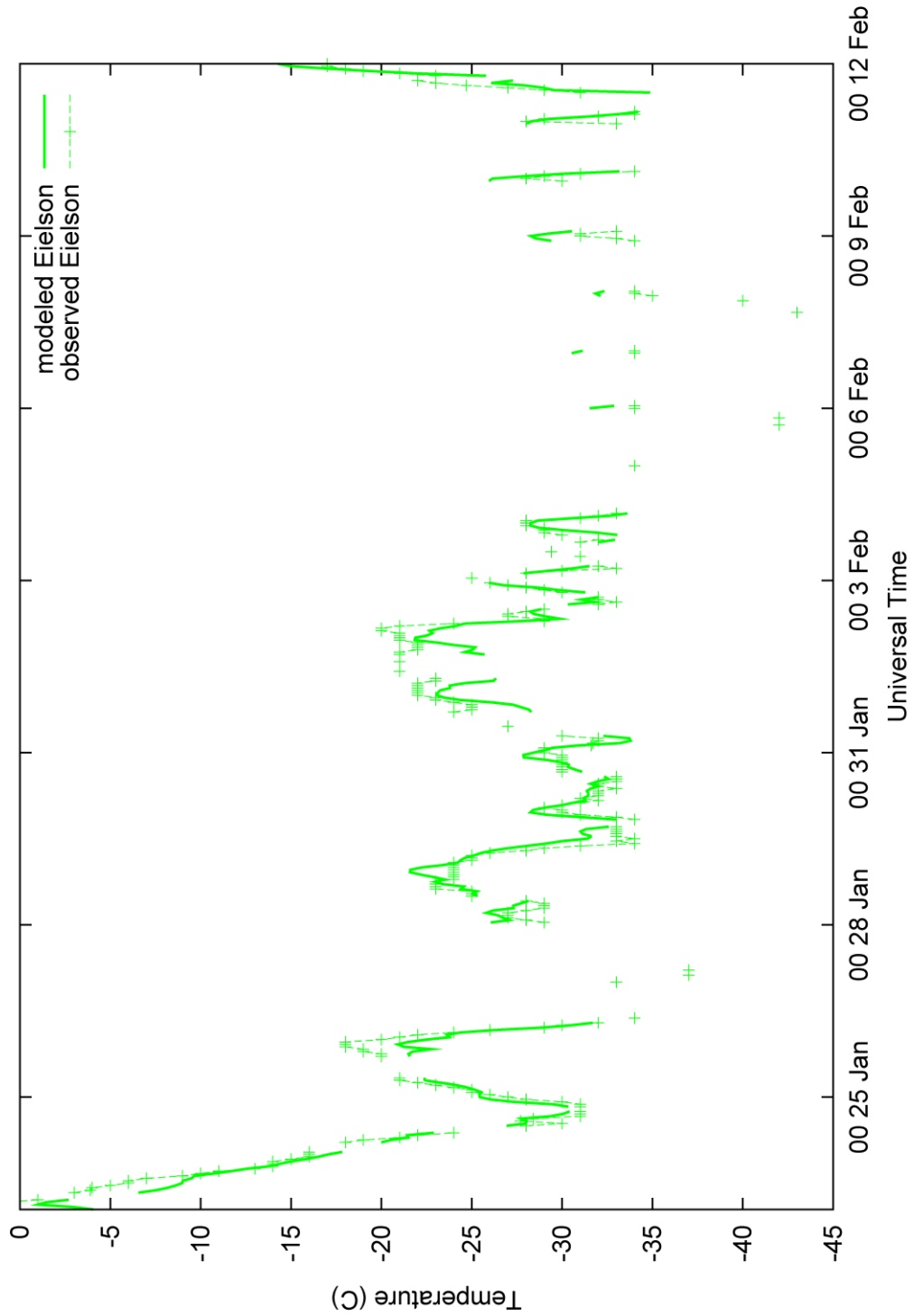


Figure 80: Time series of modeled and observed temperature for Eielson in TWIND2X30.

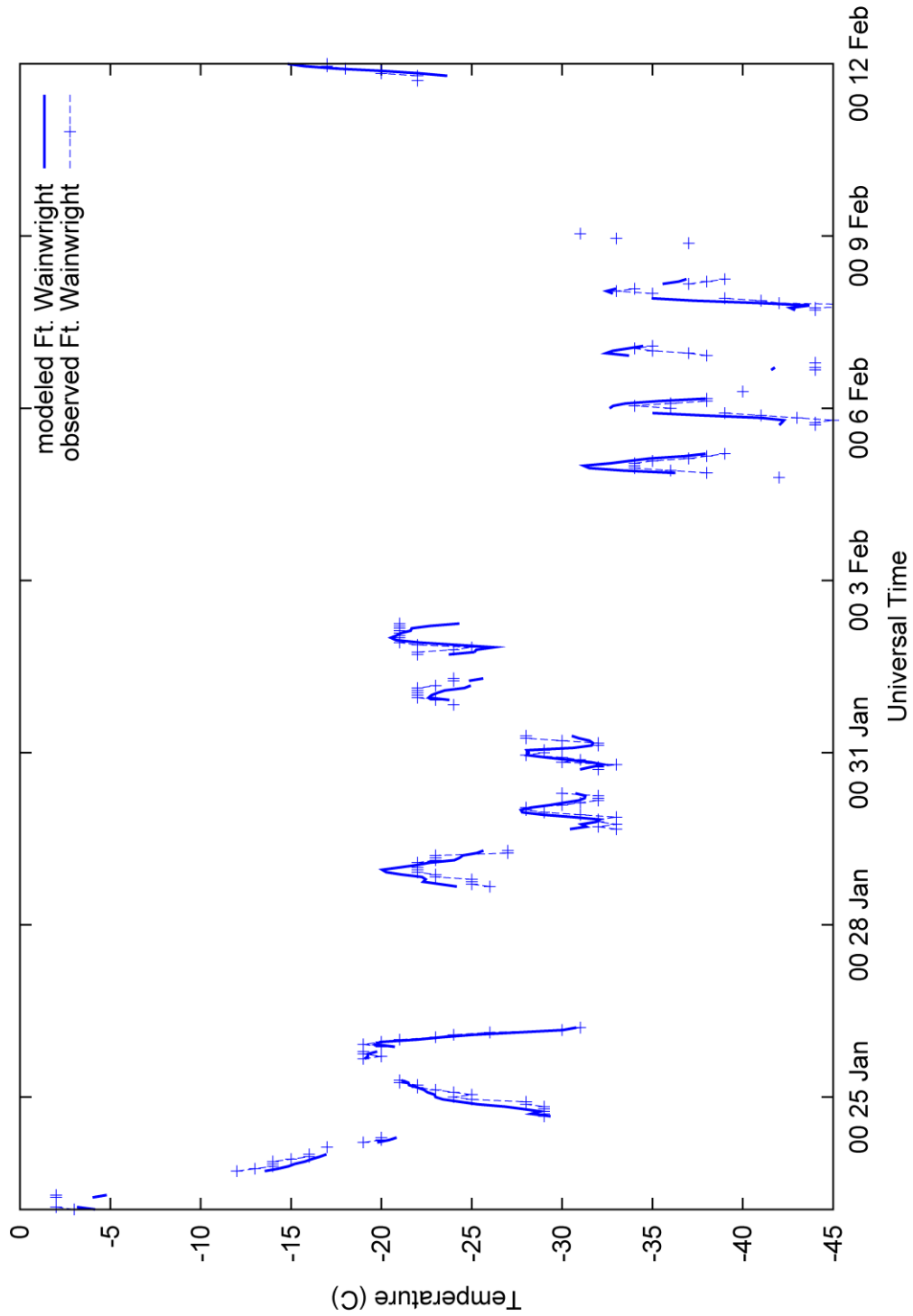


Figure 81: Time series of modeled and observed temperature for Ft. Wainwright in TWIND2X30.

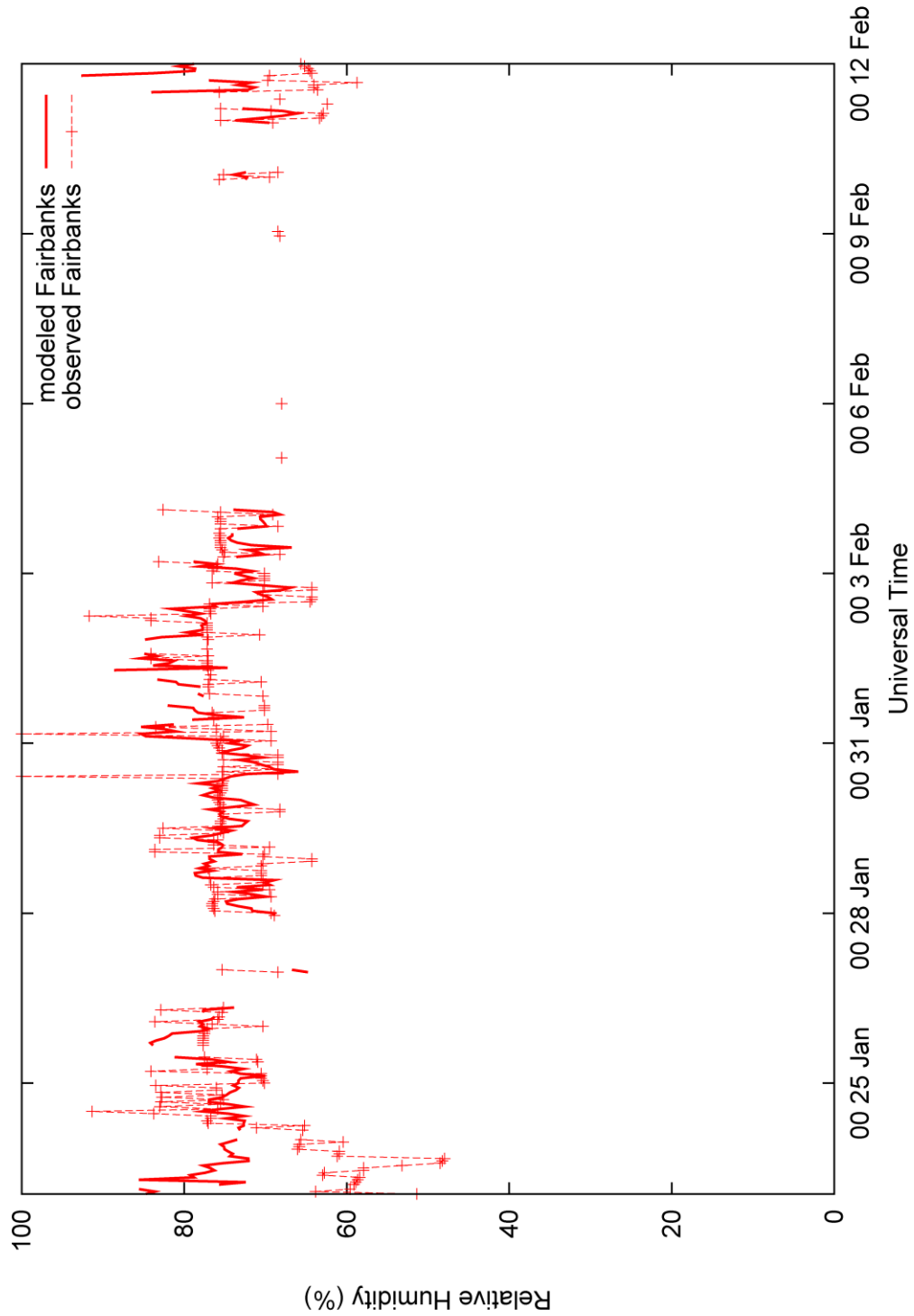


Figure 82: Time series of modeled and observed relative humidity for Fairbanks in TWIND2X30.

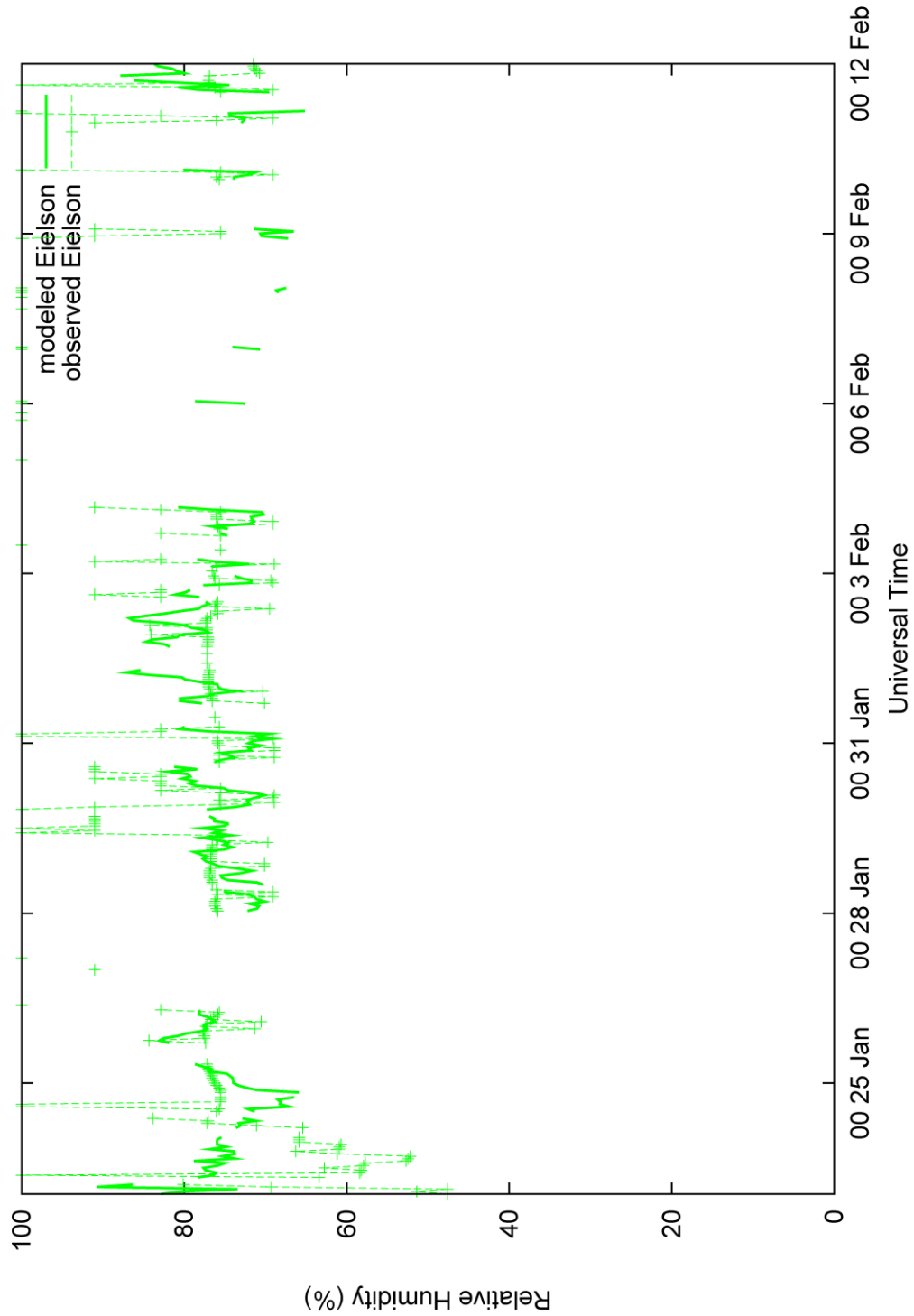


Figure 83: Time series of modeled and observed relative humidity for Eielson in TWIND2X30.

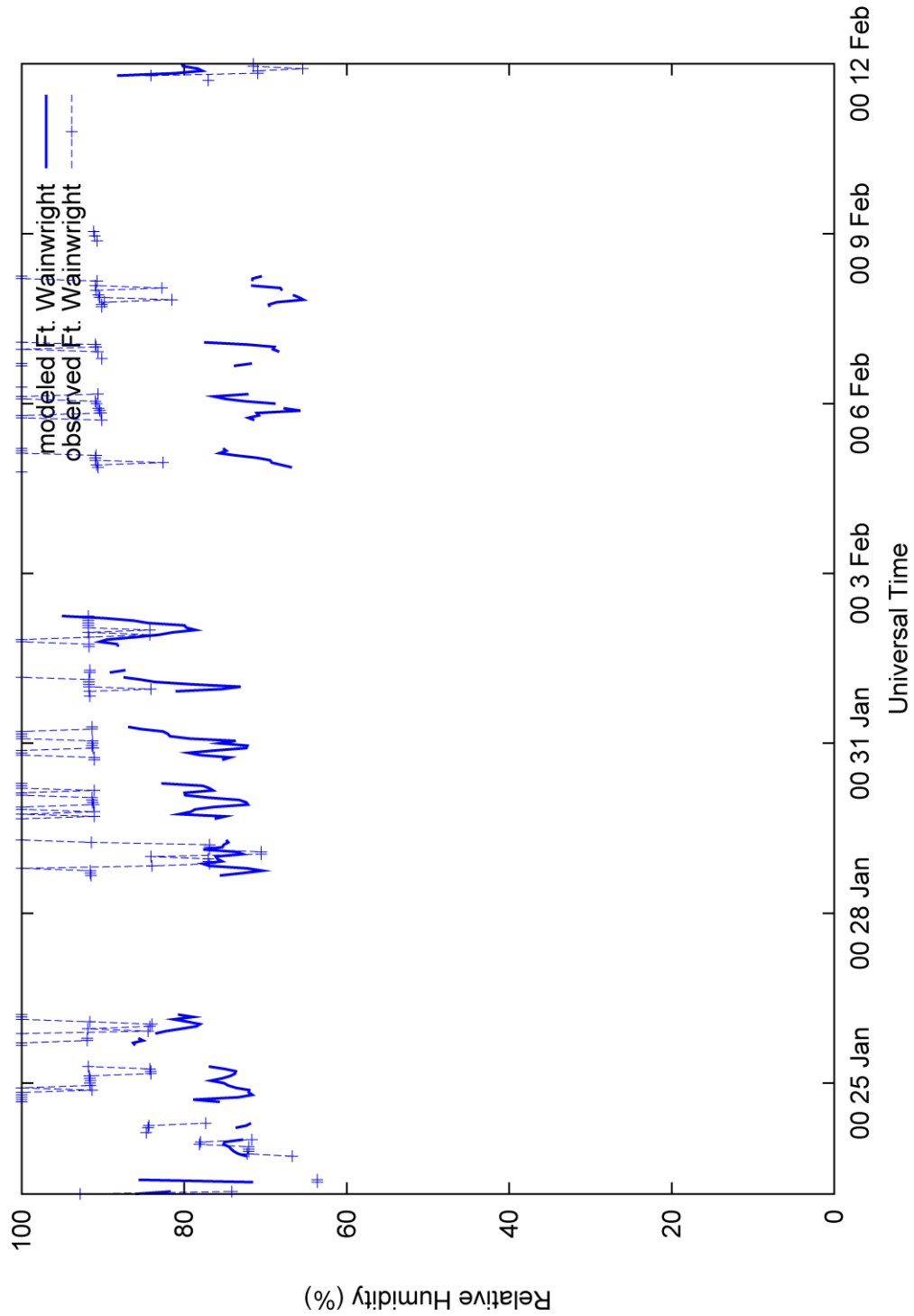


Figure 84: Time series of relative humidity for Ft. Wainwright in TWIND2X30.

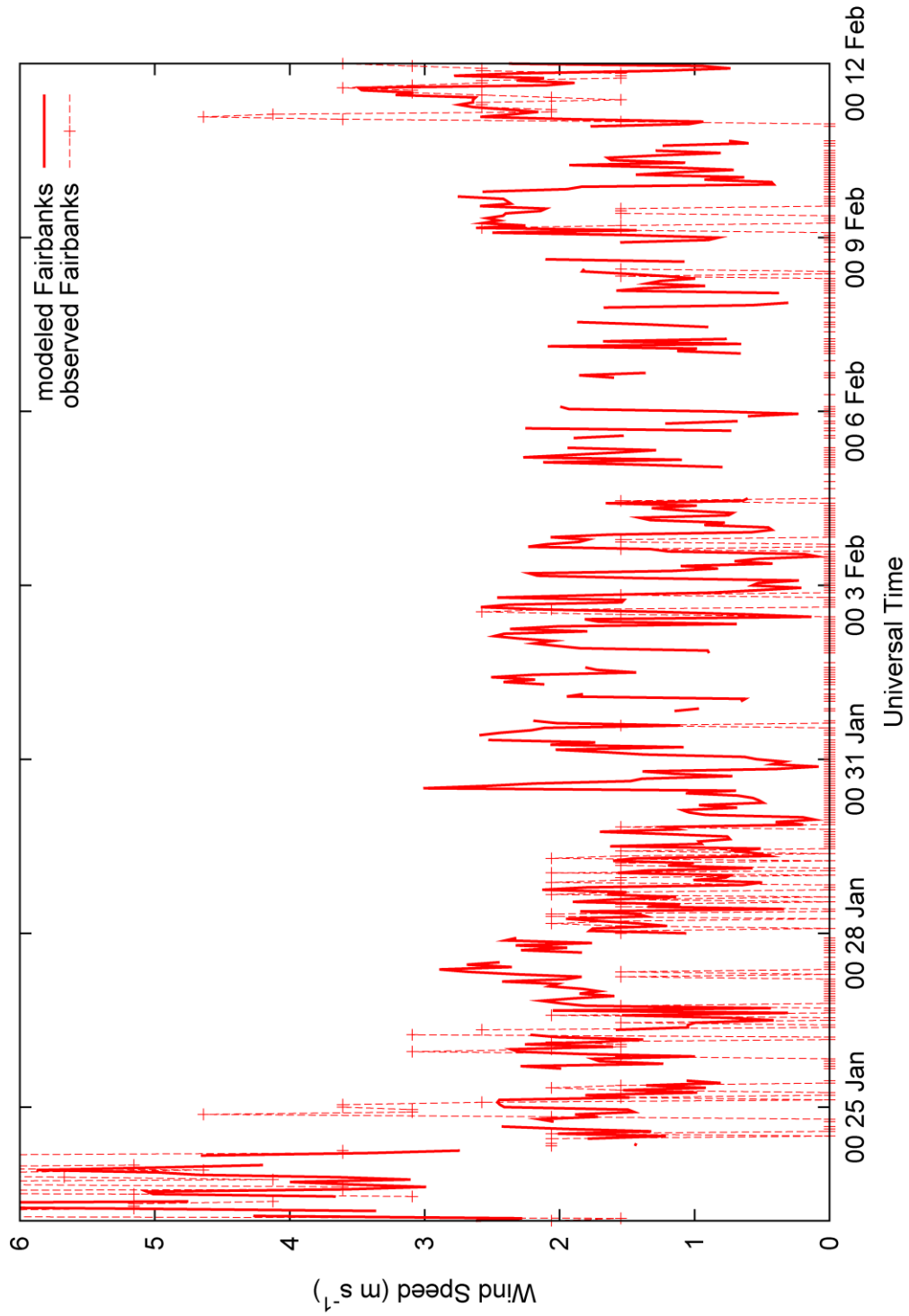


Figure 85: Time series of modeled and observed wind speed for Fairbanks in TWIND2X30.

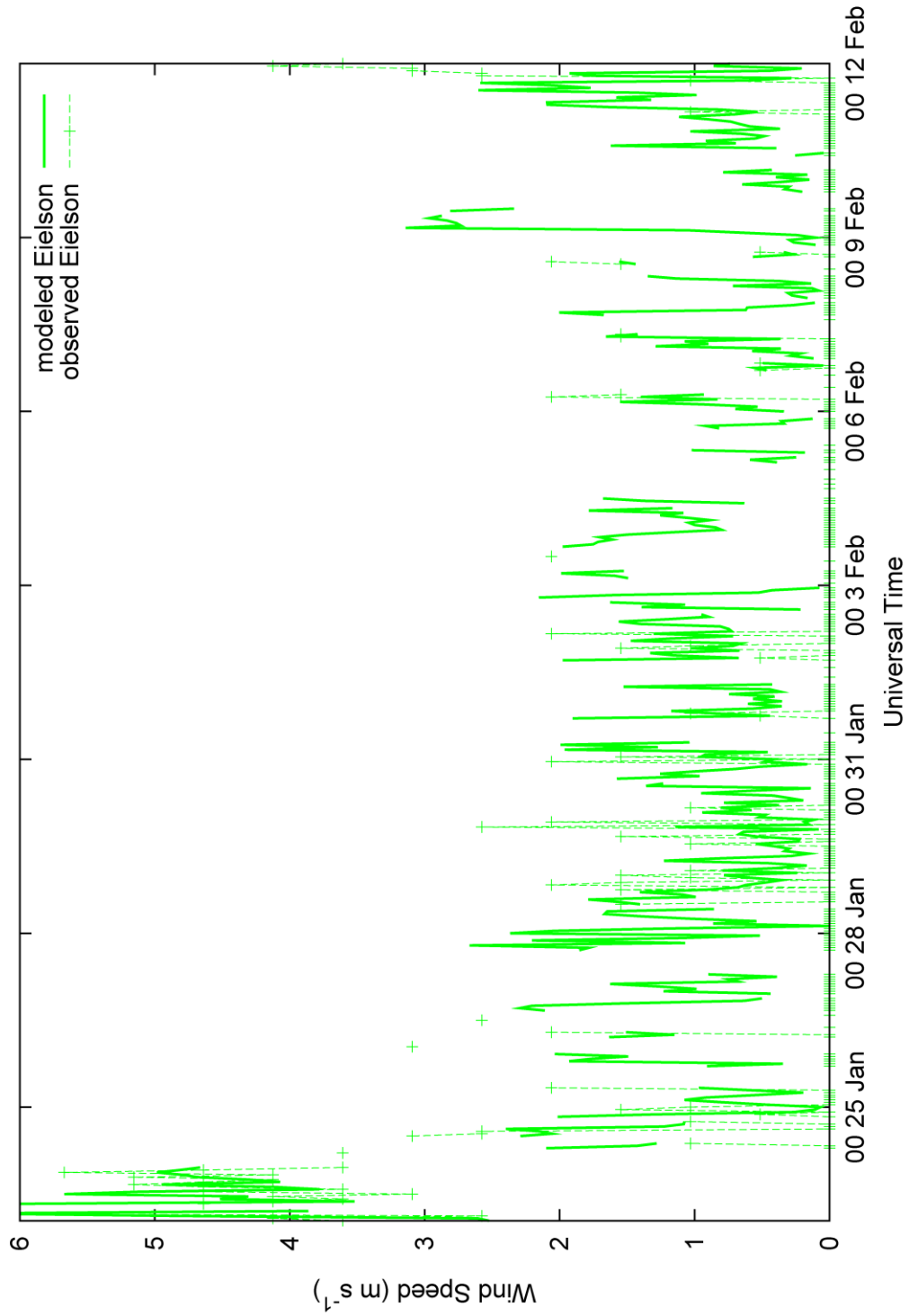


Figure 86: Time series of modeled and observed wind speed for Eielson in TWIND2X30.

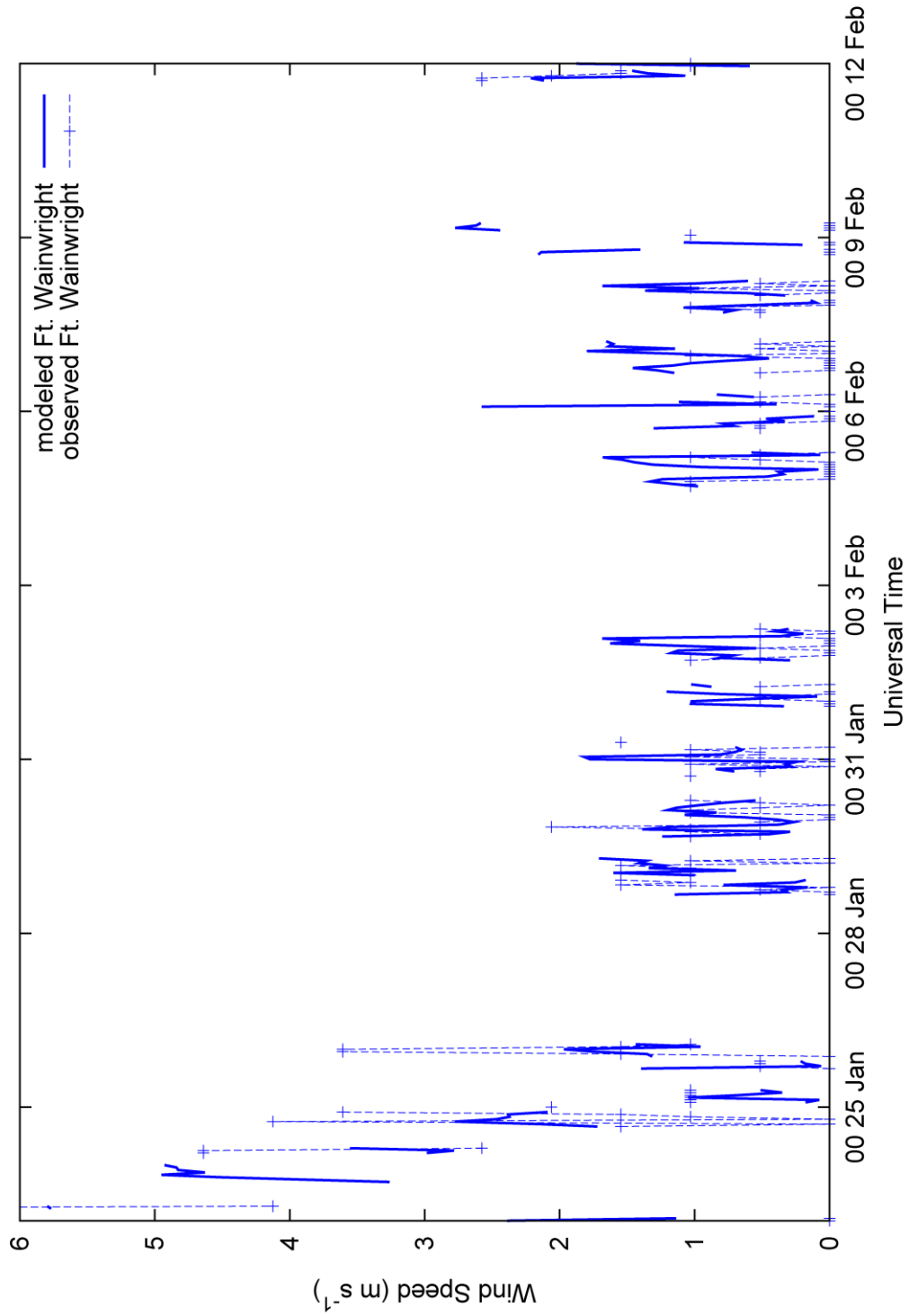


Figure 87: Time series of modeled and observed wind speed for Ft. Wainwright in TWIND2X30.

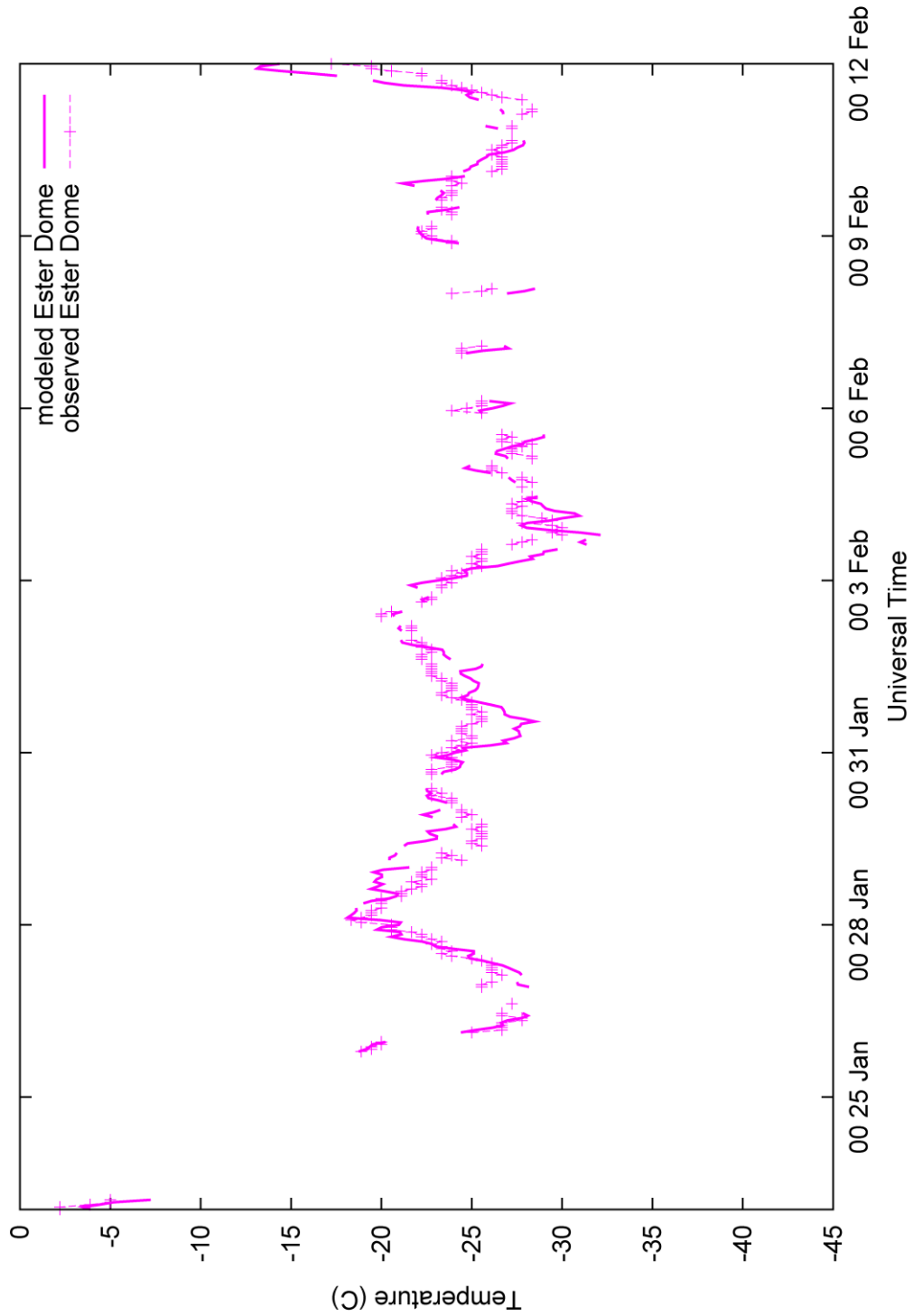


Figure 88: Time series of modeled and observed temperature for Ester Dome in TWIND2X30.

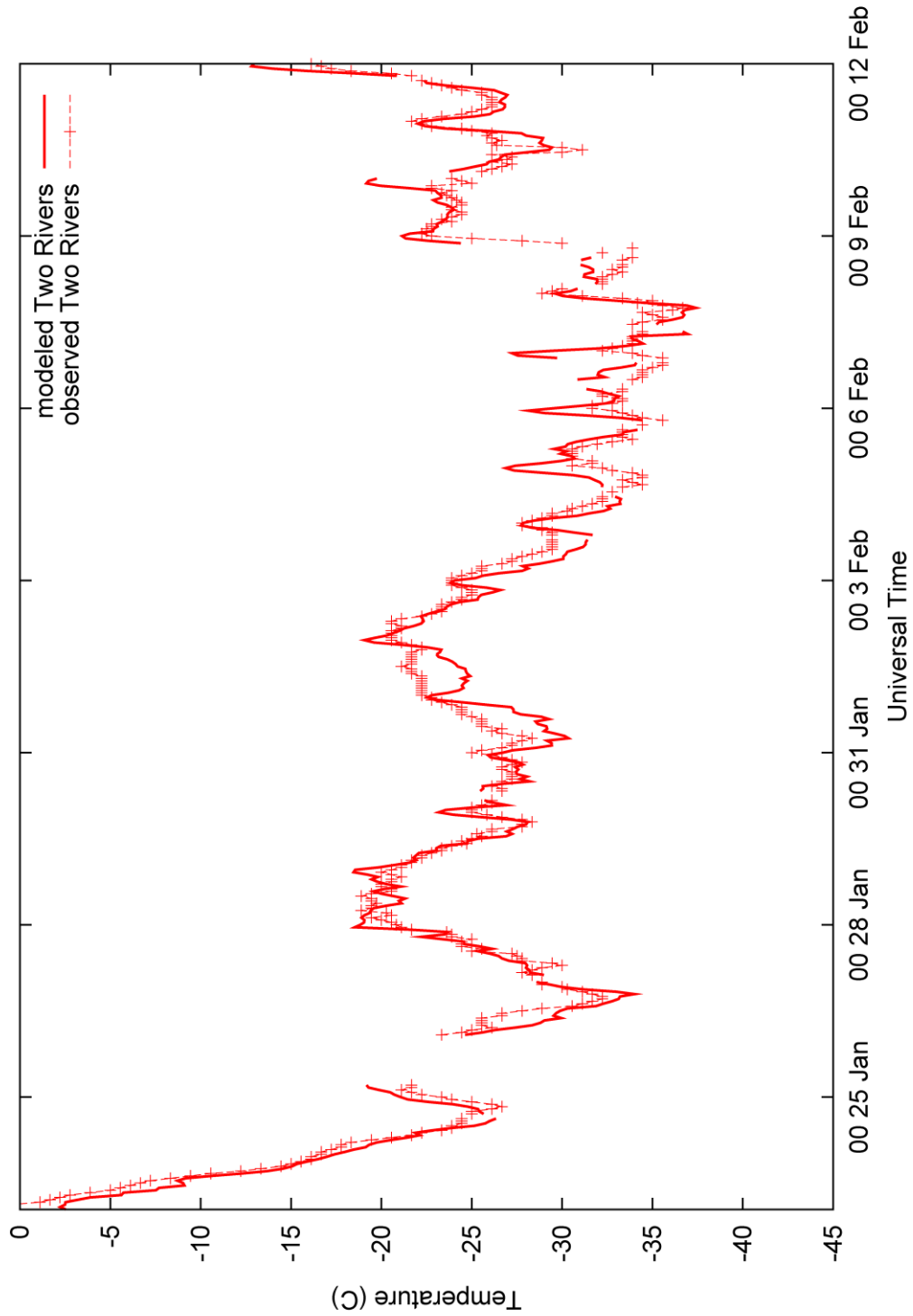


Figure 89: Time series of modeled and observed temperature for Two Rivers in TWIND2X30.

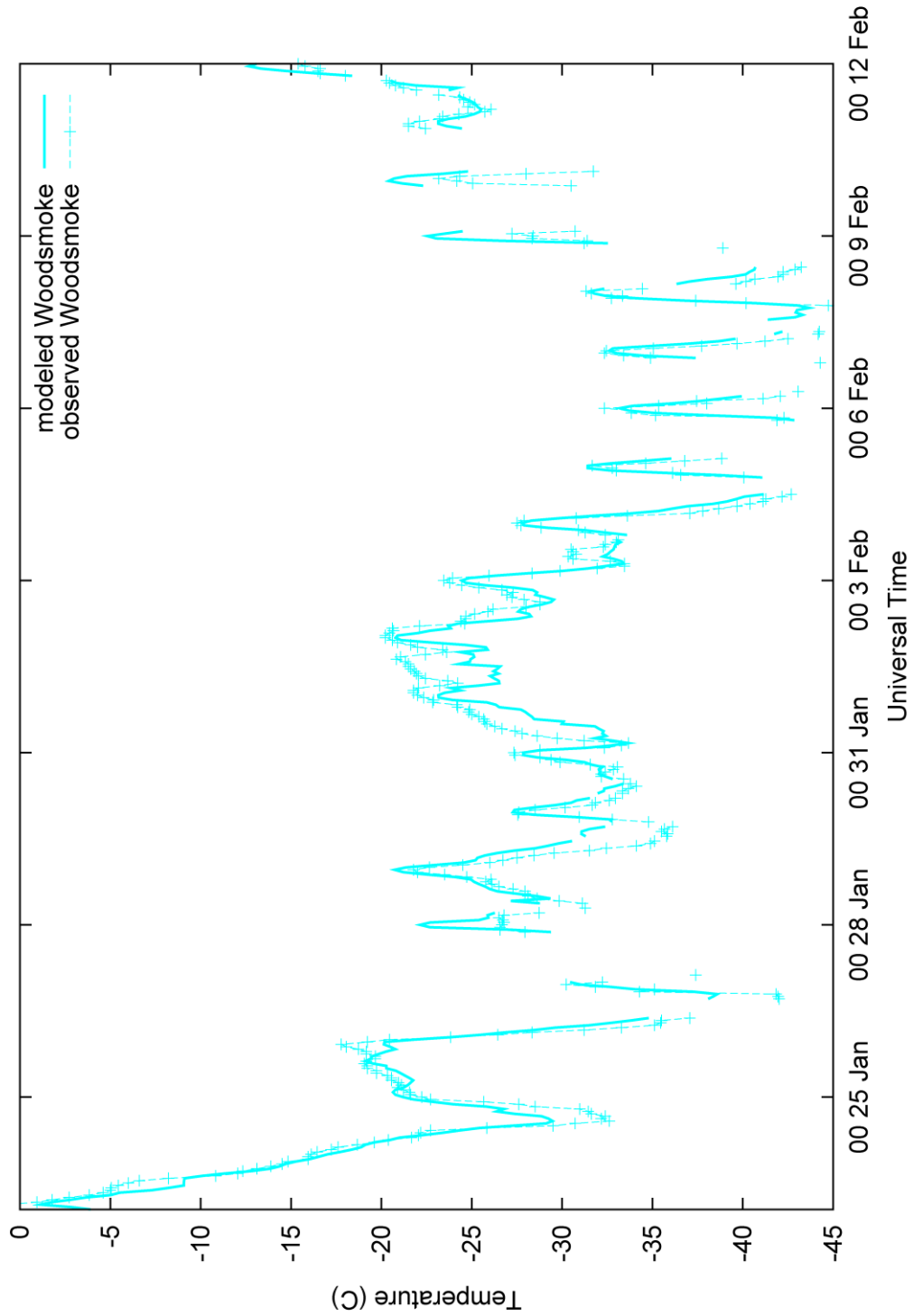


Figure 90: Time series of modeled and observed temperature for Woodsmoke in TWIND2X30.

REFERENCES

- Benjamin, S.O., and N.L. Seaman, 1985: A simple scheme for objective analysis in curved flow. *Mon. Wea. Rev.*, **113**, 1184-1198.
- Benson, C.S., 1970: Ice fog: Low temperature air pollution. Research Report 121. U.S. Army Corps of Engineers, Cold Regions Research and Engineering Laboratory, Hanover, NH, 118 pp.
- Chen, F., and J. Dudhia, 2001: Coupling an advanced land-surface/hydrology model with the Penn State/NCAR MM5 modeling system. Part I: Model implementation and sensitivity. *Mon. Wea. Rev.*, **129**, 569-585.
- Deng, A., D. Stauffer, B. Gaudet, J. Dudhia, J. Hacker, C. Bruyere, W. Wu, F. Vandenberghe, Y. Liu, and A. Bourgeois, 2009: Update on WRF-ARW end-to-end multi-scale FDDA system. *10th Annual WRF Users' Workshop*, 23 Jun 2009, Boulder, CO.
- Gaudet, B.J., and D.R. Stauffer, 2010: Stable boundary layer representation in meteorological models in extremely cold wintertime conditions. Final Report, Purchase Order EP08D000663, Environmental Protection Agency, 54 pp.
- Gaudet, B., D. Stauffer, N. Seaman, A. Deng, K. Schere, R. Gilliam, J. Pleim, and R. Elleman, 2009: Modeling extremely cold stable boundary layers over interior Alaska using a WRF FDDA system. *13th Conference on Mesoscale Processes*, 17-20 Aug, Salt Lake City, UT, American Meteorological Society.
- Janjić, Z.I., 2002: Nonsingular implementation of the Mellor-Yamada Level 2.5 Scheme in the NCEP Meso model. NCEP Office Note 437, 61 pp.
- Mlawer, E.J., S.J. Taubman, P.D. Brown, M.J. Iacono, and S.A. Clough, 1997: Radiative transfer for inhomogeneous atmosphere: RRTM, a validated correlated-k model for the longwave. *J. Geophys. Res.*, **102**, 16663-16682.
- Mölders, N. and G. Kramm, 2010: A case study on wintertime inversions in interior Alaska with WRF. *Atmos. Res.*, **95**, 314-332.
- Morrison, H., J.A. Curry, and V.I. Khvorostyanov, 2005: A new double-moment microphysics parameterization for application in cloud and climate models. Part I: Description. *J. Atmos. Sci.*, **62**, 1665-1677.
- Nuss, W.A., and D.W. Tittley, 1994: Use of multiquadric interpolation for meteorological objective analysis. *Mon. Wea. Rev.*, **122**, 1611-1631.

- Seaman, N.L., B.J. Gaudet, D.R. Stauffer, L. Mahrt, S.J. Richardson, J.R. Zielonka, and J. C. Wyngaard, 2012: Numerical prediction of submesoscale flow in the nocturnal stable boundary layer over complex terrain. *Mon. Wea. Rev.*, **140**, 956-977.
- Serreze, M.C., J.D. Kahl, and R.C. Schnell, 1992: Low-level temperature inversions of the Eurasian Arctic and comparison with Soviet drifting station data. *J. Climate*, **5**, 615-629.
- Skamarock, W.C., J.B. Klemp, J. Dudhia, D.O. Gill, M. Barker, M.G. Duda, X.-Y. Huang, W. Wang, and J.G. Powers, 2008: A description of the Advanced Research WRF version 3. NCAR Technical Note NCAR/TN475+STR.
- Smirnova, T.G., J.M. Brown, and D. Kim, 2000: Parameterization of cold-season processes in the MAPS land-surface scheme. *J. Geophys. Res.*, **105**, 4077-4086.
- Stauffer, D.R., and N.L. Seaman, 1994: Multiscale four-dimensional data assimilation. *J. Appl. Meteor.*, **33**, 416-434.
- Stauffer, D.R., N.L. Seaman, and F.S. Binkowski, 1991: Use of four-dimensional data assimilation in a limited-area mesoscale model. Part II: Effects of data assimilation with the planetary boundary layer. *Mon. Wea. Rev.*, **119**, 734-754.
- Stauffer, D.R., B.J. Gaudet, N.L. Seaman, J.C. Wyngaard, L. Mahrt and S. Richardson, 2009: Sub-kilometer numerical predictions in the nocturnal stable boundary layer. *23rd Conference on Weather Analysis and Forecasting/19th Conference on Numerical Weather Prediction*, 1-5 Jun, Omaha, NE, American Meteorological Society.
- Wyngaard, J.C., 2004: Toward numerical modeling in the ‘Terra Incognita’. *J. Atmos. Sci.*, **61**, 1816-1826.

**Fairbanks, Alaska PM_{2.5} Organic Composition and
Source Apportionment Research Study**

Final Report

August 10, 2012

by

Christopher P. Palmer, Ph.D.

**The University of Montana – Missoula
Department of Chemistry and Biochemistry
Missoula, MT 59812
Office: (406) 243-4079
Fax: (406) 243-4227**

1. Executive Summary

Fairbanks, AK experiences very high levels of ambient $PM_{2.5}$ during the winter months. Studies are currently under way to determine the sources of the $PM_{2.5}$ so that the issue might be addressed. Possible sources of the $PM_{2.5}$ include residential heating (wood, fuel oil, and/or natural gas combustion), transportation (diesel and gasoline engines), and coal combustion.

The current project is to provide a more complete characterization of the organic chemical composition of $PM_{2.5}$ from Fairbanks with the goal of identifying and quantifying chemical species that can be used to calculate and apportion ambient $PM_{2.5}$, particularly from wood and fossil fuel combustion.

Comprehensive chemical analyses for levoglucosan, hopanes, steranes and PAHs have been performed on up to 33 ambient $PM_{2.5}$ samples from Fairbanks. Analyses have also been performed on $PM_{2.5}$ generated at OMNI scientific using representative fuels and devices. The results of these analyses have been examined with special attention to compounds reported by previous authors as emissions from wood (levoglucosan) and fossil fuel sources. Emphasis has been placed on sulfur-containing compounds (dibenzothiophene and benzonaphthothiophene) which are known emissions of diesel vehicles and were hypothesized to be markers of residential oil burners and a polynuclear aromatic hydrocarbon (picene) which has been reported as a unique marker for coal combustion. A second polynuclear aromatic hydrocarbon, bibenzyl, has been identified as a potential marker for residential oil combustion.

In general, the results show that the ambient levels of levoglucosan and selected hopanes, steranes, picene and thiophenes, measured either as a concentration in air or as a fraction of $PM_{2.5}$, are high relative to previous studies. Levoglucosan results provide a reasonable estimate of the wood smoke contribution to ambient $PM_{2.5}$, and other markers provide a sense of upper bounds for the contribution of residential oil burners and coal combustion.

Levoglucosan results indicate that wood smoke contributes 26-35% of the $PM_{2.5}$ at the State Building site, 42-62% at the North Pole site, and 20-30% at the Peger Road site. These values are significantly lower than those reported by CMB analysis and similar to somewhat lower than those determined by ^{14}C analysis. The results show that wood smoke is a substantial contributor to ambient $PM_{2.5}$. The contribution of wood smoke to ambient $PM_{2.5}$ varies substantially within a season, but has had a fairly constant seasonal average or median over the past three seasons.

Polynuclear aromatic hydrocarbon results indicate that residential oil combustion is likely a minor contributor to ambient $PM_{2.5}$ levels with a median contribution of less than 1%. Sterane analysis indicates that the upper bound for the contribution from residential oil combustion is 15%, but this is likely to be an overestimate. There is significant but unquantifiable uncertainty in these results, which rely on a single sample of no. 2 fuel oil $PM_{2.5}$.

Analysis of picene levels indicates that coal combustion also contributes a minor fraction to ambient $PM_{2.5}$ of 2.7% or less. Analysis of hopanes suggests an upper bound for coal contribution of 13%, which is likely to be an overestimate. The picene and hopane shares of coal $PM_{2.5}$ are highly variable with device, however, and the contribution of coal combustion to ambient $PM_{2.5}$ could be less than 1% from coal stoves or much higher if from HH systems.

Thiophene analysis shows that these compounds are not present in residential oil emissions, and thus cannot be used as markers of residential oil combustion. The compounds do appear in the emissions from coal combustion at shares that result in estimated coal contributions to ambient $PM_{2.5}$ of 6.7% to over 100%. It is clear from this analysis that there is another significant source of thiophenes, particularly dibenzothiophene, other than residential heating. The most likely source is transportation, since thiophenes have been reported at significant levels in diesel fuel and gasoline emissions.

2. Levoglucosan

Levoglucosan, a product of incomplete cellulose combustion, has been recognized for many years as a marker of biomass combustion in PM_{2.5}. In winter urban environments such as Fairbanks, this can be equated with smoke from wood-fired residential heating devices.

The University of Montana has been analyzing ambient filters from Fairbanks for levoglucosan content since beginning in the 2008-2009 heating season and continuing through the 2010-2011 heating season. Measurements have been made on over 225 filters from four separate sampling sites during that period. This report will summarize these results, providing both the raw results and interpretation of those results in terms of the fractional contribution of wood smoke to total PM in Fairbanks.

2.1 Analytical Method and Quality Control

The Fairbanks ambient PM_{2.5} sampling program is described in detail in "The Fairbanks, Alaska PM_{2.5} Source Apportionment Research Study Final Report," July 23, 2012, by Tony Ward. Levoglucosan analyses were performed on quartz filters obtained through this sampling program as described in this report for the ¹⁴C analyses.

Ambient filters received from Fairbanks are stored at -10 C until analysis is performed. Each filter is halved before analysis to allow for a second half to be archived or analyzed for ¹⁴C or other analytes. The filter half was placed in a 30 mL vial and spiked with deuterated levoglucosan as an internal standard. The vials were left at room temperature to allow the standard to be absorbed onto the filter. After half an hour or until the standard solvent had evaporated, 20 mL of ethyl acetate with 3.6 mM triethylamine (TEA) was added and the samples were sonicated for half an hour to extract the desired compounds. After sonication, the filter was removed and the extract was filtered through a Whatman 0.45 µm nylon filter to remove particulates. The volume of the solvent was adjusted to 0.5 mL through evaporation under a stream of air in a sand bath at 45 °C. The sample was evaporated to dryness under a stream of air at room temperature and then derivatized with 75 µL N-O-bis(trimethylsilyl)trifluoroacetamide (BSTFA), 10 µL trimethylchlorosilane (TMCS), and 10 µL trimethylsilylimidazole (TMSI). The samples were heated in a sand bath at 70 °C for 1 hour to allow the derivatization to go to completion. Upon removal from the sand bath, the samples were diluted to 500 µL with ethyl acetate containing 3.6 mM TEA and were transferred to a GC vial for analysis.

Analysis was performed on an Agilent 6890N Gas Chromatograph with an Agilent 5973 Mass Spectrometer. An HP-5MS column ((5%-Phenyl)-methylpolysiloxane) was used with dimensions of 0.25 mm ID x 30 m length x 0.25 µm film thickness. A volume of 2 µL was injected for each analysis into a Split/Splitless FocusLiner™ for HP, single taper p/w quartz wool liner. Split injection was used to analyse for levoglucosan with a split ratio of 50:1. The inlet temperature was set to 250°C and the auxiliary transfer line temperature was set at 280°C. The temperature programme was started at 40°C for 1.5 minutes, ramped at 30°C/min to 190°C, 20°C/min to 210°C, and then 50°C/min to a final temperature of 300°C, which was held for 1.5 minutes. The mass spectrometer was operated with a solvent delay of

4.00 minutes and the mass range from 40-450 was scanned. Single ion monitoring was also used during detection. Highly selective quantitation was performed using the signal for representative ions for levoglucosan (217 m/e) and D-levoglucosan (220 m/e) extracted from the total ion chromatogram.

Calibration standards were prepared containing variable concentrations of levoglucosan and a fixed concentration of D-levoglucosan internal standard. The fixed concentration of deuterated internal standard (20 ppm) was selected to match the concentration expected from extraction of internal standard spiked on the filters, assuming 100% recovery. The standards were derivatized and analysed on the GCMS. The ratio of the peak area of levoglucosan to the peak area of D-levoglucosan standard was found for each calibration standard. A calibration curve was prepared by plotting the ratio of the two peak areas versus the concentration of the levoglucosan. Linearity was determined for each calibration curve, and all had R^2 values of at least 0.95. The concentration of levoglucosan extracted from sample filters was determined by measuring the ratio of the peak area for the analyte to that of D-levoglucosan, and reading the concentration from the calibration curve. Filter blanks and spiked filters were analysed on a regular basis, at least once for every 10 filters. Recoveries were determined for blank filters spiked with the analytes at known amounts corresponding to typical levels seen in actual sample filters. Recovery was consistently in the range of 95-105%, and blank filters did not give significant signals.

Wood smoke particulate obtained from OMNI Scientific was also analysed for levoglucosan content using essentially the same procedure. These filters had very high loads of $PM_{2.5}$, which required adaptations to the method. Smaller portions of the filters, typically 1/8 rather than 1/2, and extracts were often diluted before derivatization. In each case where additional dilution was necessary, the filters were spiked before extraction with sufficient deuterated levoglucosan such that the final diluted concentration would match that of other samples and standards. This ensured that the area ratios could be interpreted using the same standard curve.

In order to interpret the results for levoglucosan as a share of wood smoke $PM_{2.5}$ on the OMNI-generated filters, it was necessary to estimate the total $PM_{2.5}$. OMNI reported total $PM_{2.5}$ for quartz filter 1 (PM_{Q1}) and flow rates for quartz filters 1 (FR_{Q1}) and 2 (FR_{Q2}) for each sampling event. Quartz filter 2 was sent to UM for levoglucosan analysis. We calculated total $PM_{2.5}$ on quartz filter 2 using these data:

$$PM_{Q2} = PM_{Q1} \frac{FR_{Q2}}{FR_{Q1}}$$

This calculation assumes that the sampling time and that the $PM_{2.5}$ level in the sampling region for the two quartz filters were the same for each experiment.

2.2 Results

Raw results for all measured levoglucosan levels in ambient air (in ng/m^3) and as levoglucosan share of total $PM_{2.5}$ (in %) are provided in a spreadsheet. These data are organized by sampling site and sampling date, and total reported $PM_{2.5}$ (in $\mu g/m^3$) are also included. Based on replicate measurements, typical relative error for reported levoglucosan levels is $\pm 10\%$.

Table 1 presents averages and 95% confidence intervals for levoglucosan levels and shares by sampling site and year. Data for the RAMS site is presented only for the 2009-2010 season since other seasons have either no or insufficient data. Confidence intervals in these results are affected by actual variations in levoglucosan levels and shares as well as variations due to analytical reproducibility.

Table 1: Average levoglucosan (LG) levels and shares for four sites over the three year study period.

	State Building		Peger Road		North Pole		RAMS	
	LG Level (ng/m ³)	LG Share (%)	LG Level (ng/m ³)	LG Share (%)	LG Level (ng/m ³)	LG Share (%)	LG Level (ng/m ³)	LG Share (%)
2008-09	573 ±203	3.1 ±1.1	628 ±120	2.18 ±0.24	833 ±480	3.8 ±1.2	NA	NA
2009-10	671 ±288	2.33 ±0.63	312 ±131	1.60 ±0.41	1720 ±470	4.80 ±0.51	NA	NA
2010-11	671 ±157	2.96 ±0.32	763 ±195	2.30 ±0.36	1150 ±490	4.85 ±0.53	2680 ±1160	4.67 ±0.70
3 yr	632 ±118	2.80 ±0.46	628 ±120	2.18 ±0.24	1400 ±300	4.59 ±0.40		

Levoglucosan levels range from 600 to 2700 ng/m³ with levels at the State Building and Peger Road at the lower end and those at North Pole averaging 1400 ng/m³.

Table 2: Levoglucosan shares for various devices, fuels and burn rates.

Filter ID	Burner Type	Fuel Type	Burn Rate	Levoglucosan Share (%)
FNB 1	pellet	Pellet	single	0.24
FNB 44	conv. WS	Birch	high	1.08
FNB 40	conv. WS	Spruce	high	0.88
FNB 52	conv. WS	Birch	low	1.18
FNB 48	conv. WS	Spruce	low	0.35
FNB 4	Cert. WS	Birch	high	0.27
FNB 7	Cert. WS	Spruce	high	1.80
FNB14	Cert. WS	Birch	low	6.12
FNB 18	Cert. WS	Spruce	low	6.05
FNB 87	NQ OWHH	Spruce	high	5.86
FNB 27	EPA OWHH	Birch	high	7.46
FNB 34	EPA OWHH	Spruce	high	2.48
FNB 28	EPA OWHH	Birch	low	5.73
FNB 36	EPA OWHH	Spruce	low	11.73

The RAMS site, with an average of 2700 ng/m³ is very high, but the PM_{2.5} levels are also very high at that site. Levoglucosan share range from 1.6 to 4.7%, with the State Building and Peger Road sites averaging 2.2-2.8% and the North Pole and RAMS sites averaging 4.6-4.7%. Significant differences in levoglucosan levels and shares are observed between sampling sites, with the North Pole and RAMS sites showing higher levels and shares and the State Building and Peger Road sites having lower levels and shares. There are no significant differences or trends in levoglucosan levels or shares for any given site as

a function of heating season. Variability in the levoglucosan levels, expressed as relative 95% confidence intervals, are high, often exceeding 40%. This variation reflects the fact that levoglucosan levels increase

and diminish with PM_{2.5} levels, which also vary significantly. Relative variations in levoglucosan as share of PM_{2.5} are lower, and are typically 15% or less.

Fourteen filters generated by OMNI Scientific utilizing wood burning devices and two wood species representative of those from Fairbanks, and generated at different burn rates, were also analyzed for levoglucosan content and share. The results for levoglucosan share of the wood smoke PM_{2.5} for these filters are presented in Table 2. Based on replicate analyses of some filters, the relative uncertainty in these numbers is estimated to be ±10%.

In general, these results indicate a relatively low share of levoglucosan in the wood smoke (3.7%) compared to published values¹⁻³. No significant differences were observed in levoglucosan share based on wood species, which is also not consistent with previous studies¹⁻³. Significant differences are observed as a function of burner type and within burner types as a function of burn rate.

2.3 Interpretation and Discussion

The levoglucosan results in Tables 1 and 2 have been analyzed in an effort to provide a quantitative measure of the contribution of residential wood combustion to ambient PM_{2.5}. Recent studies have made similar efforts¹. The basic approach is to establish an experimental levoglucosan share in wood smoke, and to use this to convert levoglucosan share of ambient PM_{2.5} to wood smoke fraction of ambient PM_{2.5}. Dividing the levoglucosan share of ambient PM_{2.5} by the levoglucosan share of pure wood smoke generated using representative heating appliances and wood species should provide the fractional wood smoke contribution to the ambient PM. The levoglucosan share of wood smoke is established by analysis of PM from wood heaters and wood species used in the region of study. The levoglucosan share is generally observed to vary between wood species¹⁻³, so a representative value for the region is calculated as a weighted average based on a survey of the amount or fraction of each wood species consumed in the region¹.

There are several difficulties, however, in establishing the best conversion factor to apply to Fairbanks ambient levoglucosan results. The most relevant data for levoglucosan share of wood smoke PM_{2.5} should be those reported in Table 2. However, those data include results only for spruce and birch, and a survey of wood consumption in Fairbanks has indicated 43% aspen, 52% birch, and 6% spruce. Further, average levoglucosan share reported in Table 2 is 3.7%, which is significantly lower than typical and average levoglucosan shares measured in ambient PM_{2.5} at the North Pole and RAMS sites. Calculation of wood smoke contribution to ambient PM using these average numbers would result in average values of 124-126% for these two sites. This is clearly not a reasonable result.

There are experimental levoglucosan shares of PM reported in the literature for wood smoke from various species, including aspen, birch and spruce (Fine). These published data are generally accepted and have been used in multiple studies to interpret ambient PM levoglucosan results. The published numbers are generally higher than those reported in Tables 1 and 2, and employing them would result in more acceptable average wood smoke contributions of less than 100%. However, the published results are not specific for appliances and practices in Fairbanks, and their use thus introduces

significant uncertainty. Other published results for levoglucosan share do not include the same species as those burned in Fairbanks and/or are for PM₁₀ rather than PM_{2.5}.

We have investigated multiple approaches to generate a conversion factor to allow the calculation of wood smoke contributions from levoglucosan fractions of ambient PM_{2.5}. Each of our conversion factors is a weighted average based on the survey data for wood species consumption in Fairbanks:

$$CF = \frac{1}{0.43L_A + 0.52L_B + 0.06L_S}$$

where CF is the desired conversion factor and L_A, L_B, and L_S are the levoglucosan share for aspen, birch and spruce wood smoke respectively. A value calculated from results published by Caseiro et al. (CF=11) was rejected because those published results did not include all of the species of interest and because they were for PM₁₀. The value calculated from the published results of Fine et al. (CF=9.01) is considered the industry standard, and is based only on the assumption that the Fine results are valid for Fairbanks devices and conditions. This “Fine conversion factor” was the lowest of the calculated conversion factors and is used here as a lower limit. Two conversion factor values were calculated using, in part, the results in Table 2 for the OMNI-generated filters. The first is calculated using the average values for L_B and L_S from Table 2 under all burn conditions and the value for aspen reported by Fine et al. (L_A=0.125). The resulting “OMNI conversion factor” (CF=13.3) is strongly influenced (43%) by the published value for aspen. Working with a lower value for aspen more in line with those measured for OMNI-generated filters would result in a larger conversion factor and in many days for which wood smoke contributions in North Pole would exceed 100%. The OMNI conversion factor as calculated results in only one day for which wood smoke contribution in North Pole exceeds 100%, and three days that exceed 90%. It is thus a reasonable upper limit for the conversion factor. Finally, device type data by zip code was utilized together with wood species survey data to generate site-specific conversion factors weighted for both wood species and device type. These conversion factors were calculated using L_A from Fine et al., and L_B and L_S from Table 2 and ranged from 12.2-12.4. There was significant concern that these conversion factors were based on too many data with significant uncertainties. Because of this, and because the values are intermediate, they were rejected and were not used for additional calculations.

Using the two conversion factors it is possible to calculate a low and a high estimate of wood smoke contribution to ambient PM_{2.5} in Fairbanks. The high end estimates are nearly 48% higher than the low end estimates. Table 3 presents these results by site and season, along with results for the same sites and seasons from ¹⁴C and CMB analysis. The levoglucosan results include analyses for many sampling periods when ¹⁴C analysis was not performed. Average values are reported, but these do not differ significantly from median values. Errors are reported as presented in previous reports or as 95% confidence intervals for levoglucosan results. The results for ¹⁴C analysis are based on a subset of the samples that were analyzed for levoglucosan, and those results may thus be biased if those samples were not selected at random. Still, results calculated using the OMNI conversion factor (which includes the published Fine result for Aspen) are within the range or are not significantly different from the

results reported from the ^{14}C results. Results calculated using the conversion factor generated using only the published Fine numbers are generally lower than, and often significantly lower than, the minimum value reported from the ^{14}C results. All of the results based on levoglucosan analysis are significantly lower than those reported using CMB modeling. It should be noted that some data were eliminated for a few low PM days, where the results for levoglucosan are either below the detection limit or near the detection limit and thus have considerable error. No more than two data points were eliminated for any heating season.

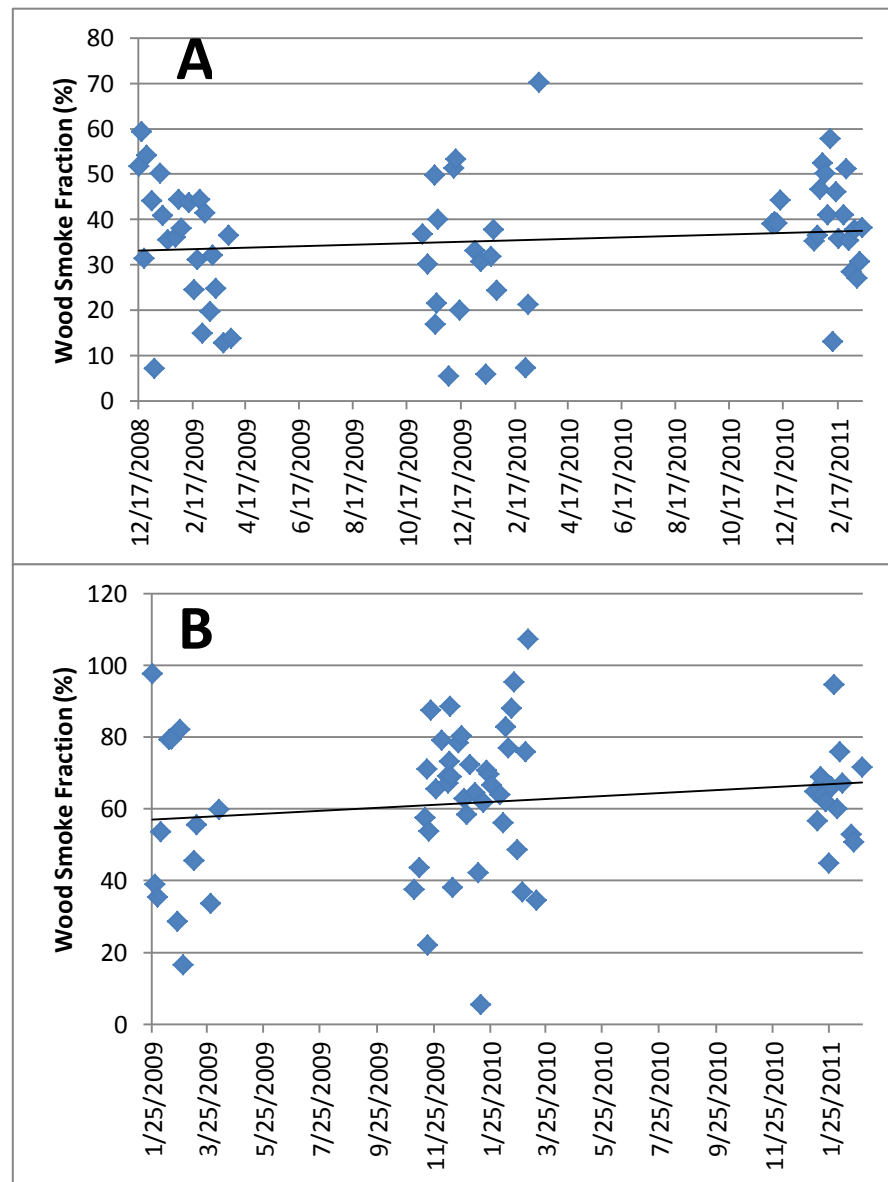
Table 3: Wood smoke contributions to ambient $\text{PM}_{2.5}$ as determined by ^{14}C analysis, levoglucosan analysis

	WS % $\text{PM}_{2.5}$ ^{14}C Minimum	WS % $\text{PM}_{2.5}$ ^{14}C Maximum	WS % $\text{PM}_{2.5}$ Levoglucosan (Fine CF=9.01)	WS % $\text{PM}_{2.5}$ Levoglucosan (OMNI CF=13.3)	WS % $\text{PM}_{2.5}$ CMB Model (OMNI)	WS % $\text{PM}_{2.5}$ CMB Model
State Bldng						
2008/2009	31.6 ± 8.0	38.0 ± 9.6	28.1±10.0	34.7±5.9	56.0	66.3 ± 10.1
2009/2010	36.7 ± 7.5	44.2 ± 9.1	21.0±5.6	31.0±8.3		69.9 ± 7.8
2010/2011	28.7 ± 4.3	34.5 ± 5.1	26.7±2.9	39.4±4.3		72.0 ± 6.3
3-yr avg	33.6 ± 7.7	40.4 ± 9.3	25.6±4.1	35.2±3.5		68.5 ± 8.6
North Pole						
2008/2009	42.9 ± 9.8	51.7 ± 11.8	36.8±10.0	54.3±14.7	73.4	72.1 ± 4.7
2009/2010	56.7± 6.3	68.3 ± 7.6	43.3±4.6	63.8±6.8		83.3 ± 10.3
2010/2011	58.4 ± 6.9	70.4 ± 8.3	43.7±4.8	64.3±7.0		73.8 ± 17.0
3-yr avg	55.0 ± 8.3	66.2 ± 10.0	42.0±3.4	61.8±5.1		79.4 ± 11.8
Peger Road						
2008/2009	23.6	28.4	14.3±3.7	21.1±5.4	51.0	62.9
2009/2010	33.9 ± 4.8	40.9 ± 5.8	21.5±2.9	31.7±4.3		69.9 ± 13.1
2010/2011	28.7 ± 6.6	34.6 ± 8.0	22.5±3.4	33.1±5.0		68.5 ± 11.3
3-yr avg	31.8 ± 5.6	38.3 ± 6.7	20.0±2.0	29.5±3.0		69.0 ± 12.1

The relatively low per sample cost of levoglucosan analysis allows multiple analyses to be run a single site in a single season and over several seasons. This, in turn, provides a means to monitor wood smoke contributions as a function of time as well as during and after efforts to reduce wood smoke emissions. A major caveat with this approach, however, is that source profiles would also need to be monitored if significant changes in fuels or devices are implemented. As an example of the approach, the wood smoke contribution to $\text{PM}_{2.5}$ at two sampling sites in Fairbanks as a function of time are presented in Figure 1. These plots show clearly that there is significant variability in the results, which is a combination of actual variability and random error in the measurements (if relative error in PM and levoglucosan measurements are each ±10%, the calculated levoglucosan share can be expected to be ±14%). The plots show no observable trend within any heating season. The data show a weak but

statistically insignificant trend of increasing contribution from wood smoke over time. Neither these plots nor the average seasonal data in Table 3 provide significant evidence of any trend of increased or diminished wood smoke contribution over this time period.

Figure 1: Wood smoke contribution to ambient $PM_{2.5}$ in Fairbanks North Star Borough, based on levoglucosan measurements and the OMNI conversion factor, at A. State Building and B. North Pole sites as a function of time.



2.4 Conclusions

Measurement of levoglucosan shares in ambient $PM_{2.5}$ in Fairbanks as well as in wood smoke particulate using representative devices and fuels allows an estimate of the residential wood smoke contribution to ambient $PM_{2.5}$. The final estimates include significant uncertainty due to both random measurement errors and lack of knowledge concerning the chemical composition of wood smoke. The effect of random measurement errors is reduced somewhat by the large number of measurements that can be made to generate averages. The effect of errors in estimation of the conversion factor is not diminished by making multiple measurements. Two conversion factors were generated that can be

reasonably expected to yield minimum and maximum wood smoke contributions, but as an indication of the uncertainty these two values differ by nearly 45%.

The resulting values for wood smoke contribution are similar to those determined from ^{14}C analysis. This lends some level of credence to both of these methods. Both of the approaches, however, yield results that are significantly lower than those obtained from CMB analysis.

Levoglucosan analysis is relatively inexpensive in comparison to either ^{14}C analysis or CMB analysis. This allows the wood smoke fraction of $\text{PM}_{2.5}$ to be determined and monitored many times over the course of a heating season or intervention program. Inspection of the data for the past three years in the Fairbanks area indicates that wood smoke contribution has not diminished but may have increased.

3. Polynuclear Aromatic Hydrocarbons

Polynuclear aromatic hydrocarbons (PAH) are found in the $\text{PM}_{2.5}$ from most combustion processes. Although the PAH are generally associated with combustion, certain PAH are reported to be strongly associated with combustion of specific fuels. Examples include retene, picene, and thiophenes, which are often associated with wood, coal and diesel fuel combustion, respectively.

Ambient and OMNI Scientific-generated $\text{PM}_{2.5}$ samples on quartz filters were submitted to the Desert Research Institute for analysis of PAH, including two thiophenes (dibenzothiophene and benzonaphthothiophene), on two dates. In the first round of analyses, eight ambient samples were analyzed for 62 PAH. In the second set, 25 ambient samples and 11 OMNI-generated samples were analyzed for 96 PAH. All of the ambient $\text{PM}_{2.5}$ samples are from the State Building site. The first eight samples were selected to be relatively high $\text{PM}_{2.5}$ days to ensure detection of the PAH, but the subsequent 25 ambient samples were selected considering meteorological conditions and represent a range of low to high $\text{PM}_{2.5}$ days. Most of the ambient samples are from the 2009-10 season. All of the raw and calculated results discussed in this report are provided in a spreadsheet.

The results for OMNI Scientific samples have been used to identify those PAH that appear at relatively high levels and shares of $\text{PM}_{2.5}$ in samples for specific fuels and devices. Those fuel-specific share data have then been used to set upper bounds on the contribution to ambient $\text{PM}_{2.5}$ from the combustion of those fuels.

3.1 OMNI Fuel and Device-Specific Samples

OMNI Scientific supplied UM with eleven quartz filter samples generated using various burners and fossil fuels. The identity of the filters, fuel and burner type are provided in Table 4. The $\text{PM}_{2.5}$ catch for each filter was calculated as described for OMNI-generated wood smoke filters as described in section 2.1. Unfortunately, no data were available to allow calculation of the $\text{PM}_{2.5}$ catch for two of the filters. Full PAH results for these filters, with analytical uncertainties, are provided in a spreadsheet.

Unfortunately, no replicate filters were provided for any fuel type or device, so it is not possible to estimate the repeatability of these experiments.

Table 4: OMNI Scientific-generated filters analyzed for PAHs.

Filter ID	Fuel	Device	PM _{2.5} Catch (µg)
FNB56	No. 1 Fuel Oil	CHIF	NA
FNB59	No. 2 Fuel Oil	CHIF	474
FNB62	Waste Oil	Waste Oil Burner	9559
FNB66	Coal	Stove	NA
FNB69	Dry Coal	Stove	16340
FNB72	Dry Coal	Stove	2950
FNB79	Coal	Stove	7536
FNB89	Coal	OWHH	93786
FNB91	Coal	OWHH	59879
FNB95	Coal	HH Cold Start	3431
FNB96	Coal	HH Hot Start	3965

3.2 Fuel and Waste Oil

Insufficient data were provided by OMNI Scientific to calculate PM_{2.5} catch for the filter generated with no. 1 fuel oil. The filter provided for no. 2 fuel oil has a relatively low catch of PM_{2.5}, and analysis was able to detect significant quantities and shares of only bibenzyl and 9-fluorenone. Bibenzyl appears at a relatively high share of no. 2 fuel oil PM_{2.5}, at 0.2%. Although a higher quantity of PM_{2.5} was caught for waste oil, analysis of this filter detected only 9-fluorenone and at a much lower share (0.0001%) compared with no. 2 fuel oil. The results for waste oil and no. 1 fuel oil do not identify any potential PM_{2.5} markers for these fuels. It is possible, however, to consider 9-fluorenone and bibenzyl as markers of no. 2 fuel oil combustion.

9-Fluorenone made up a significant but small share (0.013%) of no. 2 fuel oil PM_{2.5}, but was also detected in the OMNI generated coal PM_{2.5} samples at 0.0002% to 0.004% share. 9-Fluorenone was detected in ambient samples at similar to higher shares than in the no. 2 fuel oil PM_{2.5} sample, implying that there is another significant source of this compound in ambient PM_{2.5}. This compound was thus not considered to be a unique or useful marker for no. 2 fuel oil PM_{2.5}.

Bibenzyl, however, was not detected in any other OMNI-generated fossil fuel PM_{2.5} samples but was detected as a significant share (0.2%) in no. 2 fuel oil PM_{2.5}. Bibenzyl was not determined in the first set of eight ambient filter samples but was detected in 24 of the 25 samples submitted in the second set. Bibenzyl is found at much lower shares in ambient PM_{2.5} than in PM_{2.5} for no. 2 fuel oil. Bibenzyl was thus considered a potentially unique and useful marker for no. 2 fuel oil combustion.

An upper boundary for the contribution of no. 2 fuel oil PM_{2.5} to the ambient PM_{2.5} samples was calculated using the bibenzyl results for ambient shares and the experimental bibenzyl share in no. 2 fuel oil PM_{2.5}. **This analysis provided a median of 0.6% and a mean of 0.6 ± 0.4% (±1σ) contribution, suggesting that no. 2 fuel oil combustion is responsible for only a minor fraction of ambient PM_{2.5}.**

This is considered an upper boundary since the analysis does not take into consideration any other potential sources of bibenzyl. Further, there is significant but unquantifiable uncertainty in this result, since it is based on a single collection and analysis of PM_{2.5} from no. 2 fuel oil.

3.3 Coal

OMNI Scientific provided PM_{2.5} samples for coal combustion in various residential devices. These results provide some useful results for these devices. However, there are still no measured values for any PAH in coal emissions from power plants or other commercial facilities.

Inspection and analysis of the results for the OMNI coal PM_{2.5} samples suggests eight possible PAH markers for coal combustion. These compounds were selected because they were detected in more than half of the OMNI coal PM_{2.5} samples and because they showed at least a 200 ppm share for one or more coal PM_{2.5} samples. Table 5 lists the selected PAH with their median and average $\pm 1\sigma$ shares of PM_{2.5} over the seven usable OMNI coal PM_{2.5} samples. The very high standard deviations in these data reflect the large variability between different coal burning devices tested by OMNI scientific. In each case, PM_{2.5} from the HH systems had the lowest shares of PAH compounds. Previous studies have identified picene as a unique marker for coal combustion,⁴⁻⁶ and this compound is observed at relatively high shares in most of the coal PM_{2.5} samples in this study (although not for the HH systems).

Table 5: PAH compound shares of coal PM_{2.5} in OMNI Scientific-generated samples, and contributions of coal PM_{2.5} to Fairbanks ambient PM_{2.5} calculated using these shares.

Compound	Share of Coal PM _{2.5} (ppm)		Median Coal Fraction of Ambient PM _{2.5} (%)	
	Median	Mean $\pm 1\sigma$	by Median	by Mean
Picene	1000	1000 \pm 1200	2.7	2.7
Retene	56	250 \pm 400	72	16
Indeno[1,2,3]pyrene	320	370 \pm 350	19	16
Benzo[g,h,i]perylene	440	460 \pm 430	26	24
Anthanthrene	210	190 \pm 160	12	13
Dibenzo[a,l]pyrene	150	130 \pm 120	4.4	4.9
Coronene	160	160 \pm 150	21	21
Dibenzo(b,k)fluoranthene	160	160 \pm 150	5.7	5.8
Dibenzothiophene	2.2	11 \pm 14	234 ¹	48 ¹
Benzonaphthothiophene	6.4	19 \pm 33	20 ¹	6.7 ¹

¹Based on second set of 25 ambient PM_{2.5} samples only.

Also included in Table 5 are the median percent contributions of coal PM_{2.5} for the Fairbanks ambient PM_{2.5} samples based on either the median or the mean share of that compound in OMNI-generated coal PM_{2.5} samples. Most of these are determined for the full set of 33 ambient samples, but thiophene results are reported for only the latter 25 samples analyzed (this is discussed in detail below).

The results for coal PM_{2.5} fraction based on the PAHs are highly variable, ranging from a median contribution of 2.7% to 72%. In fact, because these compounds are also produced by other combustion processes, each of the reported values is an upper boundary for coal PM_{2.5} contribution. Retene, for example, is known to be emitted during wood combustion. Thus, the lowest of these calculated

contributions, 2.7%, which is based on picene shares, is most likely to be valid. Picene has been reported as unique to coal combustion emissions^{7,8}, lending additional confidence to this result.

Defining a coal PM fraction based on any of the markers is complicated, however, by the wide range of PM_{2.5} shares observed for each marker with different coal burning devices. Picene is no exception; picene shares range from below the detection limit (5 ppm share of PM_{2.5}) for HH systems to 3300 ppm share of PM_{2.5} for coal stoves. This suggests that the median coal PM_{2.5} contribution to ambient PM_{2.5} could range from 0.8% if the contribution were exclusively from coal stoves to >100% if the PM_{2.5} were exclusively from HH systems. A value of greater than 100% indicates a substantial contribution from a separate source, although other sources of picene have not been reported. It is possible that a single coal stove in the vicinity of the sampling site contributing less than 1% to the sampled PM_{2.5} could account for all of the observed picene.

3.4 Ratiometric Analysis

Another commonly used measure for sourcing PAH emissions is the ratio of indeno[123-cd]pyrene to the sum of indeno[123-cd]pyrene and benzo[ghi]perylene (IP/(IP+BghiP)).^{6,9,10} Typical

Table 6: Ratio of indeno[123-cd]pyrene to sum of indeno[123-cd]pyrene and benzo[ghi]perylene for various sources.

Source	IP/(IP+BghiP)
Gasoline autos	0.18
Diesel autos	0.37
Coal combustion	0.56
Wood combustion ⁹	0.54
OMNI-Coal	0.42 ± 0.05
Fairbanks PM _{2.5}	0.33 ± 0.05

values for this ratio from various fossil fuel sources, woodsmoke, and for Fairbanks are reported in Table 6. No published value is available for residential oil combustion PM_{2.5}. The ratio for OMNI-generated coal PM_{2.5} (average ± 1σ) is also included in Table 6. No value could be determined for oil burner samples since these PAH compounds were not detected. The ratio for Fairbanks ambient PM_{2.5} is reasonably consistent between samples, and is most similar to that reported for diesel fuel emissions. The observed ratio is lower than all reported ratios except gasoline autos, which suggests a significant contribution from transportation.

3.5 Thiophenes

The thiophenes are unique sulfur-containing compounds related to the PAHs that have been reported in the emissions of fossil fuel combustion. Preliminary studies of Fairbanks ambient PM_{2.5} showed high levels of these compounds. Thus, there was interest in further study of these compounds in ambient PM_{2.5} and in PM_{2.5} from fossil fuel sources.

Dibenzothiophene, benzonaphthothiophenes and alkylated derivatives of these compounds are reported to be representative of diesel fuel vehicle emissions.^{7,8} These compounds make up a significant fraction of the sulfur content of diesel fuel. Low sulfur diesel fuel has lower concentrations, and vehicles utilizing low sulfur diesel fuel emit reduced quantities of these compounds^{7,8}. Rogge *et al.*¹¹ did not report thiophenes in the emissions from residential fuel oil combustion, but Huffman *et al.* did report that typically 25-35% of the sulfur in residential fuel oil particulate is thiophenic sulfur.¹² Analysis of no. 2 fuel oil from Fairbanks at the University of Montana detected dibenzothiophene at 443 ppm, a

level that is higher than that reported previously for high sulfur diesel fuel. Given the similar composition of # 2 fuel oil and diesel fuel, and the fact that the sulfur content of # 2 fuel oil is not regulated with respect to sulfur content, it was hypothesized by us that these compounds would be found in the PM_{2.5} emissions from #2 fuel oil. Dibenzothiophene has also been reported in the emissions from gasoline vehicles¹³. In this and one report on diesel emissions⁸, dibenzothiophene was found primarily in the gas phase. Given the ambient temperatures in Fairbanks, it seems likely that the compound would be found in the particulate phase. These sulfur compounds are not present in wood smoke PM_{2.5}.

Preliminary results for eight Fairbanks ambient PM_{2.5} samples showed very high levels and shares of thiophenes when compared with published results for diesel emissions⁷ or with ambient concentrations in European urban environments¹⁴. Results for the second set of 25 Fairbanks ambient PM_{2.5} samples are much lower, however, and there is a large, statistically significant ($p < 10^{-9}$), and inexplicable difference in thiophene shares of ambient PM_{2.5} between the first eight and latter 25 samples. The share results for the latter 25 samples are lower than those reported for diesel emissions⁷. However, the ambient concentration results for the latter samples remain a factor of two to three higher than those reported for European cities¹⁴. This may be explained by different PM_{2.5} concentrations and local environments. There is concern, therefore, that the thiophene results for the initial eight samples are invalid.

It is important to note that thiophenes were not detected in the OMNI-generated PM_{2.5} from fuel oil samples. Our hypothesis that dibenzothiophene and benzonaphthothiophene might serve as markers for PM_{2.5} from no. 2 fuel oil combustion is not supported by the results, and is invalidated.

Results for two thiophenes in OMNI-generated coal PM_{2.5} are included in Table 5 and are used in subsequent calculations of coal contributions to ambient PM_{2.5}. Coal contributions based on thiophenes range from 6.7% to more than 100%. A value of greater than 100% indicates a substantial contribution from a separate source of dibenzothiophene, such as diesel or gasoline vehicle emissions.

It remains unclear what the sources of the thiophenes observed in Fairbanks ambient PM_{2.5} are. None of the OMNI samples for residential oil heating devices had detectable levels of either thiophene, so this cannot be considered a significant source. Some fraction of the thiophene shares of Fairbanks ambient PM_{2.5} may be explained by coal emissions, but these cannot explain all of the observed thiophenes. Previous studies have attributed thiophenes to diesel emissions, but this should be minimized with low sulfur diesel fuel. Previous studies have also reported relatively high concentrations of these thiophenes in the vapor phase emissions from gasoline automobiles¹³. It is possible in the winter climate in Fairbanks that these normally vapor phase emissions are associated with the PM_{2.5}, explaining a substantial fraction of the observed levels.

3.6 Conclusions

Polynuclear aromatic hydrocarbon and thiophene analysis of PM_{2.5} generated using representative fuels and devices as well as ambient PM_{2.5} does provide useful information regarding

potential contributions of fuel oil, coal and potentially other fossil fuels to Fairbanks PM_{2.5}. The results indicate no substantial contributions of fuel oil or coal combustion to ambient PM_{2.5}.

No. 2 fuel oil emissions and waste oil filters had low amounts of PM_{2.5} and the levels of nearly all compounds were below the detection limits. Bibenzyl was identified as a potential marker based on its relatively high fraction in no. 2 fuel oil PM_{2.5} and its absence in coal PM_{2.5}. Using this as a marker leads to the conclusion that combustion of no. 2 fuel oil contributes a negligible fraction to ambient PM_{2.5} of less than 1% for the 33 samples analyzed.

Picene is accepted as a unique marker for coal combustion. Zhang *et al.* reported picene as being “unique to the organic carbon emissions from coal combustion,” although picene was not detected in all coal particulate and was notably absent from bituminous coal emissions from industrial boilers.⁶ Zhang *et al.* did report picene in brown and mixed coal emissions from industrial boilers (3.7 and 2.0 ppm shares respectively) as well as much higher levels in the emissions from residential coal burners (72-284 ppm shares).⁶ Oros *et al.* reported picene and methyl picenes as bituminous coal smoke markers, and C₂ substituted picenes as more general coal-specific markers.⁴ As a large PAH, picene can be expected to be found primarily in the particulate phase.

The current results for picene support its use as a specific marker for coal combustion. Picene appears as a relatively large share of coal PM_{2.5} for certain devices. Other compounds found in the coal PM_{2.5} were detected at lower PM_{2.5} share and suggested higher contributions of coal combustion to ambient PM_{2.5}. These compounds are very likely found in the emissions of other combustion sources.

Using a median value of picene share in the various devices leads to 2.7% coal contribution to PM_{2.5}. The picene shares, however, are highly variable depending on the device. If coal combustion were primarily from devices that have a much lower PM_{2.5} share of picene, then coal PM_{2.5} would represent a much higher fraction of ambient PM_{2.5}. Alternatively, the observed picene share of ambient PM_{2.5} could result from less than a 1% contribution from devices that generate high picene shares.

The OMNI Scientific PM_{2.5} samples do not show detectable levels of thiophenes for fuel oil samples, and show only low shares for coal samples. Thiophenes are observed in ambient PM_{2.5} at levels that cannot be explained using coal combustion sources alone. It remains unclear what the sources of these thiophenes are. A fraction of the observed thiophenes might be associated with coal emissions, but it seems likely that the majority is from transportation sources.

4. Hopanes and Steranes

The hopanes and steranes are typically found and reported in distillate fossil fuel emissions, but have also been reported in coal emissions. The highest levels reported are for diesel auto emissions, and the lowest are for coal emissions. The hopanes and steranes are not present in emissions from biomass combustion, and thus provide a general indication of the extent to which an air shed is affected by fossil fuel emissions. Unfortunately, however, none of the compounds have been reported to be a specific marker of any particular fossil fuel source.

Analytical results for 23 hopane and sterane compounds have been obtained for eight Fairbanks ambient PM_{2.5} samples, and generally show high levels and shares (5-60 ppm) of certain compounds. These results, with analytical uncertainties, are presented in a separate spreadsheet. Levels of hopanes and steranes in Fairbanks are typically higher than those reported for ambient air in other airsheds^{5,15}, and Fairbanks hopane and sterane shares are greater than those reported for most specific fuel emissions^{4,6,8,11,13}. Analytical results for the same hopanes and steranes were also obtained for fossil fuel PM_{2.5} samples provided by OMNI Scientific. These results are also presented in a separate spreadsheet.

4.1 Coal

Of the compounds analyzed, several hopanes were selected as potentially useful markers of coal combustion. Compounds were considered potential markers if they were detected in all of the coal PM_{2.5} samples, if shares of three or more of the seven samples exceeded 100 ppm, and if the compounds did not have comparable shares in fuel oil PM_{2.5}. These selected hopanes, and their median and mean shares of coal PM_{2.5}, are presented in Table 7. Shares of coal PM_{2.5} are highly variable between devices, with the HH systems showing low shares and the coal stoves generally showing high shares. In comparison, previous studies have reported hopane shares of diesel PM_{2.5} of 5-60 ppm^{7,8}.

Table 7: Hopane compound shares of coal PM_{2.5} in OMNI Scientific-generated samples, and contributions of coal PM_{2.5} to Fairbanks ambient PM_{2.5} calculated using these shares.

Compound	Share of Coal PM _{2.5} (ppm)		Median Coal Fraction of Ambient PM _{2.5} (%)	
	Median	Mean ± 1σ	by Median	by Mean
17α(H),21β(H)-29-Norhopane	83	122 ± 133	50	34
17α(H),21β(H)-Hopane	111	126 ± 121	23	21
22S-17α(H),21β(H)-30-Homohopane	45	132 ± 135	39	13
22R-17α(H),21β(H)-30-Homohopane	90	137 ± 156	26	17
22S-17α(H),21β(H)-30,31-Bishomohopane	41	65 ± 62	21	13

The share data presented in Table 7 can be used to estimate coal contributions to the ambient PM_{2.5} samples. These results are also presented in Table 7, and show median coal contributions to ambient PM_{2.5} of 13 to 50%. Because the hopanes are not specific to coal emissions, these should be considered upper bounds to coal contribution. Further, the hopane shares are highly variable with coal burning device. Thus, ambient levels of PM_{2.5} could suggest an upper bound of as little as 6% contribution of PM_{2.5} from coal stoves that produce high hopane shares. Coal emissions from HH systems, on the other hand, cannot explain the shares observed in Fairbanks ambient PM_{2.5}.

4.2 Fuel Oil

The results for hopane and sterane shares of no. 2 fuel oil and waste oil PM_{2.5} were also examined for potentially useful selective markers. Hopane and sterane shares of waste oil PM_{2.5} were all less than 1.3 ppm and were equivalent or higher in coal PM_{2.5}, and thus could not be used to estimate waste oil contributions to ambient PM_{2.5}. One sterane, 20S-5 α (H),14 β (H),17 β (H)-cholestane, did appear at a relatively high share of no. 2 fuel oil PM_{2.5} (13 ppm) and at lower shares of coal PM_{2.5} (0-6 ppm). Using this compound as a marker for no. 2 fuel oil generates an extreme upper bound of 15% for the contribution of no. 2 fuel oil combustion to ambient PM_{2.5}. This is very clearly an overestimate to fuel oil contribution, since substantial quantities of this sterane would also be produced by combustion of other fossil fuels, including coal. Further, there is significant but unquantifiable uncertainty in this result, since it is based on a single collection and analysis of PM_{2.5} from no. 2 fuel oil.

4.3 Ratiometric Analysis

An alternative approach for the analysis of hopane results is to calculate the ratio of 17 α (H) 21 β (H) hopane to 22R-17 α (H), 21 β (H) homohopane.^{4,6,16} This value has been reported to be 3.7 for gasoline emissions and 2.5 for diesel emissions.¹⁶ Unfortunately, conflicting results have been reported for coal combustion emissions, with Oros *et al.*⁴ reporting values of 0.1-2.6 and Zhang *et al.*⁶ reporting values of 4.28-9.19. In the current study, the ratio for OMNI-generated coal emissions over all devices ranged from 0.76 to 1.63 with a median of 1.15 and an average $\pm 1\sigma$ of 1.13 \pm 0.33. The ratios for no. 2 fuel oil and waste oil emissions were found to be 0.57 and 1.01 respectively, but the ratio for no. 1 fuel oil emissions could not be determined because 22R-17 α (H), 21 β (H) homohopane was not detected. The average value observed for Fairbanks is 1.2 \pm 0.4. This relatively low result for Fairbanks is not significantly different from that observed for the OMNI-generated coal filters and is within the range reported by Oros *et al.* for coal. This analysis implies that coal or other low ratio emissions such as fuel oil may be a more substantial contribution to the hopanes in Fairbanks ambient PM_{2.5} than the analyses above suggest.

4.2 Conclusions

Hopane and sterane analysis of Fairbanks ambient PM_{2.5} shows levels and shares that are indicative of substantial contribution from fossil fuel combustion sources. Unfortunately, however, none of these compounds can be considered specific markers of any individual combustion source. This means that any simple calculations of contributions from a given source will overestimate the value and must be considered upper bounds. Upper boundaries for the contributions of coal and no. 2 fuel oil combustion to ambient PM_{2.5} by this approach are estimated to be 13% and 15% respectively.

Analysis based on the ratio of levels for two specific hopanes indicate that a substantial share of hopanes in ambient Fairbanks PM_{2.5} are from a low ratio source such as fuel oil or coal. This is inconsistent with the results based on hopane and sterane shares of PM_{2.5}.

A more comprehensive approach of source apportionment using full profiles of all sources and ambient PM_{2.5} is much more appropriate for this analysis. This is not recommended with the limited data available for Fairbanks sources and ambient PM_{2.5}.

5. References Cited

- [1] Caseiro, A., Bauer, H., Schmidl, C., Pio, C. A., Puxbaum, H., "Wood burning impact on PM10 in three Austrian regions," *Atmospheric Environment* **2009**, *43*, 2186-2195.
- [2] Fine, P. M., Cass, G. R., Simoneit, B. R. T., "Chemical Characterization of Fine Particle Emissions from the Fireplace Combustion of Wood Types Grown in the Midwestern and Western United States," *Environmental Engineering Science* **2004**, *21*, 387-409.
- [3] Schmidl, C., Marr, I. L., Caseiro, A., Kotianova, P., Berner, A., Bauer, H., Kasper-Giebl, A., Puxbaum, H., "Chemical characterization of fine particle emissions from wood stove combustion of common woods growing in mid-European Alpine regions," *Atmospheric Environment* **2008**, *42*, 126-141.
- [4] Oros, D. R., Simoneit, B. R. T., "Identification and emission rates of molecular tracers in coal smoke particulate matter," *Fuel* **2000**, *79*, 515-536.
- [5] Rutter, A. P., Snyder, D. C., Schauer, J. J., De Minter, J., Shelton, B., "Sensitivity and Bias of Molecular Marker-Based Aerosol Source Apportionment Models to Small Contributions of Coal Combustion Soot," *Environmental Science and Technology* **2009**, *43*, 7770-7777.
- [6] Zhang, Y., Schauer, J. J., Zhang, Y., Zeng, L., Wei, Y., Liu, Y., Shao, M., "Characteristics of Particulate Carbon Emissions from Real-World Chinese Coal Combustion," *Environmental Science and Technology* **2008**, *42*, 5068-5073.
- [7] Liang, F., Lu, M., Birch, M. E., Keener, T. C., Liu, Z., "Determination of polycyclic aromatic sulfur heterocycles in diesel particulate matter and diesel fuel by gas chromatography with atomic emission detection," *Journal of Chromatography, A* **2006**, *1114*, 145-153.
- [8] Schauer, J. J., Kleeman, M. J., Cass, G. R., Simoneit, B. R. T., "Measurement of Emissions from Air Pollution Sources. 2. C1 through C30 Organic Compounds from Medium Duty Diesel Trucks," *Environmental Science and Technology* **1999**, *33*, 1578-1587.
- [9] Schauer, J. J., Kleeman, M. J., Cass, G. R., Simoneit, B. R. T., "Measurement of Emissions from Air Pollution Sources. 3. C1-C29 Organic Compounds from Fireplace Combustion of Wood," *Environmental Science and Technology* **2001**, *35*, 1716-1728.
- [10] Stracher, G. B., Taylor, T. P., "Coal fires burning out of control around the world: thermodynamic recipe for environmental catastrophe," *International Journal of Coal Geology* **2004**, *59*, 7-17.
- [11] Rogge, W. F., Hildemann, L. M., Mazurek, M. A., Cass, G. R., Simoneit, B. R. T., "Sources of Fine Organic Aerosol. 8. Boilers Burning No. 2 Distillate Fuel Oil," *Environmental Science and Technology* **1997**, *31*, 2731-2737.
- [12] Huffman, G. P., Huggins, F. E., Shah, N., Huggins, R., Linak, W. P., Miller, C. A., Pugmire, R. J., Meuzelaar, H. L. C., Seehra, M. S., Manivannan, A., "Characterization of fine particulate matter produced by combustion of residual fuel oil," *Journal of the Air & Waste Management Association* **2000**, *50*, 1106-1114.
- [13] Schauer, J. J., Kleeman, M. J., Cass, G. R., Simoneit, B. R. T., "Measurement of Emissions from Air Pollution Sources. 5. C1-C32 Organic Compounds from Gasoline-Powered Motor Vehicles," *Environmental Science and Technology* **2002**, *36*, 1169-1180.

- [14] Saarnio, K., Sillanpaa, M., Hillamo, R., Sandell, E., Pennanen, A. S., Salonen, R. O., "Polycyclic aromatic hydrocarbons in size-segregated particulate matter from six urban sites in Europe," *Atmospheric Environment* **2008**, *42*, 9087-9097.
- [15] Zheng, M., Cass, G. R., Schauer, J. J., Edgerton, E. S., "Source Apportionment of PM_{2.5} in the Southeastern United States Using Solvent-Extractable Organic Compounds as Tracers," *Environmental Science and Technology* **2002**, *36*, 2361-2371.
- [16] Rogge, W. F., Hildemann, L. M., Mazurek, M. A., Cass, G. R., Simoneit, B. R. T., "Sources of fine organic aerosol. 2. Noncatalyst and catalyst-equipped automobiles and heavy-duty diesel trucks," *Environmental Science and Technology* **1993**, *27*, 636-651.

***Exploratory Research of Wintertime Aerosol Chemical
Composition at a Ground Location in Fairbanks, Alaska***

Richard E Peltier
University of Massachusetts
February 10, 2012

TABLE OF CONTENTS

Executive Summary	3
Introduction and Rationale for Research	4
Instrumentation	4
PILS-IC	4
Sunset Labs EC and OC	6
Filter Samples	6
Results and Discussion	7
Aerosol Ions	7
Sulfur Studies	10
EC and OC	12
XRF (Preliminary)	14
Conclusions and Future Directions	18
References	19

EXECUTIVE SUMMARY

This report summarizes quantitative chemical composition data of ambient particulate matter of less than 2.5 μm (PM_{2.5}) aerosol collected during a month-long study in Fairbanks, Alaska in February and March, 2011. The data collected include hourly measures of ions commonly found in aerosol, as well as hourly measurements of organic and elemental carbon. Daily filter samples were also collected for alternative chemical analyses. Data were collected in a small, insulated trailer that was located near the Fairbanks Borough North Star Administrative Office near 809 Pioneer Road.

Approximately 283 sets of ion samples were collected during this study, and just over 500 measurements of organic and elemental carbon were collected. 37 pairs of filters were collected as well, with one set consumed by analytical techniques and a second set collected for long-term storage and post-hoc analyses. Aerosol chemical composition appears to be dominated by organic carbon (mean = 6.5 $\mu\text{gC m}^{-3}$) and estimated organic matter, as well as elemental carbon (mean = 0.9 $\mu\text{gC m}^{-3}$) and sulfate (mean = 2.02 $\mu\text{g m}^{-3}$). Lesser measurements included ammonium, nitrate, potassium, and several light organic acids.

The data show a clear diurnal profile that is likely attributed to anthropogenic activities. Wood burning appears to be a significant contributor to the high particle loading observed during the winter in Fairbanks as indicated by the enhanced levels of organic carbon and in the relative absence of other compounds that would indicate other emission sources of PM_{2.5}. Ion information provides some confirmation of this, and a preliminary look at high time resolution XRF data provides additional confirmatory evidence in support of this hypothesis.

A particular focus of this work involved improving the understanding of sulfur in the Fairbanks airshed. Particulate sulfur (as sulfate) was detected throughout the study indicating that mechanisms that promote sulfur conversion (from gas phase to particle phase) are, in fact, present. We also examined chemical composition by complementary analytical methods – first by X-Ray Fluorescence (XRF) followed by ion chromatography for two measures of sulfur from the same filter. Results show that sulfur is measured at the same levels no matter the analytical method, which is in contrast to results reported by the United States Environmental Protection Agency (EPA) for chemical speciation measurements in Fairbanks. It is likely that a methodological difference explains the disagreement between the two methods of sulfur measurement used by the EPA speciation network.

INTRODUCTION AND RATIONALE FOR RESEARCH

Ambient fine particles are ubiquitous in the lower troposphere, and result from a variety of physical and chemical transformations. They can be formed as a primary pollutant through, among others, combustion and biogenic sources, as well as by resuspension of dust from crustal surfaces [1-3]. Secondary aerosol sources – that is, aerosol formed by a variety of secondary gas-phase chemical reactions in the atmosphere - are substantially more complex and can represent a significant fraction of ambient aerosol [2, 4]. The diversity of possible atmospheric reactions makes unequivocal identification of aerosol sources quite complex, and thus, our understanding of aerosol formation is also incomplete.

The Fairbanks region is an excellent example of unique and diverse chemical conditions that result in ambient particulates. The region is known to routinely exceed the National Ambient Air Quality Standards during the winter heating season. This is thought to arise both from significant local emissions, but also by meteorological enhancement due to strong inversions and poor regional ventilation. Aerosol source hypotheses include emissions from wood and fuel oil burning, and the formation of sulfur-containing particles from local coal-fired power generation. Because of its relatively remote location, regional transport of particle pollution is generally insignificant suggesting that most of the ambient pollution was generated within the local area. Thus, because of this unique complexity and the absolute need to maintain safe temperatures through residential heating during the winter, Fairbanks represents an excellent case for further study of ambient aerosol composition and formation.

Because of a history of demonstrated non-attainment for PM_{2.5} in the Fairbanks area, there exists a need for substantially increased expansion of fundamental understanding of aerosol chemical climatology for the community. This information will be useful in identifying suggested pathways to reduce air pollution levels in the most efficient and cost-effective manner, as well as reduce aerosol components of known health hazards for the citizens of the borough. Without this information, mitigation attempts are likely to be ineffective.

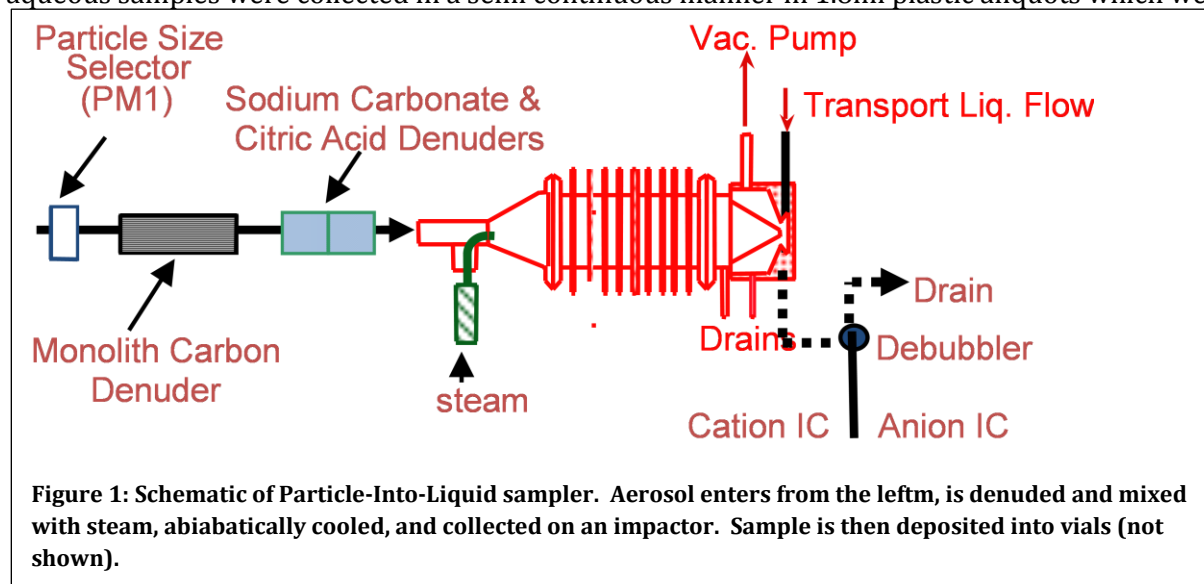
INSTRUMENTATION

A state-of-the-art instrumentation package was installed in a small, insulated utility trailer, which was situated near the N CORE site in Fairbanks, Alaska. Instrument integration was completed on February 6, 2011, and field data collection began on February 9th, 2011 at approximately 13:00 AST. The instrumentation package, described below, operated with periodic user intervention and maintenance, as described below. FNSB staff were immensely helpful in performing these duties for the duration of the study. The study continued until March 16th, 2011 at 07:05 AST when instruments were powered down and removed from the trailer.

PILS-IC

The Particle-Into-Liquid Sampler (PILS) is a device that captures all particles greater than ~10-15 nm by employing condensational growth of the particle in a supersaturated environment of water vapor. Prior to entering the PILS, a particle passes through a set of denuders which strip out gas phase organics, and any acidic or basic gases present in the aerosol stream. The particles and water vapor are adiabatically cooled, which promotes rapid particle growth to a size of 1-3 μm ; these are then accelerated and collected on an impaction wall. This wall is continuously washed with a small amount of purified water, and the effluent is then diverted by syringe pump to any number of

analytical processes. Typical detection limits are described in Table 1, and a schematic representation of the PILS system is shown in Figure 1. Rather than *in-situ* analytical chemistry, aqueous samples were collected in a semi continuous manner in 1.8ml plastic aliquots which were



mounted on a computer-controlled rotating carousel. Filled aliquots were periodically collected and frozen by local assisting staff.

Maintenance activities performed by local staff included emptying of wastewater tanks (containing a non-hazardous dilute solution), replacement of purified water, retrieval and storage of samples and replacement of new plastic vials, and inspection and removal of any ice buildup at the pump exhaust. The instruments were checked daily for normal operation. Collected samples were organized according to unique barcodes, and shipped to the investigator's lab in Massachusetts for chemical analysis.

Table 1: This is a summary of analyses of aerosol chemical composition useful for this study. Data include typical concentrations in Fairbanks, estimated liquid concentration in the PILS effluent, and typical detection limits by a variety of analytical techniques.

Compound	Typical Winter Air Concentration at Fairbanks (Jan-Feb, 2006-2009), $\mu\text{g m}^{-3}$	Estimated Liquid Concentration ($\mu\text{g L}^{-1}$)	Typical Detection Limit ($\mu\text{g L}^{-1}$)
Sulfate	4.498	3748.33	0.01 ^a
Elemental sulfur	1.63	1358.33	0.1 ^b
Ammonium	2.021	1684.17	0.1 ^a
Sodium	0.093	77.50	0.1 ^a
Nitrate	1.121	934.17	0.5 ^a
Potassium	0.150	125.00	0.2 ^a
As	0.0015	1.25	0.1 ^c
Se	0.0010	0.83	1.0 ^c
Oxalate	n/a	n/a	0.2 ^a
Zn	0.0520	43.33	0.2 ^c

^a by ion chromatography

^b by ICP-MS

^c by Flame ionization/ Atomic Absorption

Once defrosted, collected aliquots were removed from field vials and diluted to 4ml with precision pipettes and placed into 5ml autosampler vials (Environmental Express, Model K4300). Dilution matrix was 18.2M-Ohm or better purified water. The samples were then analyzed by ion chromatographic separation for 18 ion species (as a total of 13 anion and 5 cation peak) using a Dionex ICS-3000 Ion Chromatography System. In order of elution, the anion peaks are fluoride, acetate, formate, methanesulfonate, chlorite, chloride, nitrite, sulfate, bromide, oxalate, nitrate, chlorate, and phosphate. The 5 cation peaks are sodium, ammonium, potassium, magnesium, and calcium.

SUNSET LABS EC AND OC

Because of the multicomponent complexity of aerosol in Fairbanks, we also operated a Sunset Labs Model 4 semi continuous Organic Carbon and Elemental Carbon (OC/EC) analyzer. This instrument simultaneously and directly measures fine particle organic and elemental carbon at hourly integrated measurements and is a standalone instrument that requires almost no user support.

The instrument includes a sharp-cut cyclone to remove particles greater than 2.5 μm . The inlet also includes a parallel plate denuder consisting of laminar paper sheets impregnated with activated carbon which effectively removes organic vapors. The sample cycle typically includes 45 minutes of sample collection that begins on the hour, and a 12-13 minute analysis cycle. The instrument goes through a cooling cycle and then repeats an analysis at the next hour. With typical operating parameters, the detection limits of this analyzer are approximately 0.3 $\mu\text{g m}^{-3}$ for both organic carbon and elemental carbon. It requires several certified compressed gases for analysis, and this method is consistent with the NIOSH [5-7] method of OC and EC determination.

FILTER SAMPLES

37 filters samples (collected in duplicate, a total of 74 filters) were also collected for the duration of this study. The samples were collected over a nominal 24 hours (with filter changes initiated at approximately 13:00 AST), and were collected at ambient temperature and pressure and corrected to standard temperature and pressure. Samples were collected in conductive plastic filter holders that contained 37 mm ringed Teflon filters (Pall Corporation, model R2PJ037) that were sequentially labeled. Sample passed through a sharp-cut cyclone with a cut size of 2.5 μm , and through two stainless steel annular denuders in series, one of which was coated with a sodium carbonate/bicarbonate solution, and second coated with a citric acid solution. Sample flow was achieved by a 1/4hp vane pump that applied a strong vacuum to a critical orifice calibrated for choked flow at 15.0 l min^{-1} . After sampling, filters were returned to their original petri dish containers and sent to the investigator's lab in Massachusetts.

Filters were analyzed by high resolution X-ray Fluorescence Spectroscopy using analytical methods consistent with EPA speciation approaches. The method used in this analysis conforms to EPA Compendium Method IO-3.3: For the Determination of Metals in Ambient Particulate Matter Using X-Ray Fluorescence (XRF) Spectroscopy.

Filters were then returned to the lab and sent for further analysis by ion chromatography. This is a destructive technique that renders the remaining filters unusable for any further testing. Chromatographic separation methods were consistent with those described above, but filters were first digested in a vial of purified water under sonication, and then cooled for an hour to room temperature prior to analysis.

RESULTS AND DISCUSSION

AEROSOL IONS

Approximately 280 unique, hourly samples were collected over the course of this study. A number of samples were invalidated due to issues of contamination and instrument failure.

Table 2: Univariate statistics for the range of ions measured during this study. Reported values include mean, median, standard deviation, range, and the number of measurements collected during this study. Llod denotes measurements below the limit of detection.

	Mean, $\mu\text{g m}^{-3}$	Median, $\mu\text{g m}^{-3}$	Std Dev, $\mu\text{g m}^{-3}$	Range, $\mu\text{g m}^{-3}$	n
Ammonium	0.39	0.24	0.46	(llod, 3.22)	278
Potassium	0.75	0.63	0.42	(0.24, 3.5)	278
Magnesium	0.17	0.07	0.39	(0.03, 2.65)	278
Calcium	0.93	0.56	1.16	(0.17, 7.37)	273
Acetate	1.06	0.51	1.23	(llod, 8.8)	285
Formate	0.21	0.09	0.25	(0.02, 1.55)	285
Chloride	0.83	0.28	2.12	(0.08, 25.1)	285
Nitrite	0.08	0.03	0.12	(llod, 0.62)	285
Sulfate	2.02	1.55	1.56	(0.12, 12.25)	285
Oxalate	0.03	0.01	0.08	(llod, 0.56)	285
Nitrate	0.59	0.41	0.51	(llod, 2.9)	285

Table 2 shows univariate statistics describing the data collected at this location. Dominant ions throughout this study included ammonium, calcium, and potassium, as well as sulfate, nitrate and some chloride. All ions were detected at times over the course of this study. A number of light organic acids were detected, including acetate and formate; these are discussed further in the next section.

Aerosol chemical composition during this study could be characterized by high variability, as seen in relatively high reported standard deviations (Table 2) and graphically as in Figure 2. Figure 2 plots sulfate, one of the more dominant ions measured during this campaign, plotted on hourly intervals. Superimposed on this graph are measured sulfate concentrations determined from collocated 24-hour filter samples which were also analyzed by ion chromatography. Of particular note, sulfate appears with a quasi-diurnal cycle (more discussion of this follows) with minima typically in the 1-2 $\mu\text{g m}^{-3}$ range, and short term maxima in the 4-5 $\mu\text{g m}^{-3}$ range; there are notable deviations from this with clear spikes in sulfate approaching 10-12 $\mu\text{g m}^{-3}$. 24 hour filter measures show some variability in concentration data, but they lack substantial texture clearly seen with the higher time resolution data.

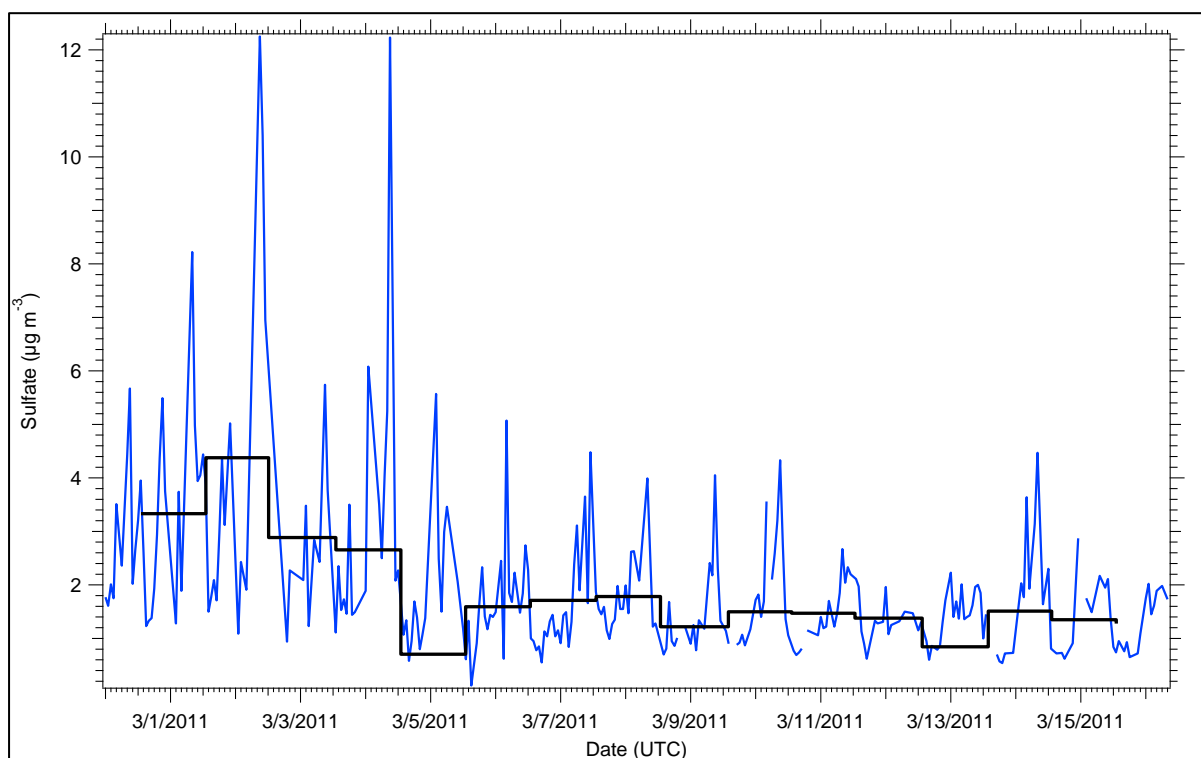


Figure 2: Time series of daily filter measures of sulfate (black lines) with hourly measures of sulfate by PILS (blue) superimposed on the figure.

Figure 3 depicts available ion data coupled with measured organic carbon, plotted against apparent charge, in microequivalents. Charge is calculated by taking the net valence charge for each measured ion, adjusted for molar concentration, and summing the positive and negative charges. This approach also includes (when available) the net charge resulting from a variety of measured light organic acids (including oxalate, formate, and acetate). If all elements are measured, one would expect a balanced charge of zero. Deviations towards a net negative charge indicate a missing cation; deviations towards a net positive charge indicate a missing anion. In typical studies, this missing cation (e.g. conditions with net negative charge) is presumed to be a hydrogen proton which can accompany acidic aerosol.

In the case of Figure 3, both positive and negative conditions appear in the data. While acidic conditions are often observed in air sheds that have significant influence from coal combustion (which normally leads to sulfuric acid formation in the aerosol), it is notable that these deviations occurred throughout a range of concentrations of OC – both high and low – and suggest that acidic influence is independent of OC concentration. Charge balance contributed by the measured light organic acids also appears to be relatively low during these periods suggesting that the aerosol climatology lacks a substantial light organic acid profile and further suggestion this acidity is linked more closely inorganic acids, such as sulfuric or nitric acid, rather than light organic acids. This does provide some weak evidence that inorganic acids are playing a role in determining aerosol charge in Fairbanks, but these results are not yet determinative; there are a number of possible explanations for this, though it does appear likely that the modest acidity results from a source unrelated to the source of organic carbon. It should also be noted that apparent acidity determined here is quite modest in the context of other studies which examined particle acidity arising from coal combustion. For example, in communities on the East Coast of the US, net charges are typically $-0.25 \mu\text{Eq}$ and lower [8, 9], which is twice as acidic as conditions observed here.

In contrast, a surprising result was that there were a number of cases where there were significant positive charges observed in the data, suggesting missing cations. This tended to occur during

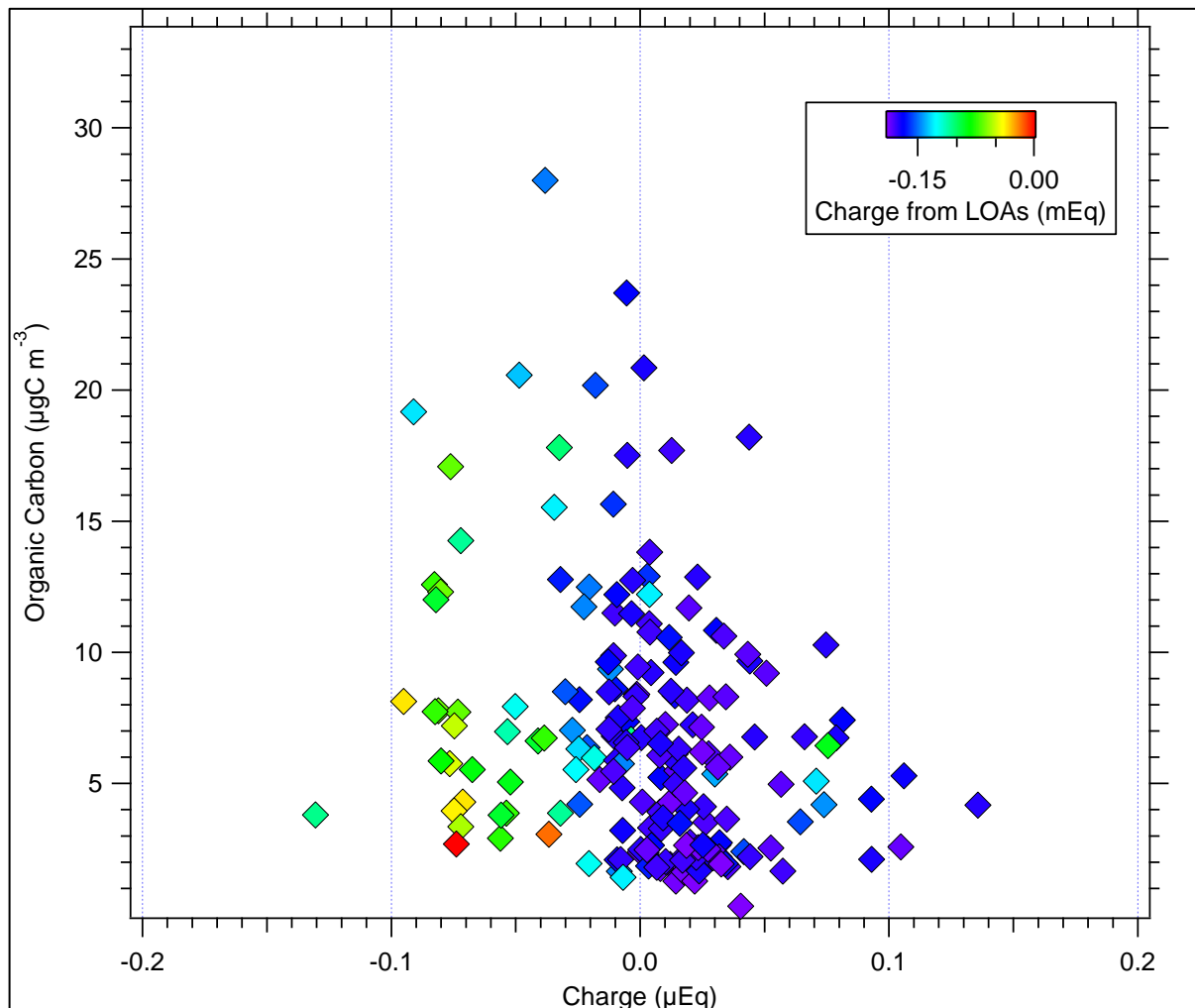


Figure 3: Net charge on aerosol plotted against organic carbon concentration. Markers are colored by apparent net charge resulting from three measured light organic acids, which include acetate, formate, and oxalate.

periods of lowest measured OC. While not yet determined, there are several possible explanations for this. For example, one explanation would be contamination of the system by a cation such as ammonium, though one would expect to see a systematic bias rather than only occasional influence. Another more likely explanation is that a negatively charged species, such as a light organic acid, may be present in aerosol only under conditions of limited OC, which is not accounted for in the charge calculation.

SULFUR STUDIES

Investigating the possible sources of sulfur was an a priori interest in this study and stems from the observation that local speciation measurements, which measure sulfate by chromatography and sulfur by XRF, suggest that there may be a non-sulfate source of sulfur present in the Fairbanks air shed. Of note, as illustrated by Figure 4, existing sulfate and sulfate data shows a substantially noisy

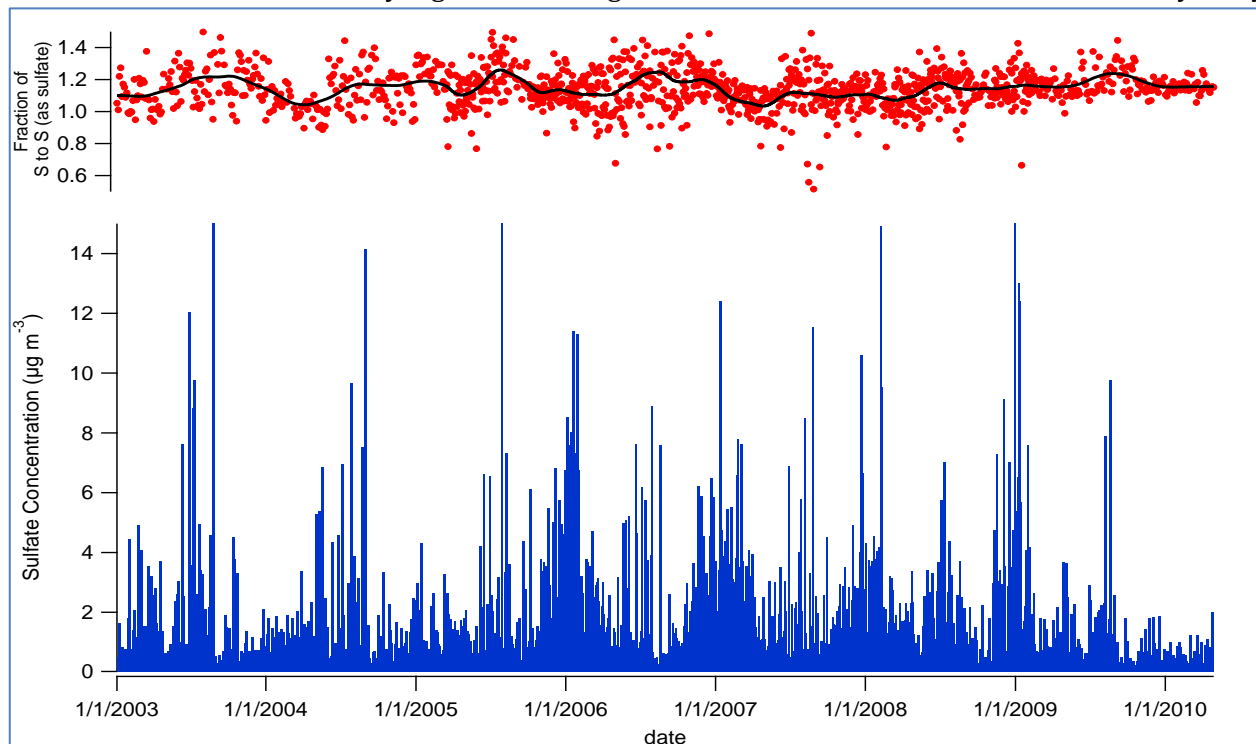


Figure 4: Time series of speciation data collected by FNSB staff since 2003. Data on bottom is daily sulfate measurements, and plot at top represents the fraction of total sulfur to sulfur calculated from measured sulfate. Total sulfur is measured directly by XRF, and sulfate is measured directly by ion chromatography.

pattern in the ratio of sulfur to sulfur (as sulfate). A clear divergence from unity can be observed suggesting that there is a possible unmeasured, stoichiometrically-adjusted sulfur source not captured in a collocated measure of sulfate. This ratio does have broad trends, but they do not appear to correspond with measured sulfate, which appears as highly variable in concentration and time.

Because this study collected its own filter measurements, we can empirically investigate the possibility of ‘missing sulfur’ by sequential analysis by non-destructive X-Ray Fluorescence Spectroscopy, followed by filter processing and chemical analysis of dissolved ions. The methods

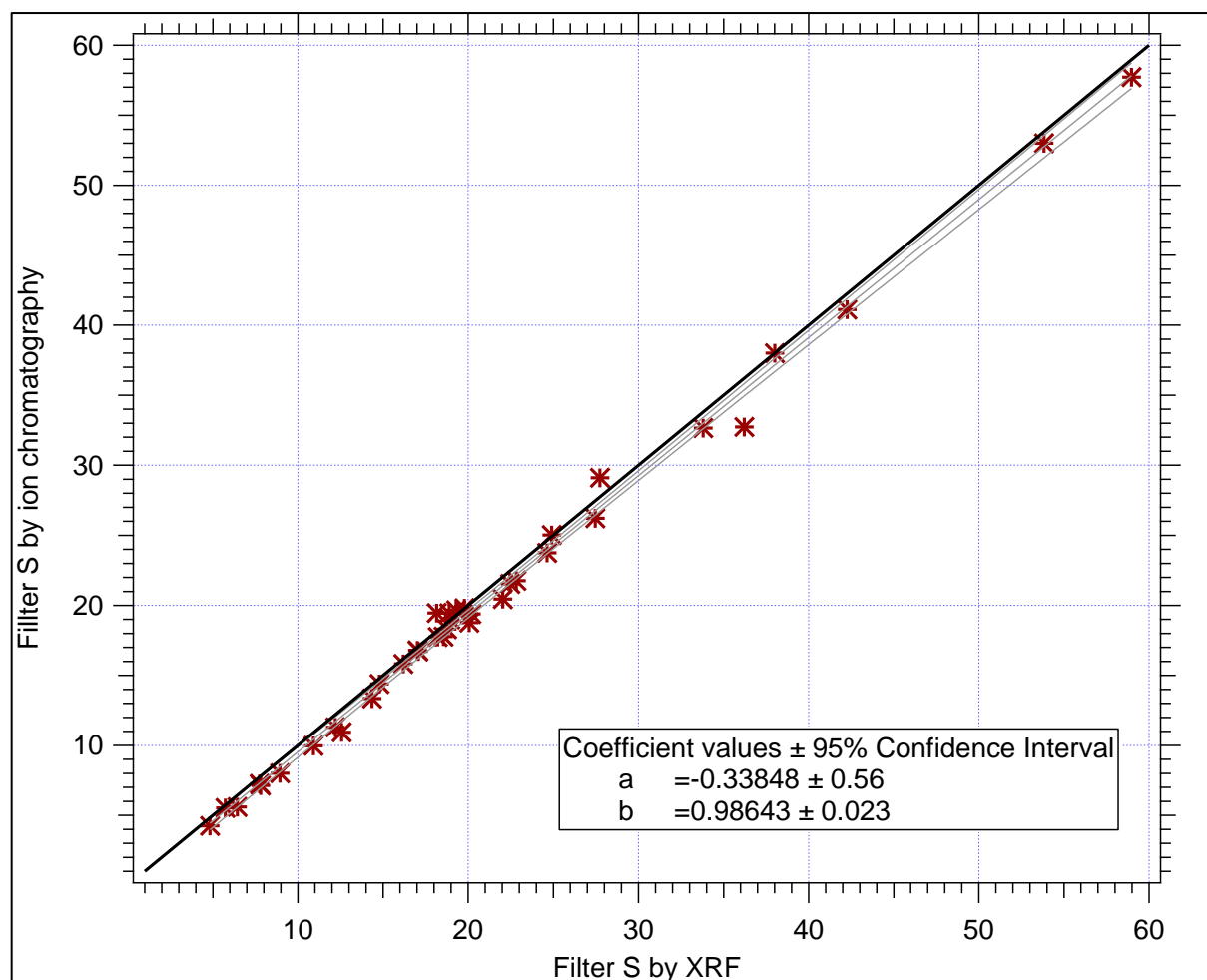


Figure 5: Regression plot of sequentially analyzed filters for sulfur concentration. Filters were first analyzed by XRF followed by ion chromatography for a measure of sulfate. Linear fit coefficients are also included and report a correlation coefficient of 0.97.

for this process were similar to the method used to analyze the aliquots collected by the PILS. The results, as shown in Figure 5, show a very high degree of correlation between measured S as sulfate and directly measured S by XRF. Regression slope approaches statistical unity, with a statistically insignificant intercept. These findings clearly suggest that any bias seen in the presence of sulfur across different measurements are not likely because of a unmeasured sources of ambient sulfur; the most likely explanation is that there is some bias introduced because of methodological reasons such as differential absorption related to different filter materials, systemic bias introduced by post-collection filter processing, or gas-phase intrusion resulting from the extreme cold experienced in Fairbanks. While the answer to this problem is still elusive, it should be noted that sulfur comprises a relatively small fraction of overall PM loading and this small bias, on average, may represent just a few tenths of percent of aerosol (by mass) in the Fairbanks region.

Further analysis follows in the section on preliminary analysis of XRF data.

EC AND OC

By mass, OC was one of the largest contributors to PM_{2.5} mass observed at this location during the study. EC, which was a much smaller fraction by mass, was well correlated with OC suggesting common sources. Of particular note as illustrated in Figure 6, OC and EC are generally well correlated with one another during this study. The OC to EC ratio was generally between 4-5,

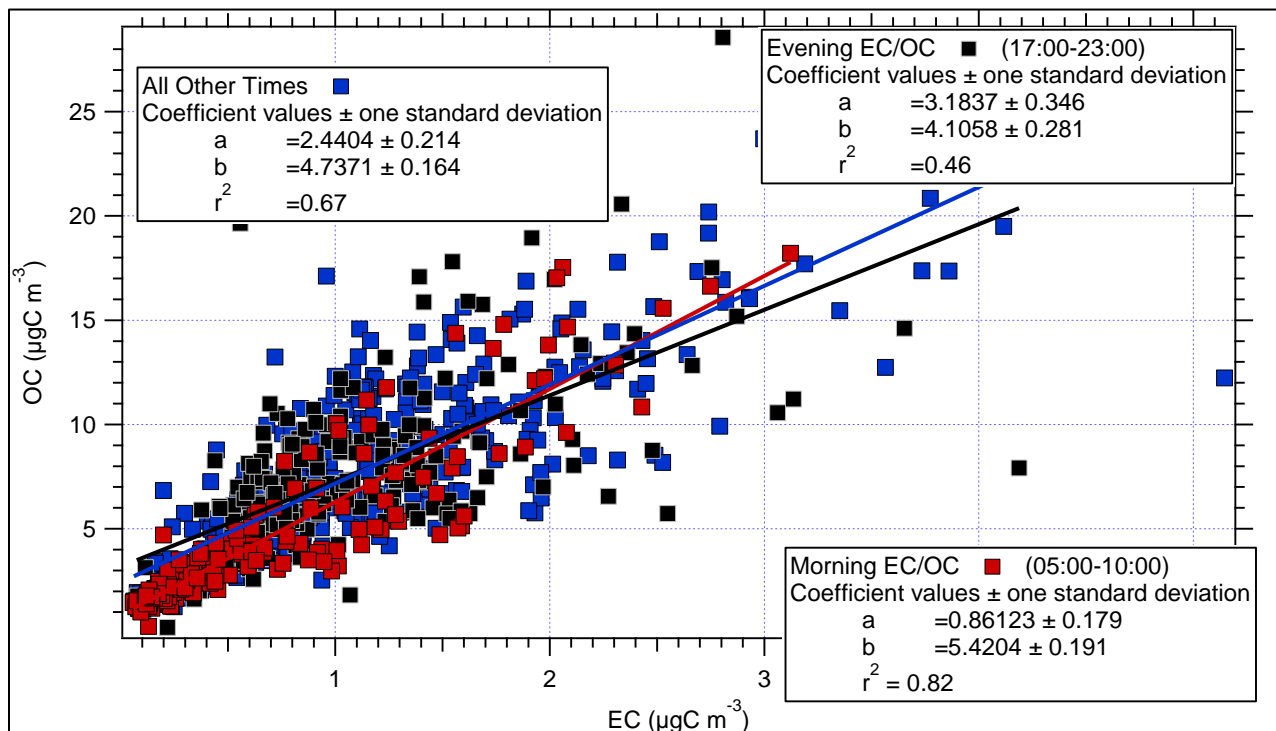


Figure 6: Measured organic carbon compared to measured elemental carbon (collected at same time). Data are binned to different time periods to show comparison between morning, evening, and all other times. Regression statistics are for a linear fit.

which is somewhat higher than urban values reported in the literature [10-14] and is more consistent with the higher values observed in biomass burning plumes [15-18], though this is an overly simplified analysis. More work is indicated to investigate these ratios further. A somewhat different regression was observed when the data were binned between morning, evening, and all other times. Tighter correlations and higher ratios were observed (Figure 6) in the morning compared to the evenings, suggested a different source process is occurring at this time. The lowest ratios and the less correlated data are observed in the evenings, with data from all other times falling between the two. This finding suggests that during morning periods, sources that are attributed to OC and EC (which themselves are tightly correlated) are more likely to emit OC per unit of EC than observed in the evenings. Possible explanations for this may include different combustion characteristics that emit OC and EC that are more conducive for OC formation in the morning compared to the evening. Likewise, combustion conditions in the evening appear to emit less OC per unit EC, providing another line of evidence suggesting different formation mechanisms.

Table 3: Univariate statistics for organic and elemental carbon measured during this study. Reported values include mean, median, standard deviation, range, and the number of measurements collected during this study. Llod denotes measurements below the limit of detection.

	Mean, $\mu\text{g m}^{-3}$	Median, $\mu\text{g m}^{-3}$	Std Dev, $\mu\text{g m}^{-3}$	Range, $\mu\text{g m}^{-3}$	n
Organic Carbon	6.47	5.92	4.62	(0.03, 33.4)	505
Elemental Carbon	0.90	0.78	0.69	(llod, 3.86)	509

While much remains to be analyzed, it appears that OC and EC in the Fairbanks region are most likely associated with biomass burning. A substantial residential heating demand is required in this community during the winter, and wood burning remains an economically efficient fuel source for the community. Unfortunately, this has resulting in a preponderance of OC and EC in the Fairbanks

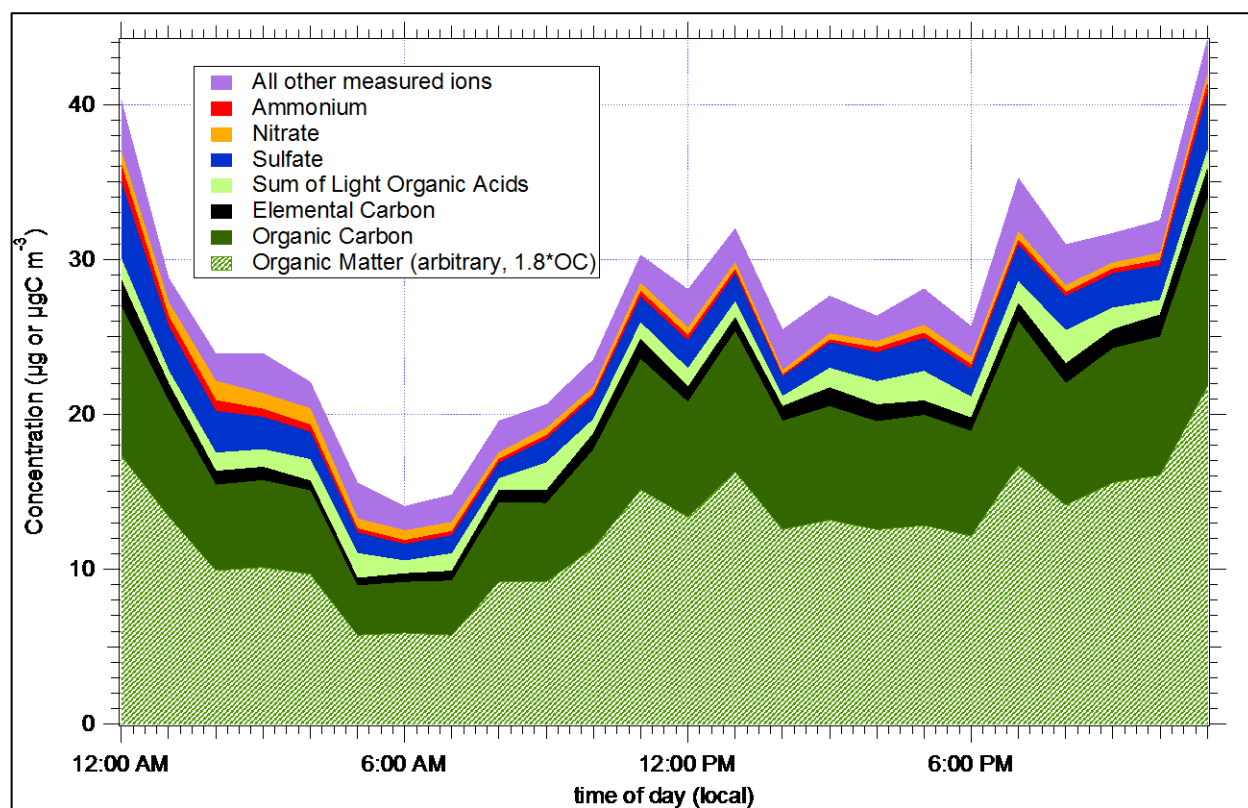


Figure 7: A composite diurnal profile for ~270 hourly measurements of OC, EC, and most ions. Organic matter is estimated as 1.8 times the measured OC value. Data are binned to each hour of the day and the mean value is presented here. Several lesser ions are binned into a separate composite group ('all other measured ions') to simplify this plot

air shed linked to these fuels, and it would be wise to investigate this issue further in hopes to better identify the mechanistic conditions leading to these different emissions profiles.

The data from this study were concatenated into a single, diurnal profile and plotted in Figure 7. While a number of components were measured during this study, organic matter – that is, the functional groups that are part of the organic particle, but not accounted for in the measure of carbon – is only estimated here. We use an arbitrary, but reasonable, value of 1.8 for the OM-to-OC ratio, and included this in the profile. Figure 7 shows a clear drop in concentration in the early

morning, with distinct peaks occurring around noon, 7PM, with highest observations around midnight local time. Ion composition is generally uniform throughout the day with some deviations in sulfate apparent throughout the day. Notable, however, is the dominance of OC and OM across the entire day, with these components reaching a minima around 6AM and a maxima at midnight.

This profile, at least subjectively, is consistent with wood burning as the dominant source of aerosol in this community. One might expect to see a declining emission rate between the evening and early morning as wood burning devices start to self-extinguish; a rapid increase in emissions follows in the morning as there is an increased demand for residential heating. The spike near midnight may be attributed to residential space heaters which are typically refueled to ensure continuous heating through the night and early morning.

XRF (PRELIMINARY)

As part of additional measurement efforts, the Borough has initiated a longer term study in the winter/spring of 2012 using a novel speciation instrument that provides hourly measurements of metal composition from PM2.5. This method is accomplished by way of a newly developed semicontinuous XRF installed at a ground location in Fairbanks. An initial look at this data is enclosed here, but does not represent a full analysis. Univariate statistics describing the dataset, as of 06 Jan 2012 are included in Table 4.

Table 4: Univariate statistics for the range of metals measured during the ongoing field study. Reported values include mean, standard deviation, max, and min values. All data are reported as nanograms per cubic meter, adjusted for standard temperature and pressure. Total number of measurements is 261 as of January 6, 2012, with data collection currently ongoing.

	Average	Stdev	Min	Max		Average	Stdev	Min	Max
SULFUR	868.169	760.360	0.076	3348.000	ZINC	42.448	42.982	0.116	254.743
POTASSIUM	158.202	100.821	0.941	568.123	GERMANIUM	0.129	0.102	<i>LLOD</i>	0.777
CALCIUM	24.719	93.944	<i>LLOD</i>	834.172	ARSENIC	0.117	0.500	<i>LLOD</i>	3.642
SCANDIUM	0.127	0.249	<i>LLOD</i>	1.486	SELENIUM	0.052	0.065	<i>LLOD</i>	0.372
TITANIUM	0.949	0.877	<i>LLOD</i>	4.754	BROMINE	3.291	3.250	0.049	24.975
VANADIUM	0.084	0.133	<i>LLOD</i>	0.729	RUBIDIUM	0.220	0.196	<i>LLOD</i>	1.122
CHROMIUM	0.087	0.240	<i>LLOD</i>	2.242	STRONTIUM	2.177	8.863	0.203	127.562
MANGANESIUM	0.525	0.821	<i>LLOD</i>	8.083	SILVER	54.473	178.273	0.204	1378.000
IRON	27.536	32.076	2.400	280.647	CADMIUM	19.157	52.453	1.096	588.461
COBALT	0.020	0.054	<i>LLOD</i>	0.504	BARIUM	0.930	1.547	<i>LLOD</i>	15.086
NICKEL	0.220	0.177	<i>LLOD</i>	1.645	MERCURY	0.001	0.010	<i>LLOD</i>	0.157
COPPER	3.997	3.263	0.918	46.591	LEAD	4.443	4.740	0.719	37.569

Transition metals are useful for source identification initiatives to provide quantitative information on elements that are released by specific sources, even if the overall concentrations of the elements are quite small. Figure 8 depicts a time series of concentration following elements with tracers through to mainly derive from coal combustion, although the important caveat that these

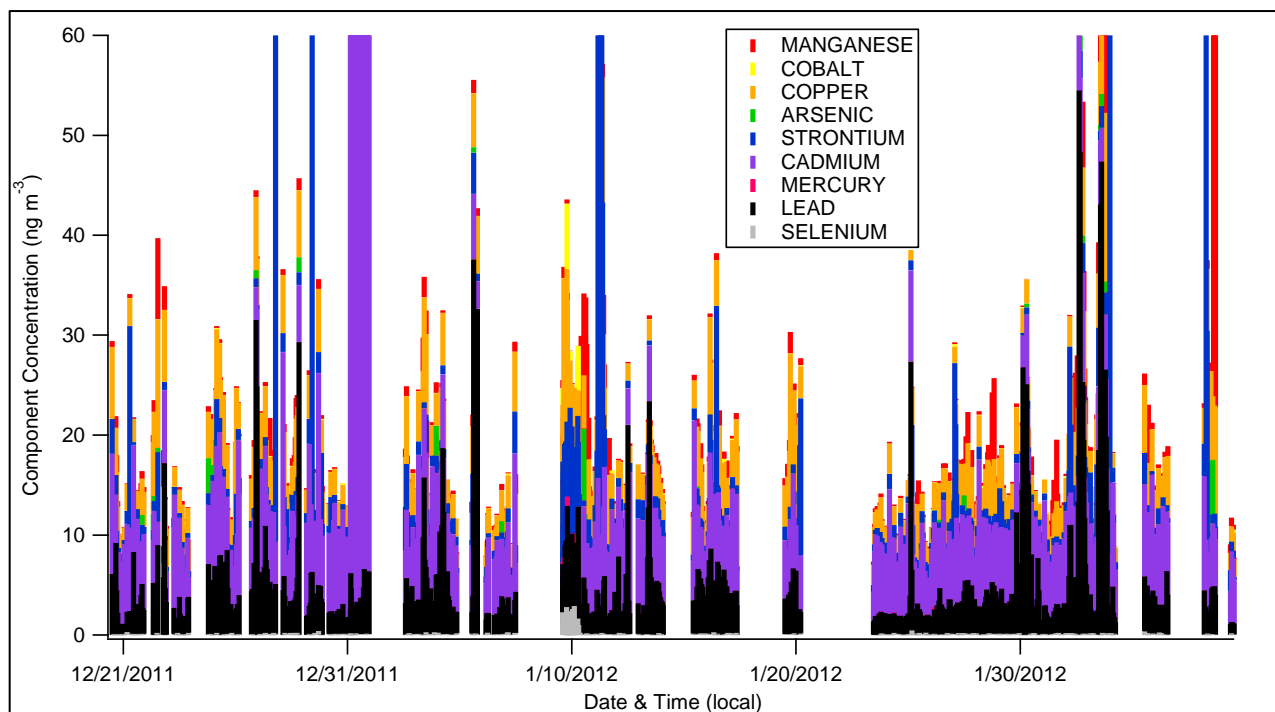


Figure 8: Time series of preliminary XRF data for selected metals thought to be linked to coal emissions. Gaps in data represent periods where the instrument was not reporting data.

components have not yet been confirmed as markers of coal combustion; further analyses to this effect are continuing.

Substantial texture in these elements suggests highly variable influence from coal combustion sources at this location. While overall elemental concentrations are in the single to 10's of nanogram per cubic meter range, some notable trends do appear in the data. For example, strontium has been anecdotally linked to spikes in PM concentration during times when air advection would suggest influence from the nearby coal power plant. Mercury and selenium also appear infrequently, but do so at clearly detectable levels well above a background concentration of less than $\sim 0.5 \text{ ng m}^{-3}$ and are generally thought to be markers of coal combustion.

At least three distinct events are shown in this figure, occurring on January 1, January 12, and Feb 2-3 that warrant greater investigation. The event on January 1 was characterized by nearly 1 microgram per cubic meter of cadmium; other elements were also substantially elevated during this time period. Because this event occurred just after midnight, it is likely that this is linked to local fireworks celebrations in the community. While this anecdote has little relevance for the broader air quality problems experienced by the borough, it does show the specificity and power of these measurements in the context of a complex aerosol setting. The other events are characterized by increases in strontium concentration, which is thought to be linked to coal emissions, though other sources may also be responsible for this emission.

It is important to point out that Figure 8 depicts a time series of densely-packed concentration for only a fraction of the elements. Though this approach provides a measure of concentration magnitude and temporal time scales, a more robust approach would be to use statistical modeling techniques to refine this data; such techniques include PMF, PCA, or other source apportionment approaches. It should also be noted that information on 13 additional elements (not plotted here) are also available, and these data are expected to be collected until the end of winter 2012. These approaches are forthcoming and not included in this report.

High time resolution data for sulfur was also exploited to begin investigating sulfur emissions and sulfate formation processes. The time period of study for this was from December 20th, 2011 through January 13th, 2012 and included 417 hourly data points measuring particulate sulfur by

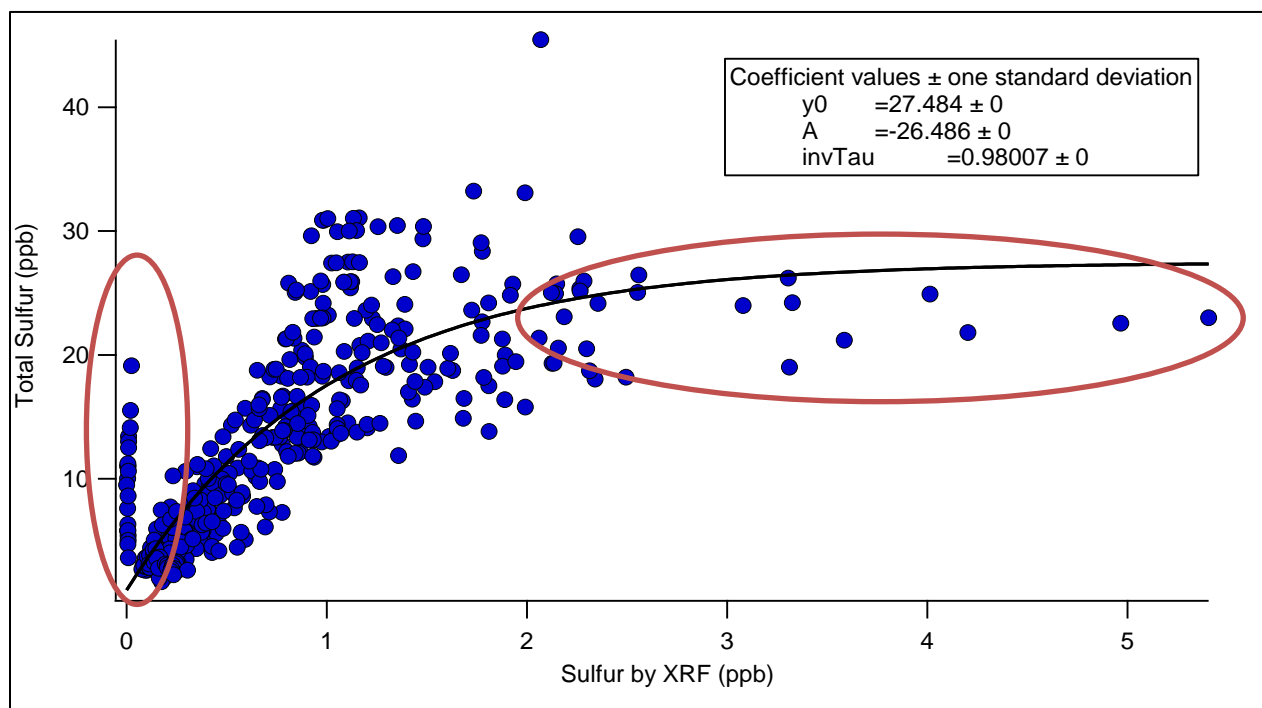


Figure 9: Total sulfur compared to sulfur measured by XRF. Total sulfur is defined as the sum of particulate sulfur by XRF with the sulfur observed in the gas phase as sulfur dioxide. Measurements are collocated. Circled regions highlight two distinct regimes; the left being a regime where particulate sulfate is absent even in the presence of gas-phase sulfur and the second regime (right) where total sulfur appears with a higher fraction in the particulate phase. This second regime may represent the most advantageous conditions for gas-to-particle conversion processes. Fit line is a simple exponential decay function.

XRF and sulfur as sulfur dioxide. Figure 9 plots total sulfur as defined by the sum of particulate sulfur by XRF and sulfur from SO₂ compared against total particular sulfur by XRF. At least two different regimes are immediately apparent from this data; one that shows conditions where no aerosol is detected (presumably during precipitation events) and a second where sulfur conversion to particles is effective. In the latter case, an exponential decay appears to describe the latter where SO₂ concentrations were generally limited to 25-30 ppb. An exponential curve fit to the data appears reasonable, but greater investigation is warranted. Under most conditions, sulfur conversion is a widely understood chemical process that occurs in the presence of sulfur dioxide, water vapor, and sunlight. The region lacks strong sunlight, and thus the typical mechanism for sulfate conversion is probably quite weak. Nonetheless, the presence of sulfate in the aerosol

stream in Fairbanks confirms that this conversion process exists, and appears to limit SO₂ concentration to less than ~30ppb.

In terms of identification of sulfur sources, it is not yet clear where these sources can be attributed. Likely sources include coal power generation, coal residential heating, or combustion of fuel oils for residential heating. Much greater analysis is indicated to develop a more robust profile.

CONCLUSIONS AND FUTURE DIRECTIONS

While data from these studies continues to be collected at the time of writing this report, it is clear from the winter 2011 studies that aerosol chemical composition is complex and unlike any other air shed in the United States. With the exception of occupational environments, it is relatively rare that greater than $20 \mu\text{gC m}^{-3}$ are observed at any time in US, yet this is typical on cold winter days in Fairbanks. Thus, Fairbanks is subjected to unique and important stressors on its airshed.

The data are consistent with a profile that fits a primary influence from biomass burning. High levels of OC and EC are routinely observed, and follow a pattern one might expect from a community that relies on wood burning to meet sizeable demands for residential heating. EC is well correlated with OC suggesting common sources, and the OC to EC ratio is consistent with sources derived from biomass combustion.

High temporal resolution measurements of ion concentrations showed relatively low (when compared with OC and EC) levels and suggest only a limited influence. Measured ions were dominated by sulfate, ammonium, and nitrate, but only at levels of approximately 10-20% of observed PM_{2.5} mass. While ions derive from a number of sources, sulfate is mainly derived from coal and non-road distillate combustion, the latter being defined mainly by home heating oil. Because we observed modest concentrations of sulfate (typically $2\text{-}4 \mu\text{g m}^{-3}$), we cannot exclude these sources as contributors to the air quality concerns in Fairbanks, but they likely play only a minor role in PM_{2.5} loading in the community.

Combining these measurements, a strong diurnal profile was observed providing further evidence of anthropogenic influence on aerosol composition in Fairbanks. While there was some hour-to-hour variability in ion concentration, the vast majority of the diurnal profile was driven by OC, and the estimated organic material component that was not measured in this study. Further limited analysis examined sulfur concentrations in both gas and particle forms and suggest that there are at least two regimes related to sulfur conversion: one where sulfur remains in the gas phase with only trivial particulate sulfur, and another where sulfur conversion to particulate form appears to follow an exponential decay pattern. This suggests that the conditions necessary for this conversion are, in fact, present.

Future work on this data is extensive. One project includes a comparative analysis with fuel source profiles collected during another investigation by FNSB. By incorporating updated fuel profiles, which provide detailed chemical component information from each type of fuel used in the region, we hope to be able to statistically connect those profiles with the observations in Fairbanks. Another project will incorporate these results into the Chemical Mass Balance modeling currently performed by investigators at the University of Montana. Additional planned analyses include investigating the high time resolution XRF data in much greater detail, with a focus on chemical mass balance and positive matrix factorization modeling, as well as coupling this data with in-progress modification of the CMAQ model for purposes of refining and validation.

REFERENCES

1. Kanakidou, M., et al., *Organic aerosol and global climate modelling: a review*. Atmospheric Chemistry and Physics, 2005. **5**: p. 1053-1123.
2. Seinfeld, J.H. and J.F. Pankow, *Organic atmospheric particulate material*, in *Annual review of physical chemistry, Volume 54, 2003*. 2003, Annual Review. p. 121-40.
3. USEPA. *Review of the national ambient air quality standards for particulate matter policy Assessment of scientific and technical information*. 2005; 514 p.]. Available from: Available online, Government web site, 2005: <http://purl.access.gpo.gov/GPO/LPS62787>
4. Jacobson, M.C., et al., *Organic atmospheric aerosols: review and state of the science*. Reviews of Geophysics, 2000. **38**(2): p. 267-94.
5. Schauer, J.J., et al., *ACE-Asia intercomparison of a thermal-optical method for the determination of particle-phase organic and elemental carbon*. Environmental Science & Technology, 2003. **37**(5): p. 993-1001.
6. Chow, J.C., et al., *Comparison of IMPROVE and NIOSH carbon measurements*. Aerosol Science and Technology, 2001. **34**(1): p. 23-34.
7. NIOSH, *Elemental carbon (diesel particulate): method 5040*, in *NIOSH Manual of Analytical Methods*, P.M. Eller and M.E. Cassinelli, Editors. 1996, National Institute for Occupational Safety and Health: Cincinnati.
8. Peltier, R.E., et al., *Fine aerosol bulk composition measured on WP-3D research aircraft in vicinity of the Northeastern United States – results from NEAQS*.

- Atmospheric Chemistry and Physics, 2007. **7**(12): p. 3231–3247.
9. Peltier, R.E., et al., *No evidence for acid-catalyzed secondary organic aerosol formation in power plant plumes over metropolitan Atlanta, Georgia*. Geophysical Research Letters, 2007. **34**(6): p. 5.
 10. Heald, C.L., et al., *A large organic aerosol source in the free troposphere missing from current models*. Geophysical Research Letters, 2005. **32**(L18809): p. 4.
 11. Heald, C.L., et al., *Concentrations and sources of organic carbon aerosols in the free troposphere over North America*. Journal of Geophysical Research, 2006. **111**(D23): p. D23S47.
 12. Na, K., et al., *Primary and secondary carbonaceous species in the atmosphere of Western Riverside County, California*. Atmospheric Environment, 2004. **38**(9): p. 1345-1355.
 13. Turpin, B.J., J.J. Huntzicker, and S.V. Hering, *Investigation of organic aerosol sampling artifacts in the Los Angeles basin*. Atmospheric Environment, 1994. **28**(19): p. 3061-3071.
 14. Turpin, B.J. and H.J. Lim, *Species contributions to PM_{2.5} mass concentrations: Revisiting common assumptions for estimating organic mass*. Aerosol Science and Technology, 2001. **35**(1): p. 602-610.
 15. de Gouw, J.A., et al., *Volatile organic compounds composition of merged and aged forest fire plumes from Alaska and western Canada*. Journal of Geophysical Research, 2006. **111**(D10): p. 20.

16. Maxwell-Meier, K., et al., *Inorganic composition of fine particles in mixed mineral dust-pollution plumes observed from airborne measurements during ACE-Asia*. Journal of Geophysical Research-Atmospheres, 2004. **109**(D19).
17. Sullivan, A.P., et al., *Airborne measurements of carbonaceous aerosol soluble in water over northeastern United States: Method development and an investigation into water-soluble organic carbon sources*. Journal of Geophysical Research, 2006. **111**(D23): p. 1-14.
18. Warneke, C., et al., *Biomass burning and anthropogenic sources of CO over New England in the summer 2004*. Journal of Geophysical Research, 2006. **111**(D23): p. 13.

Final Report

To

Environmental Protection Agency (EPA)

Purchase order EP08D000663

Reporting Period: 1 September 2008 – 31 January 2010

'Stable Boundary Layers Representation in Meteorological Models in Extremely Cold Wintertime
Conditions'

Dr. Brian J. Gaudet, co-PI

Dr. David R. Stauffer, co-PI

The Pennsylvania State University

Dept. of Meteorology

University Park, PA 16802

bjg20@met.psu.edu

12 May 2010

EXECUTIVE SUMMARY

This final report describes work performed by Penn State for the EPA-funded Purchase Order EP08D000663 titled ‘Stable Boundary Layers Representation in Meteorological Models in Extremely Cold Wintertime Conditions’. The purpose of the project was to develop, adapt, and test a methodology for stable boundary layer representation (initial onset, space/time evolution, dissipation) in three-dimensional numerical models, with a specific focus on the dark, extremely cold environments such as those in the winter in the Fairbanks, AK region. A particular concern is the frequent occurrence of very high fine particulate matter (PM_{2.5}) concentrations within the stable boundary layers that form in these conditions.

Ten tasks were defined in the Statement of Work (SOW) for this project. A summary of these tasks and a brief overview of the work completed can be found in the Appendix to this report. Two twenty-day episodes were selected from the 2007-2008 winter season to study periods of extremely cold temperatures and high PM_{2.5} concentrations and to evaluate model performance: one in near total darkness (14 Dec 2007 – 03 Jan 2008), and the other in partial sunlight (23 Jan 2008 – 12 Feb 2008). One baseline physics configuration and three physics sensitivity experiments were performed for each episode. The physics sensitivity experiments were used to assess the impact of different planetary boundary layer (PBL) parameterizations, land surface models, and atmospheric radiation schemes on the simulations. Each simulation used three nested grids: Grid 1 (12-km horizontal grid spacing) and Grid 2 (4-km) utilized the multiscale multigrid data assimilation strategy of Stauffer and Seaman (1994) in order to ensure the model and observations remain close over the extended duration of the simulations, and Grid 3 (1.3-km) did not use any direct data assimilation, and so was best-suited for quantifying the physics sensitivity. Grid 3, which is centered over the Fairbanks region, also possesses sufficient horizontal resolution to be used by the EPA as meteorological input to chemical and air transport and dispersion models. From the different physics packages one was to be recommended to the EPA for further mesoscale modeling of the region.

The major findings and impacts of this project are as follows:

- The use of the three-grid configuration with a multiscale, multigrid four-dimensional data assimilation (FDDA) strategy on the outer two grids and no direct FDDA on Grid 3 consistently produced qualitatively plausible atmospheric fields throughout the variety of meteorological conditions found in the episodes, despite the relatively sparse data density. Quantitatively, the multiscale, multigrid FDDA strategy led to improved root-mean-square-error (RMSE) scores for both wind and temperature on all grids. The FDDA on the outer domains had the desired effect of improving the simulations of Grid 3 without FDDA and used for physics sensitivity tests, by providing improved lateral boundary conditions.

- The best RMSE scores for the combination of both surface and sounding data required modification of the default FDDA procedure. These modifications included applying surface wind observational data to the third model vertical level instead of the lowest model level because wind observations are normally taken at a height of 10 m which is the height of the third level in the high vertical resolution configuration used here. The influence of surface observations was also restricted to approximately the lowest 100 m, instead of the top of the PBL, because the model-predicted PBL height in these simulations, based on the turbulent kinetic energy profile, was often found to be 1 km or higher. This correction applied the surface innovation (observation minus model value) in these predominantly stable boundary layers over a much shallower layer and produced improved statistical results in the lower troposphere.
- All model physics combinations tended to have a positive temperature bias on Grid 3, especially during the most extremely cold periods. All of the physics sensitivity tests tended to reduce the warm bias in comparison with the selected baseline physics package.
- Switching from the RRTM longwave / Dudhia shortwave radiation package to the RRTMG longwave and shortwave radiation package led to significantly reduced warm biases and better RMSE statistics. RRTMG was then used in all future physics sensitivity tests. The reduced warm bias seemed to be due to the longwave component, both because of direct examination of surface fluxes in the partial sunlight case, and due to the fact that the difference was more pronounced in the near total darkness episode.
- The simulation with the Rapid Update Cycle (RUC) land surface model, the Mellor-Yamada-Janjić (MYJ) PBL model, and the RRTMG radiation package was the coldest of the four physics suites tested, and had the lowest positive temperature bias and best statistics during those periods when the temperature was coldest. It was thus selected as the physics configuration of choice, since the coldest temperature conditions are those with the potential for the highest PM2.5 concentrations. However, there were periods in each episode, generally when the temperature was steadily decreasing in advance of an extremely cold period, during which the models had a cold bias. During these periods the RUC/MYJ/RRTMG configuration would usually be even colder and thus have worse magnitude temperature biases and RMSE scores. Thus, while this configuration was recommended, we also strongly recommended that the final fine-scale atmospheric data (i.e., from Grid 3) to be provided to EPA should come from an additional simulation in which FDDA is performed directly on Grid 3, in order to reduce some of this error.
- Wind component and wind speed statistics generally showed much less variability among the model physics sensitivity experiments than that seen for temperature. The MYJ/RUC/RRTMG (MRR) configuration usually produced slightly better wind statistics than the other configurations.
- Use of obs nudging for temperature and humidity (and not surface wind) on Grid 3 produced large improvements in the mass fields as expected, and also improvements in the wind fields

above the surface. Results were very encouraging and suggested that a smaller (larger) time window should be used for the surface (above-surface) data assimilation. This capability present in the Penn State MM5 FDDA system has been added to the new-release version of WRF.

- In addition to this final report, deliverables to the EPA will include the full three-dimensional output at relatively fine temporal resolution (every 1 hour for Grid 1; every 12 minutes for Grids 2 and 3) for the final Grid 3 nudging simulation as well as all the baseline and physics sensitivity simulations. Model namelists, initialization files, and modifications to the model source code will also be provided.
- The development and refinement of WRF FDDA capabilities and supporting software, including the surface analysis nudging, observation nudging and the OBSGRID objective analysis and obs-nudging pre-processing code, occurred concurrently with this project. This separate development effort led by PI Dave Stauffer and funded by the Defense Threat Reduction Agency (DTRA) allowed us rapid access to the most recent and robust versions of the WRF FDDA code, and this greatly benefited this project.
- The results of the default FDDA procedures not performing well in this high vertical resolution modeling study of stable boundary layer environments motivated an additional FDDA code development effort to make the vertical influence functions of surface observations within the FDDA be a function of stability regime type, as well as to provide the user with greater flexibility in specifying the vertical influence functions. These modifications were not finalized in time to be used for this project but are scheduled to appear in the next official release of the WRF model.
- An extended abstract and oral presentation were made at the 13th Conference on Mesoscale Processes (Gaudet et al. 2009), and a manuscript based on the project is in preparation.
- Since the first draft of the final report, the Grid 3 FDDA design and simulations have been completed for both twenty-day episodes. The results showed that the use of obs nudging for temperature and humidity (but not surface wind) on Grid 3 produced large improvements in the mass fields (as expected), and also improvements in the wind fields above the surface. Results were very encouraging and suggested that a smaller (larger) time window should be used for the surface (above-surface) data assimilation. This capability present in the Penn State MM5 FDDA system has been added to the new-release version of WRF.

1. INTRODUCTION

Fine particulate matter (PM_{2.5}, referring to particles with aerodynamic diameters equal or less than 2.5 microns) has been implicated in a variety of health problems, including respiratory disease. With the recent decrease in the allowable 24-hour PM_{2.5} concentration to 35 micrograms per cubic meter, there is now an even greater need to be able to determine the sources primarily responsible for exceedance events when they occur, as well as to predict the potential impact of source emission changes. Modeling the behavior of fine particulate matter typically involves coupling between an inventory of emissions sources, chemical and air transport and dispersion models, and synoptic and mesoscale atmospheric models. (Synoptic atmospheric models are designed to represent features with characteristic horizontal scales greater than about 2000 km; mesoscale atmospheric models represent features with scales of approximately 2 – 2000 km.) The purpose of the meteorological models is to use physical predictive equations and assimilation of available meteorological data to capture the evolution of the local atmospheric state over sufficiently long periods for use by the other models.

During the winter season the part of interior Alaska consisting of Fairbanks and the surrounding Fairbanks North Star Borough often have extremely cold temperatures due to the strong longwave radiative cooling, the absence of moderating marine influences, and the generally weak winds. Although this region often has a clean, relatively pristine atmosphere, the periods of coldest temperatures are often accompanied by some of the strongest low-level temperature inversions that have been observed, with temperature increases up to 20°C as one ascends from the surface (Benson 1970). The inversions cap stable boundary layers (SBLs) that can be as shallow as tens of meters in clear nocturnal conditions (Sereze et al. 1992; Vickers and Mahrt 2004). Emissions from vehicular traffic, power plants, and home heating (mostly diesel and wood fuels) remain trapped within the SBL, leading to high concentrations of particulates and other pollutants. In the extremely cold conditions of interior Alaska an additional problem that arises is ice fog that can be triggered by combustion-generated water vapor at temperatures below approximately -25°C (Benson 1970; Girard and Blanchet 2001). The dispersal of pollutants is further hindered by the fact that winds and turbulence are quite weak in these conditions. The winds and turbulence that do exist in the SBL are strongly modulated by drainage flows, gravity waves, and other less understood phenomena (Hanna 1983; Mahrt 2009). Thus predicting the behavior of SBLs becomes a complex problem involving synoptic weather patterns, topography, turbulence, surface energy budgets, and precipitation.

The tool used for the meteorological modeling component of this project is the Weather Research and Forecasting (WRF) model (Skamarock et al. 2008), more specifically, the Advanced Research WRF dynamic core (WRF-ARW, henceforth simply called WRF). WRF contains separate modules to compute different physical processes such as surface energy budgets and soil interactions, turbulence, cloud microphysics, and atmospheric radiation. Since turbulent eddies in the SBL are typically much smaller than mesoscale model horizontal grid spacing (e.g., ten meters vs. a thousand or more meters), they cannot be modeled directly (e.g., Wyngaard 2004), but typically their effect is parameterized by a Planetary Boundary Layer (PBL) scheme that predicts turbulent kinetic energy (TKE). Within WRF the user has many options for selecting the different schemes for each type of physical process. There is

also a WRF Preprocessing System (WPS) that generates the initial and boundary conditions used by WRF, based on topographic datasets, land use information, and larger-scale atmospheric and oceanic models. New software associated with objective analysis and data assimilation will be discussed later.

The goal of this project was to select and perform two twenty-day simulations down to 1-km horizontal grid spacing for two episodes from the 2007-2008 winter season characterized by high PM_{2.5} exceedance events in the Fairbanks region. One episode was to be characterized by near total darkness, while the second was to contain partial sunlight. From a set of modeling experiments including a baseline physics configuration and a series of physics sensitivity tests, modified as appropriate to be suitable to the unique Alaskan atmospheric conditions, a best performing physics suite was to be selected and delivered to the EPA, along with source code and the model output. The project had two main components: (1) creating the best possible representation of the atmosphere through the use of a mesoscale model with continuous data assimilation, and (2) determining the best set of physics parameterizations by performing a series of sensitivity tests without the direct effects of data assimilation. Both components are included in a multiscale, multigrid data assimilation procedure, which will be described in more detail below.

2. METHODOLOGY AND BASELINE EXPERIMENTAL DESIGN

2.1 Grid Configuration

The simulations presented in this report involve three one-way nested horizontal grids with horizontal grid spacing of 12 km, 4 km and 1.3 km, respectively (Table 1 and Fig. 1). Grid 1 covers the entirety of Alaska and extends from Siberia to the northwestern continental United States. Grid 2 closely coincides with the extent of the Alaskan landmass south of the Brooks range; it includes the Anchorage region and the Gulf of Alaska in the south. Grid 3, centered around Fairbanks and extending south to the Alaska Range and north past the White Mountains and other uplands just north of Fairbanks, includes all of the proposed non-attainment area within the Fairbanks North Star Borough (Fig. 2). It can be seen in the figure that Fairbanks is located next to a semicircle of low mountains that are generally a few hundred meters above the city; this tends to restrict airflow near the city and further reduce the dispersion of pollutants in stable conditions.

Grid	Dimensions	Horizontal Grid Spacing
1	401 x 301	12 km
2	202 x 202	4 km
3	202 x 202	1.3 km

Table 1: Specifications of model grids.

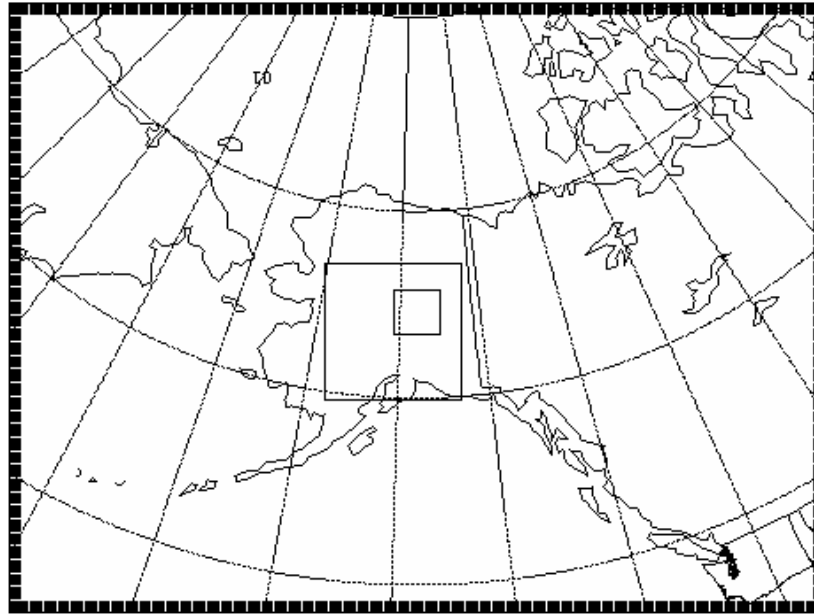


Fig. 1: Nested grid configuration of WRF, showing the 12-km Grid 1, the 4-km Grid 2, and the 1.3-km Grid 3 described in the text.

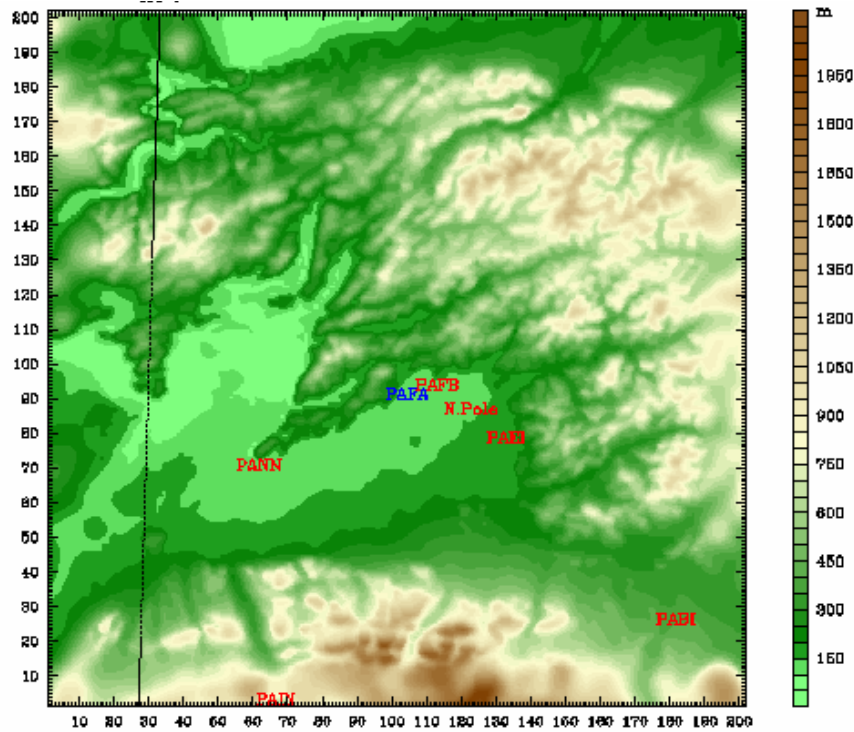


Fig. 2: Elevation on Grid 3 used in study. The location of the Fairbanks sounding is labeled in blue; other local METAR stations are shown in red.

The vertical grid spacing needed to be fine enough to resolve the structure of SBLs that can be only tens of meters deep, but not so fine that numerical instabilities arise in regions of steep topography (in particular the Alaska Range). After a series of initial tests a vertical grid configuration with 38 half layers (39 full levels) was defined, with a minimum vertical grid spacing of 4 m near the surface (see Fig. 3). Numerical stability was achieved through the use of time steps of 24 s, 8 s, and 4 s on the 12-km, 4-km and 1.3-km grids, respectively. These parameters are comparable to those used over central PA in the Seaman et al. (2008) SBL study, but with 4-m rather than 2-m vertical resolution near the surface, and slightly shorter timesteps.

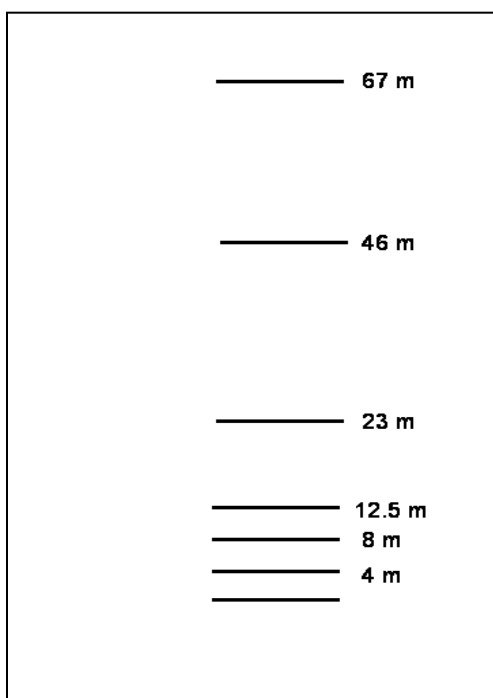


Fig. 3: Lowest few vertical full levels (i.e., locations where vertical velocity is calculated) in WRF model configuration, roughly to scale.

Two twenty-day episodes from the 2007-2008 winter season were selected for study. One episode was from 14 Dec 2007 to 03 Jan 2008, a time of year when there is little solar radiation in the Fairbanks area (approximately three hours of daylight per day near the solstice). During this episode the temperature rapidly decreased to near -40°C by 21 Dec, accompanied by rapid increases in PM_{2.5} concentrations, and then temperatures generally increased and PM_{2.5} decreased for the remainder of the episode (Fig. 4). The second episode was from 23 Jan 2008 to 14 Feb 2008, when solar insolation was more significant (between five and eight hours of sunlight per day), and provides an example of 'partial

sunlight' conditions. During this episode temperatures were initially relatively warm (near 0°C), decreased briefly to near -35°C by 27 Jan, rebounded slightly, and then decreased during the most extensive period of sub -35°C weather of the season. Consistent with the prolonged period of cold temperatures were recurring violations of the PM2.5 standard in the Fairbanks area.

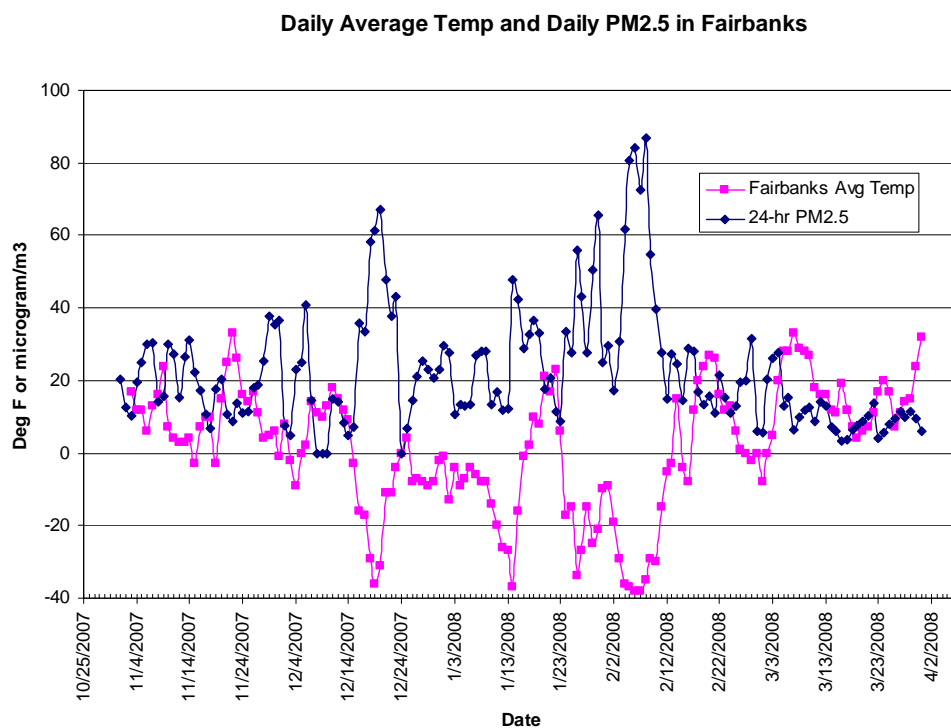


Fig. 4: Observations of daily average temperature and 24-hr PM2.5 concentrations taken in Fairbanks during 2007-2008 winter season. Courtesy Robert Dulla, Sierra Research, Inc.

In the initial period of a regional model simulation there is generally a period of several hours when the atmospheric state, whose initial conditions are usually provided by a global or coarser regional model, is still dynamically adjusting to the finer scale resolution and topography of the regional model. Therefore the model output from this initial 'spin-up' period is not completely reliable as an indicator of the true atmospheric state. However, if a regional model simulation is allowed to progress for too long without re-initialization (normally several days), it tends to drift away from the actual observed atmospheric state. Therefore, our method of obtaining realistic regional atmospheric analyses over an entire twenty-day episode was to divide each episode into four overlapping simulation segments. Each segment is around five days long with a twelve-hour overlap between each segment to avoid spin-up effects. (Specifically, the near total darkness episode was divided into successive segments of 6 days, 5.5 days,

5.5 days, and 4.5 days; the partial sunlight episode was divided into successive segments of 5 days, 5.5 days, 5.5 days, and 5.5 days).

Initial conditions and most of the Grid 1 lateral boundary conditions were obtained from the half-degree Global Forecast System (GFS) zero-hour analyses that were obtained from the NOAA National Operational Model Archive and Distribution System (NOMADS) website maintained by the National Climatic Data Center. The exceptions were some analysis times during the near total darkness episode when the half-degree GFS product was unavailable; in these instances the one-degree GFS analysis was used. All simulation segments for the near total darkness episode were selected such that all initial conditions could be obtained from half-degree global analyses.

The simulations were performed on one of two Linux clusters: one local cluster with 128 available processor cores, and the other cluster with 512 processor cores maintained by the Research Computing and Cyberinfrastructure High Performance Computing Group (RCC HPCG) at Penn State. Each 5.5 day simulation segment took 1-2 days to complete. The full 3D model output from each simulation was saved at a frequency of one hour for the 12-km Grid 1, and at a frequency of 12 minutes for the 4-km Grid 2 and 1.3-km Grid 3. For our configuration as shown in Table 1, the file size at each model output time is 500 MB for Grid 1 and 170 MB for each of Grids 2 and 3 (although this size can be approximately halved through file compression).

2.2 Four-Dimensional Data Assimilation (FDDA)

Even with the overlapping simulation segment strategy, it is difficult to ensure that the interior of a regional model simulation remains close to observations for simulations of more than a day or so. Therefore, dynamic analyses of historical cases are often performed, in which a Four-Dimensional Data Assimilation (FDDA) strategy is applied throughout the model integration. Relaxation terms based on the differences between actual observations and the corresponding model fields at the observation sites (also known as the 'innovations') are added to the model's predictive equations. In this way the model error is constrained based on available observations while the model still provides dynamic consistency and finer mesoscale structure not present in the observations. The version of FDDA used in these simulations is the multiscale, multigrid nudging FDDA strategy developed by Stauffer and Seaman (1994) for the MM5 mesoscale model. Nudging is also known as Newtonian relaxation, where the nudging relaxation terms are proportional to the innovation divided by a characteristic e-folding time inversely proportional to a nudging coefficient G . Nudging does not perform a direct insertion of observational information at a single point in space and time, but rather it applies the correction or innovation gradually in time and space based on the model terrain influences and prescribed / assumed weighting functions. For example, when a well-mixed PBL is present, one would generally want the influence of surface observations to be extended throughout the PBL, because in these conditions there is high correlation between errors in atmospheric fields at the surface and those anywhere within the PBL.

The multiscale multigrid FDDA method uses a combination of two forms of nudging: analysis nudging and observation ('obs') nudging. Analysis nudging is performed in model grid space where an objective

analysis of observations (e.g., with a modified Cressman scheme (Benjamin and Seaman 1985)) is performed using the interpolated global analyses (e.g., from the GFS) as a background field. The resultant ‘enhanced analysis’ can then be used as the basis for analysis nudging. Analysis nudging is generally applied on coarser model domains where synoptic data can be used to produce a reasonable gridded analysis. Obs nudging is more attractive for finer-scale domains and asynoptic data. It is particularly effective where observational data density is sparse and corrections are applied only in the neighborhood of the observations, allowing the model to still add value in regions without any data by propagating observation information into the data-sparse regions and creating mesoscale structure not in the observations. In this case the nudging is performed in observation space, and the model field is interpolated to the observation site to compute the innovation that is then analyzed back to the model grid over some three-dimensional neighborhood in space, and over some time window. Quality control (QC) of observations is critically important for the success of both analysis nudging and observation nudging.

In the multiscale multigrid FDDA method applied in this study, 3D-analysis nudging, as well as surface analysis nudging using higher temporal frequency surface data within the PBL (e.g., Stauffer et al. 1991), are performed on the outermost 12-km domain. Obs nudging is applied on at least the 12-km and 4-km domains. (Obs nudging is not applied on the finest 1.3-km model nest for the physics sensitivity studies described further below.) The finer domains thus have the benefit of improved lateral boundary conditions from the coarsest 12-km domain using both types of nudging, as well as the obs nudging performed directly on the 4-km nested domain.

This project was one of the first applications of the multiscale FDDA strategy of Stauffer and Seaman (1994) in WRF. It is important to note that many of the WRF FDDA capabilities were not available and still under development via a contract from the Defense Threat Reduction Agency (DTRA) to Penn State at the time that this project was proposed. In fact, the WRF 3D / surface analysis nudging and obs nudging capabilities were still being developed during this contract period. The WRF end-to-end FDDA system is shown in Fig. 5 and described in more detail in Deng et al. (2009). This contract was able to take advantage of the fact that the WRF FDDA developers at Penn State were also working on this contract.

The new OBSGRID module in the WRF end-to-end FDDA system produces gridded objective analyses and observation files similar to those produced by Rawins / Little_r in the MM5 system. These files can be used for 3D/surface analysis nudging and obs nudging within WRF. OBSGRID takes as input raw WMO observations (both surface and upper air) and the output of WPS, which consists of atmospheric initial and boundary gridded data (e.g., GFS output) horizontally interpolated to the model grid to be used in WRF. The outputs of OBSGRID relevant to this study include 1) pressure-level and surface objective analyses of the WMO observations (passing internal QC checks) using the WPS GFS output as background fields; the resultant analyses are then vertically interpolated to the WRF terrain-following “sigma” layers to be used for 3D analysis nudging; 2) surface analysis nudging files that can be directly used by WRF; 3) observation nudging files usable by WRF, and 4) files of the WMO observations including those passing the QC tests for use in the statistical verification software.

As mentioned above, for the physics sensitivity part of this study, 3D analysis nudging, surface analysis nudging, and obs nudging are performed on the 12-km Grid 1; obs nudging is performed on the 4-km Grid 2; and no nudging is performed on the 1.3 km Grid 3. Thus Grid 3 has no direct FDDA tendencies and can be used to determine physics sensitivities, while still benefitting from improved lateral boundary conditions derived from the coarser grids that do have FDDA.

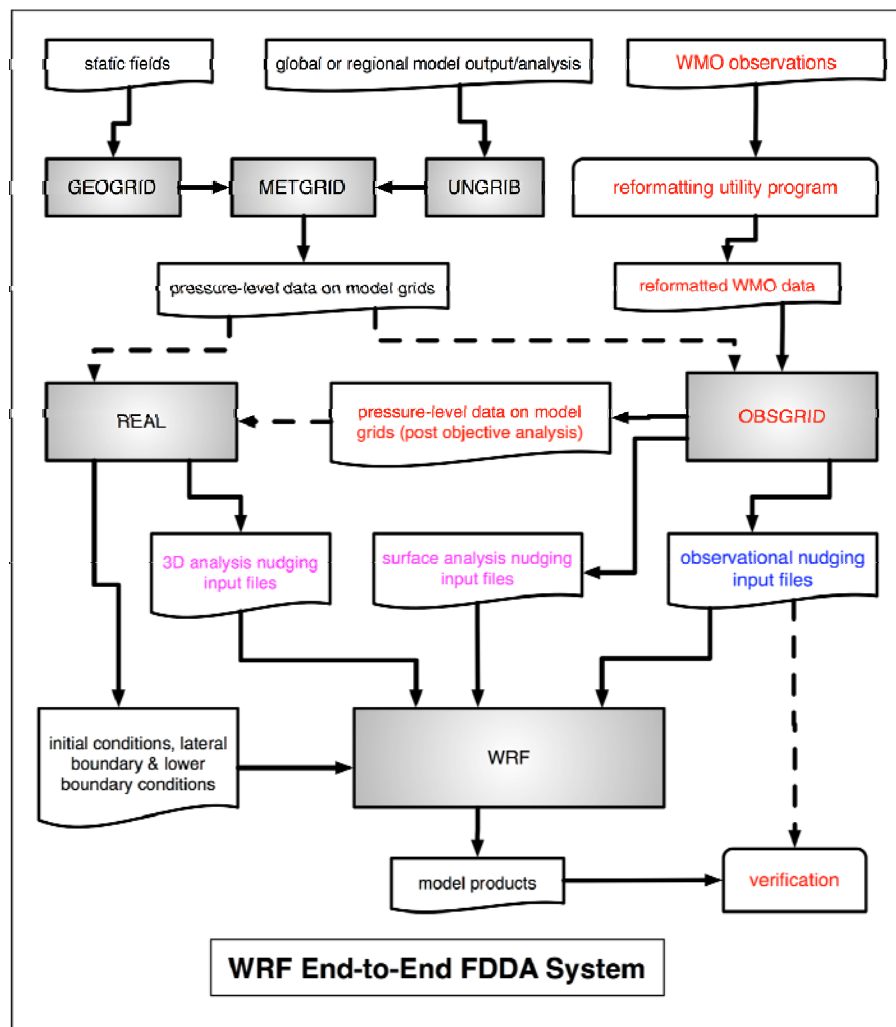


Fig. 5: Diagram of the WRF End-to-End FDDA system used for this study (from Deng et al. 2009). Items in magenta apply to analysis nudging; items in blue apply to obs nudging; items in red apply to both.

For the generation of the final dynamic analysis, obs nudging was performed on Grid 3, but with a reduced horizontal radius of influence (from 100 to 75 km), a reduced vertical pressure difference within the terrain-modified radius of influence function used for surface obs nudging (from 75 hPa to 37.5 hPa),

and obs nudging of surface data was performed on mass fields only (i.e., not winds). The values of FDDA-related WRF namelist parameters for these simulations can be found in Table 2.

Parameter	3D/Sfc Analysis Nudging			OBS Nudging		
	Grid 1 12-km	Grid 2 4-km	Grid 3 1.3-km	Grid 1 12-km	Grid 2 4-km	Grid 3 1.3-km
G (1/sec)	3×10^{-4}	Not Used	Not Used	4×10^{-4}	4×10^{-4}	(4×10^{-4})
Wind field	Yes	Not Used	Not Used	Yes	Yes	No
Mass field	Yes	Not Used	Not Used	Yes	Yes	(Yes)
RINXY (km)	N/A	N/A	N/A	100	100	(75)
TWINDO (hours)	N/A	N/A	N/A	2	2	(2 – but see Section 5)
Time Frequency of Data (hours)	6 / 3 (Sfc)	Not Used	Not Used	1	1	(1)

Table 2: List of WRF FDDA namelist parameter values used in this study. Analysis nudging parameters apply to both surface and 3D versions unless otherwise specified. Values in parentheses for Grid 3 do not apply to the physics sensitivity studies, which have no FDDA on Grid 3, but do apply to the final dynamic analysis performed in this study.

2.3 Baseline Physics Suite

Two of the most important controls on the evolution of SBLs in mesoscale models are the PBL scheme and the Land Surface Model (LSM). The former is critical for determining the effects of vertical mixing both within and outside of the PBL, and thus helps regulate how rapidly pollutants can disperse. The LSM helps to determine the details of the surface energy balance and thus the thermal tendency and stability of air near the surface. In addition to these, other physical processes that are important in these conditions are the atmospheric radiation scheme (because of the impact on the thermal cooling and temperature structure of the lower atmosphere) and the microphysics scheme (because of the interactions between radiation, latent heat, and quantities of water vapor and condensate, as well as the value of predicting such features as ice fog).

The baseline physics suite used for these simulations was originally derived from that of Seaman et al. (2008) for central Pennsylvania, but with some modifications. To determine the longwave component of radiation, the RRTM scheme of Mlawer et al. (1997) was used, whereas the Dudhia (1989) scheme was used to determine the shortwave component. The PBL scheme used was a version of the Level 2.5 Mellor Yamada scheme as modified by Janjić (2002); henceforth this will be referred to as the Mellor-Yamada-Janjić (MYJ) scheme. A Level 2.5 scheme explicitly predicts the evolution of turbulent kinetic energy (TKE) at each grid point, and uses the predicted TKE to compute the magnitude and vertical extent of mixing. The MYJ scheme used is that available in version 3.1 of WRF; however, based on subsequent work from the central Pennsylvania study, the threshold of minimum TKE within the MYJ scheme was reduced to $0.01 \text{ m}^2 \text{ s}^{-2}$, due to the extremely weak winds and turbulence expected in these stable conditions.

The LSM for the baseline was originally the 5-layer thermal diffusion model used in Seaman et al. (2008). However, we performed a series of preliminary tests with the Alaska grid configuration using the Noah LSM, originating from NCEP, Oregon State University and AFWA (Chen and Dudhia 2001). This was done because the Noah LSM includes a number of features that are potentially important in the central Alaska environment, including time-dependent snow cover, time-dependent snow density, and snow-dependent emissivities and ground conduction. Some properties of the Noah LSM that had just been incorporated into standard WRF (e.g., a more rigorous treatment of latent heat release in the presence of ice) were based on the 'Polar-WRF' and 'Polar-MM5' versions of Noah used for high latitude simulations (Bromwich et al. 2001; Hines and Bromwich 2008). A number of other features of the polar-modified Noah were not in the standard WRF at the time, but not directly relevant to central Alaska (e.g., modification of sea ice properties). Preliminary tests in the relatively mild conditions immediately prior to the partial sunlight episode revealed that the use of the Noah LSM initialized directly from the soil levels of the half-degree GFS resulted in smaller surface temperature biases. Thus, based on our preliminary favorable results, we used the version of Noah in WRF v3.1 as the LSM for the baseline simulation.

The microphysics model selected for the baseline was the Morrison et al. (2005) scheme, also new to WRF v3.1. This scheme was developed specifically for high-latitude cold temperature microphysics, and includes the prediction of two moments (mixing ratio and number concentration) for rain, snow, graupel, and cloud ice, in addition to single moment prediction of cloud water. We thus felt it was worth using this scheme in the baseline even though file sizes and computational costs were significantly increased (by 50% in time) from the simple ice scheme used previously.

3. Initial Baseline Testing and FDDA Modifications

Initial testing of the baseline WRF configuration for the two episodes began in January 2009. The purpose of the 'pre-baseline' testing was to confirm that the proposed WRF grid configuration would remain numerically stable and physically realistic for simulation segments of several days, to determine the resource and timing requirements of the simulations, and to confirm that the WRF FDDA features were working as expected. Furthermore, a number of key WRF system features to be used in this study

were still under development at the beginning of 2009; in particular, surface analysis nudging, OBSGRID, and the official WRF v3.1 release itself, which included the QNSE PBL scheme and a modified version of the Noah LSM. Thus all of these new features had to be tested and evaluated when they became available.

At the beginning many of these tests were performed on the first segment of the partial sunlight episode (23 – 28 Jan 2008). Not only was this a convenient place to begin, but it began as a time of relatively warm temperatures in central Alaska, allowing the model configurations to be evaluated in relatively mild conditions before being used in the extreme cold conditions of the high exceedance episodes. Nonetheless, a brief period of colder temperatures occurred toward the end of the 23-28 Jan 2008 period, so some evaluation of model performance in different temperature regimes could be determined.

A preliminary assessment of the skill of the FDDA components of the WRF end-to-end system for the baseline simulation of the 23-28 Jan 2008 period, made in April 2009, is shown in Table 3 for the 12-km (Grid 1) and 4-km (Grid 2) domains. Raw WMO observations from both surface METAR and rawinsonde stations were given QC codes within OBSGRID, and only those observations of sufficient quality to be used in the objective analysis were retained for verification. The table compares a simulation without FDDA, a simulation using only analysis nudging on Grid 1; a simulation using only obs nudging on Grids 1 and 2; and a simulation combining the analysis nudging and obs nudging features, corresponding to the proposed multiscale multigrid FDDA procedure. Furthermore, since the surface analysis nudging feature of WRF had only just become available from Penn State, two versions of each simulation including analysis nudging were performed: one with and one without surface analysis nudging.

The table confirms that, for virtually every grid, observation station type, and variable, the best root-mean-square error (RMSE) scores occur for multiscale multigrid FDDA, and the worse RMSE scores occur for the simulation without any FDDA. However, a more careful analysis of the table revealed a few puzzling results. While surface analysis nudging led to expected improvements in temperature on Grid 1 (vs. analysis nudging without surface analysis nudging) when verified against surface METAR stations, the RMSE scores of METAR winds and relative humidity actually became slightly worse. Furthermore, when the verification was performed against rawinsondes on Grid 1, surface analysis nudging made temperature RMSEs considerably worse, and wind RMSEs far worse, than the corresponding runs without surface analysis nudging.

For Grid 2 verified against rawinsonde data, we see the expected result that a simulation with only obs nudging improves the RMSE scores more than either version of the analysis nudging only simulation. (Since analysis nudging is always applied to Grid 1 only, the analysis-nudging-only simulations have only indirect FDDA improvements on Grid 2, through the lateral boundary conditions from Grid 1; the obs nudging simulations do have direct FDDA on Grid 2.) However, when surface METARs are used for Grid 2 verification, we have the puzzling result that obs nudging only is outperformed by analysis nudging only (except for temperature).

Verification Domain	Verification Field and Station Type	Simulation FDDA Method (O – Obs Nudging; 3DA – 3D Analysis Nudging; SA – Surface Analysis Nudging; No – No Nudging)			
		Grid 1: No Grid 2: No	Grid 1: O Grid 2: O	Grid 1: 3DA / 3DA + SA Grid 2: No / No	Grid 1: 3DA + O / 3DA + SA + O Grid 2: O / O
Grid 1 (12 km)	Surface U-Component	3.2	2.6	2.3 / 2.4	2.1 / 2.2
	Surface V-Component	3.2	2.7	2.1 / 2.3	2.0 / 2.1
	Surface Temperature	5.6	2.9	2.9 / 2.4	2.5 / 2.1
	Surface Rel. Humidity	21.0	18.7	17.7 / 18.2	17.0 / 17.5
	Sounding U-Component	4.6	2.2	1.5 / 3.3	1.1 / 2.0
	Sounding V-Component	4.2	2.3	1.5 / 2.9	1.1 / 1.9
	Sounding Temperature	3.5	1.4	1.4 / 2.0	1.0 / 1.3
	Sounding Rel. Humidity	21.2	10.2	11.2 / 16.0	8.3 / 10.5
	Grid 2 (4 km)	Surface U-Component	3.8	3.3	2.2 / 2.3
Surface V-Component		2.5	3.1	2.7 / 2.8	2.9 / 2.5
Surface Temperature		5.0	2.5	3.1 / 3.0	1.9 / 1.8
Surface Rel. Humidity		23.8	22.0	20.7 / 20.7	19.6 / 19.3
Sounding U-Component		4.5	2.2	2.6 / 2.8	1.7 / 1.8
Sounding V-Component		4.5	3.2	3.4 / 3.8	2.8 / 3.4
Sounding Temperature		3.1	1.3	2.2 / 2.2	0.9 / 1.4
Sounding Rel. Humidity		27.0	14.1	21.7 / 24.5	12.5 / 13.1

Table 3: Root-mean-square error (RMSE) values of u-component wind ($m s^{-1}$), v-component wind ($m s^{-1}$), temperature ($^{\circ}C$) and relative humidity (%) as verified within Grids 1 and 2 during test FDDA simulation of 23-28 Jan 2008 for various FDDA combinations. Verification was performed against METAR stations for the surface and rawinsonde stations for the sounding data. The best value for each row is in bold.

Investigations into the cause of these puzzling results led to the realization that a number of the components of the WRF end-to-end FDDA system probably needed to be modified to adapt the system to the special conditions of the Alaska configuration. First, in most mesoscale model simulations it can be assumed that surface wind observations, normally made at a height of 10 m above ground level (AGL), and surface temperature and moisture observations, normally made at 2 m AGL, are located within the lowest model layer. In fact, normally the problem is that the midpoint of the lowest model layer (or first half-layer height above the surface) is often tens of meters in height and still well above the height of the surface observations. A proper interpolation of model values to the height of the surface observations usually requires using similarity theory or some similar procedure. For the Alaska configuration, however, a 10-m wind would actually be located within the *third* model layer from the surface, while 2-m temperature essentially corresponds to the height of the lowest model half layer (midway between the surface and the lowest model full level). There are at least two consequences of this. The first is that, for the default procedure of verifying surface wind observations with model output from the lowest model half layer, observed 10-m winds are actually being compared to modeled 2-m winds whereas they should be verified against the modeled 10-m winds of the third model half layer. The second consequence is that the surface wind innovations used in the WRF FDDA code are by default based on the difference between 10-m observed winds and 2-m modeled winds in this case, which is wrong and may introduce erroneous biases into the FDDA simulation.

An additional issue was revealed by examining fields of PBL height produced by the PBL turbulence parameterization in various test simulations. Though, as expected, PBL heights are very low over many large areas within the model domains, especially during the colder periods, some patches of unexpectedly high PBL height values can be seen at times (Fig. 6). PBL heights of 1500 m or greater are more typical of convective boundary layers than of the nocturnal SBL conditions found in interior Alaska. Model soundings taken in the proximity of these patches (Fig. 7) confirm that the atmosphere is certainly rather stable and not well mixed in potential temperature (although some layers above show potential temperatures close to a saturated adiabat). The high PBL height zones appear to be associated with regions of elevated shear-generated TKE and cloudiness, since it is the TKE profile in the MYJ scheme that determines the PBL height. The issue is that the default WRF surface analysis and obs nudging schemes spread the influence of surface innovations throughout the depth of the PBL, but in these stable conditions this may overestimate the vertical error correlation length scale for surface innovations. This helped explain why the use of surface analysis nudging on Grid 1 made the rawinsonde-verified statistics worse.

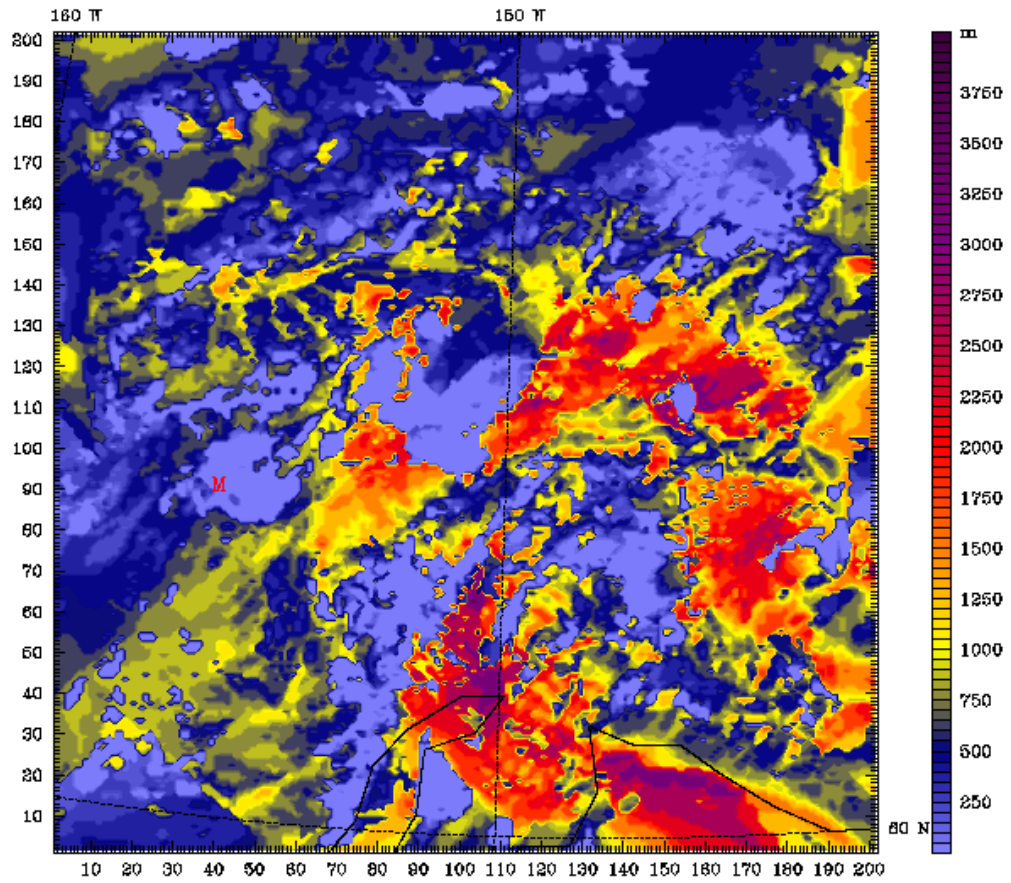


Fig. 6: WRF-predicted PBL height at 1200 UTC 25 Jan 2008 (60-hour simulation time) within the 4-km Grid 2. Simulation does not include FDDA.

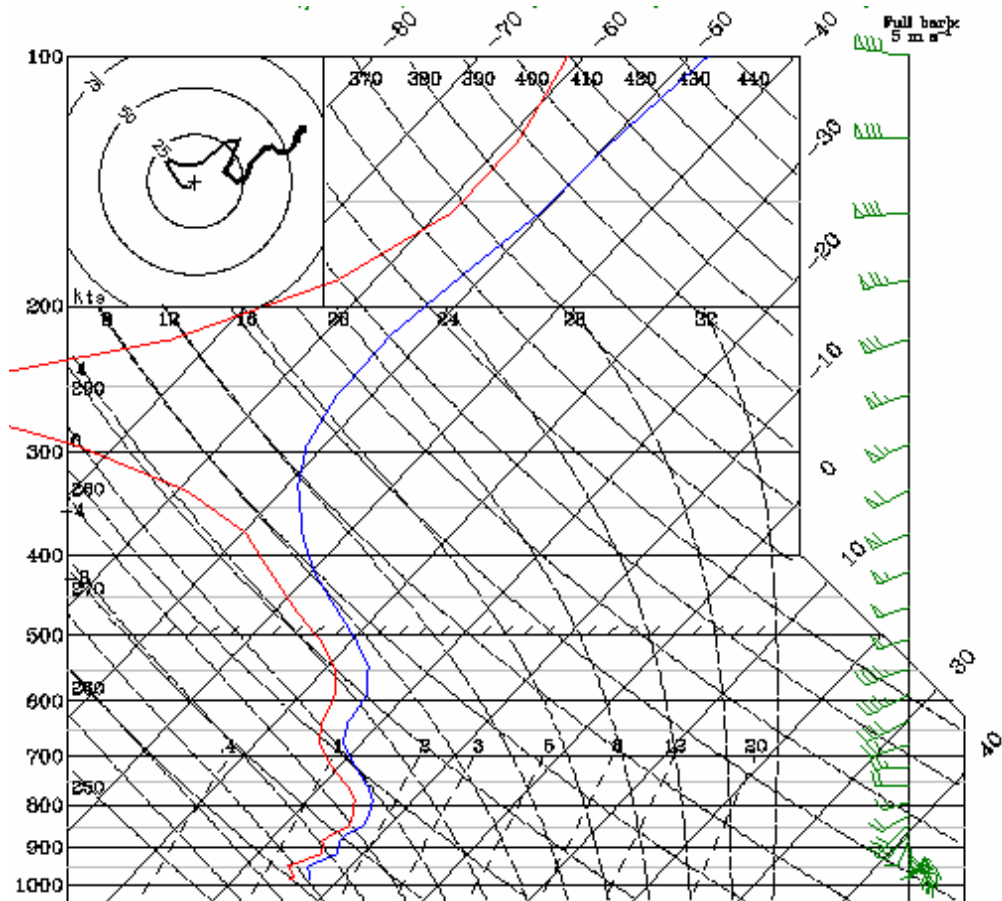


Fig. 7: WRF-predicted model sounding at Fairbanks for same time and simulation as Fig. 6.

Based on a series of similar tests, the following modifications were made to the WRF FDDA schemes for use in the baseline Alaska simulations. 1) The verification software was rewritten so that surface wind observations are verified against the third model half-layer from the ground, while surface moisture and temperature observations are verified against the lowest model half-layer. 2) A portion of the verification software that uses an assumed lapse rate to adjust model temperatures based on the difference between modeled and actual elevation was disabled, because this can lead to large errors in very stable conditions. 3) The surface analysis nudging and obs nudging codes were modified so that surface innovations for wind are computed and applied directly at the third model level. 4) Because surface wind observations directly relate to the third model layer and surface temperature and moisture observations directly relate to the lowest model layer, the similarity-based adjustments normally performed on model output for surface innovation computation was also disabled. 5) Hardwired vertical weighting functions for surface innovations were implemented into the surface analysis nudging and obs nudging codes, replacing the default functions that extend surface corrections to the model-predicted PBL height. Trial and error established that the functions shown in Fig. 8 for surface obs

nudging and analysis nudging extend the surface innovations in the vertical enough to improve surface statistics but without degrading rawinsonde-verified RMSE scores; furthermore, the vertical extent of

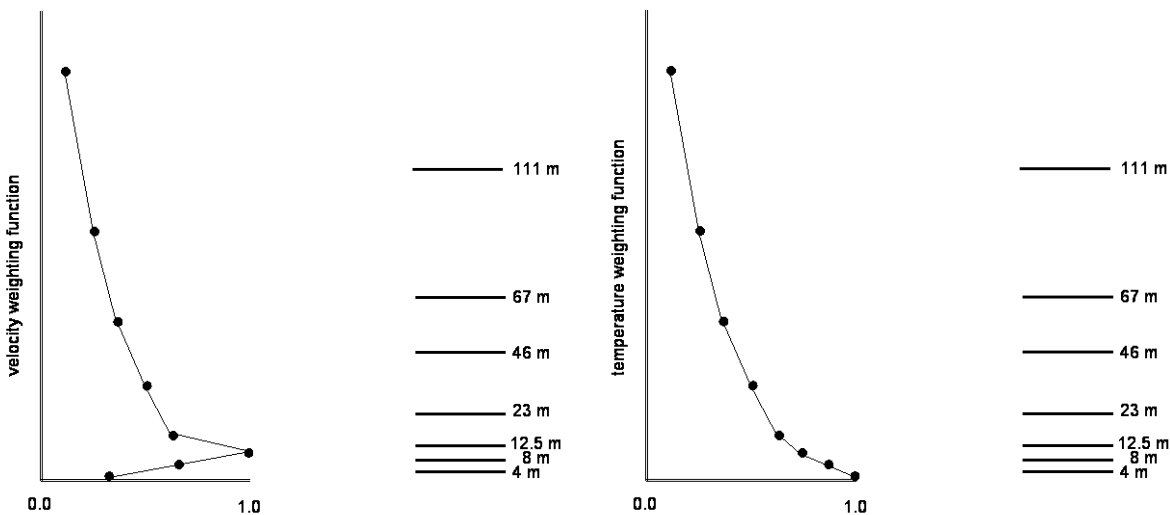


Fig. 8: Vertical weighting functions at model half-layers for wind components (left) and temperature and moisture (right), as used by modified surface analysis nudging and obs nudging FDDA procedures for Alaska simulations. Heights of model full layers are shown to the right, roughly to scale.

these functions (about 150 m) is a reasonable order of magnitude estimate for the maximum depth of nocturnal radiatively-driven SBLs.

Results from this phase of the project were presented at an oral presentation at the 13th AMS Conference on Mesoscale Processes in Salt Lake City, UT, from 17-20 Aug 2009. (Gaudet et al. 2009).

4. PHYSICS SENSITIVITY EXPERIMENTS

4.1 Experimental Design

Three modifications of the baseline physical parameterizations were evaluated in the physics sensitivity component of this project. The first involved modifying the atmospheric radiation schemes so that both the longwave and shortwave components used the new RRTMG radiation package, which uses the RRTM methodology but in a more efficient form adaptable to global climate models. This particular radiation package first became available in WRF v3.1. Though the RRTM and RRTMG longwave radiation schemes should produce very similar clear-sky fluxes, when mult-layered condensate is present the RRTMG makes use of the Monte Carlo Independent Column Approximation (McICA) to take into account 3D scattering effects.

The second involved changing the PBL parameterization from MYJ to the Quasi-Normal Scale Elimination (QNSE) scheme (Sukoriansky et al. 2005; Galperin et al. 2007). The theory behind the scheme is quite

advanced, but it is specifically designed for stable conditions, and allows both turbulent mixing and gravity wave motions to be represented in a unified framework. Dr. Boris Galperin was invited to Penn State University to give a seminar on the theory of the QNSE scheme in October 2008 before it was officially made public in WRF v3.1. The implementation of the QNSE scheme in WRF is actually similar to that of the MYJ, but with the values of vertical mixing parameters derived from the theory as a function of Richardson number (i.e., essentially the ratio of atmospheric stability to the square of the wind shear).

The third modification involved changing the LSM model from Noah to the Rapid Update Cycle (RUC) LSM. Among the features of the RUC LSM that suggest its use for this study is the presence of a snow model that potentially can have multiple layers depending on the snow depth (Smirnova et al. 2000). Other users have reported favorable results from using the RUC LSM in simulations of the Arctic (Mölders and Kramm 2010). The RUC LSM can also be initialized using soil information from the half-degree GFS after minor modification of the WRF source code. By default WRF can use either 6 or 9 soil levels, but we chose 6 because it is closer to the 4 levels of Noah and because it is the typical number of soil levels used in the RUC (e.g. Hines and Bromwich 2008).

4.2 Model Initialization and Setup

The objective analyses used for model initialization and analysis nudging were performed using the multi-quadric method within the OBSGRID software designed for WRF. The background analysis files were derived from the half-degree GFS and topographic and land use dataset through the WPS. The background fields also served as the basis for performing QC on the WMO rawinsonde and surface METAR data used for verification and obs nudging, through 'buddy-check' (excluding obs too different from their neighbors) and 'err-max' (excluding obs too different from the background) procedures. A consequence of the current QC methodology is that all observations were located at the surface or at the standard pressure levels of the GFS model.

For the baseline and sensitivity experiments the model setup was the same except for the choice of physics options. Both the near total darkness and the partial sunlight episodes were simulated in their entirety using the four overlapping simulation segments referred to above. The FDDA procedure (using the modified vertical weighting functions) was defined to use surface and 3D analysis nudging on the 12-km Grid 1, obs nudging on both the 12-km Grid 1 and the 4-km Grid 2, and no FDDA on the 1.3-km Grid 3. Physics sensitivities on Grid 3 would thus be given greater weight than sensitivities on the other grids (which would not be expected to be as large due to the influence of FDDA). (However, we left open the possibility of performing a final dynamic-analysis simulation with obs nudging also performed on Grid 3 once a best-choice physics suite was selected; this final simulation would then have our best available model analysis of the atmospheric state during the episodes, and would be appropriate for use in atmospheric chemistry or transport and dispersion models. These results have been added to the report in Section 5 below.)

For each sensitivity experiment verification was performed using model output every 3 hours (excluding the initial time). For the periods of overlapping simulation segments, the model output from the segment at the larger forecast time was used, so all of the verification model output was at least 12 hours after a model initialization (except of course for the first 12 hours of an episode). All three grids were verified against only those stations located within the boundaries of Grid 3, to ensure that statistical differences between grids are not due to the different set of stations available on each domain. As previously discussed, verification of surface METAR data is performed directly with the third model level from the surface for winds, and the lowest model level for temperature and moisture.

The first physics sensitivity test involved changing the radiation to the RRTMG scheme for both longwave and shortwave components. We all agreed that if this produced favorable results we could simply retain the RRTMG radiation scheme rather than the Dudhia shortwave / RRTM longwave radiation suite of the baseline simulation in future sensitivity experiments. An initial three-day test (23-26 Jan) was performed without FDDA on any grid so as to maximize physics sensitivity. It was indeed found that the surface METAR temperature RMSE scores were consistently improved by the use of RRTMG (Fig. 9), although winds and relative humidity were little affected (not shown). The improvement seemed to be related to reduced downward longwave fluxes beneath patches of ice condensate. Thus, the decision was made that all future physics sensitivity tests, this time with FDDA on Grids 1 and 2 as described above, would make use of the RRTMG scheme.

The combinations of physics parameterizations used in the physics sensitivity tests are summarized in Table 4. To facilitate the comparison of different physics sensitivity experiments, the baseline simulation, with the combination of MYJ PBL scheme, Noah LSM, and Dudhia shortwave / RRTM longwave radiation, will henceforth be denoted as experiment MND. Another experiment, with MYJ PBL / Noah LSM / RRTMG radiation, will be noted as MNR, and another with QNSE PBL / Noah LSM / RRTMG radiation will be denoted as QNR. Finally, the experiment with MYJ PBL / RUC LSM / RRTMG radiation will be denoted as MRR.

Experiment Name	Planetary Boundary Layer (PBL)	Land Surface Model (LSM)	Radiation
MND (Baseline)	Mellor-Yamada-Janjić (MYJ)	Noah	Dudhia Shortwave / RRTM Longwave
MNR	Mellor-Yamada-Janjić (MYJ)	Noah	RRTMG Shortwave / RRTMG Longwave
QNR	Quasi-Normal Scale Elimination (QNSE)	Noah	RRTMG Shortwave / RRTMG Longwave
MRR	Mellor-Yamada-Janjić (MYJ)	Rapid Update Cycle (RUC)	RRTMG Shortwave / RRTMG Longwave

Table 4: Names and physical parameterizations used for physics sensitivity studies.

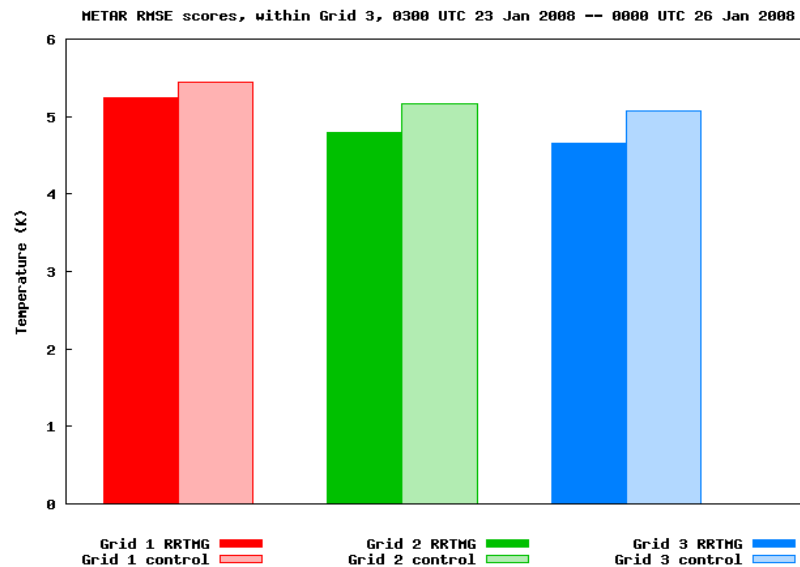


Fig. 9: Surface METAR RMSE scores for temperature compiled for those stations located within Grid 3 for simulations from 00 UTC 23 Jan 2008 – 00 UTC 26 Jan 2008. Verification statistics are computed every three hours during the period. ‘Control’ denotes baseline physics configuration; ‘RRTMG’ denotes baseline physics configuration but with the RRTMG longwave and shortwave radiation schemes. All simulations shown were performed without FDDA.

4.3 Results of Physics Sensitivity Experiments

Figures 10 and 11 present the temperature RMSE and bias scores, respectively, for Grid 3 surface METAR stations for both the partial sunlight and near total darkness episodes. First, it can be seen that the RMSE score increases from Grid 1 to Grid 2 to Grid 3, which can be explained by the fact that less FDDA forcing is being applied from Grid 1 (both analysis and obs nudging) to Grid 2 (obs nudging) to Grid 3 (no nudging). These RMSE scores are large compared to typically reported surface meteorological values (e.g., Seaman and Michelson 2000), but of course the large temperature range through the period (about 40°C for both episodes) and extreme conditions make these challenging forecasts for a numerical model. Second, we see the previously discussed result that switching the radiation to RRTMG (compare MND and MNR) leads to improved temperature RMSE scores and lower positive temperature biases; the improvement is most noticeable on the no-FDDA Grid 3. The fact that the RMSE improvement through the use of the RRTMG is greater for the near total darkness episode than for the

partial sunlight episode was not unexpected, because previous examination of the partial sunlight episode revealed that the reduced positive temperature bias with RRTMG was due to the longwave component while the shortwave component of RRTMG partially counteracted this effect (not shown).

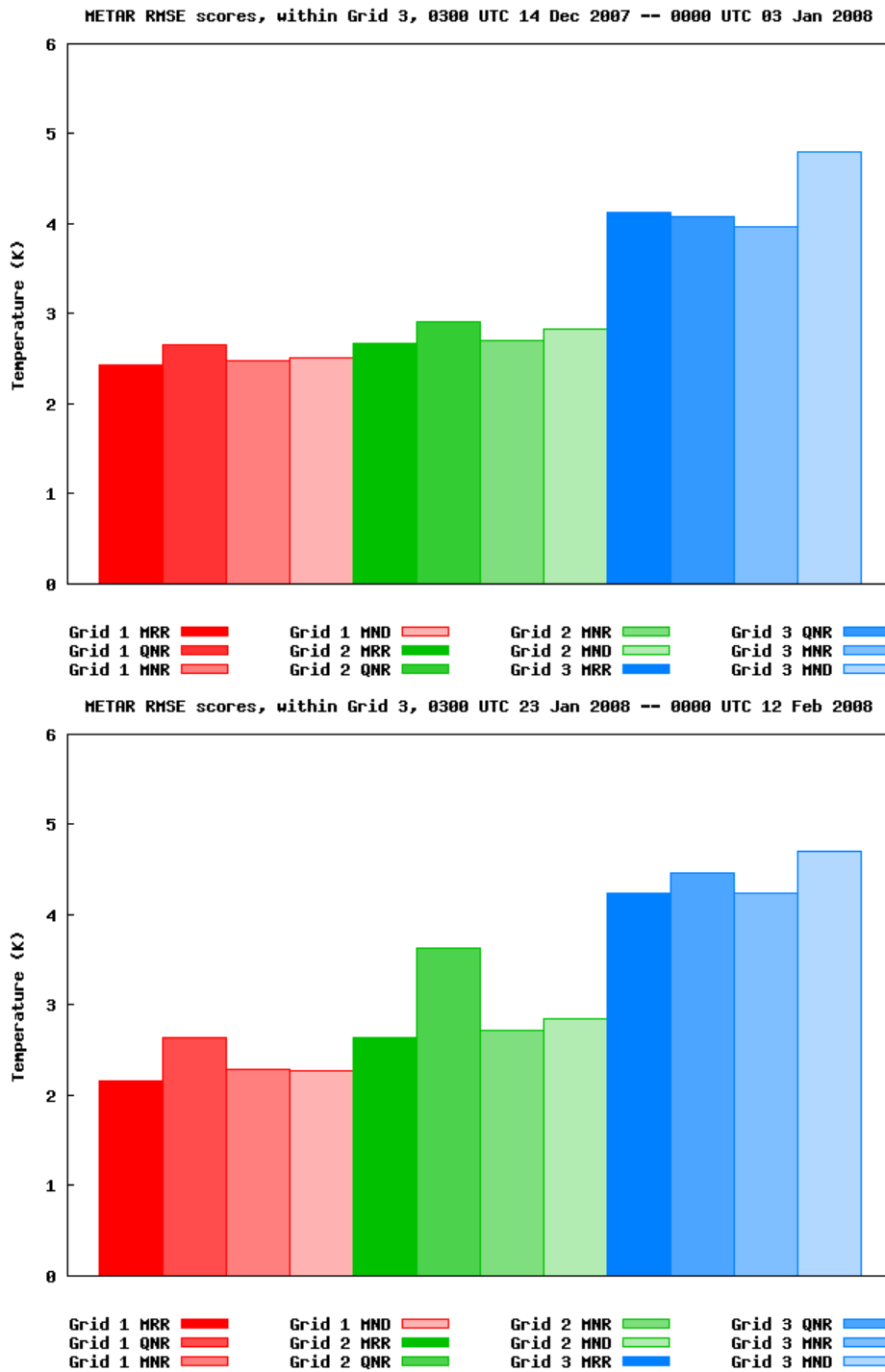


Fig. 10: Surface METAR RMSE scores for temperature for entire near total darkness episode (top) and partial sunlight episode (bottom). Labels for degree of shading refer to experiment names in Table 3. Verification statistics were computed every 3 hours during each episode as described in text.

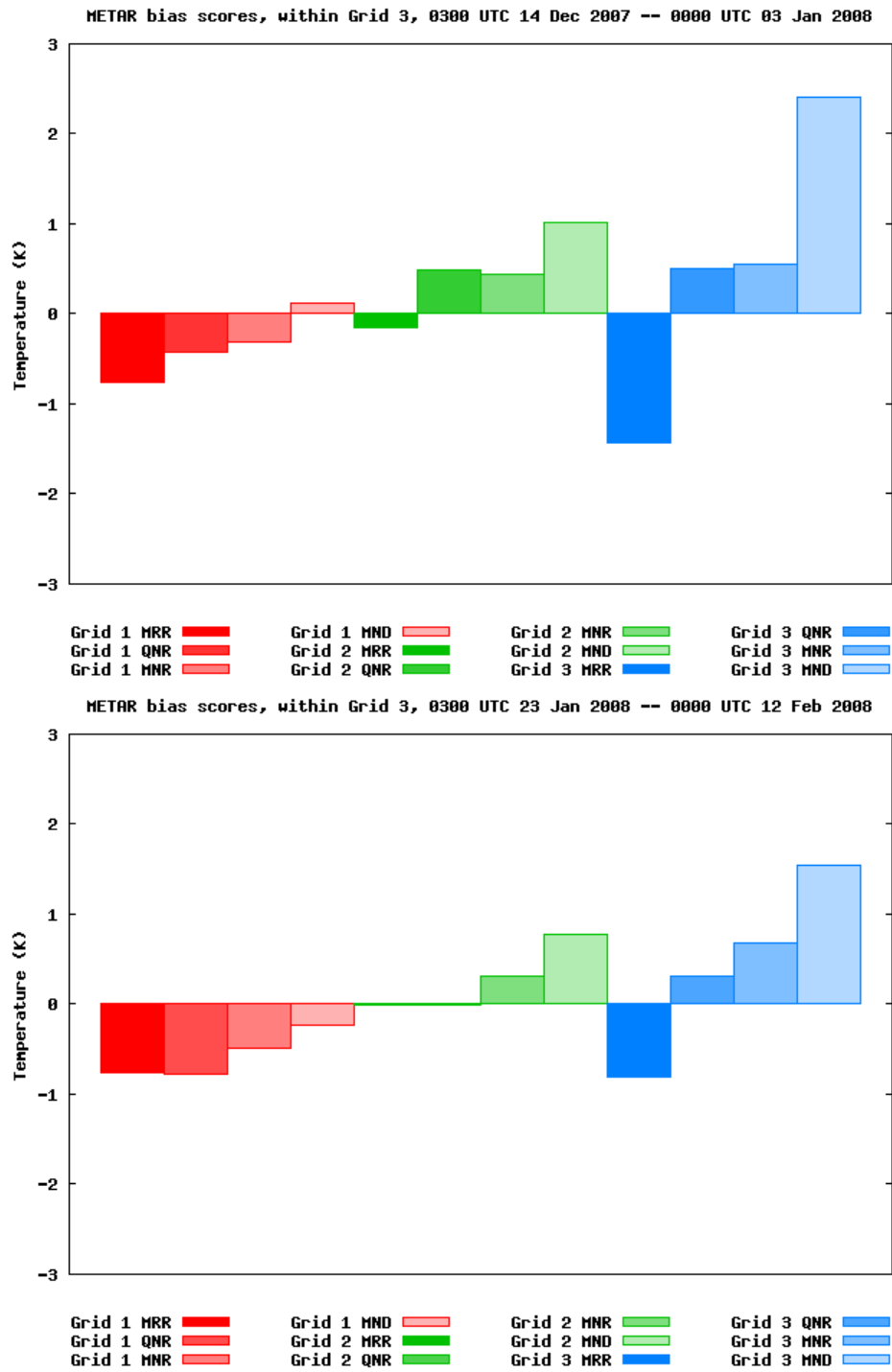


Fig. 11: Same as Fig. 10, but for surface METAR bias scores for temperature.

Switching from the MYJ to the QNSE PBL scheme (compare MNR to QNR) further reduced and improved the magnitude of positive METAR temperature bias (for Grid 3 and the Grid 2 partial sunlight episode). However, the temperature RMSE scores for QNR are consistently greater than those for MNR; so this improved bias is not reflected in more skillful forecasts. The results of the QNSE PBL scheme are encouraging and should be analyzed in greater depth in a future project. We decided that the sensitivity test introducing the RUC LSM should use the MYJ scheme due to our greater experience with MYJ in WRF.

The effect of switching from Noah to RUC (compare MNR to MRR) produces the coldest surface temperatures of any of the experiments. While this leads to the best magnitude METAR temperature biases for Grid 2, the MRR Grid 3 temperature bias is considerably more negative, especially for the near total darkness episode. The MRR temperature RMSE scores for the METARs are the best, or tied for the best, of the four physics experiments for Grid 2 and the Grid 3 partial sunlight episode, but slightly worse than MNR and QNR for the Grid 3 near total darkness episode.

In terms of surface METAR wind speed RMSE and bias errors (Figs. 12 and 13) we see that there is less variability among the different physics schemes. For virtually all variables, grids, and episodes, however, the scores for experiment MNR are slightly better than the others. The wind speed RMSE scores tend to be slightly worse on Grid 3 without FDDA than on Grid 2 with obs nudging, but better than those on Grid 1 that uses analysis nudging but with a much coarser horizontal resolution.

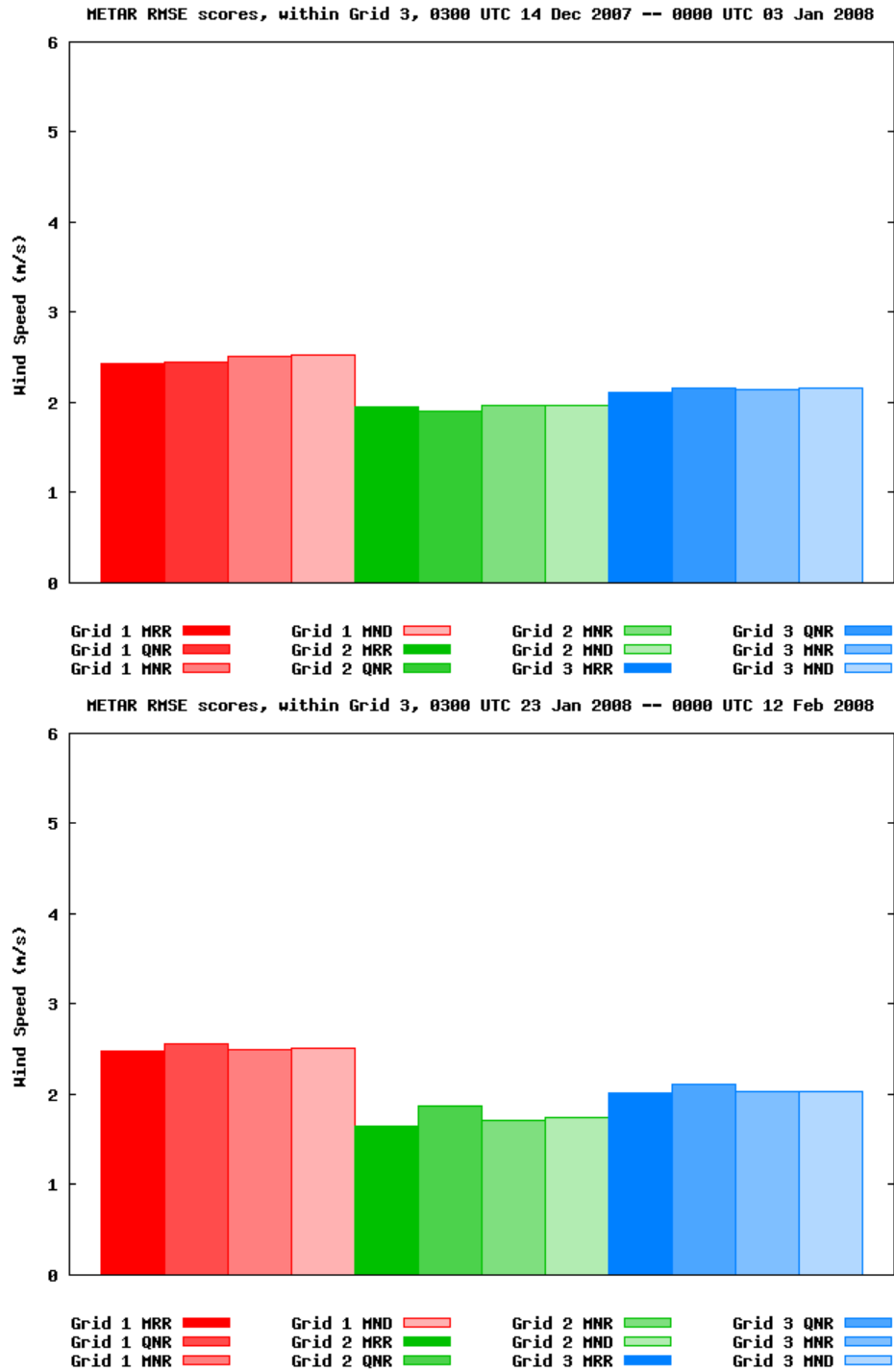


Fig. 12: Same as Fig. 10, but for surface METAR RMSE scores for wind speed.

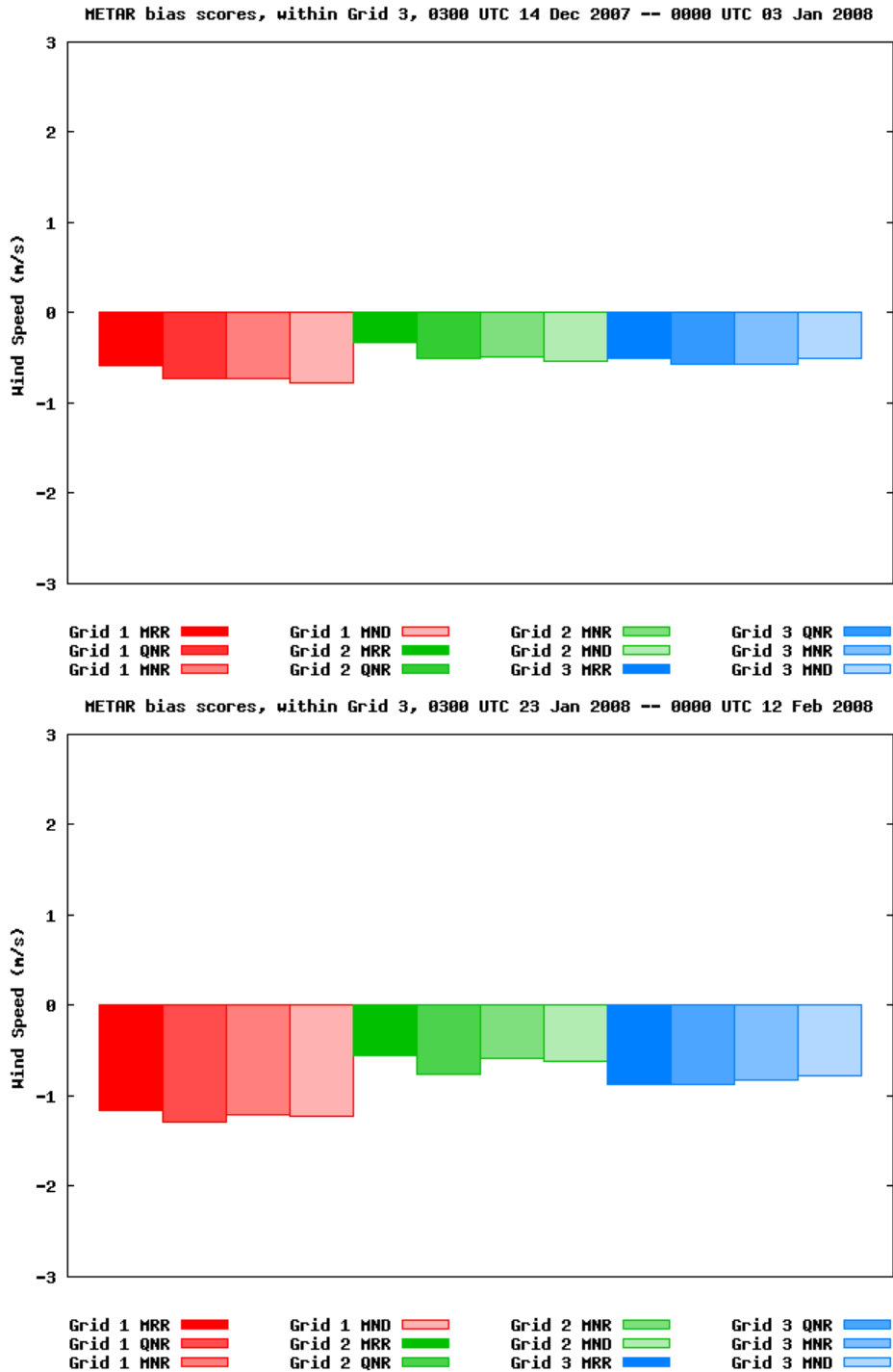


Fig. 13: Same as Fig. 10, but for surface METAR bias scores for wind speed.

In order to learn more about the nature of these biases, statistics for each episode can be compiled for each of the four 5-day (or 5.5-day or 6-day) simulation segments. One instructive comparison is between 14-20 Dec 2007 and 20-25 Dec 2007 (Fig. 14). The temperature difference between different physics configurations remains quite consistent between the two periods, but in the 14-20 Dec period the model temperature bias tends to be more negative than for the 20-25 Dec period. It can be shown that the large negative temperature biases of MRR are predominantly from the 14-20 Dec period. It should be noted that the highest exceedances / lowest temperatures for the near total darkness episode occur around 21 Dec. In general, Grid 3 tends to magnify the temperature biases of Grid 2, except for the MRR model for 20-25 Dec, where the Grid 3 temperature bias is reduced to almost zero.

A time series of the averaged observed, MNR, and MRR temperatures at the locations of the Grid 3 METARs is shown in Fig. 15. Note that the strongest MRR negative temperature biases in each episode tend to occur during times when the temperature is decreasing toward the coldest temperatures near 21 Dec in the near total darkness episode and about 05-09 Feb 2008 for the partial sunlight episode. At these times the MNR temperature bias also tends to be negative, but not by as much. However, immediately after the coldest temperatures are reached, the model biases become positive, and then the MRR configuration is preferred because temperature biases are smaller in magnitude. In particular, during the cold 5-9 Feb period MRR lacks the strong positive spikes in temperature bias that occur in the MNR simulation during the afternoons.

Verifying model features above the surface was made difficult by the scarcity of such observations in the region; the only rawinsonde sounding stations within Grid 2 are at Anchorage, McGrath, and Fairbanks, and of these only Fairbanks is located within Grid 3. No other reliable set of above-surface observations within Grid 3 was available for the episodes. A time-averaged composite of the vertical temperature structure of the Fairbanks sounding, compared to that from the different model physics configurations, is shown in Fig. 16. Since the quality-controlled observations used in the verification are located at the background GFS pressure levels, which have 25 hPa spacing near the ground, this is the effective maximum vertical resolution of the figure. The figure shows the zone from 700 hPa down to 975 hPa, which is the lowest pressure bin located entirely above the surface at Fairbanks. Note that the chosen variations in physics packages have virtually no effect above approximately 850 hPa, and all the modeled temperature profiles are extremely close to the observed profile, presumably due to the impact of Grid 2 obs nudging along the boundaries of Grid 3. From about 850 hPa to 925 hPa, the models begin to diverge from the observations for the near total darkness episode; the MND configuration is about one degree C too warm, but the models with the RRTMG radiation package reduce the positive temperature bias by about a factor of two. For the partial sunlight episode all models track the observations closely down to about 900 hPa. Below 950 hPa the MRR configuration becomes the coldest of the models, and the closest to the observed profile, especially for the near total darkness episode. At these lowest levels the RRTMG sensitivity remains much greater for the near total darkness episode than for the partial sunlight episode. The MNR and QNR configurations are always virtually indistinguishable, suggesting that choice of PBL scheme has little impact on the vertical temperature structure at 975 hPa and higher elevations.

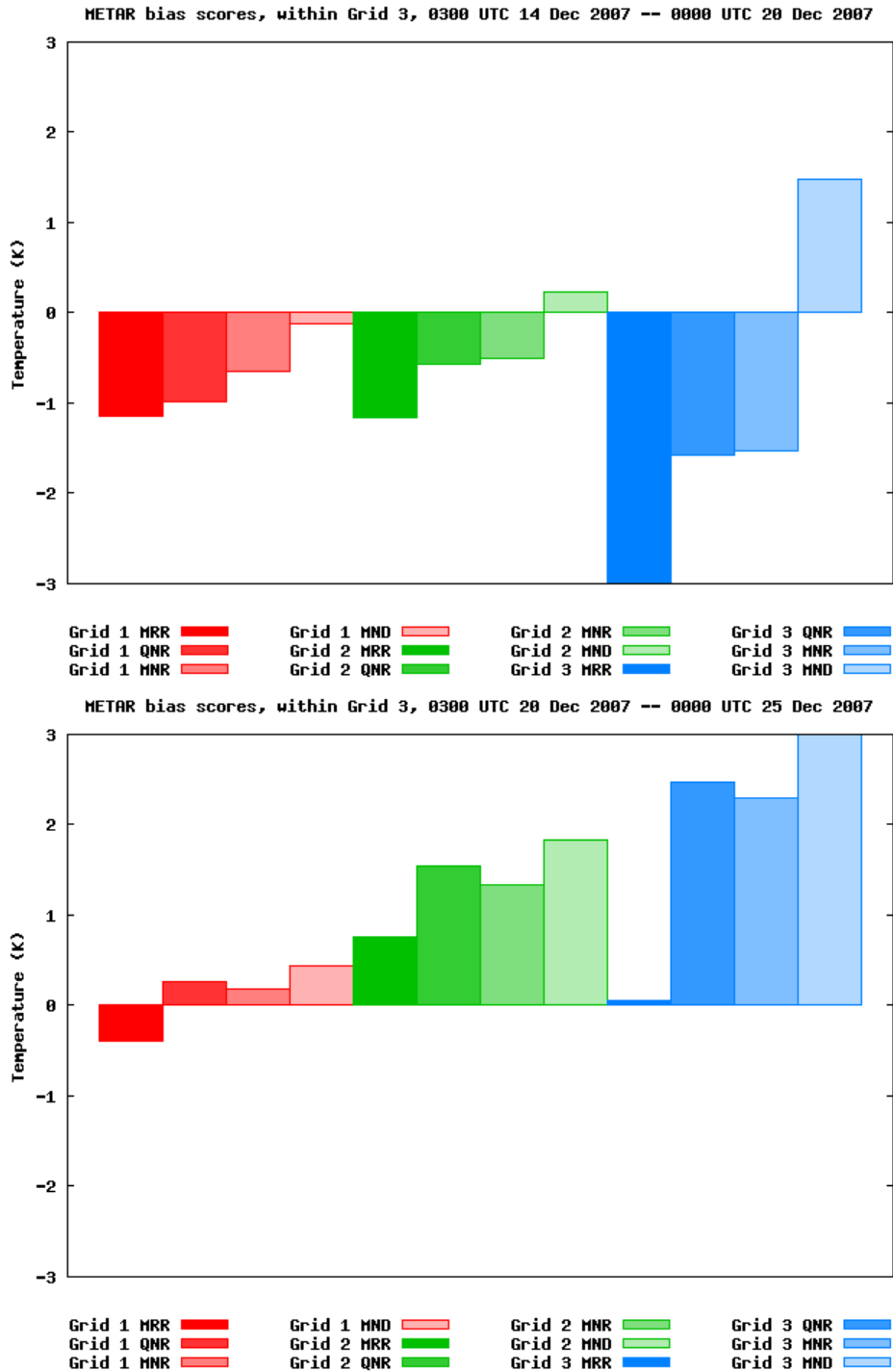


Fig. 14: Surface METAR bias scores for temperature during the near total darkness episode within the 14-20 Dec period (top) and 20-25 Dec period (bottom). Otherwise, same as Fig. 11.

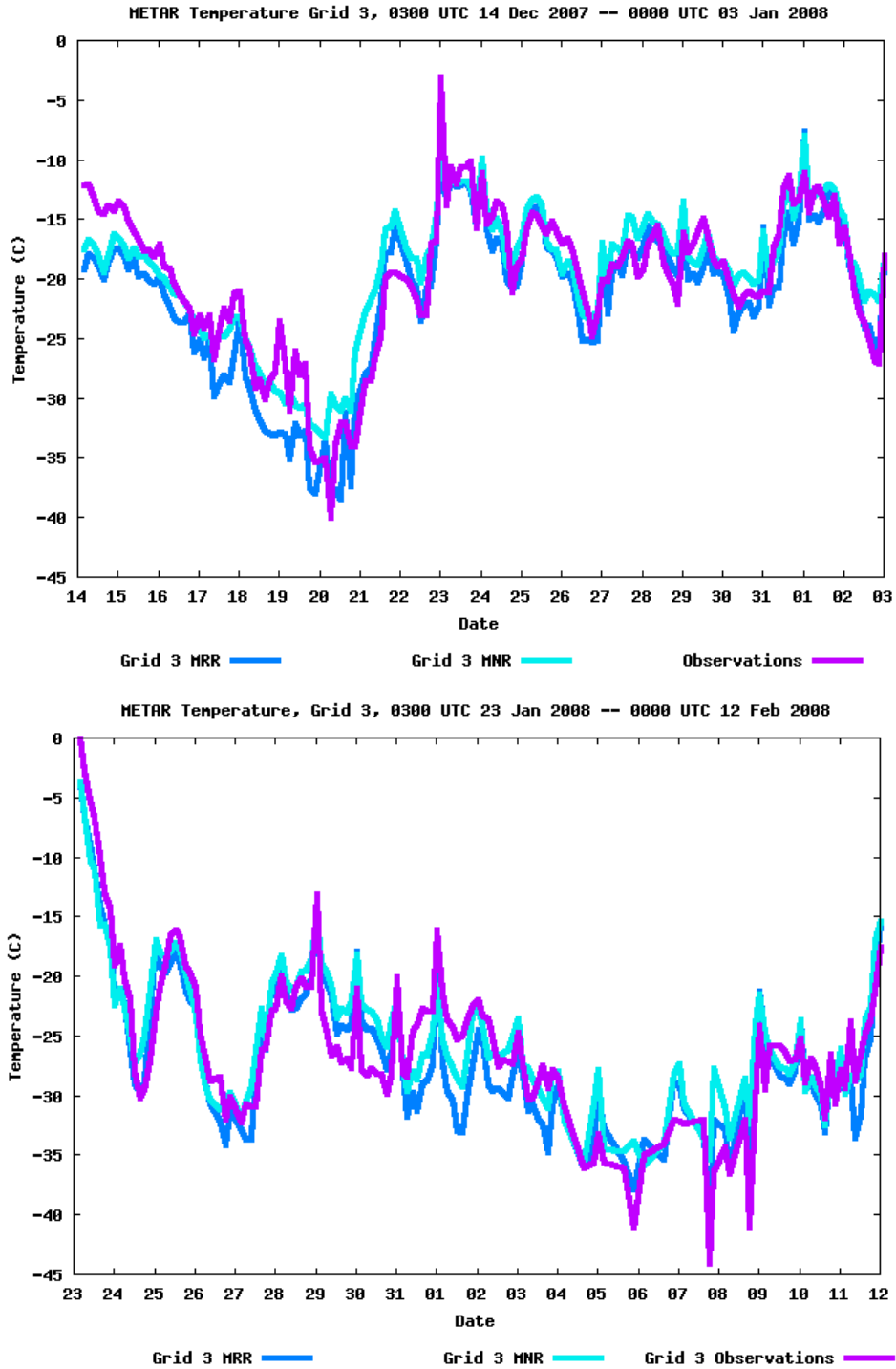


Fig. 15: Time series of temperature for near total darkness episode (top) and partial sunlight episode (bottom), averaged over the sites of all the surface METAR stations within Grid 3. Dark blue indicates value within Grid 3 from experiment MRR; light blue indicates value within Grid 3 from experiment MNR; purple indicates observed METAR value.

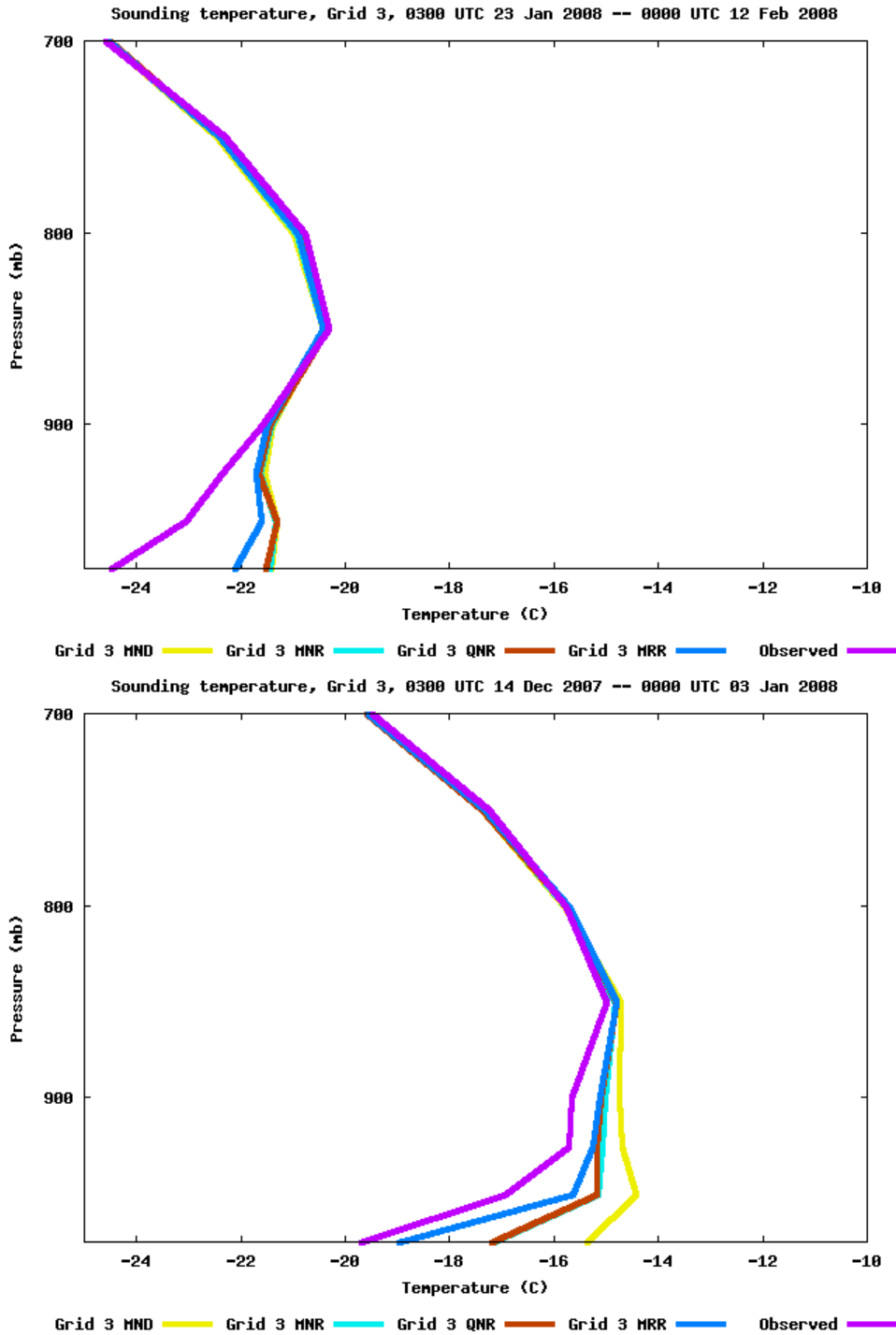


Fig. 16: Time-averaged vertical profile of Fairbanks sounding (PAFA) temperatures for near total darkness episode (top) and partial sunlight episode (bottom). Dark blue indicates value from experiment MRR; brown indicates value from experiment QNR; light blue indicates value from experiment MNR; yellow indicates value from experiment MND; purple indicates observed sounding value.

In order to learn more about the behavior of the different models, we examined the time series of the reported surface-level temperature of the raw Fairbanks sounding in comparison to the lowest-level model values at that location. When we compare the time series for the period surrounding the coldest temperatures of each episode (Fig. 17), an obvious diurnal trend appears in the partial sunlight episode observations during the coldest period from about Day 12 to Day 19 (4 – 11 Feb 2008). Little diurnal trend appears in the observations earlier in the episode; by contrast, the models all have a significant diurnal trend in surface temperature throughout the partial sunlight episode. The model diurnal amplitude during the 4-11 Feb 2008 period for the experiments other than MRR is approximately consistent with the observed amplitude, but the temperature values are consistently about 7°C too warm during this period. The MRR diurnal amplitude is somewhat larger than the others, such that it is similar to the other models for the warmer 0000 UTC times, but is much closer to the observations for the colder 1200 UTC times. For the period of rapidly falling temperatures immediately prior to 4-11 Feb the MRR experiment remains colder than the other models at the 1200 UTC times. In this case, the model 0000 UTC soundings are close to the observations, so the presence of a diurnal tendency in the model but not the observations during this time causes the 1200 UTC model soundings to be too cold, and the MRR sounding to be very cold.

During the near total darkness episode there is little diurnal variation in either the model or the observations. However, we again see the feature that when the temperatures are rapidly decreasing below -30°C, the MRR configuration has a substantial cold bias; once the coldest temperatures are achieved, however, the MRR configuration is better able to capture the low temperatures than the other models.

Finally, in order to gain as much insight as possible into the model-predicted PBL structure near the surface during the coldest episodes, we performed an alternate verification procedure using the raw Fairbanks sounding for the last ten days of the partial sunlight episode (2 – 12 Feb 2008). Instead of interpolating the model sounding to 25 hPa increments of the observed sounding, we interpolated the raw sounding to each WRF model level using some basic assumptions. (The WRF model levels are specified in terms of $(p - p_T)/(p_s - p_T)$ where p_T is the specified model top pressure, p_s is the surface pressure, and all pressures are the dry hydrostatic components; here we converted each WRF level to a pressure in the Fairbanks sounding using the observed surface pressure and the assumption that the actual pressure is approximately the dry hydrostatic pressure; the temperature at the resultant pressure was found by log-pressure interpolation. Finally, the physical height for each WRF level in the base state over ocean was used to determine the abscissa coordinate in Fig. 18.) This procedure gives us increased vertical resolution near the surface, where the model levels are much closer than 25 hPa (i.e., roughly 250 m in physical distance) apart. A plot of the temperature structure (Fig. 18) shows the same general trends as in the 25-hPa plot of Fig. 16. The two simulations using the Noah scheme (QNR and MNR) are similar, while the simulation using the RUC LSM (MRR) is consistently colder in the lowest 500 m. However, all simulations have a warm bias in the lowest 700 m. Though in the lowest 100 m the models have average vertical temperature gradients as large as, or even larger than, those in the observations, the vertical temperature gradients comprising the inversions in the observations extend to a much

greater altitude, consistent with the significantly greater temperature differences between the surface and the 1-km level found in the observations.

In summary, it appears that during periods of near total darkness and the cold, dry, calm conditions characteristic of high fine particulate concentrations, all models possess a low-level warm bias, but the bias is minimized and the statistics are generally the best in the MRR (MYJ PBL / RUC LSM / RRTMG radiation) experiment. The reason for the improved statistics in MRR for the extremely cold episodes is not precisely known at present, but it is probably related to some combination of its potentially multi-level snow model (which can serve to reduce the heat flux from the ground to the atmosphere) and the presence of a ground surface 'skin' layer in the RUC LSM (which has no thermal inertia itself and could decrease the time needed for the ground and the adjacent atmosphere to respond to a negative heat budget). A few caveats are in order, however. During the period of decreasing temperatures immediately preceding temperatures below approximately -35°C , the MRR configuration is still colder than the other models, but for these periods MRR tends to exacerbate an already cold model bias instead of improve a warm model bias. Since the observations for these falling temperature periods tend to show fairly continuous frozen precipitation (in contrast to the coldest temperature periods which tend to have ice fog and no precipitation), it is possible that all the model configurations have difficulties with modeling the microphysics/radiation interaction. For example, if the radiation scheme is not taking into account the presence of ice crystals when they exist in the actual atmosphere, the absence of their radiative heating effect on the surface during these extremely cold conditions could be significant. Another caveat is that when partial sunlight is present, MRR tends to warm more rapidly than the other models, and all models tend to have substantial warm biases in these conditions.

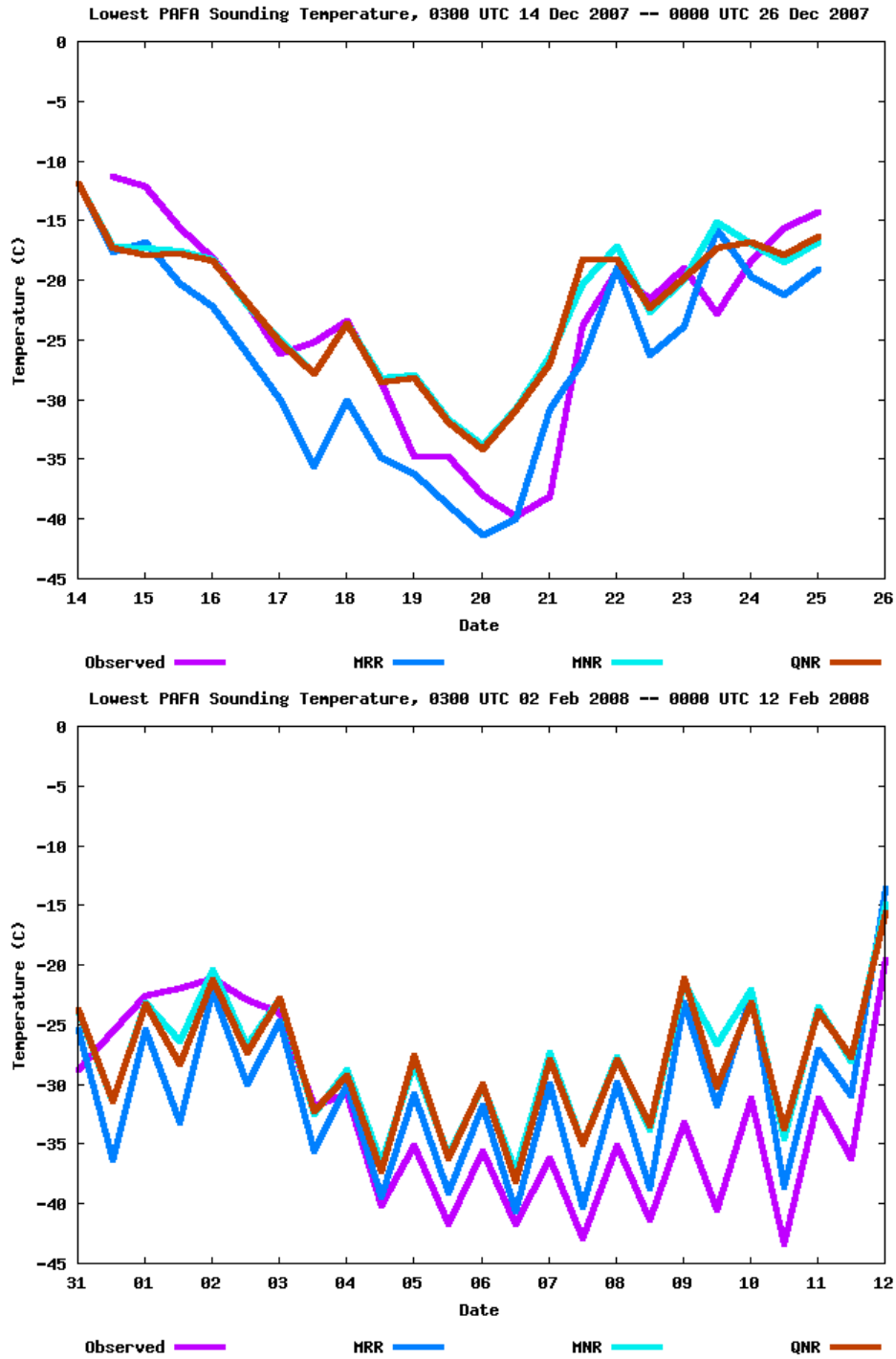


Fig. 17: Time series of raw Fairbanks surface-level reported sounding temperatures (PAFA) for 14-26 Dec 2007 period of near total darkness episode (top), and 02-12 Feb 2008 period of partial sunlight episode (bottom). Colors are same as in Fig. 16.

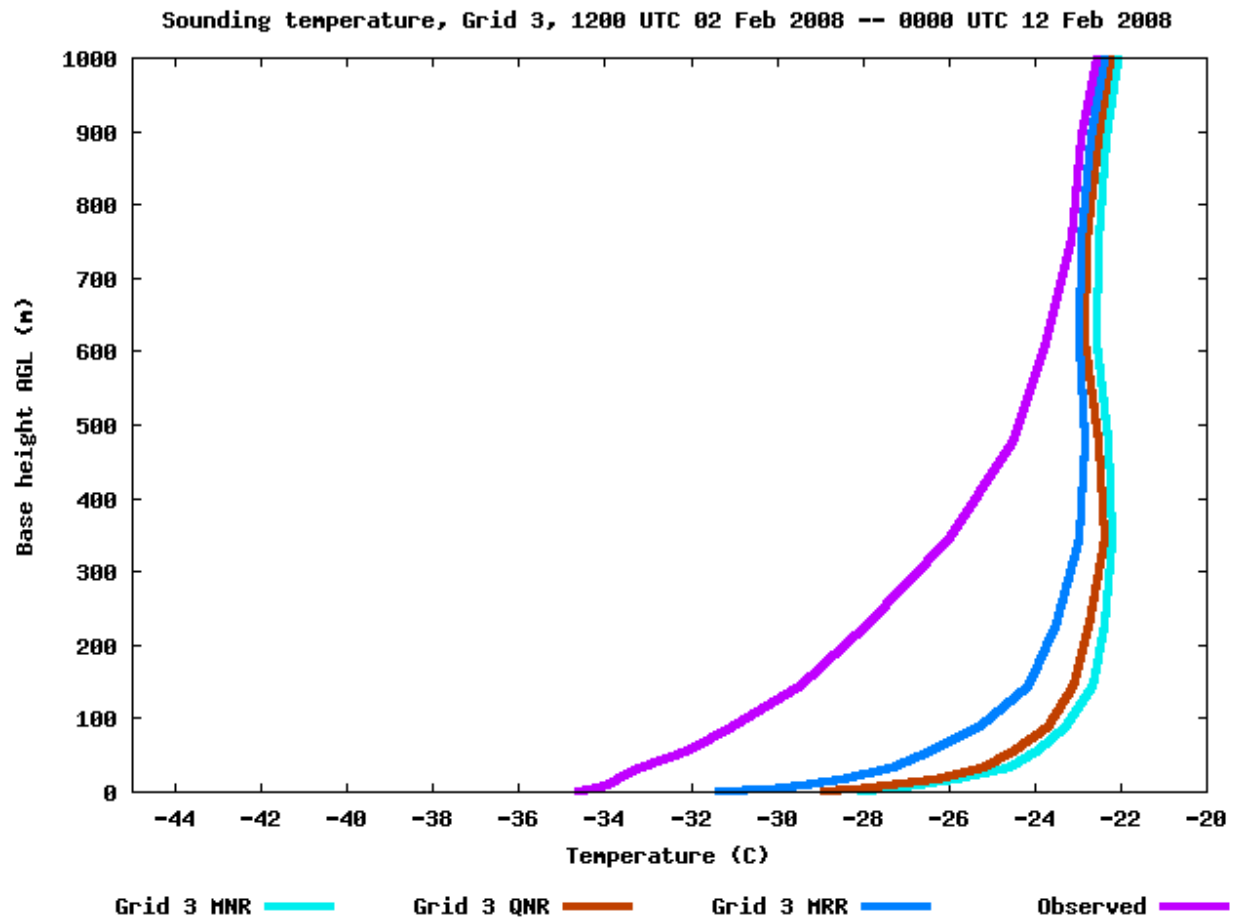


Fig. 18: Time-averaged vertical profile of Fairbanks sounding (PAFA) temperatures for 02-12 Feb 2008 period during partial sunlight episode, where observations are interpolated to WRF vertical levels as described in text. Dark blue indicates value from experiment MRR; brown indicates value from experiment QNR; light blue indicates value from experiment MNR; purple indicates observed sounding value.

5. SELECTION OF PREFERRED PHYSICS CONFIGURATION AND FINAL DYNAMIC-ANALYSIS SIMULATION

Based on the results of the physics sensitivity test, we concluded that the physics suite contained in experiment MRR (MYJ PBL, RUC LSM, and RRTMG radiation) was the best one to be used to simulate the two episodes. The high exceedance events that are of importance occur during the coldest temperature periods when the RUC LSM appeared to perform the best. However, the tendency of the MRR suite to produce significant negative temperature biases during the falling temperature periods must be noted.

We thus concluded that we should perform an additional dynamic-analysis simulation with the MRR physics package but with Grid 3 obs nudging in order to reduce the noted temperature biases and generate the best atmospheric analysis. Because the MRR Grid 2 statistics, in the presence of obs

nudging, were almost always quite good, we were optimistic that any systematic biases present in the MRR simulation on Grid 3 would be greatly alleviated through obs nudging. As noted above, however, we did not nudge the wind fields from surface data on Grid 3, whose influence is below ~ 150 m (see Fig. 8), because of concerns that the local topographic drainage flows generated by the model in the topography around Fairbanks may be smoothed out by the FDDA procedure. However, we did retain nudging of wind fields on Grid 3 for observations above the surface (i.e., from the Fairbanks sounding).

The initial specifications of the parameters used for the Grid 3 obs nudging simulation are listed within the parentheses of Table 2. They closely correspond to values on the other grids. However, the value of RINXY (a horizontal radius of influence) was decreased on Grid 3 from a value of 100 km to 75 km. This value was determined by performing a temporal correlation of the Grid 3 temperature innovations within the MRR no-FDDA simulation at the location of the METAR stations, and estimating the characteristic horizontal distance at which the Grid 3 METAR observational-based surface innovations were correlated for (see Fig. 19). The surface pressure difference parameter used in the horizontal weighting function in complex terrain (henceforth Δp_d) was also reduced from 75 hPa to 37.5 hPa based on the results of the correlation analysis (e.g., note the relationship between correlation value and the elevation difference labels in Fig. 19). This parameter controls how far the influence of a surface observation may spread along topography as the surface pressure varies from that at the obs site; our results suggested that some station pairs close in horizontal distance but with different vertical elevations were much less correlated than similar stations with little terrain difference.

An additional complication derives from the fact that the WRF method of reducing the weight of surface observations based on Δp_d is different from the MM5 method defined in Stauffer and Seaman (1994). In default WRF, if there is a difference between the model surface pressure at the location of a surface observation, p_b , and the model surface pressure at a grid point in question, p , the weight of the surface observation is reduced by a factor w given by:

$$W = \max \left[0.0, 1.0 - \frac{|p - p_b|}{\Delta p_d} \right] \left[\frac{r_0^2 - r^2}{r_0^2 + r^2} \right], \quad (1)$$

where r is the horizontal distance between the grid point and the observation, and r_0 is the surface radius of influence parameter (RINXY in Table 2). In MM5, on the other hand, the surface pressure difference is used to artificially increase the horizontal radius of influence parameter, according to:

$$W = \frac{r_0^2 - \left[r + r_0 \frac{|p - p_b|}{\Delta p_d} \right]^2}{r_0^2 + \left[r + r_0 \frac{|p - p_b|}{\Delta p_d} \right]^2} \quad (2)$$

Though the two functions are often similar, the WRF function tends to be more horizontally isotropic and less sensitive to terrain features, as well as generally nonzero over greater horizontal differences. (The WRF method will give nonzero weights to surface observations unless either $|p - p_b|$ exceeds Δp_d or r exceeds r_0 , whereas the MM5 method can give a zero weight even if neither criterion is met because the terrain difference increases the effective distance from observation to grid point.) In the final Grid 3 FDDA simulations used here, the MM5 method for surface pressure difference weighting was used.

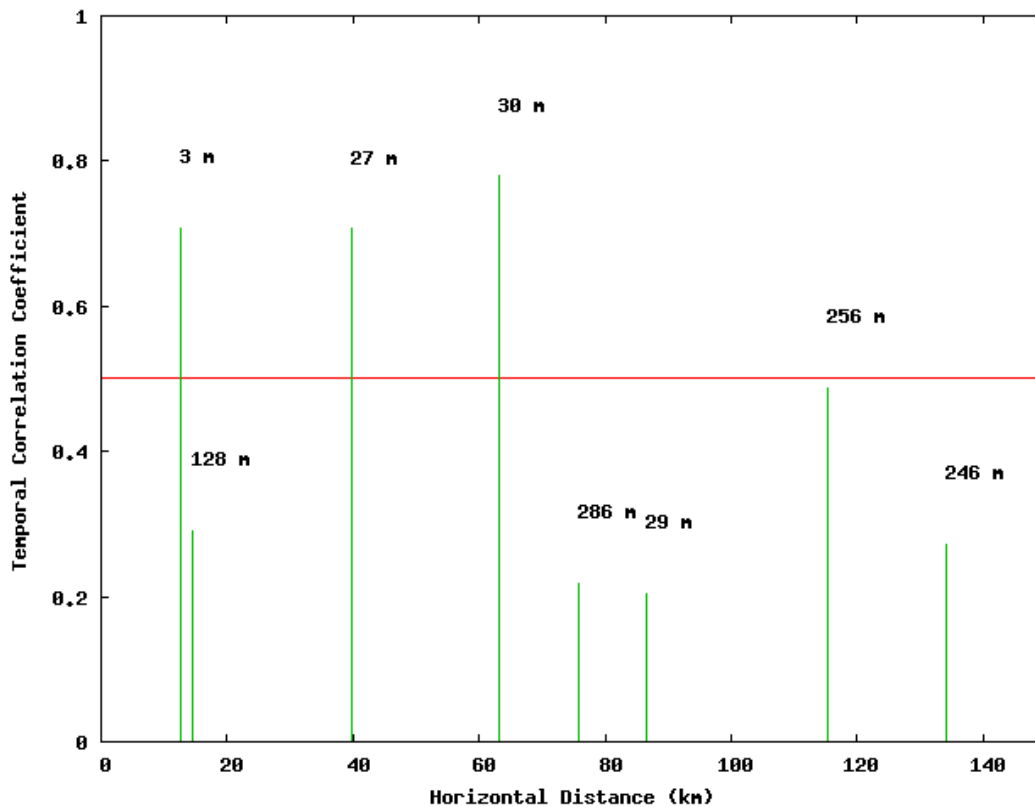


Fig. 19: Temporal correlation coefficients vs. horizontal separation distance between various pairs of surface METAR stations located within Grid 3 (green). Red line indicates a temporal correlation coefficient of 0.5. Numerical labels indicate elevation distance between stations in meters.

The value of TWINDO (Table 2), the obs nudging time window half-period defining the temporal influence of an innovation (Stauffer and Seaman 1994), should also be considered. Ideally this parameter would be a function of height and decrease in value towards the surface, to take into account the shorter temporal correlation time scales for surface data reflecting surface processes. Although this capability will be present in WRF version 3.2, in the version 3.1 that we used for this study, it is simply a constant (though it may vary with grid). Our experience suggests that the value chosen, 2.0 hours, is generally best for the assimilation of sounding data, but may be somewhat too large for the surface (Schroeder et al. 2006). For the final version of the Grid 3 FDDA simulations, we manually encoded the Penn State MM5 method used in WRF version 3.2 so that the effective value of TWINDO was 2.0 hours above the surface, but 1.0 hours at the surface.

Finally, two additional modifications were made to the default WRF version 3.1 FDDA procedure. In the default procedure the surface level observation of a sounding is treated differently than a surface observation. Specifically, a surface observation is assumed to be applicable to the lowest model level at the horizontal location of the observation, whereas all sounding observations including one at the surface level are assumed to be applicable at the vertical model location with the same pressure as the pressure of the observation. So a sounding surface level observation will not necessarily be placed at the lowest model level if the model surface pressure is not the same as the observed surface pressure. Also, the surface pressure difference is used to reduce the weight of a surface observation at remote horizontal grid points, but not the weight of a surface-level sounding observation. This inconsistent treatment becomes more of an issue in station-poor regions such as that of the Grid 3 used in this study, where the relative influence of the Fairbanks sounding to all Grid 3 METAR stations may be quite significant. In the final Grid 3 FDDA simulations, the code was modified to remove the surface-level observation from the rest of the sounding and treat it as a separate surface observation. Furthermore, to reflect the Penn State MM5 method, the Δp_d weighting function was applied to soundings as a unit, in addition to surface observations.

Figures 20-22 show the vertical profiles of RMSEs verified against the Fairbanks sounding for a series of trial simulations of the first six days of the near total darkness episode (14-20 Dec. 2007) using the MRR physics suite but different variations of the Grid 3 obs nudging procedure. First, the benefit of Grid 3 obs nudging is immediately apparent, and Fig. 21 shows in particular that the simulations with retained Grid 3 wind obs nudging above the near-surface layer have substantially reduced wind speed RMSE scores in comparison with the two simulations that don't. This helps justify our proposed procedure of retaining Grid 3 wind obs nudging above the near-surface layer but turning it off within the near-surface layer to allow the model to generate its own topographic flows. Second, for the non-wind fields shown in Fig. 20 and Fig. 22 we see that the TWINDO = 2.0 hours statistics tend to be somewhat better than the TWINDO = 0.45 hours statistics, in agreement with our past experience. The proposed Grid 3 obs nudging procedure, including, among other modifications, using TWINDO = 2.0 hours above the surface but TWINDO = 1.0 hours at the surface, produces results quite similar to the TWINDO = 2.0 hours simulation.

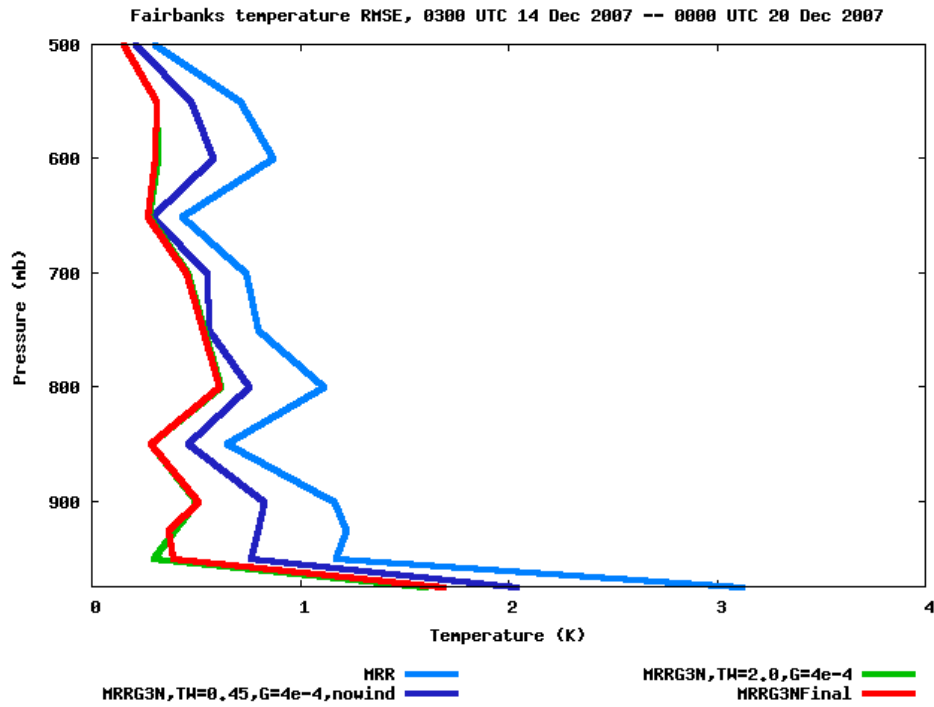


Fig. 20: Time-averaged vertical profile of Fairbanks sounding (PAFA) temperature RMSE scores for 14-20 Dec 2007 period of near total darkness episode. Blue indicates the value from experiment MRR; violet indicates the value from MRR experiment using default Grid 3 obs nudging with TWINDO = 0.45 hours and no wind nudging; green indicates the value from MRR experiment using default Grid 3 obs nudging with TWINDO = 2.0 hours and nudging of wind above the near-surface layer only; red indicates the value from MRR experiment using the final version of Grid 3 obs nudging with the modifications as described in the text.

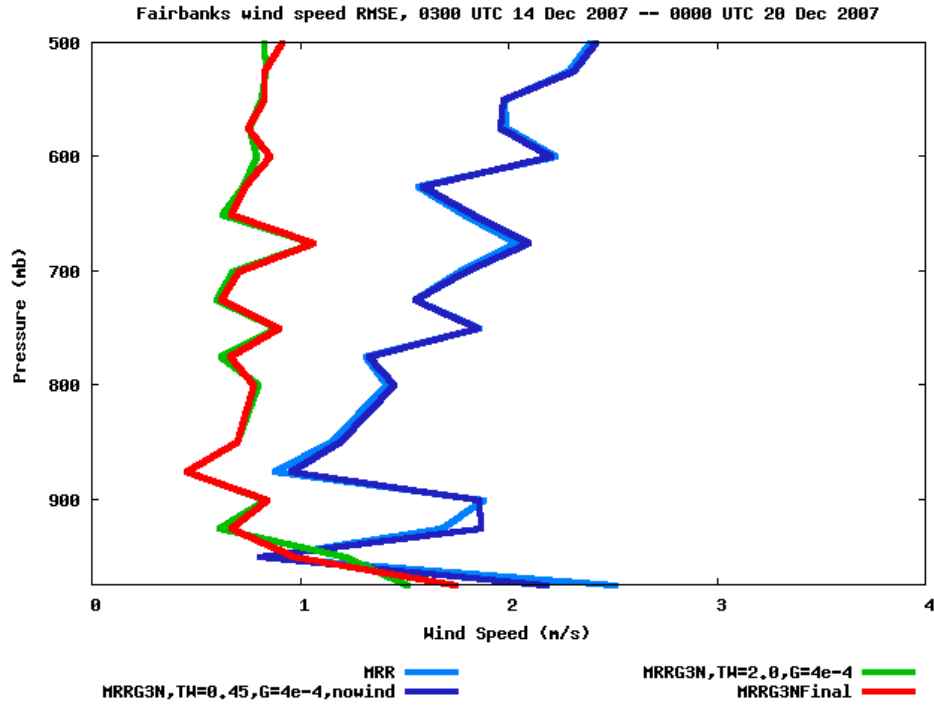


Fig. 21: Same as Fig.20, but for wind speed RMSEs.

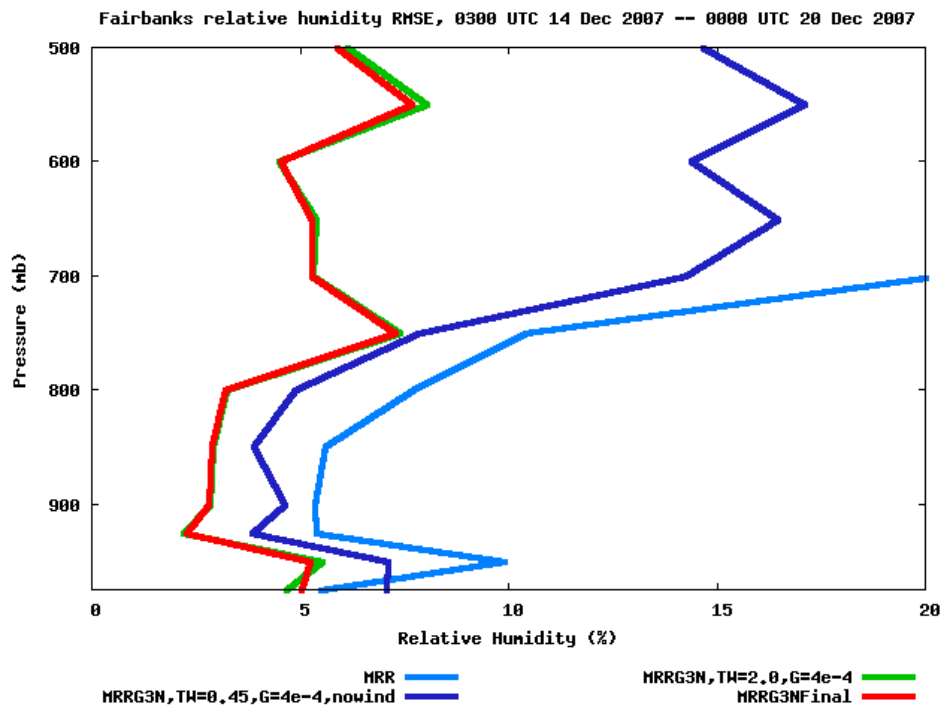


Fig. 22: Same as Fig. 20, but for relative humidity RMSEs.

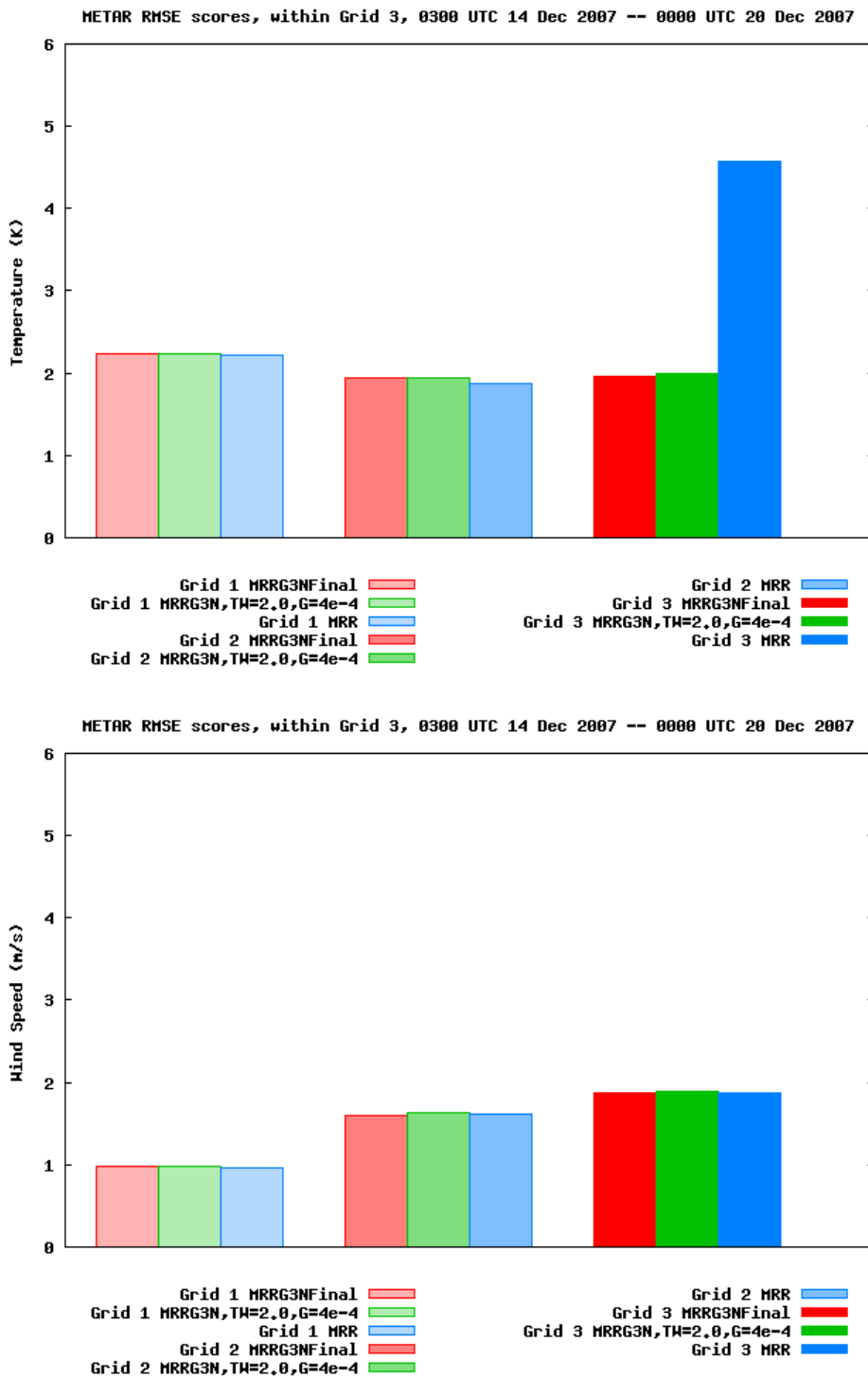


Fig. 23: Surface METAR RMSE scores for during 14-20 Dec 2007 period of near total darkness for temperature (top) and wind speed (bottom). Blue indicates value from experiment MRR; green indicates value from experiment MRR using default Grid 3 obs nudging with TWINDO = 2.0 hours and nudging of wind above the near-surface layer only (i.e., MRRG3N, TW=2.0, G=4e-4); red indicates the value from MRR experiment using the final version of Grid 3 obs nudging with the modifications as described in the text (i.e., MRRG3NFinal).

Fig. 23 shows RMSE statistics for the sample period for the surface METAR stations within Grid 3. The lightest, medium, and darkest shades in the histogram plot correspond to the dark blue, brown, and yellow curves in the vertical profile plots. In all cases the improvement of the MRR temperature RMSE scores from the Grid 3 obs nudging is quite dramatic, and shows the utility of our dynamic analysis approach. The fact that some of our modified obs nudging procedures carried over to all grids caused the Grid 1 and Grid 2 results to change from those of the MRR experiment, but the magnitudes of the changes are small. Wind speed statistics for the surface METARs show little sensitivity to the presence of either Grid 3 obs nudging of temperature and humidity, or Grid 3 obs nudging of winds above the near-surface layer. The proposed Grid 3 obs nudging procedure produces only slight differences from those of the more standardized Grid 3 obs nudging procedure shown, but to the extent there are differences they are generally slight improvements.

In summary, the use of our proposed modified Grid 3 obs nudging procedure, at least for this six-day test period, produces the desired effect of greatly improving the surface temperature statistics without significantly degrading the other statistics, and is also consistent with our past experience as to the preferred specification of obs nudging parameters. Therefore, we proceeded to perform the final dynamic-analysis simulations in their entirety using the proposed Grid 3 obs nudging procedure.

Figures 24-26 show the overall statistics for the final dynamic-analysis Grid 3 obs nudging simulation for the entire near-total darkness episode in comparison to those of the non-Grid 3 obs nudging simulation MRR. The final temperature biases in comparison to the surface METARs are below 0.5°C in magnitude, with RMSE errors 2-3°C. The temperature RMSE errors decrease below 1°C above 900 hPa. Wind speed biases are under 1 m s⁻¹ at the surface, while RMSE errors are on the order of 2 m s⁻¹ throughout the lower troposphere. Qualitatively, the statistics for the final partial sunlight episode (Figs. 27-29) show very similar tendencies.

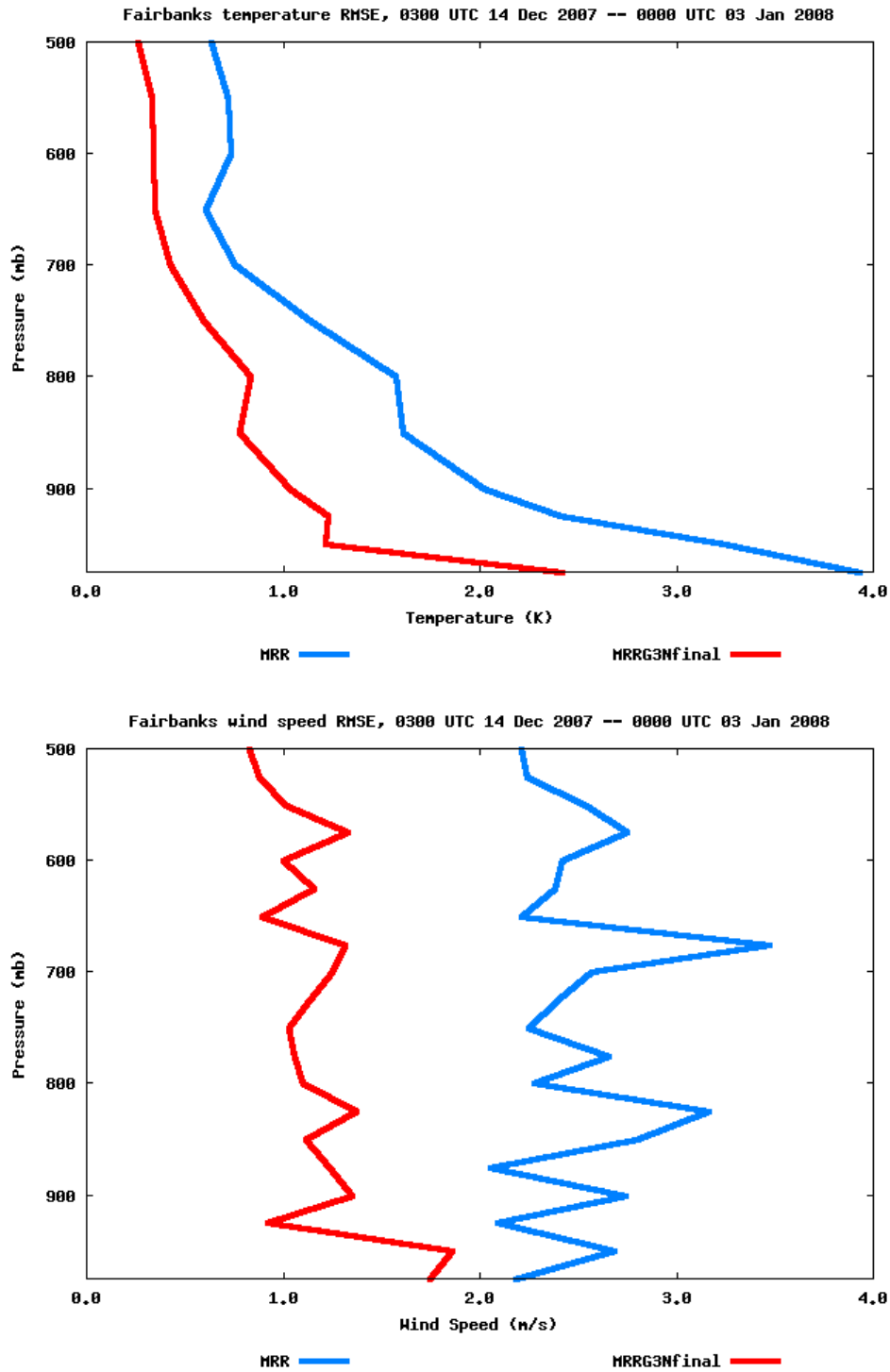


Fig. 24: Time-averaged vertical profile of Fairbanks sounding (PAFA) on Grid 3 for temperature (top) and wind speed (bottom) for 14 Dec 2007—03 Jan 2008 near total darkness episode. Blue indicates value from experiment MRR; red indicates value from final dynamic-analysis MRR simulation using Grid 3 obs nudging.

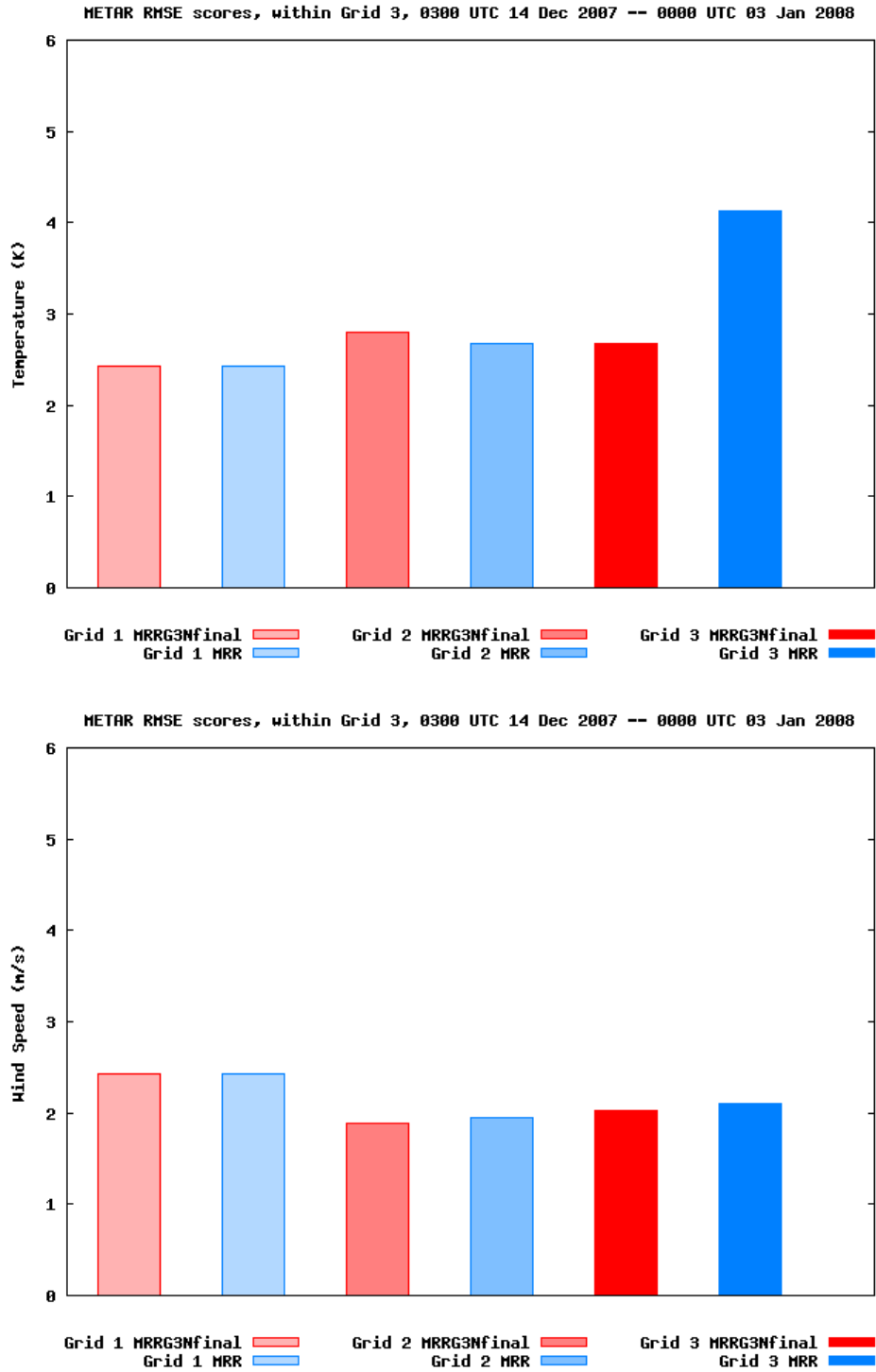


Fig. 25: Surface METAR RMSE scores during 14 Dec 2007—03 Jan 2008 near total darkness episode for temperature (top) and wind speed (bottom). Blue indicates value from experiment MRR; red indicates value from final dynamic-analysis MRR simulation using Grid 3 obs nudging.

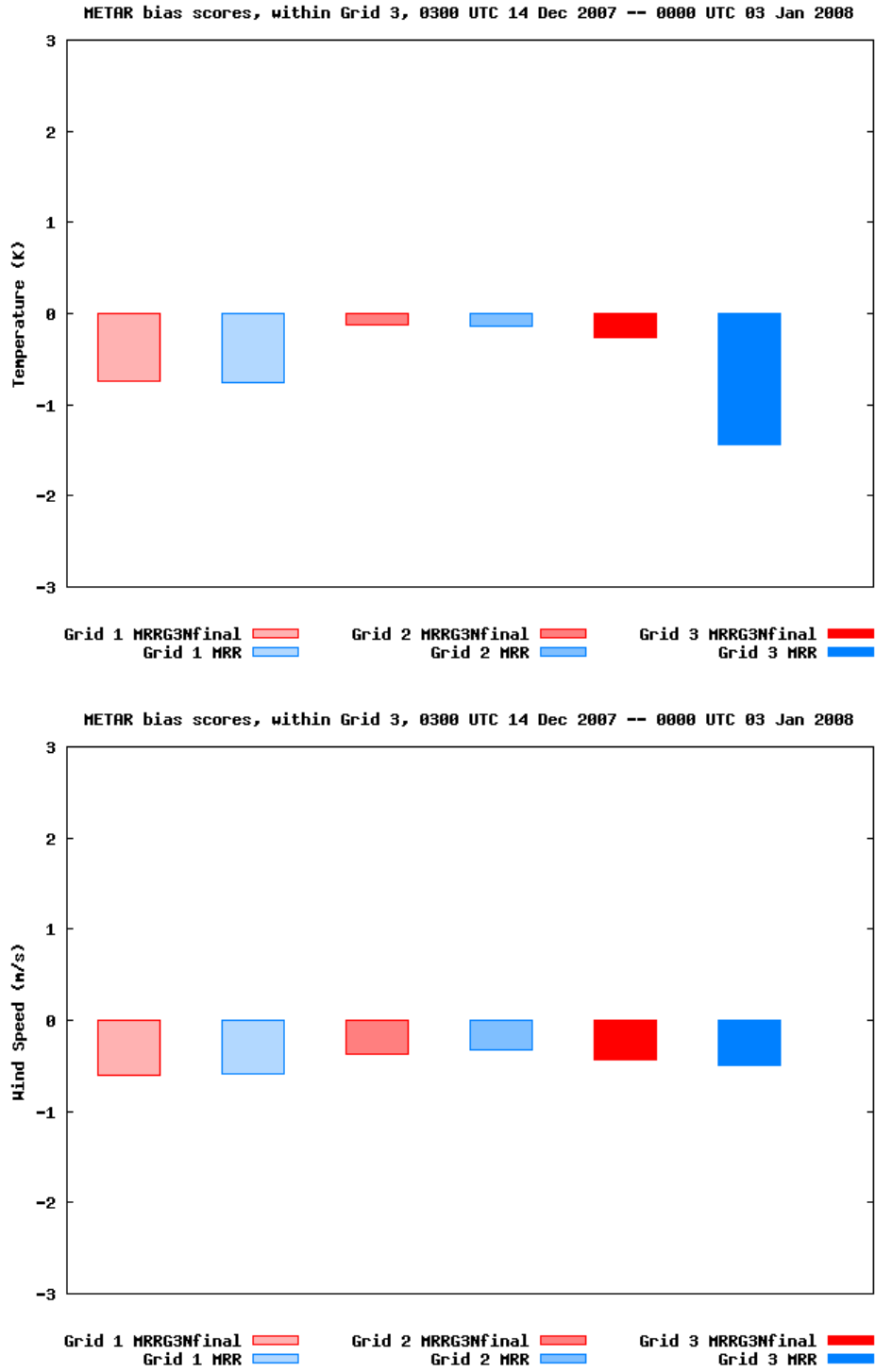


Fig. 26: Same as Fig. 25, but for bias errors.

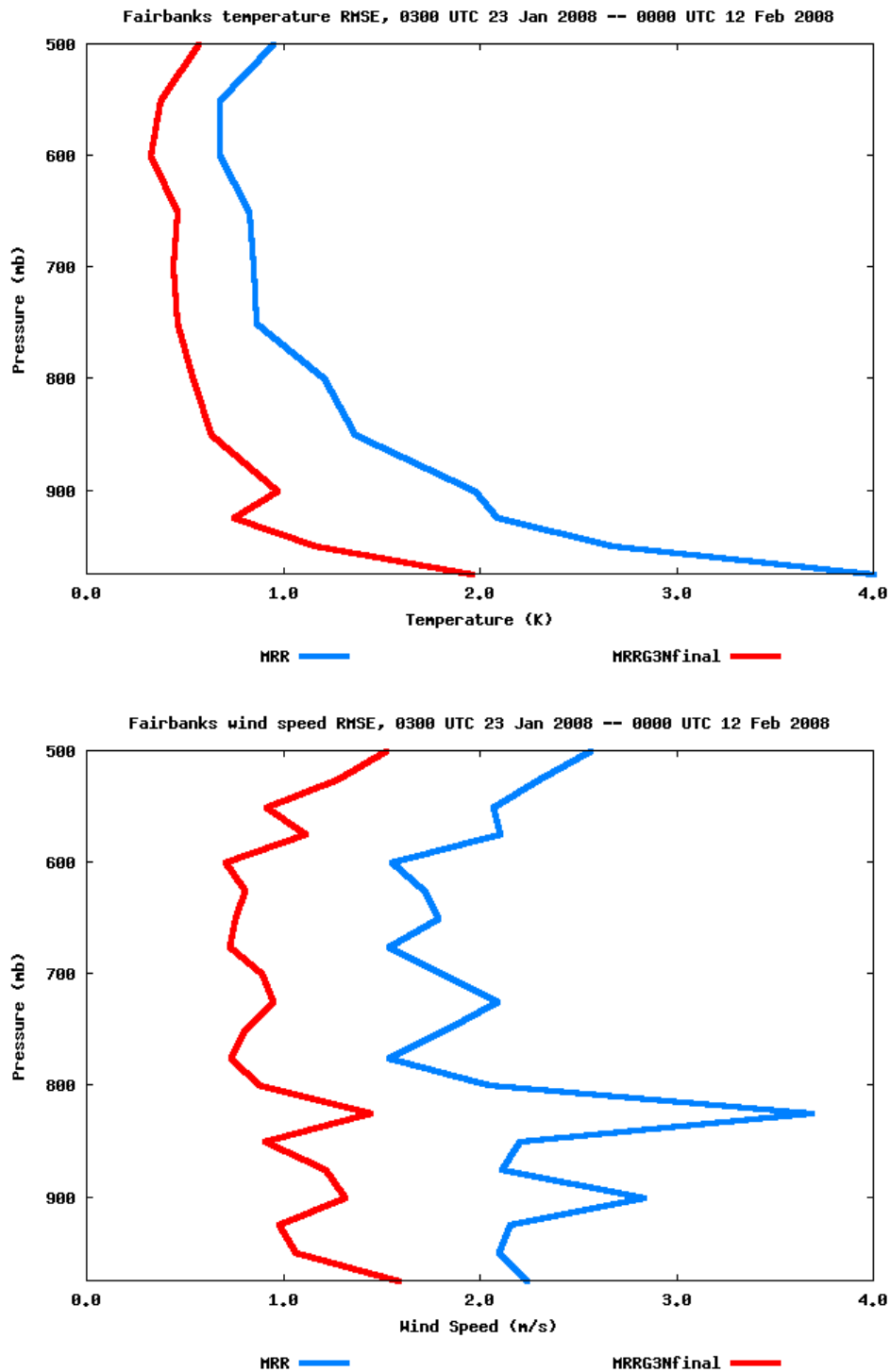


Fig. 27: Time-averaged vertical profile of Fairbanks sounding (PAFA) on Grid 3 for temperature (top) and wind speed (bottom) for 23 Jan 2008–12 Feb 2008 partial sunlight episode. Blue indicates value from experiment MRR; red indicates value from final dynamic-analysis MRR simulation using Grid 3 obs nudging.

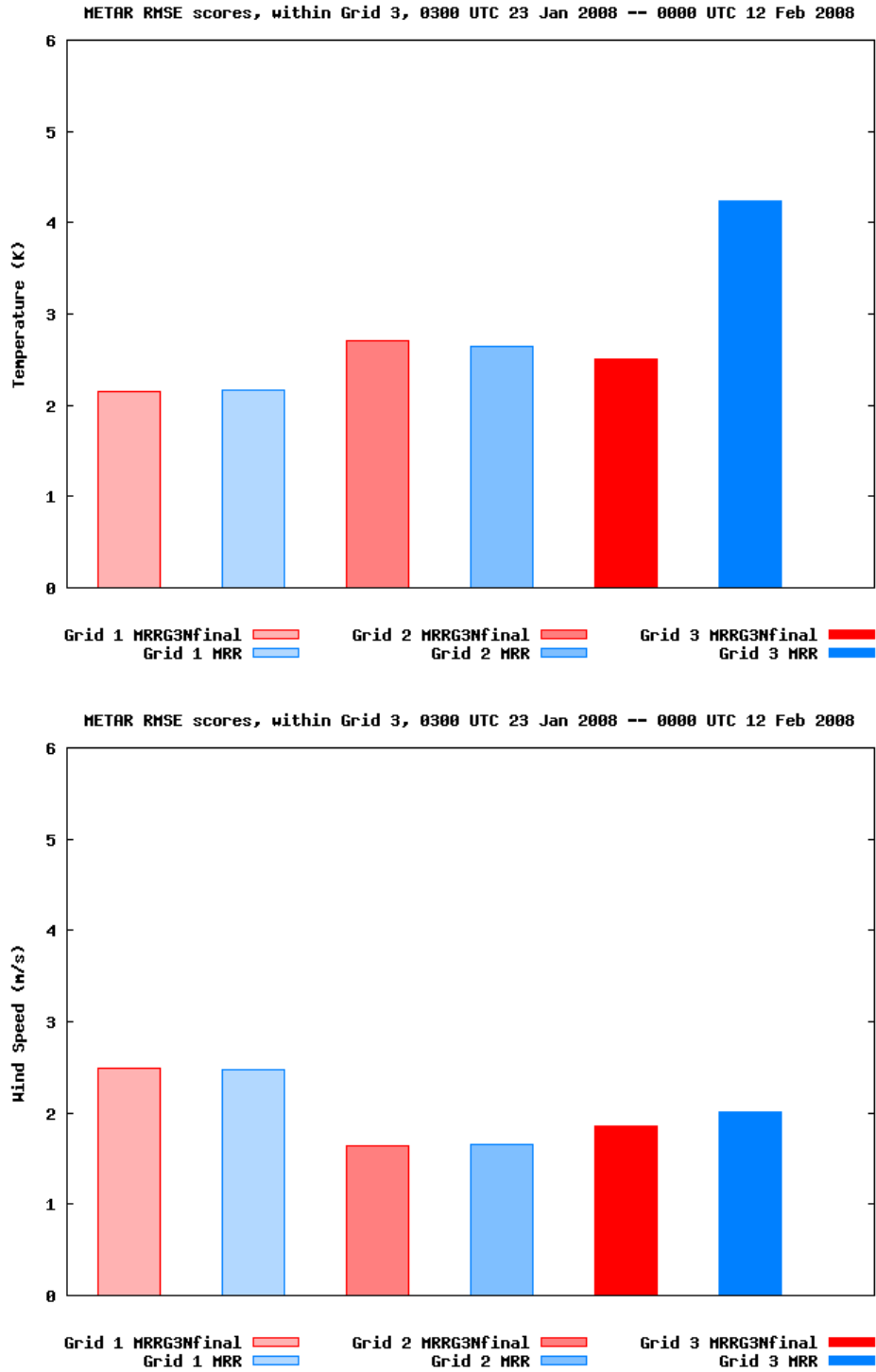


Fig. 28: Surface METAR RMSE scores during 23 Jan 2008—12 Feb 2008 partial sunlight episode for temperature (top) and wind speed (bottom). Blue indicates value from experiment MRR; red indicates value from final dynamic-analysis MRR simulation using Grid 3 obs nudging.

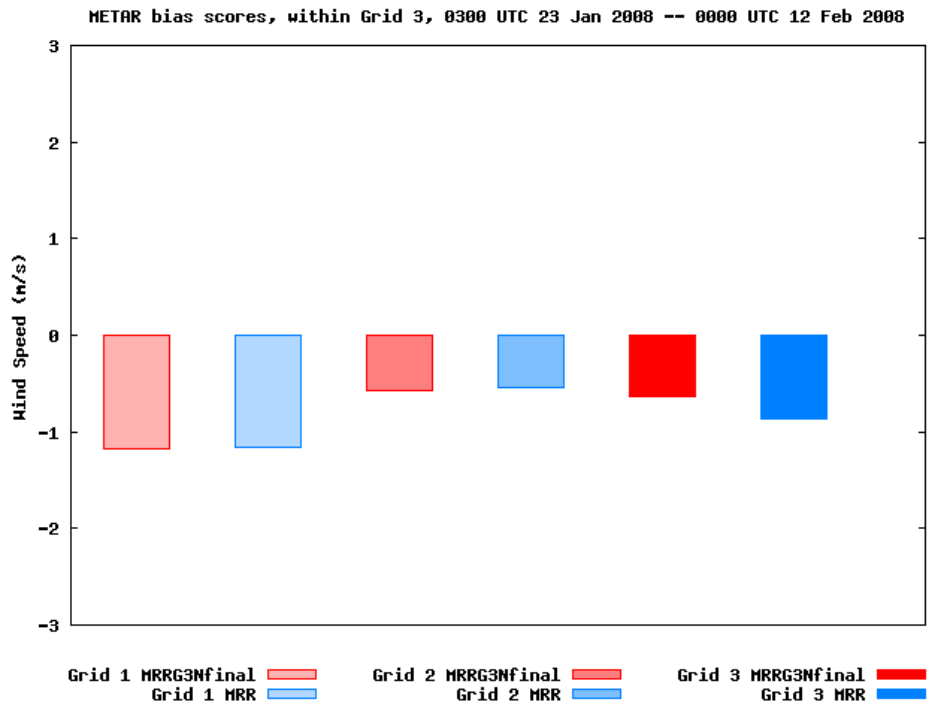
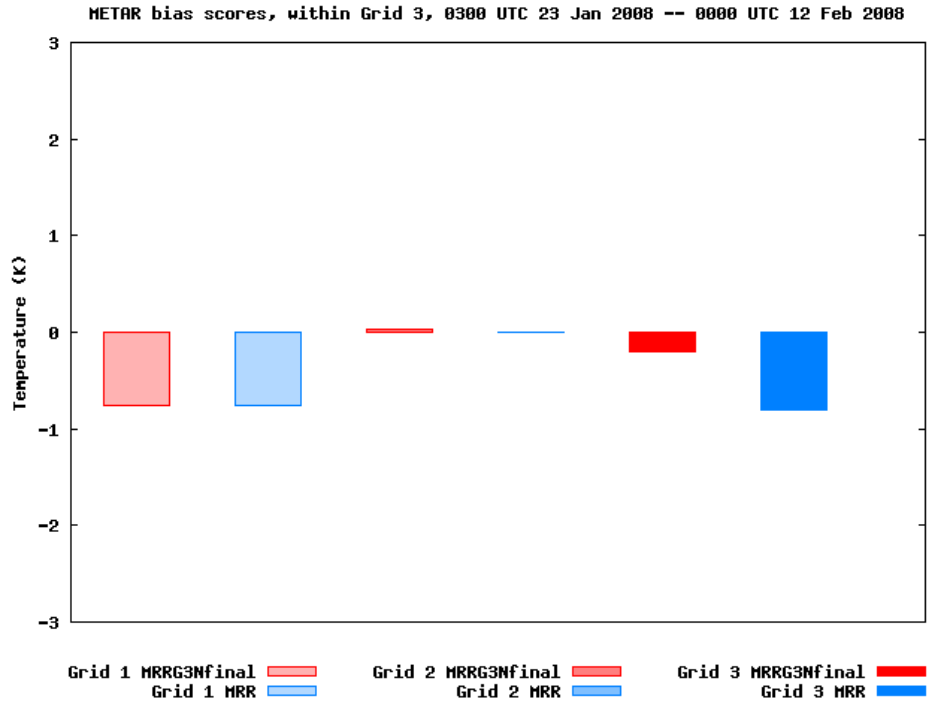


Fig. 29: Same as Fig. 28, but for bias errors.

6. CONCLUSIONS

6.1 Summary

The purpose of the project was to develop, adapt, and test a methodology for stable boundary layer representation (initial onset, space/time evolution, dissipation) in three-dimensional numerical models, with a specific focus on the dark, extremely cold environments such as those in the winter in the Fairbanks, AK region. A particular concern is the frequent occurrence of very high fine particulate matter (PM_{2.5}) concentrations within the stable boundary layers that form in these conditions.

Ten tasks were defined in the Statement of Work (SOW) for this project. A summary of these tasks and a brief overview of the work completed can be found in the Appendix to this report. Two twenty-day episodes were selected from the 2007-2008 winter season to study periods of extremely cold temperatures and high PM_{2.5} concentrations and to evaluate model performance: one in near total darkness (14 Dec 2007 – 03 Jan 2008), and the other in partial sunlight (23 Jan 2008 – 12 Feb 2008). One baseline physics configuration and three physics sensitivity experiments were performed for each episode. The physics sensitivity experiments were used to assess the impact of different planetary boundary layer (PBL) parameterizations, land surface models, and atmospheric radiation schemes on the simulations. Each simulation used three nested grids: Grid 1 (12-km horizontal grid spacing) and Grid 2 (4-km) utilized the multiscale multigrid data assimilation strategy of Stauffer and Seaman (1994) in order to ensure the model and observations remained close over the extended duration of the simulations. Grid 3 (1.3-km), centered over the Fairbanks region, did not use any direct data assimilation, and so was best-suited for quantifying the physics sensitivity; it also possesses sufficient horizontal resolution to be used by the EPA as meteorological input to chemical and air transport and dispersion models. From the different physics packages one was to be recommended to the EPA for further mesoscale modeling of the region.

The use of the three-grid configuration with a multiscale, multigrid four-dimensional data assimilation (FDDA) strategy on the outer two grids and no direct FDDA on Grid 3 consistently produced qualitatively plausible atmospheric fields throughout the variety of meteorological conditions found in the episodes, despite the relatively sparse data density. Quantitatively, the multiscale, multigrid FDDA strategy led to improved root-mean-square-error (RMSE) scores for both wind and temperature on all grids. The FDDA on the outer domains had the desired effect of improving the simulations of Grid 3 without FDDA and used for physics sensitivity tests, by providing improved lateral boundary conditions.

The best RMSE scores for the combination of both surface and sounding data required modification of the default FDDA procedure. These modifications included applying surface wind observational data to the third model vertical level instead of the lowest model level, because wind observations are normally taken at a height of 10 m which is the height of the third level in the high vertical resolution configuration used here. The influence of surface observations was also restricted to approximately the lowest 100 m, instead of to the top of the PBL, because the model-predicted PBL height in these simulations, based on the turbulent kinetic energy profile, was often found to be 1 km or higher. This

correction applied the surface innovation (observation minus model value) in these predominantly stable boundary layers over a much shallower layer than in the default FDDA procedure and produced improved statistical results in the lower troposphere.

All model physics combinations tended to have a positive temperature bias on Grid 3, especially during the most extremely cold periods. All of the physics sensitivity tests tended to reduce the warm bias in comparison with the selected baseline physics package. Switching from the RRTM longwave / Dudhia shortwave radiation package to the RRTMG longwave and shortwave radiation package led to significantly reduced warm biases and better RMSE statistics. RRTMG was then used in all future physics sensitivity tests. The reduced warm bias seemed to be due to the longwave component, both because of direct examination of surface fluxes in the partial sunlight case, and due to the fact that the difference was more pronounced in the near total darkness episode.

Though none of the four physics suites tested in the study was unambiguously superior to all of the others in terms of RMSE statistics, the simulation with the Rapid Update Cycle (RUC) land surface model, the Mellor-Yamada-Janjić (MYJ) PBL model, and the RRTMG radiation package was selected as the one to be recommended to EPA for modeling extremely cold SBLs and as the basis for producing the final atmospheric analysis. For both the near-total-darkness and partial sunlight episodes, the MYJ/RUC/RRTMG (henceforth MRR) physics suite had the lowest surface wind speed RMSE scores. For the partial sunlight episode the MRR configuration was one of two physics suites with the lowest surface temperature RMSE scores, and was among the lowest for the near-total-darkness episode. Of all the physics suites, the MRR package had the lowest warm bias during the most extremely cold periods, both when compared to the surface METAR stations and the Fairbanks sounding. The reason is not known for sure but is probably due to some combination of the effects of its snow model and top-level 'skin' layer. Since the extremely cold conditions are those with the potential for the highest PM2.5 concentrations, we took this as an additional reason to recommend the MRR physics suite for use by EPA.

However, there were periods in each episode, generally when the temperature was steadily decreasing in advance of an extremely cold period, during which all the physics configurations would tend to have a cold bias. During these periods the MRR configuration would still have colder temperatures than the other physics suites, and thus have worse magnitude temperature biases and RMSE scores. The relatively poorer performance of the MRR suite during a such a period accounts for the relatively poorer surface temperature statistics of the MRR suite compared to the MNR suite for the entire near-total-darkness episode. The reason for this behavior is not definitely known, but it is thought to be related to the interaction of radiation with the ice condensate that tends to occur during these periods. Also, the temperature biases of the MRR physics suite during the extremely cold period near the end of the partial sunlight episode were not quite as improved during daylight hours as during nighttime hours as compared to the other physics suites. Therefore, while overall we recommended the MRR configuration to EPA for these episodes, we also strongly recommended that the final fine-scale atmospheric data analysis (i.e., from Grid 3) to be provided to EPA should come from an additional simulation in which FDDA is performed directly on Grid 3, in order to reduce some of this error.

Use of obs nudging for temperature and humidity (and not surface wind) on Grid 3 produced large improvements in the mass fields as expected, and also improvements in the wind fields above the surface. Results were very encouraging and suggested that a smaller (larger) time window should be used for the surface (above-surface) data assimilation. This capability present in the Penn State MM5 FDDA system has been added to the new-release version of WRF.

In addition to this final report, deliverables to the EPA will include the full three-dimensional output at relatively fine temporal resolution (every 1 hour for Grid 1; every 12 minutes for Grids 2 and 3) for the final Grid 3 nudging simulation as well as all the baseline and physics sensitivity simulations. Model namelists, initialization files, and modifications to the model source code will also be provided.

The development and refinement of WRF FDDA capabilities and supporting software, including the surface analysis nudging, observation nudging and the OBSGRID objective analysis and obs-nudging pre-processing code, occurred concurrently with this project. This separate development effort led by PI Dave Stauffer and funded by the Defense Threat Reduction Agency (DTRA) allowed us rapid access to the most recent and robust versions of the WRF FDDA code, which greatly benefited this project.

The results of the default FDDA procedures not performing well here in this high vertical resolution modeling study of stable boundary layer environments motivated an additional FDDA code development effort to make the vertical influence functions of surface observations within the FDDA be a function of stability regime type, as well as to provide the user with greater flexibility in specifying the vertical influence functions. These modifications were not finalized in time to be used for this project but are scheduled to appear in the next official release of the WRF model.

An extended abstract and oral presentation were made at the 13th Conference on Mesoscale Processes (Gaudet et al. 2009), and a manuscript based on the project is in preparation.

6.2 Limitations of the Study and Recommendations for Future Work

Sensitivity to the microphysics parameterization was not performed here, but may be important to investigate further. In particular, results from this study suggested that both the occurrence of large negative RUC temperature biases and large differences between the RRTM and RRTMG longwave radiation schemes tended to occur when low-level ice condensate was present. Therefore, the microphysics / radiation interaction should probably be investigated further.

A fourth grid with 0.44-km horizontal grid spacing centered over Fairbanks was set up and initialized with topography, but it was not used in the sensitivity experiments here. Although this is finer horizontal resolution than the resolution requested by EPA, some of Penn State's past studies of SBLs (Stauffer et al. 2009) have suggested that the weak wind flows in these conditions may be sensitive to topographic features on these smaller scales, and it might be important to know if finer resolution is also required to resolve the topographic flows of the Fairbanks region.

The latest version of the WRF FDDA code has been designed to have more flexibility in how the temporal and spatial weighting functions are specified. Future simulations that use these new WRF FDDA options that were not yet available for this study should produce a further reduction of model error.

The availability of more meteorological observations from the immediate Fairbanks North Star Borough region, and in particular observations immediately above the surface, would allow one to make a more rigorous assessment of the accuracy of the different physics schemes (in particular, the PBL parameterizations).

More testing and analysis of the model physical parameterizations should be performed to determine the cause of the strong model biases often observed in the simulations, such as the generally persistent warm bias, and the cold RUC land surface model bias during falling temperature conditions.

7. REFERENCES

- Benjamin, S.O., and N.L. Seaman, 1985: A simple scheme for objective analysis in curved flow. *Mon. Wea. Rev.*, **113**, 1184-1198.
- Benson, C.S., 1970: Ice fog: Low temperature air pollution. Research Report 121. U.S. Army Corps of Engineers, Cold Regions Research and Engineering Laboratory, Hanover, NH, 118 pp.
- Bromwich, D.H., J.J. Cassano, T. Klein, G. Heinemann, K.M. Hines, K. Steffen, and J.E. Box, 2001: Mesoscale modeling of katabatic winds over Greenland with the Polar MM5. *Mon. Wea. Rev.*, **129**, 2290-2309.
- Chen, F., and J. Dudhia, 2001: Coupling an advanced land-surface/hydrology model with the Penn State/NCAR MM5 modeling system. Part I: Model implementation and sensitivity. *Mon. Wea. Rev.*, **129**, 569-585.
- Deng, A., D. Stauffer, B. Gaudet, J. Dudhia, J. Hacker, C. Bruyere, W. Wu, F. Vandenberghe, Y. Liu, and A. Bourgeois, 2009: Update on WRF-ARW end-to-end multi-scale FDDA system. *10th Annual WRF Users' Workshop*, 23 Jun 2009, Boulder, CO.
- Dudhia, J., 1989: Numerical study of convection observed during winter monsoon experiment using a mesoscale two-dimensional model. *J. Atmos. Sci.*, **46**, 3077-3107.
- Galperin, B., S. Sukoriansky, and P.S. Anderson, 2007: On the critical Richardson number in stably stratified turbulence. *Atmos. Sci. Lett.*, **8**, 65-67.
- Gaudet, B., D. Stauffer, N. Seaman, A. Deng, K. Schere, R. Gilliam, J. Pleim, and R. Elleman, 2009: Modeling extremely cold stable boundary layers over interior Alaska using a WRF FDDA system.

- 13th Conference on Mesoscale Processes, 17-20 Aug, Salt Lake City, UT, American Meteorological Society.
- Girard, E., and J.-P. Blanchet, 2001: Microphysical parameterization of Arctic diamond dust, ice fog, and thin stratus for climate models. *J. Atmos. Sci.*, **58**, 1181-1198.
- Hanna, S.R., 1983: Lateral turbulence intensity and plume meandering during stable conditions. *J. Appl. Meteor.*, **22**, 1424-1430.
- Hines, K.M., and D.H. Bromwich, 2008: Development and testing of polar Weather Research and Forecasting (WRF) model. Part I: Greenland ice sheet meteorology. *Mon. Wea. Rev.*, **136**, 1971-1989.
- Janjić, Z.I., 2002: Nonsingular implementation of the Mellor-Yamada Level 2.5 Scheme in the NCEP Meso model. NCEP Office Note 437, 61 pp.
- Mahrt, L., 2009: Characteristics of submeso winds in the stable boundary layer. *Boundary-Layer Meteorology*, **130**, 1-14.
- Mlawer, E.J., S.J. Taubman, P.D. Brown, M.J. Iacono, and S.A. Clough, 1997: Radiative transfer for inhomogeneous atmosphere: RRTM, a validated correlated-k model for the longwave. *J. Geophys. Res.*, **102**, 16663-16682.
- Mölders, N. and G. Kramm, 2010: A case study on wintertime inversions in interior Alaska with WRF. *Atmos. Res.*, **95**, 314-332.
- Morrison, H., J.A. Curry, and V.I. Khvorostyanov, 2005: A new double-moment microphysics parameterization for application in cloud and climate models. Part I: Description. *J. Atmos. Sci.*, **62**, 1665-1677.
- Seaman, N.L., and S.A. Michelson, 2000: Mesoscale meteorological structure of a high-ozone episode during the 1995 NARSTO-Northeast study. *J. Appl. Meteor.*, **39**, 384-398.
- Seaman, N.L., B. Gaudet, A. Deng, S. Richardson, D.R. Stauffer, J.C. Wyngaard, and L. Mahrt, 2008: Evaluation of meander-like wind variance in high-resolution WRF model simulations of the stable nocturnal boundary layer. 10th Conference on Atmospheric Chemistry, 21-24 Jan, New Orleans, LA, American Meteorological Society.
- Serreze, M.C., J.D. Kahl, and R.C. Schnell, 1992: Low-level temperature inversions of the Eurasian Arctic and comparison with Soviet drifting station data. *J. Climate*, **5**, 615-629.
- Skamarock, W.C., J.B. Klemp, J. Dudhia, D.O. Gill, M. Barker, M.G. Duda, X.-Y. Huang, W. Wang, and J.G. Powers, 2008: A description of the Advanced Research WRF version 3. NCAR Technical Note NCAR/TN475+STR.

- Smirnova, T.G., J.M. Brown, and D. Kim, 2000: Parameterization of cold-season processes in the MAPS land-surface scheme. *J. Geophys. Res.*, **105**, 4077-4086.
- Stauffer, D.R., and N.L. Seaman, 1994: Multiscale four-dimensional data assimilation. *J. Appl. Meteor.*, **33**, 416-434.
- Stauffer, D.R., N.L. Seaman, and F.S. Binkowski, 1991: Use of four-dimensional data assimilation in a limited-area mesoscale model. Part II: Effects of data assimilation with the planetary boundary layer. *Mon. Wea. Rev.*, **119**, 734-754.
- Stauffer, D.R., B.J. Gaudet, N.L. Seaman, J.C. Wyngaard, L. Mahrt and S. Richardson, 2009: Sub-kilometer numerical predictions in the nocturnal stable boundary layer. *23rd Conference on Weather Analysis and Forecasting/19th Conference on Numerical Weather Prediction*, 1-5 Jun, Omaha, NE, American Meteorological Society.
- Sukoriansky, S. B. Galperin, and V. Perov, 2005: Application of a new spectral theory of stably stratified turbulence to atmospheric boundary layers over sea ice. *Boundary-Layer Meteorology*, **117**, 231-257.
- Vickers, D., and L. Mahrt, 2004: Evaluating formulations of stable boundary layer height. *J. Appl. Meteor.*, **43**, 1736-1749.
- Wyngaard, J.C., 2004: Toward numerical modeling in the 'Terra Incognita'. *J. Atmos. Sci.*, **61**, 1816-1826.

APPENDIX – SUMMARY OF TASKS

Ten tasks were included in the Statement of Work (SOW) for this project. An overview of the tasks and a summary of the work completed on each of these tasks are provided below:

- Task 1 – Participate in kick-off teleconference in accordance with the SOW.

This took place on 11 Sep 2008. The EPA was provided with the specifications of the nested grid configuration that we proposed in the SOW, and we received in turn particular information about the period and region of study from the EPA.

- Task 2 – Prepare workplan and QA/QC plan in accordance with the SOW.

This was submitted to the EPA during Nov. 2008, along with an updated timetable of deliverables provided during the next monthly teleconference. Included was a description of our proposed simulation plan, choice of baseline physics and grid configuration, and method of simulation.

- Task 3 – Participate in monthly project teleconferences.

We held hour-long teleconferences with the project manager and other scientists at Research Triangle Park and EPA Region 10 (which includes Alaska in its jurisdiction) near the beginning of every month between the kick-off meeting and Jan. 2010. These teleconferences were indispensable for coordinating the needs of EPA with our capabilities and adapting to unforeseen developments as they arose.

- Task 4 – Prepare brief monthly progress reports.

These reports provided to the EPA at the end of every month from Oct. 2008 – Dec. 2009, contained in total most of the information and task completion history found in this report.

- Task 5 – Set up meteorological model and conduct initial baseline testing.

After some minor modifications were made to the proposed model grid configuration to maximize the utility of available data, the final specifications of Grids 1, 2, and 3 were confirmed with the EPA in Feb. 2009; more precise coordination of these grids with a parallel emissions modeling project were completed in May 2009. The data assimilation procedures required for the multiscale multigrid procedure to be used for the project were still being developed for the WRF meteorological model, led by PI Dave Stauffer also working on this contract, which helped expedite the testing and validation of these procedures. Furthermore, the testing results had to be confirmed with the version 3.1 of WRF used for most of this study, released in Apr 2009. By Jun 2009 we determined that the model components were ready to begin physics sensitivity testing.

- Task 6 – Develop and/or adapt one or more stable boundary layer and land-surface models in accordance with the SOW.

For the choice of stable boundary model in the WRF baseline physics package, we used the Mellor-Yamada-Janjić (MYJ) parameterization that we had used for our previous studies of the stable boundary layer in Alaska, with a few modifications. For the land surface model, however, we decided that we should make use of the Noah model available in version 3.1 of WRF, since it included a number of adaptations to snow-covered terrain that would be critical in this study. Using the particular Noah adaptations in version 3.1 of WRF was one reason for using that model when it became available. After we confirmed that using the Noah land surface model initialized with Global Forecast System (GFS) model data produced reasonable results, we discovered that the default WRF data assimilation procedure needed to be modified to interact properly with the stable boundary layers generated by the high-resolution model. By Jul 2009 we had decided on the baseline physics package to be used for the main simulations.

- Task 7 – Conduct up to five sensitivity tests for the selected modeling periods and evaluate results in accordance with the SOW.

Two twenty-day episodes from the 2007-2008 winter season, both with periods of extremely cold temperatures and high PM_{2.5} concentrations, were selected for evaluation of model performance: one in near total darkness (14 Dec 2007 – 03 Jan 2008), and the other in partial sunlight (23 Jan 2008 – 12 Feb 2008). In addition to the baseline physics configuration that included the MYJ planetary boundary layer (PBL) scheme, the Noah land surface model, and the RRTM longwave / Dudhia shortwave radiation package, three other physics sensitivity tests were performed for the entirety of each twenty-day episode, which involved using the RRTMG radiation package (longwave and shortwave), the Quasi-Normal Scale Elimination (QNSE) PBL scheme, and the Rapid Update Cycle (RUC) land surface model. After some discussion, the specific combinations used, in addition to the baseline, were MYJ / Noah / RRTMG, QNSE/ Noah / RRTMG, and MYJ / RUC / RRTMG. After statistical comparison with available observations, there was no clearly superior model physics combination; however, the MYJ / RUC / RRTMG option seemed to do the best job at reproducing the extremely cold temperatures characteristic of the high exceedance episodes. However, all model configurations tended to have substantial warm surface temperature biases in these conditions on the innermost 1.3-km Grid 3 when no data assimilation was performed on it. (Data assimilation was performed on the outer Grids 1 and 2 for the physics sensitivity experiments to improve the lateral boundary conditions on Grid 3.) In Jan 2009 it was decided that the MYJ / RUC / RRTMG combination was to be recommended, but that final dynamic analyses using this physics package along with Grid 3 data assimilation should be performed for each episode in order to reduce the atmospheric model errors and biases before they are used in air transport and chemistry models.

- Task 8 – Participate in 1.5-day meeting with Project Officer and scientific staff at EPA/RTP in accordance with the SOW.

This meeting occurred 19-20 Nov 2009 at Research Triangle Park (RTP), NC, between one of the co-PI's (Brian Gaudet) and the Project Officer and other scientific staff at RTP. During this meeting scientific discussion of the results occurred, and a preliminary agreement that the MYJ/RUC/RRTMG combination was the most promising was reached. The main results of the project to date were presented, and plans for bringing the project to completion were made.

- Task 9 – Prepare final report and electronic data and computer code files in accordance with the SOW.
- Task 10 – Revise draft final report and data files.

This report serves to help complete Tasks 9 and 10. A pair of 2-Terabyte external hard drives were obtained from EPA for use for transferring the data, whose cumulative size is approximately 600 Gigabytes per episode simulation. The files to be transferred consist of a full three-dimensional set of model output files, generated every hour for the 12-km Grid 1, and every 12 minutes for the 4-km Grid 2 and 1.3-km Grid 3. The output for each episode from the final dynamic initialization (i.e., with data assimilation on Grid 3) using the best choice physics package will be transferred first; later, the output from the baseline and physics sensitivity studies without Grid 3 data assimilation will be transferred to EPA. In addition, the namelist specifications for each simulation, the WRF version 3.1 code as modified for the project, and the initial, boundary condition, and four-dimensional data assimilation (FDDA) files required for each WRF simulation will be included.



Investigation of means for PM_{2.5} mitigation through atmospheric modeling

Final report Phase I
12/1/08 – 12/31/10

Prepared for the Fairbanks North Star Borough

By

Nicole Mölders, Huy N.Q. Tran and Ketsiri Leelasakultum

Geophysical Institute and College of Natural Sciences and Mathematics
Department of Atmospheric Sciences

April 2011

Summary

The Alaska adapted Weather Research and Forecasting model incline coupled with a chemistry package is used to assess the situation of PM_{2.5} concentrations in the Fairbanks PM_{2.5}-nonattainment area in the winter months, to explore two mitigation scenarios and to assess the role of point-source emissions for the PM_{2.5} concentrations at breathing level. The evaluation of the model results by the few data available suggests overall acceptable performance of WRF/Chem. WRF/Chem was chosen, as this research model was an air-quality model that was already adapted and tested for Alaska conditions.

Simulations were performed with WRF/Chem with and without consideration of point-source emissions for November 2005 to February 2006. The results suggest that point-source emissions contribute to the PM_{2.5}-nonattainment problem, but are not the main cause.

Two mitigations scenarios were performed for October 2008 to March 2009. The first mitigation scenario was a direct one as it assumed reduction of PM_{2.5}-emissions by replacing non-certified wood-burning devices with certified wood-burning devices while keeping emissions from all non-wood burning sectors the same. Comparison of the reference simulation that assumes business-as-usual, with the various simulations assuming replacement of non-certified wood-burning devices indicates that such replacements reduce the PM_{2.5}-concentrations at breathing level. However, a small replacement program that leads to only 6% reduction of PM_{2.5}-emissions on average is insufficient to achieve attainment. According to sensitivity studies, the magnitude of PM_{2.5}-concentration reductions at breathing level depends strongly on the number and kind of devices replaced, and the assumed partitioning of heating among devices in households with more than one heating device. Further uncertainty results from the unknown location of wood-burning devices.

Since PM_{2.5} is not only emitted, but also can form by physio-chemical processes (gas-to-particle conversion) in the atmosphere from precursor gases, the second mitigation scenario addressed an indirect strategy to achieve mitigation of the PM_{2.5} problem by reducing an important precursor of PM_{2.5} namely sulfur. This emission-reduction scenario assumed the introduction of low sulfur fuel for domestic heating and use in all oil-burning facilities (e.g. oil-burning power plants) if they did not already use low sulfur fuel. This simulation was also performed for October 2008 to March 2009. Comparison of the results of the simulations suggest that on average over the entire winter and nonattainment area, a slightly higher reduction of PM_{2.5}-concentrations can be achieved when introducing low sulfur fuel than for the small wood-burning device replacement program assumed in the other emission reduction scenario. However, the results also suggest that locally and temporally PM_{2.5}-concentrations may increase after introduction of low sulfur fuel due to shifts in the equilibria of precursor concentrations. The increase is due to a shift towards more formation of nitrate that has a higher mass than sulfate. Note that introduction of low sulfur fuel not only changes the emissions of SO₂, but also the emissions of other species released during the combustion of oil and hence causes a shift in the distribution of precursors. The effect of such shifts in precursors on the equilibria depends on temperature, light and moisture conditions. The aforementioned meteorological conditions all affect gas-to-particle conversion and hence the production of PM_{2.5} in the atmosphere. Since introduction of low sulfur fuel may, under certain conditions, lead to increased, instead of decreased PM_{2.5}-concentrations, a woodstove replacement program seems to be the safer way to achieve mitigation than a measure that tries to achieve mitigation indirectly.

Calculation of the relative response factors and new design values suggests that none of the scenarios assumed in this study may alone lead to attainment. Therefore, combined measures and/or other measures like enhancement of the use of gas should be examined in the future.

1. Brief description of Fairbanks' nonattainment problem

In 2006, the Environmental Protection Agency (EPA) tightened the previous 24h National Ambient Air Quality Standard (NAAQS) for particulate matter (PM)¹ with diameter $<2.5\mu\text{m}$ ($\text{PM}_{2.5}$) from $65\mu\text{g}/\text{m}^3$ to $35\mu\text{g}/\text{m}^3$. The annual $\text{PM}_{2.5}$ standard of $15\mu\text{g}/\text{m}^3$ remained. Data collected by the Fairbanks North Star Borough (FNSB) and faculty at the Geophysical Institute (GI) indicate that in the past years 24h-average $\text{PM}_{2.5}$ concentrations² exceeded the new standard frequently (cf. Fig. 1). Since in previous years, the measurements at the official PM measurement site of the FNSB at the State Building exceeded the new NAAQS for $\text{PM}_{2.5}$ repeatedly, a $\text{PM}_{2.5}$ nonattainment area was assigned.

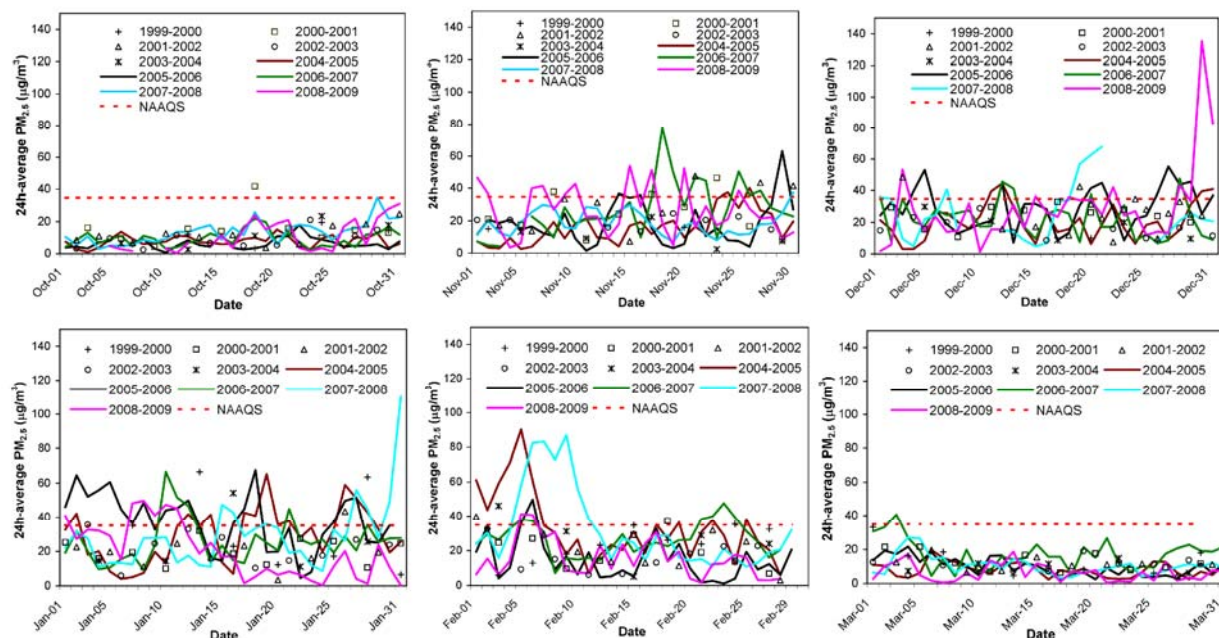


Fig. 1. $\text{PM}_{2.5}$ concentrations measured in downtown Fairbanks from October 1 to March 31 in various years from 1999 to 2009. Modified after *Tran and Mölders* [2011]

In Fairbanks, exceedances typically occur during the cold season (October to March) hereafter referred to as winter, and the fire season (summer) [*Tran and Mölders*, 2011]. In Alaska summer, fire events frequently create $\text{PM}_{2.5}$ concentrations well in excess of levels deemed “unhealthy”. However, these events may be excluded from being considered as an exceedance if it can be proven that the exceedance was due to a particular event [*EPA*, 2007]. While exceedances due to fires may be considered as “natural events” under the aforementioned circumstances, the exceedances in winter are due to anthropogenic activity.

Analysis of available data showed that there are various factors contributing to the $\text{PM}_{2.5}$ exceedances in winter: topography, weather, and emissions³ [*Tran and Mölders*, 2011].

¹ Particulate matter is often also called particulates. Here PM are tiny subdivisions of solid matter suspended in the atmosphere.

² Concentration refers to the amount of a substance per defined volume. Typically, concentration is expressed in terms of mass per unit volume (e.g. $\mu\text{g}/\text{m}^3$).

³ Emission refers to the release of gases and/or particulate matter into the atmosphere, i.e. a flow. Typically, emissions are expressed in terms of mass per unit area per time (e.g. $\text{kg}/(\text{m}^2\text{s})$).

Fairbanks' being located at the edge of an air-mass source region⁴ yields low wind-speeds, and cold air that remains in place over long time [Tran and Mölders, 2011]. In addition, wintertime radiative cooling leads to inversions, i.e. a temperature increase with height⁵. Fairbanks experiences strong semi-permanent inversions with temperature differences of 5-10K from the basis close to the earth's surface to the top of the inversion during the period from November to February [Bourne et al., 2010]. Such inversions hinder the vertical exchange of air. Consequently, if an inversion is present, PM_{2.5} and other pollutants will accumulate in the air underneath the inversion, and will potentially lead to PM_{2.5} exceedances [Tran and Mölders, 2011]. The fact that Fairbanks is surrounded by hills further contributes to the low exchange of polluted and clean air masses. Other meteorological factors affecting concentrations are mixing height, atmospheric stability, longevity and strength of inversions [Mölders and Kramm, 2010].

Heat and energy production as well as traffic are the main sources for PM_{2.5} emissions. In winter, roughly 30% of the PM_{2.5} in downtown Fairbanks may stem from traffic [Johnson et al., 2009]. Pervious studies [Davies et al., 2009] indicate that non-certified woodstoves and wood-boilers strongly contribute to the PM_{2.5} emissions from the heating sector. Another source for PM_{2.5} is gas-to-particle conversion a process that occurs naturally in the atmosphere [e.g. Kumar et al., 2010].

Trace gases that are emitted are referred to as primary pollutants. Pollutants resulting from reaction of primary pollutants and other naturally available gases are called secondary pollutants. Particulate matter that is emitted is called primary PM. Secondary PM forms already in the plumes, but also elsewhere in the atmosphere, from gas-to particle conversion. Any PM_{2.5} that results from gas-to-particle-conversion is called secondary PM_{2.5} hereafter.

The term aerosol refers to solid and liquid particles suspended in the atmosphere. Aerosols can exist in the nucleation, accumulation and coarse mode. Aerosols in the coarse mode typically stem from mineral dust and ash fly from biomass burning. The terms *nucleation mode* and *accumulation mode* denote the mechanical and chemical processes that produce aerosol particles in these two size ranges.

In the nucleation mode, the aerosols are the smallest. They are produced by *gas-to-particle conversion*. Gas-to-particle conversion produces particles when trace gases react with other gases or particles that exist in the atmosphere or when trace gases absorb solar radiation that leads to photochemical reactions. In the nucleation mode, most aerosol particles consist of sulfuric compounds, and stem from the oxidation of sulfur containing precursor gases (like SO₂, H₂S, CS₂, COS, CH₃SCH₃, and CH₃SSCH₃) to sulfate (SO₄²⁻), and subsequent condensation into particle form. This process is called homogenous gas-to-particle conversion. These tiny highly mobile sulfate aerosol particles can coagulate. Much of the sulfate aerosol from gas-to-particle conversion finally ends up in the 0.1-1.0µm size range. Sulfur dioxide (SO₂), for instance, can yield the formation of various sulfates in the presence of ammonia (NH₃) and water vapor via gas-to-particle conversion. Sources for SO₂ in the atmosphere are volcanic emissions, and emissions from fires, traffic, power-production and combustion for heating. Important anthropogenic sources for ammonia are domesticated animals and fertilizer.

⁴ An air-mass source region is a region over which air remains frequently for a long enough time that the surface affects the air mass' temperature and moisture properties substantially.

⁵ Under normal conditions, temperature decreases with height in the troposphere. Temperature inversion means that temperature increases with height. Inversion layer refers to the atmospheric layer within that such an increase exists.

Gas-to-particle-conversion forms ammonium (NH_4^+) $\text{PM}_{2.5}$ by the reaction of ammonia in the gas-phase with sulfur, nitrogen, and other acidic species forming ammonium nitrate and ammonium-sulfate particulate matter. $\text{PM}_{2.5}$ ammonium nitrate, for instance, forms from the NO_x -reaction by-product nitric acid and ammonia.

Nitrate (NO_3^-) containing aerosols typically exceed $1\mu\text{m}$ in diameter, i.e. they do not form by homogenous, but heterogeneous gas-to-particle conversion processes. They also may stem from evaporation of droplets, among other things.

In the accumulation mode ($0.1\text{-}2.5\mu\text{m}$ in diameter), *coagulation* of smaller particles and/or *heterogeneous condensation* of gases onto existing particles produce particles. The largest mass and amount of particles occur in the accumulation mode due to the lack of efficient removal mechanisms for these particles.

The term secondary aerosol refers to particles that are produced by precursor gases, condensation and other processes in the atmosphere. This means that $\text{PM}_{2.5}$ can be released in the atmosphere from emissions, or be produced in the plume of stacks or in the atmosphere by gas-to-particle conversion. Primary aerosol refers to particles directly emitted into the atmosphere as particles. Primary aerosols produced by combustion span all three size ranges.

Measurements by the FNSB show a large spatial and temporal variability in $\text{PM}_{2.5}$ concentrations (e.g. Figs. 2, 3). The reasons for the observed spatial variability in $\text{PM}_{2.5}$ concentrations are manifold. In business districts dominated by central heating, traffic usually contributes more than in low-traffic residential areas dominated by heating with coal, wood or oil. $\text{PM}_{2.5}$ emissions from traffic, power plants and home heating with oil also depend on sulfur content [e.g. *Johnson et al.*, 2009]. $\text{PM}_{2.5}$ concentrations at breathing level depend on the emissions and meteorological factors like temperature, mixing height, atmospheric stability, longevity and strength of inversions [*Dawson et al.*, 2007; *Mölders and Kramm*, 2010; *Tran and Mölders*, 2011].



Fig. 2. $\text{PM}_{2.5}$ concentrations as measured in Fairbanks by the mobile platforms (lines of dots) on 12-29-2008 during the drive starting at 1523 AST (Alaska Standard Time). Measurements have been also made in the hills and the North Pole area (not shown here). Single dots are the $\text{PM}_{2.5}$ concentrations as measured at the stationary sites. Color code: deep green $0\text{-}35\mu\text{g}/\text{m}^3$, olive $35\text{-}105\mu\text{g}/\text{m}^3$, orange $105\text{-}210\mu\text{g}/\text{m}^3$, red $210\text{-}350\mu\text{g}/\text{m}^3$, and $>350\mu\text{g}/\text{m}^3$ grey. Courtesy to *F. di Genova* [2009]

Due to the temperature dependency of chemical reaction [e.g. *Seinfeld and Pandis, 1997*] secondary pollutants, gas-to-particle-conversion and the emissions from energy and heat production differ for warm and cold atmospheric conditions. For PM_{2.5} ammonium nitrate formation not only the NO_x reaction by-product nitric acid and ammonia have to be available, but also temperatures must be low and relative humidity must be high [*Wexler and Seinfeld, 1992*]. This means that the local change rate $\partial[C]/\partial X$ in concentration [C] with changes in the meteorological quantity X can differ in winter from those in summer or in other words is different for Fairbanks' winter conditions as compared to winter conditions in a warmer climate.

As previously indicated, PM_{2.5} is a complex mixture of components – nitrate, sulfate, organic carbon, elemental carbon (EC) other primary particulate matter, ammonium and water – that show strong seasonal variations (Fig. 3) due to differences in sources, temperature and humidity. Analysis of previous measurements suggests that the burning sector and especially wood-burning strongly contribute to the high PM_{2.5} concentrations in the FNSB (e.g. Fig. 3).

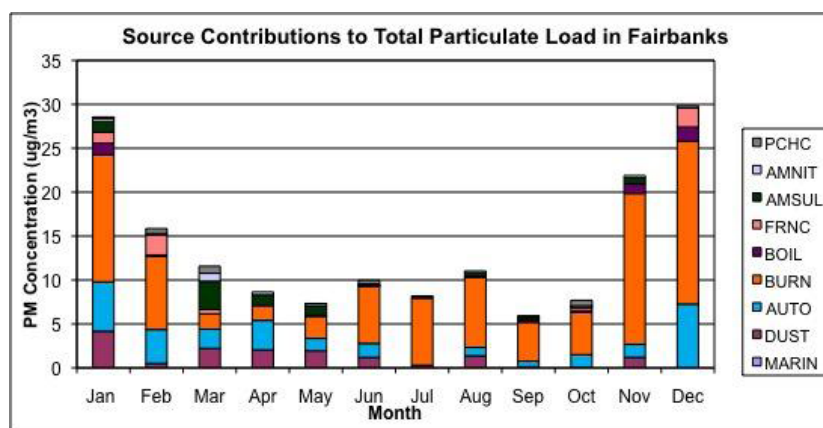


Fig. 3. PM_{2.5} composition in Fairbanks. PCHC, AMNIT, AMSUL, FRNC, BOIL, BURN, AUTO, DUST and MARINE stand for coal-fired power plant, ammonium nitrate, ammonium sulfate, furnace, industrial boilers, biomass burning, automobiles, soils, and marine PM_{2.5}. Courtesy to *C.F. Cahill and A.N. Wallace [2010]*

If no action is taken to reduce the PM_{2.5} concentrations in Fairbanks, Fairbanks will likely exceed the PM_{2.5} standard in winters in the future. Such non-compliance is expected to have significant social, health and/or economic impacts on Fairbanks, the FNSB and their citizens.

The EPA, FNSB, Alaska Department of Environmental Conservation (DEC), Alaska Health & Social Services and scientists are concerned about the PM_{2.5} concentrations in Fairbanks as PM_{2.5} has various known health adverse effects. For instance, exposure to airborne PM_{2.5} is associated with cardiovascular events and mortality in elderly and cardiac patients [*Riediker et al., 2004*]. Various studies indicate that people – especially children – living in close proximity to roadways show more respiratory symptoms, decreased lung function, more respiratory hospitalizations and increased incidence of asthma than their peer groups in other environmental conditions [e.g. *McCreanor et al., 2007*]. Climate-geographical location plays no role and a pre-existing family history of asthma is not required, i.e. living close to heavy traffic or heavily industrialized areas is the important factor [*Gordian 2010*; pers. communication]. Investigations on healthy young men who were exposed to PM_{2.5} from road traffic suggest that these men experienced pathophysiological changes that involve inflammation, coagulation and cardiac rhythm [*Riediker et al., 2004*].

2. Selection of the air quality model

Obviously, no exposure to any pollutants would avoid adverse health impacts from air pollution, but this is impossible to realize. The current NAAQS were set according to the best scientific knowledge to protect human health. These values are re-evaluated from time to time to adjust to newest scientific findings if required. Often tightening the NAAQS requires emission regulations. Such emission regulations may have enormous socio-economic impacts for both public and private stakeholders. Therefore, it is helpful to assess the effectiveness of a potential regulation and/or the contribution of an emission source sector being under suspicion to strongly contribute to the exceedance of the new NAAQS.

Photo-chemical models of various complexity have been used for a long time to examine (1) the relation between meteorological conditions and air quality, (2) the formation and distribution of acid rain, (3) air-quality issues, and (4) the role of long-range transport of pollutants for air quality [e.g. *Chang et al.*, 1989; *Mölders et al.*, 1994; *Grell et al.*, 2000, 2005; *Tetzlaff et al.*, 2002; *Otte et al.*, 2005; *Yu et al.*, 2008; *Eder et al.*, 2009; *Mölders et al.*, 2010]. The use of such air-quality models for emissions permits and/or for regulatory purposes has a long tradition not only at EPA [EPA, 2009]. Recently, ambient air-quality modeling has been used successfully to estimate individual and population exposure for human health research in mid-latitudes [e.g. *Bell* 2006].

The great advantage of photo-chemical models is that they permit easily to change emissions in the model world. The model then provides the atmospheric response, i.e. the concentrations that result in response to the altered emissions. This means photo-chemical models permit us to answer “What ...if” questions like

- “What will happen to the PM_{2.5} concentrations at breathing level if we replace a certain amount of non-certified wood-burning devices by EPA certified wood-burning devices?”
- “What will happen if we reduce the sulfur content in fuel used for domestic heating and power productions?”

They also permit us to assess the contribution of an emission source of interest to the PM_{2.5} concentrations at breathing level, and answer questions like

- “What do the power plants contribute to the PM_{2.5} concentrations at breathing level?”

Modeling is a useful tool to access in which direction emission-reduction efforts will go, how the altered emissions in combinations with the various chemical and meteorological processes affect the concentrations, and what the impact of emissions sources are. To answer such questions it is necessary to perform at least two simulations. One simulation considers the emissions as they are currently (business-as-usual). This simulation is the reference simulation and provides the baseline. The second simulation that is applied for the same meteorological condition as the first one, considers the emissions of the altered emission scenario (e.g. the change in emissions in response to a “woodstove exchange program”). Comparison of the results of the simulations permits us to assess how much the concentrations change in response to the altered emissions.

The goal of this study was to conduct photo-chemical model simulations with a complex state-of-the-art research model to quantify numerically the potential impacts of various emission reduction scenarios on the PM_{2.5} concentrations at breathing level in Fairbanks, the Fairbanks nonattainment area and its adjacent land. These modeling studies in combination with various

other investigations related to Fairbanks' nonattainment problem [e.g. *Davies et al.*, 2009; *Carlson et al.*, 2010], ongoing studies and measurements are to help policy makers in the decision making process on which measures to apply to decrease the PM_{2.5} levels in the future and to inform the public.

The Weather Research and Forecasting model inline coupled with a chemistry model commonly known as WRF/Chem [*Grell et al.*, 2005] is a state-of-the-art photo-chemical research model⁶ based on the newest scientific knowledge. It simulates the meteorology and the trace-gas and aerosol cycles from emission, through a variety of chemical reactions, to transport, and finally removal from the atmosphere by wet or dry deposition. WRF/Chem can consider feedbacks between chemistry and meteorology.

WRF/Chem was chosen as it was the only photo-chemical model that was already adapted for application in Alaska [*Mölders et al.*, 2010, 2011]. These modifications, among other things, ensure Alaska-typical values of the vertical profiles of initial background concentrations (e.g., acetylene, CH₃CHO, CH₃OOH, CO, ethane, HCHO, HNO₃, H₂O₂, isoprene, NO_x, O₃, propene, propane, SO₂) and boundary conditions. The modifications also ensure that Fairbanks and other settlements are included in the land-use data and that winter typical vegetation parameters are used from Mid-October to Mid-April. In addition, modifications concerning the stomatal behavior of Alaska vegetation and dry deposition of trace gases on snow were included [*Mölders et al.*, 2010, 2011]. Furthermore, first evaluations studies of the Alaska adapted WRF/Chem already existed that showed acceptable performance for Alaska [*Mölders et al.*, 2010, 2011]. Such studies did not exist for other photo-chemical models yet.

We used the following model setup that was capable of capturing Alaska winter conditions well in previous studies [*Mölders*, 2008; *Mölders and Kramm*, 2010; *Mölders et al.*, 2010; *Yarker et al.*, 2010]. The WRF-Single-Moment six-class scheme that allows the coexistence of super-cooled water droplets and ice-crystals and processes among the solid and liquid phase cloud and precipitation components, served to simulate resolvable cloud- and precipitation-formation processes [*Hong and Lim*, 2006; *Hong et al.*, 2006]. It is able to simulate falling snow crystals and ice fog, which are of relevance for Fairbanks in winter. To consider the impact of the cumulus convection even though it rarely occurs in Fairbanks winters, we used the cumulus-ensemble scheme [*Grell and Dévényi*, 2002] as it is well suitable for the grid-resolution at which WRF/Chem was run for this study. The Goddard two-stream multi-band scheme was used to calculate shortwave radiation processes. It considers, among other things, the impacts of clouds and ice fog on shortwave radiation. This is important as the shortwave radiation affects photolysis rates. Long-wave radiation was calculated with the **Rapid Radiative Transfer Model** [*Mlawer et al.*, 1997] that takes into account multiple spectral bands, trace gases, and cloud microphysical species (cloud-droplets, rain drops, ice-crystals, etc.), among other things. It allows considering the effects that pollution, ice fog and clouds have on long-wave radiation. The 1D-prognostic scheme by Janjić [2002] was applied to determine turbulent processes⁷ in the atmospheric boundary layer⁸ (ABL), i.e. the first 1000m or so above ground level (AGL). For the

⁶ Note that WRF/Chem is a complex state-of-the-art research model, not a regulatory model.

⁷ Turbulence refers to rapid fluctuations.

⁸ The ABL is the lowest part of the atmosphere that is directly influenced by its contact with the surface. In the ABL, turbulence and vertical mixing can be strong.

atmospheric surface layer⁹, i.e. the first 100m or so, Monin-Obukhov similarity hypotheses were used to describe the turbulent processes; the so-called Zilitinkevich thermal roughness-length concept was considered for the underlying viscous sublayer [Janjić, 1994]. Previous studies showed that out of various parameterizations available in WRF/Chem these parameterizations of ABL and surface layer processes provide the best results most of the time for Interior Alaska [e.g. Mölders and Kramm, 2010]. Simulating the ABL processes adequately is required to capture inversions and their strength and hence the accumulation of pollutants underneath. Smirnova *et al.*'s [2000] land-surface model (LSM) was used to determine the exchange of heat and moisture at the land-atmosphere interface. This LSM calculates, among other things, the soil-temperature and moisture states including frozen soil, snow conditions at various depths in the snow-pack, and vegetation impacts on the atmosphere. The LSM was chosen as it considers permafrost and snow processes. Simulating these processes adequately is important to capture the strength of inversions.

The chemical mechanism by Stockwell *et al.* [1990] served to calculate gas-phase chemistry, i.e. reactions among trace gases. This mechanism considers the chemical reactions that occur in the polluted and non-polluted atmosphere at day and night. Inorganic reactions and constants involve 14 stable inorganic compounds, four inorganic short-lived intermediates and three abundant stable species (oxygen, nitrogen, water). The organic chemistry scheme considers 26 groups of stable organic compounds and 16 groups of organic short-lived intermediates (peroxy radicals). Photolysis frequencies were calculated in accord with Madronich [1987] as even at winter solstice Fairbanks still experiences 3.7h of sunlight. These frequencies were used in the calculation of photochemical processes. Photolysis calculation considered 21 photo-chemical reactions. In mid latitudes, the chemical processes during daylight (daytime chemistry) differ from those at night (nighttime chemistry). In Fairbanks, however, the fraction of the day with daylight strongly differs over the winter. In Fairbanks, the sun is only a few hours above the horizon in January and December, while it is appreciably longer above the horizon to provide energy for photochemical processes in October, November, February and March. Thus, the importance of photochemical processes and their contribution to chemical transformations differs strongly over the winter due to the large differences in available shortwave radiation (see Fig. 11c). Thus, “daytime” and “nighttime” chemistry play a different role in January and December than the other winter months. Therefore, it was considered necessary to simulate several months rather than a short episode in the coldest month.

Various processes (transport, turbulence, evapotranspiration, sorption, desorption, biogenic activity, emission, settling, chemical reactions) are involved in the dry deposition process, i.e. the removal of trace gases from the atmosphere. Thus, dry deposition not only depends on the physical and chemical states of the atmosphere, but also on the surface on which the trace gases and particles deposit. The formulation of dry deposition [Wesely, 1989] with the modifications introduced by Mölders *et al.* [2011] considers these processes. The modifications serve to treat dry deposition of trace gases more realistically under low temperature conditions and consider dry deposition on snow. Since the stomata of Alaska vegetation often are still open at -5°C , the threshold for total stomata closure was lowered accordingly in the LSM and deposition module.

⁹ In the atmosphere, surface layer refers to the layer where the turbulent air is most affected by interaction with the surface. The characteristics of the turbulence depend on the distance from the surface. The surface layer is characterized, among other things, by large concentration gradients of any substances transported to or from the surface.

Aerosol chemistry and physics was treated based on a modified version of the Regional Particulate Model [*Binkowski and Shankar, 1995*], where the vertical transfer of particulate matter is treated in accord with *Kramm et al. [1992]*. Among other things, the aerosol module considers aerosol chemistry and physics, and aerosol formation by gas-to-particle conversion, and Secondary Organic Aerosol (SOA) formation processes [*Schell et al., 2001*] and the removal of particulate matter from the atmosphere by wet and dry deposition of aerosols. These aerosol chemistry modules have been well tested for mid latitudes. A through evaluation for Alaska is still missing due to lack of observational data. First evaluations with the limited data available [*Mölders et al., 2010, 2011*] suggest acceptable performance most of the time.

3. Model domain, initial and boundary conditions

The Alaska Emission allocation Model (AkEM) [Mölders 2009, 2010] and WRF/Chem were set up for a domain covering most of Interior Alaska with a horizontal grid increment of $4\text{km} \times 4\text{km}$. Since Alaska available land-use data did not consider any urban areas, we introduced Fairbanks, North Pole, Eielson and the villages into the WRF/Chem land-use data file (Fig. 4) based on satellite data using Google Earth. Relevant WRF/Chem-simulated concentrations and meteorological quantities were written out hourly as a function of time and space for the domain of interest. The domain of interest for the analysis encompasses $89,600\text{km}^2$ centered around Fairbanks up to 100hPa (Fig. 4).

WRF/Chem used logarithmically increasing vertical grid increments with the smallest increment being located above the ground and the largest increment reaching to the top of the model located at 100hPa . In total, there are 28 layers. In the lower troposphere, the tops of the layers were at 8, 16, 64, 113, 219, 343, 478, 632, and 824m AGL. The lowest atmospheric model layer represents the “breathing level”. This vertical and horizontal grid is a compromise to ensure still sufficient vertical and horizontal resolution, and allow for several months long simulations in a reasonable amount of time.

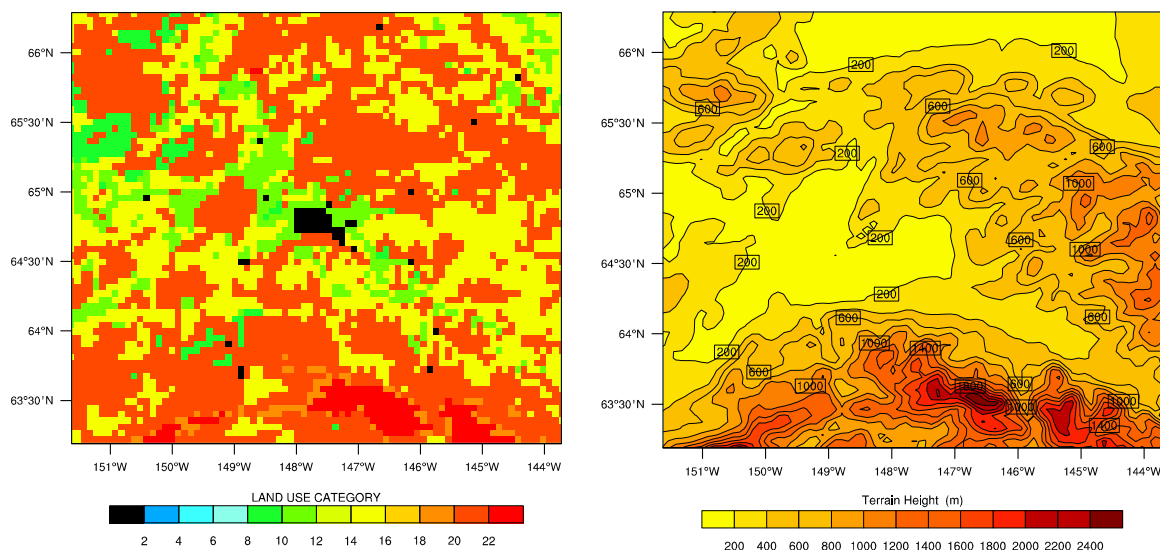


Fig. 4. Land-use (left) and topography (right) in the domain of interest for the analysis of this study. The land-use category code is 1 urban and built-up land, 2 dryland cropland and pasture, 3 irrigated cropland and pasture, 4 mixed dryland/irrigated cropland and pasture, 5 cropland/grassland mosaic, 6 cropland/woodland mosaic, 7 grassland, 8 shrubland, 9 mixed shrubland/grassland, 10 savanna, 11 deciduous broadleaf forest, 12 deciduous needleleaf forest, 13 evergreen broadleaf, 14 evergreen needleleaf, 15 mixed forest, 16 water bodies, 17 herbaceous wetland, 18 wooden wetland, 19 barren or sparsely vegetated, 20 herbaceous tundra, 21 wooded tundra, 22 mixed tundra, 23 bare ground tundra, 24 snow or ice.

The meteorological fields were initialized every five days using data downscaled from the $1^\circ \times 1^\circ$, 6h-resolution National Centers for Environmental Prediction global final analyses (FNL). At the beginning of the simulations, WRF/Chem was initialized with idealized vertical profiles of Alaska background concentrations for each chemical specie (e.g., acetylene, CH_3CHO , CH_3OOH , CO , ethane, HCHO , HNO_3 , H_2O_2 , isoprene, NO_x , O_3 , propene, propane, SO_2). For all further days, the simulated chemical fields of the previous day served as initial conditions to simulate the next day.

Since Fairbanks is far remote from any emission sources, Alaska background concentrations were used for the chemical lateral boundary conditions. The meteorological boundary conditions were downscaled and interpolated from the FNL-data.

WRF/Chem was run in forecast mode, i.e. no nudging or data assimilation was applied. The reference simulation and the simulation that was to assess the contribution of point sources to the PM_{2.5} concentrations at breathing level, start with the same meteorological and chemical initial conditions on November 1, 2005 0000 UTC (see Table 1). In the mitigation investigations, the reference simulation and all mitigation scenarios start with the same meteorological and chemical initial conditions on October 1, 2008 0000 UTC (see Table 1). This procedure ensures that differences in simulated concentrations only result in response to the changes in assumed emissions.

Emissions were considered as a function of time (month, weekday, and hour) and space (latitude, longitude and height). Various types of emission sources are considered. Point sources are fixed (immobile) facilities that emit gaseous or particulate atmospheric pollutants (e.g. smokestacks, power plants, industrial plants, steel mills). A line source is one-dimensional emission source (e.g., vehicle traffic on a highway). An area source is a two-dimensional source of diffuse emissions (e.g. the emissions from domestic heating, landfills, fires). For more details, see e.g. http://en.wikipedia.org/wiki/Air_pollution_dispersion_terminology [2011].

In the case of point sources, emissions are released into the model levels that are calculated depending on stack parameters (stack height, stack diameter, flow temperature, flow velocity, etc.). WRF/Chem, among other things, also includes plume rise [Peckham *et al.*, 2009]. In the case of area and line sources, the model level in which the emissions are released depends on the kind of emission source. For instance, emissions from city or highway traffic are released into the first model layer above ground (Fig. 5).

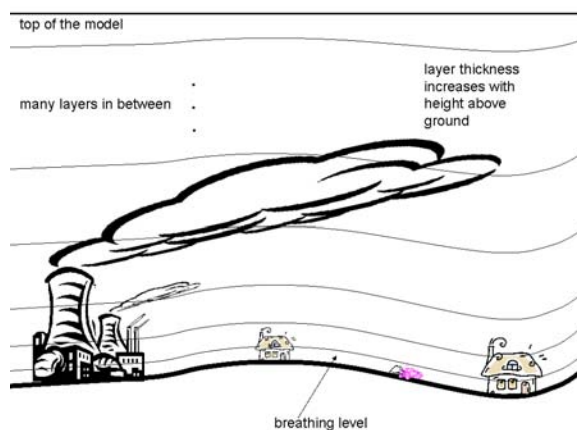


Fig. 5. Schematic view of the vertical grid structure and consideration of various emission sources. The spacing of vertical model layers increases logarithmically with height. Note that not all model layers and potential emission sources considered by WRF/Chem are pictured here.

Some Alaska plant species remain photosynthetically active up to temperatures as low as -5°C (23°F). Thus, we considered biogenic emissions of isoprenes, monoterpenes, and volatile organic compounds (VOC) by plants, and nitrogen emissions by soil as calculated by the **M**odel of **E**missions of **G**ases and **A**erosols from **N**ature [Guenther *et al.*, 1994; Simpson *et al.*, 1995] if the ground is not covered by snow.

4. Meteorological episodes simulated

At the start of the project in 2008, the most recent emission data available for the FNSB were the National Emission Inventory (NEI¹⁰) data of 2005. In December 2008, the FNSB expected that a gridded emission-data inventory with 400m spatial and hourly resolution representing the winter 2007/08 would be available for Fairbanks and its vicinity in April 2009 [Conner pers. communication, 2008]. Therefore, it was planned to switch to a more recent episode for the simulations on the impact of introduction of low sulfur fuel and a “woodstove replacement program” despite doing so would require producing an additional reference (baseline) simulation (Table 1).

4.1 Emissions

All NEI data were annual values for the various species and emission sectors in the FNSB. These emission data were allocated for use in WRF/Chem using the AkEM [Mölders, 2009; 2010]. Input data to AkEM are the EPA NEI data, stack parameters, data for the split of PM_{2.5} and VOC, allocation data of annual, daily, hourly emission percentages for area, line, and point sources, population density data, land-use and street network data as well as meteorological data. The split of PM_{2.5} emissions into ammonium (NH₄), carbon, nitrate (NO₃), potassium, sodium, and sulfate (SO₄) was made based on observations provided by the FNSB [Conner, 2009]. Due to the lack of observational data, we split the total anthropogenic VOC emissions into the various species like ethane, butane, formaldehyde, pentane, hexane, ethylene, propylene, acetylene, benzene, toluene, xylene, tri-methylbenzene, and other aromatics depending on emission-source types in accord with Mölders *et al.* [2011].

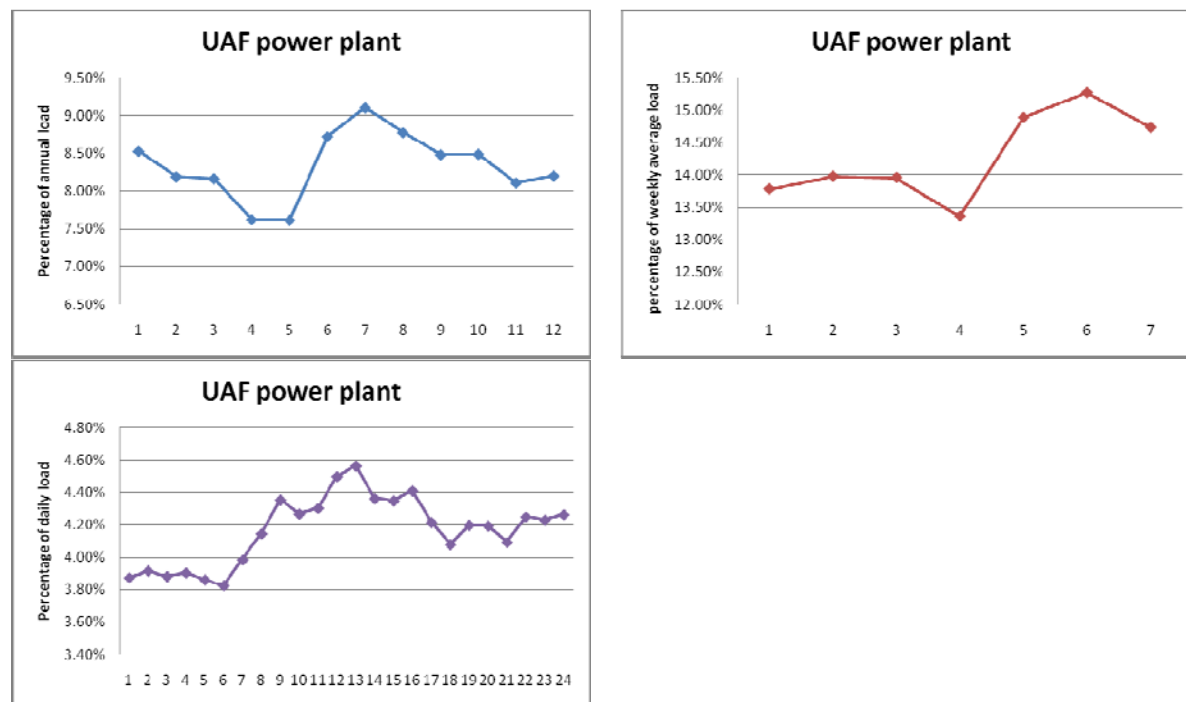


Fig. 6. Activity allocation as derived for the UAF power plant for (from upper left to lower left) monthly, weekday and hourly activity. Data courtesy by Waard [2008]

¹⁰ Typically the National Emission Inventory is abbreviated as NEI and the year is added, e.g. NEI1999 would be the NEI for 1999.

AkEM calculates hourly emission rates for each grid-cell from the annual emission E_{total} given by the NEI. In doing so, AkEM uses the spatial and temporal activity allocation functions for the various emission sources that have been recommended by EPA for Alaska with the modifications that have been derived in collaboration with local partners. Figure 6 exemplarily shows the emission-allocation functions as derived from data for the UAF power plant. Area emissions from the burning sector, for instance, are distributed spatially depending on specie, activity, population, and/or land-use, and time. The model level and grid cell into which point sources emit, depends on stack parameters, latitude, and longitude and plume raise that is calculated using Biggs formula [Peckham *et al.*, 2009].

4.1.1 Emission data for 2005/06

We performed a quality assessment and quality control (QA/QC) on the NEI2005 data for the FNSB. The QA/QC showed that for some point sources stack parameters were missing and/or the coordinates were incorrect or vice versa. We worked with the respective facility operators and EPA to fill in and/or replace the data with the correct data.

We worked with Golden Valley Electricity Association and UAF's power plant employees to obtain Alaska specific annually, daily and hourly emission profiles for 2005 (e.g. Fig. 6) and implemented them into the AkEM. We used the population-density data provided by the FNSB from the Census 2000 [data provided by Duncan, 2009] and projected them onto the model domain. AkEM requires these data for determining/distributing the area emissions.

For the winter 2005/06 simulations AkEM [Mölders, 2009] used allocations functions depending on space and time. Allocation differed with time of the day, day of the week and month. For 2006, an increase in annual emissions of 1.5% was assumed across the board.

4.1.2 Emission data for 2008/09

In December 2008, the FNSB expected that gridded spatially high resolved hourly emission data for winter 2007/08 would be available in April 2009 from SRL. The FNSB wanted to have the option to switch to a more recent episode (probably 2008/09) than 2005/06 for the “woodstove replacement” and “low sulfur emission” simulations. The reasons for this request were manifold. More observational data for model evaluation are available for this more recent winter. Moreover, since 2007, the number of woodstoves has increased notably and 2008 was discussed as a potential design year.

Early in 2010, the anticipated SRL-emission inventory for winter 2007/08 was still not available¹¹ due to unforeseen delays and difficulties in collecting the data that were beyond the control of SRL and/or the FNSB. Moreover, the QA/QC had still to be performed by EPA. Early, in 2010, the FNSB decided that we should perform the “woodstove replacement” and “low sulfur scenarios” for winter 2008/09. Meanwhile, namely, the NEI2008 became available except for point-source emissions. The NEI2008 more closely represents the current emission situation in the FNSB, as it considers emission changes between 2005 and 2008 and hence is more recent than the NEI2005. Therefore, we did a new reference simulation and the mitigation scenarios for winter 2008/09 (Table 1).

Note that the main difference between the emission data that we used for this study and those of the anticipated SRL-inventory is that the NEI2008 in combination with AkEM treat emission

¹¹ As of January 2011, we have no access to the SRL-compiled 2007/08 emission data.

data for the FNSB in a top-down approach, while the SRL-inventory treats emissions in a bottom-up approach. A top-down approach assesses emission rates based on aggregated-statistical methodologies, while the bottom-up approach compiles a site-specific emission inventory based on the detailed information for each area [e.g. *Kim et al.*, 2010]. Inter-comparison analysis suggests that standard emissions data from a top-down approach are appropriate for atmospheric model simulations [e.g. *Kannari et al.*, 2008]. The differences, advantages and disadvantages between these two types of approaches have been widely discussed in the literature [e.g. *Kannari et al.*, 2008; *Kim et al.*, 2010] and are therefore not repeated here.

Emissions of mobile and several nonpoint-emission sectors were available from the NEI2008. The NEI2008 considered aircraft emission as point sources. Other point-source sectors were not yet available in the NEI2008 and were not expected to be available before 2011. Therefore, we updated the point-source emission inventory (EI) by personal communications with the facilities holders in the FNSB whom we contacted with this request. Note that not all facilities contacted did respond. For those facilities without reported emission data, we used estimates on point-source emissions based on the previous inventory assuming a 1.5% increase per year.

The mobile emissions in the NEI2008 are less than what they were in the NEI2005, which is consistent with the lower traffic activity in 2008 as compared to 2005 [*DOT*, 2009]. Some nonpoint-emission sectors were required to be updated with the latest borough employment data. We performed these updates using the respective data from the Alaska Department of Labor and Workforce Development [<http://laborstats.alaska.gov/cgi/dataanalysis/?PAGEID=94>].

However, there were some nonpoint-emission sectors that EPA was not planning to estimate unless additional resources became available. Those sectors included industrial/commercial/institutional fuel combustion and the residential wood combustion. The latter make up a large portion of the emission in the FNSB according to the NEI2005. Therefore, the emissions from these sectors were included in the emission database used for our simulations of winter 2008/09 to obtain realistic emission conditions. For industrial/commercial/institutional fuel combustion, we assumed the 2008 emissions to be the same as in NEI2005 because they were expected to have just marginally changed over 2005-2008. Emissions from residential wood combustions were taken from *Davies et al.* [2009] as was requested by the FNSB. The outcome showed much higher emissions from residential wood combustion in 2008 as compared to that category in the NEI2005. This increase in woodstove emissions, however, is expected given the situation in the FNSB in winter 2008/09. Note that in the NEI2005, EPA estimated emissions from residential wood combustions based on the small partition of wood-burning devices as obtained from the Census 2000. Meanwhile, in response to the increasing oil prices, many residents had added wood-burning devices to reduce heating costs. The wood-cutting permits have increased threefold in 2009 as compared to 2007 [*Conner* 2010, pers. communication]. To derive the annual emissions for 2009 from those of 2008, an increase in annual emissions of 1.5% was assumed across the board.

For allocation of the winter 2008/09 emissions a modified version of AkEM [*Mölders*, 2010] was used that applied allocations functions depending on space, time and temperature. Allocation differs with time of the day, day of the week; month and deviation of the daily mean temperature from the 30-year monthly average mean temperature. This modification (calibration) of the emission model was introduced to improve the allocation functions based on our experience with the simulations for winter 2005/06 and several sensitivity studies paid from other sources. This

modification of the emission allocation permits to better consider the temperature dependency of cold start enhanced emissions (CSEE) and the increase in energy consumption for heating for temperatures below 18°C (64.4°F) using a modified equation of *Hart and de Dear* [2004]. The temperature dependency for production of electrical power was determined assuming that freezers, refrigerators and hot water production consume equal amounts of energy. The same allocation functions and temperature correction as for power plants is assumed for emissions from fuel combustion for electricity production by nonpoint sources, but these emissions are considered dependent on population density [Mölders, 2010]. AkEM assumed that the non-temperature corrected allocation function is valid for the mean temperature of the month [Mölders, 2010]. Thus, the inclusion of temperature dependency increases (decreases) the emission factors for temperatures below (above) the monthly mean temperature. The temperatures used in these corrections are the 2m-temperatures read in from the WRF/Chem initialization data. Figure 7 exemplarily shows the impact of temperature-dependent emissions for March 3, 2005 where the domain average temperature was -22.1°C (-7.8°F).

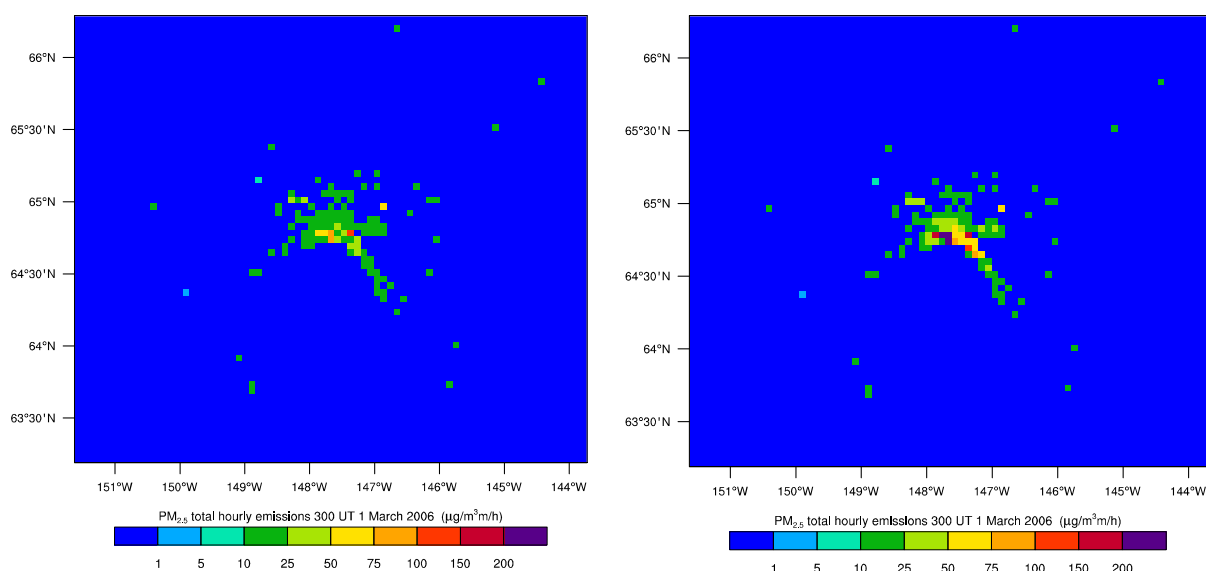


Fig. 7. Emissions of PM_{2.5} without (left) and with consideration of temperature correction. This day is colder – the daily average temperature is 22.1°C (-7.8°F) - than the climatological average March temperature of -11.7°C (10.9°F) for which the original allocation functions were valid. As expected, emissions increase in response to the low temperatures. *Davies et al.*'s [2009] emission data were used.

4.2 Emission scenarios

This section describes the emission scenarios used in the mitigation simulations. Table 1 summarized the simulations performed for this study. Throughout this report, the simulations as their results are referred to as REF and NPE, or REF, WSR and LSF, respectively.

4.2.1 Emission scenario for investigation of point source contribution

The 2005/2006 winter was chosen because at the start of the project in 2008, the most recent available emission-data inventory was the NEI2005. Since the concentrations resulting from point-source (PS) emissions alone were so low that PM_{2.5} concentrations were governed mainly by background chemistry, we performed simulations with emissions from all sectors as the reference simulation (REF). In a further simulation, we considered emissions from all sectors

except point-source emissions (NPE). This means emissions of all species emitted by point-sources were set to zero in the NPE scenario. Simulations with consideration of point-source emissions were performed for October 1, 2005 to February 28, 2006. The first 15 days performed for October 2005 served for calibration. The rest of October 2005 served to spin-up the chemical fields. Simulations without consideration of point sources were performed from November 1, 2005 to February 28, 2006. The simulations with and without consideration of point-source emissions start with the same initial conditions of the meteorological fields and chemical components on November 1, 2005 as obtained from the spin-up. Comparison of the concentrations obtained by the REF and NPE simulations for November 1, 2005 to February 28, 2006 served to quantify the contribution of the point sources (e.g. power plants) to the PM_{2.5} concentrations at breathing level.

Table 1. List and names of simulations performed with WRF/Chem for this study. Note that LSF and WSR have the same reference simulation.

Simulation name	Description	episode simulated
REF	Reference simulation with all emissions using the NEI2005	October 1, 2005 to February 28, 2006
NPE	Simulation using the NEI2005, but excluding emissions of all species from all point sources	November 1, 2005 to February 28, 2006
REF	Reference simulation with all emissions using the NEI2008 with the updates as described in the emission section	October 1, 2008 to March 31, 2009
WSS1	“Woodstove replacement” sensitivity study that assumes non-certified wood-burning devices are replaced by modern EPA-certified woodstoves using <i>Davies et al.’s</i> [2009] numbers of wood-burning devices, while keeping emissions from all other emission sectors the same as in the respective reference simulation	October, 1 2008 to October 15, 2008
WSS2	as WSS1, but using the numbers wood-burning devices from SRL’s draft report	October, 1 2008 to October 17, 2008
WSR	as WSS2, but using the numbers of <i>Carlson et al.’s</i> [2010] final report	October 1, 2008 to March 31, 2009
LSF	“Introduction of low sulfur fuel for heating and power generation”, while keeping emissions from all other emission sectors the same as in the respective reference simulation	October 1, 2008 to March 31, 2009

4.2.2 Emissions for the “woodstove replacement” scenarios

A set of simulations addressed the influence of a “woodstove-replacement action” on the PM_{2.5} concentrations at breathing level. The reference simulation (REF) considered emissions from all sectors available in the NEI2008 and the additional information described before. The simulation assuming “woodstove replacements” considered the same emissions as in REF minus the emissions from non-certified wood-burning devices that were assumed to be replaced plus the emissions that stem from the certified wood-burning devices that replaced the non-certified wood-burning devices. The reference and “woodstove replacement” simulations started with the same initial conditions of the meteorological fields and the same Alaska-typical chemical background concentrations for October 1, 2008.

To compile the emission data for the “woodstove-replacement” simulations, we analyzed *Davies et al.*'s [2009] results. We searched the literature and collected data on other species than PM_{2.5} emitted by EPA-certified woodstoves and other wood-burning devices. These data were required as not only the PM_{2.5} emissions from wood-burning devices, but also the emissions of the other species emitted by these devices will change if non-certified wood-burning devices are replaced by EPA-certified wood-burning devices. This means all species emitted by wood-burning were changed in the “woodstove-replacement scenarios”. The consideration of changes for all species emitted by wood-burning devices is required because some PM_{2.5} can form from gas-to-particle conversions once the species are in the atmosphere as explained before.

Davies et al.'s [2009] data only provide the total number of certified woodstoves (6912), but not the split between certified woodstoves with catalytic and non-catalytic equipment. The same is true for masonry heaters and pellet stoves. We assumed the same emission rates for wood-burning devices with catalytic and non-catalytic equipment.

Table 2. Number of households in Fairbanks. Data courtesy of *T. Duncan* [2010]

Year	Pre-2005	2005	2006	2007	2008	2009
Number of households	33970	34946	35910	36952	37550	38292

The number of households changed over the years (Table 2). As obvious from the sum of the devices listed in *Davies et al.* [2009] report, some households have at least two heating devices. We assumed that in the case of households with more than one heating device, woodstoves co-exist with oil furnaces. For fire-safety reasons it is unlikely that a woodstove exists in a household with gas. It is unlikely that woodstoves co-exist with hydronic or masonry heaters or pellet stoves as well. The category “others” is most likely central heating which also has a low likelihood to co-exist with woodstoves. Coal and woodstoves are unlikely to co-exist as typically people who burn coal also burn wood in the same stove. To avoid double counting of households in their emission contribution, we determined the number of households with at least two heating devices

$$N_{\text{two}} = N_{\text{devices}} - N_{\text{households}} \quad (1)$$

Where N_{devices} and $N_{\text{households}}$ are the number of heating devices and households in that particular year. After studying *Davies et al.*'s [2009] data, it seemed reasonable to assume that households with two devices use the woodstove to other device in a ratio 33.5:66.5 of the time. Sensitivity studies indicated that the total emission reduction is very sensitive to how households split their heating among their available devices. Thus, we recommend collecting data on the “split” behavior to reduce uncertainty in future modeling studies.

We determined the actual number of devices contributing at a time to wood-burning emission as

$$N'_x = N_x \left(1 - 0.665 \frac{N_{\text{two}}}{N_1 + N_2 + N_3} \right) \quad (2)$$

Where the x stands 1, 2 and 3, with 1 to 3 representing non-certified woodstoves, EPA-certified woodstoves with catalytic equipment, and EPA-certified woodstoves without catalytic equipment, respectively. Analogously, the number of devices contributing at a time to emissions from oil furnaces is determined as

$$N'_7 = N_7 \left(1 - 0.335 \frac{N_{\text{two}}}{N_7} \right) \quad (3)$$

Where the index 7 denotes oil furnaces. After this procedure, the sum $\sum_{k=1}^{11} N'_k$ equals the number of households.

Davies et al.'s [2009] data for Fairbanks' wood-burning emissions differ from those assumed in the compilation of the NEI2008. We used *Davies et al.*'s [2009] data for all wood-burning devices and oil furnaces as requested by the FNSB. We used EPA's data for the other categories, as data for these devices were not included in *Davies et al.*'s [2009] report.

The total annual emission rate of the i^{th} specie from heating after "woodstove replacement" is given by

$$E_{\text{NEI}_{yyyy, \text{WSR}}} = E_{\text{NEI}_{yyyy}} + N_{\text{exchange}} E_2 - \sum_j N_j E_j \quad (4)$$

Where N_{exchange} and E_2 are the number of wood-burning devices replaced and emission rates per certified wood-burning device, E_j are N_j the emission rates and numbers of noncertified wood-burning devices, and the index j stands for noncertified wood-burning devices, respectively.

In all "woodstove replacement" emission scenarios, we assumed emissions from all sectors to remain the same as in the reference simulation except for the heating sector. For the heating sector, we assumed the emissions from all heating devices but wood-burning devices to remain the same as in the reference simulation too. This means that in all "woodstove replacement" simulations, we only altered the emissions from the wood-burning sector.

In a first sensitivity study on "woodstove replacement", we determined the emissions remaining from wood-burning after the replacement of non-certified devices by assuming the number of residential wood-burning devices as reported in *Davies et al.* [2009]. We calculated the emissions from residential wood combustion, subtracted the contribution from non-certified devices (assumed to be replaced) and added the contribution that the certified device (that replaced the non-certified devices) would have. The simulation with this emission scenario is referred to as WSS1 hereafter. In total, 15 days (10-1-2008 to 10-15-2008) were simulated assuming this scenario.

In a second sensitivity study on "woodstove replacement", we determined the emissions remaining from wood-burning after the replacement of non-certified devices by assuming the number of wood-burning devices that became available from a draft by the Sierra Research Laboratories (SRL) group. This data based on a survey of 300 households in the nonattainment area carried out by SRL. The number of wood-burning devices reported in the draft and in the final report by *Carlson et al.* [2010] is lower than the estimates used in *Davies et al.*'s [2009] report. Note that there is high uncertainty in the actual number of wood-burning devices that exist in the nonattainment area [*Conner* 2011; pers. communication]. The draft SRL report did not include pellet stoves. *Carlson et al.*'s [2010] data only provide the total of certified woodstoves, but not the split between certified woodstoves with catalytic and non-catalytic equipment. We assumed the same emission rates for both. Again, we calculated the emissions from residential wood combustion, subtracted the contribution from non-certified devices

(assumed to be replaced) and added the contribution that the certified device (that replaced the non-certified devices) would have. The simulation performed using the emission scenario obtained this way is called WSS2 hereafter. We run this set of “woodstove-replacement” simulation from 10-01-2008 to 10-17-2008.

The final SRL report by *Carlson et al.* [2010] included pellet stoves as a separate category in the wood-burning sector. For the third “woodstove replacement” simulation, we determined the emissions remaining from wood-burning after the replacement of non-certified devices by assuming the number of wood-burning devices that were given in *Carlson et al.*'s [2010] final report. Using these numbers, we calculated the emissions from residential wood combustion, subtracted the contribution from non-certified devices (assumed to be replaced) and added the contribution that the certified device (that replaced the non-certified devices) would have. *Carlson et al.*'s [2010] data only provide the total of certified woodstoves, but not the split between certified woodstoves with catalytic and non-catalytic equipment. We assumed the same emission rates for both. A full winter simulation was performed assuming this emission scenario. This simulation is called WSR hereafter (Table 1).

Figure 8 exemplarily shows the hourly emission rates from all heating sectors for the Fairbanks area prior to and after the assumed three different “woodstove-replacement scenarios”. In all “woodstove-replacement scenarios”, we considered the impact on emissions of all species, not only $PM_{2.5}$.

The policy options recommended by *Davies et al.* [2009] estimated to reduce $PM_{2.5}$ emissions from residential heating from 874 tons/year to 422 tons/year, or 52% for their base year. The “woodstove replacement” scenario assuming *Davies et al.* [2009] numbers of wood-burning devices reduces the emissions for 2008 to 40%, while those with the SRL draft and *Carlson et al.*'s [2010] numbers reduce the emissions much less (Fig. 8). Note that changing out non-certified wood-burning devices to certified ones would reduce theoretically both primary and secondary $PM_{2.5}$ emission at the same order. In *Davies et al.* [2009], $PM_{2.5}$ accounts for both primary and secondary aerosol that forms after the emissions. WRF/Chem considers primary $PM_{2.5}$ from emissions and calculates the secondary $PM_{2.5}$ that builds in stacks and in air [*Peckham et al.*, 2009].

Note that if primary $PM_{2.5}$ emission were reduced greatly by changing noncertified wood-burning devices to oil furnaces, the secondary $PM_{2.5}$ emission might increase. Oil furnaces namely have higher emission rates of SO_x and NO_x than wood-burning devices. SO_x and NO_x are the main precursors of secondary $PM_{2.5}$ that forms through gas-to-particle conversion. Therefore, exchanging noncertified wood-burning devices to oil furnaces with current fuel sulfur content will be less effective in reducing $PM_{2.5}$ emission than exchanging them with certified wood-burning devices.

Obviously there is uncertainty in our study due to the unknown number of woodstoves that exist and that can be replaced. Unfortunately, no data were available, where what wood-burning devices are operated and when they were operated and how they were operated and how often. We simply assumed the distribution of wood-burning devices to be proportional to the distribution of population density. This assumption holds uncertainty in the spatial distribution that may affect local maximum concentrations as well as 24h-averages of $PM_{2.5}$ concentrations. *Fortun and Mölders* [2009] showed that uncertainty in the diurnal course of emission marginally affects the 24h-average $PM_{2.5}$ concentrations. However, uncertainty in the spatial distribution can

provide notable differences in the 24h-average $PM_{2.5}$ concentrations. Sensitivity studies on the emissions indicate that uncertainty in emission rates also results from the unknown partitioning of the use of wood-burning and other heating devices in households having more than one heating option. Note that the simulations on “woodstove replacement” do not consider that additional wood-burning devices have been added since 2008.

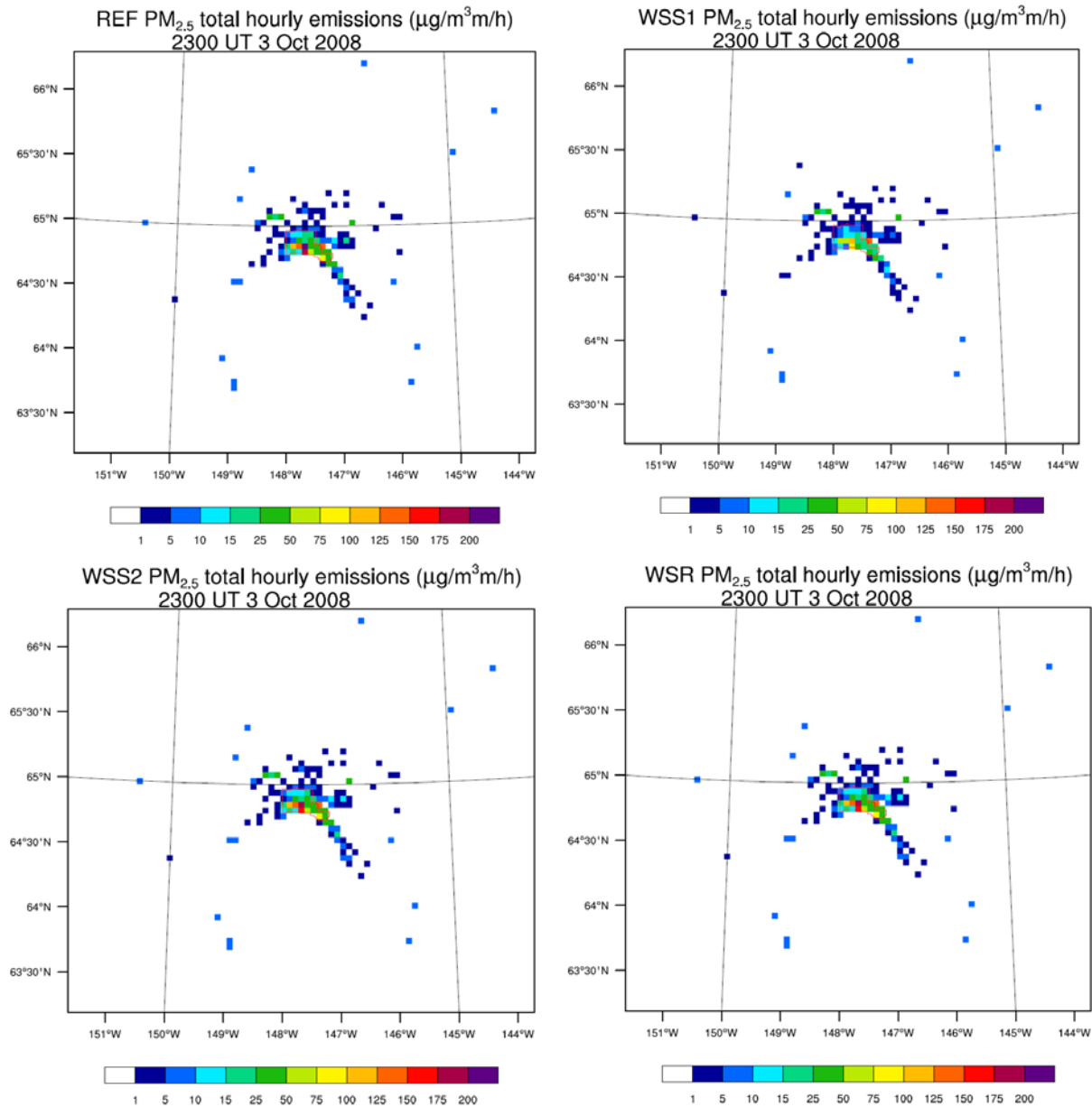


Fig. 8. Emissions of $PM_{2.5}$ as obtained with AkEM (upper left to lower right) before (REF) and after the assumed “woodstove replacement” assuming *Davies et al.*’s [2009] (WSS1), SRL’s draft report (WSS2), and *Carlson et al.*’s [2010] (WSR) data on the numbers of heating devices. All “woodstove-replacement scenarios” result in reduced emissions over the nonattainment area. The nonattainment area is schematically superimposed in red.

As pointed out above, there is uncertainty in any emission data. This uncertainty is related to the approaches used and assumptions made. *Davies et al.* [2009] developed the emission rates for wood-burning devices using the operation-emission limits of the device (grams/hour) issued by EPA multiplied with the total hours of heating per year per household. Doing so, provided a

PM_{2.5}-emission rate of 60lb/yr.hh for noncertified and of 17lb/yr.hh for certified woodstoves. *Carlson et al.* [2010] list the amount of wood used annually as 3.95 cords wood/yr.hh. If one takes the EPA AP-42 emission factors of noncertified and certified woodstoves (30.6 and 14.6lb/short tons of dry wood, respectively), one obtains for the emission rates of noncertified and certified woodstoves 145lb/yr.hh and 69lb/yr.hh, respectively. *Davies et al.*'s [2009] study is based on heating hours and emission limits, while *Carlson et al.*'s [2010] study is based on fuel used. This means *Davies et al.*'s [2009] and *Carlson et al.*'s [2010] studies use different approaches. We used the AP-42 emission factors to compare their data. Depending on the approach, one will for each replaced woodstove reduce the emissions by (60-17) lb/yr.hh = 43lb/yr.hh and (145-69) lb/yr.hh = 76lb/yr.hh, respectively.

We used *Davies et al.*'s [2009] emission-rate data for all wood devices and oil furnaces as requested by the FNSB, but used *Carlson et al.*'s [2010] data for number of devices. Note that using this data seemed to be "safer" because the amount of reduction in response to a "woodstove replacement" program is smaller than using *Carlson et al.*'s [2010] emission rates. This means that the relative response factors that we obtained from our "woodstove replacement" simulations may underestimate the actual reduction that a woodstove replacement program can provide. In the sensitivity study WSS1, we used EPA's data for the "others" category, as data for these devices were not included in *Davies et al.*'s [2009] report. In the sensitivity study WSS2, we used *Carlson et al.*'s [2010] number of devices without consideration of pellet-stoves.

4.2.3 Emission scenario for introduction of low sulfur fuel for heating oil and power generation and other oil-burning point sources

The third scenario (LSF) represents a measure that aims at mitigation of PM_{2.5} concentrations indirectly by reduction of precursors. As pointed out above sulfur can contribute to PM_{2.5} formation in the atmosphere. Thus, the third emission scenario performed for winter 2008/09 assessed the impact of the introduction of low sulfur fuel for use as heating oil and in oil-burning power plants and other point-sources on the PM_{2.5} concentrations at breathing level. The target emission categories that we considered in the "low sulfur fuel" scenario are heating oil, point source facilities and power plants that burn oil. The emissions from domestic and industrial combustion (including power plants) used in the reference simulation (REF) represent the emissions from relatively sulfur-rich fuel.

In the LSF simulation, the emissions from all sectors were kept the same as in the reference simulation except for emissions from domestic heating with heating oil, and oil-burning point sources and power plants with sulfur-rich fuel. The emissions from these sectors were replaced by emissions one would obtain with low sulfur content fuel for the same combustion amount.

To determine the amount of emission reduction due to a change from high to low sulfur-content fuels we reviewed the literature. Since the fuel-sulfur content may affect other emissions than just PM_{2.5}, we adjusted the emissions of these other species as well. Doing so is required as particles and hence PM_{2.5} may form due to gas-to-particle conversion from various species as explained earlier.

NESCAUM [2005] reported the emission reduction due to reducing the sulfur content of No. 2 distilled heating oil from 2,000-3,000ppm to 500ppm for SO₂, PM and NO_x as 75%, 80% and 10% respectively. In our study, we assumed the same transition of sulfur content in heating fuel in Fairbanks, and applied the same reduction found by *NESCAUM* [2005]. Since no reduction

benefits were reported for VOC and CO, we assumed that lowering of sulfur content in heating oil does not affect the VOC and CO emissions.

From personal communication with several power-plant operators in the FNSB, we learned that almost all power plants in the FNSB are burning No. 2 fuel oil having sulfur content about 4,000ppm. This fuel is similar to the fuel used for household heating. For the LSF simulations, we modified the point-source emissions with respect to low sulfur-fuel emissions for those oil-burning facilities that did not yet use low sulfur fuel already.

To our best knowledge, no report exists on the effects of low sulfur-fuel usage on the emissions of power plants. Therefore, we assumed a similar transition of sulfur content in heating fuel in the FNSB as reported in *NESCAUM* [2005] and applied the reduction given for power plants. Note that the actual reduction would be higher than the assumed reduction since the emission control devices in power plants become more effective as the sulfur content decreases.

In the low sulfur fuel (LSF) scenario, the emission reductions due to low sulfur fuel are only applied to those power plants and point sources that burn No. 2 fuel oil. For these facilities, a reduction rate of 75%, 80% and 10% was applied to the SO_x , PM and NO_x emissions, respectively. For power plants burning both fuel oil and coal, only emissions from burning oil were subject to the emission reduction. We only got the break-down of the fuel-type consumption for the UAF power plant. Since the UAF power plant works on economic principles as the other power-plant operators do, we assumed a similar break-down of fuel types used for those facilities that burn different fuel types. No changes in emissions were made for power plants burning only coal.

4.3 Analysis methods

We compared the results of the simulations performed with modified emissions with the results of their respective reference simulation to assess the impact of the various emission mitigation measures or the contribution of point-source emissions on the $\text{PM}_{2.5}$ concentrations in the nonattainment area and in the grid-cell holding the FNSB official measurement site. This site is located on top of the State Building.

We used the Student t-test [*von Stroch and Zwiers*, 1999] to test the $\text{PM}_{2.5}$ -concentration differences between REF and NPE for winter 2005/06, and REF and WSR or LSF for winter 2008/09 for their statistical significance at the 95% confidence level. The null hypothesis was that concentrations in REF and NPE, or REF and WSR or REF and LSF do not differ. In the following, we only use the word significant when data fail to pass this test.

Note that from a scientific point of view, it is important whether an emission source causes significant differences in the $\text{PM}_{2.5}$ -concentrations. However, from a regulation point of view it is not of relevance whether or not, an emission source contributes significantly (in a statistical sense) to the concentrations of $\text{PM}_{2.5}$. Instead, it is important whether the emission-sources' contributions are the main contributor, i.e. dominate the concentration values, and whether reducing the emissions of these sources may lead to compliance.

If a certain kind of emission sources is the dominating one, regulation on the emission may help solve the exceedance problem. Here again distinctions have to be made. An emission source far away from the nonattainment area and/or far away from any settlements will typically dominate the concentrations in its surroundings, as it is most likely the only emission source out there. Thus, the large percentage contribution of such an emission source will not be worrisome as long

as the concentrations do not exceed the NAAQS. If an emission source is located in an unpopulated area close to populated areas, its contribution also may percentagewise be the main contributor. Then one has to consider how large the impact is on the adjacent populated areas and whether this impact leads to exceedances of the NAAQS. These facts have to be kept in mind in the following discussion.

For all scenarios, we determined the relative response factors and new design values.

4.3.1 Analysis of point source contribution

Differences between the highest 24h average $PM_{2.5}$ -concentration obtained by REF and NPE were investigated to assess the impact of PS-emissions on the $PM_{2.5}$ -concentrations at breathing level. The number, frequency and locations of grid-cells with 24h-average $PM_{2.5}$ exceedances were determined for both simulations to assess the contribution of PSs to exceedances. In addition, we examined the radius of impact of the point sources on the $PM_{2.5}$ concentrations at breathing level. Grid-cells affected by PS-emission will have non-zero $PM_{2.5}$ -concentration difference between REF and NPE. Therefore, the influence of PS-emissions on the $PM_{2.5}$ -concentration at breathing level was investigated by analyzing the correlation between the PS-emissions at each emitting level with the $PM_{2.5}$ -concentration-difference. In the domain of interest, 27 PSs emit into the second (8-16m) to the seventh model layer (343-478m) due to plume raise.

The impact of each individual PS on the perturbation of $PM_{2.5}$ -concentration is difficult to identify unambiguously because in WRF/Chem, like other photochemical models, all PSs located within the same grid cell are lumped but emit into the levels into which the individual PSs would emit. After lumping, there are nine grid columns holding PSs. Due to the lumping we cannot investigate individual PS impacts on $PM_{2.5}$ -concentration at breathing level, but the cumulative impact of all PSs within a grid-column on the downwind $PM_{2.5}$ concentrations of that column. We examined the impact for each grid column holding PSs and denote these PS1 to PS9, hereafter. See Figure 14 for locations.

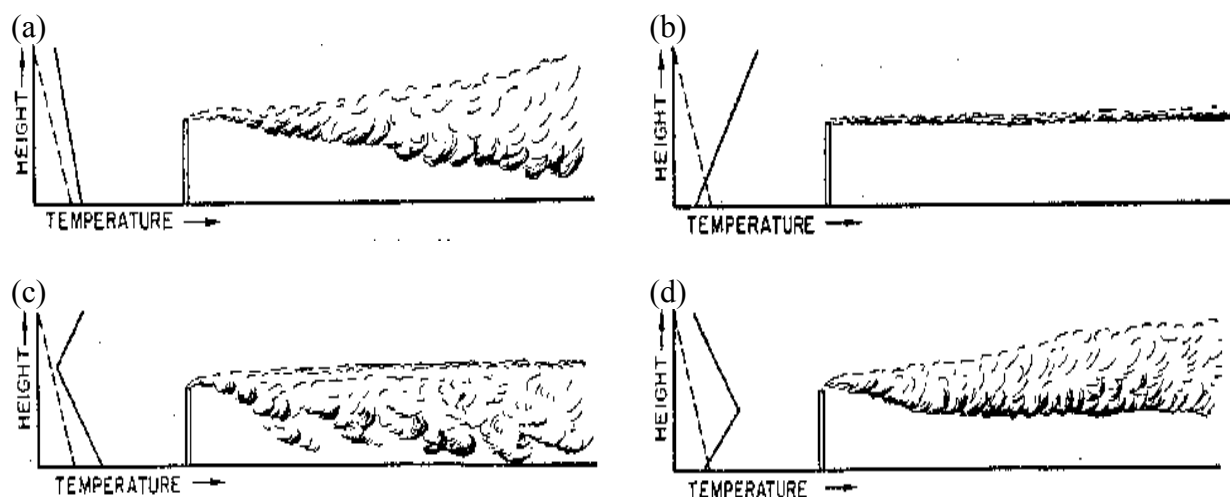


Fig. 10. Schematic view of temperature profiles and plume behavior for emissions in the case of (a) no inversion layer, (b) into an inversion layer, (c) below an inversion layer, and (d) above an inversion layer. From: <http://www.iitap.iastate.edu/gcp/acid/images/plume.gif>.

We only considered the $PM_{2.5}$ -concentration-difference distribution at grid cells located downwind of a grid-cell with PSs. At each PS1 to PS9, we used the wind direction from the first level above ground to the uppermost emitting level to identify the downwind grid cells of each level in each simulation hour. This treatment ensured that not all grid cells around the PSs, but only the grid cells impacted by the PS are considered. These $PM_{2.5}$ -concentration-difference values were used to calculate the correlation with the PS-emissions for November to February (NTF). All correlations were tested for their statistical significance at the 95% or higher confidence level using a Student-t test.

PSs in the downwind sectors of a PS-holding column may affect the $PM_{2.5}$ -concentrations in its downwind. Therefore, the correlation behavior of each PS1 to PS9 was investigated under consideration of potential impacts by other PS holding grid-columns. As atmospheric temperature inversion and wind speed affects the dispersion of the PS emissions, we investigated separately the correlation between PS-emissions and $PM_{2.5}$ -concentration-difference for different wind-speed classes at the emitting level and under conditions when PSs emitted below, above and into inversion layer (Fig. 10). We applied different time lags in determining the correlations to account for the lag in time between the actual emission and the time when the $PM_{2.5}$ reaches the downwind grid-cells at breathing level.

4.3.2 Analysis of the “woodstove replacement” scenario

We used the Student t-test to examine the $PM_{2.5}$ -concentration differences (REF-WSR) for their significance at the 95% level of confidence. To verify that the differences are really due to replacing “woodstoves”, we adopted a False Ensemble Analysis method (FEA) which was developed and applied successfully in climate model data analysis [Carpenter *et al.*, 1989; Werth and Avissar, 2002]. We performed the analysis for each month of the REF and WSR simulations. First, the true difference of 24h-average $PM_{2.5}$ -concentration between REF and WSR was determined for each month. Secondly, a set of false “REF” and “WSR” ensembles was created by randomly replacing results of simulation days of REF (WSR) with the results of the corresponding simulation days of WSR (REF). Because the emission strengths are allocated depending on the hour of the day, day of the week and month of the year, and daily mean temperature [Mölders, 2010], each randomly selected REF-day had to be replaced by the corresponding WSR-day. In this way, emissions only differ with respect to the emission changes in response to the wood-burning devices exchanged. A random generator was used to create an index array, which days of the month were to be chosen to create the false ensemble, and REF (WSR) files were replaced accordingly. The replacement was completed as the number of WSR (REF) simulation days makes up 50% of the total days of the false “REF” (“WSR”) ensemble by which the false “REF” and “WSR” can be considered as having no net difference in the mean emission.

Theoretically, $n!/[(n/2)!] \times 2$ numbers of false ensembles can be generated from n simulation days in the way described above. However, considering the time constrains and computational limitation, we generated 400 false “REF-WSR” ensembles randomly for each month. For each set of false “REF” and “WSR” ensemble the difference of 24h-average $PM_{2.5}$ -concentration was determined as was done for the true difference REF-WSR. Finally, the true and 400 false concentration differences were ranked. The above procedure was applied for each grid cell. If at a grid cell, the true difference falls in the top 5% of all values, we can conclude that the true $PM_{2.5}$ -concentration difference is real, i.e. the “woodstove replacement” actually reduced the $PM_{2.5}$ -concentration in the grid cell of interest.

4.3.2 Analysis of the “low sulfur” scenario

Emissions of PM_{2.5}, PM₁₀, SO₂, NO and VOC from the current sulfur content fuel (REF) and the use of low sulfur fuel (LSF) were analyzed and compared on a monthly and daily basis. Note that these pollutants were selected as they are primary particular matter and precursors for secondary aerosols, i.e. they can affect the PM_{2.5}-concentrations at breathing level. Since the emissions were considered temperature-dependent, the mean temperatures and their deviation from the long-term mean temperature were analyzed and used to elucidate the variations in emission reductions.

Concentrations of PM_{2.5} and other pollutants (PM₁₀, sulfate, nitrate, VOC) in the nonattainment area obtained by REF and LSF were compared. The monthly, daily, and hourly variations of PM_{2.5}-concentration reductions after introduction of low sulfur fuel were quantified and analyzed. The variations in the aerosol composition were also identified. Furthermore, mean meteorological quantities (temperature, dewpoint temperature, relative humidity, wind-speed, shortwave radiation fluxes, atmospheric boundary layer height, precipitation and cloudiness) were used in the analysis of PM_{2.5}-concentration reductions as there were feedbacks of aerosols on the meteorology.

Furthermore, we also applied the FEA to the REF and LSF data.

5. Evaluation

As pointed out above, we used the results of the WRF/Chem simulations of the first 15 days October 2005 for calibration. Within the framework of another project, WRF/Chem was evaluated by data from a Doppler Sound Detection And Ranging (SODAR) device, twice-daily radiosondes, 33 surface meteorological and four aerosol sites [Mölders *et al.* 2011].

The evaluation used the following performance skill-scores (root-mean-square error [RMSE], bias, standard deviation of error [SDE], correlation coefficient [R]) following *von Storch and Zwiers* [1999] for the meteorological quantities, and the fractional bias ($FB = (\overline{C_s} - \overline{C_o}) / [0.5(\overline{C_s} + \overline{C_o})]$), normalized mean-square error ($NMSE = (\overline{C_s} - \overline{C_o})^2 / (\overline{C_s} \cdot \overline{C_o})$), geometric mean bias ($MG = \exp(\ln \overline{C_s} - \ln \overline{C_o})$), and the fraction of simulated concentrations C_s being within a factor of two of the observed concentrations C_o (FAC2) following *Chang and Hanna* [2004] for the chemical quantities. These are standard measures typically used in the evaluation of photochemical models and hence allow us to assess how good the Alaska adapted WRF/Chem performs for Alaska winter relative to models applied for cases in mid latitudes.

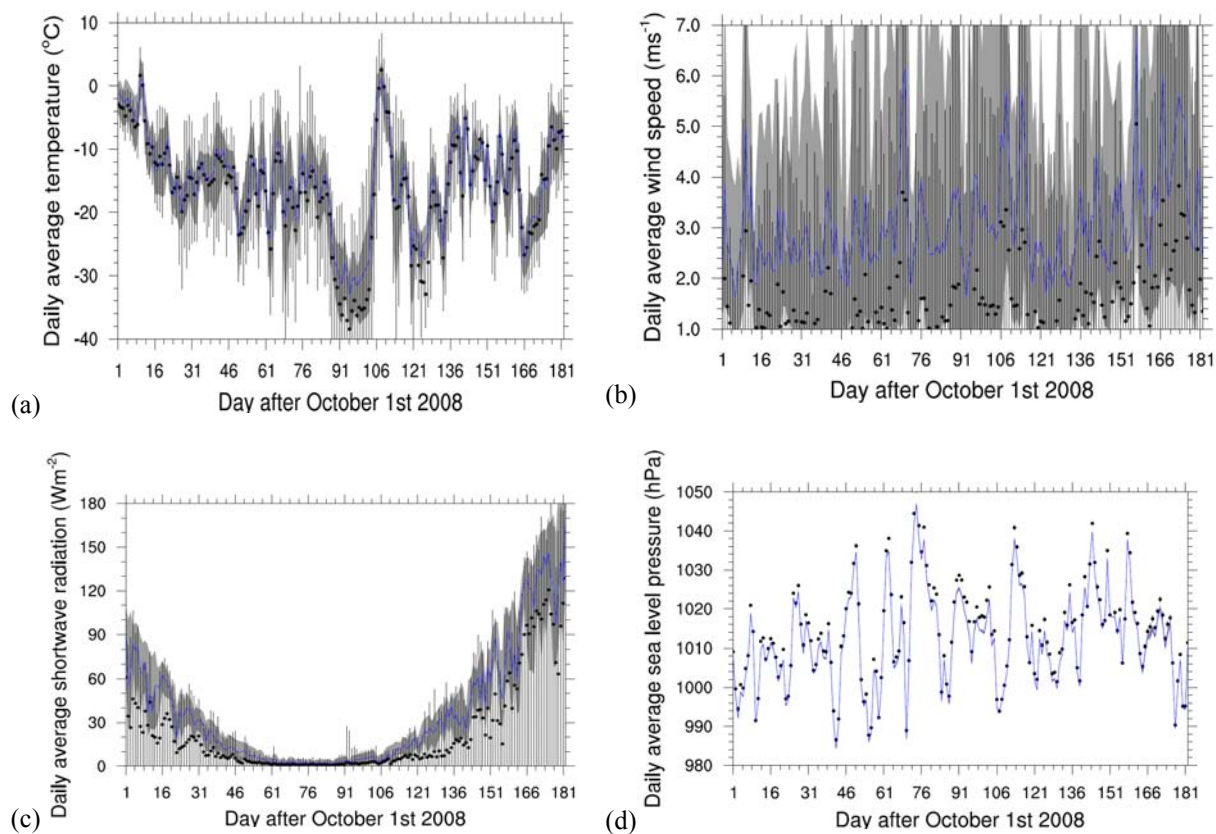


Fig.11. Temporal evolution of daily averaged of (a) air-temperature, (b) wind-speed, (c) downward shortwave radiation, and (d) pressure averaged over all sites for which data were available as simulated (blue line) and observed (dots). Plots for dewpoint (not shown) and air-temperatures look similar. Grey-shading and vertical bars indicate variance of simulated and observed quantities, respectively. Note that there were only two sites with pressure data Fairbanks International Airport and Eielson Air Force Base. Due to their relative close location, there is not much spatial variance. Therefore, no bars on the spatial variance of pressure are plotted.

All our simulations were run in "forecast" mode, i.e. no nudging or data assimilation was applied. *Mölders et al.* [2011] found that biases determined based on all available data from the 33 sites over NTF are 1.6K, 1.8K, 1.85m/s, -5° , and 1.2hPa for temperature, dewpoint temperature, wind-speed, wind-direction, and sea-level pressure, respectively, in NTF 2005/06. Figure 11 shows the average temporal evolution of simulated and observed meteorological quantities as obtained for October 2008 to March 2009 (OTM) on average over all 23 sites within the domain of interest for which data were available for that time. Note that there were less meteorological sites operating in the area covered by the domain of interest for analysis in winter 2008/09 than 2005/06. Over OTM 2008/09, the overall biases over all sites are 1.3K, 2.1K, 1.55m/s, -4° , and -1.9hPa for temperature, dewpoint temperature, wind-speed, wind-direction, and sea-level pressure, respectively. The 2005/06 temperature bias is only marginally higher than that reported by *Gaudet and Staufer* [2010] for their WRF short-term study with a 4km grid increment performed for Fairbanks using data assimilation. The wind-speed RMSE is slightly higher than the RMSE reported for their short study. Note that it is relatively easy to optimize a model for a short period of several days, while it is rather difficult to achieve a generally acceptable performance over an episode as long as four or six months like in our study.

The evaluation by means of SODAR-data revealed that WRF/Chem slightly over(under)estimates wind-speed in the lower (upper) ABL. WRF/Chem captures the frequency of low-level jets well, but overestimates the strength of moderate low-level jets [*Mölders et al.* 2011].

As aforementioned there are hardly any chemical data available for winter 2005/06. While $PM_{2.5}$ concentration data exist only at two sites (Fairbanks State Building, Denali Park) for winter 2005/06, measurements exist at 12 sites in Fairbanks for winter 2008/09. Based on the limited data available WRF/Chem simulated the maximum $PM_{2.5}$ -concentration about 6% too low for winter 2005/06. Data from four aerosol sites suggest large underestimation of PM_{10} , and NO_3 at the remote sites outside of the nonattainment area and underestimation of $PM_{2.5}$ at the State Building in winter 2005/06 [*Mölders et al.* 2011].

Averaged over the two $PM_{2.5}$ - and SO_4 -sites, 41% and 50% of the simulated values, respectively, fell within $\pm 50\%$ of the observed concentration value for winter 2005/06. The low data density – for 2005/06 only one $PM_{2.5}$ observational site exists in the nonattainment area – may falsely indicate errors due to local effects [*Mölders et al.* 2011].

The hourly $PM_{2.5}$ evaluation of winter 2008/09 shows that 29%, and 36% of the simulated and observed concentrations agree within $\pm 50\%$ for the fixed sites FNSB (site at the State Building), and Peger Road, respectively. The performance for the 24h-average $PM_{2.5}$ is better – 46% of the fixed sites agree within $\pm 50\%$. At the FNSB State Building, Peger Road, North Pole, Sadler and Denali site 35%, 58%, 38%, 39% and 58% of the simulated 24-average $PM_{2.5}$ concentrations are within $\pm 50\%$ of the observations, respectively. The scientific community considers photo-chemical models with fractional biases within $\pm 30\%$, random scatter being within a factor of two or three of the mean, and 50% of the predictions falling within a factor of two of the observations to perform well [e.g. *Chang and Hanna* 2004]. Thus, our WRF/Chem simulations for 2005/06 fall in the lower end of acceptable performance, while those for 2008/09 are slightly better. The better performance for 2008/09 than 2005/06 may be due to the introduction of a temperature-dependency of traffic, power generation and domestic heating emissions in AkEM in response to the evaluation for 2005/06.

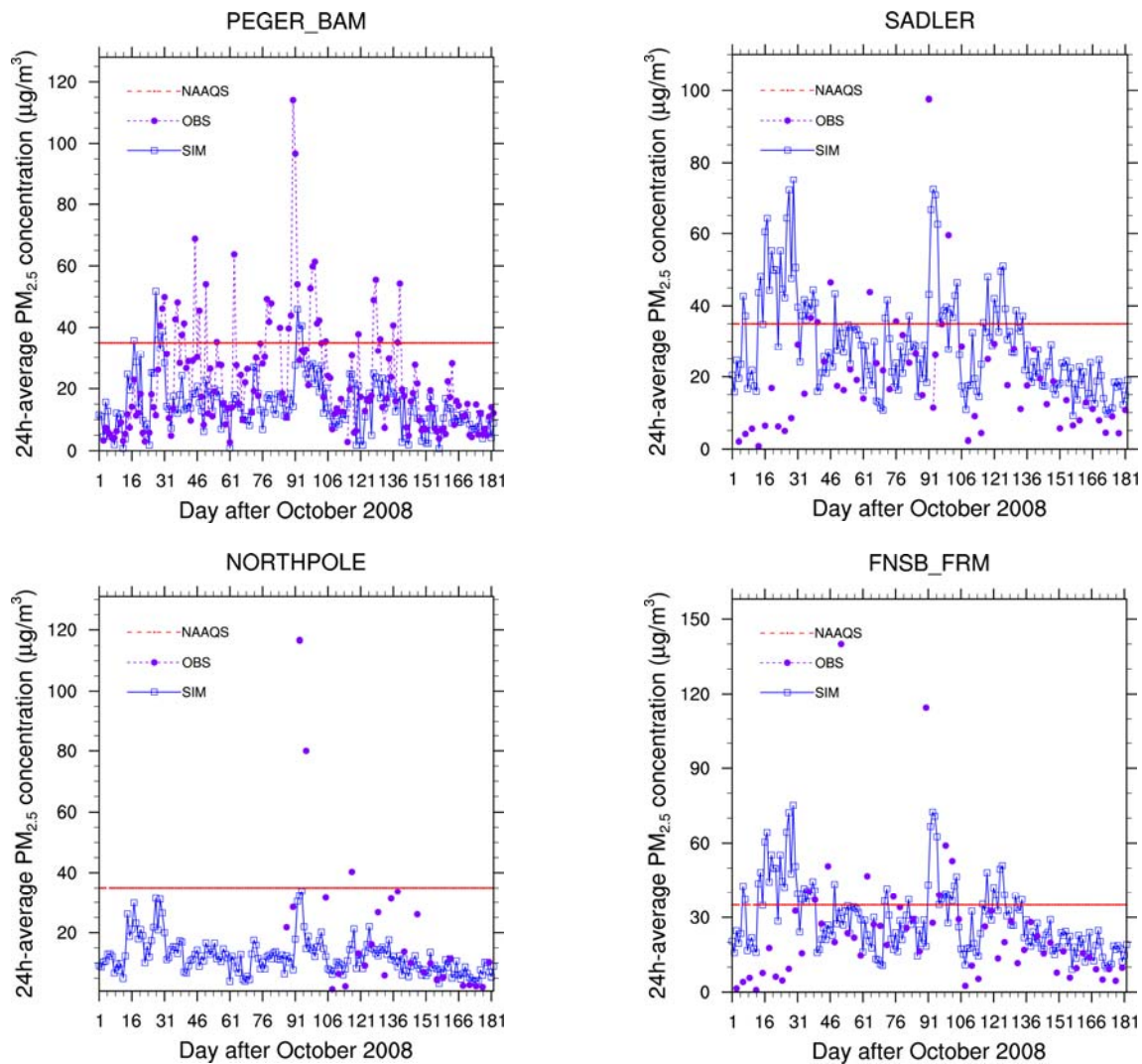


Fig. 12. Comparison of simulated and observed concentrations as obtained for winter 2008/09 for various sites. FNSB is the site at the State Building.

The evaluation of both winters indicates that WRF/Chem captures the temporal evolution of PM_{2.5} concentrations well except during sudden temperature changes, underestimation of inversion-strengths and timing of frontal passages (e.g. Fig. 12). In October, WRF/Chem underestimates the PM_{2.5} concentrations appreciably at all sites for which data are available. This behavior suggests that the assumed emissions for October 2008 are too low. Note that there are hardly any Alaska specific emission allocation functions. We used the allocation functions recommended by EPA for Alaska, which we modified to avoid obviously unreasonable emissions (e.g. emissions from lawn mowing in October), when no Alaska specific allocation functions could be obtained.

Errors in PM_{2.5}-concentrations relate strongly to temperature errors, i.e. to WRF rather than its chemical package [see also Mölders *et al.* 2011]. In October 2008, WRF/Chem underestimates the concentrations strongly at some sites (e.g. Sadler). It should be examined whether emissions are underestimated in October. On the contrary, in other months simulated and observed concentrations agree better in magnitude. The discrepancies found may also result from

channeling effects in streets or slight offsets of dispersion plumes. The occasional much higher observed than simulated concentrations are most likely due to contamination of the measurements by mobile sources at the site (e.g. busses idling at the Peger site upwind of the sampler). All these discrepancies are common in and known to occur for all photochemical models of the scale deployed here [e.g. *Chang and Hanna, 2004*].

The evaluation of winter 2005/06 suggested that simulated PM_{2.5}-concentrations may be slightly too low on average over the polluted and unpolluted site. However, averaging of polluted and non-polluted sites may be misleading due to the strong concentration differences of polluted and non-polluted sites. In both winters, WRF/Chem seems to overestimate the concentration slightly at the polluted sites. In winter 2005/06 and 2008/09, the mean biases over all available sites are 4.2 and 4.0 μg/m³, respectively. However, this bias affects the reference as well as the simulations with the emission scenarios. Since we are examining concentration differences in this study, the impact of the aforementioned errors can be considered as small.

6. Results

We examined the meteorological conditions on days with $PM_{2.5}$ exceedances. We found three distinct local circulation patterns at breathing level and five different circulation patterns higher above ground between 100 and 200 m that lead to exceedances of the NAAQS at breathing level (Fig. 13). If at breathing level, wind is very calm ($<1\text{m/s}$) and comes from various directions and the air remains in town, local exceedances will occur within the nonattainment area. The same will be true if slight drainage of the Fairbanks air occurs towards southwest, down the Tanana Valley or if air moves into town from southeast under calm wind conditions in Fairbanks. Obviously, in this case, advection of polluted air from the Salcha air shed and North Pole can contribute to causing the exceedances.

Exceedances are also related to what happens at heights between 100 and 200m or so. If at these levels, air moves out of town slowly down the Tanana Valley, air slowly travels through Fairbanks down the Tanana Valley, air moves towards North Pole and Eielson Air Force Base up the Tanana Valley, or air drains to both sides of the Tanana Valley (Fig. 13), exceedances will occur at some places in the nonattainment area at breathing level. This behavior is especially true when at the same time, winds are relatively calm over Fairbanks or the air circulates slowly over the town.

In the following, $PM_{2.5}$ -concentrations at breathing level are discussed if not mentioned otherwise.

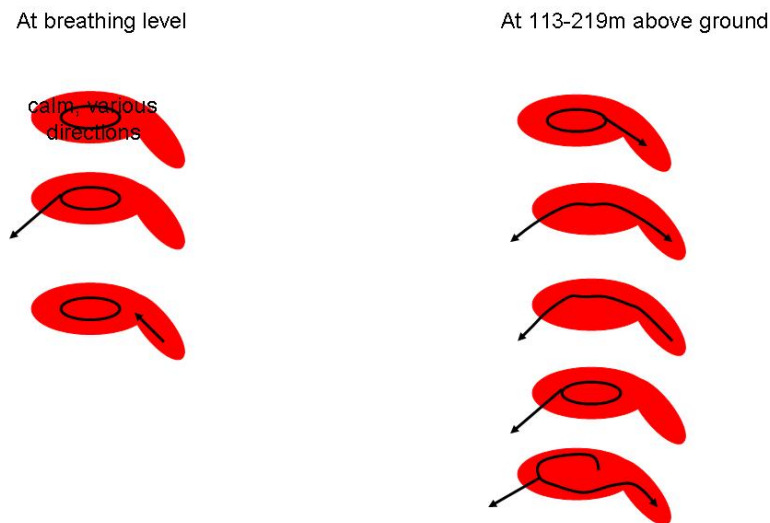


Fig. 13. Circulation pattern associated with violations at breathing level. The red area schematically illustrates Fairbanks, North Pole and Salcha air sheds. Wind-speeds must be very low.

Note that winter 2008/09 except for February and in particular October 2008 were colder than the 30-year average (Table 3).

Table 4 compares the results of the WSR, LSF and REF simulations. The results suggest that in October 2008, January, February and March 2009 the assumed “woodstove replacement” yields a stronger reduction of the $PM_{2.5}$ -concentrations at breathing level than the introduction of low sulfur fuel. In November and December 2008, introduction of low sulfur fuel, on average,

provides the higher mitigation of the PM_{2.5}-concentrations. The results suggest that “woodstove replacement” provides a temporally more constant percentage reduction of around 6% averaged over the nonattainment area than does the introduction of low sulfur fuel (Table 4).

Table 3. Monthly mean temperatures at Fairbanks International Airport in Fahrenheit. Courtesy to *H. Angelhoff* [2011]. The 30-average for 1971-2000 is taken from *Shulski and Wendler* [2007]. Values for the episode simulated in this study are high-lighted.

	Oct	Nov	Dec	Jan	Feb	Mar	Oct-Mar
2007	21.2	11.5	-3.4	-6.6	-6.7	-6.5	1.6
2008	15.1	-1.4	-7.8	-9.2	-5.9	15.4	1.0
2009	30.7	-1.2	-2.8	-12	-1.5	5.6	3.1
2010	27.5	11.9	-17.9	-13.7	2.9	10.8	3.6
2007-2009	22.3	3.0	-4.7	-9.3	-4.7	4.8	1.9
2008-2010	24.4	3.1	-9.5	-11.6	-1.5	10.6	2.6
1971-2000	24	2	-6	-10	-4	11	2.8

Table 4. Monthly average PM_{2.5}-concentration as obtained for the grid-cell holding the State Building and averaged over the nonattainment area for October 2008 to March 2009. The percentage reduction is given in brackets.

	PM _{2.5} (µg/m ³)						
	REF	State Building			Nonattainment area		
		WSR	LSF		REF	WSR	LSF
OCT	40.2	38.5 (4.2%)	39.2 (2.5%)	12.9	12.2 (5.4%)	12.5 (3.1%)	
NOV	30.3	28.8 (5.0%)	28.5 (5.6%)	11.0	10.3 (6.3%)	10.0 (9.0%)	
DEC	25.8	24.5 (5.0%)	24.4 (5.4%)	9.2	8.6 (6.5%)	8.5 (7.6%)	
JAN	33.9	32.2 (5.0%)	32.7 (3.5%)	11.0	10.3 (6.4%)	10.4 (5.5%)	
FEB	27.1	25.5 (5.9%)	26.0 (4.1%)	9.8	9.2 (6.1%)	9.3 (5.1%)	
MAR	17.1	16.1 (5.8%)	16.2 (5.3%)	5.7	5.3 (6.4%)	5.3 (7.0%)	

6.1 Impact of point-source emissions

This section discusses findings from the simulations performed for winter 2005/06. See Table 1 for details on the simulations.

The influence of emissions from elevated point sources on the PM_{2.5} concentration at breathing level was investigated by analyzing the correlation between the PSs' emissions at each level with the PM_{2.5}-concentration at the breathing level. The highest effective level reached by the plume from point-source emissions is the model layer representing the conditions between 343 and 478m. Note that the buoyancy, depending on temperature of the plume, velocity at release etc. and the environmental conditions, determine which levels the emissions from PSs can reach.

Table 5. Monthly average of PM_{2.5}-concentration at the State Building and averaged over the nonattainment area as obtained from the simulations for winter 2005/06. The percentage reduction is given in brackets.

	PM _{2.5} (µg/m ³)				
		State Building		Nonattainment area	
		REF	NPE	REF	NPE
NOV	30.5	29.2 (4.2%)	14.4	13.4 (6.9%)	
DEC	26.4	25.4 (3.8%)	12.5	12.0 (4%)	
JAN	40.9	39.7 (2.9%)	15.9	14.9 (6.3%)	
FEB	21.6	20.9 (3.2%)	9.6	9.2 (4.2%)	

Since no emissions from PSs are considered in NPE, the monthly total emission strength does not differ between REF and NPE from November 2005 to February 2006 except at the locations of the PSs. Since most of the PS and the strongest PSs are located in the highly populated

Fairbanks area, here the largest differences between REF and NPE in emissions as well as concentrations occur. Emission and concentration differences are larger in December and January as during these months emissions from PSs are higher than in November and February. The majority of the PSs are facilities that emit more in December and January to cover the higher heating and/or energy demands during the darker, colder December and January than the relatively warmer and less dark November and February.

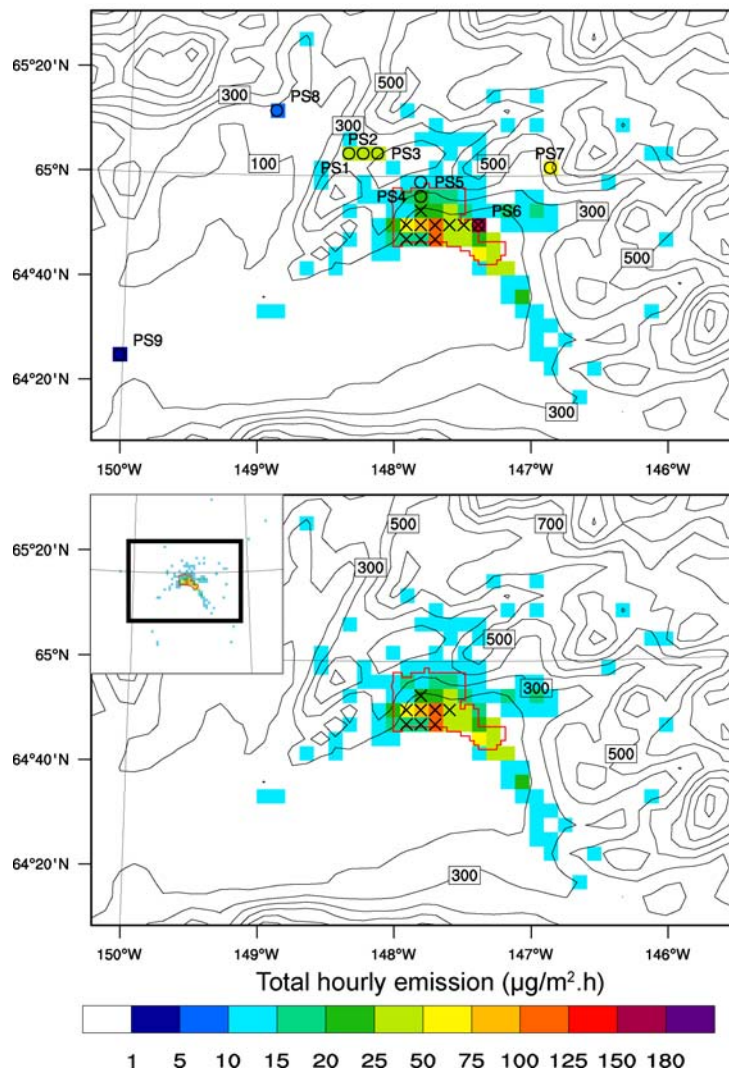


Fig. 14. Zoom-in on the spatial distribution of areas experiencing $PM_{2.5}$ -concentration exceeding the NAAQS (grid cells with crosses) in REF (top) and NPE (bottom) exemplarily superimposed on the map of total hourly emission on 0200 UTC December 1, 2005. The black box indicates the location of the zoom-in area. PS1 to PS9 indicate locations of grid columns with point sources.

$PM_{2.5}$ -concentration obtained by REF and NPE differ hardly with respect of the number of NAAQS exceedances. Within the domain of interest, the NAAQS is exceeded 10 (7), 6 (5), 22 (21) and 1(1) times in REF (NPE) in November, December, January, and February, respectively. The locations of exceedances within the nonattainment area are identical in both REF and NPE except at PS6 and the adjacent grid cell to its west (Fig. 14). Except for two events in November

2005 in REF, the grid-cell holding the State Building monitoring station experienced exceedances on all exceedance events in REF and NPE.

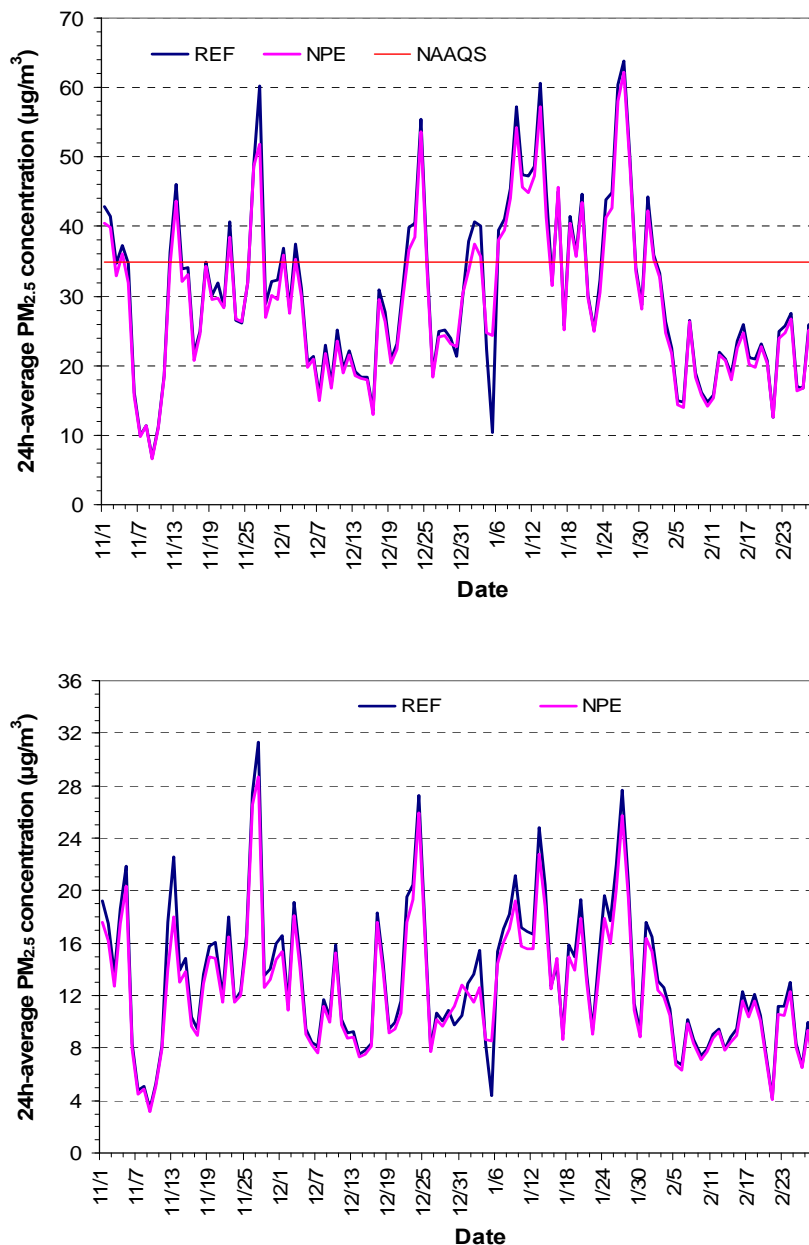


Fig. 15. Temporal evolution of 24h PM_{2.5}-concentrations as obtained for the grid-cell that holds the State Building (top) and the 24h PM_{2.5}-concentration averaged over the nonattainment area (bottom) for the simulations with (REF) and without (NPE) inclusion of point sources. NAAQS is the National Ambient Air Quality Standard of 35µg/m³.

Despite the number of exceedances in REF exceeds that in NPE occasionally, the days with exceedances in REF, but not in NPE show almost the same magnitude of PM_{2.5}-concentration (Fig. 15). Over the entire simulation period, the average differences of between REF and NPE 24h-average PM_{2.5}-concentration are 0.04µg/m³, 0.8µg/m³ and 1.0µg/m³ over the entire analysis domain, the nonattainment area and at the State Building, respectively. The average difference of

highest concentrations between REF and NPE were as low as $1.3\mu\text{g}/\text{m}^3$ and barely exceeded $3\mu\text{g}/\text{m}^3$. The most notable differences occurred at locations close to the PS-holding columns. The highest concentration differences occurred for PS6 and on 47% of 120 simulation days and amounted $7\mu\text{g}/\text{m}^3$ on average. Note that PS6 has the strongest $\text{PM}_{2.5}$ emissions among the PS-holding columns.

These findings suggest that PS-emissions do not strongly increase the $\text{PM}_{2.5}$ -concentration within the nonattainment area except for the grid-cell PS6. In the nonattainment area, on days and at the locations of exceedances, emission from PSs accounted for 4% of the 24h-average $\text{PM}_{2.5}$ -concentration on average and barely exceeded 10%. These findings mean that emissions from area sources induced high $\text{PM}_{2.5}$ -concentration in the nonattainment area and the emissions from the PSs just added the small amount needed to exceed the NAAQS. This also means that emissions from PSs play a minor role for the $\text{PM}_{2.5}$ exceedances in the nonattainment area.

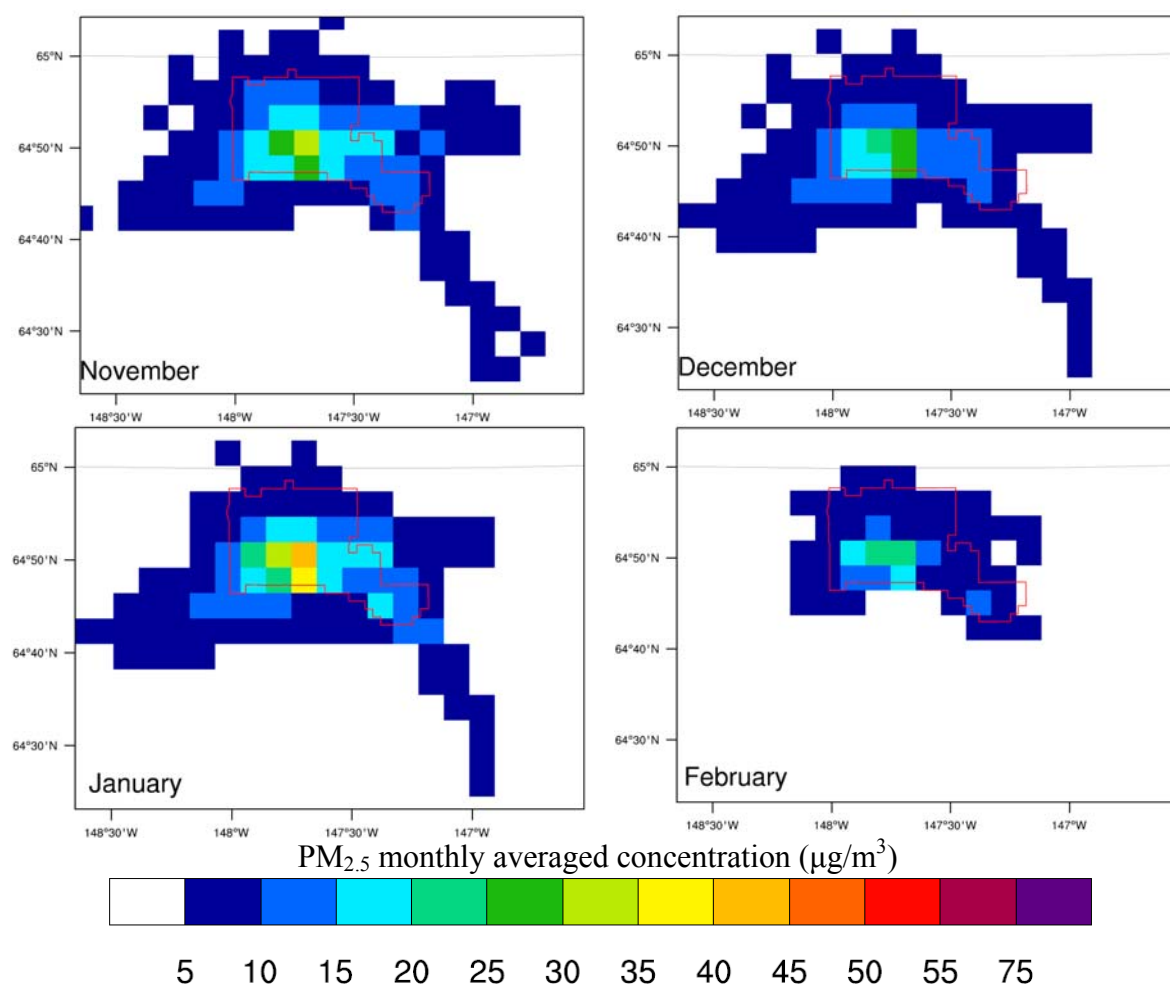


Fig. 16. Zoom-in on monthly mean 24h-average $\text{PM}_{2.5}$ concentration in NTF as obtained by REF for winter 2005/06.

Figure 16 shows a zoom on the spatial distribution monthly mean 24h-average $\text{PM}_{2.5}$ -concentrations at breathing level. The hot spots remain the same over all four months, but with different magnitude. The hot spots remain the same in the simulation without consideration of point source emissions (Fig. 17). The concentrations are only slightly lower in the simulation without consideration of point source emissions. These facts indicate that area and line sources

(e.g. domestic combustion, traffic) are the main cause emission wise for the high $PM_{2.5}$ concentrations.

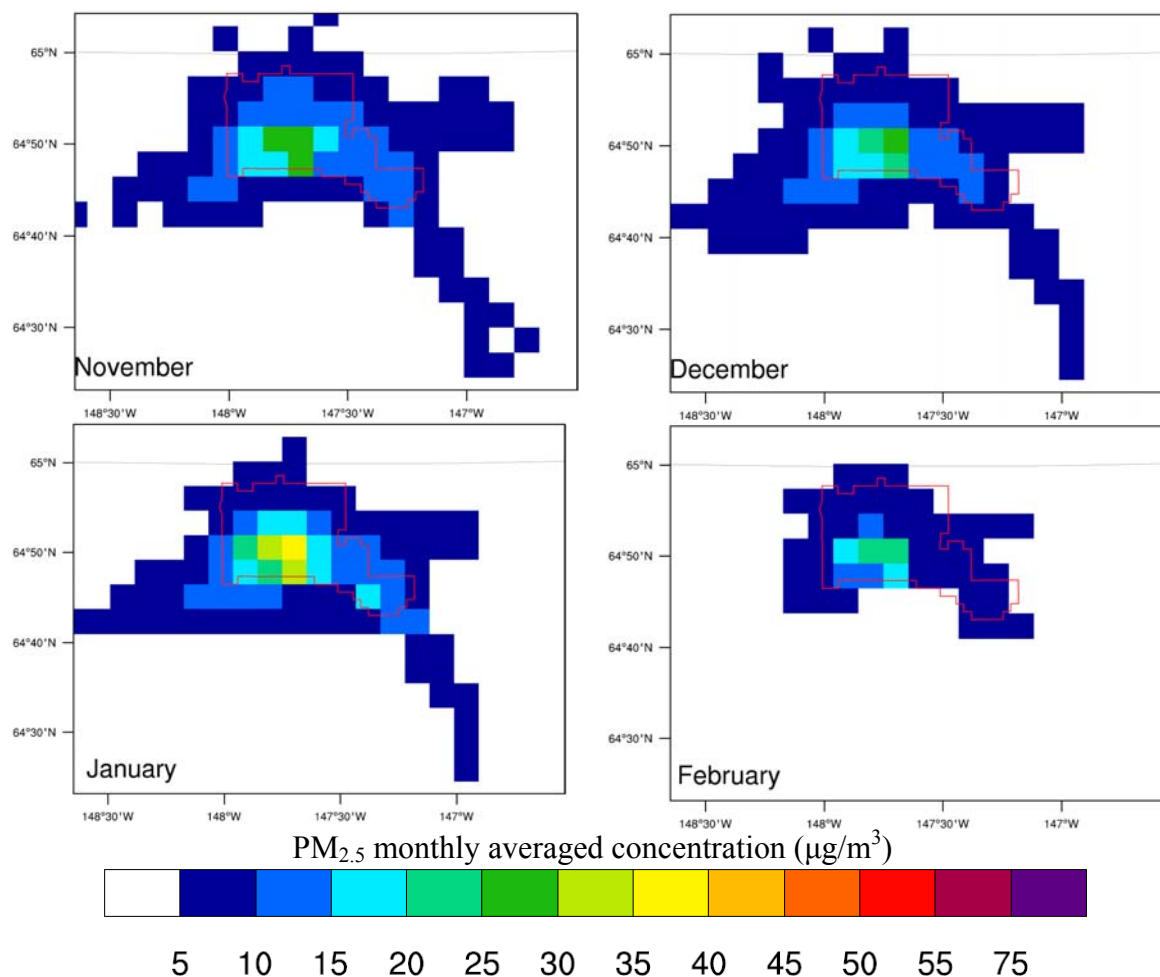


Fig. 17. Like Fig. 16, but for NPE.

Theoretically, higher $PM_{2.5}$ -concentration at breathing level are expected with higher PS-emission rates, and under normal atmospheric conditions (no inversion), the location having the highest concentration at breathing level will be farther away from the PS as the effective emission level increases. Our analysis showed statistically significant correlations between emissions and $PM_{2.5}$ -concentrations, but the correlation values are low and vary highly among PS-holding columns due to PS characteristics, location and co-location effects. In the downwind of PSs, the impact of point-source emissions on the $PM_{2.5}$ -concentration decreases rapidly with increasing distance from the PS.

Investigations show that the total emissions within a grid-column and the simulated $PM_{2.5}$ -concentrations at breathing level correlate highly in populated areas. This finding is true for both REF and NPE. The correlation between the total emissions within a grid-column and the simulated $PM_{2.5}$ -concentrations at breathing level will only marginally differ if no point-source emissions are considered in the calculation of the $PM_{2.5}$ concentrations. This finding suggests that PS emissions are not the main causes for high $PM_{2.5}$ concentrations.

We evaluated the impact-radius of PS-emissions on the $PM_{2.5}$ concentrations at breathing level. Correlation values between PS-emissions and $PM_{2.5}$ -concentration-differences at downwind grid-cells differ generally with wind-speed. Overall, under low wind-speed ($<2m/s$) conditions, the highest correlation values at breathing level occur within 2km from the PS; correlations under stronger wind-speed decrease, but are highest farther downwind (e.g. Fig. 18). The occurrence of highest correlation also shifts farther downwind when the emission-level height increases. Nevertheless, regardless of emission level and wind-speed, the highest correlations occurred within 10km from the PS. Beyond 10km from the PS, correlations are small and non-significant and small for low wind-speeds, but significant for moderate wind-speeds ($\geq 5m/s$). The strongest correlations are obtained typically with time lags of 0 or 1h.

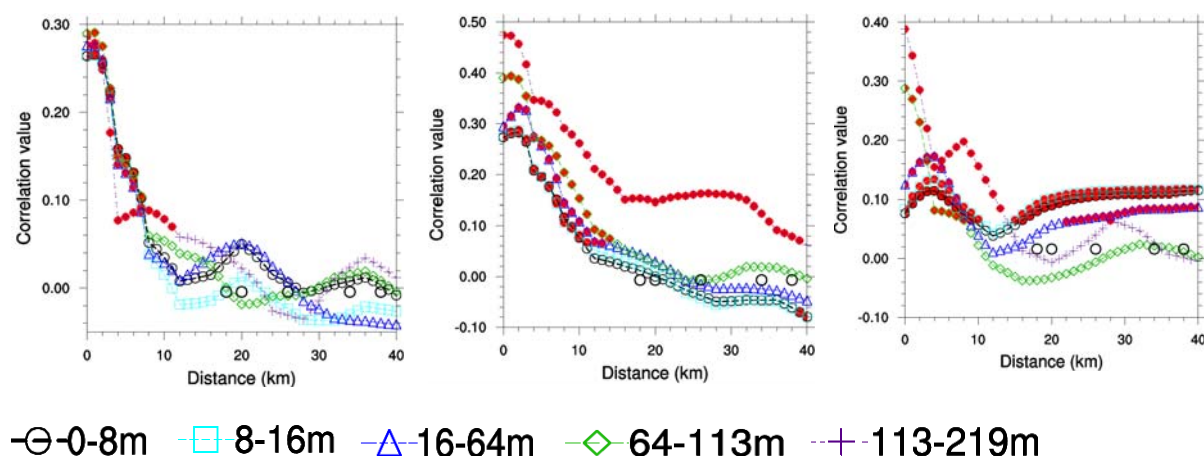


Fig. 18. Correlation of emissions at PS6 with the $PM_{2.5}$ -concentration-difference (REF-NPE) at downwind grid-cells in subsequently lower levels from the emitting level (113-219m) to the breathing level (0-8m) under wind-speeds $<2m/s$ (left), $2-5m/s$ (middle) and $\geq 5m/s$ (right). The emitting level is the highest level displayed in the figure. Open black circles indicate the relative position of grid columns holding other PSs near the PS-holding grid-column of interest. Closed red circles represent statistically significant (at the 95% confidence level) correlations.

Atmospheric temperature inversions influence the dispersion of PS-emissions (Fig. 10). As can be easily derived from Figure 10, theoretically, PS-emissions emitting into levels above, in-between and below inversion layers would have their impact on the breathing level from the lowest to highest magnitude, respectively. In the following, we talk about “no-inversion conditions” when the bottom of any inversion layer aloft is 200m above the emitting-level. “Below-inversion” refers to when the bottom of any inversion aloft is less than 50m above the highest emitting-level. On average, WRF/Chem predicted in-between-inversion, above-inversion, below-inversion and no-inversion conditions for PS-emissions in 64%, 18%, 10% and 8% of the time, respectively. Note that WRF/Chem for 2005/06 predicted the frequency of inversions acceptably [Mölders *et al.*, 2011].

In general, WRF/Chem reproduced successfully the emission-inversion relationship at all PSs. Here we only show the correlation at PS6 as an example. The strongest and significant correlations between PS-emissions and $PM_{2.5}$ -concentration-difference at breathing level occurred under “below-inversion” conditions and the highest correlation values typically occurred at 8-10km downwind depending on emission level and wind speed (e.g. Fig. 19). The second strongest (significant) correlations occurred under “in-between-inversion” conditions. Then the highest correlation values occurred within 0-12km downwind depending on wind-speed, emission level and inversion strength. The location of highest correlation typically shifts

farther downwind as the inversion strength increases and vice versa. Under both “no-inversion” and “above-inversion” conditions, PS-emissions correlate marginally and insignificantly with the breathing level $PM_{2.5}$ -concentration. Based on these findings we conclude that PSs have their highest impact on the $PM_{2.5}$ -concentration at breathing level within 10km of their location.

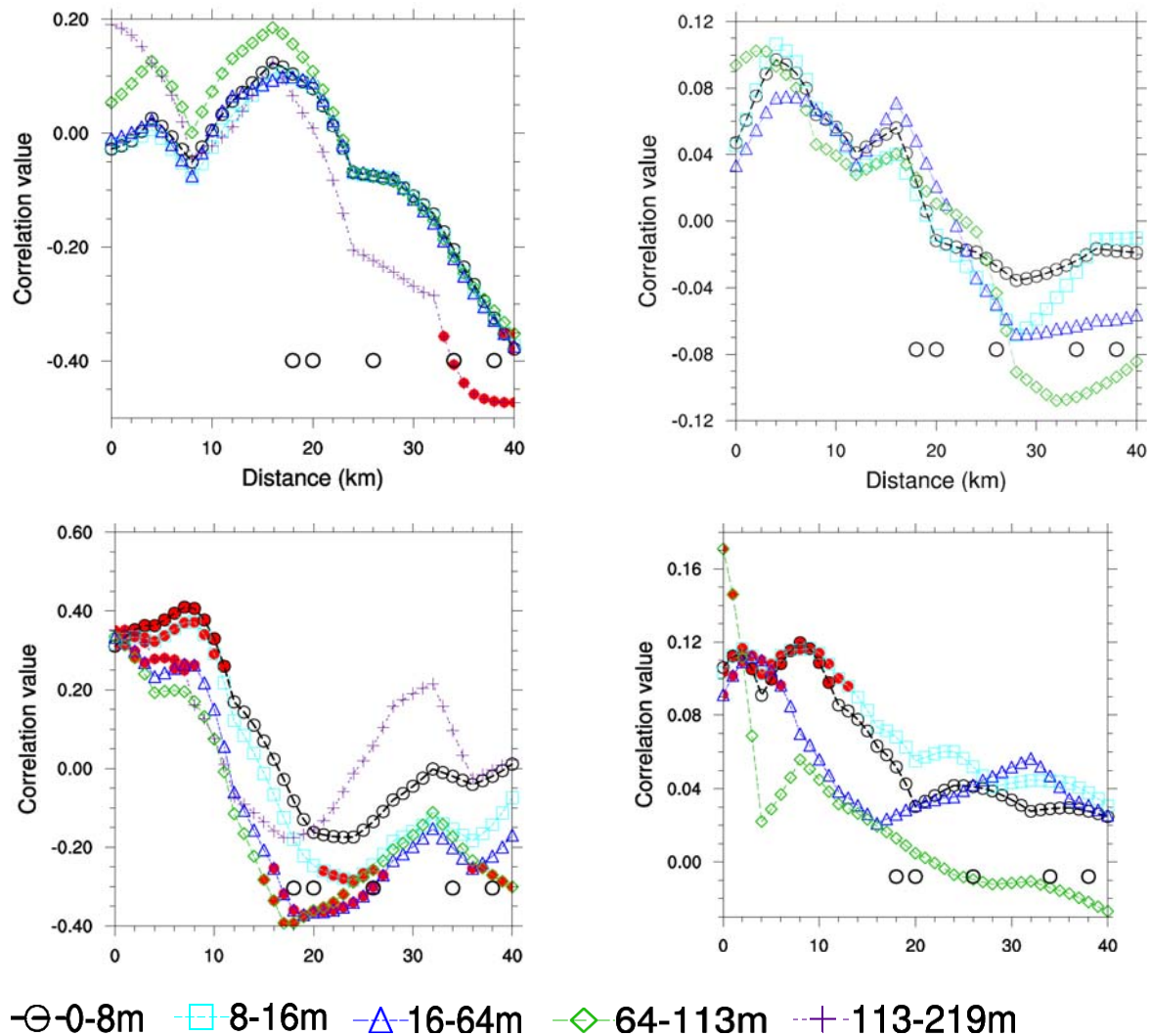


Fig. 19. Correlation of $PM_{2.5}$ emissions at PS6 with $PM_{2.5}$ -concentration-difference at downwind grid-cells in subsequently lower levels from the emitting-level to the breathing level (0-8m) under conditions when there was “no inversion”, emission into levels above, just below and in between inversion layers (top-left to bottom-right, respectively). The emitting-level is the highest level displayed in the figure. Open black circles indicate the relative position of grid columns holding other PSs in the vicinity of the PS-holding grid-column of interest. Closed red circles represent statistically significant (at the 95% confidence level) correlations.

6.2 Potential impact of “woodstove replacement” programs

As pointed out above, WSR is a very moderate “woodstove replacement” scenario in comparison with the sensitivity simulation that assumed a replacement of all non-certified wood burning devices based on the number of devices given in *Davies et al.*'s [2009] report (WSS1). The emission reduction in WSR was much lower than in WSS1 (cf. section 4). Within the nonattainment area, the emission strength in WSR was $6\mu\text{g}\text{m}^{-2}\text{h}^{-1}$ (6%) less than in REF on

average whereas in WSS1 the emission strength was 40% lower than in REF. Because of the comparably small emission difference between REF and WSR, simulated $PM_{2.5}$ -concentration of REF and WSR differ typically only slightly (Figs. 20, 21).

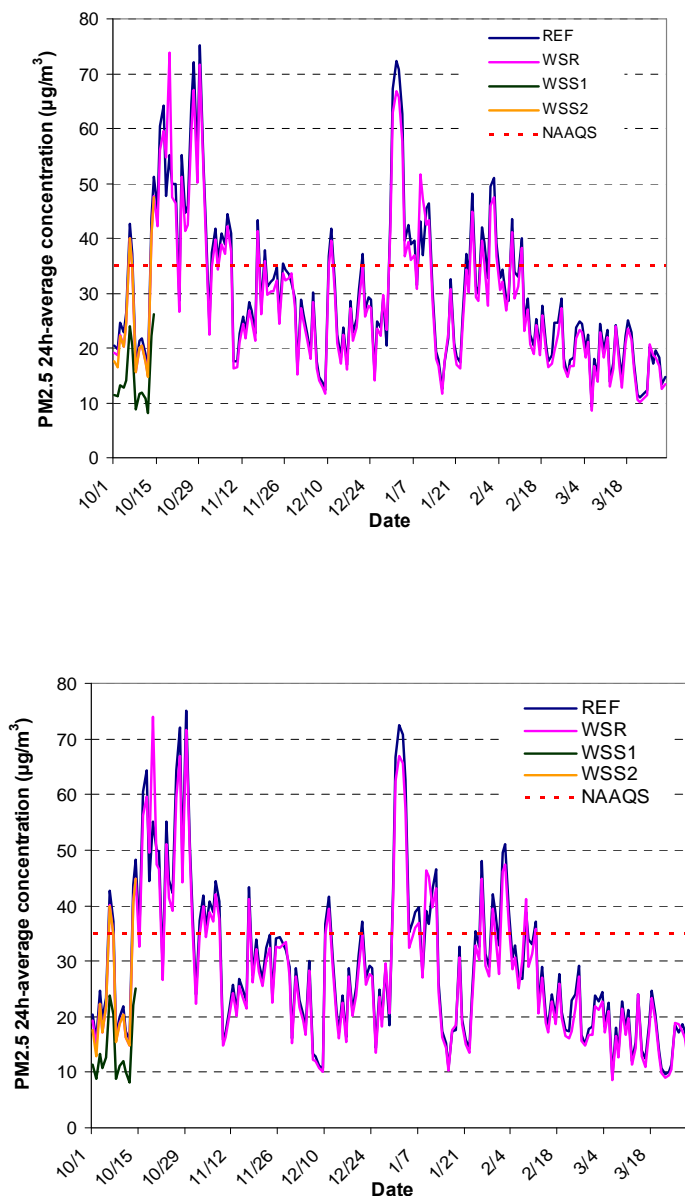


Fig. 20. Highest 24h-average $PM_{2.5}$ concentration as obtained anywhere in the model domain (top) and the 24h-average concentration at the grid-cell holding the State Building (bottom) in REF, WSR, WSS1, and WSS2. Note that the highest concentrations within the model domain occurred in the nonattainment area.

In comparison with the emissions in REF, the average $PM_{2.5}$ -emission reductions in the nonattainment area are 6%, 36%, and 7% in WSR, WSS1, WSS2, respectively. The highest 24h-average $PM_{2.5}$ -concentration difference anywhere in the domain amounts $5.7\mu\text{g}/\text{m}^3$ on February 22, 2009 (Fig. 20). Averaged over the nonattainment area, the highest ($2.1\mu\text{g}/\text{m}^3$) and the second highest ($2.0\mu\text{g}/\text{m}^3$) difference in 24h-averaged $PM_{2.5}$ -concentrations were simulated for October 27, 2008 and January 1, 2009, respectively, and the average difference over time and the nonattainment area amounts $0.6\mu\text{g}/\text{m}^3$. About 45% and 33% of the concentration differences fall

between $0.5\text{-}1\mu\text{g}/\text{m}^3$ and $0\text{-}0.5\mu\text{g}/\text{m}^3$, respectively (Fig. 22). All grid-cells with the highest concentrations are located in the nonattainment area.

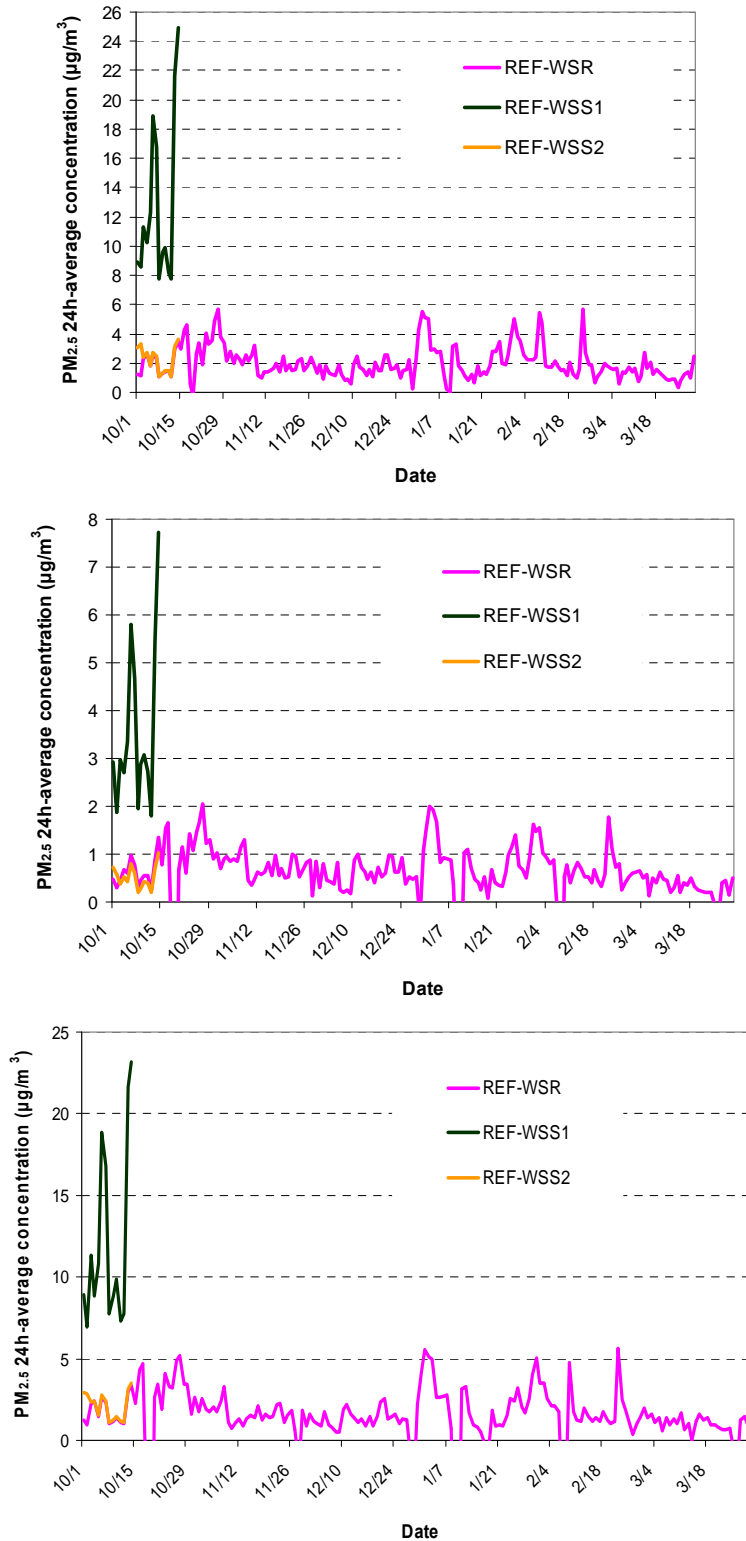


Fig. 21. Highest 24h-average $\text{PM}_{2.5}$ -concentration difference from REF for WSR, WSS1, WSS2 as obtained in the domain (top), on average over the nonattainment area (middle) and the grid-cell with the State Building (bottom).

In the nonattainment area, the monthly average $PM_{2.5}$ -concentration differences amount to $0.7\mu\text{g}/\text{m}^3$, $0.7\mu\text{g}/\text{m}^3$, $0.6\mu\text{g}/\text{m}^3$, $0.7\mu\text{g}/\text{m}^3$, $0.6\mu\text{g}/\text{m}^3$ and $0.3\mu\text{g}/\text{m}^3$ in October, November, December, January, February and March, respectively. We calculated the 24h-averaged $PM_{2.5}$ -concentration difference for each day of the 182 simulation days and sorted them from high to low differences. We picked the 20% highest and 20% lowest concentration differences from this list. Note that 20% corresponds to 36 days in our study. The investigation showed that 14 and 13 of the top 20% highest and lowest concentration differences occurred in October and January, respectively. Off the 20% lowest, nine days occurred in March. This means the highest differences typically occurred in October and January whereas the lowest differences occurred in March. This finding means that the highest mitigation of $PM_{2.5}$ -concentrations can be achieved in the months that are coldest.

The Student t-test showed statistically significant $PM_{2.5}$ -concentration differences only within the nonattainment area and some adjacent grid-cells (Fig. 23). Outside the nonattainment area, the $PM_{2.5}$ -concentration differences are very low and non-significant. Although the Student t-test shows that the concentration differences are significant, there is still a possibility that the $PM_{2.5}$ -concentration difference at a given grid-cell is not due to the reduced emission, but rather due to some variable random effects between the two simulations (e.g. truncation errors, model sensitiveness). This is especially true for very small differences in $PM_{2.5}$ -concentration. We adopted the FEA analysis [Carpenter *et al.*, 1989; Werth and Avissar, 2002] to verify that the differences are really due to the “woodstove replacement”.

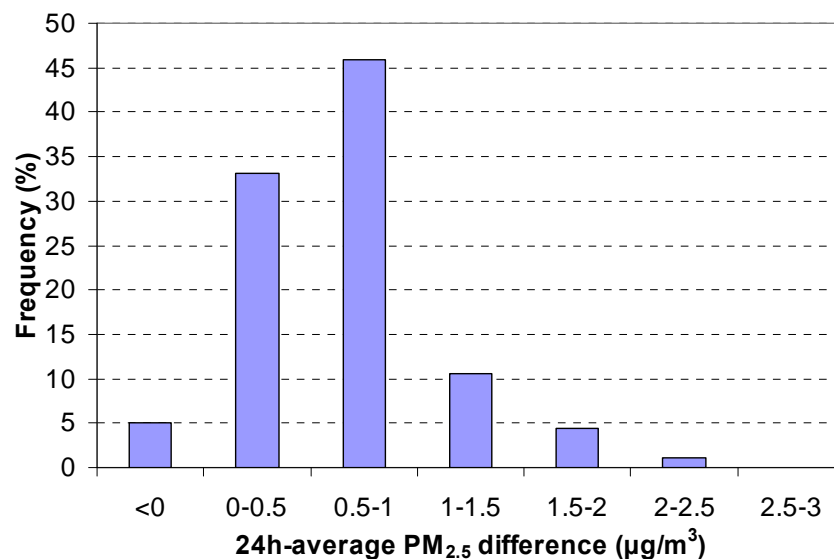


Fig. 22. Frequency distribution of 24h-average $PM_{2.5}$ -concentration difference as obtained for WSR.

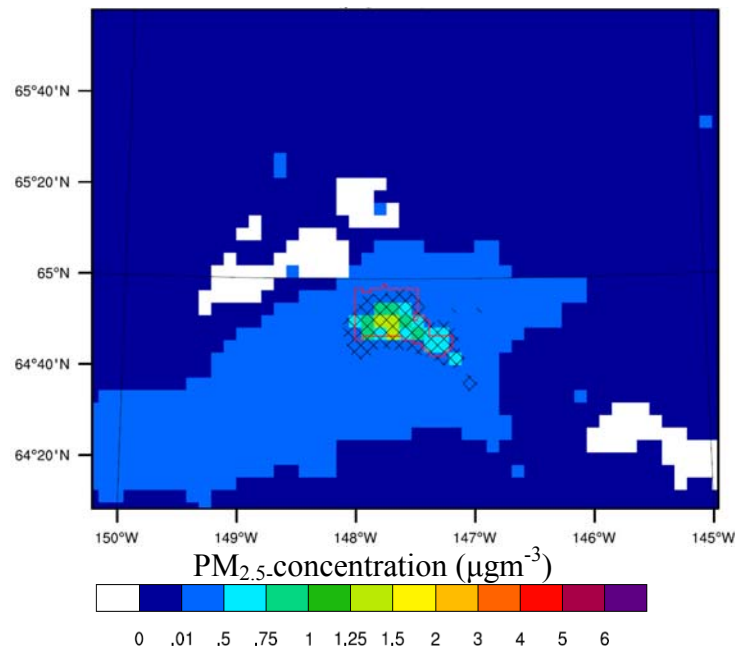


Fig. 23. Zoom-in showing the average difference of $PM_{2.5}$ -concentration between REF and WSR for October 1, 2008 to March 31, 2009. The hashed shading indicates grid cells where the difference is statistically significant at 95% or higher level of confidence

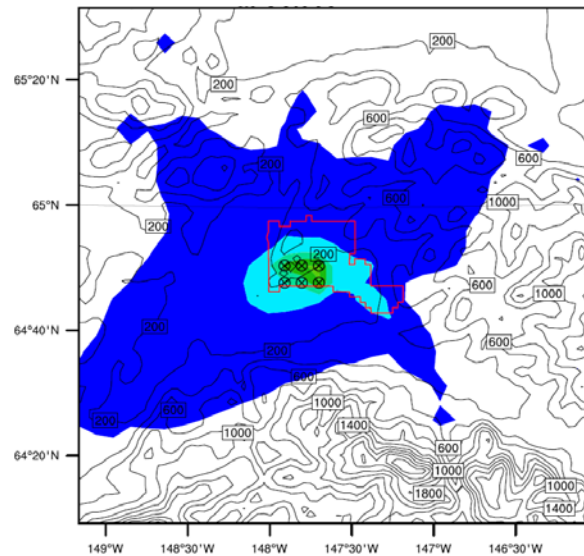


Fig. 24. Zoom-in map of grid-cells for which exceedances were simulated during October 1, 2008 to February 28, 2009 in REF. The 24h-average $PM_{2.5}$ concentration on October 1, 2008 is superimposed. The crossed circles indicate grid cells for which exceedance were simulated during OTM; the red polygon indicates schematically the nonattainment area. Grid-cells for which exceedances were simulated in WSR are identical to those for which exceedances occurred in REF (therefore not shown).

In February 2009, several grid-cells exist in the northwest of the nonattainment area that have ranks lower than the top 5%. Some of them have non-significant concentration-differences according to the Student-t test (Fig. 24). For November and December 2008, the ranks of true

concentration differences are relatively uniform anywhere in the whole model domain whereas they vary strongly in other months. This behavior coincides with the temporal evolution of the 24h-average $PM_{2.5}$ -concentration difference (Fig. 21) that indicates low variation of the difference in November and December 2008, but strong variation in the other months.

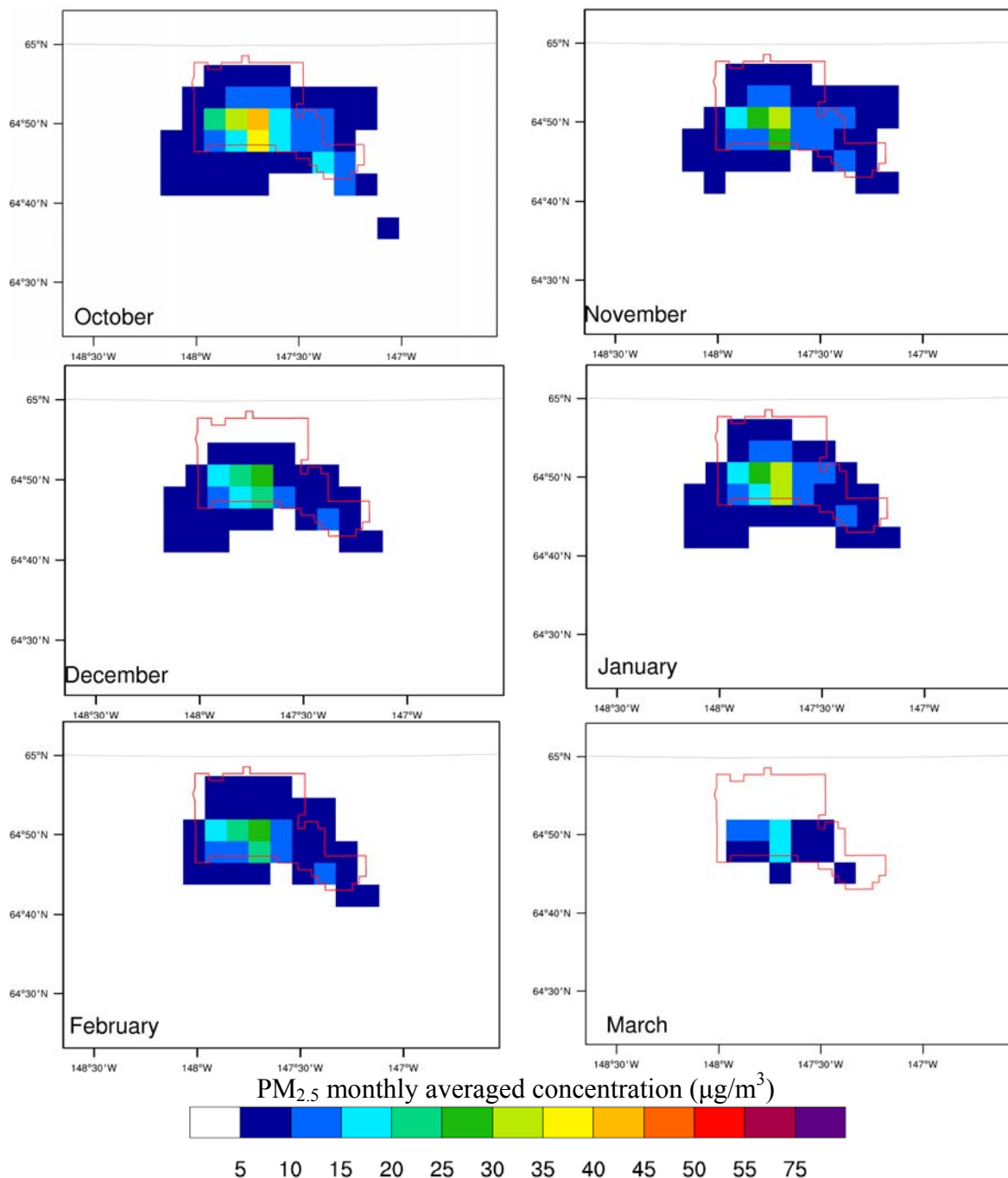


Fig. 25. Zoom-in on monthly mean 24h-average $PM_{2.5}$ concentration in OTM as obtained by REF for winter 2008/09.

According to the FEA, exchanging the noncertified wood-burning devices helped to reduce the number of exceedance days during OTM. The number of exceedance days anywhere in the nonattainment area are 20 (19), 10 (7), 5 (3), 15 (14), and 5 (5) in REF (WSR) for October,

November, December, January, February respectively. All exceedance events of OTM occurred at grid-cells in the nonattainment area. At the grid-cell holding the State Building monitoring site, exceedances were simulated for 52 (44) days in REF (WSR). At grid-cells other than that holding the official site, exceedances were simulated for 40 (34) days by REF (WSR). Despite the different number of exceedance days, locations (grid-cells) that experienced exceedances are identical in REF and WSR during OTM (Fig. 25). Days and grid-cells having the highest PM_{2.5}-concentrations during simulated exceedance events during OTM are also identical. This fact indicates that there are no offsets in the temporal and spatial distribution of exceedance events between REF and WSR.

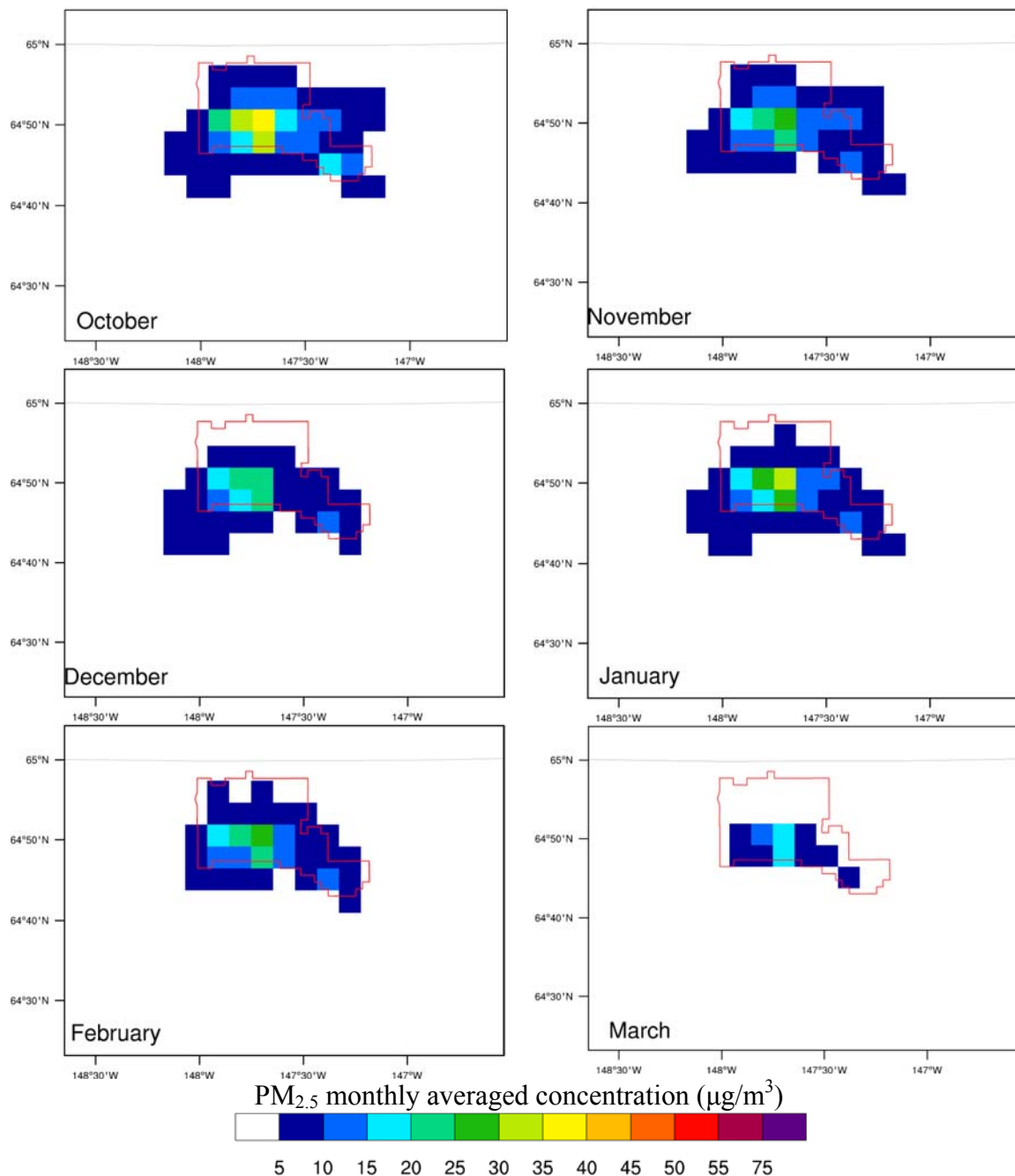


Fig. 26. Like Fig. 25, but for WSR.

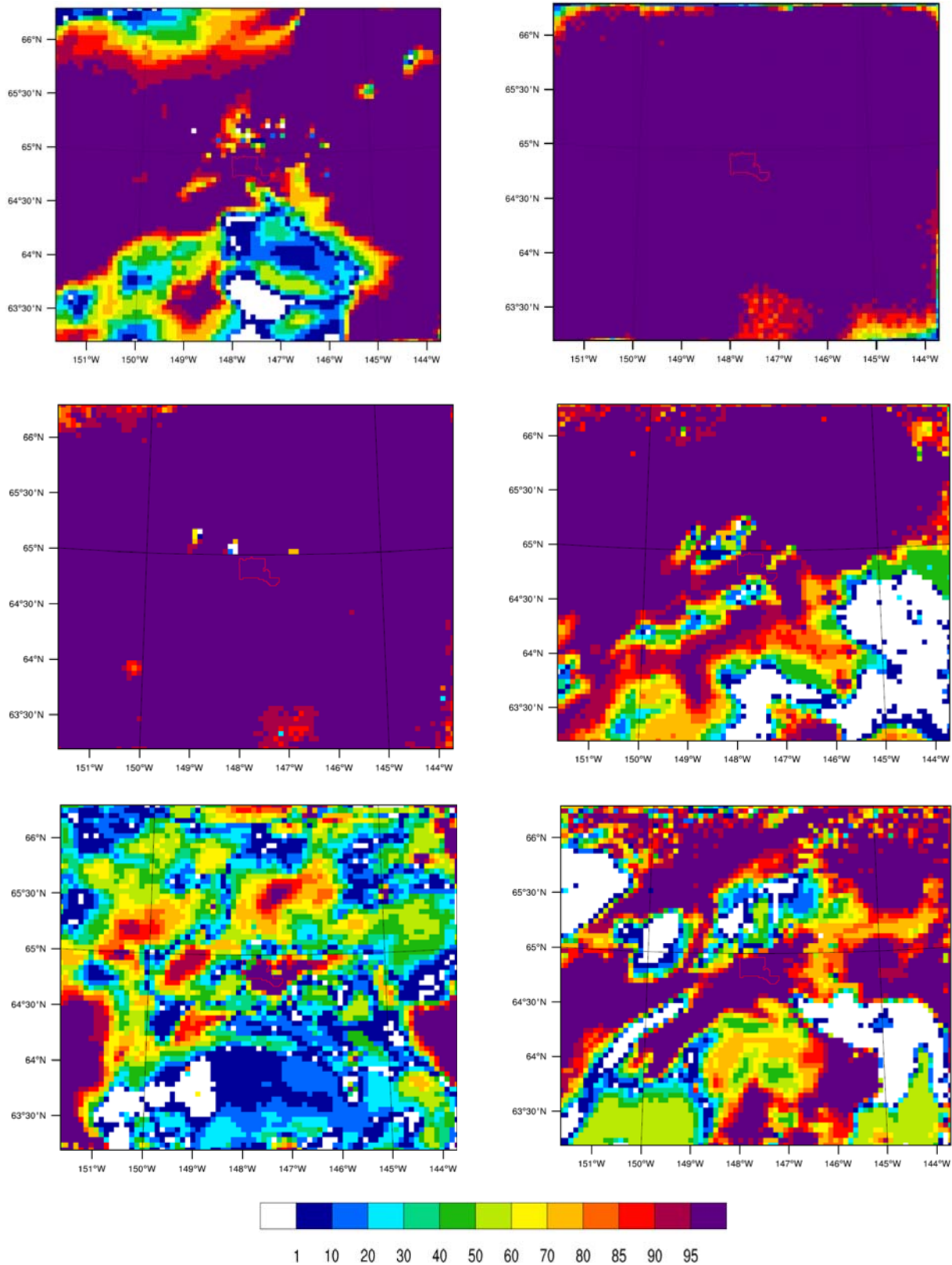


Fig. 27. Monthly rank of “true” differences over “false” differences of PM_{2.5}-concentration for October 2008 to March 2009 (from top left to bottom right). At grid-cells ranking higher than the 95% percentile, the “woodstove replacement” can be considered as the factor that actually reduced the PM_{2.5} concentrations at breathing level.

Comparison of the monthly mean 24h-average $PM_{2.5}$ concentrations obtained with REF and WSR (Figs. 25, 26) indicates that the hot spots remain the same, but with slightly lower concentrations.

The FEA was applied for every month from October 2008 to March 2009. The ranks of the true-difference concentrations varied highly at all grid-cells throughout OTM except for those in the nonattainment area (Fig. 27). The ranks of true concentration difference at grid-cells in the nonattainment area lay consistently in the top 5% of the false ensembles. This means that exchanging the non-certified wood-burning devices does really help to reduce the $PM_{2.5}$ -concentrations in the nonattainment area.

The results of the Student-t test and FEA (Fig. 27) indicate that exchanging the noncertified wood-burning devices does really help to reduce the $PM_{2.5}$ -concentration in the nonattainment area. This outcome results from the fact that wood-burning devices emit into low levels of the atmosphere. Therefore, the emitted species are not transported far away from their sources. This behavior is especially true for conditions with low wind-speeds, as they frequently exist during winter in Fairbanks [cf. *Tran and Mölders*, 2010]. Thus, the impact of emissions from wood-burning on the $PM_{2.5}$ -concentrations at breathing level remains local compared to the impacts of elevated point sources.

6.2.1 Sensitivity studies on “woodstove replacements”

We compared the emission reductions that related only to the different numbers of heating devices in WSS1, WSS2 and WSR with each other as well as with the reference simulation. Recall that the reference simulation, and the simulations assuming the “woodstove replacement” using *Davies et al.*’s number of devices, and the “woodstove replacement” using the SRL draft report and *Carlson et al.*’s number of devices were denoted as REF, WSS1, WSS2, and WSR, respectively (Table 1). Due to the tremendous CPU time required for a half-year long simulation the WSS1 and WSS2 simulations were carried out only for a limited time. While WSS1 reduces the $PM_{2.5}$ concentrations in the nonattainment area greatly, WSS2 is much less doing so (Figs. 20, 21). Within the 15 days of simulation, WSS2 reduces the 24h-average $PM_{2.5}$ concentrations by $3.6\mu\text{g}/\text{m}^3$ to the highest, while WSS1 reduces them by as much as $25\mu\text{g}/\text{m}^3$. WSS1’s reduction helped efficiently to avoid four exceedances encountered locally in REF. On the contrary, the reduction in WSS2 was not sufficient to do so. The locations of exceedances do not differ between REF, WSS1 and WSS2 and they all occur in the nonattainment area. The reduction benefit of WSS1 was higher when local exceedances existed, while the reduction obtained in WSS2 differed marginally with time.

The sensitivity studies suggested large uncertainty in the magnitude of the efficiency of a “woodstove replacement” program. This uncertainty mainly results from (1) the unknown number of wood-burning devices that exist in the nonattainment area and could be replaced, (2) the unknown partitioning of the use of wood-burning and other heating devices in households with more than one heating option, (3) the unknown temporal use of wood-burning devices, and (4) the unknown spatial distribution of wood-burning devices.

6.3 Potential impact of usage of low sulfur fuel for heating oil, power generation and in oil-burning facilities

Introducing low sulfur fuel decreased the total monthly $PM_{2.5}$ -emissions in the nonattainment area from October to March by 15.666, 17.448, 15.407, 15.447, 14.294, and 13.381 kg/km^2 ,

respectively from 140.130, 94.184, 94.118, 101.265, and 98.398 kg/km², respectively. The percentage total daily PM_{2.5}-emission reductions from October to March were 11.1%, 18.5%, 16.4%, 13.0, 14.1, and 13.6%, respectively. The decreases in monthly emissions of SO₂, NO and VOC were approximately 23%, 1% and 0%, respectively.

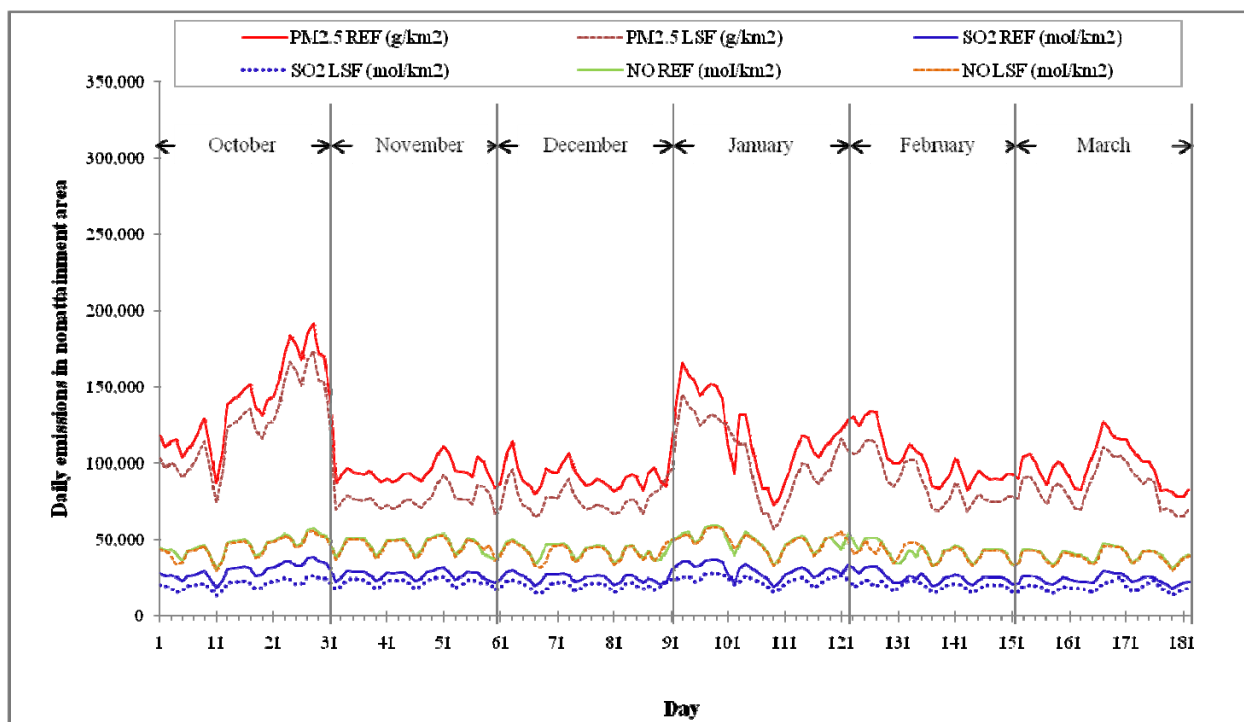


Fig. 28. Temporal evolution of daily emissions averaged over the nonattainment area for October 2008 to March 2009 as assumed in REF and LSF. The day refers to the day since start of the simulation (1 October 2008).

The daily mean temperatures are a main factor that affects the efficiency of utilizing low sulfur fuel. Low temperatures cause incomplete combustion and support the gas-to-particle conversion. During OTM, October 2008 had the highest frequency of days with daily near-surface temperatures below the 1971-2000 30-year monthly mean temperature (Table 3). Consequently, October 2008 had high emissions of particulate matter. Daily emissions in the nonattainment area with the current fuel sulfur content and after introduction of low sulfur fuel are compared in Figure 28.

In the nonattainment area, the monthly average PM_{2.5}-concentration amounted to 13.0, 11.6, 9.2, 11.0, 9.8 and 5.7 μg/m³, respectively, and 9.9 μg/m³ on average over OTM. The monthly average PM_{2.5}-concentration difference (REF-LSF) amounts to 0.4, 1.0, 0.7, 0.6, 0.5 and 0.4 μg/m³ in October, November, December, January, February and March, respectively, and 0.6 μg/m³ on average over the entire winter. The percentage reductions varied from 3% to 9% (Table 4). November had the highest assumed emission reduction and simulated concentration reductions. The daily reduction in emissions does not yield to a linearly corresponding reduction in the daily average PM_{2.5} concentrations at breathing level in the nonattainment area (cf. Figs. 28, 29).

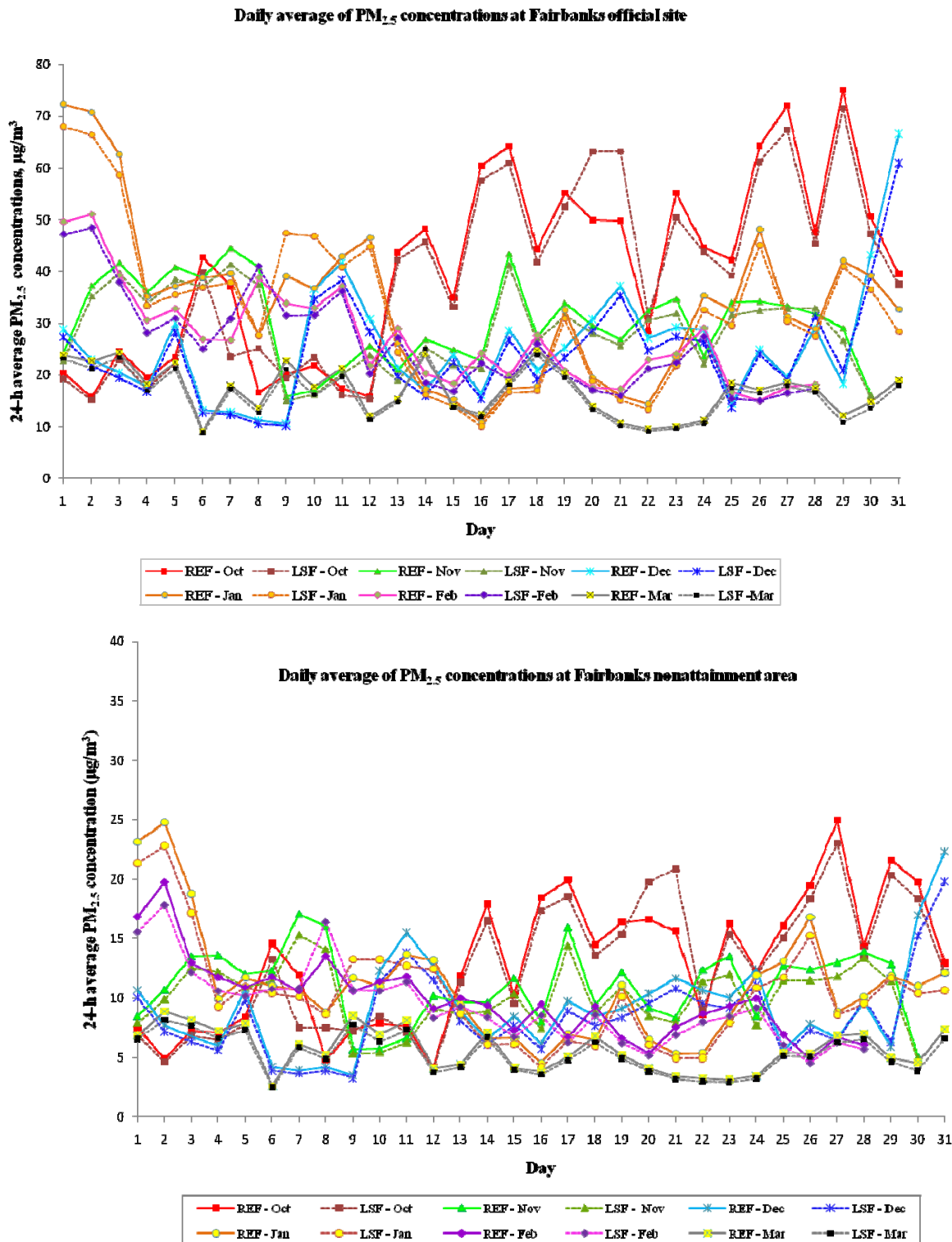


Fig. 29. Temporal evolution of simulated 24h-average PM_{2.5} concentrations as obtained for the grid-cell that holds the State Building (top) and the 24h-average PM_{2.5} concentrations averaged over the nonattainment area (bottom) in the various months of winter 2008/09. REF and LSF refer to the reference simulation and the simulation assuming the introduction of low sulfur fuel for heating oil, power generation and facilities burning oil (see Table 1).

On average, the simulated reduction of 24h-average $PM_{2.5}$ concentrations during OTM was $0.6\mu\text{g}/\text{m}^3$. The maximum 24h-average $PM_{2.5}$ -concentrations reduction of $4.4\mu\text{g}/\text{m}^3$ occurred in October (Fig. 29). Focusing on the values simulated for the grid-cell holding the official $PM_{2.5}$ -monitoring site in the nonattainment area at the State Building, the average daily concentrations reduction was $1.2\mu\text{g}/\text{m}^3$ for OTM. The maximum 24h-average $PM_{2.5}$ -concentration reduction at the State Building site was $13.6\mu\text{g}/\text{m}^3$ and was simulated for October 2008. In comparison with the $PM_{2.5}$ -concentrations obtained for other grid-cells in the nonattainment area, this site had the highest frequency of exceedance days (19, 8, 5, 15, 5, and 0 exceedance days for October to March, respectively), and most of them had the highest $PM_{2.5}$ -concentrations, when compared to other grid-cells in the nonattainment area on the same day.

We calculated the 24h-averaged $PM_{2.5}$ -concentration difference between REF and LSF for each day of the total 182 simulation days and sorted them from high to low differences. We picked the 20% highest and 20% lowest concentration differences from this list. Note that 20% corresponds to 36 days in this case. Investigation of the top 20% showed that 14 of the highest concentration differences occurred in November. Off the 20% lowest, most days (14) occurred in March. This means the highest differences typically occurred in November whereas the lowest differences occurred in March. The highest differences were mainly due to the concentration values. In this scenario, high monthly average concentrations mostly translated into high monthly average reductions. Table 4 shows that high $PM_{2.5}$ concentrations occurred in October, January, and November from the first to the third rank, respectively. In October and January, the concentrations were high, but there were some days for which $PM_{2.5}$ concentrations increased after introduction of low sulfur fuel. Therefore, in October and January, the $PM_{2.5}$ -concentration reduction was not as high as in November. The lowest difference for $PM_{2.5}$ -concentrations occurred for March as this month had the lowest $PM_{2.5}$ -concentrations.

The daily reductions in $PM_{2.5}$ -concentrations vary strongly with the meteorological conditions and over the months (Fig. 29). By reducing the fuel sulfur content of oil, the number of simulated exceedance days in October 2008 to March 2009, which amounted to 20, 10, 5, 15, 5 and 0 in REF were reduced to 19, 8, 4, 14, 5 and 0 in LSF, respectively. The simulations suggested that in total, five exceedance days could have been avoided by introduction of low sulfur fuel.

Remarkably, on several days, the 24h-average $PM_{2.5}$ -concentrations increased in the nonattainment area after introduction of low sulfur fuel. Note that similar was found also in another sulfur reduction study carried out over the North Pacific for January with another configuration of WRF/Chem [T.T. Tran, 2011; pers. communication]. In our study, on some simulated days, the increase of $PM_{2.5}$ -concentrations stemmed from the increase of $PM_{2.5}$ emissions, for example at the end of December and in mid-January (Fig. 28). The emissions increased due to the non-linear temperature dependency of emissions from power generation and domestic combustion considered in AkEM.

However, the increase of $PM_{2.5}$ concentrations on October 8, 10, 20-22, and February 7-9 and March 14 did not coincide with increased $PM_{2.5}$ emissions. These increases despite of decreased $PM_{2.5}$ emissions are due to gas-to-particle conversion. Recall that the usage of low sulfur fuel leads to a different emission spectrum for various other species. Increases of $PM_{2.5}$ concentrations occurred both inside and outside the nonattainment area (e.g. Fig. 30). The increases were related to the atmospheric chemistry of NO_x that affected the thermodynamic equilibria of sulfate-nitrate-ammonia-water in aerosols.

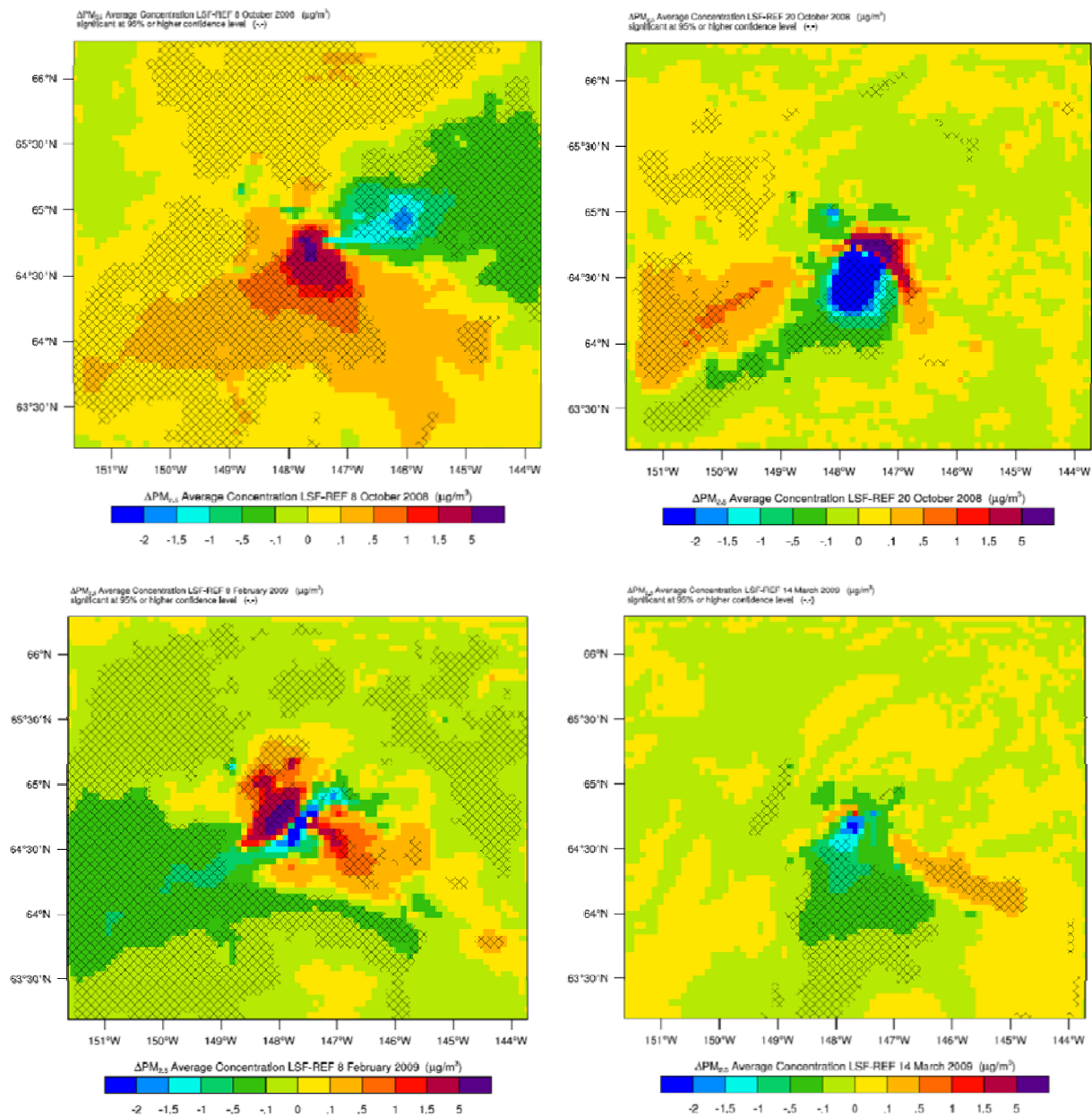


Fig. 30. Examples of PM_{2.5} concentration difference distributions on days with days with locally increased PM_{2.5} concentrations after introduction of low sulfur fuel. The hashed shading indicates grid cells wherein the difference (REF-LSF) is statistically significant at 95% or higher level of confidence.

The large number of days (12 days in the nonattainment area, 13 days for the grid-cell holding the State Building) with increased PM_{2.5} concentrations and the emission-concentration relationship (Figs. 28, 29) suggest that the locally increased PM_{2.5} concentrations after introduction of low sulfur fuel are most likely not a model artifact, but real. The reduction of SO₂ emissions and lower SO₂ concentrations in LSF reduced the sulfate-aerosol concentrations. This circumstance further resulted in partial replacement of the reduced aerosol mass by available nitric acid. The percent fraction of nitrate increased, but sulfate decreased on days with increased PM_{2.5} concentrations (Fig. 31). Note that nitrate has more mass than sulfate.

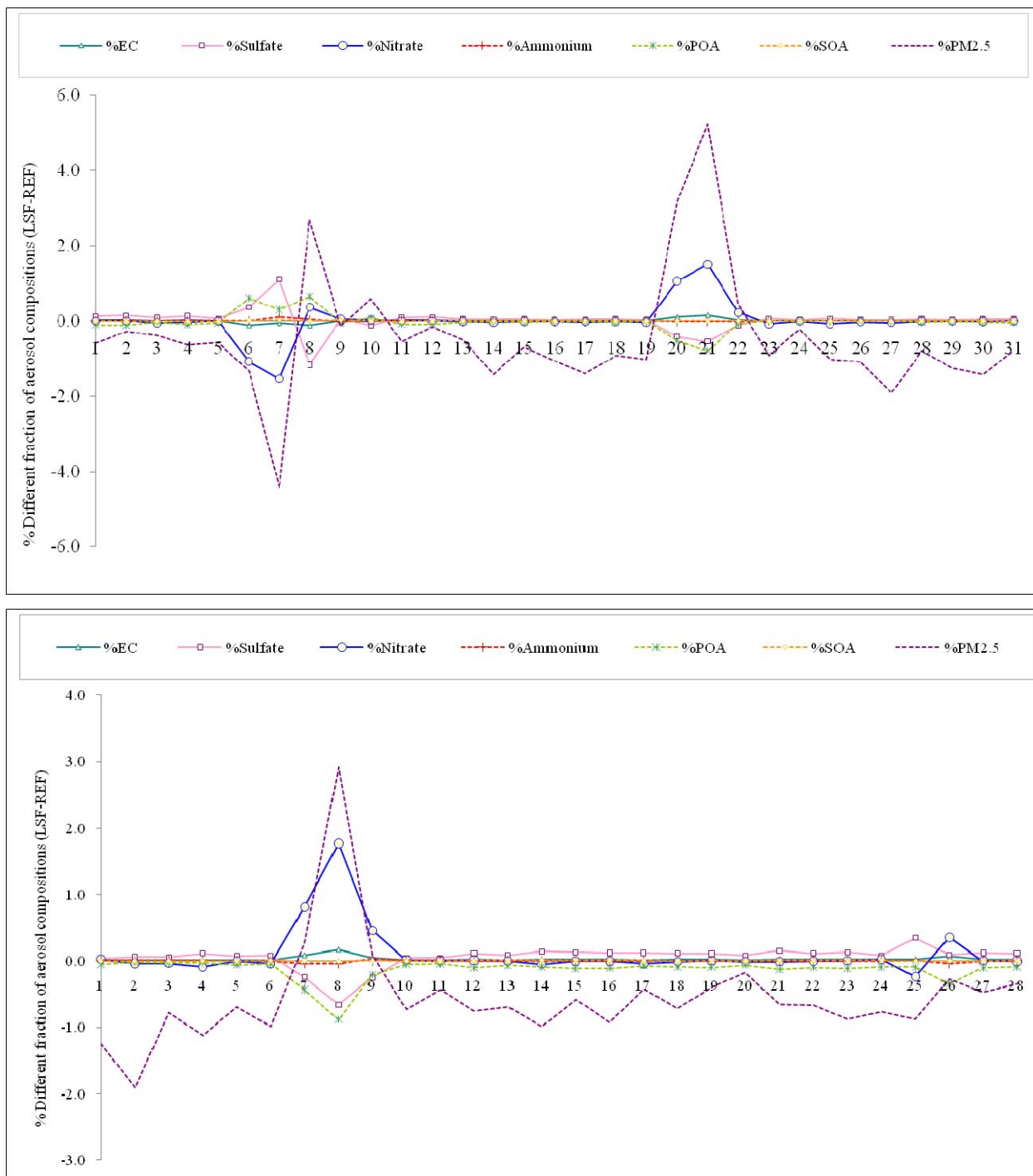


Fig. 31. Temporal evolution of daily average percentage difference of aerosol composition in the nonattainment area as obtained for October (top) and February (bottom).

The investigation of the reasons is beyond the scope of this study. However, preliminary analysis within the framework of a PhD thesis suggests that less transformation and removal of NO_x after introduction of low sulfur fuel during months with still relatively high solar radiation led to an increase of the nitrate concentrations, and increased the particulate matter concentrations accordingly (Fig. 31). The replacement of nitrate brought about a shift of the NH_4NO_3 equilibrium toward the gas-phase. Consequently, the NO_3 -concentrations increased in the

atmosphere after introducing low sulfur fuel. The fact that no such increase occurs during the months with lowest insolation (e.g. December, January) suggests that chemical processes initiated by photolysis play an important role. As explained earlier, during October, February, and March, photolysis plays a stronger role as photolysis rates are higher than in December or January. Consequently, NO, NO₂ and NO₃ concentrations increase during October, February, and March, and PM_{2.5} concentrations increased accordingly. The high aerosol concentrations fed back to meteorology. The simulated atmosphere became more stable and air quality became worse in the Fairbanks nonattainment area. The increase of nitrate, which means an increase of aerosols in the atmosphere, and the effect of chemistry on meteorology, should be analyzed for full understanding, but both tasks are beyond the scope of this study.

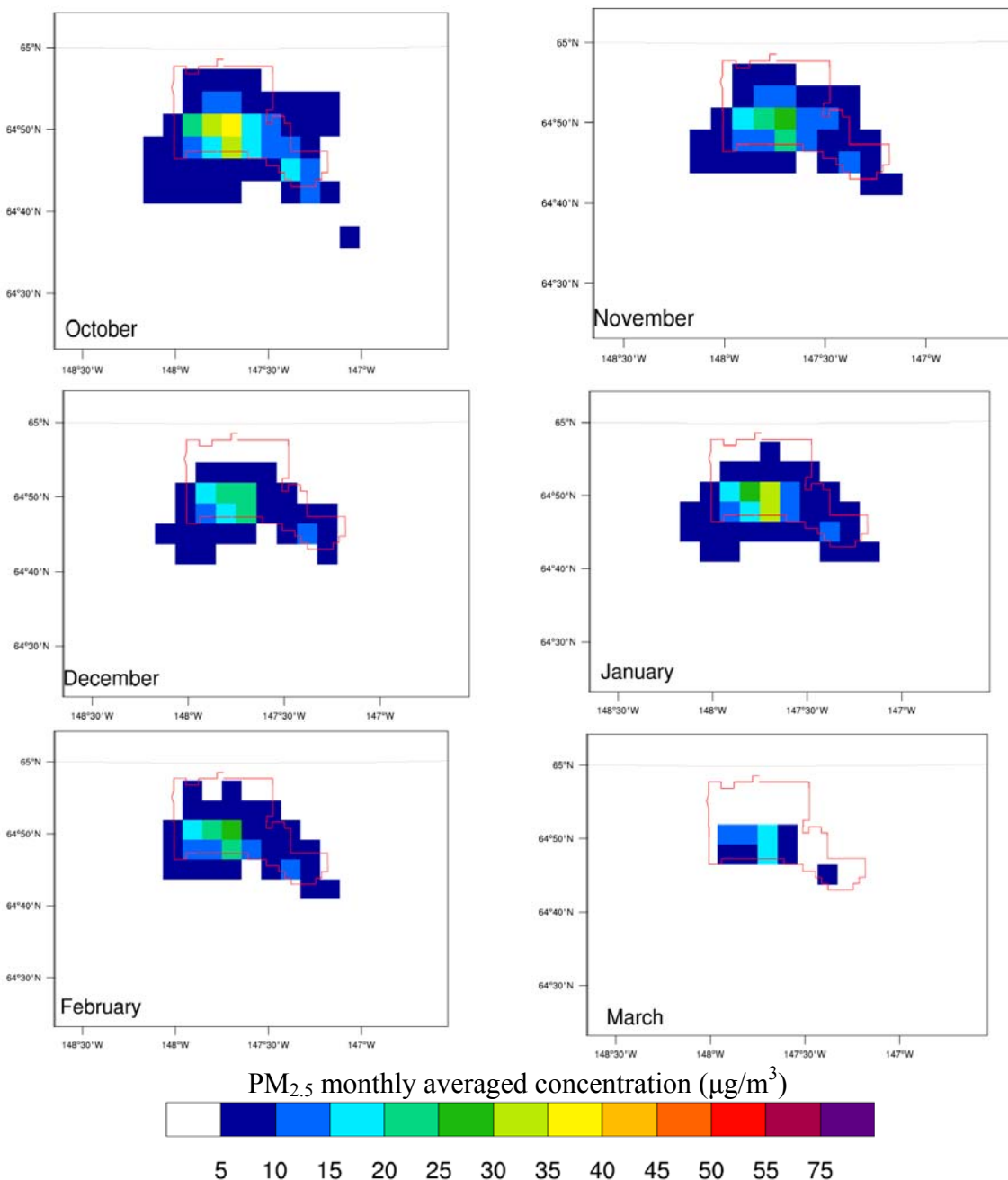


Fig. 32. Like Fig. 25 but for LSF.

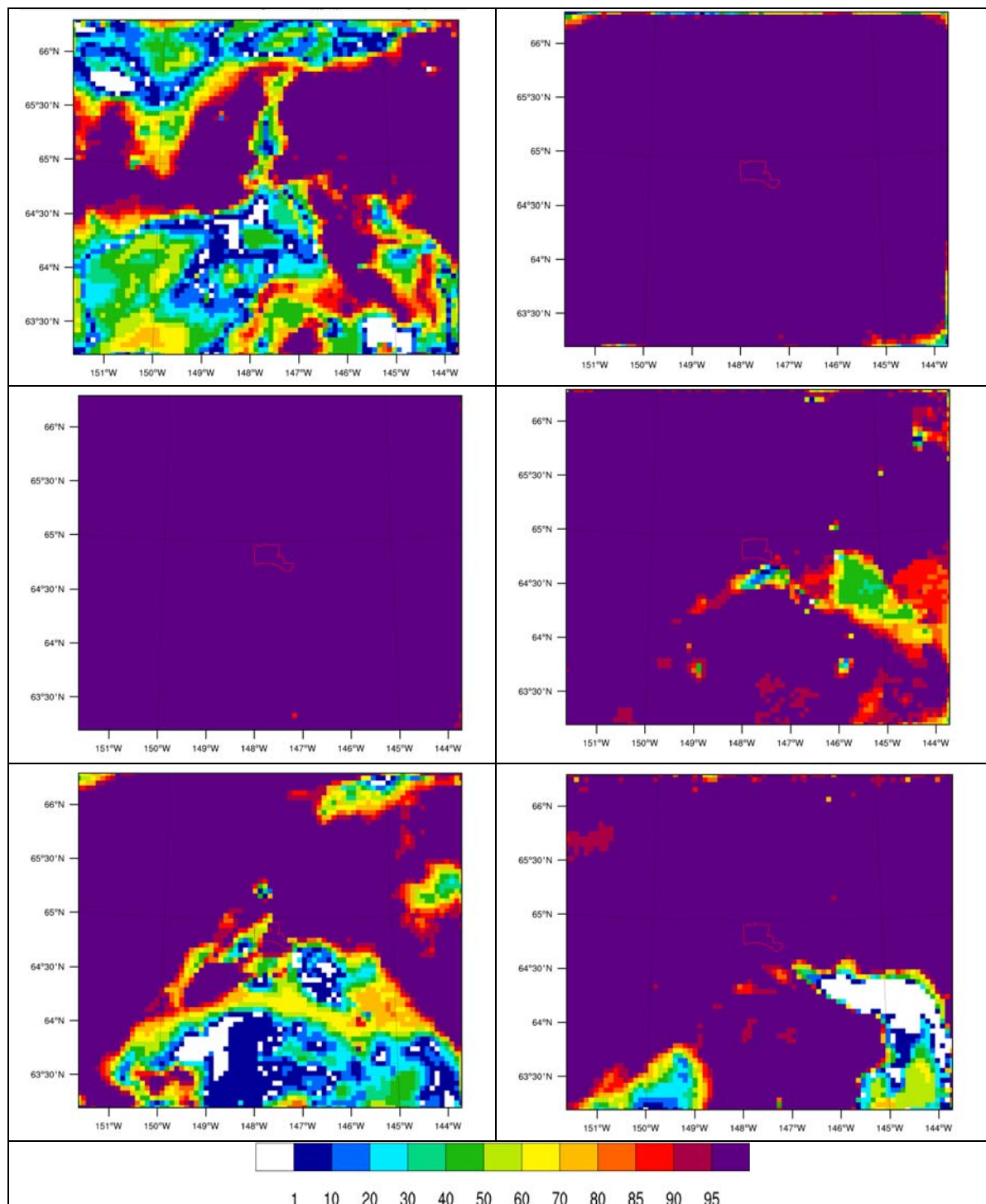


Fig. 33. Monthly rank of “true” differences over “false” differences of $PM_{2.5}$ -concentration for October 2008 to March 2009 (from top left to bottom). At grid-cells ranking higher than the 95% percentile, the low sulfur fuel scenario has high efficiency in reducing concentrations in nonattainment area only in November, December, January and March.

Comparison of the monthly mean 24h-average $PM_{2.5}$ concentrations (Figs. 25, 32) shows the same hot spots in October, January, February and March than for REF, but these hotspots have

lower values in LSF. The local reduction is smaller in February and March than in the relatively cold October. The distribution-patterns of PM_{2.5} concentrations change notably for November and December. These spatial changes suggest that gas-to-particle conversion to changes in the concentrations. Note that these processes depend on the concentrations of precursor gases, photolysis rates, temperature and humidity in non-linear ways. Thus, small changes in the concentrations of precursors may lead to much higher or lower gas-to-particle conversion rates.

Like for NPE and WSR we applied the FEA method to the data of LSF and REF. The FEA results indicate that the concentration differences (REF-LSF) in November, December, January, February and March are due to the introduction of low sulfur fuel (Fig. 33). In October, obviously random effects may play a role.

6.3 Comparison of the mitigation measures relative to each other

EPA's Office of Air Quality Planning and Standards in conjunction with the EPA Regional Offices compute design values based on observations in previous years, and review and publish them annually [EPA, 2011]. Design values are expressed as a concentration instead of an exceedance. These design values describe the air-quality status of a given area relative to the NAAQS. Consequently, design values can be used to classify nonattainment areas, develop control strategies, and assess progress towards meeting the NAAQS [EPA, 2011]. The design value for the baseline year 2008 for the Fairbanks nonattainment area is 44.5 µg/m³ [Huff, 2011; pers. communication]. The design values of 2005-2007, 2006-2008, and 2007-2009 were 39, 41, and 57, respectively [EPA, 2011]. These values partly reflect the decreasing air quality in response to the increase in wood burning.

Emissions are temperature dependent – more heating is required when it is colder than warmer outside. The winter episode 2007-2009 was about 0.7°F colder than that of 2008-2010 (Table 3). This fact explains why the 2008-2010 design value is smaller than the 2007-2009 design value. The average temperature OTM for winter 2008/09 was 0.3°F, i.e. much colder than winter 2007/08 (4.9°F) or winter 2009/10 (4.5°F).

An easy way to compare the impacts of the altered emissions on the PM_{2.5} concentrations and their composition at breathing level is to determine the relative response factors (RRF). The RRF for each simulated particulate matter component *j* at site *i* is given by [EPA, 2007]

$$RRF_{ij} = \frac{[C_{j,projected}]}{[C_{j,current}]} \quad (5)$$

Where in our study $[C_{j,projected}]$ is the mean concentration obtained from the various simulations with altered emissions (e.g. WSR or LSF), and $[C_{j,current}]$ is the respective mean concentration obtained from the reference simulation for the episode simulated. Note that the lower the RRF value is the higher is the response to the measure (e.g. “woodstove replacement”, “introduction of low sulfur fuel”).

Table 6 summarizes the RRFs for the grid-cell holding the State Building, i.e. the official monitoring site. The RRFs suggest that point sources contribute slightly to the PM_{2.5} concentration and its composition at the State Building. This finding is not surprising because several point sources are in the immediate vicinity of this site. However, as discussed above, on average over the non-attainment area, the contribution of point sources to the total PM_{2.5} concentration is relatively low. The very low RRF for NH₄ obtained for January results from the

very low NH_4 concentrations in both REF and NPE as compared to the other months. Speciation data did not become available before the end of this project. Therefore, no through analysis and interpretation of simulated vs. observed speciation is included in this report. A first screen of this data, however, supports that simulated NH_4 concentrations are too low (Fig. 34). A detailed analysis of simulated speciation was beyond the scope of our study, but should be done in the future to improve forecasts. Future studies should investigate the role of NH_4 and the emission sources of NH_3 that seem to be missing in the NEI2008 for Fairbanks.

Table 6. Relative response factors for $\text{PM}_{2.5}$ and the particulate matter composition as obtained for the scenarios without point source emissions (NPE), with woodstove replacement (WSR) and low sulfur fuel (LSF) at the grid-cell holding the official $\text{PM}_{2.5}$ site at the State Building for various periods. EC, ORG and PBW stand for elemental carbon, organic compounds, and particle bound water, respectively. Note that for the NPE scenario investigations were only to be carried out for November through February (cf. Table 1). Note that the baseline (reference) for the response factors of NPE (winter 2005/06) differs from that of WSR and LSF. WSR and LSF both use the same baseline of winter 2008/09.

	$\text{PM}_{2.5}$	SO_4	NO_3	NH_4	EC	ORG	PBW
NPE							
Nov	0.957	0.961	0.858	0.976	0.961	0.961	0.949
Dec	0.964	0.963	0.954	1.019	0.962	0.962	0.971
Jan	0.973	0.978	0.849	0.247	0.977	0.977	0.959
Feb	0.970	0.971	0.954	0.810	0.970	0.970	0.971
Nov-Dec	0.960	0.962	0.901	0.996	0.961	0.961	0.960
Jan-Feb	0.972	0.976	0.865	0.254	0.975	0.975	0.963
Winter 05/06	0.966	0.969	0.892	0.965	0.969	0.969	0.961
WSR							
Oct	0.958	0.959	0.865	1.003	0.959	0.959	0.954
Nov	0.950	0.952	0.898	1.005	0.951	0.951	0.948
Dec	0.950	0.952	1.001	1.001	0.950	0.951	0.949
Jan	0.953	0.952	0.887	1.075	0.952	0.952	0.951
Feb	0.944	0.940	1.041	0.891	0.939	0.939	0.944
Mar	0.941	0.943	0.855	1.005	0.941	0.941	0.941
Oct-Dec	0.954	0.955	0.880	1.004	0.954	0.954	0.951
Jan-Mar	0.946	0.947	0.935	0.976	0.945	0.945	0.946
Winter 08/09	0.950	0.951	0.897	0.991	0.950	0.950	0.949
LSF							
Oct	0.975	0.974	1.023	1.016	0.973	0.973	0.976
Nov	0.943	0.944	0.937	0.998	0.943	0.943	0.944
Dec	0.945	0.946	0.925	0.999	0.944	0.944	0.945
Jan	0.966	0.966	0.947	1.074	0.965	0.965	0.965
Feb	0.957	0.955	1.129	0.887	0.955	0.955	0.961
Mar	0.953	0.954	0.926	1.002	0.952	0.952	0.953
Oct-Dec	0.957	0.957	0.970	1.004	0.956	0.956	0.958
Jan-Mar	0.960	0.959	1.006	0.973	0.959	0.959	0.961
Winter 08/09	0.958	0.958	0.981	0.990	0.957	0.957	0.959

The RRFs also indicate that there is not much wiggle room related to point-source emission. Recall that in the real world, point sources cannot be “switched off”. Power plants, for instance, ensure the supply of energy. Thus, if “switching them off” in the model world does not reduce the concentration much – as indicated by the RRFs – introduction of filters to reduce the point-source emissions will not solve the problem either as the point sources still will emit even though at a lower rate.

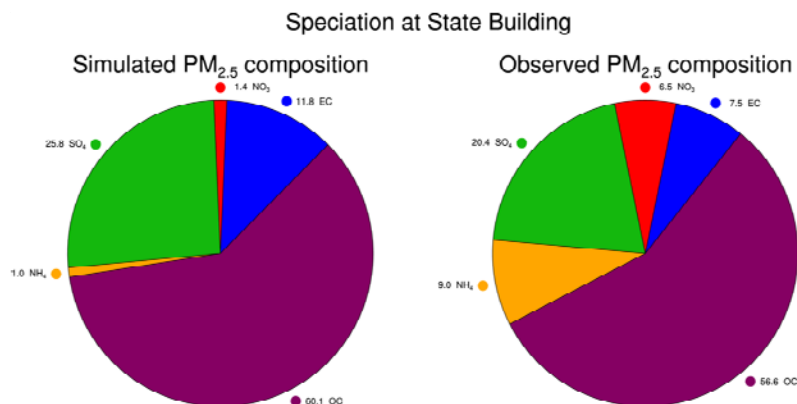


Fig. 34. Comparison of simulated and observed PM_{2.5} components for winter 2005/06. Observed data courtesy of *D. Huff* [2011].

The RRFs for the “low sulfur fuel” and “woodstove replacement” scenarios are of similar magnitude, but on average over the entire winter slightly favor a “woodstove replacement” program. The RRFs to the introduction of low sulfur fuel show a higher variability among months than to the woodstove replacement. This means that for individual months “introduction of low sulfur fuel” may yield a stronger mitigation than “woodstove replacement”. However, the latter seems to be the more temporally reliable measure as it more stably provides similar RRFs.

The RRFs of the various compounds of PM_{2.5} indicate shifts in the composition in response to the altered emissions (Table 6). This means that both measures (“woodstove replacement”, “introduction of low sulfur fuel” for heating and use in oil burning facilities) strongly affect the atmospheric chemistry and secondary aerosol formation via gas-to-particle conversion. The composition changes differ for the two measures. The “woodstove replacement” yields a shift towards more NH₄ and less NO₃ aerosols in most months. The composition shifts in response to “introduction of low sulfur fuel” vary more strongly among months than in response to “woodstove replacement”.

To calculate the future design values we multiplied the observed design value with the RRFs obtained for the various measures tested. The resulting new design values are listed in Table 7.

Table 7. Calculated PM_{2.5} “design values” (μg/m³) in response to the tested measures for the grid-cell holding the State Building for various periods. Here “winter” refers to November 2005 to February 2006 for the NPE scenario and October 2008 to March 2009 for the “woodstove replacement” and “low sulfur fuel” scenarios.

	No point source emissions	small woodstove replacement program	introduction of low sulfur fuel
Oct	--	42.6	43.4
Nov	42.6	42.3	42.0
Dec	42.9	42.3	42.1
Jan	43.3	42.4	43.0
Feb	43.2	42.0	42.6
Mar	--	41.9	42.4
Oct-Dec	--	42.5	42.6
Jan-Mar	--	42.1	42.7
Nov-Dec	42.7	--	42.6
Jan-Feb	43.3	--	43.4
Winter	43.0	42.3	42.0

The introduction of low sulfur fuel results in a slightly lower new design value than the small “woodstove replacement program” assumed in WSR. The results also showed that such a small “woodstove replacement program” reduces the design value already by $2.2\mu\text{g}/\text{m}^3$. The sensitivity studies performed on “woodstove replacement” suggested that a more rigorous replacement (WSS1) than assumed in WSR may yield much higher mitigation. Since the introduction of low sulfur fuel is very expensive, since a further reduction of sulfur content costs even more, and since the RRF and resulting new design values vary strongly among months when introducing low sulfur fuel, it seems that a rigorous replacement of non-certified wood-burning devices is the more promising way to achieve compliance.

Comparison of Figs. 25, 26, and 32 suggests that both “woodstove replacement” as well as “introduction of low sulfur fuel” reduce the concentrations in the nonattainment area. However, while hot spots remain in the same areas in the case of a “woodstove replacement” for all months, this is not the case when introducing low sulfur fuel.

7. Conclusions

We performed simulations for November 2005 to February 2006 with and without consideration of point-source emissions (Table 1) using the Alaska-adapted WRF/Chem¹² to assess the contribution of point-source emissions on the PM_{2.5}-concentrations at breathing level. The emission data for the reference simulation (business-as-usual) based on the NEI2005. The simulation without consideration of point-source emissions was run with the same meteorological input data and same emission data except that all point-source emissions were set to zero (NPE). Based on the comparison of the results of these simulations, we conclude that point sources are not the major cause for Fairbanks' wintertime PM_{2.5}-pollution problem. This conclusion is also supported by the results of the other mitigation scenarios. Eliminating the point-source emissions – as it is practically done in the NPE simulation – only led to marginal decreases in PM_{2.5} concentrations at breathing level and only five avoidances of exceedances at locations in the nonattainment area. The highest PM_{2.5}-concentrations obtained in REF and NPE only differ 1.3µg/m³ on average. The locations where simulated PM_{2.5} exceeds the NAAQS occur in the nonattainment area. According to the results of REF and NPE, PS6¹³ is the point source that often contributes to exceedances in the nonattainment area. However, in these cases concentrations without that point source were already high. Note that this point source has the highest emission rate. Emissions from point sources located in the nonattainment area may influence the PM_{2.5}-concentration at breathing level within 10km or so from the point-source-holding air column. This phenomenon is a combined effect of extreme atmospheric stable condition, weak circulation, and for some point sources the low-level in which they emit. These meteorological conditions altogether inhibit transport of the pollutants out of the area. It would be worth examining how increases in stack height and emission temperature (which also would lead to emissions into higher levels) would affect the point-sources' radius of impact and the PM_{2.5} concentrations at breathing level.

Based on or simulations with and without consideration of point-source emissions we conclude that when “switching off” of the point sources does not solve the problem, reducing point-source emissions by new techniques will not solve the problem either as the point sources still emit even though at a lower rate. For days that are close to the NAAQS, just a marginal increase in area emission would lead to an exceedance.

Some of the PM_{2.5} in the air is formed in the air from gases that transform to particles via physico-chemical processes called gas-to-particle conversion. Since gas-to-particle conversion non-linearly depends on temperature and vapor pressure of species and introducing measures to further clean the exhausts of point sources alters the composition of the point-source emission plumes, it may be worth examining whether in combination with other measures such additional filtering may nevertheless be beneficial.

In addition to the investigation on the impact of point sources on PM_{2.5}-concentrations in the nonattainment area, we performed a suit of simulations for October 2008 to March 2009 with the Alaska optimized WRF/Chem (Table 1). This suit of simulations assumed the same meteorological initial input data and boundary conditions. The reference simulation (REF) used the NEI2008 updated with point-source emissions (for details see section on emissions). Two scenarios were run. One scenario assumed a replacement program for non-certified wood-

¹² Note that WRF/Chem is a complex state-of-the-art research model, not a regulatory model.

¹³ Privacy law forbids naming facilities.

burning devices. With the assumptions made on how households with several heating devices partition heating among devices and the burning behavior and number of non-certified burning devices replaced, the $PM_{2.5}$ emissions from heating were reduced by 4% on average over the nonattainment area over the six months (WSR). Two sensitivity studies were performed assuming different numbers of non-certified wood-burning devices that could be replaced (WSS1, WSS2). In addition, sensitivity analysis was made how emissions change with the assumptions on the burning behavior (partitioning among devices, time of burning). The second scenario mitigation for winter 2008/09 assumed the use of low sulfur fuel for domestic combustion, oil-burning point-source facilities and that part of power generation that used oil-fuel in accord with the 2008 allowances for fuel-sulfur content (LSF).

The LSF and WSR mitigation studies (like the study on the contribution of point-source emissions on the $PM_{2.5}$ -concentrations at breathing level) suggest that emissions from area sources (e.g. domestic heating) and/or traffic are the main contributors to the $PM_{2.5}$ NAAQS exceedances occurring in the nonattainment area.

The “woodstove replacement” simulations indicate that a program for replacement of wood-burning devices can reduce the $PM_{2.5}$ -concentrations at breathing level in the Fairbanks $PM_{2.5}$ -nonattainment area. The study suggests that the highest mitigation of $PM_{2.5}$ -concentrations with a “woodstove replacement” can be achieved in the months that are coldest. The sensitivity studies suggest that the reduction effectiveness depends on the number of wood-burning devices exchanged and on what kinds of devices are replaced (see results of WSR, WSS1, WSS2). The average emission reduction in the heating sector calculated for October 1 to October 15, 2008 amounts 40%, 7% and 6% on average over the nonattainment area under the assumption made for the “woodstove replacement” in WSS1, WSS2, and WSR, respectively. Note that we are here talking about the emission reduction of primary $PM_{2.5}$, not the emission reductions for other species (e.g. SO_2 , NO_x , VOC) that go along with a “woodstove replacement”.

Unfortunately, no data are available, where and what wood-burning devices are operated and when and how intensively. In our study, we simply assumed the distribution of wood-burning devices as being proportional to the population density. This assumption holds uncertainty in the spatial distribution that may affect local maximum concentrations as well as 24h-averages of $PM_{2.5}$ -concentrations according to sensitivity studies. Further uncertainty is due to the unknown number of wood-burning devices that exist and that can be replaced. Sensitivity studies on the emissions indicated that uncertainty results from the unknown partitioning of the use of wood-burning and other heating devices in households with more than one heating option. Despite these uncertainties, all simulation studies on “woodstove replacement” show in common a mitigation of $PM_{2.5}$ -concentrations on average at breathing level. Note that the simulations on “woodstove replacement” do not consider that additional wood-burning devices may have been added since 2008 or might be added in the future.

Based on the studies performed on the replacement of wood-burning devices we can conclude that exchanging noncertified wood-burning devices can help to reduce the number of exceedance days during October to March. The full benefit of exceedance reduction due to the “woodstove replacement” may be underestimated by WSR because the number of woodstoves exchanged may be on the lower end of the number of woodstoves that actually could/will be exchanged. Nevertheless, the concentration offsets between the baseline simulation REF and the “future” simulation WSR (Table 6, Figs. 25, 26) imply that replacement of non-certified wood-burning devices alone when only preformed in low numbers will not be sufficient to avoid all $PM_{2.5}$

exceedances. If emissions of area and point sources only slightly increase due to increasing of traffic, population, etc. the benefit due to the “woodstove replacement” will be set off quickly. This means a high number of non-certified wood-burning devices has to be replaced.

We further conclude that there is an urgent need to collect data on the location and kind of wood-burning devices used in the nonattainment area and to obtain additional information on how households with wood-burning devices and another heating device partition their heating among these heat sources. Information is also needed on the diurnal burning behavior on weekdays, weekends and holidays. Since emissions also depend on the dryness of the wood, data on the fraction of seasoned and non-seasoned wood typically burned will be helpful in better assessing the contribution from wood-burning devices to the PM_{2.5}-concentrations at breathing level. Furthermore, it would be good to know how accurate data from surveys may be if people fear, their information could later lead to measures that may be of disadvantage to them. This means it has to be examined whether we do obtain the correct information in surveys.

Our study suggests that the introduction of low sulfur fuel can reduce the number of exceedance days. The simulations suggest that introduction of low sulfur fuel as assumed in LSF leads occasionally to higher reductions than achieved by the “woodstove replacement” (WSR) assumed in this study. However, the results also suggest that up to 20% of the days in months with relatively long daylight hours (October, February, March) may experience increases in PM_{2.5}-concentrations at breathing level in response to introduction of low sulfur fuel due to gas-to-particle conversion. This increase is related to shifts in the thermodynamic equilibrium of sulfate-nitrate-ammonia-water in aerosol during months with still or already again enough daylight. The highest temporal and local differences in simulated PM_{2.5} concentrations in response to introducing low sulfur fuel typically occurred in November whereas the lowest differences occurred in March. The reason is that October had high and February, March small increases in PM_{2.5}-concentrations after introducing low sulfur, while there were no increases in November.

The results of the simulation on the introduction of low sulfur fuel also suggest that in the case of measures aiming at mitigation indirectly by reduction of precursors it is important to simulate an entire winter emission season. Otherwise one could by accident just be lucky to have chosen a period where reduction occurs and oversee that there may be cases where despite reduced emissions of precursors the concentrations go up. Moreover, only in the case of the statistics over the entire winter it is possible to judge whether, on average, mitigation can be reached. Our study also suggests that care has to be taken in the judgment of the representativeness of the winter examined.

The simulation results showed that “introduction of low sulfur fuel” (LSF) results in a slightly lower new design value than the small “woodstove replacement program” assumed in WSR. The results also showed that a small “woodstove replacement program” such as assumed in WSR already reduces the design value by 2.2µg/m³. The sensitivity studies performed on “woodstove replacement” (WSS1, WSS2) suggested that a more rigorous replacement of wood-burning devices (WSS1) may yield much higher mitigation than the small exchange program assumed in WSR. Since the introduction of low sulfur fuel is very expensive and further reduction costs even more, and since the relative response factors and new design values vary strongly among months when introducing low sulfur fuel, it seems that a rigorous replacement of non-certified wood-burning devices is much more promising to achieve compliance.

The results of all the simulations performed for this study suggest that a single pollution-control policy may not be sufficient to help comply with the 24h-average PM_{2.5} NAAQS. Due to the high nonlinearity of chemical processes, we cannot assume that a combined “woodstove replacement” and “low sulfur fuel” program will lead to the goal. An additional study considering both measures would be required because precursors for gas-to-particle conversion are changed by both measures and interaction among the impacts of the two measures may yield to diminution or enhancement of wanted or even unwanted effects. Since changes in emissions of precursors lead to changes in gas-to-particle conversion, combinations of different control methods (i.e. “woodstove replacement” and concurrent “low sulfur fuel” programs) and other mitigation strategies (i.e. replacement of oil furnaces by gas, replacement of oil furnaces and wood-burning devices by gas) should be investigated. Future studies should also examine the impact of introducing other energy sources and/or expansion the use of gas for heating and energy generation.

The results of our study also show a stronger percentage mitigation of PM_{2.5}-concentrations on average over the entire nonattainment area than at the grid cell holding the State Building. In the future, it should be examined whether observations also show differences in changes of air quality at various sites in the nonattainment area. If so, local sources may play a role and they should be identified.

Unfortunately, the speciation data did not become available during the time of the project. Thus, an evaluation of the simulated composition of PM_{2.5} is still pending, but planned for the future. Such an evaluation of simulated speciation is an urgent need to assess the role of ammonia. Based on speciation data of prior years and a first screen of the data that became available after the end of the project (Fig. 34), various scientists are concerned that the NEI2008 may underestimate the NH₄ emissions in the FNSB.

Personnel who worked on this study:

Nicole Mölders, Ph.D., Ph.D.

Huy N.Q. Tran, M.S.

Ketsiri Leelasakultum, M.S.

Kelcy Brunner, undergraduate student

Todd Fortun, undergraduate student

References:

- Bell, M.L. (2006) The use of ambient air quality modeling to estimate individual and population exposure for human health research: A case study of ozone in the Northern Georgia Region of the United States. *Environment International*, 32, 586–593.
- Binkowski, F. S., and U. Shankar (1995), The regional particulate matter model, 1. Mode description and preliminary results, *Journal Geophysical Research*, 100, 26191-26209.
- Bourne, S. M., U. S. Bhatt, J. Zhang, and R. Thoman (2010), Surface-based temperature inversions in Alaska from a climate perspective, *Atmospheric Research*, 95, 353-366.
- Carlson, T. R., S.-H. Yoon, and R. G. Diulla (2010), Fairbanks home heating survey *Rep.*, 63 pp, Sacramento, CA.
- Carpenter, S., T. Frost, D. Heisey, and T. Kratz (1989), Randomized intervention analysis and the interpretation of whole-ecosystem experiments, *Ecology*, 70, 1142– 1152.
- Chang, J. C., and S. R. Hanna (2004), Air quality model performance evaluation, *Meteorol Atmos Phys*, 87, 167–196.
- Dawson, J.P., P.J. Adams, and S.N. Pandis (2007), Sensitivity of PM_{2.5} to climate in the Eastern U.S.: a modeling case study, *Atmos. Chem. Phys.*, 7, 6487-6525.
- Davies, J., D. Misiuk, R. Colgan, and N. Wiltse (2009), Reducing PM_{2.5} emissions from residential heating sources in the Fairbanks North Star Borough: Emission estimates, policy options, and recommendations *Rep.*, 56 pp, Cold Climate Housing Research Center.
- DOT (2009), Northern Region Annual Traffic Volume Report - Volume I 2009 *Rep.*, 200 pp, Department of Transport and Public Facilities, Alaska.
- Eder, B., D. Kang, R. Mathur, J. Pleim, S. Yu, T. Otte, G. Pouliot (2009), A performance evaluation of the National air quality forecast capability for the summer of 2007. *Atmos. Environ.*, 43, 2312-2320.
- EPA (2007) http://www.epa.gov/glo/SIPToolkit/documents/20070322_72fr_13560-13581_exceptional_events_data.pdf.
- EPA (2009) <http://www.epa.gov/>.
- EPA (2011) <http://www.epa.gov/airtrends/values.html>.
- Fortun, T., and N. Mölders (2009), Investigations on the sensitivity of predicted air quality to the uncertainty in anthropogenic emissions. *Rep.*, 18 pp, ARSC, Fairbanks, AK.
- Gaudet, B.J., D.R. Stauffer (2010) Stable boundary layers representation in meteorological models in extremely cold wintertime conditions, EPA report, pp. 60.
- Grell, G.A., S. Emeis, W.R. Stockwell, T. Schoenemeyer, R. Forkel, J. Michalakes, R. Knoche, W. Seidl (2000), Application of a multiscale, coupled MM5/chemistry model to the complex terrain of the VOTALP valley campaign. *Atmos. Environ.* 34, 1435-1453.
- Grell, G. A., and D. Dévényi (2002), A generalized approach to parameterizing convection, *Geophysical Research Letters*, 29.
- Grell, G.A., S.E. Peckham, R. Schmitz, S.A. McKeen, G. Frost, W.C. Skamarock, B. Eder (2005), Fully coupled “online” chemistry within the WRF model. *Atmos. Environ.* 39, 6957-6975.
- Guenther, A., et al. (1994), A global model of natural volatile organic compound emissions, *Journal Geophysical Research*, 100D, 8873-8892.
- Mölders, N. (2009), Alaska Emission Model (AkEM) description. *Rep.*, 10 pp, Fairbanks.
- Hart, M., and R. de Dear (2004), Weather sensitivity in household appliance energy end-use, *Energy and Buildings*, 36(2), 161-174.
- Hong, S.-Y., and J.-O. J. Lim (2006), The WRF Single-Moment 6-class microphysics scheme (WSM6), *Journal Korean Meteorological Society*, 42, 129-151.
- Hong, S.-Y., Y. Noh, and J. Dudhia (2006), A new vertical diffusion package with an explicit treatment of entrainment, *Mon. Wea. Rev.* , 134, 2318-2341.
- Janjić, Z. I. (1994), The step-mountain eta coordinate model: further developments of the convection, viscous sublayer and turbulence closure schemes, *Mon. Wea. Rev.*, 122, 927-945.
- Janjić, Z. I. (2002), Nonsingular implementation of the Mellor-Yamada level 2.5 scheme in the NCEP meso model *Rep.*, 61pp
- Johnson, R., T. Marsik, M. Lee, and C.F. Cahill (2009), Helping Fairbanks meet new air quality requirements: Developing ambient PM-2.5 management strategies, in *Transportation safety, security, and innovation in cold regions*, p. 1.
- Kannari, A., D. G. Streets, Y. Tonooka, K. Murano, and T. Baba (2008), MICS-Asia II: An inter-comparison study of emission inventories for the Japan region, *Atmospheric Environment*, 42, 3584-3591.

- Kim, J., B. Kwak, H.-S. Park, N. Kim, K. Choi, and J. Yi (2010), A GIS-based national emission inventory of major VOCs and risk assessment modeling: Part I — methodology and spatial pattern of emissions, *Korean Journal of Chemical Engineering*, 27(1), 129-138.
- Kramm, G., K.-D. Beheng, and H. Müller (1992), *Vertical transport of polydispersed aerosol particles in the atmospheric surface layer*, 1125-1141 pp., The Semonin Vol. Hemisphere Publ., Washington/Philadelphia/London.
- Kumar, P., A. Robins, S. Vardoulakis, and R. Britter (2010), A review of the characteristics of nanoparticles in the urban atmosphere and the prospects for developing regulatory controls, *Atmospheric Environment*, 44, 5035-5052.
- Madronich, S. (1987), Photodissociation in the atmosphere, 1, actinic flux and the effects of ground reflections and clouds, *Journal Geophysical Research*, 92, 9740-9752.
- McCreanor, J., et al. (2007), Respiratory Effects of Exposure to Diesel Traffic in Persons with Asthma, *New England Journal of Medicine*, 357, 2348-2358.
- Mlawer, E. J., S. J. Taubman, P. D. Brown, M. J. Iacono, and S. A. Clough (1997), Radiative transfer for inhomogeneous atmospheres: RRTM, a validated correlated-k model for the longwave, *Journal of Geophysical Research*, 102D, 16663-16682.
- Mölders, N., H. Hass, H. J. Jakobs, M. Laube, and A. Ebel (1994), Some effects of different cloud parameterizations in a mesoscale model and a chemistry transport model, *J. Appl. Meteor.*, 33, 527-545.
- Mölders, N. (2008), Suitability of the Weather Research and Forecasting (WRF) model to predict the June 2005 fire weather for Interior Alaska, *Wea. Forecast.*, 23, 953-973.
- Mölders, N. (2009), Alaska Emission Model (AkEM) description *Rep.*, 10 pp, Fairbanks.
- Mölders, N. (2010), Alaska Emission Model (AkEM) - version 1.01 description. *Rep.*, 16 pp, Fairbanks.
- Mölders, N., and G. Kramm (2010), A case study on wintertime inversions in Interior Alaska with WRF, *Atmospheric Research*, 95, 314-332.
- Mölders, N., S. E. Porter, C. F. Cahill, and G. A. Grell (2010), Influence of ship emissions on air quality and input of contaminants in southern Alaska National Parks and Wilderness Areas during the 2006 tourist season, *Atmospheric Environment*, 44, 1400-1413.
- Mölders, N., S. E. Porter, T. T. Tran, C. F. Cahill, J. Mathis, and G. B. Newby (2011), The effect of unregulated ship emissions for aerosol and sulfur dioxide concentrations in southwestern Alaska, in *North by 2020: Perspectives on a Changing North*, edited by K. Criddle, H. Eicken, A. Lovecraft and A. Metzger, p. 14, Alaska University Press, Fairbanks, in press.
- NESCAUM (2005), Low Sulfur Heating Oil in the Northeast States: An Overview of Benefits, Costs and Implementation Issues *Rep.*, Boston, MA: NESCAUM.
- Otte, T.L., G. Poulliot, J.E. Pleim, J.O. Young, K.L. Schere, D.C. Wong, P.C.S. Lee, M. Tsidulko, J.T. McQueen, P. Davidson, R. Mathur, H.-Y. Chuang, G. DiMego, N.L. Seaman, (2005), Linking the Eta Model with the Community Multiscale Air Quality (CMAQ) modeling system to build a national air quality forecasting system. *Wea. Forecast.*, 20, 367-384.
- Peckham, S. E., et al. (2009), WRF/ChemVersion 3.1 User's Guide *Rep.*, 78 pp.
- Riediker, M., W. E. Cascio, T. R. Griggs, M. C. Herbst, P. A. Bromberg, L. Neas, R. W. Williams, and R. B. Devlin (2004), Particulate Matter Exposure in Cars Is Associated with Cardiovascular Effects in Healthy Young Men, *Am. J. Respir. Crit. Care Med.*, 169(8), 934-940.
- Schell, B., I. J. Ackermann, H. Hass, F. S. Binkowski, and A. Ebel (2001), Modeling the formation of secondary organic aerosol within a comprehensive air quality model system, *J. Geophys. Res.*, 106(D22), 28275-28293.
- Seinfeld, J. H., and S. N. Pandis (1997), *Atmospheric Chemistry and Physics, from Air Pollution to Climate Change* John Wiley & Sons.
- Shulski, M., and G. Wendler (2007), *The Climate of Alaska*, 216 pp., University of Alaska Press, Fairbanks.
- Simpson, D., A. Guenther, C. N. Hewitt, and R. Steinbrecher (1995), Biogenic emissions in Europe 1. Estimates and uncertainties, *Journal Geophysical Research*, 100D, 22875-22890.
- Smirnova, T. G., J. M. Brown, S. G. Benjamin, and D. Kim (2000), Parameterization of cold season processes in the MAPS land-surface scheme, *Journal Geophysical Research*, 105D, 4077-4086.
- Stockwell, W. R., P. Middleton, J. S. Chang, and X. Tang (1990), The second-generation regional acid deposition model chemical mechanism for regional air quality modeling, *Journal Geophysical Research*, 95, 16343-16367.
- Tetzlaff, G., R. Dlugi, K. Friedrich, G. Gross, D. Hinneburg, U. Pahl, M. Zelger, and N. Mölders (2002), On modeling dry deposition of long-lived and chemically reactive species over heterogeneous terrain, *J. Atm. Chem.*, 42, 123-155.

- Tran, H. N. Q., and N. Mölders (2011), Investigations on meteorological conditions for elevated PM_{2.5} in Fairbanks, Alaska, *Atmospheric Research*, 99(1), 39-49.
- von Storch, H., and F. W. Zwiers (1999), *Statistical Analysis in Climate Research*, 484pp. pp., Cambridge University Press.
- Werth, D., and R. Avissar (2002), The local and global effects of Amazon deforestation, *Journal of Geophysical Research*, 107, 8.
- Wesley, M. L. (1989), Parameterization of surface resistances to gaseous dry deposition in regional-scale numerical models, *Atmospheric Environment* 23, 1293-1304.
- Wexler, A. S., and J. H. Seinfeld (1992), Analysis of aerosol ammonium nitrate: departures from equilibrium during SCAQS, *Atmos. Environ.*, 26A, 579–591.
- Yarker, M. B., D. PaiMazumder, C. F. Cahill, J. Dehn, A. Prakash, and N. Mölders (2010), Theoretical investigations on potential impacts of high-latitude volcanic emissions of heat, aerosols and water vapor and their interactions on clouds and precipitation, *The Open Atmospheric Science Journal*, 4, 24-44.
- Yu, S., R. Mathur, K. Schere, D. Kang, J. Pleim, J. Young, D. Tong, G. Pouliot, S.A. McKeen, S.T. Rao (2008), Evaluation of real-time PM_{2.5} forecasts and process analysis for PM_{2.5} formation over the eastern United States using the Eta-CMAQ forecast model during the 2004 ICARTT study. *J. Geophys. Res.*, 113, D06204, doi:10.1029/2007JD009226.

Fairbanks North Star Borough PM_{2.5} Non-Attainment Area CMAQ Modeling

Final Report Phase II

Reporting Period: January 1, 2012 – December 31, 2012

Project: 398831 CMAQ-DEC 2012

By Prof. Nicole Mölders (PhD, PhD) and Ketsiri Leelasakultum (MS)

University of Alaska Fairbanks, Geophysical Institute, College of Natural Science and
Mathematics, Department of Atmospheric Sciences

1. Background

The Community Multiscale Air Quality (CMAQ) model version 4.7.1 was adapted to simulate the PM_{2.5}-concentrations in Fairbanks, Interior Alaska in phase I [Mölders and Leelasakultum, 2011]. The adapted CMAQ was applied to a two-week episode in January/February, 2008 and November, 2008 each for investigations on and understanding of the PM_{2.5}-situation in the Fairbanks nonattainment area.

According to the final report of phase I [Mölders and Leelasakultum, 2011], the CMAQ model was configured to use the global mass-conserving Yamartino advection scheme, the eddy vertical diffusion module, the Carbon Bond Five (CB05) lumped gas phase chemistry mechanism, which uses the Euler Backward Iterative (EBI) as solver, the AERO5 aerosol mechanism, the photolysis inline module, and the Asymmetric Convective Method (ACM) cloud processor to compute convective mixing (cloud_acm_ae5). As described in the final report of phase I, we had made several changes to the CMAQ code to improve the prediction of PM_{2.5}-concentrations and to represent the conditions in the Fairbanks domain. Those changes were the development of Alaska specific initial and boundary conditions, modification of the dry deposition code, reducing of the minimum mixing height, replacing the minimal stomata resistances, decreasing the lowest and highest eddy diffusivity coefficients by half and scaling them according to the fraction of land-use, and reducing the wind-speed by half in valleys within the domain. The latter step has been abandoned in the further studies. This step was only done only for investigation of the magnitude of the impact of the overestimated wind-speeds obtained from the Alaska adapted WRF (see Gaudet and Staufner [2012] for details on this WRF version). This means all results reported in the current report use the original simulated wind-speed as obtained from WRF.

Based on the CMAQ's output in phase I, Sierra Research Inc. had improved the emission input data generated by using the Sparse Matrix Operator Kernel Emission (SMOKE). Penn State [Gaudet and Staufner, 2012] had updated the meteorological input data generated for the Alaska adapted CMAQ model (called adapted CMAQ hereafter) by using the Weather Research and Forecasting (WRF; Skamarock et al. [2009]) in its version adapted for Fairbanks by Gaudet and Staufner [2011]. Hereafter, we refer to the January/February episode data before and after the update as January v1 and January v2, respectively. Without the reducing wind-speed in the valleys by half, the new version of the emission inventory data and the meteorological input data brought an increase in the simulated PM_{2.5}-concentrations at the grid-cell holding the State Office Building site. Here CMAQ underestimated the PM_{2.5}-concentrations previously. Therefore, the reduction of the wind-speeds in the valleys by half is not required for the January v2 and November episode.

2. Activities

Building upon the Alaska adapted CMAQ described in the final report of phase I and the results of phase I, we incorporated the final Penn State WRF output files and the first complete emissions inventory from SMOKE which accounts for Fairbanks specific temporal and spatial variations that we obtained from Sierra Research Inc.. We prepared an assessment of the CMAQ performance, which includes using metrics established by *Boylan and Russell* [2006] and running CMAQ Process Analysis (PA). In the following sections, we describe and assess the results of these activities.

2.1 Configuration of CMAQ for the November 2008 Episode

The November episode covers November 2 to November 16, 2008. The emissions developed for the November episode were updated by Sierra Research Inc. for the emissions from mobile sources. They also included the emissions from airports. The temporal evolutions of 24h-average of simulated $PM_{2.5}$ -concentrations show that the model overestimates the 24h-average $PM_{2.5}$ -concentrations at the State Office Building site at the beginning of the episode (November 2-4); the adapted model failed to capture the peaks on November 6, 9 and 16, and shows a nonexistent temporal minimum on November 7 (Fig. 1).

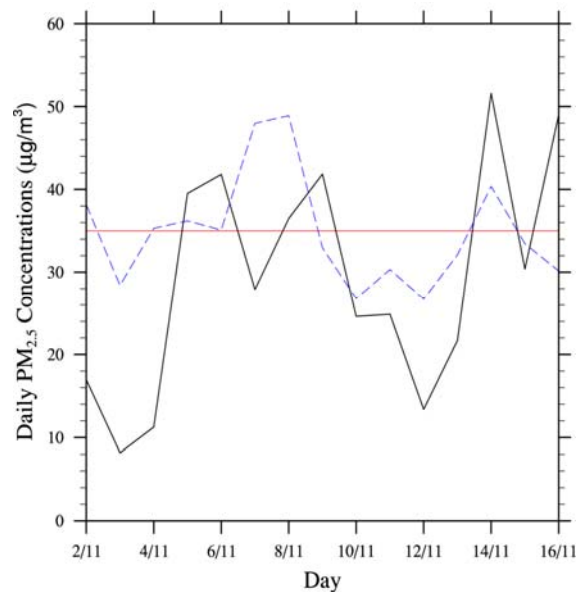


Fig. 1 Time series of simulated (blue dashed line) and observed (black solid line) 24h-average $PM_{2.5}$ -concentrations as obtained with the adapted CMAQ simulation that used the revised WRF and SMOKE input for the November episode at the State Office Building site.

The 24h-average $PM_{2.5}$ -concentrations obtained from the adapted CMAQ simulations with the observations have a correlation coefficient of 0.31. The scatter between simulated and observed 24h-average $PM_{2.5}$ -concentrations is shown in Figure 2. We also found that allowing for a time lag of one between the simulation results and the observations increases the correlation

coefficient from 0.31 to 0.37. According to the observations, there are nine days in the November episode that have $PM_{2.5}$ -concentrations below the National Ambient Air Quality Standard (NAAQS) of $35 \mu\text{g}/\text{m}^3$, and there are six days with $PM_{2.5}$ -concentrations above the NAAQS. For most of the days of the episode, the simulated and observed 24h-average $PM_{2.5}$ -concentrations agree well; there are two days with false alarm, two days of missed events and three pairs of data outside the factor of two agreement (Fig. 2).

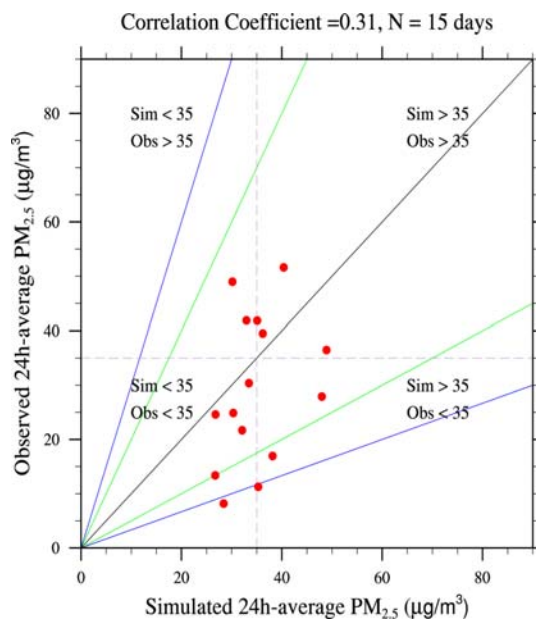


Fig.2 Scatter plot of 24h-average $PM_{2.5}$ -concentrations as obtained from the adapted CMAQ simulation that used the revised WRF and SMOKE input for the November episode and the observations at the State Office Building site. The green line indicates the factor of two and the blue line indicates the factor of three agreement.

The bugle plots and soccer plots show that the adapted CMAQ simulation has five days outside the performance criteria (Fig. 3, a-c). Three of five days are the days in the beginning of the episode, which are probably due to spin-up effects in the CMAQ model itself. Moreover, all of those five days have very low (below NAAQS) 24h-average $PM_{2.5}$ -concentrations.

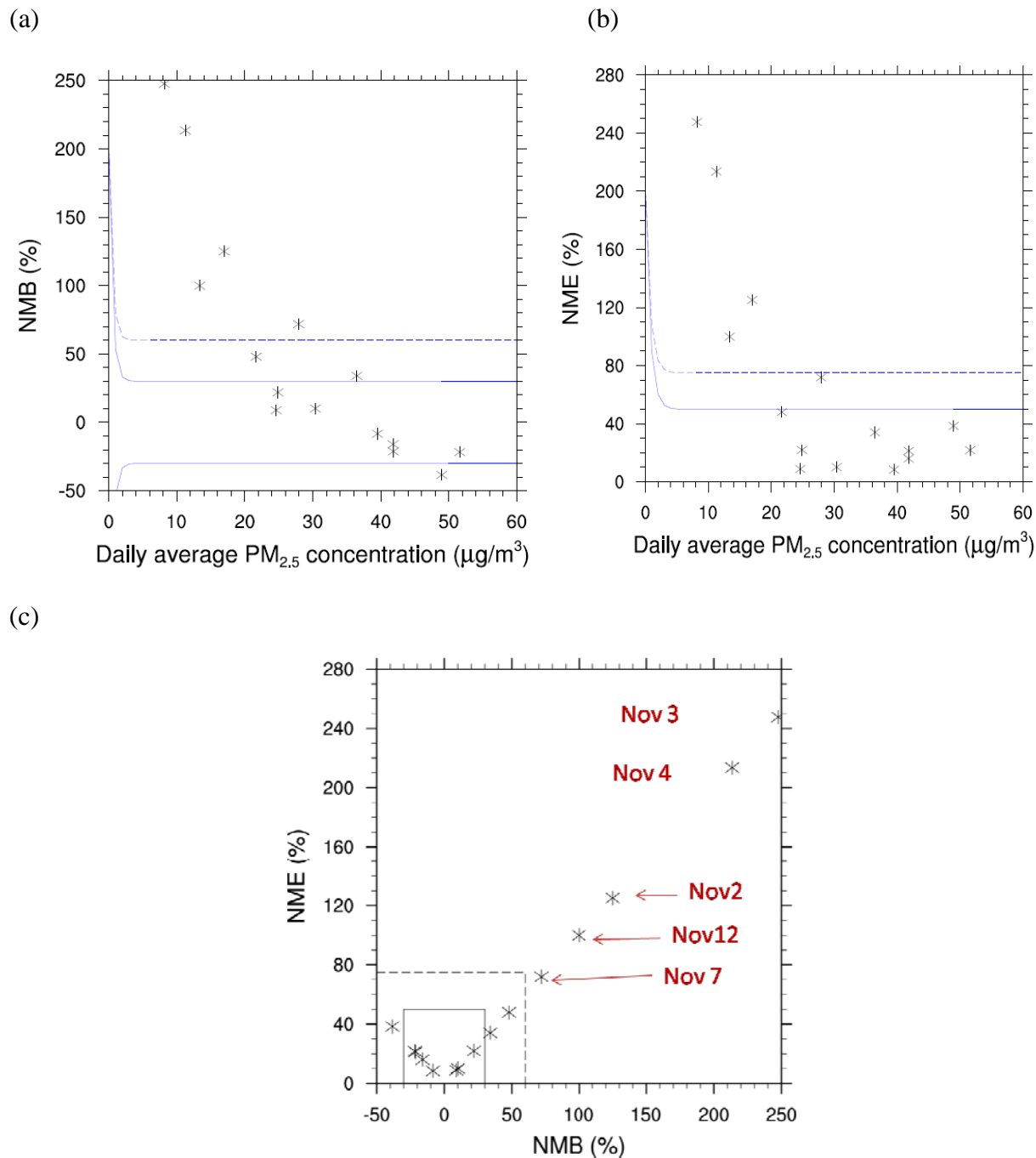


Fig. 3 Bugle plots of (a) normalized mean biases, (b) normalized mean errors, and soccer plots of (c) normalized mean errors and biases of simulated 24h-average PM_{2.5}-concentrations as obtained from the adapted CMAQ simulations that used the revised WRF and SMOKE input for the November episode at the State Office Building site.

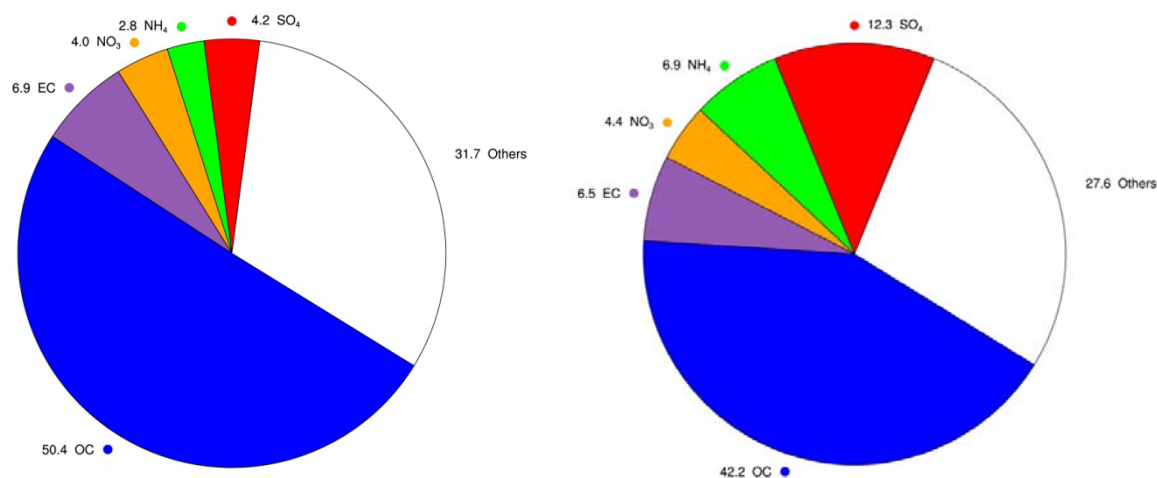


Fig. 4 Composition of simulated 24h-average total PM_{2.5} as obtained by the CMAQ with modifications on average over the November episode (left), and as observed on average over the 3 days, for which data was available during that episode, at the State Office Building site. In the observations, the category “others” includes Al, Br, Ca, Na, Cl, Cu, Fe, Pb, Ni, K, Se, Si, S, Sn, Ti, V, Zn. In the simulations, the category “others” refers to unspecified anthropogenic mass (A25i+A25j), Na and Cl.

Comparing the simulated and observed composition of 24h-average PM_{2.5} aerosol showed that the adapted CMAQ overestimated the percentage of organic carbon, but underestimated the percentage of sulfate and ammonium (Fig. 4).

Data of observed PM_{2.5}-composition data are available on a 1-in-3 day basis. The 24h-average PM_{2.5}-composition as simulated by the Alaska adapted CMAQ for the November episode were compared for each day that had observations (Fig. 5). On November 8 and 14 (with respect to Alaska Standard Time; AST), which have observed PM_{2.5}-composition data, there are small contributions from transport from outside the domain into the area [Mölders and Leelasakultum, 2012]. Note that typically advection from outside Alaska does not increase PM_{2.5}-concentrations by more than 2 µg/m³ [e.g. Cahill, 2003; Tran et al., 2011; Mölders et al., 2012]. For details, see discussion later in this report. The simulations are not able to capture the peak on November 14 well.

Simulated sulfate and ammonium are underestimated on all three days (Fig. 5). Sodium and chloride are both underestimated. A possible reason for the underestimation of sodium (Na) and chloride (Cl) is that no sea-salt is emitted into the domain as there is no ocean and that some sodium and chlorine might be advected during the episode. However, this shortcoming has no big impact on the concentrations of total PM_{2.5} as Na and Cl make up only a small amount of PM_{2.5}-composition (<1%). Simulated organic, nitrate and elemental carbon are almost in the same order of magnitude as observed.

We also conducted a process analysis. Process analysis is a technique that provides information about the impacts of individual processes on the change in a species' concentration. In the following, we refer to horizontal transport as the sum of horizontal advection and diffusion, and to vertical transport as the sum of vertical advection and diffusion. In our discussion, the term aerosol processes represents the net effects of aerosol thermodynamics, new particle formation, condensation of sulfuric acid and organic carbon on preexisting particles, and the coagulation within and between the Aitken and accumulation modes of particulate matter. Cloud processes represent the net effects of cloud attenuation of photolytic rates, aqueous-phase chemistry, below-and in-cloud mixing with chemical species, cloud scavenging and wet deposition [Liu *et al.*, 2010].

According to the process analysis, emissions were the dominant contributor to the PM_{2.5} and SO₄ concentrations, and the horizontal transport contributed to and removed PM_{2.5} and SO₄ at the grid-cell holding the State Office Building site (Fig. 6a-b). The aerosol processes played a small role here. This means PM_{2.5} is mainly composed of primary PM and SO₄ at this site. PM_{2.5} and SO₄ were mainly vented out through vertical transport. Dry deposition played a small role in the removal of PM_{2.5} and cloud process did not play any role here. Note that cloud processes are irrelevant when there are not clouds as these processes then do not occur.

Different from the findings for sulfate, the aerosol processes played the main role for nitrate formation. At the grid-cell holding the State Office Building site, horizontal transport contributed strongly to nitrate. Note that the nitrate concentrations also show an offset like found for PM_{2.5} (see discussion above). The major removal process was vertical transport, i.e. vertical mixing. Note that various studies performed with WRF for Alaska indicated that WRF has difficulties to simulate the strength of inversions with temperature gradients greater than 8K/100m and that WRF tends to overestimate vertical mixing [e.g. Mölders *et al.*, 2011, 2012, Tran, 2012]. An overestimation of the vertical transport of pollutants may lead to diluted concentrations and underestimation of the concentrations as particles are too quickly removed from the breathing level. The process analysis also revealed that dry deposition caused a small loss to nitrate. Cloud processes neither produced nor removed nitrate in this grid-cell (Fig. 6c).

For ammonium, the aerosol processes are the dominant contributor at the grid-cell of the State Office Building site. Horizontal transport contributed to ammonium on some days. The major removal process was vertical transport, and dry deposition caused only a small loss to ammonium. Cloud processes did not play a role here similar to what was found for both sulfate and nitrate (Fig. 6d).

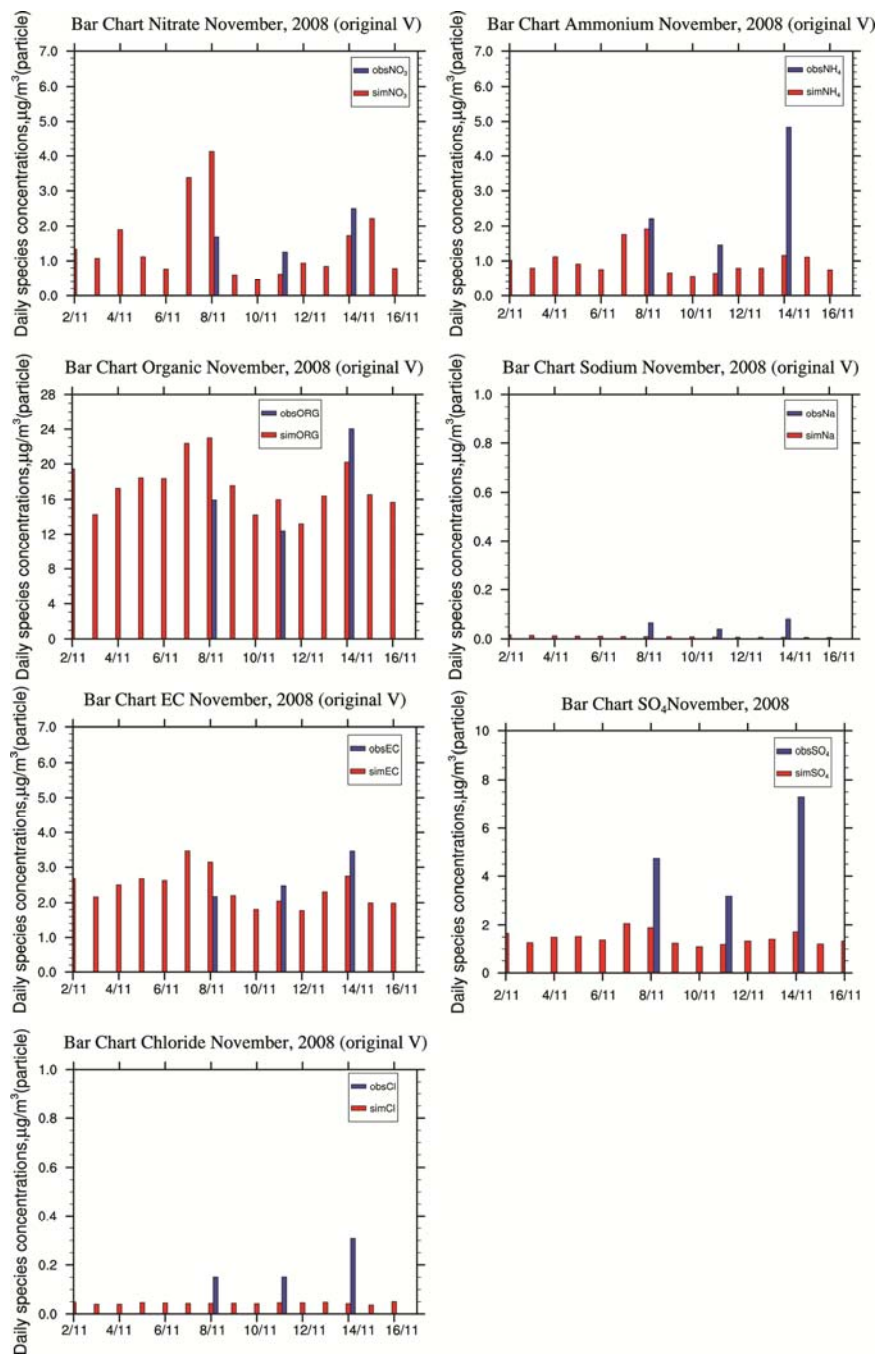


Fig. 5 Bar charts of simulated (red) and observed (blue) 24h-average PM_{2.5}-composition for NO₃, NH₄, EC, OC, Na, Cl, SO₄ as obtained for the November episode at the State Office Building site.

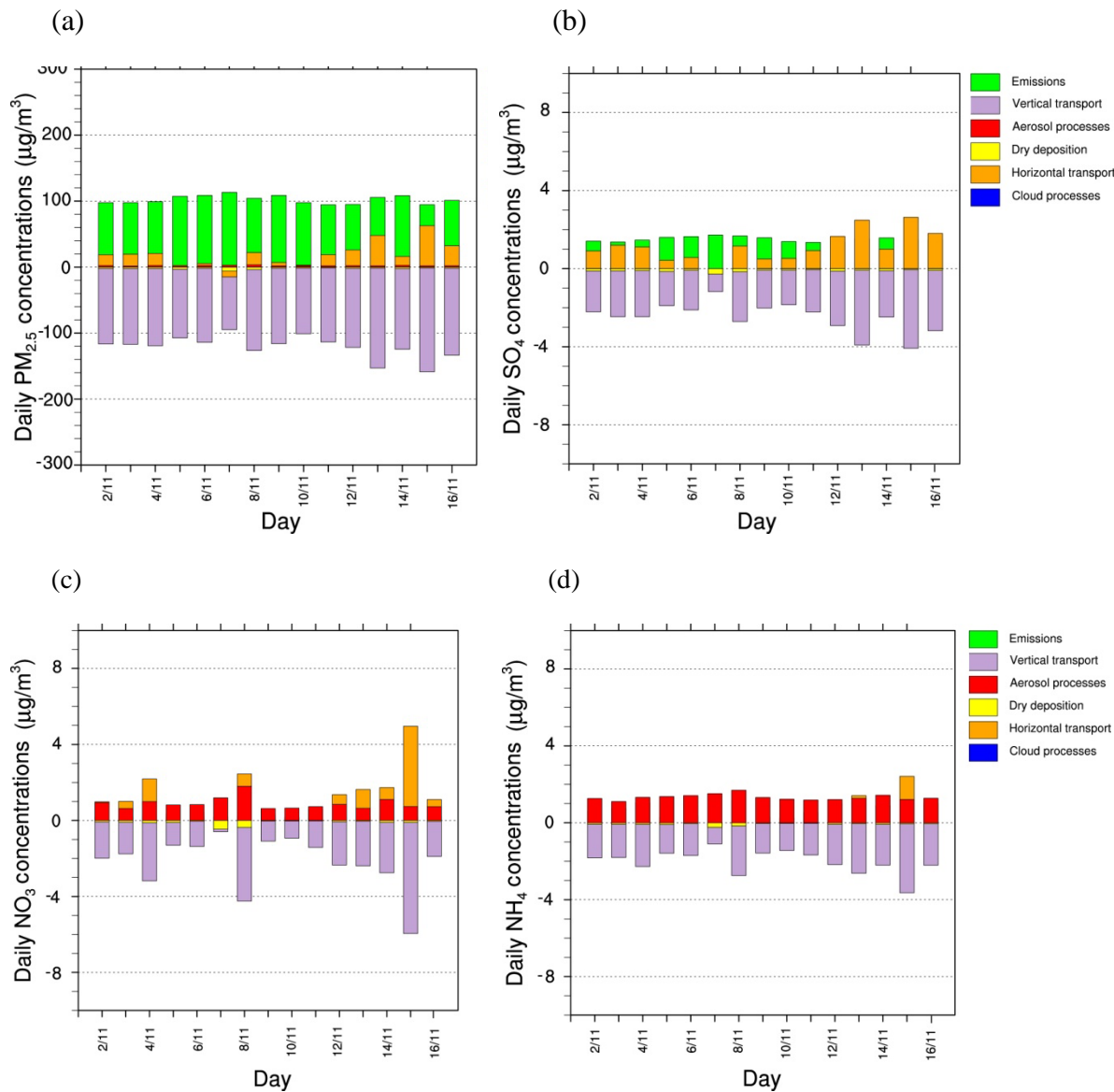


Fig. 6 Daily mean hourly contributions of individual processes to the (a) $\text{PM}_{2.5}$ -concentrations, (b) SO_4 -concentrations, (c) NO_3 -concentrations and (d) NH_4 -concentrations as obtained from the process analysis at the State Office Building site for the November episode. Simulations were performed using the revised WRF and SMOKE input.

2.2 Configuration of CMAQ for the January/February 2008 Episode (January v2)

The January episode covers January 23 to February 9, 2008. The temporal evolutions of 24h-average simulated $PM_{2.5}$ -concentrations show that the model mostly overestimates the 24h-average $PM_{2.5}$ -concentrations at the State Office Building site; the model fails to capture the peak on February 8 (Fig. 7). The model predicts a non-existing temporal minimum on February 2 (Fig. 7). The CMAQ model seems to be ahead in predicting 24h-average $PM_{2.5}$ -concentrations by about 24 hours.

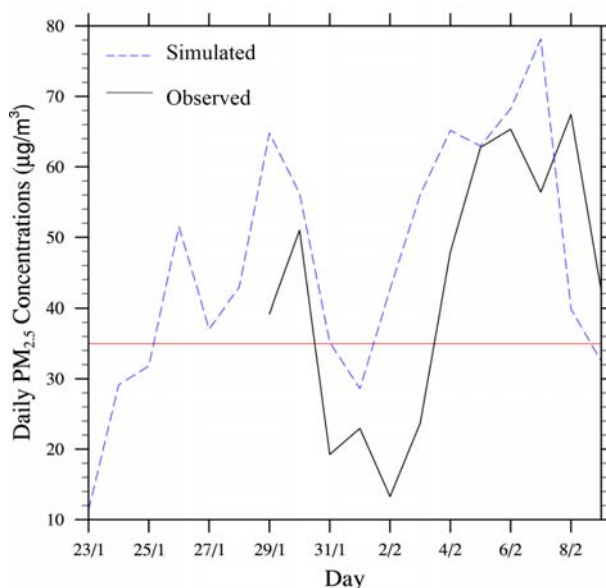


Fig. 7 Timeseries of simulated (blue dashed line) and observed (black solid line) 24h-average $PM_{2.5}$ -concentrations at the State Office Building site as obtained from the adapted CMAQ simulation that used the revised WRF and SMOKE input for the January episode.

The 24h-average $PM_{2.5}$ -concentrations obtained from the adapted CMAQ simulations correlate with the observations with a correlation coefficient of 0.52. Figure 7 shows the scatter of the simulated and observed values. To examine the reasons for the relatively low correlation we examined the timeseries. The temporal evolutions of simulated and observed hourly and 24h-average $PM_{2.5}$ -concentrations suggested an offset. To quantify the offset we calculated the correlation with various time lags. We found that allowing for a time lag for one day increases the correlation coefficient from 0.52 to 0.84 [Mölders and Leelasakultum, 2012]. Allowing a 24h-time lag can increase the correlation coefficients of the hourly average $PM_{2.5}$ -concentrations at the State Office Building site from 0.23 to 0.50, and the correlation increases even more to 0.59 when we allow a time lag of 26 hours. This means that some of the low correlation is caused by a temporal offset between simulated and observed 24h-average $PM_{2.5}$ -concentrations.

It also means that if this shift in timing would not exist, the adapted CMAQ would perform better.

According to the observations, there are four days in the January episode that have $PM_{2.5}$ -concentrations below the NAAQS, and there are eight days with $PM_{2.5}$ -concentrations above this standard. On most of the days of the January episode, the simulated and the observed 24h-average $PM_{2.5}$ -concentrations agree well; there are two days with false alarm, one day of a missed event, and two pairs of data outside the factor of two agreement (Fig. 8).

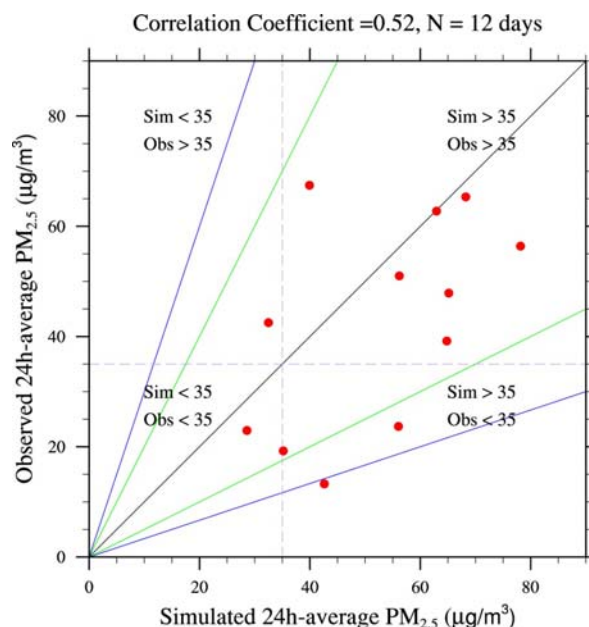


Fig.8 Scatter plots of 24h-average $PM_{2.5}$ -concentrations as obtained from the adapted CMAQ simulation that used the revised WRF and SMOKE input during the January episode at the State Office Building site. The green line indicates the factor of two and the blue line indicates the factor of three agreement.

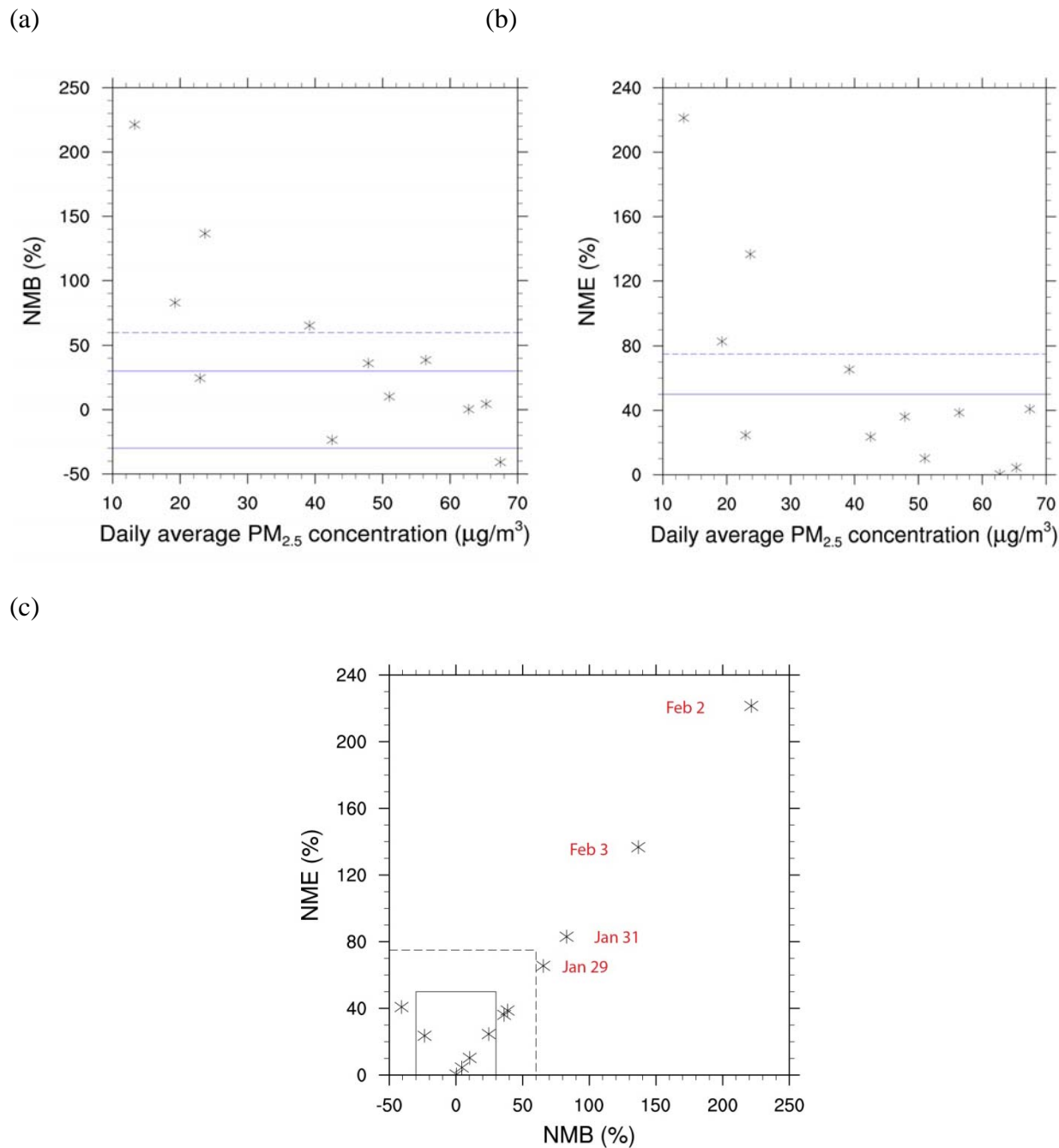


Fig. 9 Bugle plots of (a) normalized mean biases (NMB), and (b) normalized mean errors (NME) and soccer plot of normalized mean errors and biases of 24h-average $PM_{2.5}$ -concentrations at the State Office Building site as obtained from the adapted CMAQ simulations that used the revised WRF and SMOKE input for the January episode.

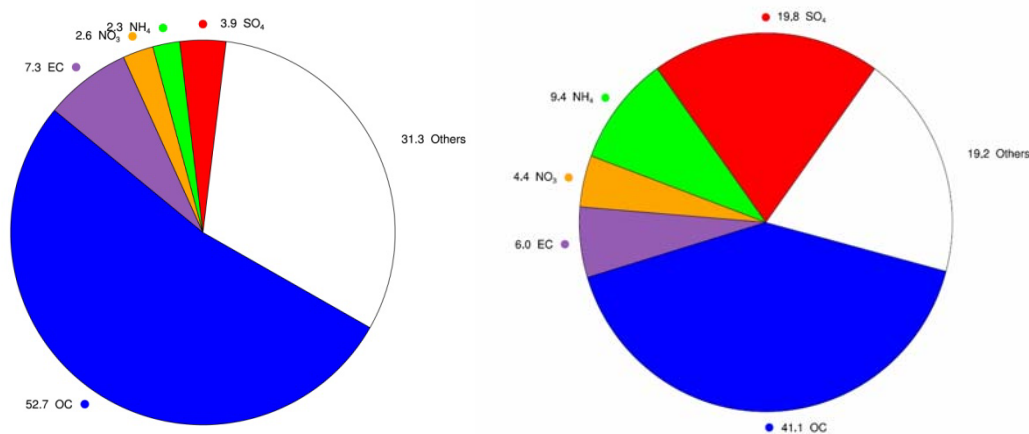


Fig. 10 Composition of simulated 24h-average total PM_{2.5} as obtained by CMAQ with the modifications on average over the January episode (left), and as observed on average over the six days, for which data was available at the State Office Building site. In the observations, the category “others” includes Al, Br, Ca, Na, Cl, Cu, Fe, Pb, Ni, K, Se, Si, S, Sn, Ti, V, Zn. In the simulations, the category “others” refers to unspecified anthropogenic mass (A25i+A25j), Na and Cl.

The bugle plots and soccer plots show that on four days the adapted CMAQ simulation provides results outside the performance criteria (Fig. 3, a-c). Three of these four days are days, on which the 24h-average PM_{2.5}-concentrations are below the NAAQS. Therefore, we conclude that the adapted CMAQ model has difficulties to capture extremely low PM_{2.5}-concentrations well. Note that it is harder to predict very low than high concentrations correctly. Thus, this behavior is typical in air-quality modeling [e.g. *Boylan and Russell, 2006*].

Comparison of the simulated and observed composition of 24h-average PM_{2.5} aerosol showed that the adapted CMAQ overestimated the percentage of organic carbon, but underestimated the percentage of sulfate, ammonium, nitrate and elemental carbon at the State Office Building site for the January episode (Fig. 10).

The 24h-average PM_{2.5}-composition as simulated by the Alaska adapted CMAQ for the January episode was compared for each day that had observed data (Fig. 11). During February 5-10, there was higher sulfur content, and on February 6 and 9 (AST), there were small contributions from long-range transport [*Mölders and Leelasakultum, 2012*]. Simulated sulfate (SO₄) and Ammonium (NH₄) are underestimated on all six days (Fig. 11). Sodium and chloride are both underestimated (see earlier discussion for reasons). Simulated organic, nitrate (NO₃) and elemental carbon (EC) concentrations are almost of the same order of magnitude as the observations and well follow the temporal evolution of the observations.

Similar to the findings of the November episode, in the January episode, emissions were the dominant contributor to the PM_{2.5}- and SO₄-concentrations at the grid-cell holding the State

Office Building (Fig. 12a-b). Horizontal transport contributed to and removed $PM_{2.5}$ and SO_4 at this site. The aerosol processes played a small role here. This fact indicates that $PM_{2.5}$ is composed mainly of primary PM and SO_4 at this site. $PM_{2.5}$ and SO_4 were mainly vented out through vertical transport. Dry deposition played a small role in the removal of $PM_{2.5}$ and cloud process did not play any role here. Note that if there are no clouds cloud processes cannot contribute to/affect the concentrations.

Like for the November episode, the findings obtained for nitrate differed from those for sulfate. The aerosol processes played the main role for nitrate formation. High contributions of nitrate also came from horizontal transport, i.e. neighbored grid-cells, but could not capture the conditions on February 9. The major removal process was vertical transport, and dry deposition caused a small loss to nitrate. Cloud processes neither produced nor removed nitrate in this grid-cell (Fig. 12c).

For ammonium, the aerosol processes are the dominant contributor at this site. Horizontal transport from neighbored grid-cells contributed to the ammonium concentrations on some days. The major removal process was vertical transport, and dry deposition caused only a small loss to ammonium. Cloud processes did not play a role here similar to what was found for both sulfate and nitrate (Fig. 12d).

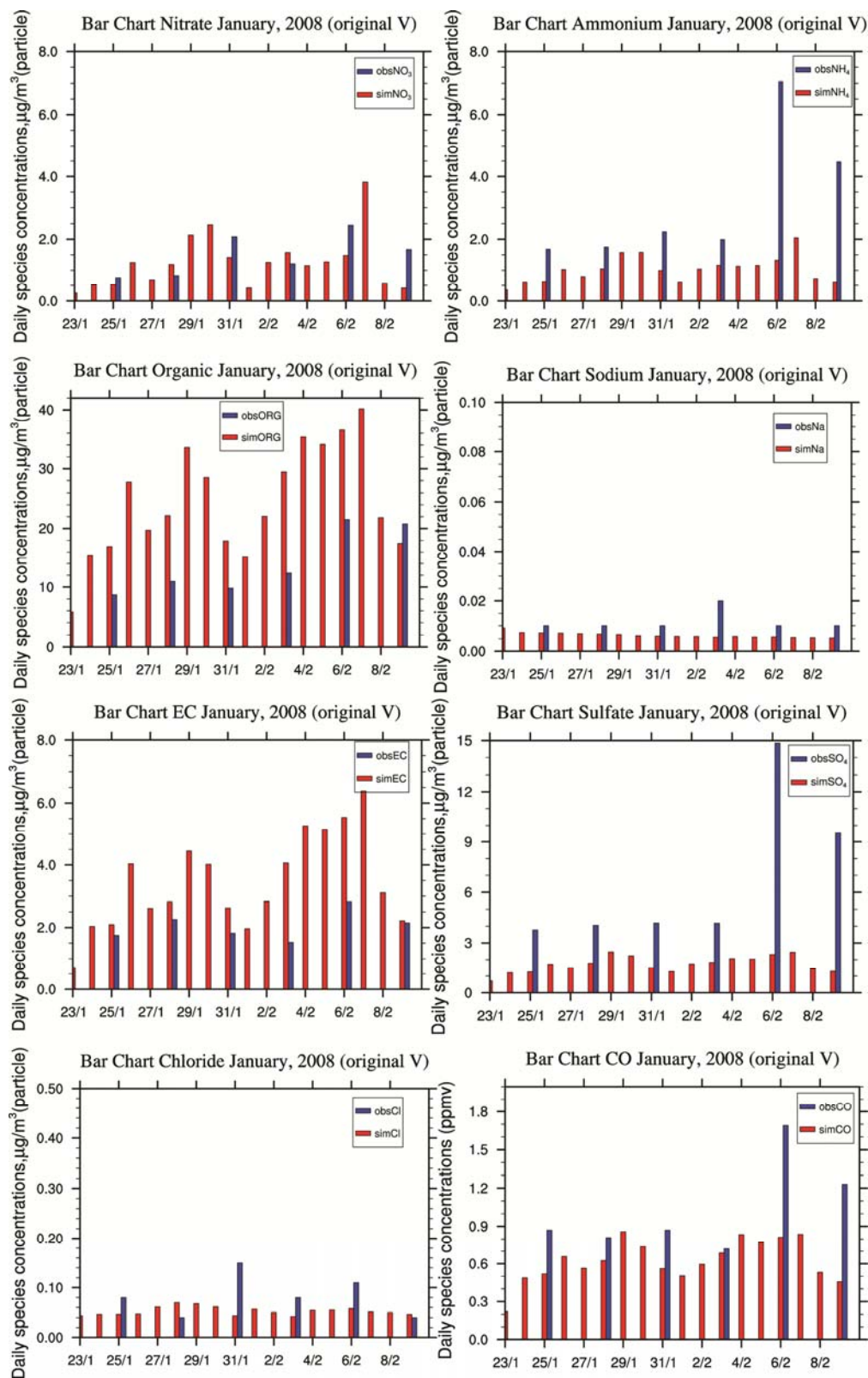


Fig. 11 Bar charts of simulated (red) and observed (blue) 24h-average PM_{2.5}-composition for NO₃, NH₄, EC, OC, Na, Cl, SO₄ as obtained at the State Office Building for the January episode.

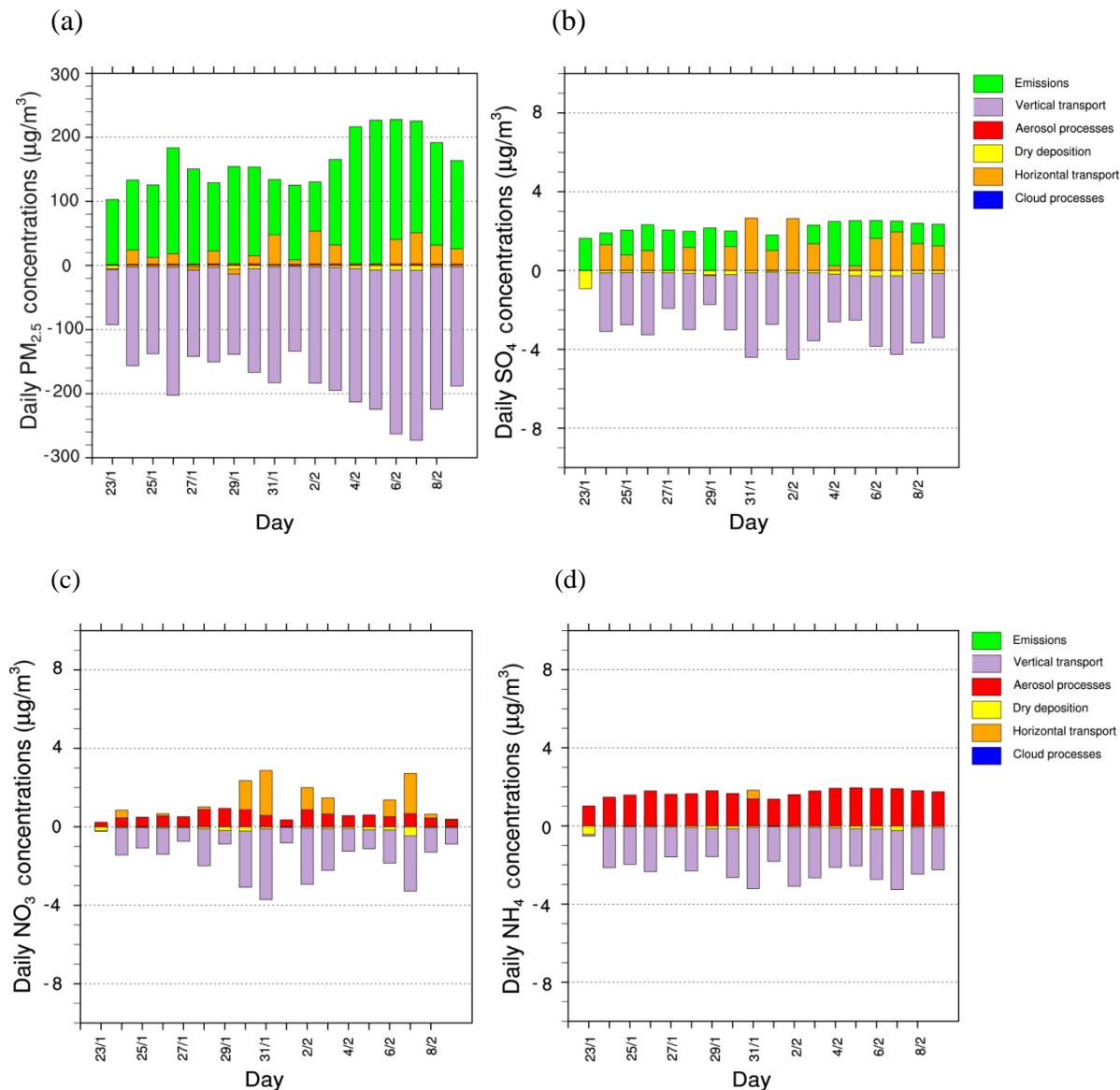


Fig. 12 Daily mean hourly contributions of individual processes to the (a) $\text{PM}_{2.5}$ -concentrations, (b) SO_4 -concentrations, (c) NO_3 -concentrations, and (d) NH_4 -concentrations as obtained at the State Office Building site from the adapted CMAQ simulation that used the revised WRF and SMOKE input for the January episode.

2.3 Documentation of Changes in CMAQ and Performance Improvements Made during Phase II

The simulations of the Alaska adapted CMAQ model underestimated sulfate (SO_4). Sulfate is the second major component in the composition of $\text{PM}_{2.5}$ in the Fairbanks nonattainment area. The simulations of the Alaska adapted CMAQ model also showed a time lag of ~24 hours in comparison with the observations at the State Office Building site for both the January and November episodes.

2.3.1 Improvements Implemented to Reduce the Sulfate-Underestimation

The performance of CMAQ in predicting fine particulate matter (PM_{2.5}) and its species has been evaluated in many studies [e.g. *Appel et al.*, 2008; *Eder and Yu*, 2006; *Mathur et al.*, 2008]. Obviously, according to these studies, CMAQ's performance tends to be lower in winter than summer for PM_{2.5} and most species. CMAQ is also likely to underpredict sulfate during winter [*Appel et al.*, 2008; *Eder and Yu*, 2006; *Mathur et al.*, 2008].

The statistical performance skills for sulfate are poorer for the Fairbanks domain than for other US states (Table 1). Slightly lower performance skills were also found for Alaska than the Lower 48 for WRF/Chem simulations [*Mölders et al.*, 2012]. Thus, based on the literature, we may conclude that air-quality models may generally have difficulty with relatively lower temperature conditions. Thus, the extremely low temperature during the winter in Fairbanks might be a reason of the sulfate underestimation. This conclusion is backed by the evaluation studies for the Lower 48 that report weaker performance for PM_{2.5}-prediction winter than summer episodes [e.g. *Appel et al.*, 2008]. Therefore, we made several changes to the code of CMAQv4.7.1 to improve the sulfate simulation.

We performed various studies to examine the reasons for and to reduce the underestimation of sulfate and PM_{2.5}. In the following, first, the changes are described and later their impact will be discussed.

1) Increase of the Default Values for Fe and Mn in AQ_PAEAMS.EXT

In aerosol and aqueous chemistry, iron and manganese can play important roles for sulfate formation. Therefore, we updated the background values of Fe (III) and Mn (II) from 0.010 $\mu\text{g}/\text{m}^3$ to 0.040 $\mu\text{g}/\text{m}^3$ and decreased Mn (II) from 0.005 $\mu\text{g}/\text{m}^3$ to 0.001 $\mu\text{g}/\text{m}^3$ following the measurement made in Fairbanks during winter 2011-2012 by *Peltier* [2012].

2) Increase of Sulfate and SO₂-concentrations for the Initial and Background concentrations (IC/BC)

The concentrations of sulfate and SO₂ of the previous initial and background concentrations were suspected to be too low. We now use the concentrations from the Clean Air Status and Trends Network (CASTNet) at the Denali site of winter 2008/09 (October–February). Thus, at the near-surface level the new SO₂-concentration is now 3.50×10^{-4} ppm. This value is closer to the default values that are used in the Eastern US. Modifying the near-surface concentration lead to ~1.7 increased near-surface SO₄-concentrations as compared to the total SO₄-concentrations obtained with the old values. The vertical profiles of SO₂ and sulfate are still based on *Jaeschke et al.* [1999] as no other vertical profile data is available to our best knowledge.

3) Change the dry deposition code back to the CMAQ v.4.7.1 original code

The modifications introduced for the dry deposition of SO₂ in phase I (deposition onto tundra, which was switched off in the original CMAQ, revised vegetation parameters for Alaska, formulations for dry deposition onto snow; see *Mölders and Leelasakultum* [2012]) led to increased removal of sulfate as compared to the original CMAQ. Therefore, we changed the parameterization of the SO₂ dry deposition processes back to their original version as it was in CMAQv.4.7.1 except that we kept the dry deposition on tundra. Note that if we would change this back to the original code it would mean that no deposition would be considered over most of the domain. Note that tundra covers most of the domain. In the original version of CMAQ, the code run over all vegetation types except for tundra to save computational time. This procedure is justifiable and makes sense for regions without tundra vegetation. However, in regions where tundra occurs, it would mean that no deposition is calculated over these tundra areas.

We want to point out that the changes that we originally made in phase I, are valid from a scientific point of view. The dry deposition over snow is quite different than over snow-free surfaces and should be dealt with similar as described in *Zhang et al.* [2003], i.e. likea we introduced it into CMAQ during phase I. The change back to the original formulation was only made to come closer to the observations and because of the philosophy to stay with the original code when changes do not lead to improvement for Alaska.

4) Reduction of the liquid-water threshold for resolvable scale clouds

Mueller et al. [2006] found that CMAQ underestimated sulfate because of a problem in the diagnosis of cloud cover. They found that reducing the liquid-water threshold values by 50% can decrease the cloud bias and lead to better results for sulfate predictions. Therefore, we decreased these threshold values by 50% in “resclD.F” of CMAQ model. The response will be discussed later.

5) Improved parameterization for the sulfuric acid – water nucleation rates

In CMAQ, the parameterization of the homogeneous nucleation rate of sulfuric acid and water is based on *Kulmala et al.* [1998]. *Vehkamaki et al.* [2002] published an extension of the formulation by *Kulmala et al.* [1998] to lower temperatures and a wider relative humidity range. CMAQ model v4.7.1 had not yet been updated to include this extension. Its formulas hold for temperatures between -43°C and 32°C, relative humidity between 0.01% and 100%, nucleation rates between 10⁻⁷ and 10¹⁰ cm⁻³ s⁻¹, and sulfuric acid concentrations of 10⁴ to 10¹¹ cm³. We coded and implemented this extended parameterization for the calculation of the nucleation rates based on *Vehkamaki et al.* [2002] and presented the results in the secondary quaterly report phase II. Later on, we updated the calculation based on personal communication with *Vehkamak* [2012]. This updated calculation is basically similar to what we have done, but the numbers include more digits. Furthermore, there are more conditions considered [*Vehkamaki*, 2012; pers. comm.]. The fortran code can be found at

http://www.atm.helsinki.fi/~hvehkama/publica/vehkamaki_hi_t_binapara.f90.

2.3.2 Response to the Improvements Made to Reduce the Sulfate-Underestimation

The introduction of the above improvements led to an increase in the percentage sulfate concentrations of total PM_{2.5} at the grid-cell of the State Office Building site. The percentage of sulfate increased from 4.2 to 5.3% and from 3.9 to 5.0% for the November and January episode, respectively (Fig. 13). The increase in the percentage of SO₄ affected the partitioning of other species. This means concurrently the percentage of NH₄ increased, while the percentage of NO₃ and organic compounds decreased. These shifts in percentage may be explained as follows. The enhancement of sulfur dioxide and sulfate affected the thermodynamic equilibrium of the aerosol system. The sulfate-related aerosol acidity may be further neutralized by NH₃ to form ammonium sulfate aerosol ((NH₄)₂SO₄) [Lovejoy, 1996; Seinfeld, 2006]. The rest of ammonia can also neutralize nitric acid (HNO₃), and forms ammonium nitrate aerosol (NH₄NO₃).

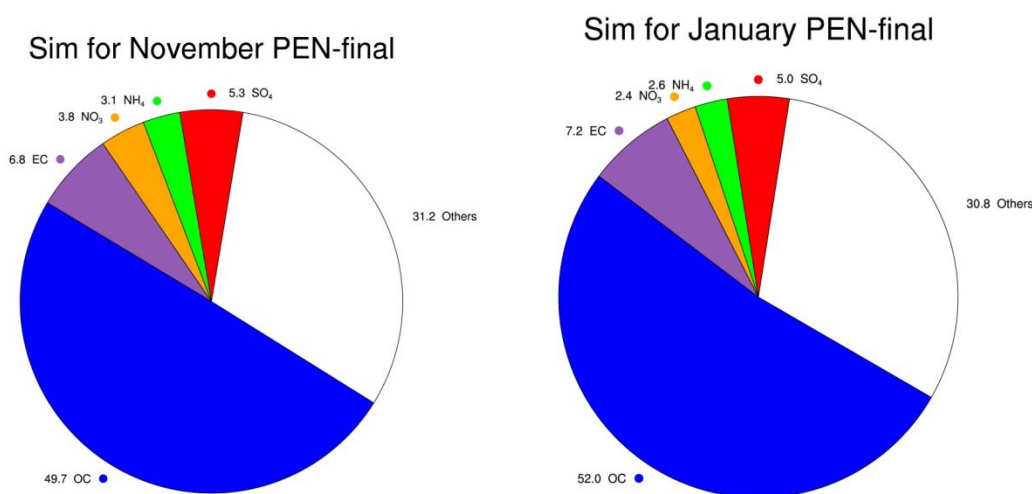


Fig. 13 Composition of simulated 24h-average total PM_{2.5} as obtained by the CMAQ simulations with the final modifications and using the PennState provided meteorology (PEN-final) on average over the November episode (left), and the January episode (right) at the grid-cell of the State Office Building site. In the simulations, the category “others” refers to unspecified anthropogenic mass (A25i+A25j), Na and Cl. In the observations, the category “others” includes Al, Br, Ca, Na, Cl, Cu, Fe, Pb, Ni, K, Se, Si, S, Sn, Ti, V, Zn.

The comparison of the absolute differences between the simulations before and after the improvements shows increases in sulfate, and ammonium and decreases in nitrate on every simulated day for both episodes (Figs. 14, 15). On average, the absolute increase of sulfate is 0.4 μg/m³ or 28-29% for both episodes. The improvements did not bring a change in the organic concentrations (Figs. 14, 15); the decreased percentage of organic compounds is due to the increase of the percentage of SO₄ and NH₄. Note that the final modifications did not change the

temporal evolutions of sulfate and $PM_{2.5}$ -concentrations, and the final version of Alaska adapted CMAQ still underpredicts sulfate aerosol.

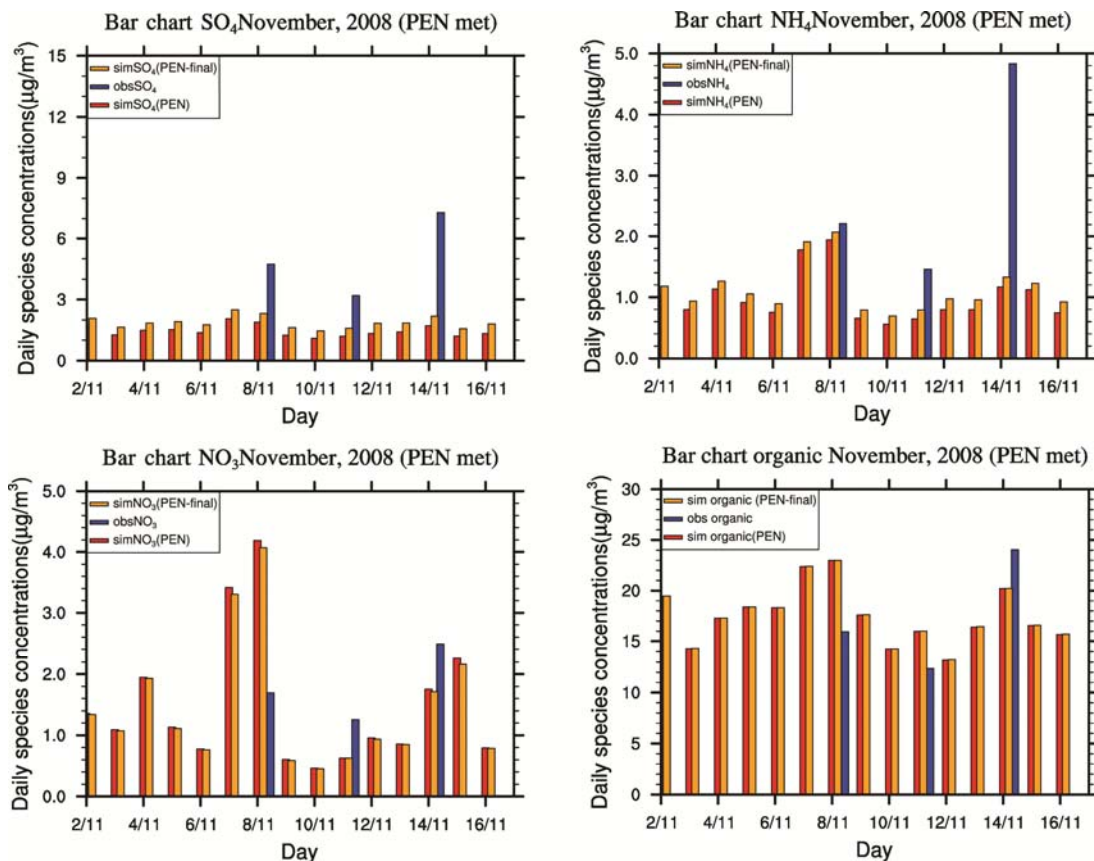


Fig. 14 Bar charts of simulated species as obtained from the previous CMAQ modification described in the final report of phase I (red), and as obtained from the final CMAQ modification described above (orange) and observed species (blue) of the 24h-average $PM_{2.5}$ -composition for SO_4 , NH_4 , NO_3 , and organic carbon for the November episode.

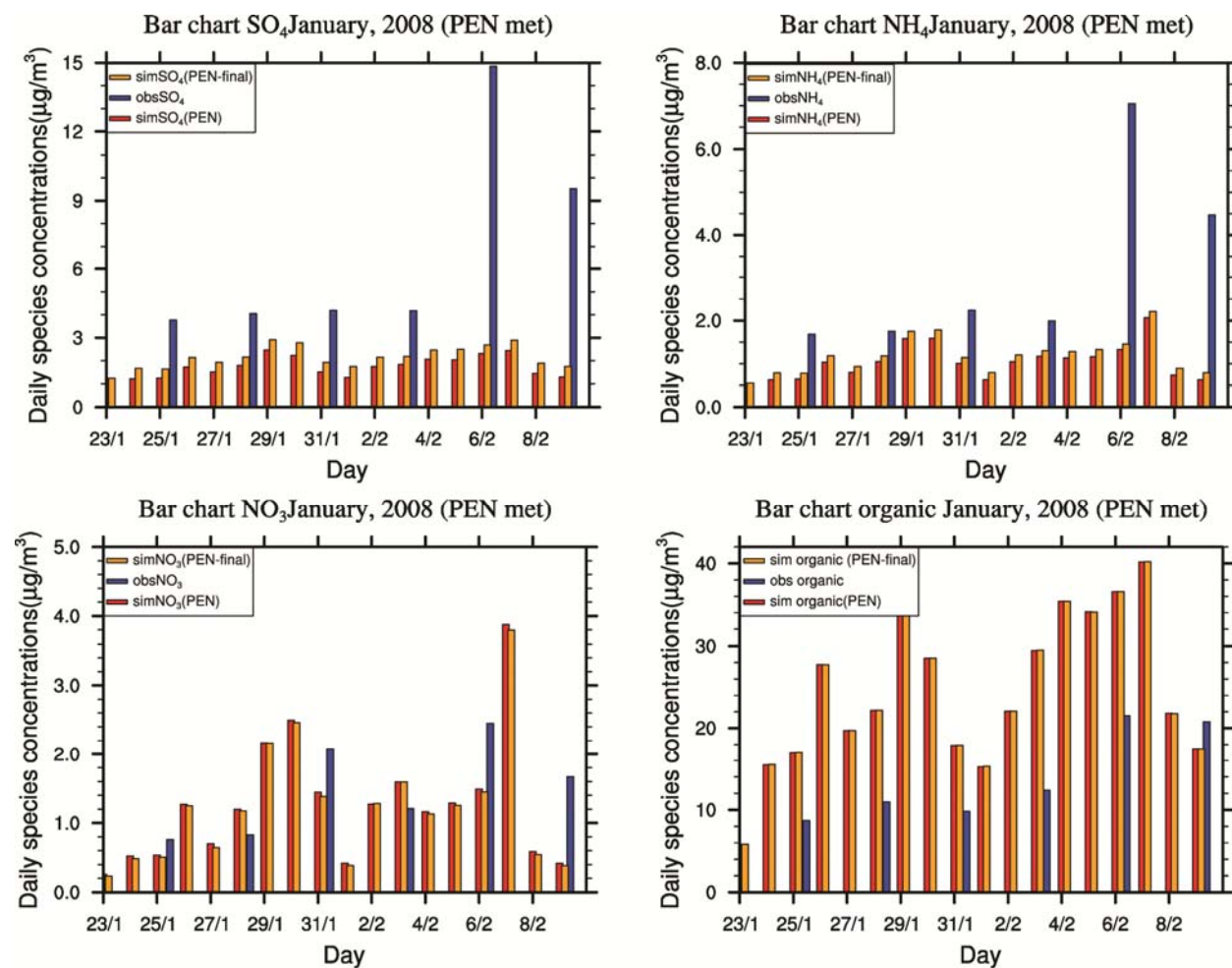


Fig. 15 Bar charts of simulated species as obtained from the previous CMAQ modification described in the final report of phase I (red), and as obtained from the final CMAQ modification described above (orange) and observed species (blue) of the 24h-average PM_{2.5}-composition for SO₄, NH₄, NO₃, and organic carbon for the January episode.

The process analysis of sulfate concentrations at the grid-cell of the State Office Building site shows that the final modifications caused changes in the horizontal and vertical transport (Fig. 16). This means that the modifications led to changes in neighbored grid-cells. These changes then led to advection of slightly modified (composition wise) air. On average in the November episode, the final CMAQ modification increased the contribution of sulfate from horizontal transport, cloud and aerosol processes by 0.39, 8.4×10^{-7} and 4.8×10^{-4} µg/m³, respectively. The contributions to sulfate from removal by dry deposition and vertical transport decreased by -0.02 and 0.28 µg/m³. There was no change in the emissions as we used the same emission inventory.

On average over the January episode, the final CMAQ modification led to increased contributions of sulfate from horizontal transport, cloud and aerosol processes by 0.30, 1.1×10^{-6} and 5.6×10^{-4} µg/m³, respectively. In the runs with the modifications, the removal of sulfate by

dry deposition and by vertical transport decreased by -0.02 and $0.37\mu\text{g}/\text{m}^3$, respectively, as compared to the run without the modifications.

Table 1. Performance statistics for sulfate species simulated by the CMAQ model that did not employ the revised WRF and SMOKE input (January v1 episode), the CMAQ model with the previous modification (January v2 episode, PEN-WRF) described in the final report of phase I, and with the CMAQ model version with the final modification (PEN-WRFFinal) for the January and November episode on the days. Statistics are based on the observed sulfate data was available at the Fairbanks State Office Building site. The statistics of the annual simulations of sulfate in other states in US as reported by *Eder and Yu* [2006] are included for comparison. Here “No.” stands for the number of days with observations. Furthermore, r, MB, RMSE, NMB and NME are the correlation skill score, mean bias, root-mean-square error, normalized mean bias, and normalized mean error.

Sulfate	No.	Mean model	Mean observed	r	MB	RMSE	NMB (%)	NME (%)
January v1 episode								
PEN-WRF	6	1.3	6.8	0.36	-5.4	6.8	-80.3	80.3
January v2 episode								
PEN-WRF	6	1.7	6.8	0.56	-5.1	6.4	-75.4	75.4
PEN-WRFFinal	6	2.1	6.8	0.61	-4.7	6.1	-69.6	69.6
November episode								
PEN-WRF	3	1.6	5.1	0.61	-3.5	3.8	-68.5	68.5
PEN-WRFFinal	3	2.0	5.1	0.66	-3.1	3.4	-60.0	60.0
Eder and Yu, 2006	6970	3.33	3.40	0.77	-0.77	2.25	-2.0	42.0

The statistical performance of the Alaska adapted CMAQ version that did not employ the revised WRF and SMOKE input (January v1), the CMAQ with the modifications that employs the revised WRF and SMOKE (January v2), and from the final CMAQ modification in simulating sulfate are compared in Table 1. Introducing the changes in the parameterizations increased the mean sulfate concentrations on the days, which had observed sulfate concentrations at the State Office Building site, in the range of 1.7 to $2.1\mu\text{g}/\text{m}^3$ and 1.6 to $2.2\mu\text{g}/\text{m}^3$ for the January and November episode, respectively. The mean biases (MB) were -4.7 and $-3.1\mu\text{g}/\text{m}^3$ for the latest changes in the parameterization for the January and November episode, respectively. The

normalized mean bias (NMB) and normalized mean error (NME) from all simulations are high (exceed 50%) in comparison with the annual NMBs in the study by *Eder and Yu* [2006]. The examination the NMB and NME for the two episodes reveals better performance in simulating sulfate with the latest modifications. Our analysis of the performance also revealed that the correlation coefficients between the observed and simulated sulfate data increase as the concentrations of sulfate increase (Table 1).

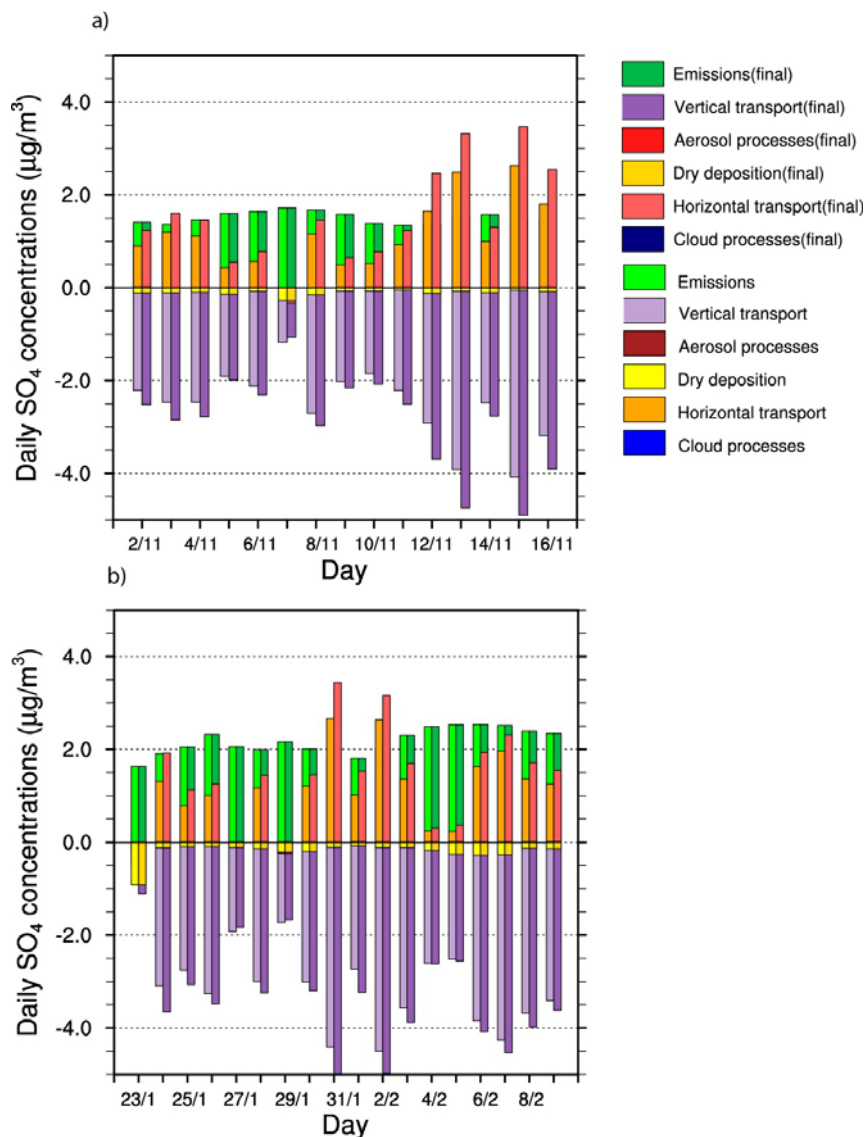


Fig. 16 Comparison of the daily contributions of individual processes to the SO_4 -concentrations as obtained by CMAQ with the previous modifications and with CMAQ with the modifications described in this report at the grid-cell of the State Office Building site for the (a) November and (b) January episode.

Table 2. Performance statistics for the 24h-average PM_{2.5}-concentrations as obtained from the Alaska adapted CMAQ with the previous modifications and the CMAQ with the final modifications at the grid-cell of the State Office Building site for the January v1, January v2 and November episodes. The small differences as compared to the 1st quarterly report of phase II are due to the use of the SMVGEAR solver instead of the EBI solver that is needed for the process analysis.

24h-average PM _{2.5} -concentrations	January v1	January v2	November	Final modifications	
				January	November
Number of pairs used in the calculation of the statistics	12	12	15	12	15
Mean simulated(μg/m ³)	35.0	52.6	34.9	53.1	35.5
Mean observed (μg/m ³)	42.6	42.6	29.3	42.6	29.3
Mean bias (μg/m ³)	-3.0	6.6	5.6	7.0	6.2
Mean fractional bias (%)	-1	17	26	18	31
Mean error (μg/m ³)	9.2	10.8	12.1	11.0	15.7
Mean fractional error (%)	24	26	42	27	54
Average difference (sim-obs)	-4.5	9.9	5.6	10.5	6.2
Simulated min max (μg/m ³)	26.6 49.7	28.6 78.2	26.8 49.0	29.3 78.8	27.3 49.4
Observed min max (μg/m ³)	13.3 67.4	13.3 67.4	8.2 51.6	13.3 67.4	8.2 51.6
Number of simulated exceedance days	7	10	7	10	7
Number of observed exceedance days	8	8	6	8	6
STDEV of simulation (μg/m ³)	7.3	16.2	6.8	16.2	6.7
STDEV of observation (μg/m ³)	19.0	19.0	13.7	19.0	13.7
Variance of simulation(μg/m ³) ²	52.8	262.2	46.0	262.0	45.5
Variance of observation(μg/m ³) ²	362.8	362.8	188.3	362.8	188.3
Correlation coefficient	0.38	0.52	0.31	0.52	0.31

The Alaska adapted CMAQ with the final modifications given in this report is still not able to simulate sulfate concentrations as high as the observations suggest. As the process analysis indicated that the emission process is the main source of sulfate at the grid-cell of the State

Office Building site, we performed simulations with the same CMAQ configuration, but used an earlier version of the emission inventory. The comparison showed that the model showed better performance in simulating sulfate at the State Office Building site with the earlier version of the emission inventory. Therefore, we compared the emission inventories to examine what changes in the emissions led to these differences in model performance. Our investigations showed that in the latest version of the emission inventory there was a decrease of sulfate from 7% to 2-3% in the partitioning of the PM_{2.5}-emissions in comparison with the earlier version of the emission inventory (see also discussion in *Mölders and Leelasakultum* [2012]). Therefore, the decrease of sulfate in the partitioning of the PM_{2.5}-emissions is probably the main cause of underestimation of sulfate concentrations. The main differences we see in these WRF-CMAQ runs that only differ by the emission inventory used, show us the sensitivity of the model to the emissions and their partitioning. However, the latest version of the emission inventory reflects the latest inventory accuracy with new woodstove changeout, census and mobile numbers. Therefore, the latest emission inventory has to be considered superior over the earlier versions from a research standpoint.

Finally, we compared the performance statistics of the 24h-average PM_{2.5}-concentrations from Alaska adapted CMAQ version that did not employ the revised WRF and SMOKE input, the CMAQ modification that employed the revised WRF and SMOKE, and the CMAQ with the final modifications (Table 2). The final modifications did not increase the correlation coefficient or change the temporal evolution. The results of soccer plot and bugle plot are similar as prior to introducing the latest changes. As the differences are not statistically relevant, they are not shown here.

2.3.3 Investigation of the Causes for the Temporal Offset

As discussed above, the time-lag effect caused the model to fail to capture the temporal evolution of PM_{2.5}-concentrations well. Consequently, the correlation coefficients between the simulated and observed PM_{2.5}-concentrations for both episodes are lower than they should be. We run a hierarchy of simulations to test the causes for the temporal offset found at the grid-cell of the State Office Building site.

In the earlier simulations, the time-steps for the operator splitting were set as follows: maximum sync time-step = 12 min, minimum sync time-step=1.5 minute, and up to sigma = 0.9. We hypothesized that the CMAQ model might be too slow in updating the chemistry, which consequently could lead to the temporal offset at the grid-cell of the State Office Building site. Therefore, we reduced the time step for the operator splitting to be as follows: maximum sync time-step = 6 min, minimum sync time-step=1minute, and up to sigma =0.7. The temporal evolution of PM_{2.5}-concentrations for the longer time-step (PEN-WRF) and the shorter time-step (PEN-WRFfinal) were compared. The comparison showed no difference in the temporal evolutions for both the January and November episode (Figs. 17, 18). The differences in concentrations might be due to the improvement of parameterizations in the PEN-final version.

Additionally, we also run the simulations by using the emission of the next day (PEN-Eshift), i.e. we shifted the emissions by one day. The temporal evolutions of simulated PM_{2.5}-concentrations showed only marginal differences from those simulations that used the emissions in sync with the meteorological data (Fig. 17).

Another reason for the temporal offset between simulated and observed PM_{2.5}-concentrations was hypothesized to be an offset in the simulated meteorology. Therefore, we ran WRF for the two episodes in a different configuration than the PennState WRF. In the following, we refer to these simulations as “UAF-WRF”. Our WRF-simulations differ in the model configuration from the WRF-simulations performed and provided by PennState. Note that the simulations provided by PennState are called “PEN-WRF”, hereafter. The new WRF simulations served to examine whether an offset in meteorology is the cause for the time lag in the PM_{2.5}-concentrations.

The domains for the simulations with the UAF-WRF are based on the domains used in the PEN-WRF for easy comparison. Our model configuration like theirs used three one-way nested horizontal grids with horizontal grid spacing of 12km, 4km and 1.3km, respectively. Domain 3 that has a 1.3km grid increment was used to provide the meteorological input data to simulate the chemical transport and transformation of species with the CMAQ model. For the UAF-WRF simulations, the initial meteorological conditions were downscaled from the 1°×1°, 6h-resolution National Centers for Environmental Prediction global final analyses. The simulations were performed in forecast mode (turning off nudging) for January 23, 2008 0000UTC to February 12, 2008 0000UTC and November 02, 2008 0000UTC to November 18, 2008 0000UTC. The selection of options in the first simulations of the UAF-WRF (UAF-WRFv1) bases on long-year experience of the PI and her research group with meteorological simulations for Alaska [e.g. Mölders and Olson, 2004; Mölders and Walsh, 2004; Mölders and Kramm, 2007; 2010; Chigullapalli and Mölders, 2008; Yarker et al., 2010; Mölders et al., 2011; 2012]. The selection of options in the second set of simulations with the UAF-WRF (UAF-WRFv2) for domain 3 is the same as those in the PEN-WRF except that we turned off the OBS nudging. The meteorological fields were initialized every day. The model configurations for both the PEN-WRF and UAF-WRFv1 and UAF-WRFv2 are compared in Table 3.

Nudging to observations (OBS nudging) is a technique that adds artificial forcing functions to a model’s prognostic equations to nudge the solutions toward the observations. Those individual observations are spread in space and time. In domain 3, there is a limited number of radiosonde sounding sites [Mölders et al., 2011]. Thus, OBS nudging might cause a temporal offset, as obviously the WRF model was unable to capture the temperature inversion at the right time and place. Therefore, we turned off the OBS nudging for a sensitivity study for both UAF-WRFv1 and UAF-WRFv2. Note that in Fairbanks, many inversions are locally forced when the right synoptic conditions exist [Mayfield, 2012].

The comparison of the temporal evolutions of the PM_{2.5}-concentrations as obtained by CMAQ with the UAF-WRFv1 and UAF-WRFv2 with those obtained with the PEN-WRF indicates that

the meteorological input data led to changes in the temporal evolutions of $PM_{2.5}$ -concentrations. However, none of the obtained changes in $PM_{2.5}$ -concentrations led a perfect fit with the observed $PM_{2.5}$ -concentrations (Figs.17, 18). The UAF-WRFv1 simulations with the *Lin et al.*'s [1983] microphysics scheme seem to provide the highest $PM_{2.5}$ -concentration peaks in the beginning of the November episode and the lowest dip in the $PM_{2.5}$ -concentrations on November 11 as compared with the other simulations (Fig. 17). For the January episode, the simulation with the *Lin et al.* [1983] microphysics scheme showed the smallest temporal shift as compared to the PEN-WRF, but still showed the offset (Fig. 18). The simulations with the Morrison 2-moment [*Morrison et al.*, 2005] scheme tend to smooth the peak and dip. As a result, the simulations with the UAF-WRFv2 clearly brought the 24h-average $PM_{2.5}$ -concentrations down.

Table 3. WRF-model configurations of the PennState University (PEN-WRF) and University of Alaska Fairbanks simulations for domain 3 version 1 (UAF-WRFv1) and version 2 (UAF-WRFv2). The main differences of model configurations are indicated in bold letters.

Model Configurations	PEN-WRF	UAF-WRFv1	UAF-WRFv2
Cumulus Parameterization	None	Grell G3	None
Microphysics	Morrison 2-moment	Lin et al.	Morrison 2-moment
Longwave radiation	RRTMG	RRTM	RRTMG
Shortwave radiation	RRTMG	Goddard	RRTMG
PBL scheme	Mellor-Yamada-Janjic (Eta)	Mellor-Yamada-Janjic (Eta)	Mellor-Yamada-Janjic (Eta)
Surface Layer scheme	Monin-Obukhov (Janjic Eta)	Monin-Obukhov (Janjic Eta)	Monin-Obukhov (Janjic Eta)
Land-surface scheme	RUC Land-Surface Model	RUC Land-Surface Model	RUC Land-Surface Model
Urban model	No urban physics	No urban physics	No urban physics
Land use classification	USGS	USGS	USGS
3D analysis nudging	OFF	OFF	OFF
SFC analysis nudging	OFF	OFF	OFF
OBS nudging	ON	OFF	ON

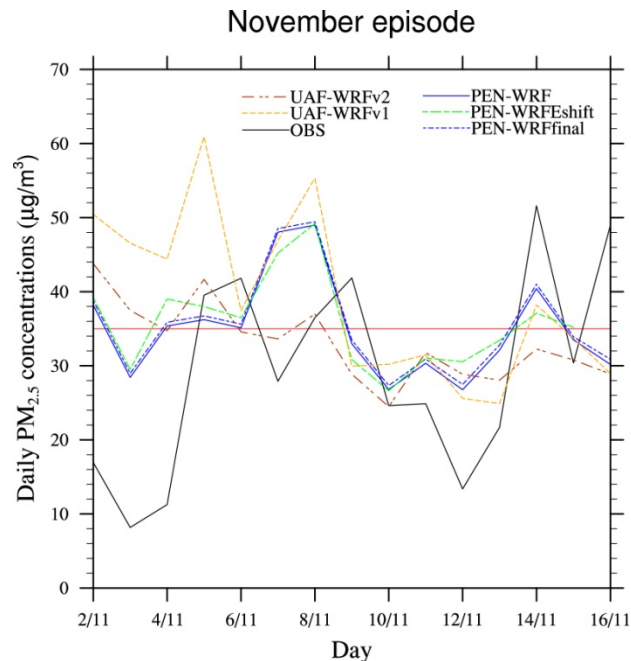


Fig. 17 Temporal evolutions of 24h-average $PM_{2.5}$ -concentrations as simulated at the grid-cell of the State Office Building site by the Alaska adapted CMAQ that uses a longer time-step (PEN-WRF) and the shorter time-step (PEN-final), emission on the next day, with the UAF-WRF version 1 (UAF-WRFv1) and version 2 (UAF-WRFv2) and as observed (OBS) at the State Office Building for the November episode.

The correlation coefficients between the simulated $PM_{2.5}$ -concentrations obtained with CMAQ using the PEN-WRF, PEN-WRFshift, PEN-WRFfinal, UAF-WRFv1 and UAF-WRFv2 and the observations are 0.31, 0.26, 0.31, -0.01 and -0.12, respectively for the November episode. For the January episode, the correlation coefficients were all 0.52 no matter whether CMAQ used the PEN-WRF, PEN-WRFfinal and UAF-WRFv1 meteorology. It can be clearly seen that the PEN-WRF is providing the best correlation coefficient of simulated and observed $PM_{2.5}$ -concentrations. However, the temporal offset of the model still exists even when we run the WRF with the OBS nudging turned off, but otherwise with the same options as used by PennState. Therefore, we recommend to do more tests and find a WRF-setup that better represents the temporal evolution of 24h-average $PM_{2.5}$ -concentrations at the State Office Building site.

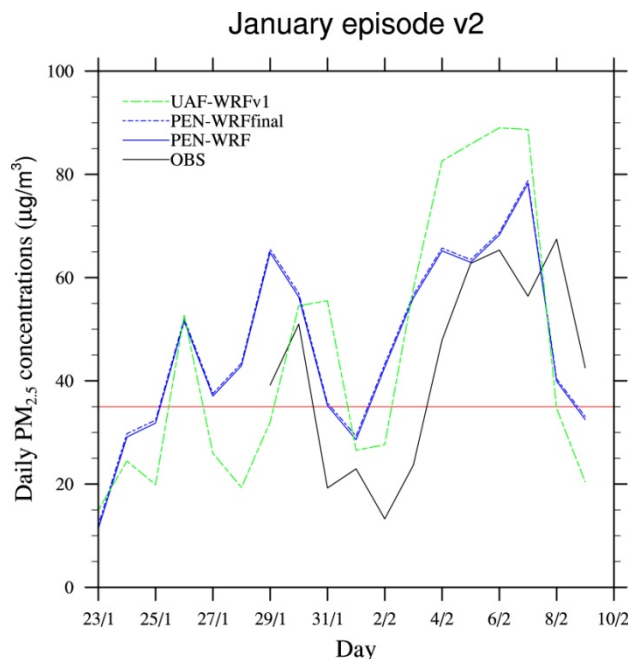


Fig. 18 Temporal evolutions of 24h-average PM_{2.5}-concentrations as simulated by the Alaska adapted CMAQ that uses a longer time-step (PEN), a shorter time-step (PEN-final), emission of the next day, with the UAF-WRF version 1 (UAF-WRFv1) and version 2 (UAF-WRFv2) and observed at the State Office Building site (OBS) for the January episode.

2.4 Investigation on the Boundary and Initial Conditions

To create the boundary conditions (BC) for domain 3, we would have had to run CMAQ on domain 2 at least. However, emission data for domain 1 and 2 were never created as various studies with WRF/Chem [Tran *et al.*, 2011; Mölders *et al.*, 2012] and observational analysis [Cahill, 2003] showed that the contribution by transport of PM_{2.5} towards Alaska are more than an order of magnitude smaller than the concentration of the NAAQS. This means that there were no issues related to the BC. Consequently, the Alaska Department of Environmental Conservation did not request Sierra Research Inc. to create an emission inventory for Alaska and did not ask us to perform CMAQ simulations on domain 2. Note that typically, the chemical fields predicted on domain 2 at the boundaries of domain 3 would serve as the BC for domain 3. For these reasons, we could not investigate the impact of the BC on the concentrations in domain 3 directly. Nevertheless, we performed a work intensive series of tests to investigate the impact of the BC on the concentrations simulated in domain 3 indirectly. These tests as their results are discussed in the following.

In the final report of phase I [Mölders and Leelasakultum, 2012], we already reported on potential impacts of BC when comparing the results at the boundaries of the smaller 66×66 domain with concentrations at these places in simulations on a 199×199 domain. The interested reader is referred to this document for further reading on BC impacts.

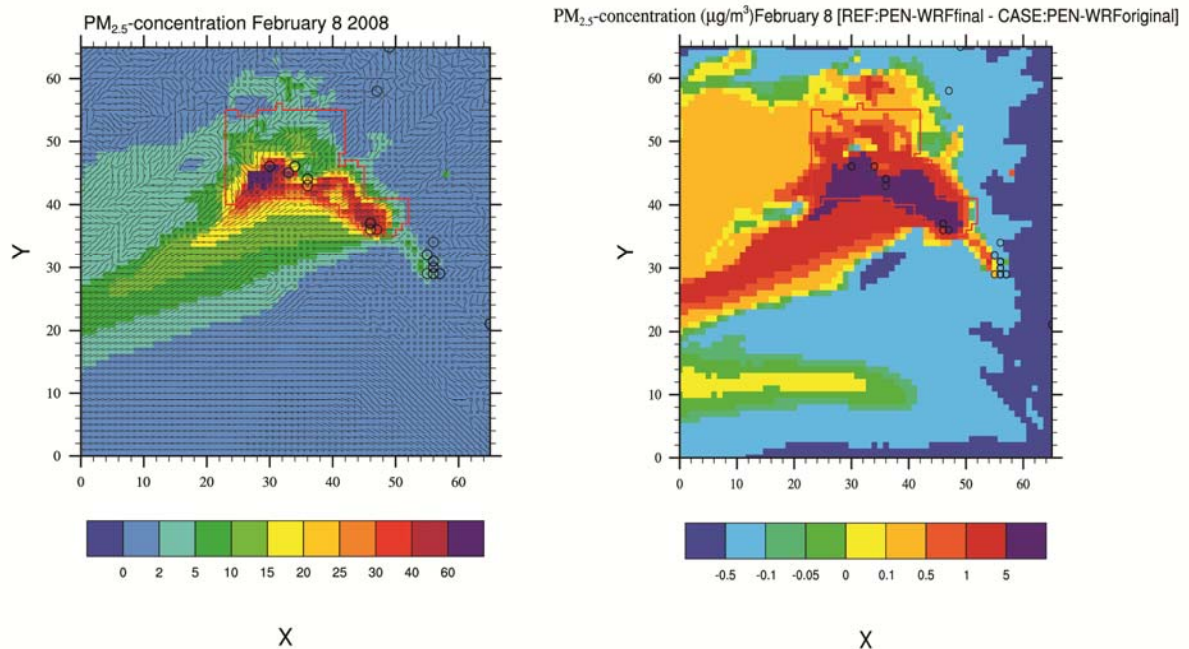


Fig. 19 Exemplary plot of (a) 24h-average $PM_{2.5}$ -concentrations as simulated by CMAQ with the PEN-WRF meteorology (PEN-WRFfinal) with the wind barbs and (b) 24h-average $PM_{2.5}$ -concentration differences at breathing level between the simulations with the final CMAQ and the PEN-WRF meteorology that uses the cleaner IC/BC conditions (see text for details) and the original CMAQ with that uses the default initial and boundary condition and PEN-WRF meteorology (PEN-WRForiginal). Differences are PEN-WRFfinal-PEN-WRForiginal.

To determine the impact of the initial conditions (IC) and BC, we compared the results from the final Alaska adapted CMAQ simulation that was generated with the PennState meteorological data (PEN-WRFfinal) with the results from the original CMAQ version with the default initial and boundary conditions that represent the background concentrations in the eastern United States. We assumed that the initial and boundary conditions developed for Alaska are “clean” background conditions. The boundary-condition impacts on the 24h-average $PM_{2.5}$ -concentrations make a difference of less than $0.5\mu\text{g}/\text{m}^3$ outside the nonattainment area (Fig. 19). For the January episode, the maximum difference due to the boundary conditions amounts $1.4\mu\text{g}/\text{m}^3$. However, on some days, effects of the boundary conditions can be found inside the nonattainment area in the range of 0.1 to $0.5\mu\text{g}/\text{m}^3$. The magnitude of the BC impacts depends on wind-speed and direction.

For example on February 8, the northeast wind blows the $PM_{2.5}$ to the southwest. This consequently results in an impact of the boundary condition on the concentrations inside the nonattainment area (Fig. 19). The difference between the clean background condition and the default BC also shows in a difference in the 24h-average $PM_{2.5}$ -concentrations about 0.1 - 0.5

$\mu\text{g}/\text{m}^3$. The results for the impact of recirculation pattern on the $\text{PM}_{2.5}$ -concentrations in the domain are shown in the Appendix.

Using IMPROVE network observations of winter 2008/09 combined with HYSPLIT [Draxler *et al.*, 2009] backward meteorological trajectories simulations at 0000 UTC on days with high $\text{PM}_{2.5}$ -concentrations ($>2\mu\text{g}/\text{m}^3$) at the Denali IMPROVE site and heights of 1000m to 8500m in steps of 500m above ground showed transport of particles from Asia to Denali Park at several levels. However, at the Denali IMPROVE site the $\text{PM}_{2.5}$ -concentrations are still far away from the NAAQS and typically below $3\mu\text{g}/\text{m}^3$. This means long-range transport may contribute to the $\text{PM}_{2.5}$ -concentrations in the nonattainment area by a couple of $\mu\text{g}/\text{m}^3$, but is not the reason for the exceedances. In winter, the advected amount of $\text{PM}_{2.5}$ is too small to cause an exceedance unless the $\text{PM}_{2.5}$ -concentrations are already close to the NAAQS.

Photochemical modeling with WRF/Chem, for which various emission datasets were available, showed that the region receives only minor amounts of pollution from long-range transport [Tran *et al.*, 2011; Mölders *et al.*, 2012]. The major sources of primary particulate matter are within the nonattainment area. Typically, $\text{PM}_{2.5}$ -exceedances occur during strong temperature-inversions on calm-wind days when the inversion traps local emissions from heating and vehicles near the surface [Tran and Mölders, 2011; Mölders *et al.*, 2012]. On these days, wind-speeds are low and advection from outside the nonattainment area is marginal.

2.5 Assessment of CMAQ Sensitivity to Secondary Chemistry

We investigated the sensitivity of the Alaska adapted CMAQ model version to chemistry before the final improvements were made for the January v1 and November episode. In the nonattainment area, the overall and average concentrations of sulfate, nitrate and organic for turning on and turning off chemistry were compared (Table 4).

The comparison of the sulfate, nitrate and organic concentrations of the two episodes shows that the concentrations of all three species are higher in the January than November episode. Turning off the chemistry decreases the sulfate concentrations by 9% and 3% for the January and November episode, respectively. Doing so, decreases the organic compound concentrations by 1% and less than 1%, and decreases the nitrate concentrations by 90% and 95% for the January and November episode, respectively (Table 4). The nitrate-aerosol production is related to the neutralization of HNO_3 vapor, which is a by-product of photochemical reactions. In the November episode, there is more sunlight than January episode. Thus, gas-phase and aerosol chemistry of nitrate play a greater role than in the January episode. For sulfate and organic compounds, the lower temperatures and dry conditions of the January episode support more gas-to-particle conversion than in the November episode. Consequently, those aqueous vapors tend to convert into particles and increase the mass of sulfate and organic particulate matter.

Table 4. Overall mass and average mass of sulfate, nitrate and organic compounds in the nonattainment area for the case of turning off the chemistry (chem_noop and aero_noop in CMAQ), turning off the gas chemistry (chem_noop), turning off the aerosol chemistry (aero_noop), and turning on the chemistry.

Nonattainment area	Sulfate ($\mu\text{g}/\text{m}^3$)	Nitrate($\mu\text{g}/\text{m}^3$)	Organic($\mu\text{g}/\text{m}^3$)
Overall mass			
January			
Turn on chemistry	152,490	103,508	713,109
Turn off gas-chemistry	148,521 (-3%)	40,787(-61%)	712,325(N)
Turn off aero-chemistry	139,856(-8%)	10,764(-90%)	708,086(-1%)
Turn off chem.	139,317(-9%)	10,161(-90%)	707,934(-1%)
November			
Turn on	125,201	189,067	1,354,795
Turn off gas-chemistry	125,413(N)	30,136(-84%)	1,354,053(N)
Turn off aero-chemistry	121,161(-3%)	10,489(-94%)	1,351,743(N)
Turn off chemistry	122,050(-3%)	10,069(-95%)	1,351,745(N)
Average mass			
January			
Turn on	0.85	0.57	3.96
Turn off gas-chemistry	0.82(-3%)	0.23(-61%)	3.95(N)
Turn off aero-chemistry	0.78(-8%)	0.06(-90%)	3.93(-1%)
Turn off chemistry	0.77(-9%)	0.06(-90%)	3.93(-1%)
November			
Turn on	0.88	1.33	9.53
Turn off gas-chemistry	0.88(N)	0.21(-84%)	9.52(N)
Turn off aero-chemistry	0.85(-3%)	0.07(-94%)	9.51(N)
Turn off chemistry	0.86(-3%)	0.07(-95%)	9.51(N)

At the grid-cell of the State Office Building site, the ratios of simulated to observed sulfate, nitrate and organic carbon and of precursors to concentrations were also investigated. On average over the January episode, the ratios of modeled SO₂/modeled aerosol sulfate are 189.0 and 154.1 for the Alaska adapted CMAQ model before and after the improvements, respectively. For the November episode, the average ratios of modeled SO₂/modeled aerosol sulfate are 184.8 and 147.5 for the Alaska adapted CMAQ model before and after the improvements, respectively. These findings mean that introducing the improvements led to more conversion of SO₂ to sulfate at the grid-cell of the State Office Building site. The ratios of emitted SO₂/emitted sulfate are 248.6 and 227.8 for the January episode v2 and for the November episode, respectively. The ratios of modeled SO₂/modeled aerosol sulfate divided by emitted SO₂/emitted sulfate are 0.62 and 0.65 for the final improvements of CMAQ for the January v2 and November episode, respectively. Note that there is no observed SO₂ data for the two episodes.

Furthermore, for the simulations that did not employ the revised WRF and SMOKE inputs, the ratio of modeled SO₂/modeled aerosol sulfate divided by emitted SO₂/emitted sulfate are very close (0.63 and 0.62). However, the ratio of emitted SO₂/emitted sulfate for the January v1 is 380.1, which is higher than for the January v2 case. The ratio of modeled SO₂/modeled aerosol sulfate divided by emitted SO₂/emitted sulfate is close to one. This finding indicates that the concentrations of SO₂ and sulfate at the grid-cell of the State Office Building site are mainly from emissions.

For organic carbon, the averaged ratios of modeled VOC/modeled organic carbon are 0.20 for both the Alaska adapted CMAQ model before and after the improvements for the January v2 episode. For the November episode, the average ratio of modeled VOC/modeled organic carbon is 0.18 for the Alaska adapted CMAQ model both before and after the improvements, i.e. it stayed the same. The introduction of the improvements does not lead to a difference in the organic carbon concentrations at the grid-cell of the State Office Building site. The ratios of emitted VOC/emitted organic carbon are 72.2 and 94.4 for the January episode v2 and for the November episode, respectively. The ratios of modeled VOC/modeled organic carbon divided by emitted VOC/emitted organic carbon are 0.19 and 0.18 for the final improvements of CMAQ for the January v2 and November episode, respectively. The simulations that did not employ the revised WRF and SMOKE inputs, have a ratio of modeled VOC/modeled organic carbon divided by emitted VOC/emitted organic carbon of 0.66. For the January v1 episode, the ratio of emitted VOC/emitted organic carbon is 30.1, which is lower than for the January v2 case. The low ratio of modeled VOC/modeled organic carbon divided by emitted VOC/emitted organic carbon indicates that there is higher gas-to-particle conversion of VOC to organic carbon than sulfate at the grid-cell of the State Office Building site.

For nitrate, the averaged ratios of modeled NO₂/modeled aerosol sulfate are 175.4 and 179.2 for the January v2 episode before and after implementation of the improved parameterizations. For the November episode, the averaged ratios are 137.8 and 140.7 before and after implementation of the improved parameterizations. The increase of sulfate concentrations after the improvement

brought about a decrease of the modeled nitrate aerosol concentrations. The averaged ratios of modeled NO_2 /modeled aerosol sulfate for the January v1 episode is 180.7.

The temporal evolutions the ratios of modeled SO_2 /modeled aerosol sulfate divided by emitted SO_2 /emitted sulfate agree with the temporal evolutions of the meteorological variables such as 2m-temperatures and 2m-water mixing ratios clearly in both episodes (Fig. 20). Lower temperature and lower water mixing ratio conditions lead to more gas-to-particle conversion. We found that on the first day of the simulations, the ratios are very low. These low ratios might be the effect of the spin-up of the chemistry in CMAQ.

a)

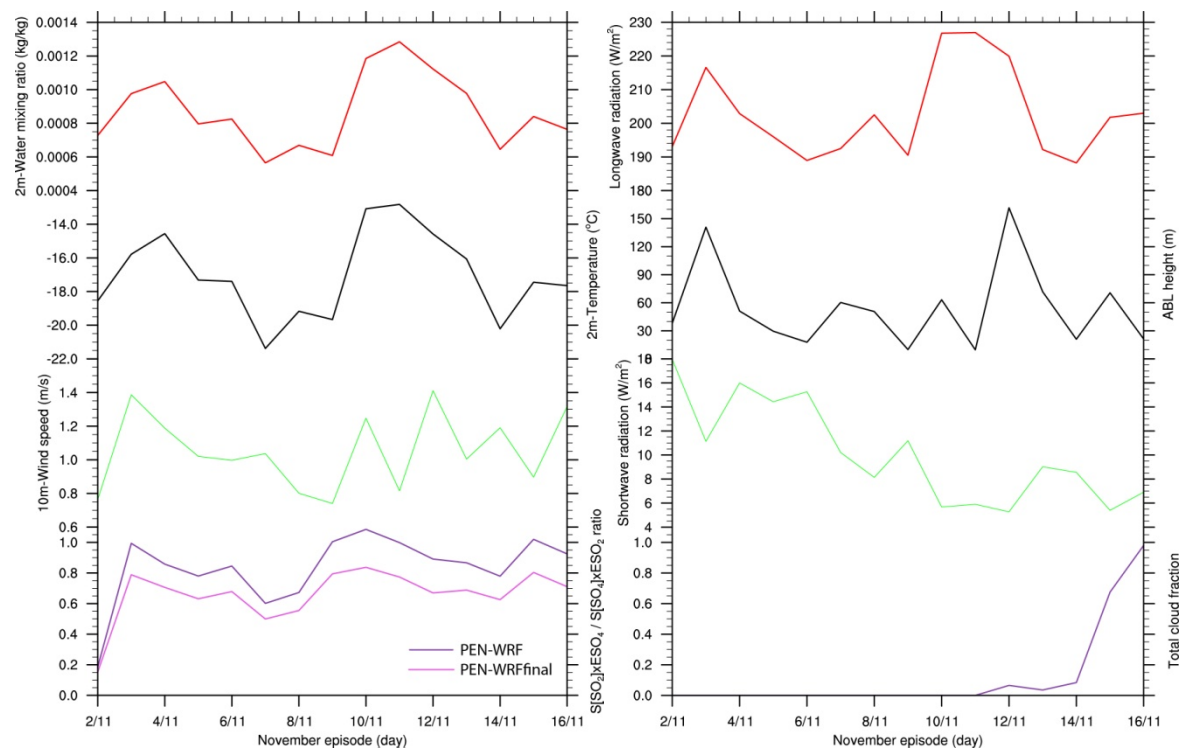


Fig. 20 continued

b)

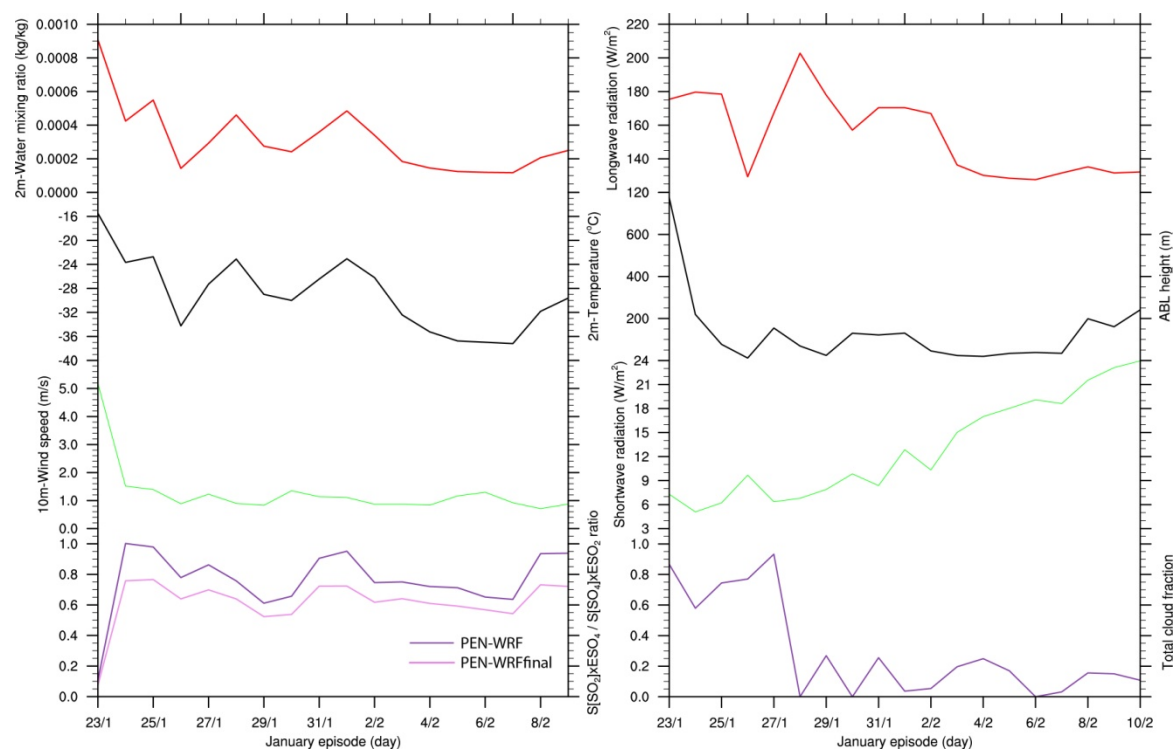


Fig. 20 Temporal evolutions of ratios of modeled SO_2 /modeled aerosol sulfate divided by emitted SO_2 /emitted sulfate as obtained from the CMAQ simulations prior to the improvements (PEN-WRF) and after the CMAQ improvements (PEN-WRFfinal) described in this report and the temporal evolutions of the meteorological variables generated by MCIP for the CMAQ model, which include 2m-water mixing ratio, 2m-temperature, 10m-windspeed, long-wave radiation, atmospheric boundary layer (ABL) height, shortwave radiation and total cloud fraction as obtained at the grid-cell of the State Office Building site for the (a) January and (b) November episode.

3. Conclusions and Recommendations

With the final improvements of the parameterizations and parameters made within the framework of this contract, the Alaska adapted CMAQ model showed an increase in the simulated sulfate concentrations at the grid-cell of the State Office Building site. Despite this success, the adapted CMAQ model still underpredicts the sulfate concentrations at the grid-cell of the State Office Building site. The normalized mean errors are 60% and 70% for the November and January episode, respectively.

We made various sensitivity simulations and tests to examine the reasons for the underestimation. These investigations and the process analysis provide strong evidence that most likely the partitioning of the emitted $\text{PM}_{2.5}$ is part of the reason for the underestimation of sulfate at the grid-cell of the State Office Building site. However, we have to use the emissions as they

partitioned in the newest version of the emission inventory as it is based on the most current insights on the emission situation in Fairbanks. Therefore, we strongly recommend further assessing and/or improving the percent partitioning of total particulate matter emissions into sulfate and other species.

Our results support the findings from other authors [e.g. *Appel et al.*, 2008] for winter cases in the Lower 48 that CMAQ underpredicts sulfate compared to observations. At UAF, currently further research is performed within the framework of a dissertation why CMAQ underestimates sulfate at low temperatures. Thus, it has to be expected that possible changes to CMAQ will become available in the future to better capture the sulfate concentrations for subarctic conditions.

Another reason for the underestimation that we cannot exclude is that in the subarctic there may be physical/chemical processes in the sulfate chemistry that are of relevance at low temperatures, low water vapor mixing ratios or both. These conditions rarely exist in the Lower 48. Thus, if such processes exist in the subarctic they may have been overlooked in studies for mid-latitudes. It is obvious that when a relevant process has not yet been found/identified, it, of course, is not considered in the code. Thus, the model cannot simulate the process and its impact on sulfate concentrations. The detection of missing processes would require long laboratory studies. Eventually, it would require long test series to derive parameterizations of the processes from the data and to implement and test the parameterizations in the model.

Our investigations and sensitivity studies also showed that the input meteorology and temporal offsets therein strongly determine the temporal evolutions of simulated 24h-average PM_{2.5}-concentrations. Therefore, we recommend further tests for the best options in the WRF setup for producing meteorological data with less temporal offset.

Our investigations suggest that the CMAQ for these episodes needs about three days to spin up the chemical fields. Therefore, we recommend to discard the first three days of simulations as spin up time and to not consider them in any assessment for the State Implementation Plan development. We further recommend that the simulation results of the first three days should be discarded from any evaluation as the chemical fields still spin-up.

We recommend that the final Alaska adapted CMAQ version presented here is tested for other episodes that have more observational data than the January and November episodes. The low data density does not permit assessment whether the occasional weak performance is related to model, emission and/or observational errors. Furthermore, with data available at just one site it is impossible to assess whether CMAQ captures the spatial distribution right. Some of the discrepancies might be just spatial offsets due to the overestimation of wind-speed. Low data availability always bears the risk to adapt a model in the wrong direction, as one can be easily right for the wrong reason at one place. This risk decreases when the amount of data increases.

A revised version of the emission inventory just became available [*Hixson*, 2012; pers. comm.]. It has to be examined how much the updated emissions will impact the simulated PM_{2.5}-concentrations and affect the simulated sulfate concentrations.

Acknowledgements

We wish to express our thanks to R. Elleman, G. Pouliot and C. Nolte for helpful suggestions regarding the CMAQ model. Special thanks also go to H. Vehkamäki for the link to the code and the suggestions on the improved parameterization for the calculation of the sulfuric acid nucleation rates. We acknowledge T. Carlson, B. Dulla and M. Hixson for providing the emission data, as well as valuable hints. We thank G. Kramm, G.A. Grell, G.J. Fochesatto, H.N.Q. Tran and D. Huff for fruitful discussions and helpful comments. We also thank D. Huff, J. Conner, J. McCormick and R.E. Peltier for providing the observational data and P. Gaudet and D. Staufer for providing the PEN-WRF-data. Computational support came from the UAF Arctic Region Supercomputing Center.

References

- Appel, K. W., P. V. Bhave, A. B. Gilliland, G. Sarwar, and S. J. Roselle (2008), Evaluation of the Community Multiscale Air Quality (CMAQ) model version 4.5: Sensitivities impacting model performance; Part II - particulate matter, *Atmos Environ*, 42(24), 6057-6066.
- Binkowski, F. S., and U. Shankar (1995), The Regional Particulate Matter Model .1. Model description and preliminary results, *J Geophys Res-Atmos*, 100(D12), 26191-26209.
- Cahill, C. F. (2003), Asian aerosol transport to Alaska during ACE-Asia, *J Geophys Res*, 108(D23), 8664.
- Draxler, R., B. Stunder, G. Rolph, A. Stein, and A. Taylor (2009), HYSPLIT4 user's guide *Rep.*, 231 pp.
- Eder, B., and S. C. Yu (2006), A performance evaluation of the 2004 release of Models-3 CMAQ, *Atmos Environ*, 40(26), 4811-4824.
- Gaudet, B. J., and D. R. Stauffer (2012) Fairbanks, North Star Borough AK PM_{2.5} non-attainment area WRF-ARW, 124 pp.
- Gipson, G. (1999), Science Algorithms of the EPA Models-3 Community Multiscale Air Quality (CMAQ) Modeling System, edited by U. S. E. P. Agency.
- Huff, D. (2012), edited.
- Jaeschke, W., T. Salkowski, J. P. Dierssen, J. V. Trumbach, U. Krischke, and A. Gunther (1999), Measurements of trace substances in the Arctic troposphere as potential precursors and constituents of Arctic haze, *J Atmos Chem*, 34(3), 291-319.
- Kulmala, M., A. Laaksonen, and L. Pirjola (1998), Parameterizations for sulfuric acid/water nucleation rates, *J Geophys Res-Atmos*, 103(D7), 8301-8307.
- Lin, Y. L., R. D. Farley, and H. D. Orville (1983), Bulk parameterization of the snow field in a cloud model, *J Clim Appl Meteorol*, 22(6), 1065-1092.
- Liu, X. H., Y. Zhang, J. Xing, Q. A. Zhang, K. Wang, D. G. Streets, C. Jang, W. X. Wang, and J. M. Hao (2010), Understanding of regional air pollution over China using CMAQ, part II. Process analysis and sensitivity of ozone and particulate matter to precursor emissions, *Atmos Environ*, 44(30), 3719-3727.
- Lovejoy, E. R., Hanson, D. R., Huey, L.G. (1996), kinetics and products of the gas-phase reaction of SO₃ with water, *J. Phys. Chem.*, 100(51).
- Mathur, R., S. Yu, D. Kang, and K. L. Schere (2008), Assessment of the wintertime performance of developmental particulate matter forecasts with the Eta-Community Multiscale Air Quality modeling system, *J Geophys Res-Atmos*, 113(D2).
- Mayfield, J. (2012) The micrometeorological effects of drainage flow in the winter atmospheric boundary layer. MS thesis, Department of Atmospheric Sciences, University of Alaska Fairbanks, pp. 216.
- Mölders, N., and K. Leelasakultum (2011), Fairbanks North Star Borough PM_{2.5} non-attainment area CMAQ modeling *Rep.*, 62 pp, Department of Atmospheric Sciences, University of Alaska Fairbanks.
- Mölders, N., H.N.Q. Tran, P. Quinn, K. Sassen, G.E Shaw, G. Kramm (2011), Assessment of WRF/Chem to capture sub-Arctic boundary layer characteristics during low solar irradiation using radiosonde, SODAR, and station data, *Atmos. Pol. Res.* 2, 283-299.
- Mölders, N., and K. Leelasakultum (2012), Fairbanks North Star Borough PM_{2.5} non-attainment area CMAQ modeling 1st and 2nd *Quarterly Rep.*, Department of Atmospheric Sciences, University of Alaska Fairbanks.
- Mölders, N., H. N. Q. Tran, C. F. Cahill, K. Leelasakultum, and T. T. Tran (2012), Assessment of WRF/Chem PM_{2.5} forecasts using mobile and fixed location data from the Fairbanks, Alaska winter 2008/09 field campaign, *Air Pollution Research*, 3(2), 180-191.
- Morrison, H., J. A. Curry, and V. I. Khvorostyanov (2005), A new double-moment microphysics parameterization for application in cloud and climate models. Part I: Description, *J Atmos Sci*, 62(6), 1665-1677.
- Mueller, S. F., E. M. Bailey, T. M. Cook, and Q. Mao (2006), Treatment of clouds and the associated response of atmospheric sulfur in the Community Multiscale Air Quality (CMAQ) modeling system, *Atmos Environ*, 40(35), 6804-6820.

- Peltier, R. E. (2012), Wintertime measurements of ambient aerosol in Alaska: High time resolution chemical components, edited by R. E. Peltier, Amherst MA.
- Seinfeld, J. H., Pandis, S.N. (2006), *Atmospheric chemistry and physics: from air pollution to climate change*, 2nd ed, 1203 pp.
- Tran, H. N. Q., and N. Mölders (2011), Investigations on meteorological conditions for elevated PM_{2.5} in Fairbanks, Alaska, *Atmospheric Research*, 99(1), 39-49.
- Tran, T. T., G. Newby, and N. Mölders (2011), Impacts of emission changes on sulfate aerosols in Alaska, *Atmos Environ*, 45(18), 3078-3090.
- Tran, H.N.Q (2012) Analysis of model and observation data for the development of a public PM_{2.5} Air-Quality Advisory Tool (AQuAT), PhD thesis submitted to the Dept. of Atmospheric Sciences, UAF, p. 308.
- Vehkamäki, H., M. Kulmala, I. Napari, K. E. J. Lehtinen, C. Timmreck, M. Noppel, and A. Laaksonen (2002), An improved parameterization for sulfuric acid-water nucleation rates for tropospheric and stratospheric conditions, *J Geophys Res-Atmos*, 107(D22).
- Zhang, L., J. R. Brook, and R. Vet (2003), A revised parameterization for gaseous dry deposition in air-quality models, *Atmos Chem Phys*, 3, 2067-2082.

Appendix 1

The following pages show an hourly sequence of plots illustrating how polluted Fairbanks air that left the nonattainment area enters the nonattainment area as aged polluted air. The wind barbs indicate wind direction. Circles mean zero wind speed and hence no wind direction. The color gives the $PM_{2.5}$ -concentrations as indicated in the legend.

Fairbanks PM_{2.5} Source Apportionment Estimates Winter 2008/2009

The University of Montana is under contract to ADEC to conduct a multi-year study of PM_{2.5} monitoring data collected in Fairbanks. The initial analysis focused on monitoring data collected during the 2008/2009 winter to determine the percent distribution of emission sources impacting each monitoring site. This information is critical to the Borough's efforts to identify which sources need to be controlled in order to reduce wintertime PM_{2.5} concentrations in Fairbanks. It is also needed to determine if the emission source contributions are consistent throughout the Borough or vary by location.

Up until the winter of 2008/2009, chemical speciation PM_{2.5} monitoring data were collected only at the State Office Building in downtown Fairbanks. To expand coverage of the Borough, three additional sites were added that winter: (1) North Pole; (2) Peger Road at the Borough Transportation Center; and (3) a field located to the northwest of the intersection between Geist Road and the Parks Highway, known as the Reindeer site. Because of delays in getting the monitors installed and operating, data collection did not begin until January 25, 2009. Thus, measurements collected at these sites did not capture the elevated concentrations recorded earlier in the winter. The State Office Building, however, collected data all winter (November 8, 2008, through April 7, 2009). A map of the location of each of the sites within the Borough is displayed in Figure 1.

The University of Montana employed several methods to analyze the data collected at each monitoring site. They first used a statistical analysis procedure, which is approved by EPA, called Chemical Mass Balance or CMB to assess relationships in the chemical compounds collected at each site to chemical compounds emitted from each emission source (e.g., automobiles, wood smoke, etc.). The second approach used was Carbon-14, which looks at the age distribution of carbon molecules found at each site. The newer carbon is generally, but not completely, associated with wood burning, while the older carbon is associated with petrochemicals or fossil fuels. The third method used was to measure an organic chemical compound known as levoglucosan, which is a unique byproduct of wood burning. Since there is some uncertainty with each method, this approach provides a broader range of insight into emission source contributions and greater comfort that the findings are correct and defensible.

The CMB analysis results for each site are displayed in Figure 2. It shows that wood smoke is estimated to be the dominant emissions source at each site, with a contribution uniformly exceeding 60% of the measured PM_{2.5} mass. The contributions of other emission sources are more variable; the second largest contributor was found to be sulfate (a compound that includes particles directly emitted during combustion and secondary particles formed in the atmosphere) and the third largest contributor to be ammonium nitrate (also a secondary particle). Generally speaking, sulfate is a function of the sulfur content of the fuels burned in the community. Recent regulations have all but eliminated sulfur from gasoline and Diesel fuel in Alaska. Therefore, the fuels contributing sulfur to the atmosphere include distillate fuel oil used in space heating and coal. Similarly,

Figure 1
Location of PM_{2.5} Monitors in Fairbanks

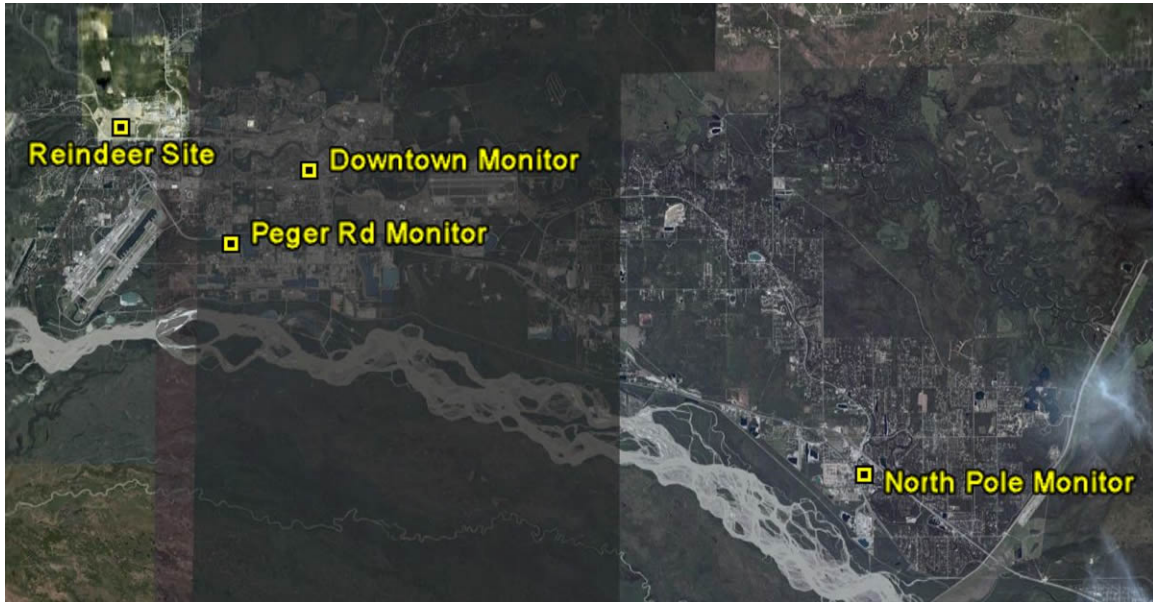
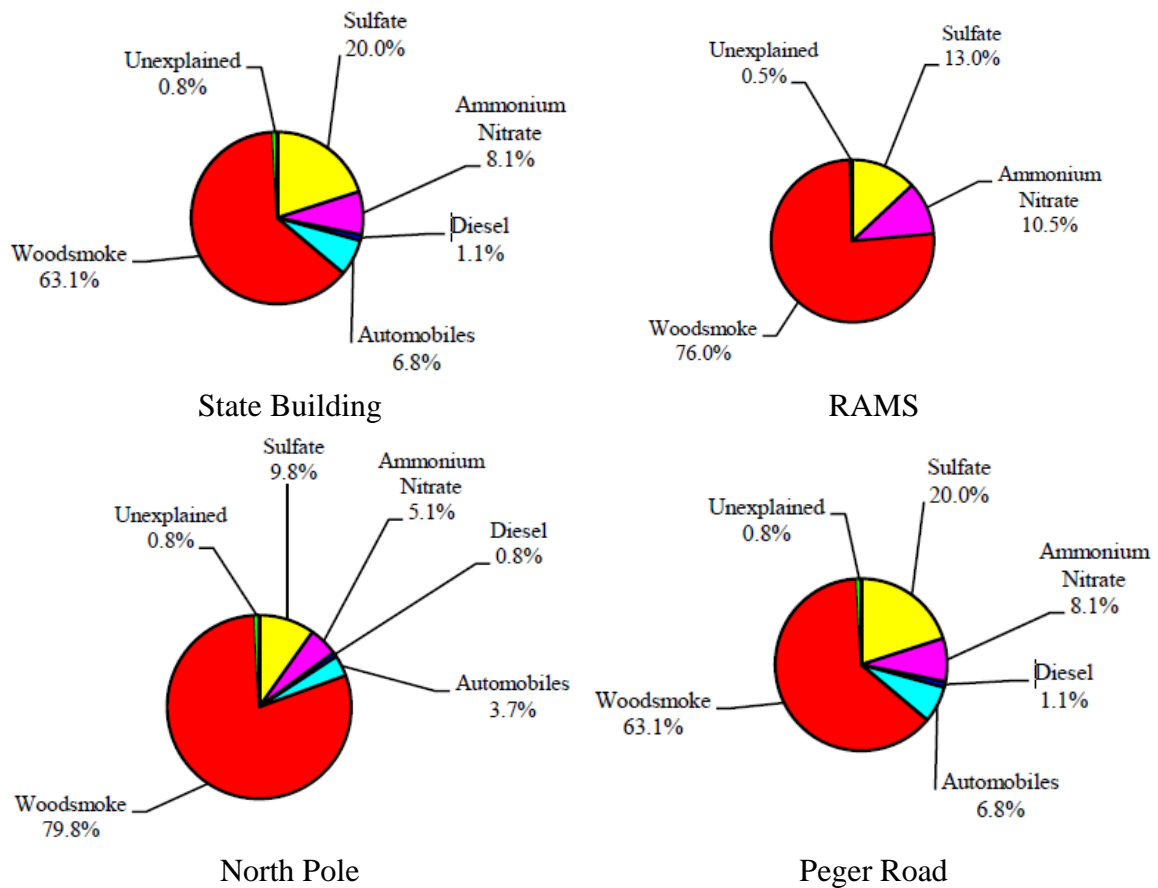


Figure 2
Emission Source Contribution Estimated from CMB Analysis



ammonium nitrate comes from ammonia and nitrogen oxide (NO_x) emissions. Sources of ammonia include waste treatment and motor vehicles. NO_x emissions come from all combustion sources.

The Carbon-14 analysis was performed on a limited sample of measurements at the three new sites and more extensively for the State Office Building. The results, which are expressed as a range, found that wood smoke values stretch from a low of 34–62% at Peger Road to high of 50–60% at North Pole. While these estimates of the wood smoke contribution are lower and more variable than the CMB results, they also support the finding that wood smoke is a major source of the PM_{2.5} mass measured at each of the monitoring sites in Fairbanks.

Levoglucosan was found to comprise 3% of the PM_{2.5} mass measured at the State Office Building, 2% at Peger Road, and 6% at the North Pole and the Reindeer sites. These values are consistent with and generally higher than those measured in other urban areas in the northwest of the U.S., including Seattle and Spokane, WA and Missoula and Libby MT. CMB analyses for the latter communities estimated the wood smoke contribution to PM_{2.5} to range from 56–82% of the wintertime PM_{2.5} mass.

In summary, the contribution of wood smoke to PM_{2.5} mass varies depending on the method used to prepare the estimate and the location. Nevertheless, three separate chemical analysis methods consistently estimate wood smoke to be a very significant source of PM_{2.5} in all areas of Fairbanks and to be potentially the largest single contributor.

Measurements of PM_{2.5} collected at monitors in Fairbanks during the entire 2009/2010 winter are currently being analyzed (i.e., chemically speciated). The results will be forwarded to the University of Montana for source apportionment analysis shortly; findings from that effort are expected to be available in October. For additional information on the results presented above, please contact Dr. James Conner at the Borough.

###

Reconciling Trends in Carbon Measurements for Fairbanks 2006-2010

Summary

A February 2009 change from the Met One SASS sampler using a NIOSH analysis methodology to the URG3000N sampler using an IMPROVE analysis methodology has resulted in an inconsistency in the particulate carbon measurement history for Fairbanks, Alaska. In order to develop a consistent history of speciated particulate matter for the region, these two carbon data sets must be reconciled. A number of journal articles and presentations have attempted to address this issue across a number of regions (Cheng 2011a, Chow 2010, Frank 2010, Schichtel 2010). Reconciliation of the total carbon (TC) and organic carbon (OC) across measurement techniques and analysis techniques proves difficult due to sampling artifacts and analysis methodology differences (McDow 1990). The elemental carbon (EC) discrepancies only occur due to the latter (McDow 1990). The design period for Fairbanks spans the years 2006 through 2010. Due to the long history of measurements with the Met One SASS sampler using a NIOSH analysis protocol, the continued usage of the Met One SASS sampler at other sites in the region, and given that the modeling episodes both occur in 2008, the best practice would be to correct the newer URG3000N IMPROVE measurements of EC/OC to reflect NIOSH-like values.

Sampler Differences

A comparison of the two samplers used in Fairbanks has shown that the higher face velocity and smaller filter area of the URG3000N reduce a positive artifact present in the SASS sampler from adsorbed OC. The positive artifact reduction reduces the overall total carbon. However, the higher face velocity of the URG3000N also results in a negative artifact due to evaporative losses of semi-volatile materials (McDow 1990). The overall difference in carbon is therefore a reduction of a positive artifact from SASS and introduction of a negative artifact from URG3000N. The magnitude of these changes is difficult to assess even with collocated samples (Chow 2010). There are multiple sites in and around Fairbanks that continue to use the Met One SASS sampler. At this time, however, there is no quantitative comparison of the magnitude of these sampling artifacts for Fairbanks, so direct comparisons cannot be made between the samplers at different sites. A value judgment of which sampler is best suited for conditions in Fairbanks is not possible as the URG3000N is not collocated with any of the Met One SASS samplers.

Analysis Differences

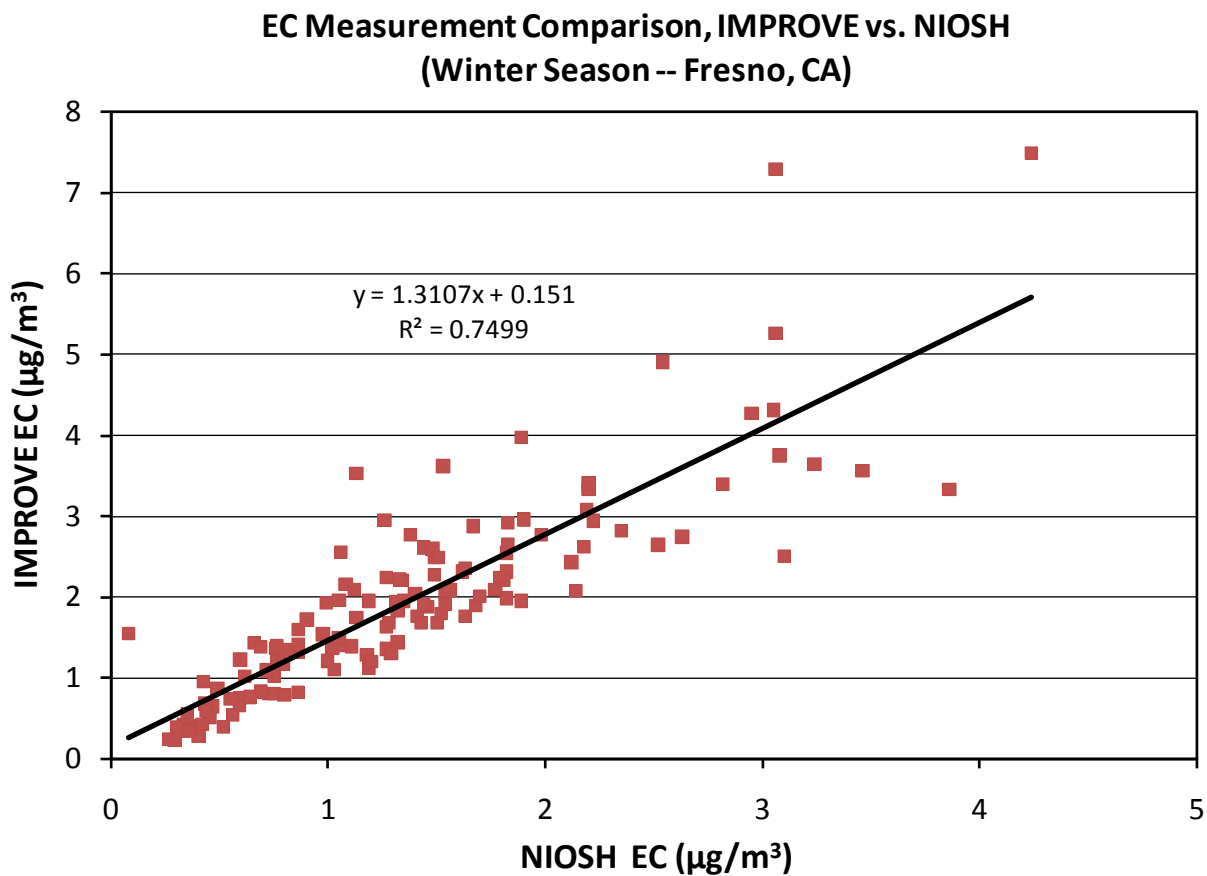
A further complication is the ongoing debate about the merits of the NIOSH and IMPROVE protocols for representing EC and OC. While the OC can be influenced by the sampler itself due to adsorption and evaporation, the EC should remain relatively the same between two samplers (McDow 1990). However, the EC (as well as OC) will vary depending on the analysis technique employed (IMPROVE, NIOSH, TOT, TOR). The literature suggests that the EC shift seen when comparing NIOSH and IMPROVE techniques is largely driven by the products of wood

combustion (Schauer 2003, Chow 2001). The choice of TOR versus TOT can also have a significant impact on the measurement of EC (Chow 2004, Cheng 2011b).

Proposed Changes

Using collocated IMPROVE and CSN sampler data from Fresno, CA from the years 2004 through 2009 an IMPROVE to NIOSH correction factor for EC has been developed. Figure 1 shows the EC concentrations as measured for the winters in Fresno, CA. The emissions source mix for Fresno, CA in the winter seems the most comparable to Fairbanks as it does include a significant amount of wood smoke as compared to other sites with collocated samplers. The conversion for IMPROVE EC to NIOSH EC would follow the equation $y=1.3107x + 0.151$, where y is the IMPROVE EC and x represents NIOSH EC. In this context, IMPROVE implies the use of the URG3000N sampler and NIOSH implies the Met One SASS. Corrected EC values would then be used to derive the corrected OC.

Figure 1
EC Correlation between the Collocated IMPROVE and CSN Samplers



Conclusion

Considering the unsettled nature of these debates, it seems the best course of action is to rely on the weight of the historical measurement data which used the Met One SASS sampler and NIOSH protocol to correct the newer IMPROVE data. This sampler and analysis technique were employed for the bulk of the design period 2006 through early 2009 and also cover the episodes in 2008 for which CMAQ simulations are already underway. An additional concern is the ability to compare the carbon measurements at the downtown site with the other monitor sites in and around Fairbanks. At present, there are no other sites using the URG3000N with IMPROVE analysis in the region. Adjusting the IMPROVE carbon measurements represents a more efficient means of comparing data gathered at multiple sites in Fairbanks. Considering that EC should differ only from the change in analysis protocol, not the change in samplers, an EC correction factor should be devised based on collocated sampler data from a region with comparable sources and meteorology to Fairbanks. Thus far the best data set appears to be from a site in Fresno, CA. The corrected EC can then be used to derive a corrected OC concentration for the period of 2009 through 2010. Going forward, the Fairbanks North-Star Borough will maintain a collocated Met One SASS sampler at the downtown site. Filters from the collocated sampler will be analyzed using the NIOSH protocol to provide a basis for comparing against the URG3000N IMPROVE sampler as well as other monitor sites in Fairbanks.

References

Cheng, Y., Zhen, M., He, K., Chen, T., Yan, B., Russell, A. G., Shi, W., Jiao, Z., Sheng, G., Fu, J., Edgerton, E. S., "Comparison of two thermal-optical methods for the determination of organic carbon and elemental carbon: Results from the southeastern United States," *Atmospheric Environment*, 45, 1913-1918, 2011

Cheng, Y., He, K., Duan, F., Zheng, M., Du, Zhen., Ma, Y., Tan, J., "Ambient organic carbon to elemental carbon ratios: Influences of the measurement methods and implications," *Atmospheric Environment*, 45, 2060-2066, 2011

Chow, J. C., Watson, J. G., Chen, L.-W. A., Rice, J., and Frank, N. H., "Quantification of PM_{2.5} organic carbon sampling artifacts in US networks," *Atmospheric Chemistry and Physics*, 10, 5223-5239, 2010

Chow, J. C., Watson, J. G., Chen, L. -W. A., Arnott, W. P., and Moosmüller, H., "Equivalence of elemental carbon by thermal/optical reflectance and transmittance with different temperature protocols," *Environmental Science and Technology*, 38, 4414-4422, 2004

Chow, J. C., Watson, J. G., Crow, D., Lowenthal, D. H., and Merrifield, T., "Comparison of IMPROVE and NIOSH carbon measurements," *Aerosol Science and Technology*, 34, 23-34, 2001

Frank, N., “Urban EC and OC Trends Using CSN, IMPROVE, SEARCH EC & OC, ‘BC’ & OCMmb via FRM PM2.5: *Findings and Issues*,” IMPROVE Carbon Workshop, Columbia Gorge, Washington, October 27, 2010

McDow, S. R. and Huntzicker, J. J., “Vapor adsorption artifact in the sampling of organic aerosol: face velocity effects,” *Atmospheric Environment*, 24A, 2563 – 2571, 1990.

Schauer, J. J., Mader, B. T., Deminter, J. T., Heidemann, G., Bae, M. S., Seinfeld, J. H., Flagan, R. C., Cary, R. A., Smith, D., Huebert, B. J., Bertram, T., Howell, S., Kline, J. T., Quinn, P., Bates, T., Turpin, B., Lim, H. J., Yu, J. Z., Yang, H. and Keywood, M. D., “ACE-Asia intercomparison of a thermal-optical method for the determination of particle-phase organic and elemental carbon,” *Environmental Science and Technology*, 37, 993-1001, 2003

Schichtel, Hand, Malm, White, Pitchford, Murphy, Frank: Exploration of IMPROVE and CSN fine particulate carbon spatial and temporal patterns,” IMPROVE Carbon Workshop, Columbia Gorge, Washington, October 27, 2010

Fairbanks North Star Borough PM_{2.5} Non-Attainment Area CMAQ Modeling

First “Quarterly” Report Phase II

Reporting Period: January 1, 2012 – April 30, 2012

Project: 398831 CMAQ-DEC 2012

By Prof. Nicole Mölders (PhD, PhD) and Ketsiri Leelasakultum (MS)

University of Alaska Fairbanks, Geophysical Institute, College of Natural Science and
Mathematics, Department of Atmospheric Sciences

1. Background

Due to deadlines that the Alaska Department of Environmental Conservation (DEC) had to meet with respect to the development of the Fairbanks State Implementation Plan (SIP), DEC had postponed the due date for the Quarterly Report. They wanted to provide time to UAF to perform investigations on questions DEC personnel needed to answer at their deadlines. Various phone conferences were held where UAF reported on the progress and the results of the investigations performed to answer DEC's urgent questions. Due to this DEC approved and requested later submission of the Quarterly Report, this report covers a longer period than three month.

The Community Multiscale Air Quality (CMAQ) model version 4.7.1 was adapted to simulate the $PM_{2.5}$ -concentrations in Fairbanks, the interior of Alaska in phase I (Mölders and Leelasakultum 2011). In the time covered by the current report, we applied the adapted CMAQ to a two-week episode in January/February, 2008 and November, 2008 each for further improvement and investigations and understanding of the $PM_{2.5}$ -situation in the Fairbanks nonattainment area.

The episode January, 2008 was first used to evaluate the performance of the CMAQ model. According to the final report of phase I (Mölders and Leelasakultum 2011), the model was configured to use the global mass-conserving Yamartino advection scheme, the eddy vertical diffusion module, the Carbon Bond Five (CB05) lumped gas phase chemistry mechanism which using the Euler Backward Iterative (EBI) as solver, the AERO5 aerosol mechanism, the photolysis inline module and the Asymmetric Convective Method (ACM) cloud processor to compute convective mixing (cloud_acm_ae5).

Several changes were made to the CMAQ code with the purpose of improving the prediction of $PM_{2.5}$ -concentrations and for representing the Fairbanks domain conditions:

1. The default initial condition and boundary conditions were replaced with the developed Alaska specific initial and boundary condition.
2. The dry deposition code were modified to made the dry deposition occurred in the tundra-typed land-use, which is the major type of land-use in Fairbanks domain. Some other changes related to the dry deposition include the adjustment for the resistance to snow of SO_2 , the soil resistance, the canopy cuticle resistance to be functioning with the low temperature, reducing of wet canopy resistance (see Mölders et al. 2011), reducing and scaling the area-to-volume ratio for buildings according to the urban fraction of Fairbanks, and increasing the pH value for snow/rain/wet surfaces to the average values found in Alaska.
3. The code in Meteorology-Chemistry Interface Processor (MCIP) version 3.6 for the minimum mixing height constant was reduced in accord with the observations in Fairbanks, and the minimal stomata resistances were also replaced.

4. The lowest and highest eddy diffusivity coefficients, which play an important role for the vertical distribution of concentrations, were decreased by half, and scaled according to the fraction of land-use.
5. The wind-speed in the valley of domain was reduced by half for calibrating the over-estimation of the simulated wind-speed by WRF.

The evaluations of the performance of the Alaska adapted CMAQ from phase I considered the January/February episode. It showed that the mean average of 24h-average $PM_{2.5}$ -concentrations at the grid-cell that holds the official monitoring site is $38.07\mu\text{g}/\text{m}^3$, whereas the mean average of observed data is $41.7\mu\text{g}/\text{m}^3$. The ratio of means (sim/obs) is 1.13. The mean bias, mean fractional bias, mean error and mean fractional error are $-3.76\mu\text{g}/\text{m}^3$, -0.32% , $13.13\mu\text{g}/\text{m}^3$, 34.51% , respectively. The CMAQ model overestimated during January 31 to February 2, and underestimated during February 5 to February 9. The correlation coefficient between the observed and simulated 24h-average $PM_{2.5}$ -concentrations is 0.39 for 13 pairs of data. Bugle plots and soccer plots indicate weak performance on February 2 and February 8, 2008 (AKT). The Alaska adapted CMAQ model simulated the speciation of total dry $PM_{2.5}$ as 48% organic carbon (OC), 6% elemental carbon (EC), 4% nitrate, 3% ammonia, 2% sulfate and 36% others. The observed speciation of total dry $PM_{2.5}$ was 41% OC, 6% EC, 5% nitrate, 9% ammonia, 20% sulfate, and 19% others. The model obviously underestimated the sulfate compositions and ammonium, slightly overestimated OC and had very good performance for nitrate and EC.

Based on the CMAQ's output in phase I, Sierra Research Inc. had improved the emission input data, and Penn State had improved the meteorological input data for the CMAQ. Hereafter, we referred to the January/February episode data before the improvements as January v1 and we referred to the January/February episode data after the improvements as January v2. This first quarterly of Phase II will cover:

1. The simulations of the adapted CMAQ for the January v1 episode including the Relocatable Air Monitoring System (RAMS) data, $PM_{2.5}$ speciation and the sensitivity tests we performed
2. The comparison of simulations and the model performance for the November episode performed with and without reduction of the wind-speed in the valleys, including the simulations for $PM_{2.5}$ speciation and various sensitivity tests
3. The comparison of simulations and the model performance for the January v2 episode with and without CMAQ modifications
4. The statistical performance of the November and January v2 episodes with the CMAQ modifications and the performance evaluation for the $PM_{2.5}$ -speciations in the January v2 episode
5. The process analysis results for the November episode and January v2 episode

2. Activities

2.1 Evaluations of the Alaska adapted CMAQ for the January v1 episode with RAMS data, PM_{2.5} speciation and the sensitivity tests

The significance tests in the final report of phase I showed that the simulated and observed 24h-average PM_{2.5}-concentrations had statistical differences due to the low sample number. Therefore, the Relocatable Air Monitoring System (RAMS) data of the PM_{2.5}-concentrations were also included for evaluating the adapted CMAQ performance. The locations of the RAMS (Fig. 1) were Julie Shelton's house (N 64.88° W147.68°) for January 18 to January 24, David Leone's house (N 64.80° W147.45°) for January 24 to January 31, Anne Ruggle's house (N 64.88° W147.82°) for January 31 to February 7, Alaska Rubber (N 64.80° W147.70°) for February 7 to February 14 (see Fig. 1).

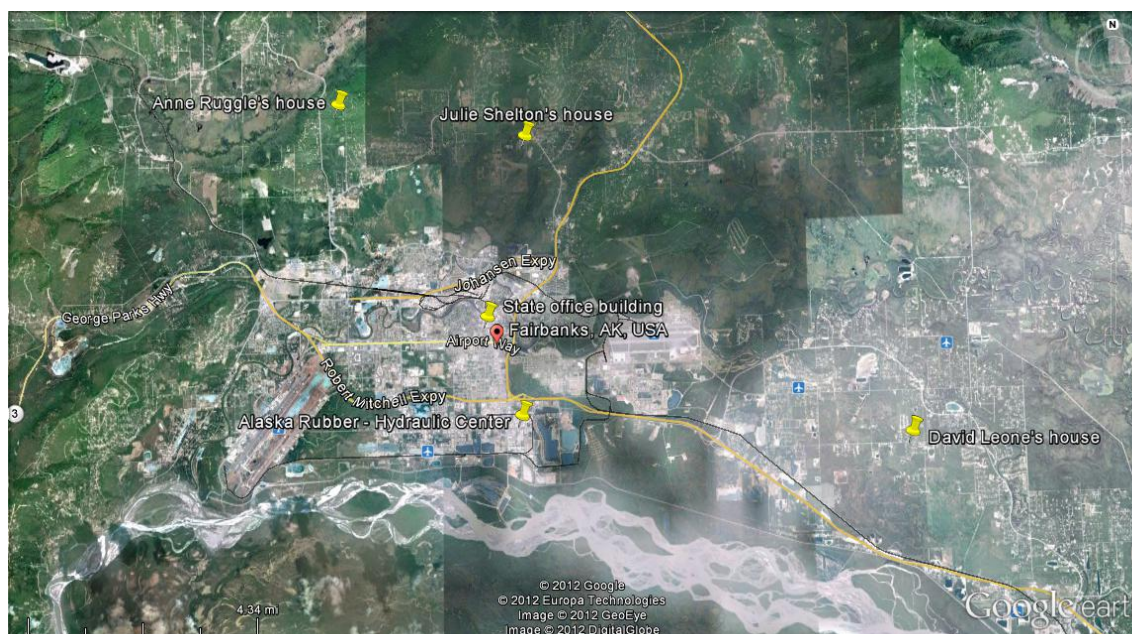


Fig. 1 Locations of the Relocatable Air Monitoring System (RAMS) and the State Building site.

The temporal evolution of the observed RAMS PM_{2.5}-concentrations were compared with the simulated PM_{2.5}-concentrations (Fig.2). The RAMS data suggested some spatial and temporal offsets during the local extremes, for instance, the adapted CMAQ model underestimated during January 26-January 28, and during February 8-10 (Fig. 2).

Combining the simulated and observed data of 24h-average PM_{2.5}-concentrations from both State Building and RAMS sites led to the increase of correlation coefficient to 0.51 for 29 pairs of data. There is no statistically significant difference at the 95% confidence level for both hourly and daily data. The scatter plot between the simulated and observed 24h-average PM_{2.5}-concentrations show the agreement of majority within the factor of two (Fig.3). For those pairs of data, that have agreement less than a factor of three, are the RAMS on January 27, February 2,

8, 9, which are sites above the inversion. Possibly, this is due to sub-grid scale effects, which are not resolved by the model.

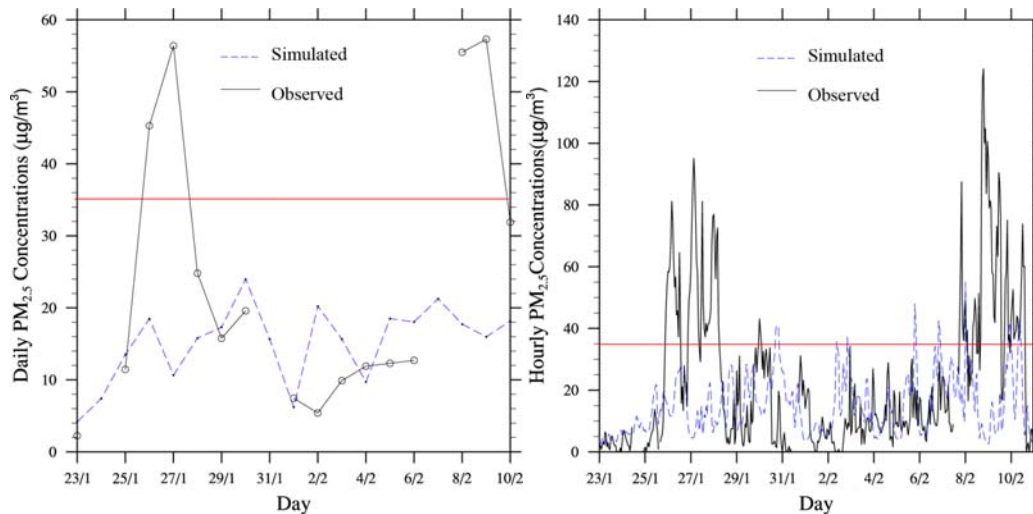


Fig. 2 Time series of the adapted CMAQ simulated (blue dashed line) and RAMS observed data (black solid line) for (a) 24h-average $PM_{2.5}$ -concentrations and (b) hourly $PM_{2.5}$ -concentrations (right) for January v1

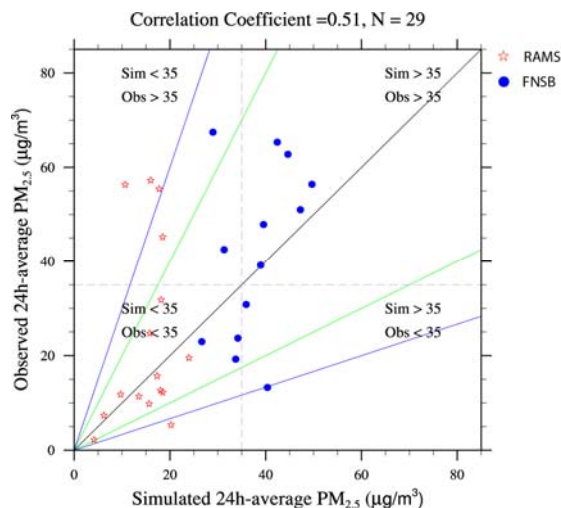


Fig. 3 Scatter plots of 24h-average $PM_{2.5}$ -concentrations for January v1. The blue dots and red stars represent the data for the State Building and RAMS sites, respectively. The green line indicates the factor of two and the blue line indicates the factor of three agreement between simulated and observed values. Note that 30% of agreement within a factor of two is considered good performance (Chang and Hanna 2004).

The bugle plots and soccer plots show the similar results as the scatter plots i.e. that most pairs of data outside the performance criteria (see Boylan and Russell 2006 for a definition of the criteria) are from the RAM sites located above the inversion (Fig. 4). Note that it is common

knowledge that models like WRF have difficulties capturing inversions in very complex terrain as they use the mean terrain height within a grid-cell as the representative height, while the measurements capture the actual terrain impacts (Mölders and Kramm 2010). At the State Building site, there are two pairs outside the performance criteria. They occurred on January 31 and February 2, when the model overestimated the $PM_{2.5}$ -concentrations and the observed data were extremely low.

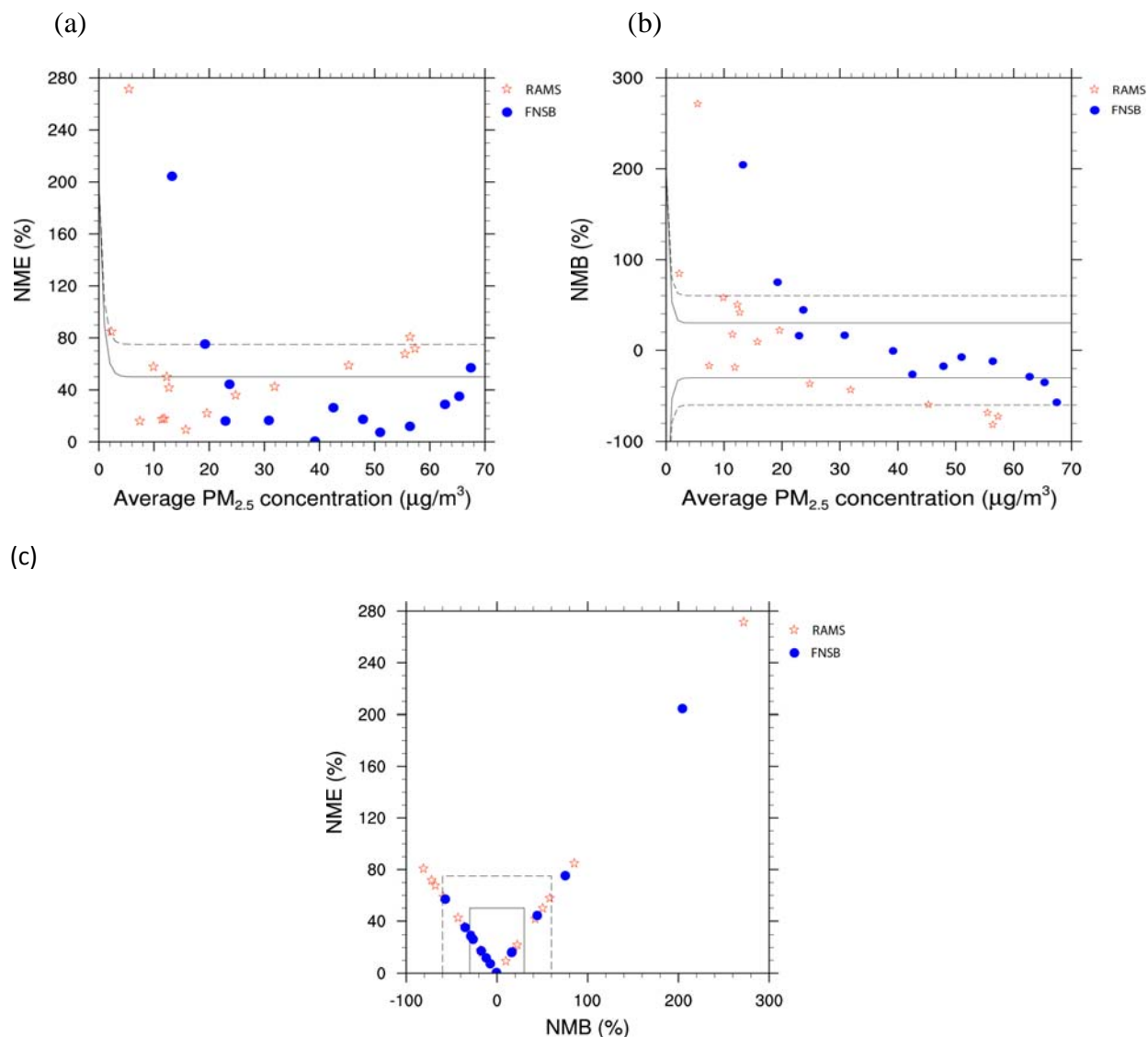


Fig. 4 Bugle plots of normalized mean (a) errors and (b) biases of simulated 24h-average $PM_{2.5}$ -concentrations and (c) soccer plot of normalized mean errors and biases all determined with respect to the observations at the State Building site (blue dots) and RAMS sites (red stars) for January v1. The dashed and solid lines indicate the performance criteria and performance goals in accord with Boylan and Russell (2006).

The observed temperatures during January 31 to February 2 were the period when temperature rebounded slightly (PennState final report, 2011). WRF estimated too low surface temperatures on these days, for example, the WRF-simulated hourly surface temperature at 15 UTC on January 31 is about -30°C (Fig. 5) in the Fairbanks nonattainment area, whereas the observed temperature at the Fairbanks International Airport at that time was about -24°C . The too low temperatures would lead to enhanced gas-to-particle conversion than actually would occur with the correct temperature and lead to further over-prediction of the $\text{PM}_{2.5}$ -concentrations at the State Building site.

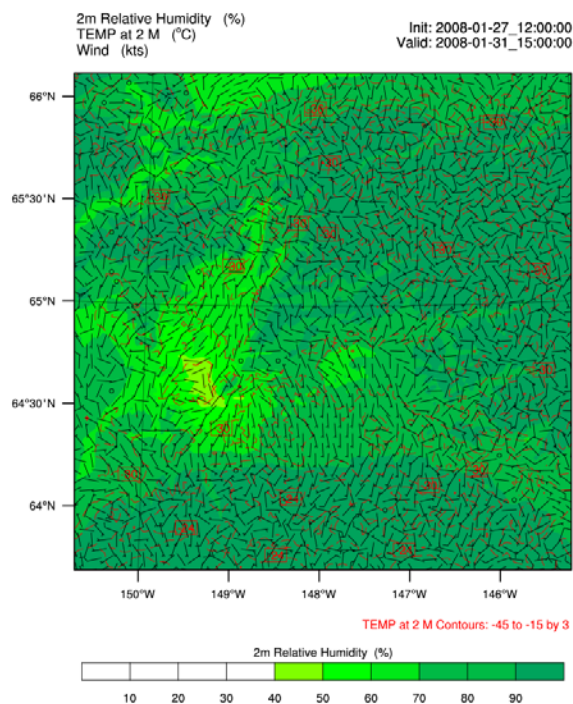


Fig. 5 Example of WRF simulated 2m temperatures (color), 2m relative humidity (contours) and 10m wind-speeds (barbs) in the Fairbanks domain on January 31 at 1500UTC.

The performance of the adapted CMAQ in simulating the $\text{PM}_{2.5}$ -compositions was evaluated. The six days with pairs of observed and simulated $\text{PM}_{2.5}$ -compositions were compared in bar charts and scatter plots (Figs. 6, 7). The adapted CMAQ model predicted best for OC and EC, which have high concentrations and make up large fractions of total $\text{PM}_{2.5}$. Simulated and observed sulfate and ammonium fail to agree within a factor of three. The bugle plots and soccer plots show similar results as the scatter plots, i.e., that most pairs of species data that fall outside the performance criteria are sulfate, ammonium and chloride (Cl) (Fig. 8). The Cl outlier occurred in the November episode as well (see later discussion), therefore we increased the initial and background Cl-concentrations at the lowest level according to the IMPROVE data in our simulations of January v2 and the November episode. The improved Cl-profiles are given in Appendix A. The NH_4 -outlier may be due to underestimation of the NH_3 emissions (for a discussion on potential reasons for the NH_3 -emission underestimation see Mölders et al. (2012).

The adapted CMAQ underestimated SO_4 by five times the observed value, which requires improvement and further investigations. Some first results of these investigations are discussed later in this report, while other investigations are ongoing.

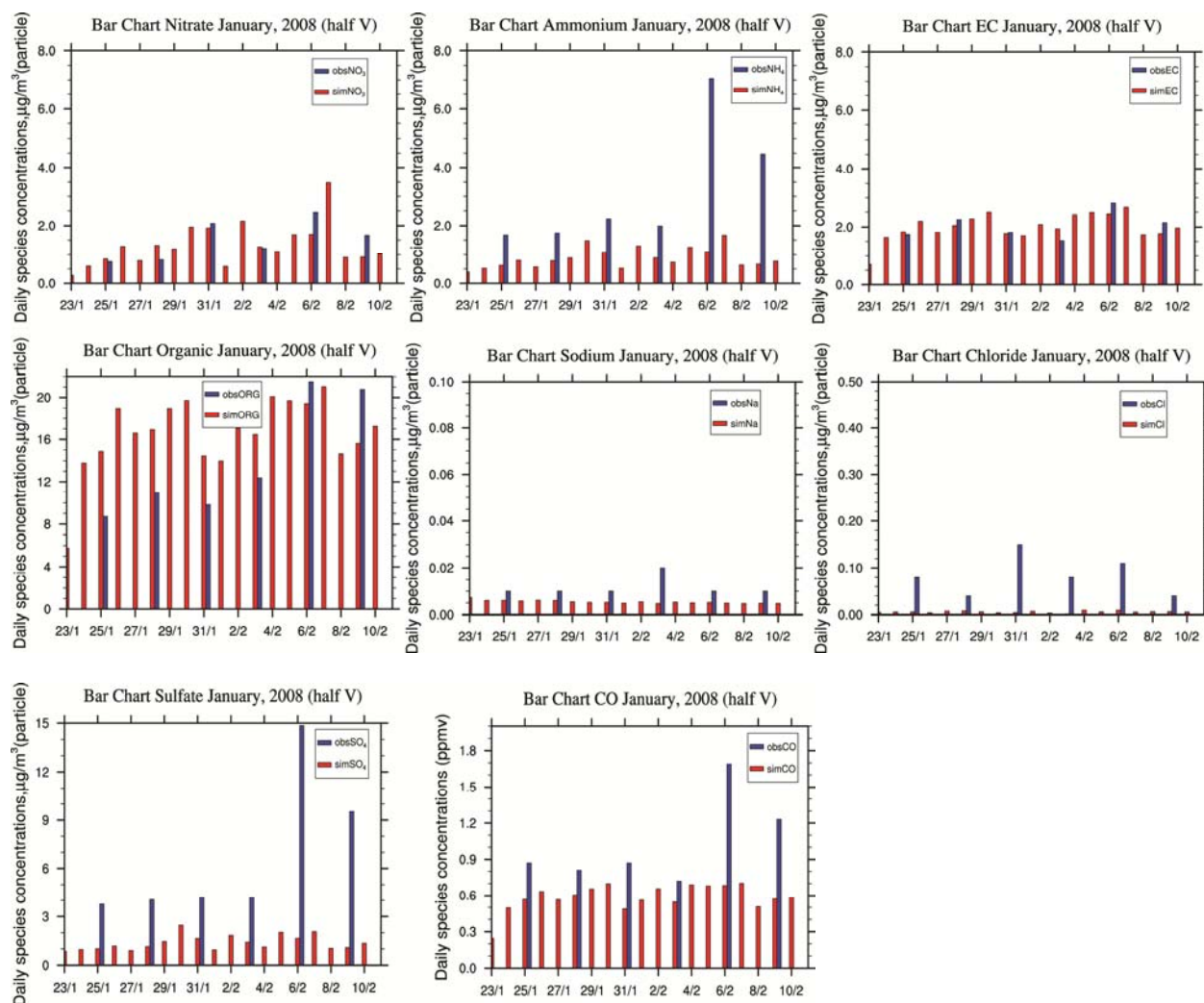


Fig. 6 Bar charts of observed (blue) and simulated (red) 24h-average PM_{2.5}-composition for NO₃, NH₄, EC, OC, Na, Cl, SO₄, CO for January v1. Note that this episode was run with 50% reduction of the near-surface wind speeds in the valleys (see Mölders and Leelasakultum 2011 for details on the simulation setup)

The 24h-average PM_{2.5}-concentrations at the State Building site were simulated for the case of without point source emissions, gas chemistry, aerosol chemistry, chemistry and compared with the observation data and the simulations, which include everything (reference/normal adapted CMAQ simulation), Fig. 9. It can clearly be seen that chemistry played a lesser role for the PM_{2.5}-concentrations than the emissions from point sources. The simulations wherein the point source emissions were turned off led to a decrease in PM_{2.5}-concentrations at State Building site of on average $3.9\mu\text{g}/\text{m}^3$ (11%), whereas the simulation with turned off chemistry, aerosol

chemistry and gas chemistry led to decreased $PM_{2.5}$ concentrations by on average 2.0 (6%), 2.0 (6%) and $1.2\mu\text{g}/\text{m}^3$ (4%), respectively. Note that in the adapted CMAQ model, turning off the aerosol chemistry resulted in the same results as turning off all chemistry. This behavior may be a hint that a process is missing in aerosol chemistry and/or aerosol chemistry is not taking place as too much water is in the ice phase.

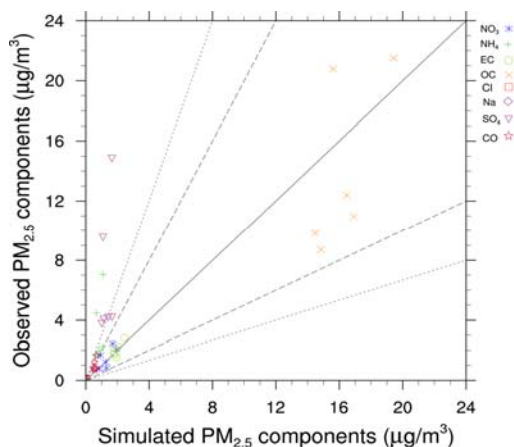


Fig. 7 Scatter plot of simulated and observed 24h-average $PM_{2.5}$ -composition for January v1. See Mölders and Leelasakultum (2011) for details on the simulation setup

On the day which simulated the highest concentrations ($49.7\mu\text{g}/\text{m}^3$ on February 7), the chemistry process had the maximum contribution to the 24h-average $PM_{2.5}$ concentrations $4.9\mu\text{g}/\text{m}^3$ (10%) at the State Building. In this $4.9\mu\text{g}/\text{m}^3$, the aerosol chemistry process contributed $3.9\mu\text{g}/\text{m}^3$ (8%) to the total aerosol production of chemistry process.

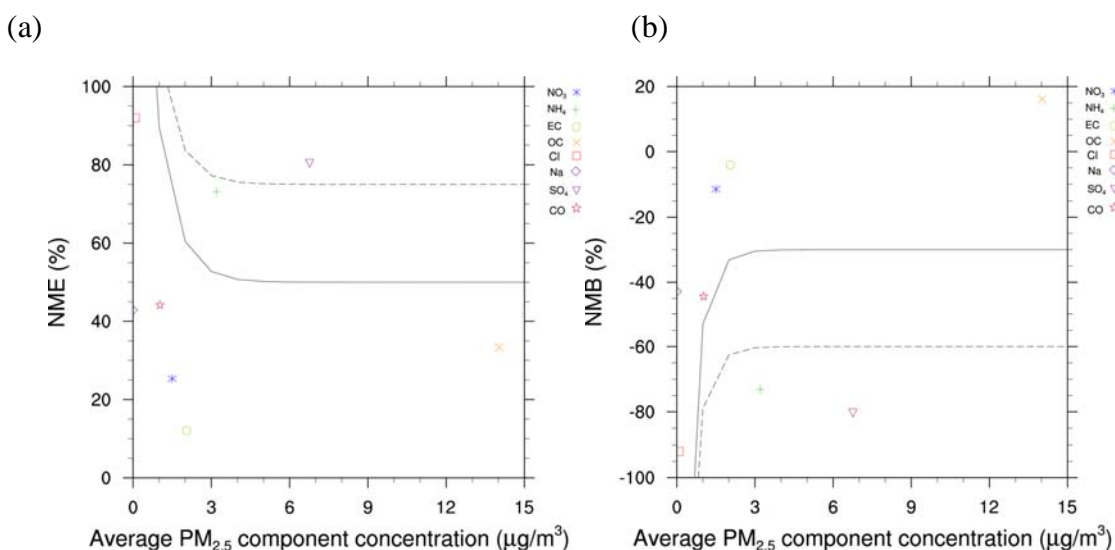
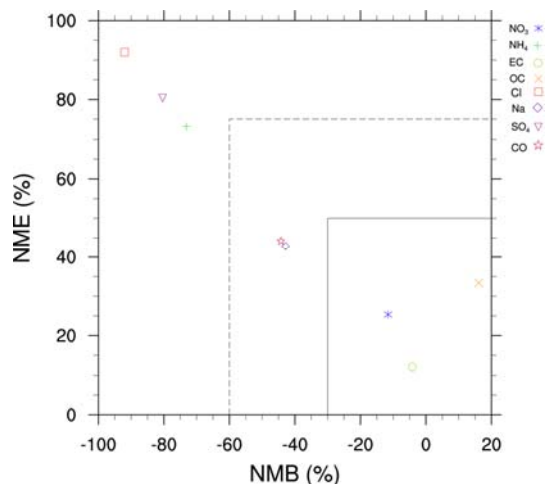


Fig. 8 continued on next page



(c)

Fig. 8 Bugle plots of normalized mean (a) errors and (b) biases of simulated 24h-average $PM_{2.5}$ -composition and (c) soccer plot of normalized mean errors and biases all determined with respect to the observations at the State Building site for January v1. The dashed and solid lines indicate the performance criteria and performance goals in accord with Boylan and Russell (2006).

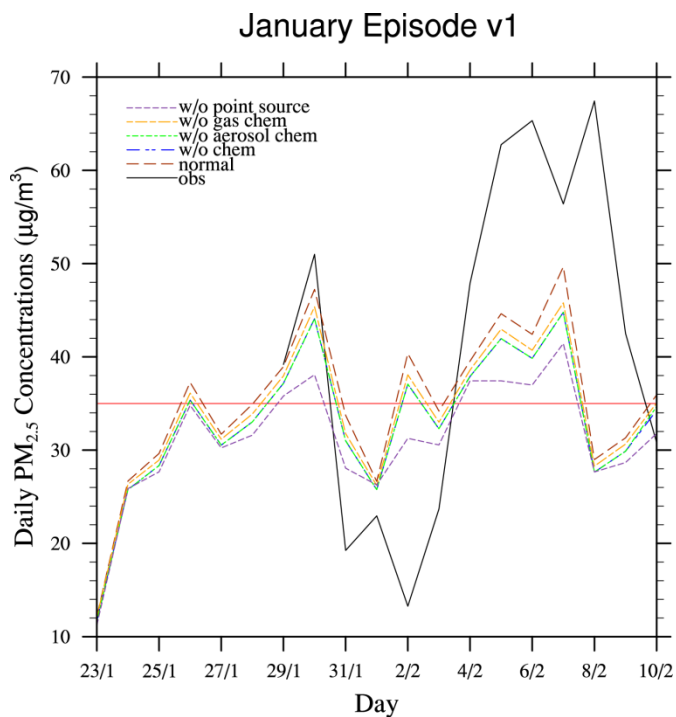


Fig. 9 Time series of observed (black solid line) and adapted CMAQ simulated data as obtained by various sensitivity tests that were performed without consideration of point sources, without consideration of gas chemistry, without consideration of aerosol chemistry, without consideration of chemistry and with consideration of all processes and emissions (reference/normal) for the 24h-average $PM_{2.5}$ -concentrations at the State Building for January v1. The red solid line indicates the National Ambient Air Quality Standard of $35\mu\text{g}/\text{m}^3$.

The highest and the second highest contribution from point source emission of 9.2 and $9.1\mu\text{g}/\text{m}^3$ was simulated on January 30 and February 2. The percent contributions from point source emissions on these two days are 19% and 22%, respectively.

2.2 Comparison of simulations and their performance for the November episode with and without reduction of wind-speeds in the valleys

The November episode covers November 2 to November 16, 2008. The emissions developed for the November episode were updated by Sierra Research Inc. for the emissions from mobile sources, and include the emissions from airports. The comparison of the spatial distribution of emissions in the January v1 and November episode showed that the magnitudes of $\text{PM}_{2.5}$ -emissions in the November episode are higher for the area north of the Fairbanks nonattainment area (Fig.10).

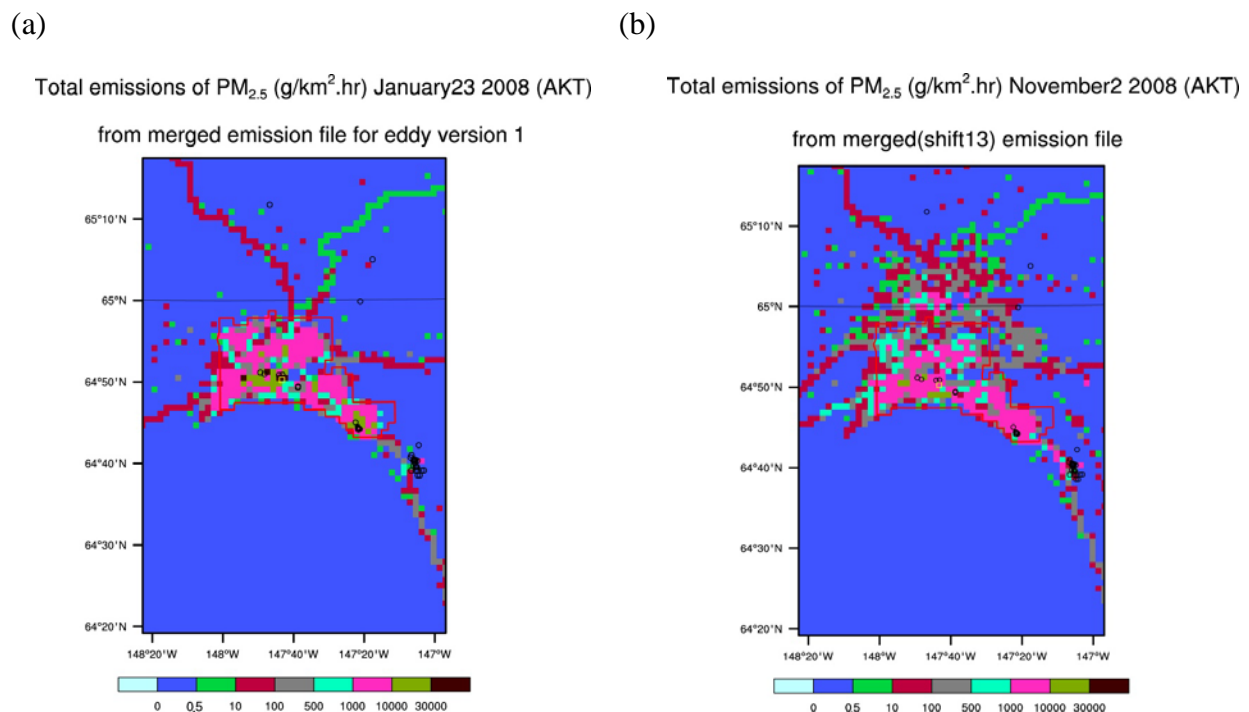


Fig. 10 Example of zoom in on the emissions as obtained from the Sierra Research Inc. emission inventory for Fairbanks for the (a) January v1 and (b) November episode. The red polygon indicates the Fairbanks nonattainment area.

In the January v1 episode, the wind-speeds in the valleys were reduced by half in order to increase the simulated $\text{PM}_{2.5}$ -concentrations at the State Building site. As discussed by Mölders and Leelasakultum (2011) this reduction violates the continuity equation and was only a test to examine whether the strong overestimation of wind-speed is a potential cause for underestimation of $\text{PM}_{2.5}$ -concentrations. Note that overestimation of near-surface wind-speeds

is a well known problem common to all meteorological models for simulations in areas with stagnant air conditions like in the Fairbanks area (see (Zhao et al., 2011), Mölders et al. 2012 for a discussion).

Our investigations showed that reducing the wind-speed by half is not required for the November episode as the emissions for November episode had been updated and increased by Sierra Research Inc. We therefore compare here the simulation results of the case study with reduction of wind-speed by half and the case study that used the original WRF-simulated wind-speeds.

The temporal evolutions of 24h-average $PM_{2.5}$ -concentrations show that the case with reduction of wind-speed by half provides higher $PM_{2.5}$ -concentrations at State Building site by on average $9.8\mu g/m^3$ than the adapted CMAQ simulation with the original wind-speed. The impacts of the wind-speed reduction on the $PM_{2.5}$ -concentrations varied with time. The highest difference in $PM_{2.5}$ -concentrations was $14.1\mu g/m^3$ on November 15, 2008 and the lowest differences in $PM_{2.5}$ -concentrations were $6-7\mu g/m^3$ during November 5 to 6 and 9 to 11 (Fig. 11). The simulated hourly $PM_{2.5}$ -concentrations in the adapted CMAQ simulation with reduction of wind-speeds showed the higher concentrations as well (Fig. 12). The reduction of wind-speed during the relatively calm wind-periods probably resulted in the little differences.

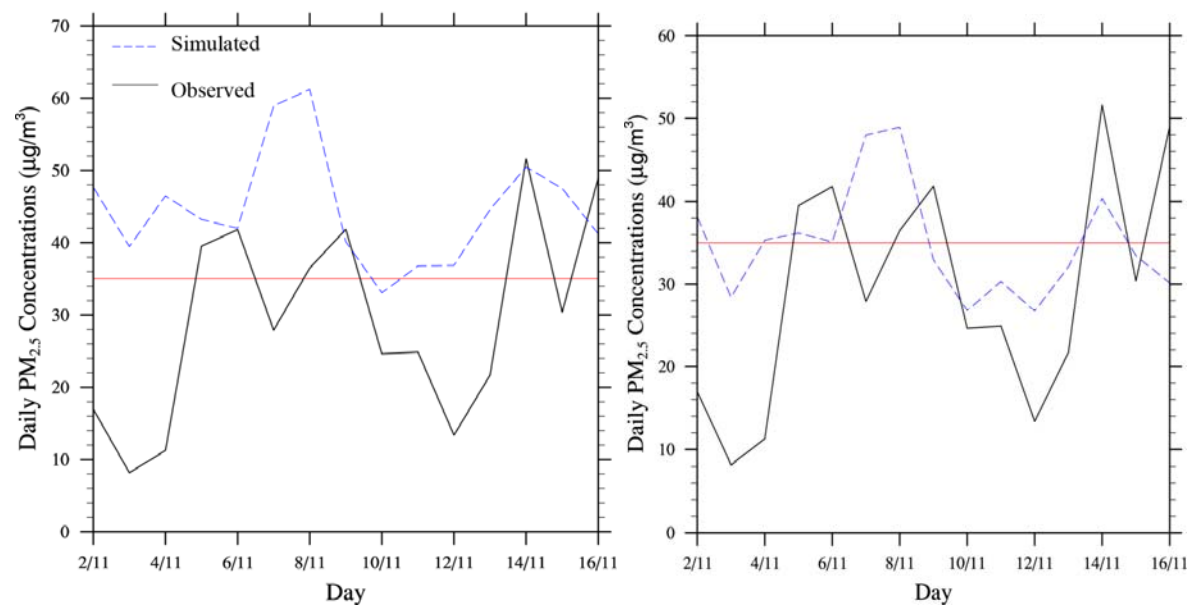


Fig. 11 Time series of simulated (blue dashed line) and observed (black solid line) 24h-average $PM_{2.5}$ -concentrations as obtained with the adapted CMAQ simulation that used reduced wind-speeds in the valleys (left) and the adapted CMAQ simulation that used the original wind-speed from WRF (right) during the November episode at the State Building site.

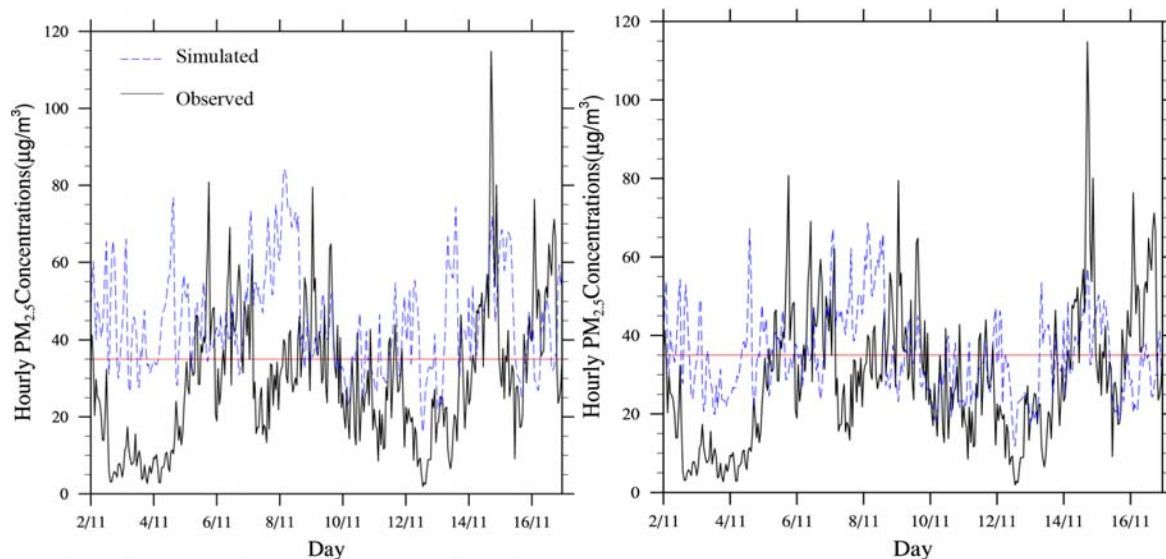


Fig. 12 Like Fig. 11, but for hourly $PM_{2.5}$ -concentrations.

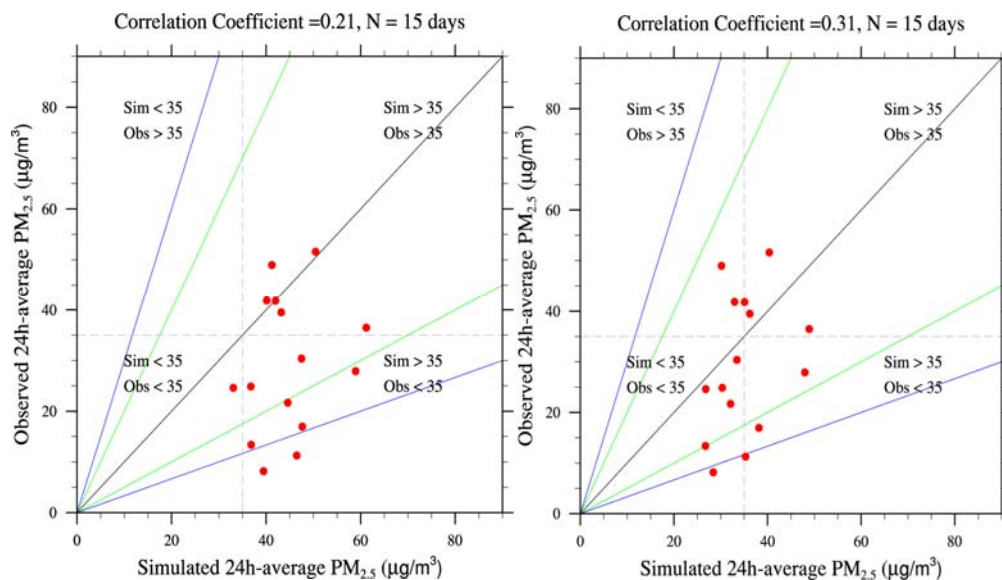


Fig.13 Scatter plots of 24h-average $PM_{2.5}$ -concentrations as obtained from the adapted CMAQ simulation with reduction of wind speed (left) and the adapted CMAQ simulation with the original WRF simulated wind-speeds (right) for the November episode. The green line indicates the factor of two and the blue line indicates the factor of three agreement.

The scatter plots of 24h-average and hourly $PM_{2.5}$ -concentrations obtained from the adapted CMAQ simulations with reduction of wind-speed and the adapted CMAQ simulation using the original WRF simulated wind-speeds have the correlation coefficients of 0.21 and 0.31, respectively (Fig. 13). The reduction of the wind-speed in the valleys resulted in six pairs of data outside the factor of two agreement. For the adapted CMAQ simulations with the original WRF-

simulated wind-speed, there were four pairs of data outside of the factor of two agreement. The scatter plot of the hourly $PM_{2.5}$ -concentrations obtained by from the adapted CMAQ simulation with the original WRF wind-speeds also shows a better correlation coefficient (0.2) for the 360 hours of data (Fig. 14).

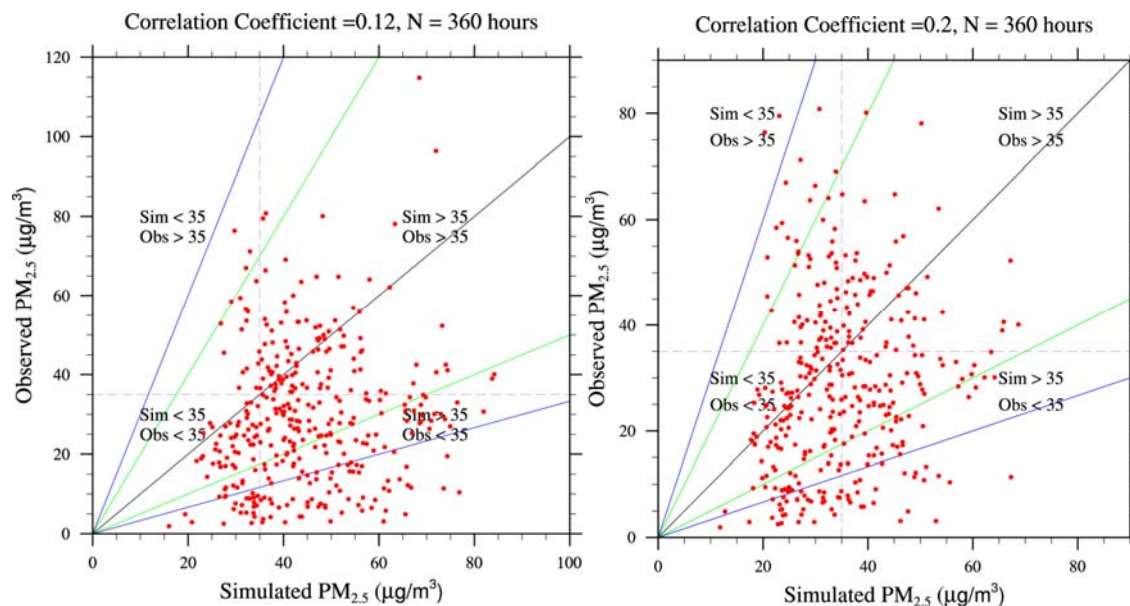


Fig.14 Scatter plots of hourly $PM_{2.5}$ -concentrations as obtained from the adapted CMAQ simulations with reduction of wind-speeds in the valleys (left) and the adapted CMAQ simulation with the original WRF simulated wind-speed (right) for the November episode. The green line indicates the factor of two and the blue line indicates the factor of three agreement.

The bugle plots and soccer plots show that the adapted CMAQ simulation with the reduction of wind-speed has seven days outside the criteria, while the adapted CMAQ simulation with the original WRF-simulated wind-speeds has five days outside the criteria (Fig. 15-17).

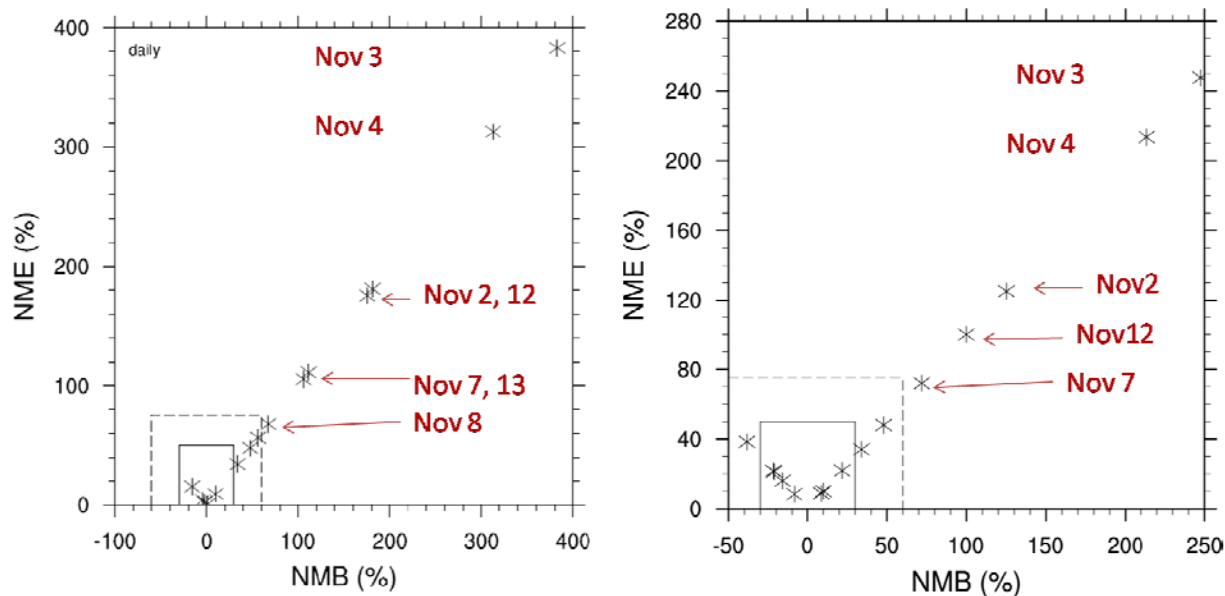


Fig. 15 Soccer plots of normalized mean errors and biases all determined with respect to the observations at the State Building site as obtained from the adapted CMAQ simulations with reduction of wind speed (left) and the adapted CMAQ simulations with the original WRF-simulated wind-speeds (right) for the November episode.

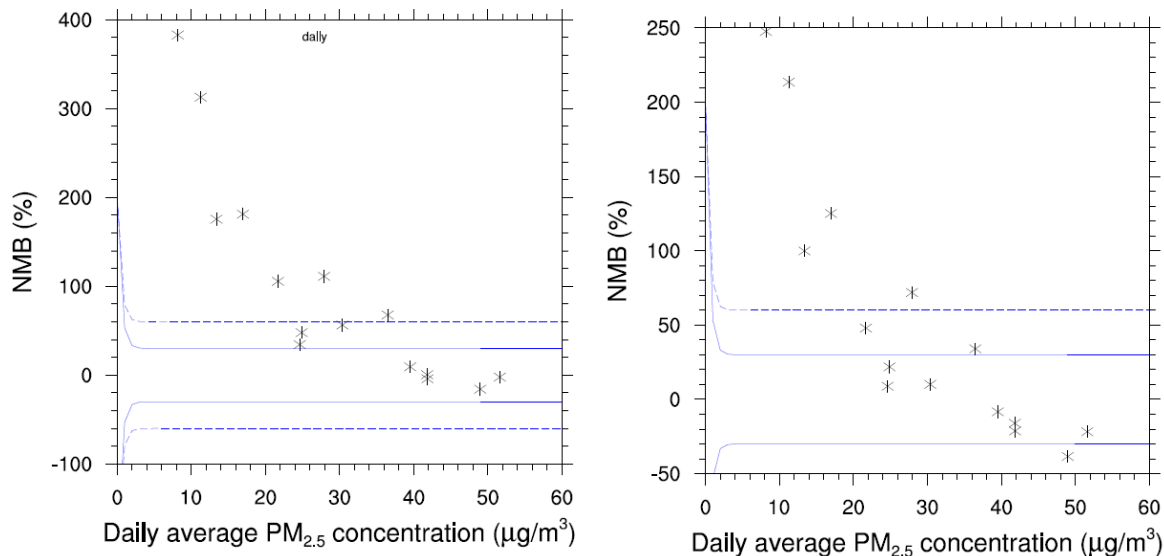


Fig. 16 Bugle plots of normalized mean biases of simulated 24h-average PM_{2.5}-concentrations at the State Building site as obtained from the adapted CMAQ simulations with reduction of wind-speed (left) and the adapted CMAQ simulation with the original WRF-simulated wind-speeds (right) for the November episode.

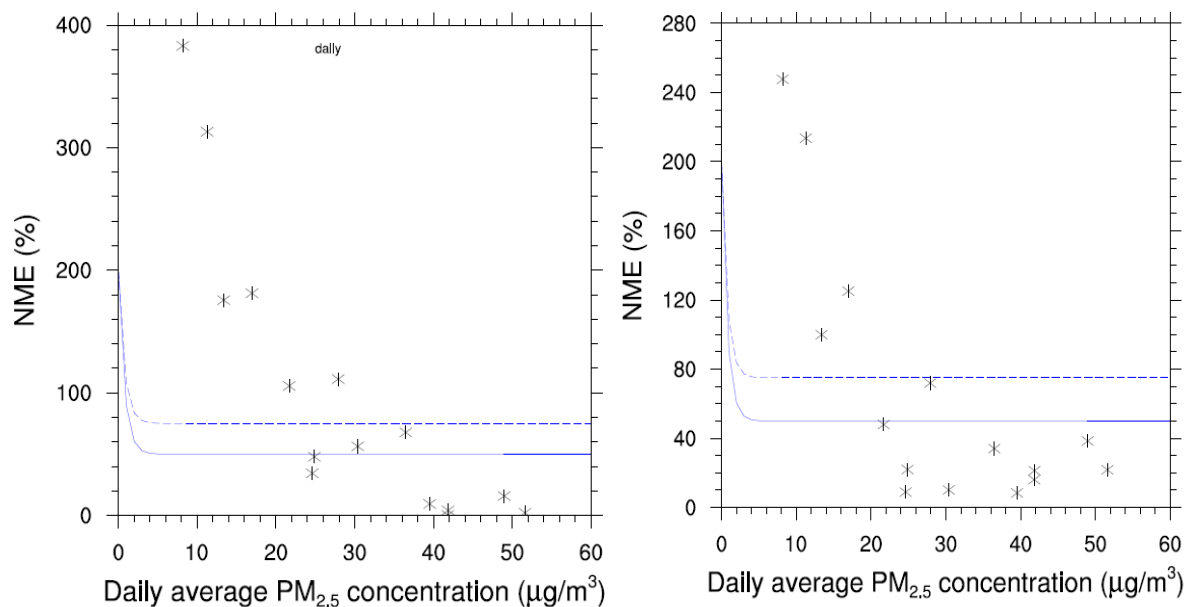


Fig. 17 Bugle plots of normalized mean errors of simulated 24h-average PM_{2.5}-concentrations at the State Building site as obtained from the adapted CMAQ simulation with reduction of wind-speed (left) and the adapted CMAQ simulation with the original WRF-simulated wind-speed (right) for the November episode.

The performance of adapted CMAQ in simulating the PM_{2.5}-composition during November was evaluated for both cases. The observed and simulated PM_{2.5}-compositions were compared in scatter plots (Fig. 18). The simulation, which used the original WRF-simulated wind-speeds, shows that sulfate and ammonium are outside of the factor of two agreement. The adapted CMAQ model predicted best for OC and EC, which have high concentrations and make up a large fraction of the total PM_{2.5}. The soccer plots for the adapted CMAQ simulation with wind-speed reduction show that sodium and chloride are outside the performance criteria. For the adapted CMAQ simulation with the original WRF-simulated wind-speeds show that sodium, chloride and sulfate are outside the performance criteria (Fig. 19). However, the increase of the Cl-concentrations for the initial/boundary conditions (IC/BC) for the adapted CMAQ simulation with the original WRF-simulated wind-speeds led to decreased NME and NMB for the Cl-species (Fig. 19) The new profile of Cl is included in the Appendix. The bugle plot of normalized mean bias for the adapted CMAQ simulations with the original WRF-simulated wind-speeds shows that sulfate is outside the criteria (Figs. 20, 21).

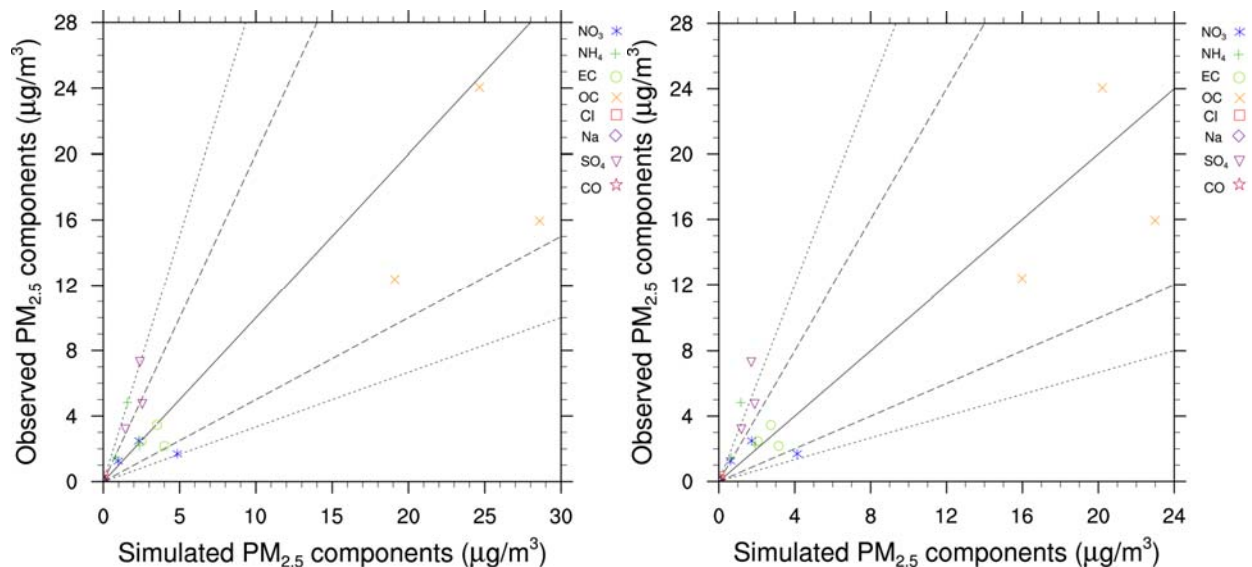


Fig.18 Scatter plot between simulated and observed 24h-average $PM_{2.5}$ -composition at the State Building site as obtained for the adapted CMAQ simulation with reduction wind-speeds in the valley (left) and the adapted CMAQ simulations using the original WRF-simulated wind-speeds (right) for the November episode.

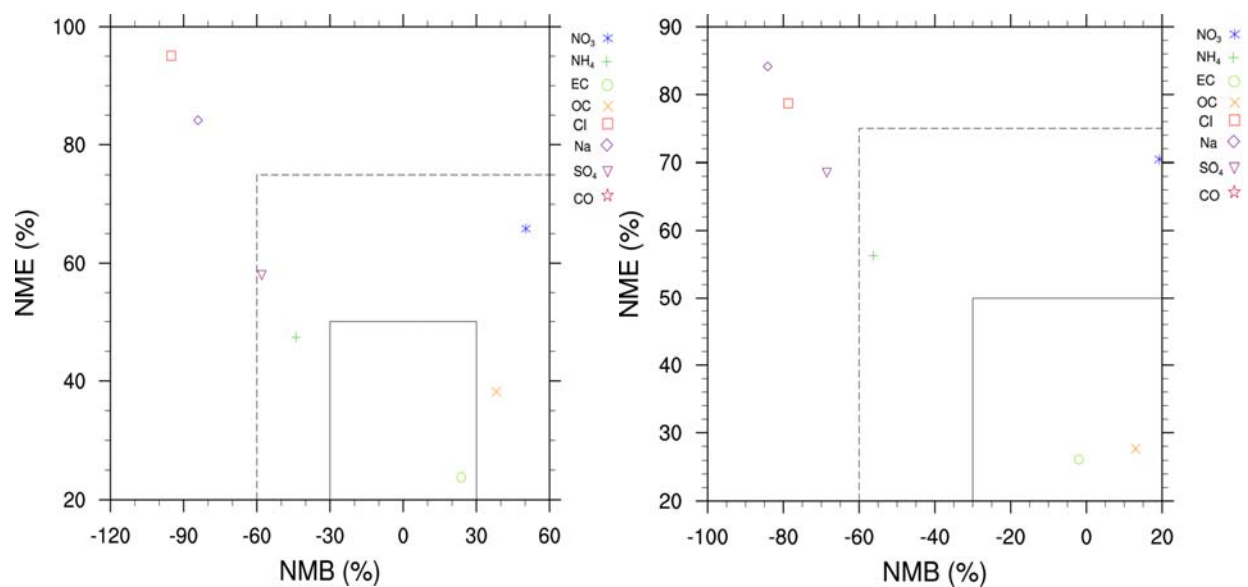


Fig. 19. Soccer plots of normalized mean errors and biases of simulated 24h-average $PM_{2.5}$ -composition simulated and observed 24h-average $PM_{2.5}$ -composition at the State Building site as obtained for the adapted CMAQ simulation with reduction wind-speeds in the valley (left) and the adapted CMAQ simulations using the original WRF-simulated wind-speeds (right) for the November episode. The dashed and solid lines indicate the performance criteria and performance goals in accord with Boylan and Russell (2006).

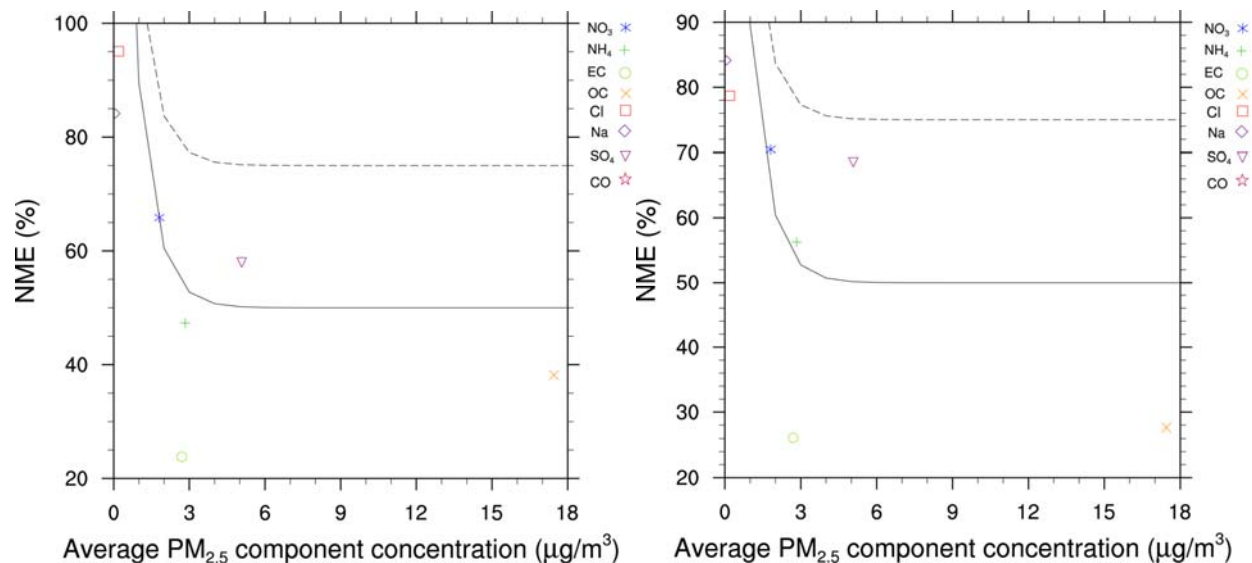


Fig. 20 Bugle plots of normalized mean errors of simulated 24h-average PM_{2.5}-composition simulated and observed 24h-average PM_{2.5}-composition at the State Building site as obtained for the adapted CMAQ simulation with reduction wind-speeds in the valley (left) and the adapted CMAQ simulations using the original WRF-simulated wind-speeds (right) for the November episode. The dashed and solid lines indicate the performance criteria and performance goals in accord with Boylan and Russell (2006).

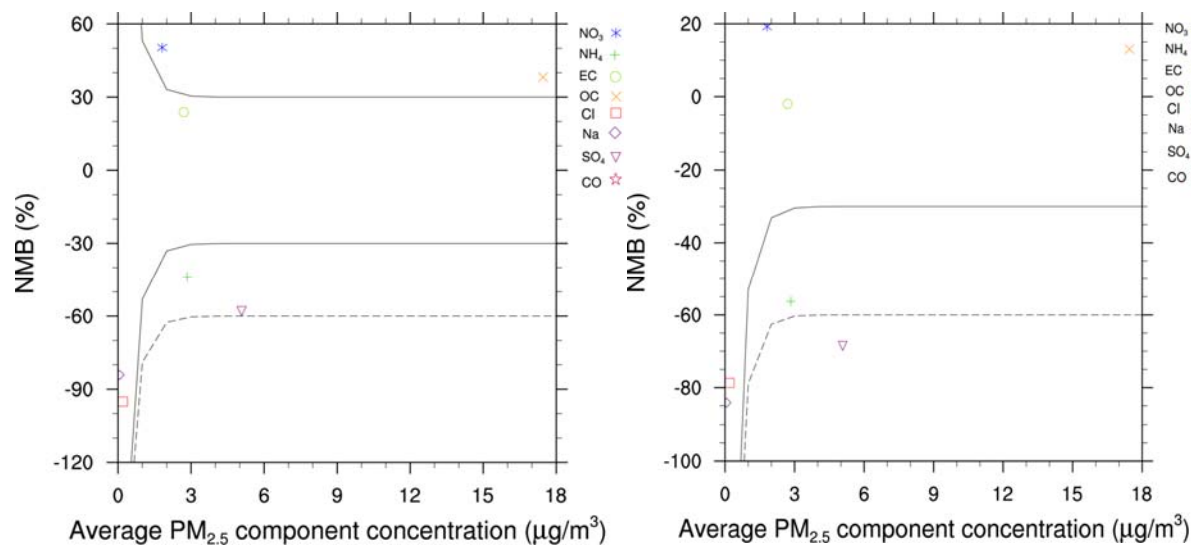


Fig. 21 Bugle plots of normalized mean biases of simulated 24h-average PM_{2.5}-composition simulated and observed 24h-average PM_{2.5}-composition at the State Building site as obtained for the adapted CMAQ simulation with reduction wind-speeds in the valley (left) and the adapted CMAQ simulations using the original WRF-simulated wind-speeds (right) for the November episode. The dashed and solid lines indicate the performance criteria and performance goals in accord with Boylan and Russell (2006).

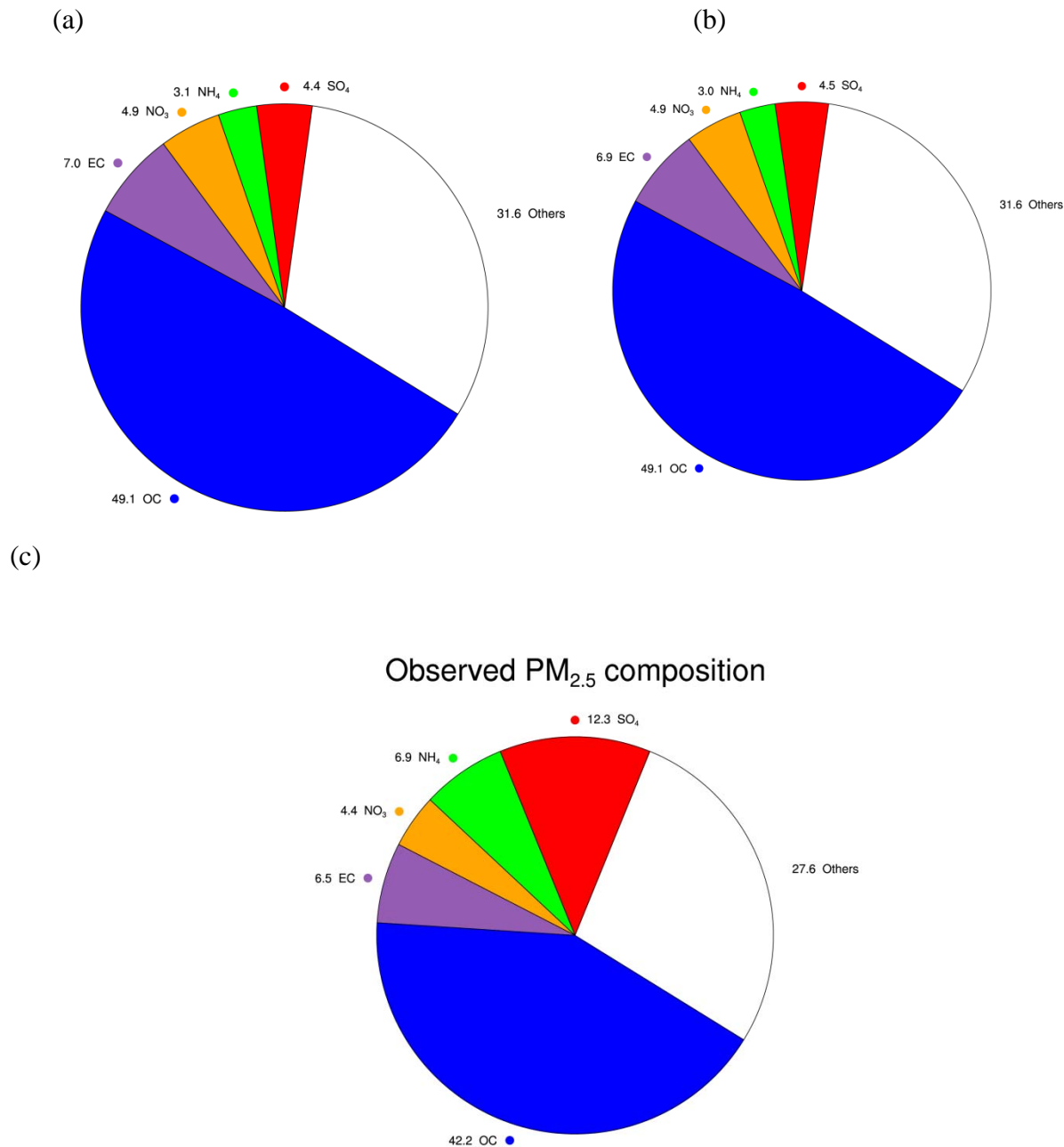


Fig. 22 The PM_{2.5}-composition at State Building site as obtained by (a) the adapted CMAQ simulation with reduction of wind-speeds in the valleys by half and (b) the adapted CMAQ simulations with modifications using the original WRF-simulated wind-speeds, and (c) observations of 24h-average PM_{2.5}-composition averaged over the 3 days with data available in the November episode. In the observations the category “others” includes Al, Br, Ca, Na, Cl, Cu, Fe, Pb, Ni, K, Se, Si, S, Sn, Ti, V, Zn. In the adapted CMAQ simulation results, the category “others” refers to unspecified anthropogenic mass (A25i+A25j).

In both case studies, in the simulated $PM_{2.5}$ -composition, the percentage of organic carbon was overestimated, but the percentage of sulfate, and ammonium was underestimated (Fig. 32). The adapted CMAQ model predicted elemental carbon and nitrate well. Note that there were only 3 days, which had the available observed $PM_{2.5}$ -composition data during the November episode.

Besides the normal case (reference simulations) with the adapted CMAQ, we performed adapted CMAQ simulations for the November episode without consideration of gas chemistry, without consideration of aerosol chemistry, and without consideration of chemistry. We compared the results of these sensitivity studies with the observed data (Fig. 23). We did not perform a sensitivity study without consideration of point-source emissions as the way Sierra Research Inc. provided the November emission data did not allow us this option. The emission file for November episode were in a merged file, not separately for area and point source emissions like the emission data provided for the January v1 episode. The interested reader is referred to Frost et al. (2006) and Tran and Mölders (2012) for a detailed discussion on point-source emission impacts.

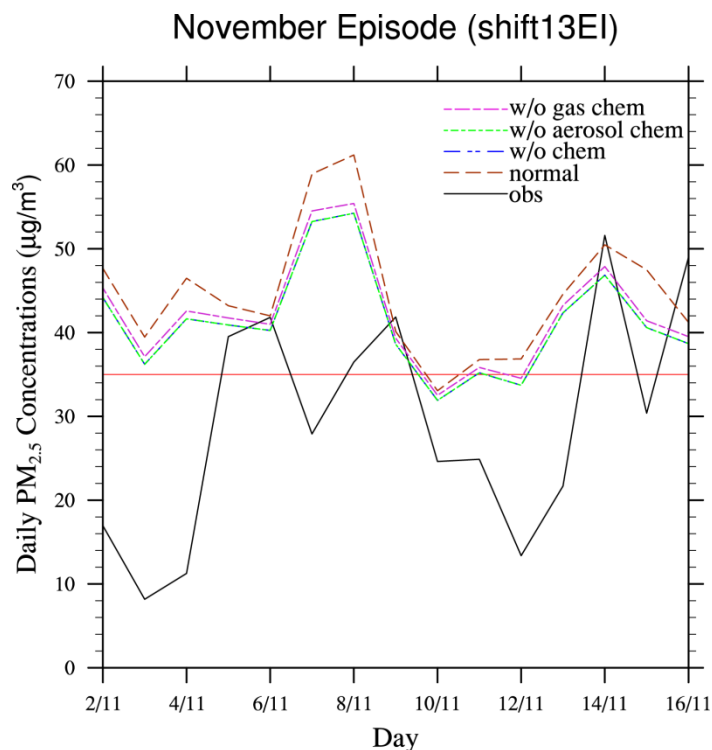


Fig. 23 Time series of observed (black solid line) and adapted CMAQ simulated 24h-average $PM_{2.5}$ -concentrations at State Building site as obtained by the various sensitivity studies without consideration of gas chemistry, without consideration of aerosol chemistry, without consideration of chemistry, and with consideration of everything (reference/normal) for the November episode. The red solid line indicates the National Ambient Air Quality Standard of $35\mu\text{g}/\text{m}^3$.

Similar to the January v1 episode, chemistry played a small role for the $PM_{2.5}$ -formation. The simulations with turned off chemistry, turned off aerosol chemistry and turned off gas chemistry led to decreases in $PM_{2.5}$ -concentrations of on average 2.2 (6%), 2.2 (6%) and $1.5\mu\text{g}/\text{m}^3$ (4%), respectively. Turning off the gas chemistry led to the same results as turning off all chemistry.

On the day, for which the highest concentrations were simulated ($48.9/\text{m}^3$ on November 8), the chemistry processes had the maximum contribution to the 24h-average $PM_{2.5}$ -concentrations $5.8\mu\text{g}/\text{m}^3$ (12%) at the State Building site. In this $5.8\mu\text{g}/\text{m}^3$, the aerosol chemistry processes contributed $4.9\mu\text{g}/\text{m}^3$ (10%) to the total aerosol production by chemistry processes.

Since the times series of simulated and observed $PM_{2.5}$ -concentrations indicated a temporal offset, we correlated the simulated 24h-average $PM_{2.5}$ -concentrations at State Building site with the observed data by allowing various time lags. We found that allowing a time lag of one day for the simulation results obtained with reduced wind-speed can increase the correlation coefficient from 0.21 to 0.46. For the reference simulation that uses the original WRF-simulated wind-speeds, allowing a time lag of one day increased the correlation coefficient from 0.31 to 0.37 (Fig. 24). This increasing of the correlation indicates that the adapted CMAQ model has a 24h delay in capturing the $PM_{2.5}$ -concentrations at the State Building site for November episode.

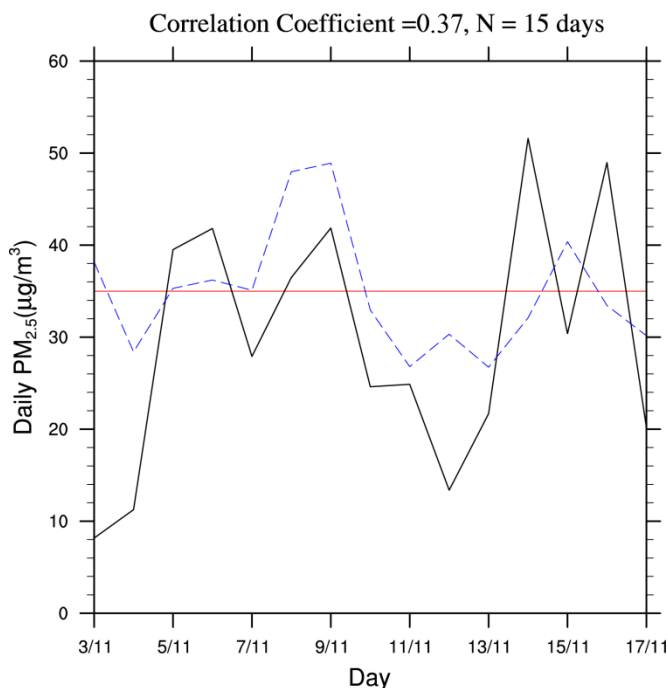


Fig. 24 Time series of simulated (blue dash line) and observed (black solid line) 24h-average $PM_{2.5}$ -concentrations that allow a one day time lag for the adapted CMAQ simulation using the original WRF-simulated wind-speed for the November episode at the State Building site.

The reduction of the wind-speed by half might demolish the continuity equation (see discussion in Mölders and Leelasakultum 2011), but it led to a clear increase of PM_{2.5}-concentrations and better performance in simulating the sulfate compositions at the State Building site (Figs. 19-21). Although, the comparison with the observed data had lower correlation coefficients than 0.5 for both cases, allowing a time lag of one day increased the correlation coefficients in both cases.

2.3 Comparison of simulations and their performance for January v2 with and without CMAQ modifications

Like January v1, January v2 covers January 23 to February 9, 2008. The emissions used for the January episode v2 were developed by Sierra Research Inc. who updated the emission inventory for emissions from mobile sources, and included the emissions from airports like in the November episode (see their reports for details and the reasoning). The comparison of the spatial distribution of emissions as used for January v1 and January v2 shows that there is the increase in emissions from the mobile sectors for the January v2, mostly outside of the nonattainment area (Fig. 25). There are both increases and decreases in emissions inside the nonattainment area for the new version of emission inventory; the increase of the emissions is mostly south of the nonattainment area (Fig. 26).

Furthermore, January v1 and January v2 also differ by the meteorological data used (Fig. 27). January v2 uses WRF simulations provided by PennState that they created with an updated data assimilation procedure (see their final report for details). On the days, for which CMAQ overestimated the 24h-average PM_{2.5}-concentrations at the State Building site, the meteorological data in January v2 tend to have lower of relative humidity in the Fairbanks nonattainment area (64°40'N- 65°N, 147°W-148°W), and the area with low temperatures covers a larger area of the domain. These changes in the meteorology in the January v2 simulations results in an increase of PM_{2.5}-concentrations as it supports the gas-to-particle conversion process. For a discussion on the impact of errors in simulated meteorological quantities on simulated PM_{2.5}-concentrations see reader is referred to Mölders et al. (2011, 2012).

With the improvements in the emission inventory and the WRF meteorological data for January v2, the adapted CMAQ 24h-average PM_{2.5}-concentrations at the State Building site increased noticeably without the need for a wind-speed reduction (cf. Figs. 9, 28). The temporal evolution of PM_{2.5}-concentrations for January v2 with CMAQ modifications shows similar trends with that obtained without modifications. Note that CMAQ without modification would not consider deposition on snow or tundra-type land as well as would have unrealistic (for Alaska) pH-value thresholds, IC/BC and other important parameters. January v2 with modifications shows that most of the times both the 24h-average and hourly PM_{2.5}-concentrations at the State Building site are overestimated (Figs. 27, 28). Note that for SIP development this behavior is preferred over underestimation.

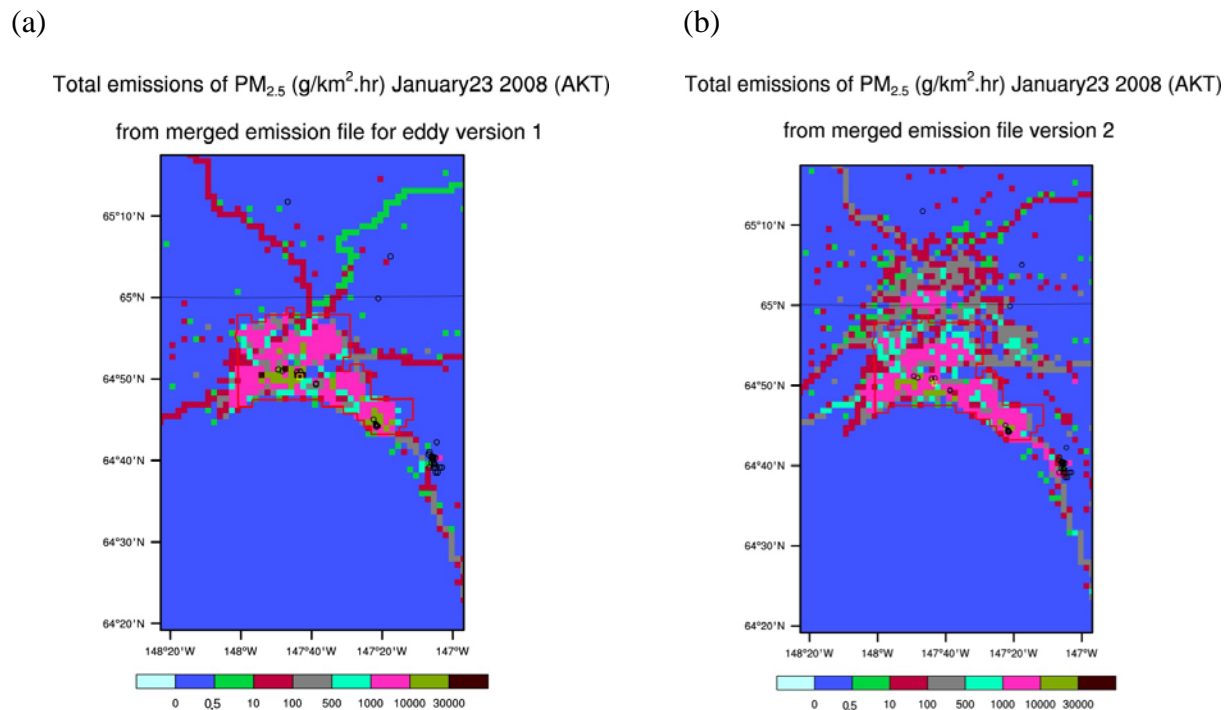


Fig. 25 Example of the emissions as obtained from the Sierra Research Inc. emission inventory for (a) January v1 and (b) January v2. The red polygon indicates the Fairbanks nonattainment area. The circles indicate point-source locations.

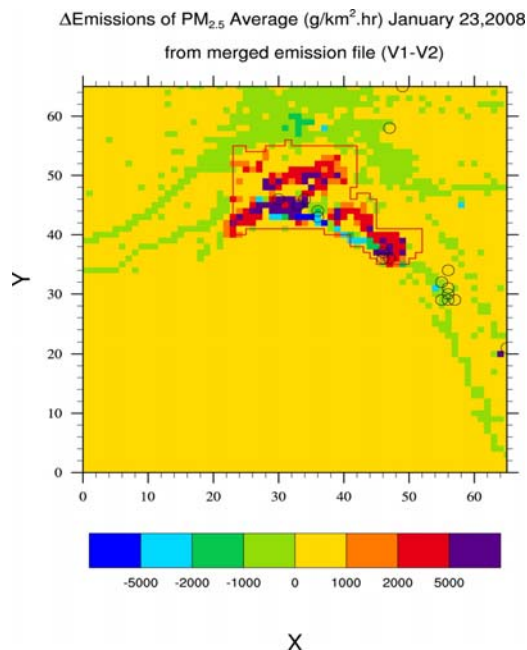


Fig. 26 Like Fig. 25, but for PM_{2.5}-emissions difference (January v1 minus January v2) at breathing level on January 23, 2008 as obtained from Sierra Research Inc. emission inventory.

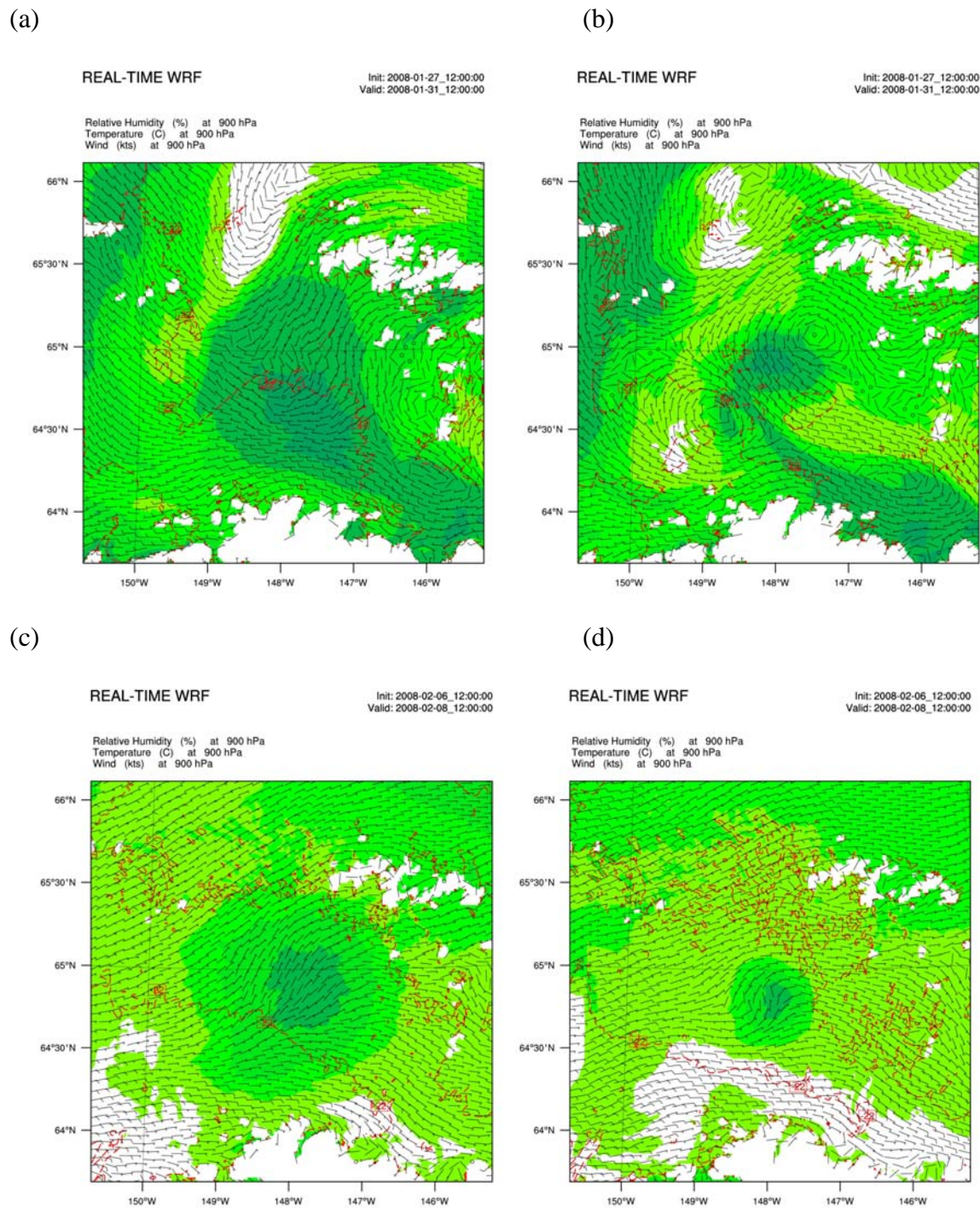


Fig. 27 Example of temperature (red contours), relative humidity (color), wind-speed and direction (barbs) at 900 hPa on January 31, 2008 1200UTC for (a) January v1 and (b) January v2, and on February 8, 2008 1200UTC for (c) January v1 and (d) January v2 as obtained from the PennState group.

The modifications of CMAQ resulted in a correlation coefficient of 0.52 for the 24h-average PM_{2.5}-concentrations, which is better than the correlation obtained for the simulation with the

CMAQ without modifications (Fig. 30). For the 12 pairs of data of the results from CMAQ with and without modifications, 83% of values lie within the factor of the two agreement (Fig. 30). However, the two points outside the factor of the two agreement for the CMAQ simulations without modifications are a “missed event” (Simulated $<35\mu\text{g}/\text{m}^3$ and Observed $>35\mu\text{g}/\text{m}^3$), and one value (simulated $<35\mu\text{g}/\text{m}^3$ and observed $>35\mu\text{g}/\text{m}^3$). Whereas, those two points in the CMAQ simulation with modifications are “false alarms” (simulated $>35\mu\text{g}/\text{m}^3$ and observed $<35\mu\text{g}/\text{m}^3$) (Fig. 30). The simulated hourly $\text{PM}_{2.5}$ -concentrations of the CMAQ with modifications also yield a higher correlation coefficient with the observed data than those obtained without CMAQ modifications (Fig. 31).

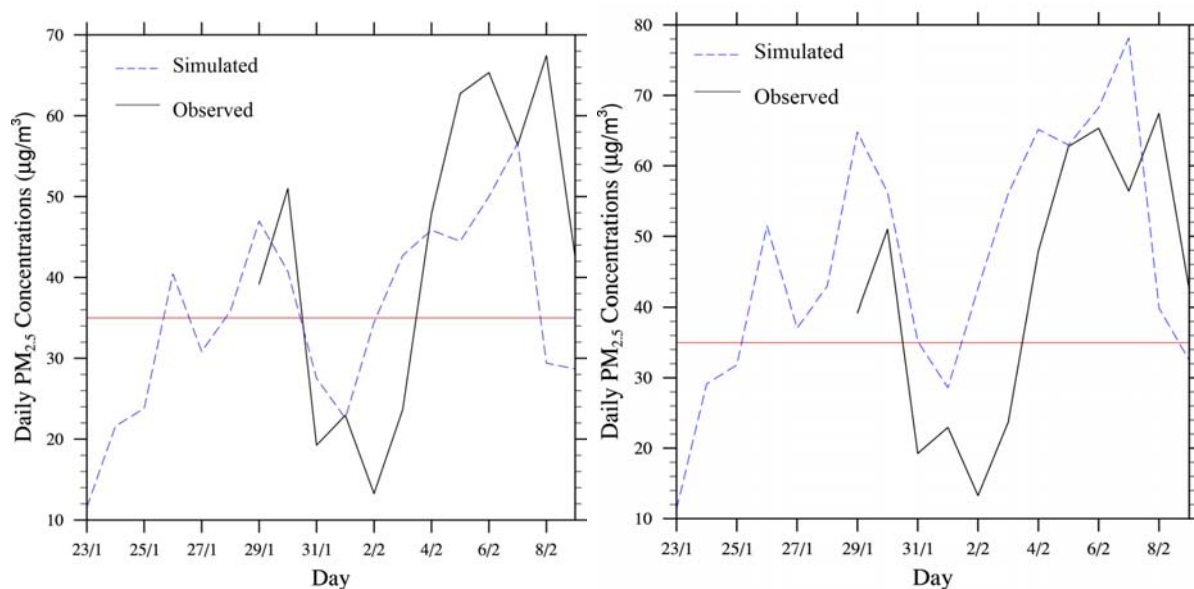


Fig. 28 Time series of simulated (blue dash line) and observed 24h-average $\text{PM}_{2.5}$ -concentrations at the State Building site (black solid line) as obtained for January v2 without modifications (left) and January v2 with modifications (right).

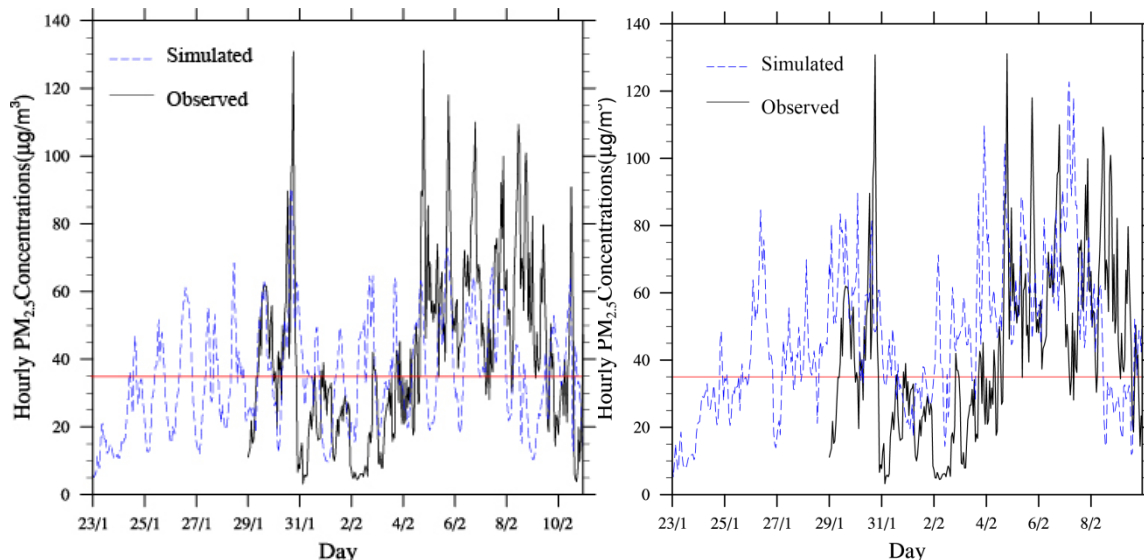


Fig. 29 Time series of simulated (blue dash line) and observed hourly PM_{2.5}-concentrations at the State Building site (black solid line) as obtained for January v2 without modifications (left) and January v2 with modifications (right).

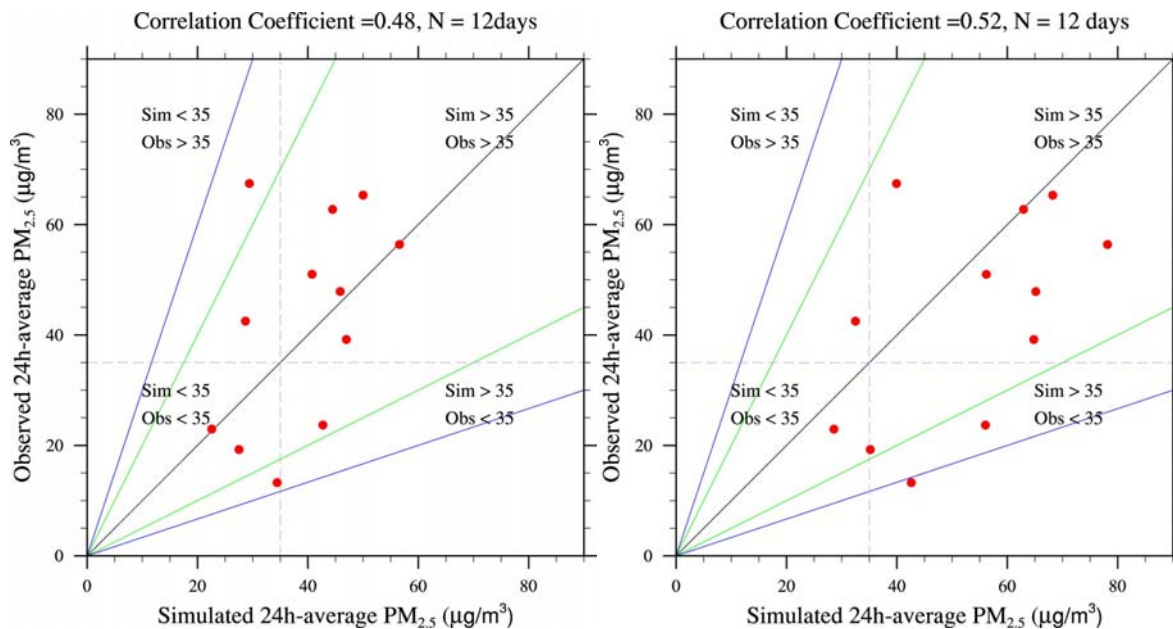


Fig. 30 Scatter plots of 24h-average PM_{2.5}-concentrations as obtained for January v2 without modifications (left) and January v2 with modifications (right). The green line indicates the factor of two agreement, and the blue line indicates the factor of three agreement.

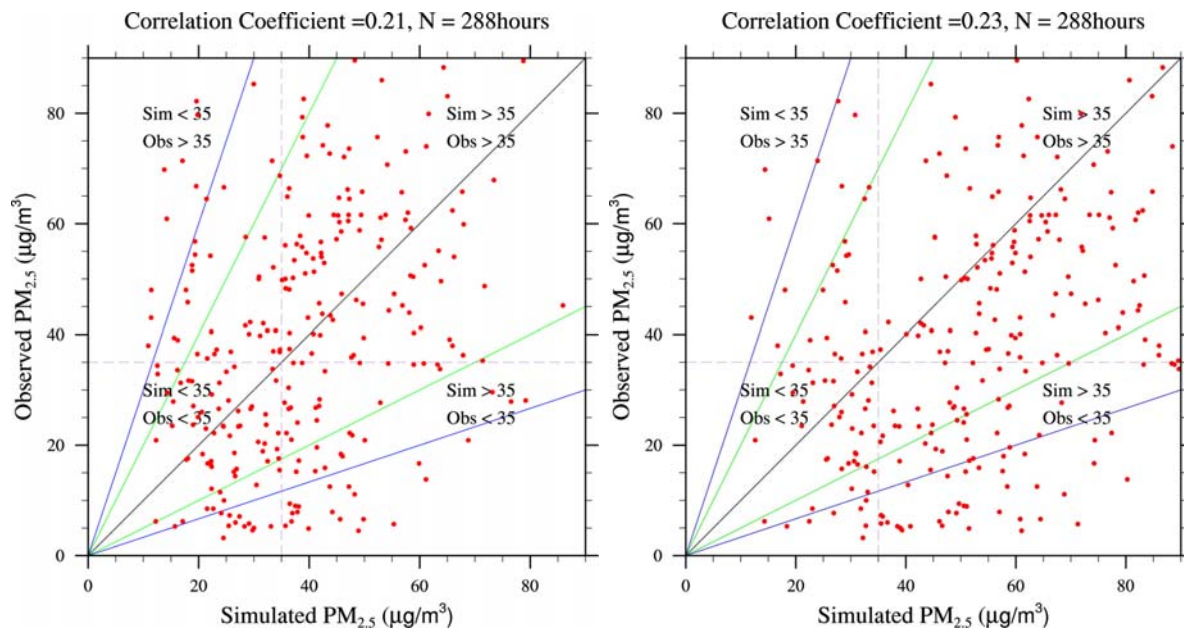


Fig. 31 Scatter plots of hourly average $PM_{2.5}$ -concentrations as obtained by January v2 without modifications (left) and January v2 with modifications (right). The green line indicates the factor of two agreement, and the blue line indicates the factor of three agreement.

Furthermore, we run the CMAQ with modifications, but without the reduction of the lowest and the highest eddy diffusivity. The hypothesis of this test is that reductions of default eddy diffusivities by half caused the over-prediction and false alarms.

The temporal evolution of simulation with all modifications except the eddy diffusivity reduction shows similar result as the case of without these modifications (Figs. 28, 29, 31). The correlation coefficient between the simulated and observed 24h-average $PM_{2.5}$ -concentrations obtained by the CMAQ with modifications, but without the reduction of the eddy diffusivity is 0.46. There are two values outside the factor of two agreement, which is similar to the CMAQ simulation of without these modifications (Fig. 31).

This means that the reduction of the default eddy diffusivities by half is the modification that led to the increase of $PM_{2.5}$ -concentrations at the State Building site. It caused the over-prediction, and false alarms, however, setting the eddy diffusivities to the default does not lead to the improvement of the correlation between simulated and observed data. The CMAQ with the modifications and the reduction of the eddy diffusivities by half shows the best correlation coefficient (0.52). Thus, we recommend this setup.

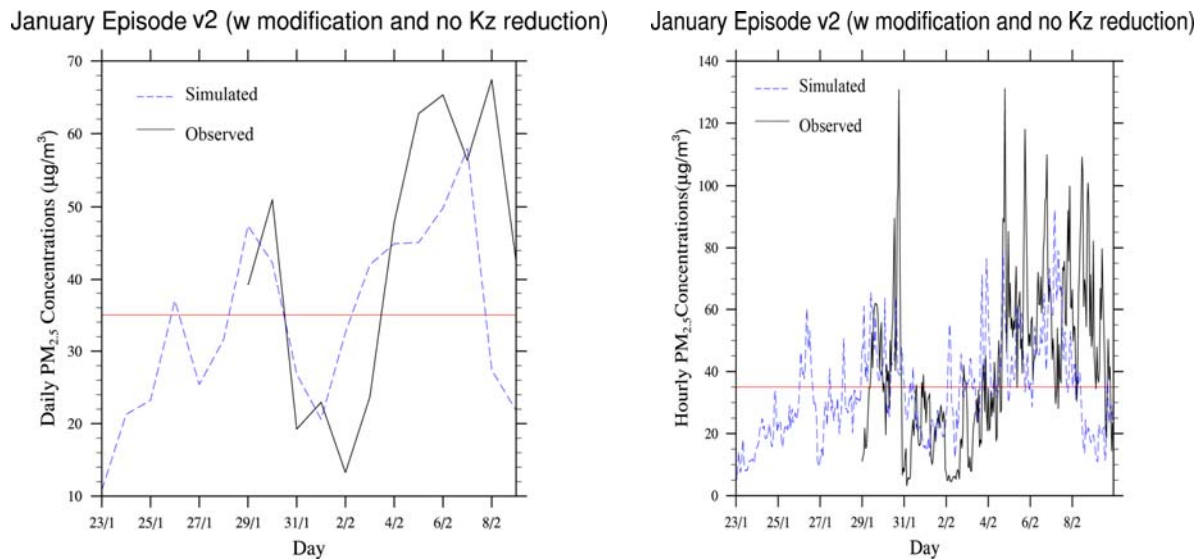


Fig. 32 Time series of simulated (blue dash line) and observed 24h-average $PM_{2.5}$ -concentrations (left) and with modifications for hourly $PM_{2.5}$ -concentrations (right) at the State Building site (black solid line) as obtained for January v2 with all modifications except the eddy diffusivity reduction.

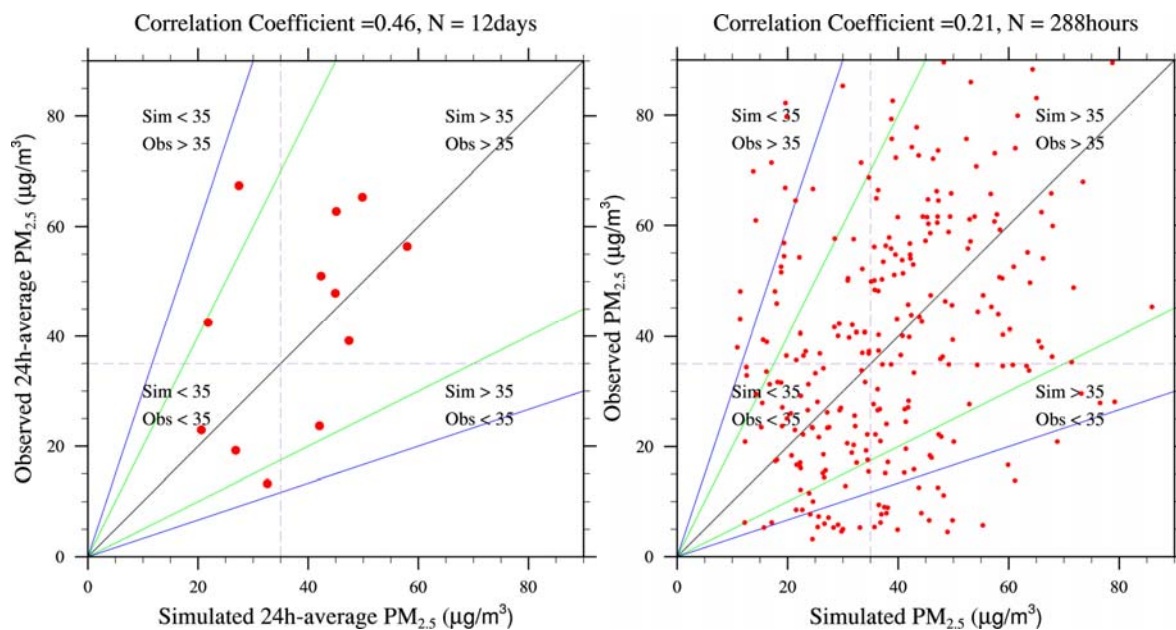


Fig. 33 Scatter plots of 24-h average $PM_{2.5}$ -concentrations (left) and hourly average $PM_{2.5}$ -concentrations (right) as obtained by January v2 with modifications, but without reduction of the eddy diffusivity. The green line indicates the factor of two agreement and the blue line indicates the factor of three agreement.

We also performed simulations for January v2 without consideration of gas chemistry, without consideration of aerosol chemistry, and without consideration of chemistry. We compared the

results of these simulations to each other, the results of the simulation that considers all processes and with the observations (Fig. 34). Similar to the January v1 episode, chemistry played a small role for the $PM_{2.5}$ -formation. The simulations with turned off chemistry, turned off aerosol chemistry and turned off gas chemistry led to decreases in $PM_{2.5}$ -concentrations of on average 2.0 (4%), 2.0 (4%) and $1.2\mu\text{g}/\text{m}^3$ (3%), respectively. Note that in the CMAQ model turning off the gas chemistry resulted in the same result with turning off all chemistry.

On the day, for which the highest concentration was simulated ($78.2/\text{m}^3$ on February 7), the chemistry processes had the maximum contribution to the 24h-average $PM_{2.5}$ -concentrations $5.6\mu\text{g}/\text{m}^3$ (7%) at the State Building. In this $5.6\mu\text{g}/\text{m}^3$, the aerosol chemistry process contributed $4.4\mu\text{g}/\text{m}^3$ (6%) to the total aerosol production of chemistry process.

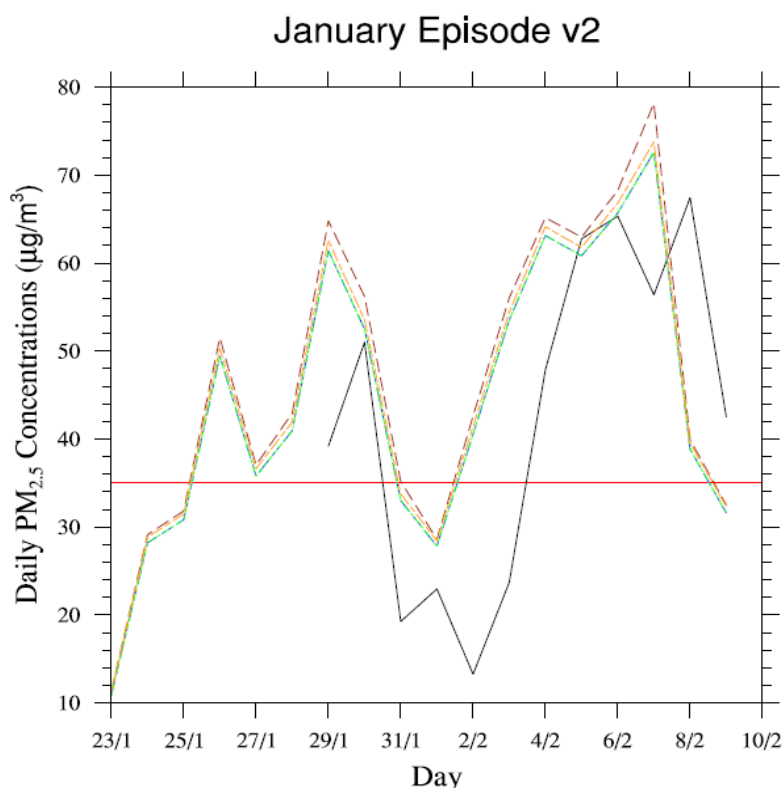


Fig. 34 Time series of CMAQ simulated and observed 24h-average $PM_{2.5}$ -concentrations at State Building for the January episode v2 (black solid line). The sensitivity studies include simulations without consideration of gas chemistry, without consideration of aerosol chemistry, without consideration of chemistry and the simulation with consideration of everything (reference/normal). The red solid line indicates the National Ambient Air Quality Standard of $35\mu\text{g}/\text{m}^3$.

Comparing between the observed and the simulated composition of 24h -average $PM_{2.5}$ aerosol, showed that simulated $PM_{2.5}$ composition with the modifications and without the modifications

reveals that the adapted CMAQ overestimated the percentage of organic carbon, but underestimated the percentage of sulfate, ammonium, nitrate and elemental carbon (Fig. 35). Note that there were only 6 days, which had the observed PM_{2.5}-composition data during the study period.

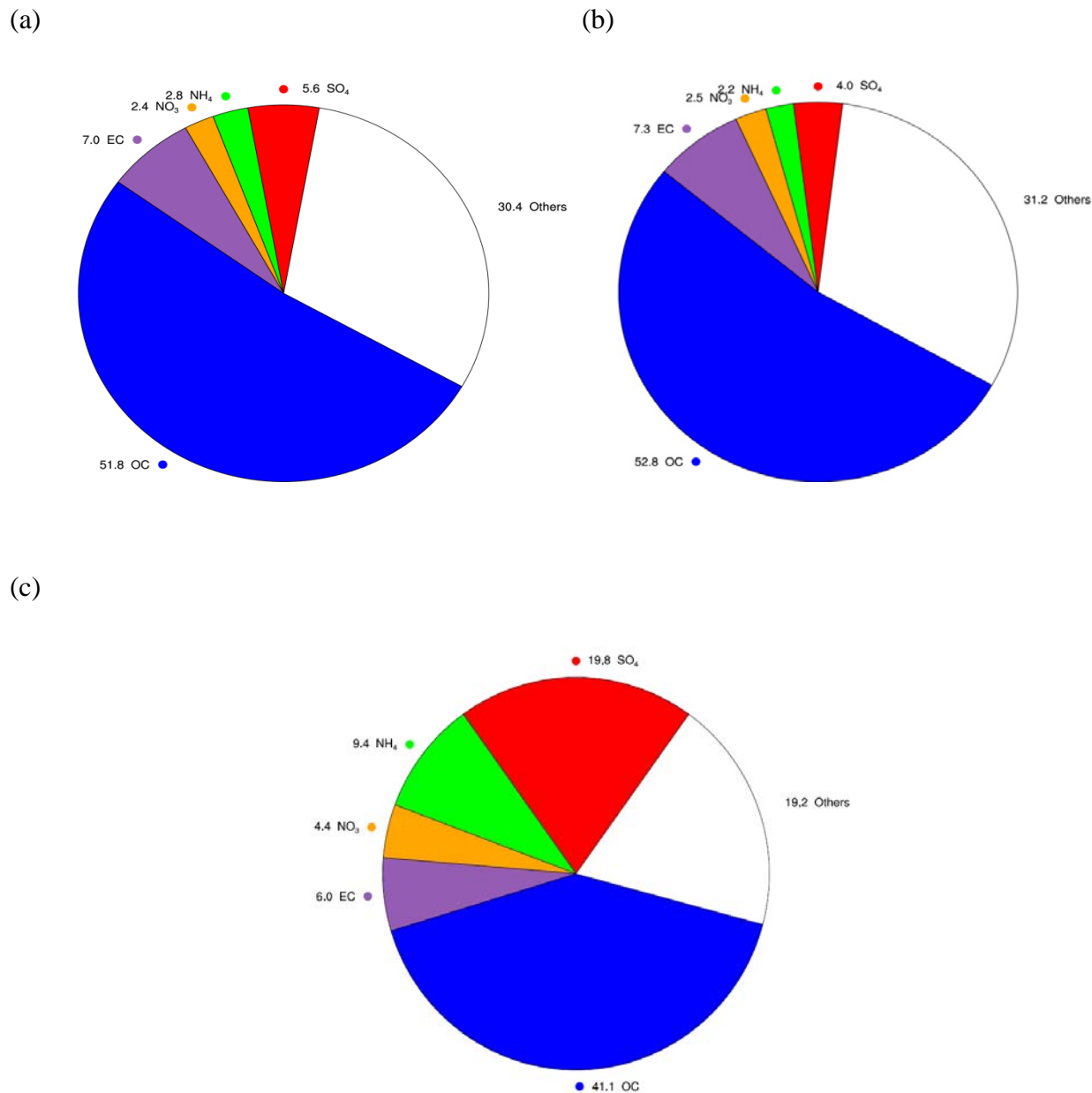


Fig. 35 Composition of simulated 24h-average total PM_{2.5} as obtained by (a) CMAQ without modifications, (b) CMAQ with modifications, and (c) as observed on average over the 6 days for which data was available at the State Building site. In the observations, the category “others” includes Al, Br, Ca, Na, Cl, Cu, Fe, Pb, Ni, K, Se, Si, S, Sn, Ti, V, Zn. In the simulations, the category “others” refers to unspecified anthropogenic mass (A25i+A25j).

For the January v2 episode, we also correlated the simulated 24h-average $PM_{2.5}$ -concentrations obtained by the Alaska adapted CMAQ model with the observed data by allowing a time lag. We found that allowing a time lag for one day increases the correlation coefficient from 0.52 to 0.84 (Fig. 36). Allowing a 24h time lag can increase the correlation coefficients of the hourly average $PM_{2.5}$ -concentrations at State Building site from 0.23 to 0.50, and the correlation increases even more to 0.59 when we allow a time lag for 26 hours. These findings clearly indicate that the discrepancies between simulated and observed $PM_{2.5}$ -concentrations are partly due to errors in simulated meteorology.

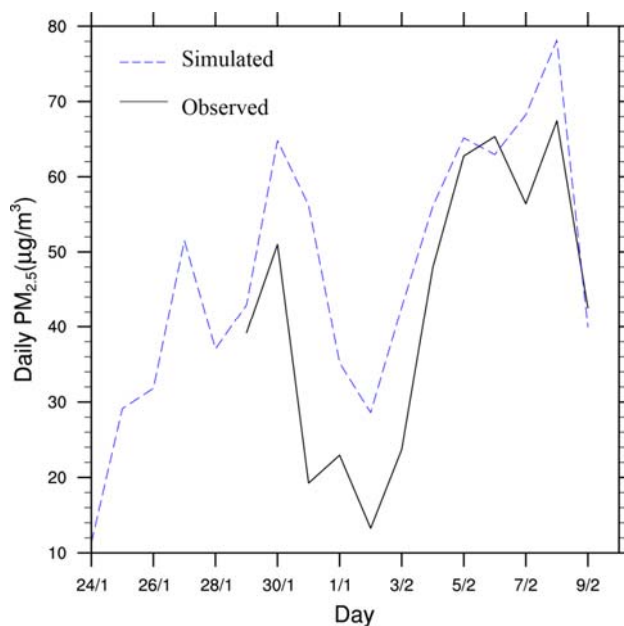


Fig. 36 Time series of simulated (blue dash line) and observed (black solid line) 24h-average $PM_{2.5}$ -concentrations with a one day time lag for the January v2 episode at the State Building site.

2.4 Statistical performance for the November episode and January episode v2 with CMAQ modification

The statistical performance of the Alaska adapted CMAQ (Mölders and Leelasakultum 2011) for the November episode and January episode v2 was determined and is shown in Tables 1 and 2, respectively.

Table 1. Performance statistics for the Alaska adapted CMAQ at the State Building site for November episode. StDev is the standard deviation.

Fairbanks official monitoring Site	# of observations	Mean CMAQ simulated ($\mu\text{g}/\text{m}^3$)	Mean observed ($\mu\text{g}/\text{m}^3$)	Ratio of Means (sim/obs)	Mean bias ($\mu\text{g}/\text{m}^3$)	Mean Fractional Bias (%)	Mean error ($\mu\text{g}/\text{m}^3$)	Mean Fractional Error (%)	Correlation coefficient
Hourly	360	34.9	29.3	1.92	5.56	30	15.51	53	0.21
24h-average	15	34.9	29.3	1.52	5.56	26	12.09	43	0.31
Fairbanks Official monitoring site	Average difference sim-obs ($\mu\text{g}/\text{m}^3$)	Simulated exceedance days	Observed exceedance days	Simulated min max ($\mu\text{g}/\text{m}^3$)	Observed min max ($\mu\text{g}/\text{m}^3$)	STDEV of simulation ($\mu\text{g}/\text{m}^3$)	STDEV of observation ($\mu\text{g}/\text{m}^3$)	Variance of simulation ($\mu\text{g}/\text{m}^3$) ²	Variance of observation ($\mu\text{g}/\text{m}^3$) ²
24h-average	5.6	7	6	26.7 48.9	8.17 51.6	6.8	13.7	45.8	188.3

Table 2. Performance statistics for the Alaska adapted CMAQ at the State Building for the January v2 episode. Note that the statistics for the January v1 episode can be found in Mölders and Leelasakultum (2011).

Fairbanks Official monitoring site	#of Observations	Mean CMAQ simulated ($\mu\text{g}/\text{m}^3$)	Mean observed ($\mu\text{g}/\text{m}^3$)	Ratio of means (sim/obs)	Mean bias ($\mu\text{g}/\text{m}^3$)	Mean Fractional Bias (%)	Mean error ($\mu\text{g}/\text{m}^3$)	Mean Fractional Error (%)	Correlation coefficient
Hourly	288	46.3	42.6	1.34	6.59	20.23	16.33	38.39	0.23
24h-average	12	46.3	42.6	0.98	6.59	17.51	10.76	26.18	0.52
Fairbanks official monitoring site	Average difference sim-obs ($\mu\text{g}/\text{m}^3$)	Simulated Exceedance days	Observed Exceedance days	Simulated min max ($\mu\text{g}/\text{m}^3$)	Observed min max ($\mu\text{g}/\text{m}^3$)	STDEV of simulation ($\mu\text{g}/\text{m}^3$)	STDEV of observation ($\mu\text{g}/\text{m}^3$)	Variance of simulation ($\mu\text{g}/\text{m}^3$) ²	Variance of observation ($\mu\text{g}/\text{m}^3$) ²
24h-average	9.9	10	8	28.6 78.2	13.3 67.4	16.18	19.05	261.88	362.82

The Alaska adapted CMAQ model shows a better performance for the January episode v2 than the November episode. The mean simulated of 24h-average $\text{PM}_{2.5}$ -concentration for the November episode is $34.9\mu\text{g}/\text{m}^3$ and the mean observed 24h-average $\text{PM}_{2.5}$ -concentration was $29.3\mu\text{g}/\text{m}^3$. The higher means of simulated 24h-average $\text{PM}_{2.5}$ -concentrations were for the January episode v2, which has lower temperatures and lower insolation. Although the average difference between the simulated and observed $\text{PM}_{2.5}$ -concentrations in January v2 is as high as $9.9\mu\text{g}/\text{m}^3$, the correlation coefficient, mean fractional bias, and mean fractional error indicate a better performance of the adapted CMAQ for the January v2 than November episode.

The performance metrics of Boyland and Rusell (2006) overlain in the soccer plot and bugle plots of the CMAQ performance for January v2 shows that four days are outside of the criteria (Fig. 37). Those four days are January 29, 31, and February 2, 3, which had 24h-average $\text{PM}_{2.5}$ -

concentrations of 39.2, 19.2, 13.3, and 23.7 $\mu\text{g}/\text{m}^3$, respectively. This means the adapted CMAQ captured well the air quality on those days that had high $\text{PM}_{2.5}$ -concentrations, but not on those days with low concentrations. Similar was found for WRF/Chem (Mölders et al. 2012).

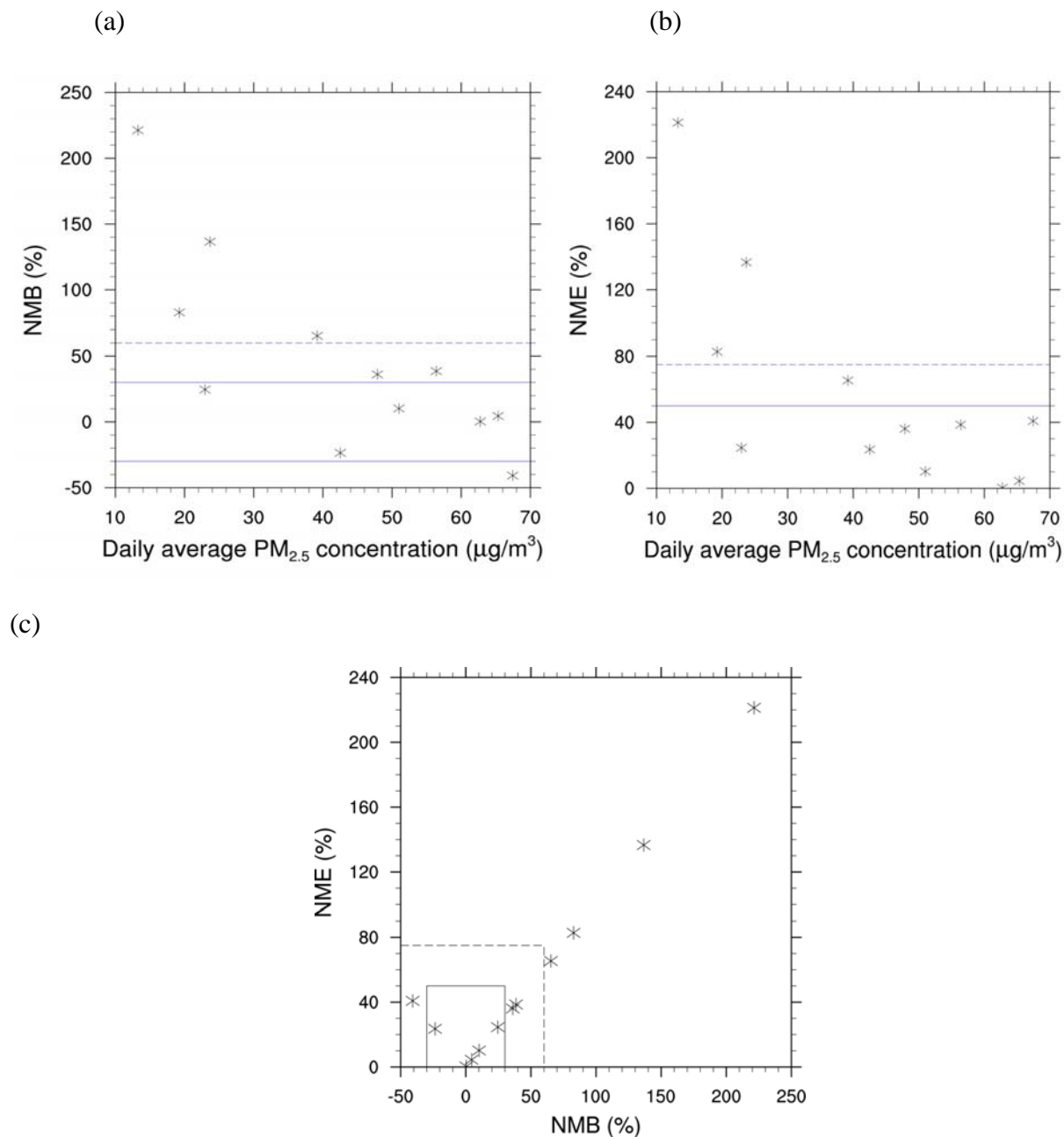


Fig. 37. Bugle plots of normalized mean (a) errors and (b) biases of simulated 24h-average $\text{PM}_{2.5}$ -concentrations, and (c) soccer plot of normalized mean errors and biases all determined with respect to the observations at the State Building site for January v2 as obtained with the CMAQ with modifications. The dashed and solid lines indicate the performance criteria and performance goals in accord with Boylan and Russell (2006).

The RAMS data of the $PM_{2.5}$ -concentrations were also included in the evaluation of the adapted CMAQ for January v2. The temporal evolutions of the RAMS-observed $PM_{2.5}$ -concentrations were compared with the simulated $PM_{2.5}$ -concentrations (Fig. 38). The RAMS data suggested some temporal offsets at times of local extremes, for instance, the adapted CMAQ model shows a drop on January 27, where the observed 24h-average $PM_{2.5}$ -concentrations peaks (Fig. 38).

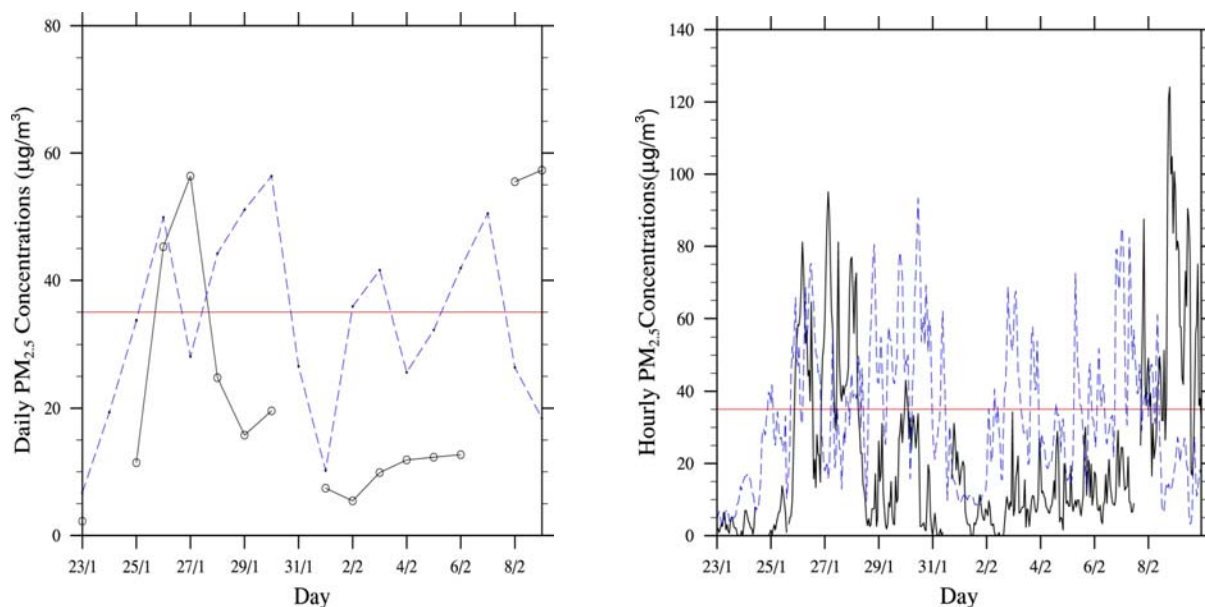


Fig. 38 Time series of simulated with the CMAQ with all modifications (blue dash line) and observed (black solid line) 24h-average $PM_{2.5}$ -concentrations (left) and hourly $PM_{2.5}$ -concentrations (right) at the State Building site as obtained for January v2.

The performance of CMAQ in simulating the $PM_{2.5}$ -compositions for January v2 was evaluated. The scatter plot of simulated and observed $PM_{2.5}$ -composition shows that one value for sulfate and one value for ammonium are not in the factor of three agreement (Fig. 39). The soccer plot and bugle plots indicate that the increased Cl-concentrations for the IC/BC led to the better performance for chloride. However, sulfate and ammonium are still outside of the criteria similar as it was found for the November episode (Fig. 40). Additionally, there was one value of OC and EC each that was outside the criteria.

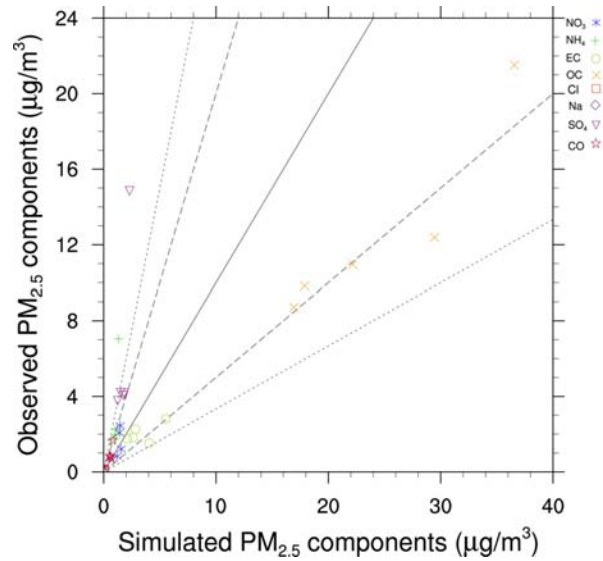


Fig.39 Scatter plot of simulated and observed 24h-average $PM_{2.5}$ -composition at the State Building site for the January v2 episode.

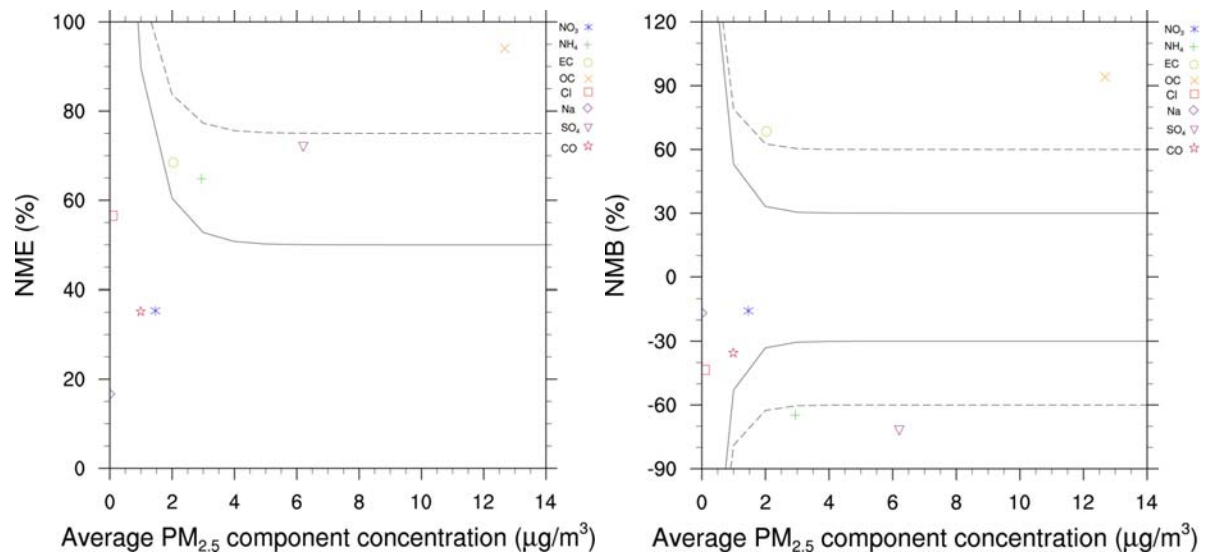


Fig. 40. Bugle plots of normalized mean (a) errors and (b) biases of simulated 24h-average $PM_{2.5}$ -composition and (c) soccer plot of normalized mean errors and biases all determined with respect to the observations at the State Building site for January v2. The dashed and solid lines indicate the performance criteria and performance goals in accord with Boylan and Russell (2006).

2.5 Process analysis for the November and January v2 episodes and investigation on boundary conditions

The 24h-average $PM_{2.5}$ -composition as simulated by the Alaska adapted CMAQ for the November episode and January v2 episode were compared for each day that had observed data (Figs. 41, 42). In the November episode, there were only three days, which had observed 24-haverage $PM_{2.5}$ -composition data. Note that there was no observed CO data on these days. Overall, the Alaska adapted CMAQ model overestimated OC and EC, but underestimated SO_4 , NH_4 , Na and Cl. The adapted CMAQ model overestimated NO_3 on one day and underestimated NO_3 on two days.

In the January episode, there were six days with observed $PM_{2.5}$ -composition data. The adapted CMAQ model shows similar results as for the November episode, i.e. it overestimated OC and EC, but underestimated SO_4 , NH_4 , Na, Cl and CO. The adapted CMAQ model overestimated NO_3 on two days and underestimated NO_3 on four days, but the trend of simulated NO_3 -concentrations seemed to follow the observed data.

Ten-day backward trajectories (http://ready.arl.noaa.gov/HYSPLIT_traj.php) were run for the days, which had observed 24h-average $PM_{2.5}$ -concentration data. The trajectories were determined starting at 00UTC and at 20m, 200m, 1000m above ground level over the Fairbanks meteorological station. The backward trajectories indicate that on the days, which had low observed 24h-average $PM_{2.5}$ -composition concentrations, i.e. November 12 and February 4, the aerosols at the low levels (20m) were from the local sources (Fig. 43). Long-range transport contributed to the peak on the days, which had high observed 24h-average $PM_{2.5}$ -composition concentrations, which CMAQ model seemed to be not able to capture. However, again the long-range is not the cause for the $PM_{2.5}$ -problem. Note that a half year study with WRF/Chem for winter 2008/09 showed only a few days that had advection from outside Alaska (Mölders et al. 2012). Investigations by Cahill (2003) based on about a decade of observations also showed that the advection of $PM_{2.5}$ by long-range transport is not the reason for the $PM_{2.5}$ -problem in Fairbanks. Investigations by Tran et al. (2011) performed for January 2000 also suggested only marginal advection of $PM_{2.5}$ from Asia to the Interior of Alaska and confirmed the results found here and by the afore cited authors.

The underestimations of SO_4 and NH_4 on every day of both episodes indicate errors, which need to be investigated and corrected. Some first steps in this direction are reported on later in this report.

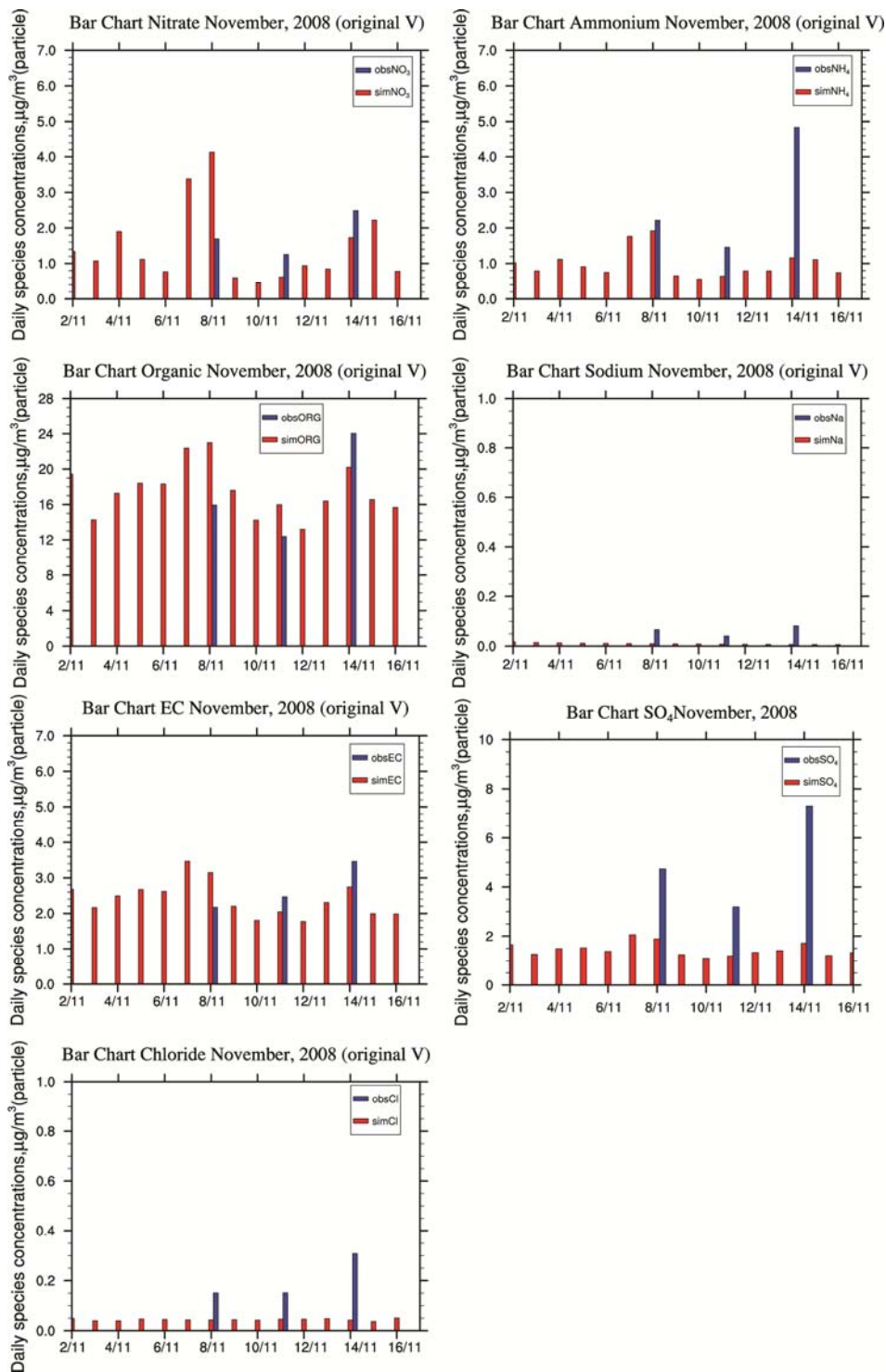


Fig. 41 Bar charts of simulated (red) and observed (blue) 24h-average $\text{PM}_{2.5}$ -composition for NO_3 , NH_4 , EC, OC, Na, Cl, SO_4 as obtained for the November episode.

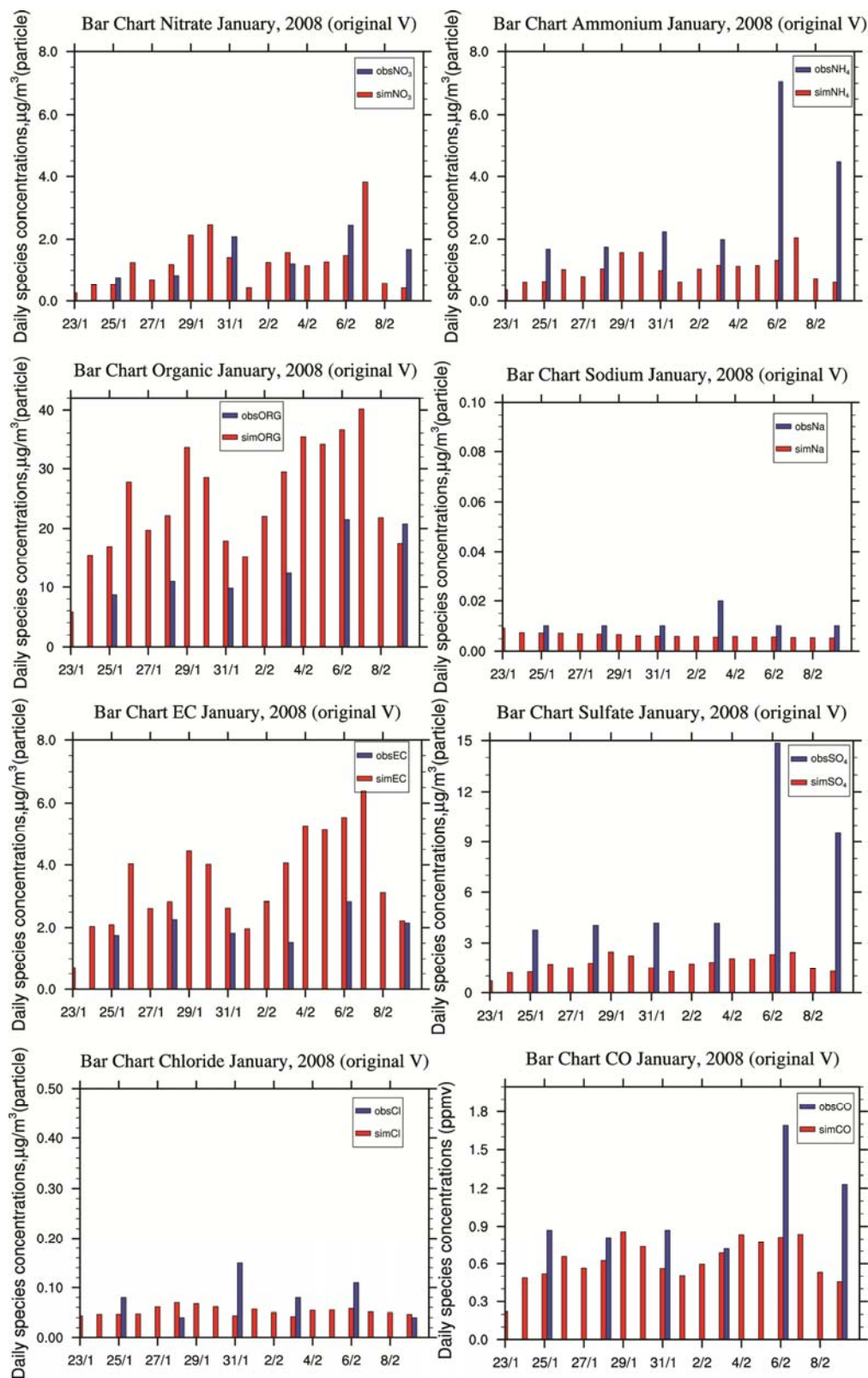


Fig. 42 Bar charts of simulated (red) and observed (blue) 24h-average PM_{2.5}-composition for NO₃, NH₄, EC, OC, Na, Cl, SO₄ as obtained for the January v2 episode.

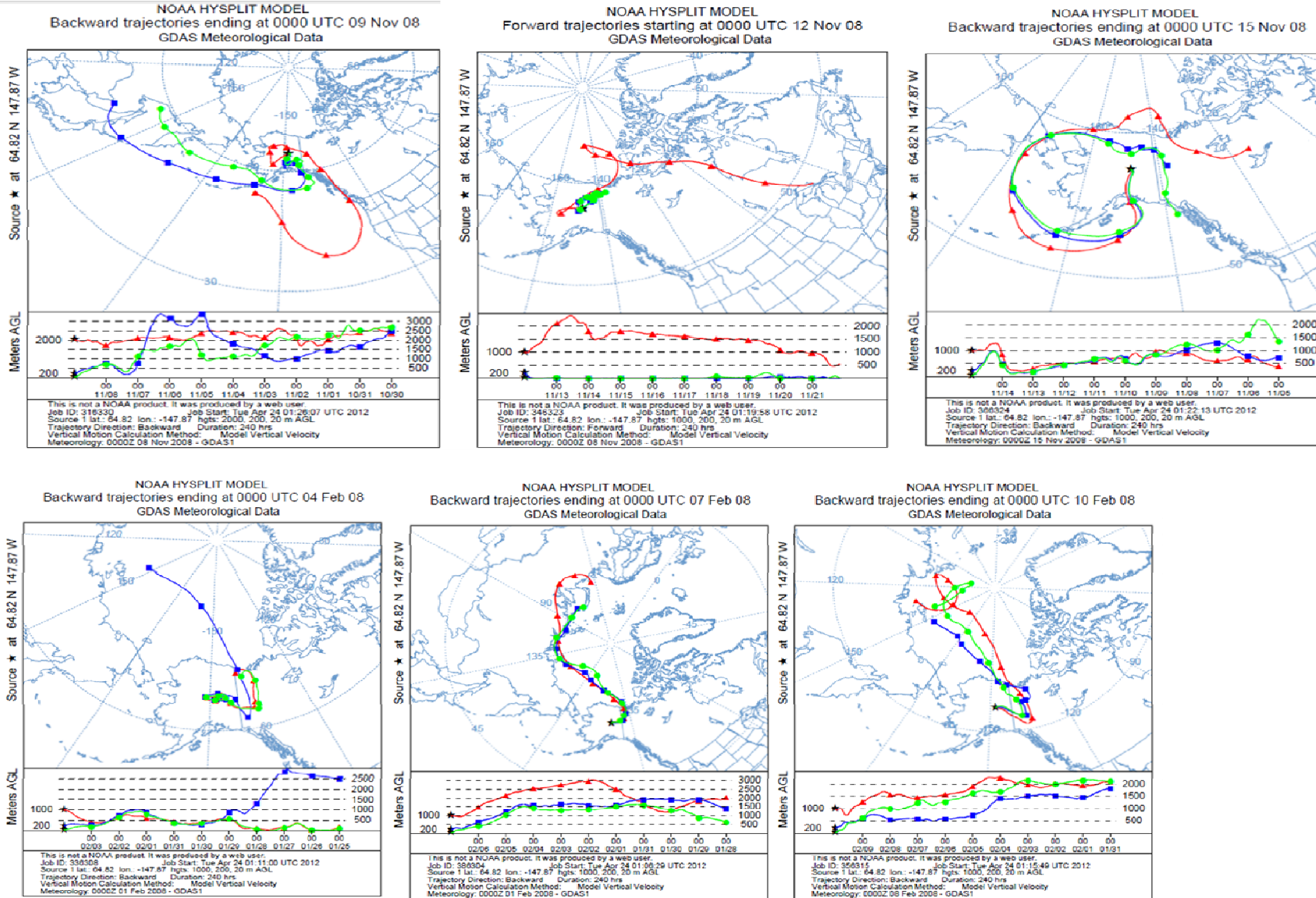


Fig. 43 Ten-day backward trajectories as calculated for November 9, 12, and 15, 2008, and February 4, 7, and 10, 2008 at 00 UTC.

To investigate the under-prediction of SO_4 at the State Building site, we conducted a process analysis. Process analysis is a technique that provides information about the impacts of individual processes on the change in a species' concentration. In the following, we refer to horizontal transport as the sum of horizontal advection and diffusion, and to vertical transport as the sum of vertical advection and diffusion. Aerosol processes represent the net effects of aerosol thermodynamics, new particle formation, condensation of sulfuric acid and organic carbon on preexisting particles, and the coagulation within and between Aitken and accumulation modes of particulate matter (PM). Cloud processes represent the net effects of cloud attenuation of photolytic rates, aqueous-phase chemistry, below-and in-cloud mixing with chemical species, cloud scavenging and wet deposition (Liu et al., 2010).

The hourly process analysis results for $\text{PM}_{2.5}$ -concentrations and other species were analyzed for the domain. In the following, the results for the grid-cell holding the State Building site are discussed. Figure 44 shows the contributions of individual processes to the 24h-average $\text{PM}_{2.5}$ -concentration in the first model layer (0-4m) at the grid-cell holding the State Building site. According to the process analysis, emissions were the dominant contributor to the $\text{PM}_{2.5}$ -concentrations, and the horizontal transport contributed and removed $\text{PM}_{2.5}$ at this grid-cell. The aerosol processes played a small role here, which indicates that $\text{PM}_{2.5}$ is composed mainly of primary PM at this site. $\text{PM}_{2.5}$ was mainly vented out through vertical transport. Dry deposition played a small role in the removal of $\text{PM}_{2.5}$ and cloud process did not play any role here.

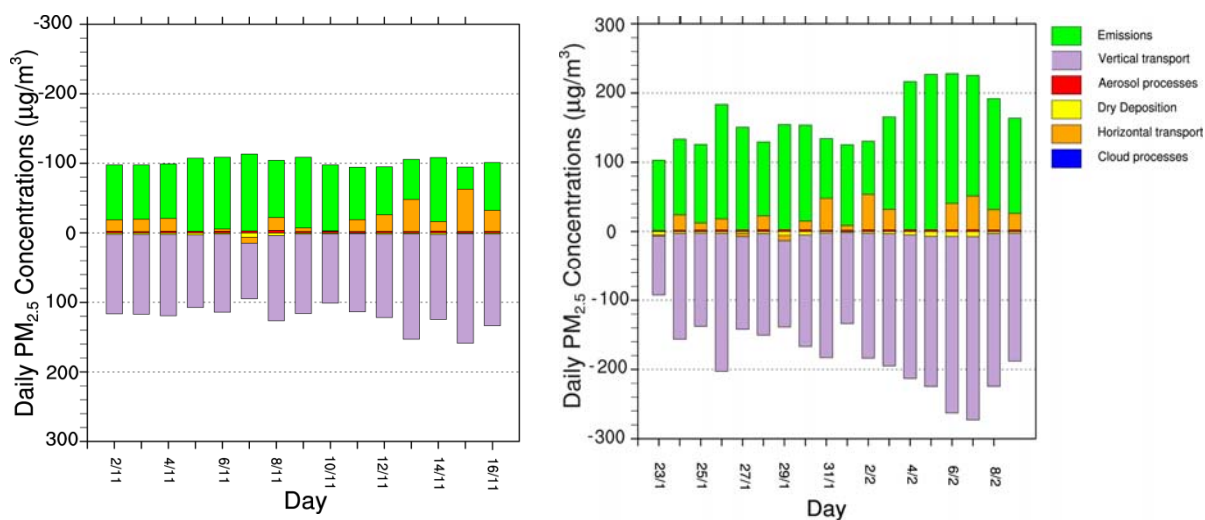


Fig. 44 Daily mean hourly contributions of individual processes to the $\text{PM}_{2.5}$ -concentrations at the State Building site as obtained for the November episode (left) and January v2 episode (right).

For the sulfate species, the major contributors were emissions and horizontal transport. Comparing the observed sulfate bar chart (Fig. 42) with the process analysis plot (Fig. 45), it

could be verified that there was some offsets for the horizontal transport. For example, on November 14 or February 6, when the observed sulfate concentrations were highest, the horizontal transport in the process analysis (Fig. 45) dropped and peaked on the following day. Similar to $PM_{2.5}$, the major removal process for sulfate at the grid holding the State Building site was vertical transport. The dry deposition processes played a small role here, and aerosol processes and cloud processes did not play a role in sulfate formation. The latter may be a hint at overlooked sulfate forming processes or too low aqueous phase processes.

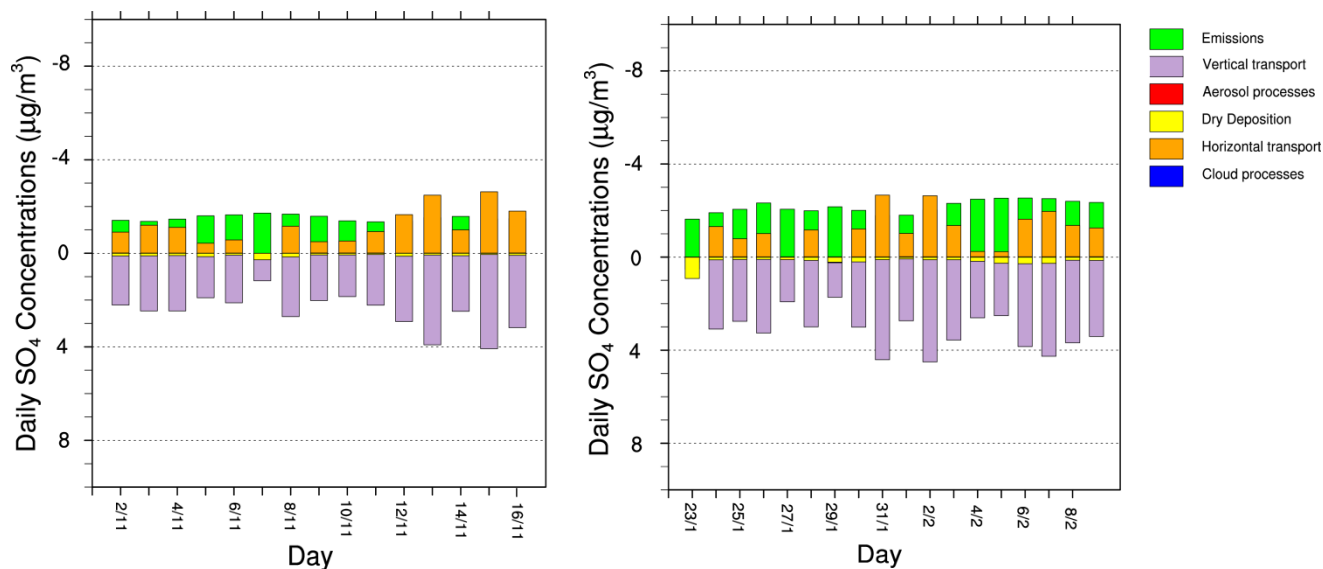


Fig. 45 Daily mean hourly contributions of individual processes to the SO_4 -concentrations at the State Building site for the November episode (left) and January v2 episode (right).

Different from sulfate, the aerosol processes played the main role for nitrate formation. High production of nitrate also came from horizontal transport, which also shows an offset. The major removal process was vertical transport, and dry deposition caused a small loss to nitrate. Cloud processes neither produced nor removed nitrate in this grid-cell (Fig. 46).

For ammonium, the aerosol processes are the dominant contributor at this site. Horizontal transport contributed to ammonium on some days. The major removal process was vertical transport, and dry deposition caused only a small loss to ammonium. Cloud processes did not play a role here similar to what was found for both sulfate and nitrate (Fig. 47).

According to the process analysis results, cloud processes did not play a role for the formation or removal of aerosols at this grid cell. In general, the aqueous-phase oxidation of SO_2 in clouds is able to increase the SO_4 -formation. Therefore, the average amount of water and ice mixing ratios simulated by WRF for both episodes were compared in vertical model column over the State Building site. Figure 48 shows that the cloud phase at this site is in the solid (ice) phase, which might affect the aqueous reactions and may be a cause for the low formation of SO_4 -aerosol. The

water phase represents the integral sum of cloud water mixing ratios and rain-water mixing ratios, and the ice phase represents the integral sum of snow, ice and graupel mixing ratios. Note that the comparison of 120 WRF-simulations over Alaska showed that the Morrison-code used in the WRF-simulations tends to produce relatively higher ice phase than liquid phase (Chigullapalli and Mölders 2008).

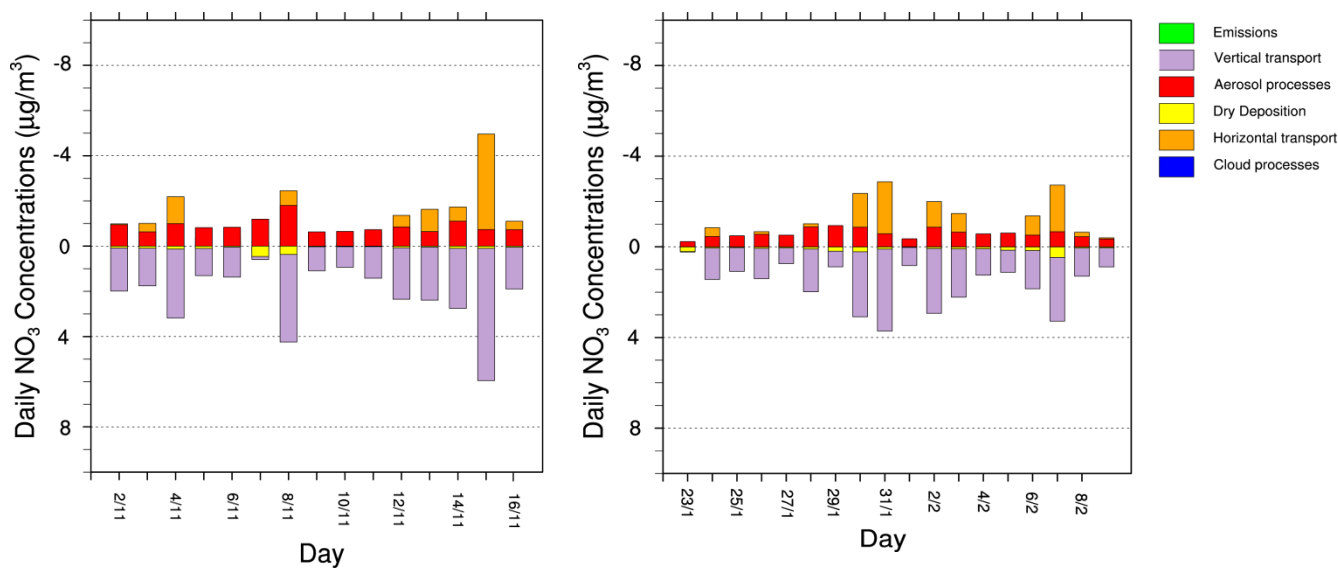


Fig. 46 Daily mean hourly contributions of individual processes to the NO₃-concentrations at State Building site as obtained for the November episode (left) and January v2 episode (right).

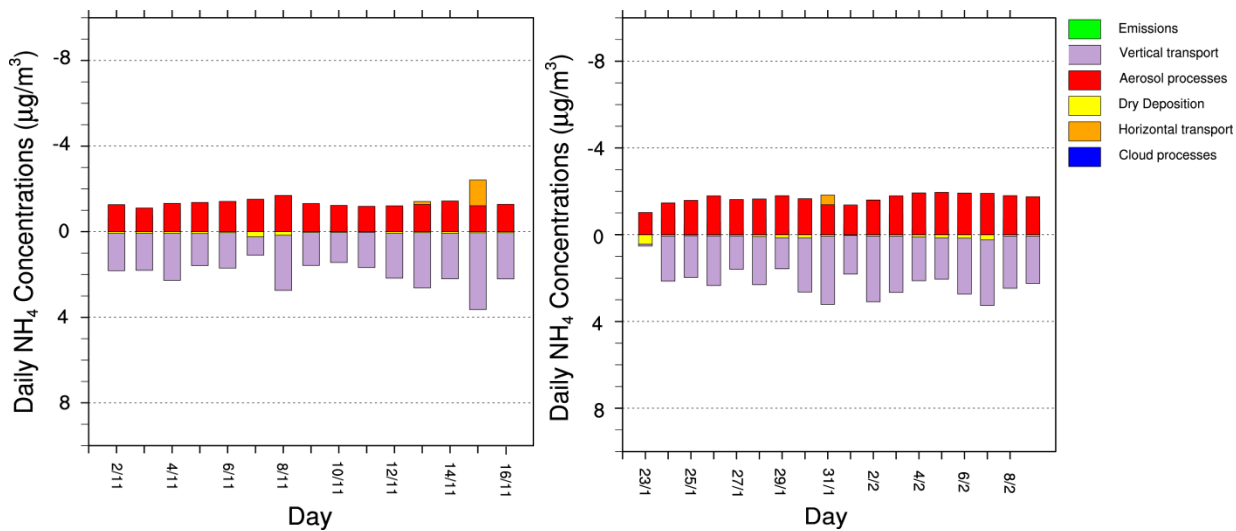
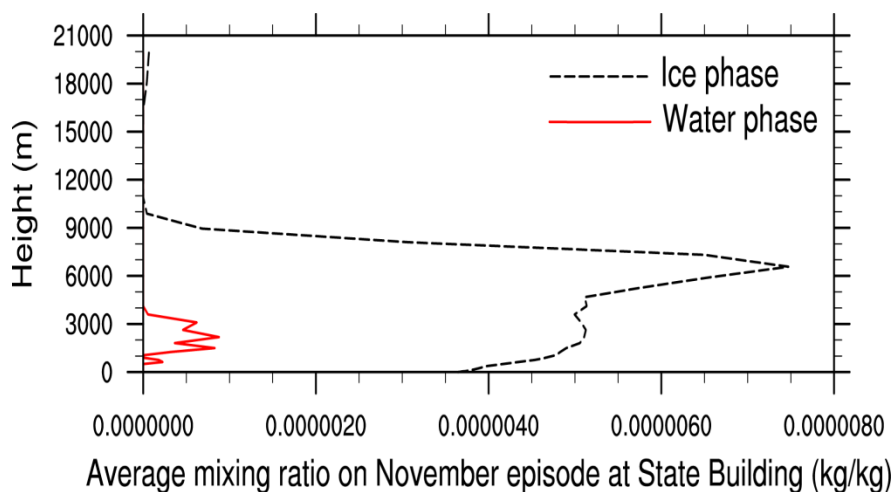


Fig. 47 Daily mean hourly contributions of individual processes to the NH₄-concentrations at the State Building site as obtained for the November episode (left) and January v2 episode (right).

(a)



(b)

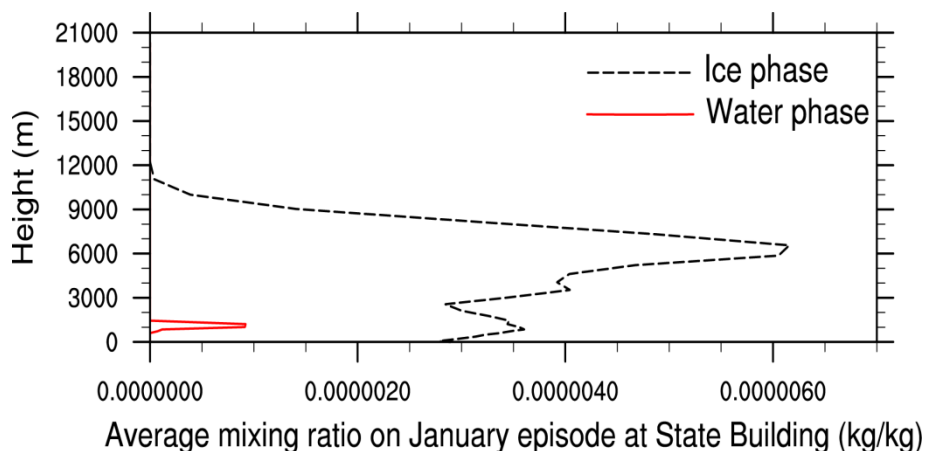


Fig. 47 Average ice phase and water phase mixing ratios at the State Building site as obtained for the (a) November episode and (b) January v2 episode.

Besides the effects from cloud processes, the underestimation of sulfate might come from too low SO_2 -emissions. To test this hypothesis, we performed adapted CMAQ simulations wherein we doubled the SO_2 -emissions that were given in the Sierra Research Inc. emission inventory. The results of this sensitivity study show that doubling the SO_2 -emissions would increase the sulfate species concentrations, but not increase them (proportionally) two times (Fig. 48).

Simulation for w modification January
double SO₂

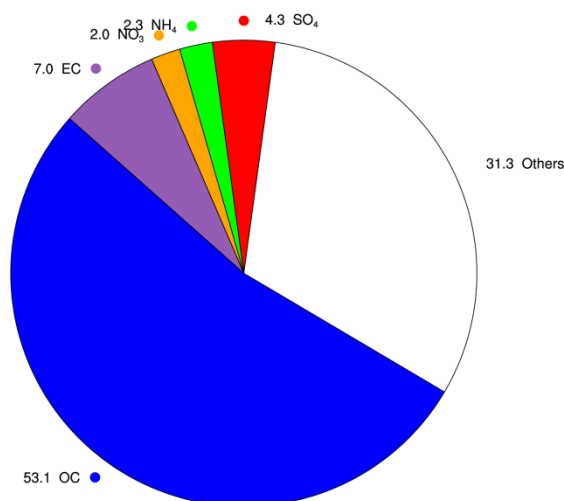


Fig. 48 Composition of total PM_{2.5} averaged for the three days with observations as obtained by the adapted CMAQ for the January v2 episode and the sensitivity study with adapted CMAQ assuming doubled SO₂ emissions.

In a nutshell, the chemical processes have the dominant role in the formation of nitrate and ammonium, but not in the sulfate formation at the grid-cell holding the State Building site. Emissions are the main contributor to sulfate and PM_{2.5}-concentrations, and horizontal transport is another main contributor. The offset of the simulated meteorology led to the delay in prediction the PM_{2.5} and its species of about 24 hours. The underestimation the sulfate composition is probably from the low amount of water in the liquid/water phase, i.e. low water content available to react with SO₂. Consequently, the cloud processes did not play a role for the aerosol formation. We recommend testing this hypothesis by adapted CMAQ simulations that use WRF simulations with a different cloud module. Studies on the impact of the parameterizations namely show that the partitioning between the solid and liquid phase in clouds differs strongly among parameterizations of cloud microphysical schemes (Möllders et al. 1995, 1997, Möllders 1999, Möllders and Kramm 2010) with consequences for the aqueous phase reactions (Möllders et al. 1994, Möllders and Laube 1994).

Acknowledgements

We wish to express our thanks to R. Elleman, G. Pouliot and C. Nolte for helpful suggestions regarding the CMAQ model. We acknowledge T. Carlson, B. Dulla and M. Hixson for providing the emission data, as well as valuable advice and assistance. We thank G. Kramm, W.R. Simpson, G.A. Grell, G.J. Fochesatto, H.N.Q. Tran, T.T. Tran and D. Huff for fruitful discussion and helpful comments. We also thank D. Huff, J. Conner, and J. McCormick for providing the observational data and P. Gaudet and D. Staufer for providing the WRF-data. Computational support came from the UAF Arctic Region Supercomputing Center.

References

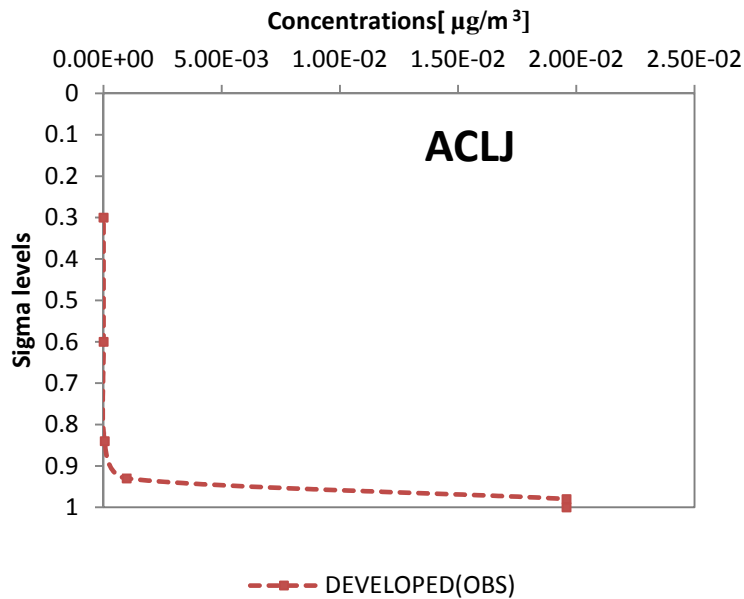
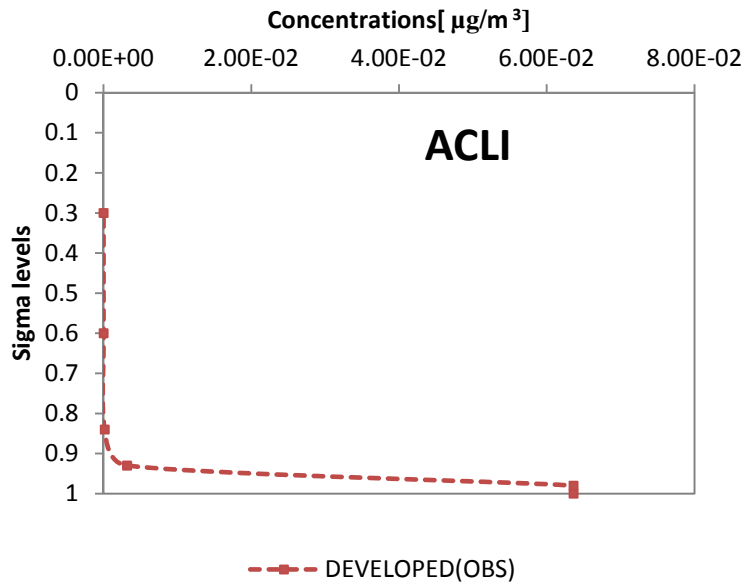
- Byun, D.W. and J. K. S. Ching, 1999. Science Algorithms of the EPAModels-3 Community Multiscale Air Quality (CMAQ) Modeling System. U.S. Environmental Protection Agency Rep. EPA-600/R-99/030, 727pp.
- Cahill, C.F., 2003. Asian Aerosol Transport to Alaska During ACE-Asia. *Journal Geophysical Research* 108, 8664.10.1029/2002jd003271.
- Chang, J. C., S. R. Hanna, 2004. Air quality model performance evaluation, *Meteorol Atmos Phys*, 87, 167–196.
- Chigullapalli, S., Mölders, N., 2008. Sensitivity studies using the Weather Research and Forecasting (WRF) model. ARSC report, pp. 15.
- Mölders, N., Hass, H., Jakobs, H.J., Laube, M., Ebel, A., 1994. Some effects of different cloud parameterizations in a mesoscale model and a chemistry transport model. *J. Appl. Meteor.*, 33: 527-545.
- Mölders, N., Laube, M., 1994. A numerical study on the influence of different cloud treatment in a chemical transport model on gas phase distribution. *Atmos. Res.*, 32: 249-272.
- Mölders, N., Laube, M., Kramm, G., 1995. On the parameterization of ice microphysics in a mesoscale α weather forecast model. *Atmos. Res.*, 38: 207-235.
- Mölders, N., Kramm, G., Laube, M., Raabe, A., 1997. On the influence of bulk parameterization schemes of cloud relevant microphysics on the predicted water cycle relevant quantities - a case study. *Meteorol. Zeitschr.*, 6: 21-32.
- Mölders, N., 1999. On the effects of different flooding stages of the Odra and different landuse types on the local distributions of evapotranspiration, cloudiness and rainfall in the Brandenburg-Polish border area. *Contrib. Atmos. Phys.*, 72: 1-24.
- Mölders, N., Kramm, G., 2010. A case study on wintertime inversions in Interior Alaska with WRF. *Atmos. Res.* 95: 314-332.
- Mölders, N., Tran, H.N.Q., Quinn, P., Sassen, K., Shaw, G.E, Kramm, G., 2011. Assessment of WRF/Chem to capture sub-Arctic boundary layer characteristics during low solar irradiation using radiosonde, SODAR, and station data, *Atmos. Pol. Res.* 2: 283-299.
- Mölders, N., Leelasakultum, K., 2011. Fairbanks North Star Borough PM_{2.5} Non-Attainment Area - CMAQ Modeling. Final report, phase I, March 1, 2011 – October 31, 2011, 62pp.
- Mölders, N., Tran, H.N.Q., Cahill, C.F., Leelasakultum, K., Tran, T.T., 2012. Assessment of WRF/Chem PM_{2.5}-forecasts using mobile and fixed location data from the Fairbanks, Alaska winter 2008/09 field campaign. *Atmos. Poll. Res.* 3: 180-191.
- Tran, H.N.Q., Mölders, N., 2012. Numerical investigations on the contribution of point-source emissions to the PM_{2.5}-concentrations in Fairbanks, Alaska, *Atmos. Poll. Res.* 3: 199-210.

Tran, T.T., Newby, G., Mölders, N., 2011. Impacts of Emission Changes on Sulfate Aerosols in Alaska. *Atmospheric Environment* 45, 3078-3090.

Zhao, Z., Chen, S.-H., Kleeman, M.J., Tyree, M., Cayan, D., 2011. The Impact of Climate Change on Air Quality–Related Meteorological Conditions in California. Part I: Present Time Simulation Analysis. *Journal Climate* 24, 3344-3361.

Appendix

The Cl-concentrations in the lowest level of the adapted CMAQ are now based on the average Cl-concentrations for January and November of 2003-2004 as observed at the Denali site (IMPROVE website). The vertical distribution assumed a reduction by 5% of the lower eta-level for every level between eta=0.93 and eta=0.30 (see panels below).



**The Fairbanks, Alaska PM_{2.5} Source
Apportionment Research Study
Winters 2005/2006-2012/2013, and Summer 2012**

**Final Report
Amendments 6 and 7**

December 23, 2013

by

Tony J. Ward, Ph.D.

**University of Montana – Missoula
Center for Environmental Health Sciences**

**Skaggs Building 176
Missoula, MT 59812
Office: (406) 243-4092
Fax: (406) 243-2807**

1.0. Executive Summary

Fairbanks, Alaska has some of the highest measured ambient PM_{2.5} (particulate matter less than or equal to 2.5 microns in diameter) concentrations in the United States, with wintertime levels often exceeding the 24-hour PM_{2.5} National Ambient Air Quality Standard (NAAQS) of 35 µg/m³. In an effort to understand the sources of PM_{2.5} in the Fairbanks airshed, source apportionment using Chemical Mass Balance (CMB) modeling was conducted at multiple locations throughout Fairbanks each winter between 2005/2006 and 2012/2013. PM_{2.5} source apportionment was also conducted at the NCORE and State Building sites during the summer of 2012 for comparison. Modeling for each of the sites/years was conducted using source profiles from both the Environmental Protection Agency (EPA) as well as Fairbanks-specific profiles developed by OMNI Environmental Services (OMNI).

Throughout the program, wintertime PM_{2.5} average concentrations ranged from 8.2 µg/m³ (RAMS, winter 2008/2009) up to 46.9 µg/m³ (NPF3, winter 2012/2013), with many of the sites having frequent exceedances of the 24-hour NAAQS on the scheduled sample days. The results of the CMB modeling using source profiles developed by the EPA revealed that wood smoke (likely residential wood combustion) was the major source of PM_{2.5} throughout the winter months in Fairbanks, contributing between ~60% to over 80% of the measured PM_{2.5} depending on site and winter / year. The other sources of PM_{2.5} identified by the CMB model were secondary sulfate (~7-21%), ammonium nitrate (3-11%), diesel exhaust (not detected-11%), and automobiles (not detected-7%). Approximately 1-2% of the ambient PM_{2.5} was unexplained.

When conducting CMB modeling with Fairbanks-specific space heater source profiles developed by OMNI, final results were somewhat similar to the sources identified using EPA profiles. Consistent with the EPA modeling, wood smoke was identified as being a large source of PM_{2.5} at the majority of the sampling sites, contributing from 30% to 77% to the ambient wintertime PM_{2.5}. In addition, the OMNI profile for No. 2 fuel oil combustion was frequently identified during the winter months, contributing anywhere from 10% to 47% to the ambient PM_{2.5} throughout the winter months at each of the sites. Combustion of No. 2 fuel oil (and contribution to ambient PM_{2.5}) was determined to be especially high at the State Building and Peger Road sites.

Summer source apportionment revealed that ambient levels of PM_{2.5} were very low at both the State Building and NCORE sites (~5.5 µg/m³). CMB modeling using both the EPA and OMNI profiles identified wood smoke as the predominant source during the summer months, likely from residential outdoor biomass waste burning and regional controlled/wildfires. In summary, CMB modeling results using both the EPA and OMNI profiles support that residential home heating (residential wood stoves and heating with No. 2 fuel oil) are the major contributors to the ambient PM_{2.5} in the Fairbanks airshed during the winter months. Wood smoke was also consistently identified during the summer months, albeit at much lower concentrations compared to winter concentrations.

2.0. Overview

The primary objective of this research study was to identify the major sources of ambient PM_{2.5} in Fairbanks, Alaska using both EPA and OMNI (Fairbanks-specific) source profiles in a CMB model. Specifically, source apportionment was conducted for the following time periods/locations:

Winter 2005/2006: State Building.

Winter 2006/2007: State Building.

Winter 2007/2008: State Building.

Winter 2008/2009: State Building, North Pole, RAMS, Peger Road.

Winter 2009/2010: State Building, North Pole, RAMS, Peger Road.

Winter 2010/2011: State Building, North Pole, Peger Road.

Winter 2011/2012: State Building, NCORE, RAMS, North Pole, NPF3.

Summer 2012: State Building, NCORE.

Winter 2012/2013: State Building, NCORE, NPF3, NPE.

Within this report, the sampling, analytical, and computer modeling methodologies are described in Sections 3.0 through 5.0, respectively. Sections 6.0 and 7.0 present the results of the PM_{2.5} sampling and CMB modeling program (using both EPA and OMNI source profiles), respectively, while Section 8.0 provides a discussion of all of the CMB modeling findings. Section 9.0 presents the results of the Quality Assurance / Quality Control (QA/QC) program. In Appendix A, the eight source profiles developed from the OMNI emissions testing are displayed, while Appendix B contains a listing of sample days excluded from CMB modeling. Finally, Appendix C presents the CMB results for each sample day (per site and season) using both EPA and OMNI profiles.

3.0. PM_{2.5} Sampling Program

3.1. Sampling Program Experimental Method

For each of the winter sampling programs (November-March), PM_{2.5} sampling was typically conducted every three days following the EPA's fixed monitoring schedule. For the winters of 2005/2006, 2006/2007, and 2007/2008, sampling was conducted at the State Building site. PM_{2.5} sampling was conducted at the State Building, North Pole, and Peger Road (also known as the Transit Yard) sites during the winters of 2008/2009, 2009/2010, and 2010/2011, respectively. A Relocatable Air Monitoring System (RAMS) collected PM_{2.5} samples only during the winters of 2008/2009, 2009/2010, and 2011/2012. From January 14-March 19, 2009, the mobile RAMS was located at the Reindeer Site (i.e. University of Alaska Fairbanks Experimental Farm property between the Parks Highway and Geist Rd). From March 19 through the end of the program, the mobile RAMS was located at Woodriver Elementary School (Palo Verde Ave/ Univ. West). In this report, results for the Reindeer and Elementary School sites are presented as one location (i.e. the "RAMS Site").

In addition to the RAMS site, samples were also collected every three days at four additional sites (State Building, NCORE, North Pole, and NPF3) during the winter 2011/2012. For the winter of 2012/2013, the RAMS and North Pole sites were discontinued while the NPE site was added. Finally, PM_{2.5} samples were collected at two locations during the summer of 2012 (State Building and NCORE) for a site comparison, as well as providing a comparison for summer results with winter results.

At each of the sites, 24-hour PM_{2.5} sampling was conducted using a MetOne (Grants Pass, OR) Spiral Ambient Speciation Sampler (SASS). During each 24-hour sampling event at each of the sites, the SASS collected ~9.7 m³ of air through Teflon, nylon, and quartz filter media, respectively (flow rate of 6.7 liters per minute (LPM)). Starting in the winter of 2009/2010, a URG 3000N Sequential Particulate

Speciation System was used to collect sample on a quartz filter at the State Building site for organics analyses. During each 24-hour event the URG collected air sample at a flow rate of 22.0 LPM.

3.2. Sampling Program Quality Assurance / Quality Control (QA/QC)

A stringent Quality Assurance / Quality Control (QA/QC) program was employed throughout this study. Prior to sampling, clean filters (Teflon, nylon, and quartz) were provided by Research Triangle Institute (RTI, Research Triangle Park, NC). Following the sampling events, exposed Teflon and nylon filters were sent back to RTI for laboratory analyses, while the exposed quartz filters were sent to Desert Research Institute (Reno, NV). During shipment of both clean and exposed filter sample media, all PM_{2.5} filters remained in their protective containers and were FedEx overnighted in a cooler containing cold packs during transport.

Throughout the sampling program, the air samplers were maintained by Fairbanks North Star Borough (FNSB) Air Quality staff, with support from Alaska Department of Environmental Conservation (ADEC) staff. During each sampling event (24-hour period), the filters were subjected to temperatures that did not exceed the ambient temperature by more than five °C for more than 30 minutes continuously. Fairbanks site personnel removed the exposed filters from the samplers within 48 hours after the episode ended, and refrigerated the exposed filters immediately upon collection. The air samplers were also audited with an independent transfer standard during the program to verify the accurate measurement of air flow rates, ambient/filter temperatures, and barometric pressures. In addition, PM_{2.5} filter field blanks were collected periodically throughout the program in an effort to determine any artifact contamination.

4.0. Analytical Program

4.1. PM_{2.5} Speciation Data

The Met One Super SASS located at each of the sites collected ambient PM_{2.5} on Teflon, nylon, and quartz filter media, respectively. The majority of the exposed SASS filter samples were analyzed by RTI. From the Teflon filter, a gravimetric analysis (RTI, 2008) was initially performed followed by an elemental analysis (RTI, 2009a) using energy-dispersive X-ray fluorescence (EDXRF) where 31 elements were quantified. From the nylon filter, ions (including ammonium, potassium, sodium, nitrate, and sulfate) were measured by ion chromatography (IC) (RTI, 2009b; RTI, 2009c). Depending on the site and year, quartz filters were either analyzed by RTI for Elemental Carbon and Organic Carbon (EC/OC) concentrations using Thermal Optical Transmittance (RTI, 2009d), or by Desert Research Institute using the IMPROVE_A method (Chow et al., 2007). Following the analyses, sample results (including analyte concentrations and uncertainties) were provided to the University of Montana for use in the CMB source apportionment model.

4.2. Analytical Program QA/QC

RTI and the Desert Research Institute were responsible for QA/QC activities within their laboratories.

5.0. Computer Modeling Program

In this project, the most recent version of the Chemical Mass Balance (CMB) computer model (Version 8.2) was utilized to apportion the sources of PM_{2.5} in Fairbanks. The CMB receptor model (Friedlander, 1973; Cooper and Watson, 1980; Gordon, 1980, 1988; Watson, 1984; Watson et al., 1984; 1990; Hidy and Venkataraman, 1996) is based on an effective-variance least squares method, and consists of a solution to linear equations that expresses each receptor chemical concentration as a linear sum of products of source fingerprint abundances and contributions.

For each sample day (from the multiple sites), the CMB modeling process began by selecting from a combination of 91 sources (see **Table 1**) and 43 chemical species (36 elements, 5 ions, OC and EC, **Table 5**) in an effort to reconstruct the measured Fairbanks ambient PM_{2.5} mass and chemical composition. As part of the CMB modeling procedure, multiple combinations would be tried for each sample run in an effort to select the best combination of sources and species, with an evaluation of the diagnostic performance measures conducted each time until an optimal fit could be obtained. The resulting output file contained the source contribution estimate (SCE) of each identified source, along with the associated standard errors (STD ERR). Unexplained concentrations were also calculated by taking the difference between the actual measured mass and the CMB predicted mass for each sample run.

5.1. CMB Model EPA Source Profiles

Discussions were held with Sierra Research, FNSB, and ADEC in an effort to identify all of the potential sources of PM_{2.5} in Fairbanks prior to setting up the CMB model. Following these discussions, a comprehensive list of sources that could potentially contribute PM_{2.5} to the Fairbanks airshed was developed. For each identified source, an attempt was made to locate a source profile. Source profiles are the fractional mass abundances of measured chemical species relative to primary PM_{2.5} mass in source emissions, and are part of the input data loaded into the CMB model. Source profiles represent a general source category rather than any local, individual, PM_{2.5} emission source.

The source profiles listed in **Table 1** (known throughout this report as “EPA Source Profiles”) were either taken directly from the most recent version of SPECIATE 4.0 (USEPA, 2006) or from previous Missoula Valley (Montana) CMB applications (Carlson, 1990; Schmidt, 1996; Ward and Smith, 2005). SPECIATE 4.0 is EPA's repository of Total Organic Compound (TOC) and Particulate Matter (PM) speciated source profiles for use in source apportionment studies. For each source found in the database, both the compound fraction and uncertainty for the source-specific compounds are presented. The profiles in **Table 1** are listed together as source groups, and can be broken down into profiles for street sand and road dust (Profiles 1- 6), pure secondary source emissions (Profiles 7-9), gasoline and diesel exhaust emissions (Profiles 10 – 40), tire and brake wear (Profiles 41 - 48), meat cooking (Profiles 49 - 53), residential wood combustion (Profiles 54 – 78), and other local sources / industry in Fairbanks (Profiles 79-91). Multiple source profiles for each source were used because source compositions can vary substantially among sources, even within a single source over an extended period of time.

Since Missoula and Fairbanks have similar topographies (i.e. valley locations impacted by temperature inversions, cold winter temperatures, etc.) and many of the same sources of PM_{2.5}, several of the CMB source profiles developed in past Missoula CMB applications were included in the Fairbanks PM_{2.5} source apportionment program. These include profiles for street sand (Profiles 1), secondary sulfate (Profile 7), secondary ammonium sulfate (Profile 8), secondary ammonium nitrate (Profile 9), diesel train (Profile 39) and diesel truck exhaust (Profile 40), and residential wood combustion (Profile 56). All SPECIATE and Missoula CMB profiles used in the Fairbanks CMB were reviewed before being loaded into the CMB model. For those chemical species known to be absent from specific source types, default values of zero for the mass fraction and uncertainty of 0.0001 were used.

One assumption of the CMB model is that compositions of source emissions are constant over the period of ambient and source sampling, and that chemical species do not react with each other. CMB is well suited for apportioning sources of primary aerosols (those emitted directly as particles). However, it is difficult to attribute secondary aerosols formed through gas-to-particle transformation in the atmosphere to specific sources. Sulfate, nitrate, and ammonium abundances in directly emitted particles are not sufficient to account for the concentrations of these species measured in the atmosphere. Therefore, to

account for secondary aerosol contributions to PM_{2.5} mass, sulfate (Profile 7), ammonium sulfate (Profile 8), and ammonium nitrate (Profile 9) were expressed as “pure” secondary source profiles, and represented by their chemical form.

Table 1: PM_{2.5} Source Profiles (“EPA Profiles”) Used in the Fairbanks CMB.

Profile	Description
1	CITY STREET SANDING PILE, STREET SAND
2	SPECIATE 411302.5, PAVED ROAD DUST – COMPOSITE
3	SPECIATE 412202.5, UNPAVED ROAD DUST – COMPOSITE
4	SPECIATE 92053, PAVED ROAD DUST – SIMPLIFIED
5	SPECIATE 92088, UNPAVED ROAD DUST – SIMPLIFIED
6	SPECIATE 92073, SAND & GRAVEL – SIMPLIFIED
7	SULFATE (SO4 IS ONLY SPECIE, THEREFORE IS ONLY NONZERO CONCENTRATION)
8	AMMONIUM SULFATE (INCLUDES NH4)
9	AMMONIUM NITRATE (INCLUDES NH4)
10	SPECIATE 311052.5 LIGHT DUTY VEHICLE-LEADED COMPOSITE
11	SPECIATE 312022.5 LIGHT DUTY VEHICLE-UNLEADED
12	SPECIATE 321022.5 LIGHT DUTY VEHICLE-DIESEL
13	SPECIATE 321032.5 LIGHT DUTY VEHICLE-DIESEL (2ND PROFILE OF THIS TYPE)
14	SPECIATE 322032.5, HEAVY DUTY VEHICLE-DIESEL
15	SPECIATE 311082.5, LIGHT DUTY VEHICLE - NON CATALYST
16	SPECIATE 311072.5, LIGHT DUTY VEHICLE - WITH CATALYST
17	SPECIATE 322022.5, HEAVY DUTY DIESEL
18	SPECIATE 322082.5, HEAVY DUTY DIESEL TRUCKS
19	SPECIATE 312012.5, LIGHT DUTY VEHICLE – UNLEADED
20	SPECIATE 312032.5, LIGHT DUTY VEHICLE – UNLEADED
21	SPECIATE 3875, GASOLINE EXHAUST - WINTER, SMOKER
22	SPECIATE 3884, GASOLINE EXHAUST - WINTER, LOW EMITTER PROFILE 1
23	SPECIATE 3888, GASOLINE EXHAUST - WINTER, LOW EMITTER PROFILE 2
24	SPECIATE 3892, GASOLINE EXHAUST - WINTER, HIGH EMITTER PROFILE 1
25	SPECIATE 3896, GASOLINE EXHAUST - WINTER, HIGH EMITTER PROFILE 2
26	SPECIATE 3900, GASOLINE EXHAUST - WINTER, NON-SMOKER
27	SPECIATE 3904, GASOLINE EXHAUST - WINTER, SMOKER PROFILE 1
28	SPECIATE 3908, GASOLINE EXHAUST - WINTER, SMOKER PROFILE 2
29	SPECIATE 3878, DIESEL EXHAUST PROFILE 1
30	SPECIATE 3879, DIESEL EXHAUST PROFILE 2
31	SPECIATE 3880, DIESEL EXHAUST PROFILE 3
32	SPECIATE 3912, DIESEL EXHAUST PROFILE 4
33	SPECIATE 3913, DIESEL EXHAUST PROFILE 5
34	SPECIATE 3914, DIESEL EXHAUST PROFILE 6
35	SPECIATE 92035, HDDV EXHAUST – SIMPLIFIED
36	SPECIATE 92042, LDDV EXHAUST – SIMPLIFIED
37	SPECIATE 92049, NON-CATALYST GASOLINE EXHAUST – SIMPLIFIED
38	SPECIATE 92050, ONROAD GASOLINE EXHAUST – SIMPLIFIED
39	DIESEL TRAIN (SENT FROM MISSOULA)
40	DIESEL TRUCK (SENT FROM MISSOULA)
41	SPECIATE 340022.5, TIRE WEAR PROFILE 1
42	SPECIATE 340032.5, TIRE WEAR PROFILE 2
43	SPECIATE 340082.5, TIRE WEAR PROFILE 3
44	SPECIATE 3156, TIRE WEAR PROFILE 4

45	SPECIATE 92087, TIRE DUST – SIMPLIFIED
46	SPECIATE 340042.5, BRAKE LINING – ASBESTOS
47	SPECIATE 3157, BRAKE WEAR
48	SPECIATE 92009, BRAKE LINING DUST – SIMPLIFIED
49	SPECIATE 160002.5, MEAT COOKING – CHARBROILING
50	SPECIATE 160012.5, MEAT COOKING – FRYING
51	SPECIATE 4383, COOKING
52	SPECIATE 91005, COOKING - CHARBROILING COMPOSITE
53	SPECIATE 92015, CHARBROILING – SIMPLIFIED
54	SPECIATE 421042.5 RESIDENTIAL WOOD SMOKE FROM MEDFORD, OR
55	SPECIATE 421052.5 RESIDENTIAL WOOD SMOKE FROM POCATELLO, ID
56	RESIDENTIAL WOOD COMBUSTION (SUPPLIED BY MISSOULA)
57	SPECIATE 423182.5, RESIDENTIAL WOOD COMBUSTION
58	SPECIATE 423032.5, RESIDENTIAL WOOD COMBUSTION, COMPOSITE
59	SPECIATE 423302.5, COMPOSITE OF RESIDENTIAL WOODBURNING SOURCES
60	SPECIATE 421022.5, WOOD STOVES - AVERAGE ALL FUELS
61	SPECIATE 421012.5, WOOD STOVES - PINE FUELS
62	SPECIATE 3235, RESIDENTIAL WOOD BURNING PROFILE 1
63	SPECIATE 3236, RESIDENTIAL WOOD BURNING PROFILE 2
64	SPECIATE 3238, RESIDENTIAL WOOD BURNING PROFILE 3
65	SPECIATE 3239, RESIDENTIAL WOOD BURNING PROFILE 4
66	SPECIATE 3240, RESIDENTIAL WOOD BURNING PROFILE 5
67	SPECIATE 3769, RESIDENTIAL WOOD BURNING PROFILE 6
68	SPECIATE 3770, RESIDENTIAL WOOD BURNING PROFILE 7
69	SPECIATE 423192.5, RESIDENTIAL WOOD COMBUSTION COMPOSITE
70	SPECIATE 423312.5, RESIDENTIAL WOODSTOVE COMPOSITE
71	SPECIATE 91031, RESIDENTIAL WOOD COMBUSTION: HARDSOFT – COMPOSITE
72	SPECIATE 91032, RESIDENTIAL WOOD COMBUSTION: HARDSOFTN/A – COMPOSITE
73	SPECIATE 91033, RESIDENTIAL WOOD COMBUSTION: SOFT – COMPOSITE
74	SPECIATE 92067, RESIDENTIAL WOOD COMBUSTION: HARD – SIMPLIFIED
75	SPECIATE 92068, RESIDENTIAL WOOD COMBUSTION: HARDSOFT – SIMPLIFIED
76	SPECIATE 92069, RESIDENTIAL WOOD COMBUSTION: HARDSOFT N/A – SIMPLIFIED
77	SPECIATE 92071, RESIDENTIAL WOOD COMBUSTION: SYNTHETIC – SIMPLIFIED
78	SPECIATE 92090, WILDFIRES – SIMPLIFIED
79	SPECIATE 92006, ASPHALT ROOFING – SIMPLIFIED
80	SPECIATE 92025, DISTILLATE OIL COMBUSTION – SIMPLIFIED
81	SPECIATE 92048, NATURAL GAS COMBUSTION – SIMPLIFIED
82	SPECIATE 92052, OVERALL AVERAGE / DEFAULT (WASTE DISPOSAL, MISC) – SIMPLIFIED
83	SPECIATE 92060, PROCESS GAS COMBUSTION – SIMPLIFIED
84	SPECIATE 92063, RESIDENTIAL NATURAL GAS COMBUSTION – SIMPLIFIED
85	SPECIATE 92072, RESIDUAL OIL COMBUSTION – SIMPLIFIED
86	SPECIATE 92075, SEA SALT – SIMPLIFIED
87	SPECIATE 92079, SINTERING FURNACE-SIMPLIFIED (ZINC PROD, FLUE DUST HANDLING)
88	SPECIATE 92082, SOLID WASTE COMBUSTION – SIMPLIFIED
89	SPECIATE 92084, SUBBITUMINOUS COMBUSTION – SIMPLIFIED
90	SPECIATE 92085, SURFACE COATING – SIMPLIFIED
91	SPECIATE 92086, TIRE BURNING – SIMPLIFIED

5.2. CMB Modeling Using Fairbanks-Specific (“OMNI”) Profiles

One limitation of using the EPA SPECIATE source profiles for CMB modeling (as described above) is that the profiles are not representative of Fairbanks-specific home heating fuel types. In other words, the

profiles were not developed using Fairbanks specific fuels or generated under Fairbanks-specific operating and meteorological conditions. To address this concern, emission testing was conducted by OMNI Environmental Services (Portland, OR) for a variety of home heating fuels and home heating devices commonly used in Fairbanks. These emissions results were provided to the University of Montana for development of Fairbanks-specific source profiles, with these profiles then used in CMB source apportionment modeling.

Prior to emissions testing, the FNSB provided OMNI with Fairbanks specific fuel types to be used in a variety of home heating devices. The goal of the OMNI testing was to generate emission profiles for the following types of heating appliances and fuel types: pellet stoves, EPA wood stoves (birch, spruce), conventional wood stoves (birch, spruce), EPA hydroponic heaters (birch, spruce), non qualified outdoor hydroponic heaters (spruce, birch, wet stoker coal), oil burners (No. 1 fuel oil, No. 2 fuel oil), waste oil burning, coal stoves (dry stoker coal, wet stoker coal, wet lump coal, dry lump coal), and coal hydroponic heaters (wet stoker coal and coal-typical moisture).

During each of the 41 trials, emission samples were collected on Teflon and quartz filter samples, respectively. From the Teflon filter, PM_{2.5} mass, ions (potassium, sodium, ammonium, nitrate, and sulfate), and elements (33 in total) were quantified. From the quartz filter, levels of Organic Carbon and Elemental Carbon were measured. The Research Triangle Institute (RTI, Research Triangle Park, NC) conducted all of the analyses, and reported results in μg of analyte/filter. Following the completion of OMNI emissions testing, results from the trials were sent to FNSB, ADEC, and Sierra Research for a comprehensive review of methodology (sampling and analytical) and completeness. From the 41 emissions trials that were conducted by OMNI, University of Montana was instructed to focus on only eight of the trials. University of Montana then took the raw emissions data from these eight source types and transformed them into source profiles that were used in the CMB model.

The Fairbanks-specific source profiles that were developed from the OMNI emissions testing are presented in **Table 2**. In developing the profiles, the raw data from OMNI had to be put into a format recognized by the CMB model. First, the raw mass, elemental, OC/EC, and ion data (in $\mu\text{g}/\text{filter}$) measured by the Teflon and quartz filters were corrected for volume (dsft^3). This volume was the amount of air collected (for each filter) during each emissions testing trial. For the Teflon filters, the collected volumes varied from 1.12 up to 22.63 dsft^3 , while for the quartz filter volumes ranged from 1.74 to 21.27 dsft^3 . These values ($\mu\text{g}/\text{dsft}^3$) were then normalized to the overall mass (units in $\mu\text{g}/\text{dsft}^3$) to give the mass fraction of each species. For uncertainty, a default value of 0.0001 was utilized, with a value of “-99” utilized for missing species.

Table 2: OMNI Source Profiles (“OMNI Profiles”) Used in the Fairbanks CMB.

Profile	Description
100	OMNI Profile, EPA Wood Stove, Birch, Low
101	OMNI Profile, EPA OWHH, Birch, Low
102	OMNI Profile, Conventional Wood Stove, Birch, Low
103	OMNI Profile, Oil Burner, No. 2 Fuel Oil
104	OMNI Profile, Coal Stove, Wet Stoker Coal, Low
105	OMNI Profile, Coal HH, Wet Stoker Coal, Single
106	OMNI Profile, WasteOil Brnr, Waste Oil, Single
107	OMNI Profile, EPA Wood Stove, spruce, low
108	OMNI Profile, Coal Stove Dry Lump Coal, low

The eight source profiles developed from the OMNI emissions testing are presented in **Appendix A**.

5.3. CMB Modeling Program QA/QC

A comprehensive QA/QC plan was applied throughout the CMB modeling program to ensure accurate results, including the use of the CMB validation protocol (Watson et al., 2004). The QA/QC protocol:

- 1) determines model applicability;
- 2) selects a variety of profiles to represent identified contributors;
- 3) evaluates model outputs and performance measures;
- 4) identifies and evaluates deviations from model assumptions;
- 5) identifies and corrects model input deficiencies;
- 6) verifies consistency and stability of source contribution estimates; and
- 7) evaluates CMB results with respect to other data analysis and source assessment methods.

For each model run, evaluations of several different combinations of source profiles were used, with the number of chemical species always exceeding the number of source types. As described in **Table 3**, statistical parameters used to evaluate the validity of source contribution estimates included TSTAT, R^2 , Chi^2 , DF, and R/U ratios. The results of these fitting parameters (for each modeling run) have to be within the EPA target ranges for the modeling results to be considered valid. It should also be noted that concentrations of species found on field/trip blanks were not subtracted (or blank-corrected) from the ambient sample concentrations before the modeling was conducted.

Table 3: Statistical Criteria for the CMB Model.

Output / Statistic	Abbreviation	EPA Target	Explanation
Std. Error	STD ERR	<SCE	The standard error of the SCE.
T-statistic	TSTAT	> 2.0	The ratio of the value of the SCE to the uncertainty in the SCE. A T-STAT greater than 2 means that the SCE has a relative uncertainty of less than 50%.
R-square	R-SQUARE (R^2)	0.8 to 1.0	A measure of the variance of the ambient concentration explained by the calculated concentration.
Chi-square	CHI-SQUARE (Chi^2)	0.0 to 4.0	A term that compares the difference between the calculated and measured ambient concentrations to the uncertainty of the difference. A perfect fit has a chi-square of 0.0, and a chi-square less than 2 usually indicates a good fit.
Percent Mass Explained	% MASS	100% \pm 20%	The ratio of the total calculated to measured mass.
Degrees of Freedom	DF	> 5	The difference between the number of fitting species and the number of fitting sources.
Ratio of Calculated to Measured	RATIO C/M	0.5 to 2.0	The ratio of the calculated to measured concentration of an ambient species. Ideally, this value should be 1.0.
Ratio of Residual to Uncertainty	RATIO R/U	-2.0 to 2.0	The ratio of the residual (calculated minus measured) to the uncertainty of the residual (square root of the sum of squares of the uncertainties).

6.0. PM_{2.5} Sampling Results

In presenting the final PM_{2.5} results (in units of microgram of analyte per cubic meter volume of air collected, $\mu\text{g}/\text{m}^3$), there were several sample days throughout the program that were excluded from the overall average calculations due to sampler malfunctions or collection errors. Sample days where a

good statistical fit was not achieved using the CMB model were also excluded from the average calculations. A complete listing of these sample days along with a description of why the data points were excluded are presented in **Appendix B**.

6.1. PM_{2.5} Mass Results

Table 4 presents the average PM_{2.5} mass that was measured from Teflon filters collected at each of the sites throughout the program. Overall, wintertime PM_{2.5} average concentrations ranged from 8.2 µg/m³ (RAMS, winter 2008/2009) up to 46.9 µg/m³ (NPF3, winter 2012/2013), with many of the sites having frequent exceedances of the 24-hour NAAQS on the scheduled sample days. Results from the summer 2012 show that PM_{2.5} mass averages were very low, averaging less than 6.0 µg/m³ at both the State Building and NCORE sites. Note that in **Table 4** there are two PM_{2.5} masses listed for the winter 2008/2009 State Building and RAMS sites. The first PM_{2.5} mass values are the average PM_{2.5} concentrations originally presented in the Final Report submitted to ADEC (dated July 23, 2012). For consistency with the CMB modeling results presented in this report, updated CMB modeling was conducted on the 2008/2009 datasets using OMNI profiles in addition to automobile and diesel source profiles (note that auto / diesel exhaust were not identified in the initial OMNI modeling). The second PM_{2.5} mass values presented for 2008/2009 (State Building and RAMS) are the average PM_{2.5} concentrations for those sample days in which updated CMB modeling was conducted. Please note that when using the OMNI profiles, there were times when a statistical fit could not be obtained for a specific sampling day, thus explaining the smaller “n” and therefore different average PM_{2.5} mass (compared to the EPA modeling runs) for specific winters/sites. For the remainder of the winters (2009/2010 through 2012/2013), a single asterisk “*” indicates the average concentrations for the days in which modeling was conducted using only the EPA profiles, while “**” indicates the average PM_{2.5} concentrations for those days in which only OMNI profiles were used for modeling. No asterisk indicates that the number of modeling runs was identical between the EPA and OMNI modeling activities (therefore PM_{2.5} averages were the same).

6.2. PM_{2.5} Chemical Speciation Results

Tables 5 through 11 present the average concentrations (in µg/m³) of elements, ions, and OC/EC, respectively, measured throughout the sampling programs at each of the sites/years. The minimum detection limits (MDL) in µg/m³ for each compound are also presented, with the bolded values (within the tables) indicating analyte concentrations measured at or above the MDL. All MDLs were provided by RTI. Also please note that **Table 6** contains the revised average speciated data for the winter 2008/2009 where CMB modeling was updated using the OMNI profiles (along with the automobile and diesel exhaust profiles). For the remainder of the speciated data results in **Tables 7-11**, a single asterisk “*” indicates the average speciated data concentrations for the days in which modeling was conducted using only the EPA profiles, while “**” indicates the average concentrations for those days in which only OMNI profiles were used for modeling. No asterisk indicates that the number of modeling runs was identical between the EPA and OMNI modeling activities (therefore speciated analyte averages were the same).

Out of the 36 elements quantified, only about 13 were consistently measured at or above their reported MDLs. Sulfur typically had the highest concentration of the measured elements (especially at the State Building and Peger Road sites), followed by chlorine and potassium. Regarding the ions that were measured, sulfate had the highest concentration at each of the sites, followed by ammonium and nitrate. Total Carbon (TC) measurements were always heavily influenced by the OC fractions at each of the sites. Results from the field and trip blanks for the species listed in **Tables 5-11** were minimal throughout the sampling/analytical program, therefore data were not blank corrected prior to using in the CMB model.

Table 4: Average PM_{2.5} Mass Concentrations (µg/m³).

Winter, Site	PM_{2.5} mass	Sampling Dates	n
2005/2006, State Building	18.9	11/3/05 – 3/30/06	36
2006/2007, State Building	19.9	11/1/06 – 3/31/07	39
2007/2008, State Building	18.7	11/2/07 – 3/31/08	40
Winter 2008/2009			
State Building	25.3, 24.4	11/8/08 – 4/7/09	47, 46
North Pole	18.9	1/25/09 – 4/7/09	21
RAMS	8.2, 8.3	1/25/09 – 4/7/09	23, 22
Peger Road	16.8	1/25/09 – 4/7/09	26
Winter 2009/2010			
State Building	28.8*, 24.5**	11/3/09 – 3/15/10	40*, 31**
North Pole	33.7	11/3/09 – 3/15/10	35
RAMS	36.7	11/15/09 – 3/15/10	29
Peger Road	29.0*, 29.5**	11/3/09 – 3/15/10	38*, 37**
Winter 2010/2011			
State Building	20.2	11/1/10 – 2/8/11	15
North Pole	26.8	1/9/11 – 2/5/11	10
Peger Road	28.6	1/9/11 – 2/5/11	10
Winter 2011/2012			
State Building	20.0*, 19.5**	11/2/11 – 3/31/12	38*, 36**
North Pole	24.2*, 23.0**	11/2/11 – 3/25/12	35*, 34**
RAMS	22.1*, 22.7**	12/20/11 – 2/27/12	16*, 15**
NCORE	19.5*, 19.3**	11/2/11 – 3/31/12	44*, 42**
NPF3	18.3	3/1/12 – 3/31/12	7
Summer 2012			
State Building	5.7	6/2/12-8/31/12	20
NCORE	5.1	6/14/12-8/31/12	17
Winter 2012/2013			
State Building	21.8	11/2/12 – 3/29/13	29
NPE	28.1*, 27.8**	11/2/12 – 3/29/13	41*, 40**
NCORE	25.5*, 25.1**	11/2/12 – 3/29/13	38*, 39**
NPF3	46.9	11/2/13 – 3/29/13	42

Note: The minimum detection limit (MDL) for the State Building site was 0.740 µg/m³, and ~0.745 µg/m³ for all of the other sites. *EPA profiles used. ** OMNI profiles used.

Table 5: Average PM_{2.5} Elemental, Ion, and OC/EC Concentrations (µg/m³) – State Building, Winters of 2005/2006, 2006/2007, and 2007/2008.

	State Building 11/3/05 – 3/30/06 n= 36	State Building 11/1/06 – 3/31/07 n=39	State Building 11/2/07 – 3/31/08 n=40	MDL
Magnesium	0.009	0.008	0.006	0.011
Aluminum	0.020	0.031	0.009	0.013
Silicon	0.063	0.042	0.048	0.011
Phosphorus	0.000	0.002	0.001	0.010
Sulfur	1.339	1.249	1.153	0.007
Chlorine	0.017	0.068	0.073	0.005
Potassium	0.083	0.081	0.102	0.004
Calcium	0.056	0.029	0.029	0.005
Titanium	0.005	0.000	0.001	0.004
Vanadium	0.001	0.001	0.000	0.003
Chromium	0.002	0.012	0.002	0.002
Manganese	0.002	0.002	0.001	0.002
Iron	0.069	0.084	0.052	0.001
Nickel	0.001	0.004	0.001	0.001
Copper	0.004	0.006	0.004	0.001
Zinc	0.043	0.040	0.039	0.003
Gallium	0.001	0.000	0.000	0.002
Arsenic	0.001	0.001	0.001	0.001
Selenium	0.001	0.000	0.000	0.002
Bromine	0.005	0.004	0.003	0.002
Rubidium	0.001	0.000	0.000	0.002
Strontium	0.006	0.006	0.002	0.002
Yttrium	0.001	0.000	0.000	0.003
Zirconium	0.001	0.001	0.000	0.004
Molybdenum	0.000	0.000	0.000	0.006
Silver	0.003	0.002	0.001	0.013
Cadmium	0.003	0.001	0.001	0.017
Indium	0.003	0.001	0.000	0.018
Tin	0.005	0.003	0.002	0.025
Antimony	0.004	0.001	0.001	0.038
Barium	0.016	0.002	0.002	0.010
Lanthanum	0.006	0.000	0.000	0.008
Mercury	0.002	0.001	0.000	0.007
Lead	0.007	0.004	0.004	0.004
Sodium	0.045	0.041	0.028	0.037
Cobalt	0.000	0.000	0.000	0.001
Sulfate	3.816	3.479	3.215	0.010
Nitrate	1.102	1.054	0.954	0.007
Ammonium	1.648	1.573	1.446	0.017
Potassium	0.072	0.064	0.095	0.014
Sodium (ion)	0.066	0.072	0.076	0.027
Total Carbon	10.4	10.9	11.1	0.24
Organic Carbon	8.7	9.3	9.2	0.24
Elemental Carbon	1.7	1.6	1.8	0.24

Note: MDL–minimum detection limit. Bolded values indicate concentrations measured at or above the MDL.

Table 6: Average PM_{2.5} Elemental, Ion, and OC/EC Concentrations (µg/m³) – Winter 2008/2009.

	State Building 11/8/08 – 4/7/09 n= 47*, 46**	North Pole 1/25/09 – 4/7/09 n=21	RAMS 1/25/09 – 4/7/09 n=23*, 22**	Peger Road 1/25/09 – 4/7/09 n=26	MDL
Magnesium	0.011	0.012	0.016, 0.014	0.018	0.013, 0.011
Aluminum	0.021	0.005	0.011	0.016	0.014, 0.013
Silicon	0.049, 0.048	0.024	0.031, 0.032	0.062	0.011
Phosphorus	0.005	0.001	0.000	0.010	0.012, 0.010
Sulfur	1.730, 1.558	0.637	0.367, 0.369	0.968	0.008, 0.007
Chlorine	0.125, 0.123	0.103	0.100, 0.076	0.151	0.007, 0.005
Potassium	0.136, 0.131	0.113	0.041, 0.042	0.069	0.006, 0.004
Calcium	0.047, 0.046	0.014	0.015	0.045	0.006, 0.005
Titanium	0.001	0.000	0.000	0.001	0.005, 0.004
Vanadium	0.000	0.000	0.000	0.000	0.003
Chromium	0.003	0.004	0.000	0.000	0.002
Manganese	0.001	0.001	0.000	0.001	0.002
Iron	0.058, 0.054	0.027	0.017	0.053	0.002, 0.001
Nickel	0.001	0.001	0.000	0.000	0.001
Copper	0.004	0.001	0.001	0.004	0.002, 0.001
Zinc	0.065, 0.062	0.015	0.008	0.058	0.003, 0.004
Gallium	0.000	0.000	0.000	0.000	0.002
Arsenic	0.000	0.000	0.001	0.001	0.001, 0.002
Selenium	0.000	0.000	0.000	0.000	0.002
Bromine	0.005	0.003	0.005	0.007	0.002
Rubidium	0.000	0.000	0.000	0.000	0.002
Strontium	0.004	0.001	0.001	0.002	0.002
Yttrium	0.000	0.000	0.000	0.000	0.003
Zirconium	0.000	0.000	0.000	0.000	0.004, 0.005
Molybdenum	0.000	0.000	0.000	0.000	0.006, 0.009
Silver	0.001	0.002	0.001	0.002	0.013, 0.015
Cadmium	0.002	0.000	0.000	0.000	0.017, 0.019
Indium	0.001	0.002	0.002	0.003	0.018, 0.022
Tin	0.005	0.002	0.002	0.003	0.025, 0.032
Antimony	0.001	0.002	0.002, 0.001	0.001	0.038, 0.042
Barium	0.001	0.000	0.000	0.000	0.015, 0.010
Lanthanum	0.000	0.001	0.000	0.000	0.014, 0.008
Mercury	0.001	0.001	0.001	0.001	0.007, 0.009
Lead	0.003	0.002	0.003	0.005	0.004, 0.005
Sodium	0.113, 0.111	0.107	0.108, 0.092	0.141	0.037, 0.040
Cobalt	0.000	0.000	0.000	0.001	0.001
Sulfate	4.585, 4.194	1.739	1.052, 1.056	2.541	0.010
Nitrate	1.282, 1.268	0.709	0.615, 0.623	1.127	0.007
Ammonium	2.160, 1.974	0.683	0.430, 0.439	1.235	0.018, 0.017
Potassium	0.137, 0.134	0.135	0.058, 0.057	0.096	0.015, 0.014
Sodium (ion)	0.126, 0.126	0.155	0.148, 0.132	0.162	0.027, 0.030
Total Carbon	14.5, 13.7	12.6	5.1, 5.2	10.0	0.24
Organic Carbon	12.9, 12.2	11.7	4.7, 4.8	8.7	0.24
Elemental Carbon	1.6, 1.5	0.9	0.5	1.3	0.24

Note: MDL–minimum detection limit. MDLs include those from both the State building, and other three sites.

Bolded values indicate concentrations measured at or above the MDL. *Average concentrations originally presented in the Final Report submitted to ADEC (dated July 23, 2012). **Average concentrations for those sample days in which updated CMB modeling (with OMNI profiles as well as auto/diesel profiles) was conducted.

Table 7: Average PM_{2.5} Elemental, Ion, and OC/EC Concentrations (µg/m³) – Winter 2009/2010.

	State Building 11/3/09–3/15/10 n=40*, 31**	North Pole 11/3/09–3/15/10 n=35	RAMS 11/15/09–3/15/10 n=29	Peger Road 11/3/09–3/15/10 n=38*, 37**	MDL
Magnesium	0.009	0.004	0.003	0.007, 0.008	0.013, 0.011
Aluminum	0.020, 0.014	0.004	0.008	0.007	0.014, 0.013
Silicon	0.054, 0.050	0.031	0.057	0.073, 0.074	0.011
Phosphorus	0.008, 0.004	0.000	0.000	0.025, 0.026	0.012, 0.010
Sulfur	1.760, 1.404	0.915	1.388	1.618, 1.654	0.008, 0.007
Chlorine	0.151, 0.116	0.151	0.154	0.290, 0.297	0.007, 0.005
Potassium	0.130, 0.114	0.202	0.185	0.132, 0.134	0.006, 0.004
Calcium	0.042, 0.039	0.014	0.028	0.058, 0.059	0.006, 0.005
Titanium	0.001, 0.002	0.001	0.002	0.003	0.005, 0.004
Vanadium	0.000	0.000	0.000	0.000	0.003
Chromium	0.002	0.000	0.004	0.001	0.002
Manganese	0.002	0.001	0.006	0.004	0.002
Iron	0.061, 0.055	0.024	0.080	0.109, 0.111	0.002, 0.001
Nickel	0.001	0.000	0.004	0.000	0.001
Copper	0.006, 0.004	0.006	0.004	0.008	0.002, 0.001
Zinc	0.072, 0.061	0.031	0.045	0.121, 0.123	0.003, 0.004
Gallium	0.000	0.000	0.000	0.000	0.002
Arsenic	0.001, 0.000	0.000	0.001	0.001	0.001, 0.002
Selenium	0.000	0.000	0.000	0.000	0.002
Bromine	0.004, 0.003	0.004	0.011	0.011	0.002
Rubidium	0.001	0.000	0.000	0.000	0.002
Strontium	0.002	0.000	0.001	0.001	0.002
Yttrium	0.000	0.000	0.000	0.000	0.003
Zirconium	0.001	0.000	0.000	0.000	0.004, 0.005
Molybdenum	0.000	0.000	0.000	0.000	0.006, 0.009
Silver	0.002	0.002	0.001	0.002	0.013, 0.015
Cadmium	0.003	0.001	0.001	0.003	0.017, 0.019
Indium	0.003	0.001	0.003	0.001	0.018, 0.022
Tin	0.004, 0.003	0.004	0.004	0.001	0.025, 0.032
Antimony	0.007, 0.008	0.008	0.008	0.006, 0.005	0.038, 0.042
Barium	0.005	0.000	0.000	0.000	0.015, 0.010
Lanthanum	0.000	0.000	0.000	0.000	0.014, 0.008
Mercury	0.000	0.000	0.000	0.000	0.007, 0.009
Lead	0.005, 0.004	0.004	0.014	0.017	0.004, 0.005
Sodium	0.084, 0.077	0.076	0.086	0.140, 0.142	0.037, 0.040
Cobalt	0.000	0.000	0.000	0.000	0.001
Sulfate	4.633, 3.911	2.452	3.890	4.173, 4.256	0.010
Nitrate	1.505, 1.417	0.888	1.029	1.706, 1.725	0.007
Ammonium	2.433, 1.894	1.232	1.822	2.420, 2.460	0.018, 0.017
Potassium	0.141, 0.129	0.184	0.170	0.123, 0.125	0.015, 0.014
Sodium (ion)	0.080, 0.079	0.117	0.135	0.134, 0.131	0.027, 0.030
Total Carbon	13.2, 11.4	22.3	24.1	16.2, 16.5	0.24
Organic Carbon	11.5, 10.0	19.8	21.5	13.4, 13.7	0.24
Elemental Carbon	1.7, 1.4	2.5	2.6	2.8	0.24

Note: MDL–minimum detection limit. MDLs include those from both the State building, and other three sites. Bolded values indicate concentrations measured at or above the MDL. *EPA runs only. **OMNI runs only.

Table 8: Average PM_{2.5} Elemental, Ion, and OC/EC Concentrations (µg/m³) – Winter 2010/2011.

Analyte	State Building 11/1/10–2/8/11 n=15	North Pole 1/9/11–2/5/11 n=10	Peger Road 1/9/11–2/5/11 n=10	MDL
Magnesium	0.001	0.000	0.000	0.013, 0.011
Aluminum	0.008	0.015	0.033	0.014, 0.013
Silicon	0.027	0.009	0.032	0.011
Phosphorus	0.002	0.000	0.014	0.012, 0.010
Sulfur	1.188	0.757	1.608	0.008, 0.007
Chlorine	0.089	0.112	0.280	0.007, 0.005
Potassium	0.089	0.184	0.142	0.006, 0.004
Calcium	0.027	0.016	0.046	0.006, 0.005
Titanium	0.001	0.000	0.001	0.005, 0.004
Vanadium	0.000	0.000	0.000	0.003
Chromium	0.002	0.000	0.000	0.002
Manganese	0.001	0.000	0.004	0.002
Iron	0.040	0.019	0.076	0.002, 0.001
Nickel	0.001	0.000	0.000	0.001
Copper	0.002	0.002	0.007	0.002, 0.001
Zinc	0.051	0.029	0.107	0.003, 0.004
Gallium	0.000	0.000	0.000	0.002
Arsenic	0.000	0.001	0.001	0.001, 0.002
Selenium	0.000	0.000	0.000	0.002
Bromine	0.004	0.002	0.010	0.002
Rubidium	0.000	0.000	0.000	0.002
Strontium	0.001	0.000	0.007	0.002
Yttrium	0.000	0.000	0.000	0.003
Zirconium	0.000	0.001	0.001	0.004, 0.005
Molybdenum	0.000	0.000	0.000	0.006, 0.009
Silver	0.001	0.000	0.000	0.013, 0.015
Cadmium	0.001	0.003	0.004	0.017, 0.019
Indium	0.002	0.005	0.001	0.018, 0.022
Tin	0.001	0.000	0.000	0.025, 0.032
Antimony	0.006	0.012	0.002	0.038, 0.042
Barium	0.000	0.000	0.000	0.015, 0.010
Lanthanum	0.000	0.000	0.000	0.014, 0.008
Mercury	0.000	0.000	0.000	0.007, 0.009
Lead	0.003	0.001	0.014	0.004, 0.005
Sodium	0.044	0.003	0.060	0.037, 0.040
Cobalt	0.000	0.000	0.001	0.001
Sulfate	3.352	2.393	5.047	0.010
Nitrate	1.158	0.755	1.790	0.007
Ammonium	1.565	0.885	2.396	0.018, 0.017
Potassium	0.084	0.165	0.147	0.015, 0.014
Sodium (ion)	0.030	0.062	0.081	0.027, 0.030
Total Carbon	8.5	16.7	15.3	0.24
Organic Carbon	7.5	14.6	12.6	0.24
Elemental Carbon	1.0	2.1	2.7	0.24

Note: MDL—minimum detection limit. MDLs include those from both the state building, and other two sites. Bolded values indicate concentrations measured at or above the MDL.

Table 9: Average PM_{2.5} Elemental, Ion, and OC/EC Concentrations (µg/m³) – Winter 2011/2012.

	State Building 11/2/11 – 3/31/12 n=38*, 36**	North Pole 11/2/11 – 3/25/12 n=35*, 34**	RAMS 12/20/11 – 2/27/12 n=16*, 15**	NCORE 11/2/11 – 3/31/12 n=44*, 42**	NPF3 3/1/12 – 3/31/12 n=7	MDL
Magnesium	0.011 , 0.009	0.019 , 0.017	0.015 , 0.016	0.017 , 0.018	0.023	0.011
Aluminum	0.009, 0.008	0.001	0.009	0.007, 0.008	0.010	0.013
Silicon	0.042 , 0.043	0.017	0.037 , 0.036	0.033 , 0.032	0.031	0.011
Phosphorus	0.000	0.000	0.000	0.000	0.000	0.010
Sulfur	1.203 , 1.153	0.655 , 0.627	0.971 , 0.998	1.049	0.584	0.007
Chlorine	0.080	0.150 , 0.145	0.113 , 0.118	0.112	0.164	0.005
Potassium	0.114 , 0.111	0.264 , 0.258	0.200 , 0.209	0.132	0.164	0.004
Calcium	0.028 , 0.027	0.017 , 0.016	0.032 , 0.033	0.026	0.014	0.005
Titanium	0.003	0.001, 0.000	0.001	0.001	0.000	0.004
Vanadium	0.000	0.000	0.000	0.000	0.000	0.003
Chromium	0.002 , 0.001	0.001	0.001	0.001	0.000	0.002
Manganese	0.001	0.001	0.002 , 0.003	0.002 , 0.001	0.001	0.002
Iron	0.042 , 0.041	0.020	0.062 , 0.064	0.039 , 0.037	0.015	0.001
Nickel	0.000	0.000	0.001	0.000	0.000	0.001
Copper	0.003	0.004	0.006	0.004	0.001	0.001
Zinc	0.041	0.023 , 0.022	0.039 , 0.041	0.037 , 0.036	0.012	0.003
Gallium	0.000	0.000	0.000	0.000	0.000	0.002
Arsenic	0.000	0.000	0.000	0.001	0.000	0.001
Selenium	0.000	0.000	0.000	0.000	0.000	0.002
Bromine	0.005	0.004 , 0.003	0.003	0.005	0.008	0.002
Rubidium	0.000	0.000	0.000	0.000	0.000	0.002
Strontium	0.003	0.002	0.006	0.003	0.000	0.002
Yttrium	0.000	0.000	0.000	0.000	0.000	0.003
Zirconium	0.001	0.001	0.002	0.001	0.000	0.004
Molybdenum	0.000	0.000	0.000	0.000	0.000	0.006
Silver	0.001	0.000	0.000	0.000	0.002	0.013
Cadmium	0.003	0.001	0.000	0.001	0.000	0.017
Indium	0.002	0.002	0.001	0.002	0.001	0.018
Tin	0.004	0.001, 0.002	0.005	0.002	0.000	0.025
Antimony	0.007, 0.006	0.008	0.005	0.008, 0.009	0.005	0.038
Barium	0.000	0.004	0.023 , 0.022	0.010	0.000	0.010
Lanthanum	0.000	0.000	0.000	0.000	0.000	0.008
Mercury	0.000	0.000	0.000	0.000	0.000	0.007
Lead	0.001, 0.002	0.001	0.002	0.002	0.000	0.004
Sodium	0.097 , 0.092	0.098 , 0.095	0.076 , 0.078	0.107 , 0.109	0.148	0.037
Cobalt	0.000	0.000	0.001	0.001	0.000	0.001
Sulfate	3.283 , 3.135	1.817 , 1.733	2.883 , 2.764	2.900 , 2.901	1.576	0.010
Nitrate	0.924 , 0.915	0.502 , 0.493	0.949 , 0.936	0.827 , 0.815	0.462	0.007
Ammonium	1.228 , 1.176	0.491 , 0.462	0.969 , 0.923	0.991 , 0.992	0.432	0.017
Potassium	0.095 , 0.093	0.237 , 0.231	0.157 , 0.159	0.105	0.114	0.014
Sodium (ion)	0.104 , 0.101	0.101 , 0.098	0.071 , 0.072	0.094 , 0.095	0.143	0.027
Total Carbon	8.5 , 8.6	13.7 , 13.4	12.4 , 12.2	10.6 , 10.9	12.5	0.24
Organic Carbon	7.3 , 7.4	12.5 , 12.3	10.6 , 10.4	9.0 , 9.2	11.3	0.24
Elemental Carbon	1.2 , 1.3	1.2 , 1.1	1.8	1.6	1.2	0.24

Note: MDL–minimum detection limit. Bolded values indicate concentrations measured at or above the MDL.

*EPA runs only. **OMNI runs only.

Table 10: Average PM_{2.5} Elemental, Ion, and OC/EC Concentrations (µg/m³) – Summer 2012.

	State Building 6/2/12 – 8/31/12 n=20	NCORE 6/14/12 – 8/31/12 n=17	MDL
Magnesium	0.001	0.000	0.011
Aluminum	0.021	0.021	0.013
Silicon	0.080	0.098	0.011
Phosphorus	0.000	0.000	0.010
Sulfur	0.143	0.146	0.007
Chlorine	0.005	0.002	0.005
Potassium	0.025	0.023	0.004
Calcium	0.018	0.020	0.005
Titanium	0.003	0.002	0.004
Vanadium	0.000	0.000	0.003
Chromium	0.002	0.000	0.002
Manganese	0.001	0.001	0.002
Iron	0.040	0.042	0.001
Nickel	0.000	0.000	0.001
Copper	0.001	0.001	0.001
Zinc	0.002	0.003	0.003
Gallium	0.000	0.000	0.002
Arsenic	0.000	0.000	0.001
Selenium	0.000	0.000	0.002
Bromine	0.001	0.001	0.002
Rubidium	0.000	0.000	0.002
Strontium	0.001	0.000	0.002
Yttrium	0.000	0.000	0.003
Zirconium	0.000	0.001	0.004
Molybdenum	0.000	0.000	0.006
Silver	0.001	0.000	0.013
Cadmium	0.002	0.000	0.017
Indium	0.002	0.000	0.018
Tin	0.005	0.001	0.025
Antimony	0.012	0.011	0.038
Barium	0.000	0.000	0.010
Lanthanum	0.000	0.000	0.008
Mercury	0.000	0.000	0.007
Lead	0.000	0.000	0.004
Sodium	0.007	0.011	0.037
Cobalt	0.000	0.000	0.001
Sulfate	0.358	0.311	0.010
Nitrate	0.181	0.207	0.007
Ammonium	0.051	0.025	0.017
Potassium	0.010	0.020	0.014
Sodium (ion)	0.017	0.059	0.027
Total Carbon	2.0	4.6	0.24
Organic Carbon	1.8	4.2	0.24
Elemental Carbon	0.22	0.4	0.24

Note: MDL—minimum detection limit. Bolded values indicate concentrations measured at or above the MDL.

Table 11: Average PM_{2.5} Elemental Concentrations (µg/m³) – Winter 2012/2013.

	State Building 11/2/12 – 3/29/13 n=29	NPE 11/2/12 – 3/29/13 n=41*, 40**	NCORE 11/2/12 – 3/29/13 n=38*, 39**	NPF3 11/2/13 – 3/29/13 n=42	MDL
Magnesium	0.007	0.010	0.006	0.010	0.011
Aluminum	0.008	0.003	0.008	0.001	0.013
Silicon	0.043	0.021	0.045, 0.044	0.029	0.011
Phosphorus	0.005	0.001	0.008	0.001	0.010
Sulfur	1.370	0.891, 0.892	1.602, 1.573	1.239	0.007
Chlorine	0.078	0.096, 0.097	0.081, 0.080	0.131	0.005
Potassium	0.154	0.310, 0.309	0.192, 0.189	0.438	0.004
Calcium	0.036	0.018	0.038	0.014	0.005
Titanium	0.001	0.000	0.001	0.001	0.004
Vanadium	0.000	0.000	0.000	0.000	0.003
Chromium	0.002	0.002	0.003	0.001	0.002
Manganese	0.001	0.001	0.001	0.001	0.002
Iron	0.051	0.031, 0.030	0.054, 0.053	0.028	0.001
Nickel	0.001	0.000	0.001, 0.000	0.000	0.001
Copper	0.003	0.002	0.003	0.002	0.001
Zinc	0.053	0.030	0.055	0.037	0.003
Gallium	0.000	0.000	0.000	0.000	0.002
Arsenic	0.000	0.000	0.000	0.001	0.001
Selenium	0.000	0.000	0.000	0.000	0.002
Bromine	0.004	0.004	0.004	0.003	0.002
Rubidium	0.000	0.000	0.000	0.001	0.002
Strontium	0.003	0.001	0.003	0.002	0.002
Yttrium	0.000	0.000	0.000	0.000	0.003
Zirconium	0.001	0.001	0.000	0.001	0.004
Molybdenum	0.000	0.000	0.000	0.000	0.006
Silver	0.000	0.001	0.001	0.001	0.013
Cadmium	0.001	0.001	0.000	0.000	0.017
Indium	0.001	0.003	0.003, 0.002	0.003	0.018
Tin	0.003	0.003	0.002	0.003	0.025
Antimony	0.007	0.001	0.001	0.002	0.038
Barium	0.002	0.001	0.004	0.001	0.010
Lanthanum	0.000	0.000	0.000	0.000	0.008
Mercury	0.000	0.000	0.000	0.000	0.007
Lead	0.002	0.001	0.002	0.002	0.004
Sodium	0.068	0.064, 0.066	0.062	0.066	0.037
Cobalt	0.000	0.000	0.000	0.000	0.001
Sulfate	3.496	2.476, 2.287	3.970, 4.088	3.004	0.010
Nitrate	1.074	0.686, 0.655	1.250	0.805	0.007
Ammonium	1.409	0.878, 0.783	1.636, 1.672	1.099	0.017
Potassium	0.118	0.288	0.177, 0.180	0.374	0.014
Sodium (ion)	0.047	0.181, 0.184	0.157, 0.155	0.130	0.027
Total Carbon	9.2	18.6, 18.3	14.3, 14.5	33.3	0.24
Organic Carbon	7.5	16.3, 16.0	12.1, 12.3	29.8	0.24
Elemental Carbon	1.6	2.4, 2.3	2.2, 2.2	3.6	0.24

Note: MDL–minimum detection limit. Bolded values indicate concentrations measured at or above the MDL.

*EPA runs only. **OMNI runs only.

7.0. Chemical Mass Balance Results

Tables 12 and 13 present the PM_{2.5} sources identified by the CMB model for each of the sites when using the EPA source profiles, including source contribution estimates (\pm standard errors) and % of total PM_{2.5}. **Tables 14 and 15** present the CMB results when using the OMNI profiles. In addition, **Figures 1-6** present the sources identified (over time) for each of the sites using the EPA source profiles, while **Figures 7-12** present the source trends for each of the sites using the OMNI profiles. Finally, CMB results are summarized as pie charts in **Figures 13-64** for both EPA and OMNI profiles for each winter/site, followed by a table comparing the results generated when using both the EPA and OMNI source profiles (**Tables 16-40**).

When using the EPA profiles, five source profile types were identified by the CMB model as contributors to the ambient PM_{2.5} throughout the winter months. Wood smoke (likely residential wood combustion) was the major source of PM_{2.5} identified, contributing between ~60% to over 80% of the measured PM_{2.5} at the monitoring sites. The other sources of PM_{2.5} identified by the CMB model were secondary sulfate (~7-21%), ammonium nitrate (3-11%), diesel exhaust (not detected-11%), and automobiles (not detected-7%). Approximately 1-2% of the PM_{2.5} was unexplained by the CMB model.

When utilizing the OMNI profiles in the CMB, the results are somewhat different. In addition to the five profiles identified using the EPA profiles, the OMNI source profile representing No. 2 fuel oil was also identified in nearly every CMB run. Wood smoke was still identified as the largest source of wintertime PM_{2.5} at the North Pole, RAMS, NCORE, NPF3, and NPE sites. However, at the State Building and Peger Road sites, No. 2 fuel oil combustion was found to be the largest source, contributing from 30-50% of the ambient wintertime PM_{2.5}.

It should be noted that the results of CMB modeling using OMNI profiles for the winter of 2008/2009 were originally presented to ADEC in a previous report (July 23, 2012). In carrying out the updated modeling using the OMNI profiles in other years (in addition to the winter of 2008/2009), it was discovered that automobiles and diesel exhaust contributed a small amount to ambient PM_{2.5} when using the OMNI profiles. To be consistent with results from the other winters, the 2008/2009 data sets were re-analyzed for the State Building, RAMS, North Pole, and Peger Road sites, with these results presented in **Table 14**. Results for the North Pole and RAMS sites remained unchanged to the previous modeling. However, for the State Building and Peger Road sites, automobiles and diesel exhaust which were not detected in the initial CMB modeling were now detected at low contributions (autos: 0.3-1.7%; diesel: 0.1-0.5%). Using this new profile combination also lowered the wood smoke contribution from 56.0% to 36.1% at the State Building, while No. 2 fuel oil contributions increased from 14.2% to 47.4%. At the Peger Road site, wood smoke was revised to 42.0% while No. 2 fuel oil was elevated from 27.2% to 38.7%. These new findings as well as those from the other winters illustrate that No. 2 fuel oil combustion is a significant source of ambient PM_{2.5} (when using the OMNI profiles) – especially at the State Building and Peger Road sites.

For the first time, CMB source apportionment modeling was conducted during the summer months in Fairbanks. Overall, ambient PM_{2.5} concentrations were very low at both sites during the summer of 2012 (5.7 $\mu\text{g}/\text{m}^3$ at the State Building, and 5.1 $\mu\text{g}/\text{m}^3$ at the NCORE site). Contributions of sulfate, ammonium nitrate, and street sand/road dust were very similar between the State Building and NCORE sites. More vehicle emissions were detected at the NCORE site compared to the State Building site when using both EPA and OMNI profiles. As expected, No. 2 fuel oil was not detected at either site. However, wood smoke was still determined to be the largest source at both sites (56-74%), likely due to residential outdoor biomass waste burning and influences from regional wildland fire events.

Table 12: Source Contribution Estimates \pm Standard Errors ($\mu\text{g}/\text{m}^3$) – EPA profiles.
 Note that percentages in parentheses are percent contributions to overall ambient $\text{PM}_{2.5}$ mass.

	Sulfate	Ammonium Nitrate	Diesel	Autos	Wood Smoke	Unexplained	$\text{PM}_{2.5}$ Mass	n	Sampling Dates
State Building 2005/2006	4.0 \pm 0.5 (21.0 %)	1.8 \pm 0.5 (9.6 %)	1.3 \pm 0.4 (7.1 %)	0.4 \pm 0.2 (2.3 %)	11.3 \pm 1.7 (59.8 %)	0.1 (0.3 %)	18.9	36	11/3/05- 3/30/06
State Building 2006/2007	3.7 \pm 0.5 (18.7 %)	1.7 \pm 0.5 (8.4 %)	1.5 \pm 0.5 (7.6 %)	1.1 \pm 0.4 (5.8 %)	11.5 \pm 2.0 (57.9 %)	0.3 (1.6 %)	19.9	39	11/1/06- 3/31/07
State Building 2007/2008	3.4 \pm 0.4 (18.2 %)	1.5 \pm 0.5 (8.1 %)	1.7 \pm 0.5 (9.0 %)	1.2 \pm 0.4 (6.2 %)	10.9 \pm 1.6 (58.5 %)	0.02 (0.1 %)	18.7	40	11/2/07- 3/31/08
2008/2009	Sulfate	Ammonium Nitrate	Diesel	Autos	Wood Smoke	Unexplained	$\text{PM}_{2.5}$ Mass	n	Sampling Dates
State Building	5.1 \pm 0.6 (20.0 %)	2.1 \pm 0.7 (8.1 %)	0.3 \pm 0.1 (1.1 %)	1.7 \pm 0.7 (6.8 %)	16.0 \pm 2.3 (63.1 %)	0.2 (0.8 %)	25.3	47	11/8/08- 4/7/09
North Pole	1.9 \pm 0.2 (9.8 %)	1.0 \pm 0.2 (5.1 %)	0.2 \pm 0.05 (0.8 %)	0.7 \pm 0.3 (3.7 %)	15.0 \pm 2.0 (79.8 %)	0.2 (0.8 %)	18.9	21	1/25/09- 4/7/09
RAMS	1.1 \pm 0.1 (13.0 %)	0.9 \pm 0.1 (10.5 %)	ND	ND	6.3 \pm 0.8 (76.0 %)	0.04 (0.5 %)	8.2	23	1/25/09- 4/7/09
Peger Road	2.8 \pm 0.3 (16.7 %)	1.5 \pm 0.4 (8.9 %)	1.2 \pm 0.5 (7.3 %)	0.7 \pm 0.2 (3.9 %)	10.6 \pm 1.6 (62.7 %)	0.1 (0.5 %)	16.8	26	1/25/09- 4/7/09
2009/2010	Sulfate	Ammonium Nitrate	Diesel	Autos	Wood Smoke	Unexplained	$\text{PM}_{2.5}$ Mass	n	Sampling Dates
State Building	5.2 \pm 0.6 (18.1 %)	2.5 \pm 0.7 (8.9 %)	0.6 \pm 0.3 (2.2 %)	0.7 \pm 0.3 (2.5 %)	19.5 \pm 1.9 (67.8 %)	0.2 (0.6 %)	28.8	40	11/3/09- 3/15/10
North Pole	2.6 \pm 0.3 (7.8 %)	1.2 \pm 0.3 (3.6 %)	0.8 \pm 0.2 (2.5 %)	1.3 \pm 0.4 (3.8 %)	27.1 \pm 3.7 (81.2 %)	0.3 (1.0 %)	33.7	35	11/3/09- 3/15/10
RAMS	4.0 \pm 0.5 (10.9 %)	0.9 \pm 0.2 (2.5 %)	2.5 \pm 0.6 (6.8 %)	2.3 \pm 0.7 (6.2 %)	26.9 \pm 4.1 (73.5 %)	0.04 (0.1 %)	36.7	29	11/15/09- 3/15/10
Peger Road	4.8 \pm 0.5 (16.5 %)	2.1 \pm 0.6 (7.4 %)	2.8 \pm 0.7 (9.6 %)	0.4 \pm 0.1 (1.3 %)	18.6 \pm 3.0 (64.4 %)	0.3 (0.9 %)	29.0	38	11/3/09- 3/15/10
2010/2011	Sulfate	Ammonium Nitrate	Diesel	Autos	Wood Smoke	Unexplained	$\text{PM}_{2.5}$ Mass	n	Sampling Dates
State Building	3.5 \pm 0.4	1.7 \pm 0.5	ND	0.4 \pm 0.1	14.6 \pm 1.1	0.004	20.2	15	11/1/10-

	(17.3 %)	(8.4 %)		(1.9 %)	(72.4 %)	(0.02 %)			2/8/11
North Pole	2.1±0.3 (8.0 %)	0.9±0.2 (3.5 %)	0.9±0.3 (3.4 %)	1.4±0.5 (5.1 %)	21.3±3.2 (79.4 %)	0.2 (0.6 %)	26.8	10	1/9/11- 2/5/11
Peger Road	4.8±0.5 (16.6 %)	2.0±0.5 (7.1 %)	0.8±0.2 (2.9 %)	0.7±0.3 (2.5 %)	20.2±3.9 (70.6 %)	0.1 (0.3 %)	28.6	10	1/9/11- 2/5/11
2011/2012	Sulfate	Ammonium Nitrate	Diesel	Autos	Wood Smoke	Unexplained	PM_{2.5} Mass	n	Sampling Dates
State Building	3.5±0.4 (17.8 %)	1.5±0.5 (7.5 %)	0.2±0.04 (1.2 %)	0.4±0.1 (2.1 %)	14.0±1.4 (70.4 %)	0.2 (1.0 %)	20.0	38	11/2/11- 3/31/12
North Pole	1.8±0.2 (7.8 %)	0.7±0.2 (3.1 %)	0.1±0.04 (0.6 %)	0.3±0.1 (1.2 %)	20.4±2.3 (85.5 %)	0.4 (1.9 %)	24.2	35	11/2/11- 3/25/12
RAMS	2.9±0.3 (13.2 %)	1.4±0.4 (6.4 %)	1.2±0.3 (5.7 %)	0.9±0.4 (4.0 %)	14.9±1.8 (69.0 %)	0.4 (1.8 %)	22.1	16	12/20/11- 2/27/12
NCORE	3.0±0.3 (15.8 %)	1.3±0.4 (6.8 %)	1.4±0.5 (7.5 %)	0.8±0.3 (4.2 %)	12.4±1.6 (64.4 %)	0.2 (1.3 %)	19.5	44	11/2/11- 3/31/12
NPF3	1.7±0.2 (9.2 %)	0.7±0.2 (3.8 %)	0.9±0.4 (4.9 %)	0.8±0.4 (4.2 %)	14.2±2.0 (77.0 %)	0.2 (1.0 %)	18.3	7	3/1/12- 3/31/12
2012/2013	Sulfate	Ammonium Nitrate	Diesel	Autos	Wood Smoke	Unexplained	PM_{2.5} Mass	n	Sampling Dates
State Building	3.9±0.5 (17.9 %)	1.7±0.5 (8.0 %)	1.2±0.4 (5.5 %)	0.1±0.04 (0.5 %)	14.7±1.5 (67.7 %)	0.1 (0.6 %)	21.8	29	11/2/12- 3/29/13
NPE	2.5±0.3 (9.0 %)	1.1±0.3 (3.8 %)	3.0±0.6 (10.9 %)	0.7±0.2 (2.6 %)	20.3±2.5 (72.8 %)	0.2 (0.8 %)	28.1	41	11/2/12- 3/29/13
NCORE	4.7±0.5 (18.4 %)	2.0±0.6 (7.9 %)	2.4±0.7 (9.6 %)	1.1±0.5 (4.4 %)	15.1±2.0 (59.3 %)	0.1 (0.3 %)	25.5	38	11/2/12- 3/29/13
NPF3	3.4±0.4 (7.4 %)	1.3±0.4 (2.8 %)	4.5±0.9 (9.8 %)	0.6±0.2 (1.4 %)	35.9±4.2 (77.6 %)	0.5 (1.0 %)	46.9	42	11/2/12- 3/29/13

ND: not detected by the CMB model. Sampling was not conducted at the RAMS site during the winter of 2010/2011.

Table 13: Source Contribution Estimates ± Standard Errors (µg/m³) – Summer 2012 EPA Profiles.

Summer 2012	Sulfate	Ammonium Nitrate	Diesel	Autos	Street Sand	Wood Smoke	Unexplained	PM_{2.5} Mass	n	Sampling Dates
State Building	0.4±0.1 (7.1 %)	0.2±0.1 (3.9 %)	0.01±0.003 (0.1 %)	0.2±0.1 (3.9 %)	0.3±0.1 (4.4 %)	4.2±0.2 (73.7 %)	0.4 (6.9 %)	5.7	20	6/2/12- 8/31/12
NCORE	0.4±0.1 (6.8 %)	0.2±0.1 (3.8 %)	0.3±0.1 (4.9 %)	1.0±0.2 (17.2%)	0.3±0.1 (4.6 %)	3.3±0.4 (56.0 %)	0.4 (6.7 %)	5.1	17	6/14/12- 8/31/12

Figure 1: State Building Source Contribution Estimates ($\mu\text{g}/\text{m}^3$) – EPA profiles.

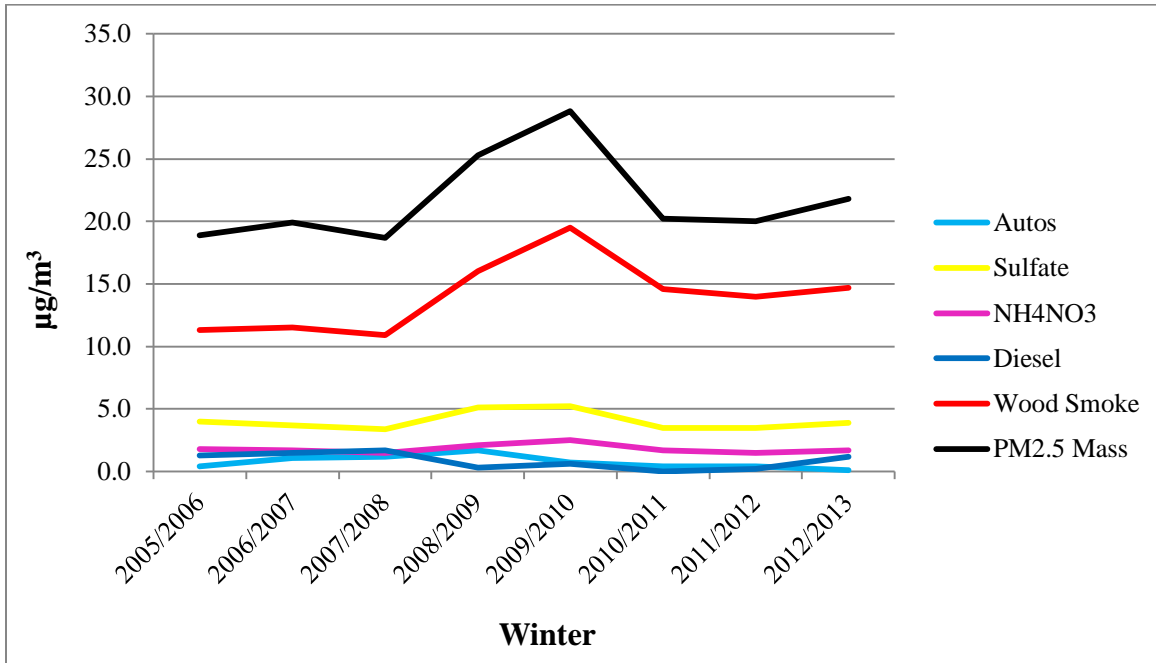


Figure 2: North Pole Source Contribution Estimates ($\mu\text{g}/\text{m}^3$) – EPA profiles.

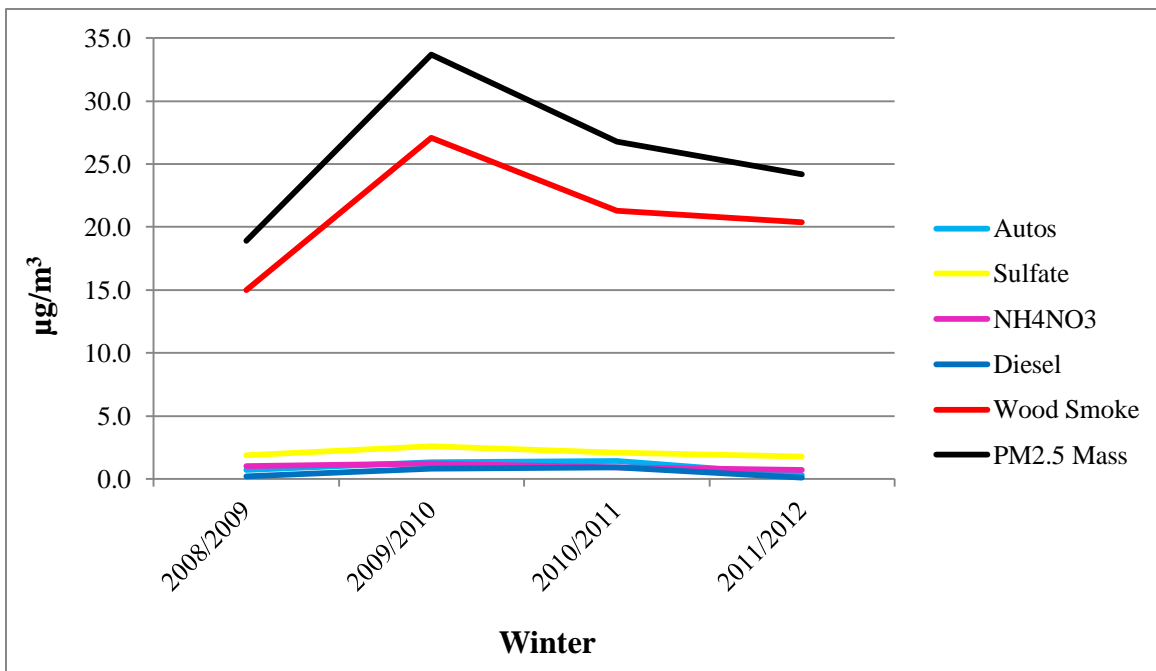


Figure 3: RAMS Source Contribution Estimates ($\mu\text{g}/\text{m}^3$) – EPA profiles.

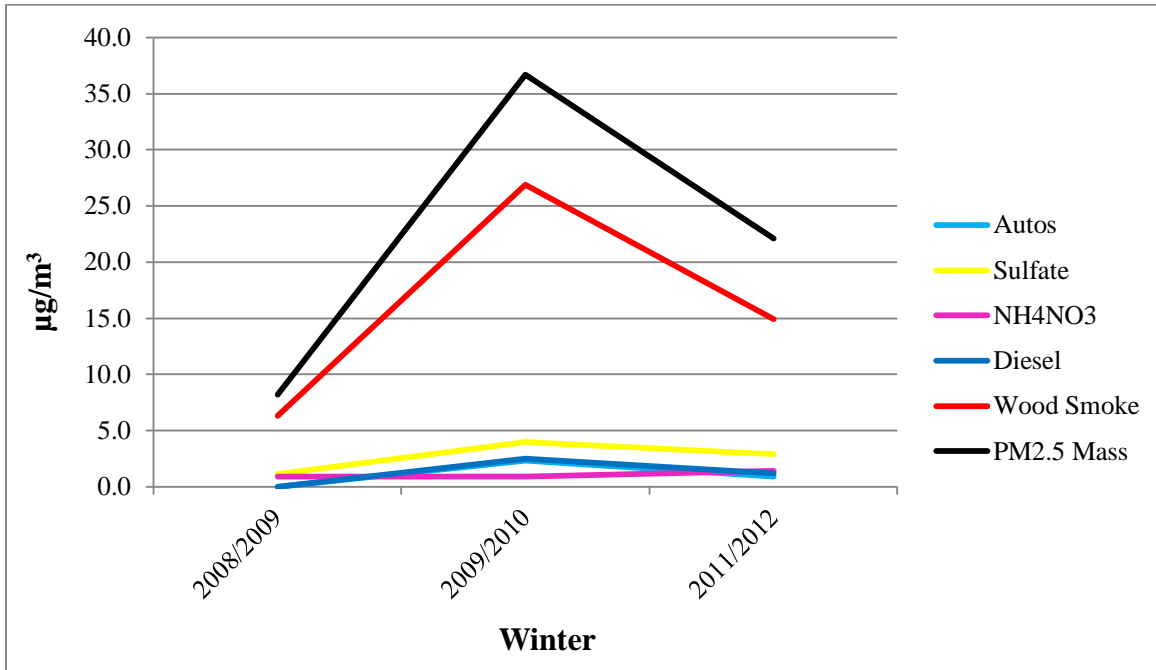


Figure 4: Peger Road Source Contribution Estimates ($\mu\text{g}/\text{m}^3$) – EPA profiles.

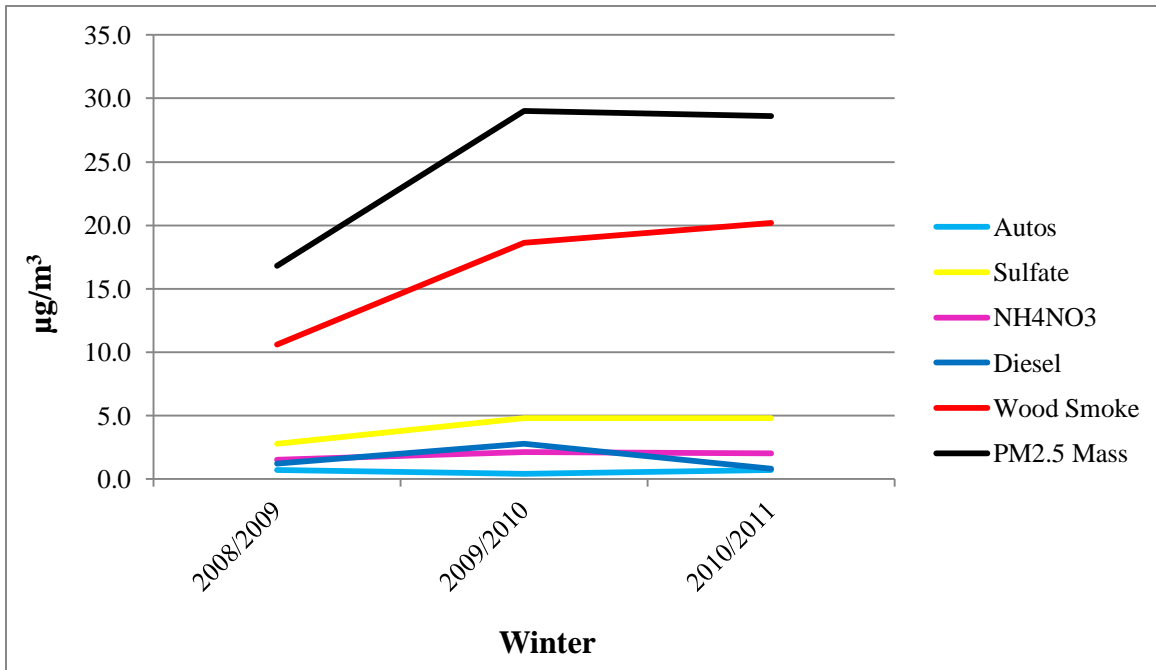


Figure 5: NCORE Source Contribution Estimates ($\mu\text{g}/\text{m}^3$) – EPA profiles.

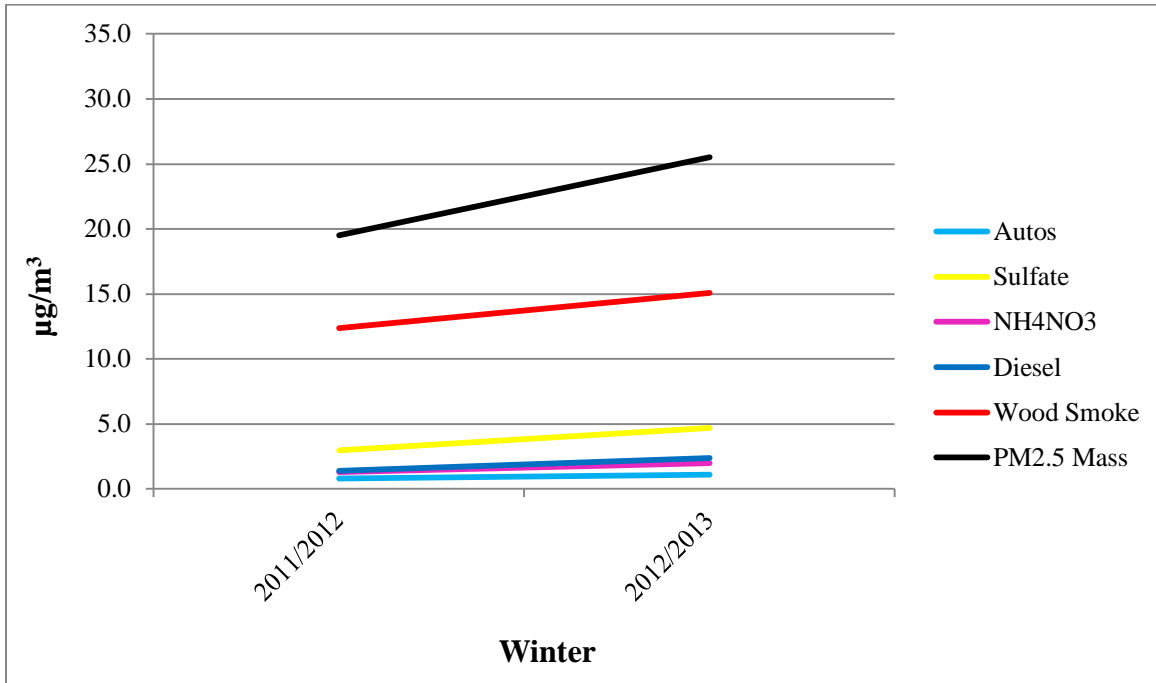


Figure 6: NPF3 Source Contribution Estimates ($\mu\text{g}/\text{m}^3$) – EPA profiles.

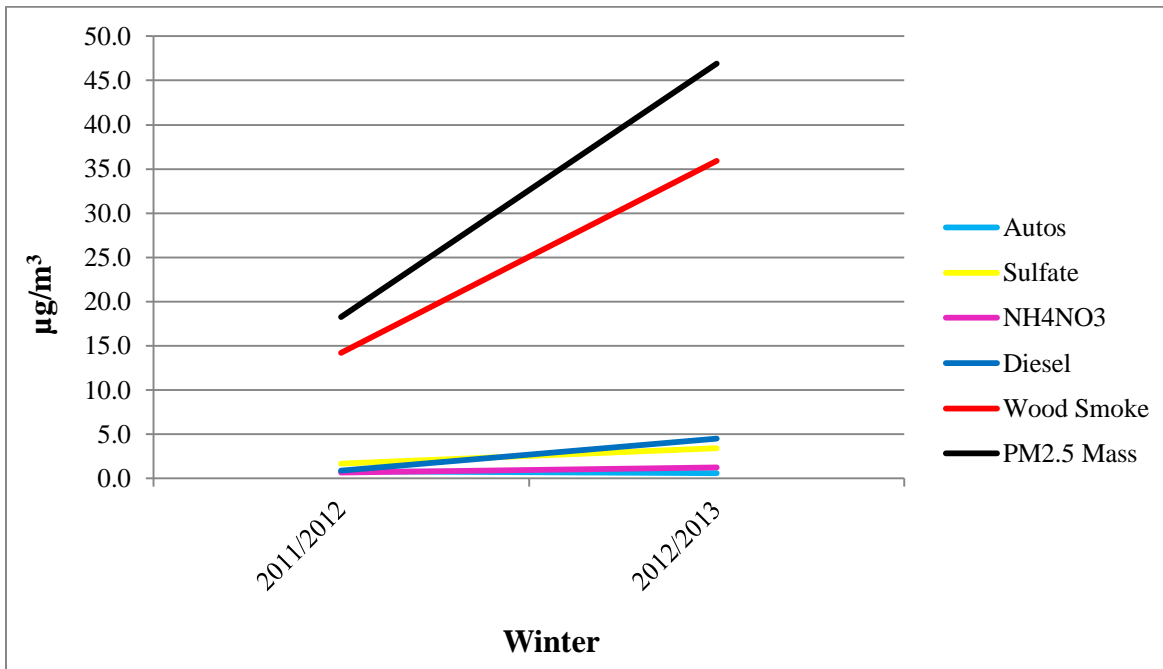


Table 14: Source Contribution Estimates ± Standard Errors ($\mu\text{g}/\text{m}^3$) – OMNI Profiles.Note that percentages in parentheses are percent contributions to overall ambient $\text{PM}_{2.5}$ mass.

	Sulfate	Ammonium Nitrate	Diesel	Autos	Wood Smoke	No. 2 Fuel Oil	Unexplained	$\text{PM}_{2.5}$ Mass	n	Sampling Dates
State Building 2005/2006	2.4±0.5 (12.8 %)	1.3 ±0.3 (6.7 %)	0.4±0.2 (2.3 %)	Not Detected	5.9±1.6 (31.7 %)	8.4±1.6 (44.7 %)	0.4 (1.9 %)	18.9	36	11/3/05-3/30/06
State Building 2006/2007	2.0±0.4 (10.1 %)	1.1 ±0.3 (5.7 %)	0.2±0.1 (0.9 %)	0.3±0.1 (1.5 %)	7.3±1.9 (36.6 %)	9.0±1.7 (45.0 %)	0.03 (0.1 %)	19.9	39	11/1/06-3/31/07
State Building 2007/2008	1.9±0.4 (10.0 %)	1.0 ±0.3 (5.5 %)	1.0±0.4 (5.5 %)	0.3±0.1 (1.6 %)	5.9±1.5 (31.9 %)	8.4±1.5 (45.4 %)	0.01 (0.1 %)	18.7	40	11/2/07-3/31/08
2008/2009	Sulfate	Ammonium Nitrate	Diesel	Autos	Wood Smoke	No. 2 Fuel Oil	Unexplained	$\text{PM}_{2.5}$ Mass	n	Sampling Dates
*State Building	4.4±0.6 (17.9 %)	1.9 ±0.6 (7.9 %)	Not Detected	Not Detected	13.8±1.7 (56.0 %)	3.5±0.7 (14.2 %)	1.0 (4.0 %)	25.3	47	11/8/08-4/7/09
**State Building	2.5±0.5 (10.4 %)	1.2 ±0.3 (5.2 %)	0.04 ±0.02 (0.1 %)	0.06 ±0.03 (0.3 %)	8.7±1.9 (36.1 %)	11.4±1.8 (47.4 %)	0.1 (0.5 %)	24.4	46	11/8/08-4/7/09
North Pole	1.4±0.2 (7.6 %)	0.9 ±0.2 (4.7 %)	Not Detected	Not Detected	13.6±1.2 (73.4 %)	2.1±0.5 (11.1 %)	0.6 (3.3 %)	18.9	21	1/25/09-4/7/09
RAMS	0.8±0.1 (9.2 %)	0.8 ±0.1 (9.2 %)	Not Detected	Not Detected	5.4±0.8 (63.9 %)	1.4±0.4 (16.8 %)	0.1 (0.9 %)	8.3	22	1/25/09-4/7/09
*Peger Road	2.0±0.3 (11.7 %)	1.4 ±0.3 (8.4 %)	Not Detected	Not Detected	8.6±1.2 (51.0 %)	4.6±0.9 (27.2 %)	0.3 (1.6 %)	16.8	26	1/25/09-4/7/09
**Peger Road	1.6±0.3 (9.6 %)	1.2 ±0.2 (7.3 %)	0.1±0.04 (0.5 %)	0.3±0.1 (1.7 %)	7.1±1.4 (42.0 %)	6.6±1.3 (38.7 %)	0.04 (0.3 %)	16.8	26	1/25/09-4/7/09
2009/2010	Sulfate	Ammonium Nitrate	Diesel	Autos	Wood Smoke	No. 2 Fuel Oil	Unexplained	$\text{PM}_{2.5}$ Mass	n	Sampling Dates
State Building	2.2±0.5 (9.3 %)	1.6 ±0.3 (6.5 %)	0.4±0.1 (1.8 %)	0.4±0.1 (1.4 %)	8.7±2.0 (36.0 %)	10.0±1.8 (41.1 %)	1.0 (3.9 %)	24.5	31	11/3/09-3/15/10
North Pole	1.1±0.2 (3.2 %)	0.9 ±0.2 (2.6 %)	1.5±0.4 (4.3 %)	1.0±0.4 (2.9 %)	22.4±2.1 (65.1 %)	7.3±0.9 (21.3 %)	0.2 (0.6 %)	33.7	35	11/3/09-3/15/10
RAMS	1.8±0.4 (4.9 %)	0.9 ±0.2 (2.5 %)	0.8±0.3 (2.3 %)	0.9±0.4 (2.5 %)	21.0±2.2 (57.2 %)	11.2±1.4 (30.5 %)	0.1 (0.1 %)	36.7	29	11/15/09-3/15/10
Peger Road	2.3±0.5 (7.8 %)	1.9 ±0.4 (6.4 %)	1.7±0.5 (5.7 %)	0.4±0.2 (1.4 %)	9.2±2.5 (31.2 %)	13.7±2.1 (46.3 %)	0.3 (1.2 %)	29.5	37	11/3/09-3/15/10

2010/2011	Sulfate	Ammonium Nitrate	Diesel	Autos	Wood Smoke	No. 2 Fuel Oil	Unexplained	PM_{2.5} Mass	n	Sampling Dates
State Building	2.0±0.4 (9.8 %)	1.3 ±0.3 (6.6 %)	0.2±0.04 (0.9 %)	0.2±0.1 (1.1 %)	6.5±1.7 (32.7 %)	8.3±1.5 (41.5 %)	1.5 (7.5 %)	20.2	15	11/1/10- 2/8/11
North Pole	1.0±0.2 (3.9 %)	0.7 ±0.1 (2.7 %)	0.9±0.3 (3.3 %)	1.9±0.5 (7.1 %)	16.6±1.9 (62.5 %)	5.3±0.8 (20.0 %)	0.2 (0.6 %)	26.8	10	1/9/11- 2/5/11
Peger Road	2.1±0.5 (7.3 %)	2.0 ±0.4 (6.7 %)	1.0±0.3 (3.3 %)	0.6±0.2 (2.2 %)	9.5±2.6 (32.7 %)	13.5±2.1 (46.4 %)	0.4 (1.3 %)	28.6	10	1/9/11- 2/5/11
2011/2012	Sulfate	Ammonium Nitrate	Diesel	Autos	Wood Smoke	No. 2 Fuel Oil	Unexplained	PM_{2.5} Mass	n	Sampling Dates
State Building	2.2±0.4 (11.0 %)	1.0 ±0.3 (5.1 %)	0.5±0.1 (2.3 %)	0.8±0.2 (4.3 %)	7.6±1.6 (38.5 %)	6.4±1.5 (32.2 %)	1.3 (6.6 %)	19.5	36	11/2/11- 3/31/12
North Pole	1.2±0.2 (5.3 %)	0.5 ±0.1 (2.1 %)	None Detected	0.6±0.2 (2.4 %)	17.3±1.6 (75.4 %)	2.4±0.7 (10.3 %)	1.0 (4.5 %)	23.0	34	11/2/11- 3/25/12
RAMS	1.9±0.4 (8.4 %)	1.0 ±0.3 (4.7 %)	0.3±0.1 (1.3 %)	0.9±0.4 (4.0 %)	11.5±1.9 (51.4 %)	4.9±1.5 (21.8 %)	1.9 (8.5 %)	22.7	15	12/20/11- 2/27/12
NCORE	2.0±0.4 (10.5 %)	0.9 ±0.3 (4.6 %)	0.2±0.1 (1.1 %)	0.4±0.2 (2.1 %)	10.1±1.7 (53.0 %)	5.4±1.4 (28.2 %)	0.1 (0.5 %)	19.3	42	11/2/11- 3/31/12
NPF3	1.2±0.2 (6.4 %)	0.5 ±0.2 (2.7 %)	None Detected	None Detected	14.1±1.3 (76.6 %)	2.2±0.7 (12.1 %)	0.4 (2.2 %)	18.3	7	3/1/12- 3/31/12
2012/2013	Sulfate	Ammonium Nitrate	Diesel	Autos	Wood Smoke	No. 2 Fuel Oil	Unexplained	PM_{2.5} Mass	n	Sampling Dates
State Building	2.9±0.5 (13.3 %)	1.3 ±0.4 (6.1 %)	0.2±0.1 (0.9 %)	0.4±0.2 (2.0 %)	8.7±1.8 (40.1 %)	6.0±1.5 (27.6 %)	2.1 (9.9 %)	21.8	29	11/2/12- 3/29/13
NPE	1.5±0.3 (5.4 %)	0.6 ±0.1 (2.0 %)	0.8±0.2 (2.8 %)	0.8±0.2 (2.9 %)	18.8±1.8 (66.6 %)	4.9±1.1 (17.1 %)	0.9 (3.1 %)	27.8	40	11/2/12- 3/29/13
NCORE	3.0±0.5 (12.1 %)	1.3 ±0.3 (5.2 %)	0.4±0.1 (1.5 %)	0.7±0.2 (2.6 %)	11.0±2.0 (44.2 %)	8.5±1.8 (34.1 %)	0.1 (0.2 %)	25.1	39	11/2/12- 3/29/13
NPF3	2.2±0.4 (4.8 %)	0.6 ±0.1 (1.3 %)	0.4±0.1 (1.0 %)	0.1±0.03 (0.2 %)	34.7±2.3 (75.2 %)	6.4±1.3 (13.8 %)	1.8 (3.8 %)	46.9	42	11/2/12- 3/29/13

ND: not detected by the CMB model. Sampling was not conducted at the RAMS site during the winter of 2010/2011. *CMB results originally presented in the Final Report submitted to ADEC (dated July 23, 2012). **Updated CMB modeling was conducted.

Table 15: Source Contribution Estimates \pm Standard Errors ($\mu\text{g}/\text{m}^3$) – Summer 2012 OMNI Profiles.

Summer 2012	Sulfate	Ammonium Nitrate	Diesel	Autos	Street Sand	Wood Smoke	Unexplained	PM _{2.5} Mass	n	Sampling Dates
State Building	0.4 \pm 0.05 (6.5 %)	0.2 \pm 0.05 (3.9 %)	0.02 \pm 0.01 (0.4 %)	0.3 \pm 0.1 (4.5 %)	0.3 \pm 0.1 (4.6 %)	3.6 \pm 0.1 (64.3 %)	0.9 (15.8 %)	5.7	20	6/2/12-8/31/12
NCORE	0.4 \pm 0.05 (6.0 %)	0.2 \pm 0.05 (3.8 %)	0.2 \pm 0.03 (2.7 %)	0.3 \pm 0.1 (5.7 %)	0.2 \pm 0.1 (3.7 %)	4.2 \pm 0.4 (70.5 %)	0.5 (7.7 %)	5.1	17	6/14/12-8/31/12

Figure 7: State Building Source Contribution Estimates ($\mu\text{g}/\text{m}^3$) – OMNI profiles.

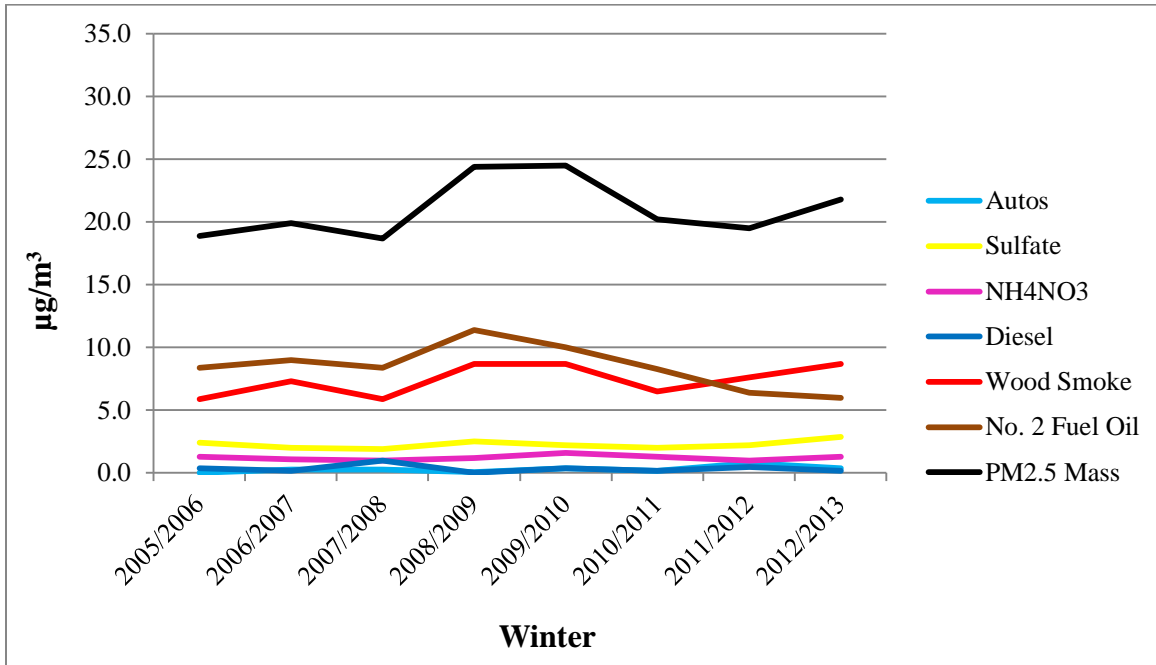


Figure 8: North Pole Source Contribution Estimates ($\mu\text{g}/\text{m}^3$) – OMNI profiles.

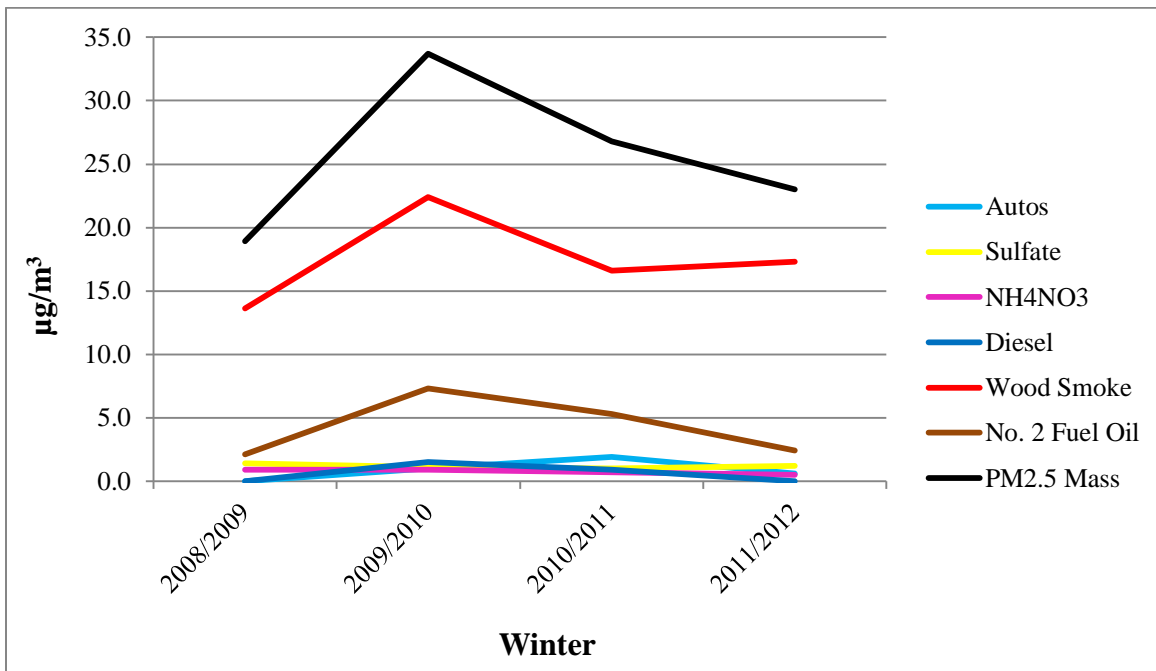


Figure 9: RAMS Source Contribution Estimates ($\mu\text{g}/\text{m}^3$) – OMNI profiles.

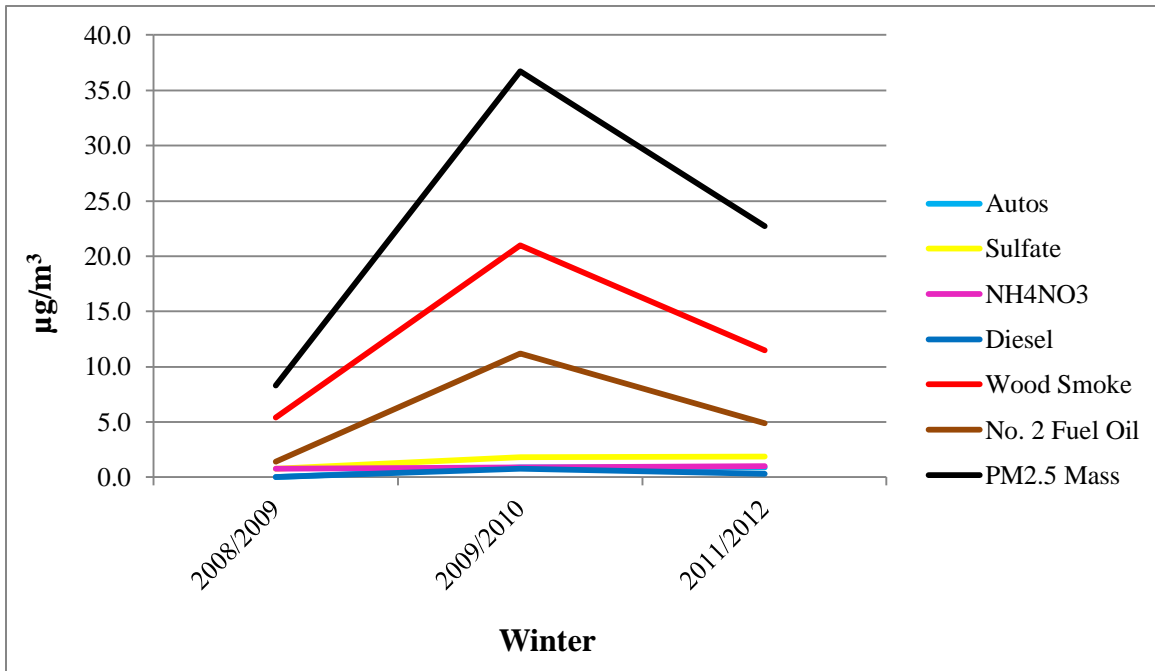


Figure 10: Peger Road Source Contribution Estimates ($\mu\text{g}/\text{m}^3$) – OMNI profiles.

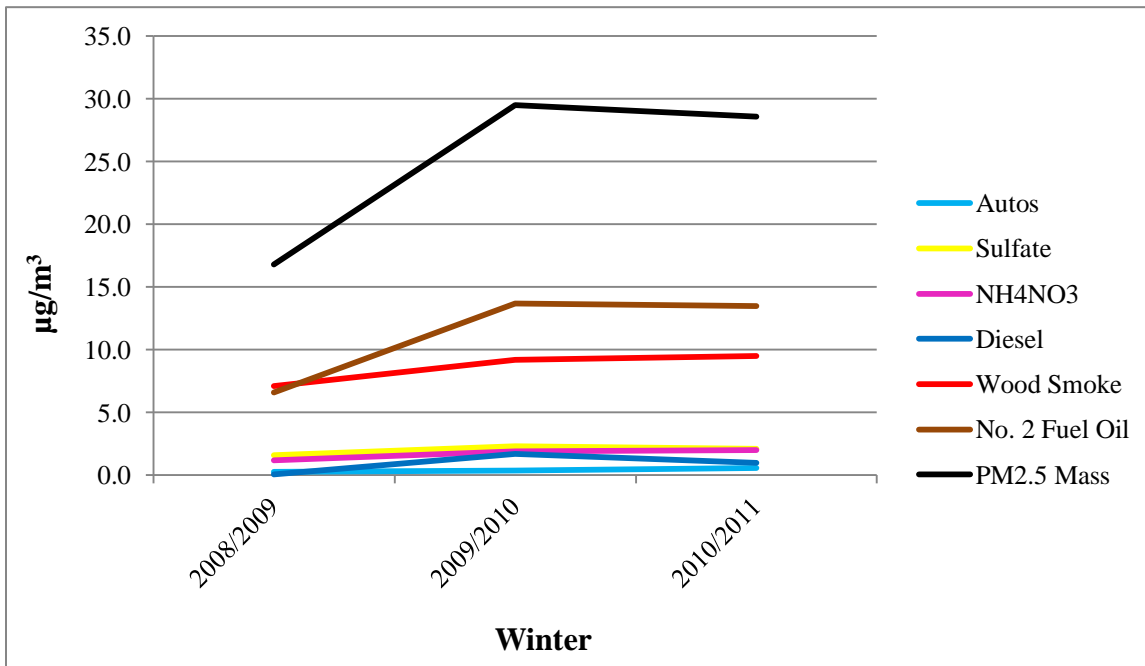


Figure 11: NCORE Source Contribution Estimates ($\mu\text{g}/\text{m}^3$) – OMNI profiles.

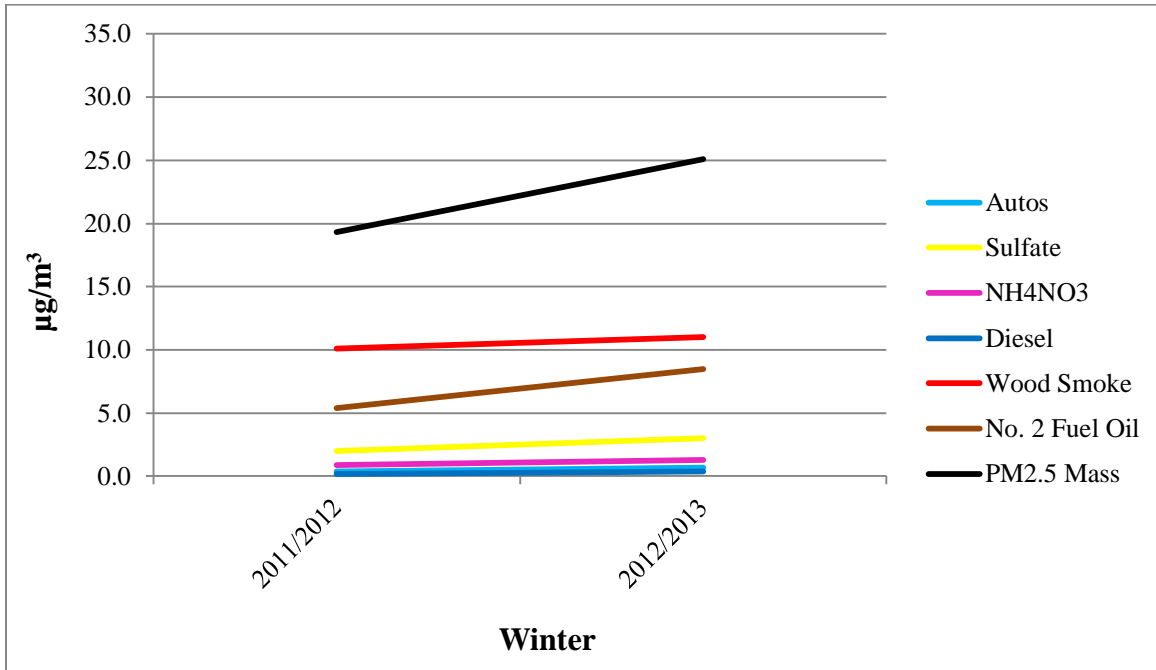
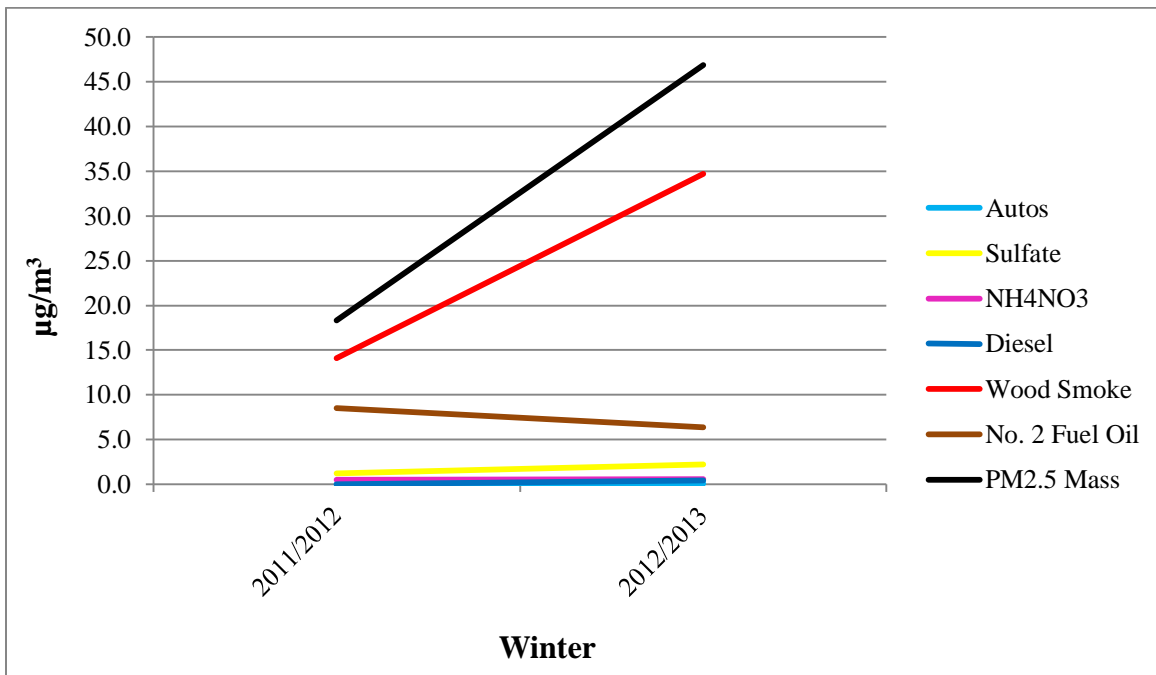
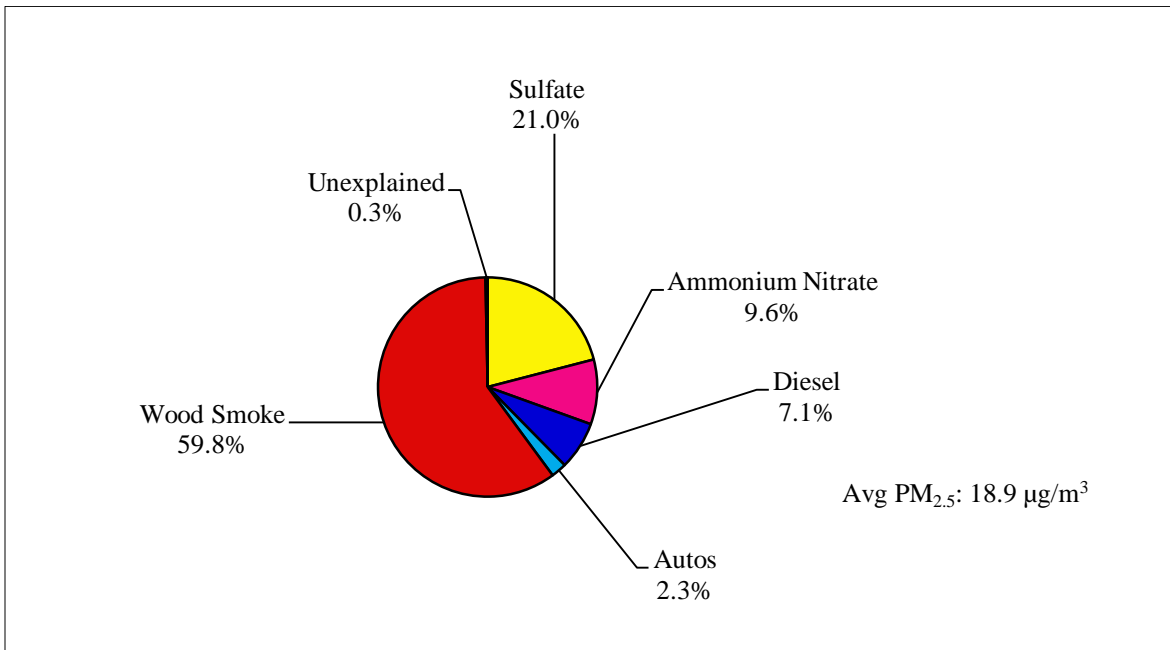


Figure 12: NPF3 Source Contribution Estimates ($\mu\text{g}/\text{m}^3$) – OMNI profiles.



**Figure 13: Winter 2005/2006, State Building.
CMB Results with EPA Source Profiles, November 3, 2005 – March 30, 2006.**



**Figure 14: Winter 2005/2006, State Building.
CMB Results with OMNI Source Profiles, November 3, 2005 – March 30, 2006.**

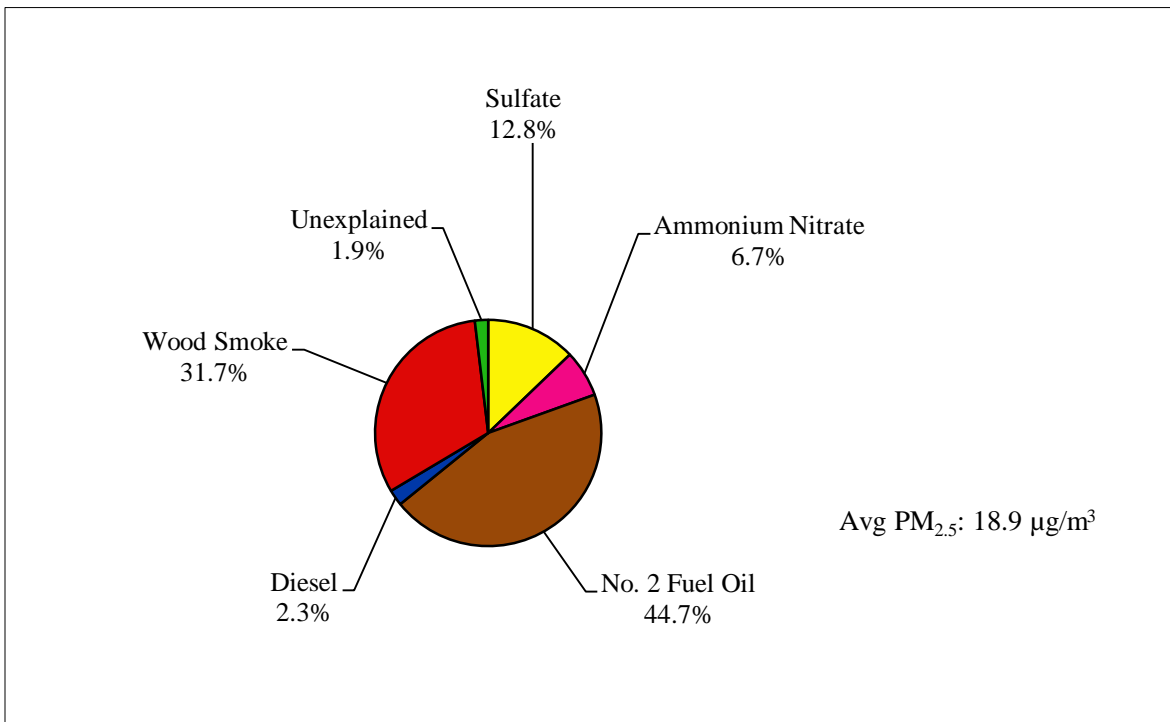


**Table 16: Comparison of CMB Results - EPA and OMNI Source Profiles.
State Building, Winter 2005/2006.**

Season:	Winter 2005/2006 (EPA)	Winter 2005/2006 (OMNI)
Dates:	11/3/05-3/30/06	11/3/05-3/30/06
n:	36	36
PM_{2.5} Mass (µg/m³):	18.9	18.9
CMB Source Estimates (µg/m³ and %)		
Sulfate:	4.0 (21.0 %)	2.4 (12.8 %)
Ammonium Nitrate:	1.8 (9.6 %)	1.3 (6.7%)
Diesel:	1.3 (7.1 %)	0.4 (2.3%)
Automobiles:	0.4 (2.3 %)	Not Identified
Wood Smoke:	11.3 (59.8 %)	5.9 (31.7 %)
No. 2 Fuel Oil:	Not Identified	8.4 (44.7 %)
Unexplained:	0.1 (0.3 %)	0.4 (1.9 %)

**Figure 15: Winter 2006/2007, State Building.
CMB Results with EPA Source Profiles, November 1, 2006 – March 31, 2007.**

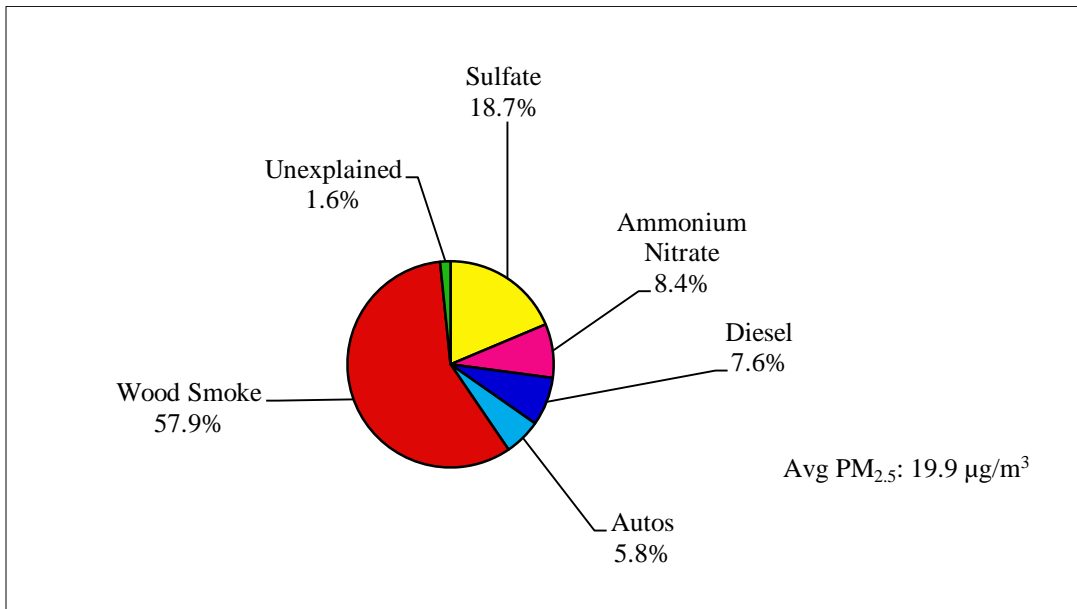


**Figure 16: Winter 2006/2007, State Building.
CMB Results with OMNI Source Profiles, November 1, 2006 – March 31, 2007.**

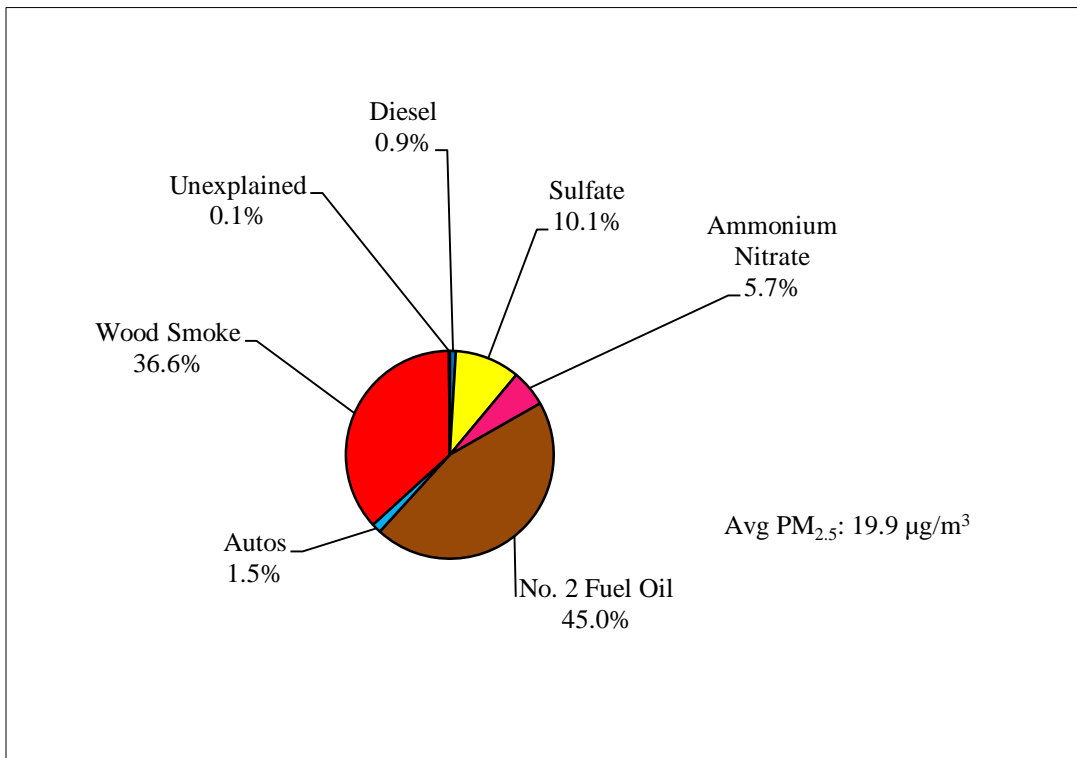


**Table 17: Comparison of CMB Results - EPA and OMNI Source Profiles.
State Building, Winter 2006/2007.**

Season:	Winter 2006/2007 (EPA)	Winter 2006/2007 (OMNI)
Dates:	11/1/06-3/31/07	11/1/06-3/31/07
n:	39	39
PM_{2.5} Mass (µg/m³):	19.9	19.9
CMB Source Estimates (µg/m³ and %)		
Sulfate:	3.7 (18.7 %)	2.0 (10.1 %)
Ammonium Nitrate:	1.7 (8.4 %)	1.1 (5.7 %)
Diesel:	1.5 (7.6 %)	0.2 (0.9 %)
Automobiles:	1.1 (5.8 %)	0.3 (1.5 %)
Wood Smoke:	11.5 (57.9 %)	7.3 (36.6 %)
No. 2 Fuel Oil:	Not Identified	9.0 (45.0 %)
Unexplained:	0.3 (1.6 %)	0.03 (0.1 %)

**Figure 17: Winter 2007/2008, State Building.
CMB Results with EPA Source Profiles, November 2, 2007 – March 31, 2008.**

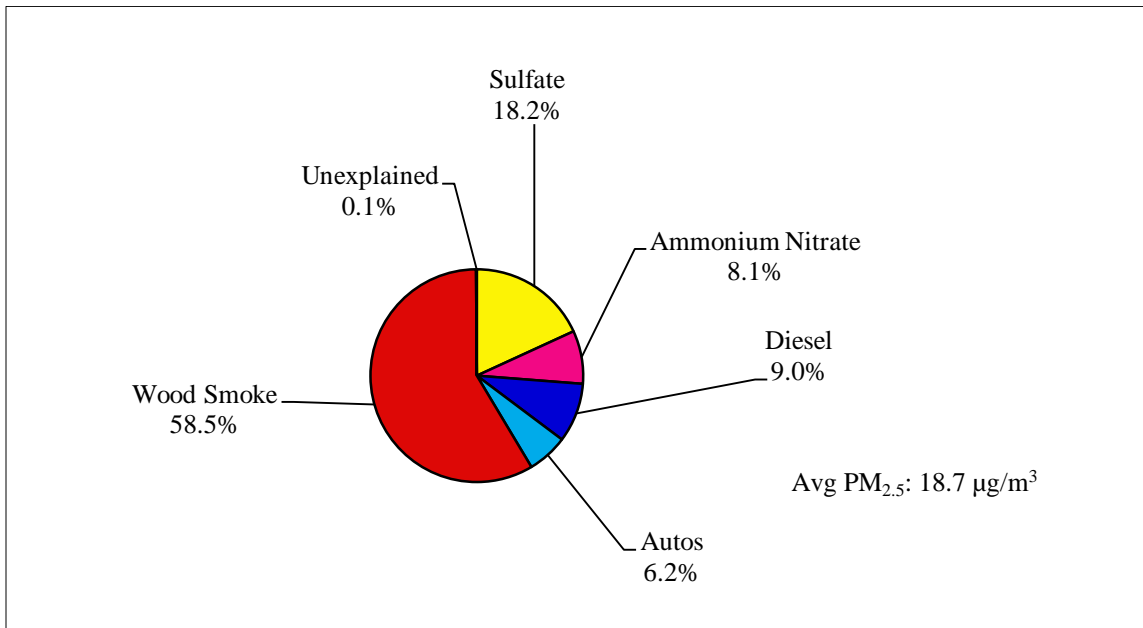


**Figure 18: Winter 2007/2008, State Building.
CMB Results with OMNI Source Profiles, November 2, 2007 – March 31, 2008.**

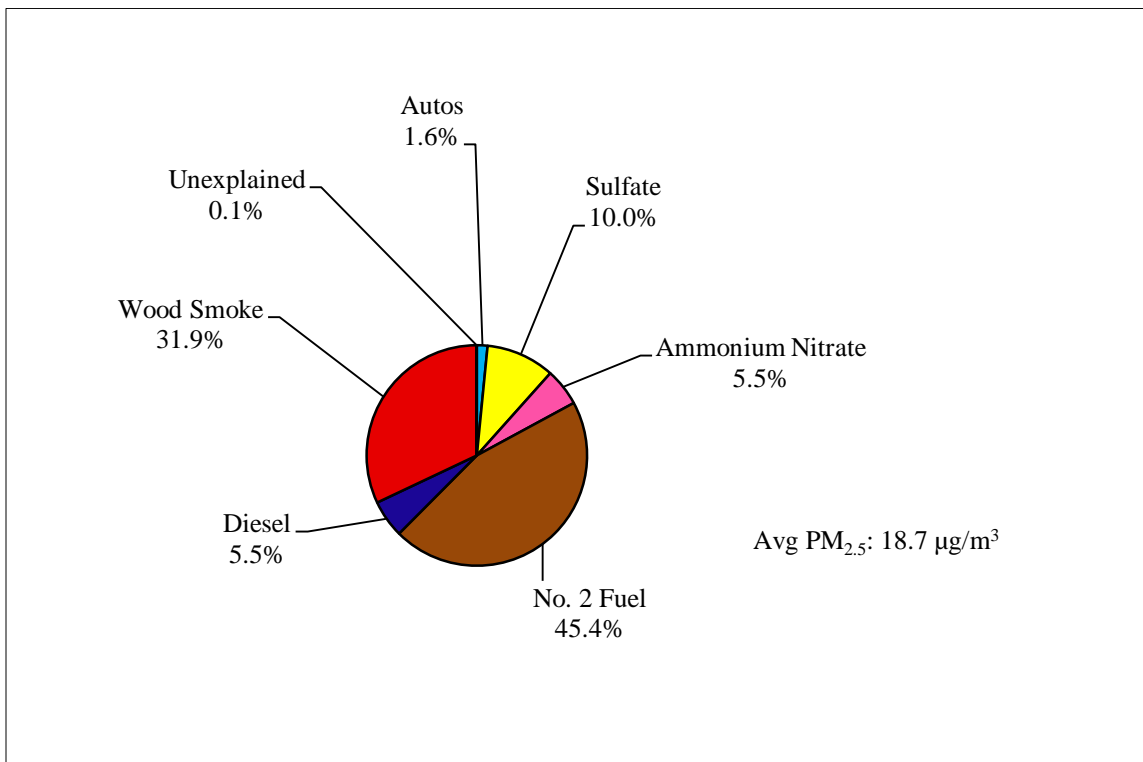


**Table 18: Comparison of CMB Results - EPA and OMNI Source Profiles.
State Building, Winter 2007/2008.**

Season:	Winter 2007/2008 (EPA)	Winter 2007/2008 (OMNI)
Dates:	11/2/07-3/31/08	11/2/07-3/31/08
n:	40	40
PM_{2.5} Mass (µg/m³):	18.7	18.7
CMB Source Estimates (µg/m³ and %)		
Sulfate:	3.4 (18.2 %)	1.9 (10.0 %)
Ammonium Nitrate:	1.5 (8.1 %)	1.0 (5.5 %)
Diesel:	1.7 (9.0 %)	1.0 (5.5 %)
Automobiles:	1.2 (6.2 %)	0.3 (1.6%)
Wood Smoke:	10.9 (58.5 %)	5.9 (31.9 %)
No. 2 Fuel Oil:	Not Identified	8.4 (45.4 %)
Unexplained:	0.02 (0.1 %)	0.01 (0.1 %)

**Figure 19: Winter 2008/2009, State Building.
CMB Results with EPA Source Profiles, November 8, 2008 – April 7, 2009.**

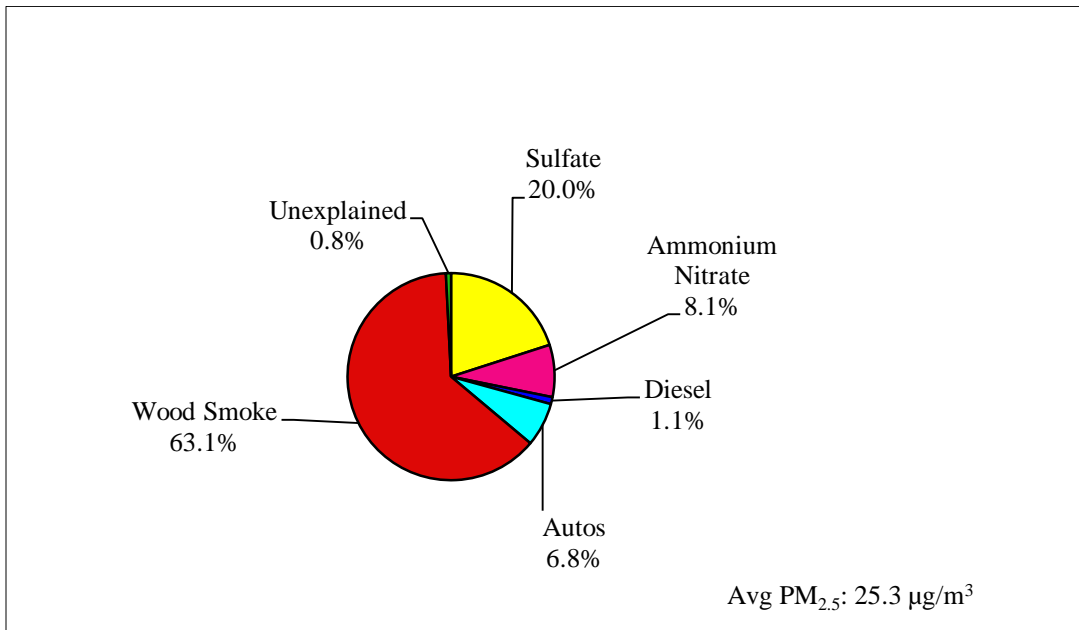


**Figure 20: Winter 2008/2009, State Building.
CMB Results with OMNI Source Profiles, November 8, 2008 – April 7, 2009.
(Submitted originally to ADEC in July 23, 2012 final report).**

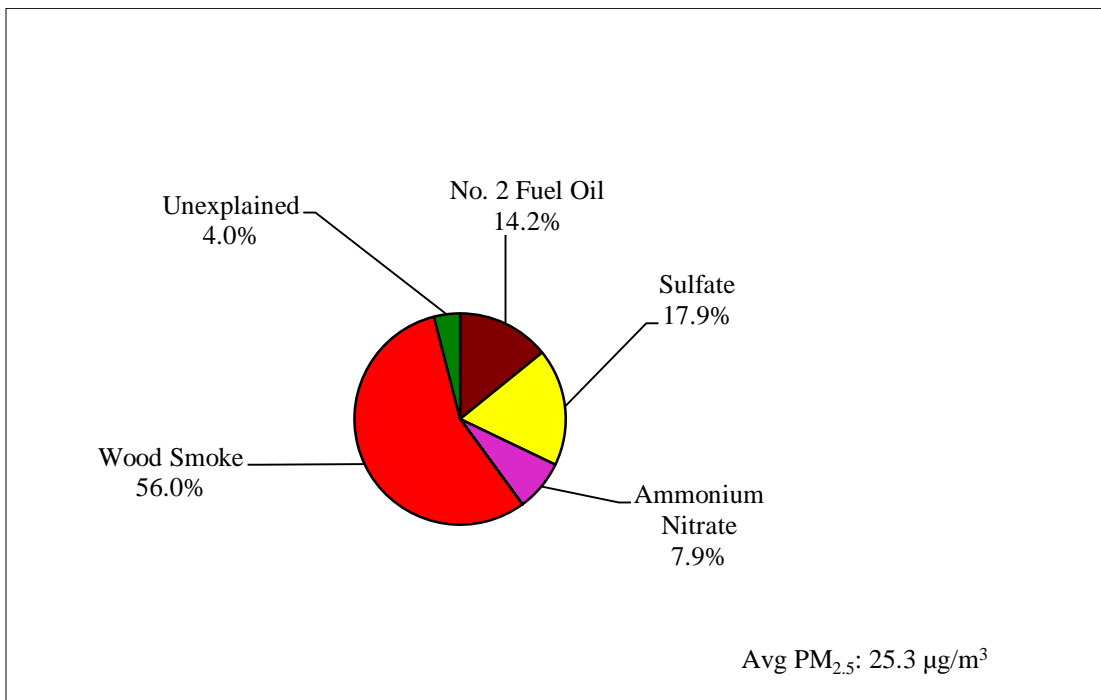


**Figure 21: Winter 2008/2009, State Building.
CMB Results with OMNI Source Profiles, November 8, 2008 – April 7, 2009.
(Updated CMB modeling using OMNI profiles and auto / diesel profiles).**

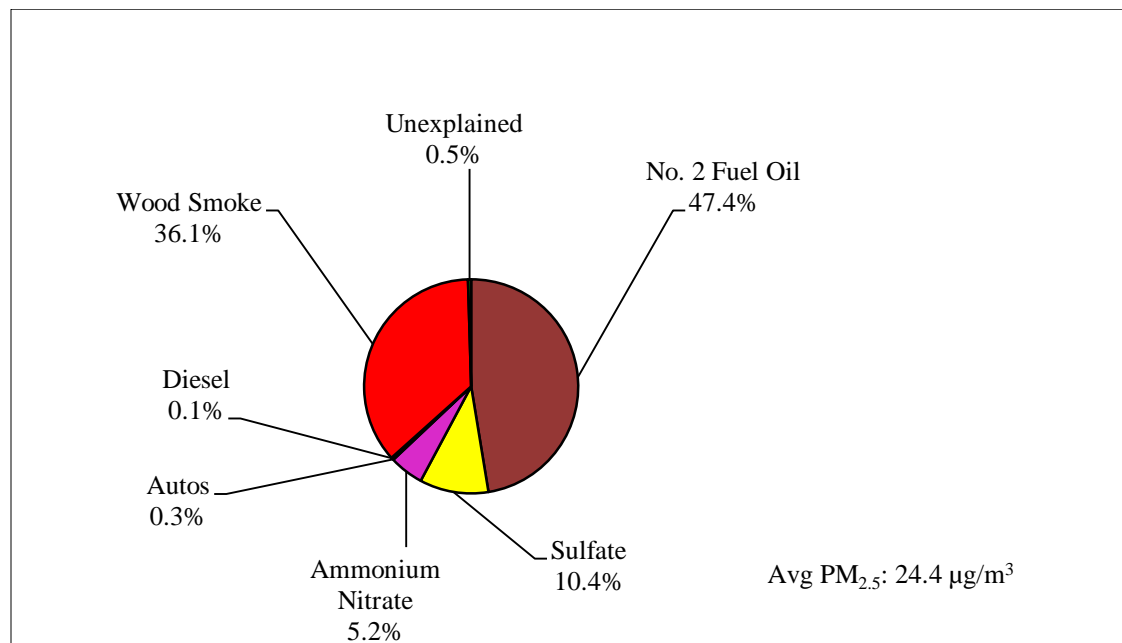


**Table 19: Comparison of CMB Results - EPA and OMNI Source Profiles.
State Building, Winter 2008/2009.**

Season:	Winter 2008/2009 (EPA)	Winter 2008/2009 (OMNI)*	Winter 2008/2009 (OMNI)**
Dates:	11/8/08-4/7/09	11/8/08-4/7/09	11/8/08-4/7/09
n:	47	47	46
PM _{2.5} Mass (µg/m ³):	25.3	25.3	24.4
CMB Source Estimates (µg/m³ and %)			
Sulfate:	5.1 (20.0 %)	4.4 (17.9 %)	2.5 (10.4 %)
Ammonium Nitrate:	2.1 (8.1 %)	1.9 (7.9%)	1.2 (5.2%)
Diesel:	0.3 (1.1 %)	Not Identified	0.04 (0.1 %)
Automobiles:	1.7 (6.8 %)	Not Identified	0.06 (0.3 %)
Wood Smoke:	16.0 (63.1 %)	13.8 (56.0 %)	8.7 (36.1 %)
No. 2 Fuel Oil:	Not Identified	3.5 (14.2 %)	11.4 (47.4 %)
Unexplained:	0.2 (0.8 %)	1.0 (4.0 %)	0.1 (0.5 %)

*Original OMNI CMB modeling (July 23, 2012 report). **Updated OMNI CMB modeling with autos and diesel profiles.

**Figure 22: Winter 2008/2009, North Pole.
CMB Results with EPA Source Profiles, January 25, 2009 – April 7, 2009.**

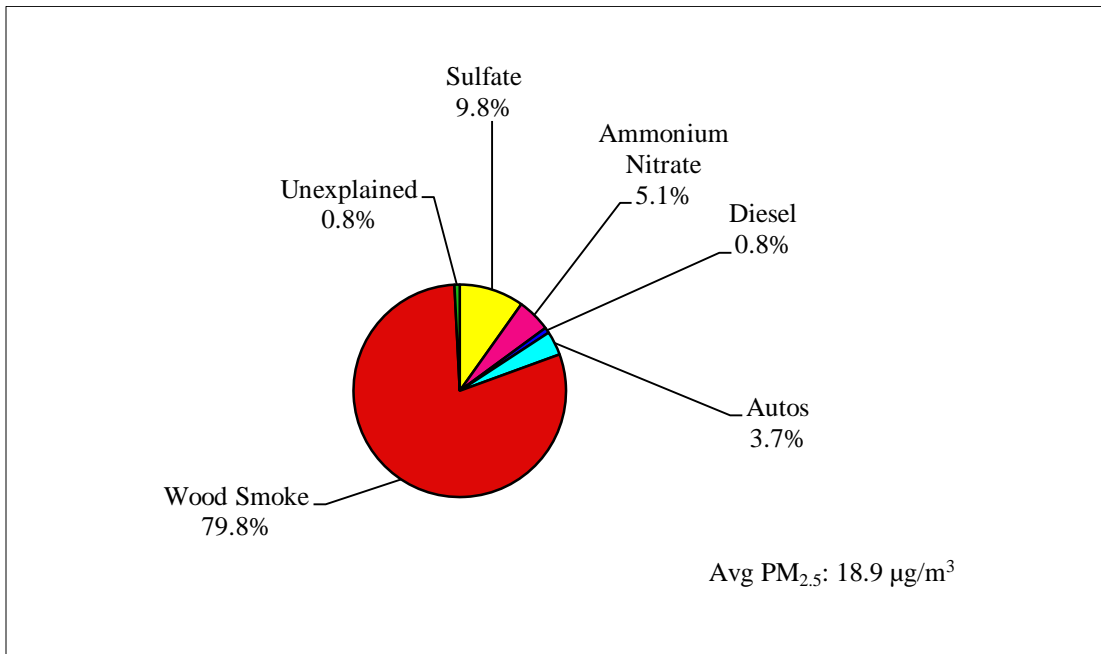


**Figure 23: Winter 2008/2009, North Pole.
CMB Results with OMNI Source Profiles, January 25, 2009 – April 7, 2009.**

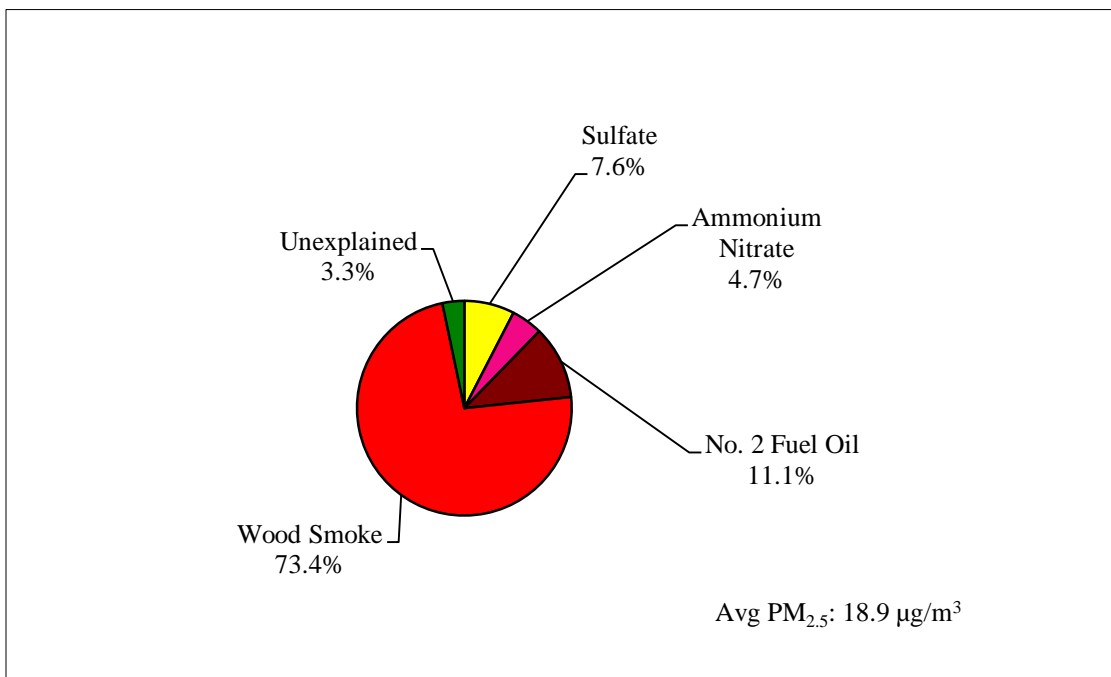


**Table 20: Comparison of CMB Results - EPA and OMNI Source Profiles.
North Pole, Winter 2008/2009.**

Season:	Winter 2008/2009 (EPA)	Winter 2008/2009 (OMNI)
Dates:	1/25/09-4/7/09	1/25/09-4/7/09
n:	21	21
PM_{2.5} Mass (µg/m³):	18.9	18.9
CMB Source Estimates (µg/m³ and %)		
Sulfate:	1.9 (9.8 %)	1.4 (7.6 %)
Ammonium Nitrate:	1.0 (5.1 %)	0.9 (4.7 %)
Diesel:	0.2 (0.8 %)	Not Identified
Automobiles:	0.7 (3.7 %)	Not Identified
Wood Smoke:	15.0 (79.8 %)	13.6 (73.4 %)
No. 2 Fuel Oil:	Not Identified	2.1 (11.1 %)
Unexplained:	0.2 (0.8 %)	0.6 (3.3 %)

**Figure 24: Winter 2008/2009, RAMS.
CMB Results with EPA Source Profiles, January 25, 2009 – April 7, 2009.**

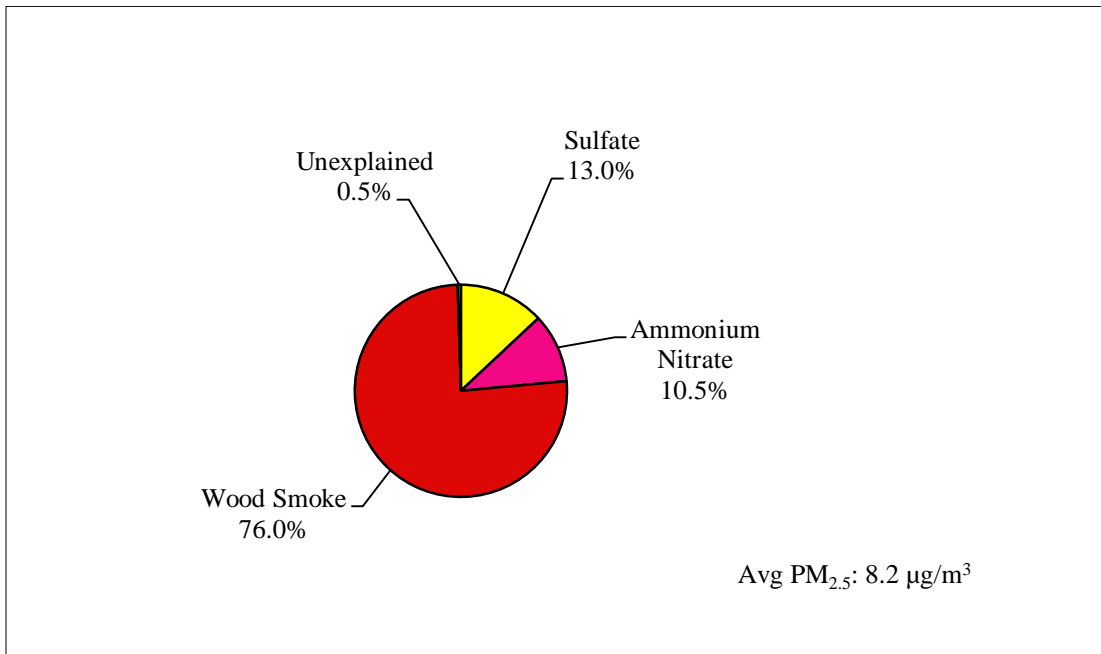


**Figure 25: Winter 2008/2009, RAMS.
CMB Results with OMNI Source Profiles, January 25, 2009 – April 7, 2009.**

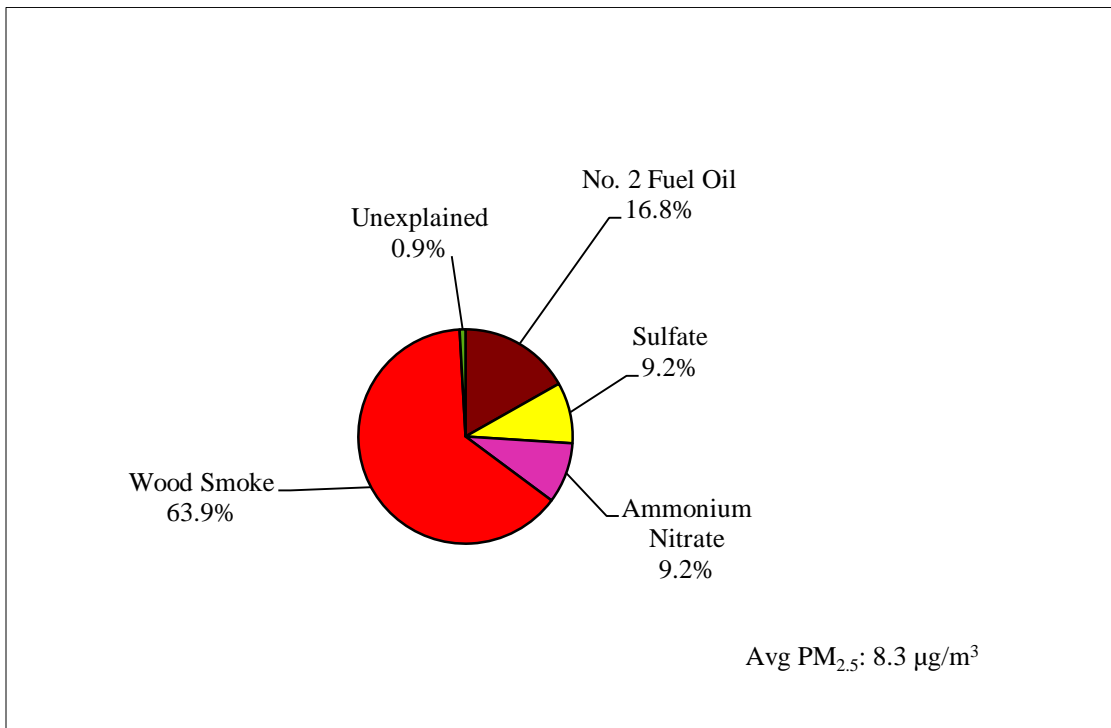
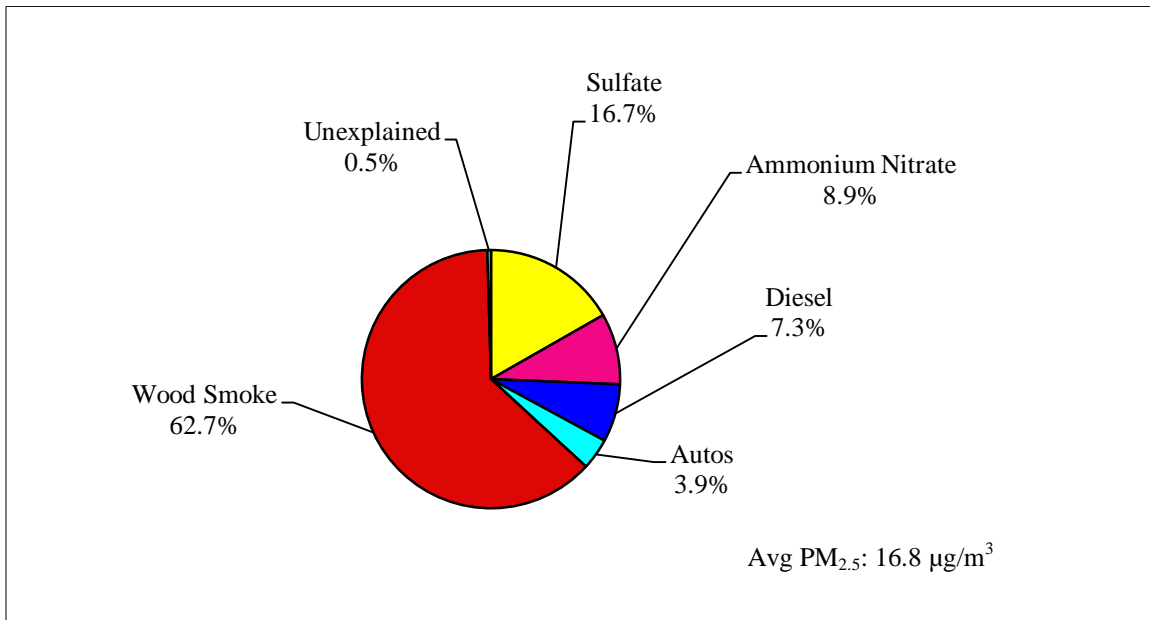


Table 21: Comparison of CMB Results - EPA and OMNI Source Profiles. RAMS, Winter 2008/2009.

Season:	Winter 2008/2009 (EPA)	Winter 2008/2009 (OMNI)
Dates:	1/25/09-4/7/09	1/25/09-4/7/09
n:	23	22
PM_{2.5} Mass (µg/m³):	8.2	8.3
CMB Source Estimates (µg/m³ and %)		
Sulfate:	1.1 (13.0 %)	0.8 (9.2 %)
Ammonium Nitrate:	0.9 (10.5 %)	0.8 (9.2 %)
Diesel:	Not Identified	Not Identified
Automobiles:	Not Identified	Not Identified
Wood Smoke:	6.3 (76.0 %)	5.4 (63.9 %)
No. 2 Fuel Oil:	Not Identified	1.4 (16.8 %)
Unexplained:	0.04 (0.5 %)	0.1 (0.9%)

**Figure 26: Winter 2008/2009, Peger Road.
CMB Results with EPA Source Profiles, January 25, 2009 – April 7, 2009.**



**Figure 27: Winter 2008/2009, Peger Road.
CMB Results with OMNI Source Profiles, January 25, 2009 – April 7, 2009.
(Submitted originally to ADEC in July 23, 2012 final report).**

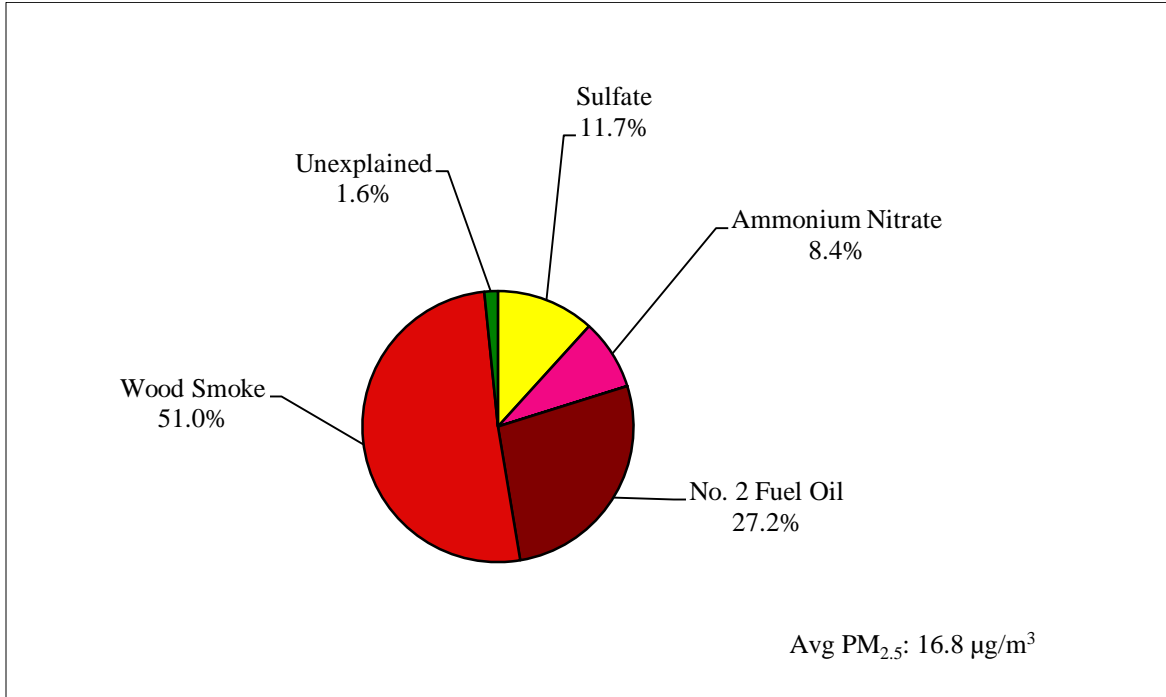


Figure 28: Winter 2008/2009, Peger Road.
CMB Results with OMNI Source Profiles, January 25, 2009 – April 7, 2009.
(Updated CMB modeling using OMNI profiles and auto / diesel profiles).

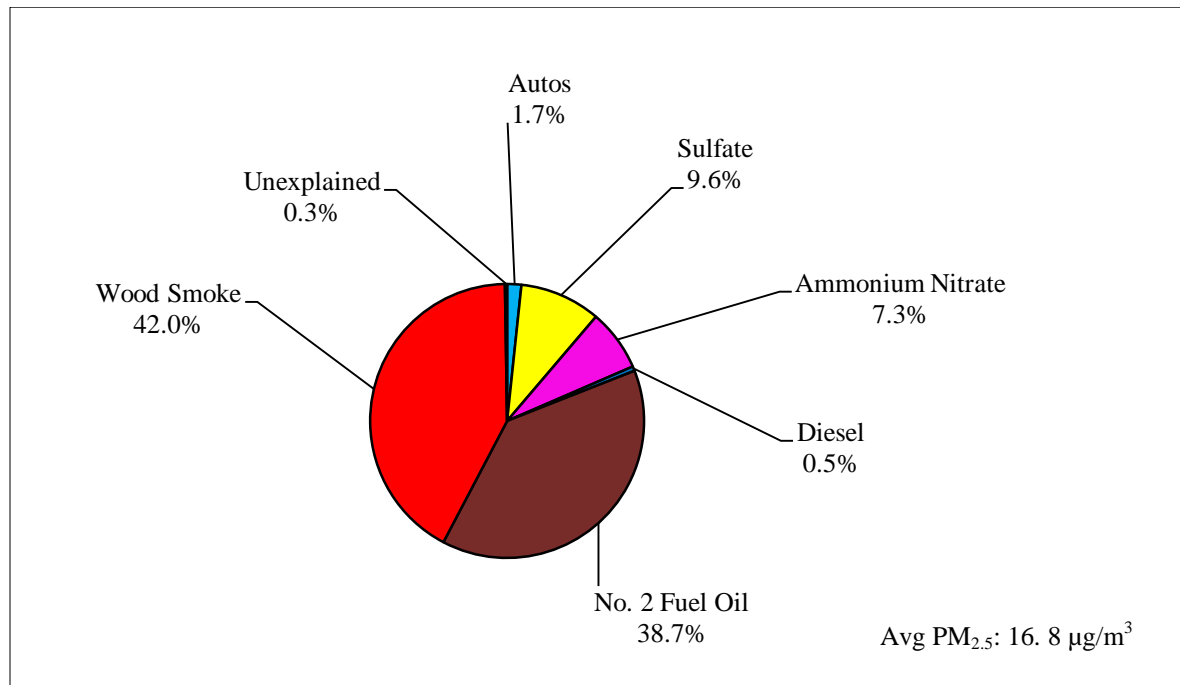
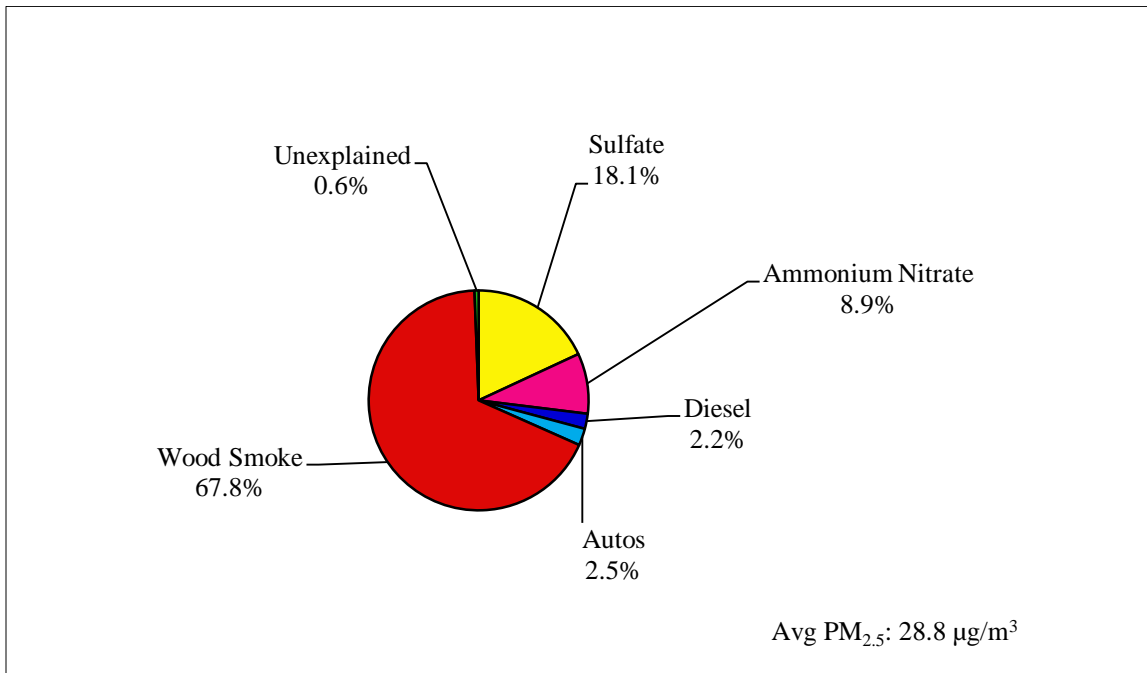


Table 22: Comparison of CMB Results - EPA and OMNI Source Profiles.
Peger Road, Winter 2008/2009.

Season:	Winter 2008/2009 (EPA)	Winter 2008/2009 (OMNI)*	Winter 2008/2009 (OMNI)**
Dates:	1/25/09-4/7/09	1/25/09-4/7/09	1/25/09-4/7/09
n:	26	26	26
PM _{2.5} Mass (µg/m ³):	16.8	16.8	16.8
CMB Source Estimates (µg/m³ and %)			
Sulfate:	2.8 (16.7 %)	2.0 (11.7 %)	1.6 (9.6 %)
Ammonium Nitrate:	1.5 (8.9 %)	1.4 (8.4 %)	1.2 (7.3 %)
Diesel:	1.2 (7.3 %)	Not Identified	0.1 (0.5 %)
Automobiles:	0.7 (3.9 %)	Not Identified	0.3 (1.7 %)
Wood Smoke:	10.6 (62.7 %)	8.6 (51.0 %)	7.1 (42.0 %)
No. 2 Fuel Oil:	Not Identified	4.6 (27.2 %)	6.6 (38.7 %)
Unexplained:	0.1 (0.5 %)	0.3 (1.6 %)	0.04 (0.3 %)

*Original OMNI CMB modeling (July 23, 2012 report). **Updated OMNI CMB modeling with autos and diesel profiles.

**Figure 29: Winter 2009/2010, State Building.
CMB Results with EPA Source Profiles, November 3, 2009–March 15, 2010.**



**Figure 30: Winter 2009/2010, State Building.
CMB Results with OMNI Source Profiles, November 3, 2009–March 15, 2010.**

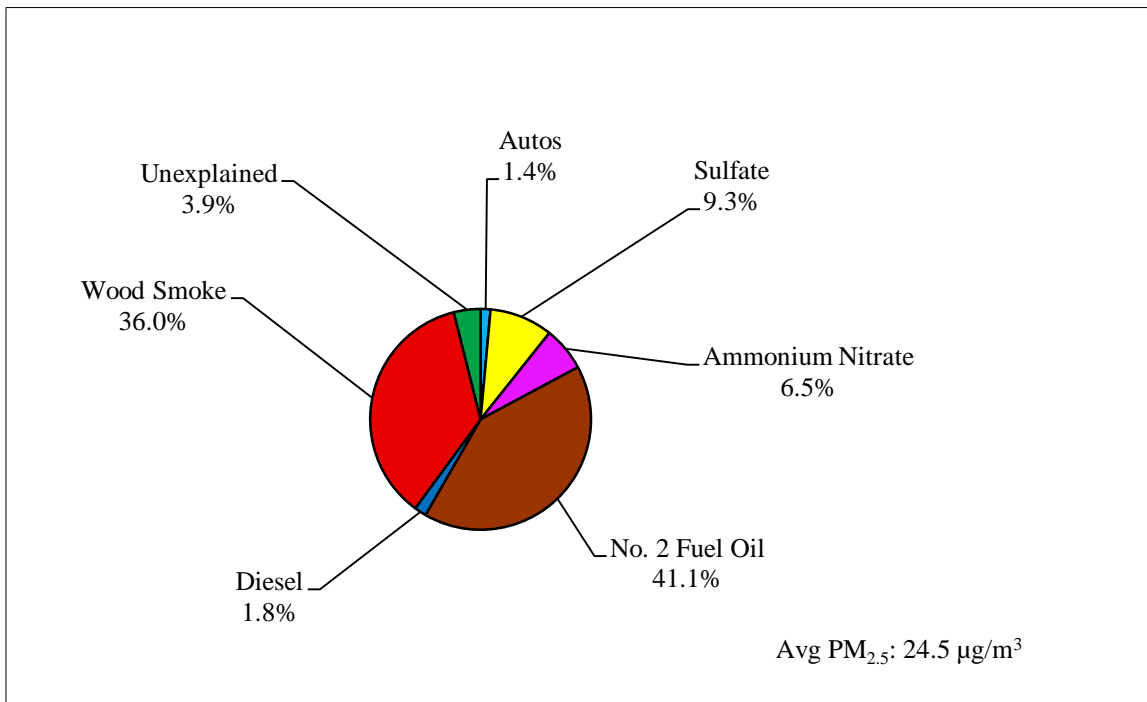


**Table 23: Comparison of CMB Results - EPA and OMNI Source Profiles.
State Building, Winter 2009/2010.**

Season:	Winter 2009/2010 (EPA)	Winter 2009/2010 (OMNI)
Dates:	11/3/09-3/15/10	11/3/09-3/15/10
n:	40	31
PM_{2.5} Mass (µg/m³):	28.8	24.5
CMB Source Estimates (µg/m³ and %)		
Sulfate:	5.2 (18.1 %)	2.2 (9.3 %)
Ammonium Nitrate:	2.5 (8.9 %)	1.6 (6.5 %)
Diesel:	0.6 (2.2 %)	0.4 (1.8 %)
Automobiles:	0.7 (2.5 %)	0.4 (1.4 %)
Wood Smoke:	19.5 (67.8 %)	8.7 (36.0 %)
No. 2 Fuel Oil:	Not Identified	10.0 (41.1 %)
Unexplained:	0.2 (0.6 %)	1.0 (3.9 %)

**Figure 31: Winter 2009/2010, North Pole.
CMB Results with EPA Source Profiles, November 3, 2009 – March 15, 2010.**

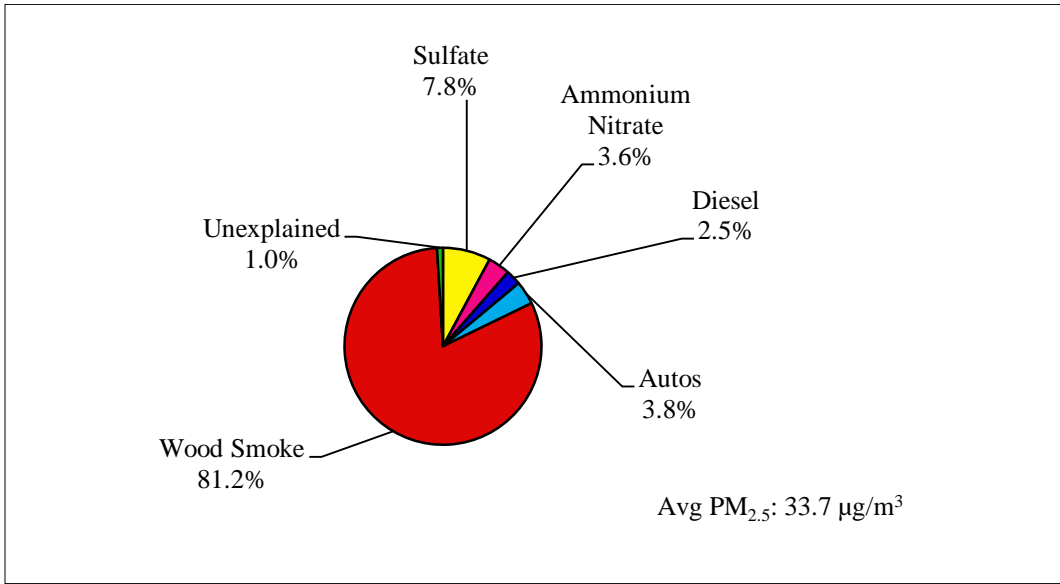


**Figure 32: Winter 2009/2010, North Pole.
CMB Results with OMNI Source Profiles, November 3, 2009–March 15, 2010.**

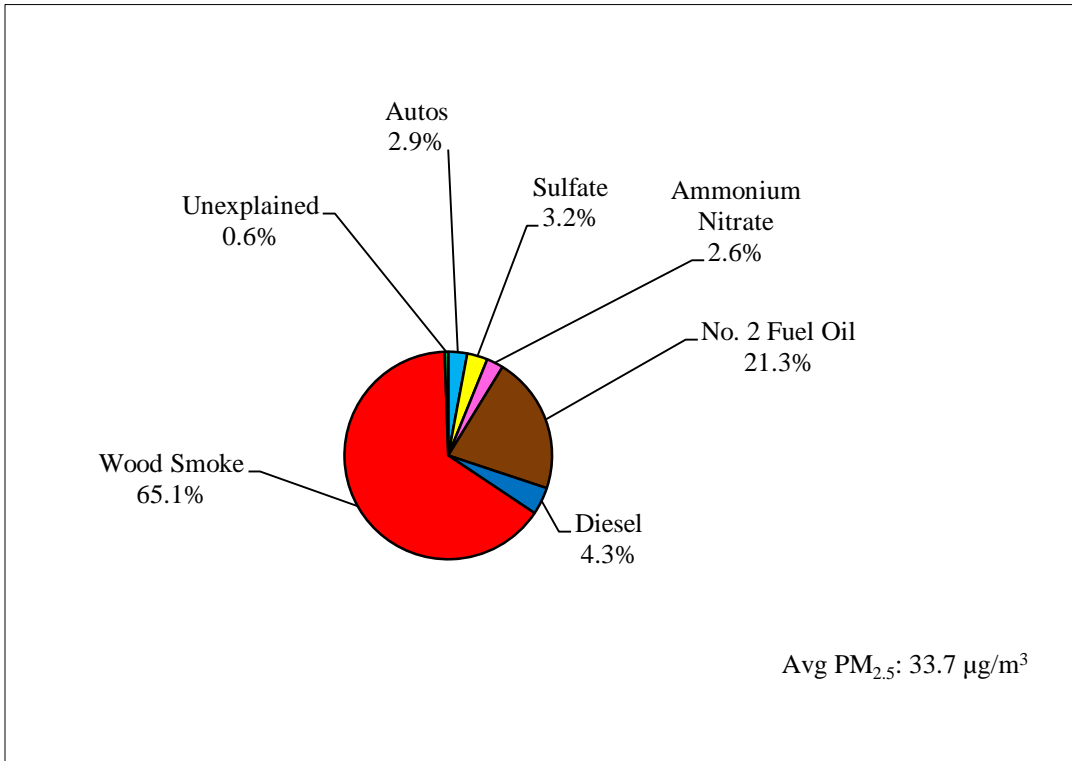


**Table 24: Comparison of CMB Results - EPA and OMNI Source Profiles.
North Pole, Winter 2009/2010.**

Season:	Winter 2009/2010 (EPA)	Winter 2009/2010 (OMNI)
Dates:	11/3/09-3/15/10	11/3/09-3/15/10
n:	35	35
PM_{2.5} Mass (µg/m³):	33.7	33.7
CMB Source Estimates (µg/m³ and %)		
Sulfate:	2.6 (7.8 %)	1.1 (3.2 %)
Ammonium Nitrate:	1.2 (3.6 %)	0.9 (2.6 %)
Diesel:	0.8 (2.5 %)	1.5 (4.3 %)
Automobiles:	1.3 (3.8 %)	1.0 (2.9 %)
Wood Smoke:	27.1 (81.2 %)	22.4 (65.1 %)
No. 2 Fuel Oil:	Not Identified	7.3 (21.3 %)
Unexplained:	0.3 (1.0 %)	0.2 (0.6 %)

**Figure 33: Winter 2009/2010, RAMS.
CMB Results with EPA Source Profiles, November 15, 2009 – March 15, 2010.**

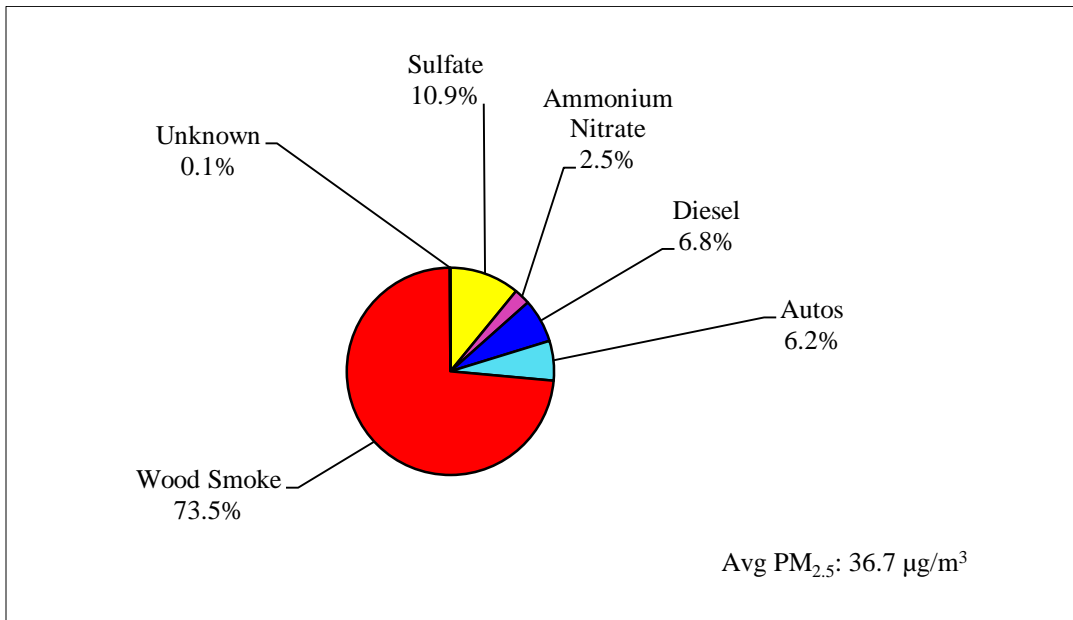


**Figure 34: Winter 2009/2010, RAMS.
CMB Results with OMNI Source Profiles, November 15, 2009 – March 15, 2010.**

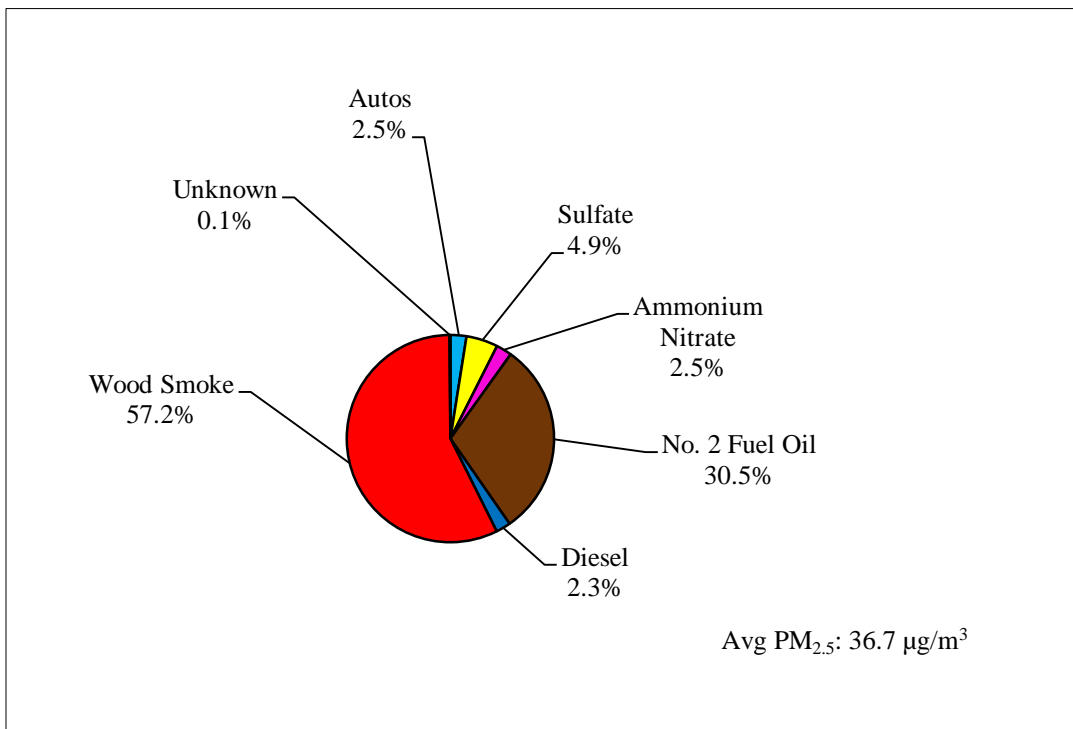


Table 25: Comparison of CMB Results - EPA and OMNI Source Profiles. RAMS, Winter 2009/2010.

Season:	Winter 2009/2010 (EPA)	Winter 2009/2010 (OMNI)
Dates:	11/15/09-3/15/10	11/15/09-3/15/10
n:	29	29
PM_{2.5} Mass (µg/m³):	36.7	36.7
CMB Source Estimates (µg/m³ and %)		
Sulfate:	4.0 (10.9 %)	1.8 (4.9 %)
Ammonium Nitrate:	0.9 (2.5 %)	0.9 (2.5 %)
Diesel:	2.5 (6.8 %)	0.8 (2.3 %)
Automobiles:	2.3 (6.2 %)	0.9 (2.5 %)
Wood Smoke:	26.9 (73.5 %)	21.0 (57.2 %)
No. 2 Fuel Oil:	Not Identified	11.2 (30.5 %)
Unexplained:	0.04 (0.1 %)	0.1 (0.1 %)

Figure 35: Winter 2009/2010, Peger Road.
CMB Results with EPA Source Profiles, November 3, 2009 – March 15, 2010.

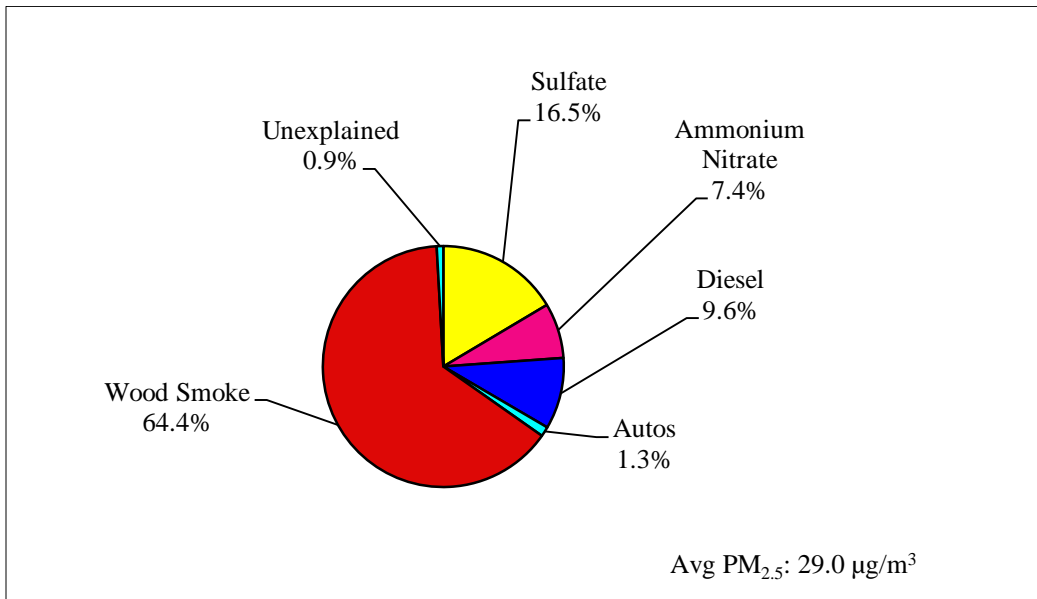
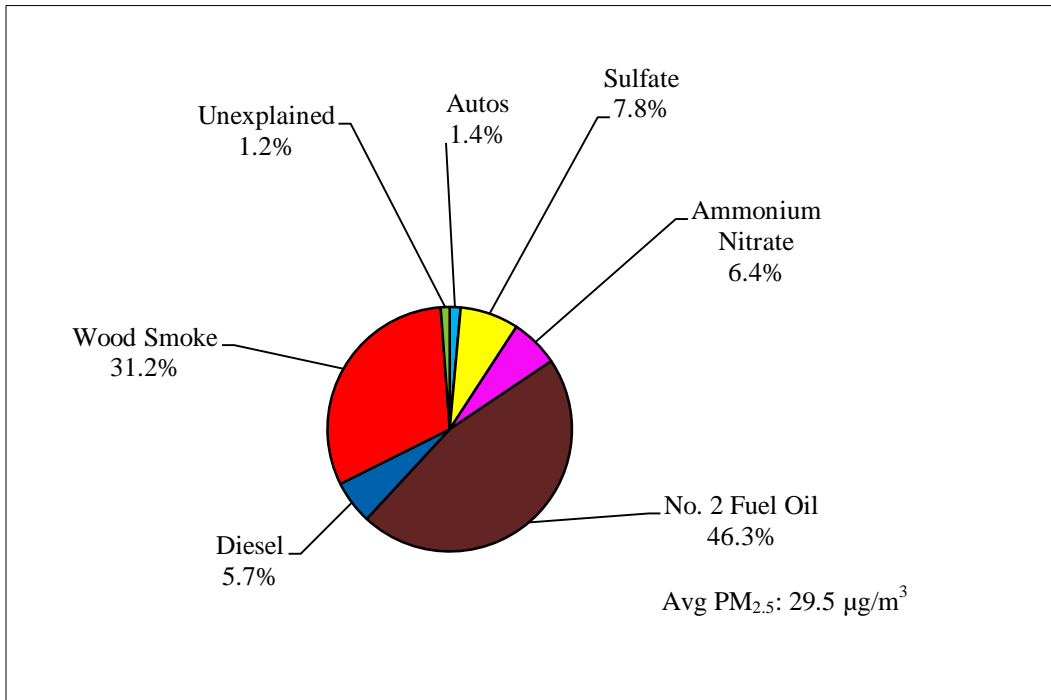


Figure 36: Winter 2009/2010, Peger Road.
CMB Results with OMNI Source Profiles, November 3, 2009 – March 15, 2010.



**Table 26: Comparison of CMB Results - EPA and OMNI Source Profiles.
Peger Road, Winter 2009/2010.**

Season:	Winter 2009/2010 (EPA)	Winter 2009/2010 (OMNI)
Dates:	11/3/09-3/15/10	11/3/09-3/15/10
n:	38	37
PM_{2.5} Mass (µg/m³):	29.0	29.5
CMB Source Estimates (µg/m³ and %)		
Sulfate:	4.8 (16.5 %)	2.3 (7.8 %)
Ammonium Nitrate:	2.1 (7.4 %)	1.9 (6.4 %)
Diesel:	2.8 (9.6 %)	1.7 (5.7 %)
Automobiles:	0.4 (1.3 %)	0.4 (1.4 %)
Wood Smoke:	18.6 (64.4 %)	9.2 (31.2 %)
No. 2 Fuel Oil:	Not Identified	13.7 (46.3 %)
Unexplained:	0.3 (0.9 %)	0.3 (1.2 %)

Figure 37: Winter 2010/2011, State Building.
CMB Results with EPA Source Profiles, November 1, 2010 – February 8, 2011.

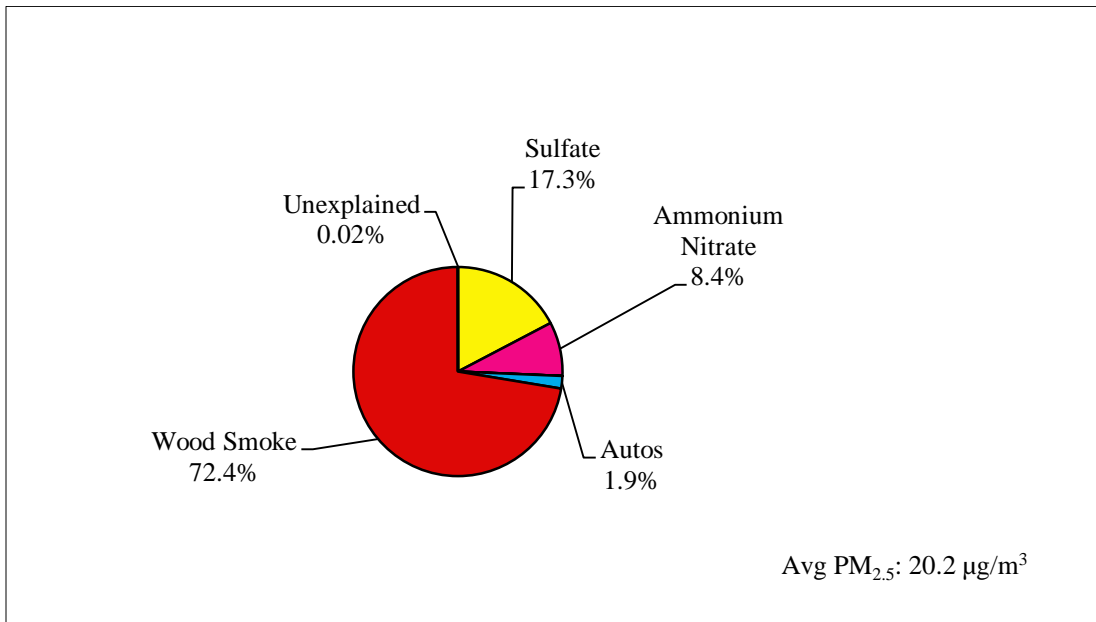
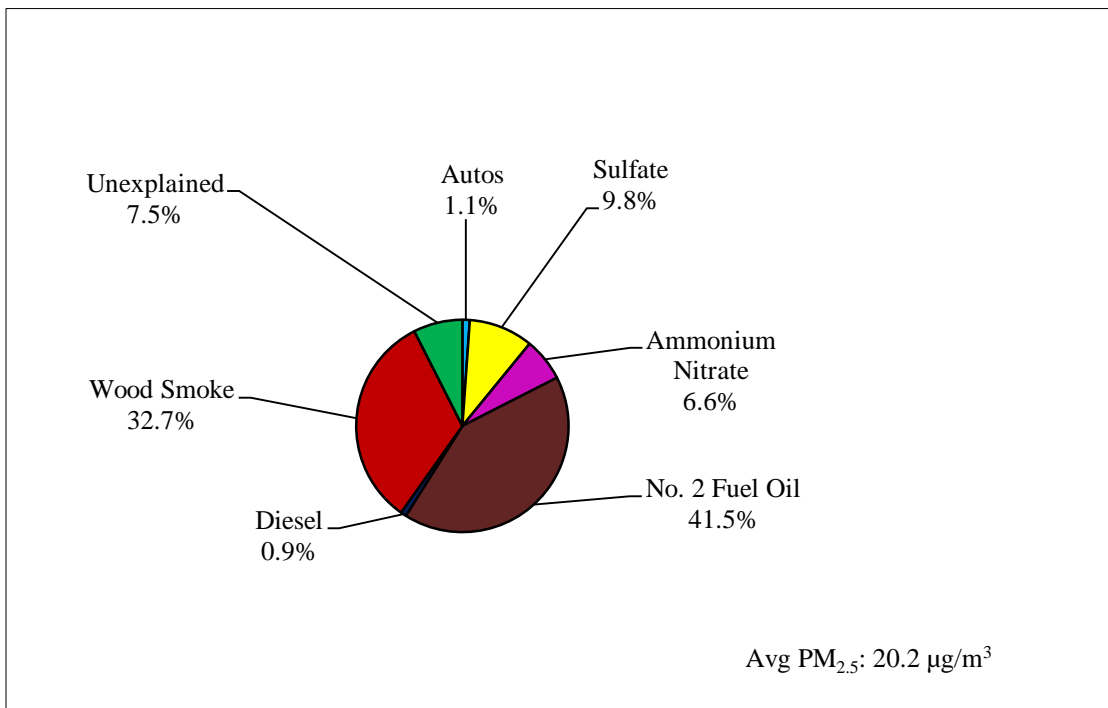


Figure 38: Winter 2010/2011, State Building.
CMB Results with OMNI Source Profiles, November 1, 2010 – February 8, 2011.



**Table 27: Comparison of CMB Results - EPA and OMNI Source Profiles.
State Building, Winter 2010/2011.**

Season:	Winter 2010/2011 (EPA)	Winter 2010/2011 (OMNI)
Dates:	11/1/10-2/8/11	11/1/10-2/8/11
n:	15	15
PM_{2.5} Mass (µg/m³)	20.2	20.2
CMB Source Estimates (µg/m³ and %)		
Sulfate:	3.5 (17.3 %)	2.0 (9.8 %)
Ammonium Nitrate:	1.7 (8.4 %)	1.3 (6.6 %)
Diesel:	Not Identified	0.2 (0.9 %)
Automobiles:	0.4 (1.9 %)	0.2 (1.1 %)
Wood Smoke:	14.6 (72.4 %)	6.5 (32.7 %)
No. 2 Fuel Oil:	Not Identified	8.3 (41.5 %)
Unexplained:	0.004 (0.02 %)	1.5 (7.5 %)

**Figure 39: Winter 2010/2011, North Pole.
CMB Results with EPA Source Profiles, January 9, 2011 – February 5, 2011.**

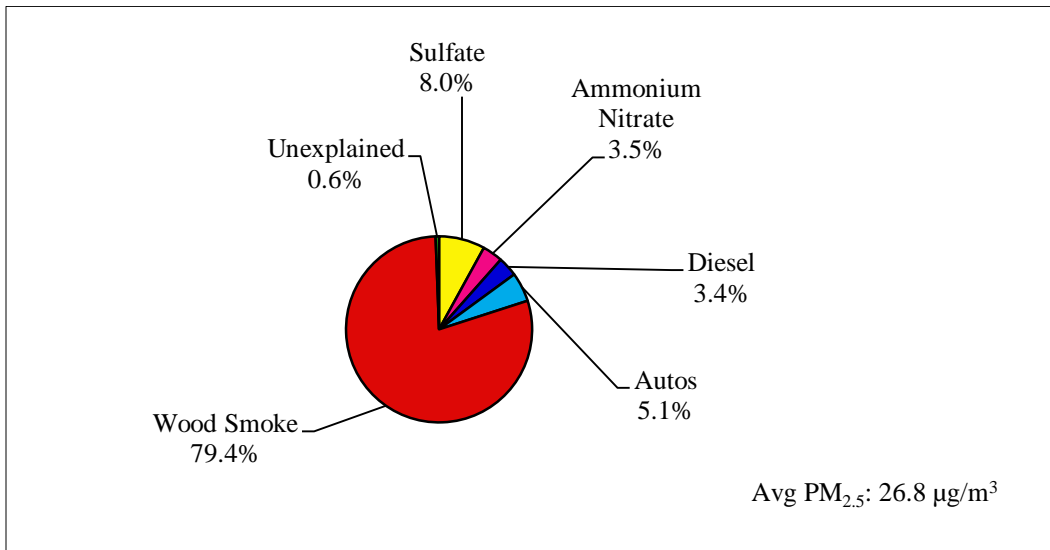


**Figure 40: Winter 2010/2011, North Pole.
CMB Results with OMNI Source Profiles, January 9, 2011 – February 5, 2011.**

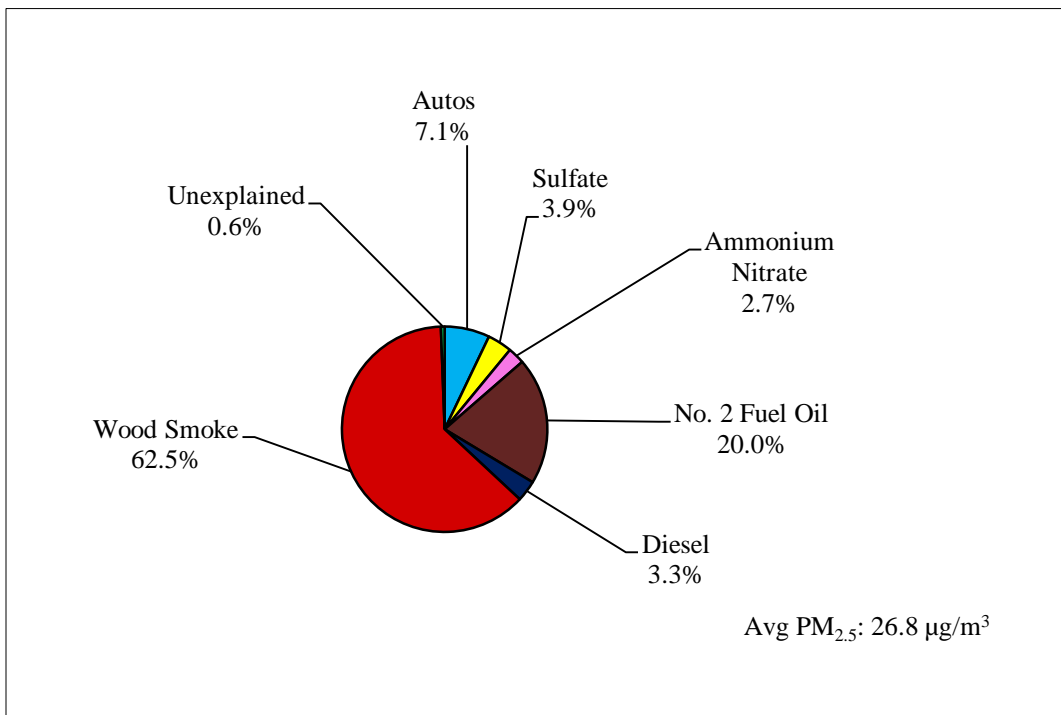


**Table 28: Comparison of CMB Results - EPA and OMNI Source Profiles.
North Pole, Winter 2010/2011.**

Season:	Winter 2010/2011 (EPA)	Winter 2010/2011 (OMNI)
Dates:	1/9/11-2/5/11	1/9/11-2/5/11
n:	10	10
PM_{2.5} Mass (µg/m³):	26.8	26.8
CMB Source Estimates (µg/m³ and %)		
Sulfate:	2.1 (8.0 %)	1.0 (3.9 %)
Ammonium Nitrate:	0.9 (3.5 %)	0.7 (2.7 %)
Diesel:	0.9 (3.4 %)	0.9 (3.3 %)
Automobiles:	1.4 (5.1 %)	1.9 (7.1 %)
Wood Smoke:	21.3 (79.4 %)	16.6 (62.5 %)
No. 2 Fuel Oil:	Not Identified	5.3 (20.0 %)
Unexplained:	0.2 (0.6 %)	0.2 (0.6 %)

**Figure 41: Winter 2010/2011, Peger Road.
CMB Results with EPA Source Profiles, January 9, 2011 – February 5, 2011.**

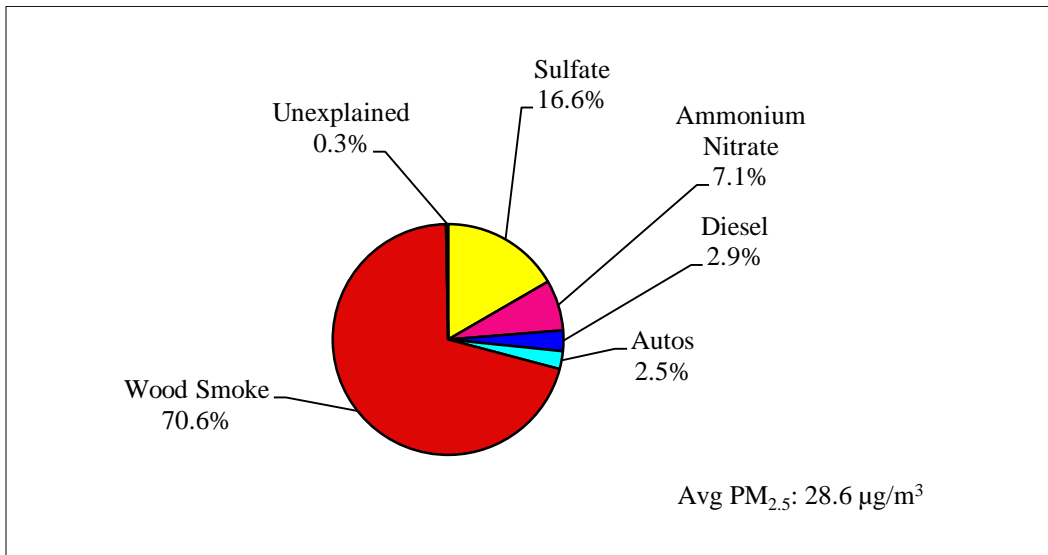


**Figure 42: Winter 2010/2011, Peger Road.
CMB Results with OMNI Source Profiles, January 9, 2011 – February 5, 2011.**

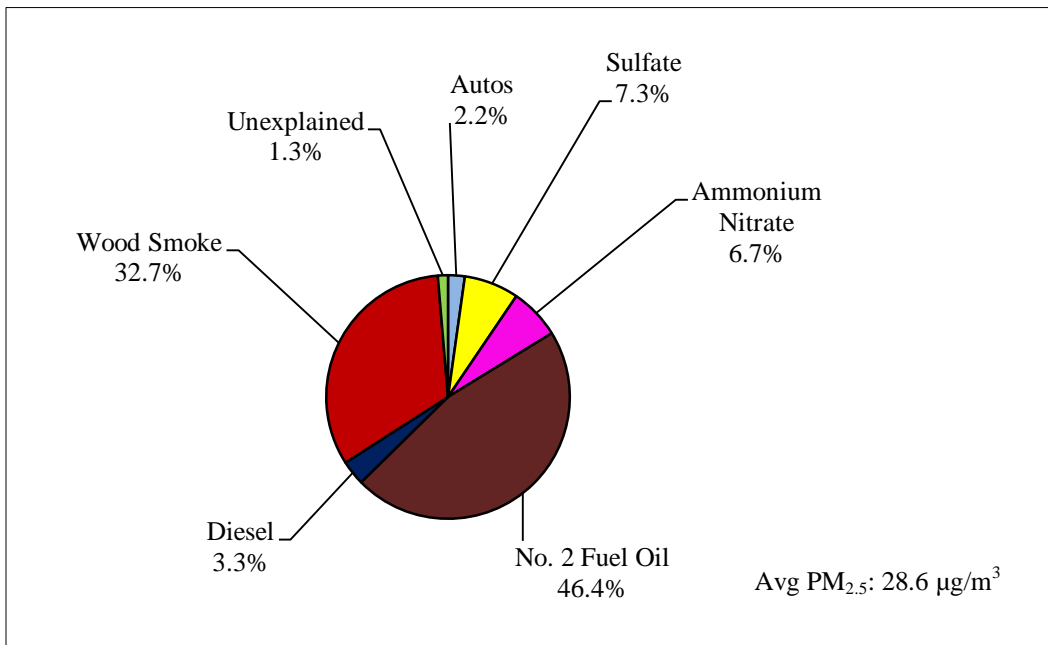


**Table 29: Comparison of CMB Results - EPA and OMNI Source Profiles.
Peger Road, Winter 2010/2011.**

Season:	Winter 2010/2011 (EPA)	Winter 2010/2011 (OMNI)
Dates:	1/9/11-2/5/11	1/9/11-2/5/11
n:	10	10
PM_{2.5} Mass (µg/m³):	28.6	28.6
CMB Source Estimates (µg/m³ and %)		
Sulfate:	4.8 (16.6 %)	2.1 (7.3 %)
Ammonium Nitrate:	2.0 (7.1 %)	2.0 (6.7 %)
Diesel:	0.8 (2.9 %)	1.0 (3.3 %)
Automobiles:	0.7 (2.5 %)	0.6 (2.2 %)
Wood Smoke:	20.2 (70.6 %)	9.5 (32.7 %)
No. 2 Fuel Oil:	Not Identified	13.5 (46.4 %)
Unexplained:	0.1 (0.3 %)	0.4 (1.3 %)

Figure 43: Winter 2011/2012, State Building.
CMB Results with EPA Source Profiles, November 2, 2011 – March 31, 2012.

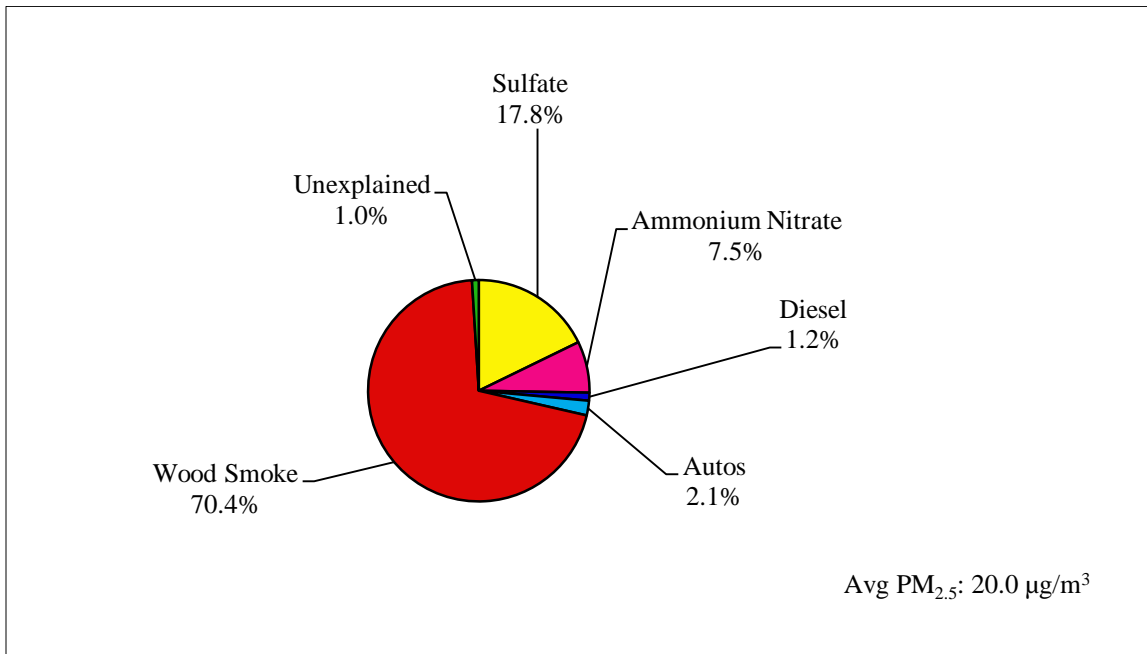
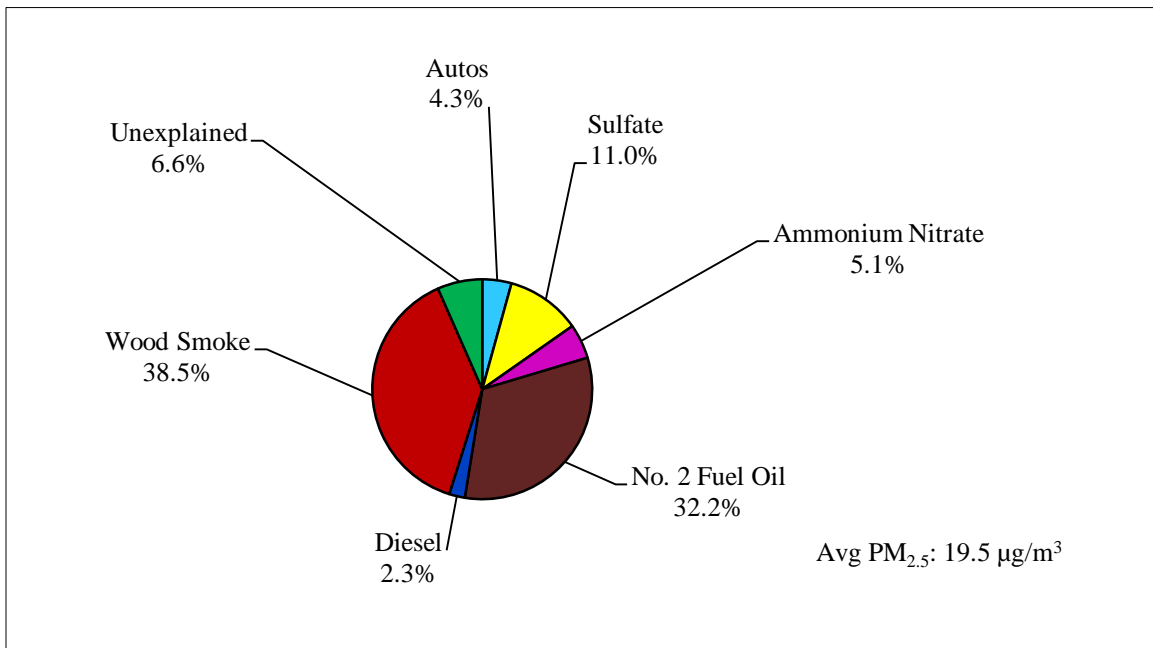


Figure 44: Winter 2011/2012, State Building.
CMB Results with OMNI Source Profiles, November 2, 2011 – March 31, 2012.



**Table 30: Comparison of CMB Results - EPA and OMNI Source Profiles.
State Building, Winter 2011/2012.**

Season:	Winter 2011/2012 (EPA)	Winter 2011/2012 (OMNI)
Dates:	11/2/11-3/31/12	11/2/11-3/31/12
n:	38	36
PM_{2.5} Mass (µg/m³):	20.0	19.5
CMB Source Estimates (µg/m³ and %)		
Sulfate:	3.5 (17.8 %)	2.2 (11.0 %)
Ammonium Nitrate:	1.5 (7.5 %)	1.0 (5.1 %)
Diesel:	0.2 (1.2 %)	0.5 (2.3 %)
Automobiles:	0.4 (2.1 %)	0.8 (4.3 %)
Wood Smoke:	14.0 (70.4 %)	7.6 (38.5 %)
No. 2 Fuel Oil:	Not Identified	6.4 (32.2 %)
Unexplained:	0.2 (1.0 %)	1.3 (6.6 %)

**Figure 45: Winter 2011/2012, North Pole.
CMB Results with EPA Source Profiles, November 2, 2011 – March 25, 2012.**

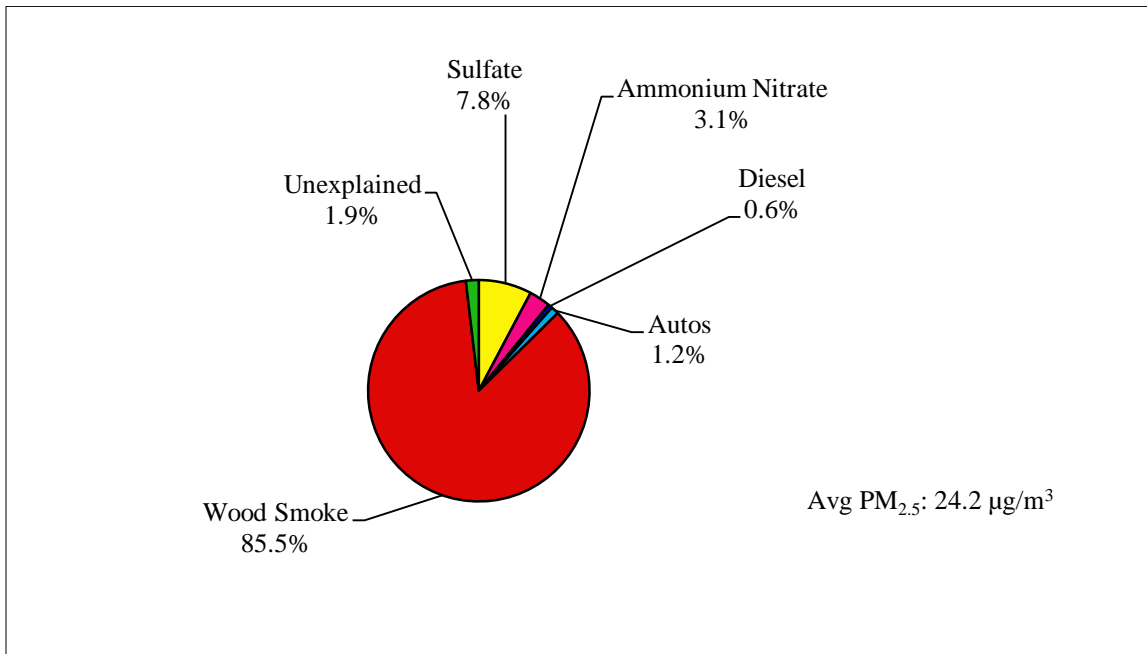


**Figure 46: Winter 2011/2012, North Pole.
CMB Results with OMNI Source Profiles, November 2, 2011 – March 25, 2012.**

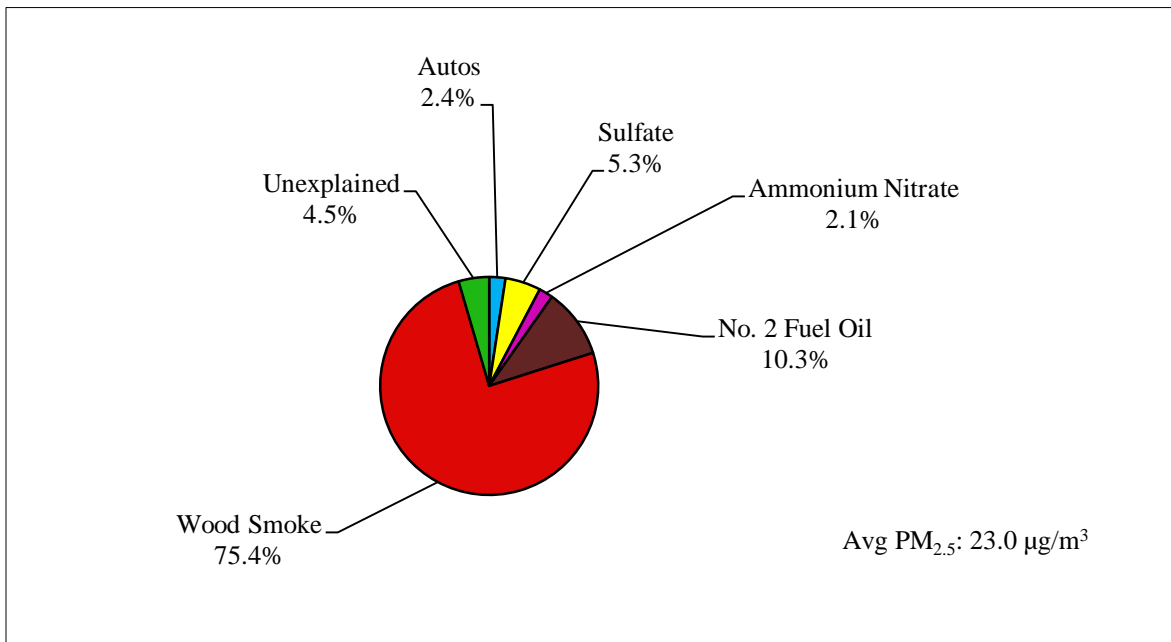


**Table 31: Comparison of CMB Results - EPA and OMNI Source Profiles.
North Pole, Winter 2011/2012.**

Season:	Winter 2011/2012 (EPA)	Winter 2011/2012 (OMNI)
Dates:	11/2/11-3/25/12	11/2/11-3/25/12
n:	36	35
PM_{2.5} Mass (µg/m³):	24.2	23.0
CMB Source Estimates (µg/m³ and %)		
Sulfate:	1.8 (7.8 %)	1.2 (5.3 %)
Ammonium Nitrate:	0.7 (3.1 %)	0.5 (2.1 %)
Diesel:	0.1 (0.6 %)	Not Identified
Automobiles:	0.3 (1.2 %)	0.6 (2.4 %)
Wood Smoke:	20.4 (85.5 %)	17.3 (75.4 %)
No. 2 Fuel Oil:	Not Identified	2.4 (10.3 %)
Unexplained:	0.4 (1.9 %)	1.0 (4.5 %)

**Figure 47: Winter 2011/2012, RAMS.
CMB Results with EPA Source Profiles, December 20, 2011 – February 27, 2012.**

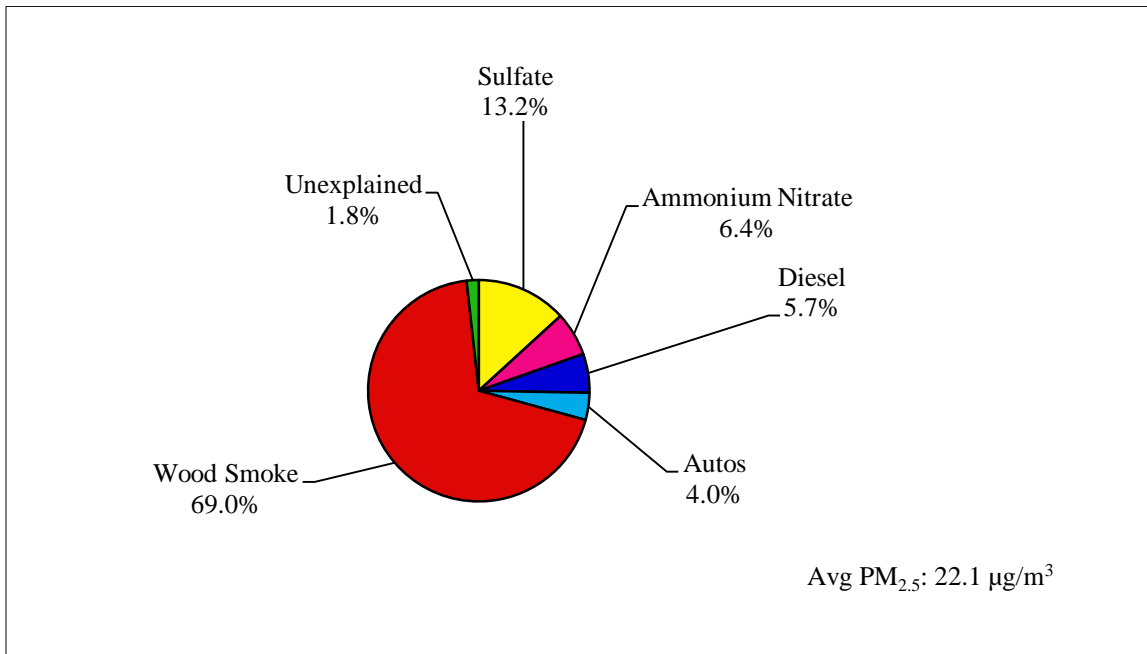


**Figure 48: Winter 2011/2012, RAMS.
CMB Results with OMNI Source Profiles, December 20, 2011 – February 27, 2012.**

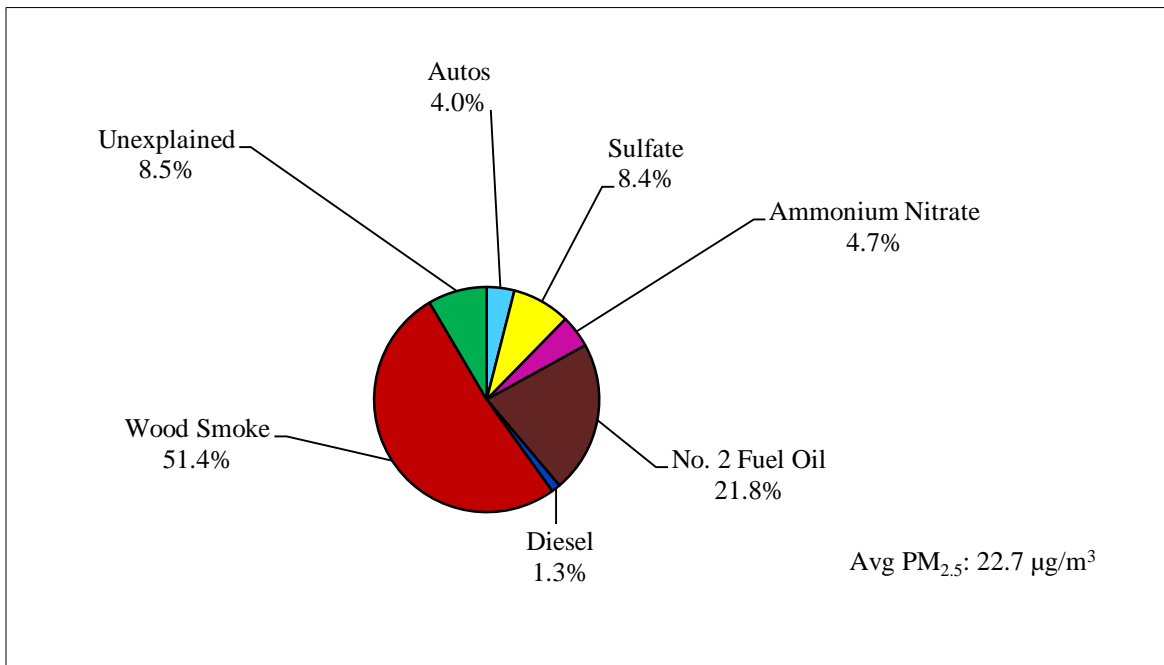


Table 32: Comparison of CMB Results - EPA and OMNI Source Profiles. RAMS, Winter 2011/2012.

Season:	Winter 2011/2012 (EPA)	Winter 2011/2012 (OMNI)
Dates:	12/20/11-2/27/12	12/20/11-2/27/12
n:	16	15
PM_{2.5} Mass (µg/m³):	22.1	22.7
CMB Source Estimates (µg/m³ and %)		
Sulfate:	2.9 (13.2 %)	1.9 (8.4 %)
Ammonium Nitrate:	1.4 (6.4 %)	1.0 (4.7 %)
Diesel:	1.2 (5.7 %)	0.3 (1.3 %)
Automobiles:	0.9 (4.0 %)	0.9 (4.0 %)
Wood Smoke:	14.9 (69.0 %)	11.5 (51.4 %)
No. 2 Fuel Oil:	Not Identified	4.9 (21.8 %)
Unexplained:	0.4 (1.8 %)	1.9 (8.5 %)

Figure 49: Winter 2011/2012, NCORE.
CMB Results with EPA Source Profiles, November 2, 2011 – March 31, 2012.

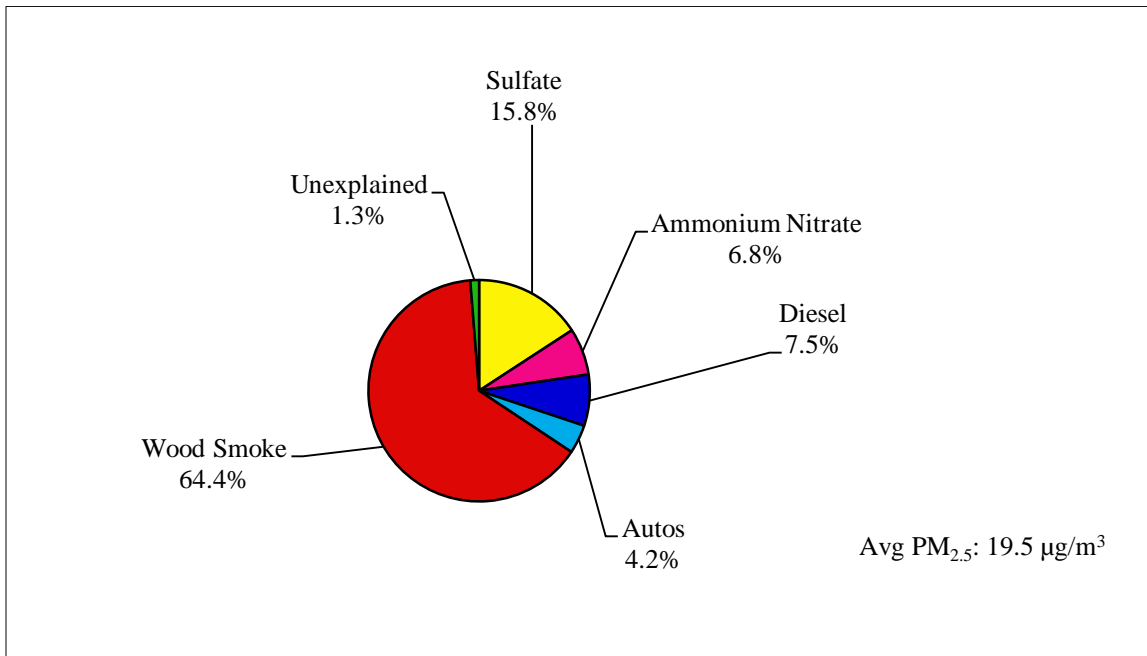


Figure 50: Winter 2011/2012, NCORE.
CMB Results with OMNI Source Profiles, November 2, 2011 – March 31, 2012.

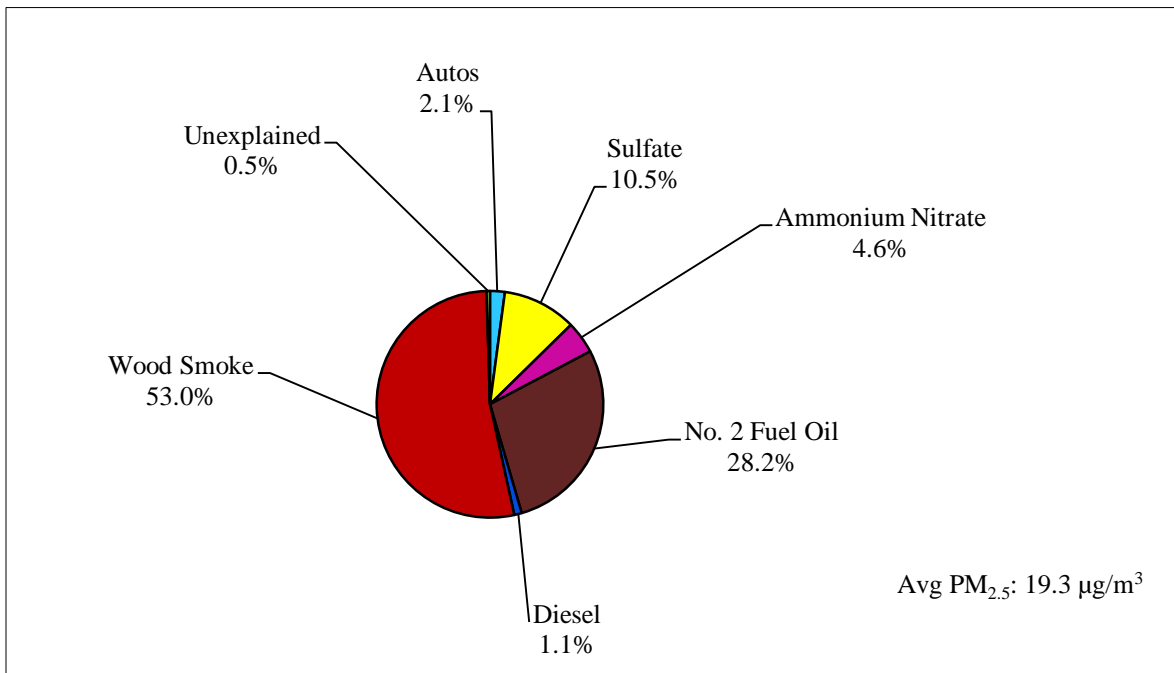
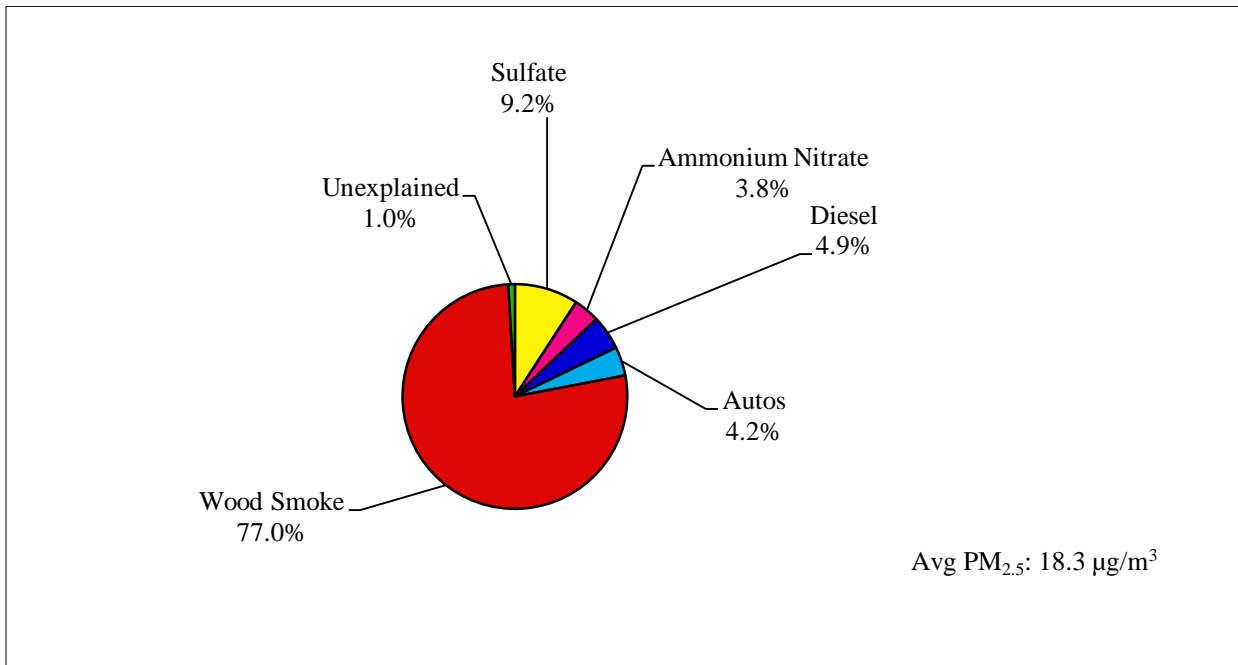


Table 33: Comparison of CMB Results - EPA and OMNI Source Profiles. NCORE, Winter 2011/2012.

Season:	Winter 2011/2012 (EPA)	Winter 2011/2012 (OMNI)
Dates:	11/2/11-3/31/12	11/2/11-3/31/12
n:	44	42
PM_{2.5} Mass (µg/m³):	19.5	19.3
CMB Source Estimates (µg/m³ and %)		
Sulfate:	3.0 (15.8 %)	2.0 (10.5 %)
Ammonium Nitrate:	1.3 (6.8 %)	0.9 (4.6 %)
Diesel:	1.4 (7.5 %)	0.2 (1.1 %)
Automobiles:	0.8 (4.2 %)	0.4 (2.1 %)
Wood Smoke:	12.4 (64.4 %)	10.1 (53.0 %)
No. 2 Fuel Oil:	Not Identified	5.4 (28.2 %)
Unexplained:	0.2 (1.3 %)	0.1 (0.5 %)

**Figure 51: Winter 2011/2012, NPF3.
CMB Results with EPA Source Profiles, March 1, 2011 – March 31, 2012.**



**Figure 52: Winter 2011/2012, NPF3.
CMB Results with OMNI Source Profiles, March 1, 2011 – March 31, 2012.**

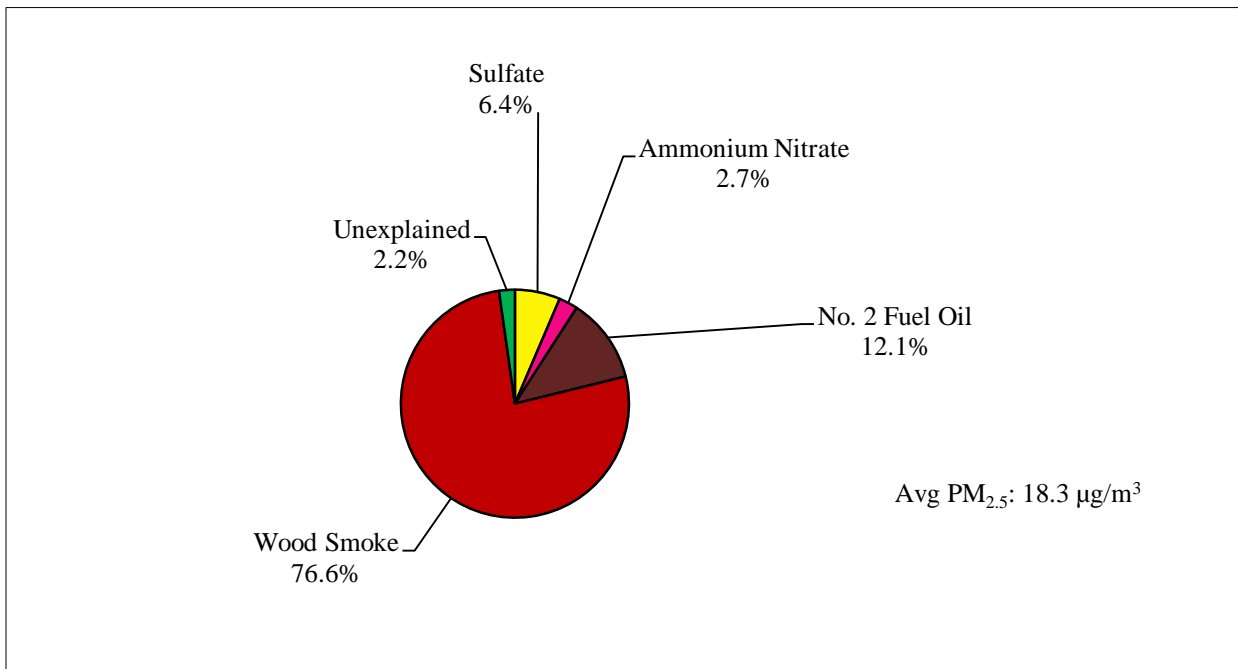
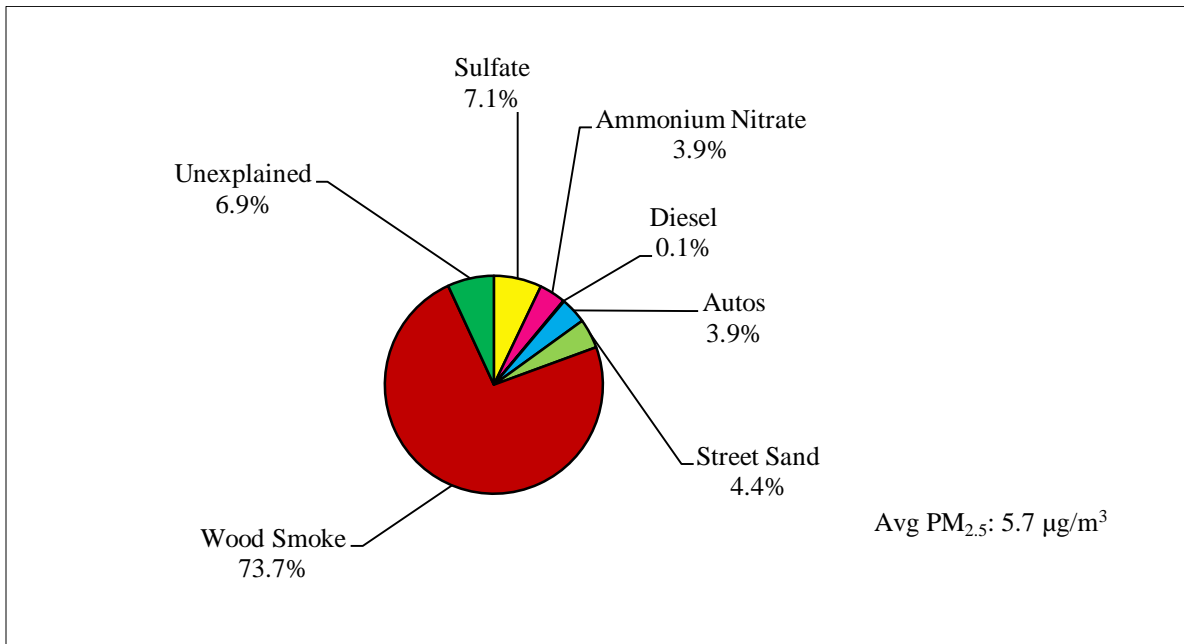


Table 34: Comparison of CMB Results - EPA and OMNI Source Profiles. NPF3, Winter 2011/2012.

Season:	Winter 2011/2012 (EPA)	Winter 2011/2012 (OMNI)
Dates:	3/1/12-3/31/12	3/1/12-3/31/12
n:	7	7
PM_{2.5} Mass (µg/m³):	18.3	18.3
CMB Source Estimates (µg/m³ and %)		
Sulfate:	1.7 (9.2 %)	1.2 (6.4 %)
Ammonium Nitrate:	0.7 (3.8 %)	0.5 (2.7 %)
Diesel:	0.9 (4.9 %)	Not Identified
Automobiles:	0.8 (4.2 %)	Not Identified
Wood Smoke:	14.2 (77.0 %)	14.1 (76.6 %)
No. 2 Fuel Oil:	Not Identified	2.2 (12.1 %)
Unexplained:	0.2 (1.0 %)	0.4 (2.2 %)

**Figure 53: Summer 2012, State Building.
CMB Results with EPA Source Profiles, June 2, 2012 – August 31, 2012.**



**Figure 54: Summer 2012, State Building.
CMB Results with OMNI Source Profiles, June 2, 2012 – August 31, 2012.**

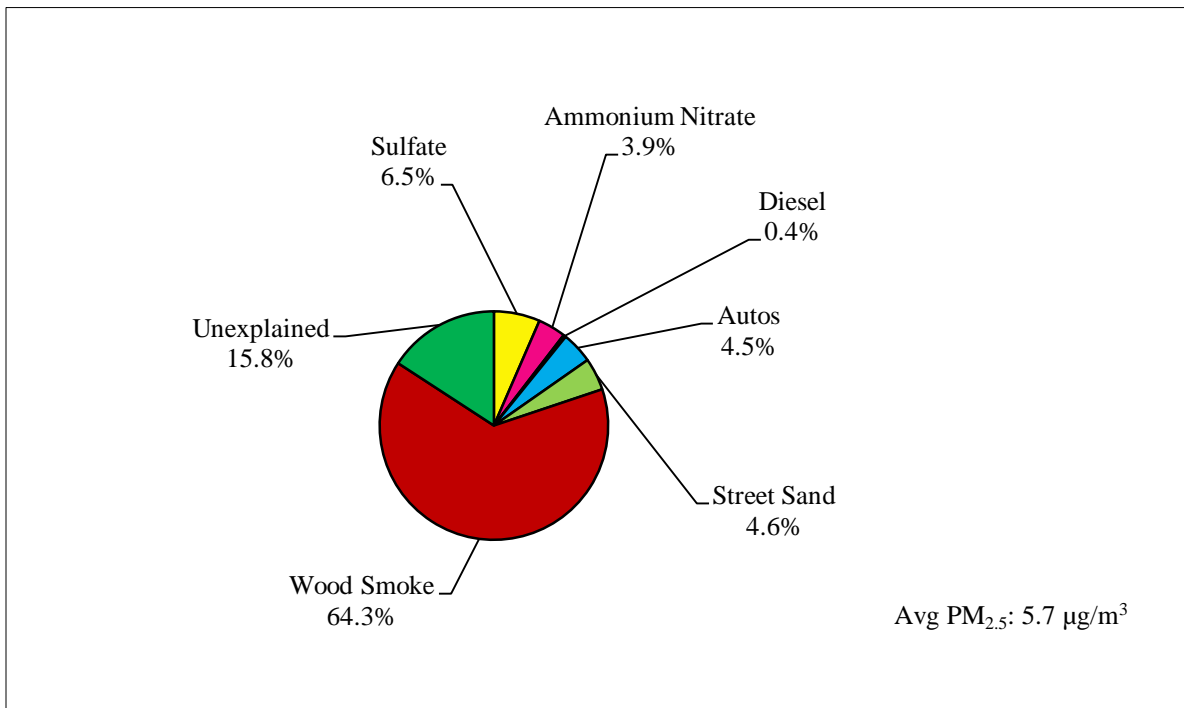


**Table 35: Comparison of CMB Results - EPA and OMNI Source Profiles.
State Building, Summer 2012.**

Season:	Summer 2012 (EPA)	Summer 2012 (OMNI)
Dates:	6/2/12-8/31/12	6/2/12-8/31/12
n:	20	20
PM_{2.5} Mass (µg/m³):	5.7	5.7
CMB Source Estimates (µg/m³ and %)		
Sulfate:	0.4 (7.1 %)	0.4 (6.5 %)
Ammonium Nitrate:	0.2 (3.9 %)	0.2 (3.9 %)
Diesel:	0.01 (0.1 %)	0.02 (0.4 %)
Automobiles:	0.2 (3.9 %)	0.3 (4.5 %)
Wood Smoke:	4.2 (73.7 %)	3.6 (64.3 %)
No. 2 Fuel Oil:	Not Identified	Not Identified
Street Sand:	0.3 (4.4 %)	0.3 (4.6 %)
Unexplained:	0.3 (6.9 %)	0.9 (15.8 %)

Figure 55: Summer 2012, NCORE.
CMB Results with EPA Source Profiles, June 14, 2012 – August 31, 2012.

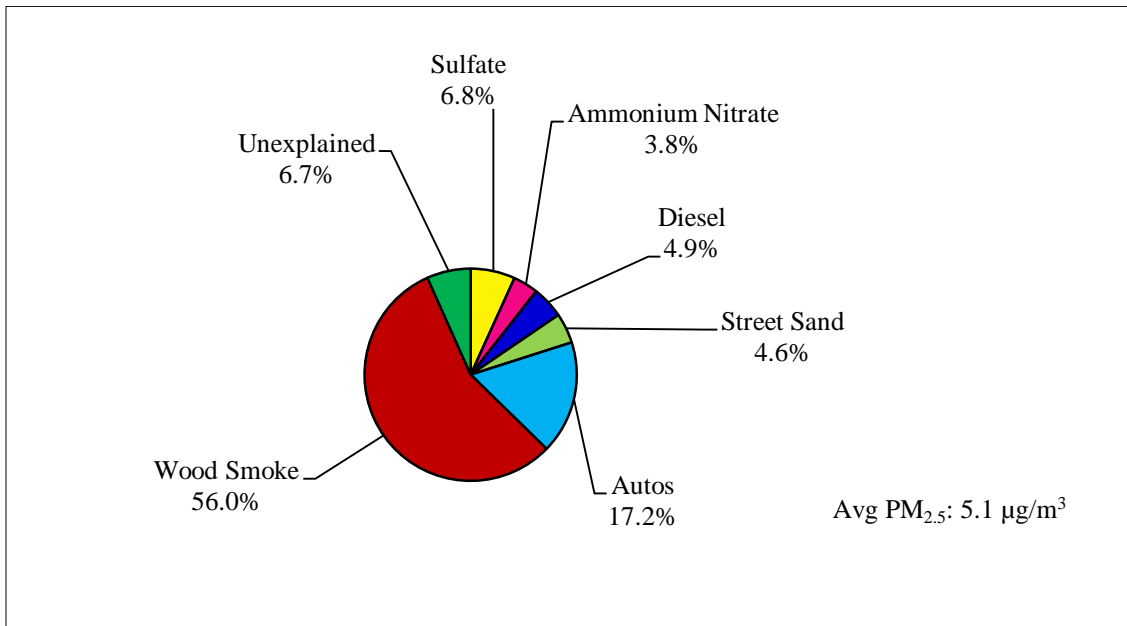


Figure 56: Summer 2012, NCORE.
CMB Results with OMNI Source Profiles, June 14, 2012 – August 31, 2012.

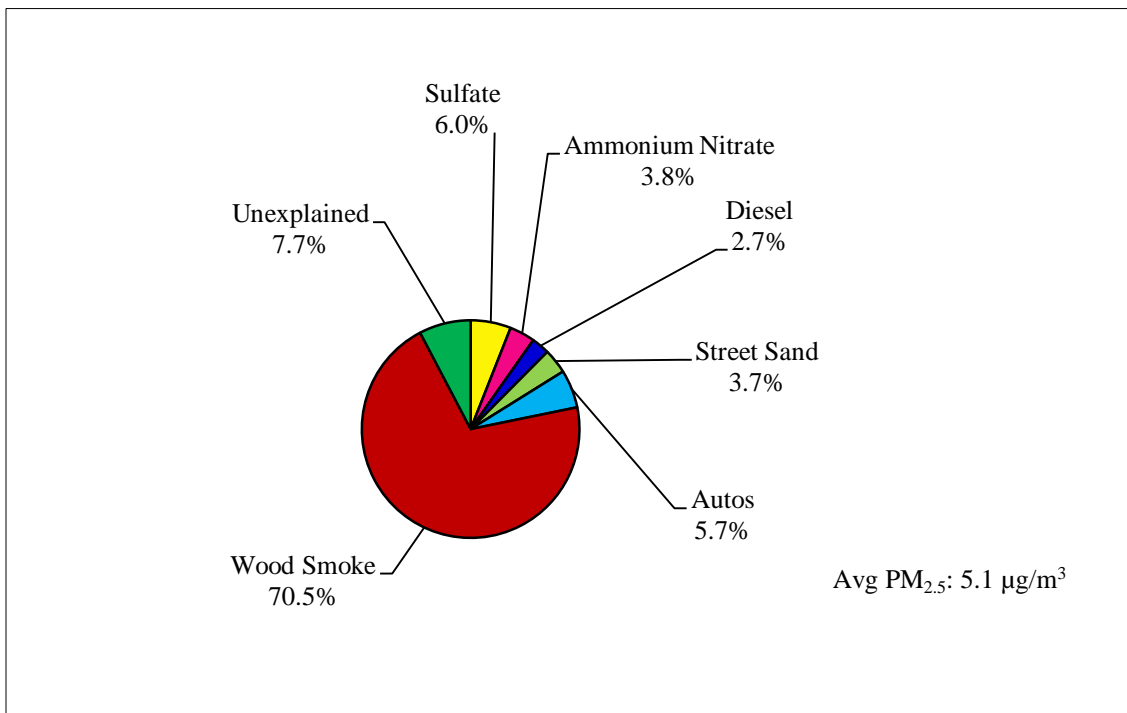


Table 36: Comparison of CMB Results - EPA and OMNI Source Profiles. NCORE, Summer 2012.

Season:	Summer 2012 (EPA)	Summer 2012 (OMNI)
Dates:	6/14/12-8/31/12	6/14/12-8/31/12
n:	17	17
PM_{2.5} Mass (µg/m³):	5.1	5.1
CMB Source Estimates (µg/m³ and %)		
Sulfate:	0.4 (6.8 %)	0.4 (6.0 %)
Ammonium Nitrate:	0.2 (3.8 %)	0.2 (3.8 %)
Diesel:	0.3 (4.9 %)	0.2 (2.7 %)
Automobiles:	1.0 (17.2 %)	0.3 (5.7 %)
Wood Smoke:	3.3 (56.0 %)	4.2 (70.5 %)
No. 2 Fuel Oil:	Not Identified	Not Identified
Street Sand:	0.3 (4.6 %)	0.2 (3.7 %)
Unexplained:	0.4 (6.7 %)	0.5 (7.7 %)

Figure 57: Winter 2012/2013, State Building.
CMB Results with EPA Source Profiles, November 2, 2012 – March 29, 2013.

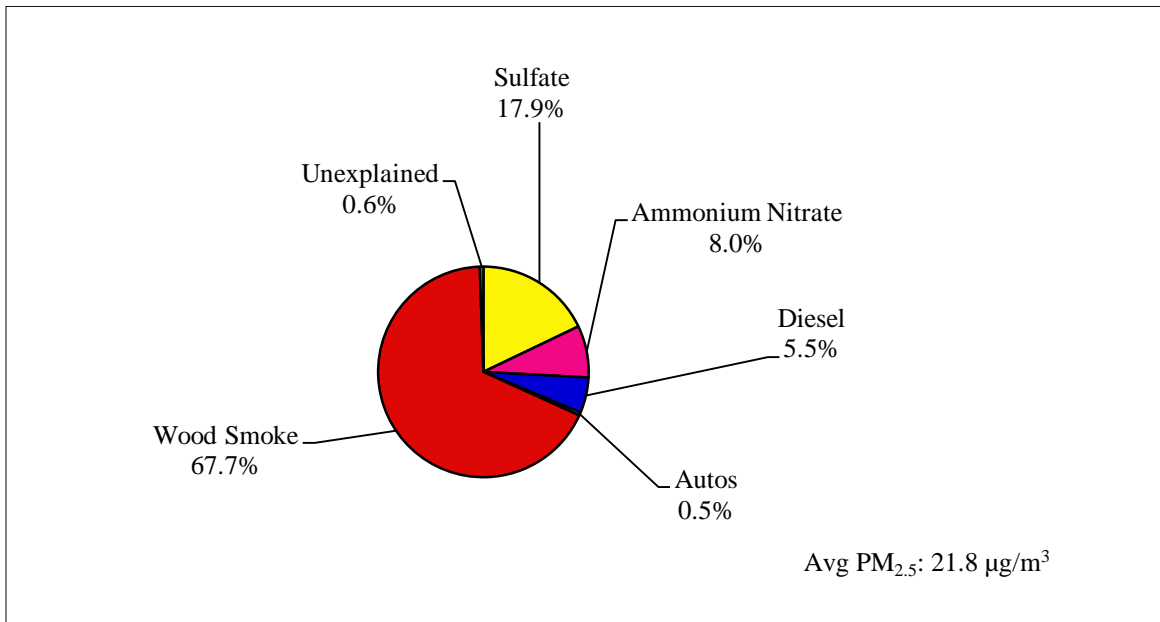
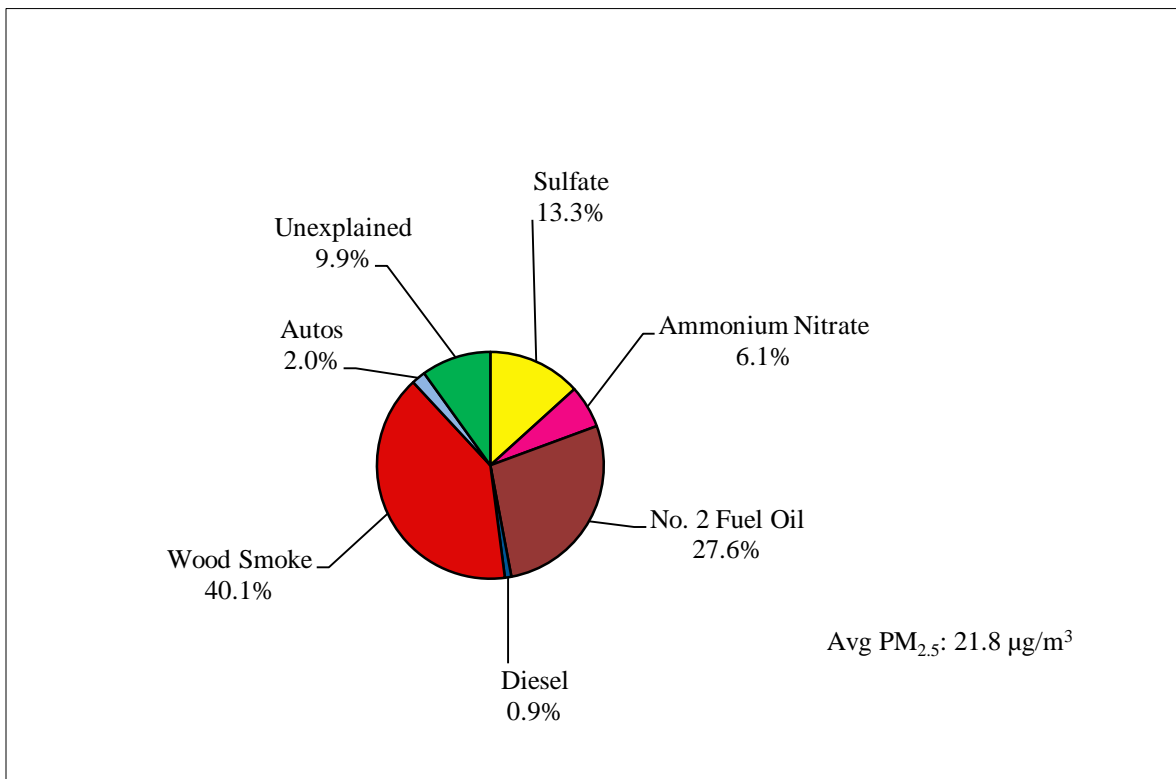


Figure 58: Winter 2012/2013, State Building.
CMB Results with OMNI Source Profiles, November 2, 2012 – March 29, 2013.



**Table 37: Comparison of CMB Results - EPA and OMNI Source Profiles.
State Building, Winter 2012/2013.**

Season:	Winter 2012/2013 (EPA)	Winter 2012/2013 (OMNI)
Dates:	11/2/12-3/29/13	11/2/12-3/29/13
n:	29	29
PM_{2.5} Mass (µg/m³):	21.8	21.8
CMB Source Estimates (µg/m³ and %)		
Sulfate:	3.9 (17.9 %)	2.9 (13.3 %)
Ammonium Nitrate:	1.7 (8.0 %)	1.3 (6.1 %)
Diesel:	1.2 (5.5 %)	0.2 (0.9 %)
Automobiles:	0.1 (0.5 %)	0.4 (2.0 %)
Wood Smoke:	14.7 (67.7 %)	8.7 (40.1 %)
No. 2 Fuel Oil:	Not Identified	6.0 (27.6 %)
Unexplained:	0.1 (0.6 %)	2.1 (9.9 %)

**Figure 59: Winter 2012/2013, NPE.
CMB Results with EPA Source Profiles, November 2, 2012 – March 29, 2013.**

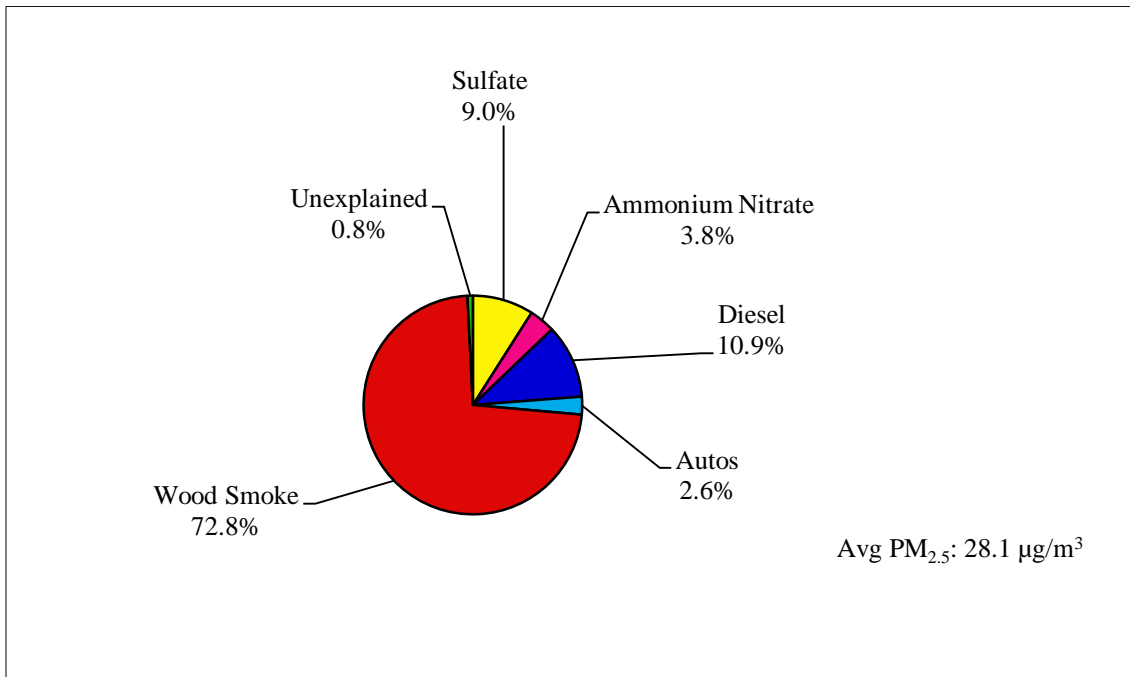


**Figure 60: Winter 2012/2013, NPE.
CMB Results with OMNI Source Profiles, November 2, 2012 – March 29, 2013.**

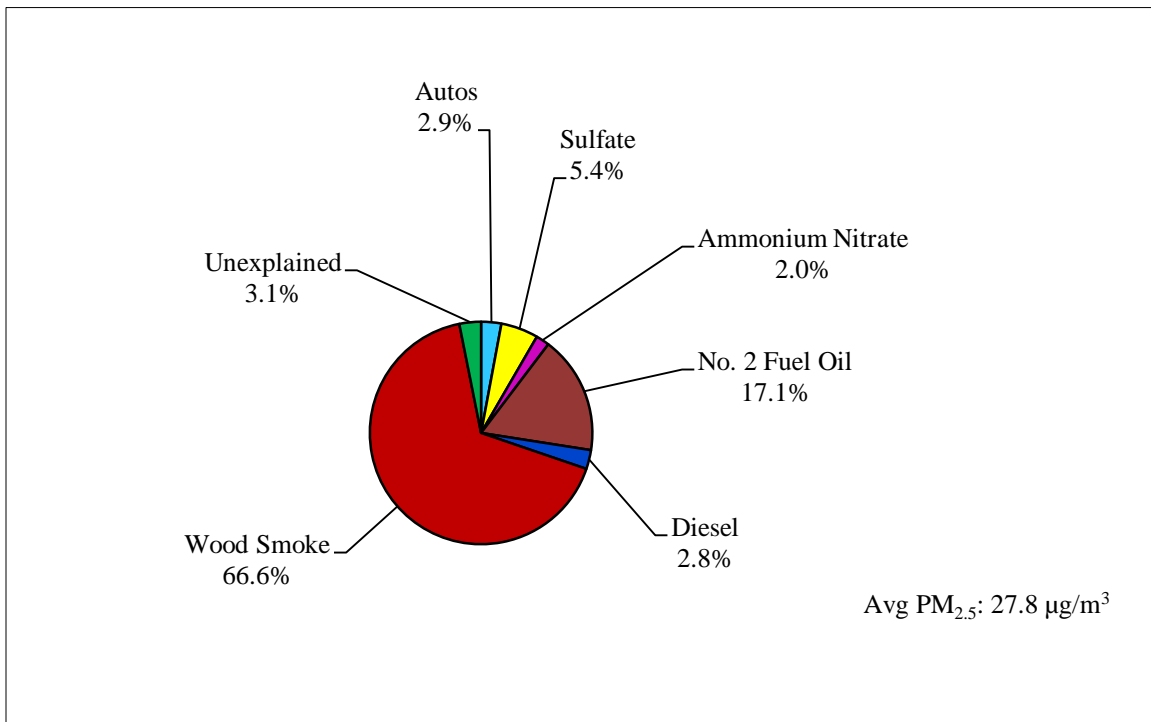


Table 38: Comparison of CMB Results - EPA and OMNI Source Profiles. NPE, Winter 2012/2013.

Season:	Winter 2012/2013 (EPA)	Winter 2012/2013 (OMNI)
Dates:	11/2/12-3/29/13	11/2/12-3/29/13
n:	41	40
PM_{2.5} Mass (µg/m³):	28.1	27.8
CMB Source Estimates (µg/m³ and %)		
Sulfate:	2.5 (9.0 %)	1.5 (5.4 %)
Ammonium Nitrate:	1.1 (3.8 %)	0.6 (2.0 %)
Diesel:	3.0 (10.9 %)	0.8 (2.8 %)
Automobiles:	0.7 (2.6 %)	0.8 (2.9 %)
Wood Smoke:	20.3 (72.8 %)	18.8 (66.6 %)
No. 2 Fuel Oil:	Not Identified	4.9 (17.1 %)
Unexplained:	0.2 (0.8 %)	0.9 (3.1 %)

Figure 61: Winter 2012/2013, NCORE.
CMB Results with EPA Source Profiles, November 2, 2012 – March 29, 2013.

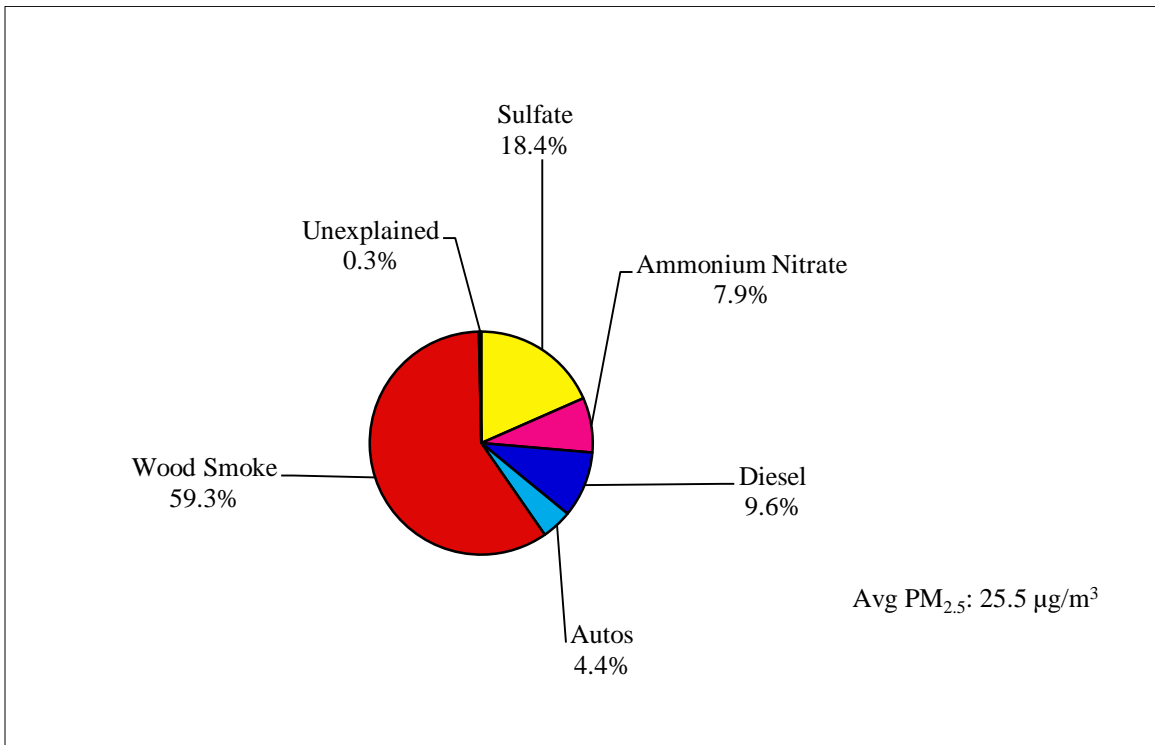


Figure 62: Winter 2012/2013, NCORE.
CMB Results with OMNI Source Profiles, November 2, 2012 – March 29, 2013.

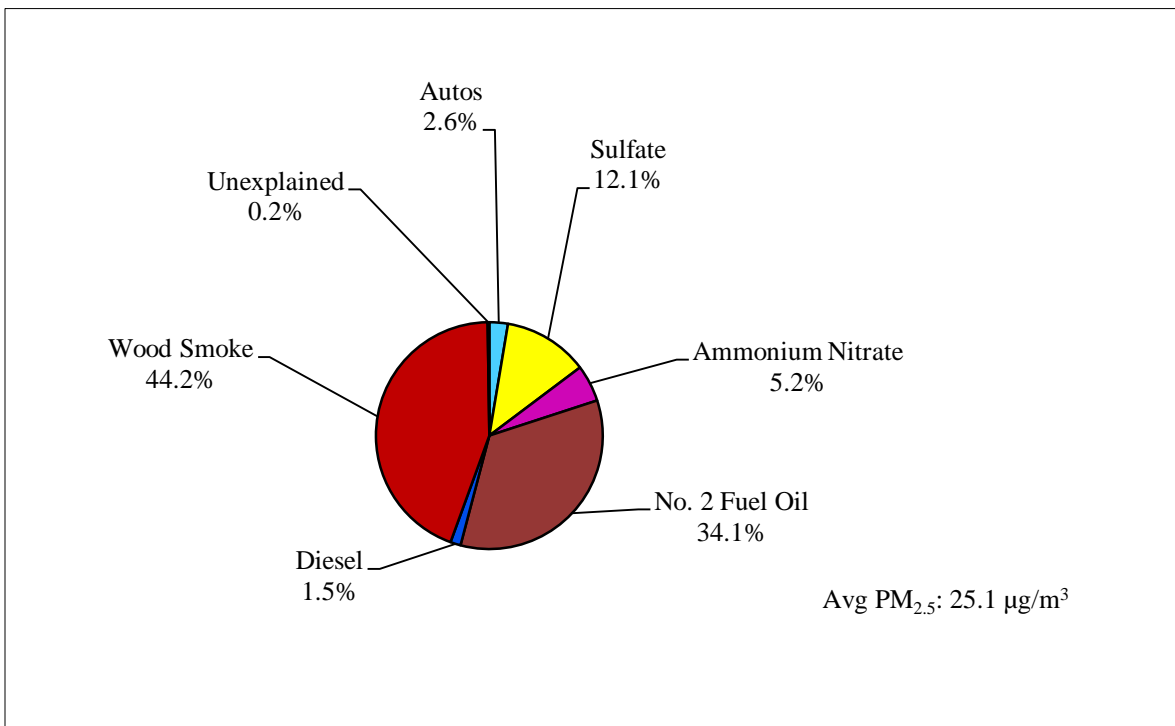
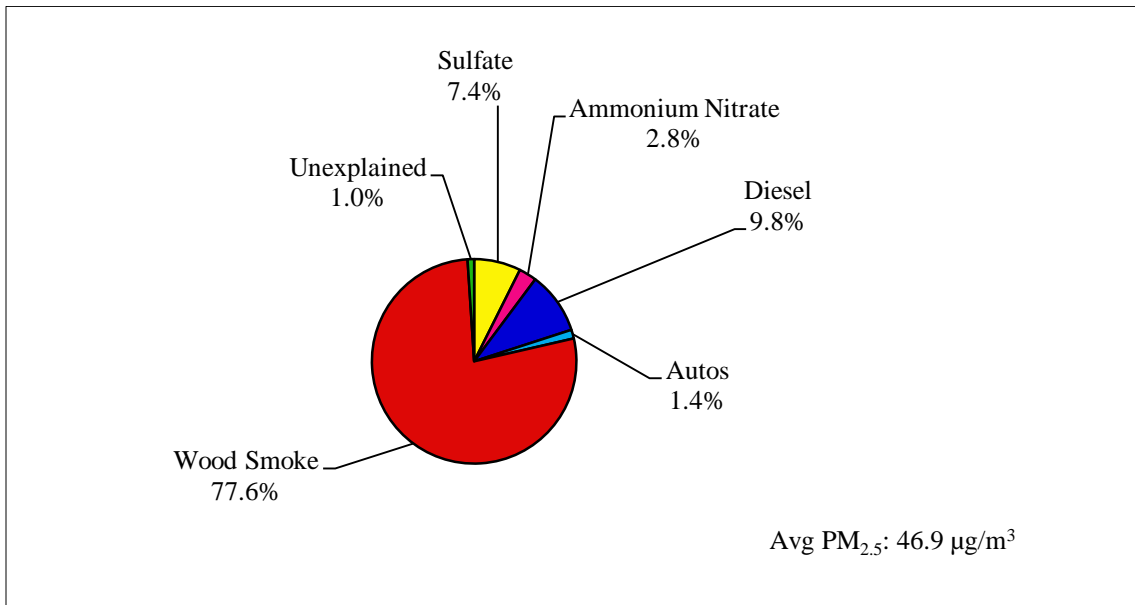


Table 39: Comparison of CMB Results - EPA and OMNI Source Profiles. NCORE, Winter 2012/2013.

Season:	Winter 2012/2013 (EPA)	Winter 2012/2013 (OMNI)
Dates:	11/2/12-3/29/13	11/2/12-3/29/13
n:	38	39
PM_{2.5} Mass (µg/m³):	25.5	25.1
CMB Source Estimates (µg/m³ and %)		
Sulfate:	4.7 (18.4 %)	3.0 (12.1 %)
Ammonium Nitrate:	2.0 (7.9 %)	1.3 (5.2 %)
Diesel:	2.4 (9.6 %)	0.4 (1.5 %)
Automobiles:	1.1 (4.4 %)	0.7 (2.6 %)
Wood Smoke:	15.1 (59.3 %)	11.0 (44.2 %)
No. 2 Fuel Oil:	Not Identified	8.5 (34.1 %)
Unexplained:	0.1 (0.3 %)	0.1 (0.2 %)

**Figure 63: Winter 2012/2013, NPF3.
CMB Results with EPA Source Profiles, November 2, 2012 – March 29, 2013.**



**Figure 64: Winter 2012/2013, NPF3.
CMB Results with OMNI Source Profiles, November 2, 2012 – March 29, 2013.**

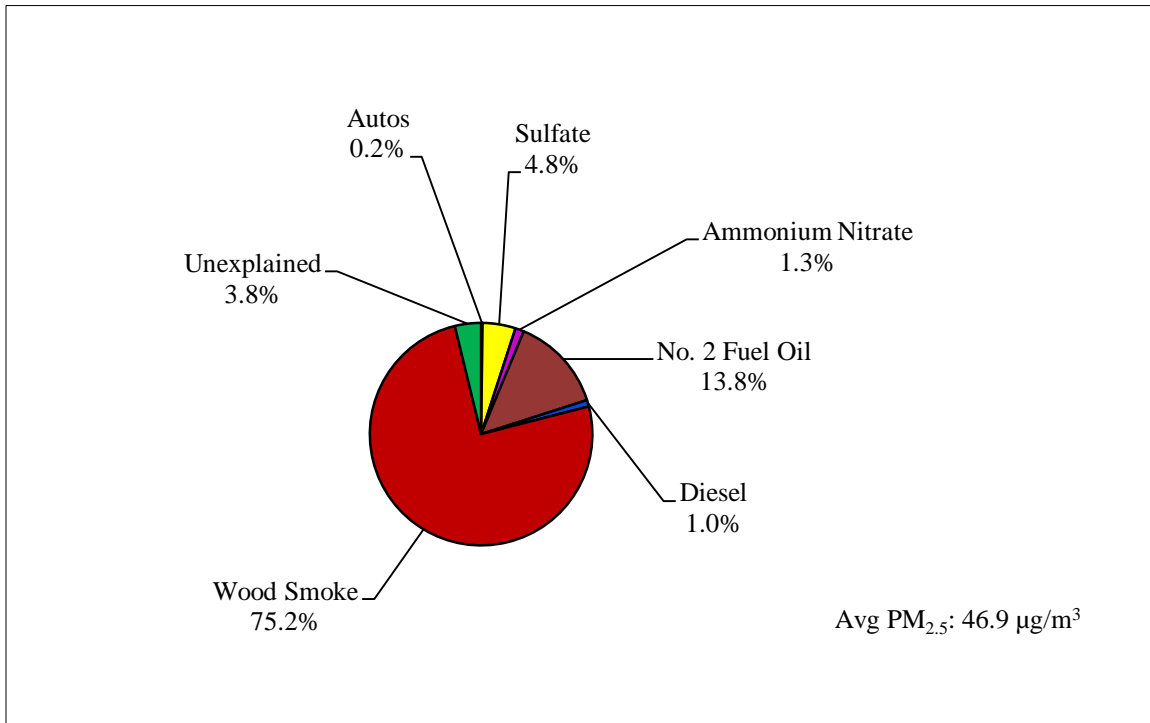


Table 40: Comparison of CMB Results - EPA and OMNI Source Profiles. NPF3, Winter 2012/2013.

Season:	Winter 2012/2013 (EPA)	Winter 2012/2013 (OMNI)
Dates:	11/2/12-3/29/13	11/2/12-3/29/13
n:	42	42
PM_{2.5} Mass (µg/m³):	46.9	46.9
CMB Source Estimates (µg/m³ and %)		
Sulfate:	3.4 (7.4 %)	2.2 (4.8 %)
Ammonium Nitrate:	1.3 (2.8 %)	0.6 (1.3 %)
Diesel:	4.5 (9.8 %)	0.4 (1.0 %)
Automobiles:	0.6 (1.4 %)	0.1 (0.2 %)
Wood Smoke:	35.9 (77.6 %)	34.7 (75.2 %)
No. 2 Fuel Oil:	Not Identified	6.4 (13.8 %)
Unexplained:	0.5 (1.0 %)	1.8 (3.8 %)

8.0. Discussion - CMB Modeling

The Tables in **Appendix C** present the $PM_{2.5}$ sources identified by the CMB model (including source contribution estimates and standard errors) for each sample day throughout the program using both EPA and OMNI profiles. The standard error is a single standard deviation. When a standard error value is multiplied by two or three times, the result may be taken as a measure of the upper and lower limit of an individual source's contribution. There is about a 66% probability that the true source contribution is within one standard error and about a 95% probability that the true contribution is within two standard errors of the source contribution estimate. Below is a more complete discussion of the individual source types identified by the CMB modeling.

8.1. Wood Smoke

The wood smoke source identified by the CMB model during the winter months should be viewed as a general source predominantly composed of wood stove emissions. In addition to residential wood stoves, other biomass combustion emission sources could have contributed to the wood smoke results in Fairbanks, including smoke from outdoor boilers, residential open burning of biomass waste, and small industrial sources. A source profile (Profile 56 in **Table 1**) developed in Missoula, Montana in the late 1980s served as a good statistically fitting wood smoke profile when using the non-OMNI profiles for each of the winters/sites when conducting the Fairbanks CMB analyses. It should also be noted that many other residential wood combustion source profiles from the EPA SPECIATE database gave good statistical fits throughout the computer modeling process for each of the sites, including the following wood smoke profiles listed in **Table 1**: 61, 62, 65, and 66. When compared to profiles of other sources, these wood smoke profiles typically had higher levels of elemental potassium, potassium ion, and OC. Generally, both elemental potassium and the potassium ion gave good fits when modeling, with the elemental form usually providing the better statistical fit.

When focusing on the OMNI profiles in the CMB model, FBK107 (EPA Wood Stove, spruce, low) gave the best statistical fit. However, other OMNI profiles for wood smoke combustion were statistically significant as well, and were used in the CMB modeling: FBK101 (EPA OWHH, Birch, Low), FBK102 (Conventional Wood Stove, Birch, Low), and FBK100 (EPA Wood Stove, Birch, Low). Given that all of these wood smoke profiles (both EPA and OMNI) provided strong statistical fits (i.e. gave the best results), this supports that wood smoke (likely from residential wood combustion) is a major source of $PM_{2.5}$ in the Fairbanks airshed throughout the winter months. It should also be noted that wood smoke was determined to be the largest source of $PM_{2.5}$ at both the State Building and NCORE sites (56-72%) during the summer of 2012, likely due to residential outdoor biomass waste burning and influences from regional wildland forest fire events.

8.2. Secondary Pollutants

“Pure secondary” aerosols such as ammonium nitrate and sulfate are actually formed through gas-to-particle transformations in the atmosphere, and are represented by their chemical form in the model. As noted earlier, one assumption of the CMB model is that compositions of source emissions are constant over the period of ambient and source sampling, and that chemical species do not react with each other. CMB is well suited for apportioning sources of primary aerosols (those emitted directly as particles). However, it is difficult to attribute secondary aerosols formed through gas-to-particle transformation in the atmosphere to specific sources. Using the secondary sulfate and the ammonium nitrate profiles allows us to account for the secondary aerosol contributions to $PM_{2.5}$ mass.

Sulfate is a large source contributor to ambient $PM_{2.5}$, representative of particles directly emitted during combustion and secondary particles formed in the atmosphere. Sulfate is a function of the sulfur content of the fuels burned in the Fairbanks community. Recent regulations have all but eliminated sulfur from

gasoline and diesel fuel in Alaska. Therefore, the fuels contributing sulfur (and sulfate) to the Fairbanks airshed likely include distillate fuel oil used in space heating and coal combustion. Ammonium nitrate (NH_4NO_3) is a secondary pollutant that was also identified frequently by the CMB model at each of the sites. Identified source contributions were very similar when using the EPA and OMNI profiles, with slightly less sulfate and ammonium nitrate identified when using the OMNI profiles. It should be noted that even though ammonium sulfate was not detected by the CMB model as a $\text{PM}_{2.5}$ source (secondary) when both sulfate and ammonium nitrate were used as fitting species, it is likely a significant contributor to the measured $\text{PM}_{2.5}$ levels. When using the secondary sulfate source profile in the model, sulfur was used as the fitting species in each model run to apportion sulfate contributions.

Ammonia (NH_3) and oxides of nitrogen (NO_x) are the precursors for ammonium nitrate particles, with just under half all NO_x emissions in the United States estimated to come from the transportation sector (Seinfeld and Pandis, 1998; Dreher and Harley, 1998). $\text{PM}_{2.5}$ has been found to correlate with gaseous emissions of NO_x from vehicles, with heavy duty vehicles contributing significantly greater amounts of NO_x and particulate matter on a per vehicle basis than light duty vehicles (Gillies et al., 2001). Between 40 and 45% of all NO_x emissions in the United States are estimated to come from transportation, with about half of this coming from light-duty gasoline trucks and cars and approximately one-quarter from heavy-duty gasoline and diesel vehicles (Seinfeld and Pandis, 1998; Dreher and Harley, 1998). Other sources of NO_x in Fairbanks might include industry, natural gas furnaces, and residential wood combustion. In other parts of the lower 48, ammonia emissions to the atmosphere can arise from many sources including the decay of livestock waste, use of chemical fertilizers, emissions from sewage waste treatment plants, and biological processes in soils (Fraser and Cass, 1998). In Fairbanks, combustion processes such as motor vehicles likely are a significant source of ammonia.

8.3. Mobile Sources

Profiles for this source group typically had higher levels of EC when compared to the wood smoke profiles. When using the EPA profiles, the CMB model determined that vehicles were a measurable source of $\text{PM}_{2.5}$ at each of the sites throughout the winter months. Automobile exhaust (gasoline-powered) contributions to $\text{PM}_{2.5}$ were detected at the sites up to 7%. Diesel exhaust was also measured at each of the sites, contributing up to 11%. When using the OMNI wood smoke and fuel oil profiles in the CMB model, mobile sources were identified as being smaller contributors to the ambient $\text{PM}_{2.5}$. For the majority of the CMB runs using OMNI profiles, both automobiles and diesel exhaust were found to typically contribute less than 6% to the overall ambient $\text{PM}_{2.5}$.

8.4. Other Sources

When conducting CMB modeling using the EPA source profiles, there were other sources identified by the CMB model as contributors to the ambient $\text{PM}_{2.5}$. However, these sources were not identified as statistically significant contributors (i.e. evaluated based on CMB model statistical criteria). These sources include the following: street sand, distillate oil combustion, natural gas combustion, residual oil combustion, and sub bituminous coal combustion. Street sand was detected by the CMB model from filters collected during the early spring, but never in concentrations that were considered statistically significant ($TSTAT > 2$). In addition, the source profile for natural gas combustion was identified on several occasions, but never in amounts that were statistically significant.

Regarding the combustion sources such as distillate oil, residual oil, and sub bituminous coal, primary $\text{PM}_{2.5}$ emissions were not identified as being statistically significant from these individual sources. To investigate this further, the CMB model was run with both the EPA SPECIATE distillate oil and coal profile in the model, and in the absence of the secondary sulfate profile (using both the sulfur and sulfate fitting species). In both instances, the model provided very poor statistical fits. Using the secondary

sulfate profile (as a potential surrogate for these sources) provided excellent statistical fits on nearly every sample run.

When using the OMNI profiles in the CMB modeling, the No. 2 fuel oil profile (FBK103) was consistently identified as a source of PM_{2.5} at each of the sites during all winters. The other OMNI profiles for coal, including FBK104 (Coal Stove, Wet Stoker Coal, Low), FBK105 (Coal HH, Wet Stoker Coal, Single), and 108 (Coal Stove Dry Lump Coal, low) were not identified in the CMB model. Similarly, the OMNI profile for waste oil (FBK106, WasteOil Brnr, Waste Oil, Single) was not identified by the CMB model to be a source of PM_{2.5} at any of the other sites (for each year).

9.0. Quality Assurance / Quality Control Results

9.1. Sampling Program QA/QC

For the Fairbanks sampling program, Alaska DEC and FNSB personnel maintained and audited the PM_{2.5} samplers at each of the sites. There were several days throughout the program where samples were not collected (and therefore CMB analyses were not conducted) due to sampler malfunctions. These sample days are identified in **Appendix B**. In addition, CMB source apportionment was not conducted on additional sample days during the winter months due to low PM_{2.5} mass. If the measured PM_{2.5} concentration is less than 7 µg/m³, the percent mass may be outside of the acceptable ranges because the uncertainty in the mass measurement is approximately 1 to 2 µg/m³. These days are also identified in **Appendix B**. These low mass days were primarily excluded for the winter days when the ambient PM_{2.5} concentrations were much higher. During the summer 2012 sample days, CMB modeling runs were conducted on all days (regardless of ambient PM_{2.5} mass concentrations) in an effort to identify the sources during these low-mass days.

9.2. Analytical Program QA/QC

RTI (speciation analyses) and Desert Research Institute were responsible for QA/QC activities within their respective laboratories. To monitor for artifact contamination in the field and in the laboratory, Teflon, nylon, and quartz filter field blanks were collected throughout the sampling programs. The results of the PM_{2.5} speciation field blank analyses show that the Teflon and quartz filters collected throughout the program did not measure significant artifacts for mass, elements, or Total Carbon. Several ions measured from the nylon filter blanks had levels above the MDLs, including sulfate, nitrate, ammonium, and sodium. Care was taken when utilizing these ions as fitting species to avoid inaccurate source apportionment to the fine PM.

9.3. CMB Program QA/QC

EPA's validation protocol (Watson et al., 2004) was followed throughout this CMB modeling program to ensure accurate results. For each model run, several different combinations of source profiles were evaluated, and the number of chemical species always exceeded the number of source types. The source contribution estimates and the statistics and diagnostic information were reviewed for each model run to determine the validity of the initial model results. The analysis was repeated by eliminating source profiles that gave negative source contribution estimates or standard errors that exceeded the source contribution estimates. When conducting the CMB model runs, only sources with TSTATs >2 were reported. If a TSTAT was <2, then the source was not considered a significant contributor for that sample day.

The majority of the CMB fitting parameters used to evaluate the validity of source contribution estimates were well within EPA target ranges. **Tables 41** (CMB with EPA profiles) **and 42** (CMB with OMNI profiles) present the program average key 'goodness-of-fit' statistics commonly evaluated for CMB models, the results for the Fairbanks CMB runs, and the EPA target ranges for each parameter.

The values for R^2 , Chi^2 , DF, and % mass explained for each CMB model run were generally well within the EPA target ranges. For the most part, the R/U ratios were all less than 2, and source collinearity (similarities between identified sources) was not a problem throughout this modeling application.

Table 41: Average Goodness-Of-Fit Parameter - EPA Profiles.

	R^2	Chi^2	Degrees of Freedom	% Mass Explained	TSTAT
EPA Target	0.8 - 1.00	0.00 - 4.0	> 5	80 - 120%	>2
State Building, 2005/2006	0.94	0.35	27	99.7	>2
State Building, 2006/2007	0.95	0.27	26	98.4	>2
State Building, 2007/2008	0.96	0.21	32	100.1	>2
2008/2009	R^2	Chi^2	Degrees of Freedom	% Mass Explained	TSTAT
State Building	0.95	0.25	28	99.3	>2
North Pole	0.98	0.11	37	99.2	>2
RAMS	0.96	0.19	37	100.5	>2
Peger Road	0.98	0.09	36	99.5	>2
2009/2010	R^2	Chi^2	Degrees of Freedom	% Mass Explained	TSTAT
State Building	0.96	0.34	37	99.4	>2
North Pole	0.97	0.17	36	99.0	>2
RAMS	0.98	0.07	36	99.9	>2
Peger Road	0.98	0.13	36	99.2	>2
2010/2011	R^2	Chi^2	Degrees of Freedom	% Mass Explained	TSTAT
State Building	0.98	0.19	38	100.0	>2
North Pole	0.97	0.15	35	99.4	>2
Peger Road	0.98	0.10	36	99.7	>2
2011/2012	R^2	Chi^2	Degrees of Freedom	% Mass Explained	TSTAT
State Building	0.96	0.25	37	99.0	>2
North Pole	0.97	0.18	38	98.1	>2
RAMS	0.98	0.13	37	98.3	>2
NCORE	0.97	0.18	37	98.8	>2
NPF3	0.98	0.10	36	101.0	>2
Summer 2012	R^2	Chi^2	Degrees of Freedom	% Mass Explained	TSTAT
State Building	0.98	0.39	38	93.1	>2
NCORE	0.89	0.56	38	107.7	>2

2012/2013	R²	Chi²	Degrees of Freedom	% Mass Explained	TSTAT
State Building	0.96	0.27	38	99.4	>2
NPE	0.97	0.17	35	99.2	>2
NCORE	0.96	0.22	36	99.7	>2
NPF3	0.97	0.21	35	99.0	>2

Note: ND: not detected by the CMB model. Sampling was not conducted at the RAMS site during the winter of 2010/2011.

Table 42: Average Goodness-Of-Fit Parameters - OMNI Profiles.

	R²	Chi²	Degrees of Freedom	% Mass Explained	TSTAT
EPA Target	0.8 - 1.00	0.00 – 4.0	> 5	80 – 120%	>2
State Building, 2005/2006	0.98	0.17	22	98.1	>2
State Building, 2006/2007	0.99	0.15	19	100.1	>2
State Building, 2007/2008	0.99	0.13	25	100.1	>2
2008/2009	R²	Chi²	Degrees of Freedom	% Mass Explained	TSTAT
*State Building	0.96	0.40	19	96.1	>2
**State Building	0.99	0.18	20	99.5	>2
North Pole	0.97	0.36	29	96.8	>2
RAMS	0.97	0.27	28	100.9	>2
*Peger Road	0.98	0.19	28	98.4	>2
**Peger Road	0.99	0.12	28	99.7	>2
2009/2010	R²	Chi²	Degrees of Freedom	% Mass Explained	TSTAT
State Building	1.0	0.13	28	96.1	>2
North Pole	0.97	0.67	27	100.6	>2
RAMS	0.98	0.49	28	100.1	>2
Peger Road	0.99	0.15	28	98.9	>2
2010/2011	R²	Chi²	Degrees of Freedom	% Mass Explained	TSTAT
State Building	1.0	0.10	29	92.6	>2
North Pole	0.97	0.65	28	99.4	>2
Peger Road	0.99	0.21	28	101.4	>2
2011/2012	R²	Chi²	Degrees of Freedom	% Mass Explained	TSTAT
State Building	1.0	0.16	27	93.3	>2
North Pole	0.97	0.37	29	95.5	>2
RAMS	0.98	0.17	29	91.6	>2

NCORE	0.99	0.13	29	99.5	>2
NPF3	0.98	0.24	29	97.8	>2
Summer 2012	R²	Chi²	Degrees of Freedom	% Mass Explained	TSTAT
State Building	1.0	0.38	30	84.4	>2
NCORE	0.90	0.62	35	108.3	>2
2012/2013	R²	Chi²	Degrees of Freedom	% Mass Explained	TSTAT
State Building	1.0	0.11	29	90.2	>2
NPE	0.98	0.35	27	96.8	>2
NCORE	0.99	0.10	27	100.2	>2
NPF3	0.98	0.39	27	96.3	>2

Note: ND: not detected by the CMB model. Sampling was not conducted at the RAMS site during the winter of 2010/2011. *Averages originally presented in the Final Report submitted to ADEC (dated July 23, 2012). **Averages for those sample days in which updated CMB modeling (with OMNI profiles as well as auto/diesel profiles) was conducted.

It is believed that all of the PM_{2.5} emission sources (or at least the source types) were identified during this CMB modeling program. Missing source types are identified by a low percent mass explained (<80%) and/or a RATIO R/U <<-2.0 for chemical species which are in the missing source. In addition, a “high negative” residual for one or more species and a large Chi² can be indicative of missing sources. The good agreement between the calculated source contributions and the measured ambient concentrations indicate that all of the major source types are included in the calculations, and that ambient and source profile measurements are reasonably accurate. CMB is intended to complement rather than replace other data analysis and modeling methods. For this project, the sensitivity of the CMB model’s results to the errors in the source profiles were evaluated by using different chemical abundances of a source type and by changing the fitting species used in the source type. The results of the sensitivity tests for each run showed that the CMB calculations carried out in this study were acceptable. Although there were a few cases where the fitting parameters were outside the EPA target range, none of these cases were considered invalid, and all of the fits were quite strong. Therefore, the source contribution estimates identified in this project can be considered valid.

10.0. References

- Carlson, J., 1990. PM₁₀ Chemical Mass Balance study for Missoula, Montana. Missoula City-County Health Department (MCCHD).
- Cooper, J.A., Watson, J.G., 1980. Receptor oriented methods of air particulate source apportionment. *JAPCA*, 30, 1116-25.
- Dreher D.B., Harley, R.A., 1998. A Fuel-Based Inventory for Heavy-Duty Diesel Truck Emissions, *J. Air & Waste Manage. Assoc.*, 48, 352-358.
- Fraser, M.P., Cass, G.R., 1998. Detection of excess ammonia emissions from in-use vehicles and the implications for fine particle control. *Environ. Sci. Technol.*, 32, 1053-1057.
- Friedlander, S.K., 1973. Chemical element balances and identification of air pollution sources. *Environ. Sci. Technol.*, 7, 235-240.
- Gillies, J.A., Gertler, A.W., Sagebiel, J.C., Dippel, W.A., 2001. On-road particulate matter (PM_{2.5} and PM₁₀) emissions in the Sepulveda tunnel, Los Angeles, California. *Environ. Sci. Technol.*, 35, 1054-1063.
- Gordon, G.E., 1980. Receptor models. *Environ. Sci. Technol.*, 14, 792-800.
- Gordon, G.E., 1988. Receptor models. *Environ. Sci. Technol.*, 22, 1132-1142.
- Hidy, G.M., Venkataraman, C., 1996. The chemical mass balance method for estimating atmospheric particle sources in Southern California. *Chem. Eng. Comm.*, 151, 187-209.
- RTI International, 2008. SOP for Particulate Matter (PM) Gravimetric Analysis, July 8, 2008, <http://www.epa.gov/ttn/amtic/files/ambient/pm25/spec/RTIGravMassSOPFINAL.pdf> (accessed 10/7/2011).
- RTI International, 2009a. SOP for the X-Ray Fluorescence Analysis of Particulate Matter Deposits on Teflon Filters, August 19, 2009, <http://www.epa.gov/ttn/amtic/files/ambient/pm25/spec/pmxfpsop.pdf> (accessed 10/7/2011).
- RTI International, 2009b. SOP for PM_{2.5} Cation Analysis, August 25, 2009, <http://www.epa.gov/ttn/amtic/files/ambient/pm25/spec/pm25cationsop.pdf> (accessed 10/7/2011).
- RTI International, 2009c. SOP for PM_{2.5} Anion Analysis, August 26, 2009, <http://www.epa.gov/ttn/amtic/files/ambient/pm25/spec/pm25anionsop.pdf> (accessed 10/7/2011).
- RTI International, 2009d. SOP for the Determination of Organic, Elemental, and Total Carbon in Particulate Matter Using a Thermal / Optical-Transmittance Carbon Analyzer, February 16, 2009, <http://www.epa.gov/ttn/amtic/files/ambient/pm25/spec/RTIOCECSOP.pdf> (accessed 10/7/2011).
- Schmidt, B., 1996. Chemical Mass Balance source apportionment of Missoula, Montana 1995/1996 winter suspended particulate matter. Missoula City-County Health Department (MCCHD).

- Seinfeld, J.H., Pandis, S.N., 1998. *Atmospheric Chemistry and Physics. From Air Pollution to Climate Change*, New York, John Wiley & Sons.
- USEPA, 2006. SPECIATE 4.0: EPA's repository of Total Organic Compound (TOC) and Particulate Matter (PM) speciated profiles for a variety of sources for use in source apportionment studies. U.S. Environmental Protection Agency OAQPS, Research Triangle Park, NC. <http://www.epa.gov/ttn/chief/software/speciate/index>.
- Ward, T.J., and Smith, G.C., 2005. The 2000/2001 Missoula Valley PM_{2.5} Chemical Mass Balance study, including the 2000 wildfire season – seasonal source apportionment, *Atmospheric Environment*, 39, 709-717.
- Watson, J.G., 1984. Overview of receptor model principles. *JAPCA*, 34, 619-623.
- Watson, J.G., Cooper, J.A., Huntzicker, J.J., 1984. The effective variance weighting for least squares calculations applied to the mass balance receptor model. *Atmos. Environ.*, 18, 7, 1347-1355.
- Watson, J.G., Robinson, N.F., Chow, J.C., Henry, R.C., Kim, B.M., Pace, T.G., Meyer, E.L., Nguyen, Q., 1990. The USEPA/DRI chemical mass balance receptor model, CMB 7.0. *Environ. Software*, 5, 38-49.
- Watson, J.G., et al., 2004. Protocol for Applying and Validating the CMB Model for PM_{2.5} and VOC. Report No. EPA-451/R-04-001, USEPA QAQPS.

Appendix A. OMNI Source Profiles

	FBK100	FBK101	FBK102	FBK103	FBK104	FBK105	FBK106	FBK107	FBK108
	OMNI_5_WS	OMNI_9_OW	OMNI_15_W	OMNI_17_O	OMNI_23_C	OMNI_29_C	OMNI_18_W	OMNI_6_WS	OMNI_38_C
	FINE								
Magnesium	0.000128902	0.000179751	6.69E-05	0	0	0.003971831	0.002287551	0	0
aluminum	8.06E-05	0	0	0.003478261	6.87E-05	0.007352113	0.000792668	0.0002849	0.000276817
silicon	0	0	0	0.001014493	0	0.01343662	0.000284456	0	0.000138408
phosphorus	0	0	0	0	0	0.00056338	0.083318258	0	0
sulfur	0.004114804	0.005342382	0.006735058	0.060289855	0.002835052	0.131014085	0.022316115	0.002393162	0.004273356
chlorine	0.002239678	0.003898264	0.002305977	0.00115942	0.000790378	0.000676056	0.213184956	0.002336182	0.00032872
potassium	0.018032226	0.026834189	0.021868867	0.001449275	0.000137457	0.03828169	0.044103785	0.008091168	0.000207612
calcium	0.00023565	0.000577158	7.14E-05	0.002753623	0.000120275	0.030732394	0.021598429	0.001168091	0.000155709
titanium	0	1.22E-06	0	0	3.44E-05	0.000450704	0	0	0
vanadium	8.06E-06	0	0	0	1.72E-05	0.000140845	0	0	0
chromium	2.62E-05	1.10E-05	0	0	0	0.000591549	0	2.85E-05	1.73E-05
manganese	3.42E-05	2.57E-05	2.68E-05	0	0	0.000507042	0	5.70E-05	0
iron	0.00012286	3.79E-05	1.78E-06	0.001449275	0.000171821	0.022	0.005232088	8.55E-05	8.65E-05
nickel	1.01E-05	1.22E-06	4.46E-06	0.000144928	1.72E-05	0.000422535	0	0.00017094	0
copper	1.61E-05	1.71E-05	0	0.000144928	0	0.003267606	0	0	0
zinc	0.003689829	0.003307655	0.003407672	2.90E-05	0.000120275	0.006704225	0.160667698	0.000826211	0.000155709
gallium	-99	-99	-99	-99	-99	-99	-99	-99	-99
germanium	-99	-99	-99	-99	-99	-99	-99	-99	-99
arsenic	0	0	4.46E-06	0	1.72E-05	0.000647887	0	0	0
selenium	0	0	0	0	0	0.000112676	0	0	0
bromine	1.81E-05	1.96E-05	2.23E-05	0	0	0.000309859	0.000217805	2.85E-05	3.46E-05
rubidium	3.02E-05	2.93E-05	2.23E-05	0	0	0.000253521	0	0	0
strontium	6.04E-06	6.11E-06	0	0	0	0.000309859	0	2.85E-05	0
yttrium	-99	-99	-99	-99	-99	-99	-99	-99	-99
zirconium	0	2.45E-06	0	0	8.59E-05	0.000422535	0	0	0
molybdenum	-99	-99	-99	-99	-99	-99	-99	-99	-99
palladium	-99	-99	-99	-99	-99	-99	-99	-99	-99

silver	-99	-99	-99	-99	-99	-99	-99	-99	-99
cadmium	0	0	0	0	0.000120275	0	0	0	0
indium	4.63E-05	0	0	0.002173913	0.000137457	0	0	0	0
tin	1.61E-05	0	0	0	0	0	0	0	0
antimony	0	0	0	0	0	0.000535211	0	0	0
barium	2.42E-05	9.78E-06	0	0	0	0.001183099	0	2.85E-05	0
lanthanum	-99	-99	-99	-99	-99	-99	-99	-99	-99
mercury	-99	-99	-99	-99	-99	-99	-99	-99	-99
lead	0.000002	0.000013	0.000009	0	0.000017	0.005352	0.001751	0.000028	0.000104
TC	-99	-99	-99	-99	-99	-99	-99	-99	-99
OC	2.115074382	0.481054286	0.687010777	0.518922229	0.649153878	0.08233928	0.009590277	0.777831363	0.666746667
EC	0.190318936	0.043286298	0.158647144	0.079583588	0.045820433	0.018000626	0.002592587	0.100578934	0.02072309
Sulfate	0.007468278	0.009576914	0.006347012	0.422985507	0.005257732	0.39943662	0.054980957	0.004928775	0.007958478
Nitrate	0.000968781	0.001228907	0.000677966	0.017057971	0.006185567	0.005380282	0.066209236	0.004245014	0.001608997
Ammonium	0.000104733	0.000132062	0	0.149318841	0.00128866	0.026225352	0	0.00017094	0.001799308
Chloride	-99	-99	-99	-99	-99	-99	-99	-99	-99
Potassium	0.015750252	0.022772071	0.016271186	0	0	0.036591549	0.040194001	0.007407407	0.000363322
Fluoride	-99	-99	-99	-99	-99	-99	-99	-99	-99
Sodium	0.000219537	0.000242113	0.000133809	0.003942029	0.000395189	0.041971831	0.06715782	0.000598291	0.000276817
Calcium	-99	-99	-99	-99	-99	-99	-99	-99	-99
Magnesium	-99	-99	-99	-99	-99	-99	-99	-99	-99
Sodium	0.0018429	0.001823184	0.00206512	0	0	0.046957746	0	0	0
Cobalt	6.04E-06	4.89E-06	4.46E-06	0	1.72E-05	0.000140845	0	1.14E-05	0

Appendix B. Days On Which CMB Modeling Was Not Conducted.

State Building Winter 2005/2006	Low PM _{2.5} Mass (µg/m ³)	State Building Winter 2006/2007	Low PM _{2.5} Mass (µg/m ³)	State Building Winter 2007/2008	Low PM _{2.5} Mass (µg/m ³)
11/9/05	*	11/1/06	5.7**	11/14/07	*
11/18/05	4.3**	11/13/06	*	12/2/07	5.4**
11/24/05	*	11/16/06	*	12/14/07	4.0**
12/3/05	*	12/16/06	*	12/20/07	*
12/13/05	*	12/19/06	*	2/24/08	*
12/27/05	*	12/25/06	*	3/1/08	5.2**
1/2/05	*	1/9/07	*	3/7/08	5.8**
1/5/06	*	1/18/07	*	3/10/08	*
1/11/06	*	2/2/07	*	3/16/08	*
1/17/06	*	2/20/07	*	3/25/08	5.7**
2/4/06	*	3/1/07	*	3/31/08	5.7**
2/13/06	5.9**	3/7/07	*		
2/19/06	4.4**				
3/24/06	4.8**				

*No, incomplete, or invalid CMB data set.

**Mass was too small to conduct a CMB analysis.

State Building Winter 2008/2009	Low PM _{2.5} Mass (µg/m ³)	North Pole Winter 2008/2009	Low PM _{2.5} Mass (µg/m ³)
12/8/08	*	2/18/09	*
1/16/09	2.3**	3/5/09	4.7**
2/6/09	*	3/17/09	3.8**
3/5/09	5.7**	3/20/09	4.6**
3/20/09	*	3/23/09	4.5**
3/26/09	*	3/26/09	3.0**

*No, incomplete, or invalid CMB data set.

**Mass was too small to conduct a CMB analysis.

Note that 12/29/08 did not give a good fit for OMNI rerun for State Building site.

RAMS Winter 2008/2009	Low PM_{2.5} Mass (µg/m³)	Peger Road Winter 2008/2009	Low PM_{2.5} Mass (µg/m³)
3/17/09	4.4**	2/6/09	*
3/20/09	*		
3/23/09	4.7**		
3/26/09	3.8**		

*No, incomplete, or invalid CMB data set.

**Mass was too small to conduct a CMB analysis.

Note that 2/21/09 had a low mass (6.2 µg/m³) and poor fit for OMNI RAMS CMB.

State Building Winter 2009/2010 EPA Runs	Low PM_{2.5} Mass (µg/m³)	State Building Winter 2009/2010 OMNI Runs	Low PM_{2.5} Mass (µg/m³)	North Pole Winter 2009/2010	Low PM_{2.5} Mass (µg/m³)
11/9/09	*	11/9/09	*	11/19/09	*
11/12/09	4.0**	11/12/09	4.0**	1/14/10	4.5**
11/18/09	4.9**	11/18/09	4.9**	1/29/10	3.3**
12/3/09	*	12/3/09	*	2/1/10	*
12/6/09	0.4**	12/6/09	0.4**	2/19/10	*
12/15/09	4.1**	12/9/09	*	2/25/10	3.8**
12/18/09	3.6**	12/12/09	*	3/6/10	*
2/25/10	3.1**	12/15/09	4.1**	3/9/10	4.1**
3/6/10	3.8**	12/18/09	3.6**		
3/9/10	3.4**	12/30/2009	*		
		1/2/2010	*		
		1/5/2010	*		
		1/20/10	*		
		1/26/10	*		
		2/4/10	*		
		2/25/10	3.1**		
		3/6/10	3.8**		
		3/9/10	3.4**		
		3/12/10	*		

*No, incomplete, or invalid CMB data set.

**Mass was too small to conduct a CMB analysis.

RAMS Winter 2009/2010	Low PM_{2.5} Mass ($\mu\text{g}/\text{m}^3$)	Peger Road Winter 2009/2010	Low PM_{2.5} Mass ($\mu\text{g}/\text{m}^3$)
11/17/09	*	11/18/09	*
11/18/09	*	11/19/09	*
11/19/09	*	2/25/10	*
1/26/10	*	3/9/10	3.6**
1/29/10	*		

*No, incomplete, or invalid CMB data set.

**Mass was too small to conduct a CMB analysis.

Note that 2/22/10 gave a poor fit for OMNI Peger Road CMB.

State Building Winter 2010/2011	Low PM_{2.5} Mass ($\mu\text{g}/\text{m}^3$)	North Pole Winter 2010/2011
11/4/10	3.3**	None.
11/25/10	*	
12/16/10	*	
12/19/10	*	
12/22/10	*	
12/25/10	*	
12/28/10	*	
12/31/10	*	
1/3/11	*	
1/6/11	*	
1/9/11	*	
1/12/11	*	
1/15/11	*	
1/18/11	*	
1/21/11	*	
1/24/11	*	
1/27/11	*	
1/30/11	*	
2/2/11	*	

*No, incomplete, or invalid CMB data set.

**Mass was too small to conduct a CMB analysis.

Peger Road Winter 2010/2011
None.

State Building Winter 2011/2012	Low PM _{2.5} Mass ($\mu\text{g}/\text{m}^3$)	North Pole Winter 2011/2012	Low PM _{2.5} Mass ($\mu\text{g}/\text{m}^3$)
11/5/11	*	11/2/11	***
11/20/11	*	12/5/11	2.5**
12/5/11	*	12/23/11	5.6**
12/11/11	*	1/22/12	***
12/23/11	6.3**	1/25/12	***
1/1/12	*	2/3/12	***
1/22/12	*	2/9/12	***
2/3/12	6.5**	2/12/12	***
2/24/12	5.0**	2/24/12	3.5**
2/27/12	4.3**	2/27/12	2.1**
3/4/12	*	3/1/12	5.1**
3/7/12	*	3/7/12	4.1**
3/31/12	5.4**	3/13/12	4.3**
		3/16/12	5.5**

*No, incomplete, or invalid CMB data set.

**Mass was too small to conduct a CMB analysis.

***Could not get a good statistical fit for CMB analysis.

Note that 1/28/12 and 1/31/12 (State Building) provided poor statistical fits for the OMNI CMB.

Note that 1/28/12 and 1/31/12 (State Building) provided poor statistical fits for the OMNI CMB, while the 1/28/12 date also provided a poor fit for the 1/28/12 North Pole CMB run.

RAMS Winter 2011/2012	Low PM _{2.5} Mass ($\mu\text{g}/\text{m}^3$)	NCORE Winter 2011/2012	Low PM _{2.5} Mass ($\mu\text{g}/\text{m}^3$)	NPF3 Winter 2011/2012	Low PM _{2.5} Mass ($\mu\text{g}/\text{m}^3$)
1/13/12	***	12/5/11	5.1**	3/1/12	4.5**
1/19/12	3.1**	12/23/11	5.6**	3/13/12	5.1**
1/22/12	0.8**	1/22/12	3.3**	3/28/12	5.2**
1/25/12	0.7**	2/24/12	5.7**	3/31/12	4.8**
1/28/12	2.8**	2/27/12	3.6**		
2/3/12	5.6**	3/25/12	***		
2/24/12	5.9**	3/31/12	5.6**		
2/27/12	3.5**				

*No, incomplete, or invalid CMB data set.

**Mass was too small to conduct a CMB analysis.

***Could not get a good statistical fit for CMB analysis.

Note that 1/16/12 (RAMS) and 2/6/12 and 2/9/12 (NCORE) provided poor statistical fits for the OMNI CMB.

State Building Summer 2012	Low PM_{2.5} Mass ($\mu\text{g}/\text{m}^3$)	NCORE Sumer 2012	Low PM_{2.5} Mass ($\mu\text{g}/\text{m}^3$)
6/2/12	***	6/26/12	***
7/2/12	***	7/5/12	***
7/8/12	***	7/8/12	***
7/14/12	***	7/11/12	***
7/17/12	*	7/14/12	***
7/23/12	***	7/17/12	***
8/4/12	***	7/23/12	***
8/16/12	***	8/25/12	*
8/22/12	***	8/28/12	***
8/28/12	***	8/31/12	***
8/31/12	***		

*No, incomplete, or invalid CMB data set.

**Mass was too small to conduct a CMB analysis.

***Could not get a good statistical fit for CMB analysis.

State Building Winter 2012/2013	Low PM _{2.5} Mass (µg/m ³)	NPE Winter 2012/2013	Low PM _{2.5} Mass (µg/m ³)
11/17/12	3.3**	11/23/12	5.3**
11/29/12	*	12/11/12	5.5**
12/5/12	***	1/19/13	5.8**
12/11/12	5.8**	1/22/13	4.4**
12/17/12	***	2/21/13	3.4**
12/20/12	***	3/5/13	*
12/23/12	***	3/14/13	2.6**
12/26/12	***	3/20/13	1.0**
1/10/13	***	3/23/13	4.6**
1/13/13	***		
1/16/13	*		
1/25/13	***		
1/31/13	***		
2/9/13	*		
2/15/13	***		
2/21/13	3.8**		
3/5/13	*		
3/14/13	*		
3/20/13	*		
3/23/13	*		
3/26/13	4.8**		

*No, incomplete, or invalid CMB data set.

**Mass was too small to conduct a CMB analysis.

***Could not get a good statistical fit for CMB analysis.

Note that 12/26/12 (NPE) provided poor statistical fits for the OMNI CMB.

NCORE Winter 2012/2013	Low PM_{2.5} Mass (µg/m³)	NPF3 Winter 2012/2013	Low PM_{2.5} Mass (µg/m³)
11/2/12	*	11/2/12	*
11/5/12	*	12/5/12	*
11/17/12	3.7**	12/8/12	*
11/26/12	*	1/22/13	4.2**
12/11/12	5.8**	2/15/13	*
1/7/13	*	2/18/13	*
1/31/13	***	2/21/13	4.0**
2/15/13	3.8**	3/14/13	3.2**
2/21/13	*		
3/14/13	3.5**		
3/23/13	5.0**		
3/26/13	5.0**		

*No, incomplete, or invalid CMB data set.

**Mass was too small to conduct a CMB analysis.

***Could not get a good statistical fit for CMB analysis.

Appendix C. CMB Results for Each Sample Day.**PM_{2.5} Source Contribution Estimates and Standard Errors (µg/m³) – EPA Profiles.
State Building – Winter 2005/2006.**

Date	PM _{2.5} Mass	Sulfate	Sulfate STD ERR	Ammonium Nitrate	Ammonium Nitrate STD ERR	Autos	Autos STD ERR	Diesel	Diesel STD ERR	Wood Smoke	Wood Smoke STD ERR
11/3/05	17.8	3.9	0.4	1.6	0.5	0.0	0.0	0.0	0.0	13.2	1.4
11/6/05	12.8	2.2	0.2	1.7	0.3	0.0	0.0	0.0	0.0	8.9	1.1
11/9/05	*	*	*	*	*	*	*	*	*	*	*
11/12/05	20.8	3.8	0.6	1.3	0.5	6.6	2.5	0.0	0.0	7.7	2.2
11/15/05	30.5	6.4	1.0	2.6	0.8	0.0	0.0	5.0	1.9	15.4	2.5
11/18/05	4.3**	**	**	**	**	**	**	**	**	**	**
11/21/05	9.1	1.9	0.2	1.3	0.3	0.0	0.0	0.0	0.0	6.3	0.8
11/24/05	*	*	*	*	*	*	*	*	*	*	*
11/27/05	26.4	4.8	0.8	2.1	0.7	0.0	0.0	3.2	1.2	14.5	2.2
11/30/05	21.7	3.7	0.6	4.6	0.7	0.0	0.0	2.4	1.0	9.9	1.6
12/3/05	*	*	*	*	*	*	*	*	*	*	*
12/6/05	17.1	2.9	0.3	2.0	0.6	0.0	0.0	3.4	1.0	9.2	1.5
12/9/05	16.1	2.7	0.3	0.0	0.0	0.0	0.0	4.4	1.0	8.4	1.5
12/13/05	*	*	*	*	*	*	*	*	*	*	*
12/15/05	25.1	5.0	0.6	1.9	0.9	0.0	0.0	4.9	1.4	12.9	2.1
12/18/05	25.8	5.2	0.8	2.2	0.8	0.0	0.0	3.6	1.3	13.8	2.2
12/21/05	25.9	4.8	0.5	1.6	0.6	0.0	0.0	6.4	1.6	12.7	2.1
12/24/05	24.4	4.2	0.5	2.2	0.5	0.0	0.0	4.4	1.4	13.2	2.0
12/27/05	*	*	*	*	*	*	*	*	*	*	*
12/30/05	34.2	7.3	0.8	3.0	0.9	0.0	0.0	0.0	0.0	25.2	3.0
1/2/06	*	*	*	*	*	*	*	*	*	*	*
1/5/06	*	*	*	*	*	*	*	*	*	*	*
1/8/06	31.4	6.1	0.7	2.7	0.8	0.0	0.0	0.0	0.0	23.8	2.2
1/11/06	*	*	*	*	*	*	*	*	*	*	*
1/14/06	18.2	3.3	0.4	1.6	0.4	0.0	0.0	0.0	0.0	12.7	1.5
1/17/06	*	*	*	*	*	*	*	*	*	*	*
1/20/06	31.1	6.5	1.0	2.3	0.8	0.0	0.0	0.0	0.0	23.9	3.1
1/23/06	26.5	5.7	0.9	1.7	0.7	9.0	4.0	0.0	0.0	12.0	2.2
1/26/06	42	12.1	1.3	2.9	1.5	0.0	0.0	0.0	0.0	27.1	3.3
1/29/06	30.7	7.5	0.8	3.6	1.0	0.0	0.0	0.0	0.0	20.0	2.4
2/1/06	7.0	1.3	0.1	1.1	0.2	0.0	0.0	0.0	0.0	5.6	0.9
2/4/06	*	*	*	*	*	*	*	*	*	*	*
2/7/06	15.3	2.9	0.5	2.0	0.6	0.0	0.0	3.3	0.9	7.1	1.3
2/10/06	7.4	1.3	0.1	0.5	0.2	0.0	0.0	0.0	0.0	5.8	0.7
2/13/06	5.9**	**	**	**	**	**	**	**	**	**	**
2/16/06	12.9	2.2	0.3	1.6	0.4	0.0	0.0	2.0	0.7	7.5	1.2
2/19/06	4.4**	**	**	**	**	**	**	**	**	**	**
2/22/06	7.1	1.6	0.2	0.6	0.2	0.0	0.0	0.0	0.0	4.4	0.7
2/25/06	15.1	3.9	0.4	1.6	0.5	0.0	0.0	0.0	0.0	9.9	2.8
2/28/06	20.1	3.4	0.4	1.4	0.4	0.0	0.0	0.0	0.0	14.2	1.7
3/3/06	23.2	5.0	0.6	3.9	0.7	0.0	0.0	5.3	1.6	8.9	1.7

3/6/06	15.1	3.6	0.4	1.7	0.5	0.0	0.0	0.0	0.0	9.6	1.2
3/9/06	7.9	2.6	0.3	0.7	0.3	0.0	0.0	0.0	0.0	4.2	0.8
3/12/06	9.4	2.8	0.3	0.7	0.4	0.0	0.0	0.0	0.0	5.5	0.9
3/15/06	8.5	2.7	0.4	1.0	0.3	0.0	0.0	0.0	0.0	4.7	0.7
3/18/06	11.3	2.5	0.4	1.1	0.3	0.0	0.0	0.0	0.0	7.0	1.0
3/21/06	9.4	2.2	0.4	1.3	0.3	0.0	0.0	0.0	0.0	5.8	0.9
3/24/06	4.8**	**	**	**	**	**	**	**	**	**	**
3/27/06	10.6	2.1	0.3	1.4	0.3	0.0	0.0	0.0	0.0	7.1	1.9
3/30/06	13.7	2.8	0.3	1.6	0.4	0.0	0.0	0.0	0.0	9.6	2.6
Average	18.9	4.0	0.5	1.8	0.5	0.4	0.2	1.3	0.4	11.3	1.7

Notes: *No or incomplete CMB data set. **Mass was too small to conduct a CMB analysis.

**PM_{2.5} Source Contribution Estimates and Standard Errors ($\mu\text{g}/\text{m}^3$) – OMNI Profiles.
State Building – Winter 2005/2006.**

Date	PM _{2.5} Mass	Sulfate	Sulfate STD ERR	Ammonium Nitrate	Ammonium Nitrate STD ERR	No. 2 Fuel Oil	No. 2 Fuel Oil STD ERR	Diesel	Diesel STD ERR	Wood Smoke	Wood Smoke STD ERR
11/3/05	17.8	3.9	0.4	1.5	0.5	0.0	0.0	0.0	0.0	13.8	1.3
11/6/05	12.8	1.2	0.2	1.3	0.2	5.2	1.0	0.0	0.0	5.0	1.1
11/9/05	*	*	*	*	*	*	*	*	*	*	*
11/12/05	20.8	2.2	0.6	0.9	0.3	8.5	1.7	0.0	0.0	7.6	1.7
11/15/05	30.5	3.3	1.0	1.5	0.5	16.6	2.6	0.0	0.0	7.7	2.3
11/18/05	4.3**	**	**	**	**	**	**	**	**	**	**
11/21/05	9.1	1.8	0.2	1.2	0.2	0.0	0.0	0.0	0.0	6.5	0.7
11/24/05	*	*	*	*	*	*	*	*	*	*	*
11/27/05	26.4	2.4	0.7	1.2	0.3	12.9	2.0	0.0	0.0	8.8	1.9
11/30/05	21.7	2.1	0.6	3.9	0.5	8.7	2.0	0.0	0.0	6.4	1.7
12/3/05	*	*	*	*	*	*	*	*	*	*	*
12/6/05	17.1	1.9	0.4	1.5	0.4	5.3	1.9	1.5	0.8	6.8	1.7
12/9/05	16.1	1.5	0.4	0.0	0.0	6.6	2.2	2.9	1.0	5.1	1.9
12/13/05	*	*	*	*	*	*	*	*	*	*	*
12/15/05	25.1	2.8	0.6	1.1	0.4	10.9	2.2	2.5	1.0	7.7	2.1
12/18/05	25.8	2.8	0.8	1.3	0.4	13.3	2.2	0.0	0.0	8.0	2.1
12/21/05	25.9	2.8	0.5	0.8	0.4	11.0	2.2	3.5	1.5	7.1	2.2
12/24/05	24.4	2.4	0.5	1.5	0.4	9.5	1.9	0.0	0.0	10.0	1.8
12/27/05	*	*	*	*	*	*	*	*	*	*	*
12/30/05	34.2	4.3	0.8	2.0	0.6	15.5	3.4	2.7	1.2	5.7	2.8
1/2/06	*	*	*	*	*	*	*	*	*	*	*
1/5/06	*	*	*	*	*	*	*	*	*	*	*
1/8/06	31.4	3.3	0.6	1.6	0.5	15.2	2.7	0.0	0.0	6.8	2.3
1/11/06	*	*	*	*	*	*	*	*	*	*	*
1/14/06	18.2	1.8	0.4	1.0	0.3	8.1	1.5	0.0	0.0	6.6	1.5
1/17/06	*	*	*	*	*	*	*	*	*	*	*
1/20/06	31.1	3.0	1.0	1.1	0.4	18.6	2.5	0.0	0.0	9.1	2.4
1/23/06	26.5	2.4	0.8	1.3	0.4	17.9	2.2	0.0	0.0	3.4	2.0
1/26/06	42	7.9	1.4	1.2	1.1	22.9	5.9	0.0	0.0	9.1	4.5
1/29/06	30.7	4.4	0.8	2.5	0.6	16.6	3.4	0.0	0.0	7.5	2.9
2/1/06	7.0	0.8	0.2	0.9	0.1	2.7	0.6	0.0	0.0	3.9	0.8
2/4/06	*	*	*	*	*	*	*	*	*	*	*
2/7/06	15.3	1.9	0.6	1.5	0.4	6.0	2.2	2.3	0.8	4.0	1.8
2/10/06	7.4	0.8	0.2	0.3	0.1	2.7	0.6	0.0	0.0	4.2	0.8
2/13/06	5.9**	**	**	**	**	**	**	**	**	**	**
2/16/06	12.9	1.5	0.3	1.3	0.2	4.5	1.2	0.0	0.0	6.2	1.2
2/19/06	4.4**	**	**	**	**	**	**	**	**	**	**
2/22/06	7.1	1.0	0.2	0.4	0.1	3.0	0.8	0.0	0.0	2.1	0.8
2/25/06	15.1	2.3	0.4	1.0	0.3	8.4	1.8	0.0	0.0	2.6	1.6
2/28/06	20.1	3.3	0.4	1.4	0.4	0.0	0.0	0.0	0.0	13.8	1.5
3/3/06	23.2	2.9	0.6	3.0	0.5	11.7	2.4	0.0	0.0	5.0	2.1
3/6/06	15.1	3.5	0.4	1.7	0.5	0.0	0.0	0.0	0.0	10.4	1.3
3/9/06	7.9	1.6	0.2	0.4	0.2	5.6	0.7	0.0	0.0	0.0	0.0
3/12/06	9.4	1.6	0.3	0.3	0.2	7.0	0.7	0.0	0.0	0.0	0.0

3/15/06	8.5	1.4	0.4	0.5	0.2	7.1	0.7	0.0	0.0	0.0	0.0
3/18/06	11.3	1.0	0.3	0.5	0.1	8.3	0.7	0.0	0.0	0.0	0.0
3/21/06	9.4	2.2	0.4	1.3	0.3	0.0	0.0	0.0	0.0	6.3	1.0
3/24/06	4.8**	**	**	**	**	**	**	**	**	**	**
3/27/06	10.6	1.3	0.3	1.1	0.2	4.0	1.0	0.0	0.0	3.3	1.0
3/30/06	13.7	1.5	0.3	1.1	0.2	7.1	1.2	0.0	0.0	3.1	1.2
Average	18.9	2.4	0.5	1.3	0.3	8.4	1.6	0.4	0.2	5.9	1.6

Notes: *No or incomplete CMB data set. **Mass was too small to conduct a CMB analysis.

**PM_{2.5} Source Contribution Estimates and Standard Errors ($\mu\text{g}/\text{m}^3$) – EPA Profiles.
State Building – Winter 2006/2007.**

Date	PM _{2.5} Mass	Sulfate	Sulfate STD ERR	Ammonium Nitrate	Ammonium Nitrate STD ERR	Autos	Autos STD ERR	Diesel	Diesel STD ERR	Wood Smoke	Wood Smoke STD ERR
11/1/06	5.7**	**	**	**	**	**	**	**	**	**	**
11/4/06	27.9	4.5	0.6	2.3	0.6	0.0	0.0	0.0	0.0	22.4	2.6
11/7/06	13.5	1.8	0.2	1.2	0.2	3.6	1.7	0.0	0.0	6.1	1.5
11/10/06	21.3	3.1	0.4	1.6	0.4	0.0	0.0	3.3	1.2	12.1	1.9
11/13/06	*	*	*	*	*	*	*	*	*	*	*
11/16/06	*	*	*	*	*	*	*	*	*	*	*
11/19/06	25.8	6.2	0.8	1.9	0.8	0.0	0.0	0.0	0.0	16.1	2.0
11/22/06	12.7	1.8	0.2	1.5	0.3	0.0	0.0	1.4	0.6	8.5	1.3
11/25/06	32.1	6.2	0.8	2.0	0.8	0.0	0.0	0.0	0.0	23.0	5.9
11/28/06	25.7	5.2	0.6	2.2	0.8	0.0	0.0	3.5	1.3	13.5	2.1
12/1/06	8.0	1.7	0.2	0.9	0.2	0.0	0.0	0.0	0.0	5.8	0.8
12/4/06	15.5	2.3	0.3	2.5	0.5	0.0	0.0	2.5	0.8	8.3	1.4
12/7/06	35.1	3.9	0.5	1.7	0.5	15.2	3.4	0.0	0.0	10.2	2.0
12/10/06	16.3	2.7	0.3	1.3	0.5	0.0	0.0	2.8	0.9	9.5	1.5
12/13/06	15.1	2.6	0.3	1.3	0.3	4.8	2.0	0.0	0.0	5.4	1.7
12/16/06	*	*	*	*	*	*	*	*	*	*	*
12/19/06	*	*	*	*	*	*	*	*	*	*	*
12/22/06	26.0	6.9	0.9	2.1	1.0	0.0	0.0	3.4	1.6	13.4	2.2
12/25/06	*	*	*	*	*	*	*	*	*	*	*
12/28/06	23.8	3.8	0.5	1.5	0.7	0.0	0.0	3.6	1.1	13.5	2.0
12/31/06	16.9	4.1	0.5	1.4	0.6	0.0	0.0	2.0	0.9	10.7	1.7
1/3/07	11.0	2.1	0.3	1.3	0.3	0.0	0.0	0.0	0.0	7.1	1.0
1/6/07	19.8	3.5	0.4	1.2	0.5	5.8	2.8	0.0	0.0	10.0	1.8
1/9/07	*	*	*	*	*	*	*	*	*	*	*
1/12/07	30.4	5.3	0.7	3.1	0.7	0.0	0.0	5.2	1.7	15.7	2.4
1/15/07	16.3	2.2	0.3	0.9	0.3	0.0	0.0	0.0	0.0	13.1	2.8
1/18/07	*	*	*	*	*	*	*	*	*	*	*
1/21/07	23.8	4.4	0.5	2.2	0.6	0.0	0.0	3.7	1.5	12.1	1.9
1/24/07	17.4	3.7	0.5	1.8	0.5	0.0	0.0	2.8	1.3	8.5	1.5
1/27/07	31.6	5.9	0.7	2.8	0.8	6.9	3.4	0.0	0.0	14.5	3.3
1/30/07	25.0	3.9	0.5	2.0	0.5	0.0	0.0	7.7	1.5	10.2	1.8
2/2/07	*	*	*	*	*	*	*	*	*	*	*
2/5/07	34.6	5.3	0.7	3.3	0.7	8.4	3.8	0.0	0.0	18.3	2.9
2/8/07	14.8	3.0	0.4	0.8	0.4	0.0	0.0	0.0	0.0	11.1	1.3
2/11/07	14.6	2.0	0.2	1.1	0.3	0.0	0.0	0.0	0.0	10.2	1.4
2/14/07	18.0	3.3	0.4	1.7	0.6	0.0	0.0	3.4	1.0	10.0	1.5
2/17/07	21.5	4.1	0.5	1.6	0.5	0.0	0.0	2.1	1.0	13.7	2.0
2/20/07	*	*	*	*	*	*	*	*	*	*	*
2/23/07	38.7	8.4	1.0	3.2	1.1	0.0	0.0	0.0	0.0	27.0	5.9
2/26/07	15.1	3.3	0.4	1.1	0.4	0.0	0.0	0.0	0.0	10.5	2.9
3/1/07	*	*	*	*	*	*	*	*	*	*	*
3/4/07	18.8	4.1	0.5	2.0	0.6	0.0	0.0	0.0	0.0	12.8	1.5
3/7/07	*	*	*	*	*	*	*	*	*	*	*
3/10/07	10.6	2.4	0.3	0.7	0.3	0.0	0.0	0.0	0.0	7.8	1.1
3/13/07	14.6	3.7	0.4	1.0	0.5	0.0	0.0	0.0	0.0	9.5	2.6

3/16/07	13.7	3.0	0.4	0.9	0.4	0.0	0.0	0.0	0.0	10.3	2.7
3/19/07	14.3	2.9	0.4	1.5	0.5	0.0	0.0	2.9	0.9	7.2	1.3
3/22/07	7.2	1.3	0.2	0.4	0.2	0.0	0.0	0.0	0.0	5.4	0.9
3/25/07	15.8	3.4	0.4	1.5	0.4	0.0	0.0	2.7	1.2	7.4	1.3
3/28/07	18.2	3.6	0.4	2.3	0.5	0.0	0.0	3.4	1.3	8.0	1.4
3/31/07	14.0	2.6	0.3	1.6	0.3	0.0	0.0	2.4	1.0	7.6	1.3
Average	19.9	3.7	0.5	1.7	0.5	1.1	0.4	1.5	0.5	11.5	2.0

Notes: *No, incomplete, or invalid CMB data set. **Mass was too small to conduct a CMB analysis.

**PM_{2.5} Source Contribution Estimates and Standard Errors ($\mu\text{g}/\text{m}^3$) – OMNI Profiles.
State Building – Winter 2006/2007.**

Date	PM _{2.5} Mass	Sulfate	Sulfate STD ERR	Ammonium Nitrate	Ammonium Nitrate STD ERR	Autos	Autos STD ERR	No. 2 Fuel Oil	No. 2 Fuel Oil STD ERR	Diesel	Diesel STD ERR	Wood Smoke	Wood Smoke STD ERR
11/1/06	5.7**	**	**	**	**	**	**	**	**	**	**	**	**
11/4/06	27.9	2.5	0.5	1.6	0.4	0.0	0.0	10.0	1.9	0.0	0.0	14.3	3.0
11/7/06	13.5	0.9	0.2	0.9	0.1	0.0	0.0	4.5	0.7	0.0	0.0	8.0	1.4
11/10/06	21.3	1.9	0.4	1.1	0.3	0.0	0.0	6.7	1.5	0.0	0.0	9.8	1.6
11/13/06	*	*	*	*	*	*	*	*	*	*	*	*	*
11/16/06	*	*	*	*	*	*	*	*	*	*	*	*	*
11/19/06	25.8	3.3	0.7	0.9	0.5	0.0	0.0	15.1	2.6	0.0	0.0	7.3	3.5
11/22/06	12.7	1.0	0.2	1.4	0.2	0.0	0.0	4.3	0.9	0.0	0.0	6.8	1.1
11/25/06	32.1	3.1	0.7	0.9	0.4	0.0	0.0	16.3	2.5	0.0	0.0	14.1	3.7
11/28/06	25.7	3.1	0.6	1.4	0.4	0.0	0.0	11.4	2.4	0.0	0.0	9.2	2.1
12/1/06	8.0	1.0	0.2	0.6	0.1	0.0	0.0	3.5	0.8	0.0	0.0	3.8	0.9
12/4/06	15.5	1.2	0.3	2.1	0.2	0.0	0.0	5.8	1.2	1.5	0.7	5.7	1.3
12/7/06	35.1	2.2	0.5	1.1	0.3	11.6	3.0	8.8	1.7	0.0	0.0	8.6	3.0
12/10/06	16.3	1.5	0.3	0.8	0.2	0.0	0.0	6.1	1.2	0.0	0.0	7.9	1.3
12/13/06	15.1	1.4	0.3	1.0	0.2	0.0	0.0	6.5	1.1	0.0	0.0	7.0	1.7
12/16/06	*	*	*	*	*	*	*	*	*	*	*	*	*
12/19/06	*	*	*	*	*	*	*	*	*	*	*	*	*
12/22/06	26.0	3.9	0.8	0.9	0.5	0.0	0.0	16.8	3.0	0.0	0.0	5.0	2.5
12/25/06	*	*	*	*	*	*	*	*	*	*	*	*	*
12/28/06	23.8	2.1	0.4	0.9	0.3	0.0	0.0	9.0	1.7	0.0	0.0	10.5	1.7
12/31/06	16.9	2.7	0.5	0.8	0.4	0.0	0.0	7.9	2.0	0.0	0.0	7.2	1.8
1/3/07	11.0	1.3	0.3	1.0	0.2	0.0	0.0	4.2	1.0	0.0	0.0	4.0	1.1
1/6/07	19.8	1.8	0.4	1.0	0.3	0.0	0.0	9.1	1.4	0.0	0.0	9.3	2.3
1/9/07	*	*	*	*	*	*	*	*	*	*	*	*	*
1/12/07	30.4	3.0	0.6	2.2	0.5	0.0	0.0	12.1	2.4	0.0	0.0	11.7	2.2
1/15/07	16.3	1.1	0.2	0.7	0.2	0.0	0.0	5.9	0.9	0.0	0.0	9.1	1.6
1/18/07	*	*	*	*	*	*	*	*	*	*	*	*	*
1/21/07	23.8	2.4	0.5	1.4	0.3	0.0	0.0	10.7	1.9	0.0	0.0	8.1	1.8
1/24/07	17.4	2.1	0.4	1.3	0.3	0.0	0.0	8.3	1.7	0.0	0.0	5.1	1.6
1/27/07	31.6	3.2	0.7	1.9	0.5	0.0	0.0	14.9	2.7	0.0	0.0	9.6	2.4
1/30/07	25.0	2.0	0.6	1.3	0.6	0.0	0.0	9.3	2.6	3.6	1.1	10.0	3.1
2/2/07	*	*	*	*	*	*	*	*	*	*	*	*	*
2/5/07	34.6	2.2	0.6	2.8	0.4	0.0	0.0	16.5	2.1	0.0	0.0	15.2	3.3
2/8/07	14.8	1.5	0.4	0.6	0.2	0.0	0.0	7.6	1.2	0.0	0.0	5.2	1.3
2/11/07	14.6	1.0	0.2	0.7	0.1	0.0	0.0	5.7	0.9	0.0	0.0	6.1	1.1
2/14/07	18.0	1.9	0.5	1.1	0.4	0.0	0.0	7.6	2.3	2.3	0.8	5.1	1.9
2/17/07	21.5	2.6	0.5	0.9	0.4	0.0	0.0	9.6	2.0	0.0	0.0	8.4	1.9
2/20/07	*	*	*	*	*	*	*	*	*	*	*	*	*
2/23/07	38.7	4.6	0.9	1.8	0.6	0.0	0.0	20.9	3.4	0.0	0.0	11.5	4.4
2/26/07	15.1	1.7	0.4	0.9	0.2	0.0	0.0	8.5	1.4	0.0	0.0	4.1	1.9
3/1/07	*	*	*	*	*	*	*	*	*	*	*	*	*
3/4/07	18.8	2.5	0.5	1.8	0.4	0.0	0.0	8.7	2.0	0.0	0.0	6.1	1.7
3/7/07	*	*	*	*	*	*	*	*	*	*	*	*	*

3/10/07	10.6	1.5	0.3	0.3	0.2	0.0	0.0	4.9	1.1	0.0	0.0	3.5	1.6
3/13/07	14.6	1.8	0.4	0.8	0.2	0.0	0.0	10.5	0.9	0.0	0.0	0.0	0.0
3/16/07	13.7	1.7	0.4	0.8	0.2	0.0	0.0	6.9	1.4	0.0	0.0	4.0	1.3
3/19/07	14.3	1.6	0.3	0.9	0.2	0.0	0.0	7.4	1.3	0.0	0.0	4.4	1.2
3/22/07	7.2	0.7	0.2	0.3	0.1	0.0	0.0	2.8	0.6	0.0	0.0	2.9	1.0
3/25/07	15.8	1.9	0.4	0.9	0.3	0.0	0.0	8.0	1.5	0.0	0.0	5.8	2.1
3/28/07	18.2	1.6	0.4	1.6	0.3	0.0	0.0	10.4	1.5	0.0	0.0	4.9	2.1
3/31/07	14.0	1.4	0.3	1.1	0.2	0.0	0.0	6.5	1.2	0.0	0.0	5.0	1.2
Average	19.9	2.0	0.4	1.1	0.3	0.3	0.1	9.0	1.7	0.2	0.1	7.3	1.9

Notes: *No, incomplete, or invalid CMB data set. **Mass was too small to conduct a CMB analysis.

**PM_{2.5} Source Contribution Estimates and Standard Errors ($\mu\text{g}/\text{m}^3$) – EPA Profiles.
State Building – Winter 2007/2008.**

Date	PM _{2.5} Mass	Sulfate	Sulfate STD ERR	Ammonium Nitrate	Ammonium Nitrate STD ERR	Autos	Autos STD ERR	Diesel	Diesel STD ERR	Wood Smoke	Wood Smoke STD ERR
11/2/07	11.0	1.5	0.2	0.8	0.2	0.0	0.0	0.0	0.0	9.4	1.0
11/5/07	23.5	3.2	0.4	1.3	0.4	0.0	0.0	0.0	0.0	19.4	1.8
11/8/07	13.1	1.9	0.2	0.6	0.3	0.0	0.0	4.4	1.0	6.0	1.1
11/11/07	23.8	3.8	0.5	2.2	0.5	0.0	0.0	5.5	1.4	11.7	1.9
11/14/07	*	*	*	*	*	*	*	*	*	*	*
11/17/07	9.1	0.7	0.2	1.5	0.3	1.7	0.8	0.0	0.0	5.2	1.1
11/20/07	18.4	2.4	0.3	0.6	0.3	0.0	0.0	3.8	0.9	11.8	1.7
11/23/07	11.7	1.3	0.2	0.6	0.2	0.0	0.0	2.3	0.7	7.4	1.1
11/26/07	12.7	1.8	0.2	0.6	0.2	0.0	0.0	3.9	1.0	6.0	1.1
11/29/07	29.3	5.0	0.6	2.0	0.6	11.6	3.1	0.0	0.0	9.7	2.8
12/2/07	5.4**	**	**	**	**	**	**	**	**	**	**
12/5/07	24.2	3.1	0.4	1.3	0.4	9.7	2.8	0.0	0.0	10.1	1.8
12/8/07	17.7	2.9	0.4	1.7	0.6	0.0	0.0	3.3	1.0	9.3	1.5
12/11/07	11.8	1.7	0.2	1.0	0.4	0.0	0.0	2.2	0.7	6.8	1.1
12/14/07	4.0**	**	**	**	**	**	**	**	**	**	**
12/17/07	25.6	4.5	0.6	1.8	0.7	0.0	0.0	2.9	1.2	16.5	2.4
12/20/07	*	*	*	*	*	*	*	*	*	*	*
12/23/07	32.5	6.3	0.8	2.4	1.2	0.0	0.0	6.7	1.6	18.0	2.8
12/26/07	13.0	3.0	0.4	1.5	0.4	0.0	0.0	1.5	0.7	7.0	1.2
12/29/07	16.4	2.7	0.3	1.8	0.6	0.0	0.0	4.1	0.9	7.9	1.4
1/1/08	24.4	5.0	0.6	1.3	0.7	7.3	3.6	0.0	0.0	10.2	1.9
1/4/08	10.2	1.4	0.2	1.3	0.3	0.0	0.0	1.2	0.6	6.9	1.1
1/7/08	20.8	4.2	0.5	1.7	0.7	0.0	0.0	3.4	1.1	11.2	1.7
1/10/08	7.3	1.5	0.2	0.6	0.2	0.0	0.0	0.0	0.0	5.2	0.7
1/13/08	8.4	1.4	0.2	0.5	0.2	0.0	0.0	0.0	0.0	6.3	0.8
1/16/08	25.1	3.9	0.5	1.9	0.5	7.5	3.1	0.0	0.0	12.4	2.1
1/19/08	26.4	4.4	0.5	2.6	0.6	0.0	0.0	5.6	1.5	13.2	2.1
1/22/08	7.8	1.4	0.2	0.5	0.3	0.0	0.0	1.6	0.6	4.6	0.8
1/25/08	18.2	4.4	0.5	1.5	0.7	0.0	0.0	2.8	1.1	9.5	1.6
1/28/08	24.4	4.3	0.5	1.4	0.5	8.3	2.7	0.0	0.0	8.5	2.4
1/31/08	26.2	4.6	0.6	2.6	0.6	0.0	0.0	0.0	0.0	19.0	1.8
2/3/08	24.2	4.6	0.6	2.1	0.6	0.0	0.0	0.0	0.0	16.5	1.9
2/6/08	68.0	17.1	2.1	5.0	2.2	0.0	0.0	0.0	0.0	48.3	6.0
2/9/08	43.7	11.1	1.4	3.5	1.4	0.0	0.0	0.0	0.0	27.4	3.7
2/12/08	9.5	2.1	0.3	0.8	0.3	0.0	0.0	0.0	0.0	7.3	1.1
2/15/08	8.7	1.8	0.2	0.6	0.2	0.0	0.0	0.0	0.0	6.1	0.9
2/18/08	14.9	2.0	0.3	1.2	0.5	0.0	0.0	3.6	0.9	8.3	1.4
2/21/08	7.5	1.1	0.1	0.8	0.2	0.0	0.0	0.0	0.0	6.2	0.8
2/24/08	*	*	*	*	*	*	*	*	*	*	*
2/27/08	17.2	3.1	0.4	1.2	0.5	0.0	0.0	2.2	0.8	11.3	1.7
3/1/08	5.2**	**	**	**	**	**	**	**	**	**	**
3/4/08	24.7	3.1	0.4	2.7	0.4	0.0	0.0	6.3	1.3	12.4	1.9
3/7/08	5.8**	**	**	**	**	**	**	**	**	**	**
3/10/08	*	*	*	*	*	*	*	*	*	*	*

3/13/08	11.0	2.1	0.3	2.0	0.3	0.0	0.0	0.0	0.0	7.1	0.9
3/16/08	*	*	*	*	*	*	*	*	*	*	*
3/19/08	6.6	1.3	0.2	0.6	0.2	0.0	0.0	0.0	0.0	4.5	0.7
3/22/08	10.1	2.3	0.3	1.0	0.3	0.0	0.0	0.0	0.0	6.4	0.9
3/25/08	5.7**	**	**	**	**	**	**	**	**	**	**
3/28/08	8.5	1.4	0.2	1.2	0.2	0.0	0.0	0.0	0.0	6.0	0.8
3/31/08	5.7**	**	**	**	**	**	**	**	**	**	**
Average	18.7	3.4	0.4	1.5	0.5	1.2	0.4	1.7	0.5	10.9	1.6

Notes: *No, incomplete, or invalid CMB data set. **Mass was too small to conduct a CMB analysis.

**PM_{2.5} Source Contribution Estimates and Standard Errors (µg/m³) – OMNI Profiles.
State Building – Winter 2007/2008.**

Date	PM _{2.5} Mass	Sulfate	Sulfate STD ERR	Ammonium Nitrate	Ammonium Nitrate STD ERR	Autos	Autos STD ERR	No. 2 Fuel Oil	No. 2 Fuel Oil STD ERR	Diesel	Diesel STD ERR	Wood Smoke	Wood Smoke STD ERR
11/2/07	11.0	0.8	0.2	0.8	0.1	0.0	0.0	3.2	0.7	0.0	0.0	7.8	1.0
11/5/07	23.5	1.2	0.4	1.1	0.3	0.0	0.0	9.8	1.8	2.1	1.0	10.6	2.3
11/8/07	13.1	1.0	0.2	0.5	0.1	0.0	0.0	4.5	0.8	2.4	1.2	4.3	1.3
11/11/07	23.8	2.2	0.5	1.6	0.3	0.0	0.0	8.9	1.8	2.9	1.3	7.4	1.9
11/14/07	*	*	*	*	*	*	*	*	*	*	*	*	*
11/17/07	9.1	0.4	0.1	1.3	0.1	0.0	0.0	2.2	0.4	1.1	0.5	4.5	0.9
11/20/07	18.4	1.3	0.3	0.4	0.2	0.0	0.0	6.7	1.1	2.0	0.8	8.3	1.4
11/23/07	11.7	0.9	0.2	0.5	0.1	5.2	2.2	3.2	0.7	0.0	0.0	1.8	0.4
11/26/07	12.7	0.9	0.2	0.5	0.1	0.0	0.0	4.6	0.8	2.6	1.0	3.7	1.1
11/29/07	29.3	2.6	0.6	1.3	0.4	0.0	0.0	12.9	2.2	3.1	1.4	7.7	2.3
12/2/07	5.4**	**	**	**	**	**	**	**	**	**	**	**	**
12/5/07	24.2	1.6	0.4	1.0	0.2	0.0	0.0	7.9	1.3	2.6	1.1	10.0	2.4
12/8/07	17.7	1.8	0.4	1.2	0.3	6.3	2.6	6.7	1.4	0.0	0.0	1.8	0.6
12/11/07	11.8	1.0	0.2	0.7	0.1	0.0	0.0	3.5	0.8	0.0	0.0	6.4	1.0
12/14/07	4.0**	**	**	**	**	**	**	**	**	**	**	**	**
12/17/07	25.6	2.2	0.5	0.9	0.3	0.0	0.0	11.9	1.8	0.0	0.0	10.3	1.9
12/20/07	*	*	*	*	*	*	*	*	*	*	*	*	*
12/23/07	32.5	3.2	0.8	1.1	0.4	0.0	0.0	18.2	2.7	7.0	1.7	2.7	1.0
12/26/07	13.0	1.9	0.4	1.0	0.3	0.0	0.0	6.3	1.5	0.0	0.0	4.1	1.3
12/29/07	16.4	1.5	0.4	1.3	0.4	0.0	0.0	6.7	2.1	2.4	0.9	5.3	2.1
1/1/08	24.4	3.8	0.7	1.2	0.5	0.0	0.0	5.6	2.6	0.0	0.0	14.9	3.3
1/4/08	10.2	0.8	0.2	1.0	0.1	0.0	0.0	3.0	0.7	0.0	0.0	6.0	0.9
1/7/08	20.8	2.4	0.6	0.9	0.4	0.0	0.0	10.3	2.3	1.9	0.9	5.3	2.0
1/10/08	7.3	0.9	0.2	0.5	0.1	0.0	0.0	3.6	0.7	0.0	0.0	2.9	0.8
1/13/08	8.4	0.9	0.2	0.5	0.1	0.0	0.0	3.1	0.7	0.0	0.0	4.6	0.9
1/16/08	25.1	1.9	0.4	1.6	0.3	0.0	0.0	10.4	1.6	0.0	0.0	12.4	2.5
1/19/08	26.4	2.1	0.5	1.8	0.3	0.0	0.0	11.5	1.9	0.0	0.0	9.9	1.9
1/22/08	7.8	1.0	0.2	0.3	0.1	0.0	0.0	2.6	0.7	0.0	0.0	3.8	0.8
1/25/08	18.2	2.6	0.6	0.7	0.4	0.0	0.0	10.3	2.1	0.0	0.0	4.7	1.7
1/28/08	24.4	2.2	0.5	0.8	0.4	0.0	0.0	11.2	2.0	1.7	0.8	8.5	2.8
1/31/08	26.2	2.3	0.5	2.4	0.4	0.0	0.0	12.3	2.0	0.0	0.0	7.3	2.7
2/3/08	24.2	2.5	0.6	1.3	0.4	0.0	0.0	11.3	2.1	0.0	0.0	8.2	2.0
2/6/08	68.0	8.5	1.6	1.9	1.1	0.0	0.0	48.1	3.5	0.0	0.0	0.0	0.0
2/9/08	43.7	6.3	1.3	1.5	0.9	0.0	0.0	27.1	5.0	0.0	0.0	9.1	4.0
2/12/08	9.5	1.1	0.3	0.4	0.2	0.0	0.0	5.0	0.9	1.3	0.6	1.3	0.4
2/15/08	8.7	1.0	0.2	0.3	0.1	0.0	0.0	4.0	0.8	0.0	0.0	3.0	0.9
2/18/08	14.9	1.1	0.3	0.8	0.3	0.0	0.0	5.2	1.6	1.9	0.7	5.8	1.6
2/21/08	7.5	0.7	0.2	0.6	0.1	0.0	0.0	2.2	0.6	2.2	0.9	1.3	0.3
2/24/08	*	*	*	*	*	*	*	*	*	*	*	*	*
2/27/08	17.2	1.8	0.4	1.0	0.3	0.0	0.0	7.6	1.4	0.0	0.0	8.2	1.5
3/1/08	5.2**	**	**	**	**	**	**	**	**	**	**	**	**
3/4/08	24.7	1.7	0.4	2.1	0.3	0.0	0.0	7.8	1.5	3.6	1.3	8.8	1.8
3/7/08	5.8**	**	**	**	**	**	**	**	**	**	**	**	**
3/10/08	*	*	*	*	*	*	*	*	*	*	*	*	*

3/13/08	11.0	1.3	0.3	1.7	0.2	0.0	0.0	3.9	1.1	0.0	0.0	4.9	1.1
3/16/08	*	*	*	*	*	*	*	*	*	*	*	*	*
3/19/08	6.6	0.8	0.2	0.3	0.1	0.0	0.0	3.0	0.6	0.0	0.0	2.5	0.7
3/22/08	10.1	1.3	0.3	0.6	0.2	0.0	0.0	5.3	1.0	0.0	0.0	2.3	1.0
3/25/08	5.7**	**	**	**	**	**	**	**	**	**	**	**	**
3/28/08	8.5	0.8	0.2	1.0	0.1	0.0	0.0	2.9	0.7	0.0	0.0	3.6	0.8
3/31/08	5.7**	**	**	**	**	**	**	**	**	**	**	**	**
Average	18.7	1.9	0.4	1.0	0.3	0.3	0.1	8.4	1.5	1.0	0.4	5.9	1.5

Notes: *No, incomplete, or invalid CMB data set. **Mass was too small to conduct a CMB analysis.

**PM_{2.5} Source Contribution Estimates and Standard Errors ($\mu\text{g}/\text{m}^3$) – EPA Profiles.
State Building – Winter 2008/2009.**

Date	PM _{2.5} Mass	Sulfate	Sulfate STD ERR	Ammonium Nitrate	Ammonium Nitrate STD ERR	Autos	Autos STD ERR	Diesel	Diesel STD ERR	Wood Smoke	Wood Smoke STD ERR
11/8/08	40.0	4.7	0.6	2.8	0.6	0.0	0.0	2.3	1.1	27.0	3.6
11/11/08	31.9	3.6	0.4	2.0	0.5	10.7	3.2	0.0	0.0	17.2	2.6
11/14/08	52.1	8.8	1.1	4.5	1.1	14.6	5.9	0.0	0.0	26.2	4.2
11/17/08	20.7	2.7	0.3	2.0	0.4	0.0	0.0	0.0	0.0	15.4	2.0
11/20/08	16.8	3.0	0.4	1.2	0.5	2.7	1.3	0.0	0.0	11.7	2.0
11/23/08	23.4	3.6	0.4	2.1	0.6	0.0	0.0	2.8	1.0	14.6	2.2
11/26/08	22.0	3.0	0.5	1.5	0.6	4.0	1.5	0.0	0.0	13.5	2.3
11/29/08	16.4	2.3	0.3	1.6	0.3	0.0	0.0	0.0	0.0	12.0	1.6
12/2/08	47.0	10.5	1.3	3.2	1.3	0.0	0.0	0.0	0.0	28.1	3.8
12/5/08	31.0	4.1	0.5	2.2	0.5	11.1	3.4	0.0	0.0	15.5	2.5
12/8/08	*	*	*	*	*	*	*	*	*	*	*
12/11/08	18.9	2.9	0.4	1.5	0.5	2.6	1.3	0.0	0.0	12.5	2.1
12/14/08	39.0	7.0	0.9	3.0	0.9	0.0	0.0	0.0	0.0	24.2	3.1
12/17/08	34.9	7.3	0.9	2.3	0.9	0.0	0.0	3.1	1.5	21.4	3.0
12/20/08	26.1	4.3	0.5	2.6	0.6	0.0	0.0	0.0	0.0	18.0	2.4
12/23/08	47.5	5.5	0.7	2.8	0.7	0.0	0.0	0.0	0.0	38.5	3.3
12/26/08	15.9	2.6	0.4	1.1	0.6	3.6	1.4	0.0	0.0	9.0	1.8
12/29/08	66.0	28.8	3.5	2.4	3.7	0.0	0.0	0.0	0.0	55.2	6.5
1/1/09	28.2	5.2	0.6	2.2	0.7	0.0	0.0	0.0	0.0	18.2	2.4
1/4/09	37.3	6.8	0.8	1.9	0.8	10.2	4.7	0.0	0.0	20.1	3.2
1/7/09	63.7	17.6	2.2	4.0	2.2	0.0	0.0	0.0	0.0	35.2	5.0
1/10/09	56.7	16.1	2.0	3.7	2.0	0.0	0.0	0.0	0.0	33.5	4.7
1/13/09	31.4	5.9	0.8	3.3	1.0	5.4	2.3	0.0	0.0	17.6	3.1
1/16/09	2.3**	**	**	**	**	**	**	**	**	**	**
1/19/09	8.2	1.7	0.2	1.4	0.2	0.0	0.0	0.0	0.0	3.9	0.7
1/22/09	6.4	1.4	0.2	0.5	0.2	0.0	0.0	0.0	0.0	5.1	0.8
1/25/09	26.7	4.3	0.5	3.7	0.6	0.0	0.0	0.0	0.0	18.2	2.4
1/28/09	31.5	8.3	1.0	2.5	1.0	0.0	0.0	0.0	0.0	20.1	2.8
1/31/09	13.4	3.0	0.4	1.3	0.4	0.0	0.0	0.0	0.0	9.1	1.3
2/3/09	18.7	4.4	0.5	1.7	0.6	0.0	0.0	0.0	0.0	13.4	1.8
2/5/09	43.1	7.2	0.8	4.6	0.9	0.0	0.0	0.0	0.0	26.9	3.2
2/6/09	*	*	*	*	*	*	*	*	*	*	*
2/7/09	32.6	6.2	0.7	3.4	0.8	0.0	0.0	0.0	0.0	22.7	2.8
2/9/09	12.3	2.0	0.2	1.3	0.3	0.0	0.0	0.0	0.0	8.5	1.2
2/12/09	18.6	2.7	0.3	2.4	0.4	0.0	0.0	1.5	0.8	12.5	1.8
2/15/09	29.6	5.3	0.7	3.4	0.7	7.6	3.8	0.0	0.0	14.6	2.4
2/18/09	23.3	4.8	0.6	1.7	0.6	0.0	0.0	0.0	0.0	16.5	4.3
2/21/09	15.6	3.0	0.4	1.2	0.4	0.0	0.0	0.0	0.0	11.7	1.6
2/24/09	19.6	3.2	0.4	2.3	0.5	4.5	2.2	0.0	0.0	9.1	2.1
2/27/09	6.9	1.6	0.2	0.6	0.2	0.0	0.0	0.0	0.0	4.7	1.4
3/2/09	15.7	2.9	0.4	1.3	0.4	4.5	2.0	0.0	0.0	6.7	1.8
3/5/09	5.7**	**	**	**	**	**	**	**	**	**	**
3/8/09	10.2	2.5	0.3	0.7	0.3	0.0	0.0	0.0	0.0	6.5	0.9
3/11/09	16.1	2.1	0.3	2.4	0.4	0.0	0.0	1.8	0.7	9.8	1.4

3/14/09	14.9	3.1	0.4	1.0	0.4	0.0	0.0	0.0	0.0	10.2	1.3
3/17/09	10.0	2.6	0.3	0.8	0.3	0.0	0.0	0.0	0.0	6.4	1.0
3/20/09	*	*	*	*	*	*	*	*	*	*	*
3/23/09	9.6	2.3	0.3	1.0	0.3	0.0	0.0	0.0	0.0	6.0	0.9
3/26/09	*	*	*	*	*	*	*	*	*	*	*
3/29/09	10.0	2.1	0.3	1.0	0.3	0.0	0.0	1.5	0.7	5.4	0.9
4/1/09	9.6	1.8	0.2	1.1	0.3	0.0	0.0	0.0	0.0	6.6	1.0
4/4/09	7.8	1.6	0.2	0.6	0.2	0.0	0.0	0.0	0.0	5.7	0.9
4/7/09	10.4	2.3	0.3	1.3	0.3	0.0	0.0	0.0	0.0	6.8	0.9
Average	25.3	5.1	0.6	2.1	0.7	1.7	0.7	0.3	0.1	16.0	2.3

Notes: *No or incomplete CMB data set. **Mass was too small to conduct a CMB analysis.

**PM_{2.5} Source Contribution Estimates and Standard Errors ($\mu\text{g}/\text{m}^3$) – OMNI Profiles.
State Building – Winter 2008/2009.**

Date	PM _{2.5} Mass	Sulfate	Sulfate STD ERR	Ammonium Nitrate	Ammonium Nitrate STD ERR	No. 2 Fuel Oil	No. 2 Fuel Oil STD ERR	Wood Smoke	Wood Smoke STD ERR
11/8/08	40.0	2.8	0.6	1.8	0.4	11.9	2.3	19.0	2.6
11/11/08	31.9	1.7	0.4	1.3	0.3	8.9	1.4	22.2	2.8
11/14/08	52.1	8.7	1.1	4.4	1.1	0.0	0.0	31.4	2.6
11/17/08	20.7	1.6	0.4	1.5	0.3	5.9	1.3	11.1	1.5
11/20/08	16.8	3.2	0.4	1.1	0.4	0.0	0.0	13.9	1.2
11/23/08	23.4	2.1	0.5	1.5	0.3	8.2	1.7	11.2	1.8
11/26/08	22.0	1.9	0.4	0.9	0.3	7.8	1.5	11.7	1.7
11/29/08	16.4	1.4	0.3	1.2	0.2	4.8	1.1	8.5	1.3
12/2/08	47.0	10.5	1.3	3.1	1.3	0.0	0.0	28.3	2.6
12/5/08	31.0	2.3	0.5	1.5	0.3	9.7	1.9	13.2	1.9
12/8/08	*	*	*	*	*	*	*	*	*
12/11/08	18.9	3.1	0.4	1.5	0.4	0.0	0.0	14.6	1.3
12/14/08	39.0	7.0	0.9	2.8	0.9	0.0	0.0	24.3	2.1
12/17/08	34.9	7.5	0.9	2.2	0.9	0.0	0.0	23.2	2.1
12/20/08	26.1	2.6	0.5	1.9	0.4	9.6	2.1	11.0	2.0
12/23/08	47.5	5.2	0.6	2.7	0.7	0.0	0.0	30.8	2.6
12/26/08	15.9	2.9	0.4	1.1	0.4	0.0	0.0	11.9	1.1
12/29/08	66.0	28.6	3.5	5.8	3.6	0.0	0.0	21.7	2.1
1/1/09	28.2	3.6	0.7	1.4	0.5	9.0	2.7	12.1	2.4
1/4/09	37.3	4.0	0.8	0.7	0.5	15.0	3.1	13.5	2.8
1/7/09	63.7	17.5	2.1	3.8	2.2	0.0	0.0	36.0	3.5
1/10/09	56.7	16.0	2.0	3.5	2.0	0.0	0.0	34.0	3.3
1/13/09	31.4	6.4	0.8	3.2	0.8	0.0	0.0	22.0	1.9
1/16/09	2.3**	**	**	**	**	**	**	**	**
1/19/09	8.2	1.2	0.2	1.2	0.2	2.5	1.0	2.6	0.9
1/22/09	6.4	1.4	0.2	0.4	0.2	0.0	0.0	5.2	0.6
1/25/09	26.7	2.4	0.5	2.9	0.4	10.7	2.2	10.3	2.1
1/28/09	31.5	8.2	1.0	2.4	1.0	0.0	0.0	20.5	1.9
1/31/09	13.4	3.0	0.4	1.2	0.4	0.0	0.0	9.2	1.0
2/3/09	18.7	4.3	0.5	1.6	0.6	0.0	0.0	13.5	1.3
2/5/09	43.1	7.1	0.8	4.5	0.9	0.0	0.0	26.9	1.9
2/6/09	*	*	*	*	*	*	*	*	*
2/7/09	32.6	3.6	0.7	2.3	0.5	14.3	2.8	13.1	2.4
2/9/09	12.3	1.3	0.3	1.1	0.2	4.1	1.0	5.8	1.1
2/12/09	18.6	2.8	0.3	2.7	0.4	0.0	0.0	13.3	1.2
2/15/09	29.6	4.9	0.6	4.1	0.7	0.0	0.0	18.1	1.6
2/18/09	23.3	4.7	0.6	2.2	0.6	0.0	0.0	13.9	1.3
2/21/09	15.6	2.9	0.4	1.6	0.4	0.0	0.0	11.6	1.1
2/24/09	19.6	1.8	0.4	2.2	0.3	7.9	1.6	7.0	1.5
2/27/09	6.9	1.0	0.2	0.5	0.1	2.9	0.8	2.0	0.8
3/2/09	15.7	1.6	0.3	1.3	0.3	6.6	1.3	5.9	1.3
3/5/09	5.7**	**	**	**	**	**	**	**	**
3/8/09	10.2	2.4	0.3	0.9	0.3	0.0	0.0	6.3	0.8
3/11/09	16.1	1.3	0.3	2.3	0.3	4.1	1.2	8.5	1.3

3/14/09	14.9	1.6	0.4	0.8	0.2	7.9	1.3	4.3	1.3
3/17/09	10.0	2.6	0.3	1.1	0.3	0.0	0.0	6.6	0.8
3/20/09	*	*	*	*	*	*	*	*	*
3/23/09	9.6	2.3	0.3	1.2	0.3	0.0	0.0	6.2	0.7
3/26/09	*	*	*	*	*	*	*	*	*
3/29/09	10.0	2.1	0.3	1.2	0.3	0.0	0.0	6.7	0.8
4/1/09	9.6	1.1	0.2	1.1	0.2	3.7	0.9	3.4	1.3
4/4/09	7.8	0.9	0.2	0.5	0.1	3.9	0.7	1.4	0.7
4/7/09	10.4	1.4	0.3	1.2	0.2	5.0	1.1	2.8	1.0
Average	25.3	4.4	0.6	1.9	0.6	3.5	0.7	13.8	1.7

Notes: *No, incomplete, or invalid CMB data set. **Mass was too small to conduct a CMB analysis.

**PM_{2.5} Source Contribution Estimates and Standard Errors ($\mu\text{g}/\text{m}^3$) – Revised OMNI Profiles (with auto / diesel).
State Building – Winter 2008/2009.**

Date	PM _{2.5} Mass	Sulfate	Sulfate STD ERR	Ammonium Nitrate	Ammonium Nitrate STD ERR	No. 2 Fuel Oil	No. 2 Fuel Oil STD ERR	Autos	Autos STD ERR	Diesel	Diesel STD ERR	Wood Smoke	Wood Smoke STD ERR
11/8/08	40.0	2.8	0.6	1.8	0.4	11.9	2.3	0.0	0.0	0.0	0.0	19.0	2.6
11/11/08	31.9	1.7	0.4	1.3	0.3	8.9	1.8	0.0	0.0	1.6	0.8	19.6	3.1
11/14/08	52.1	3.2	0.9	2.5	0.5	29.7	3.2	0.0	0.0	0.0	0.0	18.1	4.9
11/17/08	20.7	1.6	0.4	1.5	0.3	5.9	1.3	0.0	0.0	0.0	0.0	11.1	1.5
11/20/08	16.8	1.8	0.4	0.6	0.3	7.8	1.4	0.0	0.0	0.0	0.0	8.7	1.5
11/23/08	23.4	2.1	0.5	1.5	0.3	8.2	1.7	0.0	0.0	0.0	0.0	11.2	1.8
11/26/08	22.0	1.9	0.4	0.9	0.3	7.8	1.5	0.0	0.0	0.0	0.0	11.7	1.7
11/29/08	16.4	1.4	0.3	1.2	0.2	4.8	1.1	0.0	0.0	0.0	0.0	8.5	1.3
12/2/08	47.0	5.4	1.2	0.0	0.0	28.5	4.1	0.0	0.0	0.0	0.0	8.3	3.6
12/5/08	31.0	1.6	0.5	1.4	0.5	11.3	2.4	2.9	1.4	0.0	0.0	13.8	3.4
12/8/08	*	*	*	*	*	*	*	*	*	*	*	*	*
12/11/08	18.9	1.5	0.3	0.9	0.2	8.6	1.3	0.0	0.0	0.0	0.0	8.3	1.5
12/14/08	39.0	3.0	0.7	1.5	0.4	21.4	2.7	0.0	0.0	0.0	0.0	15.4	4.1
12/17/08	34.9	3.8	0.8	0.0	0.0	21.0	2.9	0.0	0.0	0.0	0.0	9.0	2.7
12/20/08	26.1	2.6	0.5	1.9	0.4	9.6	2.1	0.0	0.0	0.0	0.0	11.0	2.0
12/23/08	47.5	5.2	0.6	2.7	0.7	0.0	0.0	0.0	0.0	0.0	0.0	30.8	2.6
12/26/08	15.9	1.7	0.4	0.6	0.2	7.0	1.4	0.0	0.0	0.0	0.0	7.3	1.4
12/29/08	*	*	*	*	*	*	*	*	*	*	*	*	*
1/1/09	28.2	3.6	0.7	1.4	0.5	9.0	2.7	0.0	0.0	0.0	0.0	12.1	2.4
1/4/09	37.3	3.4	0.7	0.0	0.0	17.4	2.4	0.0	0.0	0.0	0.0	19.1	4.0
1/7/09	63.7	8.6	1.7	0.0	0.0	50.5	3.6	0.0	0.0	0.0	0.0	0.0	0.0
1/10/09	56.7	7.8	1.5	0.0	0.0	46.9	3.3	0.0	0.0	0.0	0.0	0.0	0.0
1/13/09	31.4	3.8	0.8	2.2	0.6	14.6	3.0	0.0	0.0	0.0	0.0	12.4	2.7
1/16/09	2.3**	**	**	**	**	**	**	**	**	**	**	**	**
1/19/09	8.2	1.2	0.2	1.2	0.2	2.5	1.0	0.0	0.0	0.0	0.0	2.6	0.9
1/22/09	6.4	0.9	0.2	0.3	0.1	2.6	0.7	0.0	0.0	0.0	0.0	3.4	0.8
1/25/09	26.7	2.4	0.5	2.9	0.4	10.7	2.2	0.0	0.0	0.0	0.0	10.3	2.1
1/28/09	31.5	4.2	0.9	0.0	0.0	22.3	3.0	0.0	0.0	0.0	0.0	8.8	4.3
1/31/09	13.4	1.8	0.4	0.8	0.3	6.5	1.4	0.0	0.0	0.0	0.0	4.8	1.3
2/3/09	18.7	2.9	0.6	1.1	0.4	8.4	2.2	0.0	0.0	0.0	0.0	7.8	1.9
2/5/09	43.1	3.7	0.7	3.1	0.6	19.3	3.0	0.0	0.0	0.0	0.0	13.5	2.6
2/6/09	*	*	*	*	*	*	*	*	*	*	*	*	*
2/7/09	32.6	3.6	0.7	2.3	0.5	14.3	2.8	0.0	0.0	0.0	0.0	13.1	2.4
2/9/09	12.3	1.3	0.3	1.1	0.2	4.1	1.0	0.0	0.0	0.0	0.0	5.8	1.1
2/12/09	18.6	1.7	0.4	2.2	0.3	5.9	1.4	0.0	0.0	0.0	0.0	9.1	1.5
2/15/09	29.6	2.9	0.7	3.1	0.5	12.8	2.6	0.0	0.0	0.0	0.0	8.6	2.2
2/18/09	23.3	2.9	0.6	1.5	0.4	10.0	2.3	0.0	0.0	0.0	0.0	7.2	2.0
2/21/09	15.6	1.3	0.3	1.0	0.2	9.5	1.3	0.0	0.0	0.0	0.0	5.0	1.3
2/24/09	19.6	1.8	0.4	2.2	0.3	7.9	1.6	0.0	0.0	0.0	0.0	7.0	1.5
2/27/09	6.9	1.0	0.2	0.5	0.1	2.9	0.8	0.0	0.0	0.0	0.0	2.0	0.8
3/2/09	15.7	1.6	0.3	1.3	0.3	6.6	1.3	0.0	0.0	0.0	0.0	5.9	1.3
3/5/09	5.7**	**	**	**	**	**	**	**	**	**	**	**	**
3/8/09	10.2	1.5	0.3	0.5	0.2	5.7	1.1	0.0	0.0	0.0	0.0	3.3	1.6
3/11/09	16.1	1.3	0.3	2.3	0.3	4.1	1.2	0.0	0.0	0.0	0.0	8.5	1.3

3/14/09	14.9	1.6	0.4	0.8	0.2	7.9	1.3	0.0	0.0	0.0	0.0	4.3	1.3
3/17/09	10.0	1.1	0.3	0.6	0.2	8.4	0.7	0.0	0.0	0.0	0.0	0.0	0.0
3/20/09	*	*	*	*	*	*	*	*	*	*	*	*	*
3/23/09	9.6	1.4	0.3	0.9	0.2	5.0	1.1	0.0	0.0	0.0	0.0	2.9	1.0
3/26/09	*	*	*	*	*	*	*	*	*	*	*	*	*
3/29/09	10.0	1.4	0.3	0.8	0.2	4.6	1.1	0.0	0.0	0.0	0.0	3.0	1.0
4/1/09	9.6	1.1	0.2	1.1	0.2	3.7	0.9	0.0	0.0	0.0	0.0	3.4	1.3
4/4/09	7.8	0.8	0.2	0.5	0.1	4.0	0.7	0.0	0.0	0.0	0.0	2.1	1.1
4/7/09	10.4	1.4	0.3	1.2	0.2	5.0	1.1	0.0	0.0	0.0	0.0	2.8	1.0
Average	25.3	2.5	0.5	1.2	0.3	11.4	1.8	0.06	0.03	0.04	0.02	8.7	1.9

Notes: *No, incomplete, or invalid CMB data set. **Mass was too small to conduct a CMB analysis.

**PM_{2.5} Source Contribution Estimates and Standard Errors ($\mu\text{g}/\text{m}^3$) – EPA Profiles.
North Pole – Winter 2008/2009.**

Date	PM _{2.5} Mass	Sulfate	Sulfate STD ERR	Ammonium Nitrate	Ammonium Nitrate STD ERR	Autos	Autos STD ERR	Diesel	Diesel STD ERR	Wood Smoke	Wood Smoke STD ERR
1/25/09	39.8	2.6	0.3	1.7	0.3	0.0	0.0	0.0	0.0	29.9	3.3
1/28/09	13.8	2.0	0.2	0.9	0.2	0.0	0.0	0.0	0.0	10.7	1.4
1/31/09	9.7	1.3	0.1	0.5	0.2	0.0	0.0	0.0	0.0	7.4	0.9
2/3/09	15.0	1.7	0.2	0.8	0.2	0.0	0.0	0.0	0.0	14.0	1.7
2/5/09	32.1	2.9	0.3	2.4	0.6	3.4	1.0	0.0	0.0	23.8	3.0
2/6/09	26.0	1.9	0.2	1.4	0.3	0.0	0.0	5.0	2.3	18.3	2.4
2/7/09	61.7	5.4	0.6	2.7	0.7	0.0	0.0	0.0	0.0	53.5	5.8
2/9/09	6.0	1.0	0.1	0.7	0.1	0.0	0.0	0.0	0.0	5.3	0.7
2/12/09	32.0	2.1	0.2	1.3	0.3	0.0	0.0	4.8	2.4	24.5	3.1
2/15/09	34.3	2.3	0.3	1.5	0.3	0.0	0.0	0.0	0.0	28.4	3.2
2/18/09	*	*	*	*	*	*	*	*	*	*	*
2/21/09	10.3	1.3	0.1	0.5	0.2	0.0	0.0	0.0	0.0	8.1	1.1
2/24/09	26.1	1.9	0.2	1.1	0.3	0.0	0.0	4.6	2.2	18.3	2.4
2/27/09	6.7	1.4	0.2	0.7	0.2	0.0	0.0	0.0	0.0	4.4	0.7
3/2/09	10.4	1.3	0.1	0.7	0.2	0.0	0.0	0.0	0.0	7.7	1.0
3/5/09	4.7**	**	**	**	**	**	**	**	**	**	**
3/8/09	6.1	1.1	0.1	0.4	0.1	0.0	0.0	0.0	0.0	4.6	0.7
3/11/09	12.5	1.0	0.1	0.8	0.1	0.0	0.0	0.0	0.0	11.3	2.4
3/14/09	14.1	2.0	0.2	0.6	0.3	0.0	0.0	0.0	0.0	12.1	1.5
3/17/09	3.8**	**	**	**	**	**	**	**	**	**	**
3/20/09	4.6**	**	**	**	**	**	**	**	**	**	**
3/23/09	4.5**	**	**	**	**	**	**	**	**	**	**
3/26/09	3.0**	**	**	**	**	**	**	**	**	**	**
3/29/09	11.8	1.8	0.2	0.7	0.2	0.0	0.0	0.0	0.0	9.8	2.1
4/1/09	10.6	1.3	0.1	0.5	0.2	0.0	0.0	0.0	0.0	8.2	1.7
4/4/09	7.5	1.3	0.1	0.0	0.0	0.0	0.0	0.0	0.0	5.6	1.3
4/7/09	11.4	1.5	0.2	0.0	0.0	0.0	0.0	0.0	0.0	9.2	1.2
Average	18.9	1.9	0.2	1.0	0.2	0.2	0.0	0.7	0.3	15.0	2.0

Notes: *No, incomplete, or invalid CMB data set. **Mass was too small to conduct a CMB analysis.

**PM_{2.5} Source Contribution Estimates and Standard Errors ($\mu\text{g}/\text{m}^3$) – OMNI Profiles.
North Pole – Winter 2008/2009.**

Date	PM _{2.5} Mass	Sulfate	Sulfate STD ERR	Ammonium Nitrate	Ammonium Nitrate STD ERR	No. 2 Fuel Oil	No. 2 Fuel Oil STD ERR	Wood Smoke	Wood Smoke STD ERR
1/25/09	39.8	1.2	0.2	1.2	0.2	6.3	0.9	30.0	2.4
1/28/09	13.8	1.4	0.2	0.7	0.2	3.1	1.0	8.5	1.1
1/31/09	9.7	0.8	0.1	0.4	0.1	2.2	0.6	5.6	0.8
2/3/09	15.0	1.6	0.2	0.9	0.2	0.0	0.0	13.6	1.0
2/5/09	32.1	1.7	0.3	1.8	0.3	6.5	1.4	21.7	1.8
2/6/09	26.0	0.8	0.2	1.2	0.1	4.9	0.7	20.1	1.8
2/7/09	61.7	5.3	0.6	2.5	0.7	0.0	0.0	48.4	2.7
2/9/09	6.0	1.0	0.1	0.8	0.1	0.0	0.0	5.7	0.6
2/12/09	32.0	1.3	0.2	0.9	0.2	4.0	1.0	22.2	1.6
2/15/09	34.3	1.5	0.3	1.3	0.2	4.6	1.1	22.6	1.7
2/18/09	*	*	*	*	*	*	*	*	*
2/21/09	10.3	1.0	0.2	0.5	0.1	1.6	0.7	7.0	0.9
2/24/09	26.1	1.1	0.2	0.9	0.2	3.7	0.9	16.9	1.4
2/27/09	6.7	1.3	0.1	0.8	0.2	0.0	0.0	4.3	0.6
3/2/09	10.4	1.0	0.2	0.6	0.1	1.7	0.7	6.5	0.8
3/5/09	4.7**	**	**	**	**	**	**	**	**
3/8/09	6.1	1.0	0.1	0.4	0.1	0.0	0.0	4.4	0.6
3/11/09	12.5	0.7	0.1	0.7	0.1	1.4	0.6	8.3	0.9
3/14/09	14.1	1.9	0.2	0.7	0.2	0.0	0.0	12.0	0.9
3/17/09	3.8**	**	**	**	**	**	**	**	**
3/20/09	4.6**	**	**	**	**	**	**	**	**
3/23/09	4.5**	**	**	**	**	**	**	**	**
3/26/09	3.0**	**	**	**	**	**	**	**	**
3/29/09	11.8	1.2	0.2	0.6	0.2	3.2	0.9	5.7	0.9
4/1/09	10.6	1.2	0.1	0.6	0.2	0.0	0.0	8.0	0.9
4/4/09	7.5	1.2	0.1	0.4	0.2	0.0	0.0	5.8	0.8
4/7/09	11.4	1.5	0.2	0.5	0.2	0.0	0.0	9.1	0.8
Average	18.9	1.4	0.2	0.9	0.2	2.1	0.5	13.6	1.2

Notes: *No, incomplete, or invalid CMB data set. **Mass was too small to conduct a CMB analysis.

**PM_{2.5} Source Contribution Estimates and Standard Errors ($\mu\text{g}/\text{m}^3$) – EPA Profiles.
RAMS – Winter 2008/2009.**

Date	PM _{2.5} Mass	Sulfate	Sulfate STD ERR	Ammonium Nitrate	Ammonium Nitrate STD ERR	Wood Smoke	Wood Smoke STD ERR
1/25/09	12.5	1.4	0.2	1.5	0.2	8.8	1.2
1/28/09	7.8	0.9	0.1	0.6	0.1	6.3	0.9
1/31/09	7.2	0.9	0.1	0.6	0.1	6.1	0.9
2/3/09	10.5	1.4	0.2	1.1	0.2	8.4	1.1
2/5/09	8.8	0.7	0.1	0.8	0.1	7.4	0.8
2/6/09	8.5	0.6	0.1	0.9	0.1	7.1	1.0
2/7/09	11.3	1.1	0.1	1.3	0.2	8.8	0.9
2/9/09	5.3	0.7	0.1	0.9	0.1	4.2	0.6
2/12/09	11.8	1.5	0.2	1.6	0.2	8.8	0.9
2/15/09	9.6	0.9	0.1	1.3	0.1	7.4	1.0
2/18/09	6.5	0.7	0.1	0.8	0.1	5.0	0.7
2/21/09	6.2	1.0	0.1	0.6	0.1	4.7	0.7
2/24/09	10.7	1.1	0.1	1.5	0.2	7.6	1.0
2/27/09	6.3	1.0	0.1	0.6	0.1	4.7	0.7
3/2/09	7.4	1.2	0.1	0.7	0.2	5.4	0.7
3/5/09	6.0	1.0	0.1	0.8	0.1	4.4	0.6
3/8/09	6.0	0.9	0.1	0.5	0.1	4.2	0.7
3/11/09	6.3	0.8	0.1	0.8	0.1	5.1	1.2
3/14/09	6.3	1.1	0.1	0.8	0.1	4.4	0.6
3/17/09	4.4**	**	**	**	**	**	**
3/20/09	*	*	*	*	*	*	*
3/23/09	4.7**	**	**	**	**	**	**
3/26/09	3.8**	**	**	**	**	**	**
3/29/09	7.7	1.4	0.2	0.4	0.2	5.6	0.7
4/1/09	9.3	1.7	0.2	1.1	0.2	6.8	1.0
4/4/09	8.3	1.3	0.2	0.4	0.2	6.3	0.8
4/7/09	9.2	1.6	0.2	0.6	0.2	7.6	0.9
Average	8.2	1.1	0.1	0.9	0.1	6.3	0.8

Notes: *No, incomplete, or invalid CMB data set. **Mass was too small to conduct a CMB analysis.

**PM_{2.5} Source Contribution Estimates and Standard Errors ($\mu\text{g}/\text{m}^3$) – OMNI Profiles.
RAMS – Winter 2008/2009.**

Date	PM _{2.5} Mass	Sulfate	Sulfate STD ERR	Ammonium Nitrate	Ammonium Nitrate STD ERR	No. 2 Fuel Oil	No. 2 Fuel Oil STD ERR	Wood Smoke	Wood Smoke STD ERR
1/25/09	12.5	0.9	0.2	1.2	0.2	2.5	0.7	7.2	0.9
1/28/09	7.8	0.5	0.1	0.4	0.1	1.7	0.4	5.1	0.7
1/31/09	7.2	0.8	0.1	0.6	0.1	0.0	0.0	6.2	0.6
2/3/09	10.5	0.8	0.1	0.8	0.1	3.3	0.6	6.1	0.9
2/5/09	8.8	0.4	0.1	0.7	0.1	1.0	0.3	6.8	0.7
2/6/09	8.5	0.6	0.1	0.9	0.1	0.0	0.0	7.1	0.7
2/7/09	11.3	0.6	0.1	1.1	0.1	2.0	0.5	8.2	0.9
2/9/09	5.3	0.6	0.1	0.9	0.1	0.0	0.0	4.4	0.5
2/12/09	11.8	1.4	0.2	1.5	0.2	0.0	0.0	9.9	0.8
2/15/09	9.6	0.7	0.1	1.2	0.1	1.2	0.6	6.6	0.8
2/18/09	6.5	0.6	0.1	0.8	0.1	0.0	0.0	5.9	0.8
2/21/09	6.2**	**	**	**	**	**	**	**	**
2/24/09	10.7	0.8	0.2	1.3	0.1	1.6	0.7	6.6	0.8
2/27/09	6.3	1.0	0.1	0.6	0.1	0.0	0.0	5.1	0.8
3/2/09	7.4	0.4	0.1	0.6	0.1	4.2	0.4	2.2	0.6
3/5/09	6.0	0.7	0.1	0.7	0.1	1.2	0.5	2.7	0.7
3/8/09	6.0	0.7	0.1	0.4	0.1	1.2	0.5	3.5	0.6
3/11/09	6.3	0.8	0.1	0.8	0.1	0.0	0.0	3.9	0.5
3/14/09	6.3	1.1	0.1	0.8	0.1	0.0	0.0	4.9	0.6
3/17/09	4.4**	**	**	**	**	**	**	**	**
3/20/09	*	*	*	*	*	*	*	*	*
3/23/09	4.7**	**	**	**	**	**	**	**	**
3/26/09	3.8**	**	**	**	**	**	**	**	**
3/29/09	7.7	0.9	0.2	0.3	0.1	2.4	0.6	4.4	0.8
4/1/09	9.3	1.2	0.2	0.9	0.2	2.5	0.9	4.9	1.3
4/4/09	8.3	0.8	0.1	0.2	0.1	2.9	0.6	3.6	1.0
4/7/09	9.2	0.9	0.2	0.3	0.1	3.7	0.7	4.1	1.1
Average	8.3	0.8	0.1	0.8	0.1	1.4	0.4	5.4	0.8

Notes: *No, incomplete, or invalid CMB data set. **Mass was too small to conduct a CMB analysis.

**PM_{2.5} Source Contribution Estimates and Standard Errors ($\mu\text{g}/\text{m}^3$) – EPA Profiles.
Peger Road – Winter 2008/2009.**

Date	PM _{2.5} Mass	Sulfate	Sulfate STD ERR	Ammonium Nitrate	Ammonium Nitrate STD ERR	Autos	Autos STD ERR	Diesel	Diesel STD ERR	Wood Smoke	Wood Smoke STD ERR
1/25/09	28.6	4.1	0.5	3.5	0.5	0.0	0.0	3.8	1.4	16.5	2.2
1/28/09	31.3	7.7	0.9	2.5	1.0	0.0	0.0	0.0	0.0	20.6	2.6
1/31/09	13.5	2.4	0.3	0.9	0.3	0.0	0.0	0.0	0.0	10.0	2.7
2/3/09	17.8	3.2	0.4	1.1	0.4	0.0	0.0	0.0	0.0	13.2	1.7
2/5/09	48.0	7.6	0.8	3.8	1.0	17.3	5.2	0.0	0.0	23.9	3.5
2/6/09	*	*	*	*	*	*	*	*	*	*	*
2/7/09	32.7	4.8	0.6	2.5	0.6	0.0	0.0	3.1	1.1	22.4	2.8
2/9/09	9.2	1.2	0.1	1.1	0.2	0.0	0.0	1.4	0.6	6.2	1.0
2/12/09	22.8	3.0	0.3	2.2	0.5	0.0	0.0	2.7	0.8	14.9	2.0
2/15/09	32.1	4.7	0.5	4.2	0.8	0.0	0.0	3.5	1.2	19.6	2.6
2/18/09	17.5	3.3	0.4	1.6	0.5	0.0	0.0	1.7	0.8	11.1	1.6
2/21/09	14.6	2.6	0.3	1.0	0.3	0.0	0.0	2.1	1.0	8.3	1.3
2/24/09	20.1	2.9	0.3	2.5	0.5	0.0	0.0	1.8	0.7	13.1	1.8
2/27/09	8.0	1.7	0.2	0.8	0.2	0.0	0.0	0.0	0.0	5.3	0.8
3/2/09	17.5	3.5	0.4	1.5	0.5	0.0	0.0	2.1	0.8	10.9	1.6
3/5/09	5.7	1.0	0.1	0.7	0.2	0.0	0.0	1.0	0.5	2.6	0.6
3/8/09	8.0	1.9	0.2	0.6	0.2	0.0	0.0	0.0	0.0	5.2	1.5
3/11/09	16.6	2.0	0.2	2.2	0.3	0.0	0.0	4.1	1.0	8.2	1.3
3/14/09	11.9	2.6	0.3	0.8	0.4	0.0	0.0	1.6	0.8	6.8	1.1
3/17/09	10.2	2.0	0.2	0.6	0.3	0.0	0.0	0.0	0.0	7.2	0.9
3/20/09	7.4	1.4	0.2	0.5	0.2	0.0	0.0	0.0	0.0	5.0	0.7
3/23/09	11.5	2.2	0.3	0.7	0.3	0.0	0.0	1.7	0.7	6.9	1.0
3/26/09	6.7	0.9	0.1	0.3	0.1	0.0	0.0	0.0	0.0	5.5	0.8
3/29/09	10.9	1.8	0.2	0.9	0.2	0.0	0.0	1.4	0.6	6.8	1.0
4/1/09	13.0	1.9	0.2	1.1	0.3	0.0	0.0	0.0	0.0	9.8	1.2
4/4/09	7.9	1.2	0.1	0.4	0.2	0.0	0.0	0.0	0.0	6.8	1.6
4/7/09	13.3	2.2	0.2	1.3	0.3	0.0	0.0	0.0	0.0	9.4	2.5
Average	16.8	2.8	0.3	1.5	0.4	0.7	0.2	1.2	0.5	10.6	1.6

Notes: *No, incomplete, or invalid CMB data set.

**PM_{2.5} Source Contribution Estimates and Standard Errors ($\mu\text{g}/\text{m}^3$) – OMNI Profiles.
Peger Road – Winter 2008/2009.**

Date	PM _{2.5} Mass	Sulfate	Sulfate STD ERR	Ammonium Nitrate	Ammonium Nitrate STD ERR	No. 2 Fuel Oil	No. 2 Fuel Oil STD ERR	Wood Smoke	Wood Smoke STD ERR
1/25/09	28.6	2.2	0.4	2.7	0.4	9.9	1.8	12.2	1.7
1/28/09	31.3	7.7	0.9	2.3	1.0	0.0	0.0	21.0	1.6
1/31/09	13.5	1.3	0.2	0.7	0.2	5.8	1.0	5.0	1.1
2/3/09	17.8	3.1	0.4	1.4	0.4	0.0	0.0	13.3	1.0
2/5/09	48.0	3.7	0.7	3.3	0.6	19.9	3.0	17.3	2.7
2/6/09	*	*	*	*	*	*	*	*	*
2/7/09	32.7	2.4	0.5	2.2	0.4	13.9	1.9	14.2	1.9
2/9/09	9.2	0.9	0.2	1.0	0.1	1.9	0.7	6.1	0.8
2/12/09	22.8	1.7	0.3	2.0	0.3	7.3	1.4	12.5	1.5
2/15/09	32.1	2.3	0.5	3.8	0.4	12.2	2.0	13.9	1.9
2/18/09	17.5	3.3	0.4	1.9	0.4	0.0	0.0	12.6	1.0
2/21/09	14.6	1.6	0.3	0.8	0.2	5.3	1.2	6.4	1.2
2/24/09	20.1	2.8	0.3	2.7	0.4	0.0	0.0	14.7	1.1
2/27/09	8.0	1.2	0.2	0.7	0.2	2.8	0.9	3.1	0.9
3/2/09	17.5	3.5	0.4	1.8	0.5	0.0	0.0	12.7	1.0
3/5/09	5.7	0.7	0.1	0.6	0.1	1.5	0.6	2.6	0.7
3/8/09	8.0	1.2	0.2	0.5	0.2	3.5	0.9	2.0	0.9
3/11/09	16.6	1.2	0.2	2.1	0.2	3.7	1.0	8.9	1.1
3/14/09	11.9	1.6	0.3	0.7	0.2	5.7	1.2	4.2	1.1
3/17/09	10.2	1.1	0.2	0.5	0.2	4.1	0.9	4.0	0.9
3/20/09	7.4	0.8	0.1	0.5	0.1	2.8	0.6	2.8	0.7
3/23/09	11.5	1.4	0.3	0.6	0.2	5.3	1.0	4.2	1.0
3/26/09	6.7	0.6	0.1	0.3	0.1	1.6	0.4	4.0	0.9
3/29/09	10.9	1.7	0.2	1.1	0.2	0.0	0.0	8.1	0.8
4/1/09	13.0	1.2	0.2	1.1	0.2	3.4	0.9	7.3	1.4
4/4/09	7.9	0.7	0.1	0.3	0.1	2.7	0.5	4.7	1.0
4/7/09	13.3	1.2	0.2	1.2	0.2	5.0	1.0	4.7	1.0
Average	16.8	2.0	0.3	1.4	0.3	4.6	0.9	8.6	1.2

Notes: *No, incomplete, or invalid CMB data set.

**PM_{2.5} Source Contribution Estimates and Standard Errors ($\mu\text{g}/\text{m}^3$) – Revised OMNI Profiles (with auto / diesel).
Peger Road – Winter 2008/2009.**

Date	PM _{2.5} Mass	Sulfate	Sulfate STD ERR	Ammonium Nitrate	Ammonium Nitrate STD ERR	Autos	Autos STD ERR	Diesel	Diesel STD ERR	No. 2 Fuel Oil	No. 2 Fuel Oil STD ERR	Wood Smoke	Wood Smoke STD ERR
1/25/09	28.6	2.2	0.4	2.7	0.4	0.0	0.0	0.0	0.0	9.9	1.8	12.2	1.7
1/28/09	31.3	3.9	0.7	0.0	0.0	0.0	0.0	0.0	0.0	21.3	2.8	6.7	2.4
1/31/09	13.5	1.3	0.2	0.7	0.2	0.0	0.0	0.0	0.0	5.8	1.0	5.0	1.1
2/3/09	17.8	1.9	0.4	0.9	0.3	0.0	0.0	0.0	0.0	7.2	1.4	8.4	1.4
2/5/09	48.0	3.8	0.7	3.1	0.6	7.4	3.1	0.0	0.0	19.9	3.0	17.8	5.3
2/6/09	*	*	*	*	*	*	*	*	*	*	*	*	*
2/7/09	32.7	2.4	0.5	2.2	0.4	0.0	0.0	0.0	0.0	13.9	1.9	14.2	1.9
2/9/09	9.2	0.9	0.2	1.0	0.1	0.0	0.0	0.0	0.0	1.9	0.7	6.1	0.8
2/12/09	22.8	1.7	0.3	2.0	0.3	0.0	0.0	0.0	0.0	7.3	1.4	12.5	1.5
2/15/09	32.1	2.3	0.5	3.8	0.4	0.0	0.0	0.0	0.0	12.2	2.0	13.9	1.9
2/18/09	17.5	2.1	0.4	1.4	0.3	0.0	0.0	0.0	0.0	6.3	1.6	8.4	1.4
2/21/09	14.6	1.6	0.3	0.8	0.2	0.0	0.0	0.0	0.0	5.3	1.2	6.4	1.2
2/24/09	20.1	1.8	0.3	2.3	0.3	0.0	0.0	0.0	0.0	6.1	1.4	10.6	1.4
2/27/09	8.0	1.2	0.2	0.7	0.2	0.0	0.0	0.0	0.0	2.8	0.9	3.1	0.9
3/2/09	17.5	2.2	0.4	1.2	0.3	0.0	0.0	0.0	0.0	7.3	1.7	7.8	1.5
3/5/09	5.7	0.7	0.1	0.6	0.1	0.0	0.0	0.0	0.0	1.5	0.6	2.6	0.7
3/8/09	8.0	1.2	0.2	0.5	0.2	0.0	0.0	0.0	0.0	3.5	0.9	2.0	0.9
3/11/09	16.6	1.3	0.3	2.1	0.2	0.0	0.0	2.4	1.0	3.6	1.1	6.8	1.2
3/14/09	11.9	1.6	0.3	0.7	0.2	0.0	0.0	0.0	0.0	5.7	1.2	4.2	1.1
3/17/09	10.2	1.1	0.2	0.5	0.2	0.0	0.0	0.0	0.0	4.1	0.9	4.0	0.9
3/20/09	7.4	0.8	0.1	0.5	0.1	0.0	0.0	0.0	0.0	2.8	0.6	2.8	0.7
3/23/09	11.5	1.4	0.3	0.6	0.2	0.0	0.0	0.0	0.0	5.3	1.0	4.2	1.0
3/26/09	6.7	0.6	0.1	0.3	0.1	0.0	0.0	0.0	0.0	1.6	0.4	4.0	0.9
3/29/09	10.9	1.1	0.2	0.8	0.2	0.0	0.0	0.0	0.0	4.0	0.8	5.1	0.9
4/1/09	13.0	1.2	0.2	1.1	0.2	0.0	0.0	0.0	0.0	3.4	0.9	7.3	1.4
4/4/09	7.9	0.7	0.1	0.3	0.1	0.0	0.0	0.0	0.0	2.7	0.5	4.7	1.0
4/7/09	13.3	1.2	0.2	1.2	0.2	0.0	0.0	0.0	0.0	5.0	1.0	4.7	1.0
Average	16.8	1.6	0.3	1.2	0.2	0.3	0.1	0.1	0.04	6.6	1.3	7.1	1.4

Notes: *No, incomplete, or invalid CMB data set.

**PM_{2.5} Source Contribution Estimates and Standard Errors ($\mu\text{g}/\text{m}^3$) – EPA Profiles.
State Building – Winter 2009/2010.**

Date	PM _{2.5} Mass	Sulfate	Sulfate STD ERR	Ammonium Nitrate	Ammonium Nitrate STD ERR	Autos	Autos STD ERR	Diesel	Diesel STD ERR	Wood Smoke	Wood Smoke STD ERR
11/3/09	13.8	2.1	0.3	1.1	0.3	3.5	1.3	0.0	0.0	6.4	0.8
11/6/09	5.2	0.8	0.1	0.3	0.1	0.0	0.0	0.0	0.0	4.1	0.2
11/9/09	*	*	*	*	*	*	*	*	*	*	*
11/12/09	4.0**	**	**	**	**	**	**	**	**	**	**
11/15/09	15.7	2.2	0.3	1.4	0.3	0.0	0.0	0.0	0.0	13.0	1.0
11/17/09	21.8	3.3	0.4	2.0	0.4	0.0	0.0	6.1	1.3	9.8	1.5
11/18/09	4.9**	**	**	**	**	**	**	**	**	**	**
11/19/09	10.5	1.5	0.2	1.2	0.2	0.0	0.0	0.0	0.0	7.7	0.8
11/21/09	24.9	3.9	0.5	1.6	0.5	0.0	0.0	0.0	0.0	19.0	1.5
11/24/09	34.2	6.2	0.8	2.7	0.8	0.0	0.0	3.6	1.7	21.1	1.6
11/27/09	20.9	3.1	0.4	1.1	0.4	4.5	1.8	0.0	0.0	12.2	1.8
11/30/09	14	2.7	0.3	1.3	0.3	3.3	1.6	0.0	0.0	6.3	0.9
12/3/09	*	*	*	*	*	*	*	*	*	*	*
12/6/09	0.4**	**	**	**	**	**	**	**	**	**	**
12/9/09	49	9.5	1.2	3.9	1.2	0.0	0.0	9.4	4.5	27.0	5.2
12/10/09	54.4	8.8	1.0	2.2	1.1	0.0	0.0	0.0	0.0	43.9	8.9
12/11/09	43.7	7.4	0.8	4.8	1.0	0.0	0.0	0.0	0.0	29.5	3.5
12/12/09	38.1	6.9	0.8	1.9	0.9	0.0	0.0	0.0	0.0	29.8	2.5
12/13/09	44.4	7.2	0.8	3.8	0.9	12.6	4.0	0.0	0.0	19.1	3.8
12/15/09	4.1**	**	**	**	**	**	**	**	**	**	**
12/18/09	3.6**	**	**	**	**	**	**	**	**	**	**
12/21/09	40.2	6.8	0.8	2.7	0.9	0.0	0.0	0.0	0.0	30.9	2.5
12/24/09	29.8	4.8	0.6	2.3	0.6	0.0	0.0	0.0	0.0	22.5	0.9
12/27/09	24.1	4.5	0.6	1.5	0.6	0.0	0.0	0.0	0.0	19.5	1.6
12/30/09	42.2	8.1	1.0	2.7	1.0	0.0	0.0	0.0	0.0	33.2	2.8
1/2/10	48.6	11.2	1.4	3.4	1.4	0.0	0.0	0.0	0.0	28.3	3.1
1/5/10	52.3	8.8	1.1	3.7	1.1	0.0	0.0	0.0	0.0	42.8	3.5
1/8/10	46.2	9.5	1.2	3.5	1.2	0.0	0.0	0.0	0.0	28.6	1.8
1/11/10	38.5	8.6	1.1	2.4	1.1	0.0	0.0	0.0	0.0	27.3	1.6
1/14/10	11.8	2.4	0.3	1.0	0.3	0.0	0.0	0.0	0.0	8.5	0.7
1/17/10	15.8	2.7	0.3	1.3	0.4	0.0	0.0	0.0	0.0	12.0	1.0
1/20/10	41.0	6.8	0.8	3.1	0.9	0.0	0.0	0.0	0.0	29.1	2.1
1/23/10	30.7	5.5	0.7	2.6	0.7	0.0	0.0	0.0	0.0	23.2	1.0
1/26/10	80.2	18.9	2.3	8.0	2.4	0.0	0.0	0.0	0.0	53.6	3.6
1/29/10	26.4	5.5	0.7	2.2	0.7	0.0	0.0	0.0	0.0	18.4	1.0
2/1/10	24.1	4.0	0.5	5.0	0.6	0.0	0.0	0.0	0.0	15.2	3.0
2/4/10	32.4	7.9	1.0	3.6	1.0	0.0	0.0	0.0	0.0	20.4	1.5
2/7/10	14.6	2.8	0.3	1.7	0.4	0.0	0.0	0.0	0.0	9.7	0.5
2/10/10	22.1	3.2	0.4	3.1	0.5	0.0	0.0	0.0	0.0	15.7	0.6
2/13/10	30.6	4.9	0.6	3.9	0.7	0.0	0.0	0.0	0.0	23.5	1.9
2/16/10	26.3	4.1	0.5	4.0	0.6	0.0	0.0	4.6	2.1	13.8	2.4
2/19/10	22.8	2.6	0.3	3.8	0.4	4.5	1.5	0.0	0.0	12.0	1.5
2/22/10	12.2	2.2	0.3	1.5	0.3	0.0	0.0	0.0	0.0	8.8	0.8
2/25/10	3.1**	**	**	**	**	**	**	**	**	**	**

2/28/10	10.1	1.2	0.1	2.0	0.2	0.0	0.0	0.0	0.0	7.2	0.4
3/3/10	21.3	2.8	0.3	1.8	0.4	0.0	0.0	1.8	0.8	13.9	0.8
3/6/10	3.8**	**	**	**	**	**	**	**	**	**	**
3/9/10	3.4**	**	**	**	**	**	**	**	**	**	**
3/12/10	9.1	1.3	0.2	0.7	0.2	0.0	0.0	0.0	0.0	6.7	0.4
3/15/10	6.9	1.1	0.1	1.1	0.2	0.0	0.0	0.0	0.0	4.8	1.2
Average	28.8	5.2	0.6	2.5	0.7	0.7	0.3	0.6	0.3	19.5	1.9

Notes: *No, incomplete, or invalid CMB data set. **Mass was too small to conduct a CMB analysis.

**PM_{2.5} Source Contribution Estimates and Standard Errors ($\mu\text{g}/\text{m}^3$) – OMNI Profiles.
State Building – Winter 2009/2010.**

Date	PM _{2.5} Mass	Sulfate	Sulfate STD ERR	Ammonium Nitrate	Ammonium Nitrate STD ERR	Autos	Autos STD ERR	Diesel	Diesel STD ERR	No. 2 Fuel Oil	No. 2 Fuel Oil STD ERR	Wood Smoke	Wood Smoke STD ERR
11/3/09	13.8	1.1	0.2	0.7	0.2	0.0	0.0	0.0	0.0	5.3	0.8	6.5	0.9
11/6/09	5.2	0.5	0.1	0.2	0.1	0.0	0.0	0.4	0.1	1.7	0.4	2.2	0.4
11/9/09	*	*	*	*	*	*	*	*	*	*	*	*	*
11/12/09	4.0**	**	**	**	**	**	**	**	**	**	**	**	**
11/15/09	15.7	1.2	0.2	1.1	0.2	0.0	0.0	0.0	0.0	4.5	0.9	10.5	1.0
11/17/09	21.8	1.1	0.5	1.3	0.6	4.2	1.4	0.0	0.0	9.4	2.7	5.9	2.9
11/18/09	4.9**	**	**	**	**	**	**	**	**	**	**	**	**
11/19/09	10.5	0.8	0.2	1.0	0.1	0.0	0.0	0.0	0.0	3.2	0.7	6.3	0.9
11/21/09	24.9	1.8	0.4	1.0	0.3	0.0	0.0	0.0	0.0	10.5	1.5	10.8	1.7
11/24/09	34.2	3.3	0.7	1.7	0.5	0.0	0.0	2.7	0.9	15.9	2.7	6.7	2.9
11/27/09	20.9	1.8	0.4	0.8	0.2	0.0	0.0	2.0	0.5	7.0	1.4	9.1	1.5
11/30/09	14	1.6	0.3	0.9	0.2	0.0	0.0	0.0	0.0	5.8	1.2	5.9	1.3
12/3/09	*	*	*	*	*	*	*	*	*	*	*	*	*
12/6/09	0.4**	**	**	**	**	**	**	**	**	**	**	**	**
12/9/09	*	*	*	*	*	*	*	*	*	*	*	*	*
12/10/09	54.4	5.5	0.9	0.0	0.0	0.0	0.0	5.6	2.0	17.4	3.7	26.0	5.1
12/11/09	43.7	2.3	0.6	2.8	0.4	0.0	0.0	0.0	0.0	28.4	2.4	8.8	2.4
12/12/09	*	*	*	*	*	*	*	*	*	*	*	*	*
12/13/09	44.4	2.8	0.6	2.4	0.4	0.0	0.0	0.0	0.0	23.2	2.4	13.3	2.3
12/15/09	4.1**	**	**	**	**	**	**	**	**	**	**	**	**
12/18/09	3.6**	**	**	**	**	**	**	**	**	**	**	**	**
12/21/09	40.2	3.6	0.8	1.6	0.5	0.0	0.0	0.0	0.0	16.1	2.8	18.1	3.1
12/24/09	29.8	2.6	0.5	1.5	0.4	0.0	0.0	0.0	0.0	12.1	2.0	11.7	2.2
12/27/09	24.1	2.6	0.5	0.9	0.4	0.0	0.0	0.0	0.0	9.8	1.9	12.1	2.2
12/30/09	*	*	*	*	*	*	*	*	*	*	*	*	*
1/2/10	*	*	*	*	*	*	*	*	*	*	*	*	*
1/5/10	*	*	*	*	*	*	*	*	*	*	*	*	*
1/8/10	46.2	6.4	1.2	2.4	0.9	0.0	0.0	0.0	0.0	16.8	4.3	13.7	4.7
1/11/10	38.5	5.0	1.0	1.0	0.7	0.0	0.0	0.0	0.0	20.4	3.8	7.9	4.2
1/14/10	11.8	1.6	0.3	0.7	0.2	0.0	0.0	0.0	0.0	4.8	1.2	2.7	1.3
1/17/10	15.8	1.7	0.3	1.0	0.2	0.0	0.0	0.0	0.0	4.9	1.3	8.6	1.4
1/20/10	*	*	*	*	*	*	*	*	*	*	*	*	*
1/23/10	30.7	3.1	0.6	1.7	0.4	0.0	0.0	0.0	0.0	12.9	2.4	11.6	2.7
1/26/10	*	*	*	*	*	*	*	*	*	*	*	*	*
1/29/10	26.4	3.2	0.6	1.4	0.4	0.0	0.0	0.0	0.0	13.2	2.4	5.9	2.7
2/1/10	24.1	2.1	0.5	4.2	0.5	0.0	0.0	0.0	0.0	9.9	2.0	8.5	2.2
2/4/10	*	*	*	*	*	*	*	*	*	*	*	*	*
2/7/10	14.6	1.7	0.3	1.2	0.3	0.0	0.0	0.0	0.0	6.2	1.3	3.9	1.5
2/10/10	22.1	1.5	0.4	2.5	0.3	0.0	0.0	0.0	0.0	9.2	1.4	7.2	1.5
2/13/10	30.6	2.6	0.6	3.1	0.5	0.0	0.0	0.0	0.0	11.7	2.2	14.5	2.4
2/16/10	26.3	2.5	0.5	3.3	0.4	0.0	0.0	0.0	0.0	9.2	2.1	4.8	2.3
2/19/10	22.8	1.1	0.3	3.3	0.3	0.0	0.0	1.9	0.3	7.5	1.3	8.5	1.4
2/22/10	12.2	1.3	0.3	1.1	0.2	0.0	0.0	0.8	0.4	4.6	1.0	4.3	1.1
2/25/10	3.1**	**	**	**	**	**	**	**	**	**	**	**	**

2/28/10	10.1	0.9	0.2	1.8	0.2	0.0	0.0	0.0	0.0	1.7	0.7	4.8	0.8
3/3/10	21.3	1.6	0.3	1.3	0.2	6.7	1.0	0.0	0.0	6.6	1.3	6.1	1.4
3/6/10	3.8**	**	**	**	**	**	**	**	**	**	**	**	**
3/9/10	3.4**	**	**	**	**	**	**	**	**	**	**	**	**
3/12/10	*	*	*	*	*	*	*	*	*	*	*	*	*
3/15/10	6.9	1.0	0.1	1.1	0.2	0.0	0.0	0.0	0.0	0.0	0.0	4.3	0.1
Average	28.8	2.2	0.5	1.6	0.3	0.4	0.1	0.4	0.1	10.0	1.8	8.7	2.0

Notes: *No, incomplete, or invalid CMB data set. **Mass was too small to conduct a CMB analysis.

**PM_{2.5} Source Contribution Estimates and Standard Errors (µg/m³) – EPA Profiles.
North Pole – Winter 2009/2010.**

Date	PM _{2.5} Mass	Sulfate	Sulfate STD ERR	Ammonium Nitrate	Ammonium Nitrate STD ERR	Autos	Autos STD ERR	Diesel	Diesel STD ERR	Wood Smoke	Wood Smoke STD ERR
11/3/09	6.1	0.4	0.0	0.1	0.1	0.0	0.0	0.0	0.0	5.7	0.7
11/9/09	12.9	0.8	0.1	0.5	0.1	0.0	0.0	0.0	0.0	11.0	1.0
11/15/09	16.7	0.9	0.1	0.8	0.1	0.0	0.0	0.0	0.0	13.1	1.3
11/17/09	13.3	1.3	0.1	1.3	0.2	0.0	0.0	0.0	0.0	10.9	1.1
11/18/09	6.5	0.9	0.1	0.9	0.1	0.0	0.0	0.0	0.0	4.6	0.6
11/19/09	*	*	*	*	*	*	*	*	*	*	*
11/21/09	18.5	1.9	0.2	1.0	0.2	0.0	0.0	0.0	0.0	15.0	1.3
11/27/09	27.8	1.4	0.2	0.8	0.2	0.0	0.0	0.0	0.0	25.4	5.0
12/3/09	15.3	1.1	0.1	0.6	0.1	0.0	0.0	0.0	0.0	12.1	1.2
12/9/09	83.5	5.1	0.7	1.3	0.7	0.0	0.0	0.0	0.0	81.0	15.7
12/10/09	80.5	5.9	0.7	1.4	0.8	0.0	0.0	0.0	0.0	73.3	14.3
12/11/09	58.4	4.5	0.5	1.7	0.6	0.0	0.0	0.0	0.0	48.8	5.3
12/12/09	37.9	2.7	0.3	1.8	0.4	0.0	0.0	0.0	0.0	32.6	3.6
12/13/09	54.8	4.2	0.5	1.7	0.6	0.0	0.0	0.0	0.0	46.2	5.0
12/15/09	6.2	0.5	0.1	0.5	0.1	0.0	0.0	0.0	0.0	6.0	0.7
12/21/09	45.0	4.0	0.4	1.8	0.5	0.0	0.0	0.0	0.0	36.1	2.9
12/24/09	25.2	1.5	0.2	0.9	0.2	0.0	0.0	0.0	0.0	20.0	1.7
12/27/09	17.0	1.5	0.2	0.5	0.2	0.0	0.0	0.0	0.0	13.1	1.3
12/30/09	115.4	9.9	1.1	3.1	1.2	0.0	0.0	14.0	3.2	79.0	9.6
1/2/10	53.1	5.0	0.6	1.3	0.6	0.0	0.0	0.0	0.0	44.9	5.0
1/8/10	36.6	2.9	0.3	2.2	0.4	0.0	0.0	0.0	0.0	33.2	5.8
1/11/10	17.6	1.8	0.2	0.5	0.2	5.5	2.1	0.0	0.0	10.6	1.6
1/14/10	4.5**	**	**	**	**	**	**	**	**	**	**
1/17/10	20.0	1.7	0.2	0.9	0.2	4.2	2.1	0.0	0.0	14.0	1.9
1/20/10	53.5	4.3	0.5	1.4	0.6	14.8	3.7	0.0	0.0	32.7	4.2
1/23/10	42.0	2.8	0.3	1.4	0.4	0.0	0.0	0.0	0.0	35.9	6.0
1/26/10	90.9	7.3	0.8	2.4	1.0	0.0	0.0	0.0	0.0	79.1	6.7
1/29/10	3.3**	**	**	**	**	**	**	**	**	**	**
2/1/10	*	*	*	*	*	*	*	*	*	*	*
2/4/10	31.4	3.0	0.3	1.2	0.4	0.0	0.0	7.0	1.3	18.8	2.5
2/7/10	10.3	1.3	0.1	1.1	0.2	0.0	0.0	0.0	0.0	8.2	0.9
2/10/10	32.9	2.8	0.3	1.4	0.4	0.0	0.0	8.0	1.4	18.8	2.5
2/13/10	54.6	3.3	0.4	2.0	0.4	0.0	0.0	0.0	0.0	53.6	10.4
2/16/10	39.6	2.3	0.3	1.7	0.3	12.7	2.8	0.0	0.0	25.0	3.3
2/19/10	*	*	*	*	*	*	*	*	*	*	*
2/22/10	7.0	0.8	0.1	0.8	0.1	0.0	0.0	0.0	0.0	7.0	0.8
2/25/10	3.8**	**	**	**	**	**	**	**	**	**	**
2/28/10	8.2	0.9	0.1	1.2	0.1	0.0	0.0	0.0	0.0	5.7	0.7
3/3/10	28.2	1.5	0.2	0.9	0.2	7.7	2.3	0.0	0.0	16.8	2.3
3/6/10	*	*	*	*	*	*	*	*	*	*	*
3/9/10	4.1**	**	**	**	**	**	**	**	**	**	**
3/12/10	5.6	0.8	0.1	0.5	0.1	0.0	0.0	0.0	0.0	4.3	0.6
3/15/10	7.5	0.9	0.1	0.6	0.1	0.0	0.0	0.0	0.0	6.3	1.4
Average	33.7	2.6	0.3	1.2	0.3	1.3	0.4	0.8	0.2	27.1	3.7

Notes: *No, incomplete, or invalid CMB data set. **Mass was too small to conduct a CMB analysis.

**PM_{2.5} Source Contribution Estimates and Standard Errors (µg/m³) – OMNI Profiles.
North Pole – Winter 2009/2010.**

Date	PM _{2.5} Mass	Sulfate	Sulfate STD ERR	Ammonium Nitrate	Ammonium Nitrate STD ERR	Autos	Autos STD ERR	Diesel	Diesel STD ERR	No. 2 Fuel Oil	No. 2 Fuel Oil STD ERR	Wood Smoke	Wood Smoke STD ERR
11/3/09	6.1	0.2	0.0	0.1	0.0	0.0	0.0	2.0	0.8	0.8	0.1	2.8	0.6
11/9/09	12.9	0.5	0.1	0.4	0.1	0.0	0.0	0.0	0.0	1.7	0.3	8.2	1.0
11/15/09	16.7	0.4	0.1	0.6	0.1	0.0	0.0	0.0	0.0	2.1	0.4	11.2	0.9
11/17/09	13.3	0.6	0.1	1.2	0.1	0.0	0.0	0.0	0.0	3.1	0.5	9.8	1.0
11/18/09	6.5	0.6	0.1	0.7	0.1	0.0	0.0	0.0	0.0	1.6	0.5	3.7	0.6
11/19/09	*	*	*	*	*	*	*	*	*	*	*	*	*
11/21/09	18.5	0.8	0.2	0.6	0.1	0.0	0.0	0.0	0.0	4.8	0.6	13.0	1.1
11/27/09	27.8	0.6	0.1	0.6	0.1	0.0	0.0	1.7	0.7	1.7	0.5	27.2	2.1
12/3/09	15.3	0.3	0.1	0.5	0.1	0.0	0.0	2.8	0.8	3.5	0.3	7.3	1.0
12/9/09	83.5	1.7	0.4	0.8	0.3	0.0	0.0	11.9	1.7	16.4	1.5	48.5	4.4
12/10/09	80.5	2.4	0.5	1.0	0.3	0.0	0.0	0.0	0.0	15.5	1.9	62.7	4.8
12/11/09	58.4	1.8	0.4	0.8	0.3	0.0	0.0	0.0	0.0	11.9	1.4	47.2	3.7
12/12/09	37.9	1.5	0.3	1.2	0.2	0.0	0.0	0.0	0.0	6.6	1.2	24.1	1.9
12/13/09	54.8	1.7	0.4	1.3	0.2	0.0	0.0	4.9	1.3	11.5	1.4	39.7	3.6
12/15/09	6.2	0.1	0.0	0.5	0.0	0.0	0.0	1.8	0.6	1.9	0.2	2.2	0.5
12/21/09	45.0	2.3	0.4	1.1	0.3	9.8	3.8	0.0	0.0	8.8	1.7	24.4	2.7
12/24/09	25.2	0.5	0.1	0.7	0.1	0.0	0.0	0.0	0.0	5.6	0.5	15.6	1.2
12/27/09	17.0	0.5	0.1	0.4	0.1	0.0	0.0	0.0	0.0	4.0	0.4	13.5	1.3
12/30/09	115.4	4.0	0.8	1.1	0.5	0.0	0.0	6.2	2.2	26.6	3.1	91.0	7.7
1/2/10	53.1	2.0	0.4	0.9	0.3	0.0	0.0	0.0	0.0	13.7	1.6	43.2	3.7
1/8/10	36.6	1.2	0.3	1.8	0.2	0.0	0.0	4.4	1.1	9.9	1.1	21.5	2.5
1/11/10	17.6	0.8	0.2	0.4	0.1	0.0	0.0	0.0	0.0	4.6	0.6	13.2	1.4
1/14/10	4.5**	**	**	**	**	**	**	**	**	**	**	**	**
1/17/10	20.0	1.0	0.2	0.8	0.1	0.0	0.0	0.0	0.0	3.9	0.8	12.7	1.2
1/20/10	53.5	1.4	0.4	1.0	0.3	0.0	0.0	1.9	0.8	13.4	1.8	35.4	3.3
1/23/10	42.0	1.4	0.3	1.1	0.2	0.0	0.0	9.1	1.4	8.6	1.1	24.1	2.8
1/26/10	90.9	2.6	0.6	2.1	0.4	0.0	0.0	0.0	0.0	22.0	2.2	59.2	5.0
1/29/10	3.3**	**	**	**	**	**	**	**	**	**	**	**	**
2/1/10	*	*	*	*	*	*	*	*	*	*	*	*	*
2/4/10	31.4	1.7	0.3	1.0	0.2	7.2	3.1	0.0	0.0	7.3	1.3	15.7	2.1
2/7/10	10.3	0.2	0.1	1.0	0.1	0.0	0.0	0.0	0.0	5.6	0.4	4.1	0.6
2/10/10	32.9	1.3	0.3	1.2	0.2	9.6	3.1	0.0	0.0	8.1	1.1	15.0	2.0
2/13/10	54.6	1.4	0.3	1.6	0.2	8.8	3.8	0.0	0.0	10.4	1.3	29.5	2.9
2/16/10	39.6	1.0	0.2	1.4	0.2	0.0	0.0	4.7	1.1	5.6	0.9	26.5	2.5
2/19/10	*	*	*	*	*	*	*	*	*	*	*	*	*
2/22/10	7.0	0.0	0.0	0.7	0.1	0.0	0.0	0.0	0.0	4.3	0.2	1.7	0.1
2/25/10	3.8**	**	**	**	**	**	**	**	**	**	**	**	**
2/28/10	8.2	0.5	0.1	1.2	0.1	0.0	0.0	0.0	0.0	1.8	0.4	4.7	0.7
3/3/10	28.2	0.5	0.1	0.7	0.1	0.0	0.0	0.0	0.0	5.6	0.5	15.8	1.2
3/6/10	*	*	*	*	*	*	*	*	*	*	*	*	*
3/9/10	4.1**	**	**	**	**	**	**	**	**	**	**	**	**
3/12/10	5.6	0.5	0.1	0.5	0.1	0.0	0.0	0.0	0.0	1.4	0.4	3.5	0.6
3/15/10	7.5	0.4	0.1	0.5	0.1	0.0	0.0	0.0	0.0	2.5	0.3	4.6	0.9
Average	33.7	1.1	0.2	0.9	0.2	1.0	0.4	1.5	0.4	7.3	0.9	22.4	2.1

Notes: *No, incomplete, or invalid CMB data set. **Mass was too small to conduct a CMB analysis.

**PM_{2.5} Source Contribution Estimates and Standard Errors (µg/m³) – EPA Profiles.
RAMS – Winter 2009/2010.**

Date	PM _{2.5} Mass	Sulfate	Sulfate STD ERR	Ammonium Nitrate	Ammonium Nitrate STD ERR	Autos	Autos STD ERR	Diesel	Diesel STD ERR	Wood Smoke	Wood Smoke STD ERR
11/15/09	34.6	3.0	0.3	1.3	0.4	6.2	2.8	0.0	0.0	24.7	3.2
11/17/09	*	*	*	*	*	*	*	*	*	*	*
11/18/09	*	*	*	*	*	*	*	*	*	*	*
11/19/09	*	*	*	*	*	*	*	*	*	*	*
11/21/09	50.2	4.6	0.5	0.0	0.0	11.3	3.8	0.0	0.0	34.9	4.5
11/27/09	33.7	2.4	0.3	0.8	0.3	0.0	0.0	0.0	0.0	30.1	6.0
12/3/09	22.5	2.3	0.3	0.0	0.0	5.8	2.4	0.0	0.0	14.8	2.1
12/9/09	55.4	6.4	0.7	0.0	0.0	0.0	0.0	8.3	2.1	36.0	4.5
12/10/09	72.2	7.4	0.8	0.0	0.0	0.0	0.0	4.9	2.3	56.8	6.9
12/11/09	57.6	6.2	0.7	0.0	0.0	0.0	0.0	0.0	0.0	53.2	10.5
12/12/09	59.3	7.0	0.8	2.1	0.9	0.0	0.0	0.0	0.0	49.9	5.6
12/13/09	68.7	6.7	0.8	0.0	0.0	24.1	5.2	0.0	0.0	42.0	5.5
12/21/09	52.0	5.1	0.6	0.0	0.0	0.0	0.0	7.6	1.8	35.9	4.5
12/24/09	32.2	3.0	0.3	0.9	0.4	0.0	0.0	5.1	1.3	21.6	2.8
12/27/09	6.6	0.5	0.1	0.3	0.1	0.0	0.0	2.4	0.8	3.4	0.7
12/30/09	68.8	8.5	1.0	0.0	0.0	0.0	0.0	0.0	0.0	60.9	12.1
1/2/10	64.9	8.6	1.0	0.0	0.0	18.3	5.9	0.0	0.0	41.7	5.5
1/8/10	39.0	3.9	0.5	1.1	0.5	0.0	0.0	7.7	1.2	25.2	3.1
1/11/10	52.5	8.0	0.9	0.0	0.0	0.0	0.0	0.0	0.0	45.2	9.1
1/14/10	12.5	1.4	0.2	0.8	0.2	0.0	0.0	1.2	0.6	9.2	1.2
1/17/10	24.4	1.9	0.2	0.9	0.3	0.0	0.0	2.2	0.7	20.2	2.5
1/20/10	56.7	5.5	0.7	2.1	0.7	0.0	0.0	0.0	0.0	51.2	10.1
1/23/10	55.4	5.9	0.7	1.8	0.8	0.0	0.0	11.1	2.1	33.6	4.3
1/26/10	*	*	*	*	*	*	*	*	*	*	*
1/29/10	*	*	*	*	*	*	*	*	*	*	*
2/19/10	35.9	4.5	0.5	4.9	0.7	0.0	0.0	8.1	1.6	16.6	2.3
2/22/10	21.4	2.9	0.3	2.0	0.4	0.0	0.0	2.7	0.8	13.6	1.8
2/25/10	7.2	0.8	0.1	0.3	0.1	0.0	0.0	0.0	0.0	5.8	1.1
2/28/10	17.1	1.5	0.2	2.3	0.3	0.0	0.0	0.0	0.0	13.1	2.5
3/3/10	28.4	3.6	0.4	2.1	0.5	0.0	0.0	4.8	1.3	17.2	2.3
3/6/10	5.2	0.7	0.1	0.4	0.1	0.0	0.0	0.0	0.0	4.8	0.6
3/9/10	5.3	0.6	0.1	0.4	0.1	0.0	0.0	0.0	0.0	4.1	0.6
3/12/10	12.0	1.5	0.2	0.7	0.2	0.0	0.0	3.9	0.9	5.6	1.0
3/15/10	12.0	1.2	0.1	1.3	0.2	0.0	0.0	2.3	0.6	7.9	1.1
Average	36.7	4.0	0.5	0.9	0.2	2.3	0.7	2.5	0.6	26.9	4.1

Notes: *No, incomplete, or invalid CMB data set. **Mass was too small to conduct a CMB analysis.

**PM_{2.5} Source Contribution Estimates and Standard Errors (µg/m³) – OMNI Profiles.
RAMS – Winter 2009/2010.**

Date	PM _{2.5} Mass	Sulfate	Sulfate STD ERR	Ammonium Nitrate	Ammonium Nitrate STD ERR	Autos	Autos STD ERR	Diesel	Diesel STD ERR	No. 2 Fuel Oil	No. 2 Fuel Oil STD ERR	Wood Smoke	Wood Smoke STD ERR
11/15/09	34.6	1.6	0.3	1.1	0.2	0.0	0.0	0.0	0.0	7.7	1.3	20.6	1.8
11/17/09	*	*	*	*	*	*	*	*	*	*	*	*	*
11/18/09	*	*	*	*	*	*	*	*	*	*	*	*	*
11/19/09	*	*	*	*	*	*	*	*	*	*	*	*	*
11/21/09	50.2	1.5	0.4	0.6	0.2	0.0	0.0	0.0	0.0	14.9	1.3	35.9	2.8
11/27/09	33.7	0.7	0.2	0.6	0.1	7.8	2.1	0.0	0.0	8.8	0.7	15.4	2.0
12/3/09	22.5	1.3	0.2	0.4	0.2	0.0	0.0	0.0	0.0	5.5	1.0	13.0	1.3
12/9/09	55.4	3.3	0.6	0.0	0.0	0.0	0.0	0.0	0.0	17.0	2.3	29.9	2.7
12/10/09	72.2	3.8	0.7	0.0	0.0	0.0	0.0	0.0	0.0	19.8	2.7	41.5	3.5
12/11/09	57.6	2.5	0.5	0.0	0.0	0.0	0.0	0.0	0.0	18.5	1.8	42.0	3.5
12/12/09	59.3	3.8	0.7	1.6	0.5	0.0	0.0	0.0	0.0	17.9	2.9	32.8	3.2
12/13/09	68.7	2.2	0.5	1.0	0.3	0.0	0.0	4.4	1.1	20.4	1.8	41.8	3.7
12/21/09	52.0	1.7	0.4	0.5	0.2	0.0	0.0	3.0	0.9	15.2	1.4	34.5	3.1
12/24/09	32.2	1.0	0.2	0.6	0.1	0.0	0.0	3.6	1.0	10.2	0.9	18.5	2.1
12/27/09	6.6	0.1	0.0	0.3	0.0	0.0	0.0	1.6	0.8	2.2	0.2	2.4	0.6
12/30/09	68.8	3.8	0.7	0.0	0.0	0.0	0.0	0.0	0.0	23.3	2.5	49.9	4.3
1/2/10	64.9	2.6	1.2	0.9	0.4	9.3	4.8	0.0	0.0	23.1	2.2	28.2	5.3
1/8/10	39.0	2.3	0.5	0.8	0.3	0.0	0.0	5.7	1.6	12.3	1.8	17.7	2.3
1/11/10	52.5	4.5	0.8	0.0	0.0	0.0	0.0	0.0	0.0	20.1	3.2	21.7	3.0
1/14/10	12.5	0.9	0.2	0.7	0.1	0.0	0.0	0.0	0.0	3.3	0.7	7.7	0.9
1/17/10	24.4	1.1	0.2	0.7	0.2	0.0	0.0	0.0	0.0	5.2	0.9	17.6	1.4
1/20/10	56.7	2.2	0.5	1.7	0.3	0.0	0.0	0.0	0.0	16.1	1.8	42.1	3.8
1/23/10	55.4	3.1	0.6	1.4	0.4	9.4	4.3	0.0	0.0	14.8	2.4	27.2	3.3
1/26/10	*	*	*	*	*	*	*	*	*	*	*	*	*
1/29/10	*	*	*	*	*	*	*	*	*	*	*	*	*
2/19/10	35.9	2.2	0.5	4.6	0.5	0.0	0.0	0.0	0.0	11.4	2.0	15.4	2.0
2/22/10	21.4	1.1	0.3	1.7	0.2	0.0	0.0	0.0	0.0	10.3	1.1	8.6	1.2
2/25/10	7.2	0.3	0.1	0.3	0.1	0.0	0.0	1.4	0.7	2.3	0.3	1.9	0.8
2/28/10	17.1	0.8	0.2	2.2	0.2	0.0	0.0	3.3	0.9	3.8	0.8	7.1	1.5
3/3/10	28.4	1.9	0.4	1.8	0.3	0.0	0.0	0.0	0.0	9.2	1.6	14.2	1.6
3/6/10	5.2	0.3	0.1	0.4	0.1	0.0	0.0	0.0	0.0	1.5	0.3	3.9	0.6
3/9/10	5.3	0.3	0.1	0.3	0.0	0.0	0.0	1.4	0.7	1.7	0.2	2.0	0.7
3/12/10	12.0	0.7	0.1	0.6	0.1	0.0	0.0	0.0	0.0	3.5	0.6	8.0	1.2
3/15/10	12.0	0.7	0.2	1.2	0.1	0.0	0.0	0.0	0.0	3.5	0.6	6.8	0.8
Average	36.7	1.8	0.4	0.9	0.2	0.9	0.4	0.8	0.3	11.2	1.4	21.0	2.2

Notes: *No, incomplete, or invalid CMB data set. **Mass was too small to conduct a CMB analysis.

**PM_{2.5} Source Contribution Estimates and Standard Errors ($\mu\text{g}/\text{m}^3$) – EPA Profiles.
Peger Road – Winter 2009/2010.**

Date	PM _{2.5} Mass	Sulfate	Sulfate STD ERR	Ammonium Nitrate	Ammonium Nitrate STD ERR	Autos	Autos STD ERR	Diesel	Diesel STD ERR	Wood Smoke	Wood Smoke STD ERR
11/3/09	13.7	1.7	0.2	1.0	0.4	0.0	0.0	2.4	0.8	8.2	1.2
11/9/09	12.0	1.5	0.2	1.0	0.2	0.0	0.0	2.3	0.9	6.1	1.0
11/15/09	16.2	1.7	0.2	1.2	0.2	0.0	0.0	2.2	0.9	10.4	1.5
11/17/09	13.7	1.7	0.2	1.2	0.4	0.0	0.0	2.0	0.7	8.9	1.2
11/18/09	*	*	*	*	*	*	*	*	*	*	*
11/19/09	*	*	*	*	*	*	*	*	*	*	*
11/21/09	19.1	3.6	0.4	1.1	0.5	0.0	0.0	1.8	0.8	13.0	1.8
11/27/09	16.5	2.7	0.3	1.4	0.4	0.0	0.0	0.0	0.0	15.7	1.4
12/3/09	12.9	1.5	0.2	1.0	0.3	0.0	0.0	2.2	0.6	8.1	1.2
12/9/09	66.6	12.4	1.4	0.0	0.0	0.0	0.0	0.0	0.0	56.3	5.6
12/10/09	64.0	12.0	1.3	0.0	0.0	0.0	0.0	0.0	0.0	54.0	5.4
12/11/09	58.8	10.3	1.2	2.7	1.3	0.0	0.0	4.4	2.1	38.4	4.7
12/12/09	36.8	6.3	0.7	2.6	0.8	0.0	0.0	0.0	0.0	29.0	6.0
12/13/09	40.7	6.6	0.7	2.6	0.9	0.0	0.0	0.0	0.0	30.8	7.7
12/21/09	41.7	6.5	0.7	2.1	0.9	0.0	0.0	9.2	2.1	22.1	3.1
12/24/09	28.6	4.8	0.5	2.2	0.6	11.2	3.0	0.0	0.0	10.8	2.6
12/27/09	17.8	2.8	0.3	1.3	0.4	0.0	0.0	5.7	1.2	7.1	1.2
12/30/09	49.9	9.6	1.1	0.0	0.0	0.0	0.0	0.0	0.0	41.9	3.0
1/2/10	45.6	9.5	1.1	3.7	1.2	0.0	0.0	0.0	0.0	29.9	3.7
1/8/10	39.7	7.7	0.9	2.7	1.0	0.0	0.0	0.0	0.0	28.2	7.3
1/11/10	47.1	12.1	1.3	3.1	1.5	0.0	0.0	0.0	0.0	30.3	7.8
1/14/10	9.2	1.0	0.1	0.6	0.1	3.4	1.4	0.0	0.0	3.7	1.2
1/17/10	17.6	2.3	0.3	1.4	0.3	0.0	0.0	3.5	1.0	10.0	1.5
1/20/10	29.6	5.2	0.6	2.6	0.7	0.0	0.0	7.8	1.7	12.7	2.0
1/23/10	32.2	5.0	0.6	2.3	0.7	0.0	0.0	0.0	0.0	24.4	6.2
1/26/10	64.1	11.0	1.2	4.0	1.5	0.0	0.0	0.0	0.0	49.7	4.9
1/29/10	33.9	5.7	0.6	2.2	0.8	0.0	0.0	12.6	2.0	11.5	2.0
2/1/10	23.5	3.5	0.4	3.5	0.5	0.0	0.0	0.0	0.0	16.5	4.6
2/4/10	33.9	7.4	0.8	3.1	1.0	0.0	0.0	0.0	0.0	23.3	6.1
2/7/10	11.1	1.6	0.2	1.2	0.2	0.0	0.0	1.7	0.6	6.5	1.0
2/10/10	33.5	3.8	0.4	4.2	0.6	0.0	0.0	8.5	1.5	15.5	2.2
2/13/10	32.6	4.9	0.5	5.7	1.1	0.0	0.0	6.4	1.7	15.4	2.2
2/16/10	35.9	4.6	0.5	6.2	1.2	0.0	0.0	7.8	1.9	16.8	2.3
2/19/10	33.2	2.9	0.3	6.5	0.5	0.0	0.0	9.4	1.4	14.1	2.0
2/22/10	8.9	0.8	0.1	1.3	0.3	0.0	0.0	2.2	0.7	4.7	0.8
2/25/10	*	*	*	*	*	*	*	*	*	*	*
2/28/10	9.4	0.8	0.1	1.7	0.1	0.0	0.0	0.0	0.0	7.2	1.5
3/3/10	25.8	3.1	0.3	2.1	0.4	0.0	0.0	10.7	1.5	9.4	1.6
3/6/10	6.5	0.6	0.1	0.4	0.1	0.0	0.0	0.0	0.0	5.6	0.8
3/9/10	3.6**	**	**	**	**	**	**	**	**	**	**
3/12/10	7.8	1.0	0.1	0.8	0.1	0.0	0.0	2.5	0.8	3.5	0.7
3/15/10	10.8	0.9	0.1	1.1	0.1	0.0	0.0	0.0	0.0	8.9	1.9
Average	29.0	4.8	0.5	2.1	0.6	0.4	0.1	2.8	0.7	18.6	3.0

Notes: **Incomplete filter collection, so no model run conducted.

**PM_{2.5} Source Contribution Estimates and Standard Errors ($\mu\text{g}/\text{m}^3$) – OMNI Profiles.
Peger Road – Winter 2009/2010.**

Date	PM _{2.5} Mass	Sulfate	Sulfate STD ERR	Ammonium Nitrate	Ammonium Nitrate STD ERR	Autos	Autos STD ERR	Diesel	Diesel STD ERR	No. 2 Fuel Oil	No. 2 Fuel Oil STD ERR	Wood Smoke	Wood Smoke STD ERR
11/3/09	13.7	0.8	0.2	0.7	0.1	0.0	0.0	0.0	0.0	4.4	0.6	7.3	0.9
11/9/09	12.0	0.6	0.3	0.8	0.3	1.9	0.8	0.0	0.0	3.9	1.3	4.9	1.5
11/15/09	16.2	0.9	0.2	1.0	0.1	0.0	0.0	0.0	0.0	4.1	0.8	9.0	1.0
11/17/09	13.7	1.0	0.2	1.1	0.2	0.0	0.0	0.0	0.0	4.2	0.8	7.4	1.0
11/18/09	*	*	*	*	*	*	*	*	*	*	*	*	*
11/19/09	*	*	*	*	*	*	*	*	*	*	*	*	*
11/21/09	19.1	1.9	0.4	0.8	0.3	0.0	0.0	0.0	0.0	9.6	1.5	8.1	1.4
11/27/09	16.5	1.0	0.4	1.2	0.4	0.0	0.0	3.0	0.8	8.8	2.3	2.7	0.7
12/3/09	12.9	0.7	0.1	0.7	0.1	0.0	0.0	0.0	0.0	4.0	0.6	7.6	0.9
12/9/09	66.6	6.0	1.1	2.1	0.8	0.0	0.0	0.0	0.0	33.8	4.5	27.5	6.2
12/10/09	64.0	5.9	1.1	2.1	0.8	0.0	0.0	0.0	0.0	32.0	4.4	27.0	6.1
12/11/09	58.8	5.2	1.0	2.0	0.7	0.0	0.0	0.0	0.0	30.4	4.1	19.9	3.6
12/12/09	36.8	3.4	0.7	2.2	0.5	0.0	0.0	0.0	0.0	16.1	2.7	11.8	2.4
12/13/09	40.7	3.0	0.6	2.1	0.4	6.2	2.7	0.0	0.0	19.0	2.4	12.2	4.5
12/21/09	41.7	3.4	0.7	1.6	0.5	0.0	0.0	4.3	1.7	17.5	2.6	13.4	2.6
12/24/09	28.6	1.9	0.4	2.1	0.3	0.0	0.0	0.0	0.0	15.1	1.7	9.6	1.7
12/27/09	17.8	1.2	0.2	0.8	0.2	0.0	0.0	3.1	0.7	6.8	1.0	6.9	1.6
12/30/09	49.9	4.2	0.8	1.8	0.6	0.0	0.0	5.6	1.3	27.6	3.3	11.4	4.5
1/2/10	45.6	5.2	1.0	1.9	0.7	0.0	0.0	0.0	0.0	24.0	4.0	13.0	3.3
1/8/10	39.7	3.4	0.7	2.3	0.5	0.0	0.0	3.2	1.1	22.0	2.7	7.4	3.6
1/11/10	47.1	6.2	1.1	0.9	0.8	0.0	0.0	0.0	0.0	32.2	4.6	5.3	5.7
1/14/10	9.2	0.5	0.1	0.5	0.1	0.0	0.0	0.0	0.0	2.3	0.4	6.4	1.0
1/17/10	17.6	1.1	0.2	0.9	0.2	0.0	0.0	0.0	0.0	6.2	0.9	8.4	1.1
1/20/10	29.6	2.5	0.6	1.6	0.6	0.0	0.0	3.4	1.0	13.8	3.0	8.5	3.6
1/23/10	32.2	1.9	0.6	2.0	0.5	3.2	1.4	0.0	0.0	14.9	2.7	10.8	3.5
1/26/10	64.1	5.1	1.0	3.5	0.7	0.0	0.0	4.9	2.0	31.9	4.1	16.2	5.5
1/29/10	33.9	1.9	0.4	1.8	0.3	0.0	0.0	6.8	1.0	17.9	1.7	5.6	2.6
2/1/10	23.5	1.5	0.3	3.2	0.3	0.0	0.0	0.0	0.0	11.0	1.4	4.2	1.9
2/4/10	33.9	4.0	0.7	2.7	0.6	0.0	0.0	0.0	0.0	18.6	3.1	5.0	2.6
2/7/10	11.1	0.9	0.2	1.1	0.2	0.0	0.0	0.0	0.0	4.2	0.8	5.0	0.9
2/10/10	33.5	1.7	0.4	3.9	0.4	0.0	0.0	5.1	1.4	11.5	1.7	9.9	1.9
2/13/10	32.6	2.2	0.7	4.5	0.7	0.0	0.0	4.3	1.2	15.1	3.7	6.6	2.8
2/16/10	35.9	2.0	0.7	5.2	0.8	0.0	0.0	4.5	1.4	14.0	3.7	10.2	3.2
2/19/10	33.2	1.0	0.3	5.5	0.4	0.0	0.0	4.7	1.5	9.6	1.5	10.9	2.0
2/22/10	*	*	*	*	*	*	*	*	*	*	*	*	*
2/25/10	*	*	*	*	*	*	*	*	*	*	*	*	*
2/28/10	9.4	0.6	0.1	1.4	0.1	2.6	1.2	0.0	0.0	1.9	0.5	3.1	1.5
3/3/10	25.8	0.7	0.2	1.9	0.2	0.0	0.0	6.3	0.9	9.9	0.9	8.1	1.6
3/6/10	6.5	0.3	0.1	0.3	0.0	1.8	0.8	0.0	0.0	2.0	0.2	1.7	0.8
3/9/10	3.6**	**	**	**	**	**	**	**	**	**	**	**	**
3/12/10	7.8	0.5	0.2	0.7	0.2	0.0	0.0	1.3	0.5	2.5	0.9	3.1	1.2
3/15/10	10.8	0.5	0.1	1.0	0.1	0.0	0.0	2.2	0.8	2.6	0.4	4.2	1.0
Average	29.0	2.3	0.5	1.9	0.4	0.4	0.2	1.7	0.5	13.7	2.1	9.2	2.5

Notes: **Incomplete filter collection, so no model run conducted.

**PM_{2.5} Source Contribution Estimates and Standard Errors (µg/m³) – EPA Profiles.
State Building – Winter 2010/2011.**

Date	PM _{2.5} Mass	Sulfate	Sulfate STD ERR	Ammonium Nitrate	Ammonium Nitrate STD ERR	Autos	Autos STD ERR	Diesel	Diesel STD ERR	Wood Smoke	Wood Smoke STD ERR
11/1/10	14.5	2.0	0.2	0.9	0.3	0.0	0.0	0.0	0.0	11.5	0.4
11/4/10	3.3**	**	**	**	**	**	**	**	**	**	**
11/7/10	9.6	1.9	0.2	1.2	0.3	0.0	0.0	0.0	0.0	6.5	1.0
11/10/10	8.6	1.2	0.1	0.8	0.2	0.0	0.0	0.0	0.0	6.5	0.2
11/13/10	8.1	1.0	0.1	0.7	0.1	0.0	0.0	0.0	0.0	6.5	0.2
11/16/10	22.0	3.1	0.4	1.4	0.4	0.0	0.0	0.0	0.0	18.2	1.1
11/19/10	17.6	2.4	0.3	1.5	0.3	0.0	0.0	0.0	0.0	13.9	0.5
11/22/10	11.5	2.0	0.2	0.8	0.3	5.9	1.2	0.0	0.0	2.9	0.5
11/25/10	*	*	*	*	*	*	*	*	*	*	*
11/28/10	14.4	2.4	0.3	1.2	0.3	0.0	0.0	0.0	0.0	10.4	0.5
12/1/10	43.1	8.9	1.1	3.1	1.1	0.0	0.0	0.0	0.0	31.0	1.7
12/4/10	7.0	1.3	0.2	0.7	0.2	0.0	0.0	0.0	0.0	5.0	0.7
12/7/10	36.5	7.6	0.9	1.9	1.0	0.0	0.0	0.0	0.0	26.6	3.9
12/10/10	26.1	4.5	0.6	2.2	0.6	0.0	0.0	0.0	0.0	19.1	2.8
12/13/10	15.2	2.4	0.3	1.3	0.3	0.0	0.0	0.0	0.0	11.4	1.6
12/16/10	*	*	*	*	*	*	*	*	*	*	*
12/19/10	*	*	*	*	*	*	*	*	*	*	*
12/22/10	*	*	*	*	*	*	*	*	*	*	*
12/25/10	*	*	*	*	*	*	*	*	*	*	*
12/28/10	*	*	*	*	*	*	*	*	*	*	*
12/31/10	*	*	*	*	*	*	*	*	*	*	*
1/3/11	*	*	*	*	*	*	*	*	*	*	*
1/6/11	*	*	*	*	*	*	*	*	*	*	*
1/9/11	*	*	*	*	*	*	*	*	*	*	*
1/12/11	*	*	*	*	*	*	*	*	*	*	*
1/15/11	*	*	*	*	*	*	*	*	*	*	*
1/18/11	*	*	*	*	*	*	*	*	*	*	*
1/21/11	*	*	*	*	*	*	*	*	*	*	*
1/24/11	*	*	*	*	*	*	*	*	*	*	*
1/27/11	*	*	*	*	*	*	*	*	*	*	*
1/30/11	*	*	*	*	*	*	*	*	*	*	*
2/2/11	*	*	*	*	*	*	*	*	*	*	*
2/5/11	34.9	6.8	0.8	4.4	0.9	0.0	0.0	0.0	0.0	23.3	1.3
2/8/11	33.5	5.0	0.6	3.1	0.7	0.0	0.0	0.0	0.0	26.3	1.0
Average	20.2	3.5	0.4	1.7	0.5	0.4	0.1	0.0	0.0	14.6	1.1

Notes: *No, incomplete, or invalid CMB data set. **Mass was too small to conduct a CMB analysis.

**PM_{2.5} Source Contribution Estimates and Standard Errors ($\mu\text{g}/\text{m}^3$) – OMNI Profiles.
State Building – Winter 2010/2011.**

Date	PM _{2.5} Mass	Sulfate	Sulfate STD ERR	Ammonium Nitrate	Ammonium Nitrate STD ERR	Autos	Autos STD ERR	Diesel	Diesel STD ERR	No. 2 Fuel Oil	No. 2 Fuel Oil STD ERR	Wood Smoke	Wood Smoke STD ERR
11/1/10	14.5	1.0	0.2	0.5	0.1	0.0	0.0	1.0	0.2	4.5	0.8	7.0	0.9
11/4/10	3.3**	**	**	**	**	**	**	**	**	**	**	**	**
11/7/10	9.6	1.2	0.2	1.0	0.2	0.0	0.0	0.0	0.0	3.2	0.9	3.3	1.0
11/10/10	8.6	0.7	0.1	0.6	0.1	0.0	0.0	0.0	0.0	2.7	0.5	4.1	0.6
11/13/10	8.1	0.7	0.1	0.6	0.1	0.8	0.4	0.0	0.0	1.6	0.5	4.5	0.6
11/16/10	22.0	1.8	0.4	1.3	0.3	2.6	1.2	0.0	0.0	7.2	1.5	7.6	1.6
11/19/10	17.6	1.4	0.3	1.3	0.2	0.0	0.0	0.0	0.0	5.6	1.1	9.2	1.2
11/22/10	11.5	1.8	0.2	0.8	0.2	0.0	0.0	1.5	0.3	0.0	0.0	6.8	0.4
11/25/10	*	*	*	*	*	*	*	*	*	*	*	*	*
11/28/10	14.4	1.4	0.3	0.9	0.2	0.0	0.0	0.0	0.0	5.1	1.1	5.9	1.2
12/1/10	43.1	5.0	1.0	1.7	0.7	0.0	0.0	0.0	0.0	21.4	3.9	10.7	4.3
12/4/10	7.0	0.9	0.2	0.5	0.1	0.0	0.0	0.0	0.0	2.1	0.6	2.7	0.7
12/7/10	36.5	3.8	0.8	1.6	0.5	0.0	0.0	0.0	0.0	20.9	3.1	4.5	3.4
12/10/10	26.1	2.6	0.5	2.1	0.4	0.0	0.0	0.0	0.0	10.2	2.0	8.6	2.2
12/13/10	15.2	1.4	0.3	0.9	0.2	0.0	0.0	0.0	0.0	5.5	1.0	5.7	1.2
12/16/10	*	*	*	*	*	*	*	*	*	*	*	*	*
12/19/10	*	*	*	*	*	*	*	*	*	*	*	*	*
12/22/10	*	*	*	*	*	*	*	*	*	*	*	*	*
12/25/10	*	*	*	*	*	*	*	*	*	*	*	*	*
12/28/10	*	*	*	*	*	*	*	*	*	*	*	*	*
12/31/10	*	*	*	*	*	*	*	*	*	*	*	*	*
1/3/11	*	*	*	*	*	*	*	*	*	*	*	*	*
1/6/11	*	*	*	*	*	*	*	*	*	*	*	*	*
1/9/11	*	*	*	*	*	*	*	*	*	*	*	*	*
1/12/11	*	*	*	*	*	*	*	*	*	*	*	*	*
1/15/11	*	*	*	*	*	*	*	*	*	*	*	*	*
1/18/11	*	*	*	*	*	*	*	*	*	*	*	*	*
1/21/11	*	*	*	*	*	*	*	*	*	*	*	*	*
1/24/11	*	*	*	*	*	*	*	*	*	*	*	*	*
1/27/11	*	*	*	*	*	*	*	*	*	*	*	*	*
1/30/11	*	*	*	*	*	*	*	*	*	*	*	*	*
2/2/11	*	*	*	*	*	*	*	*	*	*	*	*	*
2/5/11	34.9	3.2	0.7	3.0	0.5	0.0	0.0	0.0	0.0	20.4	2.8	3.3	3.1
2/8/11	33.5	2.5	0.6	2.9	0.4	0.0	0.0	0.0	0.0	13.6	2.1	14.0	2.4
Average	20.2	2.0	0.4	1.3	0.3	0.2	0.1	0.2	0.04	8.3	1.5	6.5	1.7

Notes: *No, incomplete, or invalid CMB data set. **Mass was too small to conduct a CMB analysis.

**PM_{2.5} Source Contribution Estimates and Standard Errors ($\mu\text{g}/\text{m}^3$) – EPA Profiles.
North Pole – Winter 2010/2011.**

Date	PM _{2.5} Mass	Sulfate	Sulfate STD ERR	Ammonium Nitrate	Ammonium Nitrate STD ERR	Autos	Autos STD ERR	Diesel	Diesel STD ERR	Wood Smoke	Wood Smoke STD ERR
1/9/11	23.4	1.3	0.1	1.3	0.2	0.0	0.0	0.0	0.0	20.8	1.5
1/12/11	11.7	1.0	0.1	0.5	0.1	0.0	0.0	2.2	0.6	8.1	1.1
1/15/11	33.8	2.6	0.3	0.8	0.3	9.8	2.7	0.0	0.0	21.9	2.9
1/18/11	26.8	2.3	0.3	1.1	0.3	0.0	0.0	3.0	1.1	18.7	2.4
1/21/11	40.8	5.0	0.6	0.0	0.0	0.0	0.0	0.0	0.0	37.0	7.4
1/24/11	6.5	0.8	0.1	0.4	0.1	0.0	0.0	0.0	0.0	5.5	0.8
1/27/11	14.0	1.1	0.1	0.7	0.1	3.8	1.9	0.0	0.0	7.8	1.2
1/30/11	58.5	3.3	0.4	1.6	0.4	0.0	0.0	0.0	0.0	54.3	10.6
2/2/11	23.3	2.0	0.2	1.5	0.3	0.0	0.0	0.0	0.0	19.4	1.4
2/5/11	28.8	2.2	0.2	1.5	0.3	0.0	0.0	4.0	1.1	19.7	2.5
Average	26.8	2.1	0.3	0.9	0.2	1.4	0.5	0.9	0.3	21.3	3.2

**PM_{2.5} Source Contribution Estimates and Standard Errors ($\mu\text{g}/\text{m}^3$) – OMNI Profiles.
North Pole – Winter 2010/2011.**

Date	PM _{2.5} Mass	Sulfate	Sulfate STD ERR	Ammonium Nitrate	Ammonium Nitrate STD ERR	Autos	Autos STD ERR	Diesel	Diesel STD ERR	No. 2 Fuel Oil	No. 2 Fuel Oil STD ERR	Wood Smoke	Wood Smoke STD ERR
1/9/11	23.4	0.7	0.1	1.1	0.1	5.3	1.9	0.0	0.0	2.9	0.6	13.0	1.6
1/12/11	11.7	0.7	0.1	0.3	0.1	0.0	0.0	0.0	0.0	1.8	0.5	8.5	0.8
1/15/11	33.8	0.8	0.2	0.6	0.1	0.0	0.0	1.8	0.7	7.3	0.7	22.8	2.1
1/18/11	26.8	0.8	0.2	0.6	0.2	0.0	0.0	1.2	0.6	6.9	1.1	17.8	1.9
1/21/11	40.8	2.6	0.5	0.0	0.0	0.0	0.0	0.0	0.0	13.4	1.9	19.6	2.1
1/24/11	6.5	0.4	0.1	0.4	0.1	0.0	0.0	0.0	0.0	1.6	0.3	4.6	0.6
1/27/11	14.0	0.6	0.1	0.5	0.1	0.0	0.0	0.0	0.0	2.1	0.5	11.4	1.1
1/30/11	58.5	1.4	0.3	1.1	0.2	13.5	2.6	0.0	0.0	8.8	1.2	35.1	4.9
2/2/11	23.3	1.4	0.2	1.3	0.2	0.0	0.0	3.8	1.0	2.5	1.1	14.0	1.9
2/5/11	28.8	0.8	0.2	1.1	0.1	0.0	0.0	1.9	0.7	5.9	0.7	19.0	1.8
Average	26.8	1.0	0.2	0.7	0.1	1.9	0.5	0.9	0.3	5.3	0.8	16.6	1.9

**PM_{2.5} Source Contribution Estimates and Standard Errors ($\mu\text{g}/\text{m}^3$) – EPA Profiles.
Peger Road – Winter 2010/2011.**

Date	PM _{2.5} Mass	Sulfate	Sulfate STD ERR	Ammonium Nitrate	Ammonium Nitrate STD ERR	Autos	Autos STD ERR	Diesel	Diesel STD ERR	Wood Smoke	Wood Smoke STD ERR
1/9/11	22.7	3.0	0.3	2.6	0.4	0.0	0.0	0.0	0.0	17.2	4.4
1/12/11	48.4	10.8	1.2	0.0	0.0	0.0	0.0	0.0	0.0	37.3	4.0
1/15/11	24.6	3.8	0.4	1.1	0.5	7.2	3.0	0.0	0.0	12.9	2.0
1/18/11	44.9	9.1	1.0	2.7	1.2	0.0	0.0	0.0	0.0	34.7	7.2
1/21/11	23.3	4.2	0.5	0.0	0.0	0.0	0.0	0.0	0.0	18.2	4.6
1/24/11	12.4	1.7	0.2	1.1	0.3	0.0	0.0	1.5	0.6	8.2	1.2
1/27/11	14.6	2.0	0.2	1.6	0.5	0.0	0.0	3.0	0.7	8.3	1.3
1/30/11	35.4	4.9	0.5	2.8	0.7	0.0	0.0	0.0	0.0	26.5	6.6
2/2/11	25.1	2.6	0.3	4.3	0.4	0.0	0.0	3.8	1.1	13.4	1.8
2/5/11	34.0	5.6	0.6	4.0	0.8	0.0	0.0	0.0	0.0	25.0	6.3
Average	28.6	4.8	0.5	2.0	0.5	0.7	0.3	0.8	0.2	20.2	3.9

**PM_{2.5} Source Contribution Estimates and Standard Errors ($\mu\text{g}/\text{m}^3$) – OMNI Profiles.
Peger Road – Winter 2010/2011.**

Date	PM _{2.5} Mass	Sulfate	Sulfate STD ERR	Ammonium Nitrate	Ammonium Nitrate STD ERR	Autos	Autos STD ERR	Diesel	Diesel STD ERR	No. 2 Fuel Oil	No. 2 Fuel Oil STD ERR	Wood Smoke	Wood Smoke STD ERR
1/9/11	22.7	1.1	0.5	2.5	0.6	4.1	1.4	0.0	0.0	7.5	2.6	7.4	2.8
1/12/11	48.4	5.1	1.0	1.8	0.7	0.0	0.0	3.2	1.3	29.4	4.0	7.5	5.0
1/15/11	24.6	1.6	0.3	0.8	0.2	0.0	0.0	0.0	0.0	11.8	1.3	11.7	2.1
1/18/11	44.9	4.2	0.8	2.1	0.6	0.0	0.0	0.0	0.0	26.9	3.2	11.0	4.3
1/21/11	23.3	2.0	0.4	0.8	0.3	0.0	0.0	0.0	0.0	11.4	1.6	11.0	2.3
1/24/11	12.4	1.0	0.2	0.8	0.1	0.0	0.0	0.0	0.0	3.7	0.8	7.0	0.9
1/27/11	14.6	1.1	0.2	1.2	0.2	0.0	0.0	0.0	0.0	5.1	0.9	7.4	1.0
1/30/11	35.4	2.0	0.5	2.5	0.5	0.0	0.0	2.5	0.9	14.6	2.4	13.7	3.2
2/2/11	25.1	0.7	0.4	3.5	0.4	2.4	1.0	0.0	0.0	8.5	1.8	11.7	2.0
2/5/11	34.0	2.2	0.5	3.7	0.4	0.0	0.0	3.9	0.9	16.3	2.0	6.8	2.8
Average	28.6	2.1	0.5	2.0	0.4	0.6	0.2	1.0	0.3	13.5	2.1	9.5	2.6

**PM_{2.5} Source Contribution Estimates and Standard Errors ($\mu\text{g}/\text{m}^3$) – EPA Profiles.
State Building – Winter 2011/2012.**

Date	PM _{2.5} Mass	Sulfate	Sulfate STD ERR	Ammonium Nitrate	Ammonium Nitrate STD ERR	Autos	Autos STD ERR	Diesel	Diesel STD ERR	Wood Smoke	Wood Smoke STD ERR
11/2/11	11.0	2.2	0.3	0.8	0.3	0.0	0.0	0.0	0.0	8.2	0.7
11/5/11	*	*	*	*	*	*	*	*	*	*	*
11/8/11	10.3	1.6	0.2	0.5	0.2	0.0	0.0	0.0	0.0	8.4	1.2
11/11/11	8.9	1.1	0.1	0.5	0.1	0.0	0.0	0.0	0.0	7.2	0.2
11/14/11	24.6	3.6	0.4	1.2	0.5	0.0	0.0	0.0	0.0	19.8	1.6
11/17/11	32.8	6.2	0.8	2.1	0.8	0.0	0.0	0.0	0.0	23.4	5.7
11/20/11	*	*	*	*	*	*	*	*	*	*	*
11/23/11	14.8	2.1	0.3	0.9	0.3	0.0	0.0	0.0	0.0	11.5	0.7
11/26/11	24.7	4.4	0.5	1.6	0.6	0.0	0.0	0.0	0.0	18.3	1.5
11/29/11	27.2	4.6	0.6	1.5	0.6	0.0	0.0	0.0	0.0	20.2	1.7
12/2/11	14.7	1.9	0.2	1.0	0.2	0.0	0.0	0.0	0.0	11.5	2.1
12/5/11	*	*	*	*	*	*	*	*	*	*	*
12/8/11	27.2	4.4	0.5	1.9	0.6	0.0	0.0	0.0	0.0	21.1	1.7
12/11/11	*	*	*	*	*	*	*	*	*	*	*
12/14/11	24.7	4.0	0.5	1.6	0.5	8.2	2.3	0.0	0.0	9.9	1.3
12/17/11	37.3	5.9	0.7	1.5	0.7	0.0	0.0	0.0	0.0	31.6	5.8
12/20/11	13.8	1.5	0.2	0.8	0.2	0.0	0.0	0.0	0.0	12.1	0.4
12/23/11	6.3**	**	**	**	**	**	**	**	**	**	**
12/26/11	23.1	4.0	0.5	1.6	0.5	8.0	2.4	0.0	0.0	10.9	1.4
12/29/11	31.8	5.7	0.7	1.6	0.7	0.0	0.0	0.0	0.0	25.5	2.1
1/1/12	*	*	*	*	*	*	*	*	*	*	*
1/4/12	14.3	2.0	0.2	1.0	0.3	0.0	0.0	0.0	0.0	11.2	0.9
1/7/12	15.6	3.2	0.4	1.1	0.4	0.0	0.0	0.0	0.0	11.0	1.0
1/10/12	24.4	4.0	0.5	1.2	0.5	0.0	0.0	0.0	0.0	18.0	2.6
1/13/12	23.2	4.8	0.6	1.2	0.6	0.0	0.0	0.0	0.0	17.9	0.9
1/16/12	29.1	6.1	0.8	2.4	0.8	0.0	0.0	8.8	1.6	12.1	1.6
1/19/12	40.5	8.1	1.0	4.0	1.0	0.0	0.0	0.0	0.0	27.3	1.5
1/22/12	*	*	*	*	*	*	*	*	*	*	*
1/25/12	9.8	1.8	0.2	0.8	0.2	0.0	0.0	0.0	0.0	6.9	0.5
1/28/12	36.8	7.6	0.9	2.2	1.0	0.0	0.0	0.0	0.0	18.3	2.0
1/31/12	18.7	4.9	0.6	1.8	0.6	0.0	0.0	0.0	0.0	11.4	1.2
2/3/12	6.5**	**	**	**	**	**	**	**	**	**	**
2/6/12	24.8	3.9	0.5	2.1	0.5	0.0	0.0	0.0	0.0	18.4	1.2
2/9/12	18.1	2.3	0.3	1.2	0.3	0.0	0.0	0.0	0.0	13.8	0.8
2/12/12	18.3	2.1	0.3	1.9	0.3	0.0	0.0	0.0	0.0	14.8	0.8
2/15/12	27.0	4.5	0.6	2.2	0.6	0.0	0.0	0.0	0.0	20.2	2.9
2/18/12	25.6	3.9	0.5	3.2	0.5	0.0	0.0	0.0	0.0	17.5	1.2
2/21/12	13.7	2.9	0.4	1.7	0.4	0.0	0.0	0.0	0.0	9.8	0.9
2/24/12	5.0**	**	**	**	**	**	**	**	**	**	**
2/27/12	4.3**	**	**	**	**	**	**	**	**	**	**
3/1/12	9.0	2.2	0.3	0.8	0.3	0.0	0.0	0.0	0.0	5.8	0.4
3/4/12	*	*	*	*	*	*	*	*	*	*	*
3/7/12	*	*	*	*	*	*	*	*	*	*	*
3/10/12	9.5	2.2	0.3	1.3	0.3	0.0	0.0	0.0	0.0	5.9	0.4
3/13/12	13.9	2.7	0.3	1.4	0.4	0.0	0.0	0.0	0.0	9.7	0.8

3/16/12	16.3	3.4	0.4	1.3	0.4	0.0	0.0	0.0	0.0	11.5	0.9
3/19/12	10.6	2.6	0.3	1.2	0.3	0.0	0.0	0.0	0.0	6.9	1.1
3/22/12	13.3	3.0	0.4	1.4	0.4	0.0	0.0	0.0	0.0	9.2	0.8
3/25/12	11.0	1.7	0.2	1.2	0.2	0.0	0.0	0.0	0.0	7.9	0.5
3/28/12	8.6	1.4	0.2	1.0	0.2	0.0	0.0	0.0	0.0	6.3	0.4
3/31/12	5.4**	**	**	**	**	**	**	**	**	**	**
Average	20.0	3.5	0.4	1.5	0.5	0.4	0.1	0.2	0.04	14.0	1.4

Notes: *No, incomplete, or invalid CMB data set. **Mass was too small to conduct a CMB analysis.

**PM_{2.5} Source Contribution Estimates and Standard Errors (µg/m³) – OMNI Profiles.
State Building – Winter 2011/2012.**

Date	PM _{2.5} Mass	Sulfate	Sulfate STD ERR	Ammonium Nitrate	Ammonium Nitrate STD ERR	Autos	Autos STD ERR	Diesel	Diesel STD ERR	No. 2 Fuel Oil	No. 2 Fuel Oil STD ERR	Wood Smoke	Wood Smoke STD ERR
11/2/11	11.0	1.6	0.3	0.6	0.2	0.0	0.0	0.0	0.0	2.4	1.1	6.8	1.3
11/5/11	*	*	*	*	*	*	*	*	*	*	*	*	*
11/8/11	10.3	1.1	0.2	0.3	0.2	0.0	0.0	0.0	0.0	2.2	0.8	6.1	0.9
11/11/11	8.9	0.8	0.1	0.4	0.1	0.0	0.0	0.0	0.0	1.4	0.5	6.3	0.6
11/14/11	24.6	2.3	0.4	0.9	0.3	0.0	0.0	0.0	0.0	5.9	1.7	16.4	1.9
11/17/11	32.8	3.8	0.8	1.2	0.5	0.0	0.0	0.0	0.0	12.9	3.0	12.4	2.0
11/20/11	*	*	*	*	*	*	*	*	*	*	*	*	*
11/23/11	14.8	1.4	0.3	0.6	0.2	0.0	0.0	0.0	0.0	3.7	1.0	6.4	1.2
11/26/11	24.7	2.7	0.5	1.1	0.4	0.0	0.0	0.0	0.0	8.2	2.0	12.5	2.2
11/29/11	27.2	2.8	0.5	0.9	0.4	0.0	0.0	0.0	0.0	8.8	2.1	13.5	2.3
12/2/11	14.7	1.4	0.3	0.9	0.2	0.0	0.0	1.0	0.3	2.2	1.1	8.5	1.2
12/5/11	*	*	*	*	*	*	*	*	*	*	*	*	*
12/8/11	27.2	2.5	0.5	1.2	0.4	0.0	0.0	0.0	0.0	9.8	1.9	13.2	2.1
12/11/11	*	*	*	*	*	*	*	*	*	*	*	*	*
12/14/11	24.7	2.5	0.5	1.1	0.3	4.2	1.6	0.0	0.0	7.5	1.9	10.3	2.1
12/17/11	37.3	3.7	0.7	0.0	0.0	7.9	2.4	0.0	0.0	13.6	2.6	12.2	2.9
12/20/11	13.8	1.4	0.2	0.8	0.2	3.1	0.9	0.0	0.0	0.0	0.0	8.2	0.5
12/23/11	6.3**	**	**	**	**	**	**	**	**	**	**	**	**
12/26/11	23.1	2.2	0.5	1.0	0.4	1.7	0.8	0.0	0.0	8.3	2.1	11.2	2.2
12/29/11	31.8	3.8	0.7	1.1	0.5	0.0	0.0	0.0	0.0	9.0	2.6	20.0	2.9
1/1/12	*	*	*	*	*	*	*	*	*	*	*	*	*
1/4/12	14.3	1.4	0.3	0.8	0.2	0.0	0.0	0.0	0.0	2.9	1.0	9.6	1.1
1/7/12	15.6	2.1	0.4	0.7	0.3	0.0	0.0	0.0	0.0	5.6	1.5	6.4	1.6
1/10/12	24.4	2.7	0.5	0.8	0.4	0.0	0.0	0.0	0.0	6.7	1.9	11.3	2.1
1/13/12	23.2	3.0	0.6	0.6	0.4	0.0	0.0	0.0	0.0	10.1	2.2	8.7	2.4
1/16/12	29.1	3.7	0.8	1.4	0.5	0.0	0.0	5.9	1.0	13.6	2.9	4.8	2.0
1/19/12	40.5	5.2	1.0	2.9	0.7	0.0	0.0	0.0	0.0	15.4	3.6	13.4	4.0
1/22/12	*	*	*	*	*	*	*	*	*	*	*	*	*
1/25/12	9.8	1.2	0.2	0.6	0.2	0.0	0.0	0.8	0.2	2.9	0.9	2.0	1.0
1/28/12	*	*	*	*	*	*	*	*	*	*	*	*	*
1/31/12	*	*	*	*	*	*	*	*	*	*	*	*	*
2/3/12	6.5**	**	**	**	**	**	**	**	**	**	**	**	**
2/6/12	24.8	2.2	0.5	1.6	0.3	0.0	0.0	4.9	0.4	7.7	1.7	4.7	1.9
2/9/12	18.1	1.6	0.3	0.9	0.2	5.4	1.1	0.0	0.0	4.2	1.2	5.2	1.4
2/12/12	18.3	1.4	0.3	1.6	0.2	4.5	0.9	0.0	0.0	4.2	1.1	6.6	1.2
2/15/12	27.0	2.4	0.5	1.5	0.4	0.0	0.0	3.0	0.5	10.4	1.9	6.7	2.1
2/18/12	25.6	2.6	0.5	2.6	0.4	0.0	0.0	0.0	0.0	7.7	2.0	7.7	2.2
2/21/12	13.7	1.9	0.4	1.3	0.3	0.0	0.0	0.9	0.4	5.2	1.6	4.3	1.7
2/24/12	5.0**	**	**	**	**	**	**	**	**	**	**	**	**
2/27/12	4.3**	**	**	**	**	**	**	**	**	**	**	**	**
3/1/12	9.0	1.2	0.2	0.4	0.2	0.0	0.0	0.0	0.0	5.8	0.2	0.0	0.0
3/4/12*	*	*	*	*	*	*	*	*	*	*	*	*	*
3/7/12*	*	*	*	*	*	*	*	*	*	*	*	*	*
3/10/12	9.5	1.6	0.3	1.1	0.2	0.0	0.0	0.0	0.0	2.7	1.2	3.5	1.3

3/13/12	13.9	1.8	0.3	1.0	0.3	0.0	0.0	0.0	0.0	5.6	1.3	2.7	1.4
3/16/12	16.3	2.1	0.3	0.7	0.3	3.8	1.3	0.0	0.0	7.8	0.7	0.0	0.0
3/19/12	10.6	1.7	0.3	0.9	0.2	0.0	0.0	0.0	0.0	4.5	1.3	2.2	1.4
3/22/12	13.3	2.0	0.4	1.0	0.3	0.0	0.0	0.0	0.0	5.6	1.5	2.4	1.6
3/25/12	11.0	1.3	0.2	1.0	0.2	0.0	0.0	0.0	0.0	2.1	1.0	4.8	1.1
3/28/12	8.6	1.0	0.2	0.8	0.2	0.0	0.0	0.0	0.0	2.3	0.8	3.1	0.9
3/31/12	5.4**	**	**	**	**	**	**	**	**	**	**	**	**
Average	20.0	2.2	0.4	1.0	0.3	0.8	0.2	0.5	0.1	6.4	1.5	7.6	1.6

Notes: *No, incomplete, or invalid CMB data set. **Mass was too small to conduct a CMB analysis.

**PM_{2.5} Source Contribution Estimates and Standard Errors ($\mu\text{g}/\text{m}^3$) – EPA Profiles.
North Pole – Winter 2011/2012.**

Date	PM _{2.5} Mass	Sulfate	Sulfate STD ERR	Ammonium Nitrate	Ammonium Nitrate STD ERR	Autos	Autos STD ERR	Diesel	Diesel STD ERR	Wood Smoke	Wood Smoke STD ERR
11/2/11	***	***	***	***	***	***	***	***	***	***	***
11/5/11	8.8	0.5	0.1	0.2	0.1	0.0	0.0	0.0	0.0	7.7	1.3
11/8/11	9.2	0.6	0.1	0.3	0.1	0.0	0.0	0.0	0.0	7.7	0.9
11/11/11	12.3	0.5	0.1	0.3	0.1	0.0	0.0	0.0	0.0	12.4	1.2
11/14/11	30.5	1.4	0.2	0.6	0.2	0.0	0.0	0.0	0.0	27.5	4.1
11/17/11	23.2	1.8	0.2	0.7	0.2	0.0	0.0	0.0	0.0	21.7	2.5
11/20/11	82.6	7.7	0.9	2.0	1.0	0.0	0.0	0.0	0.0	63.9	7.1
11/23/11	12.6	0.6	0.1	0.4	0.1	0.0	0.0	0.0	0.0	10.4	1.0
11/26/11	22.4	1.5	0.2	0.7	0.2	0.0	0.0	0.0	0.0	19.2	2.2
11/29/11	30.4	2.6	0.3	0.9	0.3	0.0	0.0	0.0	0.0	28.5	5.7
12/2/11	10.5	0.9	0.1	0.4	0.1	0.0	0.0	0.0	0.0	8.6	1.1
12/5/11	2.5**	**	**	**	**	**	**	**	**	**	**
12/8/11	42.0	2.8	0.3	1.0	0.4	0.0	0.0	0.0	0.0	38.1	3.3
12/11/11	7.9	0.4	0.0	0.1	0.1	0.0	0.0	0.0	0.0	7.0	1.3
12/14/11	16.1	1.1	0.1	0.4	0.1	0.0	0.0	0.0	0.0	14.6	3.0
12/17/11	36.4	2.8	0.3	0.8	0.3	0.0	0.0	0.0	0.0	32.2	2.1
12/20/11	12.5	0.8	0.1	0.3	0.1	0.0	0.0	0.0	0.0	11.6	1.3
12/23/11	5.6**	**	**	**	**	**	**	**	**	**	**
12/26/11	38.3	1.9	0.2	1.0	0.2	0.0	0.0	0.0	0.0	33.3	2.3
12/29/11	34.1	2.6	0.3	1.0	0.3	0.0	0.0	0.0	0.0	31.8	2.9
1/1/12	33.5	2.8	0.4	0.8	0.4	0.0	0.0	0.0	0.0	31.5	2.3
1/4/12	11.6	0.9	0.1	0.7	0.1	0.0	0.0	0.0	0.0	9.5	1.0
1/7/12	10.0	0.9	0.1	0.4	0.1	0.0	0.0	0.0	0.0	8.2	0.9
1/10/12	16.5	1.3	0.2	0.5	0.2	0.0	0.0	0.0	0.0	14.7	3.0
1/13/12	17.8	2.1	0.2	0.6	0.3	4.5	2.2	0.0	0.0	11.2	1.7
1/16/12	43.0	2.6	0.3	1.2	0.4	0.0	0.0	0.0	0.0	39.8	5.9
1/19/12	39.5	3.0	0.3	1.8	0.4	0.0	0.0	5.2	1.3	28.2	3.5
1/22/12	***	***	***	***	***	***	***	***	***	***	***
1/25/12	***	***	***	***	***	***	***	***	***	***	***
1/28/12	64.9	4.7	0.5	1.5	0.6	0.0	0.0	0.0	0.0	48.5	3.1
1/31/12	14.5	2.1	0.2	1.0	0.3	0.0	0.0	0.0	0.0	12.3	1.2
2/3/12	***	***	***	***	***	***	***	***	***	***	***
2/6/12	42.8	3.0	0.3	1.6	0.4	0.0	0.0	0.0	0.0	32.9	2.3
2/9/12	***	***	***	***	***	***	***	***	***	***	***
2/12/12	***	***	***	***	***	***	***	***	***	***	***
2/15/12	9.0	0.7	0.1	0.3	0.1	0.0	0.0	0.0	0.0	8.3	1.1
2/18/12	29.2	2.1	0.2	1.1	0.3	0.0	0.0	0.0	0.0	25.4	3.8
2/21/12	13.2	0.6	0.1	0.3	0.1	0.0	0.0	0.0	0.0	12.5	2.0
2/24/12	3.5**	**	**	**	**	**	**	**	**	**	**
2/27/12	2.1**	**	**	**	**	**	**	**	**	**	**
3/1/12	5.1**	**	**	**	**	**	**	**	**	**	**
3/4/12	26.0	2.1	0.2	0.8	0.3	5.2	2.3	0.0	0.0	18.8	2.5
3/7/12	4.1**	**	**	**	**	**	**	**	**	**	**
3/10/12	11.1	1.4	0.2	0.6	0.2	0.0	0.0	0.0	0.0	8.6	1.1

3/13/12	4.3**	**	**	**	**	**	**	**	**	**	**
3/16/12	5.5**	**	**	**	**	**	**	**	**	**	**
3/19/12	18.3	1.9	0.2	0.8	0.2	0.0	0.0	0.0	0.0	14.7	1.8
3/22/12	8.3	1.4	0.2	0.5	0.2	0.0	0.0	0.0	0.0	6.8	0.9
3/25/12	6.5	0.8	0.1	0.4	0.1	0.0	0.0	0.0	0.0	4.9	0.7
Average	24.2	1.8	0.2	0.7	0.2	0.3	0.1	0.1	0.04	20.4	2.3

Notes: *No, incomplete, or invalid CMB data set. **Mass was too small to conduct a CMB analysis. ***Couldn't get a good statistical fit during CMB modeling.

**PM_{2.5} Source Contribution Estimates and Standard Errors ($\mu\text{g}/\text{m}^3$) – OMNI Profiles.
North Pole – Winter 2011/2012.**

Date	PM _{2.5} Mass	Sulfate	Sulfate STD ERR	Ammonium Nitrate	Ammonium Nitrate STD ERR	Autos	Autos STD ERR	No. 2 Fuel Oil	No. 2 Fuel Oil STD ERR	Wood Smoke	Wood Smoke STD ERR
11/2/11	***	***	***	***	***	***	***	***	***	***	***
11/5/11	8.8	0.4	0.1	0.2	0.1	2.2	0.9	0.0	0.0	4.4	1.1
11/8/11	9.2	0.4	0.1	0.2	0.1	0.0	0.0	0.6	0.3	8.1	0.9
11/11/11	12.3	0.4	0.1	0.2	0.1	0.0	0.0	0.0	0.0	10.5	1.0
11/14/11	30.5	0.7	0.1	0.5	0.1	0.0	0.0	2.0	0.5	26.3	1.9
11/17/11	23.2	1.4	0.2	0.4	0.2	0.0	0.0	2.4	1.0	18.0	1.5
11/20/11	82.6	3.9	0.7	0.0	0.0	0.0	0.0	16.0	2.7	69.5	5.8
11/23/11	12.6	0.4	0.1	0.3	0.1	0.0	0.0	0.8	0.3	7.8	0.9
11/26/11	22.4	1.1	0.2	0.5	0.2	0.0	0.0	2.3	0.8	16.6	1.3
11/29/11	30.4	1.9	0.3	0.5	0.3	0.0	0.0	4.0	1.4	19.6	1.7
12/2/11	10.5	0.9	0.1	0.4	0.1	0.0	0.0	0.0	0.0	8.6	0.7
12/5/11	2.5**	**	**	**	**	**	**	**	**	**	**
12/8/11	42.0	1.5	0.3	0.8	0.2	0.0	0.0	4.5	1.1	36.6	2.7
12/11/11	7.9	0.3	0.0	0.1	0.0	0.0	0.0	0.0	0.0	7.2	0.9
12/14/11	16.1	0.7	0.1	0.3	0.1	0.0	0.0	1.4	0.5	14.0	1.3
12/17/11	36.4	1.8	0.3	0.5	0.2	0.0	0.0	4.0	1.3	28.9	2.5
12/20/11	12.5	0.7	0.1	0.3	0.1	2.7	1.2	0.0	0.0	8.8	1.6
12/23/11	5.6**	**	**	**	**	**	**	**	**	**	**
12/26/11	38.3	1.1	0.2	0.8	0.2	0.0	0.0	2.5	0.9	24.7	2.1
12/29/11	34.1	1.2	0.2	0.6	0.2	3.7	1.7	5.7	0.9	22.8	2.9
1/1/12	33.5	4.1	0.5	0.0	0.0	0.0	0.0	0.0	0.0	25.4	1.9
1/4/12	11.6	0.7	0.1	0.7	0.1	0.0	0.0	0.0	0.0	10.6	0.9
1/7/12	10.0	0.5	0.1	0.3	0.1	0.0	0.0	1.1	0.4	8.1	0.8
1/10/12	16.5	1.1	0.1	0.4	0.1	0.0	0.0	0.0	0.0	17.8	1.3
1/13/12	17.8	1.5	0.3	0.0	0.0	0.0	0.0	3.5	1.0	10.5	1.2
1/16/12	43.0	1.4	0.3	0.9	0.2	0.0	0.0	4.1	1.0	37.0	2.7
1/19/12	39.5	2.0	0.4	1.3	0.3	0.0	0.0	5.2	1.5	27.6	2.0
1/22/12	***	***	***	***	***	***	***	***	***	***	***
1/25/12	***	***	***	***	***	***	***	***	***	***	***
1/28/12	***	***	***	***	***	***	***	***	***	***	***
1/31/12	14.5	1.5	0.3	0.8	0.2	0.0	0.0	3.2	1.1	11.1	1.2
2/3/12	***	***	***	***	***	***	***	***	***	***	***
2/6/12	42.8	2.1	0.4	1.3	0.3	10.2	2.8	3.7	1.5	17.0	2.5
2/9/12	***	***	***	***	***	***	***	***	***	***	***
2/12/12	***	***	***	***	***	***	***	***	***	***	***
2/15/12	9.0	0.5	0.1	0.3	0.1	0.0	0.0	0.0	0.0	8.3	0.7
2/18/12	29.2	1.4	0.2	1.0	0.2	0.0	0.0	2.4	1.0	22.2	1.9
2/21/12	13.2	0.4	0.1	0.3	0.1	0.0	0.0	0.0	0.0	12.6	1.1
2/24/12	3.5**	**	**	**	**	**	**	**	**	**	**
2/27/12	2.1**	**	**	**	**	**	**	**	**	**	**
3/1/12	5.1**	**	**	**	**	**	**	**	**	**	**
3/4/12	26.0	1.6	0.3	0.5	0.2	0.0	0.0	2.9	1.1	18.2	1.5
3/7/12	4.1**	**	**	**	**	**	**	**	**	**	**
3/10/12	11.1	0.9	0.2	0.5	0.1	0.0	0.0	2.0	0.7	7.4	0.9
3/13/12	4.3**	**	**	**	**	**	**	**	**	**	**

3/16/12	5.5**	**	**	**	**	**	**	**	**	**	**
3/19/12	18.3	1.3	0.2	0.5	0.2	0.0	0.0	3.5	0.9	12.0	1.2
3/22/12	8.3	0.8	0.1	0.4	0.1	0.0	0.0	2.5	0.6	5.0	1.1
3/25/12	6.5	0.8	0.1	0.4	0.1	0.0	0.0	0.0	0.0	4.7	0.6
Average	23.0	1.2	0.2	0.5	0.1	0.6	0.2	2.4	0.7	17.3	1.6

Notes: *No, incomplete, or invalid CMB data set. **Mass was too small to conduct a CMB analysis. ***Couldn't get a good statistical fit during CMB modeling.

**PM_{2.5} Source Contribution Estimates and Standard Errors (µg/m³) – EPA Profiles.
RAMS – Winter 2011/2012.**

Date	PM _{2.5} Mass	Sulfate	Sulfate STD ERR	Ammonium Nitrate	Ammonium Nitrate STD ERR	Autos	Autos STD ERR	Diesel	Diesel STD ERR	Wood Smoke	Wood Smoke STD ERR
12/20/11	21.8	1.5	0.2	0.9	0.2	0.0	0.0	0.0	0.0	15.6	1.4
12/23/11	13.7	1.0	0.1	0.4	0.1	0.0	0.0	0.0	0.0	8.8	1.1
12/26/11	45.0	4.0	0.4	1.6	0.5	0.0	0.0	0.0	0.0	29.4	2.3
12/29/11	24.6	3.9	0.4	1.4	0.5	0.0	0.0	0.0	0.0	18.9	2.3
1/1/12	21.3	3.5	0.4	1.4	0.4	6.7	2.8	0.0	0.0	11.1	1.8
1/4/12	15.1	2.0	0.2	1.0	0.3	0.0	0.0	1.9	0.9	9.9	1.4
1/7/12	23.4	2.7	0.3	1.0	0.3	0.0	0.0	0.0	0.0	18.1	1.7
1/10/12	16.2	2.8	0.3	0.8	0.4	0.0	0.0	0.0	0.0	15.6	1.4
1/13/12	***	***	***	***	***	***	***	***	***	***	***
1/16/12	13.5	1.7	0.2	1.5	0.2	0.0	0.0	0.0	0.0	16.1	1.4
1/19/12	3.1**	**	**	**	**	**	**	**	**	**	**
1/22/12	0.8**	**	**	**	**	**	**	**	**	**	**
1/25/12	0.7**	**	**	**	**	**	**	**	**	**	**
1/28/12	2.8**	**	**	**	**	**	**	**	**	**	**
1/31/12	23.5	3.6	0.4	1.2	0.5	0.0	0.0	0.0	0.0	19.8	1.7
2/3/12	5.6**	**	**	**	**	**	**	**	**	**	**
2/6/12	24.8	4.1	0.5	1.9	0.5	0.0	0.0	0.0	0.0	18.0	4.6
2/9/12	19.4	2.3	0.3	1.2	0.3	0.0	0.0	4.3	1.1	11.0	1.6
2/12/12	18.1	2.1	0.2	1.7	0.3	0.0	0.0	3.7	1.0	9.3	1.4
2/15/12	30.8	4.4	0.5	2.1	0.6	0.0	0.0	6.9	1.5	14.5	2.1
2/18/12	25.9	3.8	0.4	2.9	0.5	7.0	3.0	0.0	0.0	13.3	2.0
2/21/12	17.0	2.4	0.3	1.2	0.3	0.0	0.0	2.9	1.0	9.6	1.4
2/24/12	5.9**	**	**	**	**	**	**	**	**	**	**
2/27/12	3.5*	**	**	**	**	**	**	**	**	**	**
Average	22.1	2.9	0.3	1.4	0.4	0.9	0.4	1.2	0.3	14.9	1.8

Notes: *No, incomplete, or invalid CMB data set. **Mass was too small to conduct a CMB analysis. ***Couldn't get a good statistical fit during CMB modeling.

**PM_{2.5} Source Contribution Estimates and Standard Errors (µg/m³) – OMNI Profiles.
RAMS – Winter 2011/2012.**

Date	PM _{2.5} Mass	Sulfate	Sulfate STD ERR	Ammonium Nitrate	Ammonium Nitrate STD ERR	Autos	Autos STD ERR	Diesel	Diesel STD ERR	No. 2 Fuel Oil	No. 2 Fuel Oil STD ERR	Wood Smoke	Wood Smoke STD ERR
12/20/11	21.8	1.3	0.2	0.9	0.2	0.0	0.0	0.0	0.0	0.0	0.0	12.1	1.1
12/23/11	13.7	0.9	0.1	0.4	0.1	0.0	0.0	0.0	0.0	0.0	0.0	6.8	0.8
12/26/11	45.0	2.3	0.4	0.9	0.3	0.0	0.0	0.0	0.0	8.5	1.7	14.3	2.4
12/29/11	24.6	2.5	0.5	0.8	0.3	0.0	0.0	0.0	0.0	7.7	1.9	13.3	1.8
1/1/12	21.3	2.5	0.4	1.1	0.3	0.0	0.0	0.0	0.0	4.3	1.8	11.5	1.7
1/4/12	15.1	1.3	0.2	0.8	0.2	0.0	0.0	0.0	0.0	3.5	1.0	8.9	1.1
1/7/12	23.4	1.7	0.3	0.6	0.2	0.0	0.0	0.0	0.0	5.5	1.2	11.8	1.9
1/10/12	16.2	1.8	0.3	0.7	0.2	0.0	0.0	4.4	1.2	5.7	1.3	3.5	0.6
1/13/12	***	***	***	***	***	***	***	***	***	***	***	***	***
1/16/12	***	***	***	***	***	***	***	***	***	***	***	***	***
1/19/12	3.1**	**	**	**	**	**	**	**	**	**	**	**	**
1/22/12	0.8**	**	**	**	**	**	**	**	**	**	**	**	**
1/25/12	0.7**	**	**	**	**	**	**	**	**	**	**	**	**
1/28/12	2.8**	**	**	**	**	**	**	**	**	**	**	**	**
1/31/12	23.5	2.3	0.4	1.0	0.3	0.0	0.0	0.0	0.0	6.9	1.7	17.0	1.8
2/3/12	5.6**	**	**	**	**	**	**	**	**	**	**	**	**
2/6/12	24.8	2.8	0.5	1.4	0.4	5.2	2.4	0.0	0.0	6.2	2.1	10.4	3.6
2/9/12	19.4	1.6	0.3	1.0	0.2	0.0	0.0	0.0	0.0	2.8	1.2	12.6	1.3
2/12/12	18.1	0.9	0.4	1.4	0.4	3.0	1.1	0.0	0.0	4.4	2.0	9.3	2.3
2/15/12	30.8	2.3	0.7	1.5	0.8	5.2	1.8	0.0	0.0	7.8	3.8	14.9	4.4
2/18/12	25.9	2.3	0.4	2.3	0.4	0.0	0.0	0.0	0.0	7.2	1.6	16.9	2.4
2/21/12	17.0	1.7	0.3	1.0	0.2	0.0	0.0	0.0	0.0	3.1	1.2	10.0	1.2
2/24/12	5.9**	**	**	**	**	**	**	**	**	**	**	**	**
2/27/12	3.5**	**	**	**	**	**	**	**	**	**	**	**	**
Average	22.1	1.9	0.4	1.0	0.3	0.9	0.4	0.3	0.1	4.9	1.5	11.5	1.9

Notes: *No, incomplete, or invalid CMB data set. **Mass was too small to conduct a CMB analysis. ***Couldn't get a good statistical fit during CMB modeling.

**PM_{2.5} Source Contribution Estimates and Standard Errors ($\mu\text{g}/\text{m}^3$) – EPA Profiles.
NCORE – Winter 2011/2012.**

Date	PM _{2.5} Mass	Sulfate	Sulfate STD ERR	Ammonium Nitrate	Ammonium Nitrate STD ERR	Autos	Autos STD ERR	Diesel	Diesel STD ERR	Wood Smoke	Wood Smoke STD ERR
11/2/11	12.8	2.2	0.2	0.8	0.3	0.0	0.0	0.0	0.0	9.5	1.0
11/5/11	7.5	1.0	0.1	0.4	0.1	0.0	0.0	0.0	0.0	6.4	1.5
11/8/11	12.7	1.6	0.2	0.6	0.2	0.0	0.0	0.0	0.0	10.3	1.0
11/11/11	14.0	1.2	0.1	0.6	0.2	0.0	0.0	0.0	0.0	13.6	1.3
11/14/11	17.8	2.7	0.3	1.1	0.3	0.0	0.0	3.2	1.1	11.0	1.6
11/17/11	38.1	5.2	0.6	1.9	0.7	0.0	0.0	0.0	0.0	30.8	2.2
11/20/11	30.4	5.8	0.6	1.7	0.7	0.0	0.0	4.0	1.8	18.4	2.5
11/23/11	12.6	2.3	0.3	0.9	0.3	0.0	0.0	0.0	0.0	9.7	1.0
11/26/11	31.9	3.7	0.4	1.5	0.5	0.0	0.0	0.0	0.0	25.6	1.8
11/29/11	22.3	3.9	0.4	1.4	0.5	0.0	0.0	1.8	0.9	15.4	2.0
12/2/11	12.8	1.7	0.2	0.9	0.2	0.0	0.0	1.5	0.6	8.9	1.2
12/5/11	5.1**	**	**	**	**	**	**	**	**	**	**
12/8/11	27.4	3.6	0.4	1.5	0.5	9.9	3.0	0.0	0.0	12.6	1.9
12/11/11	9.0	1.2	0.1	0.5	0.3	0.0	0.0	1.8	0.6	5.8	0.9
12/14/11	28.3	4.1	0.5	1.6	0.5	9.7	3.2	0.0	0.0	12.9	2.0
12/17/11	29.7	5.4	0.6	1.4	0.7	0.0	0.0	6.5	1.7	15.9	2.3
12/20/11	10.8	1.5	0.2	0.9	0.2	0.0	0.0	2.0	0.9	6.2	1.0
12/23/11	5.6**	**	**	**	**	**	**	**	**	**	**
12/26/11	24.9	4.0	0.4	1.6	0.5	9.5	3.1	0.0	0.0	12.0	1.9
12/29/11	23.6	4.1	0.5	1.5	0.6	0.0	0.0	1.9	0.9	16.4	2.2
1/1/12	28.0	3.3	0.4	1.4	0.4	0.0	0.0	0.0	0.0	23.5	2.1
1/4/12	33.6	0.8	0.2	1.1	0.1	0.0	0.0	0.0	0.0	24.0	1.8
1/7/12	14.6	2.8	0.3	1.0	0.4	0.0	0.0	0.0	0.0	11.0	1.1
1/10/12	19.6	3.8	0.4	1.1	0.5	0.0	0.0	0.0	0.0	15.3	1.4
1/13/12	19.0	4.3	0.5	1.1	0.5	0.0	0.0	0.0	0.0	13.2	1.5
1/16/12	26.4	4.9	0.6	2.0	0.6	0.0	0.0	4.9	1.6	14.4	2.1
1/19/12	38.0	6.5	0.7	3.6	0.8	0.0	0.0	6.7	2.0	19.2	2.7
1/22/12	3.3**	**	**	**	**	**	**	**	**	**	**
1/25/12	9.0	1.6	0.2	0.6	0.2	0.0	0.0	0.0	0.0	7.1	1.6
1/28/12	28.1	5.7	0.6	1.5	0.7	0.0	0.0	0.0	0.0	20.2	3.3
1/31/12	20.1	3.8	0.4	1.7	0.7	0.0	0.0	3.5	1.1	11.1	1.6
2/3/12	6.7	1.1	0.1	0.5	0.1	0.0	0.0	0.0	0.0	5.0	1.2
2/6/12	24.7	3.9	0.4	2.0	0.5	0.0	0.0	0.0	0.0	9.0	1.5
2/9/12	24.0	2.4	0.3	1.3	0.3	0.0	0.0	0.0	0.0	14.4	1.4
2/12/12	17.0	2.2	0.3	1.7	0.5	0.0	0.0	2.8	0.8	10.9	1.6
2/15/12	30.7	4.5	0.5	2.2	0.6	0.0	0.0	9.4	1.6	12.7	2.0
2/18/12	26.9	3.9	0.4	3.0	0.5	6.5	3.0	0.0	0.0	13.3	2.0
2/21/12	16.2	2.4	0.3	1.3	0.3	0.0	0.0	1.9	0.7	10.8	1.4
2/24/12	5.7**	**	**	**	**	**	**	**	**	**	**
2/27/12	3.6**	**	**	**	**	**	**	**	**	**	**
3/1/12	13.9	2.5	0.3	0.9	0.3	0.0	0.0	1.9	0.7	8.5	1.2
3/4/12	13.1	2.4	0.3	0.9	0.3	0.0	0.0	2.2	0.7	7.1	1.1
3/7/12	6.4	1.0	0.1	0.8	0.1	0.0	0.0	1.3	0.6	3.3	0.6
3/10/12	9.8	2.0	0.2	1.0	0.3	0.0	0.0	0.0	0.0	6.8	0.9

3/13/12	15.8	3.0	0.3	1.3	0.4	0.0	0.0	0.0	0.0	13.1	1.7
3/16/12	17.1	3.2	0.4	1.3	0.4	0.0	0.0	3.9	1.2	8.2	1.3
3/19/12	12.1	2.4	0.3	1.2	0.3	0.0	0.0	0.0	0.0	8.2	1.0
3/22/12	13.3	2.8	0.3	1.3	0.4	0.0	0.0	2.3	1.0	6.5	1.1
3/25/12	***	***	***	***	***	***	***	***	***	***	***
3/28/12	9.2	1.5	0.2	1.2	0.2	0.0	0.0	0.0	0.0	8.0	1.1
3/31/12	5.6**	**	**	**	**	**	**	**	**	**	**
Average	19.5	3.0	0.3	1.3	0.4	0.8	0.3	1.4	0.5	12.4	1.6

Notes: *No, incomplete, or invalid CMB data set. **Mass was too small to conduct a CMB analysis. ***Couldn't get a good statistical fit during CMB modeling.

**PM_{2.5} Source Contribution Estimates and Standard Errors (µg/m³) – OMNI Profiles.
NCORE – Winter 2011/2012.**

Date	PM _{2.5} Mass	Sulfate	Sulfate STD ERR	Ammonium Nitrate	Ammonium Nitrate STD ERR	Autos	Autos STD ERR	Diesel	Diesel STD ERR	No. 2 Fuel Oil	No. 2 Fuel Oil STD ERR	Wood Smoke	Wood Smoke STD ERR
11/2/11	12.8	1.5	0.3	0.6	0.2	0.0	0.0	0.0	0.0	3.0	1.1	7.6	1.5
11/5/11	7.5	0.9	0.1	0.4	0.1	0.0	0.0	0.0	0.0	0.0	0.0	6.9	0.8
11/8/11	12.7	1.1	0.2	0.4	0.1	0.0	0.0	0.0	0.0	2.4	0.8	8.3	1.3
11/11/11	14.0	1.1	0.1	0.5	0.1	0.0	0.0	0.0	0.0	0.0	0.0	11.1	1.1
11/14/11	17.8	1.8	0.3	0.7	0.2	0.0	0.0	0.0	0.0	4.5	1.3	10.4	1.3
11/17/11	38.1	2.9	0.5	1.1	0.4	0.0	0.0	0.0	0.0	11.9	2.1	21.0	3.2
11/20/11	30.4	3.1	0.6	0.8	0.4	0.0	0.0	0.0	0.0	13.8	2.4	11.7	2.1
11/23/11	12.6	1.6	0.3	0.6	0.2	0.0	0.0	0.0	0.0	3.8	1.2	7.6	1.1
11/26/11	31.9	2.1	0.4	0.9	0.3	0.0	0.0	0.0	0.0	8.0	1.5	18.9	2.3
11/29/11	22.3	2.7	0.5	0.8	0.4	0.0	0.0	0.0	0.0	7.5	2.0	11.4	1.8
12/2/11	12.8	1.7	0.2	0.9	0.2	0.0	0.0	0.0	0.0	0.0	0.0	10.3	0.9
12/5/11	5.1**	**	**	**	**	**	**	**	**	**	**	**	**
12/8/11	27.4	2.3	0.4	1.0	0.3	5.3	2.2	0.0	0.0	6.1	1.7	12.9	3.4
12/11/11	9.0	1.1	0.1	0.5	0.1	0.0	0.0	1.3	0.6	0.0	0.0	6.2	0.7
12/14/11	28.3	2.7	0.5	1.0	0.4	4.8	2.4	0.0	0.0	6.8	2.0	13.4	3.7
12/17/11	29.7	3.5	0.6	0.0	0.0	6.8	3.3	0.0	0.0	10.5	2.4	7.9	3.1
12/20/11	10.8	1.4	0.2	0.9	0.2	0.0	0.0	0.0	0.0	0.0	0.0	7.9	0.7
12/23/11	5.6**	**	**	**	**	**	**	**	**	**	**	**	**
12/26/11	24.9	2.2	0.4	0.9	0.3	0.0	0.0	0.0	0.0	9.2	1.6	14.5	2.4
12/29/11	23.6	2.3	0.4	0.9	0.3	0.0	0.0	0.0	0.0	9.2	1.7	11.8	1.7
1/1/12	28.0	2.6	0.4	1.1	0.4	0.0	0.0	0.0	0.0	3.9	1.8	19.5	2.6
1/4/12	33.6	1.2	0.2	0.8	0.2	0.0	0.0	0.0	0.0	3.3	0.9	15.3	1.8
1/7/12	14.6	1.8	0.3	0.6	0.2	0.0	0.0	0.0	0.0	5.5	1.4	7.9	1.3
1/10/12	19.6	2.4	0.4	0.7	0.3	0.0	0.0	2.5	0.9	6.2	1.8	9.9	1.6
1/13/12	19.0	2.6	0.4	0.0	0.0	0.0	0.0	0.0	0.0	8.7	1.8	6.5	1.6
1/16/12	26.4	3.0	0.5	1.3	0.4	0.0	0.0	0.0	0.0	9.7	2.2	11.7	2.0
1/19/12	38.0	3.7	0.7	2.6	0.5	0.0	0.0	0.0	0.0	14.7	2.8	14.4	2.5
1/22/12	3.3**	**	**	**	**	**	**	**	**	**	**	**	**
1/25/12	9.0	1.2	0.2	0.5	0.2	0.0	0.0	0.0	0.0	1.9	0.9	6.1	1.3
1/28/12	28.1	3.6	0.6	0.8	0.5	0.0	0.0	0.0	0.0	11.0	2.6	8.4	3.2
1/31/12	20.1	2.4	0.4	1.1	0.3	0.0	0.0	0.0	0.0	7.4	1.8	9.4	1.6
2/3/12	6.7	1.0	0.1	0.5	0.1	0.0	0.0	0.0	0.0	0.0	0.0	5.3	0.8
2/6/12	***	***	***	***	***	***	***	***	***	***	***	***	***
2/9/12	***	***	***	***	***	***	***	***	***	***	***	***	***
2/12/12	17.0	1.6	0.3	1.5	0.2	0.0	0.0	0.0	0.0	2.6	1.2	12.4	1.3
2/15/12	30.7	2.8	0.7	1.6	0.7	0.0	0.0	4.8	1.1	7.7	3.8	14.8	4.3
2/18/12	26.9	2.4	0.4	2.4	0.4	0.0	0.0	0.0	0.0	7.0	1.8	17.5	2.6
2/21/12	16.2	1.7	0.3	1.1	0.2	0.0	0.0	0.0	0.0	3.5	1.3	10.0	1.3
2/24/12	5.7**	**	**	**	**	**	**	**	**	**	**	**	**
2/27/12	3.6**	**	**	**	**	**	**	**	**	**	**	**	**
3/1/12	13.9	1.6	0.3	0.5	0.2	0.0	0.0	0.0	0.0	5.2	1.2	6.5	1.2
3/4/12	13.1	1.8	0.3	0.7	0.3	0.0	0.0	0.0	0.0	3.5	1.3	6.5	1.2
3/7/12	6.4	1.1	0.1	0.8	0.1	0.0	0.0	0.0	0.0	0.0	0.0	4.3	0.6
3/10/12	9.8	1.4	0.2	0.8	0.2	0.0	0.0	0.0	0.0	3.2	1.0	4.3	1.0

3/13/12	15.8	2.0	0.4	0.9	0.3	0.0	0.0	0.0	0.0	5.8	1.5	9.5	1.5
3/16/12	17.1	2.0	0.4	0.8	0.3	0.0	0.0	0.0	0.0	6.0	1.5	7.3	1.4
3/19/12	12.1	1.5	0.3	0.9	0.2	0.0	0.0	0.0	0.0	4.4	1.1	4.8	1.1
3/22/12	13.3	1.7	0.3	0.9	0.2	0.0	0.0	0.0	0.0	5.4	1.3	4.6	1.2
3/25/12	***	***	***	***	***	***	***	***	***	***	***	***	***
3/28/12	9.2	1.1	0.2	1.0	0.2	0.0	0.0	0.0	0.0	2.1	0.9	6.5	0.9
3/31/12	5.6**	**	**	**	**	**	**	**	**	**	**	**	**
Average	19.3	2.0	0.4	0.9	0.3	0.4	0.2	0.2	0.1	5.4	1.4	10.1	1.7

Notes: *No, incomplete, or invalid CMB data set. **Mass was too small to conduct a CMB analysis. ***Couldn't get a good statistical fit during CMB modeling.

**PM_{2.5} Source Contribution Estimates and Standard Errors (µg/m³) – EPA Profiles.
NPF3 – Winter 2011/2012.**

Date	PM _{2.5} Mass	Sulfate	Sulfate STD ERR	Ammonium Nitrate	Ammonium Nitrate STD ERR	Autos	Autos STD ERR	Diesel	Diesel STD ERR	Wood Smoke	Wood Smoke STD ERR
3/1/12	4.5**	**	**	**	**	**	**	**	**	**	**
3/4/12	37.4	2.7	0.3	1.1	0.3	0.0	0.0	3.3	1.2	29.7	3.7
3/7/12	6.1	0.7	0.1	0.3	0.1	0.0	0.0	1.8	0.7	3.5	0.7
3/10/12	20.5	1.9	0.2	0.8	0.2	0.0	0.0	0.0	0.0	16.9	2.0
3/13/12	5.1**	**	**	**	**	**	**	**	**	**	**
3/16/12	7.5	1.1	0.1	0.5	0.1	0.0	0.0	0.0	0.0	5.9	0.9
3/19/12	27.8	2.5	0.3	0.9	0.3	5.4	2.5	0.0	0.0	18.3	2.4
3/22/12	15.2	1.9	0.2	0.7	0.3	0.0	0.0	1.3	0.6	12.5	1.7
3/25/12	13.6	1.1	0.1	0.6	0.1	0.0	0.0	0.0	0.0	12.7	2.6
3/28/12	5.2**	**	**	**	**	**	**	**	**	**	**
3/31/12	4.8**	**	**	**	**	**	**	**	**	**	**
Average	18.3	1.7	0.2	0.7	0.2	0.8	0.4	0.9	0.4	14.2	2.0

Notes: *No, incomplete, or invalid CMB data set. **Mass was too small to conduct a CMB analysis.

**PM_{2.5} Source Contribution Estimates and Standard Errors (µg/m³) – OMNI Profiles.
NPF3 – Winter 2011/2012.**

Date	PM _{2.5} Mass	Sulfate	Sulfate STD ERR	Ammonium Nitrate	Ammonium Nitrate STD ERR	No. 2 Fuel Oil	No. 2 Fuel Oil STD ERR	Wood Smoke	Wood Smoke STD ERR
3/1/12	4.5**	**	**	**	**	**	**	**	**
3/4/12	37.4	2.0	0.3	0.6	0.3	3.9	1.4	27.8	2.0
3/7/12	6.1	0.6	0.1	0.3	0.1	0.0	0.0	4.8	0.6
3/10/12	20.5	1.5	0.3	0.5	0.2	2.2	1.1	14.8	1.3
3/13/12	5.1**	**	**	**	**	**	**	**	**
3/16/12	7.5	0.8	0.1	0.4	0.1	1.5	0.6	4.9	1.0
3/19/12	27.8	1.4	0.2	0.6	0.2	4.3	1.0	25.4	2.2
3/22/12	15.2	1.1	0.2	0.5	0.2	3.5	0.8	11.0	1.1
3/25/12	13.6	1.1	0.1	0.6	0.1	0.0	0.0	10.0	0.8
3/28/12	5.2**	**	**	**	**	**	**	**	**
3/31/12	4.8**	**	**	**	**	**	**	**	**
Average	18.3	1.2	0.2	0.5	0.2	2.2	0.7	14.1	1.3

Notes: *No, incomplete, or invalid CMB data set. **Mass was too small to conduct a CMB analysis.

**PM_{2.5} Source Contribution Estimates and Standard Errors (µg/m³) – EPA Profiles.
State Building – Summer 2012.**

Date	PM _{2.5} Mass	Sulfate	Sulfate STD ERR	Ammonium Nitrate	Ammonium Nitrate STD ERR	Autos	Autos STD ERR	Diesel	Diesel STD ERR	Street Sand	Street Sand STD ERR	Wood Smoke	Wood Smoke STD ERR
6/2/12	***	***	***	***	***	***	***	***	***	***	***	***	***
6/5/12	4.8	0.5	0.1	0.4	0.1	1.5	0.3	0.0	0.0	0.5	0.2	1.6	0.2
6/8/12	6.0	0.5	0.1	0.1	0.1	0.0	0.0	0.0	0.0	0.0	0.0	5.4	0.3
6/11/12	5.9	0.5	0.1	0.3	0.1	0.0	0.0	0.0	0.0	0.6	0.2	4.5	0.1
6/14/12	4.6	0.4	0.0	0.2	0.0	0.5	0.2	0.0	0.0	0.0	0.0	2.5	0.2
6/17/12	3.8	0.2	0.0	0.1	0.0	0.0	0.0	0.0	0.0	0.3	0.1	2.8	0.1
6/20/12	8.6	0.4	0.1	0.2	0.1	0.0	0.0	0.0	0.0	0.9	0.2	6.0	0.1
6/23/12	6.4	0.4	0.1	0.3	0.1	0.0	0.0	0.0	0.0	0.6	0.2	5.1	0.3
6/26/12	3.2	0.2	0.0	0.1	0.0	0.0	0.0	0.0	0.0	0.0	0.0	2.6	0.1
6/29/12	3.7	0.4	0.0	0.2	0.0	0.0	0.0	0.0	0.0	0.0	0.0	3.0	0.1
7/2/12	***	***	***	***	***	***	***	***	***	***	***	***	***
7/5/12	4.3	0.3	0.0	0.2	0.0	0.0	0.0	0.0	0.0	0.0	0.0	2.2	0.1
7/8/12	***	***	***	***	***	***	***	***	***	***	***	***	***
7/11/12	3.7	0.3	0.0	0.3	0.0	0.0	0.0	0.0	0.0	0.0	0.0	2.6	0.1
7/14/12	***	***	***	***	***	***	***	***	***	***	***	***	***
7/17/12	*	*	*	*	*	*	*	*	*	*	*	*	*
7/20/12	3.6	0.6	0.1	0.0	0.0	0.0	0.0	0.0	0.0	0.0	0.0	3.0	0.2
7/23/12	***	***	***	***	***	***	***	***	***	***	***	***	***
7/26/12	8.1	0.8	0.1	0.2	0.1	0.0	0.0	0.0	0.0	0.0	0.0	5.3	0.2
7/29/12	3.9	0.4	0.1	0.2	0.1	0.0	0.0	0.0	0.0	0.0	0.0	3.2	0.2
8/1/12	3.6	0.2	0.0	0.1	0.0	0.7	0.1	0.0	0.0	1.1	0.1	1.4	0.2
8/4/12	***	***	***	***	***	***	***	***	***	***	***	***	***
8/7/12	4.2	0.4	0.0	0.2	0.0	1.3	0.2	0.0	0.0	0.0	0.0	2.3	0.2
8/10/12	4.6	0.3	0.0	0.2	0.0	0.5	0.2	0.0	0.0	0.3	0.1	3.7	0.3
8/13/12	7.7	0.6	0.1	0.2	0.1	0.0	0.0	0.0	0.0	0.7	0.3	5.9	0.1
8/16/12	***	***	***	***	***	***	***	***	***	***	***	***	***
8/19/12	20.2	0.5	0.1	0.8	0.1	0.0	0.0	0.0	0.0	0.0	0.0	18.6	0.1
8/22/12	***	***	***	***	***	***	***	***	***	***	***	***	***
8/25/12	3.2	0.3	0.0	0.2	0.0	0.0	0.0	0.2	0.1	0.0	0.0	2.6	0.1
8/28/12	***	***	***	***	***	***	***	***	***	***	***	***	***
8/31/12	***	***	***	***	***	***	***	***	***	***	***	***	***
Average	5.7	0.4	0.1	0.2	0.1	0.2	0.1	0.1	0.003	0.3	0.1	4.2	0.2

Notes: *No, incomplete, or invalid CMB data set. **Mass was too small to conduct a CMB analysis. ***Couldn't get a good statistical fit during CMB modeling.

**PM_{2.5} Source Contribution Estimates and Standard Errors (µg/m³) – OMNI Profiles.
State Building – Summer 2012.**

Date	PM _{2.5} Mass	Sulfate	Sulfate STD ERR	Ammonium Nitrate	Ammonium Nitrate STD ERR	Autos	Autos STD ERR	Diesel	Diesel STD ERR	Street Sand	Street Sand STD ERR	Wood Smoke	Wood Smoke STD ERR
6/2/12	***	***	***	***	***	***	***	***	***	***	***	***	***
6/5/12	4.8	0.4	0.1	0.4	0.1	0.0	0.0	0.3	0.1	0.5	0.2	3.2	0.1
6/8/12	6.0	0.4	0.1	0.1	0.1	0.0	0.0	0.0	0.0	0.0	0.0	5.0	0.1
6/11/12	5.9	0.4	0.1	0.3	0.1	0.0	0.0	0.0	0.0	0.6	0.2	3.6	0.1
6/14/12	4.6	0.3	0.0	0.2	0.0	0.7	0.2	0.0	0.0	0.0	0.0	1.9	0.1
6/17/12	3.8	0.2	0.0	0.1	0.0	0.0	0.0	0.0	0.0	0.3	0.1	2.2	0.0
6/20/12	8.6	0.4	0.0	0.2	0.0	0.0	0.0	0.0	0.0	0.9	0.2	4.8	0.1
6/23/12	6.4	0.4	0.0	0.3	0.1	0.0	0.0	0.0	0.0	0.6	0.2	4.7	0.1
6/26/12	3.2	0.2	0.0	0.1	0.0	0.4	0.1	0.0	0.0	0.0	0.0	2.2	0.1
6/29/12	3.7	0.3	0.0	0.2	0.0	0.0	0.0	0.0	0.0	0.0	0.0	2.4	0.1
7/2/12	***	***	***	***	***	***	***	***	***	***	***	***	***
7/5/12	4.3	0.3	0.0	0.2	0.0	0.0	0.0	0.0	0.0	0.0	0.0	1.8	0.1
7/8/12	***	***	***	***	***	***	***	***	***	***	***	***	***
7/11/12	3.7	0.3	0.0	0.3	0.0	0.0	0.0	0.0	0.0	0.0	0.0	2.1	0.1
7/14/12	***	***	***	***	***	***	***	***	***	***	***	***	***
7/17/12	*	*	*	*	*	*	*	*	*	*	*	*	*
7/20/12	3.6	0.6	0.1	0.0	0.0	0.0	0.0	0.0	0.0	0.0	0.0	2.8	0.1
7/23/12	***	***	***	***	***	***	***	***	***	***	***	***	***
7/26/12	8.1	0.7	0.1	0.2	0.1	0.0	0.0	0.0	0.0	0.0	0.0	4.2	0.2
7/29/12	3.9	0.4	0.1	0.2	0.1	0.0	0.0	0.0	0.0	0.0	0.0	3.0	0.1
8/1/12	3.6	0.2	0.0	0.1	0.0	0.0	0.0	0.2	0.0	1.2	0.2	2.0	0.1
8/4/12	***	***	***	***	***	***	***	***	***	***	***	***	***
8/7/12	4.2	0.4	0.0	0.1	0.0	1.5	0.2	0.0	0.0	0.0	0.0	1.8	0.1
8/10/12	4.6	0.3	0.0	0.2	0.0	0.8	0.2	0.0	0.0	0.3	0.1	3.1	0.1
8/13/12	7.7	0.5	0.1	0.2	0.1	0.9	0.3	0.0	0.0	0.7	0.2	4.3	0.2
8/16/12	***	***	***	***	***	***	***	***	***	***	***	***	***
8/19/12	20.2	0.4	0.1	0.8	0.1	0.0	0.0	0.0	0.0	0.0	0.0	15.0	0.1
8/22/12	***	***	***	***	***	***	***	***	***	***	***	***	***
8/25/12	3.2	0.2	0.0	0.2	0.0	0.8	0.2	0.0	0.0	0.0	0.0	1.9	0.1
8/28/12	***	***	***	***	***	***	***	***	***	***	***	***	***
8/31/12	***	***	***	***	***	***	***	***	***	***	***	***	***
Average	5.7	0.4	0.05	0.2	0.05	0.3	0.1	0.02	0.01	0.3	0.1	3.6	0.1

Notes: *No, incomplete, or invalid CMB data set. **Mass was too small to conduct a CMB analysis. ***Couldn't get a good statistical fit during CMB modeling.

**PM_{2.5} Source Contribution Estimates and Standard Errors (µg/m³) – EPA Profiles.
NCORE – Summer 2012.**

Date	PM _{2.5} Mass	Sulfate	Sulfate STD ERR	Ammonium Nitrate	Ammonium Nitrate STD ERR	Autos	Autos STD ERR	Diesel	Diesel STD ERR	Street Sand	Street Sand STD ERR	Wood Smoke	Wood Smoke STD ERR
6/14/12	2.9	0.2	0.0	0.1	0.3	0.0	0.0	2.2	0.5	0.2	0.1	0.0	0.0
6/17/12	4.3	0.2	0.0	0.2	0.0	0.0	0.0	0.0	0.0	0.4	0.1	3.7	0.4
6/20/12	5.9	0.5	0.1	0.2	0.1	0.0	0.0	0.0	0.0	0.4	0.1	5.1	0.5
6/23/12	6.6	0.3	0.0	0.2	0.0	0.0	0.0	0.0	0.0	0.8	0.1	5.9	1.0
6/26/12	***	***	***	***	***	***	***	***	***	***	***	***	***
6/29/12	3.1	0.3	0.0	0.0	0.0	0.0	0.0	2.8	0.5	0.0	0.0	0.0	0.0
7/2/12	4.3	0.3	0.0	0.3	0.1	4.2	0.4	0.0	0.0	0.0	0.0	0.0	0.0
7/5/12	***	***	***	***	***	***	***	***	***	***	***	***	***
7/8/12	***	***	***	***	***	***	***	***	***	***	***	***	***
7/11/12	***	***	***	***	***	***	***	***	***	***	***	***	***
7/14/12	***	***	***	***	***	***	***	***	***	***	***	***	***
7/17/12	***	***	***	***	***	***	***	***	***	***	***	***	***
7/20/12	3.4	0.6	0.1	0.3	0.1	2.4	0.4	0.0	0.0	0.0	0.0	0.0	0.0
7/23/12	***	***	***	***	***	***	***	***	***	***	***	***	***
7/26/12	5.9	0.8	0.1	0.3	0.1	0.0	0.0	0.0	0.0	0.0	0.0	5.2	0.5
7/29/12	4.2	0.4	0.0	0.3	0.1	0.0	0.0	0.0	0.0	0.0	0.0	4.5	0.6
8/1/12	4.0	0.2	0.0	0.1	0.0	0.0	0.0	0.0	0.0	1.3	0.2	3.4	0.4
8/4/12	3.2	0.3	0.1	0.2	0.0	3.4	0.6	0.0	0.0	0.0	0.0	0.0	0.0
8/7/12	4.5	0.4	0.0	0.2	0.1	3.8	0.6	0.0	0.0	0.0	0.0	0.0	0.0
8/10/12	4.3	0.3	0.0	0.1	0.0	0.0	0.0	0.0	0.0	0.2	0.1	4.2	0.6
8/13/12	6.5	0.5	0.1	0.2	0.1	0.0	0.0	0.0	0.0	0.4	0.1	5.1	0.5
8/16/12	4.2	0.5	0.1	0.2	0.1	0.0	0.0	0.0	0.0	0.0	0.0	3.9	0.6
8/19/12	15.6	0.5	0.1	0.7	0.1	0.0	0.0	0.0	0.0	0.3	0.1	15.3	1.8
8/22/12	4.3	0.2	0.1	0.2	0.0	3.5	0.7	0.0	0.0	0.6	0.1	0.0	0.0
8/25/12	*	*	*	*	*	*	*	*	*	*	*	*	*
8/28/12	***	***	***	***	***	***	***	***	***	***	***	***	***
8/31/12	***	***	***	***	***	***	***	***	***	***	***	***	***
Average	5.1	0.4	0.1	0.2	0.1	1.0	0.2	0.3	0.1	0.3	0.1	3.3	0.4

Notes: *No, incomplete, or invalid CMB data set. **Mass was too small to conduct a CMB analysis. ***Couldn't get a good statistical fit during CMB modeling.

**PM_{2.5} Source Contribution Estimates and Standard Errors (µg/m³) – OMNI Profiles.
NCORE – Summer 2012.**

Date	PM _{2.5} Mass	Sulfate	Sulfate STD ERR	Ammonium Nitrate	Ammonium Nitrate STD ERR	Autos	Autos STD ERR	Diesel	Diesel STD ERR	Street Sand	Street Sand STD ERR	Wood Smoke	Wood Smoke STD ERR
6/14/12	2.9	0.2	0.0	0.1	0.0	0.0	0.0	0.0	0.0	0.1	0.1	2.8	0.4
6/17/12	4.3	0.2	0.0	0.1	0.0	0.0	0.0	0.0	0.0	0.3	0.1	4.2	0.4
6/20/12	5.9	0.4	0.0	0.2	0.0	0.0	0.0	0.0	0.0	0.4	0.1	5.7	0.5
6/23/12	6.6	0.3	0.0	0.2	0.0	0.0	0.0	0.0	0.0	0.8	0.1	6.6	0.7
6/26/12	***	***	***	***	***	***	***	***	***	***	***	***	***
6/29/12	3.1	0.3	0.0	0.0	0.0	0.0	0.0	2.8	0.5	0.0	0.0	0.0	0.0
7/2/12	4.3	0.3	0.0	0.4	0.0	0.0	0.0	0.0	0.0	0.0	0.0	4.4	0.4
7/5/12	***	***	***	***	***	***	***	***	***	***	***	***	***
7/8/12	***	***	***	***	***	***	***	***	***	***	***	***	***
7/11/12	***	***	***	***	***	***	***	***	***	***	***	***	***
7/14/12	***	***	***	***	***	***	***	***	***	***	***	***	***
7/17/12	***	***	***	***	***	***	***	***	***	***	***	***	***
7/20/12	3.4	0.6	0.1	0.3	0.1	2.4	0.4	0.0	0.0	0.0	0.0	0.0	0.0
7/23/12	***	***	***	***	***	***	***	***	***	***	***	***	***
7/26/12	5.9	0.8	0.1	0.2	0.1	0.0	0.0	0.0	0.0	0.0	0.0	5.9	0.4
7/29/12	4.2	0.3	0.0	0.3	0.0	0.0	0.0	0.0	0.0	0.0	0.0	4.5	0.6
8/1/12	4.0	0.1	0.0	0.1	0.0	0.0	0.0	0.0	0.0	0.7	0.1	3.2	0.3
8/4/12	3.2	0.3	0.1	0.2	0.0	3.4	0.6	0.0	0.0	0.0	0.0	0.0	0.0
8/7/12	4.5	0.4	0.0	0.3	0.1	0.0	0.0	0.0	0.0	0.0	0.0	3.6	0.5
8/10/12	4.3	0.3	0.0	0.1	0.0	0.0	0.0	0.0	0.0	0.2	0.1	3.9	0.5
8/13/12	6.5	0.4	0.0	0.2	0.1	0.0	0.0	0.0	0.0	0.5	0.2	5.6	0.4
8/16/12	4.2	0.5	0.1	0.2	0.1	0.0	0.0	0.0	0.0	0.0	0.0	4.2	0.5
8/19/12	15.6	0.5	0.1	0.6	0.1	0.0	0.0	0.0	0.0	0.4	0.1	14.3	1.0
8/22/12	4.3	0.2	0.0	0.2	0.0	0.0	0.0	0.0	0.0	0.5	0.1	3.5	0.5
8/25/12	*	*	*	*	*	*	*	*	*	*	*	*	*
8/28/12	***	***	***	***	***	***	***	***	***	***	***	***	***
8/31/12	***	***	***	***	***	***	***	***	***	***	***	***	***
Average	5.1	0.4	0.05	0.2	0.05	0.3	0.1	0.2	0.03	0.2	0.1	4.2	0.4

Notes: *No, incomplete, or invalid CMB data set. **Mass was too small to conduct a CMB analysis. ***Couldn't get a good statistical fit during CMB modeling.

**PM_{2.5} Source Contribution Estimates and Standard Errors ($\mu\text{g}/\text{m}^3$) – EPA Profiles.
State Building – Winter 2012/2013.**

Date	PM _{2.5} Mass	Sulfate	Sulfate STD ERR	Ammonium Nitrate	Ammonium Nitrate STD ERR	Autos	Autos STD ERR	Diesel	Diesel STD ERR	Wood Smoke	Wood Smoke STD ERR
11/2/12	14.9	2.2	0.3	1.0	0.3	0.0	0.0	0.0	0.0	10.8	0.4
11/5/12	19.7	3.6	0.4	1.7	0.5	0.0	0.0	0.0	0.0	14.6	1.2
11/8/12	34.9	6.3	0.8	2.6	0.8	0.0	0.0	0.0	0.0	26.1	1.2
11/11/12	13.8	1.9	0.2	0.8	0.2	0.0	0.0	0.0	0.0	10.5	0.7
11/14/12	22.2	3.4	0.4	1.6	0.4	0.0	0.0	0.0	0.0	16.7	0.6
11/17/12	3.3**	**	**	**	**	**	**	**	**	**	**
11/20/12	27.4	5.7	0.7	1.9	0.7	0.0	0.0	0.0	0.0	19.9	1.8
11/23/12	19.3	3.7	0.5	1.4	0.5	0.0	0.0	1.6	0.7	12.8	0.8
11/26/12	52.0	10.6	1.3	3.4	1.3	0.0	0.0	12.0	4.8	24.5	6.0
11/29/12	*	*	*	*	*	*	*	*	*	*	*
12/2/12	31.0	5.1	0.6	2.3	0.7	0.0	0.0	0.0	0.0	24.0	4.7
12/5/12	***	***	***	***	***	***	***	***	***	***	***
12/8/12	22.6	4.7	0.6	1.2	0.6	0.0	0.0	0.0	0.0	17.7	3.5
12/11/12	5.8**	**	**	**	**	**	**	**	**	**	**
12/14/12	10.6	1.9	0.2	0.8	0.2	0.0	0.0	1.7	0.5	7.1	0.8
12/17/12	***	***	***	***	***	***	***	***	***	***	***
12/20/12	***	***	***	***	***	***	***	***	***	***	***
12/23/12	***	***	***	***	***	***	***	***	***	***	***
12/26/12	***	***	***	***	***	***	***	***	***	***	***
12/29/12	26.9	4.1	0.5	2.3	0.5	0.0	0.0	5.4	0.8	14.6	1.2
1/1/13	7.0	0.9	0.1	0.8	0.1	0.0	0.0	0.0	0.0	5.4	1.0
1/4/13	24.4	3.3	0.4	1.4	0.4	0.0	0.0	5.9	0.6	13.4	0.7
1/7/13	29.1	5.4	0.7	1.7	0.7	0.0	0.0	2.7	1.0	20.0	1.1
1/10/13	***	***	***	***	***	***	***	***	***	***	***
1/13/13	***	***	***	***	***	***	***	***	***	***	***
1/16/13	*	*	*	*	*	*	*	*	*	*	*
1/19/13	21.5	4.7	0.6	1.7	0.6	0.0	0.0	0.0	0.0	14.3	2.2
1/22/13	22.2	4.3	0.5	1.6	0.6	0.0	0.0	0.0	0.0	15.9	2.3
1/25/13	***	***	***	***	***	***	***	***	***	***	***
1/28/13	41.4	9.1	1.1	2.7	1.1	0.0	0.0	0.0	0.0	28.3	2.3
1/31/13	***	***	***	***	***	***	***	***	***	***	***
2/3/13	23.1	3.6	0.5	1.9	0.5	0.0	0.0	0.0	0.0	17.8	1.0
2/6/13	18.0	3.3	0.4	2.4	0.4	0.0	0.0	0.0	0.0	13.0	0.9
2/9/13	*	*	*	*	*	*	*	*	*	*	*
2/12/13	27.0	4.7	0.6	2.5	0.6	0.0	0.0	3.9	1.7	14.4	2.6
2/15/13	***	***	***	***	***	***	***	***	***	***	***
2/18/13	17.8	4.0	0.5	1.8	0.5	0.0	0.0	0.0	0.0	12.2	0.8
2/21/13	3.8**	**	**	**	**	**	**	**	**	**	**
2/24/13	16.1	2.2	0.3	1.3	0.3	0.0	0.0	0.0	0.0	13.1	0.6
2/27/13	18.2	2.8	0.4	1.5	0.4	0.0	0.0	1.2	0.5	11.9	0.6
3/2/13	17.1	2.6	0.3	2.0	0.4	0.0	0.0	0.0	0.0	11.7	1.7
3/5/13	*	*	*	*	*	*	*	*	*	*	*
3/8/13	14.6	1.9	0.2	1.3	0.3	0.0	0.0	0.0	0.0	11.4	0.7
3/11/13	16.6	3.2	0.4	1.9	0.4	0.0	0.0	0.0	0.0	11.2	2.2

3/14/13	*	*	*	*	*	*	*	*	*	*	*
3/17/13	10.7	2.1	0.3	1.2	0.3	3.0	1.2	0.0	0.0	4.3	0.6
3/20/13	*	*	*	*	*	*	*	*	*	*	*
3/23/13	*	*	*	*	*	*	*	*	*	*	*
3/26/13	4.8**	**	**	**	**	**	**	**	**	**	**
3/29/13	12.2	1.4	0.2	1.3	0.2	0.0	0.0	0.0	0.0	9.5	0.4
Average	21.8	3.9	0.5	1.7	0.5	0.1	0.04	1.2	0.4	14.7	1.5

Notes: *No, incomplete, or invalid CMB data set. **Mass was too small to conduct a CMB analysis. ***Couldn't get a good statistical fit during CMB modeling.

**PM_{2.5} Source Contribution Estimates and Standard Errors (µg/m³) – OMNI Profiles.
State Building – Winter 2012/2013.**

Date	PM _{2.5} Mass	Sulfate	Sulfate STD ERR	Ammonium Nitrate	Ammonium Nitrate STD ERR	Autos	Autos STD ERR	Diesel	Diesel STD ERR	No. 2 Fuel Oil	No. 2 Fuel Oil STD ERR	Wood Smoke	Wood Smoke STD ERR
11/2/12	14.9	1.6	0.3	0.8	0.2	0.0	0.0	0.8	0.3	2.8	1.1	8.4	1.3
11/5/12	19.7	2.2	0.4	1.2	0.3	0.0	0.0	0.0	0.0	7.1	1.6	8.8	1.8
11/8/12	34.9	3.7	0.7	1.7	0.5	0.0	0.0	0.0	0.0	13.9	2.8	13.3	3.1
11/11/12	13.8	1.4	0.3	0.6	0.2	0.0	0.0	0.0	0.0	2.7	1.0	6.7	1.1
11/14/12	22.2	2.1	0.4	1.2	0.3	0.0	0.0	0.0	0.0	6.9	1.5	10.7	1.7
11/17/12	3.3**	**	**	**	**	**	**	**	**	**	**	**	**
11/20/12	27.4	3.3	0.7	1.0	0.5	0.0	0.0	0.0	0.0	12.8	2.5	8.8	2.8
11/23/12	19.3	2.4	0.5	0.9	0.3	0.0	0.0	1.3	0.5	7.1	1.8	6.5	2.0
11/26/12	52.0	10.2	1.3	3.5	1.3	0.0	0.0	0.0	0.0	0.0	0.0	32.0	2.1
11/29/12	*	*	*	*	*	*	*	*	*	*	*	*	*
12/2/12	31.0	2.8	0.6	1.4	0.4	0.0	0.0	0.0	0.0	11.8	2.2	17.7	2.4
12/5/12	***	***	***	***	***	***	***	***	***	***	***	***	***
12/8/12	22.6	2.8	0.6	0.5	0.4	0.0	0.0	0.0	0.0	9.9	2.1	7.4	1.6
12/11/12	5.8**	**	**	**	**	**	**	**	**	**	**	**	**
12/14/12	10.6	1.3	0.2	0.6	0.2	2.3	1.1	0.0	0.0	2.7	1.0	3.6	0.9
12/17/12	***	***	***	***	***	***	***	***	***	***	***	***	***
12/20/12	***	***	***	***	***	***	***	***	***	***	***	***	***
12/23/12	***	***	***	***	***	***	***	***	***	***	***	***	***
12/26/12	***	***	***	***	***	***	***	***	***	***	***	***	***
12/29/12	26.9	3.1	0.6	1.7	0.4	0.0	0.0	0.0	0.0	8.2	2.3	5.3	2.6
1/1/13	7.0	0.9	0.1	0.7	0.1	1.8	0.6	0.0	0.0	0.1	0.0	3.9	0.3
1/4/13	24.4	2.6	0.5	1.0	0.4	0.0	0.0	0.0	0.0	6.5	1.8	10.3	2.0
1/7/13	29.1	3.3	0.7	0.9	0.4	0.0	0.0	2.3	0.6	12.0	2.5	9.1	2.7
1/10/13	***	***	***	***	***	***	***	***	***	***	***	***	***
1/13/13	***	***	***	***	***	***	***	***	***	***	***	***	***
1/16/13	*	*	*	*	*	*	*	*	*	*	*	*	*
1/19/13	21.5	3.0	0.6	1.1	0.4	0.0	0.0	0.0	0.0	9.1	2.2	4.7	2.5
1/22/13	22.2	2.8	0.5	1.1	0.4	0.0	0.0	0.0	0.0	8.1	2.0	7.3	2.3
1/25/13	***	***	***	***	***	***	***	***	***	***	***	***	***
1/28/13	41.4	8.9	1.1	2.6	1.1	0.0	0.0	0.0	0.0	0.0	0.0	22.8	1.8
1/31/13	***	***	***	***	***	***	***	***	***	***	***	***	***
2/3/13	23.1	3.2	0.6	1.4	0.4	0.0	0.0	0.0	0.0	7.4	2.3	6.0	2.6
2/6/13	18.0	3.7	0.5	2.3	0.5	0.0	0.0	1.4	0.7	0.0	0.0	9.4	0.9
2/9/13	*	*	*	*	*	*	*	*	*	*	*	*	*
2/12/13	27.0	3.5	0.7	2.0	0.5	0.0	0.0	0.0	0.0	8.4	2.6	6.7	2.9
2/15/13	***	***	***	***	***	***	***	***	***	***	***	***	***
2/18/13	17.8	2.6	0.5	1.3	0.4	0.0	0.0	0.0	0.0	7.9	1.9	4.8	2.1
2/21/13	3.8**	**	**	**	**	**	**	**	**	**	**	**	**
2/24/13	16.1	2.0	0.4	1.0	0.3	0.0	0.0	0.0	0.0	4.2	1.5	5.8	1.6
2/27/13	18.2	2.1	0.4	1.3	0.3	3.9	1.4	0.0	0.0	4.0	1.6	7.5	1.7
3/2/13	17.1	1.9	0.4	1.8	0.3	2.6	1.3	0.0	0.0	3.3	1.5	6.8	1.6
3/5/13	*	*	*	*	*	*	*	*	*	*	*	*	*
3/8/13	14.6	1.3	0.3	1.1	0.2	0.0	0.0	0.0	0.0	3.0	1.0	6.7	1.1
3/11/13	16.6	2.2	0.4	1.5	0.3	0.0	0.0	0.0	0.0	5.7	1.6	4.4	1.8

3/14/13	*	*	*	*	*	*	*	*	*	*	*	*	*
3/17/13	10.7	1.2	0.2	0.9	0.2	0.0	0.0	0.0	0.0	4.5	1.0	3.7	1.1
3/20/13	*	*	*	*	*	*	*	*	*	*	*	*	*
3/23/13	*	*	*	*	*	*	*	*	*	*	*	*	*
3/26/13	4.8**	**	**	**	**	**	**	**	**	**	**	**	**
3/29/13	12.2	1.2	0.2	1.0	0.2	1.9	0.8	0.0	0.0	3.4	1.0	2.8	1.0
Average	21.8	2.9	0.5	1.3	0.4	0.4	0.2	0.2	0.1	6.0	1.5	8.7	1.8

Notes: *No, incomplete, or invalid CMB data set. **Mass was too small to conduct a CMB analysis. ***Couldn't get a good statistical fit during CMB modeling.

**PM_{2.5} Source Contribution Estimates and Standard Errors ($\mu\text{g}/\text{m}^3$) – EPA Profiles.
NPE – Winter 2012/2013.**

Date	PM _{2.5} Mass	Sulfate	Sulfate STD ERR	Ammonium Nitrate	Ammonium Nitrate STD ERR	Autos	Autos STD ERR	Diesel	Diesel STD ERR	Wood Smoke	Wood Smoke STD ERR
11/2/12	30.0	2.6	0.3	0.8	0.3	0.0	0.0	7.2	1.0	16.8	2.2
11/5/12	23.9	1.6	0.2	0.9	0.2	8.2	1.7	0.0	0.0	15.1	2.0
11/8/12	51.2	3.2	0.4	1.0	0.4	0.0	0.0	4.0	1.0	45.1	2.8
11/11/12	17.4	1.4	0.2	0.6	0.2	5.9	1.4	0.0	0.0	10.5	1.4
11/14/12	14.9	0.9	0.1	0.5	0.1	0.0	0.0	0.0	0.0	13.5	2.0
11/17/12	7.3	0.5	0.1	0.2	0.1	0.0	0.0	0.0	0.0	5.1	0.6
11/20/12	21.8	3.0	0.3	0.8	0.4	0.0	0.0	4.9	1.0	12.3	1.6
11/23/12	5.3**	**	**	**	**	**	**	**	**	**	**
11/26/12	75.2	6.3	0.7	1.8	0.8	0.0	0.0	12.4	2.1	46.9	5.7
11/29/12	68.1	6.2	0.7	1.9	0.8	0.0	0.0	11.6	2.0	44.3	5.4
12/2/12	51.7	4.0	0.4	1.2	0.5	0.0	0.0	10.7	1.5	30.1	3.7
12/5/12	32.7	2.8	0.3	1.7	0.4	0.0	0.0	9.0	1.2	20.6	2.6
12/8/12	56.8	6.9	0.8	1.8	0.9	0.0	0.0	6.9	1.5	37.4	4.5
12/11/12	5.5**	**	**	**	**	**	**	**	**	**	**
12/14/12	7.0	0.6	0.1	0.5	0.1	0.0	0.0	0.7	0.3	5.5	0.7
12/17/12	37.3	3.5	0.4	1.0	0.4	0.0	0.0	6.1	0.9	29.0	3.4
12/20/12	47.3	4.2	0.5	1.1	0.5	0.0	0.0	5.9	1.1	35.9	4.2
12/23/12	62.4	5.8	0.7	1.8	0.7	0.0	0.0	7.3	1.4	46.7	5.5
12/26/12	40.2	2.0	0.2	2.5	0.3	0.0	0.0	5.3	0.8	31.8	3.7
12/29/12	31.5	2.6	0.3	1.0	0.3	0.0	0.0	6.0	1.0	21.4	2.7
1/1/13	10.0	0.8	0.1	0.4	0.1	0.0	0.0	0.0	0.0	9.4	1.0
1/4/13	47.7	3.1	0.3	1.2	0.4	0.0	0.0	8.3	1.2	28.9	3.5
1/7/13	38.3	3.4	0.4	1.3	0.4	0.0	0.0	4.3	1.1	25.9	3.2
1/10/13	17.8	1.9	0.2	0.9	0.2	5.3	1.6	0.0	0.0	10.1	1.4
1/13/13	14.9	1.1	0.1	0.6	0.1	4.6	1.2	0.0	0.0	8.2	1.1
1/16/13	19.8	2.0	0.2	1.0	0.3	0.0	0.0	0.0	0.0	17.7	3.6
1/19/13	5.8**	**	**	**	**	**	**	**	**	**	**
1/22/13	4.4**	**	**	**	**	**	**	**	**	**	**
1/25/13	26.8	4.2	0.5	1.4	0.5	0.0	0.0	2.7	0.9	18.8	2.3
1/28/13	39.9	4.8	0.5	1.5	0.6	0.0	0.0	6.1	1.5	26.6	3.3
1/31/13	22.3	2.0	0.2	1.0	0.3	0.0	0.0	0.0	0.0	19.8	1.8
2/3/13	11.0	1.3	0.1	1.3	0.2	0.0	0.0	0.0	0.0	8.7	1.1
2/6/13	15.2	2.3	0.3	1.4	0.3	0.0	0.0	0.0	0.0	11.4	2.9
2/9/13	23.6	1.9	0.2	0.7	0.2	0.0	0.0	0.0	0.0	22.6	1.8
2/12/13	41.6	2.9	0.3	1.8	0.4	6.1	2.8	0.0	0.0	31.0	3.9
2/15/13	11.1	0.8	0.1	0.6	0.1	0.0	0.0	0.0	0.0	6.5	1.0
2/18/13	16.0	2.0	0.2	0.9	0.3	0.0	0.0	0.0	0.0	13.4	1.6
2/21/13	3.4**	**	**	**	**	**	**	**	**	**	**
2/24/13	13.9	1.6	0.2	0.7	0.2	0.0	0.0	0.0	0.0	11.2	1.0
2/27/13	20.3	1.4	0.2	1.0	0.2	0.0	0.0	2.0	0.9	15.7	2.0
3/2/13	23.6	1.8	0.2	1.5	0.2	0.0	0.0	1.1	0.5	25.6	3.0
3/5/13	*	*	*	*	*	*	*	*	*	*	*
3/8/13	12.4	0.9	0.1	0.7	0.2	0.0	0.0	1.2	0.4	9.8	1.2

3/11/13	14.4	1.6	0.2	1.0	0.2	0.0	0.0	0.0	0.0	13.0	1.6
3/14/13	2.6**	**	**	**	**	**	**	**	**	**	**
3/17/13	15.5	1.3	0.1	0.8	0.2	0.0	0.0	1.0	0.4	13.0	1.6
3/20/13	1.0**	**	**	**	**	**	**	**	**	**	**
3/23/13	4.6**	**	**	**	**	**	**	**	**	**	**
3/26/13	6.2	0.8	0.1	0.3	0.1	0.0	0.0	0.0	0.0	4.4	0.9
3/29/13	11.8	1.0	0.1	0.7	0.1	0.0	0.0	0.0	0.0	10.8	1.4
Average	28.1	2.5	0.3	1.1	0.3	0.7	0.2	3.0	0.6	20.3	2.5

Notes: *No, incomplete, or invalid CMB data set. **Mass was too small to conduct a CMB analysis. ***Couldn't get a good statistical fit during CMB modeling.

**PM_{2.5} Source Contribution Estimates and Standard Errors ($\mu\text{g}/\text{m}^3$) – OMNI Profiles.
NPE – Winter 2012/2013.**

Date	PM _{2.5} Mass	Sulfate	Sulfate STD ERR	Ammonium Nitrate	Ammonium Nitrate STD ERR	Autos	Autos STD ERR	Diesel	Diesel STD ERR	No. 2 Fuel Oil	No. 2 Fuel Oil STD ERR	Wood Smoke	Wood Smoke STD ERR
11/2/12	30.0	0.9	0.4	0.0	0.0	3.4	0.7	0.0	0.0	7.9	2.0	19.1	2.2
11/5/12	23.9	0.6	0.1	0.6	0.1	0.0	0.0	1.7	0.4	3.0	0.5	19.2	1.5
11/8/12	51.2	1.9	0.4	0.5	0.3	0.0	0.0	7.9	1.2	6.9	1.4	35.0	3.1
11/11/12	17.4	0.7	0.2	0.4	0.2	0.0	0.0	1.0	0.4	2.9	0.9	14.3	1.4
11/14/12	14.9	0.5	0.1	0.4	0.1	0.0	0.0	0.0	0.0	1.5	0.4	10.9	0.9
11/17/12	7.3	0.3	0.1	0.2	0.0	0.0	0.0	0.0	0.0	0.7	0.3	3.1	0.5
11/20/12	21.8	2.0	0.3	0.0	0.0	5.3	2.2	0.0	0.0	5.5	1.4	9.8	1.5
11/23/12	5.3**	**	**	**	**	**	**	**	**	**	**	**	**
11/26/12	75.2	2.3	0.7	0.0	0.0	0.0	0.0	4.7	1.1	17.8	3.3	55.4	5.1
11/29/12	68.1	1.6	0.7	0.0	0.0	0.0	0.0	5.2	1.1	22.5	3.4	43.1	4.3
12/2/12	51.7	2.0	0.4	0.0	0.0	13.4	2.4	0.0	0.0	8.9	1.4	34.0	4.7
12/5/12	32.7	1.8	0.3	1.2	0.3	0.0	0.0	4.7	1.1	5.3	1.4	19.7	1.9
12/8/12	56.8	4.5	0.8	0.0	0.0	0.0	0.0	0.0	0.0	15.9	3.1	31.2	3.0
12/11/12	5.5**	**	**	**	**	**	**	**	**	**	**	**	**
12/14/12	7.0	0.6	0.1	0.5	0.1	0.0	0.0	0.0	0.0	0.0	0.0	6.1	0.4
12/17/12	37.3	2.3	0.5	0.0	0.0	0.0	0.0	1.7	0.8	8.4	2.0	25.2	2.4
12/20/12	47.3	2.8	0.5	0.0	0.0	0.0	0.0	0.0	0.0	10.0	1.9	33.0	2.3
12/23/12	62.4	3.6	0.7	0.0	0.0	0.0	0.0	0.0	0.0	14.7	2.5	41.4	3.0
12/26/12	40.2	**	**	**	**	**	**	**	**	**	**	**	**
12/29/12	31.5	1.8	0.3	0.9	0.3	0.0	0.0	0.0	0.0	3.5	1.4	23.4	1.6
1/1/13	10.0	0.7	0.1	0.4	0.1	0.0	0.0	0.0	0.0	0.0	0.0	9.5	0.8
1/4/13	47.7	1.3	0.3	0.8	0.2	0.0	0.0	4.2	0.7	5.4	1.0	37.2	2.5
1/7/13	38.3	2.3	0.4	0.7	0.3	0.0	0.0	0.0	0.0	5.8	1.7	24.2	1.8
1/10/13	17.8	1.0	0.2	0.6	0.2	1.4	0.7	0.0	0.0	3.4	1.2	12.9	1.7
1/13/13	14.9	0.8	0.1	0.6	0.2	1.6	0.6	0.0	0.0	0.0	0.0	12.9	1.2
1/16/13	19.8	1.4	0.2	0.8	0.2	0.0	0.0	0.0	0.0	2.7	1.0	11.8	1.2
1/19/13	5.8**	**	**	**	**	**	**	**	**	**	**	**	**
1/22/13	4.4**	**	**	**	**	**	**	**	**	**	**	**	**
1/25/13	26.8	2.7	0.5	0.7	0.4	0.0	0.0	0.0	0.0	8.6	2.0	14.3	1.8
1/28/13	39.9	2.4	0.5	0.7	0.3	0.0	0.0	0.0	0.0	11.8	1.8	21.2	1.9
1/31/13	22.3	1.2	0.2	0.8	0.2	2.9	1.2	0.0	0.0	3.1	0.9	15.3	2.1
2/3/13	11.0	1.3	0.1	1.3	0.2	0.0	0.0	0.0	0.0	0.0	0.0	8.7	0.7
2/6/13	15.2	1.4	0.3	1.2	0.2	0.0	0.0	0.0	0.0	4.1	1.1	7.1	1.1
2/9/13	23.6	1.7	0.2	0.6	0.2	0.0	0.0	0.0	0.0	0.0	0.0	18.1	1.4
2/12/13	41.6	2.0	0.4	1.3	0.3	0.0	0.0	0.0	0.0	4.7	1.5	28.0	2.1
2/15/13	11.1	0.8	0.1	0.6	0.1	0.0	0.0	0.0	0.0	0.0	0.0	5.2	0.7
2/18/13	16.0	1.5	0.3	0.6	0.2	0.0	0.0	0.0	0.0	3.0	1.1	11.1	1.2
2/21/13	3.4**	**	**	**	**	**	**	**	**	**	**	**	**
2/24/13	13.9	1.1	0.2	0.3	0.2	5.2	1.5	0.0	0.0	2.8	0.8	4.0	1.4
2/27/13	20.3	1.3	0.2	0.9	0.2	0.0	0.0	0.0	0.0	0.0	0.0	16.7	1.1
3/2/13	23.6	1.8	0.2	1.4	0.2	0.0	0.0	0.0	0.0	0.0	0.0	23.9	1.3
3/5/13	*	*	*	*	*	*	*	*	*	*	*	*	*
3/8/13	12.4	0.9	0.1	0.7	0.1	0.0	0.0	0.0	0.0	0.0	0.0	10.9	0.7
3/11/13	14.4	1.4	0.2	1.0	0.2	0.0	0.0	0.0	0.0	0.0	0.0	12.5	1.0

3/14/13	2.6**	**	**	**	**	**	**	**	**	**	**	**	**	
3/17/13	15.5	1.0	0.2	0.6	0.1	0.0	0.0	0.0	0.0	0.0	2.0	0.7	11.8	0.9
3/20/13	1.0**	**	**	**	**	**	**	**	**	**	**	**	**	
3/23/13	4.6**	**	**	**	**	**	**	**	**	**	**	**	**	
3/26/13	6.2	0.7	0.1	0.3	0.1	0.0	0.0	0.0	0.0	0.0	0.0	0.0	3.5	0.7
3/29/13	11.8	0.6	0.1	0.6	0.1	0.0	0.0	0.0	0.0	0.0	1.3	0.5	9.4	0.9
Average	27.8	1.5	0.3	0.6	0.1	0.8	0.2	0.8	0.2	4.9	1.1	18.8	1.8	

Notes: *No, incomplete, or invalid CMB data set. **Mass was too small to conduct a CMB analysis. ***Couldn't get a good statistical fit during CMB modeling.

**PM_{2.5} Source Contribution Estimates and Standard Errors (µg/m³) – EPA Profiles.
NCORE – Winter 2012/2013.**

Date	PM _{2.5} Mass	Sulfate	Sulfate STD ERR	Ammonium Nitrate	Ammonium Nitrate STD ERR	Autos	Autos STD ERR	Diesel	Diesel STD ERR	Wood Smoke	Wood Smoke STD ERR
11/2/12	*	*	*	*	*	*	*	*	*	*	*
11/5/12	*	*	*	*	*	*	*	*	*	*	*
11/8/12	29.9	5.9	0.7	2.4	0.8	0.0	0.0	0.0	0.0	22.3	1.9
11/11/12	16.3	1.8	0.2	0.8	0.2	0.0	0.0	0.0	0.0	13.7	0.9
11/14/12	23.0	3.2	0.4	1.7	0.4	0.0	0.0	2.9	0.7	15.8	1.9
11/17/12	3.7**	**	**	**	**	**	**	**	**	**	**
11/20/12	27.2	5.1	0.6	2.2	0.6	0.0	0.0	5.0	1.1	15.4	2.0
11/23/12	29.2	4.7	0.5	1.6	0.6	0.0	0.0	0.0	0.0	23.2	5.8
11/26/12	*	*	*	*	*	*	*	*	*	*	*
11/29/12	57.4	11.2	1.3	1.0	1.4	0.0	0.0	0.0	0.0	45.4	3.2
12/2/12	35.5	6.4	0.7	2.6	0.8	0.0	0.0	8.6	1.8	15.5	2.2
12/5/12	32.2	6.5	0.7	2.9	0.8	0.0	0.0	3.7	1.8	17.0	2.4
12/8/12	25.1	4.5	0.5	1.5	0.6	0.0	0.0	3.4	1.0	13.8	1.8
12/11/12	5.8**	**	**	**	**	**	**	**	**	**	**
12/14/12	11.4	1.9	0.2	0.9	0.4	0.0	0.0	2.9	0.6	7.2	1.0
12/17/12	49.2	10.9	1.2	3.1	1.4	0.0	0.0	5.8	2.1	34.6	4.3
12/20/12	46.4	12.2	1.4	2.9	1.5	12.4	7.4	0.0	0.0	21.1	3.6
12/23/12	41.2	9.8	1.1	2.8	1.2	13.4	6.0	0.0	0.0	16.9	3.0
12/26/12	27.8	5.9	0.7	1.9	0.7	0.0	0.0	4.9	1.6	14.8	2.1
12/29/12	28.2	4.4	0.5	2.3	0.6	0.0	0.0	5.1	1.3	14.8	2.0
1/1/13	7.9	1.0	0.1	0.7	0.1	0.0	0.0	0.0	0.0	6.7	0.6
1/4/13	23.4	3.4	0.4	1.6	0.4	0.0	0.0	5.1	1.1	13.0	1.8
1/7/13	*	*	*	*	*	*	*	*	*	*	*
1/10/13	21.6	3.3	0.4	2.5	0.4	0.0	0.0	3.6	0.8	12.8	1.6
1/13/13	14.9	2.2	0.3	1.1	0.3	0.0	0.0	2.0	0.7	10.0	1.4
1/16/13	26.7	4.9	0.5	2.9	0.6	0.0	0.0	4.9	1.4	13.9	1.9
1/19/13	22.4	4.6	0.5	2.0	0.6	0.0	0.0	0.0	0.0	16.1	2.0
1/22/13	27.9	4.8	0.5	2.1	0.7	0.0	0.0	3.5	1.0	17.7	2.3
1/25/13	28.6	6.3	0.7	2.4	0.8	8.0	3.9	0.0	0.0	13.3	2.1
1/28/13	40.3	8.7	1.0	2.2	1.1	0.0	0.0	0.0	0.0	27.0	2.8
1/31/13	***	***	***	***	***	***	***	***	***	***	***
2/3/13	22.5	3.7	0.4	1.3	0.5	0.0	0.0	0.0	0.0	14.8	1.4
2/6/13	19.6	3.6	0.4	2.5	0.5	0.0	0.0	4.2	1.3	8.2	1.4
2/9/13	21.4	3.3	0.4	1.7	0.4	0.0	0.0	4.6	1.0	9.6	1.4
2/12/13	25.5	5.1	0.6	2.8	0.7	0.0	0.0	5.2	1.5	12.7	1.8
2/15/13	3.8**	**	**	**	**	**	**	**	**	**	**
2/18/13	18.4	4.1	0.5	1.9	0.5	0.0	0.0	0.0	0.0	12.2	3.1
2/21/13	*	*	*	*	*	*	*	*	*	*	*
2/24/13	15.5	2.5	0.3	1.4	0.3	0.0	0.0	0.0	0.0	12.3	1.5
2/27/13	21.4	3.4	0.4	1.9	0.4	0.0	0.0	3.6	0.9	12.9	1.7
3/2/13	24.4	2.8	0.3	2.5	0.4	9.1	2.1	0.0	0.0	9.6	1.4
3/5/13	35.4	4.9	0.6	5.2	0.7	0.0	0.0	5.7	1.6	17.8	2.5
3/8/13	17.4	2.1	0.2	1.7	0.3	0.0	0.0	4.4	0.8	7.9	1.1
3/11/13	17.5	3.1	0.3	1.9	0.4	0.0	0.0	3.3	0.9	8.8	1.3

3/14/13	3.5**	**	**	**	**	**	**	**	**	**	**
3/17/13	13.0	2.2	0.2	1.4	0.3	0.0	0.0	0.0	0.0	9.0	1.2
3/20/13	11.4	2.0	0.2	1.3	0.3	0.0	0.0	0.0	0.0	8.1	1.1
3/23/13	5.0**	**	**	**	**	**	**	**	**	**	**
3/26/13	5.0**	**	**	**	**	**	**	**	**	**	**
3/29/13	10.8	1.8	0.2	1.4	0.2	0.0	0.0	0.0	0.0	8.0	1.1
Average	25.5	4.7	0.5	2.0	0.6	1.1	0.5	2.4	0.7	15.1	2.0

Notes: *No, incomplete, or invalid CMB data set. **Mass was too small to conduct a CMB analysis. ***Couldn't get a good statistical fit during CMB modeling.

**PM_{2.5} Source Contribution Estimates and Standard Errors ($\mu\text{g}/\text{m}^3$) – OMNI Profiles.
NCORE – Winter 2012/2013.**

Date	PM _{2.5} Mass	Sulfate	Sulfate STD ERR	Ammonium Nitrate	Ammonium Nitrate STD ERR	Autos	Autos STD ERR	Diesel	Diesel STD ERR	No. 2 Fuel Oil	No. 2 Fuel Oil STD ERR	Wood Smoke	Wood Smoke STD ERR
11/2/12	*	*	*	*	*	*	*	*	*	*	*	*	*
11/5/12	*	*	*	*	*	*	*	*	*	*	*	*	*
11/8/12	29.9	3.2	0.6	2.1	0.5	5.6	2.8	0.0	0.0	14.8	2.6	4.5	0.9
11/11/12	16.3	1.0	0.2	0.6	0.1	0.0	0.0	0.0	0.0	3.4	0.8	10.9	1.2
11/14/12	23.0	2.2	0.4	1.2	0.3	0.0	0.0	0.0	0.0	6.6	1.7	13.1	1.5
11/17/12	3.7**	**	**	**	**	**	**	**	**	**	**	**	**
11/20/12	27.2	3.1	0.7	1.2	0.5	0.0	0.0	2.4	0.8	12.9	2.9	7.5	2.3
11/23/12	29.2	2.3	0.5	0.0	0.0	2.2	0.7	0.0	0.0	12.3	2.2	12.4	2.8
11/26/12	*	*	*	*	*	*	*	*	*	*	*	*	*
11/29/12	57.4	10.6	1.2	0.0	0.0	0.0	0.0	0.0	0.0	0.0	0.0	49.8	3.5
12/2/12	35.5	3.6	0.8	1.6	0.7	0.0	0.0	3.7	1.0	13.7	3.7	13.7	4.3
12/5/12	32.2	3.5	0.7	1.7	0.5	0.0	0.0	0.0	0.0	16.2	2.6	8.5	2.2
12/8/12	25.1	2.8	0.5	0.8	0.4	0.0	0.0	0.0	0.0	10.2	2.1	9.6	1.8
12/11/12	5.8**	**	**	**	**	**	**	**	**	**	**	**	**
12/14/12	11.4	1.4	0.3	0.6	0.2	0.0	0.0	3.5	0.7	3.1	1.0	2.1	0.4
12/17/12	49.2	6.2	1.1	0.0	0.0	0.0	0.0	0.0	0.0	28.7	4.3	18.7	3.6
12/20/12	46.4	6.9	1.2	0.0	0.0	0.0	0.0	0.0	0.0	28.6	4.6	10.3	5.7
12/23/12	41.2	5.3	1.0	1.1	0.7	0.0	0.0	0.0	0.0	24.7	3.9	8.2	4.8
12/26/12	27.8	3.5	0.6	1.0	0.5	0.0	0.0	0.0	0.0	12.6	2.6	10.0	2.1
12/29/12	28.2	2.6	0.5	1.7	0.4	0.0	0.0	0.0	0.0	8.6	1.9	13.2	1.7
1/1/13	7.9	0.9	0.1	0.7	0.1	0.0	0.0	0.0	0.0	0.0	0.0	8.0	0.6
1/4/13	23.4	2.1	0.4	1.0	0.3	4.6	2.0	0.0	0.0	7.3	1.6	7.9	2.1
1/7/13	*	*	*	*	*	*	*	*	*	*	*	*	*
1/10/13	21.6	2.2	0.5	1.9	0.4	0.0	0.0	1.5	0.6	7.7	2.0	8.4	1.7
1/13/13	14.9	2.2	0.2	1.1	0.3	0.0	0.0	0.0	0.0	0.0	0.0	11.6	0.9
1/16/13	26.7	2.8	0.5	2.2	0.4	0.0	0.0	0.0	0.0	10.5	2.1	10.6	1.8
1/19/13	22.4	2.7	0.5	1.2	0.4	0.0	0.0	0.0	0.0	10.5	2.0	9.1	1.8
1/22/13	27.9	2.8	0.5	1.2	0.4	0.0	0.0	0.0	0.0	11.5	2.1	13.3	1.8
1/25/13	28.6	3.5	0.6	1.4	0.5	0.0	0.0	0.0	0.0	14.9	2.6	9.9	3.2
1/28/13	40.3	8.4	0.9	2.1	1.1	0.0	0.0	0.0	0.0	0.0	0.0	21.7	2.2
1/31/13	***	1.4	0.2	1.6	0.2	0.0	0.0	0.0	0.0	0.0	0.0	9.2	0.5
2/3/13	22.5	3.5	0.4	1.3	0.4	0.0	0.0	0.0	0.0	0.0	0.0	12.1	1.1
2/6/13	19.6	2.2	0.4	2.0	0.4	0.0	0.0	1.8	0.7	7.2	2.1	7.1	2.6
2/9/13	21.4	2.3	0.4	1.2	0.3	6.3	1.8	0.0	0.0	5.2	1.6	7.1	2.8
2/12/13	25.5	3.3	0.6	2.1	0.5	0.0	0.0	0.0	0.0	9.3	2.4	10.5	2.0
2/15/13	3.8**	**	**	**	**	**	**	**	**	**	**	**	**
2/18/13	18.4	2.4	0.4	1.3	0.3	0.0	0.0	0.0	0.0	8.9	1.8	6.4	2.2
2/21/13	*	*	*	*	*	*	*	*	*	*	*	*	*
2/24/13	15.5	1.5	0.3	1.0	0.2	0.0	0.0	0.0	0.0	5.8	1.2	8.6	1.2
2/27/13	21.4	2.4	0.4	1.4	0.3	0.0	0.0	0.0	0.0	6.8	1.8	10.3	1.6
3/2/13	24.4	1.9	0.4	2.2	0.4	0.0	0.0	1.5	0.6	3.7	1.8	15.1	2.3
3/5/13	35.4	2.6	0.5	4.3	0.5	0.0	0.0	0.0	0.0	12.0	2.2	14.1	2.0
3/8/13	17.4	2.1	0.2	1.6	0.3	6.8	2.1	0.0	0.0	0.0	0.0	8.3	1.0
3/11/13	17.5	2.2	0.4	1.6	0.3	0.0	0.0	0.0	0.0	4.1	1.6	8.8	1.3

3/14/13	3.5**	**	**	**	**	**	**	**	**	**	**	**	**
3/17/13	13.0	1.5	0.3	1.1	0.2	0.0	0.0	0.0	0.0	3.5	1.1	7.2	1.1
3/20/13	11.4	1.4	0.3	1.0	0.2	0.0	0.0	0.0	0.0	3.1	1.1	6.1	1.0
3/23/13	5.0**	**	**	**	**	**	**	**	**	**	**	**	**
3/26/13	5.0**	**	**	**	**	**	**	**	**	**	**	**	**
3/29/13	10.8	1.2	0.2	1.1	0.2	0.0	0.0	0.0	0.0	3.1	0.9	6.1	1.0
Average	25.1	3.0	0.5	1.3	0.3	0.7	0.2	0.4	0.1	8.5	1.8	11.0	2.0

Notes: *No, incomplete, or invalid CMB data set. **Mass was too small to conduct a CMB analysis. ***Couldn't get a good statistical fit during CMB modeling.

**PM_{2.5} Source Contribution Estimates and Standard Errors (µg/m³) – EPA Profiles.
NPF3 – Winter 2012/2013.**

Date	PM _{2.5} Mass	Sulfate	Sulfate STD ERR	Ammonium Nitrate	Ammonium Nitrate STD ERR	Autos	Autos STD ERR	Diesel	Diesel STD ERR	Wood Smoke	Wood Smoke STD ERR
11/2/12	*	*	*	*	*	*	*	*	*	*	*
11/5/12	34.9	2.5	0.3	1.1	0.3	0.0	0.0	5.5	1.0	23.1	2.8
11/8/12	106.4	7.5	0.8	1.9	0.9	0.0	0.0	17.3	2.6	69.1	8.3
11/11/12	31.5	2.3	0.3	0.8	0.3	0.0	0.0	4.8	0.9	21.1	2.6
11/14/12	25.5	1.9	0.2	1.0	0.2	0.0	0.0	2.0	0.7	19.5	2.4
11/17/12	7.3	0.8	0.1	0.2	0.1	0.0	0.0	0.0	0.0	6.1	0.5
11/20/12	44.0	3.3	0.4	0.9	0.4	0.0	0.0	3.6	1.5	38.9	2.9
11/23/12	8.5	0.8	0.1	0.3	0.1	0.0	0.0	0.7	0.3	7.0	0.9
11/26/12	138.1	9.3	1.0	2.4	1.2	0.0	0.0	22.0	3.3	98.1	11.7
11/29/12	154.6	11.2	1.3	3.0	1.4	0.0	0.0	25.2	3.8	108.4	13.0
12/2/12	124.7	7.2	0.8	2.1	0.9	0.0	0.0	14.2	2.0	91.8	10.6
12/5/12	*	*	*	*	*	*	*	*	*	*	*
12/8/12	*	*	*	*	*	*	*	*	*	*	*
12/11/12	6.4	0.6	0.1	0.0	0.0	0.0	0.0	0.0	0.0	6.0	0.6
12/14/12	9.8	0.8	0.1	0.0	0.0	0.0	0.0	0.0	0.0	8.4	0.7
12/17/12	83.6	6.0	0.7	1.6	0.8	0.0	0.0	7.0	1.5	62.6	7.2
12/20/12	111.4	8.7	1.0	2.0	1.1	0.0	0.0	13.6	2.2	98.5	11.4
12/23/12	98.2	8.0	0.9	2.3	1.0	0.0	0.0	12.2	2.0	76.0	8.8
12/26/12	106.5	6.5	0.8	2.4	0.8	0.0	0.0	9.1	1.7	85.3	9.8
12/29/12	55.9	3.4	0.4	0.6	0.4	0.0	0.0	6.9	1.0	42.5	4.9
1/1/13	24.4	1.4	0.2	0.9	0.2	0.0	0.0	0.0	0.0	22.3	2.6
1/4/13	84.3	6.6	0.7	2.1	0.8	0.0	0.0	12.2	2.2	55.2	6.7
1/7/13	95.6	6.6	0.7	2.0	0.8	0.0	0.0	8.6	2.4	73.8	8.8
1/10/13	23.9	2.0	0.2	1.0	0.3	0.0	0.0	0.0	0.0	21.2	2.4
1/13/13	23.6	1.2	0.1	0.7	0.2	0.0	0.0	2.8	0.7	18.6	2.3
1/16/13	36.8	2.9	0.4	1.4	0.4	0.0	0.0	0.0	0.0	33.3	6.5
1/19/13	10.3	1.1	0.1	0.7	0.2	0.0	0.0	0.7	0.3	8.3	1.1
1/22/13	4.2**	**	**	**	**	**	**	**	**	**	**
1/25/13	58.1	5.7	0.7	2.2	0.7	0.0	0.0	4.2	1.3	45.5	5.3
1/28/13	66.2	5.9	0.7	1.6	0.7	0.0	0.0	4.4	1.5	57.1	6.7
1/31/13	36.1	2.8	0.3	1.6	0.4	0.0	0.0	3.6	1.2	26.6	3.3
2/3/13	24.0	1.5	0.2	1.5	0.2	0.0	0.0	0.0	0.0	21.1	2.4
2/6/13	26.0	3.1	0.3	1.9	0.4	0.0	0.0	2.8	1.0	16.9	2.1
2/9/13	30.1	1.7	0.2	0.9	0.2	6.1	1.7	0.0	0.0	21.3	2.7
2/12/13	26.6	2.5	0.3	1.4	0.3	7.0	2.5	0.0	0.0	17.5	2.4
2/15/13	*	*	*	*	*	*	*	*	*	*	*
2/18/13	*	*	*	*	*	*	*	*	*	*	*
2/21/13	4.0**	**	**	**	**	**	**	**	**	**	**
2/24/13	24.6	2.1	0.2	1.0	0.3	4.7	1.8	0.0	0.0	17.4	2.2
2/27/13	37.6	3.0	0.3	1.5	0.4	4.7	2.3	0.0	0.0	28.2	3.5
3/2/13	32.2	1.8	0.2	1.3	0.2	0.0	0.0	0.0	0.0	28.3	2.1
3/5/13	32.2	1.8	0.2	1.3	0.2	0.0	0.0	2.9	1.0	25.1	3.1
3/8/13	25.7	1.4	0.2	1.3	0.2	0.0	0.0	1.1	0.5	22.7	2.6
3/11/13	31.4	2.5	0.3	1.5	0.3	4.5	2.0	0.0	0.0	23.0	2.9

3/14/13	3.2**	**	**	**	**	**	**	**	**	**	**
3/17/13	25.3	1.7	0.2	1.1	0.3	0.0	0.0	1.5	0.5	21.2	2.5
3/20/13	9.8	1.0	0.1	0.8	0.1	0.0	0.0	0.0	0.0	8.0	0.9
3/23/13	6.6	0.8	0.1	0.5	0.1	0.0	0.0	0.0	0.0	5.8	0.7
3/26/13	6.3	0.7	0.1	0.4	0.1	0.0	0.0	0.0	0.0	5.4	0.7
3/29/13	23.5	1.2	0.1	1.2	0.2	0.0	0.0	1.6	0.5	19.9	2.3
Average	46.9	3.4	0.4	1.3	0.4	0.6	0.2	4.5	0.9	35.9	4.2

Notes: *No, incomplete, or invalid CMB data set. **Mass was too small to conduct a CMB analysis. ***Couldn't get a good statistical fit during CMB modeling.

**PM_{2.5} Source Contribution Estimates and Standard Errors ($\mu\text{g}/\text{m}^3$) – OMNI Profiles.
NPF3 – Winter 2012/2013.**

Date	PM _{2.5} Mass	Sulfate	Sulfate STD ERR	Ammonium Nitrate	Ammonium Nitrate STD ERR	Autos	Autos STD ERR	Diesel	Diesel STD ERR	No. 2 Fuel Oil	No. 2 Fuel Oil STD ERR	Wood Smoke	Wood Smoke STD ERR
11/2/12	*	*	*	*	*	*	*	*	*	*	*	*	*
11/5/12	34.9	1.7	0.3	0.7	0.2	0.0	0.0	0.0	0.0	3.6	1.3	24.5	1.6
11/8/12	106.4	2.5	0.6	0.0	0.0	0.0	0.0	8.0	1.3	18.7	1.8	80.0	5.7
11/11/12	31.5	1.7	0.3	0.5	0.2	0.0	0.0	0.0	0.0	3.2	1.2	22.2	1.5
11/14/12	25.5	1.5	0.3	0.7	0.2	0.0	0.0	0.0	0.0	2.3	1.1	18.1	1.3
11/17/12	7.3	0.5	0.1	0.2	0.1	0.0	0.0	0.0	0.0	1.1	0.4	5.3	0.7
11/20/12	44.0	1.3	0.3	0.5	0.2	0.0	0.0	5.6	0.8	6.8	1.0	30.7	2.4
11/23/12	8.5	0.6	0.1	0.2	0.1	0.0	0.0	0.0	0.0	1.0	0.4	6.9	0.6
11/26/12	138.1	5.3	1.0	0.0	0.0	0.0	0.0	0.0	0.0	20.2	3.7	100.1	5.5
11/29/12	154.6	5.9	1.1	0.0	0.0	0.0	0.0	0.0	0.0	27.6	4.1	108.2	6.1
12/2/12	124.7	4.7	0.9	0.0	0.0	0.0	0.0	0.0	0.0	18.6	3.3	88.5	4.9
12/5/12	*	*	*	*	*	*	*	*	*	*	*	*	*
12/8/12	*	*	*	*	*	*	*	*	*	*	*	*	*
12/11/12	6.4	0.5	0.1	0.0	0.0	0.0	0.0	0.0	0.0	0.0	0.0	6.8	0.5
12/14/12	9.8	0.6	0.1	0.0	0.0	0.0	0.0	0.0	0.0	0.0	0.0	9.7	0.6
12/17/12	83.6	4.0	0.7	0.0	0.0	0.0	0.0	0.0	0.0	13.6	2.8	55.2	3.6
12/20/12	111.4	5.8	1.0	0.0	0.0	0.0	0.0	0.0	0.0	20.8	4.0	91.5	5.4
12/23/12	98.2	5.0	0.9	0.0	0.0	0.0	0.0	0.0	0.0	20.8	3.5	70.0	4.5
12/26/12	106.5	4.2	0.8	0.0	0.0	0.0	0.0	0.0	0.0	16.3	2.9	75.2	4.4
12/29/12	55.9	3.8	0.4	0.0	0.0	0.0	0.0	0.0	0.0	0.0	0.0	46.8	2.3
1/1/13	24.4	1.4	0.2	0.8	0.2	0.0	0.0	0.0	0.0	0.0	0.0	20.9	1.3
1/4/13	84.3	2.7	0.6	1.1	0.4	0.0	0.0	4.8	1.1	14.0	2.1	71.4	5.1
1/7/13	95.6	4.1	0.7	0.0	0.0	0.0	0.0	0.0	0.0	13.0	2.8	65.1	4.1
1/10/13	23.9	1.5	0.3	0.7	0.2	0.0	0.0	0.0	0.0	2.6	1.1	18.2	1.5
1/13/13	23.6	1.2	0.1	0.6	0.2	0.0	0.0	0.0	0.0	0.0	0.0	19.9	1.1
1/16/13	36.8	1.6	0.3	1.0	0.2	0.0	0.0	0.0	0.0	5.2	1.2	34.4	2.5
1/19/13	10.3	0.7	0.1	0.6	0.1	0.0	0.0	0.0	0.0	1.4	0.5	7.5	0.7
1/22/13	4.2**	**	**	**	**	**	**	**	**	**	**	**	**
1/25/13	58.1	3.7	0.7	1.1	0.5	0.0	0.0	0.0	0.0	12.5	2.8	37.4	3.0
1/28/13	66.2	3.8	0.7	0.0	0.0	0.0	0.0	0.0	0.0	12.9	2.6	47.4	3.5
1/31/13	36.1	1.8	0.3	1.1	0.3	0.0	0.0	0.0	0.0	4.9	1.4	24.8	1.9
2/3/13	24.0	1.4	0.2	1.4	0.2	0.0	0.0	0.0	0.0	0.0	0.0	19.6	1.3
2/6/13	26.0	2.1	0.4	1.4	0.3	0.0	0.0	0.0	0.0	5.6	1.6	14.6	1.5
2/9/13	30.1	0.9	0.2	0.6	0.1	4.1	1.1	0.0	0.0	2.6	0.7	22.4	2.2
2/12/13	26.6	1.8	0.3	1.1	0.3	0.0	0.0	0.0	0.0	3.7	1.3	17.4	1.5
2/15/13	*	*	*	*	*	*	*	*	*	*	*	*	*
2/18/13	*	*	*	*	*	*	*	*	*	*	*	*	*
2/21/13	4.0**	**	**	**	**	**	**	**	**	**	**	**	**
2/24/13	24.6	1.6	0.3	0.7	0.2	0.0	0.0	0.0	0.0	2.8	1.1	16.5	1.3
2/27/13	37.6	2.2	0.4	1.1	0.3	0.0	0.0	0.0	0.0	4.0	1.6	24.6	1.8
3/2/13	32.2	1.3	0.2	1.1	0.2	0.0	0.0	0.0	0.0	2.1	0.9	26.6	1.9
3/5/13	32.2	1.8	0.2	1.2	0.2	0.0	0.0	0.0	0.0	0.0	0.0	25.9	1.5
3/8/13	25.7	1.4	0.2	1.2	0.2	0.0	0.0	0.0	0.0	0.0	0.0	21.1	1.2
3/11/13	31.4	2.4	0.3	1.4	0.3	0.0	0.0	0.0	0.0	0.0	0.0	23.4	1.3

3/14/13	3.2**	**	**	**	**	**	**	**	**	**	**	**	**
3/17/13	25.3	1.2	0.2	0.8	0.2	0.0	0.0	0.0	0.0	2.8	0.9	19.5	1.3
3/20/13	9.8	0.6	0.1	0.7	0.1	0.0	0.0	0.0	0.0	1.0	0.5	8.4	0.8
3/23/13	6.6	0.5	0.1	0.4	0.1	0.0	0.0	0.0	0.0	0.8	0.4	5.9	0.7
3/26/13	6.3	0.4	0.1	0.3	0.1	0.0	0.0	0.0	0.0	0.8	0.3	5.2	0.6
3/29/13	23.5	1.2	0.1	1.1	0.2	0.0	0.0	0.0	0.0	0.0	0.0	19.7	1.1
Average	46.9	2.2	0.4	0.6	0.1	0.1	0.03	0.4	0.1	6.4	1.3	34.7	2.3

Notes: *No, incomplete, or invalid CMB data set. **Mass was too small to conduct a CMB analysis. ***Couldn't get a good statistical fit during CMB modeling.

Characterization of PM_{2.5} from Fairbanks, AK: Organics Analysis for Residential Oil Burner Emissions

Interim Report: 6/2011

Christopher P. Palmer, Department of Chemistry and Biochemistry, University of Montana, Missoula, MT 59803

1. Executive Summary

Fairbanks, AK experiences very high levels of ambient PM_{2.5} during the winter months. Studies are currently under way to determine the sources of the PM_{2.5} so that the issue might be addressed. Possible sources of the PM_{2.5} include residential heating (wood, fuel oil, and/or natural gas combustion), transportation (diesel and gasoline engines), and coal combustion.

The current project is to provide a more complete characterization of the organic chemical composition of PM_{2.5} from Fairbanks with the goal of identifying and quantifying chemical species that can be used to indicate and monitor PM_{2.5} emissions from fossil fuel combustion.

A comprehensive chemical analysis for hopanes, steranes and PAHs has been performed on eight PM samples from Fairbanks, selected to represent typical or high PM_{2.5} days. The results of these analyses have been examined with special attention to compounds reported by previous authors as emissions from fossil fuel sources. Emphasis has been placed on sulfur-containing compounds (dibenzothiophene and benzo naphtho thiophene) which are known emissions of diesel vehicles and residential oil burners and a polynuclear aromatic hydrocarbon (picene) which has been reported as a unique marker for coal combustion.

The results indicate that the levels of selected hopanes, steranes, picene and thiophenes, measured either as a concentration in air or as a fraction of PM_{2.5}, are very high. These concentrations are significantly higher than those reported in previous studies for coal, diesel or residential oil burner PM emissions or for airsheds in the United States and in Europe. Given that picene is a specific marker of coal emissions, the results indicate that coal combustion emissions are likely a significant contributor to Fairbanks PM_{2.5}, specifically the sulfate/sulfur fraction. Overall, the results indicate that fossil fuel combustion, particularly of emissions from coal and residential fuel oil combustion, is a significant contributor to Fairbanks PM_{2.5}.

2. Methods

2.1 Samples selected for analysis.

Eight Fairbanks PM_{2.5} samples from the winter of 2009-2010 were selected in consultation with Alaska DEC and submitted to Desert Research Institute for comprehensive analysis of 83 PAHs (including substituted PAHs, dibenzothiophene and benzonaphthothiophene) and 23 hopanes and steranes. The samples, listed in Table 1, were all from the downtown sampling site and had a range of PM_{2.5} levels from 15.7 to 54.4 ug/m³. A laboratory blank filter was also sent for analysis, and the reported levels of all compounds are blank corrected.

Desert Research Institute (DRI) returned two spreadsheets with the analytical results for hopanes and steranes and for PAHs. The amount and estimated uncertainty of each compound found on the filter is reported in ng. These spreadsheets of the raw analytical results are included with this report.

2.2 Analysis of the Raw Results

The DRI results provide a great deal of information about the samples. However, these raw results are difficult to interpret or utilize without some context. Based on a review of relevant published studies, several specific chemical compounds were selected for further analysis. These compounds are listed in Tables 2 and 3 and are those reported as significant components of particulate matter from combustion of specific fossil fuels: residential heating oil, diesel vehicles, gasoline vehicles, and coal. Unfortunately, many of the published reports only provide levels for a subset of the compounds selected. It is not clear if those that are not reported were included in the original analysis but were not detected or if they were not subject to analysis. Blank cells indicate that no level was reported for those compounds in the cited publication, while “nd” indicates that those compounds were reported as not detected.

Table 1: Date, identity and PM_{2.5} level of the filters selected for analysis.

Date	Cassette Number	PM _{2.5} Level ug/m ³
11/15/2009	510	15.7
11/27/2009	773	20.9
12/10/2009	772	54.4
12/13/2009	215	44.4
12/27/2009	721	24.1
1/11/2010	615	38.5
1/17/2010	753	15.8
2/10/2010	735	22.1

The sampled volume and PM_{2.5} levels for each Fairbanks sample were used to determine the concentrations of the selected compounds in the ambient air (ng/m³) and as a fraction of the PM_{2.5} (ppm). These results are also reported in Tables 2 and 3 as the median and maximum for those samples for which the compounds were detected. In most cases, the compounds were detected on all or nearly all samples. The exception is 20S-5α(H),14α(H),17α(H)-ergostane, which was detected on only two samples (510 and 735).

3. Results and Discussion

The results from literature review and calculated analytical results for fourteen selected compounds are presented in Tables 2¹⁻⁶ and 3⁷⁻⁹. These compounds are classified into hopanes and steranes, thiophenes, and PAHs.

3.1 Hopanes and Steranes

The hopanes and steranes are typically found and reported in distillate fossil fuel emissions, but have also been reported in coal emissions. The highest levels reported are for diesel auto emissions, and the lowest are for coal emissions. The second column of coal results, presented as mg/kg of fuel, indicate that these compounds are present in coal emissions but do not allow direct comparison with the other values reported. The hopanes and steranes are not present in emissions from biomass

Table 2: Levels of selected marker compounds as a fraction of particulate matter (ppm).

Compound	Residential Oil Burner ³	Diesel Vehicles ^{1,4}	Gasoline Vehicles ⁵	Bituminite Coal ⁶	Bituminite Coal ^{2,b}	Fairbanks Median (Maximum)
Hopanes/Steranes (petroleum products)	17 α (H)-22,29,30-Trisnorhopane	5.3		0.4	67	16.6 (90.6)
	17 α (H),21 β (H)-29-Norhopane	2.22	14.8	2.5	85	41.3 (152)
	17 α (H),21 β (H)-Hopane	3.53	61.6	4.4	1.4	26.0 (79.8)
	22S-17 α (H),21 β (H)-30-Homohopane	1.02		nd	1.1	17.7 (55.9)
	22R-17 α (H),21 β (H)-30-Homohopane	0.64		nd	0.2	23.5 (129)
	22S-17 α (H),21 β (H)-30,31-Bishomohopane	0.58		nd	nd	8.5 (34.5)
	22R-17 α (H),21 β (H)-30,31-Bishomohopane	0.40		nd	nd	15.9 (39.5)
	20R-5 α (H),14 β (H),17 β (H)-cholestane	2.03	4.2			39.2 (45.7)
	20S-5 α (H),14 α (H),17 α (H)-ergostane	4.53	17.0			4.43 (4.97)
	20R-5 α (H),14 β (H),17 β (H)-stigmastane	1.87	20.6			4.89 (6.36)
Thiophenes	Dibenzothiophene	12.6 10.7 ^a	43 ^a			49.0 (65.8)
	2,3-Benzo[b]naphtha[1,2-d]thiophene	23.8				15.8 (29.7)
PAH	Picene			nd	94	36.2 (69.3)
	Retene			4.6	nd	44.2 (68.0)

^aFound in the gas phase only. ^bEmission factors in mg/kg of fuel.

Table 3: Levels of selected marker compounds found in ambient air (ng/m³)

	Compound	Ambient Air, Europe ⁸	Mingo Junction, OH ⁷	Zheng Southeastern USA ⁹	Fairbanks Median (Maximum)
Hopanes/Steranes (petroleum products)	17 α (H)-22,29,30-Trisnorhopane			0.06	0.53 (2.18)
	17 α (H),21 β (H)-29-Norhopane		0.1-0.6	0.36	1.26 (3.67)
	17 α (H),21 β (H)-Hopane		0.05-0.3	0.38	0.72 (1.92)
	22S-17 α (H),21 β (H)-30-Homohopane			0.20	0.47 (1.17)
	22R-17 α (H),21 β (H)-30-Homohopane			0.18	0.61 (3.11)
	22S-17 α (H),21 β (H)-30,31-Bishomohopane			0.11	0.38 (0.72)
	22R-17 α (H),21 β (H)-30,31-Bishomohopane			0.08	0.45 (0.95)
	20R-5 α (H),14 β (H),17 β (H)-cholestane				0.88 (2.49)
	20S-5 α (H),14 α (H),17 α (H)-ergostane				0.082 (0.086)
	20R-5 α (H),14 β (H),17 β (H)-stigmastane				0.12 (0.24)
Thio-phenes	Dibenzothiophene	0.029 (0.095)			0.93 (2.92)
	2,3-Benzo[b]naphtho[1,2-d]thiophene	0.012 (0.082)			0.45 (0.72)
PAH	Picene		<0.0006 - 0.2		0.76 (1.67)
	Retene				1.08 (2.58)

combustion, and thus provide a general indication of the extent to which an air shed is affected by fossil fuel emissions. Unfortunately, however, none of the compounds provide a specific marker of any particular fossil fuel source.

The results for the Fairbanks samples show very high levels of the selected hopanes and steranes. This is clear from inspection of Table 2, which shows that the hopanes and steranes typically represent a much higher fraction of PM_{2.5} than any of the reported fossil fuel sources. There are exceptions in which the Fairbanks levels are about the same as or lower than diesel emissions. These results are striking, however, since PM_{2.5} in Fairbanks is expected to be a mixture of PM from various sources including non-fossil fuel sources.

The ambient air levels of hopanes and steranes in Fairbanks also far exceed those reported for other airsheds (Table 3). Since these airsheds are impacted by automobiles and Mingo Junction Ohio is also affected by coal emissions, the very high levels in Fairbanks are notable. Clearly, fossil fuel emissions have a substantial impact on Fairbanks PM_{2.5}.

An alternative approach for the analysis of hopane results is to calculate the ratio of 17 α (H) 21 β (H) hopane to 22R-17 α (H), 21 β (H) homohopane.^{2,6,10} This value has been reported to be 3.7 for gasoline emissions and 2.5 for diesel emissions.¹⁰ Unfortunately, conflicting results have been reported for coal combustion emissions, with Oros *et al.*² reporting values of 0.1-2.6 and Zhang *et al.*⁶ reporting values of 4.28-9.19. The average value observed for Fairbanks is 1.2 \pm 0.4. This relatively low value places the result for Fairbanks within the range reported by Oros *et al.*, which implies that coal emissions may have a significant impact on Fairbanks PM_{2.5}.

The hopane and sterane results indicate that fossil fuel emissions have a substantial effect on air quality in Fairbanks. However, the results are not very helpful in more clearly identifying the specific fossil fuel source. For this reason, regular further analysis of hopanes and steranes is not recommended unless it is conducted as part of a more in-depth comprehensive source apportionment based on organic compounds.

3.2 Thiophenes

Table 4: Dibenzothiophene levels in three fuel oils from Fairbanks and in diesel fuels.

Fuel	Dibenzothiophene (ppm)
Fuel #1	34.3
Fuel #2	461
Waste Fuel	21.7
LSDF ³	15.2
HSDF ³	84.0

Dibenzothiophene, naphthobenzothiophenes and alkylated derivatives of these compounds are reported to be representative of diesel fuel vehicle emissions.^{1,4} These compounds make up a significant fraction of the sulfur content of diesel fuel (Table 4). Low sulfur diesel fuel has lower concentrations of these compounds, and vehicles utilizing low sulfur diesel fuel emit reduced quantities of these compounds. The values reported in Table 2 for diesel emissions are from vehicles utilizing low sulfur diesel fuel.^{1,4} Rogge *et al.*³ did not report thiophenes in the emissions from residential fuel oil combustion, but Huffman *et al.* did report that typically 25-35% of the sulfur in residential fuel oil particulate is thiophenic sulfur.¹¹ Given the similar composition of # 2 fuel oil and diesel fuel, and the fact that the sulfur content of # 2 fuel oil is not regulated with respect to sulfur content, it stands to reason that these compounds may be found in the PM_{2.5} emissions from #2 fuel oil as well. In fact, #2 fuel oil obtained from Fairbanks was found to have a level of dibenzothiophene much higher than that reported previously for high sulfur diesel fuel (Table 4). Waste oil fuel and #1 fuel oil from Fairbanks were found to have dibenzothiophene levels between that of low and high sulfur diesel fuels. Dibenzothiophene has also been reported in the emissions from gasoline vehicles. In this and one report on diesel emissions, dibenzothiophene was found primarily in the gas phase. Given the ambient

temperatures in Fairbanks, it seems likely that the compound would be found in the particulate phase. These sulfur compounds are not present in wood smoke, and were not reported in coal studies. It is not clear, however, whether or not they are present in PM from coal combustion.

The results in Table 2 indicate that the Fairbanks PM has high levels of thiophenes in comparison to PM emitted from vehicles burning low sulfur diesel fuel. As with the hopane and sterane results discussed in section 3.1, these results are striking given that Fairbanks PM_{2.5} is expected to be a mixture of PM from various sources and not only diesel fuel or residential fuel oil burners. The observed dibenzo- and benzonaphtho- thiophene levels do not, however, explain the relatively high levels of non-sulfate sulfur observed in Fairbanks PM_{2.5}. These compounds represent only 7.7 and 2.5 ppm S in the PM_{2.5} respectively.

The results in Table 3 show that the ambient levels of these thiophenes in Fairbanks are much higher than those reported for several European cities. The average PM_{2.5} levels in those cities varied from 11 to 30 $\mu\text{g}/\text{m}^3$, and median concentration of dibenzo- and benzonaphtho- thiophenes as a fraction of the PM_{2.5} was 1.3 and 0.48 ppm respectively. The very high levels observed in Fairbanks, considered either as ambient concentration or as a fraction of PM_{2.5}, are remarkable given that diesel powered automobiles and trucks are typically much more prevalent in European cities.

The thiophene results presented here point rather strongly to residential fuel oil burners utilizing #2 fuel oil obtained from Fairbanks (and/or possibly coal combustion) as a source of PM_{2.5} in Fairbanks. Analysis of the PM_{2.5} obtained from residential oil burner studies utilizing Fuel #2 will be especially useful in confirming this result. Fuel #2 from Fairbanks has exceptionally high levels of dibenzothiophene, suggesting that this and other thiophenes will be very useful markers of emissions from combustion of that oil. Further, combustion of this fuel in Fairbanks may explain some of the high levels of sulfur observed in the PM_{2.5}.

3.3 PAHs

Picene is a 5-ring PAH that has been reported as being representative of emissions from coal combustion.^{2,6,7} Zhang *et al.* reported picene as being “unique to the organic carbon emissions from coal combustion,” although picene was not detected in all coal particulate and was notably absent from bituminous coal emissions from industrial boilers.⁶ Zhang *et al.* did report picene in brown and mixed coal emissions from residential boilers (3.7 and 2.0 ppm respectively) as well as much higher levels in the emissions from residential oil burners (72-284 ppm).⁶ Oros *et al.* reported picene and methyl picenes as bituminous coal smoke markers, and C₂ substituted picenes as more general coal-specific markers.² As a large PAH, picene can be expected to be found primarily in the particulate phase.

Results for picene as a fraction of Fairbanks PM_{2.5} (Table 2) are relatively difficult to interpret given the scarcity of relevant information in comparable units found in the literature. By comparison to the results of Zhang *et al.*⁶, the levels in Fairbanks are much higher (by a factor of 10 or more) than would be expected from commercial boilers. The levels observed in Fairbanks are not as high as those reported by Zhang *et al.* for residential coal burners in China, but are of a similar magnitude for combustion of some types of coal in Chinese residential coal burners.

Results for ambient picene levels are also surprising. Fairbanks has much higher levels of picene than Mingo Junction, OH, which was specifically studied because of a significant impact of coal emissions. Source apportionment in Mingo Junction using organic marker profiles concluded that coal soot makes up 3 to 10% of the organic carbon in the PM_{2.5}, depending on season.⁷

Relatively high levels of picene are observed in Fairbanks when considered either as a fraction of PM_{2.5} or as ambient concentration. This is a very strong indication that coal combustion, and very likely coal combustion in a poorly designed or operated boiler, is a significant contributor to Fairbanks PM_{2.5}.

Retene is an alkyl substituted 3-ring PAH that has commonly been associated with combustion of soft woods.¹² This compound is included in this report, however, because it has also been reported as a component of coal combustion emissions.⁶ Levels in Fairbanks are relatively high compared with those reported by Zhang et al. for bituminous coal emissions from industrial boilers, similar to the level

Table 5: Ratio of indeno[123-cd]pyrene to sum of indeno[123-cd]pyrene and benzo[ghi]perylene for various sources.

Source	IP/(IP+BghiP)
Gasoline autos	0.18
Diesel autos	0.37
Coal combustion	0.56
Wood combustion ¹²	0.54
Fairbanks PM _{2.5}	0.39 ± 0.02

reported by these authors for brown coal emissions from industrial boilers (60 ppm) and much lower than those reported for residential coal burners (364-5000 ppm).⁶ Ambient levels in Fairbanks are similar to or lower than those reported for southeastern US cities.⁷ It is not clear whether the retene observed in Fairbanks PM_{2.5} is indicative of coal combustion, wood combustion, or both.

Another commonly used measure for sourcing PAH emissions is the ratio of indeno[123-cd]pyrene to the sum of indeno[123-cd]pyrene and benzo[ghi]perylene (IP/(IP+BghiP)).^{6,}

^{12, 13} Typical values for this ratio from various fossil fuel sources, woodsmoke and for Fairbanks are reported in Table 5. No value is available for residential oil combustion PM_{2.5}. The ratio for Fairbanks is quite consistent between samples, and is most similar to that reported for diesel fuel emissions.

4 Conclusions

The results of this preliminary study are very informative, but are not conclusive. It is not possible to draw unqualified or quantitative conclusions concerning the sources of Fairbanks PM_{2.5} with the limited number of samples and compounds analyzed. However, the results do show that Fairbanks PM_{2.5} is more complex chemically than was previously realized, and strongly suggest that fossil fuel combustion represents a measurable contribution to PM_{2.5} in Fairbanks. The levels of hopanes and steranes, thiophenes, and picene are all high relative to previous reports whether considered as a fraction of PM or as ambient concentrations. These compounds are all representative of fossil fuel combustion sources.

The hopanes and steranes are not representative of any particular fossil fuel source, but do indicate the overall contribution of fossil fuels. Analysis of the ratio of 17 α (H) 21 β (H) hopane to 22R-17 α (H), 21 β (H) homohopane might suggest that coal combustion is a significant source of PM_{2.5} in Fairbanks, but inconsistent literature values for this ratio cause significant uncertainty in this conclusion.

The relatively high levels of thiophenes observed in Fairbanks PM_{2.5} are a strong indication of significant transportation diesel fuel or residential oil burner contributions. Again, the levels of these compounds are higher than those previously reported for diesel PM or in cities with many more diesel vehicles than Fairbanks. The #2 fuel oil used in residential oil burners in Fairbanks also contains a very high concentration of dibenzothiophene, implying that this is a likely source. The low sulfur diesel fuel used in Fairbanks should significantly limit the contribution of diesel transportation to the thiophene concentrations. Coal combustion emissions can not be ruled out as a source of some of the thiophenes, but few if any quantitative data exist concerning the presence or absence of thiophenes in coal combustion emissions. Although the concentrations of thiophenes are relatively high, their concentrations are not sufficient to explain the sulfur content of Fairbanks PM_{2.5}.

Picene is also observed at remarkably high levels whether considered relative to the PM_{2.5} mass or as ambient concentration. This compound is considered to be a good and selective marker of coal combustion, so this result is strong evidence that coal combustion is a source of PM_{2.5} in Fairbanks. Based on literature values, however, the concentrations of picene in Fairbanks can not be explained by

industrial boiler emissions alone. This begs the question of whether the boilers operating in the Fairbanks area are being operated under suboptimal conditions, or if there are other coal combustion sources contributing to Fairbanks PM_{2.5}.

The ratio of IP/(IP+BghiP) for Fairbanks PM_{2.5} is lower than that reported previously for coal or wood combustion, and is indicative of diesel vehicle emissions. This may indicate either a significant contribution from diesel transportation, a significant contribution from residential heating oil, or a combination of wood/coal with diesel/residential heating oil and gasoline auto PM.

Further study of Fairbanks PM_{2.5} needs to be conducted before any more quantitative or conclusive source apportionment using organic tracers can be conducted. This approach would be much more informative once analyses have been performed on PM_{2.5} obtained from representative sources under controlled conditions. A comprehensive organic speciation of many more samples than were analyzed in the current study, combined with a source apportionment procedure using organic compounds as tracers,^{9, 14, 15} could lead to a more complete picture of the Fairbanks PM_{2.5} problem.

Alternatively, analysis of Fairbanks PM_{2.5} for a limited number of selected analytes could be informative. This is especially true if these analyses were used to evaluate the effects and efficacy of remediation efforts and/or in combination with local or regional mapping of concentrations. If this limited and less costly approach is to be pursued, the current study suggests that the most likely marker candidates for analysis are levoglucosan (wood smoke), picene (coal) and thiophenes (residential oil and/or diesel). Initial and preliminary studies in our laboratory indicate that these three compounds can be determined at relevant concentrations using a single extraction followed by two separate gas chromatographic separations.

5 References Cited

- [1] Liang, F., Lu, M., Birch, M. E., Keener, T. C., Liu, Z., "Determination of polycyclic aromatic sulfur heterocycles in diesel particulate matter and diesel fuel by gas chromatography with atomic emission detection," *Journal of Chromatography, A* **2006**, *1114*, 145-153.
- [2] Oros, D. R., Simoneit, B. R. T., "Identification and emission rates of molecular tracers in coal smoke particulate matter," *Fuel* **2000**, *79*, 515-536.
- [3] Rogge, W. F., Hildemann, L. M., Mazurek, M. A., Cass, G. R., Simoneit, B. R. T., "Sources of Fine Organic Aerosol. 8. Boilers Burning No. 2 Distillate Fuel Oil," *Environmental Science and Technology* **1997**, *31*, 2731-2737.
- [4] Schauer, J. J., Kleeman, M. J., Cass, G. R., Simoneit, B. R. T., "Measurement of Emissions from Air Pollution Sources. 2. C1 through C30 Organic Compounds from Medium Duty Diesel Trucks," *Environmental Science and Technology* **1999**, *33*, 1578-1587.
- [5] Schauer, J. J., Kleeman, M. J., Cass, G. R., Simoneit, B. R. T., "Measurement of Emissions from Air Pollution Sources. 5. C1-C32 Organic Compounds from Gasoline-Powered Motor Vehicles," *Environmental Science and Technology* **2002**, *36*, 1169-1180.
- [6] Zhang, Y., Schauer, J. J., Zhang, Y., Zeng, L., Wei, Y., Liu, Y., Shao, M., "Characteristics of Particulate Carbon Emissions from Real-World Chinese Coal Combustion," *Environmental Science and Technology* **2008**, *42*, 5068-5073.
- [7] Rutter, A. P., Snyder, D. C., Schauer, J. J., De Minter, J., Shelton, B., "Sensitivity and Bias of Molecular Marker-Based Aerosol Source Apportionment Models to Small Contributions of Coal Combustion Soot," *Environmental Science and Technology* **2009**, *43*, 7770-7777.
- [8] Saarnio, K., Sillanpaa, M., Hillamo, R., Sandell, E., Pennanen, A. S., Salonen, R. O., "Polycyclic aromatic hydrocarbons in size-segregated particulate matter from six urban sites in Europe," *Atmospheric Environment* **2008**, *42*, 9087-9097.

- [9] Zheng, M., Cass, G. R., Schauer, J. J., Edgerton, E. S., "Source Apportionment of PM_{2.5} in the Southeastern United States Using Solvent-Extractable Organic Compounds as Tracers," *Environmental Science and Technology* **2002**, *36*, 2361-2371.
- [10] Rogge, W. F., Hildemann, L. M., Mazurek, M. A., Cass, G. R., Simoneit, B. R. T., "Sources of fine organic aerosol. 2. Noncatalyst and catalyst-equipped automobiles and heavy-duty diesel trucks," *Environmental Science and Technology* **1993**, *27*, 636-651.
- [11] Huffman, G. P., Huggins, F. E., Shah, N., Huggins, R., Linak, W. P., Miller, C. A., Pugmire, R. J., Meuzelaar, H. L. C., Seehra, M. S., Manivannan, A., "Characterization of fine particulate matter produced by combustion of residual fuel oil," *Journal of the Air & Waste Management Association* **2000**, *50*, 1106-1114.
- [12] Schauer, J. J., Kleeman, M. J., Cass, G. R., Simoneit, B. R. T., "Measurement of Emissions from Air Pollution Sources. 3. C1-C29 Organic Compounds from Fireplace Combustion of Wood," *Environmental Science and Technology* **2001**, *35*, 1716-1728.
- [13] Stracher, G. B., Taylor, T. P., "Coal fires burning out of control around the world: thermodynamic recipe for environmental catastrophe," *International Journal of Coal Geology* **2004**, *59*, 7-17.
- [14] Schauer, J. J., Rogge, W. F., Hildemann, L. M., Mazurek, M. A., Cass, G. R., Simoneit, B. R. T., "Source apportionment of airborne particulate matter using organic compounds as tracers," *Atmospheric Environment* **1996**, *30*, 3837-3855.
- [15] Schauer, J. J., Rogge, W. F., Hildemann, L. M., Mazurek, M. A., Cass, G. R., Simoneit, B. R. T., "Source apportionment of airborne particulate matter using organic compounds as tracers," *Atmospheric Environment* **2008**, *41*, S241-S259.